

КОЛЛОИДНЫЙ
ЖУРНАЛ

20
1958

COLLOID JOURNAL

(KOLLOIDNY ZHURNAL)

IN ENGLISH TRANSLATION

545-155
8

VOL. 20

NO. 1

CONSULTANTS BUREAU, INC.

227 WEST 17TH STREET, NEW YORK II, N. Y.



an agency for the interpretation of international knowledge

INFLUENCE OF THE PREPARATION CONDITIONS OF ALUMINUM SOAPS OF NAPHTHENIC ACIDS ON THE PROPERTIES OF THEIR OLEOGELS

G. V. Belugina and A. A. Trapeznikov

Aluminum soap powders, which consist of aluminum salts of organic acids (aliphatic, naphthenic), are able to swell and dissolve in hydrocarbon liquids to form colloidal systems of various consistencies according to conditions, from mobile solutions of low viscosity to highly viscous elastic gels. The nature of the thickener, i.e., the aluminum soap, the structure and properties of which determine the oleogel properties to a considerable extent, is of particular significance for such systems.

There have been many studies of the possibility of formation, and of the structure and properties of mono-, di-, and trisubstituted aluminum soaps of fatty acids and of their gels in organic solvents. Considerably less information is available in the literature on aluminum soaps of naphthenic acids [1-10]. The purpose of the present investigation was to study and interpret the influence of individual factors in the preparation of aluminum naphthenates and their thickening power and the stability of their oleogels. Our study of the influence of precipitation conditions on the properties of aluminum soaps was based on the possible analogy between the conditions of formation of $\text{Al}(\text{OH})_3$ structures and of aluminum-oxygen networks in aluminum soaps. This approach made it possible to determine the influence of individual factors in precipitation (ratio of free to bound alkali, pH of the medium, temperature, and concentrations of the reagents) on the properties of the aluminum soaps formed, and also to establish a relationship between the stability of oleogels in the course of aging and the composition of the soaps.

The molecular weight and nature of the organic radical of the acid also have a strong influence on the thickening properties of a soap. Investigations of aluminum soaps of fatty and naphthenic acids have shown that the thickening power of soaps increases with decreasing molecular weight of the acids [11-13]. We found that this general principle was also valid in the preparation of Al soaps of naphthenic acids in factory conditions.

Oleogels of Al naphthenates in hydrocarbon solvents have peculiar structural and mechanical properties [14, 15]. These properties (high viscosity, elasticity, strength, and stability) are closely associated with the nature of the soaps, which depends in many respects on the acid radical and the conditions of preparation of the soap. The stability of oleogels, i.e., their retention of their original properties (including viscosity) during prolonged storage is a question of great practical importance. Apart from the factors mentioned above, the stability of oleogels is also influenced by the chemical nature and purity of the organic solvent, the presence of admixtures of other substances, the form and nature of the material of the container in which the oleogel is kept, and other factors.

Methods of soap preparation. The Al naphthenates were prepared by double decomposition, effected by two methods: 1) by the usual addition of $\text{Al}_2(\text{SO}_4)_3$ solution to a solution of alkaline sodium soap, with a continuous change of the pH of the medium from high to low values. This was termed the "direct precipitation" method; 2) by simultaneous pouring of solutions of $\text{Al}_2(\text{SO}_4)_3$ and alkaline sodium soap into water the pH of which had previously been brought to a definite value by means of one of these solutions. The addition rates of the two solutions were regulated so as to keep this pH constant throughout the entire precipitation. The constancy of pH was checked by means of a glass electrode or colored indicators. This method was proposed and used for the first time by A. A. Trapeznikov in 1942-1943;* in the present investigation it was improved and modified with respect to the optimum pH of the medium [16]. The precipitation was carried out in a laboratory unit (Fig. 1) equipped

* The precipitation was carried out at constant pH, which was decreased to 4.5 at the end of the precipitation.

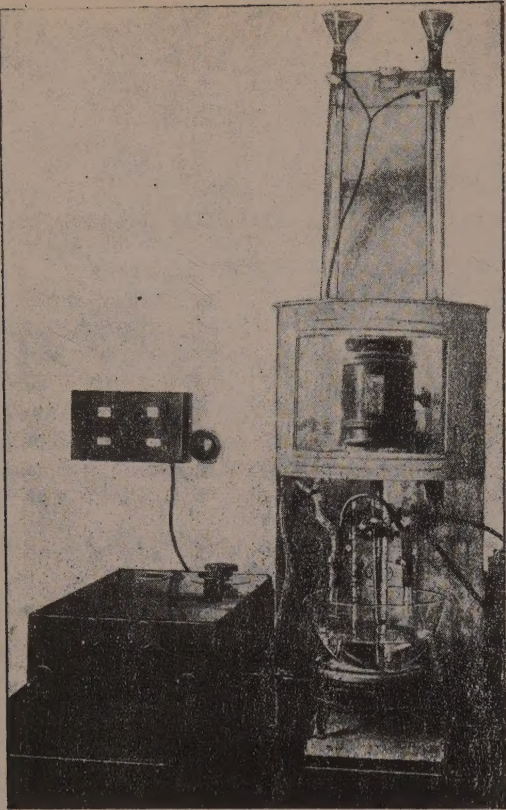
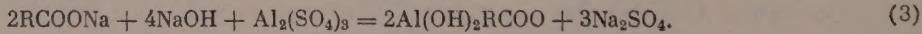
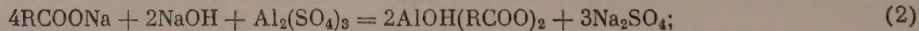
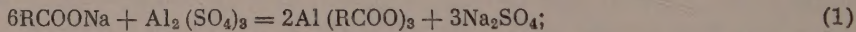


Fig. 1. Laboratory apparatus for precipitation of Al naphthenates.

is in theory possible to obtain aluminum salts of different degrees of substitution, for example:



Therefore the "basicity" of the soap, i.e., the saturation of the aluminum valences with hydroxyls, depends on the relative proportions of the free alkali and the bound alkali (i.e., the alkali used for saponification of the acid). Thus, in absence of free alkali [Equation (1)] the composition corresponds to a trisubstituted soap, which probably cannot exist owing to its easy hydrolysis [1, 3, 17]. If free alkali is present in 50% excess over the bound alkali [Equation (2)], a disubstituted soap is formed; with 200% excess of free alkali [Equation (3)], a monosubstituted soap is formed. However, owing to the complex character of the whole process of soap formation, such definite stoichiometric compounds probably constitute only a part of the whole product, while the rest consists of more complex formations of intermediate composition, and also of hydrolysis products (Al(OH)_3 , free acids). We therefore used different proportions of free and bound alkali, including intermediate ratios between those given above, and studied the properties of Al naphthenates prepared in presence of between 15 and 200% free alkali both by "direct" precipitation and by precipitation at constant pH [16].

It was found that the viscosity* of 4% oleogels in cryoscopic benzene, of Al soaps precipitated at 20° at different but constant pH values (5, 7, and 9), increases with increasing free alkali content at precipitation, and passes through a maximum at 21–36% NaOH (Fig. 2).

* The viscosity was characterized by the values of the highest constant viscosity of the undestroyed structure [14, 15], determined by a standard procedure developed by N. A. Bakh.

with a mechanical stirrer, a thermostatically controlled reaction vessel, and heated burets (the temperature of the emerging drops was determined by means of thermocouples coated with thin plastic films and placed in the buret tips).

In both methods the precipitated soap was washed to a negative reaction for SO_4^{2-} in the wash waters, and dried at a definite temperature to constant weight. It was found that precipitates formed at pH 10 and 9 coagulate badly, contain a fine fraction which passes through the filter, and are difficult to wash. The filterability and coagulation of the precipitates improves with decreasing pH, while precipitation from acid solution ($\text{pH} \sim 3.5$) gives a sticky, resinous precipitate.

The starting material was "asidolmylonraft" (GOST No. 3854-47, Grade 1) obtained in the alkaline purification of petroleum distillates, and containing naphthenic acids of the kerosene and solar oil fractions with average molecular weight $M_{av} = 250-260$. Apart from this, in some experiments naphthenic acids ($M_{av} = 250$), purified to remove the tail fraction and a large proportion of unsaponifiables by a single distillation of "asidol" in refinery conditions, were used.

Cryoscopic benzene (supplied by the Becker Company) was used as an individual nonpolar solvent; some typical industrial solvents (B-70 aviation gasoline, ordinary gasoline, etc.) were also used.

Effect of free-bound alkali ratio in precipitation of Al soaps. In the precipitation of Al naphthenates it

As the precipitation temperature increases, the viscosity maximum is shifted in the direction of higher contents of free alkali, corresponding to 75-100% NaOH.

The viscosity of 4% oleogels in cryoscopic benzene is plotted against the free alkali content in precipitation of the soaps in Fig. 3 (the soaps were precipitated at pH 5 and 66°). However, while the viscosity of the oleogels increases with increasing free alkali content at precipitation, the stability* of the gels falls rapidly, and oleogels of soaps precipitate at lower free alkali contents (15-50%) are the more stable.

Typical curves for aging of oleogels (6% solutions in cryoscopic benzene) of soaps prepared by "direct" precipitation at 80° with 50-200% of excess alkali are given in Fig. 4.

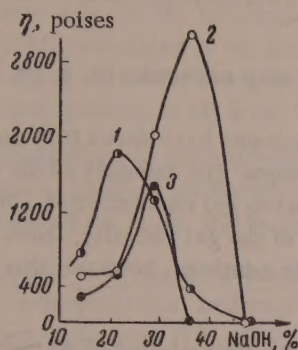


Fig. 2. Effect of the ratio of free to bound alkali in soap precipitation on the viscosity of oleogels:

1) pH 5; 2) pH 7; 3) pH 9.

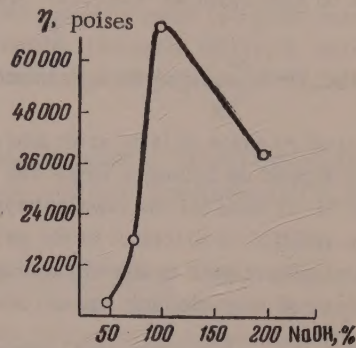
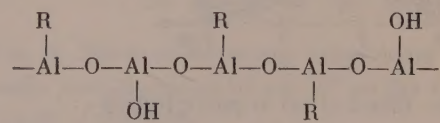


Fig. 3. Effect of the ratio of free to bound alkali in soap precipitation on the viscosity of oleogels.

The observed differences of viscosity and aging processes of oleogels of Al naphthenates precipitated at different contents of free alkali can be accounted for by the differences in their composition. The thickening properties of an Al soap are closely associated with the structure and properties of its aluminum-oxygen skeleton. By analogy with the ability of $\text{Al}(\text{OH})_3$ to "polymerize" with formation of polyhydroxide chains [18], we may assume that the primary soap particles are of elongated shape, although probably not of very large size, owing to "polymerization" through the oxygen atoms:



In a number of cases, owing to incompleteness of the precipitation process or to the presence of a large excess of alkali, such chains may include regions of $\text{Al}(\text{OH})_3$

Fig. 4. Effect of storage time on oleogel viscosity for soaps precipitated in presence of excess NaOH:

1) 50%; 2) 75%; 3) 150%; 4) 200%.

entirely devoid of acid radicals. The aluminum-oxygen skeleton of the soap chains may undergo changes in the course of time, i.e., it may age in the same way as pure $\text{Al}(\text{OH})_3$ [19], especially if it contains $\text{Al}(\text{OH})_3$.

* We studied the stability of the oleogels in relation to the various properties of the soap itself regarded as a thickener, and did not consider artificial stabilization of the oleogels by means of additives. An oleogel was taken as stable if its viscosity did not increase or decrease by a factor of more than two during prolonged storage (about a year).

regions. Consequently, increase of the free alkali content in precipitation leads to formation of Al soaps with a structure increasingly closer to the structure of $\text{Al}(\text{OH})_3$, which is therefore increasingly liable to undergo aging, leading to changes in the properties (including viscosity) of the oleogels in the course of time. The ratio of free to bound alkali in the precipitation of Al soaps is one of the main factors determining the stability of their oleogels. Moreover, the aluminum-oxygen skeleton may adsorb ions in the course of its formation, and these may influence the aging of the soap, in the same way as the aging of $\text{Al}(\text{OH})_3$. The great resemblance between the properties and preparation methods of $\text{Al}(\text{OH})_3$ itself and the Al soaps described in this paper has been recently established by A. A. Trapeznikov and A. M. Tolmachev.

Structure formation in the oleogel system may take place by different types of bonding; for example, by means of additional coordination bonds between aluminum and oxygen, RAI...O-Al , hydrogen bonds between hydroxyls attached to aluminum Al-OH...O-AlR and hydroxyls and oxygens in carboxyl groups of other

molecules Al-OH...O-C(=O)-R , and through water molecules joining individual soap molecules [2, 3, 12, 20,

25]. Recent studies of Al soaps of fatty acids and of their gels by infrared spectroscopy have shown [21] that gel formation does not depend on hydrogen bonds due to the presence of free OH groups. The intensity of the band characterizing the $\text{Al}-\text{O}$ bond (of the covalent type) was found to be proportional to gel concentration. Weakening of this band on addition of m-cresol to the gel, accompanied by a decrease of the gel viscosity, shows that the $\text{Al}-\text{O}$ band is closely related to the thickening power of the soap. It must be admitted, however, that the nature of the bonds in Al soap oleogels has not been finally established.

Effect of pH in the precipitation of Al soaps. The pH of the medium in the precipitation of Al soaps, greatly influences their composition and thickening properties [16]. The viscosity of oleogels of Al naphthenates precipitated at different pH (from 10 to 3.5) and in presence of 36% excess alkali first increases with decreasing pH, and passes through a maximum at $\text{pH} \sim 5$ (Fig. 5). This is probably associated with hydrolysis of $\text{Al}_2(\text{SO}_4)_2$

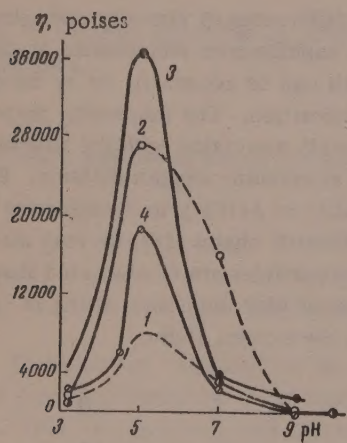


Fig. 5. Effect of pH at precipitation on the viscosity of oleogels, for soaps precipitated at different temperatures: 1) 20°; 2) 67°; 3) 80°; 4) 93°.

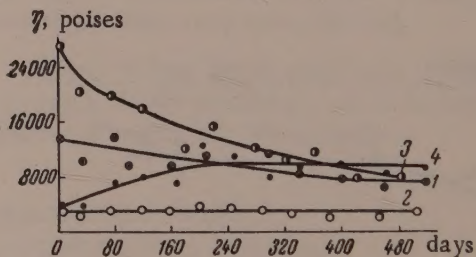


Fig. 6. Effect of storage time on the viscosity of oleogels from soaps prepared:
1) by "direct" precipitation, 36.0% excess NaOH, at 67°; 2) at pH 5, 28.8% excess NaOH, at 67°;
3) at pH 5, 36.0% excess NaOH, at 67°; 4) at pH 7, 36.0% excess NaOH, at 80°.

alkaline media ($\text{Al}(\text{OH})_3$) is predominantly formed. Moreover, in an alkaline medium OH ions are adsorbed, and possibly also molecules of the alkaline sodium soap, which greatly lowers the viscosity of oleogels [22]. Excess adsorption of H^+ (if the soap is precipitated in a strongly acid medium) also decreases oleogel viscosity. Other electrolytes (NaCl , Na_2SO_4 , Na_2HPO_4 , tartaric acid, etc.) added specially to the solution during precipitation of the soap, or introduced together with the Al soap into the oleogels, also have an appreciable effect [22]. These effects are probably caused by anion adsorption and complex formation in the course of precipitation, leading to shielding of the polar groups in the soap chains by the additives, and to peptization.

Determinations of the viscosity of oleogels of Al naphthenates precipitated at different pH showed that soaps precipitated in an acid medium at pH 3.5-5 give rise to oleogels the viscosity of which decreases with

TABLE 1

Thickening Properties of Al Naphthenates Precipitated by Different Methods
36% excess of NaOH at precipitation, temperature 93°

Method of precipitation of Al naphthenates, and pH of medium	Direct pre- cipitation	pH ~ 3.5	pH 4.5	pH 5	pH 7	pH 9
Viscosity of 4% gels in benzene after 3 days, in poises	3655	2032	6127	18,500	2400	21

time. The aging of oleogels of soaps precipitated in alkaline media (pH 7-10) follows a different course; their viscosity increases with time, probably because of additional structure formation in the system in consequence of the slow aging of the aluminum-oxygen skeleton, and also because of a more complete reaction between the free Al(OH)_3 remaining in the soap and the naphthenic acids. This is illustrated by Fig. 6, which shows several typical aging curves for oleogels (4% solutions in cryoscopic benzene) of soaps prepared by "direct" precipitation and by precipitation at pH 5 and 7.

Comparison of the thickening properties of Al naphthenates prepared by "direct" precipitation and by precipitation at constant pH showed that the latter method, under the optimum conditions (pH 5, high temperature), gives soaps of the better thickening properties (Table 1).

Influence of the temperature factor on the properties of Al naphthenates. The precipitation temperature and the subsequent heat treatment of the Al soap formed have a great influence on the structure and thickening properties of the soap [23]. It was found that with increase of the precipitation temperature (from 20 to 92°) the thickening power of the Al soaps formed increases, and passes through a maximum at $\sim 80^\circ$. Observations of viscosity variations in oleogels of Al soaps precipitated at higher temperatures did not reveal any significant differences in the nature of the aging of the oleogels, although in some instances oleogels made from soap precipitated at 92° had greater stability. Soaps precipitated at room temperature sometimes give rise to oleogels the viscosity of which increases with time; this is also the result of additional structure formation in the system.

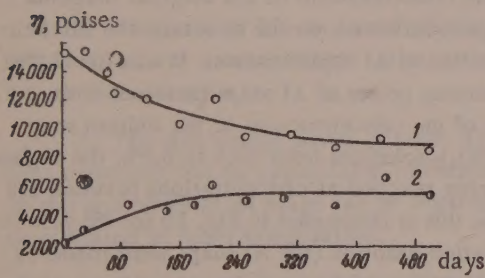


Fig. 7. Effect of storage time on the viscosity of oleogels from soaps heated at 100°:

1) soap precipitated at pH 5; 2) the same, pH 9 (36.0% excess NaOH, temperature 80°).

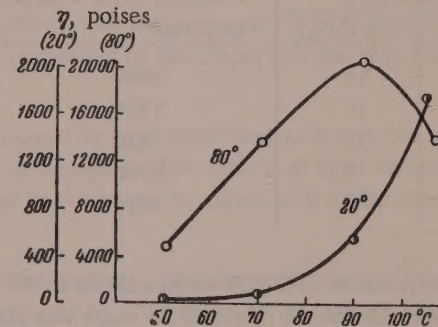


Fig. 8. Effect of the drying temperature of soaps precipitated at 20 and 80° on the viscosity of oleogels.

Heat treatment of moist soaps (for 6 hours at 80-160° in sealed tubes) increases their thickening power, especially of soaps of low thickening power precipitated at room temperature or in an alkaline medium (pH 9) [23].

The aging curves of oleogels made with soaps prepared under different conditions and subjected to heat treatment differ in character. The viscosity of oleogels of Al soaps precipitated at pH 5 and subjected to heat treatment decreases in the course of aging, as it does in the case of the same soaps without heat treatment. On the other hand, the viscosity of oleogels of soaps precipitated at pH 9 and subjected to similar heat treatment increases in the same way as for oleogels of the untreated soaps. Figure 7 shows two typical aging curves for oleogels (4% solutions in cryoscopic benzene) of Al soaps precipitated at pH 5 and 9 and heated at 100° (compare with Fig. 6). It follows that heat treatment of moist soaps has no significant influence on the stability of oleogels made from them.

Drying temperature of Al soaps. As various workers have pointed out, water has a very strong effect on the structure of metal soap oleogels, playing not only a peptizing but also a structurizing role [2, 3, 12, 24, 25]. We studied the influence of drying at various temperatures on the thickening power of Al soaps and on the stability of their oleogels (soaps precipitated at pH 5, 36% excess of NaOH). It was found that the oleogel viscosity increases with increase of the drying temperature of the Al soaps (from 50 to 105°)* (Fig. 5); in the case of the soap precipitated at 80° the viscosity passes through a maximum at ~90°. However, the variation of stability with time is not parallel to the absolute viscosity, as oleogels of soaps precipitated at pH 5, 36% excess of NaOH, at 80°, and dried at low temperatures are the more stable (Fig. 9). Increase of the drying temperature is especially significant for soaps precipitated at 20°, as the drying serves as additional heat treatment. The optimum drying temperature for Al naphthenates precipitated at elevated temperatures is in the 70-90° range.

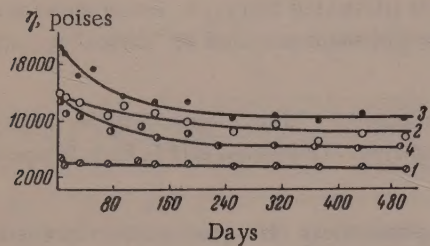


Fig. 9. Effect of storage time on the viscosity of oleogels from soaps dried at:
1) 50°; 2) 70°; 3) 90°; 4) 105°.

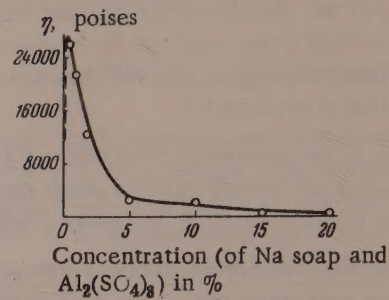


Fig. 10. Variation of oleogel viscosity with the concentrations of the reagents used in precipitation of the soaps.

TABLE 2

Thickening Power of Al Naphthenates as a Function of the Concentrations of the Reagents in Precipitation

Concentration, %		Viscosity after 3 days, in poises
sodium soap	$\text{Al}_2(\text{SO}_4)_3$	
2	10	3690
5	10	1990
10	10	216
2	2	3700
10	2	1010

"direct" precipitation with 50% excess alkali at 80°). The effect of variation of the concentration of one of the reagents on the thickening power of Al soaps was also studied (Table 2).

It follows from these results that changes of the concentration of the sodium soap have a strong influence on the thickening power of the Al soap. Variations of the $\text{Al}_2(\text{SO}_4)_3$ concentration have a more pronounced effect at high concentrations of the sodium soap, and have almost no effect at low concentrations. It must be pointed out, however, that oleogels of Al soaps precipitated at low concentrations are less stable than oleogels of soaps precipitated at higher concentrations.

The increase of the thickening power of Al soaps with increasing dilution of the reagents may be attributed, on the one hand, to hydrolysis of $\text{Al}_2(\text{SO}_4)_3$, and on the other, to dissociation of the sodium naphthenate soap micelles to molecules, when they can react more readily with aluminum in the ionic form. This finding is of great importance in relation to the preparation of Al soaps with reproducible properties.

Stability of oleogels of Al naphthenates in various solvents. To determine the influence of the nature of the solvent, we studied the thickening properties of Al naphthenates, prepared by different methods, in an individual nonpolar solvent — cryoscopic benzene — and in several typical industrial solvents. It was found that the

* The drying was continued to practically constant weight in each case.

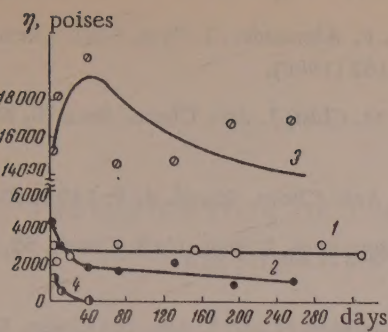


Fig. 11. Effect of storage time on the viscosity of soap oleogels in different solvents:

1) cryoscopic benzene, 2) B-70 aviation gasoline, 3) gasoline, 4) products of kerosene pyrolysis, containing considerable amounts of unsaturated hydrocarbons.

The slow decrease of viscosity in the other solvents may be a consequence of peptization of the soap particles, although the possibility of latent coagulation processes is not excluded.

SUMMARY

1. A study has been made of the precipitation of Al naphthenates by the usual double decomposition method ("direct" precipitation), and by our method in which the reacting solutions are poured into water at constant pH of the medium. The latter method, used under the optimum conditions (pH 5, elevated temperature) gives soaps of higher thickening power than the "direct" precipitation method.
2. The ratio of free to bound alkali, the pH of the medium, and the temperature in the precipitation of the Al soap have a considerable influence on the thickening properties of the soaps, and the structure and stability of their oleogels.
3. The thickening power of some Al soaps can be increased by heat treatment at a suitable temperature; heat treatment has no appreciable influence on the stability of oleogels. The effects of high-temperature drying on the properties of Al soaps can be regarded as the effects of heat treatment, especially in the case of soaps precipitated at room temperature.
4. Decrease of the concentrations of the sodium soap and $\text{Al}_2(\text{SO}_4)_3$ used for precipitation of Al soaps increases their thickening power, the greater effect being produced by a decrease of the sodium soap concentration.
5. The relationships found between the thickening properties of Al soaps in cryoscopic benzene and their formulation and preparation conditions also hold for industrial solvents. Viscosities in certain solvents (containing unsaturated hydrocarbons) are considerably lower than in benzene, and such oleogels are unstable on keeping.
6. The results of this investigation have formed the basis of recommendations for a new improved technical process for the production of Al naphthenates, developed jointly with the organizations concerned, and adopted on the industrial scale.

Academy of Sciences USSR
Moscow

Received February 20, 1957

LITERATURE CITED

- [1] E. Eigenberger and A. Eigenberger-Bittner, *Koll.-Z.* 91, 287 (1940); A. S. C. Lawrence, *J. Inst. Petrol.* 31, 303 (1945); A. S. C. Lawrence, *Trans. Faraday Soc.* 34, 660 (1938); G. H. Smith et al., *J. Am. Chem. Soc.* 70, 1053 (1948).

relationships between the thickening power and the formulation and preparation conditions of the soaps are the same in technical solvents as in benzene. The viscosity in some solvents (containing unsaturated hydrocarbons) is lower than in benzene, and the viscosity of such oleogels falls rapidly during storage. This is probably caused by oxidation products formed at the unsaturated bonds in the hydrocarbons, which break down the oleogel structure owing to their polar character.

Figure 11 shows typical aging curves for oleogels (precipitated at pH 5, 28.8% excess NaOH, temperature 67°) in various solvents; it is seen that the viscosity of oleogels in kerosene pyrolysis products, with a considerable content of unsaturated hydrocarbons, falls very rapidly, and after 40 days the system undergoes complete phase separation, with precipitation of the soap. Therefore in this case aging occurs as the result of latent coagulation, which passes into visible coagulation and culminates in complete precipitation of the thickener.

- [2] C. G. McGee, J. Am. Chem. Soc. 71, 278 (1949); G. V. Vinogradov, Progr. Chem. 20, 533 (1951).
- [3] V. R. Gray, Trans. Faraday Soc. 42 B, 196 (1946); V. R. Gray, A. E. Alexander, J. Phys. Coll. Chem. 53, 9, 23 (1949); A. E. Alexander and V. R. Gray, Proc. Roy. Soc. 200 A, 162 (1950).
- [4] J. Glaser et al., J. Chem. Soc. 2082 (1950); K. J. Mysels and D. M. Chin, J. Am. Chem. Soc. 75, No. 7, 17,506 (1953).
- [5] R. H. Coe, J. Coll. Sci. 3, 293 (1948); E. Back and K. E. Almin, Acta Chem. Scand. 4, 9, 140 (1950).
- [6] K. V. Kharichkov, J. Russ. Phys.-Chem. Soc. 691 (1897); W. Rueggerberg, J. Phys. Coll. Chem. 52, 8, 1948; D. F. Vasilyev, Coll. J. 11, 6, 377 (1949).
- [7] G. W. Shreve et al., J. Phys. Coll. Chem. 51, 963 (1947); S. S. Marsden et al., J. Am. Oil Chem. Soc. 25, 454 (1948).
- [8] R. D. Vold, and G. S. Hattiangdi, Ind. Eng. Chem. 41, 2311 (1949); 41, 2320, (1949); M. J. Vold, Ind. Eng. Chem. 41, 2539 (1949).
- [9] J. W. McBain and E. B. Working, J. Phys. Chem. 51, 974 (1947); K. J. Mysels and J. W. McBain, J. Phys. Coll. Chem. 52, 1471 (1948); S. Ross, McBain, Oil and Soap 23, 214 (1946).
- [10] S. S. Marsden et al., J. Coll. Sci. 2, 265 (1947); K. J. Mysels, J. Coll. Sci. 2, 375 (1947).
- [11] Wo. Ostwald and R. Riedel, Koll.-Z. 69, 185 (1934); 70, 67 (1935).
- [12] G. A. Parry et al., Proc. Roy Soc. 200A, 148 (1950); T. S. McRoberts and J. H. Schulman, ibid, 136; Nature 152, 101 (1948).
- [13] F. J. Licata, J. Am. Oil. Chem. Soc. 31, No. 5, 204 (1954).
- [14] A. A. Trapeznikov, Coll.: New Methods of Physicochemical Investigation of Surface Phenomena, 1, 20 (1950); A. A. Trapeznikov and E. M. Shlosberg, ibid, 39; Proc. Acad. Sci. USSR 62, 791 (1948).
- [15] A. A. Trapeznikov and V. A. Fedotova, Proc. Acad. Sci. USSR 81, 1101 (1951); 82, 97 (1952); 95, 595 (1954).
- [16] A. A. Trapeznikov and G. V. Belugina, Proc. Acad. Sci. USSR 87, 635 (1952).
- [17] J. W. McBain, and W. L. McClatchie, J. Am. Chem. Soc. 54, 3266 (1932).
- [18] R. Willstätter and H. Kraut, Ber. 56, 139 (1923); 57, 58 (1924).
- [19] H. B. Weiser, Inorganic Colloid Chemistry, Vol. II; S. P. Marion and A. W. Thomas, J. Coll. Sci. 1, 3, 222 (1946); Z. Ya. Berestneva, T. A. Koretskaia and V. A. Kargin, Colloid J. 13, 323 (1951); M. I. Lapshin and S. N. Stroganov, Chemistry and Microbiology of Potable and Waste Waters (State Construction Press, 1938), p. 104; L. K. Lepin and A. Ya. Vaivade, J. Phys. Chem. 27, 217 (1953).
- [20] H. Sheffer, Can. J. Res. 26B, 481 (1948).
- [21] W. W. Harple et al., Anal. Chem. 24, 635 (1952); F. A. Scott et al., J. Phys. Chem. 58, 1, 61 (1954); W. H. Bauer, ibid, 59; No. 1, 32, (1955).
- [22] A. A. Trapeznikov and G. V. Belugina, Proc. Acad. Sci. USSR 94, 97 (1954).
- [23] A. A. Trapeznikov and G. V. Belugina, Proc. Acad. Sci. USSR 87, 825 (1952).
- [24] C. M. Cawley et al., J. Inst. Petr. 33, 649 (1947).
- [25] A. A. Trapeznikov and E. M. Shlosberg, Colloid J. 8, 421 (1946).

* In Russian.

INVESTIGATION OF THE DISPERSITY OF SAPROPELS BY MEANS OF THE SEDIMENTOMETER AND THE ELECTRON MICROSCOPE

M. P. Volarovich and V. P. Tropin

Several papers have been published recently on determinations of the dispersity of peats, including the use of the electron microscope [1-3]. However, no special investigations of the dispersity of sapropels have been reported up to the present. Sapropels are polydisperse systems formed in lakes by deposition of dead micro-organisms of plant and animal origin [4, 5]. Since sapropels and peats differ in structural and chemical characteristics, owing to differences in their sources, the physical and mechanical conditions of their formation are also different, it was of interest to apply the procedure developed previously for peats [1-3] to determination of particle size distribution curves for sapropels. By this procedure, fractions larger than 250μ were analyzed by the wet sieving method; the weight sedimentometer was used for fractions between 250 and 1 μ , while the highly disperse colloidal fraction with particles smaller than 1 μ were studied with the aid of the electron microscope. A somewhat improved version of Churaev's weight sedimentometer [6] was used for sedimentometric analysis of sapropels. To avoid orthokinetic coagulation, the solid phase contents of the sapropel suspensions were low, of the order of 0.02-0.03%. The suspensions were prepared by the method used in the experiments with peat, the sapropel samples being dispersed in distilled water without addition of stabilizers or peptizing agents.

Sapropel particles, like peat particles, include large amounts of the dispersion medium (water); therefore their true density in suspension during sedimentation is considerably less than the density of the solid phase, and depends on the particle size. The technique developed by N. V. Churaev for peats was used to measure the sedimentation rates and particle radii in sapropel suspensions with the aid of an optical microscope with a micrometer eyepiece. Stokes' law was used to derive a relationship between the true density of the settling sapropel particles (γ , g/cc) and their effective radius (r , μ), Fig. 1. The three commonest varieties of sapropel were studied: coarse detrital No. 12, fine detrital No. 12, and calcareous No. 14.*

The experimental points are, naturally, considerably scattered; however, they are grouped around two curves as shown in Fig. 1. The deviations of the true density of the settling particles from the density of the dry sapropel substance are large. The density of the dry substance of calcareous sapropel is 2.13 g/cc, while the true density of the settling particles is considerably less. The density of the settling particles of coarse detrital and fine detrital sapropels may reach 1.01-1.02 g/cc, for densities of 2.01-2.09 g/cc for the dry substances. The anomalous density of the particles in sapropel suspensions can be explained, as in the case of peat suspensions, by different forms of bonding between water and the particle substance [7]. It is interesting to note that calcareous sapropel, over 80% of which consists of particles of calcareous origin, has anomalous density owing to the porous internal structure of the fragments of various calcaceous shells and also of occasional plant fragments, the cells of which contain osmotic water. For comparison, the dash line in Fig. 1 represents the curve obtained previously for peats [2, 3].

Figure 2 shows particle size distribution curves for No. 12 coarse detrital, No. 13 fine detrital, and No. 14 calcareous sapropels; the highly disperse fraction of the last was not studied by means of the electron microscope. This fraction is represented in the form of an aggregate rectangle on the curve for calcareous sapropel. Each of the size distribution curves has at least two maxima; this, as in the case of peats, is indicative of aggregate heterogeneity. Moreover, the distribution curves of the coarse and fine detrital sapropels are polyconic in character. Since sapropels consist of coarse and fine remains of higher plants, algae, animal

* The sapropel samples were supplied by Assistant professor A. G. Martinson of the Chair of Hydrotechnology of the Moscow Peat Institute.

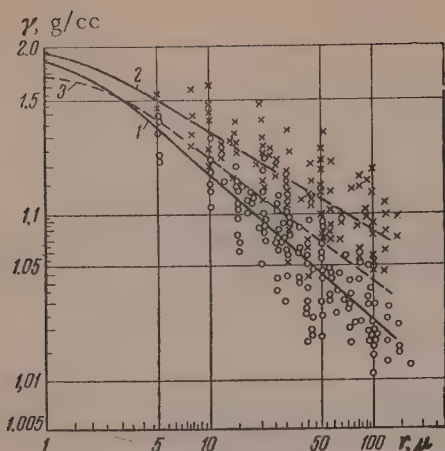


Fig. 1. Variations of true density of settling sapropel particles with their size:
1) Fine and coarse detrital sapropel (circles);
2) calcareous sapropel (crosses); 3) peats
[2, 3].

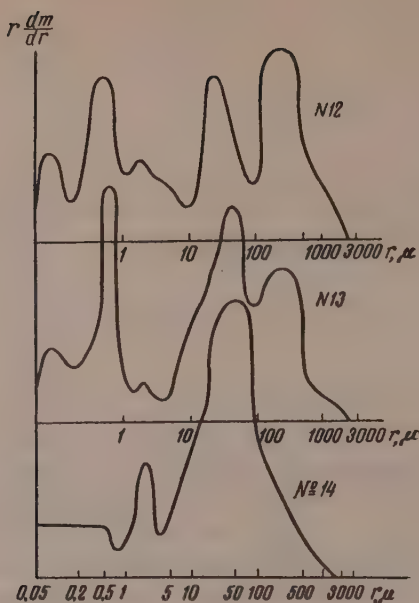


Fig. 2. Particle size distribution curves for sapropels: coarse detrital No. 12, fine detrital No. 13, and calcareous No. 14 (in semilogarithmic coordinates).

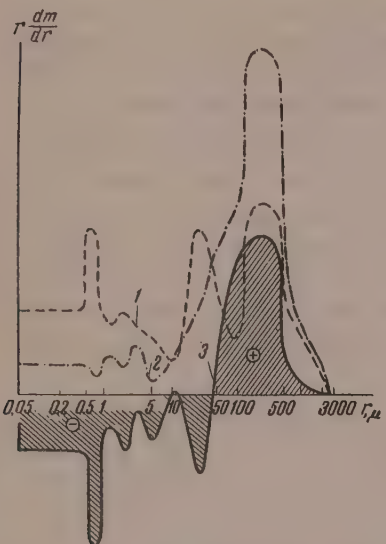


Fig. 3. Particle size distribution curves for coarse detrital sapropel No. 12.

the fractions of each sapropel sample from the results of sieve and sedimentometric analysis, on the assumption that the particles are of spherical shape of a certain effective radius. The values found were $13,892 \text{ cm}^2/\text{g}$ for coarse detrital sapropel No. 12, $12,965 \text{ cm}^2/\text{g}$ for fine detrital sapropel No. 13, and $8,168 \text{ cm}^2/\text{g}$ for calcareous sapropel No. 14. S_{sp} generally ranges between $15,000$ and $25,000 \text{ cm}^2/\text{g}$ for moderately decomposed peats. The inhomogeneity coefficient f , which is often used in soil science [8], was also calculated. The value of f increases with increasing heterogeneity of particle size in a disperse system. For coarse detrital sapropel No. 12, $f = 88$, for fine detrital sapropel No. 13, $f = 30$, and for the calcareous sapropel No. 14, $f = 9.1$. The coarse detrital sapropel was therefore the most heterogeneous with respect to particle size; this is also demonstrated by the particle size distribution curve (Fig. 2). Despite the fact that fairly similar values were found for the specific surfaces of the coarse detrital and fine detrital sapropels, the dispersity of the latter must be nevertheless regarded as somewhat higher than that of the former, as the average weighed diameter of the particles in the coarse fraction ($d_1 > 1 \mu$) was 440μ for the coarse detrital and 320μ for the fine detrital sapropel.

remains, mineral impurities, and detritus (the decomposed sapropel mass), this type of distribution is to be expected. The coarse and fine detrital sapropels have maxima between 500 and 125μ , and between 70 and 15μ , in the large-particle region. The minimum on the distribution curves in the transitional region is followed by a maximum for fine fractions between 1 and 0.25μ . The calcareous sapropel No. 14 is more homogeneous in its particle size distribution; it shows a principal maximum in the large-particle region between 124 and 15μ , and a smaller maximum in the region of intermediate particle sizes, between 3 and 1μ .

Since the distribution curves for the sapropels with several maxima reveal a size heterogeneity, the dispersity is most conveniently expressed in terms of specific surface. The aggregate specific surface (S_{sp}) was calculated for all

The aggregate specific surface (S_{sp}) was calculated for all

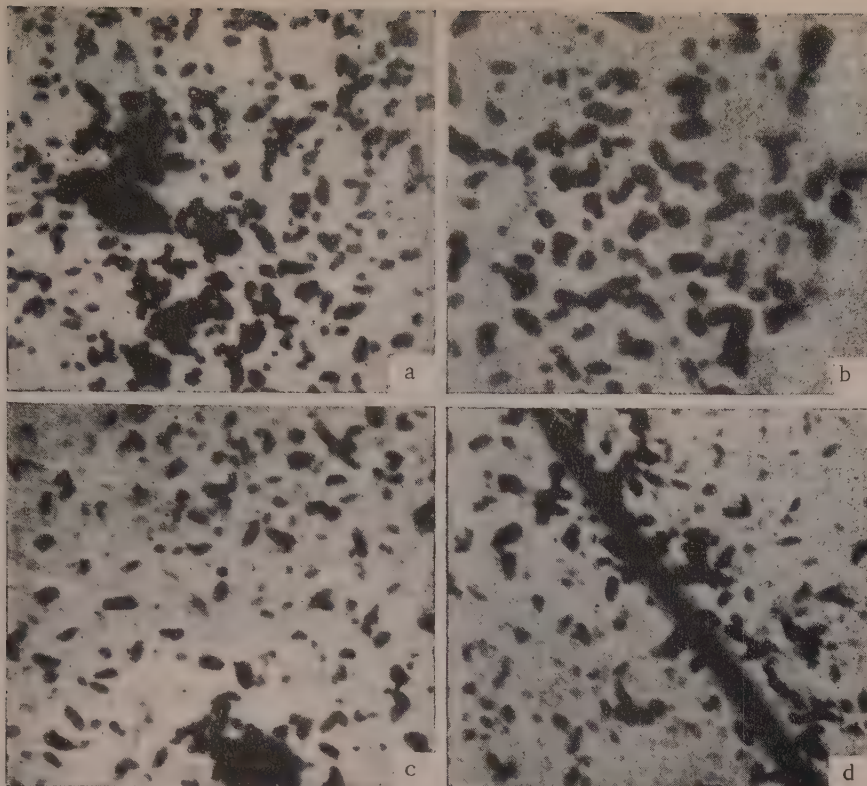


Fig. 4. Electron micrographs of sapropels:
a and b) coarse detrital No. 12; c and d) fine detrital No. 13.

TABLE 1

Particle Sizes and Masses in Highly Disperse Sapropel Fractions

Particle diameters, μ	Number of particles	Δm in %	ΔS in %	Particle diameters, μ	Number of particles	Δm in %	ΔS in %
Coarse detrital sapropel No. 12							
1.0—0.75	18	25.15	23.86	1.0—0.75	8	14.74	12.12
0.75—0.50	37	18.83	25.03	0.75—0.50	33	21.96	25.51
0.50—0.25	123	13.46	30.01	0.50—0.25	161	23.12	44.89
0.25—0.10	380	42.52	20.38	0.25—0.10	274	40.16	16.80
<0.10	167	0.04	0.72	<0.10	140	0.02	0.68
	725	100.00	100.00		616	100.00	100.00

TABLE 2

Particle Shapes in Highly Disperse Sapropel Fractions

Sapropels	Contents of particles of different shapes, %				
	circular	rounded	oval	rodlike	irregular
Coarse detrital No. 12	2.89	41.81	51.04	—	4.26
Fine detrital No. 13	0.32	64.29	34.74	—	0.65

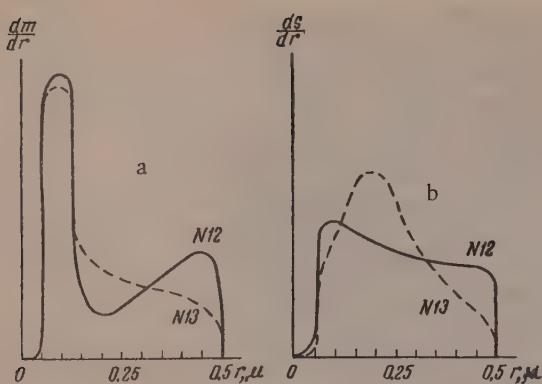


Fig. 5. Distribution curves for the colloidal fractions of No. 12 coarse detrital and No. 13 fine detrital sapropels:
a) by particle mass; b) by specific surface.

underwent coagulation on freezing, the value being 33.5%. The dispersity characteristics of the sapropel were also changed considerably by freezing. For the frozen sapropel $S_{sp} = 4739 \text{ cm}^2/\text{g}$, $f = 5.2$, $d_1 = 495 \mu$. Qualitatively, the structure of the coarse detrital sapropel became looser and more granular after freezing. When dried, it lost its strength almost entirely. Mud from lake Nero was found to have the same qualitative characteristics after freezing [10].

The electron micrographs* of the fine fractions of the sapropels in Fig. 4 were taken at magnifications of 7000-8000. The treatment of the photographs was the same as in the case of peats [1-3]. The negatives were placed in a projection lantern and projected on a screen to give $\times 50,000$ magnification; the sizes of the particles were then measured by means of a specially prepared universal transparent gage, their numerical contents were counted, and their image densities and shapes were noted. Table 1 contains data obtained from the electron micrographs of coarse detrital No. 12 and fine detrital No. 13 sapropels, with percentage mass distributions of the fractions ΔM and their percentage specific surface distributions ΔS .

The data in Table 1 were used to plot the complete distribution curves of Fig. 2, and also the mass and specific surface distribution curves for the colloidal fractions of the sapropels, shown in Fig. 5.

Examination of the curves shows that the particle mass distribution curves for the colloidal fraction of coarse detrital sapropel has two maxima, at $0.5-0.375 \mu$ and $0.125-0.05 \mu$. In the case of the fine detrital sapropel this fraction is more uniformly distributed by mass in the $0.5-0.125 \mu$ range, but it has almost the same maximum as in the coarse detrital sapropel at $0.125-0.05 \mu$. The coarse detrital sapropel has a more uniform specific surface-size distribution for all sizes between 0.5 and 0.05μ , while the fine detrital sapropel has a small maximum 0.125 and 0.05μ . In contrast to peats [3], in which most of the fine fraction consists of particles $0.25-0.5 \mu$ in radius, particles $0.125-0.25 \mu$ in radius predominate in sapropels.

Percentage distributions of particles of different shapes in coarse detrital and fine detrital sapropels are given in Table 2. It follows from Table 2 that rounded and oval particles predominate (comprising over 90%), the numbers of these being roughly equal in both types of sapropel. As regards the image density of the particles of the fine fractions in electron micrographs, this is variable in the case of peats [2, 3], and considerable numbers of particles of low density are found. Particles of low density are not found in sapropels, and nearly all the particles in the colloidal fraction of sapropels are of the type which are designated as high-density particles in peats. An interesting feature is that several of the electron micrographs of the fine sapropel fractions contained larger particles, which were diatoms or their fragments. Several such photographs, taken at 3500-6000 magnification, are given in Fig. 6. Electron micrographs of diatoms have been taken by several workers [11],

Sapropels, like peats [9], undergo considerable dispersity changes on freezing. Figure 3 shows size distribution curves for coarse detrital sapropel No. 12: the original (Curve 1), and frozen (Curve 2) at -15 and -25° for three weeks. In the same Fig. 3 is also plotted a curve (Curve 3) obtained by graphical subtraction of the distribution curve for the original sapropel from that for the frozen sapropel, and which represents the coagulation effect on freezing [9]. It follows from Fig. 3 that coagulation affected a wide range of fractions, from hundredths of one micron to 40μ , leading to the appearance of additional amounts of coarse fractions between 40 and 500μ . The fine fractions which disappeared in the course of coagulation on freezing lie under the abscissa axis (Curve 3), and are denoted by a minus sign, while the coarser fractions formed lie above the abscissa axis and are denoted by a plus sign. The shaded area represents the percentage of the sapropel mass which

* Some of the micrographs were taken by V. I. Aleksashin in the Physics Department of the Moscow Power Institute, and others in the Laboratory of Electron Microscopy of the Moscow Peat Institute.

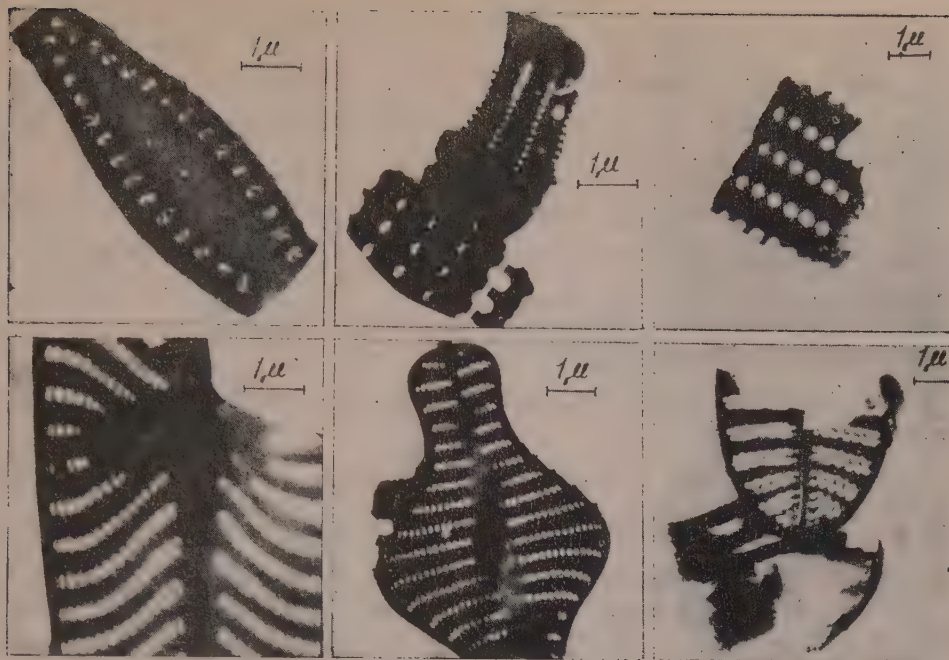


Fig. 6. Electron micrographs of diatoms ($\times 3500-6000$) found in coarse detrital and fine detrital sapropels.

as diatoms are sometimes used as "test objects" for determining the resolving power of both optical and electron microscopes. In an electron-microscopic investigation of clays, mainly of marine origin, Vikulova [12] also found fragments of diatoms. It is clear from Fig. 6 that the diatoms in sapropels vary greatly in form.

The experiments on the production of photographs of the fine fraction of sapropels by means of the electron microscope show that this method is suitable for investigations of the dispersity and microstructure of sapropels.

SUMMARY

1. For purposes of sedimentometric analysis, the true densities of settling particles in coarse detrital, fine detrital, and calcareous sapropels has been determined and their variations with particle size studied.
2. Particle size distribution curves have been plotted for the three commonest varieties of sapropels; the curves were found to have several maxima due to particle size heterogeneity and also to the heterogeneous composition of the individual components of the sapropels.
3. The specific surface of all the sapropel fractions ($8000-14,000 \text{ cm}^2/\text{g}$) has been determined; this is somewhat less than for peats of a moderate degree of decomposition. The inhomogeneity coefficient f for sapropels was found to lie in the range 9-88.
4. It was found that when sapropels are frozen* they are coagulated with a resultant considerable decrease of dispersity.
5. In order to obtain complete distribution curves, the highly disperse fractions of sapropels were investigated by means of the electron microscope.
6. The electron micrographs were used to study the shapes and densities of the particles in the fine sapropel fractions. Diatoms of various shapes were found in several of the micrographs.

The Moscow Petroleum Institute

Received May 6, 1957

* This was demonstrated for peat by A. V. Dumansky in 1936.

LITERATURE CITED

- [1] M. P. Volarovich and N. V. Churaev, *Colloid J.*, 17, 3, 200 (1955).*
- [2] M. P. Volarovich and N. V. Churaev, *Colloid J.*, 16, 4, 241 (1954).*
- [3] M. P. Volarovich and N. V. Churaev, Proc. 3rd All-Union Colloid Conference, Minsk, 1953 (Izd. AN SSSR, Moscow, 1956) p. 258.
- [4] S. N. Tyuremnov, *Peat Deposits and Their Exploration*, 2nd edition (Gosenergoizdat, 1949) p. 210.**
- [5] N. V. Korde, Trans. Laboratory of Sapropel Deposits No. 6, 5 (Izd. AN SSSR, 1956).
- [6] N. V. Churaev, *Colloid J.* 16, 3, 220 (1954). *
- [7] A. V. Dumanskii et al., *Colloid J.*, 2, 95 (1936).
- [8] V. G. Bulychev, *Physicomechanical Properties of Soils* (GISL, 1940); E. M. Sergeev, *General Soil Science* (Izd. MGU, 1952).**
- [9] M. P. Volarovich, K. F. Gusev, S. M. Markov and V. N. Propin, *Colloid J.*, 19, 4, 401 (1957).
- [10] A. V. Smirnov, Trans. Laboratory of Sapropel Deposits No. 6, 213 (Izd. AN SSSR, 1956).
- [11] M. Ardenne, *Elektronen-Übermikroskopie*, Berlin, 1940; V. N. Vertsner, Proc. Acad. Sci. USSR, 44, No. 3 (1944).
- [12] M. F. Vikulova, *Electron Microscopy of Clays* (State Geological Press, 1952).**

* Original Russian pagination. See C. B. Translation.

** In Russian.

COMPATIBILITY OF NITROCELLULOSE WITH BUTADIENE - ACRYLONITRILE COPOLYMERS

4. RELAXATION PROPERTIES OF BINARY MIXTURES

S. S. Voiutskii, V. I. Alekseenko and L. E. Kalinina

Deformation of high polymers is accompanied by complex regroupings of the flexible chain molecules, in which the forces acting between the molecules are overcome and their equilibrium positions are disturbed. Any increase of chain order during deformation brings the system into a stressed, thermodynamically unstable state. Relaxation is the process of establishment of a new state of equilibrium in a deformed body, occurring under the influence of thermal motion and leading to a decrease of internal stresses. The time required for this process increases with increasing height of the potential barriers, with increasing energy of molecular interaction, and with decreasing energy of thermal motion. The changes which take place in polymer systems as the result of plasticization are in many respects analogous to the changes produced by increases of temperatures.

The present investigation consisted of a study of relaxation of stress in films of mixtures of nitrocellulose with butadiene-acrylonitrile copolymers of different polarities, in order to clarify the mechanism of plasticization with high-molecular plasticizers. Use was made of theoretical concepts [1, 2] whereby it was possible to reveal certain characteristics of the structure of the mixtures and the nature of the intermolecular interaction.

Films used in the experiments were prepared, by the method described previously [3], from solutions of mixtures of nitrocellulose with butadiene-acrylonitrile copolymers containing the following percentages of acrylonitrile groups:

Copolymer 1-18.4%	Copolymer 3-37.7%
Copolymer 2-28.6%	Copolymer 4-44.4%

The relaxation of stress at constant deformation was determined with the aid of a Polanyi dynamometer of the usual type with a thermostatic attachment. The temperature near the specimen was measured by means of a thermocouple. The temperature fluctuations during the experiments as a rule did not exceed one degree.

The dynamometer dial was turned to lower the micrometer screw with the casing attached to the instrument table at a distance corresponding to the required elongation. The upper part of the table with the lower clamp was then raised by hand until the distance between the clamps became equal to the length of the test portion of the specimen. After the specimen had been clamped, the light spot from an illuminated mirror was directed onto the zero reading of the scale to establish the zero point. The lower clamp was then lowered to the position established earlier, by a rapid but smooth movement of the hand.

At the beginning of the experiment, when the stress decreased fairly rapidly, the scale readings were taken at intervals of 15 seconds, and subsequently at intervals of 30 seconds and more.

As an example, Fig. 1 shows curves for stress relaxation at elongation equivalent to 25% of the elongation at break, for films made from mixtures of nitrocellulose with butadiene-acrylonitrile copolymer 2. Similar relaxation curves were obtained for films containing other copolymers.

The results indicate that pure nitrocellulose has high elastic properties: the decrease of stress during 90 minutes was very small, only ~8%. There was a general tendency to an increase of the relaxation rate with increasing contents of butadiene-acrylonitrile copolymers in the mixture in all cases.

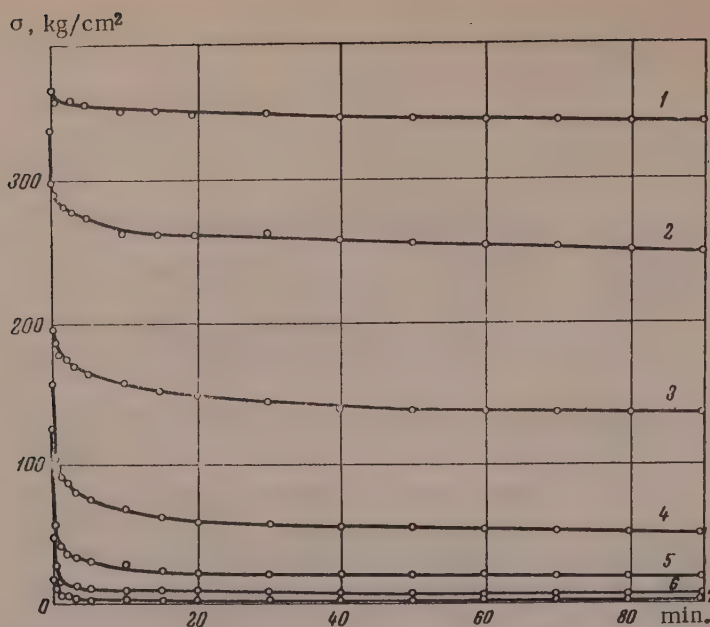


Fig. 1. Stress relaxation curves for nitrocellulose films containing butadiene-acrylonitrile copolymer 2:
1) 0%; 2) 20%; 3) 40%; 4) 50%; 5) 60%; 6) 80%; 7) 100%.

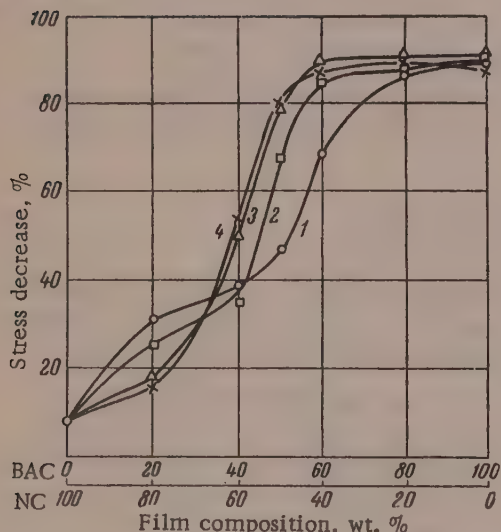


Fig. 2. Effect of film composition on stress decrease.
1) Nitrocellulose film containing butadiene-acrylonitrile copolymer 1; 2) the same, with copolymer 2;
3) with copolymer 3; 4) with copolymer 4.

Kozlov [4] established experimentally the existence of two groups of relaxation times in high polymers, and pointed out that rapid relaxation processes are the result of changes in the configuration of the chain molecules; in other words, disorientation of the chain segments occurs; slow relaxation processes, on the other hand are associated with regroupings of the whole molecules or large regions of them, and depend on the aggregate energy of interaction of all the chain segments.

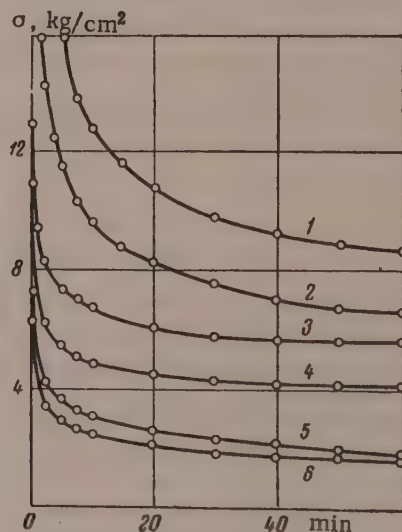


Fig. 3. Stress relaxation curves for nitrocellulose films containing 80% of butadiene-acrylonitrile copolymer 2.
1) 22° and 320% elongation; 2) 22° and 100%;
3) 40° and 300%; 4) 40° and 100%; 5) 60° and 500%; 6) 60° and 300%.

The stress-time curves at constant elongation for the systems studied descend relatively steeply at first, and then tend asymptotically to certain constant values, indicating that equilibrium slowly becomes established at the given temperature.

The data obtained for all the different mixtures were used to calculate the decrease of stress (as a percentage) in a relaxation time of 90 minutes. The decrease of stress (π) was calculated from the formula

$$\pi = \frac{\sigma_{\text{inst}} - \sigma_{90}}{\sigma_{\text{inst}}} \cdot 100. \quad (1)$$

σ_{inst} is the instantaneous value of the stress; σ_{90} is the stress after 90 minutes.

The decreases of stress as functions of the film composition are plotted in Fig. 2. It is seen that at low contents of butadiene-acrylonitrile copolymers, when they are dissolved in the nitrocellulose and the mixture is relatively homogeneous, the greatest stress decreases are found for the least polar copolymers, with the highest contents of butadiene groups which, in our view, are responsible for the plasticizing effect of these copolymers.

The situation is reversed with higher contents of butadiene-acrylonitrile copolymers in the mixtures. For equal copolymer contents in the systems, the greatest stress decreases are found with the most highly polar copolymers. The reason is that in this case an important part is played by the compatibility of the butadiene-acrylonitrile copolymers with nitrocellulose, resulting in the formation of homogeneous systems which have the greatest tendency to relaxation. Conversely, if nitrocellulose is mixed with an excess of a weakly polar copolymer, a heterogeneous mixture, a kind of emulsion of one polymer in another, is formed. In such cases the high-elastic butadiene-acrylonitrile copolymer acts as the external phase and largely determines the relaxation properties of the mixture. The decreases of stresses are therefore smaller, as is seen in the diagram in Fig. 2. It may be noted that this conclusion concerning the poor compatibility of weakly polar polymers with nitrocellulose is in full agreement with the phase separation in such mixtures in solutions [5].

The curve for nitrocellulose-copolymer 1 mixtures, with two inflection points, is noteworthy. In our opinion this form of the curve is a consequence of heterogeneity of the mixture. If the more polar copolymer 2 is mixed with nitrocellulose, the inflection points on the curve become less pronounced, while in presence of copolymers 3 and 4 they disappear entirely.

In a discussion of the mechanism of relaxation effects accompanying high-elastic deformation it was established [1] that the rate of partial or total restoration of equilibrium configuration of the molecular chains is primarily determined by the nature of the intermolecular forces. Thus, studies of the relaxation effects accompanying high-elastic deformation can reveal the relationships between relaxation properties and the nature of the intermolecular interaction in high polymers.

The authors cited [1] derived an approximate equation to represent the process of the establishment of equilibrium:

$$\frac{d(\sigma - \sigma_{\infty})}{dt} = (E'_0 - E_{\infty}) \frac{d\varepsilon}{dt} - \frac{\sigma - \sigma_{\infty}}{\tau}, \quad (2)$$

where σ and σ_{∞} are the instantaneous and the equilibrium stresses; ε is the deformation; t is the time; E'_0 and E_{∞} are the initial and the equilibrium modulus respectively; τ is the relaxation time.

Equation (2) is essentially a simple generalization of the Maxwell equation, and is suitable only for qualitative description of relaxation processes in high-elastic deformation. Even then it is suitable only for the region of temperatures, deformation rates, and observation times in which: a) the value of the modulus E'_0 remains low, indicating that the rapid relaxation process of restoration of short-range order equilibrium, ignored here, is relatively complete; b) there is no cleavage of chemical bonds, leading to irreversible changes of structure on deformation.

The authors also concluded from their results that the relaxation time as a function of the stress may be represented by the following equation:

$$\tau = \tau_0 \exp \frac{\frac{u_0}{V} (\sigma - \sigma_\infty)^2}{kT}, \quad (3)$$

where τ_0 is a constant independent of the experimental conditions; u_0 is the activation energy of an elementary structural change, which is essentially the relaxation; V is the volume of a kinetic unit of relaxation; k is the Boltzmann constant; $E_1 = E_0' - E_\infty$; T is the absolute temperature. Equations (2) and (3) can be used for approximate quantitative description of relaxation processes in high-elastic deformation of high polymers.

The coefficient of $(\sigma - \sigma_\infty)^2$ in Equation (3) has a definite physical meaning. It is particularly important that the expression contains V , the volume of the kinetic unit of relaxation, without which an uncertainty remains in the concept of the activation energy u_0 . This is because the dimensions of the structural unit to which u_0 should be referred are not known [6]. The presence of the two constants u_0 and V , which relate the mechanical properties of a polymer to its physical structure, makes it possible to characterize the structural features of the systems under consideration.

We tested the applicability of the foregoing views to mixtures of nitrocellulose with butadiene-acrylonitrile copolymers. The study had to be confined, of course, to mixtures which were in the high-elastic state under the experimental conditions, and the relaxation of which could be investigated by the usual methods. Stress relaxation was studied at temperatures between 6 and 80°, with initial deformations of 15 to 500% of the original specimen length.

As an example, Fig. 3 shows typical stress-time curves for nitrocellulose films containing 80% of copolymer 2, for different temperatures and elongations.

For stress relaxation at constant elongation, when $\frac{d\epsilon}{dt} = 0$, Equation (2) becomes:

$$\frac{d\sigma}{dt} = -\frac{1}{\tau} (\sigma - \sigma_\infty). \quad (4)$$

Equation (4) was used to analyze the experimental curves by the method of finite differences, for graphical determination of the instantaneous values of the relaxation time corresponding to the chosen stress values, in accordance with the expression

$$\tau \approx -\frac{\Delta t}{\Delta \sigma} (\sigma - \sigma_\infty), \quad (5)$$

where σ_∞ is the equilibrium stress corresponding to the given deformation and temperature. Correct determination of the equilibrium stress is very important in this method of calculation. There have been several publications on the conditions of attainment of equilibrium stresses [7-10]. The method used by us for determination of equilibrium stress was similar to that used by Meyer and Ferri [11] for rubber. This method has been improved and experimentally verified [1, 12]. The experiments showed that the equilibrium stress for all the mixtures studied, and also for the pure copolymers is, as a rule, close to zero.

Expression (3) may be simplified by writing:

$$\tau^* = \tau_0 \exp \frac{u_0}{kT}. \quad (6)$$

$$\beta = \frac{V}{2E_1 kT}. \quad (7)$$

It should be noted that τ^* and β depend on the temperature but not on the nonequilibrium value of the stress. Substituting the above expressions into Equation (3) and taking logarithms, we obtain the equation

$$\log \tau = \log \tau^* - \frac{\beta}{2.3} (\sigma - \sigma_\infty)^2. \quad (8)$$

TABLE 1

Values of τ^* and β for Butadiene-Acrylonitrile Copolymers at Different Temperatures and Elongations

Temper- ature, °C	Elonga- tion, %	τ^*	$\frac{\beta}{2.3} \cdot 10^3$	Temper- ature, °C	Elonga- tion, %	τ^*	$\frac{\beta}{2.3} \cdot 10^3$
Copolymer 1							
3	50	239.9	10.6				
10	100	138.0	15.4				
10	200	151.4	11.8				
Copolymer 2							
14	100	112.2	7.7				
14	200	107.2	4.25				
22	100	63.10	7.1				
22	150	69.18	3.62				
30	100	43.66	16.65				
Copolymer 3							
3	100	204.2	1.1				
10	100	112.2	2.1				
10	200	123.0	3.5				
22	100	562.3	5.25				
22	200	63.10	3.6				
Copolymer 4							
14	300	117.5	2.42				
22	375	69.18	2.29				
32	500	34.67	7.9				

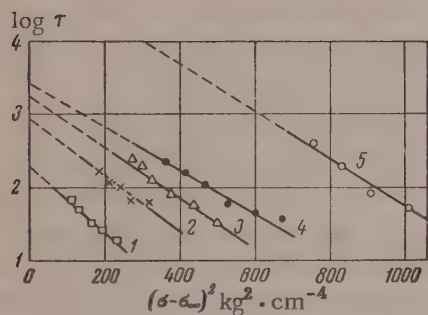


Fig. 4. Variation of $\log \tau$ with $(\sigma - \sigma_{\infty})^2$ for nitrocellulose films containing 80% of copolymer 1:
 1) temperature 22°, elongation 16%; 2) 22° and 40%; 3) 22° and 50%; 4) 10° and 32%; 5) 12° and 100%.

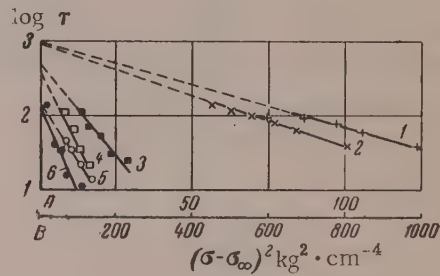


Fig. 5. Variation of $\log \tau$ with $(\sigma - \sigma_{\infty})^2$ for nitrocellulose films containing 80% of copolymer 2:
 1) temperature 6°, elongation 300%; 2) 6° and 100%; 3) 20° and 320%; 4) 20° and 100%;
 5) 60° and 500%; 6) 60° and 300%. The values of $(\sigma - \sigma_{\infty})^2$ are taken along scale B for 1-4,
 and along scale A for 5 and 6.

It was found, in agreement with this equation, that plots of the experimental values of $\log \tau$ against the square of the nonequilibrium part of the stress are satisfactorily linear both for the pure copolymers and for the mixtures of nitrocellulose with butadiene-acrylonitrile copolymers. In Figs. 4 and 5 $\log \tau$ is plotted against $(\sigma - \sigma_{\infty})^2$ for nitrocellulose films containing 80% of butadiene-acrylonitrile copolymers 1 and 2 respectively.

The experiments showed that whereas for mixtures of nitrocellulose with copolymers containing not less than 28% of polar nitrile groups in the molecule the limiting relaxation time at a given temperature is practically independent of the elongation, in the same way as for smoked sheet rubber and rubber bromide [1], mixtures containing the weakly polar copolymer 1 do not conform to this. Consequently, the foregoing theoretical quantitative relationships for relaxation processes are evidently applicable only to sufficiently homogeneous systems. The limiting relaxation time τ^* was found from the intercept cut off by the $\log \tau$, $(\sigma - \sigma_{\infty})^2$ line along the ordinate axis; β was found from the tangent of the angle formed by this line and the abscissa axis.

TABLE 2

Values of τ^* and β for Mixtures of Nitrocellulose with Copolymers 1, 2, 3, and 4 at Different Temperatures and Elongations

Temper- ature, °C	Elonga- tion, %	τ^*	$\frac{\beta}{2.3} \cdot 10^3$	Temper- ature, °C	Elonga- tion, %	τ^*	$\frac{\beta}{2.3} \cdot 10^3$				
80 % Copolymer 1											
12	100	79430	3.16	14	200	177.8	5.06				
18	32	2630	3.0	20	225	114.8	3.33				
22	16	199.5	4.6	20	540	120.2	2.03				
22	40	891.3	3.9	40	100	63.10	61.33				
22	50	1778	3.52	40	300	56.23	26.7				
80 % Copolymer 2											
6	300	955	0.72	40	50	2399	$125.2 \cdot 10^{-2}$				
6	500	912	0.69	50	75	1778	$530 \cdot 10^{-2}$				
22	100	398.4	10.0	60	100	1259	$910 \cdot 10^{-2}$				
22	320	501.2	6.10	60 % Copolymer 2							
60	300	152.4	94	60 % Copolymer 3							
60	500	144.5	62	40	50	2089	$9.1 \cdot 10^{-2}$				
80 % Copolymer 3											
3	450	645.7	0.86	22	100	1096	$47.9 \cdot 10^{-2}$				
22	350	257.0	30.8	40	100	575.4	$299.0 \cdot 10^{-2}$				
22	700	204.2	16.3	40	200	645.7	$250 \cdot 10^{-2}$				
40	100	83.18	160	60 % Copolymer 4							
40	450	95.5	89	15	50	524.9	$10.25 \cdot 10^{-2}$				
80 % Copolymer 4											
22	20	331.1	$102 \cdot 10^{-2}$								
22	60	381.1	$39 \cdot 10^{-2}$								
40	60	173.8	$56.6 \cdot 10^{-2}$								
40	150	151.4	$44.1 \cdot 10^{-2}$								

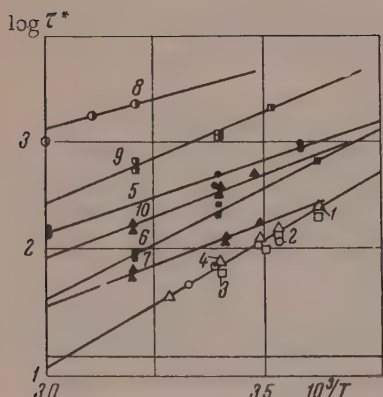


Fig. 6. Variation of $\log \tau^*$ with $1/T$ for pure copolymers and for nitrocellulose films containing various amounts of butadiene-acrylonitrile copolymers:

1-4) copolymers 1, 2, 3, and 4; 5) nitrocellulose containing 80% of copolymer 2; 6) the same, with copolymer 3; 7) the same, with copolymer 4; 8) nitrocellulose containing 60% of copolymer 2; 9) the same, with copolymer 3; 10) the same, with copolymer 4.

The terms τ^* and β characterize the values of u_0 and V . The physical meaning of τ^* and β at a given deformation and temperature is as follows. If the relaxation of a high polymer is regarded as a regrouping of the molecular bonds with relative displacements of chain segments, then τ^* represents the average time of existence of such bonds or the time interval between two elementary acts of regrouping in the case of ordinary diffusion of the structural elements of polymers. Reznikovsky states that the less frequent such regroupings are, the greater is this value. Consequently, the limiting time of relaxation is a certain measure of the stability of the elementary bonds and, as follows from Equation (6), it is directly related to the activation energy of the relaxation process. The constant β should be regarded as a measure of the effect of the external stress on the stability of such elementary bonds. This effect evidently increases with decreasing numbers of such bonds in the system. The numerical value of β is thus a measure of the concentration of elementary bonds in the polymer.

Data for films from pure copolymers and from nitrocellulose containing 80 and 60% of butadiene-acrylonitrile copolymers are given in Tables 1 and 2. It is seen that for the pure copolymers the values of τ^*

TABLE 3

Activation Energy of the Relaxation Process in kcal./mole

Copolymer 1	10.7
Copolymer 2	10.7
Copolymer 3	10.7
Copolymer 4	10.7
Nitrocellulose film,	
containing 80% of copolymer 2	6.3
containing 80% of copolymer 3	9.5
containing 80% of copolymer 4	7.12
containing 60% of copolymer 2	5.3
containing 60% of copolymer 3	7.85
containing 60% of copolymer 4	6.92

volumes of the kinetic units, and a higher relaxation rate, i.e., the plasticizing effects of copolymers 3 and 2 on nitrocellulose are considerably greater than the effects of copolymers 4 and 1. This confirms the general principles stated by us earlier [3].

On the basis of the assumption that polar polymers contain fixed and relatively stable intermolecular bonds, the relationship between the mechanical properties and the structural characteristics of the mixtures can be explained as follows. When nitrocellulose is mixed with butadiene-acrylonitrile copolymers, definite local bonds are formed between unlike molecules, analogous to the bonds between active groups of the same polymer. The hydrocarbon regions of the copolymer chains shield the polar groups and weaken the total interaction between the polymer molecules. As a result, a kind of network structure of variable character is formed in the system.

The decrease of β in the course of deformation indicates an increase of local bond concentration owing to increased interaction between the chains when the specimen is stretched. The fact that τ^* depends on the temperature means that the bonds formed by accidental localization of van der Waals forces of attraction vary in strength, so that the effect of temperature on these bonds also varies.

The fact that τ^* for polymer mixtures depends on the polarity of the components shows that interaction between the polymer molecules is determined mainly by bonds at the polar groups. Therefore polarity is the determining factor in polymer compatibility. In the mixtures studied, such bonds can be formed by the active groups present in the polymer molecules, such as polar NO_2 groups, CN, groups which cause hydrogen bond formation, etc. The fact that τ^* does not depend on elongation for the various systems shows that elementary local bond energy does not undergo any changes on deformation.

The activation energy u_0 can be determined from the relationship between temperature and the logarithm of the limiting time of relaxation, in accordance with Equation (8). These relationships for the pure copolymers and for mixtures of nitrocellulose with different copolymers are plotted in Fig. 6. The values of the activation energy calculated per nominal mole (a mole of "kinetic units of relaxation") calculated from these relationships are given in Table 3.

As was to be expected, the activation energy is the same for all the pure copolymers, as the bonds which determine the elementary regroupings or changes of molecular configuration during relaxation are of the same nature in all cases (the bond energy at nonpolar groups can be neglected in the first approximation).

The lower activation energies for mixtures are difficult to understand at first sight, as in view of the strongly polar nature of the nitro group it is difficult to believe that the activation energy of relaxation should be less for nitrocellulose than for butadiene-acrylonitrile copolymers.

However, the explanation for the experimentally observed decrease in the case of mixtures is that close approach of the polar groups of the two polymers is hindered by purely steric factors, associated with the structure of the molecules. This should decrease the energy of the bonds formed and lower the activation energy of relaxation accordingly. However, additional and detailed investigation of this is required.

depend on the temperature and change very little with deformation; the value of β decreases considerably with increasing degree of elongation in relaxation. It follows that the activation energy remains constant during the deformation process, and only the volume of the kinetic unit of relaxation changes. Increase of the nitrocellulose content in mixtures leads to a decrease of the volume of the kinetic unit of relaxation, i.e., to retardation of the relaxation process. In mixed systems β also varies with temperature, evidently owing to a decrease of the number of bonds with increase of temperature, and this should therefore be accompanied by an increase of V.

The value of β is highest for mixtures containing copolymers 3 and 2, and it is considerably lower for mixtures containing copolymers 4 and 1. Therefore in the former case the system has a smaller bond content, larger

SUMMARY

1. All the investigated binary mixtures of nitrocellulose with butadiene-acrylonitrile copolymers show a general tendency to an increase of the relaxation rate with increasing copolymer content.

2. At low contents of butadiene-acrylonitrile copolymers, when they are dissolved in the nitrocellulose and the mixture is sufficiently homogeneous, the greatest decrease of stress on relaxation is found in copolymers with the highest contents of butadiene groups, while the situation is reversed with higher contents of the butadiene-acrylonitrile copolymers. The probable reason is that at higher elastomer contents the compatibility of butadiene-acrylonitrile copolymers with nitrocellulose, which increases with increasing polarity of the copolymer, begins to be important.

3. The limiting relaxation time τ^* , which represents the time interval between two elementary acts of molecular regrouping, is independent of the degree of deformation only for mixtures of nitrocellulose with copolymers containing 28.6% of acrylonitrile groups or over, i.e., for fairly homogeneous mixtures.

4. The dependence of the constants β and τ^* on temperature and deformation, and comparisons of the values of these constants for different mixtures, have been used to establish a direct relationship between the nature of the intermolecular interaction of the components and the relaxation properties of the mixtures.

5. The activation energy of relaxation is the same, 10.7 kcal./mole, for all the pure butadiene-acrylonitrile copolymers. The reason is that the local bonds are of the same nature in all the copolymers. The activation energy for mixtures of nitrocellulose with the copolymers is somewhat lower, in the range of 5.3-7.8 kcal./mole. It is possible that this lower value of the activation energy is the consequence of purely steric factors, which prevent close approach between the polar groups of the two polymers in the mixtures.

Central Scientific Research Institute
of Leather Substitutes

Received February 18, 1957

LITERATURE CITED

- [1] B. A. Dogadkin, G. M. Bartenev and M. M. Reznikovskii, *Colloid J.* 11, 314 (1949).
- [2] B. A. Dogadkin and M. M. Reznikovskii, *Colloid J.* 12, 102 (1950).
- [3] L. I. Kalinina, V. I. Alekseenko and S. S. Voiutskii, *Colloid J.* 18, 180 (1956). *
- [4] P. V. Kozlov, Proc. I and II Conf. on High Molecular Compounds (Izd. AN SSSR, 1945).
- [5] L. E. Kalinina, V. I. Alekseenko and S. S. Voiutskii, *Colloid J.* 18, 691 (1956). *
- [6] M. M. Reznikovskii, Symposium, High Molecular Compounds, No. 12 (Goskhimizdat, 1952) p. 27. **
- [7] L. A. Wood and F. L. Roth, *J. Appl. Phys.* 15, 781 (1944).
- [8] G. Gee, *Trans. Faraday Soc.* 42, 585 (1946).
- [9] G. M. Bartenev, *Colloid J.* 13, 233 (1951).
- [10] G. M. Bartenev, *J. Tech. Phys.* 20, 461 (1950); 22, 1154 (1952).
- [11] K. Meyer and C. Ferri, *Helv. Chim. Acta* 18, 570 (1935).
- [12] B. A. Dogadkin and Z. N. Tarasova, *Colloid J.* 15, 347 (1953). *

* Original Russian pagination. See C. B. Translation.

** In Russian.

THE HEATS OF HYDRATION OF SOME CATIONS AND THE EFFECT OF THEIR ADSORPTION ON THE STRUCTURE OF SILICA GELS

Z. Z. Vysotskii and V. V. Shalia

It is known [1] that when silicic acid hydrogels are washed with solutions of different electrolytes, products of different porosity are formed; an important part is played by the pH of the medium [2], which influences the nature of the ion exchange processes involved [3]. The mechanism of porous structure formation of hydrophilic sorbents has been studied [4-9], several factors which influence the silica gel structure being investigated; however, the published data on the influence of individual cations on the pore structure of the resultant dry gel are fragmentary [10], and this question has not yet been studied systematically.

The present investigation consisted of a study of the influence of the nature of certain cations adsorbed by silicic acid hydrogels on the structure of the dry silica gel.

Preparation of silica gels. A silicic acid sol with $\text{pH} < 4.4$ was made by addition of 2.25 volumes of an aqueous solution of chemically pure Na_2SiO_3 ($d = 1.154$) to 1 volume of HCl solution ($d = 1.099$); the pH of the hydrosol and wash liquors was determined by means of a range of indicators. After gelation and aging until the start of syneresis (about 5 days), the gel was divided into portions and repeatedly washed by decantation with the following solutions: HCl (pH ≈ 3.5), 0.1 N NaHCO_3 (pH 10-11), 0.1 N KHCO_3 (pH 10-11), a solution, saturated at 20° , of $\text{Ca}(\text{HCO}_3)_2$ (pH 7.2-8.8), 0.1 N NaCl (pH 6.2-7.2) and 0.1 N CaCl_2 (pH 6.2-7.2). The washing was continued for two weeks, until the pH of the wash liquors returned to their original values. One part of each sample was then dried, and another washed with distilled water for a week before being dried. All the samples were dried at room temperature.

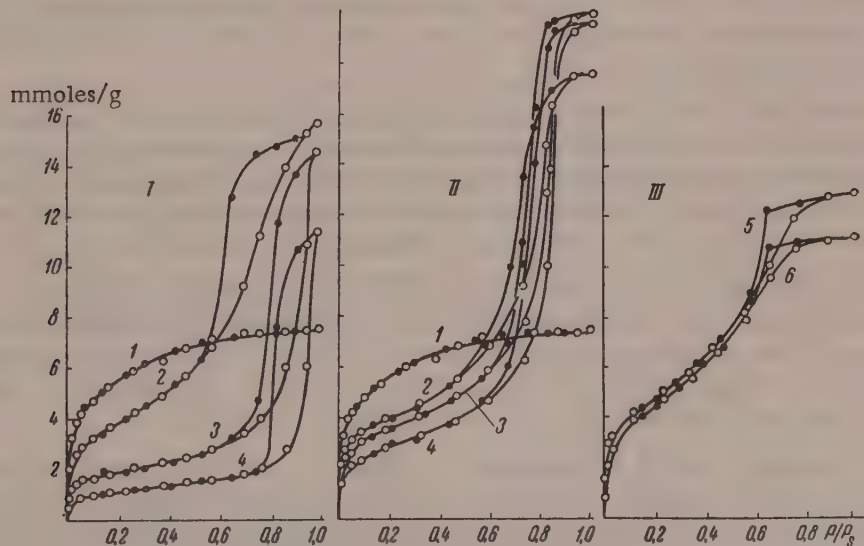


Fig. 1. Isotherms for the sorption of CH_3OH vapor on silica gels of Series I, II, and III, washed with:
1) HCl; 2) $\text{Ca}(\text{HCO}_3)_2$; 3) NaHCO_3 ; 4) KHCO_3 ; 5) CaCl_2 ; 6) NaCl . Black dots represent desorption.

TABLE 1

Structural and Sorptional Characteristics of Silica Gels Treated With Electrolyte Solutions

Series	Sample	Adsorbed cations	Volume of adsorption space in cc/g		Predominant pore radius in Å	Specific surface in m ² /g	Heat of hydration of cation, kcal./g-ion
			from adsorption of C ₆ H ₆	from CH ₃ OH isotherm			
I	1	H ⁺	0.26	0.30	10	660	255
	2	Ca ²⁺	0.61	0.62	15	470	174.5
	3	Na ⁺	0.60	0.58	35	230	97
	4	K ⁺	0.49	0.45	40	135	77
II	5	Ca ²⁺	0.67	0.71	20	495	—
	6	Na ⁺	0.74	0.80	27	435	—
	7	K ⁺	0.74	0.78	30	320	—
III	8	Ca ²⁺	0.50	0.52	15	595	—
	9	Na ⁺	0.46	0.45	17	520	—

The structural and sorptional characteristics of the silica gels were determined with the aid of isotherms for the sorption of methyl alcohol vapor at 23° in a vacuum apparatus with a quartz spring balance. The isotherms were used to calculate the adsorptional volume V_s , the specific surface S , and the predominant pore radius r of the silica gels. In addition, the static activity of each sample was determined by adsorption of benzene from saturated vapor, from which V_s could also be calculated.

The results of the determinations and the calculation data are given in Tables 1 and 2, and the isotherms of CH₃OH sorption are shown in the diagram.

The first series of silica gels in Table 1 was washed with solutions of bicarbonates (Samples 2-4) and HCl (Sample 1); the occluded electrolyte solution was not washed out before the drying; in the second series, Samples 5, 6, and 7 were washed to remove excess bicarbonates occluded with the solutions. Finally, Samples 8 and 9 of the third series were washed with chloride solutions and washed with distilled water before being dried.

It follows from Table 1 that if the wash liquor is strongly acid (pH 3.5, Sample 1), the silica gel acquires a finely porous structure. If the medium is weakly acid, neutral, or alkaline, i.e., if the aging and drying of the gel takes place under conditions when cation exchange is possible and metal cations replace H⁺ on the surfaces of the silicic acid micelles, the dry silica gels have a more coarsely porous structure. This result is in agreement with earlier findings of other authors [7-10, 11].

At the same time, as far as we are aware, the earlier workers did not correlate the influence of the cations adsorbed by the silicic acid micelles on the silica gel structure with the properties of these cations. There has only been an attempt [6] to explain the effects of electrolyte treatment of hydrogels in relation to the ionic radii of the H⁺ and Al³⁺ cations, and to attribute the formation of finely porous silica gels in acid media to weakening of hydrogen bonds between the micelles as the result of adsorption of H⁺ and AlO⁴⁻.

Our results show the existence of a direct relationship between the heats of hydration of the cations studied [12] and their influence on the pore structure of the dry silica gels (especially on the pore radii and specific surface). The lower the heat of hydration in the series H⁺ > Ca²⁺ > Na⁺ > K⁺, the more coarsely porous is the resultant silica gel, and the less is its specific surface. This is illustrated very clearly by the relative positions of the isotherms for Samples 1-4 in Fig. 1,I.

The above relationship holds for the samples of all three series of silica gels. In Table 1, data for the H⁺ ion are given once only, for Series I, as washing with distilled water after washing with bicarbonate solutions, or addition of chlorides to the acid medium with pH ≈ 3.5 does not change the structural and sorptional characteristics of the silica gels. The difference between the samples in Series I, II, and III lies in the fact that the observed relationship between the heats of hydration of the cations and the silica gel structure is most pronounced in samples which had not been washed free from occluded 0.1 N solutions (Series I). in Series II (Table 1 and

TABLE 2

Effect of Washing of Dry Silica Gels with Water and HCl (1 : 1) on Their Adsorptional Volume

Sample	Adsorbed cations	Adsorptional volume in cc/g, from adsorption of C ₆ H ₆		
		directly after drying	after washing with	
			distilled water	HCl solution (1 : 1) and distilled water
2	Ca ²⁺	0.61	0.58	0.58
3	Na ⁺	0.60	0.59	0.59
4	K ⁺	0.49	0.52	0.52

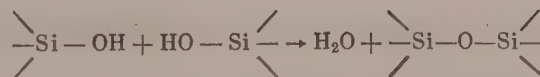
Fig. 1, II) the differences of pore structure are somewhat less, but conform to the same relationship. Finally, Samples 8 and 9, washed with chlorides (Table 1 and Fig. 1, III) also show a small increase of the specific surface as the result of adsorption of Ca²⁺ as compared with the adsorption of Na⁺ ions. The results in Table 2 show clearly that the adsorptional volume is influenced by the adsorbed cations, and not by the traces of occluded electrolytes.

We attempted to correlate this connection between the heats of hydration of the cations and the influence of their adsorption on silica gel structure with the existing theories on the formation of the pore structure in silica gels.

Poliakov et al. [4] put forward the view that the nature of the silicic acid micelles has a decisive influence on the structure of the silica gel, which is formed mainly during dehydration. Because of errors in some unimportant details, this view was unfortunately abandoned, and the theory of Veselovskii and Seliaev gained wide acceptance [5].

According to this theory, the nature of the porosity of a silica gel depends on the degree of shrinkage of the hydrogel during drying. Shrinkage of the gel framework occurs mainly under the influence of capillary pressure $P = 2\sigma/r$, where σ is the surface tension of the intermicellar liquid and r is the pore radius. The strength of the gel framework increases with increasing shrinkage, and the latter ceases when the strength becomes high enough to withstand the capillary pressure. All factors which decrease σ (temperature, surface-active agents, etc.) or increase the strength of the hydrogel framework (dehydration of the surface of the framework, increase of pH, heating, etc.) favor the formation of more porous silica gels. Therefore according to this theory the state of the micelle surface becomes less important and the decisive role is attributed to the surface tension of the intermicellar liquid which, in the view of these authors, mainly determines the capillary pressure.

In the theory advanced by Plank [6], changes of the pore structure during drying of the hydrogel are virtually ignored, and it is postulated that the structure of the dry gel is predetermined by the process which takes place during gelation, syneresis, and washing of the hydrogel with electrolyte solutions. Plank ascribes the decisive influence to intra- and intermicellar bonds which, in his opinion, are hydrogen bonds formed directly between the micelle surfaces or between the micelle surfaces and the intermediate layers of water molecules. Adsorption of cations at OH groups influences the pore structure by weakening the hydrogen bonds. According to Golderbitter [11], adsorption of cations (apart from H⁺) results in the formation of a more porous structure, because condensation of silicic acid according to the scheme



with formation of siloxane bonds and corresponding shrinkage of the framework then becomes impossible. Important experimental results were obtained by Boreskov et al. [7], and also by Neimark and his associates [8, 13].

Nevertheless, it seems probable to us that the influence of adsorbed metal cations on silica gel structure is not confined to an easing of micellar aggregation and strengthening of the gel framework. The decrease

in the hydrophilic properties of the hydrogel as the result of cation adsorption must inevitably lead to a decrease of the capillary forces which, as is known, depend not only on σ of the intermicellar liquid, but also on the degree of wetting of the micelles with this liquid. (Incidentally, it is very likely that in a number of cases the influence of the wettability of the hydrogel framework may be more important than the influence of σ). This view was put forward by one of us earlier [14]. Recently Schultze [15] has published an interesting paper in which capillary effects are explained in terms of wettability only, and the role of the surface tension of the wetting liquid is rejected entirely.

Our experimental results can be explained either in terms of decreased wetting, or in terms of an increase of micellar aggregation on adsorption of metal cations, as both these factors act in the same direction — they increase the porosity of the silica gel. Since the influence of cation adsorption on the wettability of clays, studied by Dumansky and Ovcharenko [16] is analogous to their action on silica gels, it is likely that the predominant effect of adsorbed cations is on wettability. These authors arranged cations in the following series by their influence on the wettability of clays: $\text{Ca}^{2+} > \text{H}^+ > \text{Na}^+ > \text{K}^+$. Our isotherms for the sorption of CH_3OH show that the degree of aggregation increases in the series $\text{H}^+ < \text{Ca}^{2+} < \text{Na}^+ < \text{K}^+$.

The aggregation mechanism of silicic acid micelles is still obscure. For instance, Golderbitter [11] believes that adsorption of cations prevents condensation (aggregation) of silicic acid, whereas Neimark [10] holds the directly opposite opinion. It has been reported [17, 18] that bivalent calcium ions are capable of preserving bonds of the type $\text{Si}-\text{O}-\text{Si}$ by entering them and forming $\text{Si}-\text{O}-\text{Ca}-\text{O}-\text{Si}$ bonds, but that univalent sodium can rupture such bonds; this leads to the logical conclusion that calcium ions should assist micelle growth to a greater extent than sodium (or potassium etc.) ions. However, this is not supported by published data [10] and the results in this paper. The question of the mechanism of micelle aggregation in silicic acid as the result of adsorption of metal cation therefore remains open.

SUMMARY

1. Adsorption of H^+ , Ca^{2+} , Na^+ and K^+ ions by silicic acid hydrogels influences the structure of the dry silica gels.
2. There is a direct connection between the heats of hydration of H^+ , Ca^{2+} , Na^+ and K^+ ions and their influence on silica gel structure.
3. Loss of hydrophilic properties of the hydrogel surface at regions where metal cations are adsorbed results in the formation of more coarsely porous silica gels, probably not only because of easier aggregation of the micelles at these regions, with a strengthening of the gel framework, but also because of (and probably, mainly because of) decreased wettability of the gel framework with water, and a consequent decrease of the capillary forces.

The authors consider it their duty to thank Professor M. V. Poliakov for discussion and valuable advice.

The L. V. Pisarzhevskii
Institute of Physical Chemistry
Academy of Sciences Ukraining SSR
Kiev

Received July 6, 1956

LITERATURE CITED

- [1] M. O. Kharmadarian and S. L. Kapelevich, *J. Chem. Ind.* 24, 1484 (1930); A. P. Okatov, *J. Appl. Chem.* 2, 399 (1929).
- [2] C. T. Plank and L. C. Drake, *J. Coll. Sci.* 2, 399 (1947).
- [3] B. P. Nikolskii, Dissertation (Leningrad, 1939).
- [4] M. V. Poliakov, *J. Phys. Chem.* 2, 799 (1931); M. V. Poliakov et al., *J. Phys. Chem.* 4, 454 (1933); M. V. Poliakov et al., *J. Phys. Chem.* 10, 100 (1937).
- [5] V. S. Veselovskii and I. A. Seliaev, *J. Phys. Chem.* 5, 1171 (1935).

[6] C. J. Plank, *J. Coll. Sci.* 2, 413 (1947).

[7] G. K. Boreskov, M. S. Borisova, O. M. Dzhigit, V. A. Dzisko, V. P. Dreving, A. V. Kiselev and O. A. Likhacheva, *J. Phys. Chem.* 22, 603 (1948).

[8] I. E. Neimark and R. Iu. Sheinfain, *Colloid J.* 15, 50 (1953).*

[9] I. E. Neimark, M. A. Piontkovskiaia and I. B. Sliniakova, *Colloid J.* 18, 61 (1956);^{*} G. F. Yankovskiaia, M. A. Piontkovskiaia and I. E. Neimark, *Proc. Acad. Sci. Ukrainian SSR* No. 1, 87 (1955).

[10] I. E. Neimark and I. B. Sliniakova, *Colloid J.* 18, 219 (1956). *

[11] M. S. Golderbitter, Author's Summary of Dissertation (Moscow, 1952).

[12] A. W. Dumanskii, *Bull. Acad. Sci. USSR, Div. Chem. Sci.* No. 3, 270 (1956). *

[13] I. E. Neimark, Trans. Commission on Analytical Chemistry, Acad. Sci. USSR, Vol. VI (IX), 77 (1955).

[14] Z. Z. Vysotskii, Dissertation (Kiev, 1952); *Ukrainian Chem. J.* 20, 513 (1954).

[15] K. Schultze, *Koll.-Z.* 141, 11 (1955).

[16] A. V. Dumanskii and F. D. Ovcharenko, *Colloid J.* 12, 331 (1950); F. D. Ovcharenko, *Ukrainian Chem. J.* 19, 139 (1953).

[17] J. O. M. Bockris, J. D. Mackenzie and J. A. Kitchener, *Trans. Faraday Soc.* 51, 1734 (1955).

[18] A. G. Repa, *J. Appl. Chem.* 28, 694 (1955).*

* Original Russian pagination. See C. B. Translation.

THERMOMECHANICAL INVESTIGATION OF EPOXIDE RESINS

L. I. Golubenkova, B. M. Kovarskaia, M. S. Akutin and G. L. Slonimskii

Our previous communication [1] contained the results of a study of the hardening of ED-6 grade epoxide resin (with 1:2.3 molar ratio of diphenylolpropane to epichlorohydrin) in presence of amines and resole phenol-formaldehyde resins. It was shown that in the hardened state these resins are tridimensional structures with infrequent long and flexible cross links, giving rise to high elasticity at elevated temperatures. As these resins have higher elasticity than phenol-formaldehyde resites, they can be used as lacquers, adhesives, and coatings. Recently several new grades of epoxide resins have been synthesized by condensation of diphenylolpropane and epichlorohydrin in various molar ratios. These resins have different molecular weights and epoxy group contents.

In the present investigation a thermomechanical study was made of the hardening of epoxide resins of different grades: ED-5, ED-6, ED-13, and ED-15, details of which are given in the Table.

Characteristics of Epoxide Resins

Grade of epoxide resin	Molar ratio of diphenylolpropane to epichlorohydrin	Epoxy group content, %	Molecular weight of resin
ED-5	1:5	25	400
ED-6	1:2.3	15	500
ED-13	1:1.5	8-10	1500
ED-15	1:1.2	2-5	2000

Data for the deformation-temperature (thermomechanical) curves were determined by means of the dynamometric balance [2] for the original resins, and by means of the consistometer [3] for the hardened specimens. The deformation-temperature relationship plotted in Fig. 1 (for applied constant stress $\sigma = 0.07 \text{ kg/cm}^2$) shows that the epoxide resins are of low molecular weight, i.e., they pass from the glassy into the viscofluid state without an intermediate region of high elasticity. The glass transition points of the resins are between 5 and +50°. At room temperature, ED-5 and ED-6 resins are viscous liquids, and ED-13 and ED-15 resins are brittle solids. The different states of aggregation of these resins at room temperature and the rapid hardening of ED-13 and ED-15 resins on addition of hardeners at the melting points of these resins (45-55°) makes further molding of the specimens difficult. A different method from that used in the previous study [1] was used for preparation of hardened resins of different grades under the same conditions. The hardener (polyethylene polyamine) was added to acetone solutions of the epoxide resins. Removal of the solvent and hardening of the resin took place over a period of 30-45 days at room temperature.

In a number of papers epoxide resins in their initial state are described as low-molecular thermoplastic substances, i.e., substances which do not harden without addition of suitable hardeners. However, our investigations showed that above a certain molar ratio of the original components (diphenylolpropane and epichlorohydrin) these resins acquire thermosetting properties, i.e., they become capable of hardening at temperatures of the order of 200°.

At 1:1.5 molar ratio of diphenylolpropane to epichlorohydrin (ED-13), the resin heated for 10 hours at 200° forms gelatinous products which swell strongly and partially dissolve in acetone. With decreasing proportions of

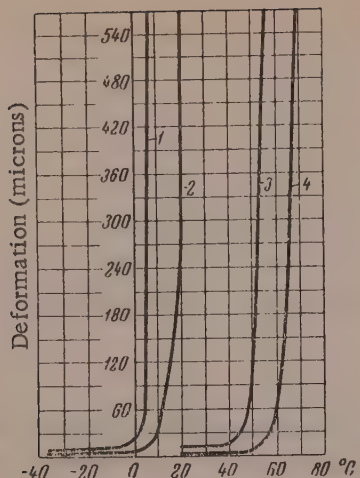


Fig. 1. Deformation-temperature curves for epoxide resins:
1) ED-5; 2) ED-6; 3) ED-13; 4) ED-15.

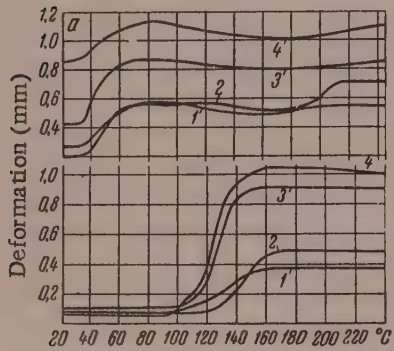


Fig. 3. Deformation-temperature curves for epoxide resins hardened with 6.5% of polyethylene polyamine (a), and additionally heated at 150° for 10 hours (b):
1) ED-5, 2) ED-6, 3) ED-13, 4) ED-15.

epichlorohydrin (starting from 1:1.2) the resins (ED-15), when heated for 10 hours at 200°, yield strong products, which are elastic at high temperatures, and which swell slightly and are practically insoluble in acetone. The physicochemical properties of ED-5 and ED-6 resins (solubility, viscosity, glass transition temperature, etc.) are not altered appreciably by the action of heat under the same conditions.

Deformation-temperature curves ($\sigma = 5 \text{ kg/cm}^2$) for ED-13 and ED-15 resins heated at 200° for 10 hours are plotted in Fig. 2. Heat treatment raises the glass transition temperature of the resins (especially of ED-15 resin, which also shows elastic behavior after heat treatment). However, as was already stated, ED-13 resin forms weak structures, which are broken down by small stresses ($\sigma = 5 \text{ kg/cm}^2$), while ED-15 resin loses its power of passing into the viscofluid state without

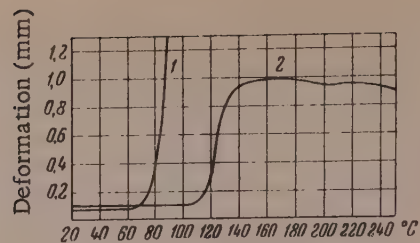


Fig. 2. Deformation-temperature curves for epoxide resins heated at 200° for 10 hours.
1) ED-13; 2) ED-15.

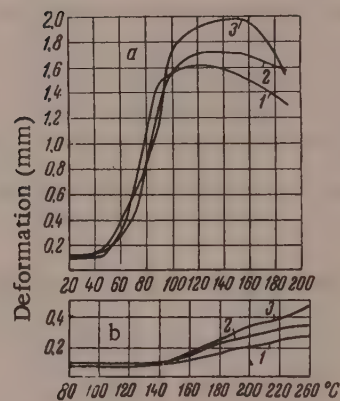


Fig. 4. Deformation-temperature curves for epoxide-resole resins (1:1), kept for 10 hours at 100° (a) and at 200° (b): 1) ED-5; 2) ED-13; 3) ED-15.

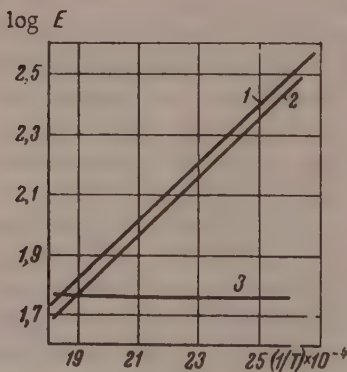


Fig. 5. Effect of temperature on the equilibrium modulus of elasticity for resins: epoxide ED-6; resole 2:1 (1); epoxide ED-5; resole 1:1 (2); and epoxide ED-5 hardened with 15% of polyethylene polyamine (3).

breakdown of the structure. ED-15 resins hardened at 200° for 10 hours without added hardeners have higher heat resistance and much better external appearance than the same resins hardened in presence of polyethylene polyamine at room temperature and additionally heated at 200° for 10 hours.

Tridimensional structures are formed in the hardening both of thermosetting and thermoplastic epoxide resins in presence of polyethylene polyamine (a mixture of homologs, from triethylenetetramine to hexaethyl-eneheptamine, with boiling point above 175°) and phenol-formaldehyde resins.* The deformation-temperature curves in Fig. 3 ($\sigma = 5 \text{ kg/cm}^2$) indicate that epoxide resins of different grades, hardened with equal amounts of polyethylene polyamine, differ in elasticity in the heated state. For example, ED-15 resin, with the lowest content of epoxy groups, has higher elasticity on deformation in the hardened state than ED-5 resin, which has the highest epoxy group content. Similar results were obtained for epoxide-resole resins ($\sigma = 5 \text{ kg/cm}^2$, weight ratio 1 : 1) (Fig. 4).**

Thus, the mechanical behavior of epoxide resins depends appreciably on their epoxy group contents. The greater elasticity which develops at high temperatures in resins of lower epoxy group content, and therefore of higher molecular weight, is clearly associated with the formation of space networks with less frequent cross links. When the hardened resin specimens are heated at 150° (Fig. 3) and 200° (Fig. 4) for 10 hours, their heat resistance increases considerably. The glass transition temperature of such specimens increases by 50-80°.

An investigation of the effect of temperature on the equilibrium modulus of elasticity of epoxide resins (ED-5, ED-6) hardened in presence of various hardeners, and of ED-15 resin previously heated at 200°, showed that the equilibrium modulus of resins hardened with amines is independent of the temperature (Fig. 5). The equilibrium modulus of elasticity of hardened epoxide-resole resins decreases with rise of temperature. Therefore the space structure of hardened epoxide resins is mainly formed by stable chemical bonds, as the presence of physical (hydrogen) bonds was detected by us only in epoxide-resole resins (Fig. 5).

The calculated bond dissociation energy [4, 5] is 6.9 kcal./mole, which corresponds to the energy of the hydrogen bond. It is very likely that the presence of hydrogen bonds in epoxide-resole resins is the consequence of their considerable contents of resole resins, in which hydrogen bonds have been shown to play an important part [5, 6].

SUMMARY

1. Epoxide resins may be either thermoplastic or thermosetting, according to the relative proportions of the original components - diphenylpropane and epichlorohydrin. Thermosetting properties begin to appear in the resins at 1 : 1.5 molar ratio of the components, and on further decrease of the epichlorohydrin content.

2. Hardened epoxide resins are tridimensional structures the mechanical behavior of which depends on the epoxy group content of the original product. Thus, hardened resins with lower epoxy groups contents (ED-13 and ED-15) have higher elasticity at elevated temperatures than resins with higher epoxy group contents (ED-5 and ED-6).

Therefore elasticity (with retention of the other properties - adhesion, mechanical strength, chemical resistance, etc.) may be one of the decisive factors in the choice of a particular resin for use in various branches of industry.

3. Thermosetting resins (ED-15) hardened without addition of hardeners, have higher heat resistance and better external appearance than the same resins hardened with amines or resole resins.

Scientific Research and Project Institute for Plastics
Moscow

Received January 25, 1957

* It should be pointed out that epoxide resins can be hardened not only under the influence of resoles, but also of novolac phenol-formaldehyde resins. For example, we found that addition of novolac (K-18) resin (in weight proportions of 10 : 1, 2 : 1, 1 : 1) to ED-6 epoxide resin results in hardening with formation of low-strength products at 200°. The epoxide-novolac resins have a low rate of hardening.

** Figure 4 shows deformation-temperature curves for epoxide-resole resins heated at 100°, and not in the original state, as owing to the presence of resoles the combined products harden at considerably higher temperatures than epoxide resins hardened in presence of amines.

LITERATURE CITED

- [1] B. M. Kovarskii, L. I. Golubenkova, M. S. Akutin and G. L. Slonimskii, *Colloid J.* 18, 6, 697 (1956).*
- [2] V. A. Kargin and T. I. Sogolova, *J. Phys. Chem.* 23, 530 (1949).
- [3] G. M. Bartenev, *J. Phys. Chem.* 24, 10, 1210 (1950).
- [4] G. M. Bartenev, *J. Phys. Chem.* 22, 7, 1154 (1952).
- [5] G. L. Slonimskii, V. A. Kargin and L. I. Golubenkova, *Proc. Acad. Sci. USSR* 93, 2, 311 (1953).
- [6] L. I. Golubenkova, G. L. Slonimskii and V. A. Kargin, *J. Phys. Chem.* 31, 1, 27 (1957).

* Original Russian pagination. See C. B. Translation.

THE STRUCTURE AND PHASE STATE OF POLYETHYLENE TEREPHTHALATE FIBERS*

V. O. Gorbacheva and N. V. Mikhailov

In recent years a new synthetic polymer, polyethylene terephthalate, has attained considerable industrial importance; it is used mainly in the production of synthetic fibers known under various trade names such as Terylene, Lavsan, etc., and also of various products such as films and plastics. These fibers have a number of valuable properties: high initial modulus, good chemical resistance to acids and oxygen, adequate mechanical strength at various temperatures, low permeability to gases, and high resistance to light and bacteria; all this accounts for the great interest taken by research workers in matters related to the production technology of this polymer, extrusion of fibers from it, etc. Most of the published investigations deal with its physical and mechanical properties [1], structure [2], and the mechanism of fiber drawing [3]. Many workers have shown that polyethylene terephthalate products can be obtained both in the amorphous and in the crystalline state. However, not enough is known about the crystallization processes and structural changes in polyethylene terephthalate and the associated changes in the properties of the polymer and of fibers made from it. It is known that a distinctive and unfavorable characteristic of this polymer, which is of great importance in relation to fiber production, is its poor susceptibility to "cold" drawing.

This paper contains the result of a study of the structure of polyethylene terephthalate and of fibers made from it, in relation to the conditions of production and subsequent stretching and heat treatment, carried out with the aid of x-ray and thermographic analysis. Samples of polyethylene terephthalate in the form of resin with specific viscosity 0.24-0.27, and fibers made from it, were investigated. The fibers were spun at 285° and stretched by 550% at 80-100°. The polymer was dissolved at 25-30° in phenol-tetrachloroethane mixture (1:1); it was precipitated and washed with diethyl ether [4]. The x-ray photographs were taken with copper radiation with β -radiation (K_{β}) filtered out by means of nickel foil, at 45 kv, 14-15 ma, at a distance of 35 mm between the specimen and film; the exposure time was 8 hours. The photometric analysis of the x-ray patterns was carried out by means of a recording microphotometer.

Figure 1,a shows the x-ray pattern of polyethylene terephthalate in the form of a solid transparent mass (resin). A similar pattern is given by the unstretched fibers. Comparison of these patterns show them to be the same for both samples, with one broad interference ring, which is a sign of amorphous structure. In the course of the investigation the isotropic fibers were stretched at 18-20°. The x-ray pattern of such fibers (Fig. 1,c) when reduced to powder diagram form (Fig. 1,b), also showed one broad interference ring.

It must be assumed that the phase states of isotropic and oriented polyethylene terephthalate fibers is the same. On the other hand, if the fibers were stretched at 80-90°, the x-ray pattern showed more interference rings (1, d). The question naturally arose, what is the origin of this new pattern - more pronounced orientation of the molecules in the fiber, or the appearance of new interferences, i.e., changes in the phase state of the polymer (fiber) during stretching? By the use of the Katz method for obtaining x-ray patterns of stretched fibers, we found that the pattern for a fiber stretched at 80-90°, in reduced form (Fig. 1,e) does not reproduce the isotropic fiber pattern and differs from the reduced x-ray pattern of a fiber stretched at 18-20° by the distinct presence of several new sharp interference rings.

This leads to the conclusion that when polyethylene terephthalate fibers are stretched at 80-90°, molecular orientation and crystallization take place in the polymer. "Cold" drawing (at 18-20°) of polyester fibers is

* X-ray technologist P. M. Larionov took part in the work.

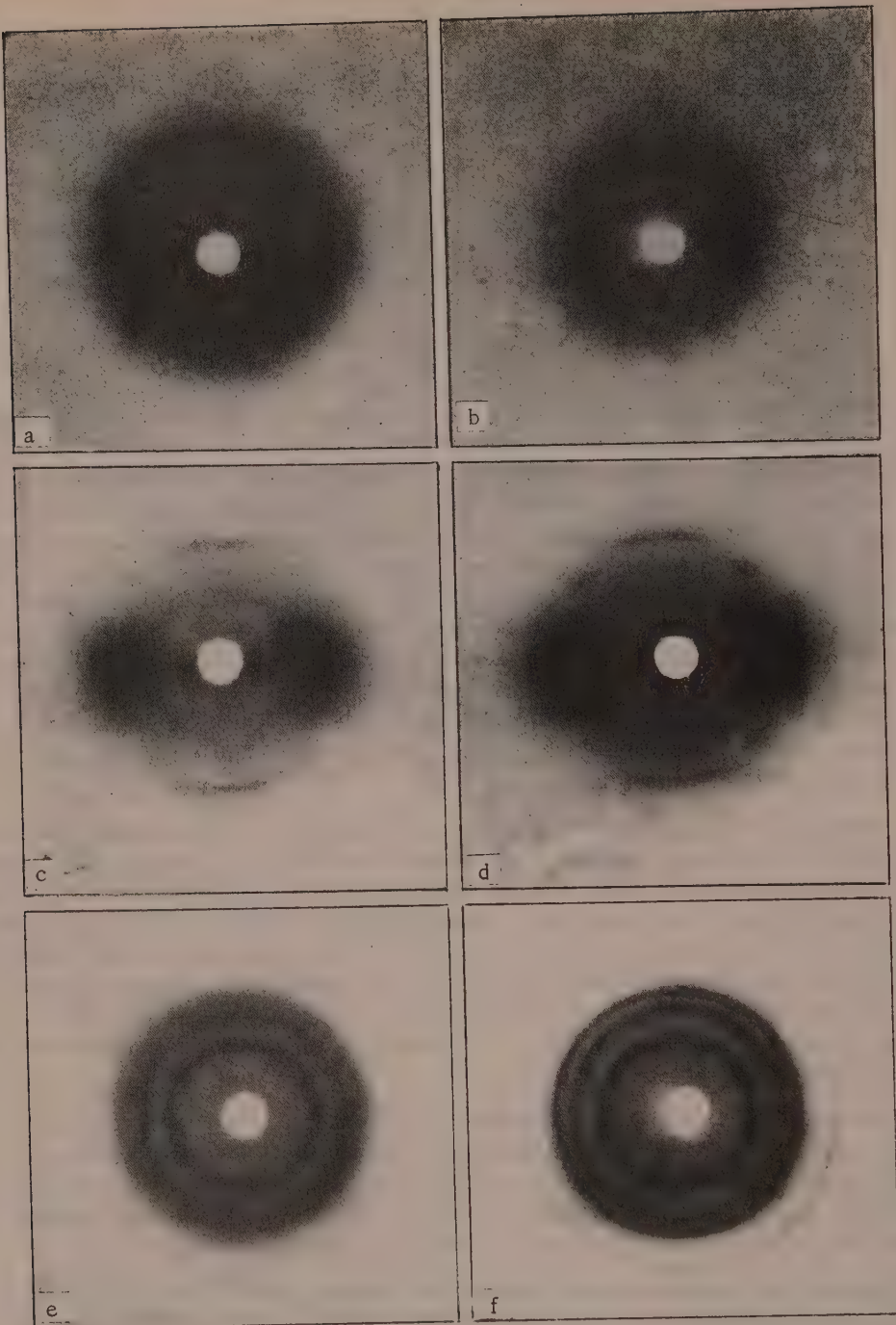


Fig. 1. X-ray patterns:

a) original polyethylene terephthalate resin; b) fiber stretched to 450% at 18-20° (reduced powder pattern); c) fiber stretched to 450% at 18-20°; d) fibers stretched to 450% at 80-90°; e) same, reduced powder pattern; f) slowly cooled polyethylene terephthalate melt.

accompanied by orientation processes only, while the phase state of the substance remains unchanged. It follows that the original polymer, the isotropic fibers, and fibers oriented at 18-20° are amorphous. Crystalline fibers can be obtained from polyethylene terephthalate only by stretching at 80-90°. Additional confirmation of this view is provided by x-ray data for the original polymer heated at 150-190°. The x-ray pattern of such a heat-treated

polymer strongly resembles the "reduced" x-ray pattern of a fiber oriented at 80-90°. The same is found in x-ray patterns of polymer samples obtained by slow cooling of melts to room temperature or by precipitation of the polymer by slow evaporation of solvent from a polymer solution (Fig. 1,f). It is known from earlier publications [5] that these are the most favorable conditions for crystallization of polyamides.

TABLE 1

Interplane Spacings of Different Polyethylene Terephthalate Specimens
(measured from the central spot of the pattern)

Polyethylene terephthalate specimen	Interplane spacings (d) in Å						
	d ₁	d ₂	d ₃	d ₄	d ₅	d ₆	d ₇
Original polymer	—	—	—	—	—	4.74	—
Unstretched fiber	—	—	—	—	—	4.76	—
"Cold-drawn" fiber	—	—	—	—	—	4.8	—
Heat-stretched fiber	—	—	2.49	4.10	4.35	—	5.47
Slowly cooled melt	2.18	2.31	2.44	4.09	4.35	—	5.50

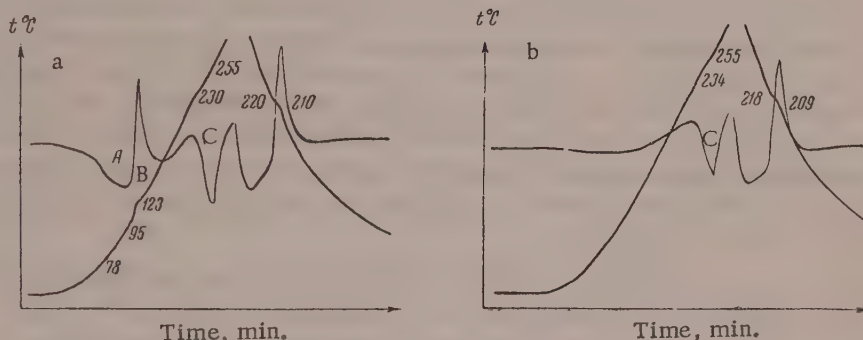


Fig. 2. Differential heating and cooling curves:
a) Unstretched Laysan fiber; b) same, stretched to 450% at 80-90°.

It follows from these results that polyethylene terephthalate fibers, when extruded with air cooling, are formed in the amorphous and glassy state. In this they differ from polyamides, which show a crystalline structure even in the original state and in the form of isotropic fibers. It should be noted that polyethylene terephthalate has a greater tendency to supercooling than polyamides. It must also be pointed out that when fibers oriented at 80-90° are additionally heated at 185°, their x-ray pattern is improved considerably: the crystal interferences become clearer and sharper. A similar effect is found in polyamide fibers but is less pronounced.

For completeness, the corresponding interplane spacings for short-range order reflections are given in Table 1.

It is known that the structural criterion alone is insufficient for evaluation of the phase state of a polymer, and therefore the above structure data were supplemented by the results of phase analysis by the thermographic method. The experimental procedure has been described previously [10]. Figure 2,a shows differential heating and cooling curves for the original polyethylene terephthalate. Unstretched fibers and "cold-drawn" fibers give similar curves. These results show that the behavior of all these materials on heating is exactly the same. The heating curve shows three effects, two endothermic and one exothermic.

However, the thermographic picture changes considerably if the original polymer and the unstretched fiber were previously heated, and the fiber was stretched at high temperature. Heating and cooling curves for such samples are shown in Fig. 2,b. Similar curves are given by polymer samples obtained by slow cooling of melts or by evaporation of solvent from a polymer solution. Figure 2,b shows that the heating curves have only one peak instead of three. The explanation is that in both cases the appearance of the endothermic effect (area C) in the 235-255° range is associated with fusion of the polymer; this is shown by the reversibility of this peak upon repeated heating and cooling of the polymer.

TABLE 2

Transition Temperature Ranges of Polyethylene Terephthalate Specimens on Heating and Cooling

Specimen of polyethylene terephthalate	Endothermic effects I and II, °C		Exothermic effects I and II, °C	
	I (A)	II (B)	(I B)	II
Original polymer	78-95	235-255	115-150	210-220
Unstretched fiber	78-95	235-255	110-123	210-220
Fiber stretched at 18-20°	80-93	235-255	110-125	210-220
Fiber stretched at 80-90°	None	235-255	None	210-220
Slowly cooled melt	None	235-255	None	210-220

The appearance of two other peaks on the heating curves in the 80-95° and 115-130° ranges (Fig. 2,a, areas A and B) may seem somewhat unexpected. However, these effects can be explained if the x-ray data obtained for polyethylene terephthalate and the published descriptions of the properties of silicate glasses and triglycerides are taken into account. It is known that silicate and organic glasses and certain other organic substances are undercooled liquids and are therefore thermodynamically unstable systems. Such compounds therefore tend to pass into the true stable crystalline state; this is effected when the substances are heated. Analogously, our undercooled polyesters also tend to pass into the true crystalline state when heated. It is likely that when the polymer was heated it softened and tended to pass from the glassy into the elastic state. This transition required a certain amount of heat, represented by the endothermic effect in the 80-95° range (Fig. 2,a, area A). This explanation of the reason for the appearance of an endothermic effect while the substance remains in the same phase state somewhat contradicts the accepted views. However, similar effects have been reported and explained in the literature [6-8]. We observed analogous but less distinct effects in polyamides and put forward tentative views on their nature [5].

The polymer is devitrified by heating, and the kinetic mobility of its chain segments is thereby increased. After devitrification of the polymer or during the process, if the substance is in the solid state, crystallization occurs. Therefore an exothermic effect in the 105-150° range appears on the heating curves (Fig. 2,a, area B).

It is quite obvious that these effects are not to be found on the heating curves of previously heated specimens. The average results of 5-6 determinations of the temperature ranges of these effects on the heating curves for different specimens of polyethylene terephthalate are given in Table 2.

The cooling curves for the polymer shown in Fig. 2,a and 2,b have one exothermic effect at 210-220°, when the polymer crystallizes. It is therefore necessary to explain why this effect occurs at a higher temperature than the corresponding effect on the heating curves (at 210-220° instead of 115-150°). The probable explanation is that in the one case the polymer crystallizes during cooling of its melt, i.e., when kinetic obstacles to structure formation in the polymer are absent or very small. When the polymer crystallizes in the solid state, i.e., in conditions of high viscosity, these obstacles are high. It seems that the influence of the kinetic factor on the crystal growth rate is greater in these polyesters than in polyamides, as the former are strongly undercooled even at room temperature, while the latter require deeper cooling. The most favorable conditions for crystallization of the polymer arise when the difference between the formation rate and the growth rate of the crystallization centers is at a minimum; this is the case in the crystallization of a very slowly cooling polyester melt (see Fig. 1,f). Crystalline specimens of polyethylene terephthalate are white and opaque; amorphous specimens are transparent.

The thermographic data obtained in this investigation were used to determine the heat of fusion of polyethylene terephthalate; the value found was 9-11 cal./g, which differs somewhat from the published value [9] or 16 cal./g for the heat of fusion. The heat of fusion was determined by the Berg and Anosov method, described by us previously [10].

SUMMARY

1. A comparison of x-ray structural and thermographic data, which were in satisfactory agreement, suggests that, in contrast to polyamides, polyethylene terephthalate is a polymer which is readily undercooled in the

usual conditions of forming from melts, and is therefore amorphous.

2. Polyethylene terephthalate is thermodynamically unstable when in the amorphous state. The polymer crystallizes at relatively low temperatures (80-110°) and at a low rate.

3. The heat of fusion of polyethylene terephthalate is 9-11 cal./g.

The Institute of Artificial Fibers
Mytishchi

Received February 9, 1957

LITERATURE CITED

- [1] A. Thompson, Nature, 4471, 9 (1955); F. Morgan, J. Appl. Chem. 4, No. 4; 160 (1954); E. Leonard, Ind. Eng. Chem. 2291 (1953).
- [2] A. Keller and G. Lester, Proc. Roy. Soc., London 247, A 921, 1-21 (1954).
- [3] J. Marschall, J. Appl. Chem. 4, No. 4, 145 (1952).*
- [4] W. Creel, Faserforschung und Textiltechnik 10, 423 (1954).
- [5] N. V. Mikhailov and V. O. Klesman, Proc. Acad. Sci. USSR 91, 1, 99 (1953).
- [6] W. Eitel, The Physical Chemistry of the Silicates (Russian Translation) (ONTI, Chem. Theoret. Moscow, 1936) p. 181.
- [7] P. P. Kobeko, Amorphous Substances (Izd. AN SSSR, 1952).**
- [8] G. B. Ravich and G. G. Tsurinov, The Phase Structure of Triglycerides (Izd. AN SSSR, 1952) p. 83.**
- [9] W. Smith and M. Dole, J. Pol. Sci. 20, No. 94 (1956).
- [10] N. V. Mikhailov and V. O. Klesman, Colloid J., 16, No. 4, 272 (1954).*

* Original Russian pagination. See C. B. Translation.

** In Russian.

THE FORMATION AND PROPERTIES OF INTERPOLYMERS OF NATURAL AND BUTADIENE - STYRENE RUBBERS

B. A. Dogadkin, V. N. Kuleznev and Z. N. Tarasova*

Angier and Watson [1] have described a number of examples of the formation of interpolymers of natural rubber with other polymers (such as polychloroprene) by joint mastication in an inert gas atmosphere. The formation of an interpolymer from natural and butadiene-styrene rubbers was not studied. However, this system is of undoubted interest, as it has been reported [2] that this pair of polymers is thermodynamically incompatible. Moreover, in our opinion an interpolymer of these rubbers, if used as an adhesive interlayer, should increase adhesive bond strength between natural and butadiene-styrene rubber vulcanizates, which is of practical importance in the production of laminated articles such as tires, which contain both natural and butadiene-styrene rubbers in their components. The theoretical grounds for this view are given in the last section of this paper. The importance of this problem caused us to initiate the present investigation.

Production of interpolymers. The mastication was carried out on specially designed microrolls [3] contained in a hermetic cabinet, so that any desired atmosphere could be provided around the material. The process was carried out with a 0.25 mm gap between the rolls in an atmosphere of purified nitrogen or argon (containing about 0.1% O₂), the rolls being strongly cooled with running water. The rubbers were previously purified by extraction with hot acetone (natural rubber) or hot methanol (butadiene-styrene rubber) for 12 hours. Data on the intrinsic viscosity [η] and plasticity measured by the Defo method in the course of milling are given in Figs. 1 and 2.

Fractional precipitation. To prove the formation of an interpolymer during joint mastication of the rubbers, we carried out fractional precipitation of solutions of the masticated rubber mixtures, and also selective vulcanization of one of the components. The natural and butadiene-styrene rubbers were present in 1:1 ratio.

The choice of a selective nonsolvent for precipitation in the system natural rubber - butadiene-styrene rubber presents considerable difficulties because these rubbers have almost equal solubilities in common solvents. We chose the binary mixture benzene - methyl ethyl ketone (1:4), in which butadiene-styrene rubber is completely soluble whereas natural rubber does not dissolve in this mixture on periodic shaking for 48 hours at 25 ± 0.5°. For comparison, in parallel with the solubility determinations on the rubbers masticated together, the solubility of a mixture of the rubbers masticated separately and then mixed together in air during 3-4 minutes with very vigorous stirring was investigated. When the solution process was completed, the solution was separated off, evaporated, and the natural-rubber content of the film was determined refractometrically. For these determinations, solutions with different proportions of the rubbers were previously prepared; films were made from these, and their refractive indices were determined by means of an Abbe refractometer, after removal of phenyl-β-naphthylamine. The results were used to plot a calibration graph for the linear relationship between the refractive index and the ratio of the rubbers in the film. This graph was then used in analysis of mixtures with unknown proportions of natural and butadiene-styrene rubbers.** Figure 3 shows that with the separately masticated polymers natural rubber begins to pass into solution after 40 minutes of milling; this is undoubtedly the consequence of the better solubility of the products of lower molecular weight formed during mastication. In the case of the jointly masticated polymers, natural rubber begins to pass into solution from the first moment of mastication. This difference in the behavior of the mixtures undoubtedly indicates the existence of chemical bonds between some of the molecules of natural rubber and the molecules of butadiene-styrene copolymer in the mixture.

* Student N. Ia. Safronov assisted in the work.

** The refractive index does not change appreciably during mastication [4].

obtained by joint milling of the rubbers. The molecules of butadiene-styrene rubber, bound to molecules of natural rubber, take some of the latter with them into the solution and thereby increase their solubility.

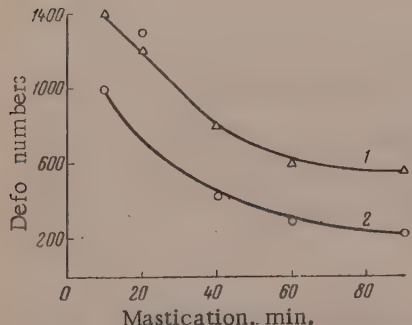


Fig. 1. Effect of mastication time of the Defo number for 1:1 mixtures of natural and butadiene-styrene rubbers:
1) extracted; 2) technical.

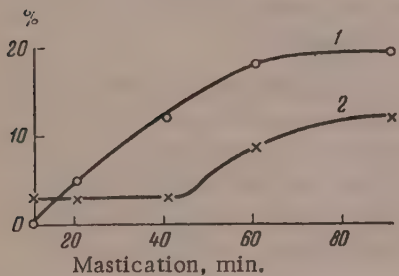


Fig. 3. Effect of mastication time on the amount of natural rubber dissolved by the binary solvent benzene-methyl ethyl ketone (1:4):
1) jointly milled mixture; 2) mixture of separately milled rubbers.

This is confirmed especially clearly by experiments on fractionation of mixtures of jointly and separately masticated rubbers from benzene solutions by addition of methyl ethyl ketone. After 90 minutes of mastication 2% solutions of both samples were made, and methyl ethyl ketone was added to each at $20 \pm 0.5^\circ$ with vigorous stirring. Figure 4 shows that, in comparison with the separately milled rubbers, slow and incomplete precipitation of natural rubber (only 64% of the amount added) and more complete precipitation of butadiene-styrene rubber (89%) occurs in the jointly milled mixture; this indicates that chemical bonds are present between the molecules of the two polymers, i.e., it is evidence of interpolymerization. The difference between the amounts of natural rubber precipitated from the products of joint and separate mastication respectively represents 30% of the total amount of natural rubber in the original sample.

Selective vulcanization. For further confirmation of interpolymerization, we vulcanized mixtures of jointly and separately milled polymers by means of polychloro compounds which, as is known [5], do not vulcanize natural rubber. The following formulation was used: 150 wt. parts of polymer, 8.0 wt. parts of

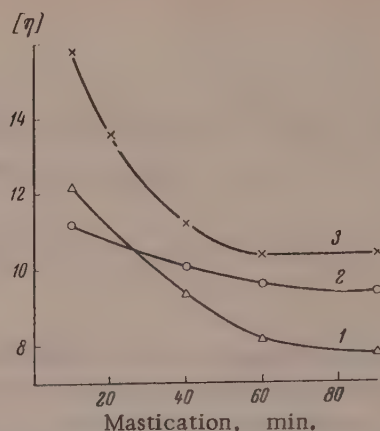


Fig. 2. Effect of mastication time of extracted natural and butadiene-styrene rubbers and of a mixture of them, on $[\eta]$:
1) natural rubber; 2) butadiene-styrene rubber; 3) 1:1 mixture.

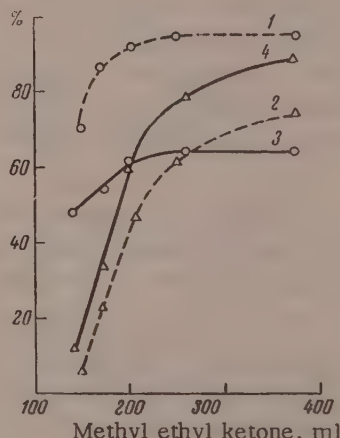


Fig. 4. Precipitation with methyl ethyl ketone from benzene solutions of mixtures of natural (1,3) and butadiene-styrene (2,4) rubbers milled for 90 minutes:
1, 2) milled separately; 3, 4) milled together.

TABLE 1

Fractional Composition of Heat-Vulcanized Mixtures of Natural and Butadiene-Styrene Rubbers

Polymers in vulcanizate	Sol fraction, %	NR in sol fraction, %	NR extracted, %	Residue, %	
				NR	BSR
Milled together	78	64	50	0	28
Milled separately	76	47	36	14	10

benzal chloride, 10.0 wt. parts of activator, and 1 wt. part of phenyl- β -naphthylamine. The activator, in two parallel experiments, was either ZnO or PbO. The vulcanization was performed for 60 minutes at 143°, and the vulcanizates were then extracted with chloroform. The amount extracted by chloroform from a mixture of the separately milled polymers with lead oxide activator was 51.5%, and from a mixture of the jointly milled polymers, 38.6%. With zinc oxide as activator, the chloroform extract from the mixture of separately milled polymers was 87.0%, and from the mixture of jointly milled polymers, 77%.

It follows that not all the butadiene-styrene rubber becomes bound during vulcanization, as with the polymer ratio used (1:1) the extract of the separately milled rubbers should not exceed 50%. It is also possible that the different rubbers can be tied to some extent in the spatial network by mechanical tangling of their molecules, so that both polymers may be present both in the vulcanizate and in the extract.* However, since the conditions of binding of the butadiene-styrene rubber into the spatial network were the same for the jointly milled and the separately milled polymers, the difference between the extracts must be ascribed mainly to different degrees of chemical bonding of the natural rubber. If the value found for the extract is referred to the total amount of natural rubber in the sample, it is found that 20-26% of the natural rubber in the mixture becomes bound in the course of mastication.

The jointly and separately milled polymers were also heat-vulcanized at 200° for 2 hours. As is known, synthetic polymers containing vinyl side chains (poly butadiene, butadiene-styrene) form structures when heated in a press, in contrast to natural rubber, which is degraded under such conditions. The degree of vulcanization in this case was again determined from the amount of chloroform extract and subsequent determinations of the rubber in it. The results are given in Table 1.

The amount of natural rubber bound with the molecules of butadiene-styrene copolymer (14%) in the jointly milled rubbers, referred to the total amount of natural rubber present (as before) is 28%. Thus, the results of fractionation, vulcanization by means of polychloro compounds, and heat vulcanization all show that interpolymerization (chemical bonding) of the molecules of natural and butadiene-styrene rubbers occurs during cold mastication in an inert medium, and 26-30% of the natural rubber present enters the interpolymer.

Variation of intrinsic viscosity with the ratio of the rubbers. If it is assumed that the degradation of polymer molecules under the influence of the shearing forces which develop in mastication is independent of the chemical nature of their neighbors, and depends only on the magnitude of the deformation, it becomes quite evident that solutions of equal concentrations of mixtures of separately and jointly milled polymers should have equal viscosity. We carried out parallel viscosity determinations on solutions of natural and butadiene-styrene rubbers in different proportions. Benzene solutions of 3% total polymer concentration were prepared, and their absolute viscosities determined by means of the Hoeppler viscosimeter. Figure 5 shows that the viscosities of the jointly milled polymers are higher than the corresponding viscosities of mixtures of separately milled polymers, the deviations being greatest in the region of intermediate ratios. In order to show that this viscosity increase is not entirely the consequence of intermolecular forces in these relatively concentrated solutions, the intrinsic viscosity of each sample was also measured by the usual method by means of the Ostwald viscosimeter. It follows from Fig. 5 that the values of $[\eta]$ (and therefore of the average-viscosity molecular weight of the mixtures) deviate considerably from the additive values for polymer mixtures. It is interesting to note that after milling in the presence of phenyl- β -naphthylamine the intrinsic viscosity of a 1:1 mixture of the two polymers is considerably lower even than the intrinsic viscosity of pure natural rubber. This indicates the possibility of direct interaction of phenyl- β -naphthylamine with the hydrocarbon radicals.

* The polymer contents could not be determined refractometrically as both the extract and the vulcanizate were opaque.

Physicochemical properties of the vulcanizates. The physicochemical properties of a series of vulcanizates made from mixtures with different proportions of polymers milled jointly and separately in an inert medium were studied. The composition of the vulcanizates (in parts by weight) was: rubber mixture 100.0, sulfur 2.2,

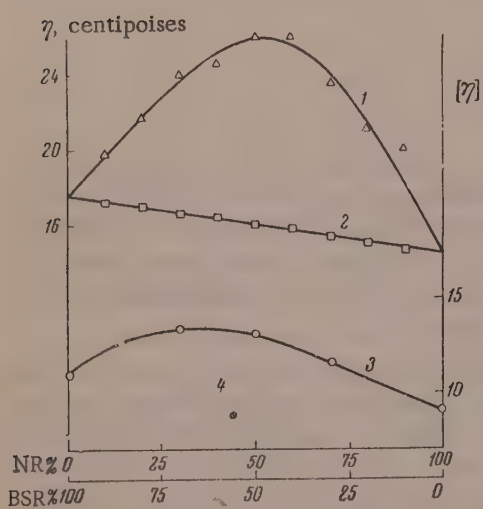


Fig. 5. Variation of intrinsic (3,4) and absolute (1,2) viscosities of 3% benzene solutions of mixtures of natural and butadiene-styrene rubbers milled for 90 minutes, with composition of the mixtures.

1, 3) Milled jointly, 2) milled separately,
4) mixture with 4% of phenyl- β -naphthylamine,
milled jointly.

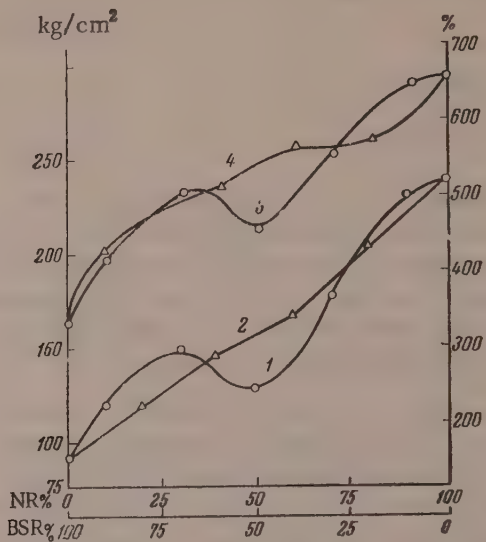


Fig. 6. Variation of tensile strength (1,2) and relative elongation (3,4) of vulcanizates with the composition of mixtures of natural and butadiene-styrene rubbers:
1, 3) milled jointly; 2, 4) milled separately.

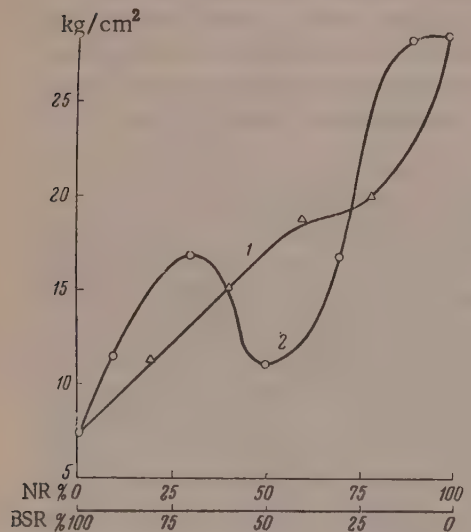


Fig. 7. Area under the load - elongation curves (energy of elasticity) of vulcanizates as a function of composition of mixtures of rubbers milled:
1) separately; 2) jointly.

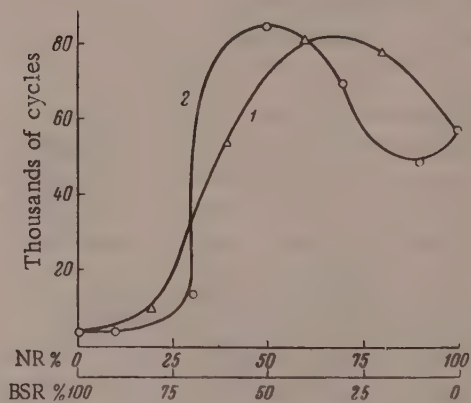


Fig. 8. Variation of fatigue endurance of vulcanizates with the composition of mixtures of natural and butadiene-styrene rubbers milled:
1) separately; 2) jointly.

tetramethylthiuram disulfide 0.5, zinc oxide 5.0. The vulcanization optimum (30 minutes for all the mixtures) was determined by determinations of bound sulfur (by the radioactive tracer method with S³⁵ isotope) and of the number of cross bonds per unit volume, calculated by the Flory - Rehner formula from the maximum swelling. The following values were determined for specimens at optimum vulcanization: tensile strength, relative

elongation, moduli at 100, 200, 300, 400%, areas under the load-elongation curves (proportional to the work of deformation of the vulcanizates), and fatigue resistance at $\epsilon = 100\%$ by means of the De Mattia machine. The moduli decrease linearly with increasing contents of natural rubber, which undergoes greater degradation than butadiene-styrene rubber during mastication (see Fig. 2), and there are no appreciable differences in this respect between vulcanizates of jointly and separately milled polymer mixtures. The tensile strength and relative elongation of mixed vulcanizates increase with increasing natural rubber content. The variations of both of these values with the composition are represented by curves with a small bend at 1:1 polymer ratio (Fig. 6).* This form of the curve is shown even more clearly on the plots of the work of deformation against the ratio of the rubbers in the vulcanizates (Fig. 7). The behavior of vulcanizates of both types of mixtures under repeated deformation was studied (Fig. 8). Here both types of vulcanizate have maxima of fatigue endurance; at 1:1 ratio for the jointly milled polymers, and with ~70% of natural rubber in the mixtures for the separately milled polymers. The higher fatigue endurance in presence of ~30% of butadiene-styrene rubber, as compared with the pure components, is in our opinion the consequence of loosening of the vulcanizate structure owing to the lower integral packing density of the mixture of these two incompatible polymers (fuller details will be given in our next communication), leading to lower internal friction and therefore lower mechanical activation of the chemical processes which develop in the course of repeated deformation. This finding is undoubtedly of practical interest, as it indicates that it is possible to obtain mixtures of natural and butadiene-styrene rubbers with higher fatigue resistance than in vulcanizates of natural rubber alone. However, this requires confirmation by tests of rubber articles in use.

The variation of cross-link concentration in vulcanizates with the ratio of the rubbers (Fig. 9) is especially interesting. For vulcanizates of mixtures of the separately milled rubbers this relationship is represented by a curve with a minimum at about 80% of natural rubber in the mixture; this can probably also be ascribed to a decreased integral packing density of a mixture of these two incompatible polymers. A decrease of packing density occurs on addition even of small amounts of disordered molecules of the noncrystallizing butadiene-styrene rubber to the crystallizing natural rubber. This causes steric obstacles to cross-link formation. In mastication, in an inert medium, of a mixture of two polymers with molecules differing in activity and mechanical strength, a process of radical degradation occurs. This process depends on the relative reactivity (both with regard to mechanical and to radical, chemical influences) of the two polymers. The more easily degraded natural rubber, with a higher content of weakened bonds between the α -methylene carbon atoms, yields more free radicals than the butadiene-styrene copolymer.

The radicals from natural rubber may act on the molecules of butadiene-styrene copolymers which are under mechanical stress, and attach themselves to these molecules, with the formation of a larger number of bonds

than are found in mixtures of rubbers milled separately. Branched molecules nearer to spherical in shape than the original molecules, and therefore of lower viscosity-average molecular weight, are also formed. The difference of bond content does not influence such relatively crude characteristics of the vulcanizates as tensile strength, elongation at break, and modulus. The fatigue endurance of mixtures of separately milled polymers in the region of maximum difference of cross-link concentration is greater than that of mixtures of jointly milled polymers.

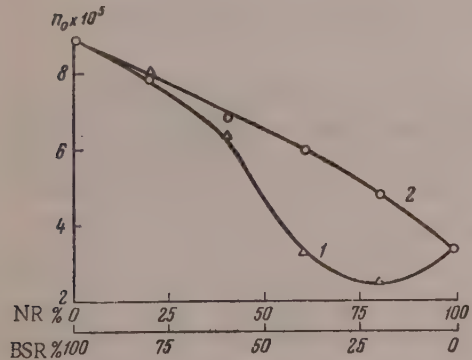


Fig. 9. Variation of cross-link concentration with composition of mixtures of rubbers milled:
1) separately; 2) jointly.

has been considered in a number of papers [6]. However, it can be easily shown that diffusional displacement of

Production of adhesives from the interpolymers and their effect on bond strength between vulcanizates of different rubbers. The autohesion of doubled polymer layers is regarded as a diffusion process, effected by displacement of individual segments of the molecular rubber chains on this basis, the influence of molecular weight, chain flexibility, etc. on the autohesion process

* The special position of the point at 1:1 ratio cannot be attributed to scattering of the experimental points, as this result is based on five parallel determinations on different specimens.

individual segments is not enough for complete coalescence of doubled layers. As has been pointed out by Dogadkin [7], a necessary condition for cohesion is the existence of true flow for bonding unlike rubbers, the thermodynamic characteristics of which do not favor spontaneous diffusional cohesion. Under otherwise equal conditions, another important effect is covulcanization of the doubled layers, i.e., formation of a space vulcanizate network consisting of molecules of different rubbers chemically bonded by the vulcanizing groups. The presence of these chemical bonds between different rubbers makes the system stable and prevents phase separation. If a specimen consisting of two doubled strips of tread and breaker butadiene-styrene rubber vulcanizates, joined by a natural rubber adhesive, is vulcanized and placed in benzene, simple swelling can break down the bond at the boundary between the natural and the butadiene-styrene rubbers. This shows the absence of a continuous vulcanization network at the boundary between the rubbers, i.e., it indicates the absence of a covulcanization effect [7]. It seems likely that if an adhesive made from the interpolymer is used, the regions (segments) of the molecules of natural rubber chemically bonded to molecules of butadiene-styrene rubber penetrate relatively easily into the layers of natural rubber, while segments of molecules of the synthetic rubber chemically bound to natural rubber molecules can penetrate easily into the synthetic rubber layer. Since the kinetic conditions of vulcanization (concentration and chemical activity of the double bonds) favor the cross linking of molecular chains of the same composition during vulcanization, the two layers of different rubbers are firmly bonded by means of the interpolymer molecules after vulcanization.

Mixtures of the two rubbers in 1:1 ratio, both purified by previous extraction and unpurified, were milled in an inert medium for different times. The milled mixtures were then compounded in air with the following ingredients:

Polymer	100 wt. parts	Pine resin	5.0 wt. parts
Dibenzothiazolyl disulfide	2.5 wt. parts	Rosin	3.0 wt. parts
Diphenylguanidine	1.5 wt. parts	Phenyl- β -naphthylamine	1.0 wt. parts
Zinc oxide	5.0 wt. parts	Channel black	25.0 wt. parts
Steric acid	0.5 wt. parts	Sulfur	3.0 wt. parts

The mixtures were then shaken in the cold with gasoline to give 10% solutions; the adhesives were tested for tackiness by the Baer test, for endurance under repeated deformation by M. M. Reznikovskii's method by means of the MRS-2 machine (shearing deformation of doubled layers with the joint at right angles to the direction of deformation), and by A. I. Kolomytseva's method by repeated compression of rectangular specimens with a diagonal joint in the "Metallist" machine. The results of the tests are given in Table 2.

TABLE 2

Effect of Adhesive Layer of Interpolymer on Bond Strength Between Natural and Butadiene-Styrene Rubber Vulcanizates

Composition of the joined rubbers	Composition of adhesive	Tackiness in g/cm	Dynamic bond strength (under repeated compression)				
			tested by MRS-2 machine	tested on "Metallist" machine	endurance, % of joint	destruction, % of joint	temperature of specimen, °C
Breaker based on natural rubber, code 23-448	Without adhesive	—	0.175	100	—	—	100-121
	Adhesive based on NR, code 1-KE-7	2410	0.208	—	240.0	66	
Tread based on SKS-30A, code 43-196	Adhesive based on technical NR and SKS-30A, milled for 90 minutes	2360	1.000	60	423.0	50	115-140
	Adhesive based on NR and SKS-30A purified by extraction and reprecipitation, milled for 60 minutes	1600	0.700	34	480.0	17	

It follows from the data in Table 2 that high bond strengths and high tackiness are found in adhesives based on a 1:1 mixture of the technical polymers after joint mastication for 90 minutes. This adhesive has nearly four times the endurance of the standard adhesive based on natural rubber, as measured by Reznikovskii's method, and nearly double as measured by Kolomytseva's method, and also conforms to the tackiness specifications. These experiments therefore confirm that a firm bond between different rubbers can be produced by means of an adhesive layer consisting of an interpolymer of these rubbers. It may also be assumed that these views, experimentally confirmed for natural and butadiene-styrene rubber, are generally applicable. An adhesive layer of an interpolymer of the appropriate composition between any pair of different polymers should have satisfactory adhesive properties.

SUMMARY

1. Joint mastication of natural and butadiene-styrene rubbers at $\sim 25^\circ$ in an inert medium yielded interpolymers of these rubbers, containing chemically bonded regions of the molecules of the different rubbers.
2. Fractional precipitation from solutions, and selective vulcanization of mixtures of jointly and separately masticated rubbers showed that the amount of natural rubber bound to the butadiene-styrene rubber does not exceed 30% of the amount present (for 1:1 initial component ratio).
3. The products of joint mastication (interpolymers) have higher intrinsic viscosities than mixtures of the separately milled rubbers of the same composition.
4. Vulcanizates of jointly milled and separately milled rubber mixtures do not differ in dynamic modulus, but differ somewhat in the course of the curves showing variations of the tensile strength, relative elongation, and work of deformation with the composition.
5. The fatigue endurance of mixtures containing 50-80% of natural rubber is higher than that of the original polymers.
6. Vulcanizates containing the interpolymer have a higher concentration of cross links than vulcanizates of simple mixtures.
7. Mixtures containing the interpolymers have been used to produce adhesives which give stable joints between different vulcanizates based on natural and butadiene-styrene rubbers respectively.

The M. V. Lomonosov Institute of Fine Chemical Technology, Moscow
Scientific Research Institute for the Tire Industry

Received July 12, 1957

LITERATURE CITED

- [1] D. J. Angier and W. F. Watson, *J. Polymer Sci.* 18, No. 87, 129, 1955.
- [2] N. F. Komskaia and G. L. Slonimskii, *J. Phys. Chem.* 30, 1529 (1956).
- [3] B. A. Dogadkin, A. V. Dobromyslova, L. V. Sapozhkovaa and I. A. Tutorskii, *Colloid J.*, 19, 421 (1957).*
- [4] A. Arnold, I. Madorsky and L. A. Wood, *Anal. Chem.* 23, 1656 (1951).
- [5] B. M. Sturgis, A. A. Baum and J. H. Trepagnier, *Ind. Eng. Chem.* 39, 64 (1947).
- [6] D. Josephowitz and H. Mark, *India Rubb.*, World 106, 30, 1942; S. S. Voyutskii and Yu. L. Margolina, *Progr. Chem.* 13, 449 (1949).
- [7] B. A. Dogadkin, *Proceedings of Conference on Bond Strength Between the Components of Rubber-Fabric Laminates in Production and Use* (in Russian) (State Sci.-Tech. Press, Chem. Lit., Leningrad, 1956) p. 26.

* Original Russian pagination. See C. B. Translation.

ELECTRON MICROSCOPIC AND ADSORPTION STUDIES OF SILICA SOLS AND SILICA GELS

A. V. Kiselev, V. I. Lygin, I. E. Neimark, I. B. Sliniakova and Chen' Ven'-han

According to the theory of the globular structure of many gels (silica, alumina-silica, and titania gels), the gel framework consists of spherical primary particles, while the spaces between these particles constitute the pores [1-5]. The size of the pores in xerogels with various pore structures is determined by the size and packing density of the particles; the packing is closer in finely porous and less close in coarsely porous xerogels. This concept of the structure of the gel framework is in harmony with the experimentally observed influence of preliminary treatment of a hydrogel on the final pore structure of the xerogel. Decrease of the surface tension of the intermicellar liquid decreases the capillary forces which compress the gel framework during drying, and leads to a looser packing of the particles [6-8]. Treatment of the hydrogel with liquids which charge the particles and strengthen the framework counteracts the capillary forces [9-11]. Xerogels with different pore structures can be obtained by variation of these factors over wide limits. Luk'ianovich and Leont'ev [12] obtained direct confirmation of the globular structure of coarsely porous xerogels by applying the replica method to studies of xerogels. The globular nature of the structure of an alumina-silica catalyst was revealed in an investigation by the pseudoreplica method [13]. Studies of xerogel structure by the pseudoreplica method also led to the opposite conclusion, that the structure consists of a solid permeated by a network of cylindrical pores [14]. In this connection it is of definite interest to use electron microscopy for studying the formation of the framework of xerogels at different stages of aging, starting with silicic acid sols. However, such investigations are complicated by experimental difficulties, primarily caused by the rapid aggregation of the sol particles. To observe the particles in the course of the formation of xerogel structures it is necessary either to prepare special uncondensed specimens [15] suitable for direct transmission electron microscopy, or to disperse dense samples by ultrasound, or to study their structure by the carbon replica technique.

In the present investigation these methods were used for electron microscope investigations of the original sols and sols obtained by peptization of hydrogels washed with liquids of different pH, dried on the supports. The structure of the xerogels obtained from these hydrogels was studied by the adsorption method as well as by electron microscopy.*

Preparation of stable sols. Silicic acid sol was prepared by the reaction between solutions of sodium silicate and sulfuric acid of sp. gr. 1.17. After the solutions had been mixed, sol samples were taken at definite intervals. After 20-fold dilution with distilled water these samples were stabilized by addition of 25% ammonia solution. After 7 days air was bubbled through the sols to remove ammonia, and the sols were then sealed in tubes.

Preparation of stable sols from hydrogels. Gelation of the main bulk of the original sol took place 9 hours after the solutions had been mixed. After gelation of the sol, the gel was aged for two days, broken into pieces, and washed with liquids of different pH. Separate portions of the hydrogel, washed under different conditions, were covered with concentrated ammonia solution. The peptization was continued for 6-7 days at room temperature. Nearly all the pieces of gel were peptized to sols. The excess of ammonia was removed by the bubbling of air. The sols were diluted with water and sealed in tubes. This method was used to prepare sols from hydrogels washed with liquids of pH 1.9; 3.0; 6.5; 8.2 and 10.2.

* The sols, hydrogels, and xerogels were prepared in the Institute of Physical Chemistry, Academy of Sciences Ukrainian SSR, by I. E. Neimark and I. B. Sliniakova, and the electron microscope and adsorption studies were carried out by A. V. Kiselev, V. I. Lygin, and Chen' Ven'-khan in the Adsorption Laboratory of Moscow University.

Preparation of xerogels. To prepare xerogels from hydrogels washed with solutions of different pH, portions were dried in a drying oven at 125°. Xerogels obtained by this method from hydrogels with pH 1.9; 3.0; 6.5; 8.2 and 10.2 were studied by the electron microscope and adsorption methods.

Electron microscope investigation of sols and hydrogels. Sols are usually examined by transmission after being dried on a support [16-20]. In the course of electron microscope investigation the specimens are acted upon by the electron beam and undergo dehydration and sometimes sintering [16]. Particular difficulties arise in investigations at the subsequent stages of sol aging, gel formation, and syneresis, as further condensation of the structure makes transmission impossible. Nevertheless, studies of the transformation of the primary sol particles

in these processes are of direct interest for the elucidation of the structure and formation of the pore structure of xerogels. A very suitable procedure for studying the primary particles in aggregates is ultrasonic dispersion of the aggregates before investigation by transmission, or they may also be studied by the indirect method of carbon replicas, free from most of the above-mentioned defects of the transmission method [21].

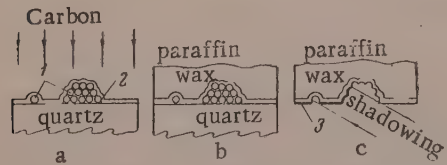
Fig. 1. Consecutive stages in the preparation of a carbon replica:

a) drying of specimen (1) on quartz surface and application of carbon film; b) fixing of carbon film (2) by means of paraffin wax; c) shadowing of carbon film with chromium (3) after solution of the quartz and specimen.

cause of the small size of the aggregated particles of a peptized hydrogel, the usual methods of replica preparation cannot be used. We developed a special technique for preparation of carbon replicas (imprints) of aggregates of the particles in the dried hydrogel [21]. The consecutive stages in the preparation of carbon replicas from aggregates of this type are illustrated in Fig. 1. The hydrosol obtained by peptization of a hydrogel is applied to a fractured surface of fused quartz and dried (Fig. 1,a); a carbon film about 100 Å thick is then applied to the quartz by thermal dispersion of carbon under the bell of the vacuum apparatus for specimen preparation (Fig. 1,a). To prevent any deformation of the carbon film during separation, it is fixed by paraffin wax, by immersion of the quartz surface covered by the carbon film into a drop of molten wax (Fig. 1,b). After the paraffin wax has solidified the quartz and the specimens are dissolved in hydrofluoric acid. The carbon replica is then shadowed with chromium (Fig. 1,c). The wax is dissolved in toluene and the carbon replica is studied on a wire screen under the electron microscope. The resolution of the carbon replicas made by this method is ~50 Å. The UEM-100 60 kv electron microscope was used for obtaining transmission micrographs of the specimens and micrographs of the replicas.

The micrograph of the original sol, dried on a collodion support (Fig. 2,a), shows a large number of partially aggregated small particles 50-100 Å in size. The particles observed on the support cannot be ascribed to the structure of the support itself, as no such structure is seen in a micrograph of such a support prepared and shadowed under the same conditions. Dried particles of sols obtained by peptization of hydrogels give a totally different picture. The micrograph of a sol dried on the support (Fig. 2,b), obtained by peptization of a hydrogel washed with acidified water shows lumpy particles 200-1500 Å in size, with a weakly defined structure. However, the observed structure of the particles, the heterogeneity of their form, and the large dimensions, considerably larger than those given by electron microscope studies of xerogels [13] or calculated from adsorption data [3, 4], suggest that they are composed of smaller particles. In fact, the micrograph of a carbon replica obtained from these lumpy particles of a peptized hydrogel (Fig. 2,c) dried on a quartz surface shows that the lumpy particles observed by transmission consist of smaller spherical particles about 100 Å in size.

A similar result is obtained after preliminary ultrasonic dispersion of the aggregates of such sols. The micrograph (Fig. 2,d) of a sol so treated and dried on the collodion support shows spherical particles similar in size to the particles seen in the micrograph of a carbon replica of the lumpy particles of this sol (Fig. 2,c).



The sols and hydrogels were investigated by the usual transmission method after being applied to and dried on a collodion support. The collodion supports were prepared by application of 1% solution of collodion in amyl acetate to the surface of distilled water [22]. The chromium shadowing of the sol dried on the support was carried out under the bell of the preparation apparatus at an angle of 30° under a vacuum of 10^{-4} mm Hg. Be-

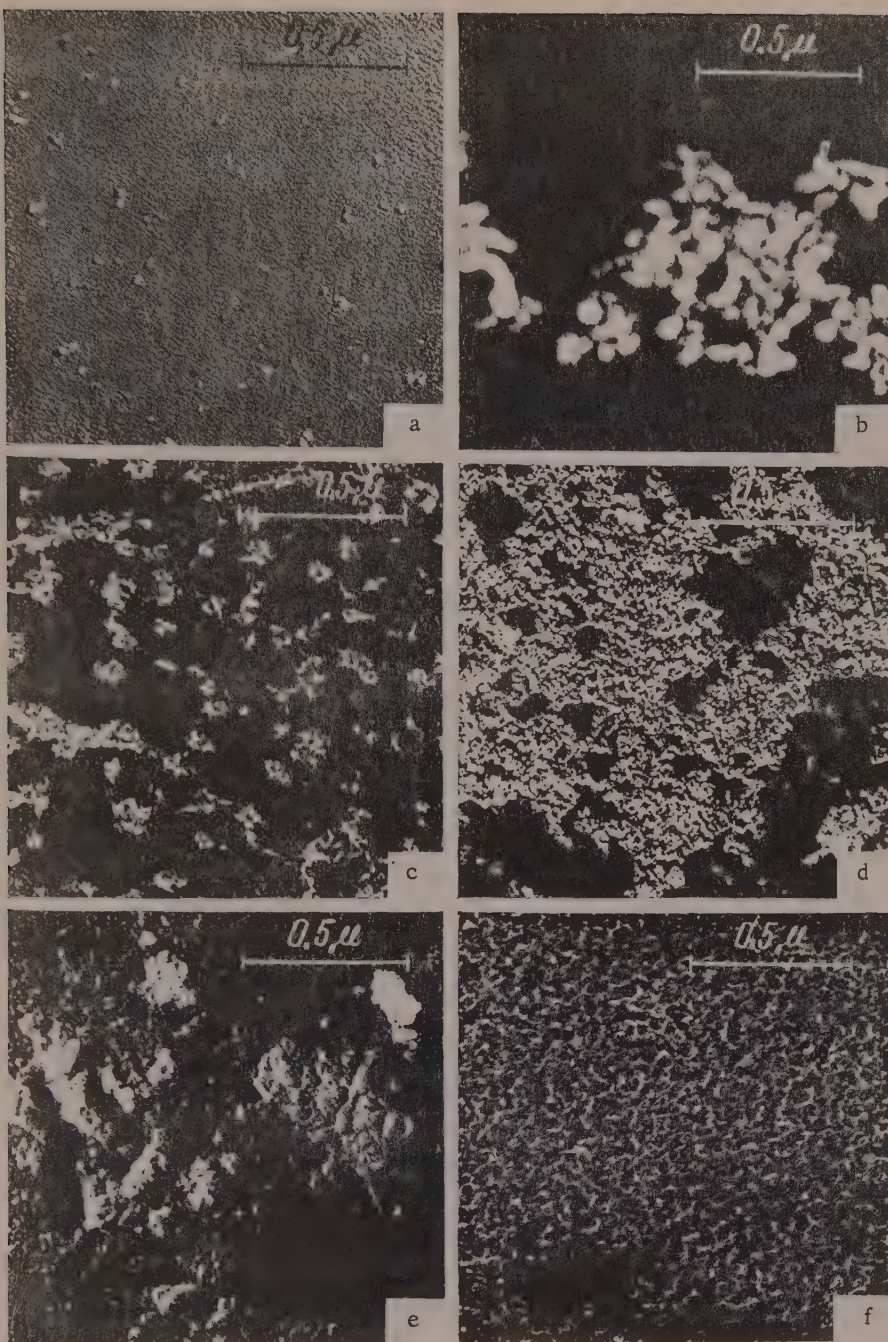


Fig. 2. Electron micrographs ($\times 45,000$):
 a) original sol dried on a collodion support (negative); b) sol obtained by peptization of a hydrogel washed with acidified water, and dried on a collodion support (negative); c) carbon replica of a sol obtained by peptization of a hydrogel washed with acidified water; d) ultrasonically treated sol obtained by peptization of a hydrogel washed with acidified water (negative); e) sol obtained by peptization of a hydrogel washed with a liquid of pH 1.9, and dried on a collodion support (negative); f) carbon replica of a sol obtained by peptization of a hydrogel of pH 1.9.

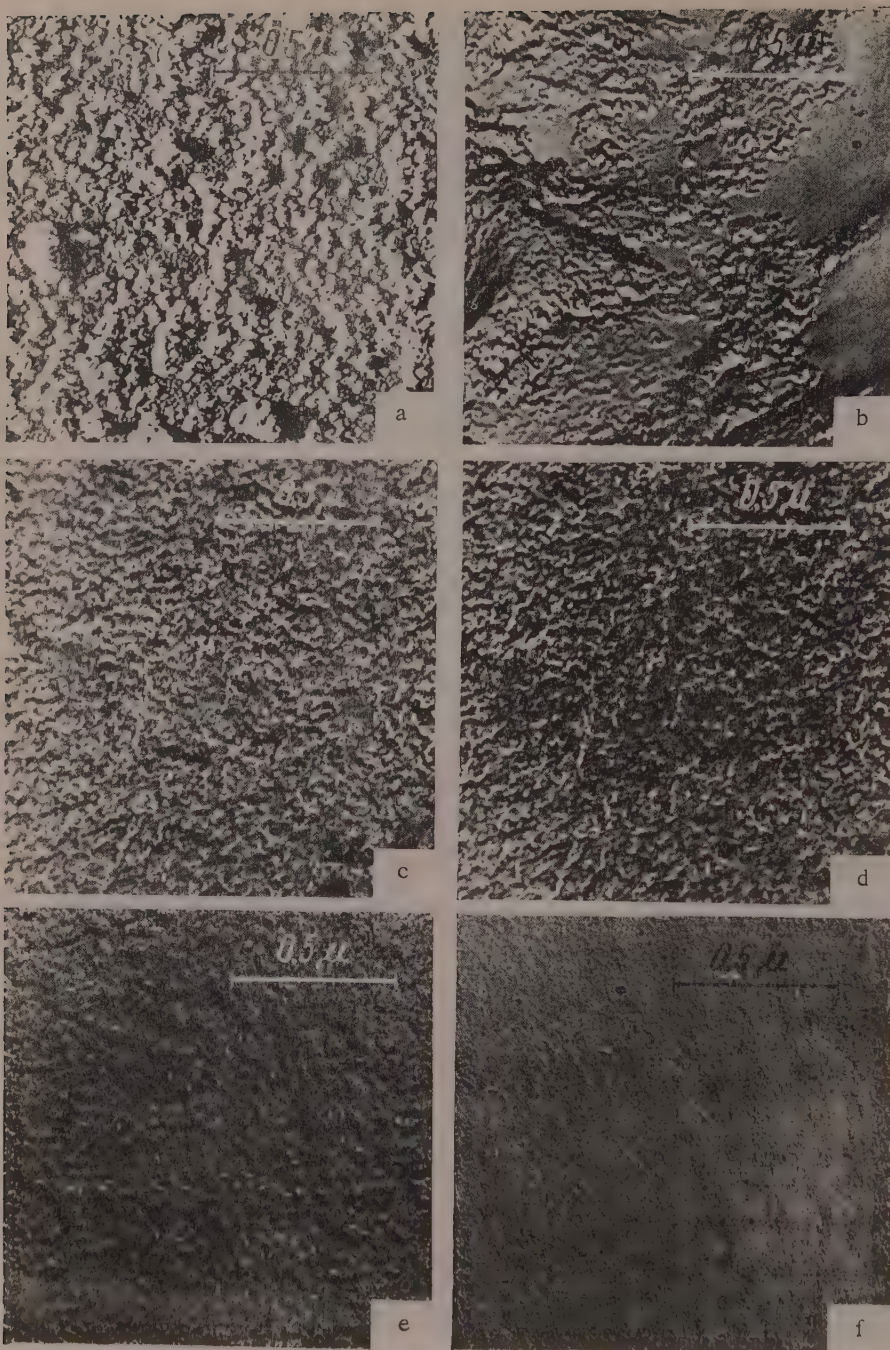


Fig. 3. Electron micrographs ($\times 45,000$):

a) Sol obtained by peptization of a hydrogel of pH 8.2 and dried on a collodion support (negative); b) carbon replica of a sol obtained by peptization of a hydrogel of pH 8.2; c, d) stereomicrograph of a carbon replica of a silica gel obtained from a hydrogel of pH 10.2; e) carbon replica of a silica gel obtained from a hydrogel of pH 8.2; f) the same, pH 3.0.

Thus, comparison of micrographs of the original sol (Fig. 2,a) and of sols obtained by peptization of hydrogels (Fig. 2,b,c,d) shows that the transition of a sol to a hydrogel is characterized by aggregation of the primary particles in the sol without any significant change in their size. This type of transition from a sol to a

hydrogel is characteristic of all the hydrogels studied irrespective of the pH of the wash liquid. Figure 2,e is a transmission micrograph of dried particles of a sol obtained from a hydrogel of pH 1.9. In addition to fine particles smaller than 100 Å, the micrograph shows larger aggregates of particles, 500-1500 Å in size. The micrograph (Fig. 2,f) of a carbon replica of such aggregates shows that they all consist of smaller particles, less than 100 Å. A transmission micrograph of a sol prepared by peptization of a hydrogel of pH 8.2 (Fig. 3,a) shows, in addition to a large number of fine particles about 100 Å in size, larger particles of 500-2000 Å. The micrograph of a carbon replica from particles of such a sol indicates that all these larger particles consist of small primary particles.

Electron microscope investigation of xerogels. Because of the high density of the framework of xerogels, to which reference has already been made, detailed analysis of their pore structure is not possible by the transmission method [23]. The replica method gives much more information about their pore structure [12]. We therefore used the carbon replica technique for studying the pore structure of xerogels. Because of the great irregularity of the outline of fracture surfaces of the xerogels, preparation of replicas of porous substances involves a number of experimental difficulties; to avoid these difficulties, we used a method developed earlier for the preparation of replicas of porous substances [24]. A carbon film is applied on the fractured xerogel surface by thermal dispersion of carbon under the bell of the vacuum apparatus for specimen preparation under a vacuum of 10^{-3} - 10^{-4} mm Hg, and fixed by means of a layer of molten paraffin wax after cooling of the specimen. Preliminary cooling of the specimen with the carbon film prevents penetration of the wax into the pores. The specimen is then dissolved in hydrofluoric acid. After two washings in pure hydrofluoric acid and distilled water the carbon replica is shadowed with chromium at an angle of 45° under a vacuum of 10^{-4} mm Hg. The carbon replicas are investigated on a wire screen under the electron microscope after solution of the wax in toluene. Stereophotography of the carbon replicas gives a three-dimensional indication of the form of the pores and of the packing of the primary particles of the xerogel framework.

Figure 3,c,d, is a stereomicrograph of a carbon replica of a xerogel obtained from a hydrogel washed with a liquid of pH 10.2. Examination of the micrographs in a stereoscope reveals the spatial distribution of loosely packed spherical particles, ~80 Å in size, in the xerogel framework. Figure 3,e is a micrograph of a carbon replica of a silica gel obtained from a hydrogel of pH 8.2. This replica reveals a similar pore structure, but with closer packing of the primary particles. Even closer packing of the primary particles is seen in replicas of xerogels prepared from hydrogels washed with liquids of low pH (Fig. 3,f). The framework particles observed on the xerogel replicas do not differ significantly in size from the primary particles of the original sol and hydrogel. It also follows from the micrographs of replicas of xerogels prepared from hydrogels of different pH (Fig. 3,c,d,e,f) that decrease of the pH of the original hydrogel results in some decrease in the size of the spherical particles of the xerogel framework.

These results confirm the earlier conclusions [12] based on electron microscope studies of xerogel structure by the replica method, according to which the xerogel structure is globular. Thus, electron microscope studies of silica gels provide direct proof of the theory of corpuscular structure of xerogel adsorbents, put forward earlier on the basis of comparisons of the adsorption properties of porous and nonporous adsorbents of similar nature [3,4].

Adsorption studies of xerogels. The adsorption isotherms of methanol vapor and the curves for pore volume distribution by effective diameters in Fig. 4 indicate that, as was shown earlier [11], decrease of the pH of the wash liquid results in formation of xerogels with smaller pores. The structural characteristics of the xerogels studied are given in the Table.

The Table shows that the limiting pore volume varies from 0.90 cc/g (pH 10.2) to 0.33 cc/g (pH 1.9). The effective diameter of the pore necks at the maximum of the volume distribution curve, calculated from Thomson's formula, decreases from 85 to 30 Å with variation of the pH of the wash liquid from 10.2 to 6.5. The specific surface of the xerogels, calculated by the BET method, varies from 400 m²/g (pH 10.2) to 650 m²/g (pH 6.5). This change of the specific surface indicates that during the preliminary treatment of the hydrogel with liquids of different pH there is not only preparation for different types of aggregation of the particles during subsequent drying, but also some change in the size of the primary particles. From the specific surface and the density of the silica framework $\delta = 2.2 \text{ g/cc}$, neglecting the elimination of a part of the particle surface at points of contact, we can estimate the particle diameter by means of the formula $D = 6/\delta s = 27,300/s \text{ Å}$, if s is in m²/g. From results obtained by this method (see Table) it follows that the average diameter of the primary particles of the xerogel framework increases from 40 Å at pH 6.5 to 70 Å at pH 10.2.

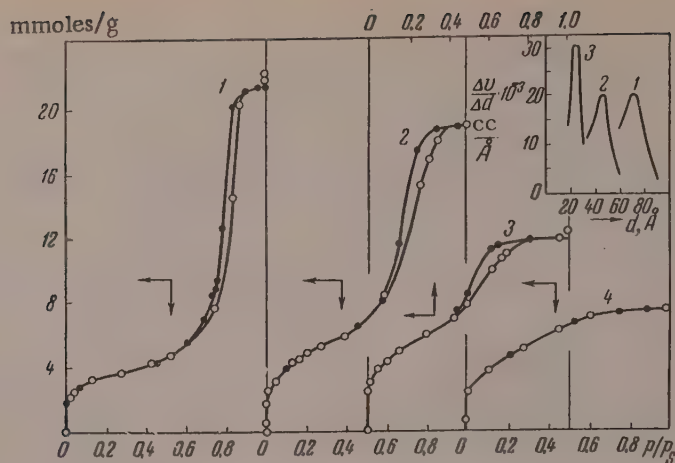


Fig. 4. Isotherms for adsorption (white circles) and desorption (black circles) of methanol vapor, and curves of pore volume distribution by effective pore diameters, for silica gels obtained from hydrogels of different pH:
 1) pH 10.2; 2) pH 8.2; 3) pH 6.5; 4) pH 1.9.

Comparison of the Structural Characteristics of Silica Gels From Electron Microscope and Adsorption Data

Silica gel specimens	Specific surface s in m^2/g		Particle diameter D in Å		Porelain d with corr. for film thickness, in Å	d/D_a	Pore volume v_s in cc/g	Number of contacts	Type of packing of framework particles — electron microscope data
	electron microscope data	adsorption data	electron microscope data D_e	adsorption data D_a					
Xerogel obtained from hydrogel of pH 10.2	~350	400	~80	70	85	1.23	0.90	4	Loose
The same, pH 8.2	~450	540	~60	50	54	1.08	0.76	5	Less loose
The same, pH 6.5	—	650	—	40	30	0.75	0.48	5.5	More dense
The same, pH 1.9	—	500	—	—	26	—	0.33	7	Dense

The decrease of the specific surface of the xerogel obtained from a hydrogel washed with the most acid liquid of pH 1.9 indicates that a part of the surface at the points of contact of the most closely packed particles is inaccessible to methanol molecules, and possibly that there is some coalescence of these particles.

DISCUSSION OF RESULTS

The micrographs of the original sols dried on collodion supports show that primary spherical particles 50–100 Å in size are formed during the early stages of existence of colloidal silicic acid before formation of the hydrogel. It is quite possible, in the light of our results, that the larger particles observed by a number of authors [17, 19, 20] in sols dried on supports, considerably larger than 100 Å, are aggregates of finer particles.

The micrographs of dried particles of sols obtained by peptization of hydrogels, and of their carbon replicas indicate that the conversion to a hydrogel is accompanied by aggregation of the primary particles without significant changes of their size. Comparison of the sizes of the primary particles of dried sols obtained by peptization

of hydrogels, and of the particles in xerogels, shows that in the transition from a hydrogel to a xerogel the particles retain their individuality and do not change significantly in size.

The variations in the structure of the xerogel framework after different preliminary treatments of the hydrogel can be revealed most fully by comparison of the results obtained by two independent methods: electron microscopy and adsorption. The specific surface of xerogels, determined by the adsorption method, can be compared with the specific surface determined by electron microscopy and calculated by means of the formula $s = 6/\delta D_e$ (where δ is the density and D_e is the diameter of the xerogel particles measured on the micrographs of the carbon replicas). In turn, the nature of the pore structure of the xerogel observed in the micrographs can be correlated with the coordination number of particle packing in the xerogel framework, determined by comparison of the ratio of the volume of the cavities v_s filled when capillary condensation is complete to the total volume of the xerogel $v_s + 1/\delta$, with the corresponding ratio for regularly packed spheres [3, 25]. It follows from the Table that the results obtained for coarsely porous xerogels by the electron microscope method are in agreement with adsorption data.*

Increase of the pH of the wash liquid gives more coarsely porous silica gels. The transition from finely porous to coarsely porous silica gels, in addition to some increase of the average particle diameter, corresponds to a decrease of the coordination number of particle packing. The decrease of the coordination number of packing of these particles in the framework in the transition to coarsely porous silica gels corresponds to the transition from a closely packed to a loosely packed xerogel structure, observed in the xerogel replicas.

SUMMARY

1. An electron microscope study has been carried out on original silicic acid sols dried on supports, sols obtained by peptization of hydrogels washed with liquids of different pH, and xerogels obtained from these hydrogels by the usual method.

2. Combination of different techniques of electron microscopy (transmission micrographs, micrographs of carbon replicas, and ultrasonic dispersion of the specimens) extends considerably the possibilities of studying sols and hydrogels, making it possible to observe the internal structure of large aggregates formed during aging and drying.

3. Sol particles 50-100 Å in size are formed during the early stages of existence of the colloid, before formation of the hydrogel. Subsequent gel formation and drying do not produce any significant changes of particle size. According to conditions, these processes are accompanied by aggregation of the particles to different extents, and this largely determines the porosity of the xerogels.

4. The results obtained by electron microscopy and by the adsorption method are in qualitative agreement: coarsely porous silica gels as indicated by electron microscope data correspond to a looser structure, and finely porous gels to a denser structure. In the case of the silica gels with the loosest packing it was possible to estimate the particle size by electron microscopy. The specific surface found from this is close to the value given by the adsorption method.

The M. V. Lomonosov State University, Moscow
The Adsorption Laboratory
Institute of Physical Chemistry
Academy of Sciences Ukrainian SSR

Received April 15, 1957

LITERATURE CITED

- [1] A. V. Kiselev, Colloid J. 2, 17 (1936).
- [2] E. Manegold, Koll.-Z. 96, 186 (1941).
- [3] A. V. Kiselev, Proc. Acad. Sci. USSR 98, 427 (1954).

* The agreement between the results obtained by these methods was noted earlier for coarsely porous silica gels [12] and alumina-silica catalysts [13].

[4] A. V. Kiselev, in the book: Surface Chemical Compounds and Their Role in Adsorption Phenomena (Izd. MGU, 1957) p. 90.*

[5] A. V. Kiselev, in the book: Methods of Investigating the Structure of Highly Disperse and Porous Bodies, No. 2 (Izd. AN SSSR, 1958).*

[6] V. S. Veselovskii and I. A. Seliaev, J. Phys. Chem. 6, 1171 (1935).

[7] I. E. Neimark and F. P. Khatset, Colloid J. 9, 289 (1947).

[8] I. E. Neimark and R. Iu. Shenfain, Colloid J. 15, 145 (1953). **

[9] G. K. Boreskov, M. S. Borisova, V. A. Dzis'ko, O. M. Dzhigit, V. P. Dreving, A. V. Kiselev and O. A. Likhacheva, J. Phys. Chem. 22, 603 (1948).

[10] I. E. Neimark and R. Iu. Shenfain, Colloid J. 15, 45 (1953).**

[11] I. E. Neimark and I. B. Sliniakova, Colloid J. 18, 219 (1956).**

[12] V. M. Luk'ianovich and E. A. Leont'ev, Proc. Acad. Sci. USSR 103, 1039 (1955).

[13] A. V. Kiselev, E. A. Leont'ev, V. M. Luk'ianovich and N. S. Nikitin, J. Phys. Chem. 30, 2149 (1956).

[14] I. Sugar and F. Guba, Acta Chim. Acad. Sci. Hung. 7, 233 (1955).

[15] N. M. Kamakin and Ia. V. Mirskii, in the book: Proceedings of the Second Scientific and Technical Conference on Well Drilling, Winning, and Processing of Oil and Gas (Chechen-Inguz Press, 1957).*

[16] O. E. Radczewski and H. Richter, Koll.-Z. 96, 1 (1941).

[17] Z. Ia. Berestneva and V. A. Kargin, and T. A. Koretskaia, Colloid J. 11, 369 (1949).

[18] G. B. Alexander and R. K. Iler, J. Phys. Chem. 57, 932 (1953).

[19] Z. Ia. Berestneva and V. A. Kargin, Progr. Chem. 24, 249 (1955).

[20] Z. Ia. Berestneva, in the book: Surface Chemical Compounds and Their Role in Adsorption Phenomena (Izd. MGU, 1957) p. 346.*

[21] V. I. Lygin and Chen Ven'-khan, J. Phys. Chem. 32, 465 (1958).

[22] Electron Microscopy, edited by A. A. Lebedev (GTTI, 1954) p. 499.*

[23] V. M. Luk'ianovich and L. V. Radushkevich, J. Phys. Chem. 24, 21 (1950).

[24] V. I. Lygin, Factory Labs. No. 3 (1958).

[25] A. P. Karnaukhov and A. V. Kiselev, J. Phys. Chem. 31, 2635 (1957).

* In Russian.

** Original Russian pagination. See C. B. Translation.

INVESTIGATION OF THE NATURE OF THE ADHESION BOND IN THE BONDING OF TWO HIGH-MOLECULAR COMPOUNDS

L. P. Morozova and N. A. Krotova

In our earlier papers [1] the view was put forward that in a number of cases the adhesion bond is formed by electrostatic interaction of the layers of the electric double layer formed at the interface during the formation of an elastic film of polymer from a solution applied to the substrate surface.

Various authors [2] have repeatedly put forward views on the role of diffusion processes in the formation of adhesion and autohesion bonds.*

The purpose of the present investigation was to carry out an experimental study of the formation of an adhesion bond between two high polymers and to determine the relative roles of electrical and diffusion processes in adhesion.

The electron-emission effects observed by one of the present authors (jointly with Karasev and Deriagin [4]) when adhesion bonds are destroyed in such systems as polymer-glass, polymer-metal, and polymer-polymer, and the electron emission from a freshly detached polymer surface, make it possible to analyze, in each individual case, the nature of the processes which occur when the adhesion bond between two polymer specimens is broken. Some information on the nature of the bonds is also obtainable from microscopical investigations of cross sections of joints, and from adhesiograms.

We showed previously [5] that the plot of the logarithm of the work of separation A against the logarithm of the separation rate v forms an adhesiogram with three linear regions (Fig. 1,a); these were explained as follows: in Region III, parallel to the abscissa axis, when separation is rapid, the observed effects conform to Paschen's law of gas discharge. Luminescence is observed in this region during separation if the experiment is performed under moderate vacuum, and electron emission under high vacuum. In Region II, where the relationship $A = f(v)$ is most pronounced, the charges of the electric double layer become neutralized during separation of the joint, by surface leakage. The slower the process of separation (in which the capacitor layers are drawn apart), the more important the process of charge leakage along the boundary of the detaching film becomes. In some cases (as in the system nitrocellulose-glass), if the separation is very slow, the charges can leak away completely, and then A becomes independent of v in Region I of the adhesiogram, parallel to the abscissa axis, and the order of magnitude of A corresponds to equilibrium adhesion, described by the Dupre-Young equation and caused by intermolecular forces.

In other cases the value of A in Region I may be greater by several orders of magnitude, but Region I itself remains parallel to the abscissa axis. Evidently charge leakage in this region is a considerably slower process than separation of the capacitor plates. Because of all this, region I for polymers of this kind, in which adhesion is determined to a considerable extent by forces of electrostatic attraction, was given the name of the pseudo-equilibrium region by Deriagin [5].

* It is stressed in G. L. Slonimskii's paper, presented at the Conference on the Strength of Bonds Between Components of Rubber-Fabric Articles (Goskhimizdat, 1956, p. 11), that the electrical theory of adhesion allegedly does not take into account the possible formation of a transition layer, conferring a cohesive character to the splitting of the adhesive. In reality, in the paper by B. V. Deriagin, S. K. Zherebkov, and A. M. Medvedeva [3] presented at the Conference on Adhesion held in the Institute of Physical Chemistry, Academy of Sciences USSR in May 1955 it was not only stated that such cases are possible, but it was rigorously proved that such cases arise if the polymers are compatible, and the adhesion may be the result of diffusion on the chains of the contacting objects rather than of the formation of an electric double layer. If the separation is purely adhesive, the electrical theory of adhesion is fully applicable.

TABLE 1

Effect of Specimen Width on the Displacement of the Middle Region of the Adhesiogram

Specimen width, mm	Separation rates in cm/sec., corresponding to the middle region of the adhesiogram
1	$1.26 \cdot 10^{-4}$ - $2.9 \cdot 10^{-2}$
3	$1.58 \cdot 10^{-3}$ - $0.25 \cdot 10^{-2}$
5	$5.63 \cdot 10^{-3}$ - $1.58 \cdot 10^{-2}$
10	$5.63 \cdot 10^{-3}$ - $1.58 \cdot 10^{-2}$

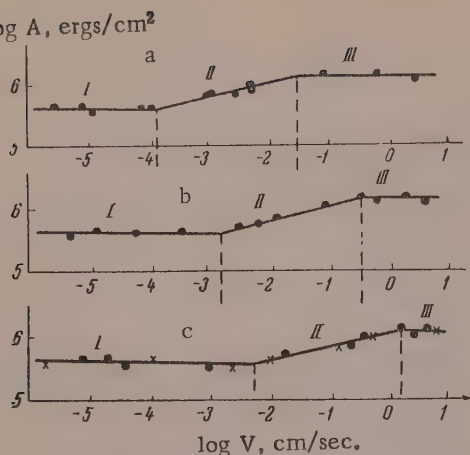


Fig. 1. Effect of specimen width on the form of the adhesiogram for chlorinated polyvinyl chloride - rubber (SKB):
a) 1 mm; b) 3 mm; c) 5 and 10 mm.

Region III is absent. It is possible that such a region does exist, but is situated in the range of high rates, where experimental determination is difficult.*

Since the surface electrification density σ can be determined only in the applicability range of Paschen's law, it is extremely important to determine the factors which influence the form of the adhesiogram and the position of the inflection points on it. Our experiments show that one such factor is the width of the specimen. Its effect is such that when the width of the specimen is altered from 1 to 5 mm the middle Region II of the adhesiogram is displaced to the right; all the other characteristics of the adhesiogram (levels of Regions I and III, the slope of the middle region) remain unchanged (Fig. 1,a, b, and c). The displacement of the middle region is shown by the data in Table 1 for the system chlorinated polyvinyl chloride - sodium butadiene rubber.

It is clear from the data in Table 1 that specimen width has an influence up to a definite limit (5 mm) only. This may be explained as follows. Dispersion of the lines of force of the electric field increases with decreasing specimen width, leading to decreased leakage of the charges under the influence of the field by the surface conduction mechanism. Because of this, in wide specimens Region II is shifted to the right, as at the same separation rates the leakage of charges from narrow specimens (1-3 mm) is considerably less, and the adhesion is therefore greater, than in wide specimens (5 mm and over). With further increase of specimen width the influence of the dispersion of the lines of force becomes small and edge effects therefore cease to influence the form of the adhesiogram.

In our experiments the electrical characteristics of adhesion (potentials, potential gradients, surface electrification density σ) were calculated from the gas discharge laws, which was possible only for adhesiograms with clearly defined Regions III. The values of σ were calculated from the values of the maximum work of separation (adhesion) A_0 corresponding to the maximum separation rates v with the aid of an auxiliary Paschen curve (Table 2). In all the cases given in Table 2, rapid separation in air and in moderate vacuum results in luminescence, and electron emission is observed in high vacuum. Electrical effects are also observed during separation with high-strength adhesives (BF-type glue, polyurethanes, polyamides), but in view of the absence of Region III in the adhesiograms it is not possible to calculate σ , and only the lower limit of the values of σ can be estimated, although there is no doubt about the electrostatic nature of the adhesion bonds in such cases.

The maximum velocities of the electrons emitted during the separation may give an idea of the potential difference of the double layer after its separation, as these electrons are dispersed by the fields which exist in the gap between the separated surfaces. After σ has been determined from the experimental data and Paschen's

* Time intervals less than 0.01 second could not be measured in our experiments.

TABLE 2

Characteristics of the Adhesion of Polymers to Various Surfaces*

Polymer	Substrate	$A \cdot 10^{-4}$ (erg/cm ² , pseudoequilibrium) at $v = 10^{-5}$ cm/sec.	$A_0 \cdot 10^{-5}$ (erg/cm ² , limiting) at $v = 1$ cm/sec.	Discharge potential in volts. $\cdot 10^{-3}$	Discharge interval μ	$\sigma \cdot 10^4$ in e.u./cm ²
Gutta-percha	Glass	1.3	1.78	6.3	1.00	1.67
Gutta-percha	Gelatin	2.9	3.55	9.0	0.96	2.52
Gutta-percha	Steel	0.56	4.00	9.3	0.94	2.64
Nitrocellulose	SKB rubber with kaolin filler	10.1	3.16	8.6	0.95	2.42
Chlorinated polyvinyl chloride	The same	10.1	5.63	11	0.93	3.10

* Separation of these specimens is accompanied by electron emission. The adhesiograms have three distinct regions. The values of σ were calculated from Region III, Fig. 1, of the adhesiograms, in the applicability range of Paschen's law.

TABLE 3

Work of Separation A_0 of Polymer Films from Various Surfaces and Velocities of Electrons Emitted During the Separation at $p = 10^{-4}$ mm Hg *

Polymer	Substrate	Electron velocities in ev $\cdot 10^{-3}$	$A_0 \cdot 10^{-4}$ in ergs/cm ²	
			experimental	calculated from electron velocity
Chlorinated polyvinyl chloride	Brass	2.45	2.45	1.04
	Glass	6.25	3.16	2.52
	Gelatin	11	31.6	28.2
	SKB rubber (kaolin filler)	25	159	56.3
Polyisobutylene	Gelatin	11	35.6	31.7

* Experiments carried out under vacuum; curves plotted for the high-rate region.

curve, the potential difference and the value of σ can be used to calculate the work of adhesion A , and the result may be compared with the value of A determined experimentally by a mechanical method (Table 3).

It is seen in Table 3 that the theoretically calculated values are in good agreement with the experimental data (apart from the system chlorinated polyvinyl chloride - SKB rubber), thus confirming the electrical theory of adhesion.

We showed earlier [6] that a polymer film after separation contains separate centers of emission. It is suggested that the adhesive film is not bound continuously to the substrate, but only to separate regions, and these emit electrons after the adhesion bond has been broken. It is to be expected that when regions of the closest and most continuous contact are separated, the emission intensity would be higher in such regions. It is well known that mechanical treatment of the substrate surface results in an increase of adhesive strength; this is generally attributed to an increase of contact area.* It was therefore of interest to find whether the emission intensity of a detached polymer film is highest at regions where the film had been in contact with a mechanically treated

* However, this effect may have other causes, such as changes in the surface properties of mechanically treated surfaces, or thinning of the oxide film.

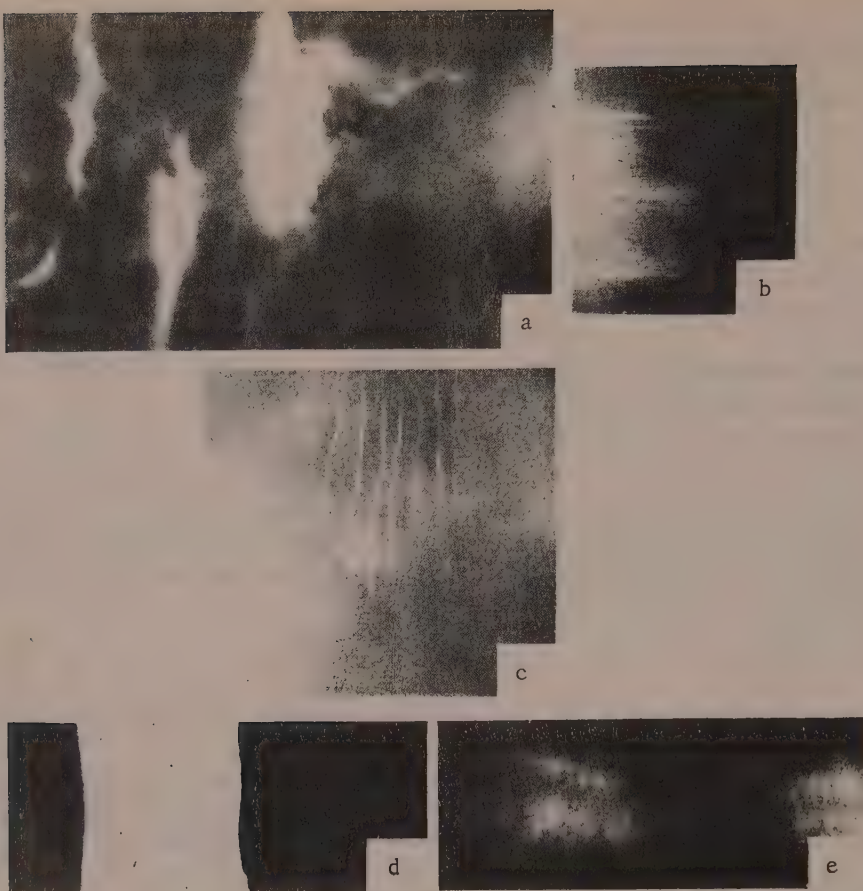


Fig. 2. Images produced by polymer films by the action of electrons, emitted during separation of the films from the substrates, on x-ray film:
 a) emission from regions of chlorinated polyvinyl chloride film attached to deep grooves on brass surface; b) same, with the letter E marked on the brass; c) lines marked on the brass; d) emission from surface of a gutta-percha film stripped from rubber filled with kaolin (no emission from regions in contact with rubber filled with carbon black); e) same, stripped from rubber filled with carbon black and treated with H_2SO_4 .

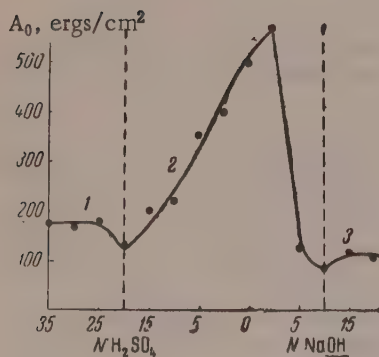


Fig. 3. Effect of the reaction of the glass surface on its adhesion to chlorinated polyvinyl chloride: 1) and 3) film positively charged after separation; 2) film negatively charged.

surface. For this, grooves were made in a metal (brass) surface by means of a file, and the surface was coated with a polymer solution. The experiments were performed in a vacuum roller adhesiometer of modified design, in which an x-ray film was placed very close to the separating polymer film and moved synchronously with it. The photographs show clearly that the electron emission was most intense at the regions of the polymer film where it was separated from the grooves in the metal (Fig. 2,a and c).

These experiments and the data in Table 3 lead to the conclusion that the magnitude of the adhesion (if it is caused by electrostatic forces) is closely associated with the velocity of the emitted electrons on the one hand, and with the intensity of electron emission on the other. This is understandable in the light of the electrical theory of adhesion.

TABLE 4

Classification of Various Film-Substrate Systems by the Nature of the Adhesion Bond

Signs of residual charges in systems separated in air	Electron emission after separation under vacuum $P = 1 \cdot 10^{-4}$ mm Hg	Work of separation at $v = 1$ cm/sec. in ergs/cm $^2 \cdot 10^{-4}$	Type of separation
Systems of the first group			
Chlorinated polyvinyl chloride (-) Steel (+)	Emission by PVC	1.04	Adhesive
Chlorinated polyvinyl chloride (-) Glass (+)	Ditto	2.52	Ditto
Polyethylene (-) SKB rubber (+) (kaolin filler)	Polyethylene	4.45	Ditto
Polyethylene (-) SKN rubber (+) (kaolin filler)	Ditto	5.63	Ditto
Gutta-percha (-) Glass (+)	Gutta-percha	1.78	Ditto
Polyvinyl butyral (-) SKB rubber (+) (kaolin filler)	Polyvinyl butyral	20.2	Ditto
Chlorinated polyvinyl chloride (-) Gelatin (+)	Chlorinated polyvinyl chloride	28.2	Ditto
Polyamide (-) SKB rubber (+) (kaolin filler)	Polyamide	30.1	Ditto
Nitrocellulose (-) SKB rubber (+) (kaolin filler)	Nitrocellulose	91.6	Ditto
Gutta-percha (-) Steel (+)	Gutta-percha	39.8	Ditto
BF-6 (-) SKB rubber (+) (kaolin filler)	BF-6	39.8	Ditto
Chlorinated polyvinyl chloride (-) Ditto	Chlorinated polyvinyl chloride	56.3	Ditto
Polyurethane (-) Ditto	Polyurethane	63.2	Ditto
Gutta-percha (-) SKB rubber (with carbon black filler) treated with H_2SO_4 (+)	Gutta-percha	65.2	Ditto
Gutta-percha (-) SKN rubber (+) (kaolin filler)	Gutta-percha	105	Ditto
Polyamide (-) Ditto	Polyamide	112	Ditto
Polyethylene (-) SKB rubber* (+) (containing 40% carbon black)	No emission	4.45	Ditto
Polyvinyl butyral (-) Ditto	Ditto	17.5	Ditto
Polyamide (-) Ditto	Ditto	28.4	Ditto
Nitrocellulose (-) Ditto	Ditto	30.4	Ditto
Chlorinated polyvinyl chloride (-) Ditto	Ditto	54.1	Ditto
BF-6 (-) Ditto	Ditto	38.7	Ditto
Polyurethane (-) Ditto	Ditto	62.3	Ditto
Nitrocellulose SKN rubber (kaolin filler)	No emission	300	Cohesive, rubber splits
Chlorinated polyvinyl chloride (-) Ditto	Ditto	300	Ditto
Polyurethane Ditto	Ditto	300	Ditto

(continued)

* No electron emission is observed on separation of polymers from this rubber with carbon black filler, although the separated surfaces carry charges of opposite sign. Electron emission occurs with lower contents of carbon black.

TABLE 4 (continued)

BF-6	SKN rubber (kaolin filler)	No emission	300	Cohesive, rubber splits
Chlorinated poly- vinyl chloride (-)	SKB rubber (with carbon black filler) treated with H_2SO_4	Ditto	300	Ditto
Systems of the second group				
Polyethylene	Polyisobutylene		119	Mixed
Polyethylene	Paraffin wax	No emission	50.4	Mixed
Gutta-percha	Paraffin wax	No emission	50.4	Mixed

The influence of the chemical structure of the bonded substances on adhesion is a highly important question. By De Bruyne's empirical rule, known to specialists, a high degree of adhesion is obtained between polymers of similar polarity, i.e., polymers with polar functional groups, or between nonpolar polymers of similar structure.

Deriagin, Zhrebkov, and Medvedeva [3] showed that in most cases there is a correlation between the adhesive shear strength of polymers and the similarity of their polarities. They regard this as the most convincing evidence of the role of polymer chain diffusion in the formation of adhesion bonds between polymers of similar nature.

The purpose of the present work was to analyze the nature of the adhesion bonds between different types of polymers, by disruption of the bonds (and by microscopical investigation of cross sections of the contact surfaces), in relation to the chemical structure of the bonded substances.

It was found that the systems studied can be divided into two main groups. The first group is characterized by electrical effects on disruption of the adhesion bond: luminescence in moderate vacuum, electron emission in high vacuum, and the presence of residual charges on the separated surfaces. The sign of the charge was determined with the aid of a simple radiometric circuit; the following rule was found to apply in all cases: the surface which emits electrons after separation has a negative residual charge, while the opposite surface, which does not emit electrons, has a positive residual charge.

Microscopical investigations of sections (micrographs are not shown here owing to lack of space) show the existence of a sharp boundary between the two polymers in such cases. Sometimes, when the adhesion is particularly great, the separation occurs along the polymer film. Neither electron emission nor residual charges on the separated surfaces are found in such cases. The work of separation is very large, and in such cases the work of adhesion is evidently greater than the work of cohesion. Microscopical investigations also reveal a distinct boundary. Systems of this kind are formed from components with strongly polar groups (BF-6 glue and acrylonitrile rubber, chlorinated polyvinyl chloride and rubber the surface of which was treated with concentrated H_2SO_4 and then washed).

The following case is of interest. If one of the components is SKB rubber with carbon black filler, no electron emission is observed when a film of any polymer is detached from it, although the separated surfaces carry residual charges of opposite sign. Separation of polymers from the same rubber, but filled with kaolin, results in very intense electron emission. A special substrate specimen consisting of alternating bands of rubber containing carbon black and kaolin was prepared, and a polymer film was stripped from it. Figure 2,d shows that emission occurs only at those regions (of the gutta-percha) which had been in contact with the rubber containing kaolin, whereas the regions in contact with the rubber containing carbon black do not emit. However, if the surface of rubber containing carbon black, heated at 120°, is treated for 3 minutes with concentrated H_2SO_4 and then washed, which leads to the formation of new polar groups in the surface, electron emission may be observed when a gutta-percha film is stripped from this surface (Fig. 2,e).

It must be pointed out with reference to these results that the presence or absence of electron emission when the polymer is detached does not in itself prove or disprove the applicability of the electrical theory of adhesion in the given instance. The sole significance of electron emission is that it can be used to estimate the potentials of the electric double layers from the velocities of the emitted electrons. At the same time, the existence of charges on the separated surfaces, representing the residual surface electrification density, which is a certain part

of the initial density σ of the double layer, is an indication of the electrostatic character of the adhesion bond.

Systems of the second group (Table 4), consisting of nonpolar components, are significantly different. When the components of these systems are separated, no electron emission occurs and there are no charges on the separated surfaces. Microscopical examination of sections shows the boundary to be diffuse. This shows that in systems of the second group the adhesive bonds are formed by diffusion of the polymer chains in the contact zone. It cannot be said that the adhesive bond strengths of either group of systems are higher than those of the other. However, the first group contains some "weak" specimens (for example, chlorinated polyvinyl chloride - steel, or polyethylene - rubber; see Table 4).

The reaction (pH) of the substrate is very significant in adhesion effects; this was demonstrated by our experiments on the adhesion of chlorinated polyvinyl chloride to glass.

The experimental procedure was as follows: small amounts (about $\frac{1}{2}$ cc) of H_2SO_4 or NaOH solutions of various concentrations were applied from a pipet to a glass surface (40 x 70 mm). The solution was spread uniformly over the whole surface and the excess was removed by means of filter paper at the edge of the plate. A polymer film was then applied in the usual way and its adhesion to glass was determined by means of an adhesiogram in the region of high stripping rates. Figure 3 shows the variation of the work of separation A_0 at $v = 1$ cm/sec. with the concentration of the solution applied to the glass surface.

Figure 3 shows that the maximum adhesion A_0 corresponds to the neutral region. The separated surfaces, in the region of maximum adhesion, carry residual charges: positive on the polymer film and negative on the glass. If the glass is covered with a film of acid or alkali solution of high concentration, then the polymer film in contact with it must evidently undergo chemical change, probably by surface oxidation in an acid medium in the first case, and an alkaline medium in the second.

When a polymer film is stripped from a strongly acid or strongly alkaline glass surface, there is a sharp decrease of the work of adhesion and a change in the sign of the charges on the separated surfaces. The glass surface acquires a negative charge, while the polymer surface is positively charged. Thus, the charge reversal is accompanied by sharp decreases of the work of adhesion both in the acid and in the alkaline regions, which can be attributed only to a decrease of the surface electrification density of the layers of the electric double layer in the charge reversal region.

The authors express their gratitude to Corresponding Member (AN SSSR) B. V. Deriagin for valuable guidance, and to V. V. Karasev for helpful advice and constant assistance in the experimental work.

SUMMARY

1. The nature of the adhesion bonds in different cases can be determined by investigations of the mechanical characteristics of adhesion, of electrical effects observed on destruction of the bond, and microscopical investigation of the separation boundaries in various systems consisting of polymer pairs, and polymer-metal and polymer-glass systems held together by forces of adhesion.

2. The adhesion bonds between polymer and metal and polymer and glass are electrical in character, as shown by the form of the adhesiogram, the occurrence of electron emission on separation, and the existence of electric charges on the separated surfaces.

3. After separation, the polymer film continues to emit electrons and carries a negative residual charge. The substrate (glass, metal) does not emit electrons and has a positive charge.

4. The breakdown of the adhesion bond between two polar polymers of different structure, or a polar and nonpolar polymer, is accompanied by the same characteristic effects as the separation of a polymer from glass or metal. A sharp boundary is observed in microscopic specimens.

5. Determinations of the velocities of electrons emitted during separation show that breakdown of a firm adhesion bond is accompanied by emission of electrons with higher velocities than those emitted in the breakdown of a weak bond. These results are in good agreement with the electrical theory of adhesion.

6. The reaction of the substrate (glass) has a strong influence on the adhesion of a polymer (chlorinated polyvinyl chloride) to it. The maximum adhesion is found in the neutral region. The detached polymer film

shows a reversal of residual charge in the strongly acid and strongly alkaline regions, accompanied by a sharp decrease of the work of adhesion; this can only be attributed to a decrease of the surface electrification density of the layers of the electric double layer in the charge reversal region.

7. Mechanical treatment of the metal surface increases the adhesion of polymers to it and intensifies electron emission from the regions of the polymer film which were attached to the treated regions of the metal surface.

8. The formation of an adhesion bond between two nonpolar polymers of similar structure is caused by diffusion processes in the contact zone. In such cases no electrical effects are observed during separation, the boundary in microscopic specimens is diffuse, and the work of separation depends relatively little on the rate of separation.

9. The systems studied can be subdivided into two groups: the adhesion bond in systems of the first group is the result of formation of an electric double layer at the boundary; in systems of the second group the adhesion bond is produced by diffusion processes at the boundary.

Institute of Physical Chemistry
Academy of Sciences USSR
Moscow

Received December 18, 1956

LITERATURE CITED

- [1] B. V. Deriagin and N. A. Krotova, Progr. Phys. Sci. 36, 387 (1948); B. V. Deriagin and N. A. Krotova, Adhesion (Izd. AN SSSR, 1949);^{*} B. V. Deriagin, N. A. Krotova, and Iu. M. Kirillova, Proc. Acad. Sci. USSR, 97, 475 (1954).
- [2] D. Josefowitz and H. Mark, India Rubber World 33, 106 (1942); S. S. Voiutskii and Iu. L. Margolina, Progr. Chem. 18, 449 (1947); B. V. Deriagin and N. A. Krotova, Adhesion (Izd. AN SSSR, 1949) p. 242; S. S. Voiutskii and V. M. Zamazii, Colloid J. 15, 407 (1953);^{*} S. S. Voiutskii and B. V. Shtarkh, Proc. Acad. Sci. USSR 90, 573 (1953); S. S. Voiutskii, A. I. Shapovalova and A. I. Pisarenko, Proc. Acad. Sci. USSR 105, 1000 (1955).
- [3] B. V. Deriagin, S. K. Zherebkov and A. M. Medvedeva, Colloid J. 18, 404 (1956).**
- [4] V. V. Karasev, N. A. Krotova and B. V. Deriagin, Proc. Acad. Sci. USSR 88, 777 (1953).
- [5] N. A. Krotova, Iu. M. Kirillova and B. V. Deriagin, J. Phys. Chem. 30, 1921 (1956); N. A. Krotova, Gluing and Adhesion (Izd. AN SSSR, 1956).*
- [6] V. V. Karasev and N. A. Krotova, Proc. Acad. Sci. USSR 99, 715 (1954).

* In Russian.

** Original Russian pagination. See C. B. Translation.

THE HYDRODYNAMIC CHARACTERISTICS AND POLYDISPERSITY OF SOME ETHYLCELLULOSE SPECIMENS

T. I. Samsonova and S. Ia. Frenkel¹

In investigations of the technical properties of high polymers it is extremely important to know their average molecular weights and molecular weight distributions. While these characteristics have been studied in considerable detail for such cellulose esters as nitrocellulose and acetylcellulose [1-4], ethylcellulose has been studied very little in this respect [3, 5]. It is known that ordinary technical ethylcellulose, with degree of substitution between 2.15 and 2.60, is a very heterogeneous product both in chemical composition and in degree of polymerization; its fractionation is based on both these characteristics and does not yield homogeneous products [6]. The heterogeneity of ethylcellulose is considerably increased by oxidation, as this not only results in depolymerization, but also alters the functional groups [7].

It is therefore highly important to determine the nature of the relationships between the hydrodynamic characteristics and the molecular weight, and in particular the relationship between the latter and easily determined parameters such as the intrinsic viscosity $[\eta]$. This would permit rapid estimation of average molecular weights both in the production of ethylcellulose and during the changes which it undergoes in the course of oxidation. In particular, it is very important in this connection to find how the shape of the macromolecules depends on the chemical composition; in other words, to determine whether the function $[\eta] = f(M)$ alters in the oxidation and other chemical conversions of ethylcellulose.

The scanty data available in the literature [5] on the $[\eta] = f(M)$ relationship give high values when used for molecular weight calculations.

It was also desired to correlate variations of the molecular weight and molecular weight distribution of ethylcellulose on oxidation with variations of the mechanical properties of films made from it.

Materials and Methods

Commercial specimens of ethylcellulose of different degrees of substitution were used; to remove mineral impurities, 1% solutions were passed through purified activated charcoal, followed by reprecipitation.

Highly substituted ethylcelluloses (N and NI grades) were reprecipitated by water from acetone solution, and the low-substituted grade (K) was precipitated by ligoine from alcohol-benzene solution.

The ethoxyl numbers, determined by the Zeisel method, were 45.5% for ethylcellulose grade K, 47.5% for grade N, and 48.5% for grade NI. The specimens were oxidized by heating in a stream of oxygen (3 liters/hour) at 110-125°. The principal solvent used in measurements of hydrodynamic properties was dried and redistilled ethyl acetate [8]. In addition, the intrinsic viscosity $[\eta]$ was measured in alcohol-benzene solutions. The partial specific volume of the polymer was determined by the usual method [3].

The diffusion coefficients (D) were determined with the aid of Lamm's apparatus, fitted with an optical scale, a thermostat for maintaining the temperature to within 0.005°, and an automatic device for photographing the scale [9]. The method of the second and zero moment was applied to the diffusion diagrams to determine the weight-average coefficient of diffusion D_{2M} , while the "average" coefficient D_A was found by the method of the maximum ordinate from the area A [10]. As is known, for polydisperse substances $D_{2M} \neq D_A$ (usually $> D_A$).

Concentration effects were eliminated by the Boltzmann-Graelen method [17] by skewness of the diffusion diagrams in normal coordinates. The values of D were reduced to 20° by means of the usual corrections.

The sedimentation constant (s) was determined with the aid of a large oil centrifuge [3] at 60,000 r.p.m. Two optical systems were used for observing the course of sedimentation: Svensson's inclined slit method [11] (which gives a direct image of the refractive-index gradient) for determination of s , and Lamm's combined scale method [12] for evaluation of molecular weight distribution.

The sedimentation coefficient s_m , corresponding to the maximum on the sedimentation diagrams (which were always almost symmetrical) was calculated from the usual formulas:

$$s_m = \frac{1}{\omega^2} \frac{d \ln x_m}{dt} \quad \text{or} \quad s_m = \frac{1}{\omega^2} \frac{\ln (x_2)_m - \ln (x_1)_m}{t_2 - t_1}, \quad (1)$$

where ω is the angular velocity of the ultracentrifuge rotor, x_m is the distance of the maximum of the sedimentation diagram from the rotation axis, and $(x_1)_m$ and $(x_2)_m$ are the positions of this maximum at times t_1 and t_2 . The values of s_m were reduced to the standard temperature of 20° and a pressure of 1 atm. [13].

The influence of concentration was eliminated by means of the standard construction

$$\frac{1}{s} = \frac{1}{s_0} + Kc, \quad (2)$$

where c is the concentration and s_0 is the sedimentation constant. As a rule, K was very small for the systems studied, while at $s_0 \leq 2$, s did not depend on the concentration at all.

Molecular weights were calculated by Svedberg's formula

$$M = \frac{s_0}{D_0} \frac{RT}{1 - V\rho}, \quad (3)$$

where s_0 and D_0 are the sedimentation and diffusion constants in the given solvent at infinite dilution; $T = 293^\circ$ abs.; R is the universal gas constant; V is the partial specific volume of the polymer (which was 0.860 ± 0.004 for the system in question, irrespective of the composition of the specimens); ρ is the density of the solvent.

In addition, M was determined by the formulas of Flory and Mandelkern [14]

$$\frac{\eta_0 N s_0 [\eta]^{1/2}}{M^{2/3} (1 - V\rho)} = \Phi^{1/3} P^{-1}, \quad (4)$$

$$\frac{\eta_0 N D ([\eta] M)^{1/2}}{RT} = \Phi^{1/3} P^{-1}, \quad (5)$$

where $\Phi^{1/3} P^{-1} \approx 2.6 \cdot 10^{-6}$ is a constant (valid for all linear polymers); η_0 is the viscosity of the solvent; N is the Avogadro number; $[\eta]$ in these formulas is expressed in deciliters per g; $[\eta]$ was determined by means of the usual hanging-level viscosimeter, and calculated by the standard method.

The original and oxidized specimens were made into films 30-40 μ thick, the mechanical properties of which were studied by the usual methods.

Experimental Results and Discussion

Molecular weights. Effect of the degree of oxidation. Table 1 gives the coefficients of diffusion, sedimentation constants, intrinsic viscosities (in two solvents), oxidation conditions, and ethoxyl numbers of the specimens. The last column of Table 1 gives the average molecular weights calculated from various combinations of the hydrodynamic parameters by means of Formulas (3, 4).

TABLE 1

Hydrodynamic Parameters and Molecular Weights of Ethylcellulose

Type of ethylcellulose	Oxidation conditions		Ethoxyl number	[η] in alcohol-benzene	[η] in ethyl acetate	$(D_{2m}) \cdot 10^7$	$(D_A)_0 \cdot 10^7$	D_{2m}/D_A	s_0	σ_0	$M_s, D_{2m} \cdot 10^{-3}$	$M_s, D_A \cdot 10^{-3}$	$M_{s,\eta} \cdot 10^{-3}$
	t °C	time, hours											
NI	—	—	48.5	2.20	1.85	5.36	4.77	1.12	2.80	0.384	58.8	66.4	65.6
NI oxidized	120	3	46.9	1.60	1.40	7.13	6.19	1.15	2.28	—	36.0	41.3	41.1
NI oxidized	120	4	44.0	0.90	0.79	7.10	6.19	1.15	2.25	0.540	35.5	40.6	30.5
NI oxidized	120	7.5	41.9	0.60	0.43	8.00	7.68	1.04	2.11	—	29.6	30.8	20.6
N	—	—	47.5	2.10	1.80	4.49	4.28	1.07	2.19	—	54.5	57.0	45.0
K	—	—	44.5	2.20	1.87	4.40	2.87	1.54	2.67	0.307	67.5	104.0	60.0
K oxidized	125	1.5	42.4	1.45	1.25	6.95	4.68	1.49	2.12	—	33.9	50.5	35.2
K oxidized	125	2.25	41.3	0.87	0.80	7.87	6.32	1.24	1.94	0.474	27.5	34.2	24.6

Note: M_s , D_{2m} and M_s, D_A are the molecular weights calculated from Svedberg's formula based on D_{2m} and D_A respectively. $M_{s,\eta}$ is the molecular weight calculated by Formula (4).

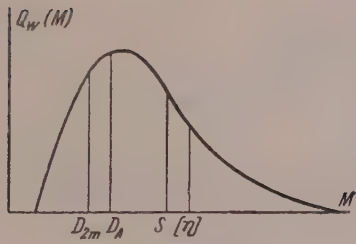


Fig. 1. Schematic representation of molecular weight distribution.

The differences between the diffusion coefficients D_{2m} and D_A are evidence of considerable polydispersity in the ethylcellulose specimens; this also accounts for the differences between the molecular weights calculated by different methods. It therefore seemed undesirable to use combinations of the intrinsic viscosity and diffusion coefficients, in accordance with Equation (5), for calculation of M . This was confirmed by quantitative estimates. The use of Equation (5) for calculation of M for polydisperse substances is undesirable for two reasons.

1. The coefficient D is considerably more sensitive than $[\eta]$ to the presence of low-molecular components.

This is shown schematically and in exaggerated form in

Fig. 1, which represents a hypothetical molecular weight distribution, with values of the molecular weight corresponding to s_0 , $[\eta]$, D_A and D_{2m} indicated on the abscissa axis. It is seen that the best correlation is to be expected from combinations of s_0 with $[\eta]$, and of s_0 with D_A .

2. Equation (5) contains the third power of the diffusion coefficient and the first power of $[\eta]$, and in consequence the influence of experimental errors on the calculation results is large.

It is clear from Table 1 that all the polymers are of relatively low molecular weight, the most probable values generally not exceeding $70 \cdot 10^3$. It also follows from Table 1 that the molecular weight decreases with progressive oxidation, i.e., oxidation results in degradation of the polymer chains.

Polydispersity of the specimens. In polydispersity analysis by the method of equivalent Gaussian distributions it is assumed more or less arbitrarily that the sedimentation curves approximate to the form of a Gaussian curve [15]. Figure 2 shows that in this instance this assumption is reasonably well justified. However, in all cases the contribution of diffusion to the broadening of the sedimentation curve is large (of the same order as that of true polydispersity), and therefore such details of the distribution as the high- or low-molecular "tails" are blurred, and the distribution functions $Q_W(M)$ given below should be regarded merely as first approximations to the truth. Because s depends little on the concentration, it may be assumed in the distribution calculations that the standard deviation σ of the equivalent Gaussian distribution by values of s at the final concentration is related to the true standard deviation (σ_0) of the distribution by the sedimentation constants in the simple proportion

$$\frac{\sigma}{s} = \frac{\sigma_0}{s_0}. \quad (6)$$

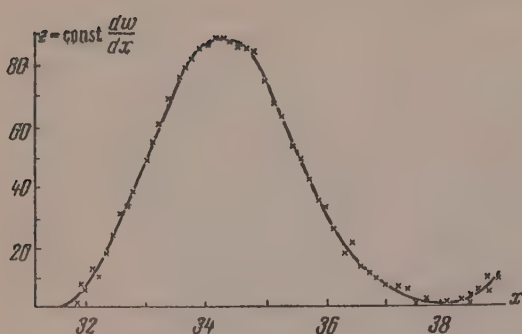


Fig. 2. Sedimentation diagram for grade K ethylcellulose oxidized for 2 hours 15 minutes at 120°.

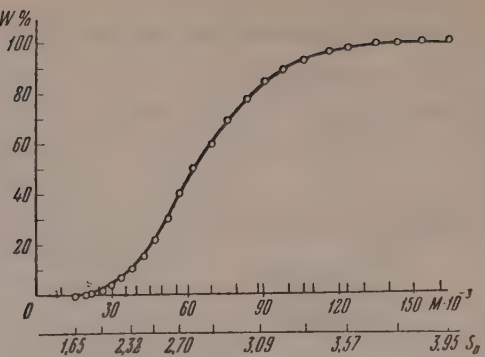


Fig. 3. Integral $W(M)$ curve for the molecular weight distribution of NI ethylcellulose.

TABLE 2

Average Molecular Weights and Coefficients of Dispersion and Asymmetry, Calculated from the Distribution Curves

Type of ethylcellulose	$M_z \cdot 10^{-3}$	$M_W \cdot 10^{-3}$	$M_n \cdot 10^{-3}$	μ_n/M_n	μ_W/M_W	γ
NI	64.8	55.2	38.0	0.213	0.132	1.56
NI oxidized	44.9	33.4	21.0	0.243	0.186	2.23
K	65.6	59.9	47.4	0.163	0.097	1.70
K oxidized	37.6	28.0	18.5	0.226	0.185	1.94

The values of σ_0 calculated in this way are used

$$\text{to plot integral distribution curves } W(s_0) = \int_0^{s_0} Q_W(s_0) ds_0,$$

and s_0 is then replaced by M in the abscissa axis (from the data of Figs. 8 and 9; see below). A specimen calculation for an original NI specimen is illustrated in Fig. 3. Differentiation of the integral curve $W(M) = \int_0^M Q_W(M) dM$ gives the required weight curve for the molecular weight distribution. Curves for specimens K and NI are given in Fig. 4.

Table 2 gives the values of the consecutive molecular weights M_n , M_W , M_z calculated from these curves, the number and wt. dispersion coefficients (μ_n/M_n and μ_W/M_W respectively, where $\mu_n^2 = M_n M_W - M_n^2$ and $\mu_W^2 = M_W M_z - M_W^2$), and the distribution asymmetry γ calculated by Jullander's method (from the ratio of the areas under the $Q_W(M)$ curves to the right and to the left of the maximum ordinate). It is seen that both the polydispersity itself, given by the dispersion coefficient, and the distribution asymmetry increase on oxidation.

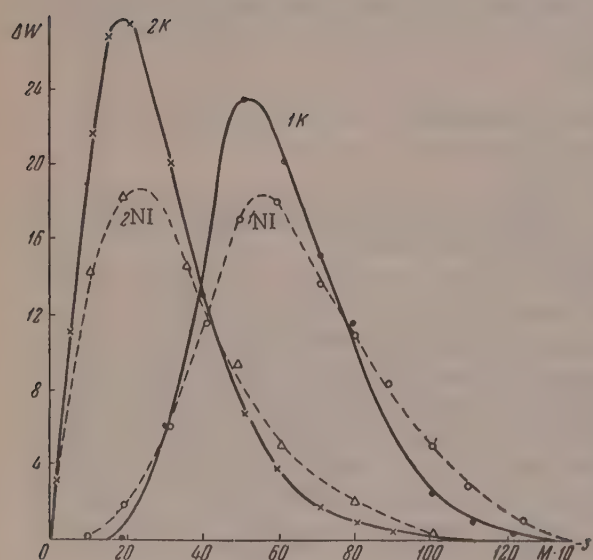


Fig. 4. Molecular weight distribution curves of K and NI ethylcellulose:
1) original; 2) oxidized.

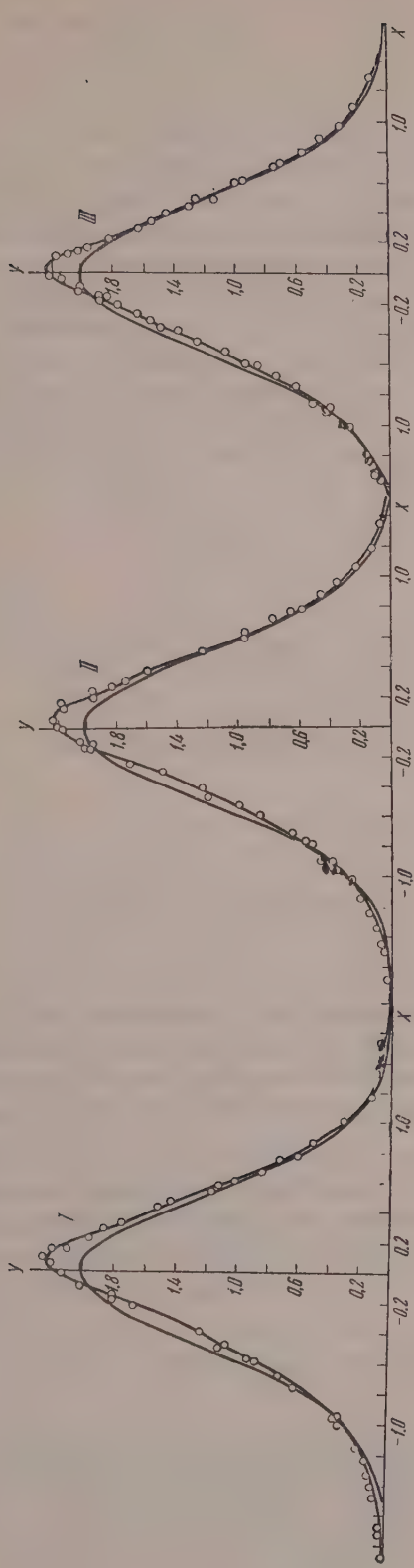


Fig. 5. Diffusion diagram in normal coordinates, for Ni ethylcellulose:
I) original; II) oxidized for 3 hours at 120°; III) oxidized for 4 hours at 120°.

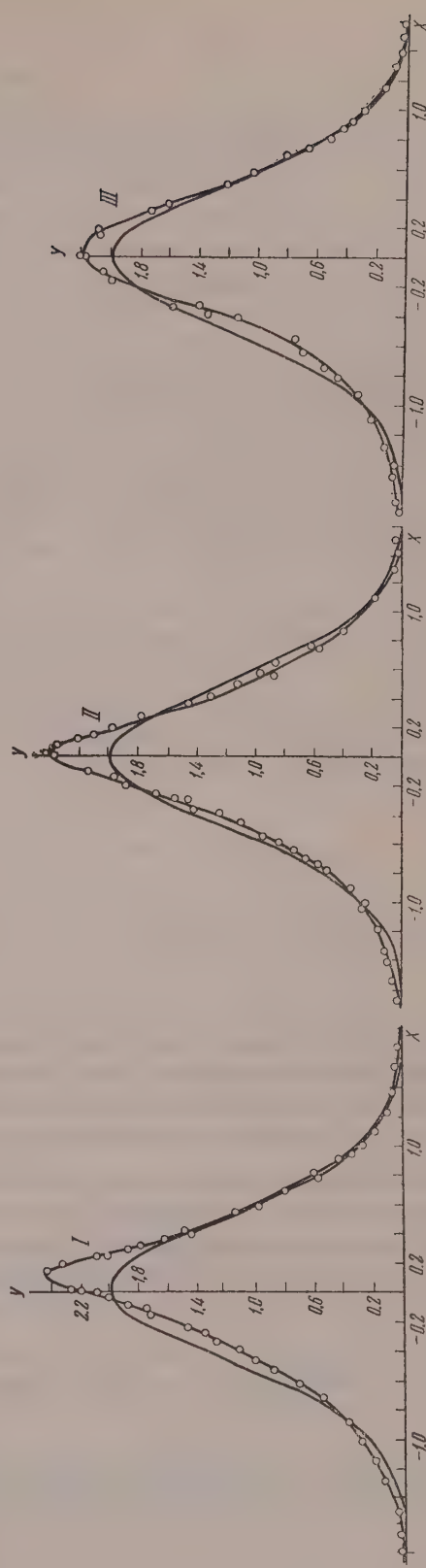


Fig. 6. Diffusion diagrams in normal coordinates, for K ethylcellulose:
I) original; II) oxidized for 1 hour 30 minutes at 125°; III) oxidized for 2 hours 15 minutes at 125°.

Another important result which follows from an examination of Table 2 is that for both oxidized specimens $M_{\text{II}} : M_W : M_Z = 2 : 3 : 4$, which corresponds to a distribution function of the form $Q_W(M) = \text{const } M^2 e^{-\alpha M}$, where α is a distribution parameter [16]. This means, on the one hand, that the oxidation process eliminates fairly rapidly traces of the initial distributions, which in this case should correspond to binomial model functions, and on the other, that the degradation accompanying oxidation is not of a purely statistical character, as this would result in the ratio $M_{\text{II}} : M_W : M_Z = 1 : 2 : 3$ [15, 16]. The possibility is not excluded, however, that such a distribution becomes established in more prolonged oxidation.

The gradual loss of the traces of the initial distribution can also be seen in the diffusion curves for K and NI ethylcelluloses, reduced to normal coordinates [17] (Figs. 5 and 6). It is seen that all the normalized curves for NI ethylcellulose are similar, whereas the curves for K change appreciably with time. After oxidation for 1.5 hours the normalized curve is still very similar to the curve for the original specimen, whereas after 2 hours 15 minutes the curve is practically of the same form as the curve for NI. The difference between the original curves and their gradual approach to the same form is in good agreement with the data in Table 2, and also with the course of the ratio D_{2M}/D_A . Indeed, the initial distributions $Q_W(M)$ for NI and K differ significantly, as is clear from a direct examination of Figs. 4 and 5, and still more evident from a comparison of the $M_{\text{II}} : M_W : M_Z$ ratios. For K this ratio is $1 : 1.27 : 1.38$ which corresponds to an irregular distribution (i.e., one which does not conform to a model function of the type $M^k e^{-\alpha M}$), narrower than that of NI. The distribution for NI is also irregular, although it is closer to the "recombination" form, with $M_{\text{II}} : M_W : M_Z = 2 : 3 : 4$. This ratio in this case is $1 : 1.45 : 1.71$.

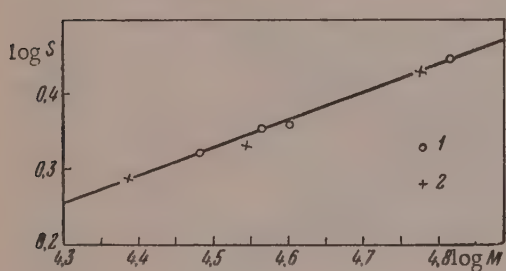


Fig. 7. $\log s$ as a function of $\log M$:
1) for NI ethylcellulose; 2) for K ethylcellulose.

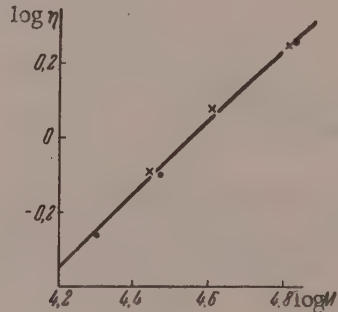


Fig. 8. $\log [\eta]$ as a function of $\log M$:
1) for NI ethylcellulose; 2) for K ethylcellulose.

The difference between the initial and final distributions is considerably less for NI than for K ethylcellulose, while the nature of the final distribution is the same for both specimens. As the nature of the polydispersity becomes the same for both, the ratios D_{2M}/D_A also converge. This does not exclude the possibility that specimen K contains a low-molecular impurity which escapes notice in the sedimentation diagram.

These differences in the initial $Q_W(M)$ functions reflect the previous history of the ethylcellulose. Milder conditions result in the production of the less polydisperse specimen K (but with a greater degree of asymmetry), the distribution function of which differs greatly from the Poisson distribution which would be found with random degradation of the chains. The degradation during the formation of specimen NI is more random in character, although the result is also still very far from a Poisson distribution.

Hydrodynamic characteristics. The variations of $\log s_0$ and $\log [\eta]$ with $\log M$ are given in Figs. 7 and 8. Because of some discrepancies in the value of M calculated by different equations, the points in Figs. 7 and 8 represent average values of M .

It is seen that the points for specimens NI and K are grouped with roughly similar accuracy around the same straight lines, i.e., any possible differences of chemical composition (ethoxyl number and modification of side chains on oxidation) are not detectable in the hydrodynamic behavior of the macromolecules.

The values of s_0 and $[\eta]$ as functions of the molecular weight, according to Figs. 7 and 8, are given by the expressions:

$$[\eta] = (2.82 \cdot 10^{-5} M) \text{ deciliters/g} \quad (7)$$

$$s_0 = (4.6 \cdot 10^{-2} M^{1-0.63}) \text{ Svedberg units } (10^{-13} \text{ CGS}). \quad (8)$$

Thus, solutions of both ethylcelluloses in ethyl acetate conform to the simple Staudinger equation. At first sight this seems somewhat unexpected, as the relationships of the parameters a_1 and a_2 in the equations

$$s = K_s M^{1-a_1} \text{ and } [\eta] = K M^{a_2} \quad (9)$$

contradict the hydrodynamic theories of Flory, Fox, and Mandelkern [14] and of Debye and Beuche [18], which predict relationships of this type between s_0 , $[\eta]$, and M .

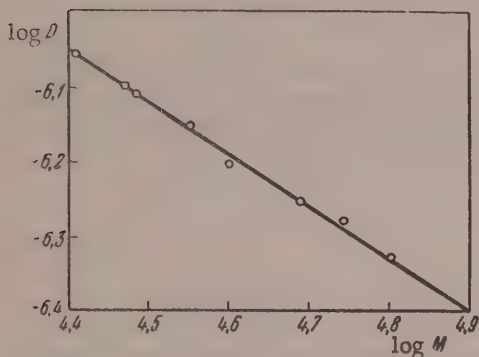


Fig. 9. Variation of $\log D$ with $\log M$.

It is postulated in the Flory-Mandelkern theory that the solvent is totally immobilized inside the molecular coils (i.e., they are impermeable to the solvent), and the linear dimensions of these coils increase, not in proportion to $M^{1/2}$ as would be the case in an ideal solvent, but in proportion to $M^{1/2}\alpha$, where α is the so-called "swelling parameter" of the macromolecules, equal to the ratio of the root mean square distances between the ends of the coil in a real and an ideal solvent; $R/R_0 \cdot \alpha$ characterizes the volume effects due to thermodynamic interaction of the macromolecule segments with the solvent. The parameter α is itself a function of the molecular weight, increasing in proportion to M^β where β is of the order of 0.1. Since $R_0 \sim M^{1/2}$,

$R \sim M^{1/2} + \beta$. Substitution of R into the equations for $[\eta]$ and s_0 gives the Equations (9), which may be written in the form

$$[\eta] = K M^{(1/2+3\beta)}, \quad (10)$$

$$s_0 = K_s M^{1-(1/2+\beta)}. \quad (11)$$

Therefore $a_1 = 1/2 + \beta$; $a_2 = 1/2 + 3\beta$, i.e., β calculated from a_1 is 0.13, and a_2 should then be 0.89, whereas the experimental value $a_2 = 1$ should give 0.67 for a_1 . These discrepancies are beyond the limits of experimental error. To account for them, it might be assumed that in the region of relatively low molecular weights, especially for rigid molecules such as those of all cellulose derivatives, a factor such as the permeability of the molecular coils to the solvent may play a significant part together with the volume effects.

This aspect of the question is considered in the Debye-Bueche theory. In this theory the treatment of viscosity is by analogy with the simple Einstein law for the viscosity of suspensions of rigid spheres, but the constant coefficient 2.5 is replaced by the variable parameter $\varphi(\sigma)$ which allows for the permeability of the macromolecules to the solvent. The frictional factor f , which enters the formulas for the sedimentation and diffusion constants

$$D_0 = \frac{RT}{f}, \quad s_0 = \frac{M(1-V\varphi)}{f}, \quad (12)$$

by analogy with the Stokes equation for rigid spheres, is $f = 6\pi\eta_0 \times R_s \psi(\sigma)$, where R_s is the radius of an equivalent hydrodynamic sphere; η_0 is the viscosity of the solvent, and $\psi(\sigma)$ is another volume factor, which also depends on the permeability of the macromolecules.

The "shielding ratio" σ , of which the factors φ and ψ are functions, also determines the values of a_1 and a_2 ; σ varies from 0 for completely permeable macromolecules (corresponding to $a_1 = a_2 = 1$) to ∞ for

impenetrable coils (when $a_1 = a_2 = \frac{1}{2}$). For intermediate values of σ , values of φ , ψ , a_1 and a_2 are tabulated in Debye and Bueche's paper [18]. It is important to note that $a_2 > a_1$ in this region in all cases. The reason is that in viscous flow the main frictional losses caused by rotation of the macromolecules [15] occur at the peripheral regions of the coils, where the distribution density of the segments is at a minimum, and which are therefore almost entirely permeable to the solvent. The inequality $a_2 > a_1$ reflects the fact that in rotational motion (i.e., in relation to viscosity) the macromolecule as a whole appears to be "more transparent" than in translational motion (with respect to s and D).

It is easy to see that our experimental data do not conform to the Debye-Bueche theory either. We see that $a_1 = 0.63$ corresponds to $\sigma \approx 3.5$, but this value of σ corresponds to $a_2 = 0.8$; conversely, if we assume that $a_2 = 1$, then a_1 should also be unity and s_0 would not depend on M . We are therefore forced to conclude that the hydrodynamic behavior of ethylcellulose molecules in the range of $M < 100,000$ can be interpreted in terms of non-compact coils, in thermodynamic interaction with the solvent and partially permeable to it. On the assumption that the effects caused by swelling and permeability of the macromolecules are additive, we obtain the best correlation between a_1 and a_2 if we assume that $\sigma = 10$. Then, as the result of permeability only, a_1 would be 0.522 and $a_2 = 0.611$; for $\beta = 0.12$, we would have $a_1 = 0.65$ and $a_2 = 0.97$. This discrepancy is now within the limits of experimental error, especially in view of the polydispersity of our specimens.

The appreciable permeability of the ethylcellulose molecules is evidently the result of the high rigidity of the chains, which prevents the formation of compact coils. We can attempt to estimate this rigidity or, which is the same thing, the degree of coiling. By the Flory-Mandelkern theory [14] the frictional coefficient of a macromolecule

$$F = \frac{M}{s_0} \frac{(1 - V\rho)}{N}, \quad (13)$$

where N is the Avogadro number, and the root mean square size of the macromolecule are related by the expression

$$F / \eta_0 = 5.1R. \quad (14)$$

For the random value $M = 5 \cdot 10^4$, which corresponds, according to Fig. 7, to $s_0 = 2.5$ Svedberg units, we have $R = 360$ Å; the same estimate can be made on the basis of Kirkwood and Riseman's hydrodynamic theory [19] in which, as in the Debye-Bueche theory, only the hydrodynamic interaction between the macromolecules and the solvent is taken into account. By this theory

$$s_0 = \frac{m_0(1 - V\rho)}{N\xi} [1 + \frac{8\lambda_0}{3} Z^{1/2}], \quad (15)$$

where m_0 is the molecular weight of the monomer, 224 in this instance (for an average degree of substitution of 2.4); ξ is the frictional coefficient of one monomer unit; Z is the degree of polymerization, and

$$\lambda_0 = \frac{\xi}{(6\pi s)^{1/2}\eta_0 b}, \quad (16)$$

where b is the effective length of a monomer unit.

A plot of s_0 against $Z^{1/2}$, according to Equation (15), where s_0 and $Z^{1/2}$ are calculated from the data in Fig. 7 gives $b = 25.2$ Å which corresponds, at $M = 5 \cdot 10^4$, to $R = 378$ Å and is in excellent agreement with the preceding estimate.

If we assume that the chains are fully extended, and use the x-ray value of $b_0 = 5.13$ [20] for the length of the pyran ring, we find the chain length $b_0 Z = 1154$ Å; the degree of coiling of ethylcellulose molecules in

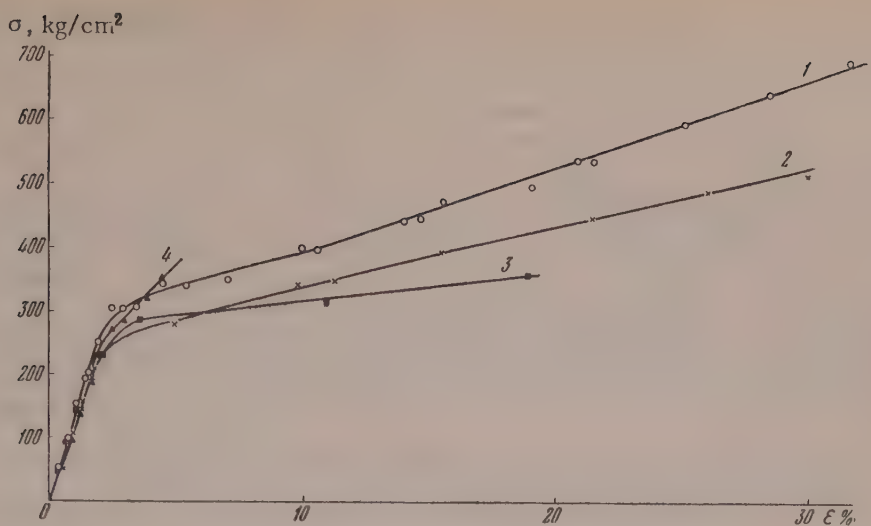


Fig. 10. Load-extension diagram for NI ethylcellulose: 1) original; 2) oxidized for 3 hours 20 minutes at 120°; 3) oxidized for 4 hours at 120°; 4) oxidized for 7 hours 30 minutes at 120°.

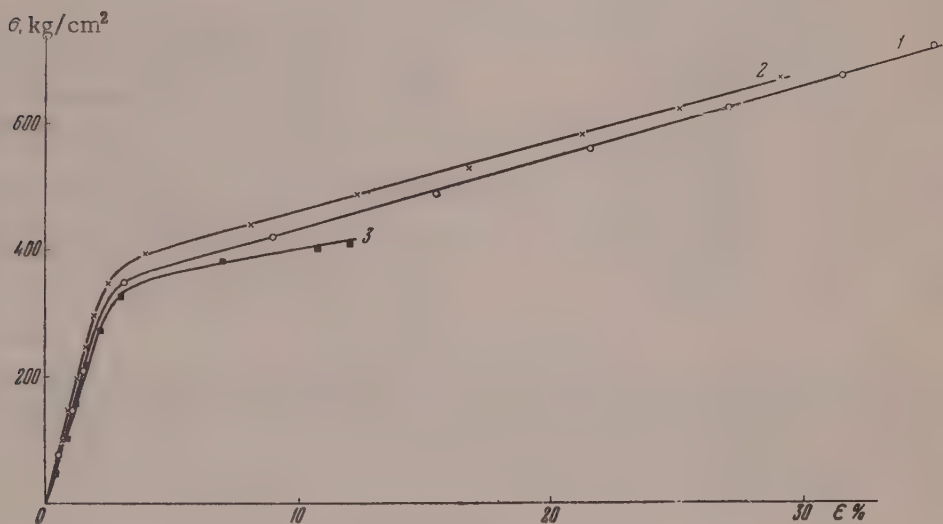


Fig. 11. Load-extension diagram for K ethylcellulose: 1) original; 2) oxidized for 1 hour 30 minutes at 125°; 3) oxidized for 2 hours 15 minutes at 125°.

ethyl acetate is therefore ≈ 3 . For nitrocellulose in the same solvent [15] $b = 52 \text{ \AA}$ (in acetone it is 37 \AA [21]), and the degree of coiling is ≈ 2 .

Thus, the configuration of ethylcellulose molecules in solution is in any event more compact than that of nitrocellulose molecules (no data for other cellulose derivatives are available). This suggests that ethylcellulose molecules are highly flexible; this is in good agreement with the macroscopic properties of ethylcellulose (the relative elongation of ethylcellulose films is 30%, and that of nitrocellulose is 5-8%).

In conclusion, it was desirable to estimate the molecular weights of the specimens for which only the diffusion coefficients were determined. By the Debye-Beuche and Flory-Mandelkern theories,

$$D = K_D M^{-a_1},$$

TABLE 3

Diffusion Coefficients and Molecular Weights of Ethylcellulose Specimens for Which s_0 Was Not Determined

Type of ethylcellulose	Oxidation conditions		Ethoxy number	$[\eta]$ in alcohol-benzene	$[\eta]$ in ethyl acetate	$(D_{2m}) \cdot 10^7$	$(D_A) \cdot 10^7$	D_{2m}/D_A	$M_s, D_{2m} \cdot 10^{-3}$	$M_s, D_A \cdot 10^{-3}$	$M_s, D_{2m} \cdot 10^{-3}$	$M_s, D_A \cdot 10^{-3}$
	t, °C	time, hours										
NI, oxidized	120	2 ^{2/3}	47.5	2.05	1.70	6.77	5.67	1.19	30.3	39.9	37.1	45.7
NI, oxidized	120	3 ^{1/3}	46.7	1.30	1.20	6.64	6.05	1.10	35.2	46.5	38.1	45.0
NI, oxidized	125	5	35.5	0.23	0.22	22.19	15.53	1.42	5.14	15.0	5.7	10.0
N, oxidized	110	8	43.0	1.40	1.12	8.28	6.81	1.21	19.5	34.9	26.9	36.7
N, oxidized	125	5	38.0	0.12	0.11	49.7	37.5	1.32	0.9	2.1	1.3	2.5

Note. M_s, D are molecular weights calculated from Equation (5). M_s, D are molecular weights obtained by interpolation in accordance with Fig. 1.

TABLE 4

Effect of Molecular Weight on the Mechanical Properties of Films

$$K_D = \frac{RTK_s}{1 - V_p} = 5.147 \cdot 10^{-4}.$$

Type of ethyl-cellulose	$M_{av} \cdot 10^{-3}$	F, kg/cm ²	$\epsilon, \%$
NI	60.9	703	31.8
NI, oxidized	41.3	527	29.0
NI, oxidized	35.5	395	17.6
NI, oxidized	30.2	339	6.4
N	55.0	680	30.0
K	67.5	780	35.0
K, oxidized	40.2	664	30.0
K, oxidized	27.5	403	11.5

Effect of molecular weight on the mechanical properties of films. Average molecular weights, tensile strengths F, and relative elongations ϵ are given in Table 4; it is seen that as the molecular weight decreases the mechanical properties of ethylcellulose films deteriorate sharply, and the load-extension diagrams change, becoming flatter (Figs. 10, 11).

SUMMARY

- The ethylcelluloses studied were of relatively low molecular weight, the probable values not exceeding 70,000; they also had considerable polydispersity. The polydispersity of specimens with molecular weight distributions which are not susceptible to the usual statistical analysis reflects, to some degree, their previous history (method of preparation).
- Oxidation is accompanied by depolymerization and a change in the nature of the polydispersity. Both the breadth and the asymmetry of the distribution increase with increasing degree of oxidation.
- Moderate differences in the chemical composition of ethylcelluloses, caused by differences in the degree of substitution or oxidation, are not reflected to a measurable extent in the hydrodynamic behavior of the macromolecules. The relationships between the intrinsic viscosity and the sedimentation constant, and the molecular weight in ethyl acetate, are of the form $[\eta] = 2.82 \cdot 10^{-5} M$, $s_0 = 4.6 \cdot 10^{-2} M^{1-0.63}$, where $[\eta]$ is expressed in deciliters per gram, and s_0 is Svedberg units.
- If the pyran ring is regarded as the kinetic unit of the chain, the effective length of an ethylcellulose chain unit is 25 Å, which is half the value for nitrocellulose in the same solvent. This shows that the molecular

This plot is shown in Fig. 9. It is seen that the experimental values of D_{2m} and D_A are grouped satisfactorily around the straight line (here $\log D_{2m}$ is plotted relative to $\log M_s, D_{2m}$, and $\log D_A$ relative to $\log M_s, D_A$, because in the ΔM range for the difference between the molecular weights corresponding to D_{2m} and D_A (compare Fig. 1) s_0 , which is only slightly dependent on M, can be regarded as approximately constant). Values obtained by interpolation from this plot are given in Table 3.

coils in ethylcellulose are more compact, and therefore that the ethylcellulose chains are more flexible, than those of other cellulose derivatives, in harmony with their macroscopic properties.

The mechanical properties of films prepared from ethylcellulose during oxidation deteriorate sharply with progressive oxidation, i.e., with decrease of molecular weight.

Institute of High-Molecular Compounds
Academy of Sciences USSR
Leningrad

Received January 31, 1957

LITERATURE CITED

- [1] E. H. Immergut, B. G. Ranby and H. F. Mark, Ind. Eng. Chem. 45, 11, 2483 (1953); G. V. Shultz and M. Marx, Makromol. Chem. 14, 1 (1954).
- [2] A. M. Sookne and M. Harris, Ind. Eng. Chem. 37, 475, 573 (1945).
- [3] T. Svedberg and K. O. Pederson, The Ultracentrifuge, (Oxford, 1940).
- [4] J. Jullander, Studies on nitrocellulose, cited through [10].
- [5] N. I. Nikurashina and S. A. Glikman, Sci. Mem. Saratov State Univ. 34 (1954).
- [6] S. N. Ushakov and I. M. Geller, Collected Papers on Plastics 3, 30 (1939).
- [7] O. P. Koz'mina and V. I. Kurliankina, Proc. Acad. Sci. USSR 114, No. 4 (1957).*
- [8] S. E. Bresler, I. A. Poddubnyi and S. Ia. Frenkel', J. Tech. Phys. 23, 1521 (1953).
- [9] P. A. Finogenov, J. Tech. Phys. 21, 167 (1951).
- [10] J. Jullander, Ark. f. Kemi, Mineral och. Geol. 21 A, No. 8 (1945).
- [11] H. Svensson, Ark. f. Kemi. Mineral och. Geol. 22 A, No. 10 (1946).
- [12] O. Lamm, Nova Acta Reg. Soc. Sci. Upsala. 4, 10, 6, 1937.
- [13] S. Ia. Frenkel', J. Tech. Phys. 24, 2169 (1954).
- [14] L. Mandelkern and P. Flory, J. Chem. Phys. 20, 212 (1952).
- [15] S. Ia. Frenkel', Progr. Phys. Sci. 53, No. 2 (1954).
- [16] S. E. Bresler and S. Ia. Frenkel', J. Tech. Phys. 23, 1502 (1953).
- [17] N. Gralen, Sedimentation and diffusion studies on cellulose and cellulose derivatives, Uppsala (1944).
- [18] P. Debye and A. M. Bueche, J. Chem. Phys. 16, 573 (1948).
- [19] J. G. Kirkwood and J. Riseman, J. Chem. Phys. 16, 565 (1948).
- [20] E. Ott, Cellulose and cellulose derivatives, 5, (New York, 1943) p. 209.
- [21] H. Benoit, A. Holtzer and P. Doty, J. Phys. Chem. 58, 635 (1954).

* See C. B. Translation.

INVESTIGATION OF THE COAGULATION OF RUBBER LATEXES
WITH THE AID OF RADIOACTIVE ISOTOPES

D. M. Sandomirskii and M. K. Vdovchenkova

The action of electrolytes on latexes is the basis of the separation of polymers from latexes in emulsion polymerization, and of a number of methods (ionic deposition, gelation) for the production of rubber goods directly from latex [1]. Calcium chloride solutions are widely used in these processes. The behavior of latex in these operations greatly depends on its stability; one method of determining this is in terms of the so-called "coagulation threshold," i.e., the minimum quantity of electrolyte required for the coagulation of a definite portion of the latex. However, for some synthetic latexes it is difficult to determine the instant of coagulation, and the results obtained may depend on the concentration of the latex and other factors [2].

Coagulation of a latex by the action of bivalent metal ions can occur both owing to a change in the electrokinetic potential of the globules, and owing to formation of water-insoluble compounds by reactions of the cations with anions of the stabilizer. In the latter case the amount of the cation irreversibly bound with 1 g of the coagulum might serve as a measure of the stability of the latex. To verify this possibility, it was first necessary to determine whether this value is sufficiently constant and independent of such factors as the concentration of the coagulant salt solution and of the latex.

To 1 ml of latex (Table 1) 1 ml of a solution of $\text{Ca}^{45}\text{Cl}_2$ of known activity and concentration was added. The coagulum was washed in water at the boil until the activity of the water ceased to increase; it was then ashed and the radioactivity of the ash was determined by the usual methods. The amounts of Ca^{2+} in meq, combined with 1 g of coagulum, was calculated. We shall term this value the calcium number.

TABLE 1

Composition and Properties of Latexes

Name of latex	Nature of polymer	Stabilizer	Original contents of solids, %
L-4	Polychloroprene	-	48.9
L-3	The same	-	48.6
VKh-2	The same	Sodium salts of tridecyclic and paraffinic acids	38.4
SKS-30n	Butadiene-styrene copolymer	Potassium naphthenate	27.2
SKS-50n	The same	Potassium naphthenate	29.4
SKS-50n	The same	Potassium paraffinate	49.14
Natural latex	Natural rubber	Natural proteins and resins	34.2
Qualitex**	The same	The same	61.6
Revultex**	Natural rubber, vulcanized	The same	60.1
Standard Revertex***	Natural rubber	Same, with alkali soap	69.5

* Tridecyclic acid tagged with C^{14} in the carboxyl.

** Concentrate obtained by centrifuging.

*** Concentrate obtained by evaporation.

TABLE 2

Effect of Concentration of the Coagulant Solution (c_s) on the Calcium Number

c_s in millimoles/liter	Calcium number in meq/g					
	L-4	SKS-50n	SKS-30n	SKS-50n	Revertex	Qualitex
6	—	0.091	0.099	0.087	0.111	0.030
8	0.054	0.091	0.099	0.086	0.109	0.030
10	0.055	0.090	0.097	0.085	0.108	0.031
12	0.055	0.093	0.097	0.086	0.108	0.033
14	0.054	0.091	0.099	—	0.110	0.032

TABLE 3

Effect of Concentration of the Latex (c_L) on the Calcium Number

Name of latex	c_L in %	Calcium number in meq/g	Name of latex	c_L in %	Calcium number in meq/g
L-4	34.2	0.021	SKS-30n	28.4	0.051
	19.5	0.022		14.0	0.050
	9.5	0.020		7.0	0.049
	5.2	0.022		3.0	0.049
L-3	35.3	0.007	Qualitex	51.2	0.006
	17.6	0.007		23.1	0.006
	1.8	0.007		17.0	0.006
VKL-2	36.0	0.032	Revertex	10.2	0.006
	18.0	0.031		54.0	0.111
	3.6	0.032		36.0	0.110
SKS-30n	25.0	0.046		18.0	0.109
	18.0	0.045		6.0	0.110
	12.5	0.046		—	—
	6.0	0.047		—	—

TABLE 4

Effects of Storage, Dialysis, and Aging of Latexes on the Calcium Number

Name of latex	Calcium number in meq/g						
	after storage			after dialysis			
	0	2 months	7 months	0	4 days	10 days	15 days
L-4	0.054	0.034	0.015	0.021	0.009	0.008	0.006
L-3	0.055	0.035	0.006	—	—	—	—
VKh-2	—	—	—	0.032	0.010	0.009	0.008
Revultex	0.034	0.009	0.002	—	—	—	—
Qualitex	0.033	0.005	coagul.	—	—	—	—

Calcium number of L-4 in meq/g after aging at 70°

0	2 days	4 days	6 days	8 days
0.047	0.028	0.027	0.025	0.024

The calcium numbers of various latexes on coagulation with $\text{Ca}^{45}\text{Cl}_2$ solutions of different concentrations are given in Table 2.

It follows from the data in Table 2 that the quantity of calcium ions required to give 1 g of coagulum does not depend on the concentration of the coagulant solution.

The data in Table 3 show that the calcium number is also independent of the concentration of the latex.*

The calcium number can therefore be used as a measure of the stability of a latex to electrolytes. The greater the calcium number, the more electrolyte is required to coagulate the latex, and therefore the higher is its stability.

It was of interest to determine the variations of the calcium number when the stability of the latex is known to decrease, as in storage or during dialysis. The relevant data are given in Table 4.

The data in Table 4 show that the calcium number can be used in studies of the variations of the sensitivity of latexes to electrolytes as the result of various treatments. It is seen in the case of natural latex and its concentrates that the introduction of additional stabilizers, as in the production of Revertex, results in a considerable increase of the calcium number. Concentration by centrifuging (Qualitex, Revultex), when a part of the protective substances is removed with the serum, decreases the calcium number. The results also agree with everyday technological experience. The technological properties of all the latexes studied, as determined by their stability to the action of electrolytes, show a correlation with their calcium numbers.

To determine what proportion of the stabilizer combines with the cation on coagulation, experiments were carried out on the coagulation of VKh-2 latex with a tagged stabilizer. The coagulant was 3% acetic acid solution or 0.4% calcium chloride solution (not radioactive). The unchanged stabilizer was extracted with alcohol from the dried coagulum, the amount being found from the activity of the dried extract. If the extract of a latex film made by drying is taken as 100% (all the sodium tridecylate being extracted), 98.7% is extracted from an acetic acid coagulum, i.e., almost the same amount; in coagulation with calcium chloride, only 73.6% is extracted. In the first case, tridecyclic and paraffinic acids are formed, which are insoluble in water but soluble in alcohol; in the second case, a part (~24%) of the tridecyclic acid is converted into the calcium salt, which is not soluble in water or alcohol. Thus, in the coagulation of rubber from a latex it is not necessary for all the stabilizers to be converted into an insoluble form.

The coagulation of a number of synthetic latexes with $H_2S^{35}O_4$ was also studied. It was found that the coagulum, after being washed, was not radioactive. Therefore anions are not adsorbed in the process.

SUMMARY

1. A new method is described for determination of latex stability with the use of $Ca^{45}Cl_2$.
2. The quantity of calcium ions combined in the coagulation of 1 g of rubber (the calcium number) does not depend on the concentrations of the coagulant solution or latex.
3. The calcium number decreases on aging, dialysis, or centrifugation of the latex.
4. When a latex is coagulated, only part of the stabilizer is converted into an insoluble form.

Scientific Research Institute
for Widely Used Rubber Goods
Moscow

Received November 14, 1956

LITERATURE CITED

[1] B. Dogadkin, Chemistry and Physics of Rubber (1947) p. 76; O. B. Litvin, Technology of Synthetic Rubbers (Chem. Press, 1950) p. 415; D. Sandomirskii and V. Charnaia, Trans. Sci. Res. Inst. Rubber Ind. 1, 20 (1954); S. S. Voiutskii, R. M. Panich, and K. A. Kal'ianova, Colloid J. 12, 50 (1950); 13, 89 (1951).

[2] S. S. Voiutskii, Colloid Chemistry of Synthetic Latexes (Chem. Press, 1946) p. 90.**

* The reason for the differences between the calcium numbers for the same latex in Tables 2 and 3 is that the determinations were carried out at different times. The effect of storage is discussed below.

** In Russian.

THE STRUCTURE AND ADSORPTIVE PROPERTIES OF SILICA GELS
PREPARED FROM ALKALINE MEDIA

I. B. Sliniakova and I. E. Neimark

When silicic acid gels are precipitated in presence of excess sodium silicate, the so-called "alkaline silica gels" are formed. The preparation and properties of these gels were studied by Kharmadar'ian and his associates [1], Markov and Nagornaia [2], and Plank and Drake [3]. Kharmadar'ian et al. [1] showed that gels obtained from alkaline media have large pores and low strength. Their explanation for this fact was that when coagulation takes place in an alkaline medium a part of the sodium silicate remains unchanged and fills the structural cavities in the silica gel; these cavities become empty when the gel is washed and give rise to a coarsely porous structure. This explanation seems to us to be improbable.

According to Kharmadar'ian's data [1] the sorptive activity of silica gels washed with hydrochloric acid solution was in two instances somewhat higher than that of a gel washed with water, and in one instance it was the same.

Markov and Nagornaia [2] noted that the number (in %) of small pores is increased when gels prepared in an alkaline medium are washed with acidified water. However, they did not have the modern methods for studying the pore structure of adsorbents at their disposal, and they based their conclusions on studies of static activity which, as is known, cannot provide a complete characterization of the pore structure of silica gels. Plank and Drake [3] found that silica gels precipitated in alkaline media have smaller specific surfaces than gels precipitated in an acid medium.

We showed earlier [4] that the pH of the wash water has a considerable influence on the pore structure of silica gels obtained from acid media. It was therefore of interest to carry out a systematic study of the influence of the pH of the wash waters on the adsorptive properties of alkaline silica gels.

The object of the present investigation was a more detailed study of the pore structure and sorptive properties of gels precipitated from alkaline media, and to determine what factors influence the pore structure of these gels.

Methods for the preparation and testing of the alkaline silica gels. A definite amount of dilute sodium silicate solution was added to sulfuric acid solution, to an alkaline reaction. In order to retard coagulation, which usually occurs instantaneously, dilute solutions of water glass and sulfuric acid (sp. gr. 1.07-1.12) were used; coagulation was observed after 1-2 minutes. This allowed time for thorough stirring of the mixture and determination of the pH of the sol by the potentiometric method with the aid of an antimony electrode. The alkaline hydrogel was aged for two days, and then broken into 1-2 cm pieces and divided into several portions; separate portions were washed by decantation with aqueous solutions of different pH. Acid wash liquors with $\text{pH} < 7.0$ were prepared by addition of different amounts of sulfuric acid to distilled water; alkaline solutions with $\text{pH} > 7$ were made by addition of ammoniacal water. The washed gels were dried in a drying oven at 125° for 6 hours.

For evaluation of the sorptive characteristics of the alkaline silica gels, isotherms for the sorption of methyl alcohol vapor were determined with the aid of a vacuum apparatus with a quartz spring balance. The sorption isotherms were used to calculate the specific surfaces, volumes of the adsorption spaces and transitional pores, and the effective pore radii. The apparent and true densities were determined, the total pore volumes being calculated from the results; the static activity corresponding to the amount of benzene sorbed from saturated vapor was also determined.

Effect of pH of the wash water on the pore structure of alkaline silica gels. Hydrogels precipitated in an alkaline medium were divided into two portions; one was washed with an aqueous solution of pH 2.0-2.5, and the other, at pH 8.5-10.3. The washing was continued for 12 days.

TABLE 1

Sorptive and Structural Characteristics of Alkaline Gels

Series	I		II		III		V		VI	
	1	2	3	4	5	6	13	16	17	22
Specimens										
pH of sol	8.2		8.5		8.6		9.2		10.3	
pH of original wash water	2.0	10.2	2.0	10.2	2.0	8.6	2.1	10.3	2.1	10.3
pH of wash water after 24 hrs.	2.5	9.8	2.0	10.0	2.2	8.6	2.0	9.8	2.2	10.2
Apparent xerogel density, g/cc	0.87	0.85	0.84	0.78	0.75	0.78	0.87	0.82	0.77	0.84
Total pore volume, cc/g	0.70	0.72	0.74	0.83	0.87	0.83	0.70	0.76	0.84	0.74
Limiting sorptive pore vol., cc/g	0.74	0.72	0.72	0.80	0.88	0.80	0.70	0.75	0.84	0.74
Vol. of adsorption space, cc/g	0.47	0.14	0.44	0.10	0.39	0.26	—	—	—	—
Effective pore radius in Å	15	22	14	26	17	26	23	31	20	37
Spec. surface in m ² /g, by BET equation	570	280	687	357	695	495	—	398	522	304
Same, Kiselev's method	580	319	668	428	675	495	—	420	515	319

The sorptive and structural characteristics of these silica gels are given in Table 1.

Comparison of the structural and sorptive characteristics of silica gels the alkaline hydrogels of which had been washed with solutions at pH 2 and pH 10.3 respectively (see Table 1) shows that their total pore volumes and limiting sorptive volumes are similar, but their specific surfaces differ. Further investigations showed that the pore volume distributions by radius are also different for these gels.

Figures 1 and 2 show isotherms for the sorption of methyl alcohol vapor on silica gels, the hydrogels of which were prepared in an alkaline medium and washed with solutions at pH 2.0 and pH 8.6-10.3 (Specimens 1, and 2; 17 and 22). The black points represent desorption. The upper portions of the diagrams give the differential curves for pore volume distribution by effective radius.

It is seen in Figs. 1 and 2 that in every instance the sorption isotherms for silica gels washed with acid water lie above the corresponding curves for gels washed with alkaline water, in the region of low relative vapor pressures. This shows that the gels washed with acid water have highly developed micropores, and therefore greater specific surfaces. The effective pore radius in these gels is low. For example, silica gel specimens 1 and 2 of Series I, which differ only in the washing conditions, have very different pore distributions: specimen 1 washed with a solution of pH 2.0, has a predominant pore radius of 15 Å, while the silica gel washed with alkaline water (specimen 2) has a value of 22 Å. The volume of the adsorption space is 0.47 cc/g in the former case, and 0.14 cc/g in the latter. The specific surface of the former specimen is double that of the latter (see Table 1).

The high specific surface and the relatively high limiting sorptive capacity of alkaline gels washed with water at pH 2.0 is noteworthy. Silica gels of mixed structure, with extensive volumes of both fine and coarse pores have not been described in the literature.

In all probability, the reason for the considerable increase of the specific surface of alkaline silica gels when their hydrogels are washed with acid solutions at pH 2.0 is that the acid of the wash water reacts with the

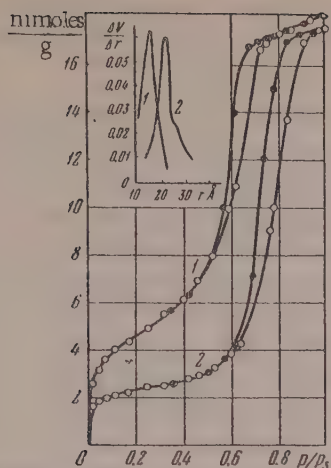


Fig. 1. Isotherms for the sorption of methyl alcohol vapor on alkaline silica gels: 1) specimen 1, washed at pH 2.0; 2) specimen 2, washed at pH 10.2.

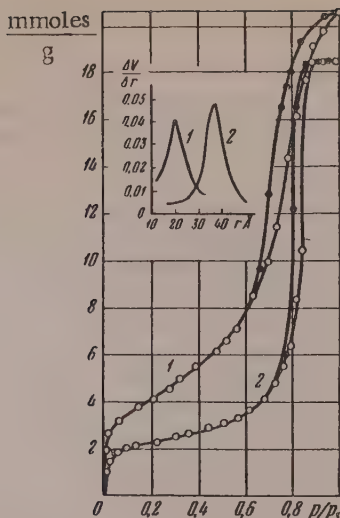


Fig. 2. Isotherms for the sorption of methyl alcohol vapor on alkaline silica gels: 1) specimen 17, washed at pH 2.1; 2) specimen 22, washed at pH 10.3.

TABLE 2

Sorptive and Structural Characteristics of Alkaline Gels Washed With Weakly Acid Waters

Series	IV			V		VI			VII		
	Specimens	8	9	10	14	15	18	19	20	24	25
pH of sol		8.1			9.2		10.3		10.3		
pH of original wash water	2.6	6.6	6.8	6.6	6.8	2.6	6.6	6.8	6.6	6.8	
pH of wash water after 25 hours	8.4	8.8	8.3	8.8	8.5	8.5	9.1	8.8	8.0	8.0	
Apparent density, g/cc	0.87	0.87	0.84	0.92	0.87	0.88	0.90	0.85	0.75	0.75	
Total pore vol., cc/g	0.70	0.70	0.74	0.63	0.70	0.68	0.66	0.72	0.86	0.87	
Limiting sorptive pore vol., cc/g	0.70	0.70	0.72	0.64	0.70	0.65	0.67	0.74	0.86	0.89	

unchanged sodium silicate retained in the intermicellar spaces, forming silicic acid sol, and then gel. As the additional precipitation of the silicic acid takes place in an acid medium, mainly fine pores are formed, giving rise to an extensive specific surface in the alkaline silica gels.

It was important to determine the influence of washing on the structure of alkaline silica gels, with the use of weakly acidic solutions ($\text{pH} > 2.0$) in which the hydrogen ion concentration is not sufficient for additional precipitation of the residual sodium silicate. For this, 4 series of silica gels were prepared, the hydrogels being washed with waters at pH from 2.6 to 6.8.

The salts formed in the precipitation of a hydrogel are usually washed out of it within 10-12 days. When alkaline hydrogels were washed with weakly acidic waters for a fairly long time (20 days), it was found that the wash waters became alkaline. Despite the fact that the hydrogel was covered daily with a fresh portion of acidified water at pH 2.6-6.5, after 24 hours this water became alkaline, and had pH 8.0-8.8 (see Table 2). The lumps of the alkaline hydrogel became loose and crumbled into smaller pieces. Silicic acid was detected in the wash waters.

Table 2 gives the changes in the reaction of the wash water after the washing of the hydrogels, and the structural characteristics of the silica gels formed.

It follows from these results that the total pore volumes of the alkaline silica gels formed differ very little from each other. The isotherms for the sorption of methyl alcohol vapor on these specimens almost coincide (see Fig. 3). The specific surface of these gels is low.

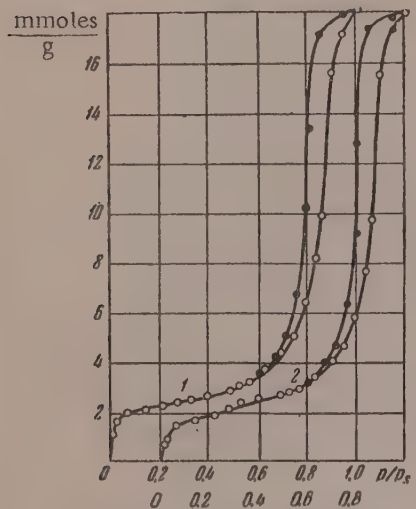


Fig. 3. Isotherms for the sorption of methyl alcohol vapor on alkaline silica gels: 1) specimen 18, washed at pH 2.6; 2) specimen 19, washed at pH 6.6.

The formation of complex silicates is possible when silicic acid gel is precipitated in an alkaline medium (with excess of sodium silicate). Evidence for this is provided by Krestinskaya's results [5], indicating the formation of complex silicates by the action of alkali on silicic acid sol, and also by the results obtained by one of us jointly with Iankovskaya and Piontkovskaya [6] in experiments with the use of tagged calcium. The complex silicate formed probably enters the nucleus of the micelle, while the simpler silicate, capable of dissociation, is on the micelle surface. When an alkaline gel is washed with a weakly acidic solution, ion exchange probably takes place between the cations of the silicate on the micelle surface and the hydrogen ions of the wash water. As a result, the wash water becomes alkaline. The alkali formed in the solution partially dissolves silicic acid from the gel surface; the silicic acid can be detected in the wash water by means of the ammonium molybdate reaction. Dubrovo's data supports this view [7].

Since all the alkaline hydrogels have the same reaction ($\text{pH} \sim 8.5$) after being washed with acid water, irrespective of the pH of the original wash water, the resultant silica gels should all have the same structure; this is found to be the case (see Table 2 and Fig. 3).

When the alkaline hydrogels were washed with acid solutions ($\text{pH} \sim 2.0$) (see Table 1), the wash waters did not become appreciably more alkaline. This is probably because the alkali formed as the result of ion exchange has little influence on the pH of the water owing to the high excess of hydrogen ions in the latter. No SiO_2 was detected in the wash liquor with which the alkaline hydrogel had been converted for a considerable time. Evidently peptization of the alkaline hydrogel does not take place in wash waters with high hydrogen ion contents.

All the alkaline hydrogels had a large volume of coarse (transitional) pores. This is probably the consequence of the definite precipitation conditions in an alkaline medium, leading to aggregation of the micelles into larger particles. When such a hydrogel is dried, the packing of the primary particles is looser and the cavities between them are larger, leading to the formation of large pores. Moreover, when waters at $\text{pH} 8.6-10.2$ are used for the washing the framework of the alkaline hydrogel is strengthened and such a gel offers a greater resistance to compression under the action of capillary forces during drying, so that a coarsely porous silica gel is formed.

These experimental results show that it is possible to prepare silica gels of mixed structure and large specific surface, containing considerable volumes of both fine and transitional pores.

Alteration of the structure of alkaline silica gels by treatment of their hydrogels with concentrated acids. It was of interest to find the effect of treatment of the washed hydrogels with concentrated acids on the pore structure of the dried silica gels. In these experiments hydrogels were precipitated in an alkaline medium, washed free of salts with ammonia solution of $\text{pH} 9.8-10.0$, and divided into several portions. One portion was immediately dried at 125° ; this provided the control specimens (Nos. 2 and 4), while the other portions were treated with 6 and 10 N sulfuric acid or 6 and 10 N hydrochloric acid for two days. After the acid treatment the hydrogels were washed with distilled water to a negative reaction for SO_4^{2-} or Cl^- and dried at 125° in a drying oven (specimens 38, 40, 43, and 51).

The structural and sorptive characteristics of alkaline silica gels the hydrogels of which were treated with acids are given in Table 3; data on the structure of the control specimens are given for comparison.

TABLE 3

Structure and Sorptive Characteristics of Alkaline Silica Gels Treated With Acids

Specimen	pH of hydrogel wash water	Acid used for treatment of washed hydrogel	Apparent density in cc/g	Total pore volume in cc/g	Effective pore radius in Å	Specific surface in m ² /g	
						BET method	Kiselev's method
2 (control)	9.8	—	0.85	0.72	22	280	319
40	9.8	6 N HCl	0.70	0.96	31	518	522
43	9.8	10 N HCl	0.72	0.94	30	568	578
38	9.8	10 N H ₂ SO ₄	0.69	1.00	35	536	534
4 (control)	10.0	—	0.78	0.83	26	357	420
51	10.0	6 N H ₂ SO ₄	0.68	1.01	35	640	660

It follows from Table 3 that impregnation of alkaline hydrogels, previously washed with ammoniacal water (pH 9.8-10.0), with fairly concentrated acids leads to increases of the total porosity and of the specific surface, the latter being roughly doubled.

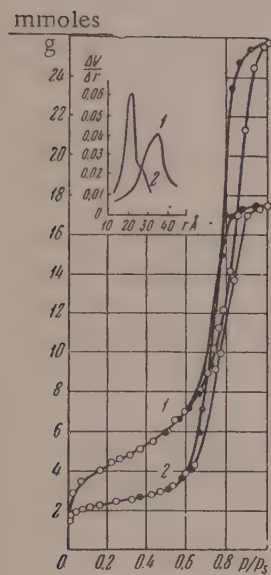


Fig. 4. Isotherms for the sorption of methyl alcohol vapor on alkaline silica gels washed with ammoniacal water: 1) specimen 2, control; 2) specimen 38, treated with 10 N H₂SO₄.

Figures 4 and 5 give the isotherms for the sorption of methyl alcohol vapor on the control specimens (2 and 4), washed with ammoniacal water, and on specimens 38 and 51, the hydrogels of which had been treated with concentrated acids after washing. It follows from these isotherms and the curves for pore volume distribution by effective radius (see the upper portions of the diagrams) that the volume of the micropores in the dry silica gels is increased as the result of acid treatment of hydrogels washed with solutions

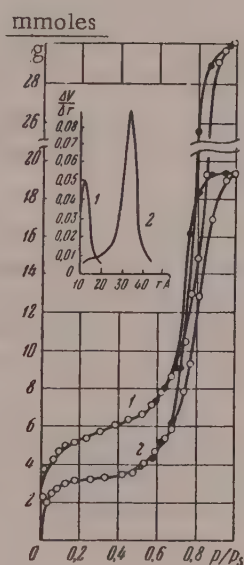


Fig. 5. Isotherms for the sorption of methyl alcohol vapor on alkaline silica gels washed with ammoniacal water: 1) specimen 4, control; 2) specimen 51, treated with 6 N H₂SO₄.

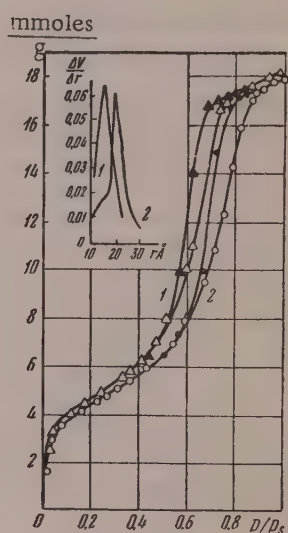


Fig. 6. Isotherms for the sorption of methyl alcohol vapor on alkaline silica gels washed with water at pH 2.0: 1) specimen 1, control; 2) specimen 36, additionally treated with 6 N H₂SO₄. Black triangles represent desorption. Curves for pore volume distribution by effective radius are shown at the top.

at pH 10.3. This is shown by the sharp ascent of the isotherms at comparatively low relative pressures. The pore diameters of these silica gels also show some increase. The limiting sorption capacity of the treated silica gels increased (see Figs. 4 and 5).

TABLE 4

Structure and Sorptive Characteristics of Alkaline Silica Gels Treated With Acids

Specimen	pH of hydrogel wash water	Acid used for treatment of hydrogel	Apparent density in g/cc	Total pore volume in cc/g	Effective pore radius in A	Specific surface in m ² /g	
						BET method	Kiselev's method
1 (control)	2.0	—	0.87	0.70	15	570	580
36	2.0	6 N H ₂ SO ₄	0.81	0.78	19	550	553
39	2.0	10 N HCl	0.81	0.78	18	595	594
3 (control)	2.0	—	0.84	0.74	14	687	668
49	2.0	6 N H ₂ SO ₄	0.82	0.76	17	700	684

The probable reason for the change in the structure of alkaline gels washed with ammoniacal water and then treated with concentrated acids is that during the washing the ammoniacal solution peptizes the gel, and silicic acid is formed in the intermicellar spaces. Treatment with concentrated acid results in secondary coagulation of the silicic acid, with a consequent increase of the specific surface of the silica gel formed. Moreover, the concentrated acid partially dehydrates the silicic acid micelles and thereby strengthens the gel framework, leading to the formation of more coarsely porous structures, with greater limiting sorptional pore volumes.

Treatment of alkaline hydrogels, previously washed with acid solutions (pH 2.0), with concentrated acids (specimens 36, 39, and 49) does not increase the already large specific surface, but merely increases somewhat the effective pore diameter (see Table 4).

Figure 6 shows the isotherms for the sorption of methyl alcohol vapor, and differential distribution curves, for control specimen 1 and for specimen 36, the hydrogel of which had been washed in a solution at pH 2.0 and then treated with 6 N sulfuric acid, followed by washing with distilled water. It is seen that the isotherms for both specimens have initial steep rises, which indicate extensive microporosity and a large specific surface. However, at higher relative pressures the sorption isotherms for specimen 36 is further to the right, indicating an increase of the pore size in the gel.

The probable reason why concentrated acid treatment of alkaline gels washed with solutions at pH 2.0 does not increase the already large micropore volume is that the secondary coagulation of silicic acid in the intermicellar spaces have already taken place during the first acid wash.

SUMMARY

- Washing of alkaline hydrogels with acid waters (pH 2) yields coarsely porous silica gels with large specific surface. The increase of the micropore volume in these silica gels is probably the result of secondary coagulation of the unreacted sodium silicate in the intermicellar spaces under the action of the acid waters.
- If alkaline hydrogels are washed with weakly acid solutions ($\text{pH} > 2.0$), the wash waters become alkaline, possibly as the result of ion exchange between the cations of the silicates in the micelles and the hydrogen ions of the acids in the wash waters. These coarsely porous silica gels have a small specific surface.
- If alkaline hydrogels, previously washed with ammoniacal water, are treated with concentrated acids, silica gels of large micropore volume and very high total porosity are formed. Treatment of alkaline hydrogels, previously washed with acid water, with concentrated acids merely increases the effective pore radius in these silica gels.

4. It has been shown for the first time that silica gels of mixed structure and of large specific surface (600 m²/g) can be prepared.

The L. R. Pisarzhevskii Institute
of Physical Chemistry
Academy of Sciences, Ukrainian SSR
Kiev

Received November 16, 1956

LITERATURE CITED

- [1] M. O. Kharmadar'ian and E. G. Kopelevich, *J. Chem. Ind.* 7, 1484 (1930); 7, 31 (1932).
- [2] V. K. Markov and N. A. Nagornaia, *J. Appl. Chem.* 10, 853 (1937).
- [3] C. J. Plank and L. C. Drake, *J. Colloid Sci.* 2, No. 1, 399 (1947).
- [4] I. E. Neimark and I. B. Sliniakova, *Colloid J.* 18, 219 (1956).*
- [5] V. P. Krestinskaia and N. E. Natanson, *Colloid J.* 2, No. 7, 599 (1936).
- [6] G. F. Iankovskaia, M. A. Piontkovskaia, and I. E. Neimark, *Proc. Acad. Sci. Ukrainian SSR* No. 1, 91 (1955).
- [7] S. K. Dubrovo and Iu. A. Shmidt, *Bull. Acad. Sci. USSR, Div. Chem. Sci.* No. 4, 597 (1953).*

* Original Russian pagination. See C. B. Translation.

PROCESSES OF STRUCTURE FORMATION IN MILK FAT AND THEIR SIGNIFICANCE IN THE PRODUCTION OF BUTTER

A. I. Titov, I. N. Vlodavets and P. A. Rebinder

The development of physicochemical mechanics [1] is continuously widening the range of important practical problems where the application of this science gives very valuable results. The necessity of conferring predetermined mechanical properties on particular materials arises not only in the development of methods for the production of new plastics, building materials, and heat-resisting alloys, but also in reassessment of technological processes for the production of substances which have long been known, where at first sight it might seem difficult to introduce an element of novelty.

The production of butter, one of the most important consumer products, is being rapidly modernized. The lengthy and laborious process of churning in cumbersome batch churning is being replaced by a continuous process, based on the cooling and mechanical treatment of high-fat cream in continuous coolers fitted with agitators. The product leaving the cooler is fed directly into packages, where it hardens and turns into butter of normal composition, excellent flavor characteristics, and adequate keeping qualities.

However, this efficient process does not always yield butter of good enough consistency, and study of methods for regulating the mechanical properties of butter is therefore of urgent importance.

The consistency of butter should conform to the following requirements: 1) the butter should not be too "soft," and a lump should retain its form, without spreading even at 20-25°; 2) the butter should not be too "hard," "brittle," "splittable," or "crumbly;" it should be fairly plastic even at 10-15°; 3) the butter should be macrohomogeneous: it should not leave a "sandy" or "floury" sensation on the tongue, and it should not separate into individual layers.

Attempts to replace these descriptive evaluations by objective determinations of mechanical properties have given rise to many different instruments and methods of measurement [2], for evaluation of the strength properties of the test samples in various ways. Most of these methods are empirical.

Characterization of the mechanical properties of milk fat and butter. Precise temperature control is particularly important in studies of the mechanical properties of butter and fats. Such temperature control is conveniently effected in the Höppler consistometer, in which the speed of immersion of a ball pushed by means of a thin rod under the action of a known load along the axis of a vertical cylinder filled with the substance under test is measured. The cylinder can be filled by direct insertion into a lump of butter; with the lower end of the cylinder closed by an air-tight lid, the mechanical properties of the specimen can be studied with its structure practically undisturbed.

Figure 1 gives curves for the deformation (ϵ) as a function of time (T) at different values of the effective shearing stress, for a milk fat sample determined at 15° in the region of creep flow by means of the Höppler consistometer. The depth of immersion was taken as the measure of deformation, and the load per unit cross section of the sphere was taken as proportional to the effective shearing stress (P). It is seen in Fig. 1 that milk fat exhibits appreciable elastic properties in this region. After a sufficiently long time, the flow process becomes steady without breakdown of the structure. At higher shearing stresses the structure breaks down very rapidly, and the flow rate rises sharply.

We investigated the extent to which the flow curves obtained with the aid of this instrument satisfy the principal criterion for the admissibility of "semiabsolute" methods — the criterion of invariancy, independence

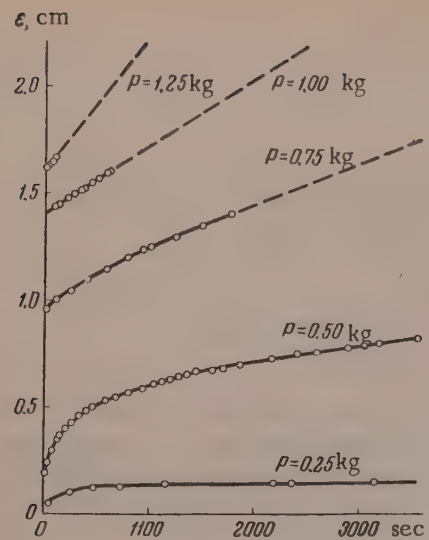


Fig. 1. Deformation - time curves.

instance it proved convenient to use the value of the effective viscosity η at a constant immersion rate of 0.01 cm/second of a sphere 0.799 cm in radius. Determination of this value requires the least number of measurements, but, as Fig. 3 shows, it is approximately proportional to η^* and P_m .

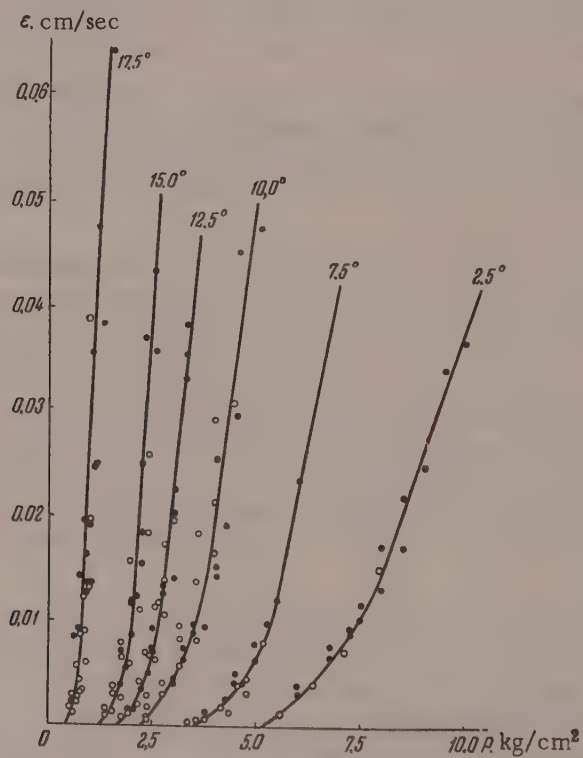


Fig. 2. Flow curves for milk fat samples:
black circles — rate of immersion of a sphere 0.799 cm
in radius; white circles — 0.278 of the rate of immersion
of a sphere 0.635 cm in radius.

of the geometrical dimensions of the instrument [3]. For a highly viscous true liquid (colophony at 60°), measurements with spheres of two different radii (0.799 cm and 0.635 cm in a cylinder of 1.008 cm radius) gave equal values of the deformation rate ($\dot{\epsilon}$), which in the case of the smaller sphere is taken as 0.278 of the steady immersion rate, at equal values of the shearing stress. The viscosities calculated in absolute units also coincided. Similar curves were obtained for milk fat cooled in a continuous flow cooler at a rate of 0.11° per second, and kept at 8°. The determinations were performed at various temperatures, at which the samples were previously conditioned for 1 hour. As Fig. 2 shows, here also the flow curves obtained by means of the Höppler consistometer with the use of spheres of different sizes are also practically invariant; the use of this instrument for the study of such systems is therefore fully justified.

The strength properties of disperse structurized systems are often characterized by the value of the dynamic limiting shearing stress P_m , determined by extrapolation of the linear portion of the low curve to the abscissa axis. The plastic viscosity η^* is usually also calculated. In the present

It is evident from Figs. 2 and 3 that the mechanical properties of milk fat vary considerably with small changes of temperature. The reason is that the state of aggregation of most of the fat changes in this particular region.

For brevity, we shall use the term effective viscosity for the quantity determined by the method described above at 12°. This was taken as the standard temperature.

Observations on a large number of samples of milk fat and butter showed the optimum consistency in relation to organoleptic evaluation corresponds to effective viscosities in the range of $2 \cdot 10^5$ - $3.5 \cdot 10^5$ poises.

Samples with effective viscosity $< 2 \cdot 10^5$ poises usually had "weak," "smearing" consistency, while samples with effective viscosity $> 3.5 \cdot 10^5$ poises had excessively hard, "brittle," or "splitting" consistency.

Characteristics of the process of crystallization of milk fat. Milk fat in the liquid state is a homogeneous mixture of fatty acid glycerides, with small amounts of carotenoids, cholesterol, fat-soluble vitamins, and free fatty acids. On cooling, the solution becomes supersaturated with respect to individual groups of components; first, the highest-melting glycerides, and on further cooling, the glycerides melting at lower temperatures.

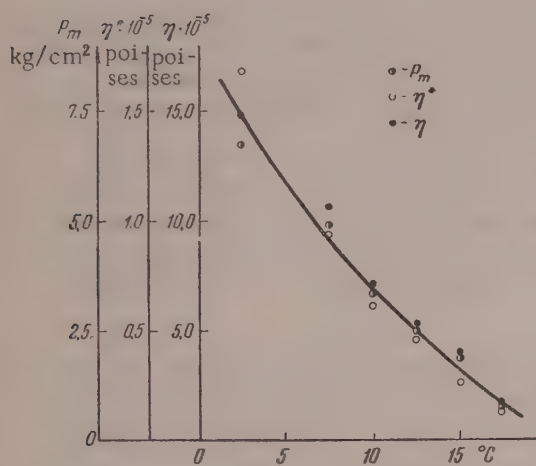


Fig. 3. Effect of temperature on the limiting shearing stress P_m , plastic viscosity η^* , and effective viscosity η at a deformation rate of 0.01 cm/second.

at $\sim 6\text{-}8^\circ$. The maximum rate of crystal growth is found at $\sim 20^\circ$.

If cooling of the fat is interrupted at 20° or somewhat higher, the low rate of formation of the crystallization centers in conjunction with the high rate of crystal growth leads to the formation of large grains, crystalline aggregates 20-60 μ in diameter. Our experiments showed that this may occur in the continuous butter-making process. If the chilling in a continuous cooler is interrupted at 20° or higher, the butter acquires a "loose" consistency, and becomes "floury" or "sandy."

When the pure fat is rapidly cooled to below 0° , it passes into an amorphous, glassy state, described by Ravich and Tsurinov [6] as the γ -phase. At temperatures above zero the γ -phase is converted relatively rapidly into metastable α -modifications, and then into stable β -forms. Unfortunately, the polymorphism of milk fat has been studied very little. Mulder [4] reports that metastable phases generally cannot be detected if the liquid phase is present. The highly interesting question of the possibility of modifying the crystallization process of the fat by means of the surface-active components present in it also requires study.

Formation of butter during the churning of cream. When in the disperse state, the fat has a great tendency to undercooling, and therefore cream containing 25-40% of fat is usually cooled to $6\text{-}8^\circ$ and kept at that temperature for about 18 hours before churning. The crystallization in a fat globule usually begins with orientation of

According to Mulder's observations [4], the lower the temperature at which the fat crystallizes, the lower will its melting point be. The reason is that milk fat can give rise to continuous series of mixed crystals of variable composition. In crystallization at low temperatures a greater proportion of low-melting glycerides enters the solid phase. The total amount of solid phase formed in nonisothermal crystallization increases with the rate of cooling. During rapid cooling, equilibrium does not become established at each given temperature, the crystallization proceeds at lower temperatures, and a greater proportion of low-melting glycerides enters the solid phase. During slow cooling, fractional crystallization takes place [5], and a larger proportion of the low-melting glycerides remains in the liquid phase.

The "melting point" of milk fat, i.e., the temperature at which the highest-melting crystals dissolve in the liquid phase, fluctuates between 28 and 36° according to composition. The "solidifying point," i.e., the temperature at which the first crystals form in the liquid fat, is in the 15-25° range. The maximum rate of formation of crystallization centers is probably found

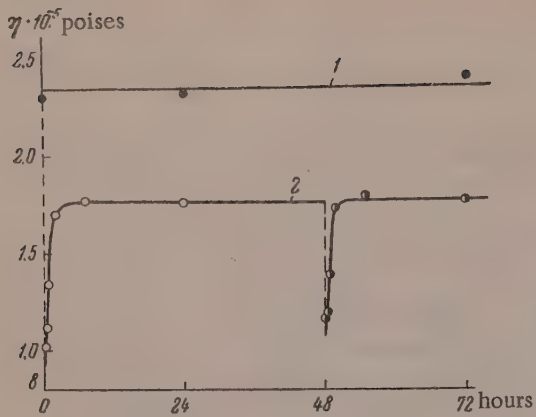


Fig. 4. Variations of effective viscosity of a butter sample as the result of structural breakdown at 12°: 1) untreated butter; 2) butter subjected to mechanical treatment twice (at 0 and 48 hours).

If, as is usually the case in production conditions, extensive cream-air interfaces are formed during the churning, flotation processes begin to play an important part; they accelerate the churning process by facilitating hydrophobization of the globule surfaces and assisting local increases in their concentration and formation of lumps [13]. Aggregation of the fat particles ultimately leads to the formation of macroscopic "grains." The mechanical treatment which follows washing of the "grains" leads to the formation of a macrohomogeneous "slab" of butter.

The microscopic picture of the colloidal structure of butter can be characterized as follows: butter is a gel-like disperse system in which liquid fat forms the continuous phase. Droplets of aqueous phase and microscopic aggregates consisting of fibrous crystals of colloidal dimensions are distributed in this phase. Some of these formations retain the form of undestroyed fat globules. Air bubbles may also be present in butter; it is also usually permeated by veins of a continuous aqueous phase.

Freshly made butter has a pastelike consistency. This becomes firmer with time. Two processes should be distinguished here: "hardening," or further crystallization of part of the milk fat, and "setting," or the development of a thixotropic coagulation structure from the disperse solid phase present. The structure of milk fat in butter is to be classified as a mixed, crystallization-coagulation structure [14].

The variation of the effective viscosity of a butter sample as the result of mechanical breakdown of its structure at a constant temperature of 12° is given in Fig. 4. After the butter had been passed through a grinder, the effective viscosity fell sharply (from $2.3 \cdot 10^5$ to $1.0 \cdot 10^5$ poises) but after several hours at rest it rose to $1.7 \cdot 10^5$ and then ceased to increase. After 48 hours the structure was again broken down in the grinder. After an abrupt decrease, the effective viscosity again rose to $1.7 \cdot 10^5$ poises. The effective viscosity of a control sample, not subjected to mechanical treatment, remained at $2.3 \cdot 10^5$ throughout. The picture was qualitatively quite analogous to that seen in a study of calcium stearate oleogels [15], although the observed changes were smaller in the case of butter. The irreversible decrease of effective viscosity — relatively small in this instance, from $2.3 \cdot 10^5$ to $1.7 \cdot 10^5$ poises — was the result of irreversible brittle destruction of the crystallization structures, which are evidently rather weakly developed in butter.

The reversible change of effective viscosity as the result of repeated mechanical treatment, and the existence of perfect thixotropy in butter subjected to such treatment, are indicative of a thixotropic structure of the coagulational type. Its breakdown is of the nature of plastic flow, and the buildup rate increases with increase of temperature, as contact between individual crystalline particles is facilitated by intensification of Brownian movement [15]. In the experiments described above the restoration of the coagulational structure

molecules of the highest-melting glycerides near the surface, leading to the formation of a birefringent layer, detectable by means of the polarization microscope [7]. The theory [8], that the phosphatides, including lecithin, present on the globule surface crystallize first is not in harmony with data on the phosphatide content of milk, according to which they could form only a monomolecular layer on the globule surface [7]. Such a thin film cannot crystallize in the ordinary meaning of the word, although, of course, the possibility is not excluded that it can give rise to surface nuclei on which the glycerides crystallize.

The fat globules in chilled cream ready for churning consist of solid "shells" with liquid or gelatinous contents. During churning the globules collide, the "shells" break down, and their contents coalesce forming lumps of fat. This process can occur at an appreciable rate in a homogeneous shear field, in absence of frothing [9, 10], especially at high fat contents in the cream. The kinetics of this process resembles the kinetics of coagulation processes [11, 12].

required only a few hours (at 12°), while according to Mulder's data [4] the setting process may continue for weeks and months at lower temperatures.

Our experiments showed that butter or milk fat with defects of consistency, such as "brittleness" or "crumbliness," i.e., with a tendency to brittle breakdown, has a structure of a pronounced crystallizational character. After mechanical treatment the effective viscosity of such samples usually decreased severalfold, and was restored, as the result of thixotropic processes, at a considerably lower level than the effective viscosity of the original sample.

On the other hand, samples of "weak," "smearing" consistency, with a tendency for the separation of liquid fat, i.e., a peculiar form of syneresis, were almost devoid of any signs of a crystallizational structure; their effective viscosity remained almost without any decrease after mechanical treatment followed by thixotropic buildup, although its level was fairly low.

Butter of optimum consistency should have a structure of a predominantly coagulational type, fairly plastic, without brittle properties. A total absence of crystallizational structures, however, is also undesirable.

Formation of butter by the chilling and mechanical treatment of high-fat cream. Continuous processes of butter making, based on chilling and mechanical treatment of high-fat cream containing ~83% fat, differ in the conditions in which the structurization processes occur rather than in the nature of the process of aggregation of the fat globules. Only the earliest stage of crystallization occurs when the fat is in a disperse state. As soon as hardening of the outside layers of the fat globules begins, rapid and almost total destabilization of the cream takes place in the continuous flow cooler under vigorous mechanical treatment. During the subsequent crystallization the continuous fat phase predominates.

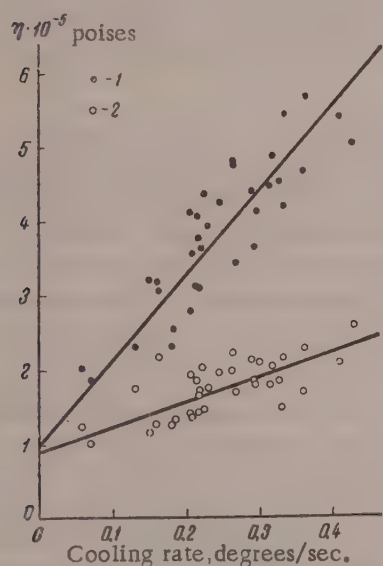


Fig. 5. Effective viscosity of milk fat cooled to 14-20° in a continuous flow cooler with a mixer at different rates:
1) after keeping at 8° for 24 hours; 2) after additional mechanical treatment and thixotropic setting at 8° for 24 hours.

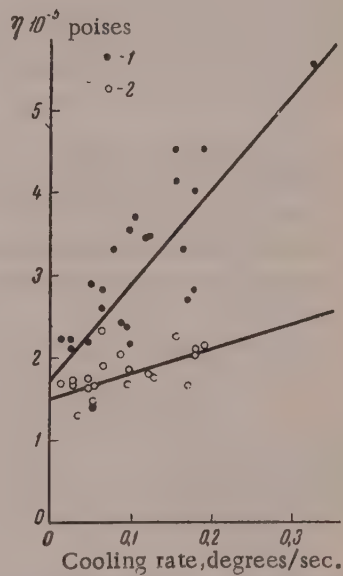


Fig. 6. Effective viscosity of butter made in an industrial continuous flow cooler at different cooling rates: 1) After keeping at 8° for 24 hours; 2) after additional mechanical treatment and thixotropic setting at 8° for 24 hours.

Figure 5 shows the results of determinations of the effective viscosity of milk fat passed through a laboratory one-cylinder cooler fitted with a mixer. The final temperature of the chilled fat varied in the fairly narrow range of 14-20°; the cooling rate, calculated as the decrease of the temperature of the fat in the cooler divided by the time the fat was present in it, was varied between 0.05 and 0.45 degrees/second. The determinations were carried out on samples which had been kept in a cooler at 8° for 24 hours. The results of measurements

of the effective viscosity of the same samples of milk fat the structure of which had been broken down in a grinder and restored over a period of 24 hours at 8° are also shown.

The regression lines in the diagram show that in both cases the effective viscosity increases approximately linearly with the rate of cooling. Curve 2, which corresponds to fat subjected to mechanical treatment after hardening, shows that the effective viscosity increases with the cooling rate even in a purely coagulatory, thixotropic structure. This is a consequence of the above-mentioned increase of the total amount of solid phase with increase of the cooling rate. The effective viscosity of fat which had not been subjected to additional mechanical treatment after cooling increases to a considerably greater extent with the cooling rate. The simultaneous increase of the difference between the effective viscosities of these samples before and after breakdown of the structure indicates an increase in the role played by the crystallizational structure.

The longer the crystallizing fat remains in the cooler, in conditions of vigorous agitation, the less fat remains capable of crystallizing and forming crystallizational structures after leaving the cooler. In the limit, with infinitely slow cooling and an infinite time in the cooler, crystallizational structures may not be formed at all, and the effective viscosity of the product should be equal to the effective viscosity of a fat with a coagulatory structure. In fact, extrapolation of both regression lines to zero rate of cooling (Fig. 5) gives approximately equal values for the effective viscosity.

Similar results were obtained when high-fat cream was cooled in an industrial continuous cooler of the All-Union Scientific Research Institute of the Dairy Industry (Fig. 6). This confirms once again that the consistency characteristics of butter are entirely determined by the crystallization conditions of the milk fat.

One of the commonest faults in butter made by the continuous process is flakiness. Our experiments showed that this fault may occur not only in butter, but also in milk fat subjected to cooling in a continuous cooler; its appearance is always associated with the formation of stable crystallizational structures. Flakiness occurs when the crystallization process passes only through its earliest stages in the cooler, i.e., when the cream or fat is passed through the cooler at a very high rate. In such cases the hardening, i.e., formation of crystallizational structures is so rapid when the product leaves the cooler that the upper layers do not have time to mix with the lower before fluidity is finally lost.

Methods of regulating the consistency of butter. The processes of butter making cannot be completely standardized, as the composition of milk fat varies in fairly wide limits according to the feeding conditions of the animals, and therefore according to the season of the year and local conditions. "Winter" fat usually has a lower content of unsaturated fatty acid glycerides, and gives a harder, crumbly, brittle butter. "Summer" fat, on the other hand, may contain an excess of low-melting unsaturated glycerides, yielding a butter of "weak," "smeary" consistency, with a tendency to separation of the liquid phase. The situation is complicated by the fact that butter should have exactly the reverse properties — maximum plasticity in winter, and higher strength in summer.

It is clear from the foregoing that undesirable changes in the properties of the fat can be compensated to some extent by modification of the technological conditions in butter making. To make "summer" butter harder and less prone to separation of the liquid phase, it should be made in such a way that, first, the maximum amounts of the low-melting glycerides enter the solid phase, and second, that stable crystallizational structures have time to develop. In the production of butter by the churning process, increased hardness can be achieved by the following procedures: 1) rapid chilling of the cream and prolonged keeping at the lowest possible temperatures (2-4°); 2) churning and washing, also at the lowest possible temperatures (not above 12°); 3) the minimum of mechanical working; 4) immediate transfer of the finished butter to a cooling chamber.

In the continuous process the same aim can be achieved by cooling of high-fat cream at the highest possible rate to the lowest possible temperatures. This should be done in such a way as not to allow crystallization to become complete in the cooler, so that the butter hardens after leaving the cooler. This will give rise to the most stable crystallizational structures.

To make "winter" butter more plastic, to lower its hardness and brittleness, it is necessary, first, to ensure that as much fat as possible remains in the liquid phase, and second, to prevent the formation of stable crystallizational structures.

In the production of butter by churning, increased plasticity can be obtained by the following sequence of operations: 1) rapid chilling of the cream to 6-8° and brief (2-4 hours) exposure at that temperature, to allow enough crystal nuclei to form in the fat but at the same time not to allow them to become too large; 2) increase of temperature to about 19°, and exposure at that temperature until crystallization is completed; 3) churning at the highest possible temperature (14-16°); 4) cooling of the grains by washing with cold water; 5) fairly vigorous working.

In the production of butter by the continuous process, the plasticity may be increased by a decrease of the cooling rate of the cream. The cream should be first rapidly chilled to 6-8°, to produce a considerable number of crystallization centers, the temperature should then be raised to 16-19°, with continuous stirring until the completion of crystallization if possible, and finally, the temperature should be lowered slowly to 10-12° with continuing mechanical working. This theoretical program, designed for the maximum utilization of the potentialities for increasing the plasticity of butter, cannot be put into practice in all continuous installations. Three- and four-cylinder coolers obviously have advantages over two- and one-cylinder coolers in this respect.

Some increase of plasticity can also be obtained by simpler means. For example, it is possible merely to decrease the cooling rate, so that the crystallization should be as complete as possible during mechanical agitation. By lowering the temperature of the cooling liquid and raising the agitation rate it is possible to make the crystallization more rapid, and therefore more complete, during agitation at relatively high temperatures.

Instead of preventing the formation of crystallizational structures during the cooling process it is possible to allow them to develop and then to break them down by vigorous mechanical treatment. Our experiments showed that additional mechanical treatment may produce a considerable improvement in the consistency of butter with excessive hardness, brittleness, and flakiness.

There is no doubt that detailed studies of structure formation in milk fat will provide the basis for a finalized theory of butter making, founded on the successes of physicochemical mechanics. Without claims to completeness, the purpose of the present work was merely to indicate the general direction of further research in this field, and the prospects of solving important technological problems.

SUMMARY

1. To conform to the consistency requirements of butter, milk fat should form a structure of a mixed crystallization-coagulation type, with a predominance of a coagulatory structure.

2. In the production of butter from cream of any fat content, the surface layers of the fat globules should crystallize and become brittle as the result of cooling, so that their breakdown by mechanical action should lead to the formation of a continuous fat phase.

In the production of butter by churning, crystallization is completed to a considerable extent during preparation of the cream for churning, in absence of a continuous fat phase; aggregation of the fat particles is facilitated by flotation processes at the strongly developed cream-fat interfaces.

In the production of butter by the chilling of high-fat cream in continuous coolers with vigorous agitation, only the earliest stage of crystallization occurs while the fat is in the disperse state; most of the crystals are formed in the continuous fat phase.

3. One of the possible methods for improving the consistency of butter is by regulation of the crystallization temperature of the milk fat. The higher the temperature at which crystallization occurs, the less is the total amount of solid phase formed, and the higher is the plasticity of the product.

4. Another method for improving the consistency is by regulation of the mechanical treatment during hardening. The more complete the crystallization in conditions of mechanical agitation, the less is the possibility of formation of brittle and strong crystallizational structures, and the higher is the plasticity of the butter.

The authors express their deep gratitude to Iu. A. Gusynina and I. I. Favstova, who assisted in the experiments.

LITERATURE CITED

- [1] P. A. Rebinder, "New Problems of Physicochemical Mechanics," Paper at the Permanent Colloquium on Solid Phases of Variable Composition, jointly with the Moscow Colloid Colloquium, January 26, 1956, Moscow.
- [2] G. W. Scott-Blair, Foodstuffs, their plasticity, fluidity and consistency (Amsterdam 1953).
- [3] B. Ia. Iampolskii and P. A. Rebinder, *Colloid J.* 10, 464 (1948).
- [4] H. Mulder, *Nederlands melk en zuiveltijdschrift* 7, 149 (1953).
- [5] M. M. Kazanskii and G. V. Tverdokhleb, *Dairy Ind.* 14, No. 11, 33 (1953).
- [6] G. B. Ravich and G. G. Tsurinov, The Phase Structure of Triglycerides (Izd. AN SSSR, Moscow, 1952).*
- [7] N. King, The Milk Fat Globule Membrane and Associated Phenomena (Russian Translation) (Food Industry Press, Moscow, 1956).
- [8] W. Mohr and E. Mohr, XIV Intern. Dairy Congr. Vol. 2, 273 (1956).
- [9] H. Mulder and J. J. Schols, XIII Intern. Dairy Congr. 2, 706 (1953).
- [10] V. N. Favstova and I. N. Vlodavets, *Dairy Ind.* 17, No. 8, 29 (1956).
- [11] A. D. Grishchenko, *Dairy Ind.* 11, No. 6, 36 (1950).
- [12] I. N. Vlodavets, *Dairy Ind.* 13, No. 12, 30 (1952).
- [13] A. P. Belousov, *Dairy Ind.* 14, No. 9, 28 (1953).
- [14] N. V. Mikhailov and P. A. Rebinder, *Colloid J.* 17, 107 (1955).**
- [15] E. E. Segalova and P. A. Rebinder, *Colloid J.* 10, 233 (1948).

* In Russian.

** Original Russian pagination. See C. B. Translation.

THE HYDROPHILIC PROPERTIES OF MONTMORILLONITE CLAY

E. T. Uskova

There have been very few investigations of the hydrophilic properties of bentonites [1]. The hydrophilic properties of montmorillonite clays were shown to be considerably influenced by adsorbed cations [2]. However, only clays saturated with one given cation were studied. The hydrophilic properties of bentonites with different ratios of two or more cations in the exchange complex were not studied.

In the present investigation the variations in the hydrophilic properties of bentonite at different ratios of univalent and bivalent cations were studied.

The material used was gumbrin from Mtis-Piri, Georgian SSR. The specimens were prepared as follows. The clay was covered with ten times its own bulk of distilled water for 24 hours. The suspension was passed through a sieve of 4900 mesh/cm². The liquid was settled for 24 hours and the sediment was treated by repeated decantation with 1 N NaCl solution to a negative reaction for Ca²⁺. NaCl was not washed out of the sodium gumbrin suspension. Separate portions of the suspension were covered for 24 hours with equal volumes of mixtures of 1 N solutions of CaCl₂ and NaCl, or MgCl₂ and NaCl. Excess electrolytes were removed by dialysis through a collodion membrane at 60-80° for 5-7 days. The suspensions were then evaporated and the residues were dried at 105°.

The adsorbed cations in the specimens were determined by the Gedroits method. The results are given in the Table.

Amounts of Adsorbed Ca²⁺ and Mg²⁺ in Different Specimens of Na-Gumbrin

Specimen No.	Calcium		Magnesium	
	mequiv/g	% of capacity	mequiv/g	% of capacity
1	0	0	0	0
2	123	11.9	97	8.8
3	176	17.1	190	17.3
4	256	24.8	332	30.2
5	462	45.8	479	43.6
6	601	58.3	637	57.9
7	756	73.4	820	74.6
8	872	84.7	950	86.3
9	1030	100	1100	100

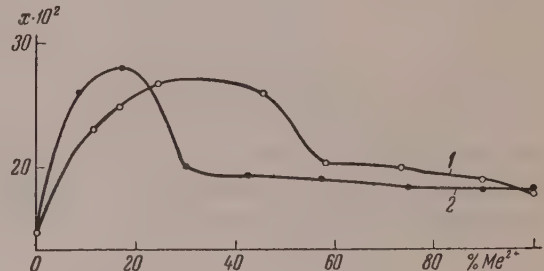


Fig. 1. Effect of the degree of replacement of sodium in sodium gumbrin on the amount of bound water:
1) by calcium; 2) by magnesium.

The amount of water bound by the surface of 1 g of a gumbrin specimen was taken as the measure of its hydrophilic nature. The bound water was found by Dumanskii's indicator method [3]. The indicator used was sucrose solution of about 13-15% concentration. In the determinations of bound water, two weighed samples of each specimen, previously dried at 110° for 12 hours, were covered with sucrose solution and distilled water respectively in weighing bottles. After thorough stirring the suspensions were left in the bottles for 15 minutes to reach equilibrium, and the solutions were then filtered under pressure with the aid of a special funnel. The results are given in Fig. 1.

It is seen in Fig. 1, that when the content of bivalent ions in Na-gumbrin is 20-40% of the exchange capacity there is a sharp increase of hydrophilic nature to a maximum. With further increase of Ca^{2+} or Mg^{2+} contents the amount of bound water decreases smoothly, up to complete saturation with calcium or magnesium.

If the hydration of cations is the only factor to influence the hydrophilic properties of clays, a steady increase of the amount of bound water would be found with increasing contents of bivalent ions in the exchange complex, in the course of substitution of Na ions by Ca or Mg ions in the gumbrin. However, the curves in Fig. 1 show that this is not the case. There is evidently some other factor, which in its turn depends on the adsorbed cations, influencing the hydrophilic properties of the clay. This factor may be the value of the zeta potential. The zeta potential was measured by the electrophoretic method [4]. The determinations were carried out on 1% suspensions of gumbrin. In more concentrated suspensions the migration rate of the suspensions was lower, probably owing to the formation of a spatial structure.

The composition and conductance of the auxiliary liquid are of great importance in electrophoresis [5]. Ultrafiltrate was used as the auxiliary liquid. It is known, however that the conductance of an ultrafiltrate is lower than that of the corresponding suspension, and this is undesirable. The ultrafiltrate was therefore obtained from a more highly concentrated suspension (6%) by pressure filtration through a dense ashless filter. The first turbid drops were rejected, and the clear liquid filtered through the clay layer was collected. The residue from the 6% suspension was diluted down to 1% concentration, and the ultrafiltrate was diluted to the same conductance as this suspension.

Some of the samples, with high contents of adsorbed calcium or magnesium, which did not give stable suspensions, were studied by the electroosmotic method. It proved possible to use both methods on one of the samples, containing 74.6% of magnesium. The values for the zeta potential were similar (8.8 mv by electrophoresis and 8.2 mv by electroosmosis).

The values of the electrokinetic potential found by the two methods are therefore comparable. Further evidence for this is the fact that the experimental data obtained by the electrophoretic and electroosmotic methods fit satisfactorily on a common curve (Fig. 2).

As in the case of kaolinite clay [6], when the amount of adsorbed calcium or magnesium increases, with a corresponding decrease of adsorbed sodium, the zeta potential does not decrease steadily but passes through a maximum. The value of the zeta potential remains relatively high all along the curve; its minimum value is 8.2 mv.

When water is bound by gumbrin, as by kaolinite clay, differences in the degree of hydration of the adsorbed cations have an appreciable influence. Increase of the contents of strongly hydrated calcium and magnesium ions results in increased hydrophilic properties — all the points on the curve lie above those for the pure sodium gumbrin.

Fig. 2. Variation of the zeta potential of gumbrin samples with the degree of substitution of sodium in sodium gumbrin: by calcium (1) and by magnesium (2); ●) electrophoresis; ○) electroosmosis.

The introduction of relatively small amounts of bivalent cations produces a sharp increase in the amount of bound water. Incidentally, it should be noted that Mg increases the hydrophilic nature of bentonite to a greater extent than calcium in the region studied. The hydrophilic maximum corresponds to a lower content of adsorbed magnesium, but its absolute value is greater than for calcium.

The existence of a hydrophilic maximum is accounted for by the existence of a maximum of the zeta potential in this region, as shown by the curves in Figs. 1 and 2. This effect confirms Dumanskii's views [7] on the hydrophilic properties of disperse systems. The thickness of the hydrate layer on the particles depends on the diffuseness of the double layer: the more diffuse the double layer, the thicker the hydrate layer will be, and the greater the zeta potential of a sample, the higher is its hydrophilic properties.

Bentonite samples with high contents of bivalent cations, in contrast to similar kaolin samples, do not show a hydrophilic increase. The probable reason is the very high value of the zeta potential in the region of the

curve under consideration. Therefore there is hardly any hydrophilic increase due to additional introduction of more highly hydrated cations into the exchange complex. The zeta potential and hydrophilic curves follow the same course throughout.

It follows from the foregoing that the zeta potential plays an extremely important role in the binding of water by bentonite clays. Because of the high values of the zeta potential (8-32 mv), its influence is even more prominent than in kaolinite clays, where its value is relatively low (1-6 mv).

SUMMARY

1. The effect of the ratio of univalent and bivalent ions in the exchange complex on the hydrophilic properties of gumbrin, a Caucasian bentonite, has been studied.
2. As sodium in the clay is replaced by increasing amounts of bivalent adsorbed cations, the amount of bound water does not increase steadily but passes through a maximum.
3. The hydrophilic curve follows the same course as the curve for electrokinetic potential throughout.
4. The value of the electrokinetic potential is an important factor in the binding of water by bentonite particles.

The author offers her deep gratitude to A. V. Dumanskii for general guidance and for valuable advice in discussion of the work.

The Ukrainian Agricultural Academy
Kiev

Received September 25, 1956

LITERATURE CITED

- [1] A. V. Dumanskii and F. D. Ovcharenko, *Colloid J.* 12, 334 (1950); F. D. Ovcharenko and S. F. Bykov, *Colloid J.* 16, 134 (1954); F. D. Ovcharenko, I. E. Neimark, and S. F. Bykov, *Proc. Acad. Sci. Ukrainian SSR* 69, 447 (1952).
- [2] F. D. Ovcharenko, *Ukrain. Chem. J.* 19, 139 (1953).
- [3] A. V. Dumanskii, *Koll.-Z.* 65, 178 (1933); A. V. Dumanskii and O. V. Neiman, *Colloid J.* 2, 625 (1936).
- [4] I. A. Uskov and E. T. Uskova, *Colloid J.* 19, No. 3, 361 (1957).*
- [5] E. T. Uskova, *Colloid J.* 19, No. 6 (1957).*
- [6] A. I. Rabinovich and E. V. Fodiman, *J. Phys. Chem.* 3, 8 (1932).
- [7] A. V. Dumanskii, *Lyophilic Properties of Disperse Systems* (Voronezh, 1940).**

* Original Russian pagination. See C. B. Translation.

** In Russian.

THE EFFECT OF PLASTICIZER ADDITIONS ON THE MECHANICAL
PROPERTIES OF VINYL CHLORIDE - VINYLIDENE CHLORIDE COPOLYMER
AND OF POLYVINYL CHLORIDE

R. I. Fel'dman, A. K. Mironova and S. I. Sokolov

In the preceding communications [1, 2] it was shown, in the case of plasticized polyvinyl chloride, that the conventional (nominal) tensile strength and modulus of a mixture in the high-elastic state can be represented, in the first approximation, by an equation of the type

$$X_m = \prod X_i^{N_i}, \quad (1)$$

where X_m is the nominal strength or nominal nonequilibrium modulus of the mixture, determined from the extension curves; X_i is the nominal strength or modulus of the components of the mixture, their molar fractions being N_i ($\sum N_i = 1$).

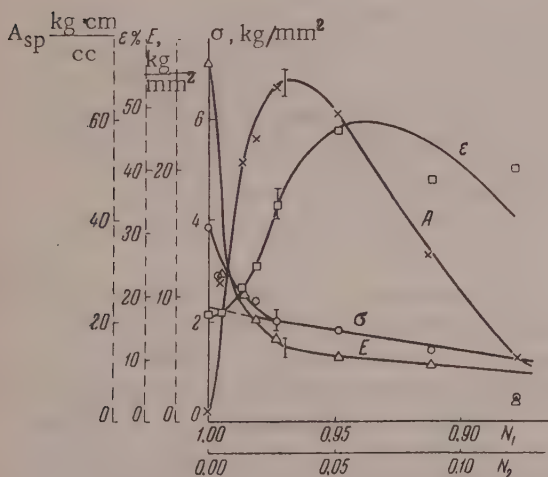
The explanation offered [1] for the similarity of the variations of nominal strength and modulus of mixtures with the molar fractions of the components was that these quantities are associated with the characteristic relaxation times of the systems. For calculations of the values of X_i we assumed that the systems conform to the principle according to which each component in a homogeneous mixture is present in the same state of aggregation as the mixture itself [3], irrespective of whether this state can be realized in practice for each of them separately under the same conditions [1].

The validity of Equation (1) was verified for binary (polymer-plasticizer) [1] and ternary (polymer-plasticizer I - plasticizer II) [2] systems. Calculations showed that the nominal tensile strengths of polyvinyl chloride and plasticizers present in the high-elastic state in a mixture are individual characteristics, independent of the presence of other components. To confirm these findings, it was desired to study specimens based on other polymers.

The materials chosen for the investigation were the plasticized polymers: Soviden, and polyvinyl chloride - Igelit K. Soviden was made by the copolymerization of vinyl chloride and vinylidene chloride in 77:23 ratio. The following systems were studied: Soviden-dibutyl phthalate, Soviden-tricresyl phosphate, Soviden-chlorinated diphenyl, Igelit K-tricresyl phosphate, and Igelit K-dibutyl phthalate. The plasticization of Soviden in various proportions was carried out on steam-heated rolls at 95-100° followed by pressing. Films of plasticized

Fig. 1. Composition-mechanical properties diagram for the systems Soviden-chlorinated diphenyl.

Igelit K were made by rolling at 160°. 2% of calcium stearate on the weight of the polymer was used for stabilization.



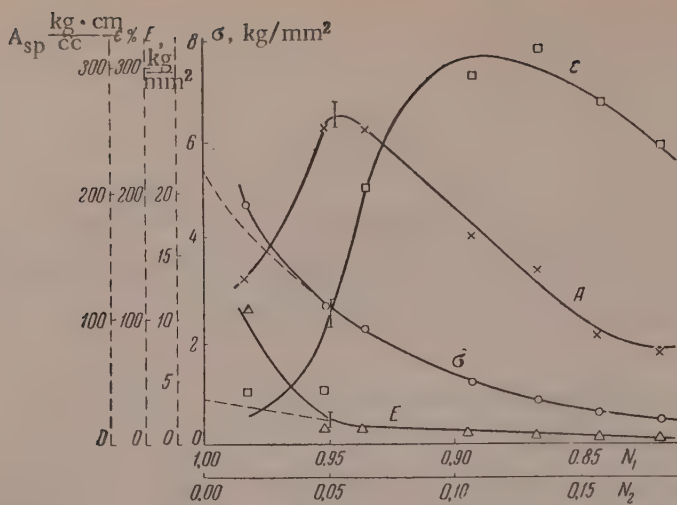


Fig. 2. Composition-mechanical properties diagram for the system polyvinyl chloride (Igelit K) - m,p-tricresyl phosphate.

TABLE 1

Nominal Tensile Strengths and Nominal Moduli of Certain Polymers and Plasticizers (in the high-elastic state)
Extension Rate 2 mm/min.

Polymer	Plasticizer	Temper- ature, °C	Nominal tensile strength, kg/mm ²		Nominal modulus, kg/mm ²	
			poly- mer	plasticizer	poly- mer	plasticizer
Copolymer (Soviden)	m,p-tricresyl phosphate	20.0	2.95	$3.39 \cdot 10^{-6}$	6.60	$2.58 \cdot 10^{-6}$
	Dibutyl phthalate	20.0	2.34	$1.12 \cdot 10^{-6}$	5.75	$2.95 \cdot 10^{-5}$
	Chlorinated diphenyl	20.0	2.29	$1.05 \cdot 10^{-2}$	—	—
Polyvinyl chloride (Igelit K)	m,p-tricresyl phosphate	20.0	5.39	$6.00 \cdot 10^{-6}$	3.71	$2.95 \cdot 10^{-6}$
	Dibutyl phthalate	20.0	5.30	$1.50 \cdot 10^{-6}$	3.76	$4.96 \cdot 10^{-5}$
Polyvinyl chloride emulsion poly- merization	m,p-tricresyl phosphate	15.5	5.82	$3.68 \cdot 10^{-6}$	10.82	$1.37 \cdot 10^{-6}$
	Dibutyl phthalate	15.5	5.02	$3.16 \cdot 10^{-6}$	7.15	$1.06 \cdot 10^{-5}$
	Chlorinated diphenyl	15.5	5.75	$3.24 \cdot 10^{-2}$	—	—

For determination of the load-extension curves, the specimens were tested at 20° on a dynamometer of the Polanyi type at a constant extension rate of 2 mm/min. The nominal tensile strength σ in kg/mm², relative extension at break ϵ in %, the specific work of extension to break, the so-called "energy of elasticity" A in kg·cm/cc, and the nominal nonequilibrium modulus E in kg/mm² were determined for mixtures of various compositions.

The composition-mechanical properties diagrams for all the systems were of the same form as those obtained earlier for plasticized polyvinyl chloride [4]. In illustration, Figs. 1 and 2 show the variations of mechanical properties with composition for the systems Soviden-chlorinated diphenyl, and Igelit K-tricresyl phosphate. The compositions are given in molar fractions of the polymer (N_1) and plasticizer (N_2). The molar fractions are calculated from the average molecular weights of the monomer units in the polymers. The vertical lines on the curves correspond to the amounts of plasticizer (N_2) which ensure high-elastic properties in the materials under the test conditions. It was found that more of the plasticizer (N_2) must be added to polyvinyl chloride than to the copolymer in order to obtain a product in the high-elastic state. This was to be expected,

TABLE 2

Values of Nominal Tensile Strength and Nominal Modulus for Plasticized Polymers,
Found Experimentally and Calculated by Means of Equation (2)
Extension rate 2 mm/min.; temperature 20°

Polymer	Plasticizer	Plasticizer contents in molar fractions $N_2 \cdot 10^2$	Nominal tensile strength, kg/mm²		Nominal modulus, kg/mm²	
			experimental	σ_m by Equation (2)	experimental	E_m by Equation (2)
Polyvinyl chloride (Igelit K)	m,p-tricresyl phosphate	4.85	2.72	2.77	(1.20)	1.83
		6.37	2.30	2.26	(0.98)	1.47
		10.62	1.20	1.26	0.86	0.84
		13.25	0.86	0.88	0.43	0.57
		15.72	0.62	0.61	0.38	0.41
		18.10	0.49	0.45	0.28	0.29
	Dibutyl phthalate	3.24	3.35	3.26	—	—
		6.33	1.73	2.00	1.60	1.85
		10.99	1.25	1.05	0.95	1.10
		16.85	0.40	0.41	0.71	0.51
		19.82	0.26	0.26	0.42	0.41
		22.60	0.18	0.18	0.51	0.29
Copolymer (Soviden)	m,p-tricresyl phosphate	0.38	2.92	2.80	—	—
		1.20	2.60	2.51	—	—
		2.40	2.05	2.13	—	—
		3.49	1.86	1.83	4.10	3.98
		4.62	1.50	1.57	3.40	3.33
		7.97	(0.32)	1.00	2.00	2.00
	Dibutyl phthalate	0.63	2.04	2.10	7.85	7.80
		1.57	1.86	1.86	—	—
		2.18	1.73	1.71	4.05	4.36
		3.05	1.39	1.48	4.13	3.98
		4.57	(0.76)	1.20	3.18	3.20
		5.97	(0.59)	0.96	2.75	2.70
	Chlorinated diphenyl	2.69	1.97	1.98	—	—
		5.15	1.79	1.73	—	—
		8.77	1.42	1.43	—	—

as Soviden is a polymer with so-called internal plasticization, requiring less added plasticizer (external plasticization) for high elasticity. It is interesting to note that films based on Soviet polyvinyl chloride and Igelit K have almost the same tensile strengths, but their relative extensions at break and moduli differ. Plasticized Igelit K has higher relative extension at break and lower modulus than plasticized Soviet polyvinyl chloride.

In the high elasticity range, variations of the logarithm of the nominal tensile strength and of the logarithm of the modulus with the composition are linear. Therefore, in the first approximation, expressions of type (1), i.e.,

$$\sigma_m = \sigma_1^{N_1} \cdot \sigma_2^{N_2} \text{ and } E_m = E_1^{N_1} \cdot E_2^{N_2}, \quad (2)$$

are applicable in this range; here σ_m , σ_1 , σ_2 , E_m , E_1 and E_2 are the nominal tensile strengths and moduli of the mixture and components respectively, and N_1 and N_2 are the molar fractions. The nominal tensile strength and moduli, calculated as the limiting values in accordance with Equations (2) for the plasticizers and polymers, are given in Table 1. Previously published data [1] are included for comparison.

Table 2 gives the values of the nominal tensile strength and modulus for plasticized polymers, calculated by means of Equations (2) and determined experimentally.

The data in Table 2 indicate that the Equations (2) are valid for the representation of the mechanical characteristics (σ , E) of the systems studied, in the high-elastic state. Comparisons of the nominal tensile strengths and moduli of polymers and plasticizers, based on data for different systems, show that their values are independent of the presence of other components, and confirm that these values can be calculated on the assumption of the additivity of their logarithms [1].

SUMMARY

1. The additivity of the logarithms of the nominal tensile strengths and moduli has been confirmed for plasticized vinyl chloride - vinylidene chloride copolymer (77:23) in the high-elastic state; the results are compared with the corresponding data for polyvinyl chloride.

2. It is shown that the tensile strength and modulus of a mixture depend on the corresponding characteristics of the individual components, and that, for the high-elastic state, they can be calculated, in the first approximation, from the equations $\sigma_m = \sigma_1^{N_1} \cdot \sigma_2^{N_2}$ and $E_m = E_1^{N_1} \cdot E_2^{N_2}$.

3. It is shown that the numerical values of these characteristics for the components are determined by the test conditions and are independent of the presence of other components in a mixture.

The Moscow Technological Institute
for the Light Industry

Received January 7, 1957

LITERATURE CITED

- [1] R. I. Fel'dman, Proc. Acad. Sci. USSR 97, No. 6, 1033 (1954).
- [2] R. I. Fel'dman and A. K. Mironova, Colloid J. 17, No. 6, 465 (1955).*
- [3] R. I. Fel'dman and S. I. Sokolov, Chemistry and Physical Chemistry of High-Molecular Compounds (Izd. AN SSSR, 1952) p. 159. **
- [4] S. I. Sokolov and R. I. Fel'dman, Investigations in the Field of High-Molecular Compounds (Izd. AN SSSR, 1949) p. 329. *

* Original Russian pagination. See C. B. Translation.

** In Russian.

THE EFFECT OF THE ACETYL GROUP CONTENT OF ACETYLCELLULOSE
ON THE PROPERTIES OF ITS SOLUTIONS

V. P. Kharitonova and A. B. Pakshver

When acetylcellulose is dissolved, the solvent molecules solvate its active groups. Ellis and Bath, and also Clement [1], who studied the infrared absorption spectra of acetylcellulose and determined the amounts of free solvent by the "method of residues," showed that various solvents interact with the ester of hydroxyl groups of acetylcellulose.

The formation of molecular compounds between acetylcellulose and solvent should alter the configuration and therefore the flexibility of the macromolecules in solution. Because of the different configurations of the macromolecules, solutions of acetylcellulose of the same degree of esterification and the same molecular weight have different viscosities in different solvents [2, 4]. In the opinion of Meerson and Lipatov [4], high solution viscosity is a sign of good solvent power, as a higher degree of solvation favors a more extended configuration of the macromolecules. In the opinion of Tager and Verhskain [3], high viscosity is a sign of poor solvent power.

The heat of solution of acetylcellulose should be different in different solvents, because the degree of solvation and the value of $E_{2,2}$ which represents the bond energy between the macromolecules are different. Regularity of the structure of the macromolecule, i.e., alternation of acetyl and hydroxyl groups along the macromolecular chain, is probably an important factor [5].

Aggregates of various sizes, depending on the acetyl content of the acetylcellulose and the nature of the solvent, may be present in solutions; these influence solution turbidity [6].

The effects of the combined acetic acid content in acetylcellulose on the following properties of its solutions were studied in the present investigation.

1. Specific (η_{sp}) and intrinsic viscosity [η], calculated by the usual methods.

2. The degree of asymmetry (b/a) which gives an approximate indication of the form of the macromolecules in solution. The values of b/a were calculated by means of Kuhn's equation [7]

$$\frac{\eta_{sp}}{cv_{sp}} = 2.5 + \frac{1}{16} \left(\frac{b}{a} \right)^2. \quad (1)$$

3. The root mean square distance ($\sqrt{\bar{h}^2}$) between the chain ends, calculated by the Flory equation [8]

$$\sqrt{\bar{h}^2} = 7.82 \times ([\eta] \bar{M}_r)^{1/2} \text{ Å}. \quad (2)$$

4. The coefficient k' which reflects the character of polymer-solvent interaction, by the Huggins equation [9]

$$\frac{\eta_{sp}}{c} = |\eta| + k' |\eta|^2 c. \quad (3)$$

5. The value of c_{lim} , the polymer concentration up to which the specific viscosity is a linear function of the concentration.

6. The integral heat of solution.

7. Solution turbidity, characterized by $1/n$, where n is the width of the slit.

TABLE 1

Effect of CH_3COOH Content on the Solution Properties of Acetylcellulose

Sample No.	Combined CH_3COOH	P/c at $c \rightarrow 0$ at temperature, °C			Molecular weight
		10°	20°	30°	
1	60.44	0.230	—	—	100 000
2	59.45	0.230	0.236	0.240	98 600
3	58.42	0.230	0.232	0.242	100 500
4	56.61	0.230	0.232	0.242	98 500
5	52.61	0.255	0.260	0.265	98 300
6	50.35	0.220	—	—	105 000

Acetylcelluloses with different combined acetic acid contents were obtained by saponification of the same batch of acetylcellulose for different times. The samples used for viscosimetric and thermochemical determinations were divided into 3 fractions by fractional precipitation of solutions in acetic acid. The first fractions were used for the determinations. The molecular weights of the fractions were determined by the osmotic method. The molecular weights of the acetylcelluloses with different acetyl contents were practically equal (Table 1); the discrepancies were within the limits of experimental error, $\pm 6.5\%$.

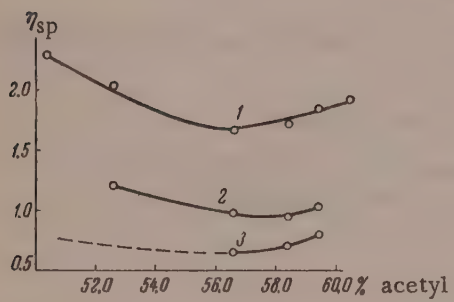


Fig. 1. Variation of specific viscosity of 0.5% acetylcellulose solutions with combined CH_3COOH content:
1) in formic acid; 2) in pyridine; 3) in acetone.

1) in formic acid; 2) in pyridine; 3) in acetone.

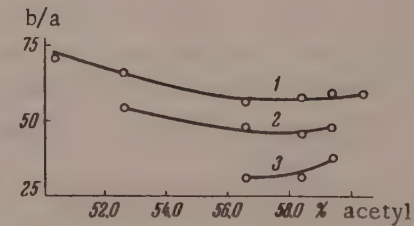


Fig. 2. Variation of b/a for acetylcellulose solutions with combined CH_3COOH content:
1) in formic acid; 2) in pyridine; 3) in acetone.

Therefore all the solution properties depended only on the acetyl group content of the acetylcellulose.

For the turbidity determinations, technical acetylcellulose of 55% acetyl value, and acetylcelluloses containing 53.05, 55.60, and 58.74% were taken. The solvents used were: acetone dried over calcined CaCl_2 , freshly distilled pyridine (chemically pure grade), and 97-98% formic acid solution (chemically pure). In the turbidity determinations, the following were also used: dioxane (chemically pure), glacial acetic acid, and nitromethane (chemically pure).

The viscosities of solutions containing 0.05; 0.1; 0.3; 0.4 and 0.5% of acetylcellulose were determined with the aid of ordinary Ostwald capillary viscosimeters at $30^\circ \pm 0.005^\circ$ in a thermostat. The relative error of the determinations did not exceed $\pm 0.9\%$. The experimental results are given in Table 2 and Figs. 1 and 2.

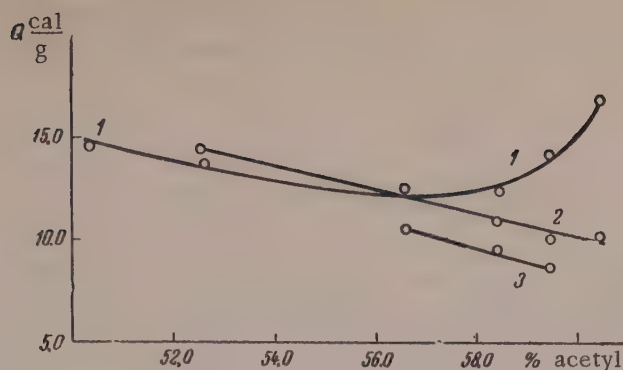


Fig. 3. Variation of integral heat of solution with combined CH_3COOH content for acetylcellulose solutions in:
1) formic acid; 2) pyridine; 3) acetone.

TABLE 2

Properties of Acetylcellulose Solutions

Acetyl group content of acetylcellulose %	Solvent	$[\eta]$	$\frac{b}{a}$ $c \rightarrow 0$	V_{h^2} in Å	k'	c_{lim}
60.44	Formic acid	1.20	59.0	385.7	2.31	0.330
59.45	Formic acid	1.17	58.8	382.5	2.32	0.330
	Pyridine	1.14	48.0	379.2	1.67	0.360
	Acetone	0.65	37.5	314.4	8.14	0.320
58.42	Formic acid	1.10	57.8	374.7	2.35	0.330
	Pyridine	1.07	46.0	371.3	1.70	0.360
	Acetone	0.48	32.0	284.2	14.0	0.320
56.61	Formic acid	1.09	56.5	373.6	2.42	0.330
	Pyridine	1.08	47.5	372.4	1.68	0.360
	Acetone	0.45	31.8	278.1	15.52	0.320
52.61	Formic acid	1.62	66.0	426.3	1.02	0.330
	Pyridine	1.58	54.0	422.8	0.80	0.360
50.35	Formic acid	1.95	71.2	453.5	0.78	0.330

TABLE 3

Effect of Final Concentration of Acetylcellulose in Solution on the Integral Heat of Solution

Sample No.	Combined CH_3COOH in %	Heats of solution in cal./g											
		in formic acid			in pyridine*			in acetone			0.1 %	0.3 %	0.5 %
		0.1 %	0.3 %	0.5 %	0.1 %	0.3 %	0.5 %	0.1 %	0.3 %	0.5 %			
1	60.44	14.20	16.92	20.67	7.50	10.09	13.75						
2	59.45	11.72	14.27	18.13	7.70	10.10	14.09	6.50	8.77	14.72			
3	58.42	9.34	12.50	15.77	8.25	11.00	15.19	7.00	9.70	15.91			
4	56.61	10.19	12.50	16.50	10.00	12.60	17.72	8.00	10.61	16.70			
5	52.61	11.57	13.68	17.23	11.31	14.57	18.41						
6	50.35	12.46	14.60	17.72									

* Data for 0.1% solutions in pyridine and acetone were obtained by extrapolation.

The heat effects were measured by means of an improved [10] microcalorimeter of the Schottky type [11] with an isothermal jacket. The action of this microcalorimeter is based on the principle of the thermal expansion of liquids, and small heat effects can be measured with low relative error. In the conditions of our experiments the error was $\pm 2.7\%$. The experimental results are given in Tables 3 and 4 and Fig. 3.

TABLE 4

Heats of Dilution of Acetylcellulose Solutions

Sample No.	Combined CH ₃ COOH, in %	ΔQ in formic acid		ΔQ in pyridine		ΔQ in acetone	
		in cal./g	in %*	cal./g	in %*	cal./g	in %*
1	60.44	6.47	31.3	6.25	45.5	—	—
2	59.45	6.41	35.4	6.39	45.5	8.22	55.8
3	58.42	6.43	40.8	6.94	45.7	8.91	56.0
4	56.61	6.51	39.0	7.72	43.6	8.70	52.1
5	52.61	5.66	32.9	7.10	38.6	—	—
6	50.35	5.26	29.7	—	—	—	—

$$* \Delta Q \% = \frac{\Delta Q}{Q_{0.5}} \cdot 100.$$

TABLE 5

Effect of Solvent on the Turbidity of Solutions of Technical Acetylcellulose

Solvent	Nephelometer reading, $\frac{1}{n}$	$\frac{1}{n}$	Turbidity after addition of 10% of water		$\Delta^* \text{ in \%}$
			n	$\frac{1}{n}$	
Acetone	1.00	1.000	1.76	0.568	43.2
Dioxane	4.30	0.230	11.70	0.085	63.1
Pyridine	25.80	0.039	11.60	0.086	-54.7**
Acetic acid	3.07	0.325	11.25	0.088	73.0
Formic acid	1.48	0.676	9.05	0.110	83.7
Nitromethane	0.27	3.703	2.10	0.476	87.1

* Δ is the decrease of turbidity on addition of water.

** Turbidity increased.

TABLE 6

Effect of Additions on the Turbidity of Solutions of Technical Acetylcellulose in Acetone.
Initial Turbidity $1/n = 1$

Reagent added	1/n after addition of reagent, %				Δ^* , in %	
	5	10	15	25	with 10%	with 25%
Formic acid	0.78	0.58	0.44	0.40	42.0	60.0
Pyridine	0.90	0.78	0.68	0.64	22.0	36.0
Acetic acid	0.81	0.63	0.53	0.45	37.0	55.0
Dichloroethane	0.93	0.86	0.78	0.68	14.0	32.0
Water	0.67	0.56	0.60	0.70	44.0	30.0
Ethyl alcohol	0.84	0.74	0.74	0.78	26.0	22.0

* Δ is the decrease of turbidity in % after addition.

TABLE 7

Effect of Combined Acetic Acid Content on the Turbidity of Solutions of Acetyl-cellulose in Acetone

Reagent added	Acetyl number	Molecu- lar wt.	1/n after addition of reagent, %					
			0	1	5	10	15	20
Water	53.05	76000	1.30	1.20	0.64	0.50	0.52	0.54
	55.60	78500	1.00	0.98	0.70	0.62	0.74	0.86
	58.74	73400	0.90	0.80	0.71	0.70	0.78	0.88
Formic acid	53.05	76000	1.30	1.14	—	0.53	—	0.35
	55.60	78500	1.00	0.94	0.68	0.58	—	0.52
	58.74	73400	0.90	0.88	0.74	0.64	—	0.56
Dichloroethane	53.05	76000	1.30	—	—	—	—	—
	55.60	78500	1.00	0.98	0.94	0.88	0.82	0.78
	58.74	73400	0.90	0.88	0.82	0.74	0.68	0.64

A Kleinmann nephelometer was used for determinations of the turbidity of 1% acetylcellulose solutions. The degree of turbidity was measured by the width of the opened slit n , and was expressed in terms of $1/n$, which increases with turbidity. The experimental results are given in Tables 5, 6, and 7.

DISCUSSION OF RESULTS

These experimental results show that the properties of acetylcellulose solutions depend on the combined acetic acid content.

As reported earlier [2], acetylcellulose has rigid chains owing to strong interaction between the polar groups. When the polar groups become solvated, the interaction weakens and the molecules can become coiled. The hydrodynamic resistance to flow then diminishes and the viscosity decreases. It is found that the degree of asymmetry (b/a) and the root mean square distance between the chain ends (\bar{h}^2), which give an approximate indication of the shape of the macromolecules, vary with variations of the acetyl group content of the acetyl-cellulose. The specific and intrinsic viscosities of acetylcellulose solutions in formic acid and pyridine, plotted against the acetyl content, pass through minima. With increasing combined acetic acid content, the viscosities in all solvents again increase owing to increasing regularity of the acetylcellulose structure. It must be remembered that in acetylcellulose solutions intramolecular forces, i.e., mutual attraction and repulsion of groups within the molecule, play an important part, in addition to intermolecular forces. Increase of the number of like groups in the molecule results in mutual repulsion between them, and the molecules become more elongated. With an irregular distribution of unlike groups, mutual attraction occurs between them, leading to coiling of the molecular chains. In such cases the degree of asymmetry and the root mean square distance between the chain ends have their lowest values. This is found for acetylcellulose containing from 56.5 to 58.5% combined acetic acid. The solution viscosity is higher in formic acid than in pyridine, and much higher than in acetone. This is accounted for by the stronger interaction between the polar groups of acetylcellulose and formic acid, as the latter solvates both acetyl and hydroxyl groups in acetylcellulose. Pyridine probably solvates only the hydroxyl groups in acetylcellulose, and the degree of solvation is lower in this solvent. Acetone solvates only the acetyl groups of acetylcellulose, by virtue of its ketone grouping. Accordingly, the degree of asymmetry and the root mean square distance between the ends of the macromolecular chains of acetyl-cellulose are higher in formic acid than in pyridine, and much higher than in acetone.

The heats of solution also show that the interaction of acetylcellulose with different solvents depends on the nature of the solvent. Thus, the heat of solution in acetone is less than in pyridine, and much less than in formic acid.

It should be pointed out that while molecular aggregates are present in dilute solutions, they are probably absent at infinite dilution, the solute being monomolecular. For example, osmometric determinations showed that the values of P/c at $c \rightarrow 0$ are approximately the same for acetylcelluloses with different combined acetic acid contents at various temperatures; the discrepancies are due to experimental error. Comparison of values

of $[\eta]$ and k' reveals an inverse relationship between them, i.e., the values of $[\eta]$ decrease while k' increases with worsening of the solvent; this means that in worse solvents the molecules are more coiled, and the possibility of association increases. The value of c_{lim} , the limiting concentration up to which the specific viscosity is a linear function of the concentration, is highest in the best solvent.

Different solvents solvate different groups in acetylcellulose, giving rise to solutions with different degrees of macromolecular association, and therefore of different turbidity. Solvents which solvate the hydroxyl groups, or hydroxyl and acetyl groups of acetylcellulose simultaneously (pyridine, dioxane, formic and acetic acids) yield solutions of a lower degree of association, and therefore of lower turbidity, than solvents which solvate the acetyl groups only, such as acetone and nitromethane.

The turbidity of the solutions decreases on addition of small amounts of water, as the latter has an additional solvating effect on the hydroxyl groups in acetylcellulose. However, water exerts its disaggregating effect only up to a certain limit, beyond which the turbidity begins to increase owing to desolvation and aggregation of the macromolecules. We see that addition of 10% of water to solutions of acetylcellulose in pyridine produces a strong increase of turbidity. The turbidity of acetone solutions decreases with increasing acetyl group content in the acetylcellulose, since acetone solvates the acetyl groups, and the degree of macromolecular association diminishes with increasing acetyl group content. Thus a 2.55% increase of the combined CH_3COOH in acetyl-cellulose decreases the turbidity by 23.1%, while at 5.69% increase of the CH_3COOH content decreases the turbidity by 30.8%.

Thermochemical determinations showed that, with increasing dilution of the solutions from 0.5 to 0.1%, Q decreases by about 30% in formic acid, by about 42% in pyridine, and by about 50% in acetone, i.e., additional disaggregation takes place and the energy of bond rupture in the aggregates increases. The greatest disaggregation occurs in acetone, and the least in formic acid. The maximum energy of bond rupture and disaggregation on dilution in all solvents corresponds to 56.5-58.5% combined acetic acid. In acetone and pyridine the heat effect diminishes with increasing combined acetic acid in the acetylcellulose, as with an increase of the number of CH_3CO groups the number of contacts between them increases, and more energy is required to break the bonds. Moreover, because of the decrease in the number of hydroxyl groups, the value of Q in pyridine is less. The heat effect is greatest in formic acid as solvent, and is independent of the acetyl group content, as all the polar groups in acetylcellulose are apparently solvated equally and the heat of solvation is considerably greater than the energy of rupture of the intermolecular bonds.

SUMMARY

1. The viscosity of acetylcellulose solutions depends on the combined acetic acid content of the acetyl-cellulose.
2. The minimum viscosity corresponds to the greatest degree of coiling of the macromolecules, which is found with the least regular distribution of polar OH and CH_3CO groups along the chains. For secondary acetyl-cellulose, the least regular distribution of the polar groups corresponds to 56.5-58.5% combined acetic acid.
3. The heat of solution of acetylcellulose depends on the ratio of acetyl to hydroxyl groups and the nature of the solvent. The greatest heat effect is found in formic acid, and the least in acetone.
4. The turbidity of acetylcellulose solutions depends on the degree of solvation of the polar groups by the solvent molecules. The turbidity of solutions of the same concentration in different solvents may vary by a factor of 100.
5. Small amounts of substances which cause additional solvation of the polar groups of acetylcellulose decrease the turbidity of acetone solutions of technical acetylcellulose by 40-60%.
6. The turbidity of technical acetylcellulose solutions increases, and the quality of spinning dopes probably decreases, with increasing content of fractions of low acetyl group content.

LITERATURE CITED

- [1] Ellis and Bath, *J. Am. Chem. Soc.* 62, 2859 (1940); P. Clement, *Ann. Chim.* 2, 420 (1947).
- [2] A. B. Pakshver and R. I. Dolinin, *J. Appl. Chem.* 23, No. 7, 775 (1950).*
- [3] A. A. Tager and R. Vershkain, *Colloid J.* 13, No. 2, 123 (1951).
- [4] S. I. Meerson and S. M. Lipatov, *Colloid J.* No. 6, 435 (1952).*
- [5] S. M. Lipatov, *Proc. Acad. Sci. USSR* 48, 408 (1945); P. M. Doty, *J. Phys. Coll. Chem.* 5, 32 (1947).
- [6] S. I. Meerson and E. Grimm, *Colloid J.* 18, No. 2, 199 (1956). *
- [7] R. Powell and H. Eyring, *Progr. Phys. Sci.* 27, 265 (1945).
- [8] P. Flory and T. Fox, *J. Am. Chem. Soc.* 73, 1904 (1951).
- [9] M. L. Huggins, *J. Phys. Chem.* 42, 439 (1939); *J. Am. Chem. Soc.* 64, 2716 (1942).
- [10] K. B. Iatsimirskii and V. V. Kharitonov, *J. Phys. Chem.* 6, 799 (1953).
- [11] Schottky, *Z. Phys. Chem.* 64, 425 (1908).

* Original Russian pagination. See C. B. Translation.

BRIEF COMMUNICATIONS

SWELLING OF SILICATE MELTS AND BLISTERING OF ENAMEL COATINGS ON STEEL

K. P. Azarov

Determination of the conditions which favor or hinder the formation of blister structures is of importance for many silicate industries, and in particular in relation to blistering of boronless ground coatings. The sources of the gases causing blistering are constant and abundant, and cannot be eliminated in the usual enameling practice. However, practical experience shows that boronless ground coatings are damaged considerably more than coatings with boron by the liberated gases.

Comparison of the available data on the properties of borate and boronless ground coat enamels reveals considerable differences between them. Thus, the surface tension of the former (210-240 dynes/cm) is lower than that of the latter (250-280 dynes/cm) [1]. Iron oxide is wetted much better by borate than by boronless enamels [1-3]. The solubility of iron oxide in the latter is ~10%, while in the former it is 23%. The nature of the viscosity variation in the softening range on addition of iron oxide is especially important. Experiments carried out in connection with the present investigation showed that the viscosity of boronless ground enamels increases sharply, and that of borate enamels decreases with increasing iron oxide contents.*

For elucidation of the causes of blistering and of the role played by scale, comparative experiments** were carried out on artificial blistering in typical borate (b) enamels Nos. 18, 124, 1 and 2; boron-free (b/f) enamels Nos. 35, 27, and 16; and titanium (Ti) enamels Nos. 121 and 445, all for ground coats. Tablets pressed from mixtures of the enamel frits with various additives were heated in the furnace of the apparatus for determination of contact angle. The shadows of the swelling specimens were projected onto paper, and outlined in pencil for subsequent planimetric measurement of the shadow area.

The experiments showed that none of the enamels tested swelled on heating, either in absence of additives, or with additions of 15% of iron oxide or 10.5% of metallic iron powder. Additions of 2% of graphite as gas former caused some swelling, which was greater in the boronless enamels. Additions of 15% of iron oxide with 2% of graphite (Fig. 1), or of 10.5% of previously carburized iron powder (Fig. 2) produced very vigorous swelling of the boronless and titanium enamels, and much less in the borate enamels. The strong swelling of boronless enamels is probably the result of the sharp increase of viscosity produced by dissolution of the iron oxide.

Comparison of the data obtained on the swelling of ground-coat enamels with the technological characteristics of the corresponding ground coats on steel showed that a high degree of swelling in an enamel corresponds to a low quality of the ground coat: boronless coatings show more blisters and faults than borate coatings.

The existence of a connection between the dissolution of iron oxide, the swelling of enamels, and the tendency of coatings to form blisters is also confirmed by the following experiment. A tube of heat-resistant steel was filled with a gas-forming mixture of iron oxide and graphite, and its ends were then flattened and welded. The outside of the tube was divided into four regions, coated respectively with boron-free enamel b/f 35 and borate enamel b 18, and also the same enamels which had previously been melted with 15 or 30% of iron oxide. An electric current was passed through the tube walls to fire the coatings. The liberated gas passed through the tube walls into the zone of contact between the enamel and the steel; blistering was found only in the boron-free coating containing iron oxide. The boron-free coating without iron oxide did not blister, as the heat-resistant steel remained practically free from oxidation.

* The surface tension and viscosity determinations were carried out with the assistance of S. B. Grechanova, and the iron oxide solubility determinations, with the assistance of V. V. Balandina.

** With the assistance of G. V. Berdova.

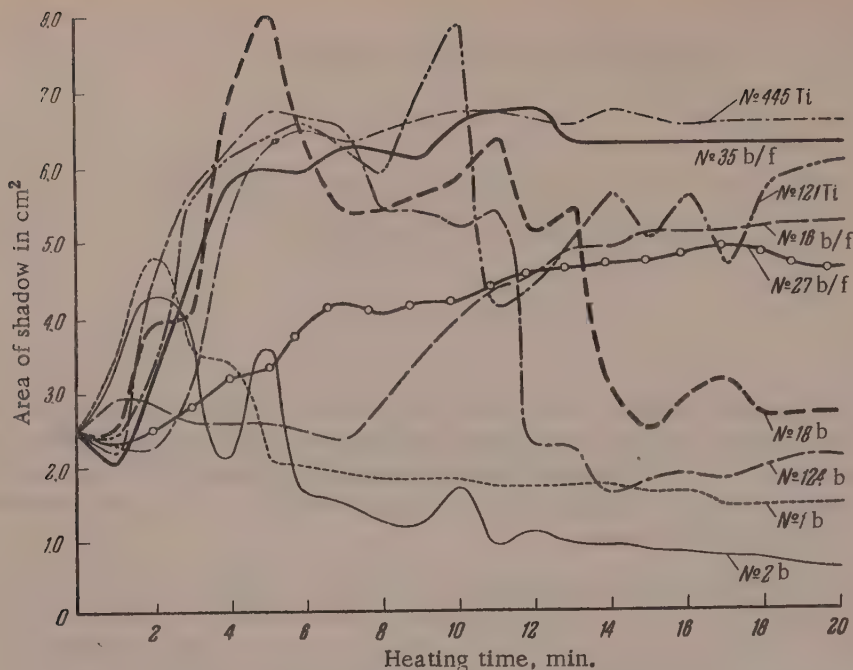


Fig. 1. Swelling of borate, boron-free, and titanium ground enamels with additions of a mixture of 15% iron oxide and 2% graphite (temperature 750°).

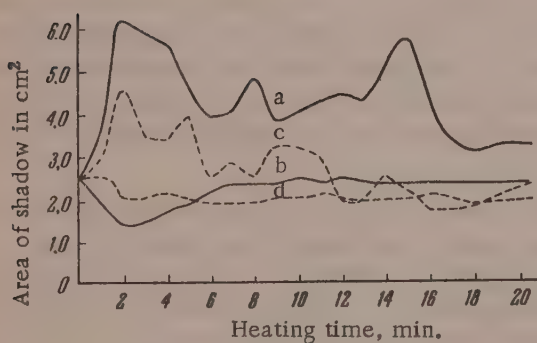


Fig. 2. Swelling of enamels with additions of 10.5% metallic iron powder:

a) Ground No. 35 b/f with carburized iron; b) ground No. 35 b/f with noncarburized iron; c) ground No. 18 b with carburized iron; d) ground No. 18 b with noncarburized iron.

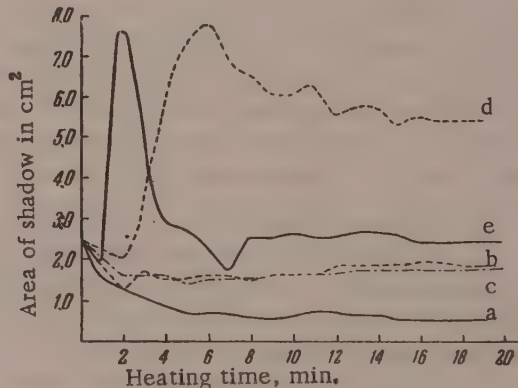


Fig. 3. Swelling of window glass at 800°:
a) without additions; b) with 2% graphite;
c) with 15% iron oxide; d) with 15% iron oxide
and 2% graphite; e) with 2% marble (from
Kitaigorodskii's data [4]).

The results were applied to experiments on the swelling of foam glass. It was to be expected from the previous results that additions of iron oxide in presence of a gas former should favor the swelling of ordinary boron-free glasses. Figure 3 shows that a mixture of iron oxide and graphite produces the most stable swelling and gives a higher final degree of swelling.

The dimensions and mobility of the gas bubbles depend on the properties of the ground coat melt. It is known [5] that the force of adhesion of a gas bubble to a surface depends on the diameter of the circle along which the bubble is attached to the solid surface, on the surface tension at the melt-gas interface, and on the contact angle. The high surface tension of boron-free melts, and their lower wetting action on iron oxides (oxidized steel!), favor the formation of larger gas bubbles in the ground coats, less easily detached than the bubbles

in borate enamels. Incidentally we may note that additional experiments showed that small additions of surface-active substances (FeS) to the mixtures reduce swelling. The resistance of a liquid to the motion of a gas bubble increases with increasing viscosity of the liquid and bubble size. Therefore the sharp increase in the viscosity of boron-free ground coat melts produced by the dissolution of scale in the region of contact with oxidized steel leads to the formation of large bubbles which emerge with difficulty, and this in its turn favors blistering and faults.

We must point out that titanium borate enamels have much in common with boron-free ground coat enamels. They are also characterized by vigorous swelling on addition of mixtures of iron oxide and graphite, a sharp increase of viscosity on addition of iron oxide, and the formation of numerous large blisters on the coatings.

The S. Ordzhonikidze Polytechnic Institute
Novocherkassk
Enamels Laboratory

Received March 17, 1957

LITERATURE CITED

- [1] K. P. Azarov, Factory Labs. No. 3, 355 (1954).
- [2] K. P. Azarov, Refractories No. 12, 551 (1950).
- [3] K. P. Azarov, J. Appl. Chem. 27, No. 1 (1954).*
- [4] I. I. Kitaigorodskii and T. N. Keshish'ian, Foam Glass (Industrial Construction Press, Moscow, 1953).**
- [5] A. N. Frumkin, V. O. Bagotskii, Z. A. Iofa and B. N. Kabanov, Kinetics of Electrode Processes (Izd. MGU, Moscow, 1952).**

* See C. B. Translation.

** In Russian.

AN APPARATUS FOR DETERMINING THE DISPERSITY OF EMULSIONS

B. M. Babanov and V. V. Kafarov

In the processing of heterogeneous systems such as emulsions it is often necessary to determine their dispersity. In this paper an apparatus is described for direct determinations of particle size in emulsions in the course of agitation, extraction, etc. The advantage of our apparatus is that aggregation of the emulsion droplets is eliminated. This is because a small amount of the sample is uniformly distributed in a relatively large volume of liquid in the apparatus. The apparatus is suitable for investigation of emulsions in which the density of the disperse phase is less than that of the dispersion medium.

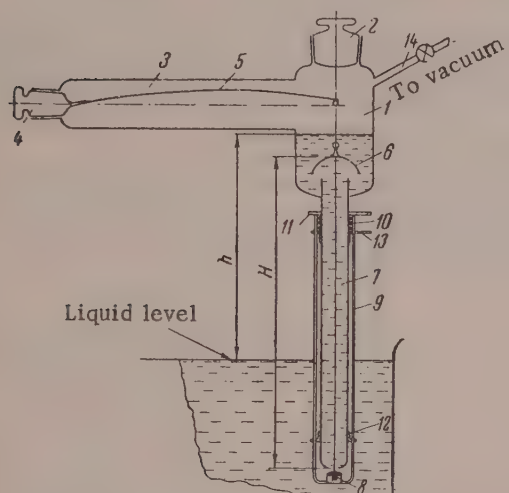


Fig. 1. Diagram of the apparatus.

Deflection of pointer in scale divisions

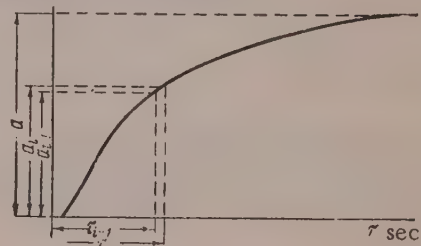


Fig. 2

The design and principle of the apparatus are as follows. To a glass container 1 (Fig. 1), fitted with a ground glass stopper 2, is welded a tube 3, with a stopper 4 carrying a pointer 5 welded to it, at the other end. The other end of the pointer is bent in the form of a hook from which is suspended a cap 6. The glass cap is in the form of a hemisphere 28-30 mm in diameter, with walls 0.2-0.3 mm thick, and weighs 0.5-0.7 g. To the top of the cap there is welded a glass loop, which is used for suspending the cap from the pointer 5 by means of a platinum wire 0.1-0.2 mm in diameter. A tube 7, with a valve 8 at its lower end, is welded to the bottom of the container 1. The valve 8 closes the orifice in the lower end of the tube 7 with the aid of the coupling rods 9 and spring 10. The coupling rods 9 are welded to the ring 11 which can move freely along the tube 7. The tube 7 also carries two directing collars 12 and 13, with holes through which pass the coupling rods 9. The upper part of the container has a side tube 14 for evacuation of the apparatus. The whole apparatus is clamped on a stand, which also carries a microscope eyepiece with an inserted measuring scale, or a special measuring microscope of the MPB-2 type, used for measurements of the pointer deflections. The tube 7 must first be lowered into the emulsion to be studied, and filled with the liquid used as the dispersion medium in the emulsion. The tube 7 can be filled with the liquid through the opening in its lower end with the aid of a vacuum, or, if the tube 7 has already been put into the emulsion, it can be filled through the opening closed by the stopper 2. A vacuum equivalent to h (3-5 cm H₂O) (Fig. 1) must be created in the apparatus. To take a sample, the ring 11 is pressed; this descends, compresses the spring 10, and opens the valve 8. The time clock

0.2-0.3 mm thick, and weighs 0.5-0.7 g. To the top of the cap there is welded a glass loop, which is used for suspending the cap from the pointer 5 by means of a platinum wire 0.1-0.2 mm in diameter. A tube 7, with a valve 8 at its lower end, is welded to the bottom of the container 1. The valve 8 closes the orifice in the lower end of the tube 7 with the aid of the coupling rods 9 and spring 10. The coupling rods 9 are welded to the ring 11 which can move freely along the tube 7. The tube 7 also carries two directing collars 12 and 13, with holes through which pass the coupling rods 9. The upper part of the container has a side tube 14 for evacuation of the apparatus. The whole apparatus is clamped on a stand, which also carries a microscope eyepiece with an inserted measuring scale, or a special measuring microscope of the MPB-2 type, used for measurements of the pointer deflections. The tube 7 must first be lowered into the emulsion to be studied, and filled with the liquid used as the dispersion medium in the emulsion. The tube 7 can be filled with the liquid through the opening in its lower end with the aid of a vacuum, or, if the tube 7 has already been put into the emulsion, it can be filled through the opening closed by the stopper 2. A vacuum equivalent to h (3-5 cm H₂O) (Fig. 1) must be created in the apparatus. To take a sample, the ring 11 is pressed; this descends, compresses the spring 10, and opens the valve 8. The time clock

is switched on at the instant when the ring 11 is pressed. The valve 8 should be open for only a short time, as the amount of emulsion to be taken should only be such as to contain enough disperse phase to raise the cap within the range of the microscope scale. This amount depends on the sensitivity of the pointer, the content of disperse phase in the emulsion, and the difference between the densities of the disperse phase and the dispersion medium; it is usually 1-2 cc. The time during which the valve should be open, and the degree of vacuum, are determined from the results of two or three trial determinations.

To determine the dispersity of a polydisperse emulsion, the whole disperse phase must be fractionated by particle size and the average particle diameter in each fraction determined. This fractionation actually takes place in the apparatus itself, as all the droplets of the sample taken, starting from the same level, have time to separate while passing along the tube 7 (from the valve 8 to the cap 6) because of their different velocities, determined by their size. Therefore the largest droplets reach the cap first, followed by progressively smaller droplets. Therefore the rise of the cap over a given interval corresponds to the weight of the droplets which have passed from the valve 8 to the cap 6 during the period starting with the instant when the sample was taken and ending with the start of the given interval. For determination of the dispersity of an emulsion with the aid of this apparatus it is convenient to plot a graph (Fig. 2), where a is the total deflection of the pointer in microscope scale divisions; $a_i - a_{i-1}$ is the deflection of the pointer in scale divisions, corresponding to the fraction i ; $100 \times \frac{(a_i - a_{i-1})}{a}$ is the content of fraction i as a percentage of the total disperse phase present; $\frac{(\tau_i + \tau_{i-1})}{2}$ is the time of ascent of a droplet of fraction i in seconds; H is the path in centimeters transversed by the droplet in the apparatus (Fig. 1); $W = \frac{2H}{(\tau_i + \tau_{i-1})}$ is the velocity of the droplet in centimeters per second.

The diameter of a droplet is calculated from its velocity in a viscous medium by means of Oseen's equation [1], which covers the widest range of droplet sizes, or the simplified Stokes equation. These equations are normally used for suspensions, but it has been shown, Nordlund [1], that the deviations due to the existence of the disperse phase particles in the liquid state are so small as to be of no practical significance.

Our apparatus, described in this paper, based on the balance principle, was used in investigations of the efficiency of various stirrers for mixing two immiscible liquids, and also for studying the extraction process in injection equipment. The apparatus proved quite reliable in all cases, the droplets measured ranged from 20μ to 2 mm.

Scientific Research Institute of
Organic Intermediates and Dyes, Moscow

Received October 25, 1956

LITERATURE CITED

- [1] N. A. Figurovskii, Sedimentometric Analysis (Izd. AN SSSR, Moscow-Leningrad, 1948) p. 308.*

* In Russian.

DETERMINATION OF THE BOUND WATER CONTENT IN PEAT BY THE
METHOD OF THE NEGATIVE ADSORPTION OF A RADIOACTIVE TRACER

M. P. Volarovich, F. D. Sysoeva, V. V. Cherniavskaya and N. V. Churaev

Investigations of bound water are very important in relation to studies of the hydric properties of peat, which determine the course of such important technological processes as the drying of peat deposits, processing and drying of peat, etc. Various methods have been used for determination of physically and chemically bound water in peat: negative adsorption of sugar, freezing, and tensimetry [1]. However, because these methods are complicated, lengthy, and require special equipment, they are not used for large-scale investigations.

The method described below can be used for fairly rapid serial determinations of bound water content with the use of standard radiochemical laboratory equipment. The method is based on the negative adsorption of the radioactive tracer $\text{Na}_2\text{S}^*\text{O}_4$, containing the S^{35} radioactive sulfur isotope, and is essentially a variation of Dumanskii's method [2]. It was shown earlier [3] that $\text{Na}_2\text{S}^*\text{O}_4$ can also be used as a radioactive tracer for determination of the content of static water, not involved in filtrational motion, in peat.

Relative Contents of Bound Water in Different Peat Samples

Peat type	Degree of decomposition, %	Bound water content (w_b) in %	
		by radioactive tracer method	by negative adsorption of sugar
Medium peat No. 37	15	34.7	34.7
Medium peat No. 36	20	14.8	7.3
Same, processed once	—	26.0	21.4
Same, processed twice	—	28.2	24.6
Medium peat No. 79	25	13.6	13.7
Sedge peat No. 77	40	21.0	19.8
Scheuchzeria-sphagnum peat No. 40	20	22.6	25.4
Pine-cotton grass peat No. 34	60	24.1	21.7
Sedge-Lypnum peat No. 80	35	48.2	38.1
Same, processed once	—	28.4	27.4
Same, processed 3 times	—	14.0	15.2
Sedge peat No. 75	35	50.6	47.5

For the experiments, peat samples 100 g in weight (M) were taken, with a natural moisture content (w) 80-90%, determined previously by drying at constant temperature. The samples were placed in beakers, and distilled water was added in amounts (M_d) such that the relative moisture content of the resultant suspension was 95%. This gives a more exact comparison of the bound water contents of different peat samples. To each beaker 20 g (M_0) of $\text{Na}_2\text{S}^*\text{O}_4$ solution was added, and the suspension was stirred mechanically for 15 minutes. Samples taken from the beakers after stirring were centrifuged. The initial and final $\text{Na}_2\text{S}^*\text{O}_4$ concentrations were determined by measurement of the activity of samples of the original solution and the dispersion medium after centrifugation. Samples 1 ml in volume were taken (in duplicate) with a micropipet into metal foil cups and dried under the infrared lamp. The activity was determined by means of an end-type counter and the B-2 radiometric apparatus. The relative error in the activity determinations did not exceed 0.5%. In calculations of the counts, the counter background was taken into account in the usual way.

The bound water content (M_b) was calculated by means of the formula:

$$M_b = \frac{Mw}{100} + M_d + M_0 - M_0 \cdot \frac{N_0}{N},$$

where N_0 and N are the average counting rates (in pulses/minute) for the original solution and the dispersion medium. Calculations showed that the relative error in determinations of the bound water M_b by this method, with experiments in triplicate, did not exceed $\pm 5\%$.

The results obtained by this method were compared with the data obtained by determinations of the bound water in the same peat samples by the method of negative adsorption of sugar. The initial sugar concentration and the filtrate concentration were determined by means of the IRF-23 refractometer (of the Pulfrich type) with the aid of Schönrock's table. The temperature of the prism and solution was kept constant to within $\pm 0.5^\circ$. In calculations of the sugar concentration, the water-soluble substances in the peat water were taken into account.

The results of parallel determinations of the relative contents of bound water w_b (as percentages of the sample weight) obtained by the two methods for different samples are given in the Table.

Comparison of the tabulated data shows that the values obtained for the bound water contents of different types of natural and processed peat are fairly close. The radioactive tracer method can therefore be regarded as no less accurate than the method of negative adsorption of sugar.

The Moscow Peat Institute
Chair of Physics

Received October 16, 1957

LITERATURE CITED

- [1] N. N. Kulakov, Introduction to the Physics of Peat (Gosenergoizdat, 1947).*
- [2] A. V. Dumanskii, Lyophilic Properties of Disperse Systems (Voronezh State University Press, 1940);* Colloid Science (Goskhimizdat, 1948).*
- [3] M. P. Volarovich, N. V. Churaev and B. Ia. Minkov, Colloid J. 19, No. 2 (1957);** Proc. Acad. Sci. USSR 114, No. 5 (1957).**

* In Russian.

** See C. B. Translation.

THE ACTION OF METAL OXIDES IN THE VULCANIZATION OF
RUBBER BY TETRAMETHYLTHIURAM DISULFIDE

B. A. Dogadkin and V. A. Shershnev

Rubber is usually vulcanized with the aid of the so-called activators, metal oxides, zinc oxide being the one most often used. In vulcanization in presence of mercaptobenzothiazole or diphenylguanidine as accelerators it was found [1] that vulcanization activators have almost no effect on the rate of addition of sulfur to rubber, but have a significant influence on the rate and degree of cross linking of the rubber molecules. Special interest attaches to studies of the action of metal oxides in vulcanization with tetramethylthiuram disulfide (TMTD), as it is known from technological practice that in absence of zinc oxide this accelerator does not bring about vulcanization.

Vulcanization with TMTD was studied on mixtures of natural rubber* and of synthetic isoprene rubber (SKI) masticated on microrolls, of the following compositions (in parts by weight):

Mixture No.	1	2	3	4	5	6	7	8
NR*	100	100	100	—	—	—	—	—
SKI	—	—	—	100	100	100	100	100
TMTD	2.5	2.5	2.5	4	4	4	4	4
Stearic acid	—	—	0.5	1	1	1	1	1
Zinc oxide	—	5	5	5	1	—	—	—
Magnesium oxide	—	—	—	—	—	0.5	—	—
Calcium hydroxide	—	—	—	—	—	—	1.4	—
$\text{Ca}(\text{OH})_2 \cdot 2\text{H}_2\text{O}$	—	—	—	—	—	—	—	—

The vulcanization was effected in a press at 143° under a hydraulic pressure of 100 atm. Under these conditions the interaction of TMTD with rubber is accompanied by the addition of sulfur and nitrogen to the rubber, probably in the form of radicals, together with other elements of TMTD. At the same time TMTD is reduced to dithiocarbamic acid [2] which forms zinc dithiocarbamate in presence of zinc oxide. As the result of these reactions chemical cross links are formed between the molecular chains of the rubber; the concentration of these cross links, determined from the maximum swelling, can serve as a measure of the degree of vulcanization.

It is seen in Fig. 1 that the accumulation of sulfur in the vulcanizates is represented by curves with pronounced maxima; this means that part of the added sulfur is split off from the rubber during subsequent heating. This removal of sulfur is the consequence of the formation of volatile products, as the ratio of the total sulfur in the rubber to the amount of sulfur introduced in the form of TMTD, decreases appreciably as heating proceeds (Fig. 2). Metal oxides have little influence on the amount of sulfur added to the rubber. The influence of metal oxides on the amounts of volatile substances formed is more pronounced: in presence of zinc oxide the loss of sulfur is slight, whereas in absence of zinc oxide (and also in mixtures with magnesium oxide) up to 60% of the sulfur of the added TMTD is liberated in the form of volatile compounds. Calcium hydroxide occupies an intermediate position. The influence of metal oxides on the formation of the spatial structure in the vulcanizates is

* Natural rubber (NR) was extracted with cold acetone in a stream of nitrogen for 50 hours.

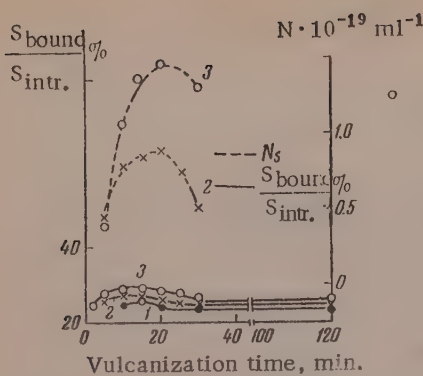


Fig. 1. Variation of the amount of bound sulfur $S_{\text{bound}}/S_{\text{intr.}}$ from thiuram, and of the density of the spatial network N of vulcanizates of natural rubber with TMTD:
1) Mixture No. 1; 2) mixture No. 2; 3) mixture No. 3.

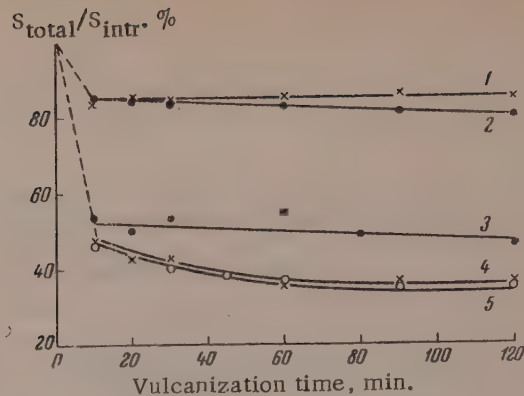


Fig. 2. Variation of total thiuram sulfur in vulcanization of technical SKI rubber with TMTD:
1) Mixture No. 4; 2) mixture No. 5; 3) mixture No. 7; 4) mixture No. 6; 5) mixture No. 8.

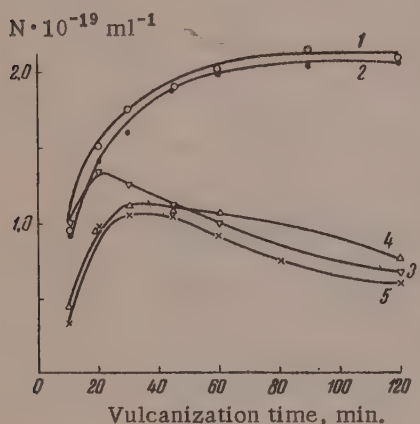


Fig. 3. Variation of the density of the spatial network in the vulcanization of technical SKI with TMTD:
1) Mixture No. 4; 2) mixture No. 5; 3) mixture No. 7; 4) mixture No. 6; 5) mixture No. 8.

very significant: in absence of metal oxides a very thin network is formed (the maximum swelling cannot be measured) in natural rubber mixtures at the vulcanization optimum, after 15-20 minutes of heating. Further heating leads to reversion — the vulcanizate again becomes completely soluble in hydrocarbons. Introduction of zinc oxide (5 wt. parts) into the mixture favors a rapid increase of the cross link content (at the vulcanization optimum in mixtures containing 5 wt. parts $ZnO N_s = 0.9 \cdot 10^{19} \text{ ml}^{-1}$) and decreases reversion of vulcanization. In mixtures based on SKI containing ZnO practically no reversion occurs (Fig. 3), but the effect is pronounced in mixtures containing MgO and $Ca(OH)_2$, and in mixtures without oxides. Therefore, as in the previously investigated cases [1] of sulfur vulcanization in presence of mercaptans and diphenylguanidine, in vulcanization with TMTD, metal oxides primarily influence the formation rate and concentration of chemical cross links. In presence of zinc oxide (or zinc salts of fatty acids) dithiocarbamic acid is bound in the form of the zinc salt; its accumulation as vulcanization proceeds is shown graphically in Fig. 4. In mixtures without zinc oxide, dithiocarbamic acid (or the rubber complex containing the dithiocarbamyl radical) decomposes with liberation of carbon disulfide, leading to a considerable decrease of the total and bound sulfur in the vulcanizate (Fig. 2). The formation of carbon disulfide was detected by means of the qualitative reaction with ammonium molybdate [3]. The liberation of carbon disulfide is accompanied by formation of dimethylamine according to the equation

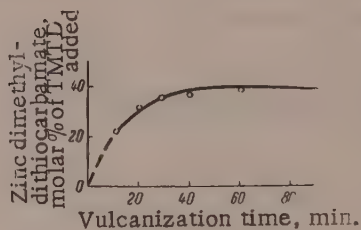
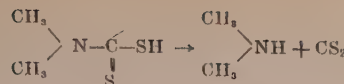


Fig. 4. Kinetics of the formation of zinc dimethyldithiocarbamate in vulcanization of the following mixture:
SKB (30% of 1-2 structural units) 100 wt. parts; TMTD, 4 parts; ZnO , 5 parts; stearic acid, 1 part; phenyl- β -naphthylamine 1 part.



The formation of dimethylamine was detected by means of Nessler's reagent.

It is known that, under certain conditions, some secondary amines and similar compounds favor thermal and thermooxidative degradation of natural rubber and its vulcanizates. For example, phenylhydrazine sharply lowers the viscosity of rubber solutions on heating [4]; phenyl- β -naphthylamine (in conjunction with xylol mercaptan) favors the degradation of sodium butadiene rubber vulcanizates [5]. Therefore it seems likely that the formation of the decomposition products of dithiocarbamic acid in the course of vulcanization also intensifies breakdown of the vulcanization structure; in other words, it decreases the degree of cross linking and leads to reversion.

Zinc dimethyldithiocarbamate is fairly stable under vulcanization conditions, and therefore binding of the acid by means of zinc oxide tends to increase the density of the vulcanization network and retards reversion. An indirect indication of this effect of zinc dimethyldithiocarbamate was obtained in our experiments on the viscosity changes of natural milled rubber on heating in an inert gas and in air at 143°. Zinc dimethyldithiocarbamate has no effect on the variation of the viscosity of rubber under these conditions; but in presence of butyric or benzoic acid, which themselves do not influence the viscosity of natural rubber, dimethyldithiocarbamate produces a considerable increase in the fall of viscosity on heating. The degradation in this case is probably associated with the formation (in an exchange reaction with the acids) and decomposition of dithiocarbamic acid.

Magnesium dithiocarbamate is not found in vulcanization in presence of magnesium oxide; this leads to the conclusion that magnesium oxide does not combine with dithiocarbamic acid formed. Therefore in mixtures with magnesium oxide the same reversion occurs as in mixtures without oxides added as vulcanization activators.

In addition to the main action of zinc oxide in the vulcanization of rubber with TMTD, described in this paper, some of the processes described previously [1] may also take place.

The direction of the reactions between TMTD and rubber depends to a considerable extent on the type of rubber. It was found that in the vulcanization of butadiene rubbers the amount of zinc dimethyldithiocarbamate formed and the amount of bound sulfur increase with increasing relative contents of the 1-2 structure in the polymer. This means that the mobile hydrogen at the tertiary carbon atom in the molecular chain takes part in the reduction of TMTD. At the same time the degree of cross linking, as was shown earlier for other types of vulcanization [6], increases with increasing contents of the 1-4 structure in the polymer. Therefore the spatial structure is formed mainly from the principal chains in the rubber. The mechanism of the presumed reactions will be discussed in a future communication.

The M. V. Lomonosov Institute of
Fine Chemical Technology, Moscow

Received August 14, 1957

LITERATURE CITED

- [1] B. Dogadkin and I. Beniska, Colloid J. 18, 167 (1956); R. T. Armstrong et al., Rub. Chem. Techn. 17, 788 (1944); Hull et al., Rub. Chem. Techn. 21, 553 (1948).
- [2] W. Scheele, Kautschuk u. Gummi 7, IT-273 (1954).
- [3] F. I. Berezovskaya and Zh. F. Solomko, Sci. Mem. Dnepropetrovsk State Univ. 43, 31 (1952); see also Referat. Zhur. Khim. 16829 (1954).
- [4] L. F. Sapozhkova, Dissertation, Moscow Inst. Fine Chem. Technol., Moscow (1947).
- [5] Z. N. Tarasova and B. A. Dogadkin, Report of the Moscow Inst. of Fine Chemical Technology (1948); see also Blace and Bruce, Ind. Eng. Chem. 33, 1198 (1941).
- [6] B. A. Dogadkin, A. V. Dobromyslova, F. S. Tolstukhina and N. G. Samsonova, Colloid J. 19, 188 (1957).*

* Original Russian pagination. See C. B. Translation.

THEORY OF THE OPTICAL RECORDING OF MIXTURE COMPOSITIONS BY AN INCLINED CYLINDRICAL LENS ARRANGEMENT

Ia.M. Bikson

Optical recording methods are widely used in electrophoretic analysis of proteins. Svensson [1] proposed a recording method which he termed the crossed-slit method. An optical system assembled in accordance with Svensson's scheme, comprising two crossed slits and a cylindrical lens with a vertical axis, makes it possible to obtain curves by a photographic method, from which the concentrations of the components of a mixture can be easily found. However, the accuracy of this method is limited by the crossed slits: wide slits give a diffuse concentration curve, while narrow slits lead to the same effect owing to diffraction of light. Troitskii [2,3] attempted to eliminate the defects of Svensson's method and at the same time to simplify the optical recording system by the use of an inclined cylindrical lens arrangement. Some use has been made recently of this new method [4-6]; however, in absence of a theory it is not possible either to make a rational choice of the design constants of the apparatus, or to compare the inclined cylindrical lens arrangement with the Svensson system (the theory of which has been worked out in detail). A theory of the Troitskii method is advanced in the present paper.

Figure 1 is a schematic representation of the optical system for recording the concentration distribution in the electrophoresis vessel C.

If the cell C contains a homogeneous mixture, it has no refracting effect and the lens system B and D gives an image of the point light source A at some point O. After electrophoresis, a refractive-index gradient is set up along the vertical axis in the cell C; its action can be likened to the action of a cylindrical lens with a horizontal axis. The image of the point A will now take the form of a vertical line in the plane E.* The screen G (photographic plate) is arranged in such a manner that an image of the cell C** is formed on it by means of the lens D (in absence of the cylindrical lens F). The inclined cylindrical lens F introduces astigmatism into the optical system; its position between the planes E and G is so chosen that the foci of the sagittal beams from the points of plane E and the foci of the meridional beams from the cell C coincide on the screen G. The rays of light from the source A are then expanded on the screen in the form of a curve.

Formation of the concentration diagram. The analysis of the composition of the mixture is based on the geometrical properties of the curve formed on the screen G (we shall term this the concentration diagram) (Fig. 1). We denote by θ the angle formed between the geometrical axis of the cylindrical lens and the vertical (the angle θ lies in a plane perpendicular to the axis of the optical system). We now introduce the following three coordinate systems. In the plane of the cell C: the x coordinate axis in the direction parallel to the geometrical axis of the cylinder F, and the coordinate axis z , taken along the vertical (i.e., in the direction of the concentration gradient); the coordinate origin is situated at the point O_1 , where the refractive-index gradient $dn/dz = 0$. In the plane of the screen G: the coordinate axis X, taken in a direction parallel to the coordinate axis x , and the coordinate axis Y, in a direction perpendicular to the coordinate axis X; the coordinate origin is at the point corresponding to the image of the point O_1 obtained by means of the single lens D. In the plane E: the y axis, in a direction parallel to the Y axis; the Z axis, taken parallel to the z axis, and the w axis, taken along the horizontal; the coordinate origin is at the point O. The point in the cell C with coordinate x will appear on the screen G as a thin line parallel to the Y axis, and at a distance X from it. The point in the plane E with

*Here and subsequently the curvature of the focal planes is ignored.

**This means one of the cell faces; the front face, for the sake of definiteness.

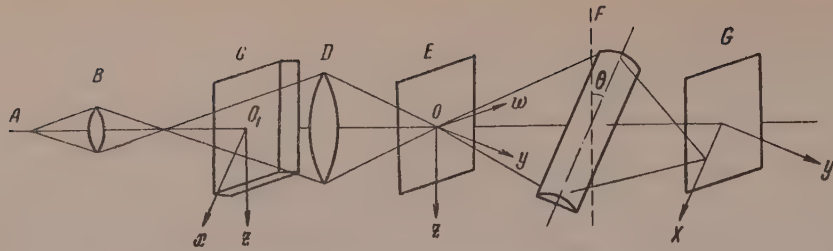


Fig. 1. Diagram of optical recording system.

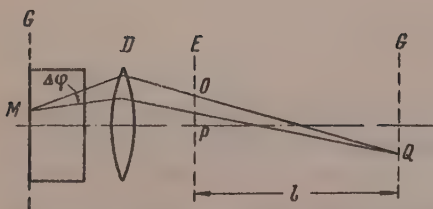


Fig. 2. Effect of the concentration gradient in the solution in the cell on the path of a ray of light.

the coordinate y will be represented as a thin line parallel to the X axis and at a distance Y from it. Thus, a ray of light which crosses the plane C at a point with coordinate x and the plane E at a point with coordinate Y will give a bright point with coordinates X, Y on the screen G .

We denote the magnifying powers of lenses D and F by K_1 and K_2 respectively.* The relationships between the coordinates x and y , and the coordinates X and Y are given by the expressions

$$X = K_1 x, \quad (1)$$

$$Y = K_2 y. \quad (2)$$

The formation of a concentration gradient along the O_1z axis blurs the point image of O in the lane E , along the OZ axis. The relationship between the above coordinates in the plane C is given by

$$x = z \cos \theta, \quad (3)$$

and in the plane E , by

$$y = Z \sin \theta. \quad (4)$$

These four equations contain six variables: x, y, z, X, Y and Z . In order to obtain the equation to the curve $Y(X)$ by elimination of the other variables, we must find a fifth equation connecting z and Z . For this we use the equation derived by Lamm [7] for the variation of the angle of deviation $\Delta\varphi$ of the ray in the cell with the refractive-index gradient of the solution and the thickness of the cell a , taken along the optical axis.

$$\Delta\varphi = a \frac{dn}{dz}. \quad (5)$$

Figure 2 explains the relationship between the coordinate Z and the angle $\Delta\varphi$, where C is the front face of the cell, D is a long-focus lens, E is the plane of the light-source images, and G is the screen (photographic plate). In the absence of a refractive-index gradient, a ray from the point M travels along the path MOQ , an image of the point M being formed at the point Q , and an image of the light source at the point O . With the formation of a refractive-index gradient the ray takes the new path MPQ . Owing to the low optical strength of the cell, the image Q does not deviate significantly from its previous position, while the image of the light source is displaced from O to P . The displacement OP is equal to the product of the distance l between the planes E and G , and the angle OQP . In turn, the angle OQP is equal to the ratio $\Delta\varphi/K_1$.

*The magnifying power K_2 is the magnifying power of the cylindrical lens with respect to the sagittal rays.

Thus,

$$Z = \frac{l}{K_1} \Delta\varphi \quad (6)$$

and, by virtue of Equation (5),

$$Z = a \frac{l}{K_1} \frac{dn}{dz}. \quad (7)$$

Combining Equations (2, 3 and 7) we have

$$Y = al \frac{K_2}{K_1} \frac{dn}{dz} \sin \theta. \quad (8)$$

From Equations (1) and (3) we obtain

$$dX = K_1 \cos \theta dz. \quad (9)$$

Multiplication of Equations (8) and (9) and integration of the resultant equation with respect to n gives

$$\int_{X_1}^{X_2} Y dX = alK_2 (n_2 - n_1) \sin \theta \cos \theta. \quad (10)$$

On the assumption that the increment of the refractive index is proportional to the increment of concentration c

$$\Delta n = m \Delta c \quad (11)$$

(where m is a constant) we can write Equation (10) in the form

$$S = \frac{m}{2} alK_2 (c_2 - c_1) \sin 2\theta, \quad (12)$$

where S is the area of the screen contained between the curve Y(X), the X axis, and the lines X = X₁, X = X₂.

Estimation of the resolving power of the optical system. In this theory of optical recording we neglect the dimensions of the light source, considering it as a geometrical point, which corresponds to the concept of the Y(X) curve as an infinitely thin line. In reality the curve on the screen G has finite width, and this limits the sensitivity of the method.

Assume that the luminous surface A is a circle of diameter ϵ . Since both the plane C and the plane E are projected onto the screen G, there are two causes for the spreading of the Y(X) curve into a band of finite width.

1. The cell C is entered in the direction φ not by one ray which reaches the point z, but by a beam which passes through the plane C between z and z + Δz .

2. In the plane E along the Z axis, we have the image not of an infinitely thin line, but of a band of width

$$\Delta w = K\epsilon, \quad (13)$$

where K is the magnifying power of lenses B and D.

These two factors apparently overlap to some extent. However, we shall consider the least favorable case, when the effect of the two factors is additive. We represent the width ΔN of the line Y(X), taken along the normal, as the sum $(\Delta N)_1 + (\Delta N)_2$ (here and subsequently the subscript indicates one of the two spreading factors considered above). Analogously, the width ΔX of the line Y(X), taken in a direction parallel to the X axis, and the width ΔY , in a direction parallel to the Y axis, can also be represented as sums of two intercepts

$$\Delta X = (\Delta X)_1 + (\Delta X)_2, \quad (14)$$

$$\Delta Y = (\Delta Y)_1 + (\Delta Y)_2. \quad (15)$$

We shall use the approximate equations

$$\frac{(\Delta Y)_1}{(\Delta X)_1} = \frac{(\Delta Y)_2}{(\Delta X)_2} = \frac{\Delta Y}{\Delta X} = \frac{dY}{dX}. \quad (16)$$

The value of dY/dX can be found by differentiation of Equation (8) with respect to \underline{z} and elimination of \underline{dz} from the resultant equation and Equation (9)

$$\frac{dY}{dX} = al \frac{K_2}{K_1^2} \frac{d^2n}{dz^2} \tan \theta. \quad (17)$$

The spreading of the coordinate \underline{z} by the amount Δz will determine the spreading of the coordinate \underline{x}

$$\Delta x = \Delta z \cos \theta. \quad (18)$$

From this and Equation (1) we have

$$(\Delta X)_1 = K_1 \Delta z \cos \theta. \quad (19)$$

We find Δz from the condition that the rays passing through the cell over the interval Δz form, in the plane E, an image with diameter

$$\Delta Z = K\epsilon. \quad (20)$$

From Equations (7), (19) and (20) we obtain

$$(\Delta X)_1 = \frac{KK_1^2 \epsilon}{ald^2n/dz^2} \cos \theta. \quad (21)$$

Substitution into the first of Equations (16) of the values of $(\Delta X)_1$ from (21) and dY/dX from Equation (17) gives

$$(\Delta Y)_2 = KK_2 \epsilon \sin \theta. \quad (22)$$

The value of $(\Delta Y)_2$ is determined by the spreading of the coordinate \underline{y} .

$$(\Delta Y)_2 = K_2 \Delta y = K_2 \Delta w \cos \theta, \quad (23)$$

which, because of Equation (13) gives

$$(\Delta Y)_2 = KK_2 \epsilon \cos \theta. \quad (24)$$

By adding Equations (22) and (24) term by term, and taking Equation (15) into account, we find

$$\Delta Y = KK_2 \epsilon (\sin \theta + \cos \theta). \quad (25)$$

We now use Svensson's concept [1] of the resolving power of the optical system. The resolving power is taken to mean the value Δc_1 of the concentration increment in the cell at which the area S enclosed by the curve $Y(X)$ becomes equal to the area σ of the curve itself.

An element of the area of the curve is represented by the expression $d\sigma = \Delta Y dX$, which gives, by virtue of Equations (25) and (9)

$$d\sigma = KK_1K_2\epsilon (\sin \theta + \cos \theta) \cos \theta dz,$$

and, after integration

$$\sigma = KK_1K_2\epsilon (\sin \theta + c \cos \theta) \cos \theta \Delta z, \quad (26)$$

where Δz is the distance over which the concentration changes by Δc (i.e., in practice, the width of the boundary layer in which a concentration gradient of a given component is formed after electrophoresis). Equating the right-hand sides of Equations (12) and (26) and solving the resultant equation for Δc , we have

$$\Delta c_i = \frac{KK_1\epsilon}{mal} (1 - \cot \theta) \Delta z. \quad (27)$$

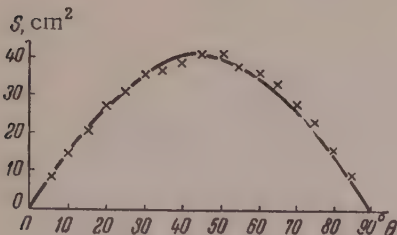


Fig. 3. Area of the concentration diagram as a function of the inclination of the cylindrical lens.

continuous line represents the $S-\theta$ curve calculated from Equation (12), and the points represent experimentally determined areas.

In comparisons of the two methods of optical recording it should be remembered that numerous variations in the arrangement of individual components of the optical system are possible in both methods.*

Figure 1 corresponds to a definite variation of the crossed-slit method, in which there is a horizontal slit in place of the light source A, and an inclined slit in the plane E. In the horizontal slit an image of the line source of width ϵ is formed; the angle between the second slit and the vertical is θ . For these conditions, Svensson's theory gives

$$S = malK_2(c_2 - c_1)\tan\theta, \quad (12a)$$

$$\Delta c_i = \frac{KK_1\epsilon}{mal} \Delta z + \Phi(\lambda), \quad (27a)$$

where Φ is a certain function of the wavelength.

Comparison of Equations (12) and (12a) shows that the crossed-slit method can give a concentration diagram of considerably greater area than the inclined cylindrical lens method. The importance of this should not, however, be exaggerated, as the scale of the curve can always be enlarged as desired by ordinary photographic enlargement.

Comparison of Equations (27) and (27a) is significant. It was shown by Svensson [1] that in Equation (27a) the term $KK_1\epsilon/mal$ is small relative to $\Phi(\lambda)$. Therefore, comparison of Equations (27) and (27a) leads to the conclusion that the inclined cylindrical lens method, which eliminates diffraction effects, makes it possible in principle to obtain high resolving power in a system for recording the distribution of concentrations in the cell.

Equation (27) clearly illustrates the role of the individual parameters of the optical system; its resolving power increases with decreasing K and K_1 and with increasing a and l . These parameters play the same role in Troitskii's apparatus as in Svensson's apparatus. In this connection, we may refer to the statement by Troitskii and Rodionov [5] that their instrument is transportable. To increase the sensitivity of the optical system, portability should be abandoned and the optical path increased considerably.

*However, different versions of the same method are analyzed similarly.

SUMMARY

1. A theory is presented for the optical registration of the composition of a mixture with the aid of an inclined cylindrical lens system.
2. The resolving power of the optical system in this method is estimated.
3. It is shown that with suitably chosen parameters of the optical system the resolving power of the new method may exceed that of systems used previously.

In conclusion, the author expresses his gratitude to Professor G.V. Troitskii, who suggested this investigation and who kindly placed at our disposal the experimental data given here, prior to publication.

LITERATURE CITED

- [1] H. Svensson, Electrophoresis by the Moving Boundary Method (Uppsala, 1946).
- [2] G.V. Troitskii, Biochemistry 15, 426 (1950).
- [3] G.V. Troitskii, Biochemistry 16, 592 (1951).
- [4] N.A. Troitskaia, Biochemistry 18, 151 (1953).
- [5] G.V. Troitskii and I.I. Rodionov, Biochemistry 20, 431 (1955).
- [6] G.V. Troitskii and D.A. Sorokina, Proceedings of the Scientific Session of the Crimean Medical Institute (Simferopol, 1956), p. 8.
- [7] O. Lamm, Zs. f. Phys. Chemie 138 A, 313 (1928).

Received January 4, 1957

The Borisoglebsk Pedagogic Institute

CHARACTER OF THE RELAXATION OF NONVULCANIZED RUBBER MIXES

K. Weber

We have designed a plastometer which can be used, with the minimum expenditure of time, for characterization of the technological properties of viscoelastic materials. The present investigation was confined to nonvulcanized rubber mixes.

To be effective, the method must conform to the requirements of the control of technological processing of the stocks. In the rubber industry, the plastometer designed by Baader and manufactured by the "Continental" company is widely used; the principle of this instrument is based on determination of the load which produces an axial compression of 4 mm in 30 seconds in a cylindrical specimen (10×10 mm). The value of this load is checked for four specimens. Immediately after the determination the load is removed from the specimen and its elastic recovery is measured after 30 seconds. It is possible to vary the temperature. The determinations are

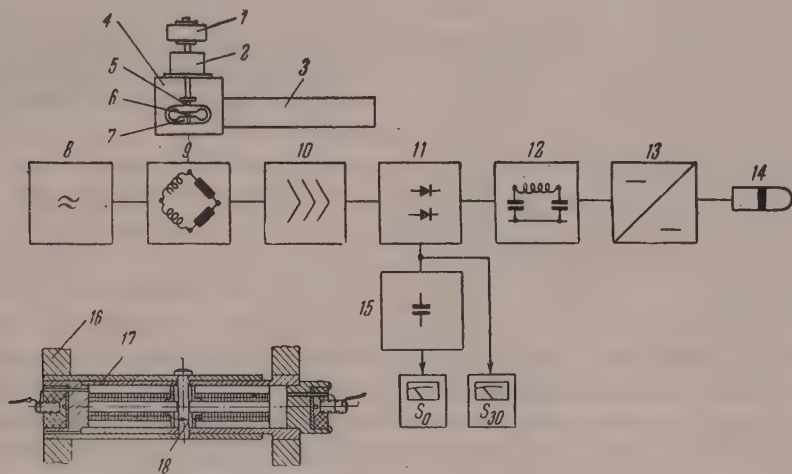


Fig. 1. Design of the plastometer: 1) motor; 2) drive; 3) preheating chamber; 4) heating chamber; 5) specimen; 6) force detector; 7) dynamometer spring; 8) tube generator; 9) modulator; 10) amplifier; 11) discriminator; 12) filter; 13) direct-current transformer; 14) loop oscillograph; 15) battery; 16) dynamometer spring; 17) force detector; 18) air gap.

usually made at 80° . The rate of deformation is not constant during the measurement; its average value is 0.2 mm/second. Because of the viscosity of the material, its deformational properties depend on the rate of loading (in milling, calendering, mixing, etc.). However, this rate is about two orders of magnitude greater than the rate used in the tests, which lowers the effectiveness of the method. Our aim was to design an instrument in which resistance to deformation could be measured at relatively high deformation rates, and relaxation of stress at constant deformation could also be determined. A block diagram of the instrument is given in Fig. 1.

A cylindrical specimen (10×10 mm) is deformed by axial compression at a constant rate (usually 10

mm/second) to a predetermined extent; the maximum resistance to deformation can be measured in absence of any significant displacements in the measuring instrument. Stress relaxation is recorded immediately after the deformation. It is possible to observe the kinetics of relaxation or, in serial tests, it is possible to measure the stress corresponding to a given time (say 30 seconds) in the deformed state. The results of the tests for each specimen are interpreted independently. The force is transmitted through a plate (dynamometer spring) carrying the specimen, and the curvature of the spring is recorded by an induction force detector. The dynamometer spring is so designed that a force of 20 kg (the maximum value) produces a deformation of less than 0.01 mm. The electronic measuring circuit operates on the carrier frequency. The tube generator produces oscillations at a frequency of 5 kc, and at an amplitude modulated by means of an alternating-current bridge. The induction detector is situated in one arm of this bridge, and a resistance in another. The modulated-amplitude oscillations

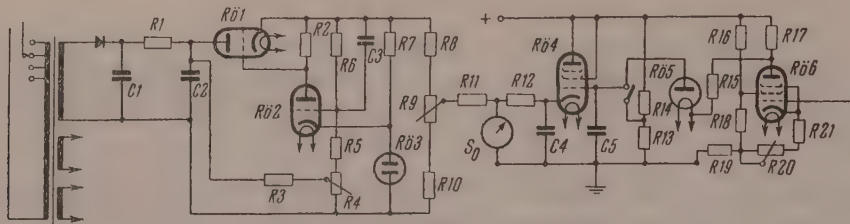


Fig. 2. Auxiliary measuring device.

tions are amplified, demodulated by means of a ring discriminator, and fed into a direct-current amplifier through a filter. This amplifier produces signals recorded by a cathode-ray (± 200 v) or loop oscillograph. In order to ensure that the instantaneous value of the maximum resistance to deformation (S_0) is measured, an auxiliary measuring device was constructed, with an instrument the pointer of which is set to a reading corresponding to the maximum resistance to deformation. The circuit of this device is given in Figure 2. When the bridge is balanced, we have the same voltage at the anode of the tube 6 as at the grid of tube 4. If the bridge is out of balance, the grid voltage of tube 6 is more positive, the anode current of tube 6 increases and the anode voltage diminishes. As a result, the capacitor C5 is discharged by means of tube 5 by the same amount. The change of the cathode current of tube 4 determines the pointer reading at S_0 . If the grid voltage of tube 6 now becomes more negative (this depends on the behavior of the induction detector during relaxation of stress in the specimen), the anode current of this tube decreases, and the anode voltage increases. However, the capacitor C5 can no longer be charged by the same amount, as tube 5 is cut off. At the end of the measurement, after the compression plate has been raised again, the capacitor C5 is again charged through a relay by means of the voltage distributors R13 and R14, and is switched over to "measurement" shortly before the next measurement. In parallel with this device, another measuring instrument is connected before the direct-current amplifier, the pointer of which indicates the stress at any instant after deformation. The amplification can be varied to give three-measurement ranges: the full sweep of the pointer (100 scale divisions) can represent 5, 10 or 20 kg.

A photograph of the instrument is shown in Figure 3. Figure 4 is an oscillogram obtained in tests of a tread stock based on Buna S. This shows an ascending region corresponding to the deformation period, a sharp stress maximum, and a relaxation curve. It was found during analysis of the results that the relaxation of stress measured by this method in pure natural and synthetic rubbers and mixtures with fillers, plasticizers, etc., based on these rubbers does not conform either to an exponential or to a logarithmic law. It may be expressed as the sum of three or more exponents, but such an expression requires the use of at least three time constants and three constants with the dimensions of force or stress. Thus, the expression for the stress-time relationship involves at least six mathematical constants which, moreover, depend on the measurement points chosen for the calculations.

We found a fairly simple empirical interpolation formula, which represents the results of our experiments very satisfactorily. This equation contains only two constants, and is of the form

$$\frac{S_0 - S}{S - S_\infty} = \sqrt{\frac{t}{\tau}},$$

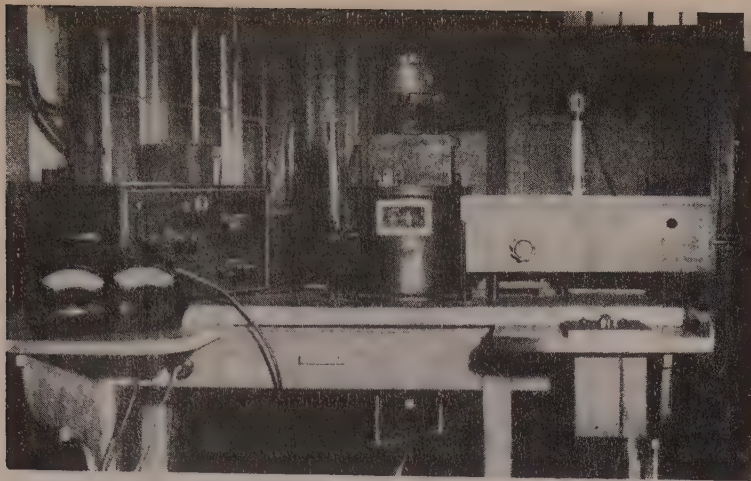


Fig. 3. General view of plastometer.

where S_0 is the maximum stress at the instant the deformation process is ended; t is the time; S_∞ and τ are constants. The relative relaxation of stress S/S_0 is given, after rearrangement, by the expression

$$\frac{S}{S_0} = R(t) = \frac{1 + R_\infty V t / \tau}{1 + V t / \tau}.$$

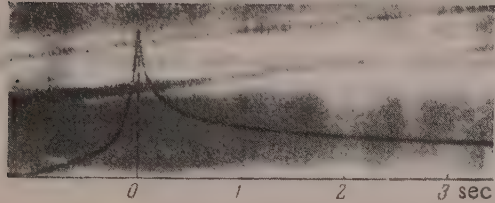


Fig. 4.

This expression can be readily verified by plotting $R(t)$ as a function of $1 - R(t)/\sqrt{t}$. If the expression is valid, a straight line should be obtained cutting off an intercept R_∞ along the ordinate axis, and with slope $\sqrt{\tau}$. It is found in all cases that the relative relaxation of stress $R(t)$, both for pure rubbers and for complex mixtures, is independent of the shape of the specimen or the magnitude of the deformation; this is true for all measurement temperatures from 20 to 100°.

Figure 5 gives the results of measurements carried out with butyl rubber (A_1) and Buna S4 (A_2) at 20, 50 and 80° (see page 132) interpreted with the aid of the above expression. The deformation behavior of the two polymers varies in different ways with the temperature; this suggests differences in the internal mobility of the molecules. Indeed, the internal mobility of the molecules of butadiene-styrene copolymer is hindered to some extent by the presence of styrene. Natural rubber (NR) exhibits similar relaxation behavior to butyl rubber, while other Buna types resemble Buna S4 in this respect. Figure 6 gives the results of a series of measurements on three types of rubber mixes, differing only by the nature of the rubber: mix B_1 was based on pure NR, B_2 — on NR with Buna S4 (50:50), and B_3 — on pure Buna S4. All three mixes contained thirty parts of finely divided channel black E. Here the nature of the rubber again determines the differences in the effect of temperature on relaxation; the behavior of a mix based on two rubbers is found to be intermediate relative to the respective pure rubbers. The nature of the relaxation of six different mixes is shown in Figure 7. The relative stress relaxation after 60 seconds (S_{60}/S_0) is plotted against the maximum resistance to deformation S_0 . Each curve corresponds to one mix and to different temperatures, varied in the range of 20 to 80°. This is an unusual way of plotting the graphs, but it illustrates very clearly the influence of temperature on the resistance to deformation and relaxation of stress in the rubber. As both these factors are significant in evaluation of the processing characteristics of a given mix, this method quickly gives a fairly complete picture of its technological properties. B_1 , B_2 and B_3 are the above-mentioned mixes containing channel black E, while B_4 , B_5 and B_6 contained the semireinforcing acetylene black P 1250, which ensures good extrusion properties. The continuous curves represent mixes B_1 , B_2 and B_3 with channel black E; the dash lines represent mixes B_4 , B_5 and B_6 . Mix B_3 , based on Buna with channel black E, shows an increase of the relative stress relaxation at 80°. This reflects the elasticity of this mix, which determines its very poor extrudability.

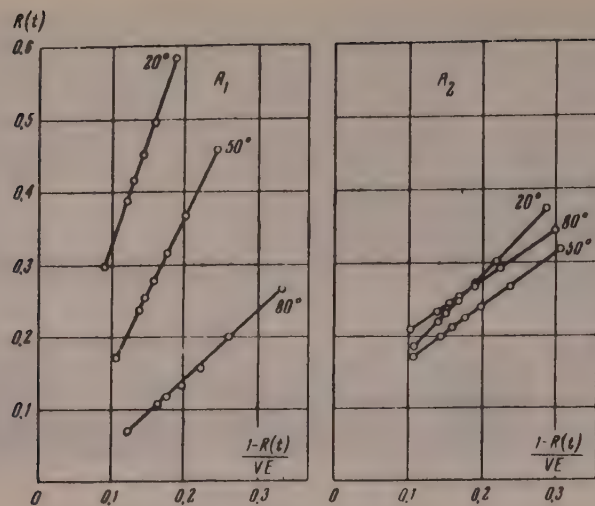


Fig. 5.

On the other hand, the mix B₆ based on Buna and containing P 1250 black shows a further decrease of the relative stress relaxation at 80°, which is fully consistent with its good extrudability. It is seen that mixes based on pure NR (B₁ and B₄) do not show this effect while their technological properties are just as good. However, in mixes B₂ and B₄, based on combinations of rubbers, the influence of the carbon black differs from its influence in mixtures based on pure Buna. These combined mixes are intermediate in their properties between mixes based on the individual rubbers. The results of these tests on other mixes are given in the table. The deformation,

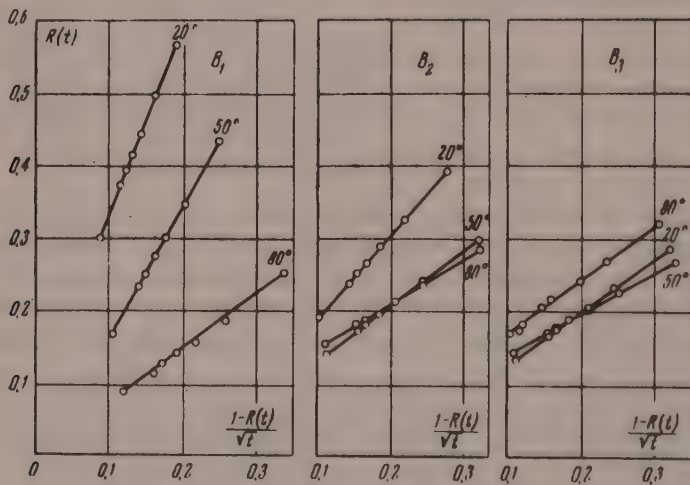


Fig. 6.

test temperature, S_0 , and the constants R_∞ and τ of the relaxation equation are given for each mix. Mixes A₁ to B₆ have already been mentioned. The types of rubber and carbon black exert an influence in these mixes. Mixes C₁ and C₂, based on Buna 3, differ only in the degree of degradation of the rubber, that is, in the Defoe hardness, with values of 1400 and 400 respectively. The very large differences of the effects of temperature on τ and R_∞ indicate the strong influence of the degree of degradation on the nature of the relaxation. The more "elastic" mix based on hard rubber is more difficult to work than a mix with soft rubber. The increase of the constant τ with temperature for the soft mix suggests that temperature has a negative influence on extrudability; this is in harmony with practical experience. The mixes D₁ and D₂ based on NR have the same composition, and

Mix	Test tem- perature, °C	Deforma- tion, mm	S, kg	Relaxation con- stants		Composition of mixes	
				τ (sec)	R	components	contents in wt. parts
A ₁	20	5	6.95	8.87	+0.0256	Butyl rubber	Not filled
	50	5	5.43	4.43	-0.0529		
	80	5	4.27	0.93	-0.0530		
A ₂	20	5	7.78	1.40	+0.075	Buna S4	Not filled
	50	5	5.10	0.60	+0.090		
	80	5	3.32	0.46	+0.138		
B ₁	20	3	4.04	6.65	+0.0825	NR Carbon black E	100 30
	50	3	2.84	3.37	-0.0325		
	80	3	2.00	0.54	-0.0038		
B ₂	20	3	4.17	1.353	+0.0701	NR Buna S4 Carbon black E	100 50 30
	50	3	2.72	0.576	+0.0594		
	80	3	1.60	0.432	+0.0778		
B ₃	20	3	3.63	0.527	+0.0509	Buna S4 Carbon black E	100 30
	50	3	2.12	0.380	+0.0733		
	80	3	1.16	0.618	+0.0791		
B ₄	20	3	4.30	5.64	+0.0684	NR Carbon black P 1250	100 30
	50	3	3.26	2.71	-0.0234		
	80	3	2.52	1.047	-0.0241		
B ₅	20	3	4.23	1.368	+0.064	NR Buna S4 Carbon black, P 1250	50 50 30
	50	3	2.96	0.804	+0.0391		
	80	3	1.84	0.416	+0.0403		
B ₆	20	3	3.68	0.552	+0.0444	Buna S4 Carbon black P 1250	100 30
	50	3	2.19	0.295	+0.0521		
	80	3	1.16	0.569	-0.0031		
C ₁	20	3	5.26	2.92	+0.101	Buna S3 Carbon black E	100 (* 1400) 30
	50	3	4.10	1.217	+0.126		
	80	3	3.02	0.923	+0.137		
C ₂	20	3	3.68	0.781	+0.058	Buna S3 Carbon black E	100 (* 400) 30
	50	3	2.06	0.781	+0.058		
	80	3	1.19	1.601	+0.031		
D ₁	20	5	6.14	5.64	+0.100	NR Carbon black E (unmilled stock)	100 30
	50	5	4.87	2.80	-0.019		
	80	5	3.76	1.83	-0.062		
D ₂	20	5	4.89	2.80	+0.014	NR Carbon black E (milled stock)	100 30
	50	5	3.38	1.16	-0.041		
	80	5	2.24	0.56	-0.040		
E ₁	20	3	4.30	2.32	+0.033	NR Buna S3 Carbon black E	80 20 15
	50	3	2.07	0.706	+0.015		
	80	3	1.28	0.257	+0.036		

* Hardness.

TABLE (continued)

Mix	Test tem- perature, °C	Deform- ation, mm	S ₀ , kg	Relaxation con- stants		Composition of mixes	
				τ (sec)	R	components	contents in wt. parts
E ₂	20	3	8.10	1.382	+0.063	NR	80
	50	3	4.80	0.488	+0.068	Buna S3	20
	80	3	3.20	0.250	+0.125	Carbon black E	60
F ₁	20	3	3.26	0.756	+0.066	Buna S3	100
	50	3	1.45	0.530	+0.074	Carbon black E	30
	80	3	0.80	0.658	+0.154		
F ₂	20	3	7.85	0.782	+0.076	Buna S3	100
	50	3	3.20	0.450	+0.093	Carbon black E	60
	80	3	1.80	0.404	+0.162		

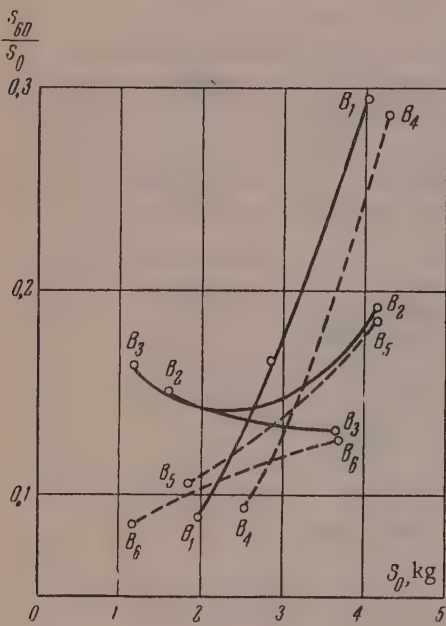


Fig. 7.

only differ in the degree of mastication. It is readily seen that the unmilled mix is more elastic. E₁ and E₂ are two combined mixes with a predominance of NR, and they only differ in the carbon black content: E₁ contains 15 parts and E₂ 60 parts of carbon black E. The dependence of the relaxation on temperature diminishes with increasing temperature with increasing active black contents. The relatively high value of R_∞ indicates that the elasticity increases with increasing concentration of the active black. F₁ and F₂ are mixes based on pure Buna S3 with different concentrations of active carbon black E (30 and 60 parts). The influence of the carbon black content is less here than in the corresponding mixes based on NR. The more pronounced effect of temperature on the constant τ is a sign of better extrudability as the result of the higher carbon black content; however, the change of R_∞ in the opposite direction indicates that the shrinkage should be greater. This is also in full agreement with technological experience. If the relaxation of stress is represented as the sum of a very large number of elementary exponential processes, for the limiting case we have the following expression

$$R(t) = \int_0^\infty L(t) e^{-t/\tau} d \ln \tau,$$

where L(t) is the relaxation spectrum in a logarithmic time scale, which may be calculated, with the aid of the Laplace transform, from the empirical formula which is in good agreement with the experimental data. A method of successive approximations has been given by Schwartzel for integral transforms of this type. In the first approximation, the equation has the form

$$L_1(t) = dR(t)/d \ln t.$$

If we solve this equation, we obtain the following formula for the spectrum from our expression for the relaxation

$$L_1(t) = \frac{1 - R_\infty}{2} \frac{V_{t/\tau}}{(1 + V_{t/\tau})^2}.$$

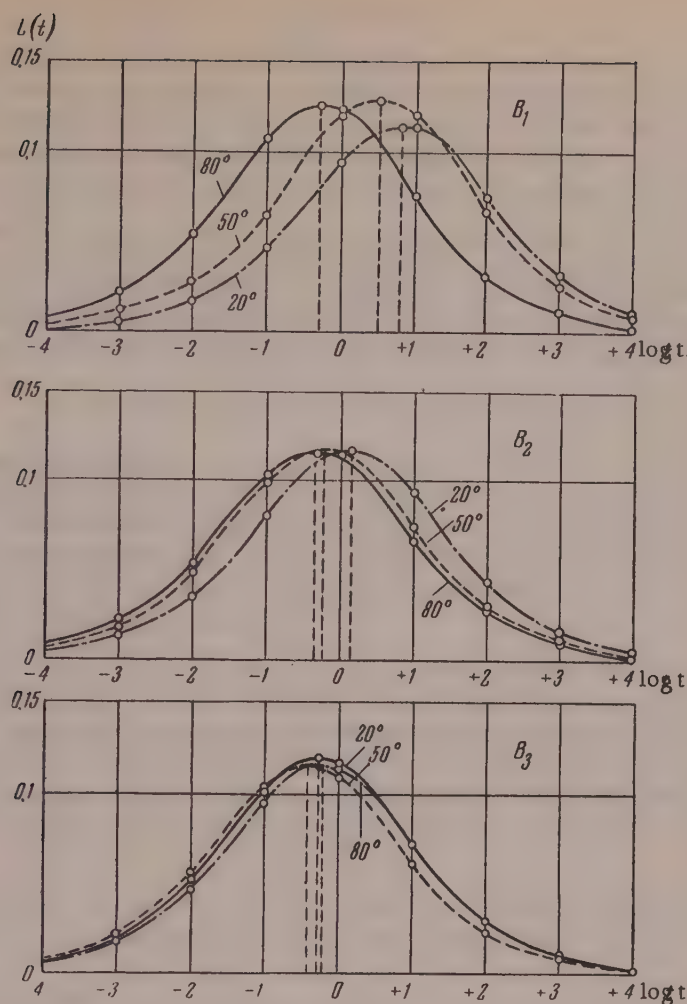


Fig. 8.

It follows from this equation that the spectrum has a maximum at the point $t = \tau$. The constant τ in our equation for the relaxation proves to be the relaxation time corresponding to an elementary process occurring at the maximum intensity. Figure 8 gives the approximate spectra for mixes B_1 , B_2 and B_3 as functions of the temperature. Both the spectral intensities and the relaxation times of the maximum intensity reveal a very obscure picture of the effects of temperature, which cannot be explained kinetically or thermodynamically as yet. The question arises whether this is due to the approximate nature of our calculations or whether the composition of the mixtures, which are complex multicomponent systems, has a fundamental significance.

In conclusion, I wish to express my gratitude to the Director of the Central Scientific Research Center of the Tire Industry of the German Democratic Republic Dr. A. Springer for his guidance in this investigation. I also offer my thanks to Engineer Heinz Luckner, who constructed the instrument, and to all my associates.

SUMMARY

A description has been made of a new plastometer by means of which the viscoelastic properties of rubbers are characterized by load-deformation curves (during the axial compression of cylindrical specimens at 10×10 mm at a constant rate of approximately 10 mm/sec) and load-time curves (at arbitrary constant compression) obtained in a single run. The electrical arrangement including an induction detector and a cathode ray or loop oscillograph provides for a high degree of accuracy and for the automatic recording of the results. The empirical formula

$$\frac{S_0 - S}{S - S_\infty} = \sqrt{\frac{t}{\tau}},$$
 where S is the instantaneous stress at the time t reckoned from the moment of cessation of the deformation, S_0 is the initial stress value (at $t = 0$) and S_∞ and τ are empirical constants, has been proposed for describing the relaxation curves. Data have been presented to illustrate the correlation between the values for the constants and their temperature dependence on one hand and the technological properties of the rubbers on the other.

Received September 15, 1957

Central Scientific Research Center of
the Tire Industry
Fürstenwalde
German Democratic Republic

INVESTIGATION OF THE TRUE FLUIDITY AND ELASTICITY OF RUBBERS AND RAW RUBBER MIXES

B.I. Gengrinovich and G.L. Slonimskii

As is known, the deformation of rubbers and raw rubber mixes under the action of external forces develops in two different forms,* because of the ability of polymeric substances to undergo reversible, high-elastic deformation, and irreversible deformation or true flow. The mechanical properties of such substances are therefore determined by their capacity to undergo both types of deformation, and should be studied in such a way as to take into account the simultaneous manifestation of both.

Detailed studies of the subject [1-3] have been carried out relatively recently, and relate only to pure undiluted rubbers. If the laws governing the development of the individual components of the total deformation of raw rubber mixes could be established, this would provide insight into the dependence of the mechanical properties both on the molecular structure of the rubber, and on the nature of the ingredients introduced into the mix. This insight, in its turn, is necessary for the development of the physical principles governing the composition of rubber mixes with required technological properties, and for the selection of rational methods for the laboratory testing of raw mixes.

The present communication contains certain data obtained in an investigation of the properties of raw mixes with the object of determining the laws which govern the development of the different components of the total deformation.

Method of investigation and interpretation of the results. The mechanical properties of rubbers and mixes were studied by the method of uniaxial compression of cylindrical specimens 10 × 10 mm.

The rubbers, and also the milled mixes, contained considerable numbers of pores, which could distort the results of the determinations. To remove the pores, the materials were rolled to give the thinnest possible films, which were stacked into sheets of the required thickness. Each sheet was placed in the middle of a cylindrical mold, where it was slowly pressed under a hydraulic press until excess of the mixture flowed out through the gap between the plunger and the mold. After 2-3 days under pressure, the sheet was removed from the mold and then stored for several days at room temperature to allow the stresses to decay. To complete the relaxation, the sheet was placed for 3 hours in a thermostat at 55-60°. Specimens cut from the sheets were subjected to additional relaxation at room temperature for several days.

The specimens were assumed to be at equilibrium when their height became constant as measured by means of a micrometer with 0.01 mm divisions. It must be pointed out that this cannot be regarded as a strict enough criterion; it merely indicates that the stresses which arose during preparation of the specimens had relaxed to the extent which is possible at room temperature. For true equilibrium the specimens must be kept for a long time at elevated temperatures, which gives rise to pore formation. Moreover, experiments showed that exposure to high temperatures apparently causes chemical changes in the raw mixes, so that consistent results cannot be obtained in measurements of the mechanical properties. As the specimens were not quite in equilibrium, this introduced some degree of uncertainty into the quantitative studies. However, we considered that it was preferable to study specimens containing certain internal stresses rather than specimens of changed chemical composition.

* We disregard elastic (Hookean) deformation, which is very small.

A Hüppler consistometer, modified for our purposes, was used for the determinations. The specimens were placed in a cylinder 20 mm in diameter, contained in a thermostat, and were compressed by means of a piston to which a load was applied through a rod. To diminish end effects, the ends of the specimens were smeared with glycerol. After the specimens had been held for 15 minutes at the temperature of the experiment, they were compressed at constant load. The displacement of the piston during compression was recorded as a function of time. At the end of the predetermined time of action the specimen was removed and restored by treatment in boiling water for 30 minutes. The experiments were performed at 40, 70, 100, and 120°. The mechanical properties at a given load were calculated from the following data: initial height of the specimen H_1 , height under load after a definite time H_2 , and height after restoration of the deformed specimen at 100° followed by 24 hours at room temperature, H_3 ; H_1 and H_3 were measured by means of a micrometer at room temperature, and H_2 was read off on the consistometer scale at the temperature of the experiment. The deformability was assessed as the true deformation, defined as the integral, between the initial and final lengths, of the ratio of an infinitesimal length change at a given instant to the actual length H at the same instant:

$$D = \int_{H_1}^{H_2} \frac{dH}{H} = \ln \frac{H_2}{H_1},$$

In accordance with the accepted designations, we have the following expressions for the total (D), plastic (D_p) and high-elastic deformation.

$$D = \ln \frac{H_2}{H_1}; D_p = \ln \frac{H_3}{H_1}; D_{he} = \ln \frac{H_2}{H_3}.$$

It is seen that

$$D = D_p + D_{he}.$$

As the true stress varied during deformation, the "coefficient of viscosity" was calculated as the ratio of the integral $\int_0^{\tau} \sigma(\tau) d\tau$ to the value of the plastic deformation which developed during the whole time of action of the load τ . The integration was performed graphically by measurement of the area of the experimentally found curve for the variation of the total relative deformation with the time τ ,

$$\int_0^{\tau} \sigma(\tau) d\tau = \int_0^{\tau} A(1 - \epsilon) d\tau = \int_0^{\tau} A\lambda(\tau) d\tau = A \int_0^{\tau} \lambda(\tau) d\tau,$$

where the stress $\sigma(\tau)$ at the given instant, the total relative deformation $\epsilon(\tau)$ at the same instant, and the stress A calculated for the initial cross section are connected by the expression $\sigma = A(1 - \epsilon)$ or $\sigma = A\lambda$, which is valid if the volume remains unchanged during the deformation; λ is the relative length of the specimen.

Thus, the viscosity was calculated by means of the formula*

$$\eta = \frac{\int_0^{\tau} \sigma(\tau) d\tau}{D_p} = \frac{A \int_0^{\tau} \lambda(\tau) d\tau}{D_p}$$

* It may be noted that if $\eta = \text{const}$, from $\eta = \frac{\int_0^{\tau} \sigma d\tau}{D_p}$ we have $\sigma = \eta \frac{dD_p}{dt}$, which is Newton's generalized viscosity equation. This was the reason for our choice of η for characterization of the plastic properties.

To characterize the high-elastic properties, we determined the elasticity modulus, defined as the ratio of the stress acting on the specimen before removal of the load to the true high-elastic deformation

$$E_{he} = \frac{A\lambda}{D_{he}}.$$

The initial stress was varied from 0.13 to $1.86 \cdot 10^6$ dynes/cm², and the deformation time, from 3 to 300 minutes. Rubber mixes based on SKB-50_{av} were used in the study. The mixes did not contain vulcanizing groups. The mixes contained, in parts by weight, 100 rubber, 5 each of Rubberax, asphalt, and zinc oxide, 2 of oleic acid, and 45 carbon black (channel black in Mix 1 and lamp black in Mix 2). Experiments were also performed on rubbers without added ingredients and on three-component mixtures containing 100 parts of rubber,

2.5 of stearic acid, and 45 of carbon black (channel in Mix 3 and lamp in Mix 4). The deformation conditions for the rubbers and three-component mixtures are given in the account of the experimental results. The results of the determinations are given in CGS units.

Experimental results and discussion. Figure 1 gives the curves for the development of total deformation and the individual components of the deformation in SKB-50_{av} rubber and mixes containing channel (Mix 3) and lamp (Mix 4) black. It would have been desirable to compare the behavior of these systems under the same compression conditions; however, owing to the sharp change of properties produced by introduction of carbon black this condition could be only partially satisfied with the experimental procedure used. The greatest deviations from uniform deformation, which could distort the results, were found in the original rubber.

It follows from Figure 1 that the pure rubber is deformed more easily than its mixtures, and this is due to high-elastic deformation, as the plastic component of the deformation is small. Introduction of carbon black decreases the total deformation. The two blacks differ little in their effect on the reversible high-elastic deformability, the absolute values of the high-elastic deformation of Mixes 3 and 4 being similar. The nature of the black mainly influences the plastic deformation. As a result, the deformation components are in a different ratio in the two mixes. Under equal experimental conditions, mixes containing channel black are characterized by a higher ratio

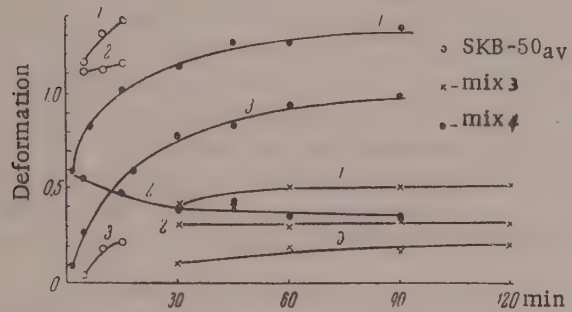


Fig. 1. Development of deformation of SKB-50_{av} rubber and of Mixes 3 and 4; $t = 70^\circ$; $A = 0.62 \cdot 10^6$ dynes/cm²; 1) total deformation; 2) high-elastic component; 3) plastic component.

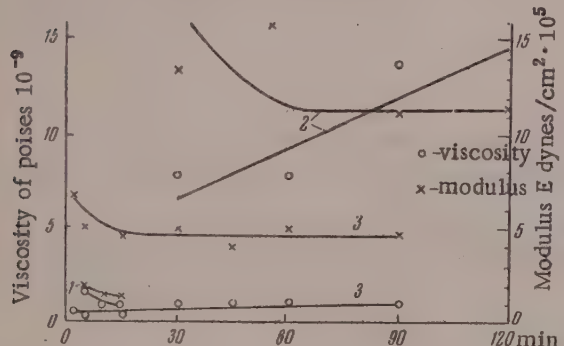


Fig. 2. Effect of the time of deformation on the viscosity and modulus of elasticity of SKB-50_{av} rubber and Mixes 3 and 4; $t = 70^\circ$; $A = 0.62 \cdot 10^6$ dynes/cm²; 1) SKB-50_{av}; 2) Mix 3; 3) Mix 4.

of the high-elastic to plastic component in the total deformation, as compared with mixes containing lamp black. Accordingly, the coefficient of viscosity and elasticity modulus are higher in mixes with channel black than in mixes with lamp black (Figure 2). Thus, although the two blacks decrease the high-elastic component of the deformation to approximately the same extent, they confer different elasticoplastic properties on the mixes.

The variations of the elasticoplastic characteristics of Mix 2 with the time of deformation and the load at different temperatures are given in Figures 3 and 4; similar relationships hold for Mix 1.

It follows from these results that the elasticity modulus can either decrease or increase with time. The direction of the change of the elasticity modulus depends on a number of factors. At temperatures below 70°

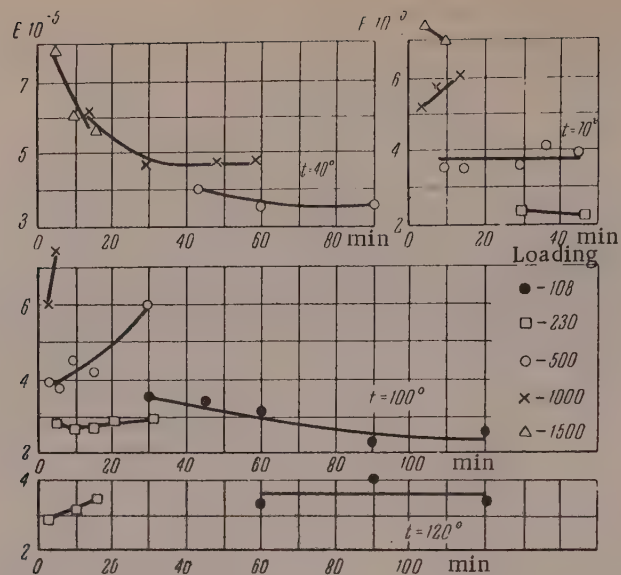


Fig. 3. Effects of time, temperature, and stress on the modulus of high elasticity of Mix 2.

the elasticity modulus decreases with time at all the stresses used. At higher temperatures, the elasticity modulus increases with time. The greater the compressive force, the greater is this increase; it is evidently the result of chemical or physicochemical structural changes in the material under these conditions. Decrease of temperature and of the stress diminishes the role played by these changes and thereby favors relaxation processes which lead to a decrease of the elasticity modulus. These results suggest that the modulus of elasticity of raw rubber mixes as a

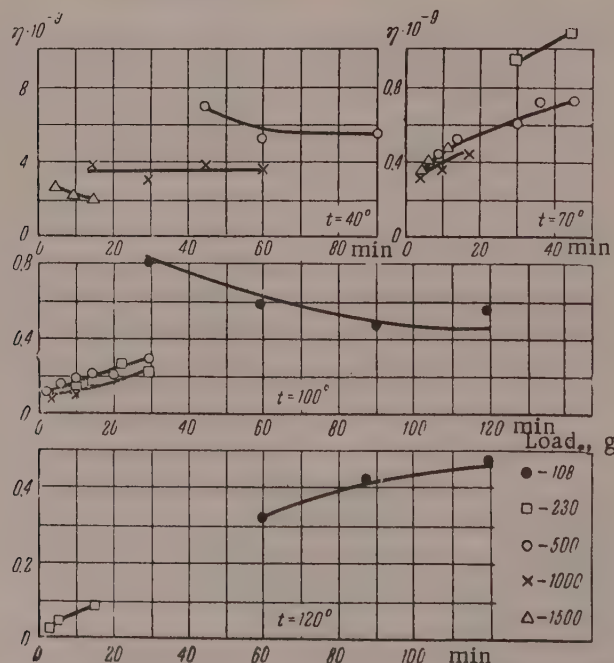


Fig. 4. Effects of time, temperature, and stress on the coefficient of viscosity of Mix 2.

function of the time of action of the force has a minimum. It seems that in our experiments only isolated portions of this general function were observed; it depended on the temperature and the force which portion of the complete curve (descending or ascending) was actually observed in a particular experiment. At lower temperatures, when chemical and physicochemical processes develop slowly, relaxation of stress with time is the predominant effect. At high temperatures these processes become appreciable, while the relaxation is so rapid that it is complete at the very start of the experiment. Therefore the modulus increases with time; the rate of increase naturally depends on the temperature and the force, which are the principal factors governing the mechanochemical processes which develop.

Examination of Figure 4 shows that the variations of viscosity with the time of action of the force, the magnitude of the force, and the temperature are also of a complex character. At 40° the viscosity decreases with time for small acting forces. At higher temperatures and at larger stresses the viscosity nearly always increases with time. It is possible that the complete viscosity-time curve also shows a minimum. Under the action of the applied force the structure of the raw rubber mix gradually breaks down, and the viscosity therefore decreases with time. During flow, however, the chain molecules are straightened, and chemical and physicochemical processes altering the structure also develop. These changes produce a gradual increase of viscosity. Naturally, at low temperatures and small stresses the predominant process is the gradual breakdown of the structure of the raw rubber mix, and therefore the viscosity decreases with time in such conditions. Conversely, the structure breaks down rapidly at high temperatures or large stresses, and the only effect actually observed is the development of chemical and physicochemical processes leading to structurization. At low temperatures and large stresses the viscosity increase may be attributed to the development of elastic deformation.

The effect of temperature on the stress-viscosity and stress-modulus relationships is very peculiar. The influence of the stress on the modulus of elasticity increases at higher temperatures, whereas the viscosity only depends on the stress at lower temperatures.

All these peculiarities of the mechanical behavior of raw loaded rubber mixes indicate that their characteristic feature is the variability of structure in the course of deformation. Little is known as yet about the mechanism of the variations of the structure of raw loaded rubber mixes during deformation, but it is quite evident that it depends on the chemical reactivity of the raw mixes and the variability of the structure formed by the rubber-carbon mixes.

SUMMARY

1. Data have been obtained on the mechanical properties of rubbers, two-component rubber-carbon black systems, and loaded raw rubber mixes at various temperatures and under different stresses.

2. The true viscosity and the elasticity modulus of a raw rubber mix depend on the time, temperature, and the magnitude of the applied force; it is suggested that this is a consequence of the variability of the structure of the mix under stress and on heating.

LITERATURE CITED

- [1] L. Treloar, Trans. Faraday Soc. 36, 538 (1940).
- [2] V.A. Kargin and T.I. Sogolova, J. Phys. Chem. 23, 540, 551 (1949).
- [3] G.M. Bartenev, J. Phys. Chem. 24, 1210 (1950).

Received November 20, 1956

Scientific Research Institute for the
Tire Industry — Moscow

THE COAGULATION OF LYOPHOBIC SOLS BY THE ACTION OF MIXTURES
OF ELECTROLYTES. COMMUNICATION II.

Iu.M. Glazman, I.M. Dykman and E.A. Strel'tsova

Our previous paper [1] on this problem dealt with the coagulation of lyophobic sols by the action of mixtures of two symmetrical electrolytes, of the $1 - 1 + 2 - 2$ type. It was shown on the basis of Deriagin's theory of stability of lyophobic colloids [2] that if the coagulation process is not complicated by subsidiary effects, synergism should occur on the addition of such pairs of electrolytes to a sol, over almost all of their concentration range.

In discussing the causes of the antagonism which is experimentally observed in coagulation, we made the suggestion that the nature of this effect is predominantly associated with adsorptive interaction between the ions and the colloid particles, which occurs in the system when coagulant electrolytes are added to the sol and which, as a rule, probably decrease the surface potential of the disperse phase. However, in the light of certain literature data on antagonism [3, 4], and also of our calculations [1], we noted that the possibility of antagonism is not excluded even in absence of such adsorption effects. This must primarily apply to the special cases in which the "unloading effect" of the colloid particles [5] caused by the electrostatic action of ions of similar charge to them, is fairly pronounced. Pauli and Valko [5] showed that, in consequence of this effect, the presence of multivalent foreign ions may lead to a considerable decrease of the coagulating action of the second electrolyte added to a colloidal solution.

When a mixture of two electrolytes acts on a sol, two opposing factors, determined by different aspects of the mechanism of the coagulation process, are apparently always superposed. On the one hand, we have synergism, which is probably the consequence of compression of the diffuse ionic atmospheres which occurs when electrolytes are added to the system. On the other hand, there is always some tendency to antagonism, because of the influence exerted by electrolytes on the shielding by gegenions of the electric field on the inner layer of the double layer. The degree of this antagonism must evidently depend considerably on the "unloading effect" of the colloid particles [5] under the action of similarly charged ions. As both these factors are taken into account in Deriagin's theory, the results of calculations based on it must evidently depend on which of these factors predominates. In the case considered previously [1], the latter factor is weak, as the presence of a 1 - 1-valent electrolyte produces the "unloading effect" [5] to only a small extent; therefore a 1 - 1-electrolyte has relatively little influence on the decrease of the coagulating action of the bivalent ion of the second component of the mixture. Because of this, calculation in this case shows synergism, and only in the very beginning the curve lies a little above the additivity line. With other combinations of electrolytes, where, owing to the "unloading effect" [5], the suppression of the coagulating action of the multivalent ion is more pronounced, this effect may prevail over synergism, and, in such cases, the theoretical curves can naturally be expected to correspond to antagonism. The present investigation was undertaken to verify these considerations. We therefore repeated the calculations reported previously [1], extending them to the coagulation of a sol by a mixture of two electrolytes of the type $1_2 - 2 + 2 - 2$ (if the colloid particles of the sol are negatively charged, the ions of different valence in these electrolytes are assumed to be positive, and vice versa). The significant difference between this electrolyte system and the system considered previously [1] is that here the second ion of the first of these electrolytes is bivalent, and therefore the "unloading effect" [5] is more pronounced. Accordingly, the coagulating action of the bivalent gegenion of the symmetrical electrolyte should be decreased to a greater extent in presence of the first component of the pair, than in mixtures of two electrolytes of the type $1 - 1 + 2 - 2$. Otherwise, the calculations are based on the same reasoning as before [1].

Suppose that unit volume of the solution contains n_1 positive ions of the first electrolyte, each carrying a charge $2e\underline{z}$, and $2n_1$ negative ions each carrying a charge $e\underline{z}$ (here \underline{z} , as usual, is the valence of the ion). Moreover, the solution also contains n_2 positive and n_2 negative ions of the second electrolyte, of charge $2e\underline{z}$. If we assume, as before [1], that the colloid particles are fairly large and can be regarded for the purpose of our problem as pairs of infinite parallel planes at a distance \underline{h} apart, then to determine the potential ψ at any point in the volume we can use an equation analogous to Equation (2) of the previous paper [1]

$$\frac{d^2\psi}{dx^2} = \frac{8\pi e z}{\epsilon} \left[n_1 \exp\left(\frac{e z \psi}{\theta}\right) - n_1 \exp\left(-\frac{2 e z \psi}{\theta}\right) + 2n_2 \operatorname{Sh}\left(\frac{2 e z \psi}{\theta}\right) \right]. \quad (1)$$

The previous notation is retained: e is the unit charge; ϵ is the dielectric constant of the solution; $\theta = kT$, the product of the Boltzmann constant and the absolute temperature. It is assumed, for the sake of clarity, that the potential ψ_1 on the plate surfaces ($x = \pm h/2$) is positive.

It is easy to find the first integral of Equation (1) and, by the reasoning given previously [1], to determine the integration constants (C). They are, for the inner and outer parts of the space respectively:

$$C_1 = n_1 \left[2 \exp\left(\frac{e z \psi_0}{\theta}\right) + \exp\left(-\frac{2 e z \psi_0}{\theta}\right) \right] + 2n_2 \operatorname{ch}\left(\frac{2 e z \psi_0}{\theta}\right), \quad (2)$$

$$C_2 = 3n_1 + 2n_2, \quad (3)$$

where ψ_0 is the potential at the point $x = 0$.

The square of the field strength (E^2) at any point in the volume is:

$$E^2 = \left(\frac{d\psi}{dx} \right)^2 = \frac{8\pi\theta}{\epsilon} \left[2n_1 \exp\left(\frac{e z \psi}{\theta}\right) + n_1 \exp\left(-\frac{2 e z \psi}{\theta}\right) + 2n_2 \operatorname{ch}\left(\frac{2 e z \psi}{\theta}\right) - C \right] \quad (4)$$

The values of C must be substituted into Equation (4) in accordance with Equations (2) or (3), depending on whether the field strength is determined in the inner or outer regions.

We now use Equations (2), (3) and (4) to find, as in Equation (6) of the previous paper [1], the force of repulsion P acting on unit area of the plates

$$P = \theta \left\{ n_1 \left[2 \exp\left(\frac{e z \psi_0}{\theta}\right) + \exp\left(-\frac{2 e z \psi_0}{\theta}\right) - 3 \right] + 2n_2 \left[\operatorname{ch}\left(\frac{2 e z \psi_0}{\theta}\right) - 1 \right] \right\}. \quad (5)$$

For the subsequent integration of Equation (4), it is convenient to replace ψ by a new function u , defined as

$$u = \exp\left(\frac{e z \psi}{\theta}\right). \quad (6)$$

We can then put

$$u_0 = \exp\left(\frac{e z \psi_0}{\theta}\right); \quad u_1 = \exp\left(\frac{e z \psi_1}{\theta}\right). \quad (7)$$

Substituting the Function (6) into Equation (4) with an arbitrary constant, given by Equation (2), and integrating Equation (4) with respect to x between 0 and $h/2$ and with respect to u between u_0 and u_1 respectively, we obtain the following relationship between u_0 and h after some simple rearrangement:

$$h \sqrt{\frac{2\pi e^2 z^2}{\epsilon \theta}} = \int_{u_0}^{\infty} \frac{du}{[n_1(2u^3 - 2u^2 u_0 - u^2 u_0^{-2} + 1) + n_2(u^4 - u^2 u_0^2 - u^2 u_0^{-2} + 1)]^{1/2}}. \quad (8)$$

Since we are considering strongly charged sols, $u_1 \gg 1$, and in the integral of Equation (8) the upper limit can be regarded as infinite.

The Integral (8) cannot be calculated in terms of elementary functions. It is important, however, that not the whole range of the possible values of the concentrations n_1 and n_2 , regarded as fixed parameters in Equation (8), is of equal significance for our problem. It was particularly stressed in the previous paper [1] that, in the case of symmetrical electrolytes, values above the additivity line are obtained only in the initial region of the $n_{2C} = n_{2C}(n_{1C})$ curve. It follows that, for the asymmetric electrolytes considered here, the same initial portion of the $n_{2C} = n_{2C}(n_{1C})$ curve is of the most interest. Therefore, to simplify the subsequent calculations, we shall assume that n_1 is infinitely small, tending to zero, and only expressions which are linear with respect to it will be taken into consideration in resolution. With this approximation, Equation (8) reduces to two integrals in the right-hand side:

$$h \sqrt{\frac{2\pi e^2 z^2}{\varepsilon \theta}} = \frac{1}{V n_2} \int_{u_0}^{\infty} \frac{du}{(u^4 - u^2 u_0^2 - u^2 u_0^{-2} + 1)^{1/2}} - \\ - \frac{n_1}{2 V n_2^3} \int_{u_0}^{\infty} \frac{(2u^3 - 2u^2 u_0 - u^2 u_0^{-2} + 1)}{(u^4 - u^2 u_0^2 - u^2 u_0^{-2} + 1)^{3/2}} du. \quad (9)$$

The first of the integrals in (9) is expressed in terms of a complete elliptic integral of the first kind (see Mathematical Supplement I)

$$\frac{1}{V n_2} \int_{u_0}^{\infty} \frac{du}{(u^4 - u^2 u_0^2 - u^2 u_0^{-2} + 1)^{1/2}} = \frac{u_0}{V n_2 (u_0^2 + 1)} K(k), \quad (10)$$

where the modulus k is given by the ratio

$$k = \frac{2u_0}{u_0^2 + 1}. \quad (11)$$

The second integral in the right-hand side of (9) is written as the sum of three integrals

$$\frac{n_1}{2 V n_2^3} \int_{u_0}^{\infty} \frac{(2u^3 - 2u^2 u_0 - u^2 u_0^{-2} + 1)}{(u^4 - u^2 u_0^2 - u^2 u_0^{-2} + 1)^{3/2}} du = \\ = \frac{n_1}{2 V n_2^3} \left[\frac{2u_0^4}{u_0^4 - 1} I_1 + \frac{u_0^2 - 2u_0 - 1}{2u_0 (u_0^2 - 1)} I_2 - \frac{(u_0 - 1)^2}{2u_0 (u_0^2 + 1)} I_3 \right], \quad (12)$$

where

$$I_1 = \int_{u_0}^{\infty} \frac{du}{(u + u_0) [(u^2 - u_0^2)(u^2 - u_0^{-2})]^{1/2}}; \\ I_2 = \int_{u_0}^{\infty} \frac{du}{(u + u_0^{-1}) [(u^2 - u_0^2)(u^2 - u_0^{-2})]^{1/2}}; \\ I_3 = \int_{u_0}^{\infty} \frac{du}{(u - u_0^{-1}) [(u^2 - u_0^2)(u^2 - u_0^{-2})]^{1/2}}. \quad (13)$$

The calculation of the Integrals (13) is given in Mathematical Supplement II. The final result is

$$I_1 = \frac{1}{u_0^2 + 1} F(\varphi, k) + \frac{1}{u_0^2 - 1} [E(\varphi, k) - 1], \quad (14)$$

$$I_2 = \frac{u_0^2}{u_0^4 - 1} + \frac{u_0^2}{2(u_0^2 + 1)} K(k) - \frac{u_0^2}{2(u_0^2 - 1)} E(k), \quad (15)$$

$$I_3 = \frac{u_0^2}{u_0^4 - 1} - \frac{u_0^2}{2(u_0^2 + 1)} K(k) + \frac{u_0^2}{2(u_0^2 - 1)} E(k), \quad (16)$$

where the argument φ is

$$\varphi = \arctan\left(\frac{u_0^2 + 1}{u_0^2 - 1}\right)^{1/2}. \quad (17)$$

We substitute Equations (10-17) into (9). This gives the relationship between h and u_0 in explicit form.

To determine the critical value of h_c and the critical concentrations n_{2c} and n_{1c} , we use the Deriagin-Landau equation (see Equation (24) in [1])

$$\frac{h}{P} \frac{dP}{dh} = -3, \quad (18)$$

which, in this instance, is conveniently written in the form

$$h \frac{dP}{du_0} = -3P \frac{dh}{du_0}. \quad (19)$$

The derivative dP/du_0 in Equation (19) is easily found if we substitute (7) into Equation (5) for the force P . This gives:

$$\frac{dP}{du_0} = \frac{2\theta}{u_0^3} [n_1(u_0^3 - 1) + n_2(u_0^4 - 1)]. \quad (20)$$

Determination of the derivative dh/du_0 involves rather more cumbersome calculations (see Mathematical Supplement III), which give

$$\begin{aligned} \frac{dh}{du_0} = & \sqrt{\frac{\varepsilon_0}{2\pi e^2 z^2}} \left\{ -\frac{1}{V n_2 (u_0^2 - 1)} E(k) + \right. \\ & \left. + \frac{n_1}{2\sqrt{n_2^3}} \times [a_1 K(k) + a_2 E(k) + a_3 F(\varphi, k) + a_4 E(\varphi, k) + a_5] \right\}. \end{aligned} \quad (21)$$

Here the coefficients a_i are:

$$\begin{aligned} a_1 &= \frac{u_0^8 - 4u_0^7 - 2u_0^4 - 4u_0^3 + 1}{2(u_0^4 - 1)^2 (u_0^2 + 1)}; \quad a_2 = -\frac{u_0^8 - 8u_0^7 + 2u_0^4 - 8u_0^3 - 3}{2(u_0^4 - 1)^2 (u_0^2 - 1)}; \\ a_3 &= \frac{8u_0^3}{(u_0^4 - 1)^2 (u_0^2 + 1)}; \quad a_4 = \frac{4u_0^3 (u_0^4 + 3)}{(u_0^4 - 1)^2 (u_0^2 + 1)}; \\ a_5 &= -\frac{4u_0 (u_0^8 + u_0^6 + 6u_0^4 + 3u_0^2 + 1)}{(u_0^4 - 1)^3}. \end{aligned} \quad (22)$$

We now use Equations (5), (20) and (21), and also the results of substitution of Equations (10-17) into (9), to obtain Equation (19), used for determination of the "critical" value of u_0 in the form:

$$\frac{3}{2} E(k) - K(k) = f [b_1 K(k) + b_2 E(k) + b_3 F(\varphi, k) + b_4 E(\varphi, k) + b_5], \quad (23)$$

where $f = n_1/n_2$. The coefficients b_i are:

$$\begin{aligned}
b_1 &= \frac{u_0^8 - 4u_0^6 + 24u_0^5 - 14u_0^4 - 12u_0^2 - 3}{8(u_0^4 - 1)(u_0^2 + 1)^2}; \\
b_2 &= -\frac{u_0^8 + 4u_0^7 - 40u_0^6 + 56u_0^5 - 54u_0^4 + 4u_0^3 - 8u_0^2 + 5}{8(u_0^4 - 1)^2}; \\
b_3 &= -\frac{u_0^3(u_0^4 + 2u_0^2 - 5)}{(u_0^4 - 1)(u_0^2 + 1)^2}; \quad b_4 = \frac{2u_0^3(u_0^4 - u_0^2 + 4)}{(u_0^4 - 1)^2}; \\
b_5 &= -\frac{2u_0(u_0^8 + 7u_0^4 + 3u_0^2 + 1)}{(u_0^4 - 1)^2(u_0^2 + 1)}. \tag{24}
\end{aligned}$$

When $f = 0$, Equation (23) becomes the Deriagin-Landau equation [2]

$$\frac{3}{2} E(k) - K(k) = 0, \tag{25}$$

the root of which is $k_0 = 0.77394$, which, according to Equation (11), corresponds to $u_{00} = 2.1103^*$ (u_{00} is the value of u_0 when $f = 0$).

When f is not zero, the solution of Equation (23) is found in the form

$$u_0 = u_{00} + u_{01}. \tag{26}$$

Since we restricted ourselves from the start to infinitesimal values of f , the root u_{01} need only be determined with an accuracy down to terms of the first power of f . For this, we substitute u_{00} into the right-hand side, and $u_{00} + u_{01}$ and $k_0 + k_1$ into the left-hand side of Equation (23). Resolution (with an accuracy down to linear terms) of the function $K(k)$ and $E(k)$ into Taylor's series gives an equation of the first degree with respect to u_{01} (see Mathematical Supplement IV)

$$\left[-\frac{u_{00}^2 - 1}{2u_{00}(u_{00}^2 + 1)} K(k_0) + \frac{u_{00}^4 - 10u_{00}^2 + 1}{2u_{00}(u_{00}^4 - 1)} E(k_0) \right] u_{01} = f \Phi(u_{00}), \tag{27}$$

where $\Phi(u_{00})$ is the expression in the square brackets of the right-hand side of Equation (23). The requisite calculations give $u_{01} = 0.1379f$. Thus we have the following final value for the root of Equation (23) (see Mathematical Supplement V):

$$u_0 = 2.1103 + 0.1379f. \tag{28}$$

This root, in the form of (28) or (26), is substituted into Equations (5) and (9) [with (10-17) taken into account], giving the "critical" values of the force P_c and the distance between the plates h_c . Retaining only the terms linear with respect to f , we have

$$P_c = n_2 \theta \left[\frac{(u_{00}^2 - 1)^2}{u_{00}^2} + \frac{2(u_{00}^4 - 1)}{u_{00}^3} u_{01} + \frac{2u_{00}^3 - 3u_{00}^2 + 1}{u_{00}^2} f \right]; \tag{29}$$

$$\begin{aligned}
h_c &= \sqrt{\frac{\varepsilon \theta}{2\pi e^2 z^2 n_2}} \left\{ \frac{u_{00}}{u_{00}^2 + 1} K(k_0) - \frac{u_{01}}{u_{00}^2 - 1} E(k_0) - \right. \\
&\quad \left. - \frac{f}{2} \left[\frac{2u_{00}^4}{u_{00}^4 - 1} I_1(u_{00}) + \frac{u_{00}^2 - 2u_{00} - 1}{2u_{00}(u_{00}^2 - 1)} I_2(u_{00}) - \frac{(u_{00} - 1)^2}{2u_{00}(u_{00}^2 + 1)} I_3(u_{00}) \right] \right\}. \tag{30}
\end{aligned}$$

*The calculations were performed with the aid of Stirling's interpolation formula and seven-figure tables of complete elliptic integrals [6].

The "critical" concentration n_{2c} can now be found by substitution of (29) and (30) into Equation (22) of the paper [1]

$$P_c = \frac{\pi A}{6h_c^3} \quad (31)$$

(A is the constant of mutual molecular attraction).

We do not give the analytical form of Equation (31) after substitution of (29) and (30) into it, as it is extremely cumbersome. It is simpler to use the root (28) to perform the numerical calculations and to substitute into Equation (31), instead of P_c and h_c , the expressions

$$\begin{aligned} P_c &= n_2 \theta (2.678 + 1.998 f); \\ h_c &= \sqrt{\frac{\epsilon \theta}{2\pi e^2 z^2 n_2}} (0.7540 - 0.1765 f). \end{aligned} \quad (31a)$$

Simple calculations then give

$$\alpha + \beta f = B \sqrt{n_{2c}}, \quad (32)$$

where

$$B = \frac{\pi^2 A e^3 z^3}{3 \epsilon \theta^2} \sqrt{\frac{2\pi}{\epsilon \theta}}. \quad (33)$$

Equation (33) gives the critical concentrations n_{2c} and n_{1c}

$$n_{2c} = \frac{1}{B^2} (\alpha^2 + 2\alpha\beta f); \quad n_{1c} = \frac{\alpha^3}{B^3} f. \quad (34)$$

At the point $n_{1c} = 0$ the derivative dn_{2c}/dn_{1c} is

$$\frac{dn_{2c}}{dn_{1c}} = \frac{dn_{2c}/df}{dn_{1c}/df} = \frac{2\beta}{\alpha} = 0.088. \quad (35)$$

The positive sign of the derivative dn_{2c}/dn_{1c} means that if a sol is coagulated with a mixture of two electrolytes of the type $1_2 - 2 + 2 - 2^*$ antagonism should occur, at least in the region of low concentrations (relative to the critical value n_{2c}) of the first component of this pair.

Thus, in full agreement with the above considerations, the laws governing the coagulation of lyophobic sols by mixtures of electrolytes of the type $1 - 1 + 2 - 2$ and $1_2 - 2 + 2 - 2$ respectively differ not only qualitatively [3]; they are opposite to each other quantitatively. Whereas in the former case theoretical calculations indicate the existence of synergism, in the latter case they point to sharply pronounced antagonism.**

It is relevant in this connection to point out that up to the present time antagonism has been regarded by nearly all workers as antagonism between the coagulant ions, despite the different explanations advanced for the effect. The results of our calculations show that this concept is essentially erroneous. Comparison of the results in this and the preceding [1] paper shows convincingly that the relationships observed in coagulation by a mixture of electrolytes can be quite different (the deviations from additivity of the coagulant action may differ not only in magnitude but also in sign) even with the same combination of gegenions. The antagonistic effect therefore depends on the electrolyte system as a whole, and not on any particular combination of coagulant

*Here, as previously, the first of the electrolyte ions is assumed to be the coagulating ion, while the second is charged similarly to the colloid particles.

**In fact, since the critical concentration n_{1c}^0 of the first electrolyte is much higher (about 64 times) than the coagulating concentration n_{2c}^0 of the second, even a small change in the absolute value of n_{2c} , in accordance with Equation (35), corresponds to a large relative increment in this value.

ions. The laws governing the coagulation of lyophobic sols differ significantly, depending on whether the coagulation is effected by the action of individual electrolytes or mixtures.

While in the former case the concept of a principal (coagulating) ion and a secondary ion (with the same charge as the colloid particles) is fully justified, this classification of the ions is quite unfounded in the latter case. Indeed, the nature of the action of electrolyte mixtures on lyophobic colloids is sometimes entirely determined, as we have seen, by the valence of the ion which is usually regarded as subsidiary. The probable reason for this very strong influence of the valence of the "subsidiary" ion on the coagulant action of electrolyte mixtures is that the critical concentration of an electrolyte with a univalent coagulant ion is many times higher (conforming to a sixth-power law [2]) than the concentration of the second electrolyte of the pair in question. Accordingly, the "loosening of the electric double layer" and the "unloading effect" of the colloid particles associated with it [5], which ultimately determine the coagulating effect of an electrolyte mixture, should depend much less on the charge of the subsidiary ion of "its own" electrolyte than on the valence of the similarly charged ion of the second electrolyte, present at a considerably higher concentration in the solution. It is this "unloading effect," caused by the subsidiary ions in the electric field of the colloid particles which is the probable cause of antagonism in a number of instances of coagulation reported in the literature [3, 4], and similar to that considered in this paper.

Despite the importance of this conclusion, it must be remembered that this is by no means the only cause of antagonism, and in all probability it is not the main cause. It must be emphasized that the results in this paper are based on calculations in which various adsorption effects which usually accompany coagulation and which undoubtedly influence the process are completely disregarded. At the same time, antagonism between electrolytes is often determined, as follows from our previous paper [1], by just these additional effects.

All the foregoing considerations lead to the conclusion that antagonism in the coagulation of lyophobic sols is a complex phenomenon, the nature of which differs in different cases. There are apparently two types of antagonism in the coagulation of lyophobic colloids:

1. Antagonism between the coagulant ions associated with competition for sites of adsorption on the surfaces of the colloid particles. The higher the specific adsorption potential of the gegenion of lower valence added to the sol, the more pronounced should the antagonism between the coagulant electrolytes be.

2. Antagonism caused by electrostatic interaction of the ions within the volume of the solution and in the electric field of the colloid particles. The greater the difference between the critical (i.e., coagulating) concentrations of the two electrolytes, and the higher the valence of the "subsidiary" ion in the electrolyte with the weaker coagulating action, the more pronounced the "unloading effect" should be; accordingly, the coagulating action of a multivalent gegenion in the electrolyte mixture should be suppressed to a greater extent, and antagonism should accordingly be more pronounced.

If, in addition to these considerations, it is also taken into account that the purely electrostatic mechanism of the coagulation process may lead to synergism in certain cases [1], the great variety of the effects observed in the coagulation of lyophobic sols by various electrolyte mixtures [7] becomes understandable.

In conclusion, it is the authors' pleasant duty to express their gratitude to Corresponding Member (AN SSSR) B.V. Deriagin for his interest in the work, for valuable advice, and for discussion of the results.

Mathematical Supplements

I. The first integral in the right-hand side of Equation (9), after the substitution $u = u_0/\sin \varphi$, reduces to a complete elliptic integral of the first kind

$$\int_{u_0}^{\infty} \frac{du}{(u^4 - u^2 u_0^2 - u^2 u_0^{-2} + 1)^{1/2}} = \frac{1}{u_0} K(u_0^{-2}). \quad (I,1)$$

For the subsequent calculations it is more convenient to transform this integral, with modulus $k_1 = u_0^{-2}$, into an integral with the modulus k given by Equation (11). The formula (see [8], 6. 126. 3)

$$K\left(\frac{2V k_1}{1+k_1}\right) = (1+k_1) K(k_1) \quad (I,2)$$

at once gives (10).

II. The integral I_1 , as the result of the substitution

$$u = \frac{u_0 [(u_0^2 + 1) + (u_0^2 - 1)v^2]}{(u_0^2 + 1) - (u_0^2 - 1)v^2} \quad (\text{II}, 1)$$

reduces to the following integral

$$I_1 = \frac{1-m}{2} \int_0^{1/\sqrt{m}} \frac{(1-mv^2) dv}{[(1+m^2v^2)(1+v^2)]^{1/2}}, \quad (\text{II}, 2)$$

which is the difference between the two tabulated integrals of type 3.144.1 and 3.149.1 [8]. Here $m = (u_0^2 - 1)/(u_0^2 + 1)$.

Elementary calculations then lead to the result (14). As regards the integrals I_2 and I_3 , it is easy to see that they can be written as $I_2 = G_1 - u_0^{-1}G_2$ and $I_3 = G_1 + u_0^{-1}G_2$, where

$$\begin{aligned} G_1 &= \int_{u_0}^{\infty} \frac{udu}{(u^2 - u_0^{-2}) [(u^2 - u_0^2)(u^2 - u_0^{-2})^3]^{1/2}}; \\ G_2 &= \int_{u_0}^{\infty} \frac{du}{[(u^2 - u_0^2)(u^2 - u_0^{-2})^3]^{1/2}}. \end{aligned} \quad (\text{II}, 3)$$

By replacement of the variables $u^2 - u_0^{-2} = z^{-1}$ the first of these integrals reduces to an elementary integral; it is

$$G_1 = \frac{u_0^5}{u_0^4 - 1}. \quad (\text{II}, 4)$$

The second integral G_2 is of the type 3.146.4 given in standard tables [8]. We give its value, as the work cited contains a misprint

$$G_2 = \frac{u_0^5}{u_0^4 - 1} E(u_0^{-2}) - u_0 K(u_0^{-2}). \quad (\text{II}, 5)$$

Then, by applying the formulas for the transformation of complete elliptic integrals, namely (I, 2) and formula 6.126.4 [8]

$$E\left(\frac{2\sqrt{k_1}}{1+k_1}\right) = \frac{1}{1+k_1} [2E(k_1) - (1-k_1^2)K(k_1)], \quad (\text{II}, 6)$$

we readily obtain the values of I_2 and I_3 given in the text.

III. The derivatives of the elliptic integrals with respect to u_0 are calculated as follows:

$$\frac{dF}{du_0} = \frac{\partial F}{\partial \varphi} \frac{d\varphi}{du_0} + \frac{\partial F}{\partial k} \frac{dk}{du_0}; \quad \frac{dE}{du_0} = \frac{\partial E}{\partial \varphi} \frac{d\varphi}{du_0} + \frac{\partial E}{\partial k} \frac{dk}{du_0}. \quad (\text{III}, 1)$$

From the values of k and φ in accordance with (11) and (17), and with the aid of the formulas for the differentiation of elliptic integrals with respect to the modulus (see 6.123 [8]), we have

$$\frac{dF}{du_0} = \frac{u_0^2 - 1}{u_0(u_0^2 + 1)} F(\varphi, k) - \frac{u_0^2 + 1}{u_0(u_0^2 - 1)} [E(k) - E(\varphi, k)] - \frac{1}{u_0(u_0^2 - 1)}; \quad (\text{III}, 2)$$

$$\frac{dE}{du_0} = \frac{u_0^2 - 1}{u_0(u_0^2 + 1)} [F(\varphi, k) - E(\varphi, k)] - \frac{1}{u_0(u_0^2 + 1)}; \quad (\text{III},3)$$

$$\frac{dK}{du_0} = \frac{u_0^2 - 1}{u_0(u_0^2 + 1)} K(k) - \frac{u_0^2 + 1}{u_0(u_0^2 - 1)} E(k); \quad (\text{III},4)$$

$$\frac{dE}{du_0} = \frac{u_0^2 - 1}{u_0(u_0^2 + 1)} [K(k) - E(k)]; \quad (\text{III},5)$$

Substituting (III,2-III,5) into (9) and taking (10-16) into account, we find, after elementary although rather laborious calculations, the value of dh/du_0 given in the text.

IV. Equation (23), with an accuracy down to terms linear in f , can be written in the form

$$\frac{3}{2} E(k_0) - K(k_0) + u_{01} \frac{d}{du_0} \left[\frac{3}{2} E(k) - K(k) \right]_{u_0=u_{00}} = f \Phi(u_{00}). \quad (\text{IV},1)$$

If we substitute Equations (III,4-III,5) into this expression and take (25) into account, we at once obtain (27).

V. For the root $u_{00} = 2.1103$, the numerical values of the elliptic integrals are as follows: $K(k_0) = 1.9485$; $E(k_0) = 1.2990$; $F(\varphi_0, k_0) = 0.97424$; $E(\varphi_0, k_0) = 0.83286$.

The remaining calculations leading to (28) do not require explanation.

SUMMARY

1. The question of the coagulation of lyophobic sols by the action of mixtures of electrolytes has been examined on the basis of B.V. Deriagin's theory of stability of lyophobic colloids. Calculations made earlier for $1 - 1 + 2 - 2$ mixtures of electrolytes were extended to coagulation of sols by mixtures of two electrolytes of the type $1_2 - 2 + 2 - 2$.

2. It is shown that if a pair of electrolytes of the type $1_2 - 2 + 2 - 2$, with coagulant ions of different valences, is added to a sol, antagonism should occur at least in the initial portion of the curve.

3. The causes of antagonism in the coagulation of lyophobic sols by mixtures of electrolytes have been examined. It is suggested that the nature of the antagonistic effect differs in different cases.

LITERATURE CITED

- [1] Iu.M. Glazman and I.M. Dykman, Colloid J. 18, 13 (1956).*
- [2] B.V. Deriagin, Bull. Acad. Sci. USSR, chem. ser. 1155 (1937); Colloid J. 6, 201 (1940); 7, 285 (1941); B.V. Deriagin and L.D. Landau, J. Expt.-Theoret. Phys. (USSR) 1, 802 (1941); 15, 663 (1945); B.V. Deriagin, Colloid J. 16, 425 (1954)*; Proc. Third All-Union Conference on Colloid Chemistry, Acad. Sci. USSR (1956), page 225.
- [3] C.F. Vester, Dissertation (1935); cited through H.R. Kruyt, Kon. Akad. Wet. 38, 464 (1935).
- [4] Y. Doucet and G. Watelle, J. Chim. Phys. 52, 65 (1955).
- [5] Wo. Pauli and E. Valko, Elektrochemie der Kolloide, Wien 141, 193 (1929).
- [6] Ia.N. Shpilrein, Tables of Special Functions (GTTI, Moscow-Leningrad, 1933).**
- [7] Iu.M. Glazman, Colloid J. 8, 299, 387 (1946).
- [8] I.M. Ryzhik and I.S. Gradshtein, Tables of Integrals, Sums, Series, and Products (GTTI, Moscow-Leningrad, 1951).**

Received February 23, 1957

Kiev Technological Institute of the
Light Industry

*Original Russian pagination. See C.B. translation.

**In Russian.

THE FORMATION OF ULTRATHIN LAYERS OF DISPERSE PHASE AT
THE HYDRASOL-ORGANIC LIQUID INTERFACE

T. A. Degtareva and S. G. Mokrushin

The spontaneous formation of thin layers on the surfaces of colloidal solutions has been described by one of us [1] for hydrosols of iron, chromium, and aluminum hydroxides. The hypothesis was put forward that this process is the consequence of surface coagulation of the sol [2]. According to Frumkin [3], the surface of an aqueous solution is negatively charged owing to orientation of water dipoles and preferential adsorption of anions in the surface layer. Therefore, positively charged colloidal particles in the sol, reaching the surface by Brownian movement, become partially discharged and dipolar, and are fixed in the surface layer. The concentration of the colloidal particles in the surface layer therefore increases relative to their concentration in the volume of the sol. This leads to coagulation of particles in the surface layer with formation of islets, while no visible coagulation occurs in the volume of the sol. The islets gradually become denser and form a film in the form of a network, the spaces in which become filled with colloidal particles emerging on the sol surface. To confirm this hypothesis, the kinetics of formation of monolayer films on the surfaces of hydrosols of the hydroxides of iron [4], titanium, and thorium [5] had been studied earlier.

If the hydrosol-air interface is replaced by a hydrosol-condensed organic phase interface, the colloidal particles are held more firmly in consequence of the interfacial tension at the colloidal particle-liquid surface [6]. Further, the organic liquid may affect the stability of the sol and favor its coagulation [7]. The present investigation is a continuation and extension of our studies of this effect. We studied the kinetics of film formation at interfaces between nickel hydroxide hydrosols and organic liquids in relation to the sol concentration and the nature of the nonaqueous phase.

Colloidal particles of nickel hydroxides are hexagonal plates several molecular layers thick [8], and between 280 and 1000 Å in diameter [9]. The particles are positively charged (the sign of the charge was determined by electrophoresis), and experiments have shown that the property of spontaneous formation of thin films is found mainly in positively charged sols.

The sol was prepared by peptization of freshly precipitated nickel hydroxide, by the method described in the literature [10]. The sol was filtered to remove unpeptized particles, diluted with boiled distilled water to the required concentration (0.158 g of Ni per liter), and kept for 24 hours. This was used as the stock sol for preparation of sols of other concentrations. The nonaqueous phases were benzene, o-xylene, toluene, chlorobenzene, and nitrobenzene.

The experimental procedure was as follows: 0.5 liter of the sol was put into a glass crystallizing dish (332 cm² area), the surface was cleaned by means of a strip of filter card, the nonaqueous phase was introduced dropwise until lens-shaped droplets formed in the surface without spreading, and the dish was covered with a ground glass lid. After a definite time the dish was opened, the organic liquid was evaporated, and the film was transferred from the liquid surface to a chromium-plated plate by the Langmuir-Blodgett method [11].

The thickness of the films was calculated by means of Mokrushin's formula [12]:

$$\delta_1 = \delta_2 \frac{n_2}{n_1} = k\delta_2,$$

where δ_1 is the thickness of a multilayer film of nickel hydroxide of a given color; δ_2 is the thickness of a mul-

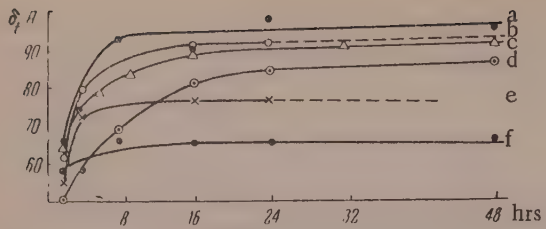


Fig. 1. Effect of the organic phase on the kinetics of formation of a nickel hydroxide film: a) benzene; b) o-xylene; c) toluene; d) chlorobenzene; e) nitrobenzene; f) film at the air interface.

TABLE 1

Thickness of Multilayer Films of Calcium Stearate and Nickel Hydroxide

Interference color of multilayer film	Thickness of multilayer in Å	
	calcium stearate	nickel hydroxide
Brown	512.4	467.6
Dark blue	1000.4	912.6
Sky blue	1488.4	1358
Yellow	1976.4	1803
Red	2464.4	2249

TABLE 2

Effect of the Nature of the Nonaqueous Phase on the Formation of Films of Colloidal Nickel Hydroxide

Nonaqueous phase	Dipole moment $\mu \cdot 10^{18}$	Limiting film thickness δ_{CO} in Å	Limiting film area S_{CO} in cm^2
Benzene	0	97	57
Toluene	0.40	92	55
o-Xylene	0.70	93	55
Chlorobenzene	1.57	77	44
Nitrobenzene	3.93	65	35

ide particles at the interface; this influence is more pronounced with increasing difference of polarity between the hydrosol and the nonaqueous phase, in full harmony with Rebinder's rule of equalization of polarity [13].

The differences between the limiting thicknesses of films formed under different organic liquids can be accounted for by the differences in the coagulating power of the latter.

According to the mechanism of film formation postulated by Mokrushin, such a film is a monolayer and its limiting thickness should not depend on the concentration of the sol if the degree of dispersion of the sol particles remains unchanged on dilution. To confirm this view of film structure, we studied the effect of sol concentration on the kinetics of film formation. Sols of different concentrations were obtained by two-, four- and

tilayer film of calcium stearate of the same color; n_1 is the refractive index of the nickel hydroxide film ($n_1 = 1.614$); n_2 is the refractive index of the calcium stearate film ($n_2 = 1.471$). The refractive index of the nickel hydroxide film was found from the angle of maximum polarization of light reflected from the film surface (Brewster's method), giving $n_1 = 1.610$; from measurements of the Becke line in the polarization microscope $n_1 = 1.617$. The average value of the refractive index as given by these two methods was used for calculations of the film thickness.

The thickness of the multilayer films was determined from the interference colors produced after repeated immersion of a chromium-plated plate into the sols. From the known thickness of a multilayer film of a definite color and the number of layers applied consecutively to the plate to produce this color, we were able to calculate the thickness of the monolayer formed on the sol surface (Table 1). The thickness of the monolayer was calculated for each color, and the average thickness was found from the results.

In our studies of the kinetics of formation of films at sol-organic liquid interfaces, the times of contact of the two liquid phases were 2, 4, 8, 16, 24 and 48 hours. The results of the determinations are given in Figure 1, where the film thickness in Å is plotted against the time in hours. It is clear from Figure 1 that the nonpolar condensed phase favors not only more rapid film formation, but also the formation of thicker films than those formed at the sol-air interface. Under layers of the more polar liquids (chlorobenzene, nitrobenzene) the limiting thickness of the films is less than under layers of nonpolar liquids.

In addition to the thickness, the area of the film was measured; for this, it was first compressed by the "oil piston" method [11]. Castor oil ($P = 16$ dynes/cm) was used as the piston liquid. The experiments show that the limiting film area, like the limiting thickness, is greatest under nonpolar liquid and increases with increasing polarity of the nonaqueous phase (Table 2).

It is seen from the data in Table 2 that the nonaqueous phase assists the fixation of nickel hydroxide particles at the interface; this influence is more pronounced with increasing difference of polarity between the hydrosol and the nonaqueous phase, in full harmony with Rebinder's rule of equalization of polarity [13].

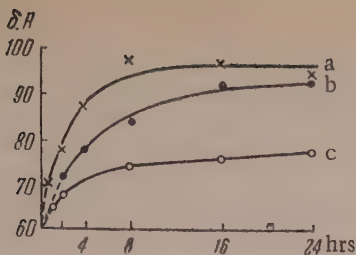


Fig. 2. Effect of dilution on the kinetics of formation of a nickel hydroxide film: a) original sol; b) sol after twofold dilution; c) after fourfold dilution; d) after eightfold dilution.

Comparison of this value with the value obtained by electron microscopy for the diameter of colloidal nickel hydroxide particles [9] indicates that our measurements gave the thickness of the particles in the film, and that the nickel hydroxide particles in the films are oriented with their flat sides toward the interface.

SUMMARY

1. The formation of a film at the hydrosol-organic liquid interface occurs as the result of passage of the particles from the volume of the sol to the interface, followed by coagulation and fixation in the surface layer.
2. The limiting thickness of the film and the time required for its formation depend on the difference between the polarities of the two liquid phases.
3. The colloid particles in the film are oriented with their flat sides toward the interface.

LITERATURE CITED

- [1] S.G. Mokrushin, Bull. Mendeleev All-Union Chem. Soc. 7, 38 (1941).
- [2] S.G. Mokrushin, J. Gen. Chem. 16, 11 (1946).
- [3] A.N. Frumkin, Collected Papers on Pure and Applied Chemistry No. 2, 3, No. 3, 3 (The L.Ia. Karpov Chemical Institute Press, 1924).
- [4] S.G. Mokrushin and M.I. Miliutina, Colloid J. 15, No. 3 (1953).*
- [5] S.G. Mokrushin and Z.G. Sheina, Colloid J. 16, 376 (1954).**
- [6] W. Reinder, Koll.-Z. 13, 235 (1913); F. Hoffmann, Z. phys. Chem. 83, 385 (1913).
- [7] H.B. Weiser and G.L. Mack, J. Phys. Chem. 34, 101 (1930).
- [8] Es.J. Longuet and J. Mering, Comptes. rend. 236, 1683 (1953).
- [9] W. Feitknecht and H. Studer, Koll.-Z. 115, 13 (1949).
- [10] W. Feitknecht, H. Studer and H. Meyer, Koll.-Z 139, 131 (1954); Tower, J. Phys. Chem. 28, 176 (1924).
- [11] K. Blodgett, J. Am. Chem. Soc. 57, 1007 (1935); S.G. Mokrushin, Proc. Acad. Sci. USSR 47, 2 (1945).
- [12] S.K. Mokrushin and P.S. Koniaev, J. Phys. Chem. 6, 95 (1935).
- [13] P.A. Rebinder, Z. phys. Chem. 129, 163 (1927).

Received December 4, 1956

S.M. Kirov Polytechnic Institute of
the Urals — Sverdlovsk

* See C.B. translation.

** Original Russian pagination. See C.B. translation.

eightfold dilution of the original sol. Benzene was used as the non-aqueous phase in each case. The results are given in Figure 2; it is seen that the film on the original sol ceases to increase in thickness after 8 hours of contact; with two- and fourfold dilution of the sol this time increases to 16 hours; the limiting film thickness is practically the same in all cases. In this dilution range the sol concentration does not influence the limiting thickness of the film; it only affects the kinetics of the process.

After eightfold dilution, the thickening of the film is much slower and the film does not reach its limiting thickness even after two days. This can be attributed to the considerable decrease in the concentration of the colloid particles in the sol after eightfold dilution.

Since the film consists of particles formed by coagulation of the primary colloid particles which emerged at the interface, the thickness of a monolayer film can be regarded as one of the dimensions of the particles forming the film. According to our measurements, this thickness is 97 Å under a layer of benzene.

BINDING OF WATER BY FINELY DIVIDED SEDIMENTS

1. CALCULATION OF THE AMOUNT OF BOUND WATER FROM THE ELECTROLYTE CONCENTRATION IN THE EQUILIBRIUM SOLUTION

O.I. Dmitrenko

When finely divided sediments interact with electrolyte solutions, they adsorb molecules of the solutes and solvent simultaneously. The adsorption of solutes by finely divided sediments and soils has been studied much more fully than the adsorption of the solvent (water).

It is known that the adsorption of solutes is associated with hydration and solubility effects [1, 2]. Adsorbability increases with decreasing solubility [3]. An inverse relationship between the amounts of molecularly adsorbed substances and the temperature has also been reported [1, 4]. A correlation between the degree of adsorption and solubility is found not only for different salts in the same solvent, but also for the same salt in different solvents [1, 5]. A direct dependence of the degree of adsorption and the concentration of the added electrolyte is characteristic for the molecular adsorption of electrolytes [6]. A very important relationship between the amounts of molecularly adsorbed electrolytes and the amounts of bound water in soils has also been reported [5].

It follows from these literature data that both electrolytes and nonelectrolytes are involved in molecular adsorption on soils. Consequently, the adsorption of sparingly soluble electrolytes, capable of replacing molecules of bound water [5], introduced into the system, will be directly dependent (under equal conditions) on the bound water content of the soil; this was confirmed by Iarusov [5]. Iarusov estimated the bound water content of soils from their hygroscopic moisture, as it had been shown by Dumanskii [7] that the bound water content and hygroscopicity of a soil have fairly similar values.

The purpose of the present work was to devise a rapid and accurate method for the determination of bound water in natural sediments. In contrast to earlier work [8], the main condition which we attempted to satisfy is the retention of the structure and the natural moisture contents of the sediments.

The materials chosen for the study were aleuritic-clay and clay finely divided sediments from the Bering Sea. These sediments, extracted by means of a hydrostatic tube from a depth of 3882 meters, have high contents (up to 90%) of a pelite fraction with particles smaller than 0.01 mm, and low carbonate contents. The organic carbon content of the sediments varied between 0.3 and 2% (Table 1).

Detailed chemical characteristics of these sediments have been given by Bruevich and Zaitseva [10].

The determination of the bound water, also known as "water of the nonsolvent volume," was carried out, at S.V. Bruevich's suggestion, by the "indicator anion" (chloride ion) method, from three variables:

- 1) the total moisture content of the sediments (ΣH_2O), determined by drying of the deposits in a thermostat at 110°;
- 2) the amount of chloride leached out (ΣCl) by washing of the sediments with an electrolyte solution free from chloride ions;
- 3) the chloride concentration in the soil solution (c_{Cl}).

The main advantage of this method is that all the analytical operations are performed on samples of nat-

TABLE 1

Brief Characteristics of the Properties of the Marine Sediments

Deposit	Sampling level* in cm · 10 ⁻¹	Water, as % on the dry material	pH of de- posits**	Eh at 16°, in mv
Gray mud with brown inclu- sions	20-30	219.48	7.37	349.0
Gray mud	400-410	95.86	8.26	61.5
Gray clay	1160-1170	100.71	7.78	111.7
Same	1850-1860	81.49	8.34	182.2
"	2780-2790	69.23	7.97	80.0
"	3324-3334	64.45	7.64	90.5

* Tables 1 and 3 give the results of experiments on samples of the same marine sediments, in the sequence given in Table 1.

** The pH determinations were carried out directly in the deposits by means of the unbreakable glass electrode designed by Dmitrenko and Zhupakhina [9].

ural sediments with intact structure, which is very important; it can be used to calculate, in addition to the amount of bound water in the intermicellar liquid, also the amounts of bound water in the interlayer spaces, channels, and cavities of the clay mineral lattices. A great merit of this method is its high degree of accuracy; in parallel determinations of the bound water in sediments the variations do not exceed ~0.5% of the free water content (see Table 2).

TABLE 2

Control Experiments on the Determination of Bound Water in Marine Sediments

Weight of moist sediment in g	Water in samples, %	Cl in mg per sample	Chloride concentration in g per 1000 g of		Water content in g			Bound water, as % of moist material
			soil solution, cC _l	water, c	total	free	bound	
63.2	74.4	938.2	19.8	20.5	47.0	45.5	1.5	2.3
62.3	74.5	925.8	19.9	20.6	46.4	44.8	1.6	2.6
52.0	81.1	838.7	19.6	20.3	42.2	41.2	0.9	1.8
51.2	81.1	823.7	19.6	20.3	41.5	40.4	1.1	2.1

However, the theoretical basis of the proposed method is not free from certain defects. In calculations of the bound water from the difference between total and free water, all the errors influence a much smaller quantity, the amount of the bound water which is being found. In calculations of the amount of water occupying the nonsolvent volume, it is assumed that there is a sharp boundary between the nonsolvent water in immediate proximity of the particle, and the rest of the solution, with a certain constant electrolyte concentration. This is a conditional assumption, as there is no sharp boundary between the bound water and the intermicellar solution. The results obtained by the indicator anion method can be quite accurate only when equi-ionic (molecular) absorption of the electrolyte containing the indicator anion is absent or reduced to a minimum. If this condition is satisfied, the amount of chloride leached out (ΣC_l) will not be equal to the amount of chloride present in the equilibrium (soil) solution.

The value of cC_l is taken into account only for that part of the soil solution in which the chloride concentration is constant. If the equilibrium chloride content is nominally referred to the volume occupied by the free water, the chloride concentration for each system will be less than would be found if the total amount of chloride leached out is referred to the same volume.

If this last condition is not satisfied and the colloidal particles are capable of exchanging chloride ions

and of giving up chloride adsorbed in equi-ionic (molecular) form, the total chloride leached out will be increased by an amount representing the chloride adsorbed by the particles.

The amount of bound water, by the S.V. Bruevich method, is found from the following expression (our notation, O.D.)

$$W_h = 100 - \frac{\Sigma_{Cl} (1000 - c_{Cl} \cdot 1,806) 10}{c_{Cl} \Sigma_{H_2O} \alpha} \quad (1)$$

where Σ_{Cl} is the amount of chloride leached out in mg; c_{Cl} is the chloride concentration in the equilibrium solution; α is the weight of natural material in grams; 1.806 is the factor for converting the chloride content to the content of salts in sea water*; Σ_{H_2O} is the total percentage of water in the moist material.

It follows from Equation (1) that the amount of free water increases with increase of Σ_{Cl} . Consequently, the difference between total and free water decreases, i.e., there is less bound water. A high value obtained in determination of c_{Cl} leads to a high value for the bound water. If the amount of free water found exceeds, by Equation (1), the total water in the system, taken as 100%, minus values will be found for all the bound water contents. This can serve as an indication of the reactivity of the given colloid, which releases the adsorbed indicator ion into the solution.

The proposed method can be recommended for determinations of bound water in most finely divided sediments (and also soils), if they are negatively charged and do not exchange chloride ions under natural conditions.

EXPERIMENTAL

The total moisture in the marine sediments was determined by drying in a thermostat at 110°. For determination of Σ_{Cl} the deposit was held for 24 hours in 0.5 N $MgSO_4$ (or Na_2SO_4) solution, washed by decantation, transferred without loss to a filter funnel, and washed for a long time on the filter with the same solution. The filtrate (~900 ml) was made up to 1 liter with distilled water, and its chloride content was determined (by Mohr's method). The total chloride contents were calculated in milligram-equivalents and in grams per kilogram of the soil solution (Table 3).

TABLE 3

Determination of Bound Water in Finely Divided Marine Sediments by the Indicator Chloride Ion Method

Weight of moist sample, g	Moisture content of natural sample, %	Σ_{Cl} in mg in sample	c _{Cl} in g per 1000 g	Bound water calculated by Bruevich method				Bound water calculated by the Dmitrenko method			
				water as % of total water		bound water, % on the material		water in g in sample		bound water, % on the material	
				soil solution	water	free	bound	moist	dry	total	free
34.3	68.7	468.3	19.2	19.9	99.2	0.7	0.5	1.7	23.6	23.4	0.186
52.0	48.9	511.2	19.7	20.4	98.2	1.8	0.8	1.7	25.4	25.0	0.444
45.6	50.1	457.8	20.0	20.7	96.2	3.7	1.8	3.7	22.7	22.0	0.831
36.9	44.9	352.7	23.1	24.0	87.9	12.0	5.3	9.7	16.5	14.6	1.899
55.0	40.9	451.6	20.5	21.2	94.0	6.0	2.4	4.1	22.5	21.2	1.303
47.6	39.1	392.7	21.3	22.1	94.6	5.3	2.0	3.4	18.6	17.7	0.931

All the chloride determinations in the solutions pressed out of the samples were carried out in duplicate with an interval of two weeks. We observed that samples of the solutions carefully protected against evapora-

*Instead of the expression $(1000 - c_{Cl} \cdot 1.806)$ we have, for the general case: $1000 - \Sigma_C$, where Σ_C is the total of all the mineral salts in the system.

tion and access of atmospheric CO_2 nevertheless developed slight turbidity owing to deposition of carbonate crystals and precipitation of ferric and manganese sesquioxides. However, the differences between duplicate determinations in most cases were very slight, not in excess of 0.04% chloride on the average, which is quite permissible.

We calculated the bound water contents of samples of gray marine clays (by the Bruevich method) by means of Equation (1) as percentages of total water, and (by the Dmitrenko method) as percentages of the absolutely dry material. The second version differs from the classical method, as our reasoning was based on the concept of the molecular capacities of finely divided sediments.

The generally accepted basis is that bound water is the term applicable to the layers of water adjacent to the surface of a colloidal particle and consisting of regularly oriented molecules. However, it is not possible to draw a definite boundary between bound water (the structure of which approximates to the structure of ice [11]), and the loosely packed layers of water at some distance from the particle, or a boundary between the loosely bound water and the intermicellar liquid.

These concepts are somewhat one-sided, as they ignore the water which impregnates the colloidal particle and fills its pores if the particle is in a hydrogel, and the water present in the form of so-called free water in mineral masses (in the cavities of the crystal lattices, in the channels, and in the interlayer spaces of the crystals) if the particle is in a colloidally disperse mineral. In our opinion, neither of these forms can be segregated from the external layers of water bound by the colloidal particles. Thus, if the surface of the colloid is regarded as a certain boundary, the zone in which bound water is present extends on both sides of it, into the intermicellar solution and into the colloidal micelle.

In the light of these views we may assume that in the efflorescence of a crystal or in its interaction with various salt solutions the molecules of bound water may be replaced by salt molecules. The "growth" of a colloidal micelle can probably proceed with equal probability both by orientation of salt molecules in aqueous salt solutions, and by orientation of water molecules. The oriented layers of the salt or water molecules in a sense supplement the crystal lattices and acquire a structure approximating to the structure of the adsorbents themselves [11]. It is therefore desirable to verify experimentally the existence of salt layers "bound" by the colloidal particles, i.e., of molecularly adsorbed electrolytes. Here we introduce the concept of the molecular capacity of finely divided sediments, denoted by Σ_m . In our view, the molecular capacity is determined by multimolecular layers retained by the solid particles, the sum of the molecules of bound water and of the adsorbed electrolyte being constant.

It does not follow, however, that when water molecules are displaced by an electrolyte all the sites can be occupied by electrolyte molecules. When a finely divided deposit (such as a marine clay) interacts with an electrolyte solution, part of the electrolyte (depending on its concentration) is adsorbed in the form of whole molecules (displacing the adsorbed water) and part will be present in the salt solution permeating the clay. Therefore, the free fraction of the electrolyte molecules can be expressed as the difference $\Sigma M - M_{\text{ads}}$, where ΣM is the total electrolyte content of the clay and M_{ads} is the amount present in the molecularly adsorbed state.

The active part of the water, i.e., the free water dissolving the electrolytes, is expressed as the difference $\Sigma H_2O - H_2O_b$, where ΣH_2O is the total water, and H_2O_b is the bound water in the clay. The concentration of electrolyte in the intermicellar (soil) solution (c), i.e., the amount of salt in grams in a definite amount of water, is given by the expression

$$c = \frac{\Sigma M - M_{\text{ads}}}{\Sigma H_2O - H_2O_b} \quad (2)$$

It follows from Equation (2) that the distribution of electrolyte and water molecules adsorbed by the colloidal particles can be estimated if the concentration of electrolyte in the soil solution is known. Here, according to our hypothesis, the sum of the bound water and electrolyte molecules is constant for a given system

$$H_2O_b + M_{\text{ads}} = \Sigma m = \text{const.} \quad (3)$$

If c and Σm are known, Equations (2) and (3) give the required values of M_{ads} and H_2O_b . Therefore, the

object of the investigation should be to determine the molecular capacities of finely dispersed sediments (ΣM).

If this value is not known, the bound water content of a colloidal sediment can be determined only with a certain degree of error, by arbitrarily assuming that $M_{ads} = 0$; the bound water content is then given by the equation

$$H_2O_b = \Sigma_{H_2O} - \Sigma_{Cl} / c, \quad (4)$$

where H_2O_b and Σ_{H_2O} are in grams in the sample, Σ_{Cl} is in milligrams in the sample, and c is the electrolyte concentration in the soil solution in grams per 1000 g of water.

Rearrangement of Equations (4) and (2) gives for the adsorption of chloride

$$c = \frac{\Sigma_{Cl} - Cl_{ads}}{\Sigma_{H_2O} - H_2O_b}. \quad (5)$$

Assuming in Equation (5) that $Cl_{ads} = 0$, we have

$$c = \frac{\Sigma_{Cl}}{\Sigma_{H_2O} - H_2O_b}, \quad (6)$$

where Σ_{Cl} corresponds to ΣM [Equation (2)].

Rearrangement of Equation (6) gives

$$H_2O_b = \frac{c\Sigma_{H_2O} - \Sigma_{Cl}}{c} = \Sigma_{H_2O} - \frac{\Sigma_{Cl}}{c}. \quad (7)$$

It is seen that Equation (7) is identical with Equation (4).*

Table 3 gives the complete calculations of the bound water contents, determined by the two methods described above, of samples taken at various levels from the sediments of the Bering Sea.

These results show that our concepts of the molecular capacity of finely divided deposits can be verified by the classical method for the calculation of bound water; the results obtained by the two methods coincide if equi-ionic (molecular) adsorption of the electrolyte of which the indicator anion is a component is absent or reduced to a minimum.

On the basis of our investigation it is possible to recommend the "indicator anion" (chloride ion) method for determinations of bound water in finely dispersed sediments: soils, marine sediments, lake muds, and organic and organomineral components of soils.

SUMMARY

1. Intermicellar solutions in contact with the colloidal particles in finely divided deposits are not homogeneous, but have structural elements.

2. The "growth" of a colloidal micelle in an aqueous solution, by our theory, may take place with equal probability either by adsorption of salt molecules or by binding of water dipoles, the distribution of which between the solid and liquid phases can be estimated if the electrolyte concentration in the intermicellar solution (soil solution, ground and mud water) is known. It must be taken into consideration that the sum of the bound water and electrolyte molecules (ΣM) is probably a constant quantity for a given system.

3. The classical method for calculation of bound water, and the method described in this paper, can be used if the equi-ionic (molecular) adsorption of the electrolyte of which the indicator anion is a component is absent or reduced to a minimum.

* The calculated amounts of bound water should more correctly be expressed as percentages on the weight of the dry material.

4. The results of the calculations show that Equations (1) and (7) may be used for determination of bound water in sediments; it is more correct to calculate the bound water relative to the dry material in the sediment [Equation (7)].

LITERATURE CITED

- [1] I.M. Kolthoff, J. Phys. Chem. 40, 8, 1027 (1936).
- [2] I.M. Kolthoff and W.M. McNevin, J. Am. Chem. Soc. 58, No. 9, 1543 (1936); N. Shilov and L. Lepin*, Bull. Lomonosov Phys.-Chem. Soc. Vol. 1 (Moscow, 1919), page 1.
- [3] O.I. Dmitrenko, J. Chemization of Soc. Agric. No. 5, 46 (1940); V.A. Kargin, P.S. Vasil'ev and O.I. Dmitrenko, J. Phys. Chem. 13, No. 12, 1838 (1939); V.A. Kargin, P.S. Vasil'ev and O.I. Dmitrenko, J. Phys. Chem. 14, No. 12, 1628 (1940).
- [4] S. Mattson, Soil Colloids* (State Agricultural Press, Moscow, 1938); V.P. Mishin and A.N. Karpov, Colloid J. 2, 305 (1936); V.P. Mishin and E. Polochanskaia, Colloid J. 2, 317 (1936).
- [5] S.S. Iarusov, J. Chemization of Soc. Agric. No. 6, 49 (1940).
- [6] L. De Bouchere, J. Chim. Phys. 26, 250 (1929); Ann. de Chim. 19, 73 (1933); Comptes rend. de 2-me Congr. Nat. de Sci (Bruxelles, 1935), page 582; V.A. Chernov, Chemical Studies of Soils, Trans. V.V. Dokuchaev Soil Inst. 20 (Izd. AN SSSR, Moscow-Leningrad, 1939), page 33.
- [7] A.V. Dumanskii, Bull. State Sci.-Res. Inst. Colloid Chem. No. 2, 3 (Voronezh, 1934); A.V. Dumanskii and A.P. Dumanskaia, ibid, page 43.
- [8] A.V. Trofimov, Scientific Agronomic J. No. 10, 613 (1925); A.V. Trofimov, ibid. No. 9, 560 (1927); I.S. Dolgov, Repts. Lenin Acad. Agric. Sci. No. 2, 3 (1948); A.A. Rode, Soil Moisture* (Izd. AN SSSR, Moscow, 1952).
- [9] O.I. Dmitrenko and E.S. Zhupakhina, Pedology No. 1, 111 (1947).
- [10] S.B. Bruevich and E.D. Zaitseva, Trans. Inst. Oceanology Acad. Sci. USSR 26, 8 (1958).
- [11] J.D. Bernal, J. Chim. Phys. et phys.-Chim. Biol. 50, C1-C12 (1953).

Received January 3, 1957

Institute of Oceanology
Academy of Sciences USSR — Moscow

*In Russian.

THE SURFACE TENSION OF DISPERSE SYSTEMS

S.N. Zadumkin

Several experimental facts indicate that the surface tension is greater in small than in large drops and crystals. It has been found, for example, that the evaporation rate of substances of low volatility (mercury drops, solid particles, etc.) increases sharply with increasing dispersion. The boiling point of water condensed in micropores depends on the pore size. It was shown [1] that for pores greater than 10 Å in radius the boiling point of water agrees with the value calculated from the Kelvin equation, while for finer pores the calculated values differ appreciably from the experimental results. Shereshevsky [2] found that the surface tension of a liquid, determined from the rise in narrow capillaries, depends on the diameter of the latter. Gorbachev [3, 4] was the first to give a theoretical explanation of the dependence of the surface tension of a liquid on the radius of curvature of the interface. On the assumptions that each particle on the surface of a small droplet is more deficient in nearest neighbors than a particle on a plane surface, and that the surface tension must be directly proportional to the number of missing neighbors of a particle on the liquid surface, Gorbachev derived the following expression for the surface tension of small spherical liquid droplets

$$\sigma = \sigma_0 \left(1 + K \frac{\rho_m}{r} \right), \quad (1)$$

where σ_0 is the surface tension of a plane liquid surface; ρ_m is the radius of molecular action; r is the radius of the droplet; K is an empirical constant which depends on the nature of the liquid.

Equations analogous to (1) were subsequently derived by other workers on the basis of different considerations.

Martynov [5], on the assumption that the volume of a liquid varies with its dispersity (as the density of a substance in the surface layer differs from its density in the volume), used known thermodynamic relationships to derive the equation

$$\sigma = \sigma_0 \frac{r}{r - 2A\delta}, \quad (2)$$

where $A = 1 - D/D_0$; D_0 is the density of the volume phase; D is the average density of the intermediate over its thickness δ .

Resolution of Equation (2) into series by powers of $2A\delta/r$ (when $2A\delta \ll r$) gives an equation analogous to (1).

We have shown that the surface tension of metals [6, 7] and the surface energy of ionic crystals of the NaCl type [8] are, in the first approximation, directly proportional to the relative number of missing nearest neighbors of the particles in the surface. For example, in the paper [7] the surface tension of a metal is considered in the light of an ion-electronic polar model of the metal. The surface tension is defined as the excess free energy of unit surface of the metal at the boundary with vacuum

$$\sigma = n_s (F_s - F_v), \quad (3)$$

where n_s is the number of particles per unit surface area; F_v and F_s is the free energy of one particle within the metal and on the surface respectively.

The free energy of vibration of the particle on the metal surface, F_s , is calculated as follows. The vibration of an ion within the metal is regarded as $f_{kv}/2$ partial linear vibrations of average frequency ν , the total free energy of which is F_v , where f_{kv} is the coordination number of the cation with respect to the "anion" in our polar model of the metal [7]. Then, evidently, a particle on the metal surface will have $f_{ks}/2$ tangential

vibrations of frequency ν and Δf partial vibrations with half-broken bonds, and therefore of average frequency $\nu/\sqrt{2}$, where f_{ks} is the coordination number of the cation with respect to the "anion" in the plane network, and Δf is the number of missing nearest "anions" of a cation at the metal surface.

On the basis of these considerations, we have

$$F_s = \frac{F_v}{f_{kv}} f_{ks} + \frac{2F'_v}{f_{kv}} \Delta f, \quad (4)$$

where F'_v is the vibrational free energy which a particle would have within the metal if its average vibrational frequency was $\nu/\sqrt{2}$. For the Einstein model of a solid at $kT \gg h\nu$, we have, as is known,

$$F_v = -3kT \ln \frac{kT}{h\nu} + E_0, \quad (5)$$

Variation of σ with the average curvature of the interface.

$$F'_v = -3RT \ln \frac{kT}{h\nu} \sqrt{2} + E'_0. \quad (6)$$

Substitution of Equation (6) into (4) and also (5) into (3) gives

$$\sigma = -n_s \frac{\Delta f}{f_{kv}} [3kT \ln 2 - 2(E'_0 - E_0)]. \quad (7)$$

Similar considerations have been given in the derivation of an equation for σ for alkali halide crystals [8]. It follows that, in our view, Gorbachev's basic assumption in the derivation of Equation (1) is correct. Gorbachev's equation can be easily extended to the case when the average curvature of the interface is $C = 1/r_1 + 1/r_2$, where r_1 and r_2 are the radii of curvature of mutually perpendicular normal cross sections.

Let the plane of the diagram (see figure) represent one of the normal sections of the interface. By simple calculations we find the distance h_1 from the plane $z = 0$ to the point of intersection of the sphere with radius ρ_m with the circumference with radius r_1 ; $h_1 = \rho_m^2/2r_1$ and, analogously, for another section $h_2 = \rho_m^2/2r_2$. Therefore the volume enclosed by the plane $z = 0$, the sphere of radius ρ_m , and the interface when $\rho_m \ll r_1$ and $\rho_m \ll r_2$ is approximately $\Delta V = \frac{1}{8}\pi\rho_m^4(1/r_1 + 1/r_2)$ and therefore

$$\sigma = \sigma_0 (1 + \frac{3}{16} \rho_m C). \quad (8)$$

However, in order to obtain agreement between the calculated and the experimental values of σ we introduce a certain constant K into Equation (8) in place of the coefficient $\frac{3}{16}$, as was done by Gorbachev [4]. The value of K must be found experimentally, and depends on the nature of the liquid.

Equation (9) then correctly represents the relationship between σ and the curvature of the interface:

$$\sigma = \sigma_0 (1 + K \rho_m C). \quad (9)$$

It is known that the surface energy varies for different faces of a crystal. In a highly disperse crystalline phase a relatively large number of particles are present at corners and edges of individual crystals, and these particles differ in their free energy contents from the surface particles. Therefore, for small crystals, we can only speak of some average value of the surface energy, which naturally depends on the size of the crystals.

Let us establish this relationship for ionic crystals of the NaCl type. It was shown by x-ray analysis of finely divided rock salt with specific surface $S = 10-15 \text{ m}^2/\text{g}$ [9] that finely divided NaCl consists mainly of cubes, i.e., the subdivision occurs along the (100) cleavage planes. If the length of the edge of such a cube is l , each cube evidently contains 8 particles at the corners, $12(l/a - 1)$ particles along the edges, and $6(l/a - 1)^2$ particles lying wholly in the (100) planes, where a is half the lattice constant.

As the excess free surface energy per particle [6-8] is directly proportional to the number of missing nearest neighbors, the corner, edge, and surface particles have the following respective free energies: $3\alpha\Delta f$, $2\alpha\Delta f$, and $\alpha\Delta f$, where α is a quantity independent of Δf , the number of deficient neighbors of the opposite sign of an ion in the (100) face.

The total excess free surface energy of a cube of edge l is

$$W = 6\alpha\Delta f \left(1 + \frac{l}{a}\right). \quad (10)$$

For the average surface energy $\bar{\sigma} = W/6l^2$ when $l \gg a$ we have

$$\bar{\sigma} = \sigma_{100} \left(1 + 2\frac{a}{l}\right), \quad (11)$$

where σ_{100} is the surface tension for the (100) face. Equation (11) may be written in the form

$$\bar{\sigma} = \sigma_0 \left(1 + K \frac{a}{l}\right), \quad (12)$$

where K is a constant which must be regarded as being dependent only on the nature of the substance if $\bar{\sigma}$ is coordinated with experimental data, as in Equations (1) and (9).

We may note that Equations (1), (9), and (12) can be written in exactly the same form

$$\sigma = \sigma_0 (1 + \beta S), \quad (13)$$

where S is the dispersity (cm^2/g) and β is a constant which differs for different substances; $\beta = \frac{D}{3} \rho_m k$ for small spherical droplets and $\beta = \frac{D}{6} ak$ for fine crystals; D is the density of the substance. If K is assumed to be 2, then, by Equation (13), the deviation of $\bar{\sigma}$ from σ_{100} for NaCl will be several percent at a dispersity of $100 \text{ m}^2/\text{g}$.

SUMMARY

1. S.V. Gorbachev's equation for the surface tension of small spherical droplets as a function of the radius has been extended to more complex configurations, when the interface is characterized by an average curvature.

2. The surface tension of disperse systems (small droplets, crystals, etc.) is a linear function of their specific surface.

LITERATURE CITED

- [1] M.L. Lankhanpal, R.K. Sud and B.R. Puri, J. Phys. Chem. 59, No. 2, 160 (1955).
- [2] L.J. Shereshevsky, J. Am. Chem. Soc. 50, 2916 (1928).
- [3] S. Gorbachev, Koll.-Z. 75, 263 (1935).
- [4] S.V. Gorbachev, Bull. Acad. Sci. USSR, chem. ser. No. 5, 843 (1936).
- [5] V.M. Martynov, J. Phys. Chem. 23, No. 3, 278 (1949).
- [6] S.N. Zadumkin, Proc. Acad. Sci. USSR 100, No. 3, 507 (1955).

- [7] S.N. Zadumkin, Proc. Acad. Sci. USSR 112, No. 3, 453 (1957).*
- [8] S.N. Zadumkin, Sci. Mem. Kabardino-Balkar Pedagogic Inst. No. 10 (1956).
- [9] C.C. Benson and G.W. Benson, Canad. J. Chem. 33, No. 2, 202 (1955).

Received October 12, 1956

The Kabardino-Balkar State University
Chair of Experimental and Theoretical
Physics

*Original Russian pagination. See C.B. translation.

GELATINIZED EMULSIONS

15. LIMITING-CONCENTRATION EMULSIONS OF PARAFFIN WAX IN WATER.

STRUCTURE OF PROTECTIVE LAYERS.

L.Ia. Kremnev and A.I. Perelygina

The introduction of small amounts of water-repellent substances, and, in particular, paraffin wax, into paper pulp makes the paper considerably more waterproof and improves other properties. Paraffin wax emulsions have been studied by numerous workers [1]. The technological process for the production of paraffin wax emulsions developed by Perelygina [2] has been adopted in one paper mill [2]. Wider utilization of paraffin wax in the paper industry is prevented by the inadequacy of the available information on the preparation conditions and properties of stable wax emulsions; the present investigation was undertaken for this reason.

The emulsions were prepared by Kremnev's method [3]. The emulsification was carried out in a thermostat, usually at $75 \pm 2^\circ$. A measuring cylinder containing pieces of the wax, the volume of which was recorded after it melted, was placed in the thermostat. A known volume of stabilizer solution contained in a second cylinder in the thermostat was foamed by means of a spiral for 1 minute. The molten wax was then introduced into this cylinder, with a to and fro movement of the spiral, dropwise at first, and then in a thin stream, with a gradual increase of the stroke of the spiral with the height of the emulsion column formed. The addition of wax was continued until a limiting-concentration emulsion was formed, i.e., until the last addition of about 0.5 ml was no longer emulsified.

The limiting-concentration emulsions were diluted with 5% gelatin solution and examined under the microscope with a $\times 60$ objective and a $\times 17$ eyepiece. The sizes of the droplets were measured with the aid of a micrometer eyepiece with 1.9μ scale divisions. The droplets were fractionated over narrow ranges of diameter. At least 1000 droplets were counted for each emulsion to ensure reliable results. The results were used to plot differential droplet size distribution curves.

The emulsions were stabilized with sodium stearate, gelatin, and mixtures of these. Sodium stearate was made by saponification of the acid with caustic soda (Stearate I) or borax (Stearate II). The emulsions were made with the use of "acid" soaps containing 70% of the alkali theoretically required to neutralize the fatty acid. According to our findings, both limiting-concentration and less concentrated emulsions have the highest stability under these conditions, and confer good waterproof qualities on the paper.

Stable emulsions of paraffin wax can only be obtained with the aid of aqueous highly concentrated solutions of stabilizers.

The dispersity of limiting-concentration emulsions in water in presence of gelatin as stabilizer is fairly high; this is illustrated in Figure 1,a. The distribution curves for emulsions of paraffin wax in presence of Stearates I and II as stabilizers are similar in character. The maximum on the distribution curves corresponds to a droplet size of about 1μ (Figure 1) for all the emulsions, both with individual and with mixed stabilizers, and for all the concentrations studied. This very small particle size is also characteristic of the water-in-oil and oil-in-water emulsions studied earlier [4]; it is substantiated by kinetic analysis of the principal processes leading to the formation of stable emulsions [5].

Figure 1,b gives distribution curves for limiting-concentration emulsions with a mixture of Stearate II and gelatin as stabilizer (the distribution curves for emulsions containing a mixture of gelatin and Stearate I are

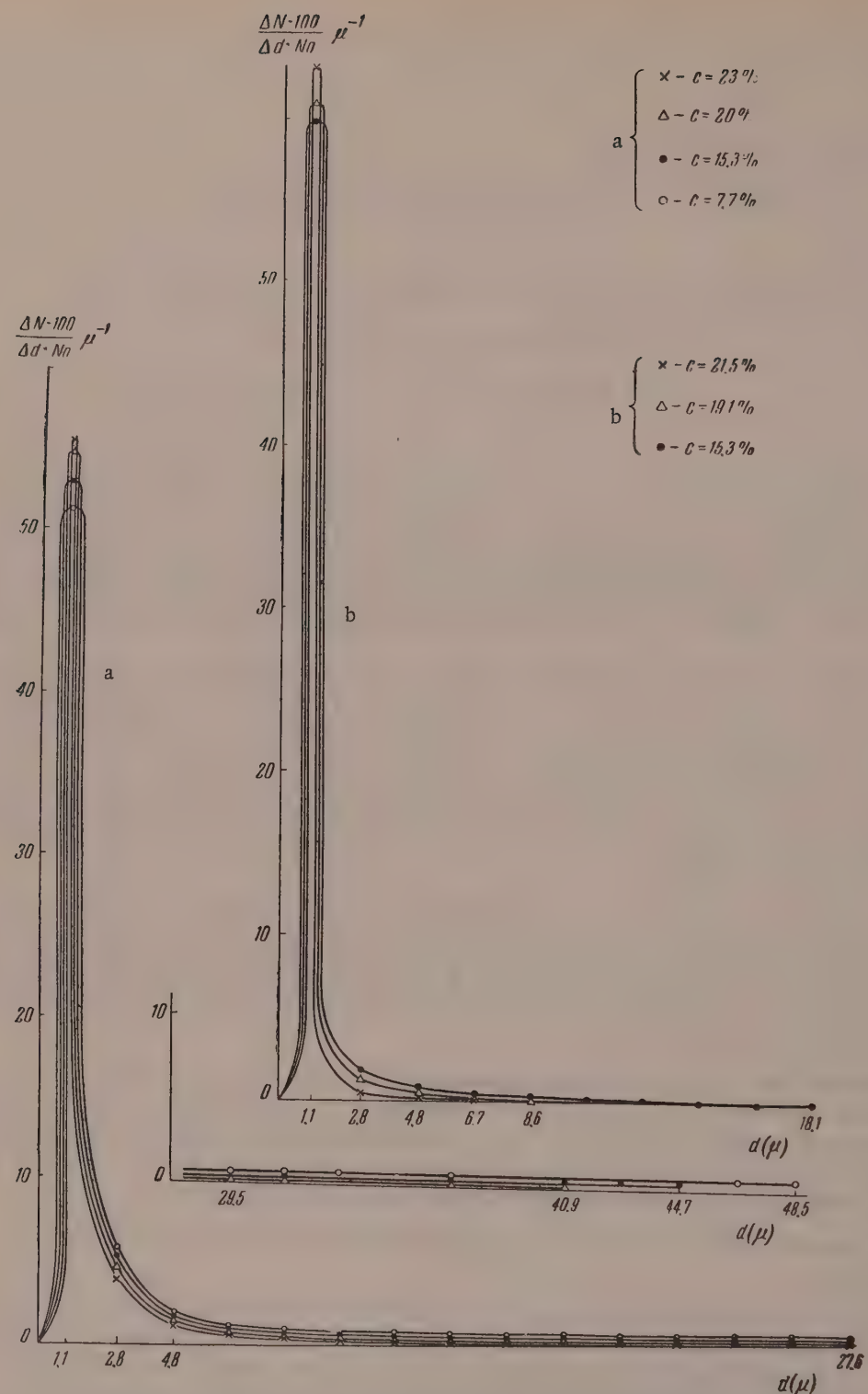


Fig. 1. Differential droplet size distribution curves for limiting-concentration emulsions of paraffin wax in water: a) stabilized with gelatin; b) stabilized with a mixture of Stearate II and gelatin.

similar to these). Mixed stabilizers give a somewhat higher dispersity than individual stabilizers.

The dispersity of the emulsions changes little with increase of the temperature of emulsification from 60 to 90°. The maximum on the distribution curves remains unchanged at the same very small droplet-size.

The results of the dispersion analysis were used to determine the characteristics of the protective layers in the limiting-concentration emulsions. The following were calculated: the surface area S_{∞} per 1 ml of dispersion medium at different concentrations of the stabilizer, the layer thickness δ_{crit} under the same conditions, and the surface area S_0 per stabilizer molecule in the interface. The results of these calculations for emulsions with stearates, gelatin, and a mixture of Stearate II with gelatin, are given in the table.

Characteristics of Protective Layers in Limiting-Concentration Emulsions Containing Stearates, Gelatin, and a Mixture of Stearate II with Gelatin

Emulsifier	Emulsifier concentra-tion in wt. %	S_{∞} in m^2	δ_{crit} in μ	δ_0 in \AA	S_0 in \AA^2
Stearate I	7.7	10	0.10	—	7
	15.3	20	0.05	—	7
	20.0	24	0.04	—	6
	23.0	24	0.04	—	5
Stearate II	5.0	7	0.14	—	7
	7.7	10	0.10	—	7
	10.0	13	0.08	—	7
	12.0	13	0.08	—	5
	15.0	13	0.08	—	4
Gelatin	7.7	4.2	0.23	130	—
	15.3	5.4	0.19	200	—
	20.0	4.8	0.21	300	—
Mixture of Stearate II and gelatin	15.3	19	0.054	—	—
	19.1	22	0.045	—	—
	21.5	22	1.045	—	—

These results show that the limiting surface area S_{∞} of the protective layers increases with increasing concentration of soap in the water, and reaches a practically constant value at high concentrations. At yet higher concentrations (not given in the table) S_{∞} decreases, probably because not enough water is available for the formation of protective layers. The emulsifying power, as represented by the highest value of S_{∞} , decreases considerably with increase of temperature [4]. There is a corresponding considerable increase in the thickness δ_{crit} of the protective layers preventing coalescence of the droplets.

In this connection special interest attaches to data on the area S_0 per soap molecule in the liquid interface. If we assume that all the soap is concentrated in the droplet surfaces, then S_0 is $4-7 \text{ \AA}^2$. The cross section of a carboxyl group in a fatty acid molecule has an area of $\sim 20 \text{ \AA}^2$. However, the polar groups of the soap molecules are hydrated and their hydrocarbon chains are simultaneously solvated in the adsorption layers at the interface between the two liquids; this is shown by the results of determinations of the heats of hydration and solvation of alkali soaps (both dry, and previously hydrated or solvated with a nonpolar liquid) [6]. Owing to the interaction of the soap molecule with both liquids in the interface, the area per molecule in the adsorption layer is considerably higher [7].

In the light of the foregoing there is no doubt that the protective layers on the droplets in paraffin wax emulsions are multimolecular. This is a very important conclusion, as it solves the question of the principal factors which determine the stability of paraffin wax emulsions. It is known [4] that oil-in-water and water-in-oil emulsions of limiting-concentration containing alkali soaps are stabilized, at room temperature, by unimolecular or even thinner adsorption layers. At higher temperatures stabilization of emulsions by monolayers

becomes impossible. This is probably caused by the disorienting influence of thermal motion on the protective layers.

In accordance with Rebinder's theory [8], such multimolecular protective layers should be regarded as gel films with high anomalous viscosity and mechanical strength. In fact, concentrated solutions of the individual and mixed stabilizers in question have structural viscosity and high thixotropy; in consequence, the space structures broken down during emulsification are rapidly restored and extremely small droplets are stabilized.

The table also gives the results obtained by emulsification of paraffin wax with the aid of gelatin, the emulsifying power (S_{∞}) of which is low, about 5 m^2 . Correspondingly the protective layer thickness δ_{crit} becomes considerable, of the order of 0.2μ .

It is known [9] that the thickness of films of isolectric gelatin on a mercury surface is $\sim 7 \text{ \AA}$. The thickness δ of dry gelatin films in limiting-concentration paraffin wax emulsions is $130-300 \text{ \AA}$, according to concentration (see table). Evidently at higher temperatures gelatin also stabilizes the emulsions by forming multimolecular layers, i.e., gel films with high structural-mechanical strength. This explains why at high temperatures the emulsions can be stabilized only by highly concentrated solutions of the stabilizers. As the table shows, the characteristics of the protective layers do not undergo any important changes with the use of mixtures of stabilizers.

Limiting-concentration emulsions of paraffin wax, obtained with the use of stabilizers at high concentrations, can be diluted with water to give less concentrated emulsions which are aggregatively and sedimentationally stable. To prevent phase separation, the dilution should be performed in two stages: 1) at the end of emulsification, with continuing movement of the spiral, an equal volume of water heated to the temperature of the limiting-concentration emulsion is added to the latter; 2) the emulsion is allowed to cool naturally to $30-35^\circ$, and water warmed to this temperature is added to the desired dilution.

The diluted emulsions of paraffin wax stabilized with gelatin or with a mixture of Stearate II and gelatin ensure good sizing of the paper.

SUMMARY

1. Limiting-concentration emulsions of paraffin wax in water, stabilized with sodium stearate, gelatin, and mixtures of these, have been prepared.
2. The paraffin wax emulsions are highly disperse systems. The maximum on the size distribution curves corresponds in all cases to droplets about 1μ in size.
3. The emulsifying power of the stabilizers studied, expressed in terms of the maximum surface area of the protective layers per 1 ml of the dispersion medium, increases with increasing concentration of the stabilizer up to a certain limit.
4. The paraffin wax emulsions are stabilized by multimolecular protective layers which consist of gel films with strongly pronounced structural-mechanical properties.
5. The limiting-strength emulsions of paraffin wax can be diluted with water. The diluted emulsions ensure a high degree of sizing of the paper and can be recommended for industrial use.

LITERATURE CITED

- [1] S.A. Zaitsev, in the book: "Theory and Practice of Paper Sizing" (State Wood Technology Press, 1935), page 150; V.A. Grabovskii and V.V. Iakimanskii, Mater. Inst. Paper No. 3-4, 90 (1935); B.G. Milov and E.E. Nikolaevskia, Symposium on Problems of the Cellulose and Paper Industry (Central Scientific Research Institute of Paper Press) No. 1-2 (1943); V.I. Mudrik, Paper Ind. No. 10, 11 (1954); N.P. Veselovskia, Paper Ind. No. 7, 17 (1955).
- [2] A.I. Perelegina, Paper Ind. No. 4, 16 (1949).
- [3] L.Ia. Kremnev, Proc. Acad. Sci. USSR 79, No. 4, 655 (1951); Colloid J. 13, 394 (1951).
- [4] L.Ia. Kremnev and S.A. Soskin, Colloid J. 9, 269 (1947); L.Ia. Kremnev and R.N. Kagan, ibid. 10, 436 (1948); L.Ia. Kremnev and N.I. Kuibina, ibid. 13, 38 (1951); 16, 358 (1954); 16, 447 (1954).

*In Russian.

[5] L.Ia. Kremnev and A.A. Ravdel, *Colloid J.* 16, 17 (1954).*

[6] A.V. Dumanskii and P.A. Demchenko, *Proc. Acad. Sci. USSR* 78, 277 (1951); P.A. Demchenko, A.V. Dumanskii and L.G. Demchenko, *Colloid J.* 14, 164 (1952).*

[7] A.B. Taubman, *Proc. Acad. Sci. USSR* 29, 23, 106, 215 (1940); *Proc. All-Union Conference on Colloid Chemistry* (Kiev, 1952), page 52; "The Structure of Adsorption Layers in Solutions," Doctorate Dissertation (Moscow, 1948).

[8] P.A. Rebiner, *Colloid J.* 8, 157 (1946); introductory chapter to the book: W. Clayton, *Emulsions* (Russian Translation) (IL, Moscow, 1950).

[9] Shepperd and Keenan, *Nature* 121, 982 (1929); 130, 259 (1931).

Received February 28, 1957

Central Scientific Research Institute
of the
Cellulose and Paper Industry
Leningrad

* Original Russian pagination. See C.B. translation.

EFFECT OF THE STRUCTURE OF CERTAIN SURFACE-ACTIVE SUBSTANCES
ON THE FOAMING OF AQUEOUS GELATIN SOLUTIONS

S.M. Levi and O.K. Smirnov

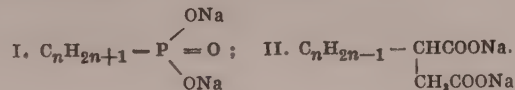
The mechanism of foaming and emulsification has been studied in detail in a number of investigations [1-3]. It follows from these investigations that the formation of stable foams and emulsions occurs in presence of surface-active substances adsorbed at the interfaces. The foam stability is primarily determined by the structural and mechanical properties of the surface layers of the disperse medium, i.e., of the two-sided films in the foam [1, 4].

It is known that there is a definite correlation between the structure and surface activity of surface-active substances; this is exemplified by the Du Claux-Traube rule. Dervichian and Lachampt [5] put forward certain considerations of the influence of the structure of surface-active substances on their wetting, emulsifying and foaming properties.

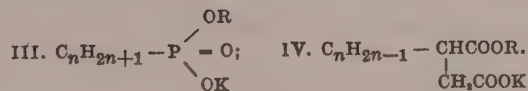
Several authors [6-9] studied the influence of individual factors on the foaming properties of certain surface-active substances, but the influence of the structure of surface-active substances on foaming is not considered in any of these papers. This led us to study the relationships between the structure of certain surface-active substances and the foaming power of aqueous gelatin solutions containing these compounds. Certain derivatives of alkylphosphonic and alkenylsuccinic acids were chosen for the investigation.

For the investigation of foaming properties, several groups of surface-active substances were specially synthesized, with systematic variations of the nonpolar hydrocarbon radicals or of the polar parts of the compounds. The following groups of surface-active compounds were used:

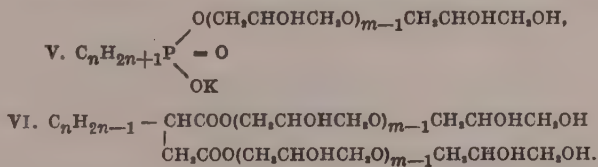
a) Salts of alkylphosphonic and alkenylsuccinic acids:



b) Esters (K salts) of alkylphosphonic and alkenylsuccinic acids (with mono- and polyhydric alcohols)



c) Polyglycerides of alkylphosphonic and alkenylsuccinic acids



These derivatives of alkylphosphonic and alkenylsuccinic acids were prepared by saponification (Groups I and II) [10, 11], esterification (Groups III and IV) [12, 13], or polyesterification (Groups V and VI) [16] of anhy-

TABLE 1

Disodium Salts (I and II)

C_n	t_1 (min)	K_f	t_2 (min)
Gelatin solution	4.3	1.1	72
Alkylphosphonic acids			
C_6	4	2.3	4.5
C_7	4.5	1.5	30
C_8	2	4	72
C_{12}	1.9	9	210
C_{16}	1.5	24	210
C_{18}	2.0	19	210
$C_6 - C_8$	4.0	1.8	34
$C_6 - C_{10}$	2.3	4	60
$C_8 - C_{10}$	3	4	60
$C_8 - C_{11}$	3	3	70
Alkenylsuccinic acids			
$C_8 - C_9$	5	0.6	8.5
$C_{12} - C_{16}$	1	2	90

In order to obtain branched nonpolar hydrocarbon chains in the molecules of the surface-active substances, saturated hydrocarbons and their mixtures (synthines) [10] were used in the former case, and certain mixtures of "polymer distillate" olefins [11] in the second, for synthesis of the corresponding acid anhydrides.

The total length of the hydrocarbon chains in the molecules of the surface-active substances was determined by the number of carbon atoms (C_n) in the original hydrocarbons. The length of the polar, polyglyceride portion in polyesters was determined by the number of glycerol molecules (m) involved in the polyesterification of the acid anhydrides.

For determination of the foaming properties, a current of air was passed under a pressure of 80 mm Hg through a No. 4 schott filter [16] into 6% aqueous gelatin solution at 35°. The surface-active substances were added to this solution, in the form of 0.1 M aqueous solutions (10 ml/liter). The foaming power of the solutions was characterized by the following values:

1. The time required to fill a cylinder 500 ml in volume with a mixture of foam and liquid (t_1 minutes).
2. The volume ratio of the foam to the liquid phase when the cylinder was filled — the "foam coefficient" (K_f).
3. The disappearance time of the foam up to the formation of a mirror surface on the liquid (t_2 minutes).

The experimental data obtained in determinations of the foaming power of gelatin solutions containing surface-active substances of different structure are given in Tables 1-6.

TABLE 3

Esters of Alkenylsuccinic Acids and Monohydric Alcohols (IV)

R	$C_8 - C_{10}$			$C_{12} - C_{16}$			C_{18}		
	t_1 (min)	K_f	t_2 (min)	t_1 (min)	K_f	t_2 (min)	t_1 (min)	K_f	t_2 (min)
Gelatin solution	2.3	9.0	18	2.3	9.0	18	2.3	9.0	18
$-C_2H_5$	3.0	2.3	16	14	0.82	21	Foam not formed	—	—
$-C_4H_9$	3.6	1.3	25	Foam not formed			Foam not formed		
$-C_8H_{17}$									

TABLE 2

Esters of Alkylphosphonic Acids (III)

R	$C_6 - C_7$		
	t_1 (min)	K_f	t_2 (min)
Gelatin solution	2.3	9.0	18
$-CH_2CH_2CH_2OH$	3.5	1.5	26.1
$-CH_2CH_2CH_2CH_2OH$	4.0	2.3	10
$-CH_2CH_2OCH_2CH_2OH$	2.75	2.3	31.6
$-CH_2CH_2CH_2CH_3$	Foam not formed*		
$-CH_2CH(C_2H_5)(CH_2)_3CH_3$	Foam not formed*		

*Foam not formed with $C_{10} - C_{12}$.

drides of the corresponding acids or certain mixtures of them (Groups VII, VIII) prepared by known methods [14, 15].

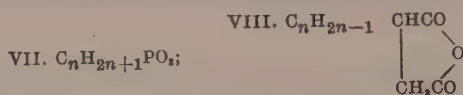


TABLE 4

Esters of Alkenylsuccinic Acids and Glycols (IV)

R	C ₁₈ —C ₁₈			C ₁₈		
	t ₁ (min)	K _f	t ₂ (min)	t ₁ (min)	K _f	t ₂ (min)
Gelatin solution	2.3	9.0	18	2.3	9.0	18
—CH ₂ CH ₂ OH	2	4.0	240	2.25	1.85	215
—CH ₂ CH ₂ OCH ₃	3	2.3	85	3	1.5	40
—CH ₂ CH ₂ OCl, CH ₂ OH	5	30	180	4	3.0	160
—CH ₂ CH ₂ OCH ₂ CH ₂ OCH ₃	3.5	4.0	55	Foam not formed		

TABLE 5

Esters of Alkylphosphonic and Alkenylsuccinic Acids and Glycerol (III and IV)

C _n	t ₁ (min)	K _f	t ₂ (min)
Gelatin solution	5	5.5	12
Alkylphosphonic acids			
C ₆ —C ₇	4.5	3.5	8
C ₇	2.5	—	8
C ₆ —C ₈	3	4	6.5
C ₈ —C ₉	3.5	1.5	90
C ₁₀ —C ₁₁	3.5	2.3	90
C ₁₂	9	0.67	210
Alkenylsuccinic acids			
C ₈ —C ₉	2.5	3.5	235
C ₁₂ —C ₁₈	3.3	4.0	260

It follows from these experimental results that surface-active substances of different molecular structure have different effects on the foaming of gelatin solutions. In some cases the surface-active substances increase the stability and durability of foams, and in others they decrease considerably or completely prevent foaming, i.e., they have foam-breaking properties. For example, the foam-breaking properties of salts and monoglycerides of alkylphosphonic and alkenylsuccinic acids diminish with increasing length of the hydrophobic radical.

The salts and monoglycerides which act as foam breakers in gelatin solutions when the radical length is less than C₈ confer better foaming properties on these solutions with increasing length of the alkyl chain. Foam formation is more rapid in presence of alkylphosphonic acid monoglycerides than in pure gelatin solutions. However, esters of alkenylsuccinic acids and monohydric alcohols decrease foaming of gelatin solutions with increasing length both of the hydrocarbon radicals of the original acid and of the alcohol. These esters, with not less than 16 carbon atoms in the sum of the acid and alcohol hydrocarbon radicals, make gelatin solutions incapable of foaming and act as foam breakers in such solutions.

Esters of alkylphosphonic acids and monohydric alcohols have a similar foam-breaking effect. With glycols in place of the monohydric alcohols the esters have foaming power. This is probably because of the presence of terminal polar hydroxyl groups in the molecules of glycol esters.

TABLE 6

Polyglycerides of Alkylphosphonic and Alkenylsuccinic Acids (V and VI)

C _n	m	t ₁ (min)	K _f	t ₂ (min)	C _n	m	t ₁ (min)	K _f	t ₂ (min)					
Gelatin solution		2.3	9.0	18.0	Alkylphosphonic acids									
Alkenylsuccinic acids										Alkenylsuccinic acids				
C ₆ —C ₇	6	2.0	4.0	32.0	C ₁₀ —C ₁₂	6	2.5	1.9	330	C ₆ —C ₉	4	7.0	0.4	188
The same	8	2.5	9.0	28.3	The same	12	3.5	2.3	360	C ₁₂ —C ₁₆	4	3.2	4.0	250
»	12	2.25	9.0	31.6	»	16	2.5	4.0	180	»	25	1.2	9.0	98
»	16	2.0	19.0	12.0	»	30	1.6	5.1	80	»	40	1.6	5.7	54
C ₈ —C ₉	8	3.2	1.9	145	Alkenylsuccinic acids									
The same	12	2.5	2.3	110	C ₆ —C ₉	4	7.0	0.4	188	C ₁₂ —C ₁₆	4	3.2	4.0	250
»	20	3.2	4.5	47.0	»	4	3.2	4.0	250	»	4	3.2	4.0	250

The polyglycerides of alkylphosphonic and alkenylsuccinic acids are also devoid of foam-breaking action on aqueous gelatin solutions. The foaming power increases with increasing length of the hydrocarbon chain of the polyesters for a given length of the polyglyceride chain. At the same time, polyglycerides of alkylphosphonic acids decrease the stability of gelatin foams with increase of the length of the polar polyglyceride chain (Table 6).

On the basis of these experimental results, these groups of alkylphosphonic and alkenylsuccinic acid derivatives can be arranged in the following series of decreasing foam-breaking power in aqueous gelatin solutions:

Esters of monohydric alcohols → (foam not formed)	Disodium salts (foam not formed → when R < C ₈ –C ₁₀)	Glycerol esters (foam not formed → when R ≤ C ₈ , m = 1)	Polyglycerides (foam formers)
--	--	--	----------------------------------

where R is the hydrocarbon radical, and m is the number of glycerol molecules.

These results lead to the conclusion that changes in the structure of surface-active agents influence the structural bonds which determine foam stability. Compounds which suppress foaming by adsorption in gelatin solutions break down the bonds between the gelatin molecules, thereby weakening the foam films.

SUMMARY

1. The influence of the structure of surface-active substances — salts, esters, and polyglycerides of alkylphosphonic and alkenylsuccinic acids — on the foaming of aqueous gelatin solutions has been studied.

2. The surface-active substances form the following series in order of increasing foaming power:

Esters of monohydric alcohols → (foam not formed)	Disodium salts (foam not formed → when R < C ₈ –C ₁₀)	Glycerol esters (foam not formed → when R ≤ C ₈ , m = 1)	Polyglycerides (foam formers)
--	--	--	----------------------------------

N.I. Grineva, A.I. Rybnikova and T.K. Stepanova took part in the experimental work.

LITERATURE CITED

- [1] P.A. Rebinder, Colloid J. 8, 157 (1946).
- [2] P.A. Rebinder and I.A. Pospelova, Preface to: W. Clayton, Emulsions (Russian translation) (1950).
- [3] W. Clayton, Emulsions (Russian translation) (IL, 1950).
- [4] P.A. Rebinder, J. Phys. Chem. 2, 254 (1931).
- [5] D. Dervichian and F. Lachampt, Bull. Soc. Chim. de France 486 (1946).
- [6] Foulk, Ind. Eng. Chem. 23, 128 (1931); 24, 277 (1932); 31, 722 (1939); Koll-Z. 60, 115 (1932).
- [7] Bartsh, Koll. Ber. 20, 1 (1925); Koll-Z. 38, 177 (1926).
- [8] Wo. Ostwald and Steiner, Koll.-Z. 36, 342 (1925).
- [9] D.L. Talmud and S. Sukhovol'skaia, J. Phys. Chem. 154, 277 (1931).
- [10] O.K. Smirnov, S.M. Levi and N.I. Grineva, Authors' Certificate No. 103162 (November 25, 1955).
- [11] F.N. Stepanov and O.K. Smirnov, Authors' Certificate No. 81713 (June 23, 1949).
- [12] O.K. Smirnov, S.M. Levi, N.I. Grineva and T.I. Stepanova, Authors' Certificate No. 107060 (December 20, 1955).
- [13] O.K. Smirnov, A.N. Rybnikova and S.M. Levi, Authors' Certificate No. 105345 (May 30, 1955).
- [14] O.K. Smirnov and S.M. Levi, Authors' Certificate No. 102550 (April 15, 1954).

[15] O.K. Smirnov, Author's Certificate No. 104890 (March 2, 1955).

[16] I.N. Putilova, Practical Manual of Colloid Chemistry* (Goskhimizdat, 1952).

Received January 15, 1957

Scientific Research Institute of
Organic Intermediates and Dyes,
Moscow

* In Russian.

THE STRUCTURAL AND MECHANICAL PROPERTIES OF CLAY SUSPENSIONS USED IN DIFFICULT DRILLING CONDITIONS

A.K. Miskarli and T.G. Gasanova

Investigations of the structural and mechanical properties of clay suspensions are very important for elucidation of the mechanism and the principal laws governing thixotropic structure formation. A knowledge of these properties is necessary for evaluation of the most important technological properties of drilling suspensions, which influence to a considerable extent the rate of sinking of oil and gas wells in the difficult geological conditions in the south of our country, especially in turbine drilling.

The structural and mechanical properties of clay suspensions have been studied in detail by the P.A. Rebinder school. As the result of the physicochemical researches of Zhigach, Serb-Serbina, and their associates, and also of foreign scientists [1-3], the mechanism of thixotropic structure formation and the laws governing the mechanical properties of drilling muds have been largely clarified. The mechanical properties of clay suspensions, as of other structurized disperse systems, are mainly determined by the formation of coagulation network structures. The formation and growth of these structures in clay suspensions is the consequence of the asymmetry of the clay particles and the high degree of dispersion. However, a number of questions relating to the rheology and structural and mechanical properties of clay suspensions still remain to be solved. Particular attention should be devoted to further studies of the dependence of the plasticoviscous properties of clay suspensions on the mineralogical composition, the colloidocochemical nature of the clays, and the composition of the dispersion medium (water). The investigations which have been carried out in this direction deal mainly with simpler and more highly structurized suspensions of bentonite clays.

However, in oil well drilling in the Azerbaidzhan oil fields the clay suspensions used are made in sea water from low-colloidal calcium clays. Under these conditions the improvement and regulation of the rheological properties of the clay suspensions presents a difficult problem.

To solve this problem it is necessary to use modern research methods for clarifying the role and significance of the principal factors which influence the structural and mechanical and other important technological properties of the clay suspensions used in difficult geological conditions of drilling.

The purpose of our investigation was a quantitative study of the relationship between the nature of structure formation and the stability of the structures in concentrated clay suspensions, and the mineralogical composition, capacity and chemical composition of the exchange complex, the colloidocochemical nature of the clays, and the kind, concentration, and fractional composition of the weighting materials. The effects of the nature and concentration of the solid phase and the composition of the aqueous phase on the thixotropy and structural and mechanical properties of clay suspensions were studied over a fairly wide range of limiting shearing stress, which is a very important and scientifically substantiated characteristic of structurized liquids. Rebinder's cone plastometer [4] was used for quantitative evaluation of aging processes and thixotropic structure formation in concentrated clay suspensions. New versions of the cone plastometer were successfully used by Volarovich and Markov [4] for studying the mechanical properties of peat.

However, the structural strength of clay suspensions is relatively low, and we therefore studied the plasticoviscous properties of concentrated clay suspensions with the aid of a somewhat lighter and modified cone plastometer: the metallic cone was replaced by a very light glass cone with a grooved surface to eliminate wall slippage. The counterpoise used for loading the cone was 10-20 times lighter, which made it possible to replace the

metallic disc by a lighter disc or organic glass. The increase of the limiting shearing stress (shear strength) as a function of time [$P_m(\tau)$ and $dP_m/d\tau$] was a measure of the increase of the structural strength of the clay suspensions with time, i.e., it characterized the kinetics of structure formation. The limiting shearing stress was calculated from the equation

$$P_m = K_\alpha \frac{F}{h^2},$$

where P_m is the shear strength in grams per cm^2 ; F is the load in grams; h is the maximum immersion of the cone in mm; K_α is the cone constant.

Investigation of the colloidochemical nature and mineral composition of the original clays. Gekmalin and Zykh clays were chosen for studying the effects of the colloidochemical nature and mineral composition of clays on the type of structure formation and the strength of the structures formed in clay suspensions. These are two of the most typical clays of the Apsheronskii Peninsula. The original clay samples were subjected to analysis, which is important in relation to the preparation of clay suspensions.

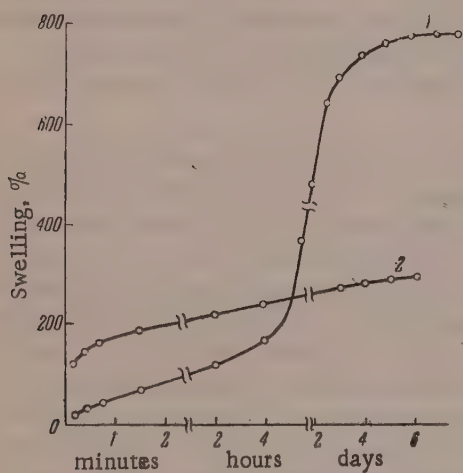


Fig. 1. Kinetics of swelling of Gekmalin (1) and Zykh (2) clays.

relatively low swelling — 286 wt. %. The swelling of Gekmalin clay in sea water is much lower, and approaches that of Zykh clay, which indicates the very high sensitivity of the highly colloidal Gekmalin to the electrolytes present in sea water.

The maximum hygroscopicity of clays, like the swelling, characterizes to a considerable extent their hydrophilic properties or tendency to hydration. In an investigation of the hydrophilic properties of certain bentonite and kaolinite clays [7], determined from their maximum hygroscopicity and calculated from the heats of wetting, it was concluded that either of these methods can be successfully used for quantitative characterization of the hydrophilic properties of clays.

The maximum hygroscopicity was determined from the adsorption of water vapor. A clay sample was dried to constant weight at 105–110° and placed in a desiccator over saturated K_2SO_4 as the vapor pressure of a saturated solution of this salt varies by only 2–4% over a very wide temperature range (from 10 to 100°). The desiccator was kept in a Höppler thermostat at 25°. After 24 hours the weighing bottles containing the clay were weighed and the weight increase due to adsorption of water vapor was determined. This was repeated until complete saturation was reached.

The clays studied differ in their adsorptive capacity for water vapor, in accordance with their colloidal character. The maximum hygroscopicity of Gekmalin clay is very high (27.7%), and equilibrium is only reached after 12 days. The hygroscopicity of Zykh clay is very low (12.1%); it reaches saturation within 6 days, after which its hygroscopicity remains unchanged.

Thus, the selected clay specimens differ in swelling and hygroscopicity, and therefore in hydrophilic properties, and it is therefore to be expected that they would differ greatly in their structuring power in aqueous suspensions.

The total capacity and chemical composition of the exchange complex of the original clays were determined by the Gedroits universal method [9]. The results are given in Table 1.

TABLE 1

Composition of Exchange Cations

Clay	Composition of exchange complex				
	in meq per 100 g			% %	
	total capacity	Na ⁺ (K ⁺)	Ca ²⁺ (Mg ²⁺)	Na ⁺ (K ⁺)	Ca ²⁺ (Mg ²⁺)
Gekmalin	60.6	41.8	18.5	69.0	31.0
Zykh	23.3	8.8	14.5	37.5	62.3

It follows from the data in Table 1 that, by the total capacity and the chemical composition of the exchange complex, Gekmalin clay should be classified with the highly colloidal sodium bentonite clays. The total capacity of the exchange complex of this clay is about 3 times that of the Zykh clay. Zykh clay has a very low sorption capacity, and by the composition of its exchange complex it belongs to the less colloidal calcium clays; it therefore has poor hydrophilic properties, and the production of a normal clay suspension requires about 35-40% of Zykh clay as compared with 5-8% of askangel or Gekmalin clay.

The mineral composition of the clays was determined by Avdusin's method [10], and by Vedeneev and Vikulova's method [11] of staining with organic dyes. The results of these analyses show that Gekmalin clay belongs to the montmorillonites, and Zykh clay to the hydromica-kaolinite clays. The comparative technological characteristics of clay suspensions of equal viscosity, made from these clays in distilled, fresh, and sea water, are given in Table 2.

TABLE 2

Characteristics of Clay Suspensions

Clay	Suspension medium	Sp. gr. in g/cc	Sediment, %	Water loss in ml/30 min	Cake thickness, mm	Static shear stress in mg/cm ²	
						1'	10'
Gekmalin	Distilled water	1.07	0	14	1.5	26.5	63.8
	Fresh water	1.08	0	15	1.5	23.4	85.4
	Sea water	1.20	2	34	4.0	78.6	80.2
Zykh	Distilled water	1.31	2	36	3.5	75.2	82.0
	Fresh water	1.32	2	37	4.0	58.4	74.8
	Sea water	1.36	3	39	4.0	54.4	56.6

It follows from the data in Table 2 that Gekmalin clay gives high-quality suspensions in distilled or fresh water of low water loss and with a thixotropic structure of high strength, with a low clay consumption; it differs in this respect from Zykh clay. However, both clays give equally unsatisfactory suspensions in sea water; the technological properties of these suspensions can be improved only by treatment with peptizing and stabilizing agents.

These investigations show that the local Gekmalin clay, which is a highly colloidal sodium bentonite, has a high specific surface, a high exchange capacity and hygroscopicity, and is therefore highly hydrophilic. Zykh clay, on the other hand, is a less colloidal hydromica-kaolin calcium clay; it has a very low specific surface, low sorption capacity, and its hydrophilic properties are very poor. Thus, the two clays, chosen for the investigation of the plasticoviscous properties of clay suspensions, have very different chemical, mineralogical, and colloidocochemical properties.

Investigation of aging and thixotropic structure formation in concentrated clay suspensions. For the studies of the type of structure formation and of the strength of the structures formed in clay suspensions in relation to the mineral composition and the colloidocochemical nature of the clays, clay samples were thoroughly kneaded with a little water for 25 minutes to a consistency of thick dough. After complete homogenization of the thick mass the remaining water was added, and the mass was agitated for 10-15 minutes more until a liquid homogeneous mass was formed. The concentrated clay suspension was then placed in 50 × 20 mm vessels and kept in a desiccator over water to prevent drying. The course of structure formation in these suspensions was then investigated by determinations of the limiting shear stress at definite time intervals.

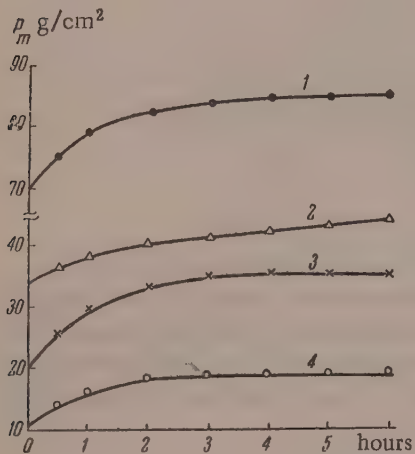


Fig. 2. Kinetics of structure formation in Gekmalin clay suspensions; volume % contents: 1) 10%; 2) 12.5%; 3) 15%; 4) 15%; 1, 2 and 3) in fresh water; 4) in sea water.

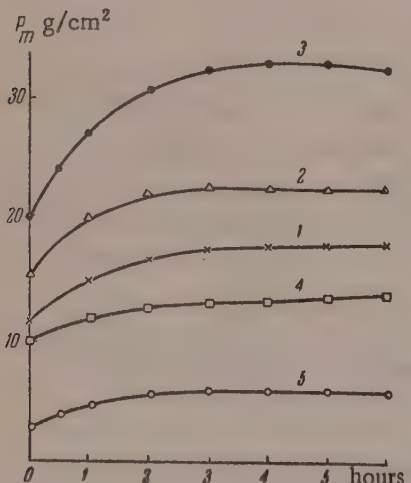


Fig. 3. Kinetics of structure formation in Zikh clay suspensions; volume % contents: 1) 25%; 2) 30%; 3) 35%; 4) 30%; 5) 25%; 1, 2 and 3) in fresh water; 4 and 5) in sea water.

Since sea water is used in a number of the Azerbaidzhan oil fields for the preparation of clay suspensions, we studied the kinetics of structure formation in clay suspensions made both in fresh and in sea water. Figure 2 gives curves representing the kinetics of structural strength increase and the type of structure formed in suspensions made from Gekmalin clay.

It is seen in Figure 2 that the strength of the structure in these clay suspensions rises sharply during the first 3 hours of aging (the strength of the previously formed structure varies little after that), and that the initial strength and the strength of the thixotropic structure formed increase sharply with increasing concentration of the solid phase. For example, an increase of the clay concentration from 10 to 15% produces an approximately 2.2-fold increase of the structural strength of the suspensions. The structural strength of the clay suspensions is much lower if sea water is used instead of fresh. This is the result of aggregation and dehydration of the clay particles owing to saturation of their exchange complex with multivalent ions from sea water, so that the hydrophily and dispersity of the bentonite clays decrease sharply, with a corresponding decrease in the number of structure-forming clay particles per unit volume of the suspension.

Suspensions of Gekmalin bentonite clay made in sea water are almost devoid of thixotropic properties even at very high concentrations.

In contrast to suspensions of Gekmalin bentonite clay, suspensions of Zikh hydromica-kaolinite clay (Figure 3) have very low structural strength even at high concentrations, indicating absence of thixotropic properties. An increase of the concentration of Zikh clay from 25 to 35% produces only a 1.5-fold increase in the structural strength of the suspensions.

From the curves in Figure 4 it is easy to determine the concentrations of different clays, according to their mineral and chemical composition and colloidocochemical nature, which give clay suspensions of equal strength, by drawing lines from the ordinate axis parallel to the abscissa axis. For example, clay suspensions with a shear strength of 20 g/cm² can be made with 7.5% of Gekmalin bentonite clay in fresh water, and 15% in sea water; 25% of Zikh hydromica-kaolin clay in fresh water and 33% in sea water, etc. Thus, curves showing the variation of the structural strength, in terms of the shear strength, with the clay concentration in the suspensions are very convenient and simple to use for estimating the characteristics of clays.

TABLE 3

Effect of the Colloidochemical Nature of the Clays on the Structural Strength of Clay Suspensions

Clay	Specific surface in m ² /g	Swelling, %	Hygroscopicity, %	Exchange capacity		Concentration of clay in suspension, %	Structural strength from P _{m,max} in g/cm ²
				total	Na ⁺		
Gekmalin	231	833	27.8	60.6	69	8 10 15	20 40 92
Zykh	93	286	12.2	23.3	37	25 30 35	21 25 32

In Table 3 are shown the greatest values attainable in the given time in terms of the shear strength of the clay suspensions.

These investigations demonstrate the pronounced interdependence of the mineral composition and the colloidochemical nature of the clays, and structure formation in their aqueous suspensions.

Investigation of thixotropic structure formation in weighted clay suspensions. To counteract difficulties in drilling caused by tectonic disturbances in the strata and by particularly high rock pressure, weighted clay suspensions are widely used. The weighting power of disperse materials depends to a considerable extent on the influence of the weighting materials on the rheological and colloidal properties of the clay suspensions. In this connection we carried out a quantitative study of the dependence of thixotropic structure formation in weighted clay suspensions on the type, concentration, and fractional composition of the disperse weighting materials. The following typical disperse weighting materials were used: Krivoi Rog hematite, pyrite cinders from the Baku sulfuric acid works, and natural carbonate rocks. The characteristics of the disperse weighting materials used are given in Table 4.

TABLE 4

Characteristics of Weighting Materials

Weighting materials	Moisture, %	Density, g/cc	Content of soluble salts, %	Maximum hygroscopic moisture content, %
Hematite	4.80	4.0	0.50	1.75
Pyrite ash	2.51	3.6	1.25	2.36
Limestone	0.15	2.7	0.10	0.63

The chemical composition of the weighting materials is given in Table 5.

To investigate the effect of fractional composition of the weighting material on the structural strength of clay suspensions, we prepared, by the sieving method, 3 fractions of each material with the following grain sizes: 102-74μ; 74-53μ; <53μ. Weighted clay of the same composition was made by the same procedure, but with different fractions of the weighting materials, and the kinetics of structure formation in them was studied (Figure 5). The results show that the structural strength of weighted clay suspensions depends on the fractional composition of the weighting materials. The finer fractions of the weighting materials, because of their greater specific surface, produce greater increases in the structural strength of the clay suspensions. The structural strength of clay suspensions decreases steadily with increasing grain size of the weighting material.

The variations of the structural strength of weighted clay suspensions with the nature and concentration of the disperse weighting materials (Figure 6) show that clay suspensions containing limestone in various concen-

TABLE 5

Chemical Composition of Weighting Materials

Weighting material	Chemical composition, %						
	Fe ₂ O ₃	Al ₂ O ₃	CaO	MgO	SO ₃	SiO ₂	Ignition loss
Hematite	76.05	—	2.29	1.08	1.64	18.27	—
Pyrite cinders	71.03	3.65	2.15	1.10	1.85	20.15	—
Limestone*	1.28	0.35	50.95	1.19	0.74	—	40.45

* Insoluble residue 4.55%.

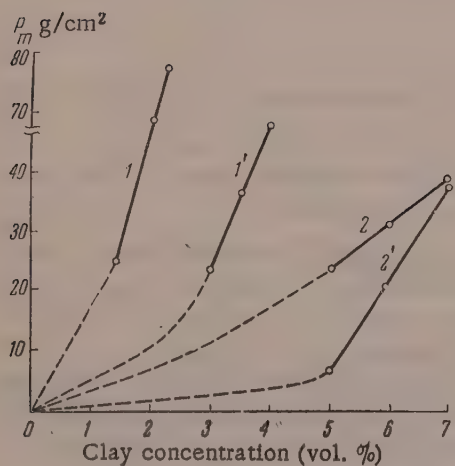


Fig. 4. Variation of shear strength of suspensions with clay concentration: 1) Gekmalin, in fresh water; 1') the same, in sea water; 2) Zykh, in fresh water; 2') the same, in sea water.

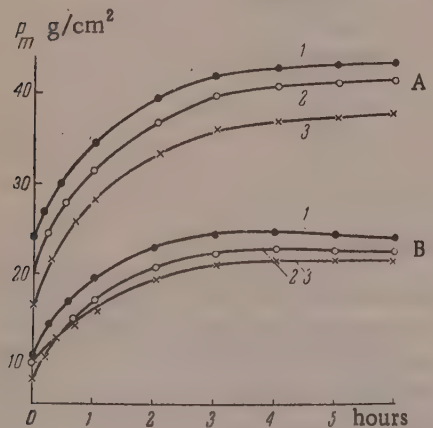


Fig. 5. Kinetics of thixotropic structure formation in clay suspensions weighted with pyrite cinders (A) and limestone (B), of grain size: 1) 59 μ; 2) 53-74 μ; 3) 74-104 μ.

trations have low structural strength, which varies very little during aging, so that it is possible to increase the carbonate concentration in the suspension and to obtain, after suitable treatment with the usual chemical reagents, high-quality weighted clay suspensions of density 1.7-1.85 g/cc [13-17]. The pyrite cinder particles have a high structuring effect on clay suspensions, which is largely due to their high content of water-soluble salts with multivalent cations, which have a strong coagulating action on clay suspensions. Therefore, clay suspensions containing pyrite cinders at the same concentrations as limestone or hematite have extremely high structural strength, viscosity, and water loss; this leads to difficulties in their use for drilling oil and gas wells.

It is known that in absence of any theoretical analysis the fundamental and decisive factor determining the weighting power of disperse materials is density. The results of our researches [16, 17] and certain literature data show that the density of a weighting material is not sufficient for determination of its weighting power. Apart from density, the weighting power of a disperse material depends on its influence on the colloidal and rheological properties of clay suspensions. It was shown that substances having anisodiametric particles, capable of a high degree of hydration and structure formation in the disperse state, tend to increase the effective volume of the disperse phase and therefore to decrease the concentration of the disperse phase in a suspension for a given viscosity. This leads to a decrease of the weighting power of the material, and suspensions of acceptable viscosity obtained with it have low density. Disperse materials which may be recommended as weighting materials for clay suspensions should have fairly low affinity for water, water repellency, and weak structuring power owing to the isodiametric form of their particles. In addition to the widely used weighting materials (hematite, baryte, etc.), natural carbonate rocks (dolomite, limestone, marl, spheroidalite [13-17]) may be included among such materials.

SUMMARY

1. The effects of the mineral composition, chemical

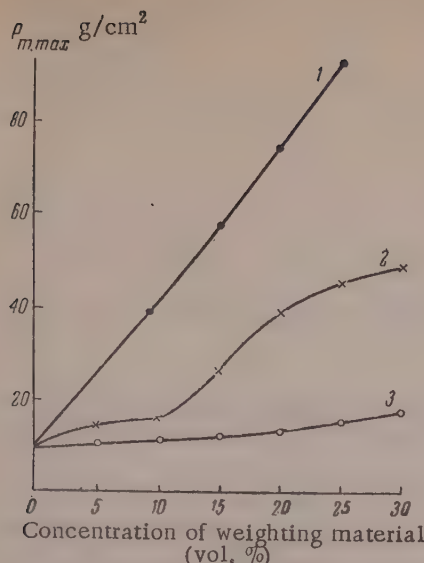


Fig. 6. Variation of shear strength of clay suspensions with the type and concentration of weighting material: 1) pyrite cinders; 2) hematite; 3) limestone.

composition of the exchange complex, and the colloidochemical nature of clays on the plasticoviscous properties of clay suspensions have been studied with the aid of a modified cone plastometer, which can be successfully used for studying the nature of structure formation and thixotropic structure strength in concentrated clay suspensions.

2. The form and strength of the structures formed in aqueous clay suspensions depend on the mineral and chemical composition of the exchange complex of the clay. Aqueous suspensions of Gekmalin bentonite clay have a very strong thixotropic structure, whereas aqueous suspensions of Zykh hydromica-kaolinite clay are almost devoid of thixotropic properties.

3. Clay suspensions made in sea water have weak structure, without thixotropic properties, because of the strong coagulating action of the multivalent cations in sea water on the clay particles, with a consequent deterioration in the hydrophilic properties and the dispersity of the clay, so that structure formation in the suspensions is sharply reduced. In such conditions it is important to improve the structural and other technological properties of clay drilling fluids by treatment with various peptizing and stabilizing agents.

4. The effects of the nature, concentration, and fractional composition of disperse weighting materials on the strength of thixotropic structures in weighted clay suspensions used in difficult drilling conditions have been studied.

a) It is shown that the finer fractions of the weighting material increase the structural strength of clay suspensions to a greater extent, owing to their greater specific surface and wettability. The structural strength of a weighted clay suspension decreases regularly with increasing particle size of the weighting material.

b) It was found that disperse weighting materials vary greatly in their structurizing power. In contrast to the high structurizing power of pyrite cinders and hematite, the structural strength produced by native carbonates (limestone, dolomite, etc.) is low. It is therefore possible to use higher concentrations of carbonates, and to obtain, after suitable treatment with stabilizers, high-quality nonabrasive weighted clay suspensions for use in turbine drilling.

5. Rheological investigations showed that disperse materials suitable for use as weighting agents for clay suspensions should have fairly low affinity for water, and weak structurizing power owing to the isodiametric shape of their particles.

The authors express their deep gratitude to Academician P.A. Rebinder for valuable advice in the course of this work.

LITERATURE CITED

- [1] P.A. Rebinder, In the book: New Methods of Physicochemical Investigation of Surface Phenomena* (Izd. AN SSSR, 1950).
- [2] S.Ia. Veiler and P.A. Rebinder, Proc. Acad. Sci. USSR 49, 5 (1945).
- [3] N.N. Serb-Serbina and P.A. Rebinder, Colloid J. 9, 381 (1947); L.A. Abduragimova, P.A. Rebinder and N.N. Serb-Serbina, Colloid J. 17, 184 (1955)*; K.F. Zhigach, Doctorate Dissertation (Moscow, 1942); K.F. Zhigach and D.E. Zlotnik, Proc. Acad. Sci. USSR 72, 3 (1950); A. Buzag, Koll.-Z. 47, 223 (1929); C.F. Good-eve and G.W. Whitfield, Trans. Faraday Soc. 34, 3, 511 (1938); W. Winkler, Koll.-Z. 105, 29 (1943); A. Engelhardt, Koll.-Z. 102, 3, 217 (1943); M.M. Gurvich, Colloid J. 18, 666 (1956).**

*In Russian.

**Original Russian pagination. See C.B. translation.

- [4] P.A. Rebinder and N.A. Semenchenko, Proc. Acad. Sci. USSR 64, 6 (1946); M.P. Volarovich and S.N. Markov, Factory Labs. 12, 1461 (1951); Peat Industry 10 (1951).
- [5] E.V. Alekseevskii, T.M. Belotserkovskii and T.T. Plachenov, Practical Work in Chemical Defense* (Defense Press, Moscow, 1940).
- [6] E.G. Kister, Petroleum Economy No. 12, 23 (1947).
- [7] F.D. Ovcharenko and S.K. Bykov, Colloid J. 16, 2 (1954).**
- [8] V.S. Baranov, Doctorate Dissertation (Moscow, 1954).
- [9] K.K. Gedroits, Chemical Analysis of Soils (State Press, Colloid Soviet Literature, 1935).
- [10] P.P. Avdusin, Sedimentary Clays* (Izd. AN SSSR, 1953).
- [11] N.E. Vedeneeva and M.F. Vikulova, Method of the Investigation of Clay Minerals With the Aid of Dyes and its Use in Lithology* (State Geology Press, 1952).
- [12] A.I. Tsurinov, New Data on Clays and Clay Suspensions Used in Oil Well Drilling (State Fuel Tech. Press, 1940).
- [13] A.K. Miskarli and M.M. Gurvich, Authors' Certificate No. 13805, June 8, 1950.
- [14] A.K. Miskarli, M.M. Gurvich, G.Kh. Efendiev and P.I. Denisov, Authors' Certificate No. 932, January 30, 1951.
- [15] A.K. Miskarli, Azerbaijhan Petroleum Economy No. 6, 18 (1953).
- [16] A.K. Miskarli, Trans. Inst. Chem. Acad. Sci. Azerb. SSR 10, 41 (1953).
- [17] A.K. Miskarli, Doctorate Dissertation (Moscow, 1955).

Received February 9, 1957

Institute of Chemistry
Acad. Sci. Azerbaijhan SSR — Baku

*In Russian.

** See C. B. Translation.

THE EFFECT OF CATIONS ON THE PROPERTIES OF BLACK SEA AGAROID

A. A. Morozov and S. N. Stavrov

The extensive use of agar, agaroid, carrageenin, and other substances extracted from red algae depends mainly on the formation of firm gels, which change little in the course of time, from their aqueous solutions. A particularly promising material of this kind, in relation to the possibility of its production in our country, is the agaroid obtained from the Black Sea alga, *Phyllophora nervosa* [1]. The agaroid obtained from it, like other extracts from red algae, is a natural cation exchanger. Some of the most important properties of agaroid may be modified to a considerable extent in the desired direction by means of cation exchange [1, 2].

The effects of the replacement of one kind of cation by another on the properties of algal extracts are by no means fully understood. According to some reports [4] replacement of calcium by univalent cations does not lead to any significant changes in the gelling power of agar, while, according to others, it results in a considerable decrease of this power. Solutions of the sodium salt of carrageenic acid, unlike solutions of the calcium salt, do not form gels [5].

We studied various cation-substituted forms (Li, Na, K, Ca, Ba) of agaroid. Studies of the viscosity of aqueous solutions (Figure 1), gel strength (Figure 2), swelling in water (Figure 3) and electrical conductance of aqueous solutions (Figure 4) of cation-substituted agaroid revealed a close relationship between the magnitude of the molecular charge and the physical and mechanical properties.*

The variations of the equivalent conductance of agaroid solutions with dilution are represented by curves which are typical for weakly dissociated low-molecular compounds. According to these curves, the agaroid samples can be arranged in the following series according to their tendency to dissociate: Li > Na > K > Original > Ca > Ba. The higher the degree of dissociation of a given sample (Figure 4), the greater is the viscosity of its dilute solutions (Figure 1), and the swelling in water (Figure 3), and the lower is the gelling power (Fig. 2).

Black Sea agaroid, like agar [6-8] and carrageenin, is a salt of an acid sulfuric ester of a polysaccharide. It is a polyelectrolyte, and behaves similarly to many other compounds of this class [10]. The observed increase of the reduced specific viscosity of agaroid solutions (Figure 1) with increasing dilution should probably be attributed to an increase of the hydrodynamic volume of the molecules as the result of straightening of the molecular chains by the action of repulsion forces between similarly charged centers (SO_4 groups) arranged in a definite manner along the molecular chains. The forces of repulsion and the straightening of the molecules increase with increasing dissociation of the compounds on progressive dilution.

The decrease of the degree of dissociation in the transition from Li-agaroid to Ba-agaroid results in a corresponding intensification of the interaction between the molecules in solution, leading to coiling in dilute solutions, and to structure formation in concentrated solutions. It is also possible that in either case aggregates of large number of molecules, behaving subsequently as independent kinetic units, may be formed.

Fixation of molecular aggregates in the junctions of the spatial network of a gelling system may occur as the result of intermolecular forces of mutual attraction [11, 12]; it is effected through the water oriented around the hydrated polar groups (by hydrogen bonding), despite the repulsion of the ionic atmospheres surrounding the colloidal particles (molecular aggregates). Mutual attraction between the particles or individual macromolecules increases with decreasing electrolytic dissociation, with compression of the electric double layer, and with increasing dehydration [13, 14] of the polar groups of the agaroid.

*The experimental procedure was described previously [21].

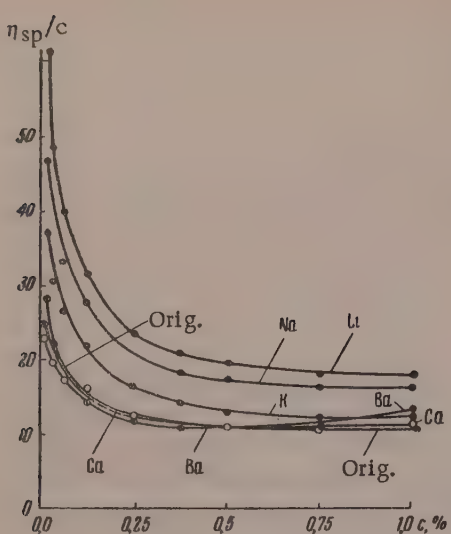


Fig. 1. Variation of reduced viscosity with concentration (at 25°) of aqueous solutions of cation-substituted agaroid samples and the original agaroid.

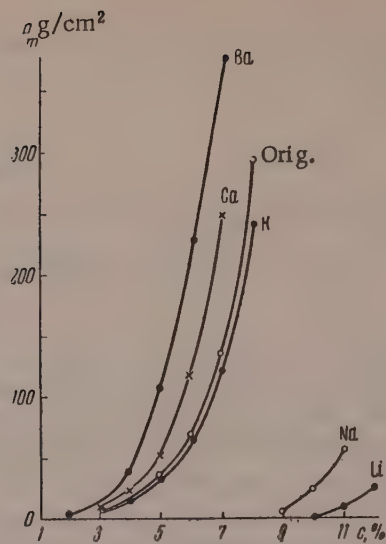


Fig. 2. Variation of shear strength (at 18-20°) with concentration of gels of cation-substituted agaroid samples and the original agaroid.

It seems that the influence of bivalent cations on gelling of agaroid solutions does not reduce to the formation of "bridge" bonds between the agaroid molecules to form a space network, as was shown to be the case in nitrocellulose and acetylcellulose solutions [15], and as is thought by some authors [8] to be the case in agar solutions. This is shown by the fact that cation-substituted Li-, Na-, and K-agaroids can also form gels. The valence of the ion influences the behavior of the agaroid in solution mainly by altering the tendency of the given cation-substituted specimen to undergo electrolytic dissociation.

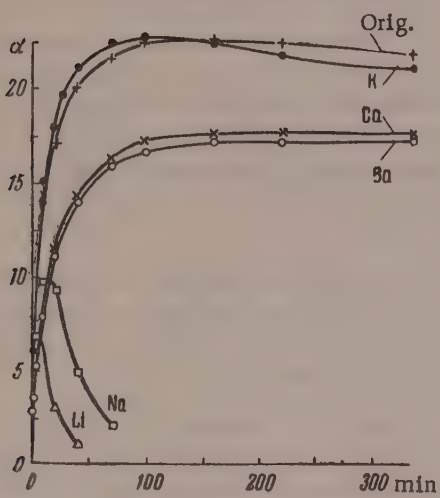


Fig. 3. Kinetics of the swelling in water (at 20°) of cation-substituted agaroids and the original agaroid.

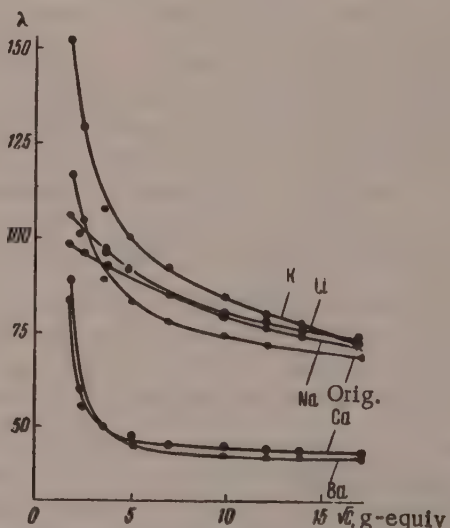


Fig. 4. Variation of equivalent conductance (at 25°) of solutions of cation-substituted agaroids and the original agaroid with the square root of the concentration.

A comparison of our experimental data on the properties of various cation-substituted agaroid samples with the properties of extracts obtained from red algae [1, 2] and various agar fractions [7, 16] as described in the literature reveals identical relationships. In particular, the swelling power in water decreases with decreasing sulfur content in the extracts; for a given gel strength, the concentration is higher for agaroid (the S content calculated as SO_4 is 21.6% on the dry substance) than for agar (containing not more than 6% SO_4). There is a well-defined correlation between the properties of different agar fractions and the number of galactose residues per SO_4 group.

As has already been noted [7, 17], the molecular weight of the extracts is not the decisive factor in their gelling power. An agaroid with molecular weight 5000 [18], in presence of small amounts of low-molecular electrolytes, forms stronger gels than those formed by Japanese agar under the same conditions [19]; we found that the former approach the strength of gels formed by White Sea agar, the molecular weight of which reaches 30,000 [20]. Moreover, carrageenin of molecular weight 2,500,000 [9] yields gels at higher concentrations than agar [2]. It appears that beyond a certain value increase of molecular weight does not have any decisive influence on the properties of the extracts.

The differences in the physicochemical properties of cation-substituted agaroid samples containing the same anion are caused by differences in the degree of dissociation. With different extracts and agar fractions, these differences in the properties arise because the substances are polyelectrolytes containing mainly calcium and different anions; the latter differ in the numbers of SO_4 groups per gram molecule.*

Extracts of red algae are classified into two groups: agars and agaroids, depending whether their swelling in water is limited or unlimited [1]. By this classification, cation-substituted Ba- and Ca-agaroids must be considered as agar merely because their swelling in water is limited and an increase of temperature is needed to dissolve them. We consider that this classification is inappropriate. In the final analysis, the differences in the properties of extracts of red algae are primarily determined by the magnitude of the charge of the high-molecular anion. Therefore, the most important characteristic of such extracts must be the sulfate group content per unit weight; this quantity determines the physicochemical and physicomechanical properties of the solutions and gels. The role of the cation present in a given agaroid is significant in the sense that it determines the electrolytic dissociation of the sample and influences the magnitude of the charge of the high-molecular anion.

SUMMARY

1. The investigated properties of solutions and gels of cation-substituted agaroids (viscosity, shear strength, swelling, etc.) are clearly dependent on their degree of electrolytic dissociation in an aqueous medium.
2. The most important characteristic of agaroid and other extracts of red algae is the magnitude of the charge of the high-molecular anion, which depends on the sulfate group content per unit molecular weight* of the substance and on the nature of the cation.
3. Views are put forward concerning the nature of the interaction of dissociated agaroid molecules in an aqueous medium, and are used to explain the formation of molecular aggregates, internal structure in the solution, and gelation.

LITERATURE CITED

- [1] I.V. Kazivetter, Bull. Pacific Scientific Res. Inst. of Pisciculture and Oceanography 36, 1 (1952); S.I. Lebedev and I.A. Iartseva, Proc. Acad. Sci. USSR 109, 160 (1956).**
- [2] C.K. Tseng, Phycocolloids. Useful Seaweed Polysaccharides, in the book: Colloid Chemistry, collected and edited by Jerome Alexander (New York, 1946), No. 6, page 629.
- [3] T. Currie, Chem. and Ind. 116 (1955).
- [4] H. de-Waele, Ann. Physiol. et physicochim. Biol. 5, 877 (1929); Fairbrother and Mastin, J. Chem. Soc. 123, 1412 (1923).
- [5] J. Buchanan, E.E. Percival and G.V. Percival, J. Chem. Soc. 51 (1943).
- [6] S.A. Glikman and V.L. Shanogina, Sci. Mem. Saratov State Univ. 24, 71 (1949).

*As in original — Publisher's note.

**Original Russian pagination. See C.B. translation.

- [7] I.T. Shubtsova, Author's Summary of Dissertation (Saratov, 1955).
- [8] S. Basu and A.K. Sircar, J. Coll. Sci. 9, 574 (1954).
- [9] R. Masson and D.A.J. Goring, Can. J. Chem. 33, 895 (1955).
- [10] R.M. Fuoss, Science 108, 545 (1948); A. Katchalsky, J. Pol. Sci. 12, 159 (1954).
- [11] B. Deriagin and M. Kusakov, Bull. Acad. Sci. USSR, div. chem. sci. 5, 1119 (1937); Colloid J. 6, 291 (1940); 7, 285 (1936); B. Deriagin and L. Landau, J. Exptl.-Theoret. Phys. (USSR) 11, 802 (1946); 15, 662 (1945); B. Deriagin and A. Malkina, Colloid J. 12, 431 (1950).
- [12] I.F. Efremov, Colloid J. 18, 276 (1956).*
- [13] V.P. Rudi and A.A. Morozov, Colloid J. 15, 117 (1953)*; Sci. Mem. State Univ. Chernovitskii 11, chem. ser. No. 2, 21 (1955); A.A. Morozov and V.P. Rudi, Bull. Acad. Sci. Belorussian SSR No. 4 (1956).
- [14] S.M. Lipatov, Problems of the Science of Lyophobic Colloids (Acad. Sci. Belorussian SSR Press, Minsk, 1941).**
- [15] V.A. Kargin and E.Ia. Vinetskaia, J. Phys. Chem. 10, 788 (1937); S. Papkov, J. Phys. Chem. 10, 418 (1937); Z.A. Rogovin and M.Ia. Shliakhover, J. Gen. Chem. 6, 1749 (1936).
- [16] S.M. Lipatov and A.A. Morozov, J. Gen. Chem. 5, 1119 (1935); A.A. Morozov, J. Gen. Chem. 5, 1359 (1935).
- [17] S.A. Glikman and M.A. Lipovskii, Sci. Mem. Saratov State Univ., chem. issue 30, 46 (1952).
- [18] V.S. Griuner, Colloids in the Food Industry, Vol. 2 (Food Industry Press, 1949), page 184.**
- [19] P.N. Pavlov and M.A. Engel'shtein, Colloid J. 2, 821 (1936).
- [20] V.P. Rudi, "Influence of Additions of Monohydric Saturated Alcohols on the Properties of Agar Gels," Author's Summary of Dissertation (Chernovitskii, 1954).
- [21] S.N. Stavrov and A.A. Morozov, Ukrain. Chem. J. 23, 721 (1957).

Received January 3, 1957

The I.I. Mechnikov State University
Odessa
The State University, Chernovitskii

* Original Russian pagination. See C.B. translation.
** In Russian.

THE STRUCTURE OF GELS

12. PREPARATION OF GELS FROM SOLUTIONS OF METHYL METHACRYLATE - METHACRYLIC ACID COPOLYMER

N.F. Proshliakova, P.I. Zubov and V.A. Kargin

The nature of the bonds in gel systems has been repeatedly discussed [1-5], but it is still far from clear. There is a lack of data on the relationship between gel formation and the numbers of the intermolecular bonds formed. Investigations of such structurized systems as protein gels could not provide a conclusive answer to this question in view of the complexity of the protein molecule, which contains a large number of groups differing in nature.

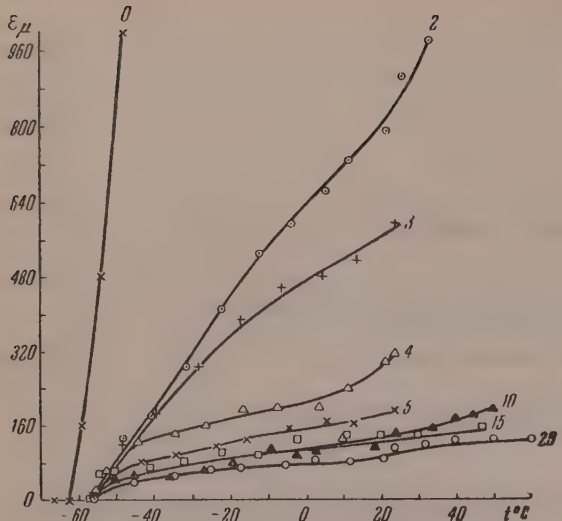
The purpose of the present work was a study of the properties of gels obtained from a synthetic polymer of well-known composition and structure. In this case it is possible to know in advance what groups and what bonds will cause gelation. By varying the number of bond-forming groups it is possible to obtain gels with networks of different density, and thus approach to a solution of the problem of the influence of the number and type of bonds on the properties of gels.

The material used for the study was a copolymer of methyl methacrylate (MMA) and methacrylic acid (MAA) in a weight % ratio of 83 : 17; this is a linear amorphous polymer. The presence of a definite number of carboxyl groups in the polymer molecules makes it possible to produce network structures by the introduction of bivalent metal oxides into the solutions. Solutions and gels of MMA-MAA copolymer with different amounts of additives were studied. Cyclohexanone was the solvent used. Dilute gels were obtained by introduction of the gel-forming additives in the form of alcoholic solutions with thorough stirring. To establish equilibrium in the systems, the samples were held at 70° for 30 hours in hermetically closed vessels. The dilute solutions and gels were studied by means of the dynamometric balance [6]. It was found in preliminary experiments that dilute solutions of MMA-MAA copolymer in a mixture of cyclohexanone and methyl alcohol pass into the gel state in presence of oxides and hydroxides of bivalent metals (Ca, Ba, Sr).

The figure shows the results of a thermomechanical investigation of dilute (4.5 g/100 ml) solutions and gels in 4:1 mixture of cyclohexanone and methyl alcohol in presence of different amounts of SrO. The deformation produced in 10 seconds at a constant stress of 0.5 g/cm² was measured at various temperatures.

It is seen in the diagram that in solutions without added SrO an increase of temperature results in a sharp increase of deformation, indicating that the system passes into the viscofluid state. Introduction of 2 or 3% SrO* displaces the deformation-temperature curves into the region of higher temperatures. With 4% of the additives and over, the displacement of the curves is accompanied by a sharp change in their form. A region characteristic of the high-elastic state appears on the curves. This region becomes more extensive for gels with higher contents of the additives. It proved impossible to detect a transition from the high-elastic to the viscofluid state in gels with more than 4% SrO by this method. The behavior of the gels at higher temperatures was therefore studied by observations of falling spheres in gels contained in sealed tubes. Steel balls 0.0326-0.0329 g in weight and 2 mm in diameter were used. The stress produced by the weight of the ball was ~1 g/cm². The results of the experiments are given in the table.

*The SrO contents of the gels are given in equivalent percentages on the carboxyl groups in the dissolved polymer.



Variation of the deformation of MMA-MAA copolymer gels with temperature. (The numbers on the curves represent the SrO contents as % of the MAA in the copolymer.)

Time Required for a Ball to Fall 10 mm in Gels Containing 4.5 g Polymer per 100 ml at Various Temperatures

SrO content, %	Temperature, °C		
	20	50	100
2	1.3 min	—	—
4	15 hours	—	—
5	94 hours	4 hrs 15 min	—
~10	—	26 hours	42 min

On the one hand, introduction of a bivalent metal oxide into a solution of a polymer containing carboxyl groups is accompanied by the formation of both intermolecular and intramolecular bonds. The latter are not involved in the creation of a spatial structure, which may account for the large amount of oxide which must be added before gelation begins. However, the probability of intramolecular bond formation decreases sharply with increasing concentration of the solution. At our concentration of 5 g/100 ml in the original solution, the relative proportion of intramolecular bonds is negligibly small. On the other hand, reactions between the bivalent metal compounds and the carboxyl groups may give rise to basic salts. These groups cannot form chemical bonds, but the possibility of nonchemical action by them is not excluded. It is true that basic salts are usually formed in presence of large excess of the bivalent metal oxides. In the present instance the formation of salt linkages owing to the excess of carboxyl groups should be expected. However, the formation of gels in presence of more than the theoretical amounts of SrO, and the high lability of the bonds in such systems, manifested in the fluidity of the gels at elevated temperatures, indicate that bonds of a different type from the usual chemical salt type are present.

These results indicate that gels with 4% SrO have some degree of fluidity even at 20°. In gels with 5 and 10% SrO the fluidity increases with rise of temperature. The behavior of the gel with 10% SrO is particularly striking; it is completely elastic at 20°, and is transformed into a viscofluid system at 100°. The appearance of viscofluid properties in the gels indicates breakdown of the stable bonds between the molecules at higher temperatures.

It follows from these results that introduction of small amounts of strontium oxide into solutions of MMA-MAA copolymer results in a gradual increase in the elasticity of the systems. The nature of the thermomechanical curves (see figure) suggests that a continuous spatial structure is formed in the polymer solutions in presence of 4% SrO.

It follows from the theory of the random formation of cross links that gelation begins in a mono-disperse system when the number of cross links reaches half the initial number of molecules, i.e., when one cross link is formed per two polymer molecules; an abrupt transition occurs from a true fluid solution to a brittle gel [7]. In a solution of MMA-MAA copolymer in presence of 2% SrO four cross links are formed per one thousand monomer units. Since the degree of polymerization of methyl methacrylate polymers is not less than 1000, the number of cross links formed in this instance is evidently larger than is theoretically required for gel formation. However, elastic properties appear in the presence of double this amount of SrO, and the elasticity increases gradually. This indicates that in the presence of SrO the carboxyl groups are not merely linked with the metal to form bonds of the neutral salt type.

SUMMARY

1. Gels have been prepared from solutions of synthetic methyl methacrylate-methacrylic acid copolymer by addition of bivalent metal oxides.

2. Gel formation is observed in presence of a larger number of bonds than is required by theory.
3. The bonds in the gels have high lability at elevated temperatures.
4. The presence of bonds of a different type from the chemical salt type is postulated.

LITERATURE CITED

- [1] P.I. Zubov, Z.N. Zhurkina and V.A. Kargin, Colloid J. 16, No. 2, 109 (1954).*
- [2] A.T. Walter, J. Pol. Sci. 13, 207 (1954).
- [3] J. Bisschops, J. Pol. Sci. 12, 585 (1954).
- [4] S.M. Lipatov, The Physical Chemistry of Colloids (1948).**
- [5] S.E. Bresler and D.L. Talmud, Proc. Acad. Sci. USSR 43, 367 (1944).
- [6] T.I. Sogolova, Candidate's Dissertation (Moscow, 1947).
- [7] P.J. Flory, J. Am. Chem. Soc. 63, 3083, 3096 (1941).

Received June 25, 1957

The L.Ia. Karlov Physicochemical
Institute — Moscow

*Original Russian pagination. See C.B. translation.

**In Russian.

THE STRUCTURE OF GELS

13. INVESTIGATION OF THE PROPERTIES OF GELS OF METHYL METHACRYLATE - METHACRYLIC ACID COPOLYMER CONTAINING UNIVALENT METALS

N.F. Proshliakova, P.I. Zubov and V.A. Kargin

It was shown in the previous communication [1] that the spatial structures formed on addition of bivalent metal oxides to solutions of methyl methacrylate-methacrylic acid copolymer contain bonds which have unexpectedly high lability at elevated temperatures. Since the nature of these structures is not clear, it was of interest to study the changes in the properties of the copolymer solutions in presence of additives which do not form chemical bonds between the molecules. Alkali metal hydroxides were used as the additives. Preliminary experiments showed that additions of alkali metal hydroxides (NaOH , KOH , TlOH) to dilute solutions of the copolymers cause gelation at room temperature. The gels melt when heated to 60° ; the solutions gel again on cooling. The dilute solutions and gels were studied with the aid of the dynamometric balance. The procedure used for preparation of the gels was the same as in the production of gels with added bivalent metal oxides.

Figure 1 gives data obtained in a study of solutions and gels of methyl methacrylate-methacrylic acid copolymer containing 4.5 g per 100 ml, in a 4:1 mixture of cyclohexanone and ethyl alcohol in presence of various amounts of sodium hydroxide. The deformation produced in 10 seconds at a constant stress of 0.5 g/cm^2 at different temperatures was measured. It follows from these results that addition of NaOH to the copolymer solutions displaces the temperature-deformation curves into the region of higher temperatures (with 3 and 5% NaOH).* With 10% NaOH the character of the curves changes: a region typical of high-elastic systems appears, but with increase of temperature a bend appears on the curves indicating transition of the system into the viscofluid state. The extent of the region of high elasticity on the temperature-deformation curves increases with increasing NaOH concentration in the gel (15, 20 and 25% NaOH), as the temperature of transition of the system into the viscofluid state increases; the solidification point of the solution remains almost unchanged.

Similar effects were observed in studies of more highly concentrated copolymer solutions and gels (7.5 g/100 ml). These results are shown in Figure 2. It is seen from a comparison of Figures 1 and 2 that the character of the deformation-temperature curves does not change with increase of the concentration of the polymer solutions. With the same caustic soda content, the temperature of the transition from the high-elastic to the viscofluid state is higher for the more highly concentrated gels.

Figure 3 represents the variations of deformation with the stress (acting for 20 minutes) at various temperatures, for a gel with a concentration of 4.5 g/100 ml, containing 20% caustic soda. It follows from Figure 3 that a linear relationship is retained at three different temperatures between the deformation and the stress, for loads between 0.25 and 25 g/cm^2 .

Figure 4 shows the results of a study of the development of deformation in a gel (4.5 g/100 ml) in the course of application and removal of a load producing a stress of 6.4 g/cm^2 ; it is seen that before the system enters the viscofluid region the deformation is completely reversible (curves for -44° , -30° , and -14°). Above this limit, both high-elastic and plastic deformation are found (curve for 0°).

*The caustic soda contents are given throughout in equivalent percentages of the methacrylic acid content of the polymer.

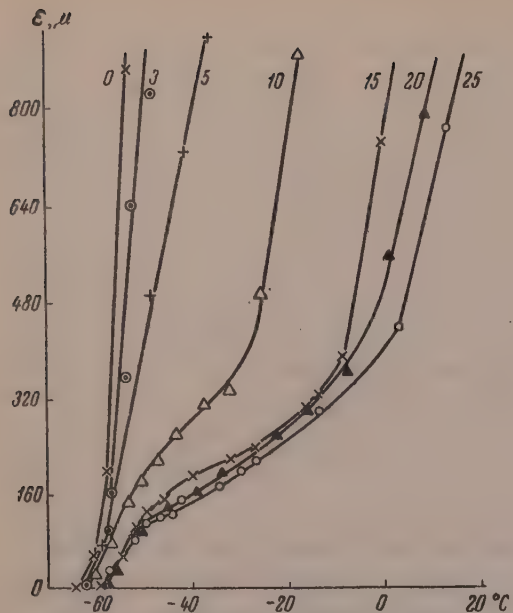


Fig. 1. Effect of temperature on the deformation of solutions and gels of MMA-MAA copolymer containing various amounts of NaOH. The numbers on the curves are the NaOH contents.

Equilibrium is established very rapidly both on application and on removal of the load. These results show that in the region of high elasticity the copolymer gels behave as ideal elastic equilibrium systems conforming to Hooke's law.

Figure 5 shows deformation-temperature curves obtained for different times of action of a constant load of 6.4 g/cm^2 on a gel with a concentration of 4.5 g/100 ml , containing 20% NaOH. It is seen in Figure 5 that the transition into the viscofluid state is characterized not only by an appearance of irreversible deformation; but also by a dependence of the deformation on the time of action of the load.

These experimental results show that gels made from a solution of methyl methacrylate-methacrylic acid copolymer in presence of sodium hydroxide have properties characteristic of elastic systems. This is evidence of the formation of a spatial network structure with relatively stable bonds. The formation of chemical bonds between the molecules is excluded in presence of univalent metal compounds, and therefore the cause of bond formation leading to the formation of the network gel structure must be nonchemical interaction of polar salt groups.

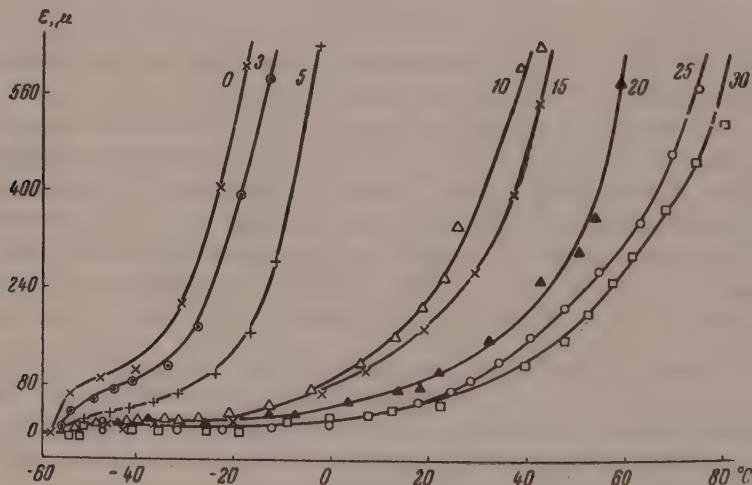


Fig. 2. Effect of temperature on the deformation of solutions and gels of MMA-MAA copolymer containing various amounts of NaOH. The numbers on the curves represent the % NaOH contents.

It was of interest to determine the causes of the interaction of the salt groups, leading to gel formation. It follows from the data on the influence of different amounts of caustic soda on the behavior of solutions of methyl methacrylate-methacrylic acid copolymer that small amounts of NaOH (up to 10%) increase the viscosity of solutions containing 4.5 g copolymer per 100 ml (Curves 2 and 3, Figure 1). In presence of 10 to 25% NaOH gelation occurs in a definite temperature range. With over 25% NaOH, phase separation takes place in the solution: the system still consists of two phases even after prolonged heating at 70° . In a solution of higher concentration (7.5 g/100 ml), separation occurs on addition of over 30% NaOH. It is known that phase separa-

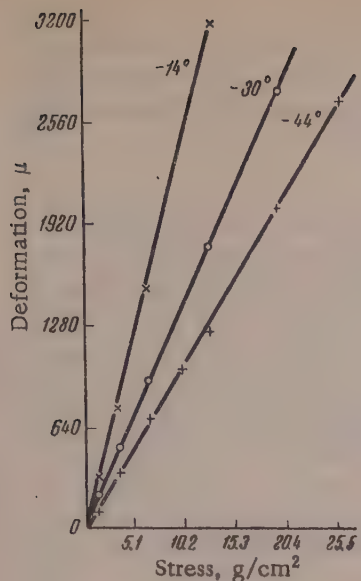


Fig. 3. Variation of gel deformation with the stress at various temperatures.

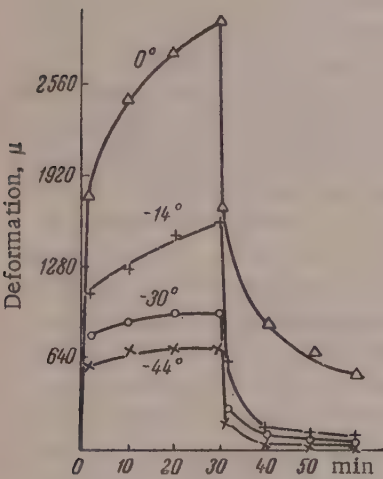


Fig. 4. Variation of deformation with time on application and removal of load.

determined from the variations of the logarithm of the equilibrium modulus with the reciprocal temperature [3]. If the network junctions are of the same structure and are therefore energetically equivalent, this relationship is represented by a straight line. For a gel of a concentration of 5.5 g/100 ml containing 30% NaOH the $\log E_{\infty} - 1/T$ relationship is not linear.

This form of the curve indicates that the junctions of the gel network structure are not energetically equivalent. At higher temperatures the junctions with the higher energies of formation are retained. The bond energy of the junctions broken down in this temperature range is between 2 and 11 kcal/mole. The presence of energetically nonequivalent junctions in the network and the fact that gelation commences in presence of a

tion takes place in a polymer solution if the solubility of the polymer in the given solvent is limited. Consequently, the introduction of salt groups into the molecules of methyl methacrylate-methacrylic acid copolymer must decrease its solubility in the solvents used. The phase separation and gelation effects occur in presence of different amounts of the same additives. From this it may be concluded that these effects are both of the same nature — they depend on the predominant interaction of groups of limited solubility in the polymer molecule with each other rather than with the solvent molecules.

This conclusion is also confirmed by the results of observations of the behavior of solutions of low-molecular acids of analogous structure (isobutyric and adipic acids). Alcoholic solution of caustic soda was added to solutions of these acids in cyclohexanone. The concentration of the acid solutions corresponded to the carboxyl group content of a copolymer solution containing 7.5 g of the copolymer in 100 ml. It was found that addition of caustic soda to solutions of the low-molecular acids caused precipitation owing to the poor solubility of the sodium salts of these acids. Phase separation in the acid solutions begins when the amount of the caustic soda added is such as leads to gelation in the polymer solutions.

Salt formation in the low-molecular acid-solvent system results in separation of the solution into two phases, while the introduction of the same quantity of salt groups into the polymer molecules in the same solvent induces gelation. This effect is a consequence of the specific structure of the polymer molecules. The sections of the polymer molecule containing salt groups have poor solubility in the solvent and tend to separate out as another phase, as is the case in solutions of low-molecular acids. Very many more sections of the same molecule have good solubility, preventing the precipitation of the salt sections. As a result of superposition of these two factors, microseparation takes place in the solution, i.e., separation of the badly soluble sections in microvolumes, while the molecule as a whole remains in solution. The groups of the badly soluble salt groups are the junction points of the gel network structure. This effect is analogous to the microseparation observed in mixtures of mutually insoluble rubbers, where complete separation is prevented by the enormous viscosity of the polymers [2]. In this case, microseparation increases the microheterogeneity of the rubbers and causes the appearance of anomalous mechanical properties in such systems.

In order to clarify the question of the structure of the junction points of the gel network structure, the dependence of the equilibrium modulus on the temperature was studied. The equilibrium modulus of elasticity depends on the number of junctions in the network structure. If such a structure contains unstable bonds, which break down on increase of temperature, the energy of formation of the junctions can be

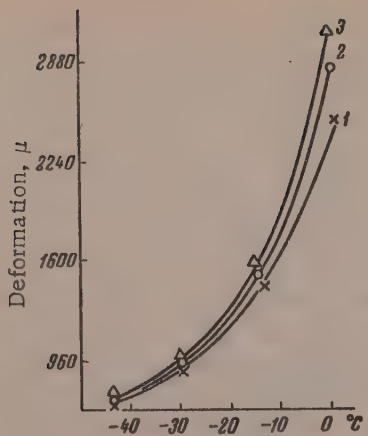


Fig. 5. Effect of temperature on deformation for various times of action of the load: 1) 10 minutes; 2) 20 minutes; 3) 30 minutes.

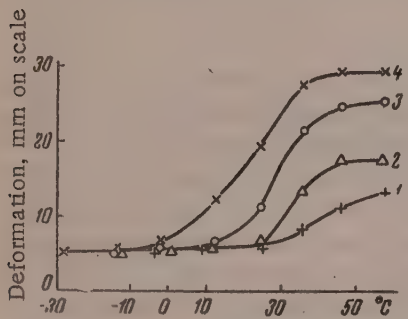


Fig. 6. Gel deformation as a function of temperature at various deformation rates: 1) 1000 rpm; 2) 100 rpm; 3) 10 rpm; 4) 1 rpm.

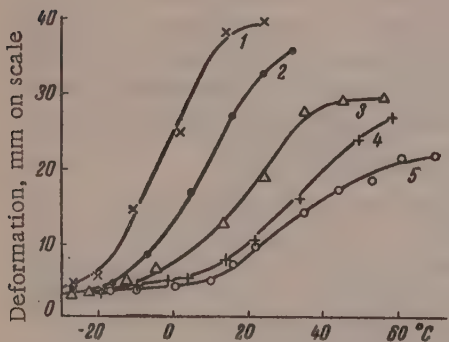


Fig. 7. Effect of temperature on deformation of gels containing different amounts of NaOH: 1) 5%; 2) 10%; 3) 15%; 4) 25%; 5) 50% NaOH (deformation rate 1 rpm).

The influence of added NaOH on the specific viscosity of a solution of the copolymer in cyclohexanone at a concentration of 0.2 g/100 ml at 20° is shown graphically in Figure 8. Curve 3 represents the variation of the specific viscosity of this solution with the caustic soda content. It is seen that the specific viscosity of the solu-

large excess of the bond-forming groups (20 salt groups per 1000 monomer units are formed on addition of 10% NaOH) lead to the conclusion that the junctions of the network structure of methyl methacrylate-methacrylic acid copolymer are swarmlike formations containing different numbers of interacting polar groups.

The behavior of dilute gels of methyl methacrylate-methacrylic acid copolymer shows great resemblance to the behavior of structurized systems made from typical gelling polymers (gelatin, etc.). A similar analogy is observed in the properties of concentrated gels. Concentrated gels of methyl methacrylate-methacrylic acid copolymer were prepared in film form. The required amount of caustic soda was added to a solution of the copolymer (2.5 g/100 ml) in 1:1 cyclohexanone-ethyl alcohol mixture. The films were made by evaporation of this solution at room temperature. The polymer concentration in the film was checked at intervals by weighing. To attain equilibrium, the films were heated at 100° and kept in a hermetically sealed vessel at room temperature for a month. The frequency apparatus [4] was used for the experiments on the concentrated gels.

Figure 6 shows the effect of temperature on the deformation of a concentrated gel (50 wt. %) containing 15% caustic soda, at various deformation rates. It is seen in Figure 6 that the deformation of the gel increases with decreasing deformation rate. At low deformation rates the transition from the glassy into the high-elastic state occurs at lower temperatures. Deformation of the relaxational type is also observed in gels with other contents of caustic soda (5-50%). Variations of the NaOH content in concentrated gels (50 wt. %) have an appreciable influence on their mechanical properties. It is seen in Figure 7 that an increase of NaOH content in the gel raises the temperature of transition from the glassy into the high-elastic state. The gels with higher caustic soda contents also melt at higher temperatures. Examination of these curves shows that the maximum deformation produced in the gel decreases with increase of caustic soda content. For example, in presence of 5% NaOH the deformation is 39 arbitrary units, whereas in presence of 50% NaOH it is 21 units.

All these results indicate that the behavior of concentrated gels of methyl methacrylate-methacrylic acid copolymer is similar to that of concentrated gelatin gels [5]. The similarity between the properties of solutions of this copolymer and of typical gelling polymers is also revealed by investigations of greatly diluted solutions of the copolymer in presence of NaOH. It is known that in dilute solutions the molecules of such polymers change their form and become globular.

tion decreases with increasing NaOH content, the greatest viscosity decrease being produced by additions of up to 30% NaOH. Subsequently, the specific viscosity remains almost unchanged.

These results indicate that caustic soda in the copolymer solution causes coiling of the molecules. Curves 1 and 2 in Figure 8 represent the viscosity variations of a solution without added caustic soda, with dilution with cyclohexanone and alcohol.

The specific viscosity of the solutions in presence of NaOH decreases up to a concentration of 1 g/100 ml. In solutions of higher concentrations the viscosity increases in presence of NaOH. Figure 9 shows the effect of temperature on the specific viscosity of a solution containing 0.175 g of copolymer in 100 ml of 88:12 cyclohexanone-ethyl alcohol mixture. Curve 1 represents a solution of the copolymer in cyclohexanone without additions, and Curve 2, a solution in cyclohexanone-alcohol mixture. Curve 3 represents a copolymer solution with addition of 100% NaOH. It follows from these results that the change in the configuration of the polymer molecules produced by the added caustic soda is fairly stable, as the specific viscosity remains low even on heating to 70°.

SUMMARY

1. Gels of methyl methacrylate-methacrylic acid copolymer containing sodium hydroxide have been prepared.
2. Over a certain temperature range these gels are ideally elastic systems.
3. It is shown that the structural network of such gels is formed only by physical interaction of the polar salt groups, which have poor solubility in the solvent used. The junctions of the network are formed by swarmlike formations containing different amounts of salt groups.
4. The properties of gels of various concentrations, containing NaOH, and of dilute solutions of the copolymer, are similar to the properties of gelatin gels and solutions.

LITERATURE CITED

- [1] N.F. Proshliakova, P.I. Zubov and V.A. Kargin, *Colloid J.* 20, 199 (1958) [this issue, page 191].
- [2] N.F. Komskaia and G.L. Slonimskii, *J. Phys. Chem.* 30, No. 7, 1529 (1956).
- [3] G.L. Slonimskii, V.A. Kargin and L.I. Golubenkova, *Proc. Acad. Sci. USSR* 93, No. 2, 311 (1953).
- [4] A.P. Aleksandrov and Iu.S. Lazurkin, *J. Tech. Phys. (USSR)* 9, No. 14, 1249 (1939).
- [5] P.I. Zubov, Doctorate Dissertation (L.Ia. Karpov Institute, Moscow, 1949).

Received June 25, 1957

L.Ia. Karpov Physicochemical Institute,
Moscow

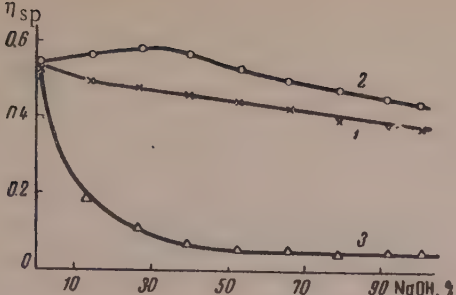


Fig. 8. Variation of the specific viscosity of MMA-MAA copolymer solutions with NaOH content and dilution with alcohol and cyclohexanone.

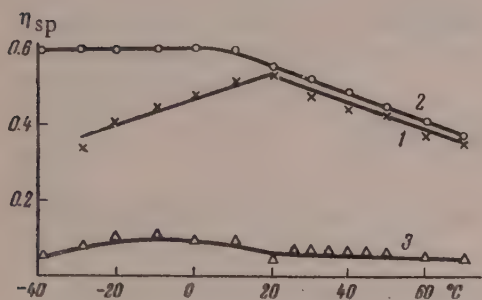


Fig. 9. Variation of the specific viscosity of copolymer solutions with temperature, with and without additions.

EQUATION FOR THE SORPTION ISOTHERM OF AMINO ACIDS ON
ION EXCHANGE RESINS IN THE HYDROGEN FORM

G. V. Samsonov and N. P. Kuznetsova

Our studies of the equivalence relationships in the exchange of dipolar ions of amino acids with other ions, and primarily with hydrogen ions, led to the conclusion that dipolar ions can be adsorbed in appreciable amounts only on conversion into cations. This conclusion was confirmed experimentally [1]. It is evident that the exchange of dipolar ions by a mechanism different from the mechanism of metal ion exchange must conform to a different exchange equation. It was shown [1] that the sorption of amino acids in neutral solutions may be represented by the equation:



where RSO_3^-H^+ is a sulfonic cation exchanger in the hydrogen form; R_1 is the hydrocarbon radical of the amino acid.

In acid solutions, exchange of amino acid cations and hydrogen ions proceeds with equivalent displacement of the one type of ion by the other according to the equation:



In the pH region close to pK_1 (K_1 is the dissociation constant of the carboxyl group of the amino acid), the sorption of amino acids should conform partly to the first and partly to the second equation. For derivation of the expression for the ion exchange isotherm it is necessary to calculate the change of thermodynamic potential for the sorption of one mole of the amino acid. Whereas by Equation (1) α moles are adsorbed, according to Equation (2) $1-\alpha$ moles are adsorbed. The change of the thermodynamic potential can be calculated from the chemical potentials of the substances involved in the process

$$\begin{aligned} \Delta\Phi_{T,p} = & [\bar{\mu}_{\text{R}^+} - \alpha\bar{\mu}_{\text{H}^+} - \alpha\bar{\mu}_{\text{R}\pm}] + [(1-\alpha)\bar{\mu}_{\text{R}^+} + \\ & + (1-\alpha)\bar{\mu}_{\text{H}^+} - (1-\alpha)\bar{\mu}_{\text{H}^+} - (1-\alpha)\bar{\mu}_{\text{R}^+}] \end{aligned} \quad (2a)$$

or

$$\Delta\Phi_{T,p} = \bar{\mu}_{\text{R}^+} - \bar{\mu}_{\text{H}^+} - \alpha\bar{\mu}_{\text{R}\pm} + (1-\alpha)\bar{\mu}_{\text{H}^+} - (1-\alpha)\bar{\mu}_{\text{R}^+}, \quad (3)$$

where the respective chemical potentials are: of the adsorbed amino acid, $\bar{\mu}_{\text{R}^+}$; of the hydrogen ions in the resin, $\bar{\mu}_{\text{H}^+}$; of the dipolar ions (zwitterions) of the amino acid in solution, $\bar{\mu}_{\text{R}\pm}$; of the amino acid cations in solution, $\bar{\mu}_{\text{R}^+}$; and of hydrogen ions in solution, $\bar{\mu}_{\text{H}^+}$.

Using the equation which relates chemical potentials with activities

$$\mu_i = \mu_i^0 + RT \ln a_i, \quad (3a)$$

and equating (3) to zero ($\Delta\Phi_{T,p} = 0$), we have

$$[\bar{\mu}_{R^+}^0 - \bar{\mu}_{H^+}^0 - \alpha \mu_{R^+}^0 - (1-\alpha) \mu_{H^+}^0 + (1-\alpha) \mu_{H^+}^0] + \\ + [RT \ln \bar{a}_{R^+} - RT \ln \bar{a}_{H^+} - \alpha RT \ln a_{R^\pm} - \\ - (1-\alpha) RT \ln a_{R^+} + (1-\alpha) RT \ln a_{H^+}] = 0. \quad (4)$$

Denoting the expression in the first square brackets, divided by RT, by $A' + B'\alpha$, we can reduce Equation (4) to the form

$$\ln \frac{\bar{a}_{R^+} \cdot a_{H^+}^{1-\alpha}}{\bar{a}_{H^+} \cdot a_{R^\pm}^\alpha \cdot a_{R^+}^{1-\alpha}} = A' + B'\alpha. \quad (5)$$

The relationship between the activities of the dipolar ions of amino acids and the cations is given by the expression

$$k_1 = \frac{a_{R^\pm} \cdot a_{H^+}}{a_{R^+}}. \quad (6)$$

With the aid of Equation (6), Equation (5) is reduced to the more convenient form

$$\ln \frac{\bar{a}_{R^+} \cdot a_{H^+}}{\bar{a}_{H^+} \cdot a_{R^+}} = A + B\alpha. \quad (7)$$

In the derivation of Equation (7) it was assumed that the concentrations of the substances in the sorption process remained constant, from which it follows that α can be calculated as follows

$$\frac{\alpha}{1-\alpha} = \frac{c_{R^\pm}}{c_{R^+}} \quad (8)$$

or

$$\alpha = \frac{c_{R^\pm}}{c_{R^\pm} + c_{R^+}}. \quad (9)$$

In dilute solutions, the activities used in Equation (7) are equal to the concentrations of the amino acid cations and hydrogen ions (c_{R^+} and c_{H^+}).

In a number of cases it is also possible to use concentrations in gram equivalents per gram of resin instead of activities for the components bound with the resin. Equation (7) then becomes

$$\ln \frac{m_{R^+} \cdot c_{H^+}}{m_{H^+} \cdot c_{R^+}} = A + B\alpha. \quad (10)$$

Putting

$$k_1 = \frac{c_{R^\pm} \cdot c_{H^+}}{c_{R^+}} \quad (11)$$

and comparing Equation (11) with Equation (8), we obtain the following equation for dilute solutions

$$\alpha = \frac{k_1}{k_1 + c_{H^+}}. \quad (12)$$

The ion-exchange Equation (10) was verified for the system alanine-hydrogen on SDV-3 sulfonic resin. Through a column containing 1 g of the resin in the hydrogen form 0.01 N alanine solutions of different acidities were passed, the acidity being regulated by addition of hydrochloric acid. 12 ml fractions of the eluate were collected, and the alanine concentration in them was determined by the ninhydrin reaction [2]. The process was

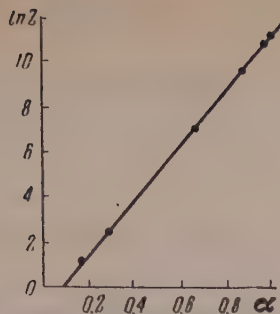


Fig. 1. Isotherm for the exchange of alanine ions and hydrogen ions on SDV-3 resin.

$$\alpha = \frac{m_{R^+} \cdot c_{H^+}}{m_{H^+} \cdot c_{R^+}}; \quad \alpha = \frac{k_1}{k_1 + c_{H^+}}$$

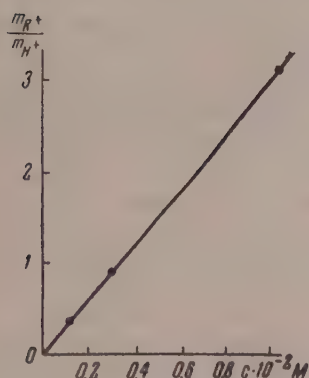


Fig. 2. Linear form of the adsorption isotherm of alanine on SDV-3 resin in the H form at pH 6.2.

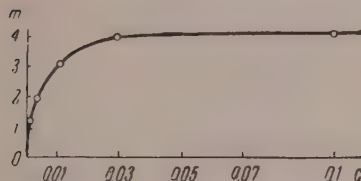


Fig. 3. Isotherm for the sorption of alanine by SDV-3 resin in the H form at pH 6.2; pK 2.3.

continued until the resin was in equilibrium with the solution. All the quantities in Equation (10) were calculated from the results of these experiments.

Figure 1 shows that the sorption of alanine by SDV-3 resin in the hydrogen form conforms to Equation (10). The constants A and B can be found graphically or calculated analytically. The specific characteristics of the sorption of amino acids by ion-exchange resins are clearly revealed on examination of the sorption isotherm for constant hydrogen ion concentration or when $pH \gg pK$. In the latter case the condition that c_{H^+} must be constant is not essential; Equation (10) then becomes

$$\frac{m_{R^+}}{m_{H^+}} = k c_R, \quad (13)$$

where c_R is the total amino acid concentration in the solution.

In Equation (13), instead of c_R we can use the concentrations c_{R^+} or $c_{R\pm}$. The constant k will then have different values.

The sorption of alanine by SDV-3 resin at pH 6.2 is represented by Equation (13) in graphical form in Figure 2. Equation (13) can be reduced to a form corresponding to the Langmuir equation

$$m_{R^+} = \frac{k \cdot m \cdot c_R}{1 + k \cdot c_R}. \quad (14)$$

Figure 3 shows that the amount of alanine adsorbed increases with increase of its concentration in solution. These experiments, like those described above, were carried out under dynamic conditions and were continued until the resin was in equilibrium with the original solution. It must be pointed out that the hydrogen ion concentration was several thousands of times lower than the alanine concentration, and the competitive effect of the hydrogen ions was therefore negligible. Under these dynamic conditions, with the usual exchange mechanism, the ions present in the resin are completely displaced by the ions introduced into the column. The limiting amount of adsorbed ions of one definite kind does not depend on the concentration in absence of competing ions. In contrast to this, when alanine is adsorbed from neutral dilute solutions it cannot occupy all the active centers in the resin owing to the specific sorption mechanism represented by Equation (1).

The sorption of alanine takes place without displacement of hydrogen ions. Similarly, the desorption of alanine does not necessitate a displacing effect by hydrogen ions.

With increase of concentration, the limiting amount of adsorbed alanine rises to 4.1 meq/g; this is equal to the total exchange capacity of SDV-3 resin determined by $\text{Na}^+ - \text{H}^+$ ion exchange, i.e., it corresponds to the number of active centers (sulfo groups) in the resin.

In solutions of high hydrogen-ion concentration the exchange of amino-acid cations with hydrogen ions conforms to Equation (2). In these conditions $\alpha = 0$ and Equation (10) therefore becomes

$$\frac{m_{R^+}}{m_{H^+}} = e^A \cdot \frac{c_{R^+}}{c_{H^+}}. \quad (15)$$

From the experimental results (Figure 1) the constant A for the system alanine-hydrogen on SDV-3 resin is

-0.9, and therefore the exchange constant in Equation (15) is $e^A = 0.408$. In other words, the selectivity of the sorption of alanine cations is very low.

This constant is hundreds of times smaller than the constant for the exchange of univalent organic cations of the tetracyclines aureomycin and terramycin with hydrogen ions [3].

SUMMARY

1. The equation for the isotherm for sorption of amino acids by hydrogen forms of sulfonic resins has been derived by a thermodynamic method.

2. The exchange of alanine ions with hydrogen ions on SDV-3 sulfonic resin has been studied experimentally. It is shown that at constant concentration of hydrogen ions in the solution the amount of amino acid adsorbed depends on its concentration.

LITERATURE CITED

- [1] G.V. Samsonov and N.P. Kuznetsova, Proc. Acad. Sci. USSR 115, No. 2 (1957).*
- [2] Stein and Moore, J. Biol. Chem. 176, 307 (1948).
- [3] G.V. Samsonov, L.M. Shuvalova, M.P. Shesterikova, et al., Colloid J. 18, No. 4, 454 (1956).**

Received January 12, 1957

Institute of High-Molecular Compounds
Academy of Sciences USSR — Leningrad

* See C.B. translation.

** Original Russian pagination. See C.B. translation.

A RADIOACTIVE ISOTOPE STUDY OF THE IONIC DEPOSITION OF RUBBER FROM LATEX

D.M. Sandomirskii and M.K. Vdovchenkova

Many technological processes for the production of rubber goods directly from latex are based on the formation of rubber gels. These can be obtained by slow destabilization of latex by the formation of coagulant ions in it, which is known as gelation [1], or by diffusion of ions into the latex from the surface of a form coated with electrolyte solution - ionic deposition [2], or from a metallic anode under the action of an electric current - electrodeposition [3]. The globules may be destabilized either by changes of the electrokinetic potential, or by the formation of water-insoluble compounds by the interaction of the electrolyte with the protective coatings on the globule surfaces.

The ionic deposition method is widely used for the production of such articles as balloons, gloves, etc. [2, 4, 5], but several problems remain unsolved. In particular, the relationship between latex stability and the degree of deposition is not quite clear, the distribution of the coagulant salt in the growing deposit is not known, the nature of the interaction of the salt with the protective substance of the latex is not understood, etc.

We showed [6] that the number of milliequivalents of calcium ions combined with 1 g of coagulum can be used as a measure of the stability of latexes to the action of electrolytes. This value, which we termed the calcium number, is determined by coagulation of the latex with $\text{Ca}^{45}\text{Cl}_2$ solution. It was desired to apply this method to a study of the ionic deposition process.

Composition and Properties of Latexes

Name of latex	Nature of polymer	Protective substance	Dry solids content, %
L-4	Polychloroprene	-	48.9
L-3	"	-	43.6
L-6	"	-	48.2
SKS-10n	Butadiene-styrene copolymer	Potassium naphthenate	26.5
SKS-30n	"	-	27.2
SKS-50n	"	"	29.4
SKS-50p	"	Ammonium paraffinate	49.14
Qualitex*	Natural rubber	Natural proteins and resins	61.6
Revultex	Vulcanized rubber	"	60.1

*Concentrate obtained by centrifuging.

The characteristics of the latexes studied are given in the table. The coagulant salt solution consisted of 59% water, 16% calcium chloride (calcined) and 25% cosmetic kaolin. The coagulant salt, to which $\text{Ca}^{45}\text{Cl}_2$ was previously added, was dissolved in the requisite amount of water. The solution was filtered through two layers of silk gauze, and kaolin was then added with thorough stirring. The activity of the coagulant solution was determined by the usual methods.

0.1 ml of the coagulant solution was placed on a glass slide of fixed size (3 x 2.3 cm). The slide was then

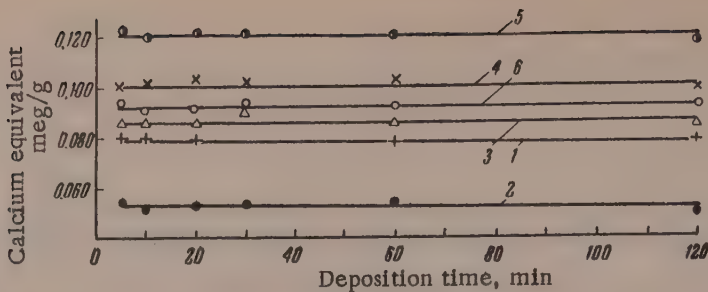


Fig. 1. Variation of calcium equivalent with the time of deposition:
1) L-4; 2) Qualitex; 3) SKS-50n; 4) SKS-30n; 5) SKS-10n; 6) SKS-50p.

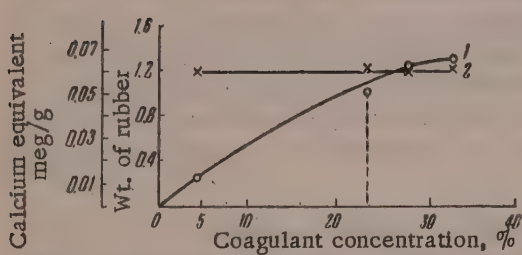


Fig. 2. Effect of coagulant concentration on the calcium equivalent and the amount of rubber deposited: 1) rubber deposited; 2) calcium equivalent.

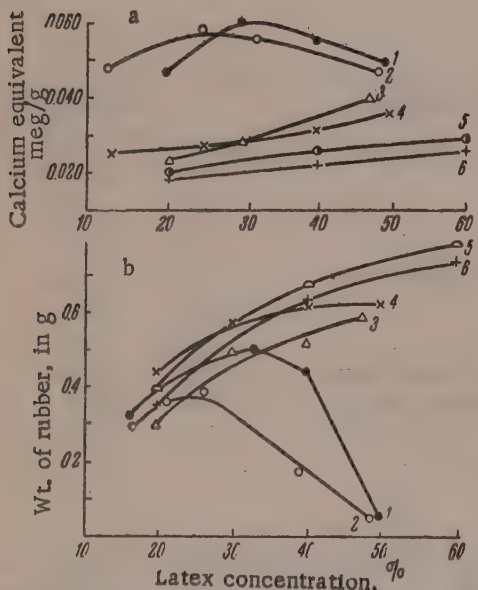


Fig. 3. Effects of latex concentration on: a) calcium equivalent; b) amount of rubber deposited; 1) L-3; 2) SKS-50p; 3) L-6; 4) L-4; 5) Qualitex; 6) Revultex.

dipped into the latex and kept there for a definite time. Rubber was deposited on the glass in the form of a gel. The gel was removed from the glass, boiled for 30 minutes in water to remove free calcium chloride, dried, and weighed. It was then burned in a muffle furnace and the activity of the ash was determined by the usual method. The calcium chloride content of the gel was calculated from the known amount of the coagulant solution taken, its activity, and the activity of the gel. The amount deposited was expressed in grams of dry solid per area of the form (glass slide) which was 6.9 cm^2 in all the experiments.

The activities of the gels formed, i.e., their contents of bound calcium chloride per 1 g of dry solid deposited, are plotted in Figure 1. The amount of bound calcium chloride is a constant value for a given latex, independent of the deposition time.

To determine how far this quantity (which we shall term the calcium equivalent, as distinct from the calcium number [6]) can serve for characterization of the behavior of the latex in ionic deposition, it was necessary to find how it depends on the concentrations of the coagulant and the latex, and on factors known to influence latex stability — temperature, dialysis, and natural or artificial aging.

It is seen in Figure 2 that the concentration of the coagulant solution does not influence the calcium equivalent (these experiments were carried out with L-4 latex and specially prepared coagulant solutions containing different amounts of calcium chloride). The amount of rubber deposited increases with coagulant concentration.

Thus, the existence of the presumed [2] "electrochemical equivalent" or a definite quantity of cations necessary for the deposition of a definite quantity of rubber has been proved experimentally.

We showed earlier [6] that the calcium number in latex coagulation does not depend on the concentration

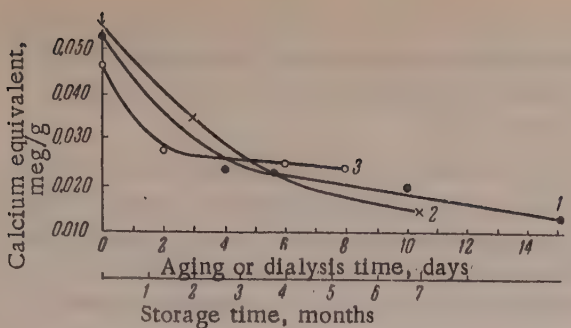


Fig. 4. Effects of storage, artificial aging, and dialysis of the latex on the calcium equivalent: 1) dialysis; 2) storage; 3) artificial aging.

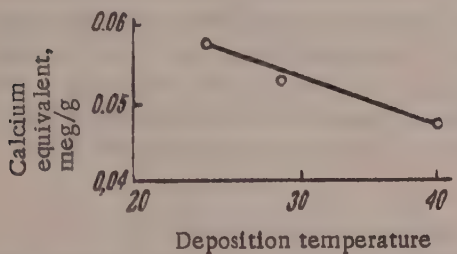


Fig. 5. Effect of deposition temperature on the calcium equivalent.

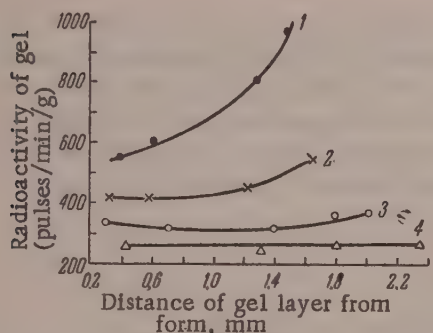


Fig. 6. Distribution of coagulant salt in the forming gel. Duration of deposition: 1) 30 minutes; 2) 40 minutes; 3) 60 minutes; 4) 120 minutes.

The electrolyte which diffuses into the latex from the surface of the form reacts mainly with the protective substance adsorbed on the globule surfaces; most of the protective substance in the serum takes no part in this interaction. Since the amount of protective substance on the globule surfaces decreases on dilution of the latex owing to desorption, the calcium equivalent must naturally decrease also. The extent of this decrease can serve as a measure of the degree of desorption.

The probable explanation for the decrease of the calcium equivalent with increasing concentration of some latexes is that, as stated above, ionic deposition ceases in these cases, and is replaced by coagulation.

The data in Figures 4 and 5 (for experiments with L-4 latex) show that the calcium equivalent greatly depends not only on the content of protective substance in the latex, but also in the stability of the latex. During natural or artificial aging of the latex the amount of protective substance in it remains constant, but its stability

of the latex. This is not the case with regard to the calcium equivalent in ionic deposition (Figure 3a). Here the calcium equivalent decreases with dilution of the latex. Latexes L-3 and SKS-30p are exceptions; with these the calcium equivalent increases at first, and begins to decrease only beyond a definite concentration. This is probably because these latexes conform to a peculiar relationship between the amount of rubber deposited (in 60 minutes) and the concentration (Figure 3b), characteristic for latexes containing salts of carboxylic acids as emulsifiers [2]. If the form coated with coagulant is dipped into latex above a definite concentration a gel is not formed, but a thin dense film is deposited on the form, making further diffusion of electrolyte into the latex impossible. As a possible explanation of this effect, one of us suggested that it is caused by differences in the solubility of the calcium salts of carboxylic and sulfonic acids [2].

However, the results of the present investigation show that in the course of ionic deposition insoluble calcium salts are formed in latexes containing salts of both carboxylic and sulfonic acids, and proteins (natural latex). It seems that a more probable explanation is that based on differences in the character of the structures formed in the interaction of the emulsifier with the electrolyte [7]. The different effects of the latex concentration on the calcium number and the calcium equivalent can be attributed to partial desorption of the emulsifier from the globule surfaces into the serum, which takes place on dilution of the latex. During coagulation the electrolyte reacts with all the emulsifier irrespective of its location. The amount of bound calcium must therefore remain constant. If the latex is subjected to dialysis as well as dilution, when the emulsifier in the serum is removed from the system, the calcium number should decrease; this was found to be the case [6].

The concentration of the gel formed by ionic deposition is considerably higher than that of the original latex [2], i.e., the latex becomes diluted and relatively richer in serum during the deposition.

decreases steadily owing to evolution of HCl, with a corresponding decrease of the calcium equivalent. This can probably be attributed to the decrease of the specific surface of the disperse phase which occurs during destabilization of the latex, owing to aggregation of the particles. Some of the protective substance is then trapped within the aggregates and does not interact with the coagulant electrolyte.

A comparison of the effects of various factors on the calcium equivalent and the kinetics of ionic deposition shows that the lower the calcium equivalent, the higher is the deposition rate and the more rubber is deposited on the form. However, this relationship does not hold for deposition from latexes of different concentrations (Figure 3). In this case, dilution of the latex results in a simultaneous decrease both of the calcium equivalent and the amount of rubber deposited. This is because of the less efficient utilization of the coagulant in dilute latexes. The formation of nonuniform gels confirms this.

In comparisons of latexes with different protective substances, their behavior in ionic deposition (deposition rate, amount of rubber deposited) cannot be predicted from a comparison of their calcium equivalents. This is only valid for similar latexes. A comparison of the variations of the calcium equivalent and technological properties of L-4 latex during artificial aging showed a satisfactory correlation between the calcium equivalent and the tensile strength of the gel [8]. A less satisfactory correlation is obtained with the yield of good-quality product, which varies much more rapidly than the other characteristics. The explanation is that the technological properties of the raw gels (for example, during stripping from the forms [9], inflation, etc.) depend in a very complex manner on all their physical and mechanical properties. They are therefore much more sensitive (especially in the production of pilot balloons) to variations of the colloidochemical properties of the latexes during storage, artificial aging, etc. [10].

By the use of a radioactive tracer, it was possible to study the distribution of the coagulant salt in the rubber gel growing on the form. For this, gels deposited for different times from L-4 latex were dried without washing and cut into several pieces across their thickness. These pieces were weighed, their thickness was measured in order to determine the average distance of the given gel layer from the form, burned, and the activity of the ash was determined, calculated per 1 g of gel.

The results, given in Figure 6, show that the electrolyte diffuses very rapidly from the surface of the form through the growing gel, forming a salt layer, which ensures further growth of the gel, on the surface in contact with the latex. A part of the electrolyte becomes bound with the protective substance of the latex and takes no part in subsequent diffusion. The proportion of the bound salt increases with time of deposition. When all the salt has become bound (after 120 minutes in our experiments), further deposition ceases. The gradual decrease in the amount of salt diffusing into the latex accounts for the continuous decrease of the deposition rate with time [2].

SUMMARY

1. The ionic deposition of rubber from latexes has been studied with the aid of $\text{Ca}^{45}\text{Cl}_2$.
2. The amount of calcium bound by one gram of rubber (the calcium equivalent) does not depend on the duration of deposition or the concentration of the coagulant salt solution.
3. The calcium equivalent decreases with increasing dilution of the latex owing to the desorption of stabilizer from the globule surfaces.
4. The calcium equivalent bears a relationship to the stability of the latex. Owing to aggregation of the particles, the calcium equivalent decreases on dialysis, storage and artificial aging of the latex, and also on increase of the deposition temperature.
5. There is a correlation between the variations of the calcium equivalent during aging of latex and the variations of gel strength.
6. The distribution of the coagulant salt in the growing gel was studied.

LITERATURE CITED

- [1] R.M. Panich, K.A. Kal'ianova and S.S. Voiutskii, Colloid J. 12, 50 (1950).

- [2] D. Sandomirskii and V. Chernaia, Trans. Sci. Res. Inst. Rubber Ind. No. 1, 20 (1954).
- [3] B.A. Dogadkin and D.M. Sandomirskii, Proc. VIth Mendeleev Conference, Vol. 2, No. 3 (1933).
- [4] R. Noble, *Latex in Industry* (1953).
- [5] H. Morris and R. Hinderer, *Rubber Age* 63, 144 (1948).
- [6] D.M. Sandomirskii and M.K. Vdovchenkova, *Colloid J.* 20, No. 1 (1958).*
- [7] Ia. Iabko and S.S. Voiutskii, *Colloid J.* 12, 303 (1950).
- [8] A.I. Medalia, *Anal. Chem.* 26, 697 (1954).
- [9] D.M. Sandomirskii, in the book: Production and Use of Synthetic Latexes (Moscow-Leningrad, 1953), page 30.**
- [10] V. Chernaia, *ibid*, page 57.

Received December 28, 1956

Scientific Research Institute of
Rubber and Latex Products — Moscow

* See C.B. translation.

** In Russian.

THE STATES OF AGGREGATION OF HIGH POLYMERS

1. STUDY OF THE LINEAR EXPANSION OF POLYMETHYL METHACRYLATE, POLYSTYRENE, POLYVINYL CHLORIDE, AND VINYL CHLORIDE-VINYL ACETATE COPOLYMER

R.I. Fel'dman

The question of the states of aggregation of high polymers has been attracting considerable attention recently. New data are available whereby it is possible to determine in greater detail the characteristics of the states of aggregation which distinguish high-molecular from low-molecular compounds. However, neither the terminology nor many of the concepts in this field have been finalized. Some authors include the glassy and high-elastic states on an equal level with the liquid and crystalline states among the states of aggregation, whereas others merely regard them as physical states, although this is too general a term. We consider the most apt term to be "state of aggregation," which is determined from the standpoint of molecular physics, first, by the spatial coordination of the structural units (atoms, monomer units, separate sections, and whole macromolecules); second, by the nature and intensity of the forces and bonds between the structural units, and finally, by the nature and intensity of thermal motion. Although this definition may also seem general, it excludes numerous physical states which do not conform to these criteria, such as the state of an electrified body, etc. The states of aggregation may vary continuously and steadily with temperature or change of concentration of an additional low-molecular component (solvent, swelling agent). In practice the variations are as a rule continuous only within certain limits. In phase transitions in low-molecular systems the variations become discontinuous, and the system enters abruptly into another state with a different course of variations. In polymer systems the transitions are diffuse owing to the relaxational nature of the processes leading to changes of state. This makes the identification of the individual states and determination of the boundaries between them somewhat arbitrary. The degree of detail in description and classification of different states and the transition points corresponding to their boundaries is determined by practical requirements. Theoretical considerations, on the other hand, often lead to obliteration of the boundaries between individual states and unification of them in single concepts. For example, the glassy, high-elastic, and viscofluid states are unified in the single concept of the amorphous state. In the discussion which follows we consider the accumulated data on various details of changes in the states of aggregation, characterized by discontinuities of the variations of the properties with the conditions determining the state. Such transitions are sometimes difficult to detect and often depend on the kinetics of the process.

States of aggregation are studied with the aid of measurements of specific volume, linear dimensions, heat capacity, and mechanical, optical, and other properties as functions of the temperature. The thermographic method and studies of the effects of the concentration of a low-molecular component in the system are sometimes applicable [1-5]. The fundamental and more direct methods of structure study such as x-ray and electron diffraction, molecular spectroscopy, etc., unfortunately can be used only rarely for clarification of the states of aggregation of amorphous polymers. We used mainly two modifications of the dilatometric method: determinations of the volume and linear expansion. In the simplest cases, for isotropic materials, these modifications give the same results. Anisotropic materials give more complex relationships, and the coefficients of linear expansion depend on the direction of the orientation. The configuration of an oriented polymer with "frozen" deformation may alter within a certain temperature range without change of volume or independently of the volume change. Therefore linear dilatometry provides a more detailed picture of the behavior of materials.

In such investigations we find a variety of states which by some criteria may be regarded as equilibrium states; more detailed study reveals their nonequilibrium nature. They occur as the result of retardation of cer-

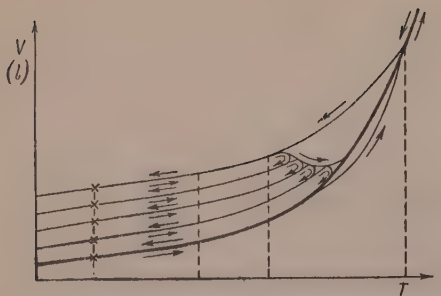


Fig. 1. Generalized schematic representation of the specific volume-temperature relationship for amorphous substances.

to reproducible states regardless of direction, if the temperature during heating does not exceed a certain value, characteristic for the given substance. Heating above this temperature favors a transition into another state of lower specific volume and evidently of lower enthalpy. Depending on the previous treatment of the material, the maximum heating temperature, and the rates of heating and cooling, it is possible to obtain hysteresis effects in the volume or linear dimensions, in either a positive or a negative direction. This is evidence of the great significance of the history of the specimen in various tests and in practical utilization. Results of a similar nature are obtained in experiments on swelling followed by evaporation of the solvent at different rates. Analogous but more complicated effects in anisotropic or previously deformed materials are more conveniently observed by studies of changes of the linear dimensions of the specimens in different directions. Spontaneous changes of volume and shape, leading to shrinkage of the articles under certain conditions, are of great practical importance. Thermal and other treatments of the tempering or annealing type are no less important for polymeric materials than for metals. The experimental results given below have a direct bearing on these practical problems.

EXPERIMENTAL

The investigations were primarily based on dilatometric determinations. A mercury dilatometer of the usual type with a graduated capillary was used. However, most of the determinations consisted of measurements of the linear expansion of specimens of different shapes (rods, films, threads) and of various origins. A dynamometer of the Polanyi type, designed by N.V. Smirnov, was used as the dilatometer. An important feature of the instrument was the accurate cutting of the thread of the main guide screw. Backlash of the guide nut with the dial was almost entirely eliminated by means of a weight suspended from the screw. The scale was read with the aid of a vernier to an accuracy of 1μ . The length was generally measured at 1° intervals. The temperature-control devices consisted of a separable shell with hollow walls, through which liquid was pumped from a thermostat, and an electric heater with a massive internal copper cylinder which ensured uniform temperature distribution inside the heater. The pitch of the screw and the thermometer placed near the specimen were calibrated before the determinations and at intervals between series of experiments. Length changes of specimens in the form of massive rods may be measured at zero load, or, if desired, with compensation of the weight of the specimen; changes in the dimensions

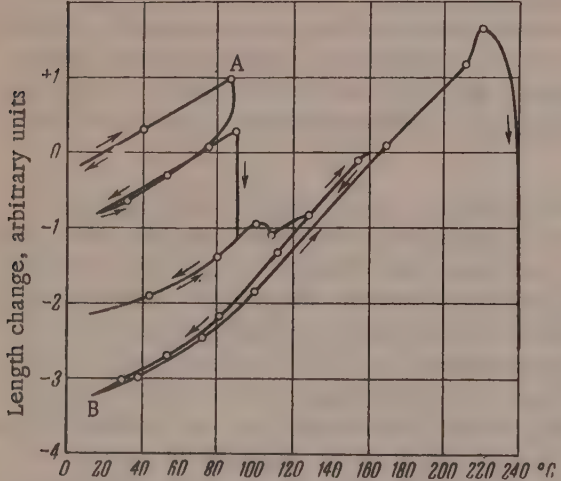


Fig. 2. Effect of temperature on the length of a polymethyl methacrylate specimen; $P = 0.025$.

of films and threads can only be measured under load. To take this factor into account, experiments were carried out under different loads (P in g/mm^2).

Polymethyl methacrylate. Anisotropic strips of the material, with internal stresses produced during industrial production, were tested. The results of tests over five heating and cooling cycles (total duration of the experiments was 13.5 days) are given in Figure 2. The decrease in the length of the strips with change of temperature from 85° (A) to 16° (B) was 3.1%. The coefficient of linear expansion α ($\text{cm}/(\text{degree} \cdot \text{cm})$) under these test conditions in the temperature range from ~5° to ~100° had a maximum value of $1.2 \cdot 10^{-4}$. It is seen in Figure 2 that as the result of heat treatment the thermal stability of the material increased, the contraction began at higher temperatures (85, 89, 99°), and annealing became complete. The length-temperature relationship resembles the volume-temperature relationship shown in Figure 1, and reflects the transition of the system from one state into another of a different degree of stability. At 85–102° there is evidently a significant change in the state of the system. The chain molecules change their configuration, and the individual segments are more easily mobile relative to each other. This transition is of practical importance, as pressed articles lose their shape at 85–100° and return to their initial shape.

Polystyrene. The length variations of industrial pressed polystyrene specimens with temperature are shown in Figure 3; it is seen that the material passes from a less to a more stable state (Figure 3,a) and that it can be obtained in the less stable state if heated above 104° (Figure 3b). The system cannot be removed from a given

state either by prolonged exposure to room temperature, or by variation of temperature if this does not exceed the first transition point of the experiment. Heat treatment decreases shrinkage, and raises the temperature at which the shrinkage begins. The decrease in the length of the specimen from the beginning (A) to the end (B) of the tests was 0.50%, and with variation of the temperature from 98 to 103° it was 0.43% (Figure 3a). During the first heating from 94 to 99° the specimen shrank by 0.13%, and in the second, between 99 to 104°, by 0.04%. The change in the length of the specimen during heating from 10° (A) to 116° (B) was 5.84% and from 10° (A) to 16.5° (K), it was 4.7% (Figure 3b). The value of α in the range between 10 and 116° is between $0.63 \cdot 10^{-4}$ and $2.15 \cdot 10^{-4}$.

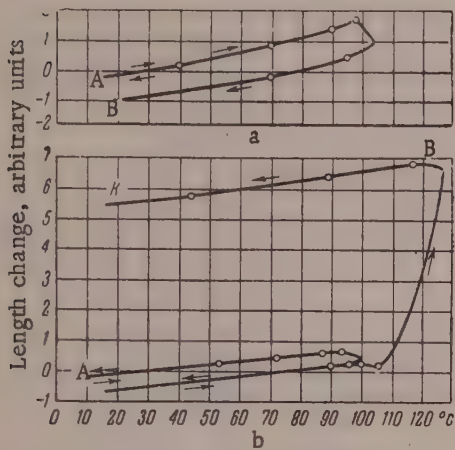


Fig. 3. Effect of temperature on the length of polystyrene specimens: a) without load; b) $P = 0.33$.

The orientation caused by previous stretching or in the preparation of the films alters the appearance of the curve. The contraction which begins at a definite temperature shows that the polymer chains become fairly mobile and can be regrouped. The system passes into a more stable state, closer to a state of relative equilibrium at these temperatures. This mobility may arise by breakdown of certain weak bonds while stronger bonds are retained. The elongation which follows the contraction indicates the elimination of another group of bonds, resulting in even greater mobility and decrease of the relaxation time. Increase of the load in the tests gives regions of almost constant length on the heating curves (Figure 4, Curve 4, temperature range 40–47°). No contraction occurs on heating in isotropic films cast on mercury or glass with subsequent heat treatment. The following experimental results illustrate the changes of linear dimensions. After two cycles of cooling and heating, a rolled film (Figure 4, Curve 1) contracted by 11%. The coefficient of linear expansion varied between $0.77 \cdot 10^{-4}$ and $1.49 \cdot 10^{-4}$ in the temperature range from 14 to 97°. Film II, cast from solution on glass (Figure 4, Curve 3) contracted by 5.54% on heating from 47 to 90°; $\alpha = 0.93 \cdot 10^{-4}$, in the temperature range from 10 to 47°. The unstretched film III, cast from solution (Figure 4, Curve 4), lengthened by 130% from the start to the end of the tests, while a stretched film with a residual elongation of 6% (Figure 4, Curve 7) contracted by 10.5%. Previous heating decreased the extension of unstretched specimens to 25% (Figure 4, Curves 5 and 6). The value of α in these test conditions, in the temperature range between 19 and 95°, varied from $0.45 \cdot 10^{-4}$ to $2.07 \cdot 10^{-4}$.* Figure 5 gives

Polyvinyl chloride. Films cast on glass and on mercury from solutions of PVC in dichloroethane and in chlorobenzene, and films made from the resin with a stabilizer by rolling and pressing, were tested. The average molecular weight of the polymer was 62,000. The results of tests for specimens with different histories are shown in Figure 4.

*The general course of the length variations with temperature is shown in Figs. 2–4 and 6. The curves are drawn to different scales, and comparison of the absolute values for different specimens is not possible.

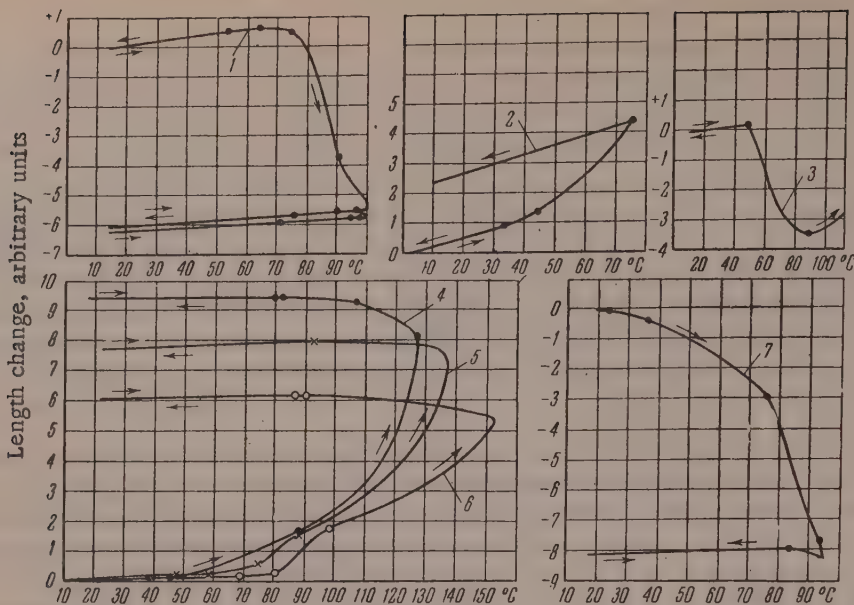


Fig. 4. Effect of temperature on the length of polyvinyl chloride film specimens (rolled and I-III): 1) rolled, oriented; $P = 4.02$; 2) I, from solution in chlorobenzene cast on glass, heated at 100° ; $P = 1.7$; 3) II, from solution in dichloroethane cast on glass; $P = 18.5$; 4) III, from solution in dichloroethane cast on glass; $P = 61.6$; 5) III, heated at 120° ; $P = 24$; 6) III, heated at 160° ; $P = 17.3$; 7) stretched; $\epsilon_{res} = 6\%$; $P = 60.3$.

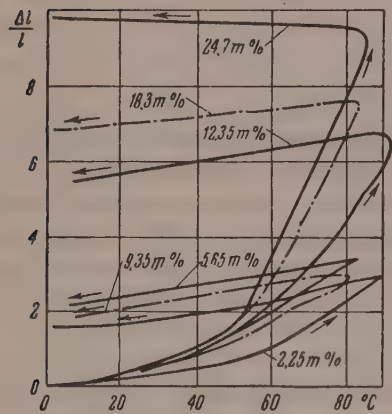


Fig. 5. Effect of temperature on the relative elongation of plasticized polyvinyl chloride; $P = 5$:

— polyvinyl chloride + dibutyl phthalate; - - polyvinyl chloride + tricresyl phosphate.

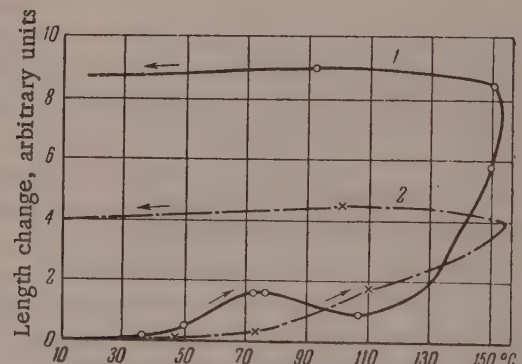


Fig. 6. Effect of temperature on the length of specimens of vinyl chloride-vinyl acetate copolymer films: 1) not previously heated; $P = 10.7$; 2) after heating; $P = 7.5$.

the relative elongation-temperature relationships for films of plasticized PVC made on rolls with subsequent pressing. The transition points are displaced toward lower temperatures and the hysteresis loops increase with increasing plasticizer contents.

Copolymer of vinyl chloride (85 wt. parts) and vinyl acetate (15 wt. parts). The length-temperature relationships were studied with anisotropic films cast on glass from solution in dichloroethane (Figure 6). Heat treatment at 160° eliminates orientation; this is reflected in the form of the relationship (Figure 6, Curve 2). The elongation from the start to the end of the tests decreased from 22.5 to 9.9%; α varied between $0.86 \cdot 10^{-4}$ and $1.84 \cdot 10^{-4}$ in the range from 23 to 101° .

Transition Temperature Points and Regions

Transition, method of determination	t°	Literature source
Poly methyl methacrylate		
T_b by induced elasticity	20	[6]
By form of tensile failure	45	[7]
T_g - glass transition temperature	57	[8]
T_g - thermal expansion (start of break in curve)	57	[9]
Proton magnetic resonance	\sim 60	[32]
T_f - thermal expansion (end of break in curve)	68	[9]
T_m - 2nd order transition, by refractive index	72	[10]
T_g - solidification temperature; dilatometry	82	[15]
T_n - from coefficient of diffusion	from 84 to 86	[15]
T_E - elasticity temperature; mechanical properties	\sim 90	[8]
Softening temperature; dilatometry	98	[11]
Modulus (torsion)	\sim 100	[35]
T_g - glass transition temperature	105	[30]
Softening temperature	107	[38]
Proton magnetic resonance	from 125 to 130	[32]
Softening point	125	[8]
Polystyrene		
Change of the sign of birefringence	from 20 to 25	[12]
T_b - induced elasticity	45	[6]
Maximum relaxation time; birefringence	from 44 to 48	[13]
Thermal volume expansion	from \sim 60 to \sim 85	[9]
E.T. - "freezing temperature"	from 70 to 80	[14]
Change of constant; birefringence	from 70 to 90	[13]
Softening point (density from 1.04 to 1.065)	from 70 to 100	[36]
T_m - 2nd order transition, by refractive index	75 \pm 4	[10]
T_b - brittle point	80	[20]
Appearance of rubberlike properties	\sim 80	[17]
Softening temperature; dilatometry	81	[11]
T_m - 2nd order transition; thermal expansion	81	[18]
T_g - transition temperature; thermal expansion	81	[19]
T_g - " " "	82	[9]
T_g - solidification temperature; dilatometry	82	[15]
T_g - glass transition temperature; dilatometry	85	[34]
T_n - from coefficient of diffusion	from 86 to 88	[15]
T_m - 2nd order transition; thermal expansion (density 1.049)	87	[20]
T_g - glass transition temperature (M.W. 19300 to 1675)	from 89 to 40	[31]
T_m - 2nd order transition; heat capacity	90	[21]
Modulus (torsion)	from \sim 100 to \sim 110	[35]
Transition temperature of precipitated material; thermal expansion	108.5	[19]
t_g - dynamometric balance (M.W. from 794000 to 360)	from 109 to 17	[22]
Birefringence becomes constant	110	[13]
Change of constant; birefringence	from 120 to 140	[13]
Maximum loss factor; frequency 1 kc	127.5	[34]
" " frequency 10 kc	138.5	[34]
t_f - dynamometric balance (M.W. from 794000 to 360)	from 163 to 23	[22]
Polyvinyl chloride		
Frost resistance	0	[37]

Transition, method of determination	t°	Literature source
T_g - stretched under load of 2 kg/mm ²	50	[23]
t_g - dilatometry	70	[24]
2nd order transition	70	[8]
T_m - 2nd order transition; thermal expansion	75	[25, 26]
Modulus (torsion)	from ~75 to ~96	[35]
T_g - unstretched	77	[23]
E.T. - "freezing temperature"	77	[27]
Proton magnetic resonance	~80	[32]
Heat endurance	80	[37]
Region of transition into high-elastic state; Aleksandrov-Gaev functiometer	from 80 to 100	[28]
T_b - brittle point	81	[16]
t_g - dynamometric balance (M.W. from 183000 to 3100)	from 85 to 12	[22]
Temperature of anomalous dispersion of dielectric constant; frequency 50 cps	90	[27]
t_g - dilatometry	92	[11]
Dielectric loss maximum at 60 cps	98	[8]
T_E - start of high elasticity	~100	[8]
Softening point	130	[33]
Proton magnetic resonance	~135	[32]
t_f - dynamometric balance (M.W. from 133000 to 3100)	from 169 to 17	[22]
Softening temperature	180	[29]

Control measurements of the lengths of the polymer specimens, carried out for several days (up to 60) after the main tests, confirmed that the state reached was relatively stable and that the individual points were fully reproducible with small temperature fluctuations. Analysis of the graphs for the length-temperature relationships, given here only in part, provided extensive numerical data on the coefficients of linear expansion over definite temperature ranges, and on the transition points corresponding to discontinuities in the curves. All this material is primarily of practical interest.

Analysis of this material leads to the following general conclusion. The coefficients of linear expansion and the transition temperatures are not very constant, and primarily depend on the previous history of the specimens and the kinetics of the changes leading to the state in question. Some of the transition points may be identified with the glass transition and flow temperatures determined by the usual methods. However, the curves contain many other transition points, which indicate the existence of numerous states of aggregation in polymeric compounds, and which do not fit into the simple scheme of three states generally accepted for amorphous polymers. For these reasons, the literature data given in the table also differ considerably. Our method is fairly convenient for determinations of transition points of every type, and for investigations of their dependence on various factors, relating both to the materials themselves and to the test conditions. The experimental data obtained in this investigation confirm conclusively the view, stated earlier, that nonequilibrium states of various degrees of relative stability are very common in high polymers. These results also emphasize the necessity for taking into account, in all investigations of the behavior of polymer materials, the previous thermal and mechanical history of the specimens used.

SUMMARY

- The states of aggregation of high polymers were studied by measurements of the linear dimensions of specimens during heating and cooling to various temperatures, a dynamometer of the Polanyi type being used as the measuring instrument. Data were obtained for polystyrene, polymethyl methacrylate, unplasticized and plasticized polyvinyl chloride, and vinyl chloride-vinyl acetate copolymer. The following values were determined: a) coefficients of linear expansion; b) hysteresis effects in the establishment of states of different degrees of

stability; c) shrinkage in relation to previous heat treatment (chilling and annealing), and previous deformation.

2. The transition temperatures so found were compared with literature data.

3. It was found that the nonequilibrium states can persist for considerable periods of time; a system in such a state can only be brought into another state by alteration of conditions (such as temperature) beyond a certain limit. "Frozen" states can be regarded as sufficiently stable states for practical purposes within definite limits.

4. The development of nonequilibrium states in polymers is associated with various hysteresis effects on the heating and cooling curves.

5. These results can serve as a basis for practical methods of thermal tempering and annealing of articles made from polymers, in order to avoid undesirable shrinkage and spontaneous changes of shape in use.

I offer my sincere thanks to Prof. S.I. Sokolov for his great interest in my work and for valuable guidance.

LITERATURE CITED

- [1] R.I. Fel'dman, Proc. Acad. Sci. USSR 97, No. 6, 1033 (1954).
- [2] S.I. Sokolov and R.I. Fel'dman, Investigations of High-Molecular Compounds*(Izd. AN SSSR, 1949), page 329.
- [3] R.I. Fel'dman and A.K. Mironova, Colloid J. 17, No. 6, 465 (1955).**
- [4] R.I. Fel'dman, A.K. Mironova and S.I. Sokolov, Colloid J. 20, 106 (1958).**
- [5] S.I. Sokolov, S.A. Reitlinger and R.I. Fel'dman, Colloid J. 19, 624 (1957).**
- [6] Iu.S. Lazurkin and R.L. Fogel'son, J. Tech. Phys. (USSR) 21, No. 3, 267 (1951).
- [7] C.A.W. Hoff, J. Appl. Chem. 2, No. 8, 441 (1952).
- [8] V.L. Simril, J. Pol. Sci. 2, No. 2, 142 (1947).
- [9] F.E. Wiley, Ind. Eng. Chem. 34, 1052 (1942).
- [10] R.H. Wiley and G.M. Brauer, J. Pol. Sci. 3, No. 3, 455 (1948).
- [11] S.N. Zhurkov, Doctorate Dissertation (Leningrad, 1947).
- [12] R. Houwink, Physikalische Eigenschaften und Feinbau von Natur- und Kunsthären (Leipzig, 1934).
- [13] O.N. Trapeznikov, J. Phys. Chem. 22, 395 (1948).
- [14] E. Jenckel, Kunststoffe 40, No. 3, 98 (1950).
- [15] S.N. Zhurkov and G.Ia. Ryskin, J. Tech. Phys. (USSR) 24, No. 5, 797 (1954).
- [16] J.J. Russel, Ind. Eng. Chem. 32, 509 (1940).
- [17] C.W. Bunn, The Chemistry of Large Molecules [Russian translation] Vol. 2 (IL, 1948), page 179.
- [18] W. Patnode and W.J. Scheiber, J. Am. Chem. Soc. 61, 3449 (1939).
- [19] E. Jenckel and K. Überreiter, Z. phys. Chem. A 182, 361 (1938).
- [20] R.F. Boyer and R.S. Spencer, The Chemistry of Large Molecules Vol. 2 [Russian translation] (IL, 1948), page 9.
- [21] R.F. Boyer and R.S. Spencer, J. Appl. Phys. 15, 398 (1944).
- [22] Iu.M. Malinskii, Candidate's Dissertation (Moscow, 1948).
- [23] F.H. Müller, Koll.-Z. 95, 138 (1941).
- [24] K. Überreiter, Z. Phys. Chem. B45, 361 (1940); Koll.-Z. 102, 272 (1943).

* In Russian.

** Original Russian pagination. See C.B. translation.

- [25] R.F. Clash and L.M. Rynkiewicz, Ind. Eng. Chem. 36, 279 (1944).
- [26] E. Hunter and W.G. Oakes, Trans. Faraday Soc. 41, 49 (1945).
- [27] Anonymous, Kunststoffe 40, No. 5, 158 (1950).
- [28] V.A. Kargin and I.Ia. Petrov, J. Phys. Chem. 25, No. 3, 345 (1951).
- [29] P.B. Stickney and L.V.E. Cheyhey, J. Pol. Sci. 3, No. 2, 231 (1948).
- [30] M.G. Fox and S. Loshaek, J. Pol. Sci. 15, 371 (1955).
- [31] Cited through M. Williams, R. Landel and J. Ferry, Problems of Modern Physics No. 12 [Russian translation] (IL, 1956), page 20; J. Am. Chem. Soc. 77, No. 14, 3701 (1955).
- [32] A. Odajima, J. Sohma and M. Koike, Problems of Modern Physics No. 12 [Russian translation] (IL, 1956), page 133; J. Chem. Phys. 23, No. 10, 1949 (1955).
- [33] Fibers from Synthetic Polymers [Russian translation] (IL, 1957), page 12.
- [34] K.Z. Fattakhov, J. Tech. Phys. (USSR) 22, No. 2, 313 (1952).
- [35] K. Wolf, Kunststoffe 41, No. 3, 89 (1951).
- [36] J. Hearle, Chemistry and Technology of Polymers No. 1 [Russian translation] (IL, 1957), page 96; Skinners Silk and Rayon Record 30, No. 4, 354 (1956).
- [37] W. Steiner, Chemistry and Technology of Polymers No. 1 [Russian translation] (IL, 1957), page 121; Plastics 141, 174, 207 (1956).
- [38] A.Ia. Drinberg, A.M. Bocharova and A.D. Iakovlev, Factory Labs. 8, 996 (1956).

Received April 15, 1957

Moscow Technological Institute of the
Light Industry

FRACTIONATION OF AMYLOSE ACCORDING TO THE DEGREE OF POLYMERIZATION

J. Hollo and J. Szejtli

As is known, the principal (carbohydrate) portion of starch consists of amylopectin and amylose. The amylopectin molecules are highly branched chains, approaching to the spherical in form, while amylose molecules have an unbranched or slightly branched chain structure. Both components are considerably heterodisperse. For complete characterization of heterodisperse substances it is necessary to have their molecular weight distribution (dispersion) curves or to know their dispersity limits. For example, in order to obtain definite physical properties for a given average molecular weight, the relative proportions of fractions of high and low molecular weight in a substance are not without significance.

A knowledge of the molecular weight distribution of a substance is of great importance in studies of degradation and its mechanism, in comparison of the values of molecular weight found by different methods, and in determinations of the mechanical properties of materials [1]. The molecular weight distribution curve of a substance is usually determined as follows: the substance is separated into fractions, the average molecular weights of the separate fractions are found, and the molecular weights of the fractions are plotted against the amounts of them present. The preparation of standard samples with narrower limits of molecular weight is also carried out by the fractionation method.

This paper deals with the fractionation of amylose. In determinations of the degree of polymerization from the intrinsic viscosity, and in other instances when the molecular weight must be determined accurately, it is necessary to obtain fractions with the narrowest possible molecular weight limits. Fractionation is especially important because films of excellent quality can be made from amylose [2] and its derivatives [3]. If an economical method for the production of amylose could be found [2], such films could be used industrially. Several workers have studied this problem recently [4, 5, 6]. Since all the properties of amylose films are determined by the average degree of polymerization and the molecular weight distribution, the development of relatively simple methods for the determination of these characteristics is an important problem. There are several methods for the fractionation of amylose.

1. Meyer's method [7] is based on the separation of amylose, at the preparation stage, into two fractions of different solubility in water. However, this method is not suitable for the purposes discussed above.

2. Kerr's method [8, 9] is as follows. Diethyl ether is added to a solution of amylose in ethylenediamine until two liquid phases are formed. The upper phase contains amylose fractions of lower degrees of polymerization. Ether is added in such a manner that the weights of the individual fractions are approximately equal. The upper phase is separated from the lower. Excess of diethyl ether, causing separation of amylose, is then added to the upper phase.

3. The method of Lansky, Kooi and Schoch [10]. To 10 liters of 1% amylose solution warmed to 80-85°, 1.5 ml of normal octyl alcohol is added. The mixture is cooled with continuous stirring, and the precipitated fraction is extracted by centrifugation. The solution is warmed again; after addition of octyl alcohol it is again cooled with continuous stirring, and the next fraction is extracted from it. This process is repeated until the required number of fractions has been obtained. Among the defects of this method are its lengthiness and the possibility of contamination of the fractions as the result of the retrogradation which takes place simultaneously.

4. Other methods. Mention should be made of Jirgensons' titration-precipitation method [11]. The prin-

inciple of the method is that the solubility of a substance in a given solvent depends on the molecular chain length. Jirgensons found that the concentration of the cooling agent required for separation of a given fraction is a linear function of the reciprocal molecular weight of the fraction. Fractionation can also be effected by solution of a nitrated or acetylated polysaccharide in a nonpolar solvent with subsequent precipitation of the separate fractions by addition of a polar solvent. Only this last method can be used for cellulose [1].

We developed a method for the fractionation of amylose, based on the formation of an amylose-iodine complex.

The amylose-iodine complex. Of the components of starch, only amylose is colored blue by the action of iodine. Amylose molecules in aqueous solution are coiled in the form of deformed spirals [12], with iodine molecules contained in the individual turns. The arrangement of the spirals depends on the degree of saturation with iodine. When the saturation is complete, a complex is formed in which the spiral molecules of amylose form turns each consisting of six glucose rings, with the iodine molecules arranged singly in the planes of the individual turns. The iodine molecules contained in the turns are acted upon by two different forces: on the one hand, the iodine molecule forms hydrogen bonds with the secondary trans hydroxyl groups of its surrounding glucose rings, and on the other, a polyiodine resonance chain is formed along the axis of the amylose helix. The dipole moments of the individual members of this chain are additive, and therefore its stability is a function of the number of members [14]. The amylose-iodine complex is in equilibrium with the free iodine present in solution. The longer the amylose helix, the lower will be the equilibrium iodine concentration at which it can absorb iodine. It follows from this relationship between the equilibrium iodine concentration and the degree of polymerization of amylose, and from the reversible nature of the equilibrium that when iodine is added to amylose solution it is first absorbed by molecules of higher degrees of polymerization. This is confirmed by conductometric and potentiometric titration data.

The amylose-iodine complex is an unstable colloid which separates out of solution under the action of electrolytes. We used this fact for the fractionation of amylose.

Fractionation of amylose by formation of its complexes with iodine. The principle of the proposed fractionation method is based on the fact that amylose-iodine complexes are not formed simultaneously with amylose molecules of different degrees of polymerization. When iodine solution is added to a solution of amylose, complexes are first formed with the molecules of the highest degree of polymerization; molecules of lower degree of polymerization do not react with iodine until the saturation of the former is complete. If an electrolyte is present in the solution, the complex formed separates out immediately.

The fractionation was performed as follows.* 60 g of a complex of moist potato starch with butanol, containing 4.16% dry solids, was dissolved in 1100 ml of distilled water. The solution was evaporated down to 1000 ml under vacuum, butanol being removed in the process. 20 g of NaCl was added to the cooled solution, followed by 5 ml of 0.1 N I₂ solution in small portions with stirring. The solution was stirred for ten minutes and then centrifuged. The precipitate was the first fraction. To the clear solution 5 ml of 0.1 N I₂ solution was added again, the solution was stirred and centrifuged, and the second, third, fourth, and fifth fractions were consecutively separated in a similar manner. After removal of the fifth fraction the blue color of the solution disappeared, and the solution became yellow on addition of excess iodine, indicating absence of amylose in the solution.

Before the subsequent treatment the fractions were kept in a refrigerator, no signs of retrogradation being observed. (According to our observations, the amylose-butanol complex can also be kept for several months at a low temperature without retrogradation.) The individual fractions were then treated as follows.

5 ml of 0.1 N Na₂S₂O₃ solution was added to each fraction. All the fractions dissolved on stirring, forming colorless opalescent solutions. These were filtered through G-3 glass filter crucibles. The filtered solutions were weighed. A 10 g sample was taken from each fraction for determinations of the carbohydrate content after hydrolysis by the Bertrand method. The amounts of amylose in each fraction and the concentrations of the solutions were found in this way. 2.5 ml was taken from the solution of each fraction. Each portion of 2.5 ml was introduced into an Ostwald capillary viscosimeter; 2.5 ml of 2 N KOH solution was added, the liquids were mixed,

* This method cannot be used for fractionation of starch solutions obtained by decomposition in an autoclave, as the amylopectin which is present in large amounts acts as a protective colloid and the iodine-amylose complex does not separate out in the pure state.

and the viscosity determined. To the 5 ml of solution in the viscosimeter a further 5 ml of 1 N KOH solution was added, the liquids were mixed, 5 ml of the mixture was removed by means of a pipet, and the viscosity of the 5 ml of solution remaining in the viscosimeter was determined.

This dilution and determination procedure was repeated 5 or 6 times, which gave the solution viscosity as a function of concentration. The intrinsic viscosity $[\eta]$ was found by extrapolation to zero of the plot of the logarithm of the specific viscosity against the concentration. The results obtained are given in the table, which also gives the approximate degree of polymerization of amylose in each fraction, calculated from the values of $[\eta]$ by means of the Potter and Hassid equation [15].

Characteristics of Potato Amylose Fractions

Serial number of fraction	Amount of solution, in g	Concentration of solution, in mg/g	Amount of fraction, in mg	Fraction as % of total	$[\eta]$	Degree of polymerization [15]
Original, unfractionated amylose	1000	2.49	2498	100.0	1.49	900
I	17.61	24.0	423	19.1	1.78	1070
II	19.64	22.60	444	20.0	1.54	930
III	19.31	23.30	450	20.2	1.41	850
IV	23.97	18.88	452	20.3	1.35	814
V	21.45	21.06	452	20.3	0.58	350
	Total		2221	99.9		

Wheat and maize amyloses were fractionated by a similar procedure. However, as these amyloses exhibit more rapid retrogradation than potato amylose under the same conditions, they must be treated within 1-2 minutes after being dissolved in thiosulfate solution.

It is also interesting to note that the narrower the fraction, the greater is its tendency to retrogression.

SUMMARY

1. Amylose in aqueous solution reacts with starch to form a complex compound which is in equilibrium with free iodine in the solution. The higher the molecular weight of the amylose, the lower is the equilibrium concentration at which iodine is absorbed.
2. Amylose is a heterodisperse substance. The formation of amylose-iodine complexes proceeds consecutively; iodine first combines with amylose molecules of the highest degree of polymerization, and then with molecules of lower degrees of polymerization as the iodine concentration is increased.
3. A simple method for the separation of amylose into fractions of different degrees of polymerization is proposed; the method is based on the above-mentioned consecutive formation of amylose-iodine complexes, and separation of the latter with the aid of electrolytes present during the formation.
4. This method was used to separate potato amylose with average degree of polymerization 900, into five fractions with different degrees of polymerization, from 1070 to 350. Wheat and maize amyloses were fractionated similarly.

LITERATURE CITED

- [1] E. Ott and H. Spurlin, *Cellulose and Cellulose Derivatives* 3 (New York, 1955).
- [2] I.A. Wolf et al., *Ind. Eng. Chem.* 43, 915 (1951).
- [3] I.A. Wolf et al., *Ind. Eng. Chem.* 43, 911 (1951).
- [4] P. Hiemstra, W.O. Bus and J.M. Mutgeert, *Die Stärke* 8, 235 (1956).

- [5] R.W. Kerr and W.J. Katzbeck, *Die Stärke* 5, 2 (1953).
- [6] T.J. Schoch, U.S. patents 2515095-6 (1950).
- [7] K.H. Meyer and H. Mark, *Makromolekulare Chemie* (Leipzig, 1950).
- [8] R.W. Kerr, *Chemistry and Industry of Starch* (New York, 1950).
- [9] R.W. Kerr, *J. Am. Chem. Soc.* 67, 2268 (1945).
- [10] S. Lansky, M. Kooi and T.J. Schoch, *J. Am. Chem. Soc.* 71, 4066 (1949).
- [11] B. Jirgensons, *J. Pr. Chem.* 159, 303 (1942); 160, 21, 65 (1942).
- [12] J. Hollo and J. Szejtli, *Zucker und Süßwarenwirtschaft* 10, 520 (1957).
- [13] J. Hollo and J. Szejtli, *Die Stärke*. In press (1958).
- [14] J. Hollo and J. Szejtli, *Periodica Polytechnica* 1, 223 (1957).
- [15] A.L. Potter and W.Z. Hassid, *J. Am. Chem. Soc.* 73, 593 (1951).

Received October 15, 1957

Technical University of Budapest
Chair of Agricultural Chemical Technology — Hungary

INFLUENCE OF ELECTROLYTES ON THE COAGULATION OF COLLOIDAL PARTICLES AT THE LIQUID-GAS INTERPHASE

R. V. Shveikina and S.G. Mokrushin

One of the authors of the present paper [1] used gelatin foam for the removal of colloidal substances from solutions. This method was used for extraction of colloidal particles of silver, gold, arsenic, antimony, mercury, antimony sulfide, and other sols. The method proved to be suitable for the separation of colloidally and molecularly dissolved substances. In particular, it was found to be possible to separate mixtures of ferric hydroxide, gold, silver, mercury, and antimony sulfide sols and true solutions of the sulfates of cobalt, copper, and nickel. On addition of gelatin to the solution, the colloidal particles became surface-active and passed spontaneously to the liquid-gas interface. Because of their high concentration on the bubble surfaces, the sensitized colloidal particles coagulated [2] and were removed from the solution with the foam.

In a study of the kinetics of the capture of colloidal particles by air bubbles, and of the influence of the amount of gelatin added, it was found [3] that there is a certain optimum amount of gelatin which gives the highest rate and degree of extraction. The degree of extraction decreases with an excess of gelatin.

The extraction process is also influenced by a number of other factors; in particular, electrolytes cause quite appreciable changes. The extraction process is closely associated with foaming, which also greatly depends on the presence of electrolytes. Reference must be made in this connection to investigations [4-6] in which it was shown that electrolytes increase the foaming of solutions by making the foams more stable.

The aim of the present investigation was to determine the influence of certain electrolytes on the kinetics of the extraction of colloids from solutions by means of gelatin foam. Hydrosols of antimonious sulfide, gold, and ferric and titanic hydroxides were used. 100 ml of the colloidal solution, with the electrolyte and 1% gelatin solution added, was placed in a vertical glass tube about 1 meter high and 40 mm in diameter, with a porous plate at the lower end. Air was blown through the solution at a constant pressure of 100 mm Hg. The foam which was formed removed the colloidal particles adsorbed on the bubbles. The degree of extraction was determined at equal time intervals by means of a photoelectric colorimeter.

In the experiments with antimonious sulfide and gold sols, which have negatively charged particles, solutions of the following salts were used as the electrolytes: KNO_3 , NaNO_3 , LiNO_3 , $\text{Ba}(\text{NO}_3)_2$, $\text{Sr}(\text{NO}_3)_2$, $\text{Ca}(\text{NO}_3)_2$, $\text{Al}(\text{NO}_3)_3$, $\text{Th}(\text{NO}_3)_4$, $\text{Zr}(\text{NO}_3)_4$.

The results of the experiments are given in Figure 1; it is seen that the degree of extraction of the disperse phase of a hydrosol increases in presence of electrolytes. The extraction is greater in presence of salts with bivalent cations than of salts with univalent cations.

It might be expected that the positive influence of cations on the extraction process should increase with increasing valence of the cation, as is the case in coagulation. The experiments showed, however, that the effects of tri- and quadrivalent ions are different from those expected (Figure 1). For example, the degree of extraction in presence of $\text{Al}(\text{NO}_3)_3$ is less than in presence of bivalent ions, while with thorium or zirconium salts the degree of extraction is even less than it is in absence of electrolytes. The acceleration of the extraction of the disperse phase from hydrosols may be attributed to growth of the colloidal particles under the influence of electrolytes, which lower the zeta potential of the particles. However, growth of the particles accelerates the extraction only up to a certain limit.

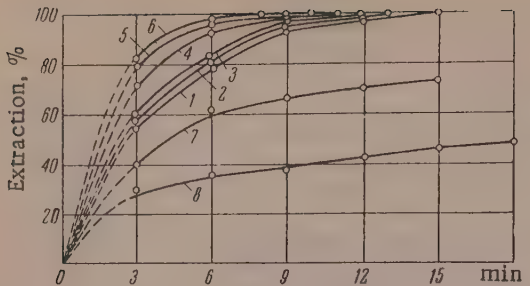


Fig. 1. Kinetics of extraction of 0.0025% Sb₂S₃: 1) without electrolyte; containing 1 millimole of: 2) KNO₃; 3) LiNO₃; 4) Al(NO₃)₃; 5) Ca(NO₃)₂; Ba(NO₃)₂; 6) Sr(NO₃)₂; 7) Th(NO₃)₄; 8) Zr(NO₃)₄.

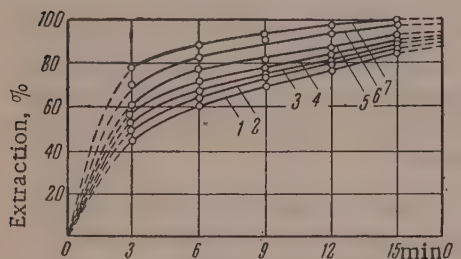


Fig. 2. Effects of electrolyte concentrations on the kinetics of extraction of 0.005% Sb₂S₃: 1) without electrolyte; containing the following electrolytes (in millimolar concentrations): 2) 0.5 of KNO₃; 3) 2 of KNO₃; 4) 5 of KNO₃; 5) 0.2 of Ca(NO₃)₂; 6) 0.5 of Ca(NO₃)₂; 7) 1 of Ca(NO₃)₂.

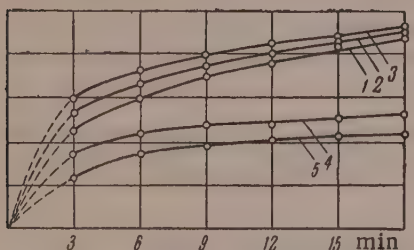


Fig. 3. Effects of electrolyte concentrations on the kinetics of extraction of 0.005% Sb₂S₃: 1) without electrolyte; containing the following electrolytes (in millimolar concentrations): 2) 0.01 of Al(NO₃)₃; 3) 0.1 of Al(NO₃)₃; 4) 0.01 of Th(NO₃)₄; 5) 0.1 of Th(NO₃)₄.

of extraction of the colloids, K₂SO₄ being the more effective (Figure 4). At low concentrations (0.01 millimolar), K₃[Fe(CN)₆], a salt with a trivalent anion, had a somewhat stronger effect than K₂SO₄ on the extraction process. However, the degree of extraction fell appreciably when the concentration of this salt was increased 10-fold (Figure 4).

It was found in the experiments that when visible coagulation occurs with fairly large colloidal aggregates present, the degree of extraction decreases because transfer of the large particles to the liquid-gas interface becomes more difficult. This accounts for the decreasing effect produced by the following salts: Al(NO₃)₃; Th(NO₃)₄; Zr(NO₃)₄.

The influence of electrolytes on foaming must be noted. In the presence of most electrolytes foaming is intensified, the effect increasing with increasing electrolyte concentration. The foam becomes more finely cellular and abundant, and the height of the foam column increases. The salts of quadrivalent cations, Th(NO₃)₄ and Zr(NO₃)₄, have a specific action on gelatin, lowering its foaming power and the extraction of the colloid. This was confirmed by experiments with gelatin solutions containing added electrolytes. Similar results were obtained in experiments with gold hydrosols.

Ions of the same valence but differing in the degree of hydration have different effects on the foam extraction of colloids; Li⁺, Na⁺ and K⁺ were studied. The lithium ion proved to be the most effective (Figure 1); this ion has a smaller radius than the sodium or potassium ions, and is the most highly hydrated. This evidently accounts for the increase of the foaming power of gelatin produced by the Li⁺ ion, and for the associated acceleration of the extraction of the disperse phase. The bivalent ions Ca²⁺, Sr²⁺ and Ba²⁺ did not show any great differences in their influence on the kinetics of extraction. However, Sr²⁺ produces a somewhat greater effect than the others (Figure 1). This ion favors the formation of more stable and abundant foam [6].

Figure 2 shows that the extraction of the disperse phase increases with increasing concentrations of the added salts. The same is found with additions of Al(NO₃)₃, as is seen in Figure 3. However, Th(NO₃)₄ is an exception. The experiments showed that the degree of extraction in presence of this salt is lower at higher concentrations (Figure 3). This is probably associated with the influence of thorium ions on the foaming power of gelatin, which becomes very weak. On the other hand, the multivalent thorium ion can decrease the zeta potential of the colloidal particles considerably, and this leads to their excessive growth. As was stated above, this hinders extraction.

Hydrosols of Fe(OH)₃ and Ti(OH)₄, which have positively charged particles, were used in studies of the effects of salts with different anions. It was found that in this case also the effect depends on the valence of the ion. It was found that KCl and K₂SO₄ increase the degree

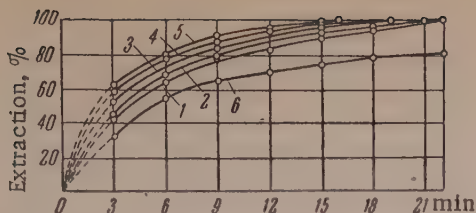


Fig. 4. Kinetics of extraction of $\text{Fe}(\text{OH})_3$: 1) without electrolyte; containing the following electrolytes (in millimolar concentrations): 2) 0.1 of KCl ; 3) 0.01 of K_2SO_4 ; 4) 0.01 of $\text{K}_3[\text{Fe}(\text{CN})_6]$; 5) 0.1 of K_2SO_4 ; 6) 0.1 of $\text{K}_3[\text{Fe}(\text{CN})_6]$.

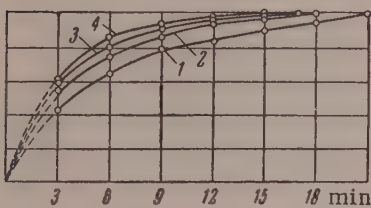


Fig. 5. Kinetics of extraction of $\text{Fe}(\text{OH})_3$ from solutions: 1) without electrolyte; containing: 2) KCl ; 3) KBr ; 4) KI .

The results of experiments on the influence of KI , KBr and KCl on the kinetics of extraction are given in Figure 5. The strongest effects were produced by KI and KBr . Similar results were obtained in experiments with $\text{Ti}(\text{OH})_4$ hydrosol. The ions can be arranged in the following sequence according to their effects on the degree of extraction of colloids: $\text{I}^- > \text{Br}^- > \text{Cl}^-$. It is possible that in this case the increase of the negative charge of the surface at the phase boundary in presence of these ions has an effect by facilitating the transfer of positively charged colloidal particles to the bubble surfaces, followed by surface coagulation. This is in agreement with Frumkin's paper [7], where it is stated that anions accumulate preferentially on surfaces of solutions, particularly the less hydrated ions, and the negative potential of the surface is accordingly increased in presence of halide anions in the following sequence: $\text{F}^- < \text{Cl}^- < \text{Br}^- < \text{I}^-$.

SUMMARY

1. The influence of certain electrolytes on the extraction of the disperse phase from colloidal solutions has been studied.
2. The influence of salts on the extraction process depends on the valence and the degree of hydration of their constituent ions.
3. The degree of extraction is associated with the aggregation of colloidal particles under the action of electrolytes and with the foaming power of gelatin.

LITERATURE CITED

- [1] S.G. Mokrushin, Bull. Mendeleev All-Union Chem. Soc. 2, 26 (1953).
- [2] N.F. Ermolenko and G.N. Plenina, Colloid J. 5, 193 (1939).
- [3] S.G. Mokrushin and K.G. Potaskuev, Colloid J. 18, No. 2, 215 (1956).*
- [4] P.A. Rebinder, The Physical Chemistry of Detergent Action (Food Industry Press, 1935), page 93.**
- [5] S.G. Mokrushin, V.I. Borisikhina and K.G. Potaskuev, J. Appl. Chem. 1, 107 (1955).*
- [6] A.M. Shkodin and L.D. Shaposhnikova, Trans. Chem. Sci. Res. Inst. State Univ. Kharkov 10 (1953); 11 (1954).
- [7] A.N. Frumkin, Z. Phys. Chem. 109, 34 (1924).

Received January 5, 1957

S.M. Kirov Polytechnic Institute of the
Urals — Sverdlovsk

*Original Russian pagination. See C.B. translation.

**In Russian.

THE SITE OF POLYMERIZATION OF UNSATURATED COMPOUNDS IN SYSTEMS CONTAINING PROTECTIVE COLLOIDS

A.S. Shevliakov and K.S. Minsker

One of the widely used methods for polymerization of unsaturated compounds is polymerization in aqueous emulsions. The degree of dispersion and the properties of the polymers formed depend on the nature of the protective colloid used. The mechanism of polymerization in presence of substances of the soap type has been studied in a number of investigations [1-5] from which it follows that the elementary processes: chain initiation propagation, transfer, and termination, may take place in different parts of the colloidal system - in a true solution of the monomer in water, in the emulsifier micelles, at the interphase boundary, within the monomer droplets, and on polymer particles.

The no less important method of polymerization in presence of protective colloids of the gelatin or polyvinyl alcohol type has not been studied sufficiently from this aspect [6], while it was concluded on general kinetic considerations that the process takes place within the droplets of the emulsion by a mechanism identical to that of block or bulk polymerization [7-10]; this method is therefore sometimes described as the microblock method. However, our experimental results obtained in a study of the polymerization process in presence of various emulsifiers and catalysts contradict this concept of the mechanism of microblock polymerization. It was found that in such cases the polymerization may occur both in the monomer droplets and in the aqueous solution of the monomer, and the site of polymerization evidently depends primarily on the nature of the monomer and catalyst and much less on the nature of the emulsifier.

The method consisted of the polymerization of monomers, colored with dyes insoluble in water, in presence of various catalysts and emulsifiers, followed by analysis of the polymer formed. It was presumed that if polymerization takes place in the monomer droplets the polymer should be colored, while if the reaction occurs in solution the polymer should be colorless. If the polymerization takes place in different parts of the system, the coloration of the polymer particles should vary.

2 kg of water containing the emulsifier, 0.5 kg of the monomer colored with 0.1 g of dye, and 0.03 molar % of catalyst was placed in an autoclave fitted with a stirrer and completely immersed in a thermostat. The polymerization temperature was 45° in all cases. Sudan Red was used as the dye; this is soluble in the monomer and insoluble in water. This dye is not affected by catalysis under the polymerization conditions used, it is almost insoluble in emulsifier solutions, and has little inhibiting effect on the polymerization process. The stability of the dye in presence of catalysts and its insolubility in emulsifier solutions was confirmed by special experiments in which the optical densities of the solutions were determined.

The effect of the solubility of the catalyst was studied in the polymerization of vinyl chloride (VC) in presence of gelatin and the following catalysts: potassium persulfate (PPS), azobisisobutyronitrile (ABN), and benzoyl peroxide (BP). PPS, which is insoluble in the monomer but soluble in water, gave a white, uncolored polymer with a small number of larger colored particles. The dye was displaced from the system to the surface of the aqueous phase. When ABN, which has limited solubility in water, was used, the polymer formed consisted of a mixture of colored and colorless particles. Investigation under the microscope revealed that about half the particles were bright red. A few single and aggregated particles had different degrees of coloring. With BP, which is insoluble in water, a colored polymer containing only rare white grains was obtained.

Both the colored and the colorless particles were roughly from 5 to 100 μ in size, and consisted of clumps

of closely adhering and even coalescing smaller particles of irregular rounded shape. The colored particles included a small number of transparent, apparently monolithic grains in which individual constituent particles could not be detected. All the uncolored white grains consisted of smaller particles. The intrinsic viscosity in cyclohexanone of the white grains isolated from the general mass was 0.9 poise; of the red grains, containing some white as an impurity, owing to the difficultly of separating them, 0.69 poise; and of the polymer as a whole, 0.74 poise. The viscosity of the colored polymer, corrected by extrapolation, should be about 0.6 poise.

The intrinsic viscosities of polymers obtained by bulk polymerization of colored and uncolored VC differed by 0.03, the absolute value being about 0.6 poise.

Experiments were carried out with the aid of an apparatus [1] consisting of two evacuated glass vessels connected at the top in order to establish the possibility of polymerization of the monomer in emulsifier solution without formation of an emulsion.* One vessel contained a filtered solution of the emulsifier, and the other, the monomer. The vessel was shaken in a thermostat; the monomer distilled over isothermally into the emulsifier solution and polymerized there. These conditions corresponded to polymerization in absence of monomer droplets [2].

The rate of polymer formation in 1% gelatin solution at 50° was 18 g/liter·hour with the water-soluble catalyst PPS, 16 g/liter·hour with the partially soluble ABN, and 0.5 g/liter·hour with the insoluble BP. Because of the negligible solubility of BP and the low solubility of ABN, the vessel with the emulsifier contained a reserve supply of the catalyst sewn in a cotton bag. At the end of the experiment the bag with BP increased in volume owing to formation of polymer on the catalyst crystals, while the emulsifier solution remained clear. When ABN and PPS were used, the polymer was in suspension in the aqueous phase.

The effect of the nature of the emulsifier was studied on solutions of photographic gelatin, polyvinyl alcohol, and the so-called MK emulsifier, which is a mixture of sodium salts of aliphatic sulfonic acids containing from 12 to 18 carbon atoms. The first two emulsifiers are typical for the production of polymers by the micro-block or suspension methods; the latter is one of the most powerful emulsifiers which gives latexes of a fairly high degree of dispersion.

The polymer obtained with the use of polyvinyl alcohol had larger particles, and contained somewhat more completely colored particles, than the polymer obtained in presence of gelatin. Polymerization in presence of MK with PPS catalyst yielded an entirely uncolored highly disperse polymer, while the dye was displaced from the system to the surface of the aqueous phase. A small amount of dye crystals remained in the polymer, but the dye was easily removed by washing the polymer with a solvent, in contrast to the colored polymer grains, which remained unchanged when so washed.

The emulsifier concentration was varied between 0 and 2% in the polymerization of vinyl chloride with ABN and PPS. Polymerization with ABN in absence of emulsifier gave lumps of colored polymer floating in transparent water; it contained very occasional white particles. The polymer obtained with PPS was very fine, pinkish in places, partially aggregated into fairly hard globules the size of peas. The pinkish regions were easily decolorized by treatment with solvent. The rate of polymerization differed little from the rate when emulsifiers were used.

In 0.5% gelatin solution with ABN an intensely colored polymer was formed, with a small number of colorless grains. In 1% solution more than half of the polymer consisted of colorless grains, which were all larger than the colored. The polymer formed in 2% gelatin solution was almost the same as this, but its dispersity was somewhat greater. With PPS, the polymer particles were small and only a small proportion of them was colored.

Different monomers, such as vinyl chloride, methyl methacrylate, and styrene, when polymerized under the same conditions, yielded polymers which differed in dispersity and the ratio of colored to uncolored particles. The dispersity of the colored and colorless grains of vinyl chloride polymer was of the same order. Methyl methacrylate polymer consisted of a large number of large colored particles, 3-4 times as large as the highly disperse white particles suspended in the aqueous phase. Polymerization of styrene gave a similar result.

DISCUSSION OF RESULTS

In all the experiments on the polymerization of intensely colored monomers varying amounts of completely

* The determinations were performed by B.F. Teplov.

colorless polymers were obtained, both by latex and by microblock polymerization.

The results of experiments on polymerization with different catalysts and emulsifiers are given in the table; it is seen that the ratio of colored to colorless particles is primarily determined by the nature of the catalyst. The greater the solubility of the catalyst in water, the larger is the amount of uncolored polymer formed.

A similar relationship between the solubility of the catalyst and the ratio of the colored to colorless polymer formed was found in the polymerization of methyl methacrylate and of styrene.

The formation of a considerable amount of colorless polymer from a colored monomer in coarse emulsions in presence of partially water-soluble catalysts is evidence of the important part played by the mechanism of polymerization in solution, and refutes the earlier view that the reaction proceeds in microblocks only. If the catalyst is insoluble in the monomer and readily soluble in water, the reaction proceeds exclusively in solution and a colorless polymer is obtained, the dye being displaced from the system. It is hard to believe that in this case chain initiation and growth occur at the phase boundary, as with such close contact between the polymer molecules and the droplets of colored monomer the polymer would inevitably retain some colored monomer and would itself be colored.

Polymerization of the monomer in solution also easily accounts for the long-known fact that most of the polymer particles formed are considerably smaller than the emulsion droplets.

Influence of the Nature of the Catalyst on the Ratio of Colored to Uncolored Particles in the Polymerization of Vinyl Chloride in Presence of Various Emulsifiers

Emulsifier	Appearance of polymers obtained in presence of different catalysts (BP, ABN, PPS)		
	BP	ABN	PPS
1% gelatin	All particles brightly colored; very few white particles; particle size 5-100 μ	Colored particles, ~40%; white, ~60%; white particles somewhat larger than red; particle size 5-100 μ	All polymer white; a small number of large colored particles; small particles <5 μ
1% polyvinyl alcohol	Same	Same, somewhat larger particles	
2% MK	All grains colored, but color less intense; a few large white grains; dispersity as of latex	—	All the polymer white and highly disperse
Without emulsifier	—	All the polymer colored; a few white inclusions	All the polymer white, fine, partially aggregated into peas

A comparison of the polymerization rates in emulsifier solutions without formation of emulsions, with vapor-phase feeding of the system, and in emulsions without emulsifiers gave values of the same order as the rate of ordinary microblock polymerization. The determining factor in polymerization in aqueous solutions is probably the rate of polymer formation. The monomer concentration should be restored much more rapidly in solution, as only in this case can the rates of polymerization in emulsions, in aqueous solutions without emulsifier, and with vapor-phase feeding of the monomer be approximately the same.

In emulsion polymerization the monomer can pass from the droplets into micellar or molecular solution both through the vapor phase which is always present over the emulsion, and by a mechanism analogous to isothermal distillation in the liquid [11]. As was shown above, the rate of these processes is evidently greater than the rate of polymer formation. Since the rate of polymerization in molecular solutions (in emulsions made mechanically without the use of emulsion stabilizers) differs little from the rate of emulsion polymerization, it may be assumed that the role of polymerization of the monomer in true solution is quite important.

By separation of the polymer according to its formation mechanism (in microblocks or in solution) it was possible to evaluate each type separately. The considerable difference between the intrinsic viscosities of these

parts of the polymer confirms the nonuniform distribution of the inhibitors and other factors which determine chain termination. Under equal conditions this nonuniformity should affect the increase of the polymerization rate in solutions.

SUMMARY

1. The topochemistry of the polymerization of certain monomers in aqueous emulsions with different catalysts and emulsifiers was studied.
2. It is shown that in microblock polymerization (by the suspension method) the polymer is formed not only in the monomer droplets but also in solution.
3. The amount of monomer formed in solution depends primarily on the nature of the catalyst. If water-soluble catalysts are used, the polymer is formed predominantly in solution. In presence of catalysts soluble in the monomer and water, the amount of polymer formed in solution depends on the solubility of the catalyst.
4. By polymerization of monomers containing dyes, it is possible to separate the polymer according to the site of its formation in the system.
5. The important role played by polymerization of monomers in true aqueous solution is demonstrated.

LITERATURE CITED

- [1] A.P. Sheinker and S.S. Medvedev, Proc. Acad. Sci. USSR 97, 111 (1954); J. Phys. Chem. 29, 250 (1955).
- [2] E.V. Zabolotskaia, I.G. Soboleva, N.V. Makletsova and S.S. Medvedev, Colloid J. 18, 420 (1956).*
- [3] Fikentscher, Ang. Chem. 51, 433 (1938).
- [4] Hohenstein, Siggia and Mark, India Rubber J. 111, 173 (1944).
- [5] N.P. Khomikovskii, E.V. Zabolotskaia and S.S. Medvedev, in the book: Investigations of High-Molecular Compounds** (Izd. AN SSSR, 1949).
- [6] B.N. Rutowskii, G.S. Goncharov and Ia.G. Muravin, Trans. MIKhM 1 (9), 36 (1950).
- [7] Aelion and Hohenstein, Ind. Plast. Mod. 1, 30 (1949).
- [8] G.V. Tkachenko, Collected Papers on Polymerization (Bureau of Technical Information, Ministry of Chemical Industry, 1953).
- [9] E.I. Barg, Technology of Synthetic Plastics (Goskhimizdat, 1954).**
- [10] A. Ward and W. Roberts, in the book: Monomers [Russian translation] Vol. 2 (IL, Moscow, 1953).
- [11] A.A. Ravdel' and L.Ia. Kremnev, Colloid J. 16, 17 (1954)*; Proc. Acad. Sci. USSR 90, 599 (1953).

Received February 4, 1957

Dzerzhinsk

*Original Russian pagination. See C.B. translation.

**In Russian.

THE ADSORPTION OF SIMILARLY CHARGED IONS IN THE COAGULATION OF SOLS BY ELECTROLYTES

1. RADIOMETRIC MEASUREMENTS

A.M. Shkodin and L.D. Shaposhnikova

There is no agreement concerning the nature of the adsorption of electrolytes by Fe_2O_3 , Al_2O_3 and other sols during their coagulation. Kargin and his associates [1, 2] concluded that the adsorption of electrolytes is molecular in character. Krestinskaia and Khakimov [3, 4] hold the opposite view. According to their data, the micelles of Fe_2O_3 , Al_2O_3 and SiO_2 sols adsorb ions of opposite charge only; ions of the same sign are not adsorbed. Glazman, Strazhesko and Tartakovskaya [5, 6] used a tracer atom method to establish in contradiction to published data [7] that sols of As_2S_3 , HgS , AgI , V_2O_5 , and MnO_2 adsorb only negligible amounts (1-2 micro-moles per g of disperse phase) of similarly charged ions when coagulated with solutions of NaH_2 , P^{32}O_4 and $\text{K}_2\text{S}^{35}\text{O}_4$.

We were interested in this question in connection with a study of the effects of the nature of electrolytes on the foaming of ferric, aluminum and chromium hydroxide sols. It had been shown [8-10] that in presence of certain electrolytes (for example, the acetates of copper, lead, zinc, or cobalt) abundant and stable foams are formed by sols of Fe(OH)_3 , Al(OH)_3 and Cr(OH)_3 . In these cases a surface film is formed very rapidly on the solution-air interface. The processes of foaming and film formation are associated with coagulation of the sols [9, 11], and the optimum foaming conditions precede visible coagulation. Both according to our data and to the results of others [12], anions as well as cations influence the foaming of sols.

Al(OH)_3 sol prepared from aluminum chloride by Vasil'ev and Rabinovich's method was used for the investigation. The sol was dialyzed until free from chloride ions. The coagulating electrolyte was zinc acetate tagged with radioactive zinc isotope. We determined the adsorption of the similarly charged ion in the surface film formed at the sol-air boundary, and not in the coagulation product as was done by other authors. This film, as was stated above, is formed almost instantaneously in presence of certain metal acetates, and can be easily transferred to a glass or metal plate [8-11], as was done by Blodgett, Langmuir and Schaefer in their investigations of fatty acid and protein monolayers. In our opinion, experiments with films are more definite than experiments with coagulant. For a number of reasons it would be interesting to use copper acetate as the coagulant, but the half life of Cu^{64} is so short (12.8 hours) that this salt could not be used in our experiments. The Zn^{65} isotope with a half life of 250 days is more convenient from this point of view, and it was therefore used in our experiments.

The experiments were performed as follows: a mixture of 10 ml of aluminum hydroxide sol (the sol concentration was 0.876 g Al_2O_3 per liter) and 20 ml of 0.2 N zinc acetate solution was put into a Petri dish. The film which was formed was transferred to a thoroughly polished glass plate by flatwise contact ("immersion") of the plate with the surface of the solution. The plate was fitted with a glass holder. After the application of each monolayer the film on the glass plate was washed with distilled water. The volume of water was determined by preliminary experiments with tests for absence of radioactive zinc in the last portions of the wash water. The plate with the film was then dried to an air-dry state at room temperature. After the drying, the next monolayer was applied, and the film was washed and dried again. The operation was repeated 130 times.

The adhesion of the film to the glass plate is shown clearly by changes of the interference colors and by the increase in the weight of the plate. The increase in weight after 130 immersions was 0.96 mg (a microbalance was used for the weighing).

The activity of the zinc present in this amount of film was 176 pulses/minute. For determination of the specific activity of the original zinc acetate solution tagged with the radioactive isotope, two drops (0.118 ml) of the solution were placed on the plate. This volume contained 1.543 mg of zinc, the activity of which was 20,670 pulses/minute, i.e., the specific activity of the original solution was 175,170 pulses/minute per ml.

The amount of zinc in 0.96 mg of film was calculated from these data; this was 0.0131 mg or 1.4% on the weight of the film, or 42 meq per 100 g of dry film. This is of the same order as the value found by Dmitrenko, Kargin and Riabinina [1] in the molecular adsorption of silver nitrate by ferric oxide gel.

It might be suggested that zinc is adsorbed on the glass. However, in our experiments adsorption on glass was possible only in the first immersion of the plate in the sol and zinc acetate solution. In subsequent immersions adsorption of glass is impossible, as the glass surface is already covered with a film of aluminum hydroxide. Nevertheless, we tested for the adsorption of zinc on the glass. A glass plate was immersed in a solution of zinc acetate without sol, washed with 50 ml of water, and dried. No activity was detected on the plate after the first immersion, and the activity was only 30 pulses/minute after 130 immersions. This is only double the background activity, indicating that the adsorption of zinc on glass is negligible if the contact between the glass and the solution is brief. The experiments were carried out at a pH value which excluded the formation of zinc hydroxide (the zinc acetate solution was acidified with acetic acid) and therefore insoluble $Zn(OH)_2$ could not be present in the film.

Analogous experiments were performed to study the adsorption of silver from silver acetate solution by ferric hydroxide sol prepared from $FeCl_3$. Radiometric determinations showed that up to 4-6% of silver, calculated on the film weight, was adsorbed. However, in this case silver chloride may be formed and enter the film.

We do not attribute our result to adsorption of similarly charged ions, i.e., of hydrated zinc ions. As has already been reported [8], in studies of the influence of electrolytes on the coagulation of sols (in this instance, on the formation of boundary films) it is necessary to take into account the form in which the ions of the coagulant electrolyte are present in the solution.

It is known [13], for example, that halides of zinc, cadmium, copper, and other metals are present in solutions not only as simple hydrated ions, but also as complex hydrated ions of the types MHy^+ , MHy_3^- , and MHy_4^{2-} . These metals form similar complex ions with acetate ions. For example, the existence of the following ions has been established [14] for copper: $[Cu(CH_3COO)(H_2O)_3]^+$; $[Cu(CH_3COO)_3H_2O]^-$; $[Cu(CH_3COO)_4]^{2-}$, and it was found that the most stable of these is $[Cu(CH_3COO)_4]^{2-}$, with an instability constant of $\approx 10^{-14}$. We therefore consider that in our experiments the positive $Al(OH)_3$ sol adsorbed zinc in the form of complex negatively charged ions: $[Zn(CH_3COO)_3H_2O]^-$ and $[Zn(CH_3COO)_4]^{2-}$.

In our opinion, Krestinskaya and Khakimov [4] failed to detect the adsorption of zinc in the coagulation of aluminum hydroxide sol by zinc sulfate not only because the method used was not precise enough, but also because the complex $[Zn(SO_4)_2]^{2-}$ ion, like the $[Ni(SO_4)_2]^{2-}$ and $[Co(SO_4)_2]^{2-}$ ions, is extremely unstable [15], its instability constant being $\approx 2-3 \cdot 10^{-2}$; i.e., dilute solutions are almost free of such complex ions.

The results of these experiments on the adsorption of zinc, and the available data on the formation of complex ions of copper, lead, zinc, cadmium, and mercury, of the type MeA_3^- , and especially MeA_4^{2-} , confirm our view [8] that the rapid formation of surface films and stable foams in mixtures of $Al(OH)_3$, $Fe(OH)_3$, $Cr(OH)_3$ sols and salts of these metals is the consequence of structure formation in the surface layers and the volume of the sols. A particularly important part in structure formation is played by the multivalent (the most stable) complex ions, which act as bridges between the micelles in the sols.

SUMMARY

1. A radiometric method was used to study the adsorption of zinc in the coagulation of positively charged aluminum hydroxide sols by zinc acetate. The zinc was determined in the films formed at the solution-air interface on addition of zinc acetate to aluminum hydroxide sols.

2. The films were found to contain 42 meq of zinc per 100 g of dry film. Adsorption of zinc by the sols is interpreted as the adsorption of complex negatively charged $[Zn(CH_3COO)_3H_2O]^-$ and $[Zn(CH_3COO)_4]^{2-}$ ions by the micelles of the positively charged $Al(OH)_3$ sols.

LITERATURE CITED

- [1] V.A. Kargin, P.S. Vasil'ev and O.I. Dmitrenko, *J. Phys. Chem.* 14, 12 (1940); V.A. Kargin and G.V. Klimovitskaia, *J. Phys. Chem.* 6, 467 (1938); V.A. Kargin, *Progr. Chem.* 8, 998 (1939); O.I. Dmitrenko, V.A. Kargin and A.A. Riabinina, *Colloid J.* 8, 3 (1951).
- [2] O.I. Dmitrenko and A.A. Riabinina, *Colloid J.* 15, 29 (1953).*
- [3] V.N. Krestinskaia and Z.V. Khakimov, *J. Gen. Chem.* 14, 70 (1944).
- [4] V.N. Krestinskaia and Z.V. Khakimov, *J. Gen. Chem.* 14, 129 (1944).
- [5] Iu.M. Glazman and D.N. Strazhesko, *Proc. Acad. Sci. USSR* 75, No. 3, 411 (1950).
- [6] Iu.M. Glazman, D.N. Strazhesko and B.E. Tartakovskaya, *Colloid J.* 15, 161 (1953).*
- [7] H.B. Weiser, *J. Phys. Chem.* 30, 20 (1926); S. Ghosh and N.R. Dhar, *J. Phys. Chem.* 31, 649 (1927).
- [8] A.M. Shkodin and L.D. Shaposhnikova, *Trans. Chem. Faculty, Kharkov Univ.* 10, 101 (1953).
- [9] A.M. Shkodin, L.D. Shaposhnikova and S.G. Teletov, *Trans. Chem. Faculty, Kharkov Univ.* 11, 33 (1953).
- [10] A.M. Shkodin and L.D. Shaposhnikova, *Trans. Chem. Faculty, Kharkov Univ.* 15, 9 (1956).
- [11] S.G. Mokrushin, *J. Gen. Chem.* 16, 11 (1946).
- [12] S.A. Durov, *Physicochemical Principles of Foam Entrainment in Boiler Water* (Izd. AN SSSR, Moscow-Leningrad, 1948)**; Ia.M. Nemirovskii, *Hydrochemical Materials* (Izd. AN SSSR, 1950).**
- [13] S.A. Shchukarev, L.S. Lisich and V.A. Latysheva, *J. Inorg. Chem.* 1, 225 (1956).
- [14] A.S. Tikhonov and L.A. Bashkirov, *Trans. Voronezh Univ.* 28, 40 (1953).
- [15] Ia.A. Fialkov and Z.A. Sheka, *J. Inorg. Chem.* 1, 1238 (1956); R.M. Flid and I.I. Moiseev, *J. Appl. Chem.* 27, 1144 (1954).*

Received March 1, 1957

A.M. Gorkii University, Kharkov

*Original Russian pagination. See C.B. translation.

**In Russian.

IVAN PLATONOVICH LOSEV

(ON HIS 80th BIRTHDAY)

Ivan Platonovich Losev was born January 16, 1878 in the hamlet of Frolov in the Ust'-Medveditskii district, in the family of a Cossack peasant. Losev's life took a peculiar course from his earliest days.

Having lost his father early (Losev was less than one year old when his father died), he grew up in the care of his mother, at whose wish he first entered a four-class theological school, and then the theological college of Novocherkassk. The revolutionary movement of the start of the century gripped the young student, and in 1901 Losev was expelled from the college for taking part in college disturbances. However, in 1904 he successfully passed his matriculation examinations at the Kazan Men's Gymnasium and entered the State University of Kazan.



However, two years later, in 1906, when on vacation in his home Ust'-Medveditskii district, Losev took part in the revolutionary movement and was legally prosecuted. In the same year, 1906, Losev was sent as a delegate

of the Kazan Committee of the RSDRP (Bolsheviks) to the First Tammerfors Conference of the Military and Battle Organizations of RSDRP (Bolsheviks). In 1910, when taking his State examinations, Losev was arrested and sentenced to imprisonment. His graduation therefore had to be postponed until 1914, when he was given permission to take the State examinations. After leaving the University, Losev began to teach chemistry and the science of staple commodities at the Kazan Commercial School. In 1919 Losev went to Moscow and began work as assistant to Prof. P.P. Shorygin at the Moscow Veterinary Institute, while from 1923 to the present day Prof. I.P. Losev has worked at the D.I. Mendeleev (Order of Lenin) Moscow Institute of Chemical Technology.

In 1932 he organized the first Department of Plastics at the Mendeleev Institute of Chemical Technology; this was joined by the most eminent specialists of the day — Professors G.S. Petrov, N.M. Nastyukov, B.N. Rutovskii, and I.A. Livshits. From the time when Losev took charge of the Department of Plastics, all his scientific interests have been associated with polymer chemistry and technology. His research on polymerization reactions characterizes Losev as a research specialist in the field of polymer synthesis. It includes work on the polymerization of vinyl chloride, the copolymerization of vinyl derivatives, the polymerization of vinyl ethers and derivatives of α -chloroacrylic acid, and the condensation of phenol and aniline with various aldehydes. These investigations showed that condensation resins are in reality complex mixtures or organic substances which are mutually soluble and similar in structure. Since 1943 the scientific interests of Prof. Losev have been associated with synthesis and investigation of polyurethanes, polyamides, polyureas, and cation-exchange resins.

Work in these directions became particularly intensive from 1948 when Prof. Losev, with his characteristic energy and enthusiasm, organized a new department in the Mendeleev Institute of Chemical Technology — the Department of Polymer Technology, and in 1957 he established a laboratory for ion-exchange resins.

Professor Losev, being a deep and purposeful research worker, never segregates the so-called pure science from applied science. In all his work the most abstract theoretical questions are always interwoven with very important technological problems. This is the reason for his close association with various specialized scientific research institutes.

Prof. Losev, who carries out extensive research work personally and with his associates, is a rare and remarkable teacher, a man of splendid nature. These remarkable qualities constantly attract young scientists of the Soviet Union and the People's Democracies to him.

The outstanding scientific work of Prof. Losev has been repeatedly recognized at the highest level. For example, the Presidium of the Supreme Soviet RSFSR awarded I.P. Losev the honorary title of Distinguished Worker in Science and Technology; in 1951 he was decorated with the Order of Lenin, and in 1957, with the Order of the Red Banner of Labor.

The scientific community of the Union has recognized the valuable activities of I.P. Losev by electing him in 1956 to be President of the D.I. Mendeleev All-Union Chemical Society.

On his glorious anniversary, let us wish him many years of life and beneficent scientific and social activity.

O.V. Smirnova

DISCUSSION

THE FLUIDITY AND STRENGTH OF STRUCTURIZED DISPERSE SYSTEMS

G.V. Vinogradov and V.P. Pavlov

During the past two years there has been a discussion in the press [1, 2] on a number of topical questions of modern rheology. This discussion, which reflects the various viewpoints existing within the framework of the Rebinder school, cannot be regarded as complete if it does not represent the opinions of specialists in other fields and if it does not take into account the experience obtained in investigations of systems different from those studied by Mikhailov and Trapeznikov. We must also participate in the discussion because Mikhailov and Trapeznikov made reference, in their polemical articles, to some individual data obtained by Klimov and Lebedev in our laboratory. Unfortunately, no account was taken of our fundamental investigations carried out during the last ten years; these results could be very useful in the analysis of many obscure rheological problems to which the discussion refers.

Mikhailov [1] bases his discussion on experiments with bitumens, which are highly viscous, weakly elastic, weakly structurized disperse systems. Trapeznikov [2] primarily makes use of the properties of low-viscosity, highly elastic, strongly structurized systems. The only common feature of these systems is that they are all liquids. In many respects they are not comparable; this was not given due consideration in the discussion.

The discussion is primarily concerned with the shear stress (τ) - deformation (γ) curves, which are determined by experiments in which the shear stress increases continuously (up to a definite value). These curves may ascend steadily or have maxima. The maximum on the $\tau(\gamma)$ curve for a plastic system was first interpreted as the flow limit (τ_f) or the yield value (τ_y) in papers published by our laboratory [3]. The concept of yield value was introduced instead of, or, more accurately, for more precise definition of, the term "limiting shear stress"; it generalized the concept of the yield value in relation to the resistance of materials and extended it to the breakdown of a three-dimensional structural framework formed by the disperse phase, which determines the complex combination of mechanical properties (elastic after-effects, etc.) of disperse systems.

In his examination of the $\tau(\gamma)$ curves, Mikhailov writes: "As our investigations showed, disruption of structure (orientation, bond rupture) takes place on the ascending branch of the curve . . . The descending branch of the curve . . . is the consequence of a purely relaxational process . . . and therefore does not contain any disruption factors" [1, page 75]. His evidence for this is the fact that ". . . when a repeat test is carried out on the same system at the same velocity gradient, the $\tau(\gamma)$ curve (our notation is used here and subsequently - V. and P.) was reproduced completely" [1, page 73]. We cannot agree with this statement or the evidence for it.

In 1947 Vinogradov and Klimov demonstrated for the first time in the USSR [4] the value of investigations of the mechanical properties of disperse systems by means of curves for γ as a function of t and constant τ ; they devoted special attention to a comparison of the $\tau(\gamma)$ and $\gamma(t)$ relationships and introduced the concept of rapid breakdown of the structural framework in disperse systems when $\tau = \tau_f$ [5]. It was shown that the transition of the yield value is accompanied or, rather, induced by this sudden breakdown of the structure in the system, when the processes of bond rupture between the particles of the disperse phase not only occur more rapidly than the processes of bond restoration, but they involve the bonds which determine the strength of the structural framework. In relation to the strength properties of the system, this rapid breakdown of the structure does not terminate, as Mikhailov asserts, but only starts when values of τ close to τ_y are reached, and it leads to a decrease of shear strength. After the yield value has been passed, the process of structural breakdown continues to develop in the system, and its restoration develops at an increasing rate. This last process is revealed very clearly by changes of the shear modulus (g) with increasing deformation, both when $\gamma < \gamma_f$ and when $\gamma > \gamma_f$.

This restoration of the structure primarily involves ranges of weak, relatively easily relaxing bonds, which do not confer rigidity to the structural framework and therefore do not influence its shear strength.

In cases in which particularly strong bonds in the structural framework are broken down irreversibly or are restored slowly, transition through the yield value results in a permanent or temporary decrease of τ_f . If there is no brittle destruction of the structure, and the bonds between the particles of the disperse phase are highly mobile (as is the case in the experiments with bitumens described by Mikhailov) the same results will be obtained in the first and subsequent determinations.

These general considerations of the behavior of disperse systems under deformation at a constant rate, or in tests with continuously increasing stress, may be supported by experimental data obtained with the aid of special methods developed in our laboratory, whereby it is possible to follow the variations of elastic and strength properties of structurized materials as functions of the deformation.

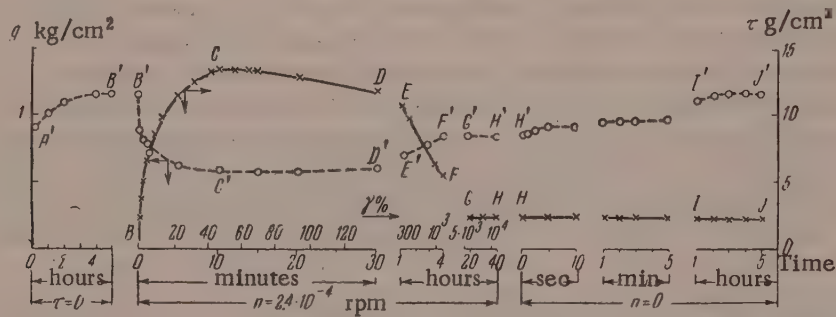


Fig. 1. Curves for the relationships between shear stress (continuous line) and shear modulus (dash line), and the deformation and time, for Solidol grease, determined by means of a rigid dynamometer.

Let us consider the nature of one of these methods, as used for the investigation of plastic greases. The Solidol grease described previously [6] was fed at 20° into the annular gap of an instrument with rifled surfaces [7], and values of g were then measured periodically under static conditions in an apparatus with a rigid dynamometer [8], the modulus of which was $4.9 \cdot 10^5 \text{ g} \cdot \text{cm} \cdot \text{radian}^{-1}$, until constant values were obtained after restoration of the structure, broken down to some extent when the instrument was being filled. The inner cylinder of the elastoviscosimeter (the heterogeneity of the stress field in the gap was 6%) was then rotated at $n = 2.4 \cdot 10^{-4}$ rpm, and g was again determined at intervals under continuous deformation while τ increased to τ_f and then fell to τ_{st} (Curve BC...H in Figure 1). After 40 hours the core of the instrument was stopped, and the determinations of g were continued for a long time with the specimen still under stress, i.e., with simultaneous relaxation and thixotropic restoration of its structure. The variations of g during this cycle of tests are represented in Figure 1 by the line A'B'...I'.

In this example, the value of g began to decrease rapidly from the very start of the deformation, which resulted in increases of τ and γ in accordance with the Curve BC...H; after 10 minutes the value of g fell to a half of its initial value, and reached a minimum at $\tau = \tau_f$ (Point C'). Subsequently, despite the fact that the same rotation rate was maintained, g began to increase slowly, and after 4 hours it reached a stable value (Point F) which remained unchanged during the subsequent 36 hours. In other words, the breakdown of the bonds of the structural framework which determine the elastic properties of plastic bodies does, in fact, occur along the ascending branch of the $\tau(\gamma)$ curve, and is completed when τ_f is reached.

An examination of the results obtained in tests of the same Solidol sample by another method leads to a different conclusion. The conditions corresponding to Figure 1 were retained in these experiments. The Curve OA...G (Figure 2), which represents the $\tau(\gamma)$ relationship for Solidol at 20° was first obtained. A fresh portion of the sample was then taken to a certain value τ_A (Point A on the Curve OA...G), the stress was then removed from the sample (indicated by the dash line and arrow at Point A), and the experiment was repeated. In this and similar tests the time interval between the applications of the load was about 5 minutes. In this repeated experiment the values of τ and γ were again read off from the Point O, and the $\tau(\gamma)$ curve coincided with the

Curve OA...G. A fresh (third) portion of Solidol was tested up to $\tau = \tau_B$, when the load was removed and the test was repeated. The $\tau(\gamma)$ relationship in this test is again represented by the Curve OA...G. Thus it was shown that at $\tau < \tau_f$ not only is there no decrease in the shear strength of plastic bodies, but that even the form of the $\tau(\gamma)$ curve remains unchanged. Deformation of a fresh portion of Solidol to $\gamma = \gamma_C = \gamma_f$, removal of the load, and a repeated loading yielded the Curve O₁C...G; examination of this curve shows that preliminary deformation of the sample to $\gamma = \gamma_f$ does not decrease the value of τ , but after this τ_f is attained more rapidly in the repeated test (6 minutes instead of 10) or, which is the same thing, the value of γ_f is smaller.

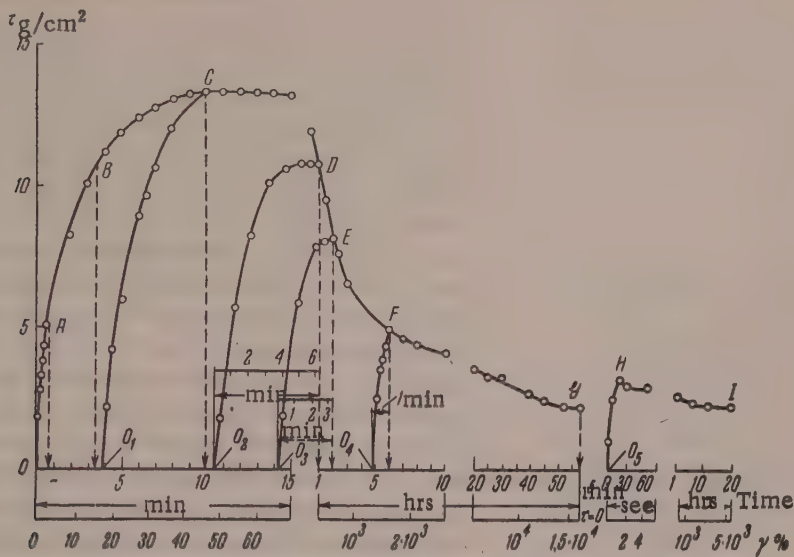


Fig. 2. Curves for the relationships between the shear stress and the time and deformation, for Solidol grease, determined by means of a rigid dynamometer.

Successive experiments were then performed, with a fresh portion of Solidol each time, up to deformations γ_D , γ_E , γ_F , and the method described above was used to obtain the corresponding Curves O₂DEFG, O₃EFG, O₄FG. The time intervals in which the maximum values of τ were reached on these curves are shown on separate scales. It follows from these experiments that breakdown of the structure of pseudogels, accompanied by a decrease of their shear strength, occurs only when $\gamma > \gamma_f$, and the relationship between the yield values and γ is represented accurately by the region CDEFG of the $\tau(\gamma)$ curve. In fact, if the preliminary deformation represented by the section OABCD is stopped at a value of τ corresponding to the point D(τ_D), the subsequent loading is graphically represented by the Curve O₂DEFG with a well-defined maximum at the point D, or, in other words, at $\tau = \tau_D$. The yield values determined similarly after γ_E and γ_F had been reached were equal to τ_E and τ_F respectively, i.e., to the values of τ reached in the preliminary test. This last conclusion is fully valid for the section of the right-hand branch of the Curve OA...G, where τ is close to or equal to τ_{st} , provided that the interval between removal of the stress and the start of application of the new load does not exceed a few seconds. Otherwise thixotropic buildup of the structure of the pseudogels results in considerable strength increase. For example, in the case of Solidol, 5 minutes of rest after removal of the load (Point G) was enough to give the Curve O₅HI with a quite distinct maximum in the subsequent test.

If we accept Mikhailov's viewpoint and assume that "... the descending branch of the curve ... is the consequence of a purely relaxational process ... and therefore does not contain any disruption factors," then the values of τ_D , τ_E , τ_F obtained in these experiments should be exactly the same and equal to τ_G (or to τ_{st} for weakly thixotropic systems), which was not the case for any of the greases.

Thus, it has been demonstrated by direct experiments that the structure of a plastic body breaks down, or, more accurately, the rate of its breakdown exceeds the rate of buildup, from the start of the experiment until a steady value of τ is reached. When $\tau \leq \tau_f$ the bonds which determine the elastic properties are broken down

more rapidly than they are restored, while the bonds determining the shear strength of the system remain unchanged. At $\tau = \tau_f$ the observable breakdown of the former is completed and that of the latter only just commences, and therefore the strength of a plastic body, which does not decrease up to γ_f , decreases on further deformation from τ_f to τ_{st} , while the $\tau_f(\gamma)$ and $\tau(\gamma)$ relationships remain unchanged.

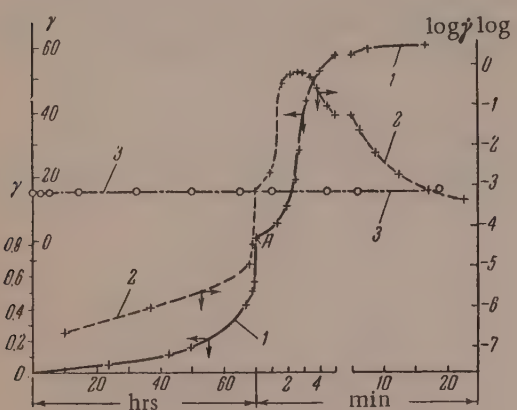


Fig. 3. Curves for the deformation (1) and deformation rate (2) of Solidol as functions of time, determined by tests by the method of continuously increasing deformations. Curve (3) represents the deformation rate as a function of time determined under the same conditions by means of a rigid dynamometer.

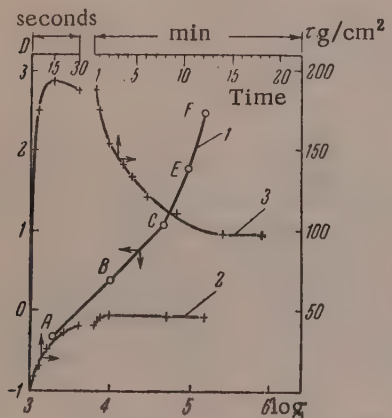


Fig. 4. Curves for the deformation rate as a function of the shear stress (1) and shear stress as a function of time (2, 3) for polyisobutylene, determined with continuously increasing stresses.

curve. It is obvious that the highest rate of deformation cannot correspond to absence of structural breakdown. It follows from Lebedev's experiments, that, in general, Mikhailov's assertion that "... the maximum, the yield point τ_f is reached in a time which corresponds to the establishment of the given velocity gradient" [1, page 70] is wrong. This is shown most convincingly by the results of our experiments on such a typical plastic system as Solidol (Figure 3). The tests were performed in conditions corresponding to Figures 1 and 2, not only with a rigid but also with a flexible dynamometer, the modulus of the latter being $29 \text{ g} \cdot \text{cm} \cdot \text{radian}^{-1}$. In Figure 3 the ordinate axes give γ , the relative deformation in the annular gap of the elastoviscosimeter, and $\log \dot{\gamma}$, the

This conclusion clearly refutes Mikhailov's view that "... it is not correct to associate the absence or presence of a maximum on the $\tau(\gamma)$ curves with destruction of structure in the system" [1, page 70]. It is clear from the facts presented above that the presence of maxima on the $\tau(\gamma)$ curves is direct evidence that there is a certain critical state, at least for plastic systems, associated with breakdown of their structure. Even if the $\tau(\gamma)$ curves are without maxima it does not follow that there is no structural breakdown; this was demonstrated by Mikhailov himself [1, Figure 6], and it also follows from investigations performed in our laboratory. Klimov, Gvozdev and Lebedev [6-9] established experimentally for plastic systems which give curves with sharp maxima at room temperature that at lower temperatures these maxima are less pronounced or disappear entirely. There are no grounds for believing that the structural framework becomes weaker with decrease of temperature. As the result of the increase in the viscosity of the dispersion medium and of the system itself, the strength characteristics are merely masked by the high viscous resistance. For the same reason, when the experiments are repeated under continuously increasing load the decrease of τ_f and τ_{st} in consequence of the breakdown of structure is slight, i.e., the systems approach in their properties to non-Newtonian liquids of low thixotropy.

In general, therefore, absence of structural breakdown cannot be assumed from the absence of maxima on the $\tau(\gamma)$ curves, or even from the identity or close similarity of $\tau(\gamma)$ curves obtained in repeated experiments. Moreover, it must be remembered that for a plastic system with a highly viscous dispersion medium, especially at low temperatures, a fairly sharp maximum on the $\tau(\gamma)$ curve can be obtained only at very low rates of load, when the resistance to viscous flow is sharply decreased.

Mikhailov [1, page 74] considers that Lebedev's experiments [9] prove that the structure in plastic systems breaks down along the ascending branch of the $\tau(\gamma)$ curves. In reality, this is not correct, as Lebedev was the first to show [9] that for plastic disperse systems tested under continuously increasing stress the maximum deformation rate is reached on the descending branch of the $\tau(\gamma)$

logarithm of the deformation rate. The left-hand ordinate axis (Figure 3) carries two scales for γ . Deformations until τ_f is reached at the point A are shown below on the left. Values of γ found after the yield point has been reached are shown above on the right.

Figure 3 shows the transition from elastic deformation to rapid breakdown of the system, corresponding to the steep portions of the $\gamma(t)$ and $\dot{\gamma}(t)$ curves. The rapid increase of γ (when the yield point is passed) corresponds to an increase by nearly 5 tenth-powers in the deformation rate, and the maximum deformation rate is found, as in Lebedev's experiments [9, 10] with hydrocarbon systems, on the descending branch of the $\tau(\gamma)$ curve. In the light of this, it is not clear why Mikhailov [1, Figure 4b] finds no maximum on the $\dot{\gamma}(t)$ curve when such a maximum exists on the corresponding $\tau(\gamma)$ curve.

The data in Figure 3 indicate once again that the whole process of structural breakdown in plastic systems develops along the descending branch of the $\tau(\gamma)$ curves. At very low rotation speeds of the core, owing to the abrupt decrease of the deformation rate after the maximum on the $\tau(\gamma)$ curve has been reached, deformation of the system may cease [11]. Trapeznikov and Mikhailov missed the very important fact that the yield point (the maximum on the $\tau(\gamma)$ curves) can be detected immeasurably more sensitively by the increase of the deformation rate than by the increase of deformation.

The next question relates to the connection between the $\tau(\gamma)$ and $D(\tau)$ curves, where D is the velocity gradient. We studied the rheological properties of fluid low-molecular polyisobutylenes, synthesized by Iu.Ia. Gol'dfarb in the Institute of Petroleum, Academy of Sciences USSR. These are non-Newtonian liquids of very high viscosity and relatively small but quite distinct elasticity. Figure 4 shows the flow curve at 20° for polyisobutylene of average molecular weight ~5000. The points on Curve 1 correspond to values of τ_{st} found in experiments with continuously increasing shear stresses. In Figure 4 there are also given $\tau(\gamma)$ curves corresponding to the points C (Curve 2) and E (Curve 3) for the $D(\tau)$ relationship. It should be noted that the points A and B on Curve 1 correspond to $\tau(\gamma)$ curves without maxima, while point E corresponds to a $\tau(\gamma)$ curve with a maximum. It is clear from Figure 4 that the transition from a linear to a nonlinear relationship between D and τ is associated with the appearance of maxima on the $\tau(\gamma)$ curves; this supports Trapeznikov's views on this question. It is quite evident that for systems of different nature the sharpness of the transition from a linear to a curved region in the $D(\tau)$ curve, and the corresponding sharpness of the transition from steady $\tau(\gamma)$ curves with maxima may and should differ.

Mikhailov's statement that the deformation rate influences the form of the $\tau(\gamma)$ curves and the value of τ_f is trivial, and gives no ground for the assertion that "the concept of yield point τ_f will lose all meaning" [1, page 71]. On the contrary, the characteristics of the strength properties of disperse systems can best be evaluated from the nature of the relationship between τ_f and the deformation rate.

Trapeznikov writes that in the papers published by our laboratory ". . . the rigidity of the dynamometers was not stated, and all these investigations (to speak objectively) might also have been carried out with nonrigid dynamometers . . ." [2, page 496]. This was indeed the case. However, the investigations in our laboratory to which Trapeznikov refers dealt with plastic systems, for which it was found [2, 3] that the deformation rate has little effect on τ_f . It follows directly from this that the deformability of the dynamometer should not play any significant role in such cases. Therefore, Trapeznikov's reference to the work of our laboratory is unjustified. It has been shown recently in direct experiments with 10^5 -fold variations of dynamometer rigidity (including the use of an almost absolutely rigid dynamometer) [8, 14] that apart from its influence on the deformation rate the rigidity of the dynamometer used for testing plastic disperse systems has no appreciable influence on the value of τ_f or the form of the $\tau(\gamma)$ curves. The conclusions drawn by Klimov and Gvozdev in the papers cited above concerning the relatively small influence of the rate of loading on τ_f for plastic disperse systems were confirmed in experiments with approximately 10^8 -fold variations of the deformation rates.

In conclusion it must be pointed out that the elementary theory of deformation used in the papers under discussion is only applicable to systems in which elastic deformations are small, and cannot always be used for calculations of rheological processes in high-elastic bodies. Therefore the comparisons, made in the discussion, between the mechanical properties of systems exhibiting very large (aluminum naphthenate gels, etc.) and very small (bitumens, etc.) elastic deformation should be regarded with considerable caution.

LITERATURE CITED

- [1] N.V. Mikhailov, *Colloid J.* 17, 68 (1955).*
- [2] A.A. Trapeznikov, *Colloid J.* 18, 496 (1956).*
- [3] G.V. Vinogradov and K.I. Klimov, *Proc. Acad. Sci. USSR* 58, 1677 (1947).
- [4] G.V. Vinogradov and K.I. Klimov, *Proc. Acad. Sci. USSR* 57, 911 (1947).
- [5] G.V. Vinogradov and K.I. Klimov, *J. Tech. Phys. (USSR)* 18, 355 (1948).
- [6] G.V. Vinogradov and M.M. Gvozdev, *Proc. Acad. Sci. USSR* 86, 341 (1952); G.V. Vinogradov and K.I. Klimov, *Proc. Acad. Sci. USSR* 71, 307 (1950).
- [7] V.P. Pavlov, in the book: "Annotations of Papers on the Chemistry and Technology of Petroleum and Gas, 1956" (Institute of Petroleum, Academy of Sciences USSR, 1957), page 69.**
- [8] V.P. Pavlov and G.V. Vinogradov, *Proc. Acad. Sci. USSR* 114, 997 (1957).*
- [9] V.G. Lebedev, "Investigation of the Mechanical Properties of Paraffinic Oils" Dissertation (Moscow, 1954).**
- [10] G.V. Vinogradov, V.G. Lebedev and V.A. Protod'jakonov, *Colloid J.* 18, 633 (1956).*
- [11] V.P. Pavlov and G.V. Vinogradov, *Proc. Acad. Sci. USSR* (in press).
- [12] K.I. Klimov, "Elasticoplastic Properties of Lubricant Greases," Dissertation (Moscow, 1950).**
- [13] M.M. Gvozdev, "Elasticoplastic Properties and Behavior of Lubricant Greases in Roller Bearings" Dissertation (Moscow, 1952).**
- [14] V.P. Pavlov and G.V. Vinogradov, *J. Tech. Phys. (USSR)* (in press).

Received July 12, 1957

Moscow

*Original Russian pagination. See C.B. translation.

**In Russian.

BRIEF COMMUNICATIONS

INFLUENCE OF THE RATIO OF FREE TO BOUND ALKALI IN THE PRECIPITATION OF ALUMINUM SOAPS ON THEIR THICKENING PROPERTIES

A.A. Trapeznikov, G.V. Belugina and F.M. Rzhavskaya

The composition and thickening properties of Al soaps are determined by the molecular weight and the nature of the organic radical of the acid on the one hand, and by the formulation and the conditions for the preparation of the soap on the other. For example, by variations of the pH of the medium in precipitation, of the temperature, of the concentrations of the reactants, and of other factors, it is possible to obtain Al soaps differing greatly in composition and in thickening effects on organic solvents [1]. A specially important factor is the ratio of free to bound alkali in precipitation, which determines the "basicity" of the soap, i.e., the saturation of the aluminum valences with hydroxyl groups. It has been reported in papers on Al soaps of fatty acids that disubstituted soaps of the AlOHR_2 type have the highest thickening power [2, 3]. The formulation of such a soap

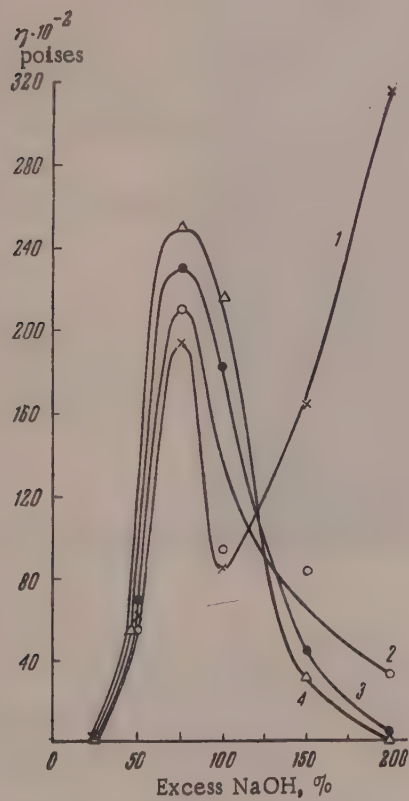


Fig. 1. Variations of the viscosity of oleogels with the excess of alkali in precipitation of the soap: 1) 3 days after preparation of the oleogel; 2) 7 days; 3) 30 days; 4) 60 days.

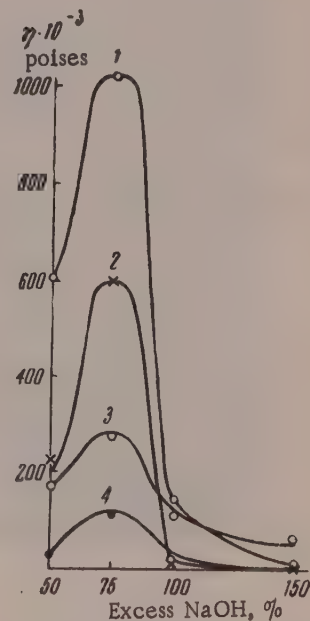


Fig. 2. Variations of the viscosity of oleogels with the excess of alkali in precipitation of soaps from naphthenic acids of different molecular weight: $M_{av} = 213.7$; gel concentration 5% (2); 6% (1); $M_{av} = 224.5$; gel concentration 5% (4); 6% (3).

may be characterized by an excess of free alkali relative to the bound alkali (i.e., the alkali consumed in neutralization of the acid); for a disubstituted soap this excess is 50% [1, 4]. It was of interest to determine whether this ratio is valid for Al soaps of naphthenic acids, since the nature of the organic acid radical has a considerable influence on the properties of the soaps. We therefore studied the properties of Al naphthenate soaps, obtained not only by precipitation with strictly stoichiometric proportions of acid to alkali, corresponding to mono-, di-, and trisubstituted soaps, but also with intermediate ratios, because in view of the complex nature of the whole process of soap formation the final product may contain more complex substances, and also hydrolysis products [Al(OH)₃, free acids].

The Al soaps were made by double decomposition (a method which we describe as "direct" precipitation [1, 4]) from naphthenic acids of average molecular weight $M_{Av} = 250$, at 80°, with between 25 and 200% of free alkali in the precipitation. Figure 1 shows the viscosity* of 6% gels of these soaps in cryoscopic benzene; the maximum corresponds to 75% of free alkali. This agrees with the value for the maximum thickening properties at 75%, found by A.A. Trapeznikov in 1942-1943; he also pointed out that this maximum represents a higher content of free alkali than that required for a disubstituted soap.

During the first few days after preparation of the oleogels, the oleogel made from soap precipitated with 200% excess alkali, corresponding to a monosubstituted soap, had the highest viscosity; this is probably because of the slow solubility of this soap in benzene, which decreases the fluidity of the gel; subsequently the viscosity of this gel fell rapidly with time. The oleogels of Al soaps precipitated with 25-75% free alkali showed almost no changes of viscosity and remained stable for a long time.

This relationship between the thickening properties and the free-bound alkali ratio was tested for Al soaps prepared from naphthenic acids with average molecular weights (M_{Av}) 213.7 and 224.5. Naphthenic acids with $M_{Av} = 224.5$ were isolated from naphthenate soaps obtained from kerosine distillates of petroleum. Further fractional distillation of these acids gave acids with $M_{Av} = 213.7$. The aluminum soaps were prepared by double decomposition under identical conditions as described above; the free alkali contents varied in the 50-150% range. The viscosities of 5 and 6% gels in a nonpolar technical solvent 30 days after preparation are plotted in Figure 2. Each curve has a sharply defined maximum for the viscosity of the Al soap oleogel at 75% excess free alkali, irrespective of the molecular weight of the naphthenic acids. It follows from these results that the relationship which has been found between the thickening properties of Al soaps of naphthenic acids and the free-bound alkali ratio in precipitation holds for naphthenic acids of different molecular weights (M_{Av} from 214 to 250); the optimum content of free alkali is 75%.

Thus, the ratio of free to bound alkali in the precipitation of Al soaps is one of the principal factors determining the viscosity and stability of their oleogels.

LITERATURE CITED

- [1] A.A. Trapeznikov and G.V. Belugina, Proc. Acad. Sci. USSR 87, 635, 825 (1952); 94, 97 (1954).
- [2] A.E. Alexander and V.R. Gray, J. Phys. Coll. Chem. 53, 9, 23 (1949); Proc. Roy. Soc. 200A, 162 (1950).
- [3] T.S. McRoberts and J.H. Schulman, Proc. Roy. Soc. 200A, 135 (1950).
- [4] G.V. Belugina and A.A. Trapeznikov, Colloid J. 20, 3 (1958) [see C.B. translation].
- [5] A.A. Trapeznikov and V.A. Fedotova, Proc. Acad. Sci. USSR 81, 1101 (1951); 82, 97 (1952); 95, 595 (1954).

Received July 6, 1957

Institute of Physical Chemistry
Academy of Sciences USSR
Moscow Branch of the All-Union Scientific
Research Institute of Fats, Moscow

*This is the maximum constant viscosity of the undestroyed structure [5], which we determined by the method of N.A. Bakh.



BORIS ARISTARKHOVICH DOGADKIN

ON THE SIXTIETH BIRTHDAY OF BORIS ARISTARKHOVICH DOGADKIN

S. M. Lipatov, S. S. Voiutskii, and V. E. Gul'

Professor Boris Aristarkhovich Dogadkin, Doctor of Chemical Sciences, was sixty years old on March 20 of this year. Nearly 35 years of this was devoted by Dogadkin to scientific and teaching work, which he began, when he was still a student in the University of Moscow, as lecturer in natural history in the Moscow Party School, and as a scientific assistant in the Timiriazev Biological Institute. Here he performed his first research, on periodic precipitation of calcium phosphates; the results were published in *Kolloid Zeitschrift*. In 1929 he joined the Institute of the Rubber (now Tire) Industry, where he organized the laboratory of the physics and chemistry of rubber. He is now the head and scientific director of this laboratory.

Dogadkin's university work began in 1930, when he became an assistant in the Department of Colloid Chemistry of the Moscow State University. In 1932 he was appointed, by competition, to be Assistant Professor and Head of the Department of Physical and Colloid Chemistry of the Moscow Petroleum Institute, and in 1933 he became Professor and head of the newly established Department of Chemistry and Physics of Rubber in the M. V. Lomonosov Institute of Fine Chemical Technology, Moscow.

Dogadkin was confirmed in the title of Professor in 1935, and awarded the degree of Doctor of Chemical Sciences in 1937. In 1941 he was awarded a Stalin prize for work on the production and industrial synthesis of synthetic latex. He was awarded the Order of Lenin and the Order of the Red Banner of Labor for outstanding success in training technologists and scientists.

Dogadkin's scientific activity has been mainly concerned with the physical chemistry of natural and synthetic rubbers, and rubber technology.

Dogadkin was the founder of USSR research on emulsion polymerization, and the originator of the industrial process for the production of synthetic latex. As the result of his investigations he was able to formulate, for the first time, the basic laws governing emulsion polymerization in relation to the properties of synthetic rubbers; he showed that the variations of the mechanical strength of vulcanizates with the course of polymerization can be represented by a curve with a maximum. Dogadkin introduced the concept of an "optimum" rubber and showed that the yield and quality of optimum rubber are higher with decrease of the polymerization temperature. The significance of the work of Dogadkin as one of the first workers in the field of emulsion polymerization is noted in a number of foreign monographs, such as Whitby's "Synthetic Rubber," etc.

Since 1940 Dogadkin and his associates have carried out systematic research on the vulcanization process, which revealed the mechanism of this important technological process. The important practical problem of reversion of vulcanization, and of the vulcanization optimum, was satisfactorily explained for the first time by Dogadkin, on the basis of the concept of two mutually-opposing processes taking place during vulcanization—structure formation under the action of the vulcanizing agent, and degradation under the influence of oxygen and thermal factors. In his development of this concept Dogadkin carried out detailed investigations of the structure of vulcanizates and its influence on the heat resistance and fatigue of rubber.

By the development of original new methods for studying vulcanization (the thermomechanical method, the isotope-exchange method with the use of S^{35}) it was possible to establish that in presence of a number of accelerators (Antax, Captax, Sulfenamide BT) vulcanization proceeds by a radical mechanism. The reactions of the addition of sulfur and accelerator to rubber were shown to be interdependent, and the mechanism of sulfur activation in presence of a number of accelerators was elucidated. Recently Dogadkin has been working on the problem of irradiation vulcanization of rubber.

Dogadkin has given a correct picture of the state of rubber in solution, and has proposed a surface-tension method for investigation of this problem. He was the first to apply light scattering to determination of the molecular weight of rubber. He designed an osmometer which has been widely adopted in the laboratories of the Union. Finally, Dogadkin studied and determined the mechanism of the structural changes in rubber in solution under the influence of light.

In their studies of the swelling kinetics, electrical conductivity, and dielectric properties of filled rubbers, Dogadkin and his associates demonstrated the existence of thixotropic chain structures in such rubbers. As long ago as 1938 Dogadkin described the formation of a carbon-rubber gel; this effect is associated with the chemical interaction between the active filler and the rubber. Later, Dogadkin studied the chemical interaction of sulfur with the active regions of the carbon black surface. All these investigations represent a substantial contribution to a correct understanding of the mechanism of rubber reinforcement and the influence of the structure of filled rubbers on their mechanical properties. Dogadkin and his associates succeeded in developing the theoretical principles and finding the conditions of rubber reinforcement by addition of fillers (active blacks) directly to latexes. The solution of this problem opens up the possibility of the development of a new technological process for the production of rubber goods from latex.

A number of investigations carried out by Dogadkin and his associates dealt with the kinetics of the elastic deformation of rubber and vulcanizates. Dogadkin devoted special attention to intermolecular forces in determining the relationships which accurately describe the properties of real materials — technical vulcanizates and rubber. In studies of the influence of swelling and softeners on the relaxational properties and strength of vulcanizates, Dogadkin and his associates established that the static and dynamic strength do not vary steadily with the softener content.

Dogadkin was one of the first to introduce new technological processes for the production of rubber goods directly from latex in the Soviet Union; these processes are more progressive both technically and economically. The technical procedure and formulations for the production of latex goods in the "Krasnyi Rezinshchik" factory in Kiev were developed under his guidance. Dogadkin is the inventor of a process, used in one of the chemical works, for the production of microporous ebonite from latex. This series of investigations includes the development of the theory and method for the production of aqueous dispersions of rubber.

It must be emphasized that the great majority of Dogadkin's investigations are original; they pose and solve new problems or provide new interpretations. At the same time, this work is not detached from the practical problems of the rubber industry. Because of his connection with industry and his scientific authority, Dogadkin constantly participates in the work of the Scientific and Technical Councils of the Ministry of the Chemical Industry, State Technology, and Ministry of Higher Education, and in the work of various special commissions and the councils of various institutes.

By his intensive teaching work Dogadkin has established a Soviet school of research scientists who work in the field of the chemistry and physics of rubber. Dogadkin's pupils and associates include 5 doctors and 31 graduates. He has published 148 scientific papers, has received over 20 author's certificates for inventions, and has written four books; of these "The Chemistry and Physics of Rubber," although a text book, is in the nature of a monograph and is an excellent summary of the chemistry and physics of rubber. The publication of this book was the opening of a new epoch for rubber scientists. It is used not only by students; but by engineers and scientists working in rubber-using industries. The success of the book was also furthered by its literary qualities—a good style, simple and precise presentation, a high scientific level and, above all, the author's single-minded approach to problems of the properties of rubber and the chemistry of the principal processes in the rubber industry.

Dogadkin constantly takes an active part in social life. From 1936 to 1938 he was Chairman of the Bureau of the Scientific and Technical Society of Rubber. He is now a member of the Presidium of the Moscow Section of the D. I. Mendeleev Chemical Society, Chairman of the Colloid Section and member of the Bureau of the Chemical Section of the Society for the Propagation of Scientific Knowledge of the RSFSR. Since 1945 he has been Deputy Editor of Colloid Journal. He was a delegate of the Frunze Regional Soviet in Moscow in three elections.

Thus, in the person of B. A. Dogadkin we have a combination of an eminent university teacher, an outstanding research worker, and an active scientific social worker.

We wish our dear Boris Aristarkhovich, from the depth of our hearts, many years of life, health, and creative success in his fruitful scientific and social activity for the good of our great country.

THE STRUCTURE AND PROPERTIES OF RUBBERS PRODUCED IN IRRADIATION VULCANIZATION

B. A. Dogadkin, Z. N. Tarasova, M. Ia. Kaplunov, V. L. Karpov,
and N. A. Klauzen

In recent years there have been great advances in studies of the action of high-energy radiations on various substances and processes. In particular, there has been great interest in the utilization of nuclear radiations for the vulcanization of polymers [1-4]. The reason for this interest is that, according to the available literature data, vulcanizates obtained under the influence of ionizing radiations have structural characteristics which distinguish them from ordinary products obtained by chemical vulcanization. According to Jackson et al. [2], irradiation vulcanizates have high resistance to thermal and thermo-oxidative aging, to the action of solvents and softeners at high temperatures, and to the action of chemically active media.

The method of vulcanization with the aid of ionizing radiations also differs from the ordinary thermochemical methods in a number of respects; the vulcanization can be effected without the use of heat or vulcanization agents. Ionizing radiations can bring about the vulcanization of saturated polymers which cannot be vulcanized by any other known methods. The interest in the vulcanization of such chemically inert polymers is due to their high resistance to various forms of aging and corrosive media. One advantage of irradiation vulcanization is the possibility of the production of homogeneous massive articles, owing to the high penetration of the radiation. All the technological processes can be accelerated, as vulcanization agents which may cause premature vulcanization (scorching) are not used. The vulcanization time can also be shortened by the use of powerful sources of radiation, as the degree of cross linking is determined by the integral dose of radiation absorbed.

The object of the present investigation was a study of the structural characteristics of irradiation vulcanizates and their physicochemical and technical properties, and the development of formulations and technological procedures in the use of ionizing radiations in technical vulcanization.

Irradiation vulcanization was effected in a nuclear reactor and in a Co^{60} unit of 20,000 curie power. The integral dose of the absorbed energy was in the range 10^7 – 10^8 roentgen; the dose rate was between 1.36 and $0.43 \cdot 10^6$ r/hour. During the cobalt irradiation the temperature of the specimens did not rise above room level. Special determinations of the temperature in the specimens in the reactor were not carried out. The temperature was probably 100–150° in the stated dose range. The irradiation vulcanizates made in the nuclear reactor had residual radioactivity. These specimens were tested 2–3 weeks after preparation; the residual radioactivity decreased to near the background level during this period.

The Irradiation Vulcanization of Rubber

The irradiation vulcanization of purified and technical specimens of natural (NR), butadiene-styrene (SKS-30A), isoprene (SKI), and sodium butadiene (SKB) rubbers was studied.

Films 0.1–0.2 mm thick were made on cellophane from the sol fractions of solutions of the above-named rubbers in benzene. After evaporation of the benzene, the films on their cellophane supports were placed in aluminum cases of a standard type for vulcanization in the nuclear reactor, or in glass test tubes for irradiation with Co^{60} . The cases were always put into the same tube of the reactor to the same depth, at a given constant power of the reactor.

When the irradiation vulcanization was performed in oxygen-free conditions, the rubbers were first purified by extraction in acetone and reprecipitation from benzene solutions in a nitrogen atmosphere. The films were formed on cellophane and dried also in a nitrogen atmosphere, then placed in glass bulbs, repeatedly evacuated at 10^{-4} mm Hg, and the tubes were sealed under vacuum. The density of the vulcanization network in the irradiation vulcanizates was estimated from the maximum swelling in xylene (see Table 1) and from the value of the modulus determined at 60% deformation at 130°. Under these conditions the modulus approached the equilibrium value.

TABLE 1

Maximum Swelling in Xylene, of Technical Rubbers after Irradiation Vulcanization in Presence of Air in a Nuclear Reactor

Composition of mixture	Maximum swelling in xylene, %	Composition of mixture	Maximum swelling in xylene
Integral radiation dose $38 \cdot 10^6$ r		Integral radiation dose $50 \cdot 10^6$ r	
SKS-30A + 40 wt. parts channel black	314	Smoked sheet	362
SKS-30AM + 40 wt. parts channel black	321	SKS-30A	432
NR + 40 wt. parts channel black	353	SKB	260
NR + 40 wt. parts furnace black	369	SKI	754
SKS-30A + 40 wt. parts furnace black	329		
SKS-30AM + 40 wt. parts furnace black	348		

According to Table 1, the technical rubbers form the following series in order of effectiveness of formation of a vulcanization network during irradiation vulcanization: SKB > NR > SKS-30A > SKI. This order may vary according to the initial weight, degree of purification of the rubber, nature of the medium, etc. In fact, the degree of cross linking of purified butadiene-styrene rubber not containing phenyl- β -naphthylamine was considerably higher than that of purified natural rubber.

The presence of oxygen plays a very important part in cross linking during irradiation vulcanization. For both the rubbers studied — natural and butadiene-styrene (SKS-30A) — the degree of cross linking estimated from the maximum swelling and modulus at 130° is greater after irradiation in air than in vacuum, even in purified rubbers (Figs. 1 and 2, and Table 2). It is interesting to note the considerably lower degree of cross linking in technical SKS-30A containing phenyl- β -naphthylamine, in comparison with rubber purified by extraction (Fig. 2).

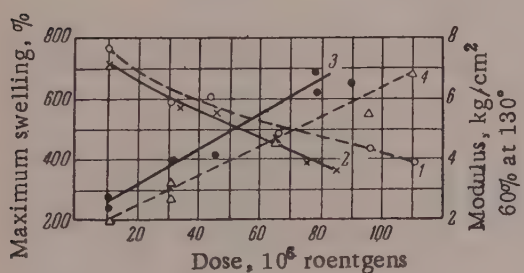


Fig. 1. Influence of the medium during irradiation on the degree of cross linking of purified natural rubber during irradiation vulcanization in a Co^{60} source: 1 and 2) Maximum swelling in xylene, %; 3 and 4) 60% modulus at 130°, in kg/cm^2 ; 1,4) in vacuum; 2,3) in air.

of acids, aldehydes, and ketones; in the 2.8μ region, the absorption band of the hydroxyl group appears; the considerable decrease in transmission in the long-wave region of the spectrum between 7 and 11μ indicates the appearance of ester ($8\text{-}9.0 \mu$ region) and ether ($7.5\text{-}8 \mu$ and $8.7\text{-}9.4 \mu$ regions) groups. The band for alcohol hydroxyls is also in this last region.

The following results were obtained in studies of the infrared absorption spectra of purified and technical SKS-30A irradiated in a Co^{60} source in presence of air. The spectrum of purified SKS-30A contains strong bands of oxygen-containing groups after irradiation with a dose of $36 \cdot 10^6$ r (Fig. 3,a). In the 5.8μ region a broad absorption band appears, corresponding to carbonyl groups

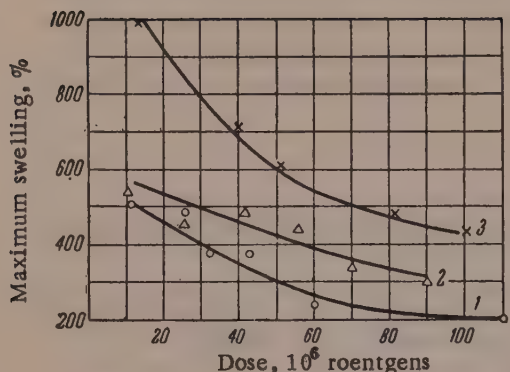


Fig. 2. Influence of the medium during irradiation vulcanization of SKS-30A in a Co^{60} source:
 1) Purified SKS-30A in air; 2) ditto, in vacuum;
 3) technical SKS-30A in air.

With increase of the irradiation dose up to 10^8 r the absorption bands of the carbonyl groups become stronger and are displaced in the direction of shorter wave lengths, indicating the appearance of ester carbonyl groups. At the same time, on a background of decreasing transmission in the long-wave region, a band appears at 8.5μ , corresponding to vibrations in the C-O-C groups of esters. The intensity of the hydroxyl group absorption band also increases with increasing radiation dose.

Quantitative estimation of changes in the unsaturation of the purified specimens is difficult owing to the decreased transmission in the long-wave region of the spectrum. For quantitative estimation of the unsaturation from the strength of the absorption bands at 10.3μ and 11.0μ , all the spectra were raised to coincide at the transmission maximum (Fig. 4). With this arrangement it is clear from Fig. 4 that irradiation with a dose of $36 \cdot 10^6$ r the unsaturation decreases sharply both at the 1-4 and the 1-2 groups. When the dose is increased to $63 \cdot 10^6$ r, the unsaturation disappears almost entirely. When the dose reaches $\sim 10^8$ r, the number of double bonds in 1-4 groups increases again.

TABLE 2

Influence of the Medium During Irradiation Vulcanization of Rubbers in a Co^{60} Source

Rubber	Irradiation dose, roentgens $\times 10^{-6}$	Cross links per 100 ev during irradiation	
		in air	in vacuum
SKS-30A, technical	15	2.17	—
	30	2.24	—
	60	2.57	—
	90	2.62	—
SKS-30A, extracted	15	12.2	9.0
	30	9.0	6.0
	60	12.3	5.14
	90	15.5	4.97
NR, extracted	15	6.87	6.2
	30	3.89	4.0
	60	3.89	2.92
	90	4.37	2.82

Comparison of data on the number of cross links (Table 2) formed during irradiation, with the loss of double bonds shows that the decrease of unsaturation cannot be attributed only to polymerization cross-linking processes. The excess loss of double bonds is evidently the result of formation of intramolecular rings. These structural changes are one of the causes of the thermal resistance of irradiation vulcanizates.

The changes in the infrared absorption spectra of nonextracted technical SKS-30A (containing phenyl- β -naphthylamine) during irradiation are substantially different (Fig. 3,b).

The spectrum of the original technical rubber already shows the presence of a small number of oxygen-containing groups. This is indicated by the presence of a weak hydroxyl group absorption band in the 2.9μ region, and traces of carbonyl groups in the 5.9μ region (Fig. 3,b). When technical SKS-30A is irradiated with

doses of $36 \cdot 10^6$ r and over, up to 10^8 r, there is a very slight increase in the intensity of these absorption bands, with a somewhat more pronounced decrease of transmission in the long-wave region.

The decrease of unsaturation as the result of irradiation is considerably less pronounced in nonextracted SKS-30A (Fig. 4,b) than in the purified rubber. After irradiation with $60 \cdot 10^6$ r the number of double bonds in the 1-4 groups decreases by about 30% of the original content; the content of 1-2 type double bonds remains almost uncharged (Fig. 4,b). The data on changes of unsaturation must be regarded as approximate because SKS-30A rubber contains styrene groups, which also give absorption bands at 10.3 and 11.0 μ , and the results of the unsaturation determinations are therefore somewhat distorted.

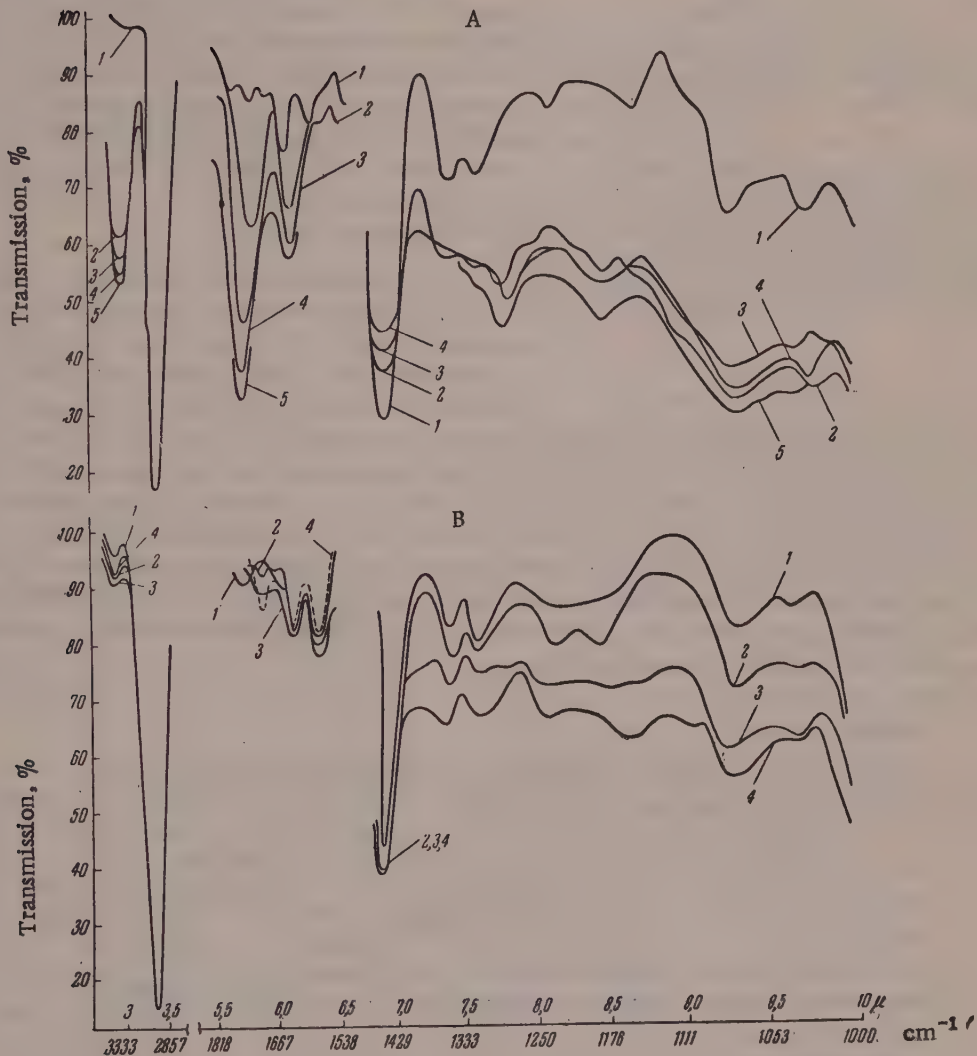


Fig. 3. Infrared spectra of SKS-30A after irradiation in air in a Co^{60} source: A) Purified SKS-30A; B) SKS-30A with phenyl- β -naphthylamine; 1) raw rubber; 2) after irradiation with $36 \cdot 10^6$ r; 3) ditto, $63 \cdot 10^6$ r; 4) ditto, $93 \cdot 10^6$ r; 5) ditto, $123 \cdot 10^6$ r.

Comparison of the infrared spectroscopic data with the results of cross-link determinations indicates that the increased cross linking in presence of oxygen is associated to some extent with formation of cross links of the ether type.

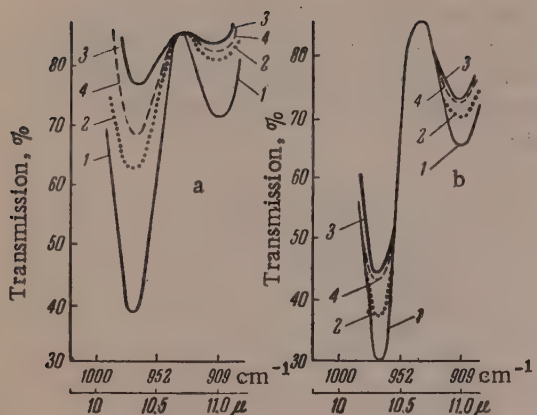


Fig. 4. Variation of the unsaturation of SKS-30A during irradiation in a Co^{60} source in air. a) Purified SKS-30A; b) SKS-30A with phenyl- β -naphthylamine; 1) raw rubber; 2) after irradiation with $36 \cdot 10^6$ r; 3) ditto, $63 \cdot 10^6$ r; 4) ditto, $93 \cdot 10^6$ r.

This is an important difference between irradiation and sulfur vulcanizates; for the latter it was shown [5] that the rate of relative relaxation of stress in not very hard vulcanizates does not depend on the number of cross links. The probable reason for the difference is a difference in the type of cross links. Whereas in the case of sulfur vulcanizates stress relaxation is the result of breakdown at branch points, in irradiation vulcanizates, which contain C-C cross links of higher stability than the diallyl bonds in the molecular chains, breakdown of the vulcanization network during chemical relaxation may occur not only at the branch points, but along the chains. In the latter case the rate of stress relaxation is inversely proportional to the number of branch points per unit volume of the vulcanizate [6].

The protective role of phenyl- β -naphthylamine in irradiation vulcanization is apparently associated with scattering of the absorbed energy and with suppression of oxidative cross linking.

The nature of the vulcanization bonds in irradiation vulcanizates was determined by a method developed previously [5], in which the rate of stress relaxation is measured at constant deformation at 130° in absence of oxygen. It was shown that under these conditions the relaxation rate is determined by the energy of the vulcanization bonds.

Figure 5 shows that the irradiation vulcanizate of natural rubber is superior in thermomechanical resistance to sulfurless vulcanizates with thiuram. The irradiation vulcanizates attain lower residual deformations and lower swelling maxima during relaxation under the conditions described than do the sulfur vulcanizates (Table 3). The results show that the cross links formed in irradiation vulcanization are more resistant to heat than the cross links in sulfur vulcanizates.

Figure 6 shows the variation of the relaxation rate constant in irradiation NR vulcanizates with the number of cross links per unit volume, determined from the maximum swelling in xylene. It is seen that the relaxation rate constant decreases with increasing density of the network.

TABLE 3

Changes in the Properties of Natural Rubber Vulcanizates During Relaxation of Stress in a Nitrogen Atmosphere at 130°

Vulcanizates	Maximum swelling In xylene, %			Residual elongation, %
	Initial Q_0	after relaxa- tion Q_1	$\frac{\Delta Q}{Q_0}$	
NR with thiuram, without sulfur	447	765	+ 70	43.0
NR, integral dose $50 \cdot 10^6$ r	331	344	+ 4	6.7

It must also be noted that the relaxation curves of irradiation NR vulcanizates are almost linear (Fig. 7), with the exception of a small initial region, in contrast to the relaxation curves of sulfur vulcanizates, which conform to an exponential law. This provides further confirmation that chemical relaxation in irradiation vulcanizates involves rupture of the molecular chains. Indeed, if it is assumed that the breakdown of chemical bonds in the chains is a first-order reaction, the relaxation rate should remain almost constant, as the breakdown of only a small proportion of the bonds in the molecular chains is sufficient for total destruction of the

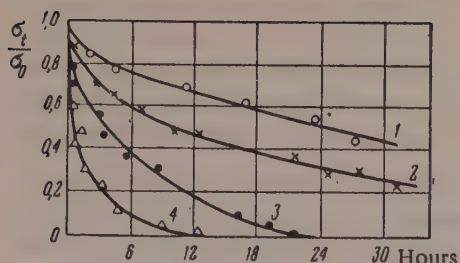


Fig. 5. Stress relaxation of rubbers (at 130°, $\epsilon = 60\%$, in nitrogen) subjected to irradiation vulcanization in air in a nuclear reactor, dose $50 \cdot 10^6$ r: 1) NR irradiation vulcanizate; 2) NR with thiuram without sulfur; 3) SKS-30A irradiation vulcanizate; 4) SKS-30A with sulfenamide and sulfur.

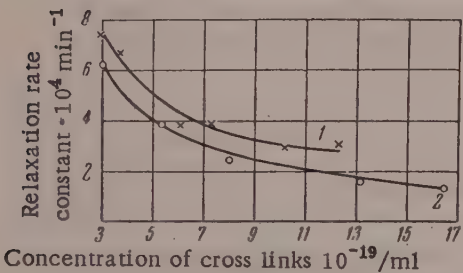


Fig. 6. Variation of the stress-relaxation rate constant with the density of the vulcanization network in irradiation vulcanizates of purified natural rubber, obtained: 1) In vacuum; 2) in air.

may be attributed to addition of oxygen at some of the soluble bonds, with a consequent increase of the thermomechanical stability of the chains.

The tendency to crystallization under tension of irradiation vulcanizates of natural rubber was determined. The crystallinity of the stretched specimens was estimated by Field's method. It follows from the data in Table 4 that irradiation vulcanizates made under the action of radiation with relatively small integral doses (up to $20 - 30 \cdot 10^6$ r) have the same degree of crystallinity as sulfur vulcanizates of the same network density. The crystallinity of the irradiation vulcanizates decreases with increasing radiation dose and increase of cross link concentration.

Irradiation Vulcanization of Filled Rubber Mixtures

It has been shown [3, 4] that the usual vulcanizing agents, sulfur and accelerators, have no accelerating effect on irradiation vulcanization or even act as inhibitors (sulfur, thiuram). On the other hand, many investigators have noted that fillers have a strong effect both in irradiation and in chemical vulcanization. Therefore in the development of recipes for filled mixtures we used rubber-filler mixtures without chemical vulcanizing agent.

network. An approximate calculation performed by Priss [7] gives the following relationship between time and the number of chains per unit volume in the network:

$$N \approx 2v_0 [(1 - M_{av}/M) - kt/v_0]. \quad (1)$$

From this an expression for stress relaxation is easily derived:

$$\frac{\sigma_t}{\sigma_0} = 1 - \frac{kt}{v_0 (1 - M_{av}/M)}. \quad (2)$$

In Equations (1) and (2) v_0 is the number of branch points per unit volume of the original vulcanize; M_{av} is the average molecular weight of the chains in the original vulcanize; k is the constant; σ_t and σ_0 are the values of the stress at time t and 0 respectively.

Equation (2) shows that if chain rupture takes place the relaxation curves should be linear and the constant rate of stress relaxation $k/v_0 (1 - M_{av}/M)$ should be inversely proportional to v_0 ; this is in qualitative agreement with the relationship found for irradiation vulcanizates.

A more exact calculation [7] shows that at the last stage of the process (at $\sigma/\sigma_0 < 0.25$) the relaxation rate decreases and the linear relationship breaks down. The experimental data at our disposal are not sufficient to check this. The deviation from linearity at the start of the relaxation process should probably be attributed to relaxation processes associated with chain regrouping.

It also follows from Fig. 6 that irradiation vulcanizates of purified natural rubber, obtained in air, have somewhat higher thermomechanical stability (lower relaxation rate constant) than vulcanizates with the same network density obtained in absence of oxygen. This

253

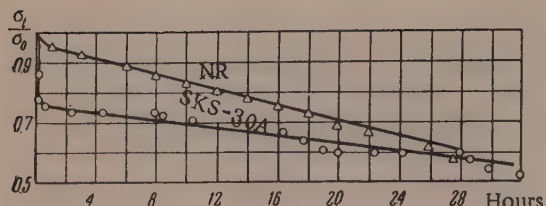


Fig. 7. Stress relaxation of irradiation vulcanizates of NR and SKS-30A of the same network density ($12 \times 10^{19} \text{ ml}^{-1}$), obtained in air; Co^{60} source; NR, dose $75 \cdot 10^8 \text{ r}$, maximum swelling 429%; SKS-30A, dose $90 \cdot 10^8 \text{ r}$, maximum swelling 434%.

tures of rubber with 50 parts of channel blacks not only failed to produce the increase of hardness which is to be expected from literature data [3, 4], but even lowered the hardness somewhat and increased the maximum swelling (Fig. 8). This effect is probably analogous to that observed in rubbers highly loaded with inactive fillers [8]. The hardness of irradiation vulcanizates increases steadily with the channel black content up to 100 wt. parts.

TABLE 4

Degree of Crystallinity of Natural Rubber Vulcanizates Under Tension

Vulcanizates	Vulcanization time, min.	Radiation dose in roentgens $\times 10^{-6}$	Max. swelling in xylene, %	Intensity ratio of crystalline interferences to amorphous scattering	Crystallinity at 400% extension
3.0% thiuram, without sulfur	10	—	525	1.2	44.5
Ditto	50	—	495	1.6	49
Diphenylguanidine 1.0% + sulfur 2.0%	10	—	720	1.0	41
Ditto	50	—	470	1.45	48
Irradiation vulcanization	—	30	759	1.1	42.5
Ditto	—	40	570	0.93	40

TABLE 5

Uniformity of Irradiation Vulcanization of a Mixture of NR with 50 wt. Parts of Channel Black, Dose $32 \cdot 10^8 \text{ r}$, Co^{60} Source

Distance from upper surface, mm	0	5	10	15	20	25	30	35
Maximum swelling in xylene, %	455	463	468	489	484	426	441	431

The filled mixtures, in the form of calendered sheets 0.2-0.3 mm thick interleaved with cellophane were placed in aluminum cases for irradiation vulcanization in the nuclear reactor, or in glass test tubes for vulcanization in the Co^{60} source. Technical vulcanizates were made by vulcanization in aluminum molds in the reactor, or in steel molds in the Co^{60} source.

Table 5 shows that irradiation vulcanization results in the formation of a uniform vulcanization network at all the thicknesses studied down to 40 mm, because of the high penetrating power of the radiation.

The introduction of carbon black gives irradiation vulcanizates with denser networks than in unfilled vulcanizates (Table 1). The relative effects of different fillers on the density of the vulcanization network are the same as in ordinary chemical vulcanization. Active blacks of the channel type are the most effective. The introduction of fillers containing heavy atoms into mix-

It was shown in our earlier investigations that both filled and unfilled sulfur vulcanizates made under the same vulcanization conditions have the same rate of chemical relaxation of stress. In contrast to this result, mixtures of rubber with carbon black have a considerably lower relaxation rate than unfilled mixtures, after irradiation vulcanization (Fig. 9). The thermomechanical stability is higher in specimens with channel black than in specimens with the same amounts of furnace black. These results indicate that chemical bonds are formed between the rubber and the carbon black during irradiation vulcanization.

The effect of resins of the styrene and epoxide type on the properties of mixtures based on NR and SKS-30AM mixtures containing channel black was studied. In contrast to sulfur vulcanizates, where the addition of resins results in an appreciable increase of hardness, in irradiation vulcanization these resins decreased the modulus and maximum swelling (Fig. 10).

The irradiation temperature in irradiation vulcanization is significant. In a number of experiments increase of temperature increased the degree of cross linking and the hardness of the vulcanizate.

Figure 11 shows variations of tensile strength, modulus, and relative elongation for irradiation vulcanizates of natural and of oil-filled butadiene-styrene (SKS-30AM) rubbers, containing 50 wt. parts of channel black, with the dose of energy absorbed. It is seen that the maximum tensile strength is found in vulcanizates made with the use of a dose of $40-50 \cdot 10^6$ r (in a Co^{60} source).

Table 6 gives comparative data on the physico-mechanical properties of irradiation vulcanizates made in the nuclear reactor, and of sulfur vulcanizates of the tire-rubber type, containing equal amounts of carbon black. The tire rubbers and the irradiation vulcanizates were tested under the same conditions, and the test specimens were all of the same size. The values for the irradiation vulcanizates are somewhat low, because molds were not used for vulcanization in this case.

Rubbers vulcanized by the action of nuclear radiations have low residual deformations, low dynamic loss and dynamic modulus, and high endurance in repeated extension. At the same time, irradiation vulcanizates have somewhat lower strength characteristics, especially those based on natural rubber. Irradiation vulcanizates have high resistance to oxidative degradation. Whereas the tensile strength of the best sulfur vulcanizates of natural rubber falls to 15% of the initial value, and the relative elongation to 18%, after 12 hours at 130° , the corresponding values for irradiation vulcanizates are 58 and 81% respectively. After 50 hours of aging at 130° the sulfur vulcanizates lose all their elastic properties, whereas the aging coefficients of irradiation vulcanizates under these conditions are 0.30 with respect to tensile strength and 0.70 with respect to relative elongation. The brittle point (-57°) of irradiation vulcanizates does not change during 12 hours of aging at 130° , whereas the brittle point of sulfur vulcanizates rises from -55 to -45° .

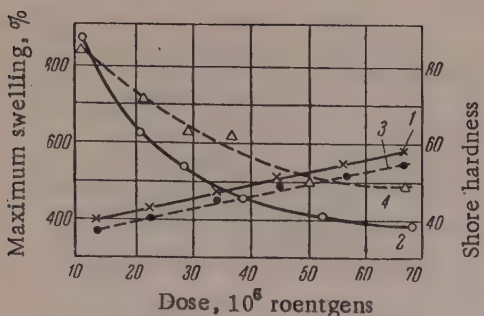


Fig. 8. Effect of fillers on the properties of NR irradiation vulcanizates; Co^{60} source: 1,3) Shore hardness; 2,4) maximum swelling in xylene; 1,2) rubber containing 50 wt. parts of channel black; 3,4) ditto with 30 wt. parts of chalk.

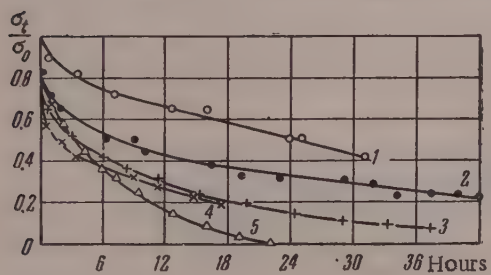


Fig. 9. Relaxation of stress in rubbers and mixtures with carbon black (at 130° , $\epsilon = 60\%$, in nitrogen) after irradiation vulcanization in air in a nuclear reactor. 1) NR without carbon black, $50 \cdot 10^6$ r; 2) NR + 40 wt. parts of channel black, $38 \cdot 10^6$ r; 3) SKS-30A + 40 wt. parts of channel black, $38 \cdot 10^6$ r; 4) SKS-30AM + 40 wt. parts of channel black, $38 \cdot 10^6$ r; 5) SKS-30A without carbon black, $50 \cdot 10^6$ r.

radiations have low residual deformations, low dynamic loss and dynamic modulus, and high endurance in repeated extension. At the same time, irradiation vulcanizates have somewhat lower strength characteristics, especially those based on natural rubber. Irradiation vulcanizates have high resistance to oxidative degradation. Whereas the tensile strength of the best sulfur vulcanizates of natural rubber falls to 15% of the initial value, and the relative elongation to 18%, after 12 hours at 130° , the corresponding values for irradiation vulcanizates are 58 and 81% respectively. After 50 hours of aging at 130° the sulfur vulcanizates lose all their elastic properties, whereas the aging coefficients of irradiation vulcanizates under these conditions are 0.30 with respect to tensile strength and 0.70 with respect to relative elongation. The brittle point (-57°) of irradiation vulcanizates does not change during 12 hours of aging at 130° , whereas the brittle point of sulfur vulcanizates rises from -55 to -45° .

TABLE 6

Physicomechanical Properties of Rubbers

Mixtures	Irradiation vulcanization dose $38 \cdot 10^6$ roentgens						Tire rubbers				
	SKS-30A+ + 40 wt. parts carbon black		SKS-30AM + + 40 wt. parts car- bon black		NR + 40 wt. parts carbon black		SKS-30A+ + 40 wt. parts carbon black		NR + 40 wt. parts carbon black		
	channel	furnace	channel	furnace	channel	furnace	channel	furnace	channel	furnace	
Tensile strength in kg/cm ²	130	112	115	78	150	157	294	236	261	274	321
Relative elongation, %	680	680	800	850	500	540	580	716	644	636	612
Residual elongation, %	16	12	16	20	8	8	24	21.6	33.6	33.2	32
Modulus at 200%, kg/cm ²	15.6	23.6	8.3	21.4	35.6	28.5	49.0	32.0	34.7	26.8	53
Modulus at 400%, kg/cm ²	62.6	69.0	39.0	53.5	136.5	132	152	85	102.5	104	100
Mechanical loss factor	15.3	15.8	9.5	9.5	7.3	7.0	35	18.5	24	17	10.6
Dynamic modulus	33.2	35.6	21.6	23.8	29	20.3	77	46.4	53	40.5	43
Endurance, in 1000 cycles in repeated extension E = 100% at 25°	127	336	285	1000	51.25	45.0	98	222	410	140	84

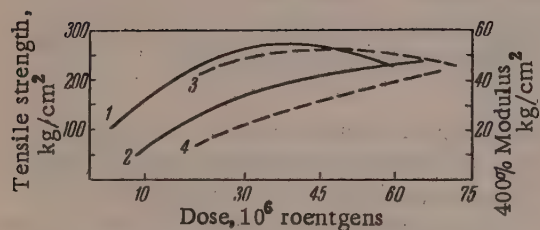


Fig. 10. Effect of fillers on the properties of NR irradiation vulcanizates; Co⁶⁰ source: 1,3) tensile strength in kg/cm²; 2,4) 400% modulus in kg/cm²; 1,2) rubber with 50 wt. parts of channel black; 3,4) ditto, with 20 wt. parts of Polymer SS.

The data in Fig. 12 also demonstrate the high stability of irradiation vulcanizates based on butadiene-styrene polymers. Under these conditions, sulfur vulcanizates show 50% decreases of tensile strength and relative elongation.

SUMMARY

1. The structure and properties of irradiation vulcanizates of technical and purified SKB, NR, SKS-30A, SKS-30AM, and SKI rubbers with and

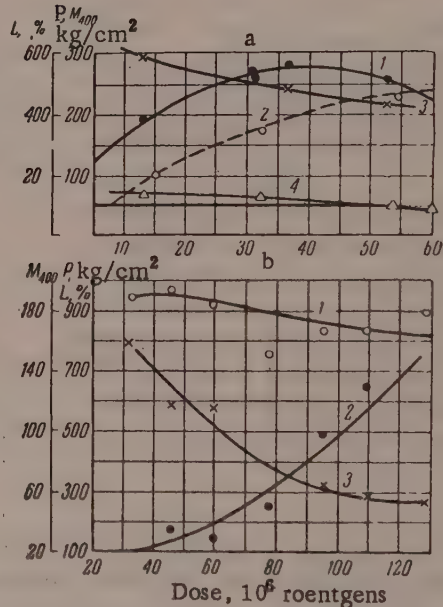


Fig. 11. Effect of quantity of energy absorbed on the properties of irradiation vulcanizates containing 50 wt. parts of channel black: a) NR; b) SKS-30AM, Co⁶⁰ source; 1) tensile strength in kg/cm²; 2) modulus at 400%, in kg/cm²; 3) relative elongation, %; 4) residual elongation, %.

without fillers, made by irradiation in a nuclear reactor and in a cobalt source, with integral doses of 10^7 – 10^8 r., have been studied.

2. The density of the network formed in irradiation vulcanization is determined by the quantity of energy absorbed, the type of rubber, the irradiation conditions (medium, temperature), and certain other factors.

The yield of cross links per 100 ev in air is ~ 12 for extracted butadiene-styrene rubber, ~ 4 for extracted NR, and 2.5 for technical SKS-30A. The cross-linking effect increases with increase of temperature and decreases in presence of an oxidation inhibitor (phenyl- β -naphthylamine).

3. The thermomechanical stability of irradiation vulcanizates is superior to that of vulcanizates made with thiuram without sulfur, and such vulcanizates undergo the least changes in properties during chemical relaxation.

In contrast to sulfur vulcanizates, the relative rate of stress relaxation in irradiation vulcanizates depends on the density of the vulcanization network. This indicates that C-C type bridges are formed in the course

Fig. 12. Variation of the properties of irradiation vulcanizates of SKS-30AM with 50 wt. parts of channel black during aging: 1) tensile strength; 2) 200% modulus; 3) relative elongation; 4) maximum swelling; 1', 2', 3', 4') the same properties after aging.

of irradiation vulcanization. The thermomechanical stability of irradiation vulcanizates is raised by the introduction of active blacks.

4. The presence of carboxyl, hydroxyl, ether, and ester groups in irradiation vulcanizates of natural, butadiene-styrene, and sodium butadiene rubbers vulcanized in presence of air has been demonstrated by infrared spectroscopy. A dose of $60 \cdot 10^6$ r causes almost complete disappearance of double bonds from extracted butadiene-styrene rubber. In the technical rubber, containing phenyl- β -naphthylamine inhibitor, this dose reduces the degree of unsaturation by about 30% of the initial value.

5. The tendency to crystallization on stretching was studied in irradiation vulcanizates of natural rubber. The crystallinity of irradiation vulcanizates made by irradiation with relatively small doses, up to $20-30 \cdot 10^6$ r., is the same as that of sulfur vulcanizates of the same network density. The degree of crystallization decreases with increasing radiation dose.

6. Conditions for the production of massive multilayer specimens by irradiation vulcanization were investigated. It was found that a uniform vulcanization network can be obtained irrespective of the thickness of the specimen (in the range 0.1–40 mm).

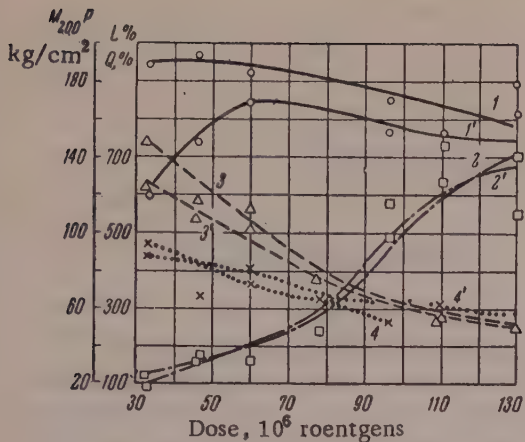
7. The physicomechanical and technical properties of irradiation vulcanizates were studied.

In comparison with the best sulfur with the same filler contents, irradiation vulcanizates have a higher resistance to aging (4–5 times as high at 130°), low residual deformations, low hysteresis, high endurance to repeated deformation, and high heat resistance.

The tensile strength of irradiation vulcanizates, as a function of the radiation dose, passes through a maximum, but does not reach the values found in the best sulfur vulcanizates.

LITERATURE CITED

- [1] A. Charlesby, Proc. Roy. Soc. A 222, No. 1148, 60 (1954); A. Charlesby, Rubber Chem. and Technol. 28, 1 (1955); A. Charlesby, Nucleonics 14, No. 9, 82 (1956).
- [2] W. Jackson and D. Hall, Rubber Age, 77, 865 (1955).



- [3] S. Gehman and J. Auerbach, Inter. J. Rad. and Isotopes, 1, No. 1, 2, 102 (1956).
- [4] A. S. Kuz'minskii, T. S. Nikitina and V. L. Karpov, Atomic Energy No. 9 (1956).
- [5] B. A. Dogadkin and Z. N. Tarasova, Colloid J. 15, No. 5, 347 (1953).*
- [6] A. Tobolsky, J. Appl. Phys. 27, No. 7, 673 (1956).
- [7] L. S. Priss, Colloid J. 19, No. 5, 607 (1957).*
- [8] K. Bryant and D. Bisset, Rubber Chem. and Technol. 30, No. 2, 610 (1957).

Scientific Research Institute
for the Tire Industry
Moscow

Received October 30, 1957

*Original Russian pagination. See C. B. Translation.

THE CHEMICAL INTERACTION OF SULFUR AND CARBON BLACK

B. A. Dogadkin, Z. V. Skorodumova, and N. V. Kovaleva

When channel black is heated with a solution of sulfur in toluene, a chemical reaction occurs and the sulfur combines with the carbon surface [1]. This effect is of undoubted interest in relation both to the vulcanization process and to the reinforcement of rubber by carbon blacks. It is known that the reinforcement effect and the influence of carbon blacks on vulcanization kinetics depend to a considerable extent on the surface properties, and in particular on the nature and number of oxygen-containing functional groups on the carbon black surface. It became necessary in this connection to find what types of carbon black are the most active toward sulfur and what surface groups and regions of the carbon interact with the sulfur.

Influence of the type of carbon black. The conditions used for the interaction of sulfur with carbon black were the same as those described previously [1]. A weighed sample of the black was heated with a saturated solution of radioactive sulfur in toluene at 145° in presence of A100 accelerator. The amount of chemically bound sulfur was found from the activity of the carbon black after extraction with chloroform. The characteristics of the carbon blacks are given in Table 1. It follows from Fig. 1,a that the highest activity toward sulfur, per unit weight of carbon black, is found in channel black, and the lowest in thermal black. However, if the amount of chemically bound sulfur is calculated per unit surface (Fig. 1,b), the carbon blacks form the following series in order of increasing chemisorptive activity toward sulfur: channel < furnace < thermal < lamp. This series is the reverse of the series of the carbon blacks in order of their oxygen contents; the higher the surface oxygen content, the less sulfur does the carbon black bind. These results lead to the conclusion, that the chemical interaction of sulfur with carbon does not, in the main, occur through oxygen-containing functional groups.

TABLE 1

Characteristics of Carbon Blacks

Type of black	Sp. surf. from phenol adsorp- tion, in m ² /g *	pH	Colori- metric number	Elementary composition, %			
				C	H	O by differ- ence	ash
Ukhta channel	110	3.47	29.6	93.04	1.25	5.71	—
Ukhta thermal	7.4	8.45	—	99.26	0.65	0.09	—
Kudinovo lamp	10.2	7.5	—	99.54	0.39	0.07	—
Dashava furnace	24.2	8.5	5.24	97.45	0.68	1.37	0.5
Channel, hydrogenated at 300°	123	7.1	28.0	94.84	1.46	3.7	—
Hydrogenated at 500°	128	7.2	28.2	94.80	1.66	3.54	—
Heated at 900°	99.5	9.0	20.6	99.32	0.67	0.01	—
Oxidized at 350°	270	2.66	20.1	82.77	1.57	15.66	—

* The specific surface was determined without preliminary blowing of the carbon blacks.

To test this conclusion, experiments were carried out in which the carbon blacks were subjected to treatments increasing or reducing their surface oxygen contents. Thus, in the first series of experiments channel black was oxidized by the action of heat in air at 350° for 3.5 hours*, and reduced by hydrogenation at 350-500° and hydrogen pressure 200-225 atm **, or heated in hydrogen at 900***. It is clear from Fig. 2 that oxidation of channel black reduces its chemisorptive activity with regard to sulfur; decrease of the amount of oxygen on the carbon black surface increases the amount of chemically bound sulfur. Channel black heated at 900° in hydrogen is an exception. Analysis showed that this treatment removes oxygen almost completely from the carbon surface, and yet the chemisorption of sulfur is reduced as a result. The explanation of the peculiar behavior of the heated carbon black is that a secondary structure is formed at 900°, as shown by the change of the colorimetric number. The secondary structure probably arises by contact of the carbon particles at points where the oxygen-containing groups have been removed.

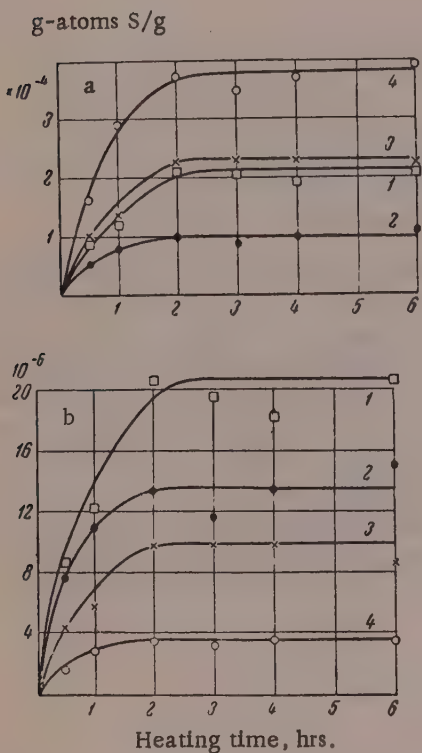


Fig. 1. Kinetics of sulfur addition to commercial carbon blacks at 145°. A100 accelerator; a) Calculated on the weight of carbon (g-atoms sulfur/g); b) calculated per unit area (g-atoms sulfur/m²): 1) lamp; 2) thermal; 3) furnace; 4) channel.

adsorption of water vapor on carbon black were carried out in order to determine the sites of chemical interaction of sulfur with the carbon. It was shown by Kiselev et al. [2] that water vapor is adsorbed mainly by the oxygen-containing groups of the carbon black. Figure 5 shows the isotherms for adsorption of water vapor on commercial channel black and on the same black after reaction with sulfur (the sulfur content was 0.7%). It is seen that the adsorption isotherms coincide for the two specimens in the initial region, corresponding to a monomolecular layer of water. This shows that sulfur does not affect the activity of the oxygen-containing groups; this is possible only if the sulfur is attached to other regions of the carbon surface, not containing oxygen. The isotherms diverge only over the regions corresponding to thicker layers of adsorbed water.

* Carbon black supplied by K. A. Pechkovskaya.

** Carbon black supplied by N. V. Lukin.

*** Carbon black supplied by P. A. Tesner.

If the secondary structure so formed is broken down by means of ultrasonic vibrations, the chemical activity of the carbon black toward sulfur is increased (approximately doubled):

Bound sulfur before ultrasonic treatment	0.48%
Ditto, after treatment at 15 kc/sec.	0.88%
Ditto, after treatment at 25 kc/sec.	0.80%

In the second series of experiments with channel black, the black was evacuated under high vacuum at 800°, and the vacuumized black was oxidized in air at 400°, or heated at 1700° in hydrogen. The results of the experiments are given in Fig. 3 and Table 2; it is seen that the carbon black with the lowest oxygen content binds most sulfur per unit surface. The action of heat at 1700° in hydrogen results in total removal of oxygen and formation of secondary structures which are not broken down by ultrasonic vibrations at frequencies up to 25 kc/second. The chemical activity toward sulfur is reduced by such heating.

The third series of experiments was carried out with an active American furnace black, Philblack O. Philblack O was heated in air at 400 and 500°, and then blown through with nitrogen to pH ~ 8. Under these conditions secondary structures are not formed (the colorimetric number remains unchanged; see Table 3), and only the specific surface and the oxygen content change. Figure 4 shows that the amount of sulfur bound per unit area decreases with increasing oxygen content in this type of carbon black also.

Adsorption of water vapor. Experiments on the adsorption of water vapor on carbon black were carried out in order to determine the sites of chemical interaction of sulfur with the carbon. It was shown by Kiselev et al. [2] that water vapor is adsorbed mainly by the oxygen-containing groups of the carbon black. Figure 5 shows the isotherms for adsorption of water vapor on commercial channel black and on the same black after reaction with sulfur (the sulfur content was 0.7%). It is seen that the adsorption isotherms coincide for the two specimens in the initial region, corresponding to a monomolecular layer of water. This shows that sulfur does not affect the activity of the oxygen-containing groups; this is possible only if the sulfur is attached to other regions of the carbon surface, not containing oxygen. The isotherms diverge only over the regions corresponding to thicker layers of adsorbed water.

Liberation of hydrogen sulfide. One possibility is that the chemical addition of sulfur to carbon black occurs as the result of oxidation-reduction reactions involving hydroxyl groups or hydrogen directly linked to the carbon surface of the blacks. If so, hydrogen sulfide should be liberated in the reaction of carbon black with sulfur. Studebaker [3] reported that H_2S is evolved when molten sulfur is heated with carbon black. We did not observe the liberation of hydrogen sulfide [1]. For clarification of this problem, experiments were carried out as follows. 2 g of elemental sulfur, 2 g of channel black, and 120 ml of toluene were put into a flask; the mixture was heated at 145° for 6 hours. Nitrogen was passed through the system during the whole time, and the gas was bubbled through a solution of cadmium acetate in acetic acid. Hydrogen sulfide was not liberated in the normal course of the sulfur-carbon black reaction (the amount of sulfur added was 0.7% of the weight of the carbon). Likewise, we did not detect the liberation of hydrogen sulfide when a melt of 2 g of sulfur with 2 g of channel black was heated for 6 hours at 145° in a bulb fitted with a side tube with a stopcock. When the gas phase was blown out of the bulb, it gave a negative test with moist lead acetate paper.

TABLE 2

Characteristics of Carbon Blacks after Vacuum Treatment

Carbon black	Sp. surf. from N adsorption, m^2/g	Colorimetric num- ber after ultrasonic treatment		Elementary composition, %		
		15 kc/sec	25 kc/sec	C	H	O by difference
Channel black, vacuumized at 800°	150	22.5	25.2	97.26	0.47	2.27
Ditto, then oxidized at 400° in air	270	18.7	22.0	93.58	1.05	5.37
Ditto, then heated at 1700° in hydrogen	100	21.4	21.4	99.65	0.36	—

Isotope exchange of sulfur attached to carbon black. The sulfur present in polysulfide $-S-S_x-S-$ groups enters fairly readily into isotope exchange with elemental sulfur [4, 5]. Mono- and disulfide sulfur exchanges with more difficulty or not at all, according to the nature of the radicals. Isotope exchange experiments were therefore carried out in order to determine the character of the sulfur attached to carbon black as the result of heating at 145°. Weighed 0.06 g samples of carbon black, containing radioactive sulfur S^{35} , were heated at 130 and 150° with 7 ml lots of a solution of ordinary elemental sulfur S^{32} in toluene. After the heating, the sulfur was extracted with chloroform and its activity was determined [1]. It follows from the data in Table 4 that the activity of the sulfur-containing carbon black remains unchanged; this means that the sulfur is present on the carbon surface in the form of stable compounds of the mono- and disulfide type. The presence of HS groups in the carbon black is equally unlikely, as these groups exchange sulfur relatively easily in many compounds.

On the assumption that the chemically bound sulfur is present in the form of monoatomic groupings in the carbon surface, it is possible to calculate the surface area of the carbon black occupied by sulfur atoms for equilibrium values of the added sulfur. If the radius of a sulfur atom is taken as 0.97A, this surface (see Table 5) varies between 0.06 and 0.35 m^2/m^2 .

DISCUSSION OF RESULTS

These results leave no doubt that chemical interaction may occur between elementary sulfur and carbon black in a hydrocarbon medium at the vulcanization temperature. It was shown earlier [1] that vulcanization accelerators influence both the kinetics of sulfur addition and the maximum amount of sulfur added. This suggests that sulfur may also be added to the carbon in the form of an active complex formed by interaction of the sulfur and the accelerator, for example, in the form of sulphydryl or persulphydryl groups [6]. The activation energy of the addition of sulfur to carbon black is close to the activation energy of the sulfur-rubber reaction; its value is approximately 15 kcal./mole for the reaction in presence of accelerator A100.

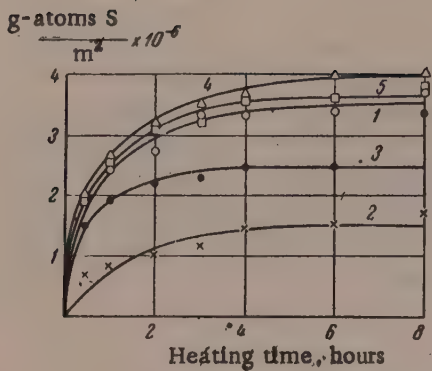


Fig. 2. Kinetics of the addition of sulfur to channel black treated under different conditions: 1) Commercial; 2) oxidized at 350° in air; 3) heated at 900° in hydrogen; 4) hydrogenated at 500° under 225 atm hydrogen pressure; 5) hydrogenated at 350° under 200 atm hydrogen pressure.

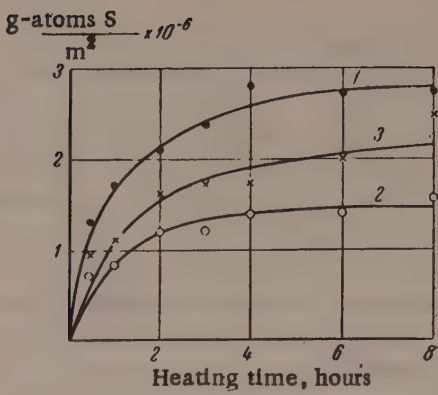


Fig. 3. Kinetics of the addition of sulfur to channel black treated under different conditions: 1) Channel black vacuumized at 800°; 2) ditto, then oxidized at 400° in air; 3) ditto, then heated at 1700° in hydrogen.

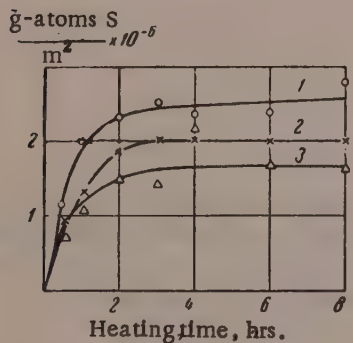


Fig. 4. Kinetics of sulfur addition to Philblack O furnace black: 1) Commercial; 2) oxidized at 400° for 15 minutes, then blown through with nitrogen to pH ~ 8; 3) oxidized at 500° for 30 minutes, then blown through with nitrogen to pH ~ 8.

With the exception of blacks heated in hydrogen at temperatures above 900°, the amount of chemically bound sulfur (per unit area) in carbon blacks increases with decreasing content of oxygen groups on the carbon surface. The isotope-exchange data indicate that the sulfur is present on the carbon surface in the form of stable monosulfide groupings. On this assumption it is possible to calculate the carbon surface occupied by sulfur at equilibrium. The carbon surface occupied by sulfur is plotted in Fig. 6 against the amount of oxygen contained in the carbon. As already noted, these quantities are in an inverse relationship.

It may be concluded from these results that sulfur mainly reacts with the active regions of the carbon surface which are not occupied by oxygen groups. Olefinic double bonds in the surface six-membered carbon rings in the carbon black structure may act as such active regions [7]. The decreased chemisorption of sulfur after

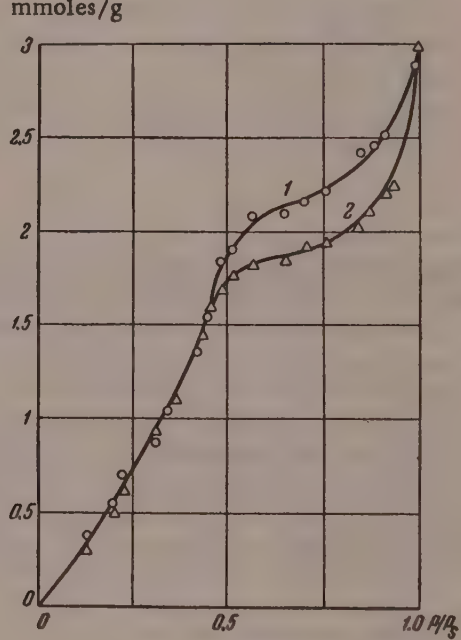


Fig. 5. Isotherm for water vapor adsorption: 1) On channel black; 2) ditto, after addition of 0.7% sulfur.

TABLE 3

Characteristics of Samples of Philblack O

Carbon black	Sp. surf. from N adsorption, m^2/g	pH	Colori- metric No.	Elementary composition, %			
				C	H	S	O by difference
Philblack O	75	8.4	21.7	96.23	1.13	0.80	1.89
Ditto, but heated to 400° for 15 minutes	127	8.7	21.7	96.01	0.46	0.6	2.93
Ditto, but heated to 500° for 30 minutes	137	8.6	22.5	95.4	0.64	0.6	3.36

TABLE 4

Isotope Exchange in Carbon Black Containing Bound Sulfur

Activity I/I_0 before exchange	Exchange time, min.	Activity I/I_0 after exchange		Activity I/I_0 before exchange	Exchange time, min.	Activity I/I_0 after exchange at 130°	
		130°	150°			130°	150°
Without accelerator							
0.05	30	0.064	—	0.24	30	0.222	
	60	0.067	—		60	0.222	
	120	0.060	0.056		120	0.225	
With accelerator A100							

TABLE 5

Surface Occupied by Chemisorbed Sulfur in Various Carbon Blacks

Carbon blacks	Elementary composition, %			Surface occu- pied by added S, in m^2/m^2 of carbon black
	C	H	O by difference	
Ukhta channel	93.04	1.25	5.71	0.064
Ukhta thermal	99.26	0.65	0.09	0.25
Kudinovo lamp	99.54	0.39	0.07	0.35
Dashava furnace	97.45	0.68	1.87	0.172
Channel, hydrogenated at 300°	94.84	1.46	3.7	0.067
Ditto, at 500°	94.80	1.66	3.54	0.073
Channel, heated in hydrogen at 900°	99.32	0.67	—	0.046
Channel, oxidized in air at 350°	82.77	1.57	15.66	0.029
Channel, vacuumized at 800°	97.26	0.47	2.27	0.0485
Ditto, then oxidized in air at 400°	93.58	1.05	5.37	0.029
Ditto, then heated in hydrogen at 1700°	99.65	0.36	—	0.045
Philblack O	96.23	1.13	1.99	0.046
Ditto, heated for 15 minutes at 400°	96.01	0.46	2.93	0.037
Ditto, heated for 30 minutes at 500°	95.4	0.64	3.36	0.030

THE MECHANISM OF VULCANIZATION IN PRESENCE OF 2-MERCAPTOBENZOTHIAZOLE

B. A. Dogadkin and I. A. Tutorskii

One of the commonest vulcanization accelerators is 2-mercaptopbenzothiazole (MBT), known to technologists under the name of Captax. In 1953 two-thirds of the total quantity of accelerators used by the rubber industry of the USA was made up by Captax and its derivatives [1]. This extensive use of MBT as an accelerator has naturally aroused increased interest in the mechanism of its action.

Despite the large number of papers on this subject, the mechanism of vulcanization in presence of MBT is still not clear, and the literature data on the subject are highly contradictory. Some authors [2, 3] consider that MBT interacts with sulfur with formation of H_2S which is added at the double bonds to give polymeric thiols; oxidation of the latter leads to formation of cross links in the vulcanizate. Another viewpoint, associated with the action of the so-called vulcanization activators, is that MBT forms a zinc salt during the vulcanization process, and this salt exerts the accelerating action. These views, based on Bruni and Romani's well-known disulfide theory [4], have been developed by the work of Zaide and Petrov [5], and were recently upheld by Auerbach [6].

It has been shown [7, 8] that the sulfur of the sulphydryl group of MBT is exchanged for elemental sulfur at vulcanization temperatures, and hence the initial stage of the vulcanization process is considered to be identical with the exchange reaction. All these theories either have inadequate experimental basis, or do not take into account all the different effects taking place in vulcanization, or are based on erroneous views which have been refuted by subsequent experimental tests.

The object of the present work was a systematic study of vulcanization in presence of MBT, and an attempt to develop a theory of the action of this accelerator from the experimental results obtained. A detailed study of the nature of the individual reactions taking place in the highly complex vulcanization process was commenced with an investigation of the nature of the reaction between MBT and sulfur. A brief communication on the reaction between MBT and sulfur was published by us earlier [9].

The reaction of MBT with sulfur. This reaction, at the vulcanization temperature, results in the formation of hydrogen sulfide, which was removed from the reaction zone by a continuous current of nitrogen and absorbed in $CdCl_2$ solution. The CdS precipitate was determined iodometrically. The reaction was carried out in melts and in inert solvents—vaseline oil and xylene.

The reaction of H_2S evolution in these conditions proceeds at a constant rate (Fig. 1), which may be attributed to the very slight changes in the concentrations of the reacting substances during the whole reaction time (only 1.5% of the MBT present reacts in 10 hours at 140°). The course of H_2S evolution from a melt of MBT and sulfur at 140° almost coincides with the course of the reaction in solution (see the curve for 141° in Fig. 1). The reaction of H_2S evolution conforms to the Arrhenius equation; the activation energy, determined graphically, is 33.5 kcal/mole.

As a result of the reaction, MBT is converted into a polysulfide, the elementary composition of which corresponds to the formula of dibenzothiazolyl pentasulfide. The absorption spectrum of this substance has a maximum in the 330 m μ region, characteristic of linear polysulfides (Fig. 2, Curve 3).

These results contradict Fisher's view that the principal intermediate reaction in vulcanization is formation of hydrogen sulfide when the accelerator reacts with sulfur. The activation energy of the reaction of

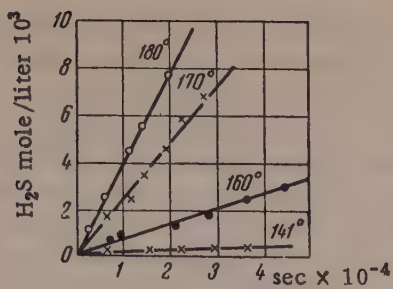


Fig. 1. Kinetics of hydrogen sulfide evolution during the heating of sulfur (0.625 g-atom/liter) with MBT (0.06 mole/liter) at various temperatures in vaseline oil solution.

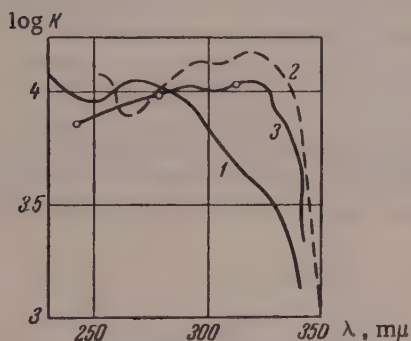


Fig. 2. Absorption spectra of the conversion products of MBT: 1) Altax; 2) reaction product of chlorobenzothiazole and H_2S_2 ; 3) conversion products of MBT.

H_2S formation from sulfur and MBT is 33.5 kcal/mole. The accurate value of the activation energy of the reaction of sulfur addition to purified natural rubber* in absence of accelerator is 33.5** kcal/mole (Fig. 3,a), and that of the reaction of sulfur addition in presence of MBT, 20.9 kcal/mole (Fig. 3,b). Thus, the activation energy of H_2S formation is close to the activation energy of the vulcanization process in absence of accelerator, and is considerably greater than the apparent activation energy of vulcanization in presence of MBT. Because of the high value of the activation energy and the very low rate constant of the reaction of H_2S evolution, the evolution of H_2S cannot be regarded as the principal intermediate reaction in vulcanization.

The chemical interaction of MBT with sulfur is manifested not only in the reaction of H_2S evolution studied by us, but in the isotope exchange reaction of MBT with elemental sulfur, first reported by Miklukhin and Blokh [8], and studied in detail by Gur'ianova [7]. There are indications that in rubber stocks the exchange between MBT and sulfur is retarded [8] or does not proceed at all [6]. To settle this problem, we studied the exchange between MBT and elemental sulfur under vulcanization conditions. Stocks of the following composition (in wt. parts): natural rubber (NR) (purified) 100, S (tagged with S^{35} isotope) 5, MBT 3, Neozone D 1, were vulcanized in a press at 120, 140, and 160°. MBT was separated from sulfur by solution in cold 5% Na_2CO_3 solution followed by precipitation with 10% HCl solution. The course of the exchange reaction was determined from the appearance of radioactive sulfur atoms in the MBT. The kinetics of sulfur addition was studied radiometrically at the same time.

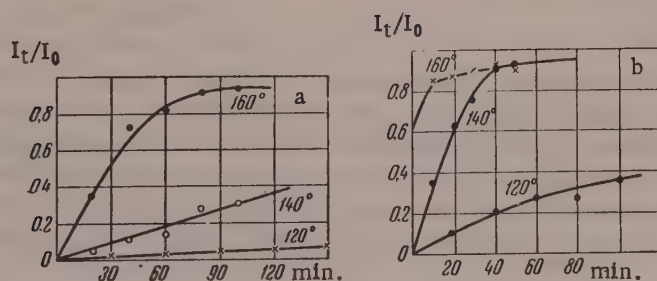


Fig. 3. Kinetics of sulfur addition in stocks of the composition (in wt. parts): a) NR 100, S 5, Neozone D 1; b) NR 100, S 5, MBT 3, Neozone D 1.

* The rubber was purified by extraction with cold acetone for 20 hours in a nitrogen atmosphere, followed by reprecipitation from 1% solution in benzene by addition of methyl alcohol. The bound sulfur was determined radiometrically [10].

** As in original — Publisher's note.

The variations of MBT activity can be represented by curves with maxima (Fig. 4). The dependence of the activity variations on the temperature is anomalous; the curve for 140° lies above the curve for 160°. The course of the variation of MBT activity during vulcanization is indicative of the existence of intermediate compounds with higher relative sulfur contents than MBT. These compounds were extracted in Na_2CO_3 solution together with the unreacted MBT, which shows that they contain thiol groups. The absorption maximum at 330 m μ found for these compounds (Fig. 5) indicates the presence of a polysulfide group. Elementary analysis showed that the S content of these compounds is over 50.2% (the S content of MBT is 38.4%).

The change in the activity of MBT extracted from the stock after vulcanization, which depends both on the rate of the isotope exchange reaction and on the rate of formation and decomposition of intermediate compounds of the polysulfide type, also depends on the concentration of free elemental sulfur. Therefore the curve for the variation of the activity of MBT at 160° lies below the corresponding curve for 140°. If a correction for the sulfur concentration is introduced, the curves assume a normal relative position but retain their maxima.

Therefore the intermediate compound formed by the reaction of MBT with sulfur under vulcanization conditions is a polysulfide of the composition:

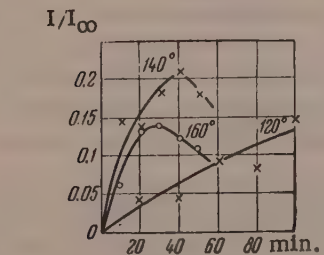


Fig. 4. Variation of the activity of MBT extracted from stocks of the composition: NR 100, MBT 3, S 5, Neozone D 1 wt. part.

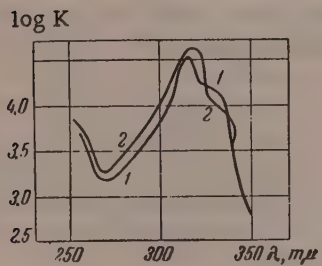
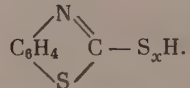


Fig. 5. Absorption spectra of MBT extracted in Na_2CO_3 solution, after reaction with sulfur: 1) In stock; 2) in melt.

Hydrogen polysulfides, a solution of sodium polysulfides was poured into concentrated HCl with cooling [12]. The mixture of hydrogen polysulfides was distilled; the disulfide distilled at 75°. 2-Benzothiazolyl hydrodisulfide was prepared as follows: 5 g of 2-chlorobenzothiazole was added dropwise with stirring to 4.13 g of freshly prepared H_2S_2 dissolved in CS_2 . After 5 minutes a yellow precipitate was formed and the bulb became warm. CS_2 was then distilled off and the product was recrystallized from absolute ethyl alcohol. The melting point of the product was 86°. The results of elementary analysis are given below:

Calculated for $\text{C}_7\text{H}_5\text{NS}_3$ %		Found %
C	42.70	42.60
H	2.52	2.43
N	7.05	7.27
S	48.33	47.35



A representative of this class of compounds (2-benzothiazolyl hydrodisulfide) was synthesized from 2-chlorobenzothiazole and hydrogen polysulfides, and identified by elementary analysis and spectrophotometrically. A characteristic absorption maximum was found at 330 m μ (Curve 3, Fig. 2).

2-Chlorobenzothiazole was synthesized from MBT and PCl_5 in POCl_3 [11]. For preparation of hydrogen polysulfides a solution of sodium polysulfides was poured into concentrated HCl with cooling [12]. The mixture of hydrogen polysulfides was distilled; the disulfide distilled at 75°. 2-Benzothiazolyl hydrodisulfide was prepared as follows: 5 g of 2-chlorobenzothiazole was added dropwise with stirring to 4.13 g of freshly prepared H_2S_2 dissolved in CS_2 . After 5 minutes a yellow precipitate was formed and the bulb became warm. CS_2 was then distilled off and the product was recrystallized from absolute ethyl alcohol. The melting point of the product was 86°. The results of elementary analysis are given below:

The molecular weight of the substance, determined cryoscopically in thymol solution, was 191 (the theoretical value for 2-benzothiazolyl hydrodisulfide is 199). An attempt to obtain a substance with a higher sulfur content was not successful, apparently owing to the instability of the polysulfide groups.

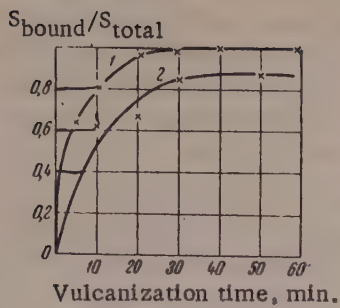


Fig. 6. Kinetics of sulfur addition in the vulcanization of SKB stocks at 143° in presence of MBT (1) and its zinc salt (2).

canization of these mixtures at 143° is plotted in Fig. 6. It is seen that the rate of sulfur addition is lower in presence of the zinc salt of MBT than in presence of MBT itself. Therefore, in contradiction of Auerbach's views, the formation of the zinc salt cannot be regarded as the determining factor in the accelerating action of MBT.

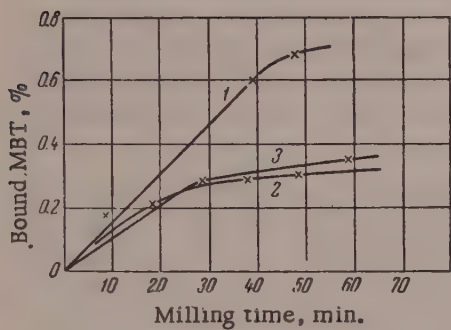


Fig. 7. Addition of MBT during mastication of natural rubber: 1) in air; 2) in nitrogen containing 0.5% O₂; 3) in nitrogen.

Reaction of MBT with rubber. It was shown by Dogadkin et al., [14, 15] that derivatives of Captax — Altax and Sulfenamide BT — react chemically with rubber; this is a very important factor in vulcanization in presence of these accelerators. It was therefore of interest to determine the extent to which interaction of MBT with rubber influences the vulcanization process in presence of this accelerator. Our experiments showed that addition of MBT to rubber occurs even at the first stage of the technological process, during mastication. The amount of MBT added to rubber was determined radiometrically and by oxidation with a mixture of HNO₃ and Br₂ in presence of MgO with subsequent determination of SO₄ as barium sulfate [16]. Structural changes in the rubber were determined viscosimetrically.

Addition of MBT to rubber proceeds at the highest rate during mastication in air (Fig. 7); the solution viscosity decreases at the highest rate under the same conditions (Fig. 8). This confirms that the action of MBT is associated with activation of oxidation processes [17]. However, the viscosity of the rubber solution decreases (Fig. 8) and MBT is added to rubber (Fig. 7) even during mastication in pure nitrogen (Fig. 7).

The reaction of 2-benzothiazolyl hydrodisulfide with sodium butadiene rubber causes extensive degradation of the latter under mastication conditions, with a decrease of the rate and degree of cross linking during vulcanization.

Effect of the zinc salt of MBT on the vulcanization process. As was noted above, a number of investigators consider [4, 6] that the accelerating effect of MBT is associated with its conversion into the zinc salt. Others [13] have shown that vulcanization activators — zinc oxide and stearic acid — have almost no effect on the rate of sulfur addition, but greatly increase the rate of cross linking. It was therefore desirable to compare the accelerating effects of MBT and its zinc salt. Mixtures of sodium butadiene rubber without fillers, containing 1 wt. part of MBT or its zinc salt, were prepared for this purpose. The course of sulfur addition during vul-

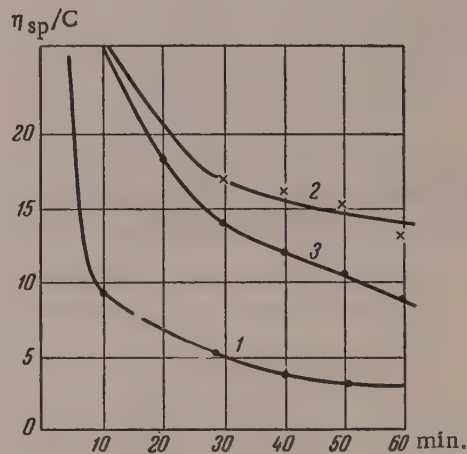


Fig. 8. Variation of intrinsic viscosity during mastication of natural rubber: 1) in air; 2) in nitrogen containing 0.5% O₂; 3) in nitrogen.

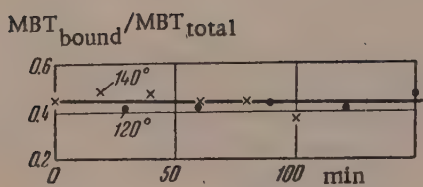


Fig. 9. Heating of MBT with natural rubber in the press at 120 and 140°.

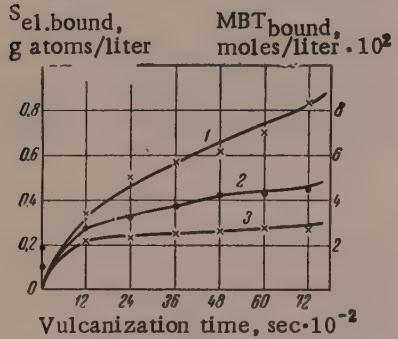


Fig. 10. Addition of sulfur and MBT during vulcanization of natural rubber at 120°: 1) sulfur; 2) MBT with ZnO; 3) MBT without ZnO.

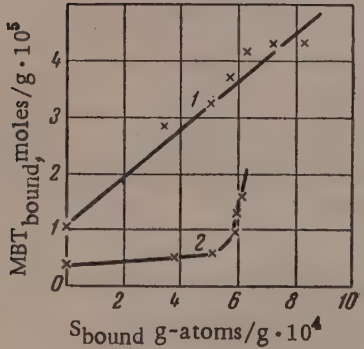


Fig. 11. Amount of bound sulfur as a function of bound MBT: 1) NR; 2) SKB.

cally, and the sulfur (elemental and combined in the accelerator) bound with the rubber was determined by oxidation of the vulcanizate with a mixture of HNO_3 and Br_2 in presence of MgO , followed by determination of SO_4^{2-} as barium sulfate.

Moreover, MBT decreases the viscosity and is added to the polymer during cold mastication of saturated polymers such as polyisobutylene. The only explanation for these facts is that the free radicals formed by mechanical rupture of the covalent bonds of the rubber molecule (polymeric radicals) react with the MBT molecule, saturating their free valences, so that their recombination is hindered and the molecular weight falls sharply.

Natural rubber, masticated with 1 wt. part of MBT in a nitrogen atmosphere, was fractionated; it was found that the fractions of lower molecular weight had considerably higher MBT contents. This suggests that MBT is added mainly at the ends of the radicals formed by mechanical rupture of the molecular rubber chains.

When the masticated product was heated in a press at vulcanization temperatures, very little addition of MBT to the rubber took place (Fig. 9); this is in agreement with reports in the literature that mercaptans do not add on to olefins in absence of catalysts [18].

Thus, addition of MBT to the rubber already takes place during mastication. Addition of MBT to rubber does not take place on heating in absence of sulfur. The interaction of MBT with rubber has a complex mechanism, and depends on a combination of mechanical, thermal, and oxidative processes. The interaction of MBT with rubber has been considered in greater detail elsewhere [19].

Conversions of MBT in vulcanization conditions. For determination of the mechanism of the reactions in rubber-sulfur-accelerator ternary systems, a sample of MBT tagged with S^{35} radioisotope in the thiazole ring was synthesized. The synthesis was carried out as follows: MBT was synthesized from phenyl mustard oil and elemental S^{35} by Jacobson's method [20]. Gur'yanova and Kaplunov [21] showed that both the sulfur atoms are tagged under these conditions. The MBT was then heated at 140° with excess of elemental inactive sulfur for 6 hours. The exchange reaction reaches equilibrium during this time, and the MBT formed is tagged in the thiazole ring only. The activity of the MBT was halved. The MBT molecule was therefore tagged with a sulfur atom which does not exchange with elemental sulfur under vulcanization conditions; it was thus possible to follow the course of sulfur addition and of the reaction of addition of the accelerator to the rubber. The MBT so prepared was used for vulcanization of NR and SKB stocks without fillers, with and without zinc oxide. The amount of MBT added to the rubber was determined radiometrically, and the sulfur (elemental and combined in the accelerator) bound with the rubber was determined by

The reactions of addition of sulfur and accelerator to the rubber occur in parallel (Fig. 10). Rather more MBT is added in presence of zinc oxide (Curve 2, Fig. 10) than in its absence (Curve 3, Fig. 10). The ratio of bound sulfur to bound MBT remains constant during the vulcanization; this is shown by the linear relationship between the bound sulfur and the MBT added (Fig. 11). There is a linear relationship between the number of cross links and the amount of bound MBT (Fig. 12).

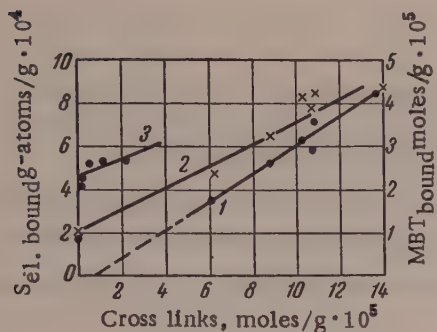


Fig. 12. Dependence of the number of cross links on: 1) amount of bound sulfur: bound MBT; 2) NR; 3) SKB.

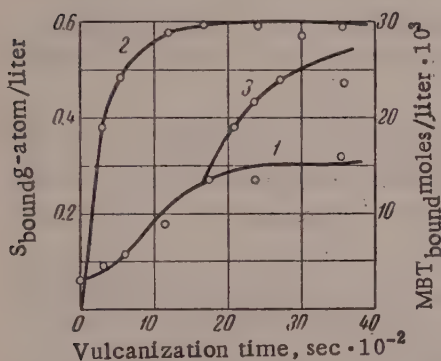


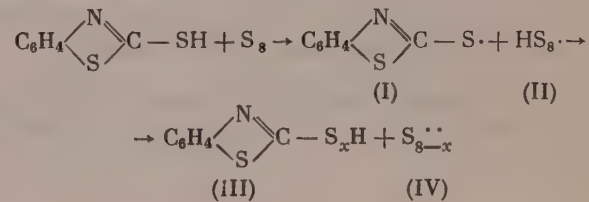
Fig. 13. Kinetics of the addition of sulfur (1) and MBT (2) in the vulcanization of SKB at 143°. Sulfur introduced into the vulcanizate by swelling (3).

The reactions of sulfur and accelerator addition also follow a similar course in the vulcanization of SKB stocks (Fig. 13). After the addition of sulfur to the rubber is complete, the addition rate of MBT is also retarded sharply, although its concentration in the mixture is still relatively high. This fact indicates that there is a direct connection between the reactions of sulfur and accelerator addition to the rubber, and is in agreement with literature data on the catalytic action of sulfur on the addition of mercaptans to olefins. Direct confirmation of the fact that addition of MBT to rubber proceeds at an appreciable rate only in the presence of sulfur is provided by an experiment on the introduction of sulfur into the vulcanizate by swelling. Introduction of sulfur into the vulcanizate (at the stage of complete sulfur addition) increases the rate of MBT addition to the rubber (Curve 3, Fig. 13). Thus, when sulfur and MBT react with rubber, the reagents activate each other, i.e., reactive forms (probably free radicals) of the sulfur and accelerator are formed simultaneously.

DISCUSSION OF RESULTS

On the basis of the above experimental data, we consider that the following mechanism of vulcanization in presence of MBT is probable.

When MBT reacts with sulfur, 2-thiobenzothiazolyl and persulphydryl radicals are formed simultaneously.



The $\text{C}_6\text{H}_4 \begin{array}{c} \text{N} \\ \diagup \\ \text{S} \end{array} \text{C} - \text{S}\cdot$ reacts with sulfur, with scission of the eight-atom ring, or (as was examined

by one of the present authors [14]) with rubber, with removal of hydrogen from the α -methylene group, and is reduced to MBT or added at the double bond.

The $\text{HS}_8\cdot$ radical can be added on at double bonds with formation of polymeric permercaptans; oxidation of the latter or their interaction with double bonds results in the formation of polysulfide bonds. By this reaction mechanism the number of sulfur atoms in the sulfide bonds in the vulcanizate, large at the start of the process, should gradually decrease owing to breakdown and regrouping of the polysulfide bonds. This is in agreement with the findings that the amount of sulfur involved in isotope exchange decreases steadily as vulcanization proceeds [22].

Recombination of the benzothiazolyl and persulphydryl radicals results in the formation of 2-benzothiazolyl hydropolysulfide, liberating a variable number of sulfur atoms in the form of $S_8\cdot\cdot_x$ biradicals, which directly join the rubber molecular chains.

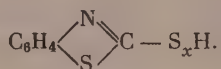
This mechanism is in agreement with our data [23] according to which the rate constant for the addition of sulfur is a linear function of the accelerator concentration. Therefore the determining stage in the vulcanization process in presence of MBT is reaction of the accelerator with sulfur according to the scheme described above.

SUMMARY

1. The kinetics of hydrogen sulfide evolution during the interaction of MBT with sulfur in the 140-180° range was studied. The activation energy of the process is 33.5 kcal/mole. Because of its high activation energy, this reaction cannot be regarded as the main intermediate reaction in vulcanization.

2. The isotope exchange reaction of MBT with sulfur was studied under conditions of practical vulcanization. The activity of the MBT extracted from the vulcanize is represented by a curve with a maximum.

3. One of the intermediate compounds formed in the reaction of MBT with sulfur under vulcanization conditions is a polysulfide of the composition:



4. 2-Benzothiazolyl hydrodisulfide was synthesized from 2-chlorobenzothiazole and hydrogen disulfide.

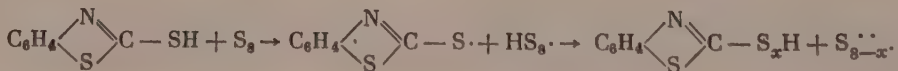
5. Addition of MBT occurs during the cold mastication of natural, sodium butadiene, and polyisobutylene rubbers in different gaseous media; the rate is greatest during mastication in air. The solution viscosities decrease sharply under the same conditions.

6. Almost no addition of MBT to rubber takes place on heating in a press at vulcanization temperatures.

7. The kinetics of sulfur addition to purified natural rubber in absence of accelerator and in presence of MBT was studied in the 120-160° range. The activation energy of sulfur addition was found to be 35.5 and 20.95 kcal/mole respectively.

8. In the vulcanization of natural or sodium butadiene rubber stocks, the addition of sulfur and of MBT are coupled reactions. Addition of MBT to rubber occurs only in presence of sulfur. Consequently, mutual activation of sulfur and MBT takes place under vulcanization conditions, i.e., reactive forms (probably free radicals) of sulfur and the accelerator are formed simultaneously. The amount of MBT added to the rubber is a linear function of the amount of sulfur added.

9. It is suggested that the mechanism of the accelerating action of MBT depends on the formation of 2-thiobenzothiazolyl and persulphydryl radicals according to the scheme:



10. The zinc salt of MBT is not a more active accelerator than MBT itself in the vulcanization of SKB stocks.

LITERATURE CITED

- [1] Report of Conference on Accelerators, Akron, USA, April 6, 1956; Rubber Age 79, 459 (1956).
- [2] H. Fisher, Ind. Engng. Chem. 31, 1381 (1939).

- [3] I. T. Taranenko, Light Industry, No. 3, 24 (1955).
- [4] G. Bruni and E. Romani, India-Rubber J. 62, 63 (1921).
- [5] D. A. Zaide and K. D. Petrov, J. Rubber Ind. 12, 665 (1935).
- [6] J. Auerbach, Ind. Eng. Chem. 45, 1526 (1953).
- [7] E. N. Gur'ianova, Proc. Acad. Sci. USSR 98, 229 (1954).
- [8] G. A. Blokh, E. A. Golubkova and G. P. Miklukhin, Light Industry 7, 25 (1952); Proc. Acad. Sci. USSR 90, 201 (1953).
- [9] B. Dogadkin and I. Tutorskii, Proc. Acad. Sci. USSR 108, 259 (1956).*
- [10] B. A. Dogadkin, Z. N. Tarasova and M. Ia. Kaplunov, Factory Labs. 4, 296 (1955).
- [11] N. Drozdov and V. Stavrovskaya, J. Gen. Chem. 7, 2813 (1937).
- [12] J. Bloch and F. Hohn, Ber. 41, 1965 (1908).
- [13] B. Dogadkin and I. Beniska, Colloid J. 18, 167 (1956).*
- [14] B. A. Dogadkin, M. S. Fel'dshtein, A. V. Dobromyslova, V. V. Shkurina and M. Ia. Kaplunov, Proc. Acad. Sci. USSR 92, 61 (1953); B. A. Dogadkin, V. V. Seliukova, Z. N. Tarasova, A. V. Dobromyslova, M. S. Fel'dshtein and M. Ia. Kaplunov, Colloid J. 17, 215 (1955).*
- [15] B. A. Dogadkin and M. S. Fel'dshtein, J. Appl. Chem. 28, 533 (1955).*
- [16] J. Franta, Gumarenska technologia (Praha, 1953).
- [17] B. A. Dogadkin, B. K. Karmin, A. V. Dobromyslova and L. F. Sapozhkova, Colloid J. 10, 268 (1948); E. P. Kheraskova and A. P. Gamaianova, Colloid J. 12, 146 (1950).
- [18] S. O. Jones and E. E. Reid, J. Amer. Chem. Soc. 60, 2452 (1938).
- [19] B. A. Dogadkin, A. V. Dobromyslova, L. F. Sapozhkova and I. A. Tutorskii, Colloid J. 19, 421 (1957).*
- [20] P. Jacobson and A. Frankenbacher, Ber. 24, 1402 (1891).
- [21] E. N. Gur'ianova and M. Ia. Kaplunov, Proc. Acad. Sci. USSR 94, 53 (1954).
- [22] B. A. Dogadkin, Paper at International Symposium on Macromolecular Chemistry, Prague (1957).**
- [23] B. A. Dogadkin, I. A. Tutorskii and D. M. Pevzner, Proc. Acad. Sci. USSR 112, 449 (1957).*

The M. V. Lomonosov Institute
of Fine Chemical Technology, Moscow

Received March 2, 1958

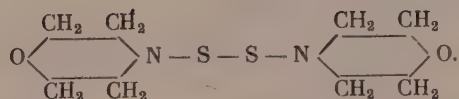
*Original Russian pagination. See C. B. Translation.

**In Russian.

THE VULCANIZING ACTION OF CERTAIN HETEROCYCLIC DISULFIDES

M. S. Fel'dshtein, I. I. Eitingon, D. M. Pevzner, and B. A. Dogadkin

The possible use of organic di- and polysulfides [1, 2], which are simultaneously accelerators and independent vulcanization agents, is of considerable interest in relation to intensification of technological processes in rubber production. The present communication contains the results of a study of the action of heterocyclic disulfides containing $>N-S-S-N<$ bonds in the molecule. Compounds of this type include N,N'-dithiodimorpholine



The vulcanizing action of N,N'-dithiodimorpholine was studied in stocks based on SKS-30A butadiene-styrene rubber without elemental sulfur. For comparison, the course of vulcanization of stocks containing sulfur was studied in parallel experiments. In the former case 7.4 wt. parts of N,N'-dithiodimorpholine was introduced into the stock; this corresponded to 2 wt. parts of sulfur per 100 wt. parts of rubber — the amount generally used in rubber stocks containing vulcanization accelerators. The data in Fig. 1 show that N,N'-dithiodimorpholine produces a much greater vulcanization effect than is found in stocks containing elemental sulfur (in absence of accelerator).

The strength characteristics of dithiodimorpholine vulcanizates at the vulcanization optimum are quite comparable with those of vulcanizates made with the use of sulfur and an accelerator — benzothiazolesulfen-diethylamide (Sulfenamide BT). The vulcanizing action of N,N'-dithiodimorpholine is greatly increased in presence of such accelerators as mercaptobenzothiazole (MBT), dibenzothiazole disulfide (DBTD), and Sulfenamide BT. The vulcanization systems obtained by the combined use of N,N'-dithiodimorpholine and the above-named accelerators are so effective that the concentration of the vulcanization agent introduced into the stock can be reduced considerably. It follows from the data in Fig. 2 that the vulcanization system N,N'-dithiodimorpholine — DBDT (without sulfur) yields, at the vulcanization optimum (40–50 minutes at 138°), vulcanizates of equal modulus to those obtained with the use of Sulfenamide BT and considerable amounts (3.0 wt. parts) of sulfur. During the first stage of the process (in the first 30 minutes) the vulcanization rate in stocks containing N,N'-dithiodimorpholine is lower than in sulfur stocks containing Sulfenamide BT.

Because of this course of vulcanization in systems with N,N'-dithiodimorpholine, such systems have less tendency to scorching at higher curing temperatures. Thus, stocks with N,N'-dithiodimorpholine, like stocks with Sulfenamide BT, have shown no tendency to scorching at 110°. Data on the variation of the Mooney plasticity (Fig. 3) show that the viscosity curve at 130°, which represents the vulcanization effect in a stock containing Sulfenamide BT, ascends steeply, whereas the stock containing N,N'-dithiodimorpholine gives a much flatter curve. Thus, the vulcanization process occurs rapidly at temperatures above 130° in stocks containing N,N'-dithiodimorpholine as vulcanization agent (with DBDT accelerator).

Because of this peculiarity in the course of vulcanization of stocks containing N,N'-dithiodimorpholine as accelerator and vulcanization agent, the systems retain their viscofluid state for a longer time during the initial stage of vulcanization. This fact, and also the absence of free sulfur, which therefore cannot migrate

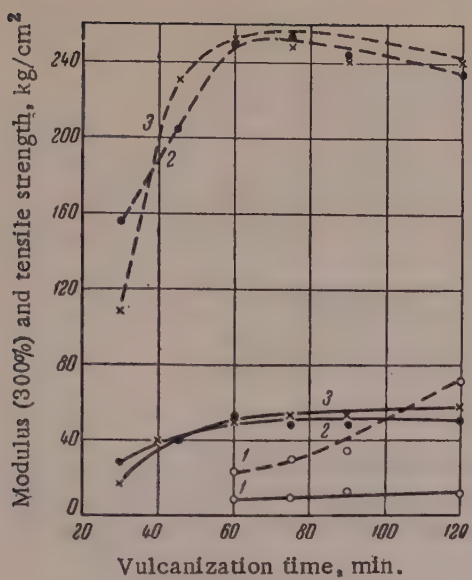


Fig. 1. Strength characteristics of vulcanizates with channel black, containing: 1) 5 wt. parts sulfur; 2) 7.4 wt. parts N,N'-dithiodimorpholine; 3) 2 wt. parts sulfur and 1 wt. part Sulfenamide BT. —— modulus; --- tensile strength.

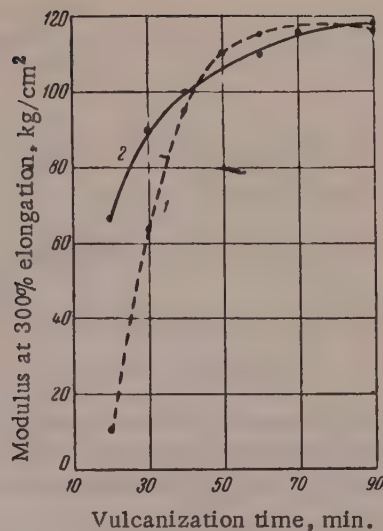


Fig. 2. Effect of N,N'-dithiodimorpholine in stocks of the breaker type, containing: 1) 3.7 wt. parts N,N'-dithiodimorpholine and 1 wt. part DBDT; 2) 3 wt. parts sulfur and 1 wt. part Sulfenamide BT.

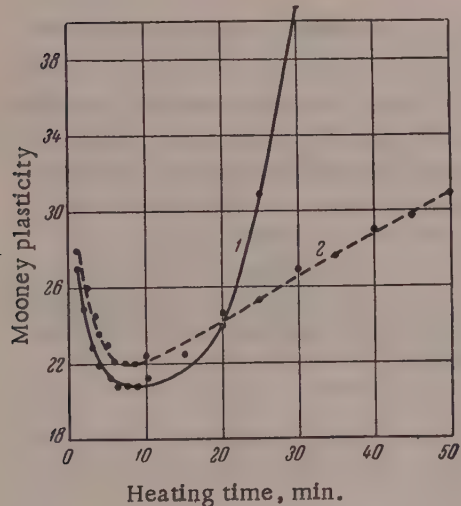


Fig. 3. Variation of Mooney plasticity in stocks of the breaker type at 130°, containing: 1) 3 wt. parts sulfur and 1 wt. part Sulfenamide BT; 2) 3.7 wt. parts N,N'-dithiodimorpholine and 1 wt. part DBDT.

to the surface of the raw rubber stocks, has a favorable influence on the continuity of multilayer rubbers. Thus, replacement of sulfur vulcanizing systems by N,N'-dithiodimorpholine increases the dynamic endurance of plied vulcanizates from 1000 to 1700 cycles. N,N'-dithiodimorpholine also has a favorable influence on the resistance of vulcanizates to the spread of cracks during repeated flexing; this value increases from 117,500 (for ordinary vulcanization systems) to 225,000 cycles. The higher fatigue resistance of vulcanizates made with the used of N,N'-dithiodimorpholine is probably the result of the presence of stable vulcanization bonds.

The above results therefore show that the use of heterocyclic disulfides, in particular N,N'-dithiodimorpholine, produces a considerable improvement in a number of important technical properties of vulcanizates. In these systems the vulcanization is effected at higher temperatures, and the possibilities for intensifying the processing of rubber stocks are thereby increased. The economic aspects of the use of these vulcanization agents depend primarily on the possibility of using them in smaller quantities. It is therefore necessary to find activators which would make it possible to use them in the quantities usual for the common vulcanization accelerators.

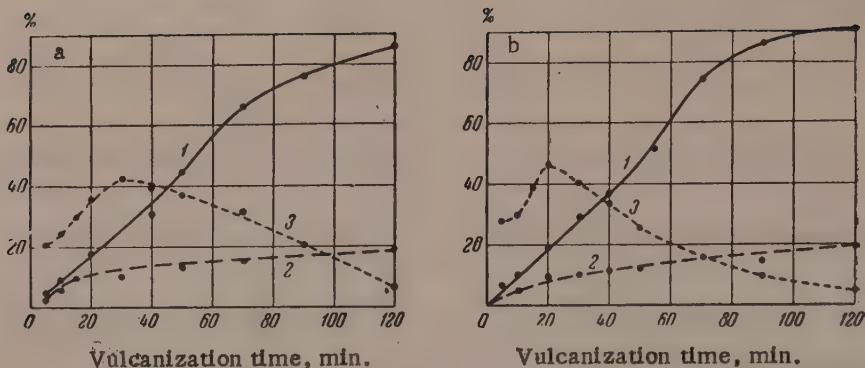
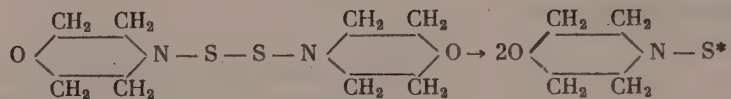


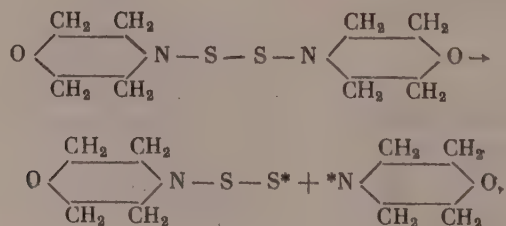
Fig. 4. Addition of sulfur and nitrogen during vulcanization of fillerless stocks with N,N' -dithiodimorpholine (a) and N,N' -dithiodipiperidine (b) 1) bound sulfur $S_{\text{bound}}/S_{\text{total}}$, %; 2) bound nitrogen $N_{\text{bound}}/N_{\text{total}}$, %; 3) "true" free sulfur $S_{\text{free}}/S_{\text{total}}$, %.

The independent vulcanizing action of N,N' -dithiodimorpholine may be the consequence of its decomposition at the S-S bond to give free radicals

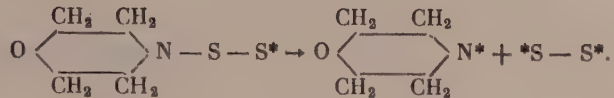


followed by their interaction with the rubber molecules by the mechanism described by us for dibenzothiazole disulfide and benzothiazolesulfendiethylamide [3, 4].

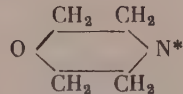
If so, vulcanization should result in the formation of structures the sulfur and nitrogen contents of which should correspond to the sulfur and nitrogen contents in the thiomorpholine radical. To test this, in addition to the studies of the kinetics of sulfur and nitrogen addition (after acetone extraction), changes in the content of the so-called "true" free sulfur in vulcanizates made with N,N' -dithiodimorpholine in the course of vulcanization were determined. The "true" free sulfur was determined by the Schulte method [5] in the same vulcanizate specimens, but without previous extraction. It follows from Fig. 4 that both sulfur and nitrogen are added to the rubber during vulcanization. The curves for the addition kinetics ascend steadily, but considerably more sulfur than nitrogen is added. The excess of added sulfur indicates that asymmetrical decomposition of N,N' -dithiodimorpholine also occurs, according to the scheme:



subsequently this may lead to liberation of "free" sulfur in the form of a biradical

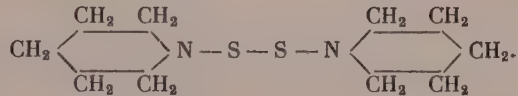


The liberation of sulfur and its subsequent interaction with the rubber is reflected in the course of Curve 3, Fig. 4. The radicals



are stabilized, either by recombination or by acceptance of hydrogen from the rubber molecules. The explanation for the maximum on the kinetic Curve 3 (Fig. 4) is that in the initial stage of vulcanization the rate of decomposition of N,N'-dithiodimorpholine exceeds the rate of addition of sulfur to the rubber.

To determine whether this vulcanizing action is characteristic of N,N'-dithiodimorpholine only, or whether it is also found in other heterocyclic compounds of this type, containing $>\text{N}-\text{S}-\text{S}-\text{N}<$ bonds, the vulcanization activity of N,N'-dithiodipiperidine



was studied.

The results showed that the structuring (vulcanizing) effect of N,N'-dithiodipiperidine is even greater than the effect produced by N,N'-dithiodimorpholine. Data on the course of addition of sulfur and nitrogen and liberation of free sulfur during vulcanization of rubber with the use of N,N'-dithiodipiperidine are plotted in Fig. 4. The kinetic curves for vulcanization with N,N'-dithiodipiperidine are similar to the curves obtained with the use of N,N'-dithiodimorpholine.

SUMMARY

1. The kinetics of vulcanization (structure formation) of rubber by the action of N,N'-dithiodimorpholine is described.
2. Vulcanization with N,N'-dithiodimorpholine is accompanied by addition of sulfur and nitrogen; the amount of bound sulfur is considerably greater than the amount of bound nitrogen (calculated as equivalents).
3. The vulcanizing action of N,N'-dithiodimorpholine is considered to be the result of unsymmetrical decomposition of this compound into free radicals.

LITERATURE CITED

- [1] D. Beaver and M. Throdahl, Rubber Chem. Techn. 17, 4, 896 (1944); 18, 1, 110 (1945).
- [2] R. Sibley, Rubber Chem. Techn. 24, 1, 211 (1951).
- [3] B. Dogadkin, M. Fel'dshtein, A. Dobromyslova, V. Shkurina and M. Kaplunov, Proc. Acad. Sci. USSR 92, 1 (1953).

[4] B. Dogadkin, M. Fel'dshtein and D. Pevzner, J. Appl. Chem. 28, 5, 533 (1955).*

[5] A. Dymov, Technical Analysis of Ores and Metals (State Tech. Press, 1949).**

Scientific Research Institute
for the Tire Industry
Moscow

Received January 23, 1958

*Original Russian pagination. See C. B. Translation.

**In Russian.

IONIC DEPOSITION FROM CARBOXYLIC DIVINYL - STYRENE REFLEXES

D. M. Sandomirskii, Iu. L. Margolina, B. A. Dogadkin and L. S. Krokhina

The production of rubber articles directly from latex by ionic deposition is based on the interaction of the electrolyte cations diffusing into the latex, with the protective membranes of the globules. This interaction results in destabilization of the globules and formation of a gel [1]. In practice, this method is suitable only for latexes which give fairly strong gels and vulcanizates without fillers. Until recently only natural and chloroprene latexes satisfied this condition, and the industrial adoption of the ionic deposition method was therefore restricted. As is known, synthetic rubbers containing carboxyl groups in the molecule give very strong vulcanizates without fillers [2]. Preliminary experiments showed that carboxylic latexes yield fairly strong gels by ionic deposition. It was therefore desired to carry out a systematic study of ionic deposition from carboxylic latexes.

Two carboxylic divinyl-styrene latexes, differing in their contents of metacrylic acid, were studied. The composition and certain properties of these latexes are given in Table 1.

TABLE 1
Composition and Properties of KL-4 and KL-10 Latexes

Latexes	Constituents				pH	Dry solids, %	Sp.g.	Surface tension, dynes/cm	Viscosity centipoises
	butadiene	styrene	meth- acrylic acid	water					
KL-4	70	30	4	200	4.0	19.90	0.998	54.2	2.04
KL-10	70	30	10	200	3.0	18.04	1.01	38.8	2.16

The pH of these latexes may be varied over a wide range by additions of different amounts of concentrated ammonia solution; these cause appreciable variations in the properties of the latexes. For example, as the pH is increased from 4 to 10.1, the surface tension of KL-4 latex decreases from 54.2 to 40.1 dynes/cm. Viscosity changes in latexes containing 4 and 10% of methacrylic acid are slight.

The coagulant used for the ionic deposition had the following composition (parts by weight): calcium chloride 18, kaolin 25, phenol 1, water 56. The extent of deposition was determined from the thickness of a dried (3-4 hours at 60°) and vulcanized (30 minutes at 104°) film.

The course of deposition from the two latexes at different pH is plotted in Fig. 1. It follows from these results that the rate of ionic deposition depends considerably on the pH of the latex, decreasing with increasing pH. This is especially noticeable in the case of KL-10 latex.

It was stated above that the physical, mechanical, and other properties of the gels formed by ionic deposition largely determine the practical applicability of this method. In particular, the use of divinyl-styrene latex with Nekal as emulsifier is impossible because very loose and weak gels are formed. The carboxylic

* The authors thank B. E. Kutsenok for preparation of the latex samples.

latexes under investigation gave quite a different result. The gels formed were fairly strong, and could be subjected to further processing.

The effects of latex pH on the tensile strength and relative elongation of gels made from KL-4 latex are plotted in Fig. 2. These properties were determined by Medalia's method [3], with certain modifications. The

syneresis was effected in air at room temperature. The latex pH has little effect on the strength of fresh gels, but has a strong influence on gels subjected to longer syneresis and drying. The tensile strength rises sharply with increase of pH. (It is possible that the dynamometer used was not sensitive enough to detect the influence of pH on gel strength after 3 hours of syneresis.)

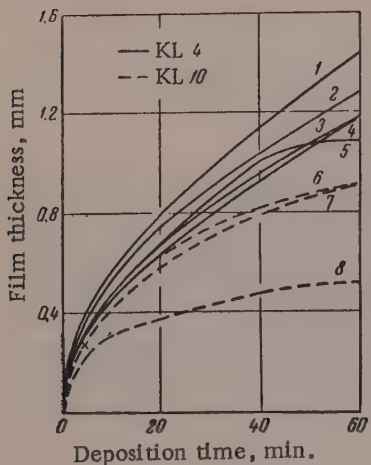


Fig. 1. Course of deposition from carboxylic latexes at different pH: 1) 4; 2) 7.6; 3) 8.7; 4) 9.6; 5) 10.1; 6) 7.9; 7) 9.4; 8) 10.4.

As it was found that latex pH has a considerable influence on the physical and mechanical properties of dried films (the moisture content of the gels after 24 hours of syneresis in air varied in the range 9.7-11.4%), it was of interest to determine whether this applies to vulcanizates. To avoid excessive complication of the system, thermal vulcanizates were used in these experiments. The gel was subjected to syneresis in water for 2 hours without removal from the form, dried for 12 hours at room temperature, and then vulcanized at 104° for 30 minutes. The results, plotted in Fig. 3, show that the influence of the pH of the original latex is even more pronounced in vulcanizates than in dried films. This influence increases with increase of methacrylic acid content. To determine the cause of this effect, the nominal equilibrium modulus*, swelling in benzene, and tensile strength at 100° of the vulcanizate films were determined. Parallel determinations were carried out on films obtained by ionic deposition and by drying. The results are given in Figs. 3 (Curve 2), 4, and 5.

The experimental results clearly show that the pH of the latex has a significant influence on the properties of films made by ionic deposition but has almost no effect on the properties of films made by drying.

Increase of pH increases the tensile strength (both at room and at elevated temperatures) and the nominal-equilibrium and equilibrium moduli, and decreases the relative elongation and maximum swelling. All this indicates that structure formation takes place, and it seems likely that the structurizing agent consists of the calcium ions which diffuse into the latex during ionic deposition, in the same way as calcium oxide acts as a vulcanizing agent in carboxylic rubbers [2]. As the coagulant diffuses into a carboxylic latex, the calcium ions interact not only with the protective membranes of the globules (as is the case in other latexes), but also with the carboxyl groups in the polymer molecules. The calcium atoms may react with carboxyls contained in different polymer molecules and join them by stable chemical cross links to form a single spatial network.

If this supposition is correct, then films formed by ionic deposition from latexes of different pH should differ in their contents of combined calcium. Films were made by ionic deposition from KL-4 and KL-10 latexes at pH 3.5 and 10.4; they were washed thoroughly in boiling water [4], and their calcium contents were determined. The results are given in Table 2.

The combined calcium undoubtedly includes both the calcium which reacted with the carboxyl groups of the polymer molecules, and the calcium in the insoluble compounds formed by reaction with the emulsifier [4]. However, the amount of emulsifier can hardly depend on the pH of the latex. The main cause of the

* The equilibrium modulus was also determined for films obtained by ionic deposition from KL-4 latex.

TABLE 2
Combined Calcium Contents

Latex	Combined calcium, %	
	pH 3.5	pH 10.4
KL-4	0.4	1.4
KL-10	0.8	2.5

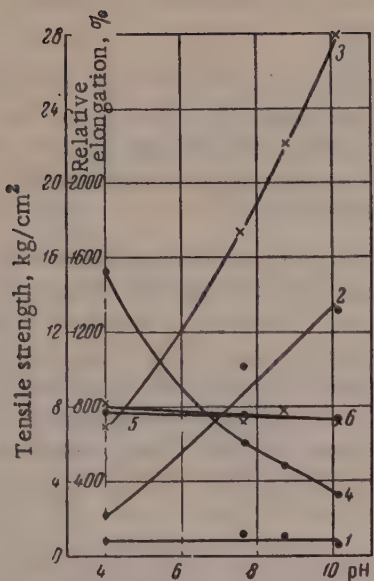


Fig. 2. Effect of pH of KL-4 latex on the mechanical properties of gels after different syneresis time: tensile strength: 1) 3 hours; 2) 6 hours; 3) 24 hours. Relative elongation: 4) 3 hours; 5) 6 hours; 6) 24 hours.

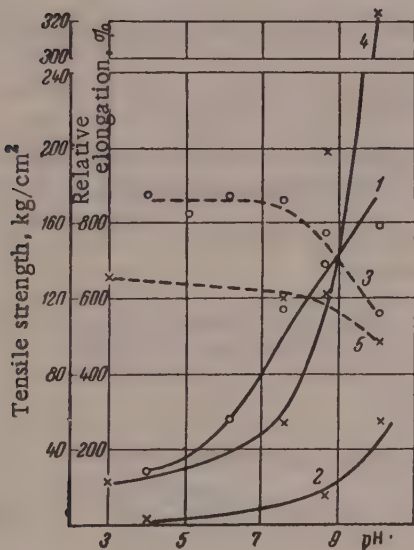


Fig. 3. Effect of pH on the mechanical properties of vulcanizates made from KL-4 and KL-10 latexes: KL-4 latex: 1) tensile strength at room temperature; 2) ditto, at 100°; 3) relative elongation. KL-10 latex: 4) tensile strength; 5) relative elongation.

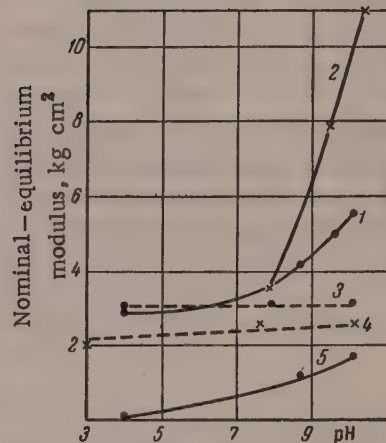


Fig. 4. Influence of pH on the modulus of vulcanizates made from KL-4 and KL-10 latexes. Nominal-equilibrium modulus: 1) ionic deposition from KL-4; 2) ditto, from KL-10; 3) drying from KL-4; 4) ditto, from KL-10; 5) equilibrium modulus, ionic deposition from KL-4 latex.

dependence of the amount of combined calcium and of the properties of the films formed on the latex pH is evidently the influence of pH on the number of carboxyl groups which react with the calcium ions; this number and the density of the cross-linked network increase with increasing pH.

A polymer molecule containing carboxyl groups can be regarded as an acid of high molecular weight. At low pH such an acid is dissociated very little, and its reaction with calcium chloride is hindered, as it would lead to the formation of strongly dissociated product, HCl. In an alkaline ammoniacal medium the polymeric acid is converted into the corresponding ammonium salt, which dissociates into ammonium cations and polymeric anions; the latter react with calcium cations and form weakly dissociated calcium salts.

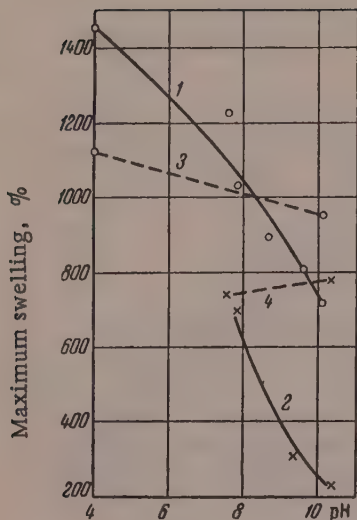


Fig. 5. Influence of pH on the maximum swelling of vulcanizates from KL-4 and KL-10 latexes in benzene. 1) Ionic deposition from KL-4; 2) ditto, from KL-10; 3) drying from KL-4; 4) ditto, from KL-10.

Therefore at high pH the coagulant ions are used not only in the reaction with the emulsifier, but also in a reaction with the polymer. This decreases the deposition rate and increases the density of the spatial network in the product.

In an acid medium, interaction of the coagulant ions with the polymer is considerably less important, but it nevertheless occurs. This is shown, in particular, by the existence of an equilibrium modulus in films made from acid latexes.

Increase of the methacrylic acid content also decreases the deposition rate, probably because of a decrease in the proportion of calcium chloride which interacts with the protective membranes of the globules. At the same time, the influence of pH on the film properties naturally becomes greater with increasing carboxyl group content in the polymer, as the proportion of calcium chloride to interact with the latter increases correspondingly.

In practice, the gels formed by ionic deposition always contain unreacted calcium chloride. During the subsequent operations — syneresis, drying, and vulcanization — it interacts with an increasing number of carboxyl groups in the polymer molecules; this accounts for the observed increase in the influence of pH on structure formation in the vulcanized films as compared with the fresh gels.

SUMMARY

1. Ionic deposition by the action of calcium chloride on butadiene-styrene latexes containing 4 and 10% of methacrylic acid was studied at different pH.
2. The deposition rate decreases with increasing methacrylic acid content and latex pH.
3. The latex pH has a significant influence on the properties of gels and of raw and vulcanized films made by ionic deposition, and has almost no influence on the properties of films made by drying.
4. Increase of the latex pH increases the tensile strength and equilibrium modulus, and decreases the relative elongation and maximum swelling of films made by ionic deposition.
5. In ionic deposition from carboxylic latexes, calcium chloride apparently reacts not only with the protective membranes of the latex globules, but also with the carboxyl groups of the polymer molecules.

LITERATURE CITED

- [1] D. Sandomirskii and V. Chernaia, Trans. Sci. Res. Inst. Rubber Ind. No. 1 (1954).
- [2] H. P. Brown and H. G. Duke, Rubber World 130, 784 (1954); H. P. Brown and C. F. Gibbs, Ind. Engng. Chem. 47, 1006 (1955); B. A. Dolgoplosk et al., Caoutchouc and Rubber No. 3, 11, No. 6, 1 (1957).
- [3] A. J. Medalia, Analyt. Chem. 26, 697 (1954).
- [4] D. Sandomirskii and M. Vdovchenkova, Colloid J. 20, No. 1, 80 (1958).*

The Lomonosov Institute of Fine Chemical Technology
Scientific Research Institute of Rubber and
Latex Products, Moscow

Received March 1, 1958

*Original Russian pagination. See C. B. Translation.

THE HEAT OF ADSORPTION OF HYDROCARBONS ON CARBON BLACKS
OF DIFFERENT DEGREES OF GRAPHITIZATION

N. N. Avgul¹, G. I. Berezin, A. V. Kiselev, and A. Ia. Korolev

Theoretical calculations of the energy of adsorption of a number of hydrocarbons on graphite are given in our earlier papers [1-6]. The theoretical values were compared with experimental values for the heat of adsorption determined calorimetrically for carbon blacks previously heated at 1700° in a current of hydrogen. It was of interest to determine the heats of adsorption of hydrocarbons on carbon blacks graphitized at higher temperatures. The heat of adsorption of argon vapor on carbon blacks of various degrees of graphitization has been studied by Beebe and Young [7]. It was shown that the initial steep decrease of the heat of adsorption, caused by heterogeneity of the surface, diminishes with increasing degree of graphitization, and the rise of the heat of adsorption to a maximum near the point at which a dense monolayer is completed becomes greater. At moderate degrees of cover of the monolayer, the differential heats of adsorption for carbon blacks heated at various temperatures between 1000 and 2700° were similar. No investigations of this type have been reported for hydrocarbons. In the present investigation we determined the differential heats of adsorption of two hydrocarbons: 3-methylhexane (isoheptane) and benzene, on carbon black graphitized at 2800°. These hydrocarbons were chosen because they differed sharply in the course of their differential heats of adsorption on carbon black graphitized at 1700°, with progressive covering of the surface [2, 6].

The starting material was Spheron 6 carbon black, graphitized at 1700° in a current of hydrogen for 1.5 hours, the same as used in the previous investigations [1, 2, 4-6]; its specific surface determined from the low-temperature adsorption of nitrogen vapor by the BET method was 92 m²/g.*

Another sample of graphitized carbon black was prepared as follows: as in the preparation of the first sample, Spheron 6 previously evacuated at 950° was taken. This carbon black was put into an induction furnace and evacuated at $5 \cdot 10^{-2}$ mm Hg. The furnace was then filled with helium to 300 mm Hg pressure. The carbon was heated up to 2800° in 15 minutes, and held at the maximum temperature for 10 minutes; the furnace was then slowly cooled.

TABLE 1
Constants of the Hydrocarbons Used

Hydrocarbon	Density in g/cc d_4^{20}	Refractive index n_D^{20}	Vapor pressure in mm Hg P_s	B. p. in °C at 760 mm
3-Methylhexane	0.6870	1.3887	47.3 (19.4°)	91.5
Benzene	0.8788	1.5011	65.2 (17.1°)	80.1

* According to Biscoe and Warren [8], the crystallite dimensions in this carbon black are $L_a = 47$ Å; $L_c = 27$ Å.

The specific surface of this sample was determined by the BET method from the low-temperature adsorption of nitrogen vapor; it was found to be $89 \text{ m}^2/\text{g}$.*

The constants of the hydrocarbons used are given in Table 1.

The amounts adsorbed were determined by means of an apparatus with liquid capillary vacuum micro-burets, and the heat of adsorption was measured in a calorimeter with constant heat transfer [10].

Figure 1 shows the absolute adsorption isotherms for 3-methylhexane and benzene on Spheron 6 carbon black previously heated at 1700° and 2800° , in two different relative-pressure scales. The adsorption isotherm for benzene on Spheron 6 heated at 1700° was taken from [2], and the adsorption isotherm for 3-methylhexane on the same carbon black was taken from [6], a further series of experiments being carried out to check the values. In studies of adsorption on Spheron 6 heated at 2800° two series of experiments were carried out for each vapor; the results of the different series coincided, and the isotherms were reversible.

It follows from Fig. 1 that the adsorption of both vapors is only slightly greater ($\sim 2\%$) on the more strongly graphitized carbon; the difference is close to the possible errors in determinations of the specific surface of these blacks.

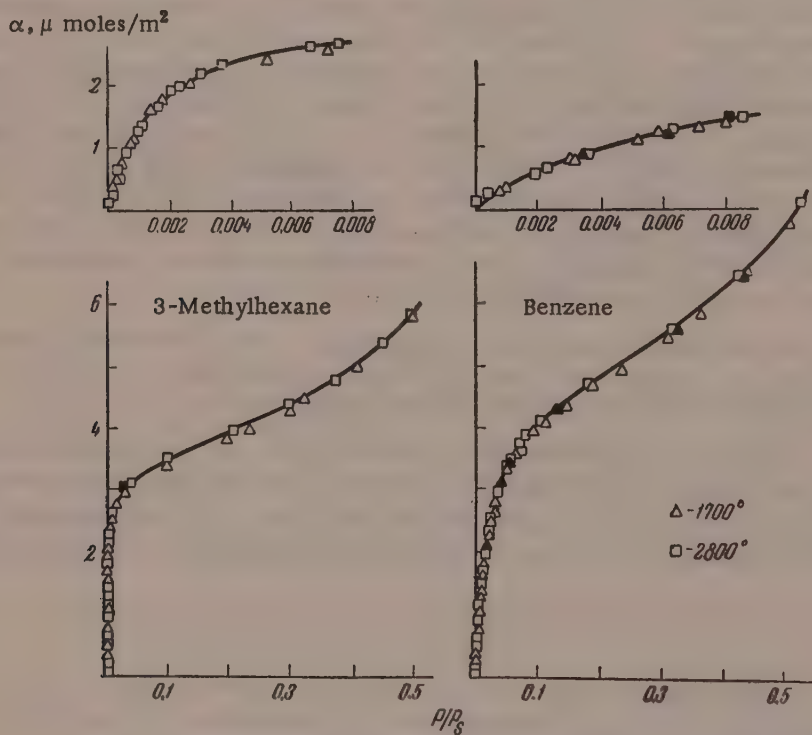


Fig. 1. Adsorption isotherms of 3-methylhexane and benzene vapors on Spheron 6 carbon black heated in hydrogen at 1700° and in helium at 2800° (black points represent desorption).

The variations of the differential heats of adsorption of the vapors with the absolute adsorption on both blacks are plotted in Fig. 2. The heats of adsorption of benzene, and one series of determinations of the heats of adsorption of 3-methylhexane on Spheron 6 heated at 1700° , are taken from the papers [2] and [6] respectively. In view of the difficulties involved in the calorimetric determinations at very low pressures, before

* It has been shown [9] that ten minutes of exposure is enough for crystallite growth, and the crystallite size changes little on further exposure at the same temperature. According to Biscoe and Warren [8] the crystallite dimensions of this carbon black are $L_a = 65 \text{ \AA}$ and $L_c = 40 \text{ \AA}$.

of $\sim 1 \cdot 10^{-3}$ mm Hg without a calorimetric determination being carried out. About 3-4% of the carbon surface was covered as a result. All the subsequent adsorption experiments were accompanied by completely reliable calorimetric determinations.

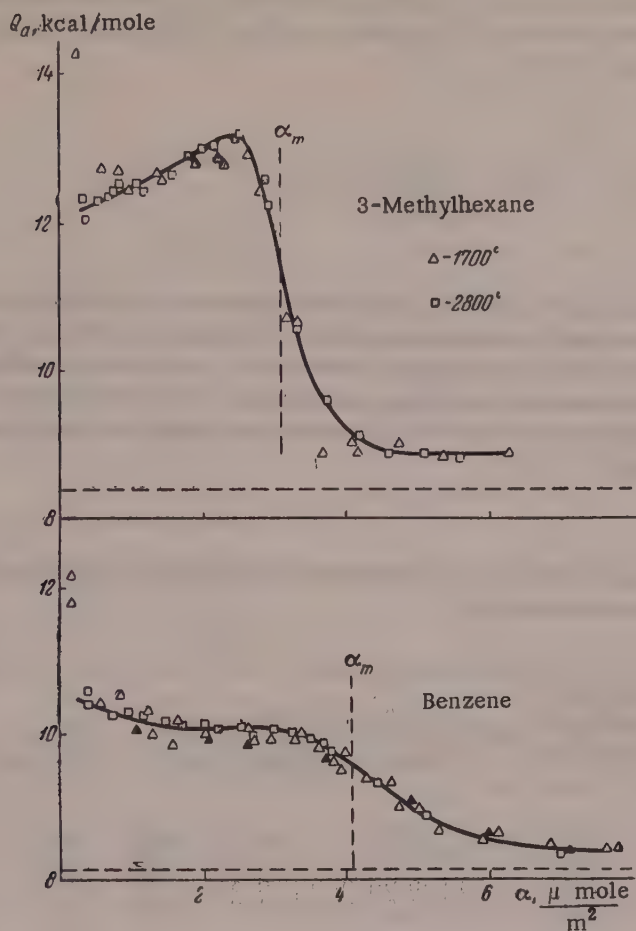


Fig. 2. Variations of the differential heats of adsorption of 3-methylhexane and benzene vapors with the amounts adsorbed on Spheron 6 heated in hydrogen at 1700° and in helium at 2800°. (black points — desorption; horizontal dash lines — heat of condensation L; vertical dash lines — capacity of monolayer α_m).

It follows from the course of the heats of adsorption of 3-methylhexane as the surface becomes covered that with the more strongly graphitized carbon the region of the initial decrease of adsorption was smaller and the maximum heat of adsorption was somewhat greater, indicating molecular attraction in the monolayer. In the adsorption of benzene, the heats of adsorption differed very little, and the initial decrease was again somewhat less on the more strongly graphitized carbon. In the adsorption of benzene on graphitized carbon blacks the course of the variation of the heat of adsorption with the degree of surface cover differs from that found for alkanes and cyclanes [6]. In the case of benzene the differential heat of adsorption does not pass through a maximum during completion of the monolayer. The initial fall of the heat of adsorption of benzene may be attributed to the high sensitivity of benzene to surface inhomogeneity, noted by us earlier [2]. The absence of a maximum on the curve for the heat of adsorption is probably due to the fact that, by virtue of the structural characteristics of the electron shells of aromatic molecules, when such molecules are packed fairly closely in a horizontal plane, additional repulsive forces may arise between them, caused by C-H dipoles in the plane of the ring, and also partially by π -electron orbits of adjacent molecules in parallel orientation [11].

Thus, the general course of the curves for the heats of adsorption of these adsorbates was not greatly changed by an increase of the graphitization temperature from 1700 to 2800°.

Thermodynamics of Adsorption

Because of the high energy of adsorption of 3-methylhexane and benzene on carbon black, high values of the surface covering θ are reached even at low relative pressures p/p_s , and therefore the equation for a monolayer adsorption isotherm derived by one of the present authors [12-14], with adsorbate-adsorbate interaction approximately taken into account

$$\theta = \frac{K'_1 p / p_s (1 - \theta)}{1 - K'_1 K_n p / p_s (1 - \theta)} \quad (1)$$

becomes similar to the Langmuir equation, and the corresponding equation for multilayer adsorption approaches the BET equation [14, 15] (in Equation (1), K'_1 is the equilibrium constant for adsorbate-adsorbent interaction; K_n is the equilibrium constant for adsorbate-adsorbate interaction). Therefore the isotherms found for the adsorption of 3-methylhexane and benzene also conform satisfactorily to the BET equation. The surface areas ω_0 per molecule in a dense monomolecular layer on the carbon black, calculated from these isotherms by the BET equation, are given in Table 2.

TABLE 2

Thermodynamic Characteristics of the Adsorption of Hydrocarbons on Different Samples of Graphitized Carbon Blacks at 20°

Hydrocarbon	Treatment temperature of carbon, (°C)	ω_0 , A ²	$Q_{a=0}$, kcal/mole	Q_q^* , kcal/mole	ΔU^* , kcal/mole	ΔF , kcal/mole	ΔS^* , cal/mole · deg.	ΔS_m , cal/mole · degree
3-Methylhexane	1700	54.0	12.4	12.7	-4.25	-3.85	-1.4	-1.8
	2800	53.7	12.1	12.7	-4.30	-3.85	-1.5	-1.8
Benzene	1700	40.3	10.0	10.0	-1.85	-2.40	+1.9	+1.6
	2800	39.8	10.2	10.1	-2.0	-2.45	+1.5	+1.8

Table 2 shows that the values of ω_0 for the same substance on different blacks coincide within 1%. The value of ω_0 for 3-methylhexane is intermediate between the values of ω_0 for n-hexane and n-heptane [5]. The explanation is that in the adsorption of 3-methylhexane four CH₂ groups and two CH₃ groups are in the surface, and one CH₃ group is at an angle to the surface; the projection of this group occupies half the area occupied by such a group in the plane of the C-C bond.

The value of ω_0 for benzene (average value 40.0 A²) coincides with the area per benzene molecule in the liquid, which is close to $\frac{147 \text{ A}^3}{3.7 \text{ A}} = 39.7 \text{ A}^2$ (3.7 A is the van der Waals thickness of the benzene molecule [16]).

Figure 3,a is a plot of the adsorption isotherms of benzene vapor in coordinates of the linear form of the equation for multimolecular adsorption [14, 15]:

$$\frac{\theta (1 - p/p_s)^2}{p/p_s [1 - \theta (1 - p/p_s)]} = K'_1 + K'_1 K_n \theta (1 - p/p_s) \quad (2)$$

The equation is satisfied from $\theta \approx 0.4$, and $K'_1 = 60$ and $K_n = 0.2$. At lower values of θ , in harmony with the higher heats of adsorption of benzene (Fig. 2), the experimental points deviate upward because the values of

θ are too high. In Fig. 3, b the experimental points are compared with the isotherm plotted in the usual θ ; p/p_s coordinates, calculated from Equation (2) with the values of K_1' and K_n given above. It follows from Fig. 3, b that in the initial region the experimental values for the adsorption are higher than the values calculated for a homogeneous surface.

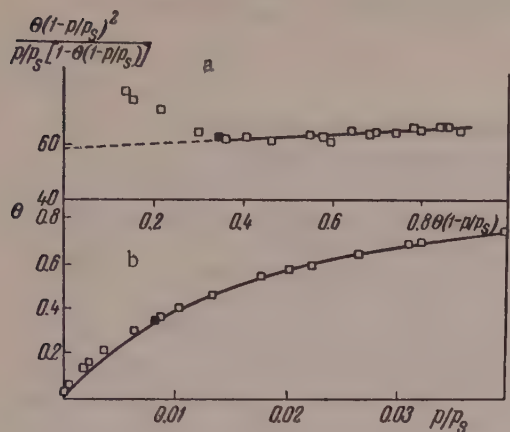


Fig. 3. Adsorption isotherms of benzene vapor on carbon black graphitized at 2800°: a) in coordinates of the linear form of Equation (2); b) in θ , p/p_s coordinates. The continuous line is calculated from Equation (2); the points represent experimental data.

Comparison of the dependence of the differential heats of adsorption of 3-methylhexane on the degree of surface covering of different carbon blacks shows that the highly graphitized carbon has the more homogeneous surface. By extrapolation of the middle regions of the heat of adsorption curves to zero covering it is possible to eliminate the influence of inhomogeneity [1] and to obtain values for the differential heats of adsorption which represent the interaction of individual molecules with a homogeneous carbon surface, $Q_a=0$. In the case of 3-methylhexane the difference between the values of $Q_a=0$ for the carbons studied does not exceed 0.3 kcal/mole, and in the case of benzene the difference is even smaller (see Table 2).

The adsorption isotherms and the differential heats of adsorption were used to calculate the following thermo-

dynamic values [17]: $\frac{\partial \Delta U}{\partial a} = - \left(Q_a - L \right)$, change of free energy $\partial \Delta F/\partial a = RT \ln p/p_s$ and change of the entropy of adsorption $\frac{\partial \Delta S}{\partial a} = \frac{\partial \Delta U/\partial a - \partial \Delta F/\partial a}{T}$.

Curves for the change of the entropy of adsorption with increasing surface cover θ are given in Fig. 4. The course of the curves for the adsorption of 3-methylhexane on the two blacks is very similar; the minimum on the curve for the more highly graphitized black is merely somewhat deeper. The curves for the change of entropy of adsorption of benzene on the two graphitized blacks are also very similar.

If the standard state of the adsorption layer is taken to be 50% cover of the surface, $\theta = 0.5$, we find the standard thermodynamic characteristics [1, 2, 5]:

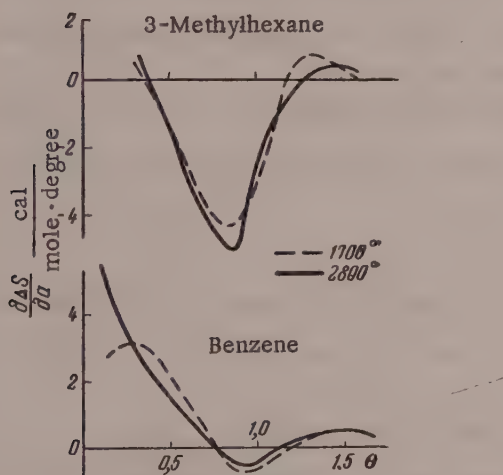


Fig. 4. Variation of the differential change of the entropy of adsorption of 3-methylhexane and benzene with the degree of surface cover of Spheron 6 previously heated in hydrogen at 1700° and in helium at 2800°.

ΔS_m^0 in the adsorption of a dense monolayer of 3-methylhexane and benzene on the two graphitized blacks. It follows from Table 2 that a considerable increase of the degree of graphitization produces almost no change in the standard values for adsorption, i.e., near $\theta = 0.5$ the surface becomes fairly homogeneous even after heating to 1700°.

$$Q_a^0; \Delta U^0 = \left(\frac{\partial \Delta U}{\partial a} \right)^0;$$

$$\Delta F^0 = \left(\frac{\partial \Delta F}{\partial a} \right)^0; \Delta S^0 = \left(\frac{\partial \Delta S}{\partial a} \right)^0.$$

Table 2 contains these standard thermodynamic characteristics, and also the mean molar entropy change

An earlier paper [6] gave a theoretical calculation of the dispersion* force potentials, with consideration of three interaction terms and of repulsion according to an exponential law, Φ_0' , and according to a power law, Φ_0'' . The calculated values for the adsorption potential of isolated hydrocarbon molecules on the graphite surface were compared with values of $Q_{a=0}$ found from the experimental heats of adsorption of hydrocarbons on Spheron 6 carbon black graphitized at 1700°. Table 3 gives a comparison of the theoretical values of the potential with the repulsion forces calculated by an exponential law for three positions of the molecule on the surface of the graphite lattice Φ_{0c}' , Φ_{0b}' and Φ_{0h}' , and the mean value $\bar{\Phi}_0'$, and also the average value of the potential with the repulsion forces calculated according to a power law, $\bar{\Phi}_0''$. The theoretical results are compared with values of $Q_{a=0}$ found from calorimetric experiments with Spheron 6 graphitized at 2800°.

TABLE 3

Comparison of Calorimetrically Determined Differential Heats of Adsorption $Q_{a=0}$ with Theoretically Calculated Adsorption Force Potentials on Graphite (kcal/mole)

Hydrocarbon	$Q_{a=0}$	$-\Phi_{0c}'$	$-\Phi_{0b}'$	$-\Phi_{0h}'$	$-\bar{\Phi}_0'$	$-\bar{\Phi}_0''$
3-Methylhexane	12.1	11.7	12.3	15.0	13.0	11.9
Benzene	10.2	10.1	10.6	13.4	11.4	10.6

It follows from Table 3 that the experimental values for the heat of adsorption lie within the limits of the theoretically calculated values of the potential for different positions.

SUMMARY

1. The adsorption isotherms and differential heats of adsorption of 3-methylhexane and benzene of Spheron-6 carbon black graphitized at 2800° were determined.
2. It is shown that these isotherms and the standard thermodynamic characteristics of adsorption of the hydrocarbons on carbon black change little with increase of the graphitization temperature above 1700°.
3. The heats of adsorption of hydrocarbons determined on carbon black graphitized at 2800° are close to the previously calculated theoretical values of the adsorption force potentials.

The authors thank B. V. Fedin and A. A. Kal'nitskii for help in graphitization of the carbon black.

The authors are happy to dedicate this paper to B. A. Dogadkin, who has a lively interest in the surface properties of carbon blacks.

LITERATURE CITED

- [1] N. N. Avgul', G. I. Berezin, A. V. Kiselev and I. A. Lygina, J. Phys. Chem. 30, 3106 (1956).
- [2] N. N. Avgul', G. I. Berezin, A. V. Kiselev and I. A. Lygina, Bull. Acad. Sci. USSR, Div. Chem. Sci. 1304 (1956).**
- [3] N. N. Avgul' and A. V. Kiselev, Proc. Acad. Sci. USSR 112, 673 (1957).**
- [4] A. V. Kiselev, Proceedings of the Second International Congress on Surface Activity, Vol. II (London, 1958).
- [5] N. N. Avgul', T. I. Berezin, A. V. Kiselev and I. A. Lygina, Bull. Acad. Sci. USSR, Div. Chem. Sci. 1021 (1957).**

* As in original — Publisher's note.

** Original Russian pagination. See C. B. Translation.

- [6] N. N. Avgul', A. A. Isirikian, A. V. Kiselev, I. A. Lygina and D. P. Poshkus, Bull. Acad. Sci. USSR, Div. Chem. Sci. 1314 (1957). *
- [7] R. A. Beebe and D. M. Young, J. Phys. Chem. 58, 95 (1954).
- [8] J. Biscoe and B. E. Warren, J. Appl. Phys. 13, 364 (1942).
- [9] M. H. Polley, W. D. Shaeffer and W. R. Smith, J. Phys. Chem. 57, 469 (1953).
- [10] N. N. Avgul', G. I. Berezin, A. V. Kiselev, I. A. Lygina and G. G. Muttik, J. Phys. Chem. 31, 1111 (1957). *
- [11] A. V. Kiselev, Proc. Acad. Sci. USSR 106, 1046 (1956). *
- [12] A. V. Kiselev, News Acad. Sci. USSR, No. 10, 43 (1957).
- [13] A. V. Kiselev, Proc. Acad. Sci. USSR 117, 1023 (1957). *
- [14] A. V. Kiselev, Colloid J. 20, 338 (1958). *
- [15] A. V. Kiselev and D. P. Poshkus, Bull. Acad. Sci. USSR, Div. Chem. Sci. 520 (1958). *
- [16] L. Pauling, Nature of the Chemical Bond (Russian translation) (Goskhimizdat, Moscow—Leningrad, 1947).
- [17] A. V. Kiselev, J. Phys. Chem. 20, 239 (1945).

Institute of Physical Chemistry
Academy of Sciences USSR
Laboratory of Sorption Processes

Received March 15, 1958

*Original Russian pagination. See C. B. Translation.

THE GAS PERMEABILITY AND STRUCTURE OF VULCANIZED RUBBERS

G. M. Bartenev

The influence of vulcanizate structure on gas permeability has been studied little. Nevertheless, gas permeability is of great technological and technical significance, being one of the most important characteristics of rubber [1-3]. It has been shown [4, 5] that the gas permeability of rubbers is closely associated with their frost resistance. The concept of vulcanizate structure includes, in addition to the chemical structure of the molecular rubber chains themselves, the spatial network which depends on the number, distribution, and type of chemical cross links, the distribution density of various polar groups, etc. Studies of the influence of structure on the gas permeability of rubber [6, 7] have shown that permeability is highly sensitive to variations of the density of the space network of the vulcanizate. It was shown [6, 7] that the permeability and diffusion constants decrease with increasing contents of sulfur in a vulcanizate. However, these results do not provide more detailed information on the connection between the permeability and structure of network polymers, as the bound sulfur content of a vulcanizate does not uniquely determine the number of cross links, since part of the sulfur combines with the rubber without formation of cross links [8]. Moreover, the number of sulfur atoms in the cross links depends on the type of accelerator [9], and the influence of this on gas permeability likewise has not been studied.

This paper presents data which make it possible to determine the influence of the density of the spatial network of the type of cross links on the gas permeability of vulcanizates of natural rubber (NR) and butadiene-styrene rubber (SKS-30).

TABLE 1
Composition of Stocks Based on SKS-30 and NR

Ingredients	Composition, in wt. parts									
	based on SKS-30					based on NR				
Rubber	100	100	100	100	100	100	100	100	100	100
Stearic acid	2	2	2	2	2	2	2	2	2	2
Zinc oxide	5	5	5	5	5	5	5	5	5	5
Captax	2	1	1	0.6	0.5	3	2.3	1.1	0.7	0.33
Sulfur	10	5	3	1.5	1.0	10	7	3.5	2.0	1.0
Amount of bound sulfur, as % of the mixture	6.76	3.65	1.89	0.99	0.49	5.8	5.0	2.5	1.65	0.8
Nominal-equilibrium modulus, E kg/cm ²	41	32	25	13	9	29	26.6	18	15.6	8.6

Vulcanizates with different contents of sulfur and accelerator (mercaptobenzothiazole) were made from these rubbers. The compositions of the vulcanizates are given in Table 1. It is seen that the amount of sulfur

was varied from 1-10 wt. parts. The vulcanization was carried out at 143°, the cure time being 20 minutes for NR and 60 minutes for SKS-30. These times corresponded to the maximum values of the equilibrium modulus.

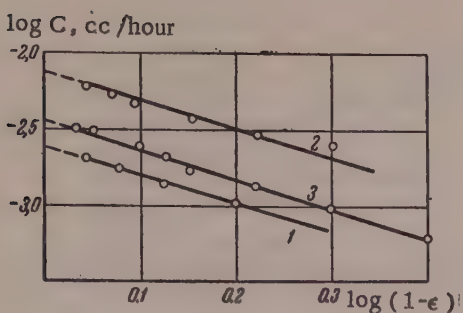


Fig. 1. Flow rate of air diffusing through a rubber membrane as a function of the compression, in logarithmic coordinates: 1) SKS-30 vulcanizates with 6.76% sulfur; 2) SKS-30 with 1.89% sulfur; 3) Buna S-3, data from [3].

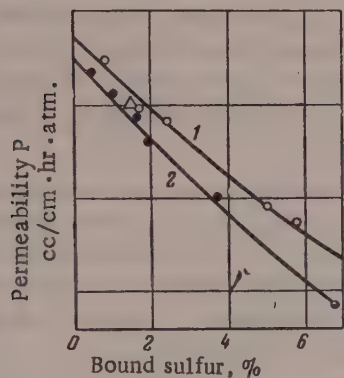


Fig. 2. Permeability to air at 25° as a function of the amount of bound sulfur in vulcanizates of: 1) NR, 2) SKS-30.

It follows from Fig. 1, which gives data for SKS-30, and from analogous data for natural rubber, that the plot of the flow rate against the compression deformation in logarithmic coordinates is linear. The index n determined from the slopes of the lines had the following values: for SKS-30 and Buna S-3, $n = 2.0$; for NR, $n = 1.7$. These results agree with the values found earlier [3]. The rate of flow of gas by diffusion through the undeformed membrane was determined by extrapolation, and the permeability constant was then found from Formula (1) for $\epsilon = 0$.

The permeability constants (at 25°) of the two vulcanizates are plotted against the amount of bound sulfur in Fig. 2. The slight deviation from linearity is in agreement with earlier data [7]. The value for the permeability of NR vulcanizate with 1.5% sulfur (Fig. 2, triangle) was calculated from Amerongen's data on the permeability to nitrogen and oxygen [10]. Extrapolation of the curves in Fig. 2 shows that the permeability constants of nonvulcanized rubbers at 25° are $3.7 \cdot 10^{-4}$ for NR and $3.5 \cdot 10^{-4}$ cc/cm hr atm. for SKS-30.

For determination of the density of the spatial network, we used the nominal-equilibrium modulus (E), which was determined for the stretched vulcanizates by the method of relaxation during 24 hours at 25°.

The air permeability of the vulcanizates was determined by the method described previously [2, 3]. Rubber membranes, compressed by 15-20% between steel plates, almost completely eliminate leakage of gas at the points of contact between the rubber and the metal. At high compressions the gas penetrates only through the volume of the membrane, i.e., by diffusion, and the amount of gas passing through the membrane is proportional to the pressure difference between the internal and external spaces.

The following formula was derived for the relationship between the amount of gas passing through the membrane and its gas permeability:

$$C = P \frac{2\pi R}{b_0} d_0 (1 - \epsilon)^n \Delta p, \quad (1)$$

here C is the rate of flow of the gas through the membrane in cc/hour; P is the permeability constant in cc/cm hr atm.; R is the average radius of the membrane in cm; d_0 and b_0 are the thickness and the width of the membrane in cm; Δp is the gas-pressure difference in atm.; ϵ is the compression deformation in relative units; here $1 - \epsilon = d/d_0$, where d is the thickness of the membrane in the compressed state. The amount of gas passing through the membrane is determined in cubic centimeters reduced to standard conditions. The rate of flow is taken to mean the amount of gas in cubic centimeters (reduced to standard conditions) passing through the membrane per unit time.

Formula (1) has been thoroughly tested [3]. The permeability constant at deformations up to 50% does not depend on the compression, within the limits of experimental error. This was confirmed by experimental data (Fig. 1) for the vulcanizates studied, and provided a simple method for determination of the permeability constant.

(see Table 1). Analysis of the data showed that there is no proportionality between E and the amount of bound sulfur, but $E^{3/2}$ is roughly proportional to the amount of bound sulfur; this justifies the choice of $E^{3/2}$ as an index of the cross-link content of the vulcanizates [11]. The gas-permeability constant - modulus relationship is plotted in Fig. 3 in two different coordinate systems.

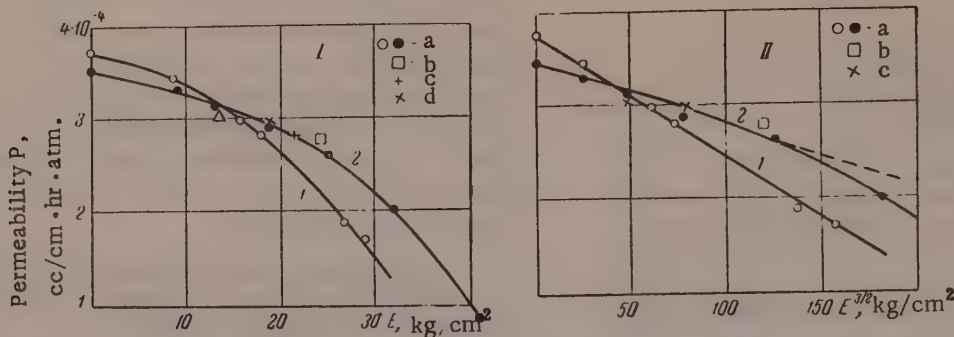


Fig. 3. Variation of the air permeability of NR (1) and SKS-30 (2) vulcanizates with the nominal-equilibrium modulus (I) and the cross-link index (II). Vulcanizing groups: a) sulfur with Captax; b) thiuram without sulfur; c) sulfur with diphenylguanidine; d) dihydroxyquinone without sulfur. The triangle denotes Amerongen's data.

Comparison of the curves given in Fig. 2 and Fig. 3, (I) shows that the dependence of permeability on the bound sulfur content and the number of cross links differs in the two rubbers. For example, it follows from Fig. 2 that the permeability constant of SKS-30 is lower than that of NR at all bound sulfur contents. Figure 3 shows that the permeability constant of SKS-30 is lower than that of NR in low-modulus vulcanizates, and higher in high-modulus vulcanizates, i.e., the permeability constant decreases more steeply with increase of the number of cross links in NR than in SKS-30.

It was therefore desirable to determine the influence of the type of cross links present on the permeability constant. SKS-30 vulcanizates were used for these experiments. The compositions of the mixtures and the vulcanization times are given in Table 2. Three vulcanizates were made with different accelerators: tetramethyl-thiuram disulfide, mercaptobenzothiazole, and diphenylguanidine. The vulcanizing agent in these three cases is sulfur. In the fourth vulcanizate dihydroxyquinone was used as the cross-linking agent. These vulcanizates therefore contained different types of cross links: monosulfide, polysulfide, and C-C bonds.

As the permeability constant depends on the number of cross links, the compositions of the vulcanizates had to be chosen so that their cross-links contents were approximately equal. This choice was made with the use of the nominal-equilibrium modulus as the measure of the cross-link content. Table 2 shows that the moduli of all the vulcanizates were approximately equal. The permeability constants given in Table 2 also proved to be approximately equal.

Figure 3 shows clearly that the permeability constant of SKS-30 is independent of the type of cross links. All the points fit satisfactorily on a single curve.

It follows from Fig. 4 that, with equal contents of bound sulfur, the nominal-equilibrium moduli of NR and SKS-30 are different. Hence the proportion of cross links in the total quantity of chemical bonds added to the rubber during vulcanization is higher in SKS-30 than in NR. In other words, the cross-link index discussed in an earlier paper [8] is higher in SKS-30 vulcanizates.

If it is assumed that in SKS-30 nearly all the bound sulfur is used for formation of cross links, then only about half the bound sulfur in NR forms cross links, while the rest of the bound sulfur combines without cross-link formation. This "nonbridge" sulfur probably causes additional intermolecular forces of the polar type to arise between the rubber chains, and also leads to the formation of five- or six-membered intramolecular rings. It was shown by Dogadkin [9] that such rings are formed in NR vulcanizates owing to the peculiarities of the chemical structure of the natural rubber molecule. Intramolecular rings with a small number of atoms cause some loss of chain flexibility and hence lead to a decrease of gas permeability.

TABLE 2

Composition of Stocks Based on SKS-30 with Different Vulcanization Agents and Accelerators

Ingredients	Composition, in wt. parts			
SKS-30 rubber	100	100	100	100
Stearic acid	2	2	2	2
Zinc oxide	5	5	5	5
Captax	0.8	—	—	—
Diphenylguanidine	—	2	—	—
Thiuram	—	—	3	—
Dihydroxyquinone	—	—	—	3
Sulfur	2.5	2.5	—	—
Vulcanization time, min.	80	80	40	80
Nominal-equilibrium modulus $E, \text{kg}/\text{cm}^2$	19	24	21	19
Air permeability at 25° in $\text{cc}/\text{cm} \cdot \text{hr} \cdot \text{atm.}$	$2.89 \cdot 10^{-4}$	$2.78 \cdot 10^{-4}$	$2.83 \cdot 10^{-4}$	$2.94 \cdot 10^{-4}$

The steeper decrease of permeability with increase of the number of cross links in NR (Fig. 3) can probably be attributed to this influence of "nonbridge" sulfur. The amount of bound sulfur increases considerably more rapidly with increase of the number of cross links in NR than in SKS-30, and accordingly the permeability decreases more rapidly in NR. Consequently, in NR the gas permeability depends not only on the density of the spatial network, but also on the amount of bound sulfur which does not form cross links. It follows from Fig. 3

that a simple relationship $P = P_0 - aE^{3/2}$, where P_0 is the permeability of the unvulcanized rubber, exists between the permeability P and the modulus E . The deviations from this formula shown by SKS-30 at high values of the modulus are the consequence of the deviation from direct proportionality between the amount of bound sulfur and the index $E^{3/2}$ in Fig. 4. In the case of NR the value of the coefficient a is greater owing to the influence of the "nonbridge" sulfur, the amount of which is approximately proportional to the amount of "bridge" sulfur; this results in an almost linear relationship (Fig. 3).

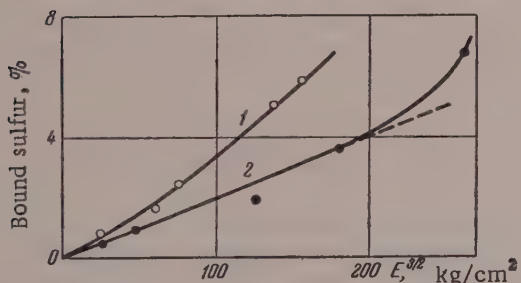


Fig. 4. Relationship between the bound sulfur content and the cross-link index (Captax accelerator): 1) NR; 2) SKS-30.

[5] of butadiene-nitrile rubbers of the SKN-18, SKN-26, and SKN-40 types, which at 25° have permeability constants 33; 8.5, and 3.4% relative to that of NR, taken as 100%.

SUMMARY

1. The degree of cross linking has a significant influence on the gas permeability of vulcanizates. For example, with an increase of bound sulfur to 7%, the air permeability of NR is decreased by a factor of 3, and that of SKS-30, by a factor of 4.5.
2. The type of vulcanization agent or accelerator has almost no influence on the permeabilities of SKS-30 vulcanizates with equal cross-link contents (equal modulus).

3. All the chemical bonds formed in the course of vulcanization influence the gas permeability, but cross links have the greatest effect.

4. The equilibrium modulus, regarded as an index of the number of cross links, is not a direct measure of the permeability of NR vulcanizates, as it does not take into account the influence of the other chemical bonds formed during vulcanization.

The author thanks L. E. Peregudova, who assisted in the experimental work, and B. A. Dogadkin and S. A. Reitlinger for discussion of the experimental results.

LITERATURE CITED

- [1] S. A. Reitlinger, Progr. Chem. 20, 213 (1951).
- [2] G. M. Bartenev, Chem. Ind. No. 8, 463 (1955).
- [3] G. M. Bartenev and L. E. Peregudova, Trans. Ind. Rubber Ind. No. 2, 56 (1955).
- [4] G. M. Bartenev, S. A. Reitlinger and B. E. Rubinstein, J. Phys. Chem. 30, 532 (1956).
- [5] G. M. Bartenev, Chem. Ind. No. 6, 344 (1955).
- [6] G. Amerongen, Rev. gen. caoutchouc 21, 50 (1944).
- [7] R. Barrer and G. Skirrow, J. Polymer Sci. 3, 549 (1948).
- [8] B. Dogadkin, G. Bartenev and N. Novikova, Colloid J. 10, 94 (1948).
- [9] B. A. Dogadkin and Z. N. Tarasova, Colloid J. 15, 347 (1953).*
- [10] G. Amerongen, J. Polymer Sci. 5, 307 (1950).
- [11] G. M. Bartenev, Vulcanization of Rubbers (Goskhimizdat, 1954) p. 196.**

Scientific Research Institute
of the Rubber Industry
Moscow

Received November 30, 1957

*Original Russian pagination. See C. B. Translation.
**In Russian.

A STUDY OF THE RHEOLOGICAL PROPERTIES OF LOW-MOISTURE PEATS

M. P. Volarovich and N. I. Malinin

In recent years a number of workers, and in particular Solopov, demonstrated the advisability of winning lump peat from deposits at a low operational moisture [1, 2]. Further advances in this field are hindered because questions of processing and forming of low-moisture peats have not been sufficiently studied [1]. Investigations of the deformational (rheological) properties of low-moisture peats are therefore of considerable interest.

Although F. N. Shvedov laid the foundations of the rheology of disperse systems as long ago as 1889, by his discovery of anomalous viscosity and elasticity in colloids, the rheological properties of easily deformable materials such as clays, paints, greases, peats, etc., have been extensively studied only during the past 20-30 years. Processes of viscoplastic flow [3] and elastic after-effects and stress relaxation [5-10] in various disperse systems have been studied in the Soviet Union. Similar work has been done abroad; here we shall cite only the most recent foreign publications in this field [11-14].

However, the rheological properties of low-moisture peats, which are typical solid-like disperse systems in Rebinder's classification [15], have been studied little. Volarovich, Kulakov et al. [16] showed that aqueous suspensions of high-moisture peat are viscoplastic materials which conform to the Shvedov-Bingham equation in flow. Later Kulakov and Samarina, and then Volarovich and Lazovskaia [18], showed that limiting shear stress (yield value) varies more sharply than the plastic viscosity with variations of moisture content of peat. Subsequently the yield value of peat, which is its most important deformational characteristic and which determines the plasticity of the material, was studied very extensively [19-20]. An investigation of the elastokinetic properties of peat was commenced by Volarovich and Branopol'skaiia [5]. However, this paper [5] and the subsequent investigations [21 and 22] contained very little experimental data, and it was not possible to draw any general conclusions concerning the deformation behavior of various peats.

The volume rheological properties of low-moisture peat were studied by means of the recording of complete rheological diagrams determined for homogeneous (or approximately homogeneous) stress and deformation fields. The complete rheological diagram of a material [21] is the name given to a series of curves showing the development of deformation under constant load, and disappearance of deformation during the subsequent removal of the load, plotted in shear deformation-time coordinates ($\gamma - t$). Complete rheological diagrams for peat at low rates of shear deformation were plotted with the aid of Tolstoi's apparatus [23] in which the material is subjected to shear between two parallel plates, and also by the method of compression of cylinders.

By mathematical analysis of the complete rheological diagrams it is possible to determine invariant (independent of stress) rheological characteristics, which can be used for describing fairly fully the rheological (deformational) properties of the system. Two types of complete rheological diagrams, designated as Types I and II, were found for low-moisture peats. A complete rheological diagram of Type I, for pine-cotton grass crude peats, is given in Fig. 1,a. It is seen in Fig. 1, a that at fairly low shear stresses, below a certain critical value θ_s , known in the rheological literature as the static yield value, the creep curves are of the form represented by Lines 1, 2 and 3. The total deformation may be subdivided into the nominally instantaneous γ_0 , which develops almost instantaneously (within the first second) on application of the load, and which disappears as rapidly on removal of the load; and the elastic deformation or deformation of elastic hysteresis which develops and disappears gradually. The deformation-time relationship for $\tau = \text{const}$, $\tau < \theta_s$ can be represented by the equation

$$\gamma = \gamma_0 [1 + K \log(C + t)], \quad (1)$$

where t is the time in seconds; K and C are constants. The value of γ_0 is a function of the applied stress. For thoroughly decomposed and well-worked peats γ_0 may be taken as being approximately proportional to the applied stress. Therefore $\tau = G_1 \gamma_0$, where G_1 is the nominally instantaneous modulus [5-7]. Equation (1) was derived by the Japanese worker Fukada [24] for methyl methacrylate polymer. Even earlier, Rebinder [25] derived a similar relationship in the form: $\epsilon = \epsilon_0 (1 + k \log t)$, where ϵ is the relative elongation, for mica plates. The determinations showed that C does not depend on the moisture content, the degree of processing, or any other factors, and is approximately equal to 1 second. Fig. 1,b shows the $\gamma - \log t$ relationships for the same pine-cotton grass peat. It is seen that at low $\tau < \theta_s = 30.7 \text{ g/cm}^2$ the $\gamma - \log t$ graphs are linear (see Lines, 1, 2, 3). Extension of these lines to the ordinate axis cuts off the nominal-instantaneous deformation along the latter, so that this deformation can be separated from the deformation of elastic hysteresis.

At $\tau > \theta_s$, the $\gamma - t$ curves could be divided into two regions — an initial, curvilinear region, when deformation of elastic hysteresis was predominantly developing, and a linear region, in which steady flow predominated. The rate of shear $\dot{\gamma}_{\text{res}}$, equal to the velocity gradient v/z , as follows from Fig. 2, where $\dot{\gamma}_{\text{res}}$ is plotted against τ for the same peat, changes very considerably over a relatively narrow range of shear stresses, in harmony with the Shvedov equation:

$$\tau - \theta_s = \eta_0^* \dot{\gamma}_{\text{res}}, \quad (2)$$

where θ_s is the flow limit analogous, on the one hand, to the static flow limit [7] and on the other, to the static limiting shear stress [26]; $\eta_0^* = (\dot{\gamma}_{\text{res}} / d\tau)^{-1}$ at $\tau > \theta_s$ — is the plastic (Shvedov)* viscosity of the structure after preliminary breakdown, analogous to Rebinder's maximum plastic viscosity.

The total shear deformation γ is the sum of the initial (nominal-instantaneous) deformation γ_0 , the deformation of elastic hysteresis $\gamma_e = \gamma_0 K \log(1+t)$, and the irreversible plastic deformation;

thus

$$\begin{aligned} \dot{\gamma}_{\text{res}} &= \frac{\tau - \theta_s}{\eta_0^*} t. \\ \gamma &= \gamma_0 [1 + K \log(1 + t)] + \frac{\tau - \theta_s}{\eta_0^*} t. \end{aligned} \quad (3)$$

The considerable increase of the velocity gradient in the plastic flow of peat (from 0 to 10^{-1} second and over) over a relatively narrow range of shear stress can only be attributed to breakdown of the original peat structure under the action of shear stresses greater than θ_s . We termed this the preliminary breakdown.

When $\tau > \theta_s$, the $\gamma - t$ curves are usually S-shaped. Convexity of the $\gamma - t$ curve toward the abscissa axis corresponds to the start of a new, more extensive breakdown of the peat structure, described in the rheological literature as shear breakdown. During such breakdown the effective viscosity of the peat falls even more sharply (by 4-5 tenth powers). Structures broken down in this manner were studied by means of the RV-4

* Rebinder and his school [6-7] established the existence of two plastic viscosities. The maximum plastic viscosity observed in the flow of disperse systems with velocity gradients $\dot{\gamma}_{\text{res}} \ll 1 \text{ sec}^{-1}$ was named the Shvedov plastic viscosity in honor of F. N. Shvedov, who was the first to derive Equation (2) for low rates of shearing deformation. The minimum plastic viscosity, observed at velocity gradients $\dot{\gamma}_{\text{res}} \gg 1 \text{ sec}^{-1}$ (see below) is known as the Bingham plastic viscosity in honor of E. Bingham, who derived an analogous equation for high velocities of viscoplastic flow. The Shvedov and Bingham viscosities differ sharply in value. Whereas the Shvedov viscosity of low-moisture peat is between 10^5 and 10^7 poises, the Bingham viscosity is between 30 and 500 poises.

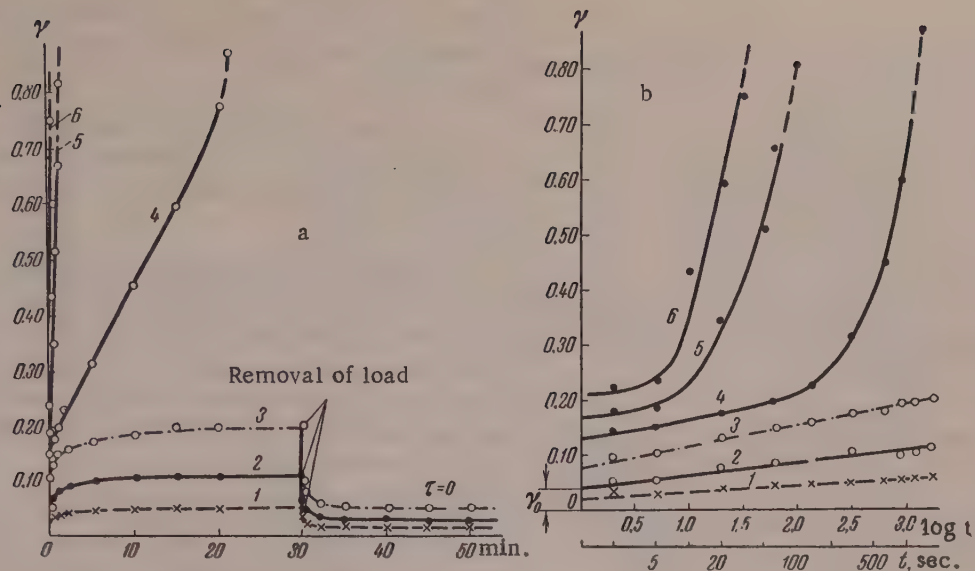


Fig. 1. Complete rheological diagram of Type I for crude pine-cotton grass peat of degree of decomposition $R = 60\%$ and moisture content $W = 80.3\%$. Determined with the use of Tolstoi's apparatus (a); the same diagram in semilogarithmic coordinates (b): 1) $\tau = 6 \text{ g/cm}^2$; 2) $\tau = 12 \text{ g/cm}^2$; 3) $\tau = 20 \text{ g/cm}^2$; 4) $\tau = 25.6 \text{ g/cm}^2$; 5) $\tau = 35 \text{ g/cm}^2$; 6) $\tau = 38.5 \text{ g/cm}^2$.

rotational viscosimeter [27]. In Fig. 3 the angular velocity Ω of the rotating cylinder of the viscosimeter is plotted against the load P (with a correction for friction) for the peat the complete rheological diagram of which is given in Fig. 1,a. The Ω curve conforms to the equation for the motion of a viscoplastic medium between the cylinders of a rotational viscosimeter for the case when the shear does not extend to the end [3, 27]. Hence it may be concluded that peat after shear breakdown of the structure is a viscoplastic body which conforms to the Bingham equation in flow:

$$\tau - \theta_d = \eta_m^* \dot{\gamma}_{\text{res}}, \quad (4)$$

where θ_d is the flow limit of the peat structure after shear breakdown analogous, on the one hand, to the nominal dynamic (Bingham) yield value [7] and, on the other, to the dynamic limiting shear stress; η_m^* is the minimum (Bingham) plastic viscosity. The dynamic yield value, calculated in the usual way from the value of P_0 (see Fig. 3) was found to be 19 g/cm^2 ; this is below the static value, in harmony with the findings of Volarovich and Kulakov [16, 26].

As the moisture content of peat decreases and its consistency passes from the normally plastic into the semisolid (in the classification used for peat consistency [1, 2, 19]), the character of its complete rheological diagrams changes. The complete rheological diagram of Type II, determined from data for the compression of cylindrical peat specimens, characteristic for the semisolid consistency of peat, is given in Fig. 4. It is clear from Fig. 4 that peat of semisolid consistency has no appreciable fluidity. The peat becomes more resilient and elastic. Breakdown of the structure occurs at considerably smaller deformations than in peats of normally plastic consistency, and is of a totally different character. The breakdown does not penetrate to any great depth into the volume, but is localized near the slippage surface. The breakdown produces discontinuity, and the specimen separates into two or more parts. It may be said that the breakdown of peat specimens of semisolid and solid consistency is brittle in

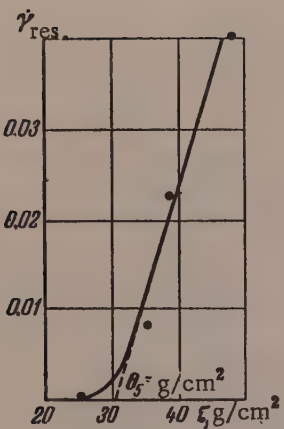


Fig. 2. Curve for the velocity gradient $\dot{\gamma}_{\text{res}}$ as a function of the shear stress τ for crude pine-cotton grass peat; $R = 60\%$; $W = 80.3\%$. Determined by means of the Tolstoi apparatus.

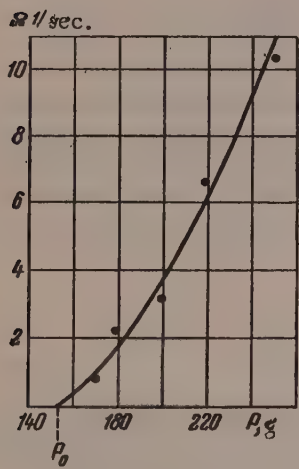


Fig. 3. Angular velocity Ω - load P curve for pine-cotton grass peat; $R = 60\%$; $W = 80.3\%$, determined by means of the RV-4 rotational viscosimeter.

3. The Shvedov viscosity η_0^* , determined from flow curves of the type shown in Fig. 2; here

$$\eta_0^* = \left(\frac{d\dot{\gamma}_{\text{res}}}{d\tau} \right)^{-1} \quad \text{at} \quad \tau > \theta_s.$$

character. The equations of the mechanics of continuous media are applicable at small deformations and stresses provided, of course, that the ultimate strength of the peat is not exceeded. The concepts of yield value and of Shvedov and Bingham viscosities become meaningless.

The data of Fig. 4, a are plotted in Fig. 4, b in $\epsilon - \log t$ coordinates. It is clear from Fig. 4, b that Equation (1) is also applicable to peat of semisolid consistency.

It must be noted that the transition from a consistency corresponding to rheological diagram Type 1 to a consistency corresponding to a rheological diagram Type 2, effected by variation of the moisture content of the peat, is rather diffuse. Measurements of the viscoplastic properties of peat in these intermediate regions are very difficult.

In conclusion, to conform with the decisions made at certain conferences [15, 28], seven rheological constants are proposed for the description of the deformation properties of low-moisture peats.

1. The nominal instantaneous shear modulus

$G_1 = \tau/\gamma_0$. The value of γ_0 , for stresses $\tau < \theta_s$, is cut off along the ordinate axis on extrapolation of the $\gamma - \log(1+t)$ relationship to $\log(1+t) = 0$. Compression experiments can give the nominal instantaneous Young's modulus $E_1 = \sigma/\epsilon_0$, where σ is the normal applied stress; ϵ_0 is the nominal instantaneous relative elongation, determined from the $\epsilon_0 - \log t$ relationships, analogously to γ_0 . The value of G_1 can be calculated from the usual formula $G_1 = \frac{E_1}{2(1+\mu)}$, where

μ is the Poisson ratio. For materials such as peat the value of μ is very close to 0.5 and $G_1 \approx E_1/3$.

2. The constant K is the Rebinder-Fukada equation (1), applicable at shear stresses $\tau < \theta_s$. The value of K determines the rate of development of elastic deformation γ_e . It should be noted that usually another quantity, T_n , the time of elastic hysteresis, is used for this purpose. However, since the creep equation for peat differs from the usual equation for creep in a Kelvin-Voigt body it is not possible to use a single time T_n for description of retardation processes in peat, as this would be a very crude approximation to reality. In this case it is possible to consider a distribution of retardation times, as is done, for example, by Alfrey [29].

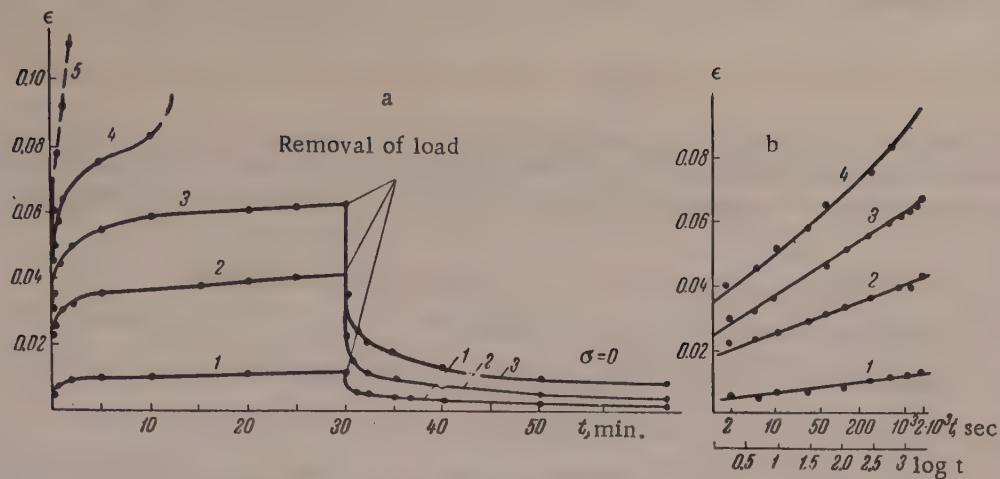


Fig. 4. Complete rheological diagram of Type II for crude sedge peat of degree of decomposition $R = 30\%$ and moisture content $W = 72.1\%$.

Determined by the cylinder-compression method (a); the same diagram in semilogarithmic coordinates (b): 1) $\sigma = 22.6 \text{ g/cm}^2$; 2) $\sigma = 57.5 \text{ g/cm}^2$; 3) $\sigma = 90.6 \text{ g/cm}^2$; 4) $\sigma = 122 \text{ g/cm}^2$; 5) $\sigma = 150 \text{ g/cm}^2$.

4. The Bingham viscosity η_B . Methods for the determination of Bingham viscosity (and the dynamic yield value) have been thoroughly worked out and described in detail in a number of papers and monographs [26, 27].

5. The static yield value (flow limit) or the strength of the structure θ_s . The value of θ_s is cut off along the abscissa axis on extrapolation of the linear region of the $\gamma_{\text{res}} - \tau$ flow curve to $\gamma_{\text{res}} = 0$.

6. The dynamic yield value θ_d .

7. The ultimate strength of the system—equal to the stress which causes shear breakdown of the specimen. The value of τ_n depends also on the time of application of the load. We take the ultimate shear strength τ_n to be equal to the load which results in almost instantaneous shear destruction of the specimen.

SUMMARY

1. The rheological properties of peats were studied by the method of homogeneous shear in the D. M. Tolstoi apparatus with a moving plate, in the RV-4 rotational viscosimeter, and by the method of cylinder compression.

2. Complete rheological diagrams were obtained for the peats; each such diagram consists of a series of curves representing the development of deformation (in deformation-time coordinates) under constant load and after removal of the load.

3. Two types of complete rheological diagrams have been found for peats. A Type I diagram is given by a peat of plastic consistency, which was capable of undergoing, at stresses in excess of the static yield value, considerable deformations at relatively high velocities (up to 100^*sec^{-1} and over) without disturbance of the continuity of flow. A peat of semisolid consistency, which gives a complete rheological diagram of Type II, did not exhibit any appreciable plastic flow. Destruction of a semisolid peat took place with breakdown of continuity and separation of the specimen into two or more parts.

4. An equation for the creep of low-moisture peat has been derived.

5. For peat giving a Type I complete rheological diagram it proved possible to calculate both the Shvedov viscosity (by the Rebinder method) at low velocity gradients, and the plastic (Bingham) viscosity at high velocity gradients. The latter is smaller than the former by several orders of magnitude.

* As in original — Publisher's note.

6. The deformation properties of low-moisture peats may be described in terms of seven rheological parameters.

LITERATURE CITED

- [1] S. G. Solopov, "Principles of Multiple Mechanization of the Winning of Peat for Fuel by the Excavator Process with Decrease of the Operating Moisture," Doctorate Dissertation* (Moscow Peat Institute, Moscow 1955); Summaries of Papers at the Scientific-Technical Conference of the Moscow Peat Institute* (Moscow, 1956) p. 3.
- [2] V. G. Goriachkin, Trans. Inst. Peat, Acad. Sci. Belorussian SSR 4, 20 (1955).
- [3] M. P. Volarovich, Colloid J. 16, No. 3, 227 (1954).**
- [4] M. P. Volarovich and S. M. Levi, Colloid J. 18, No. 2, 129 (1956).**
- [5] M. P. Volarovich and R. A. Branopol'skaia, Colloid J. 10, No. 6, 406 (1948).
- [6] P. A. Rebinder and E. E. Segalova, Colloid J. 10, No. 3, 233 (1948); L. A. Abduragimova, P. A. Rebinder and N. N. Serb-Serbina, Colloid J. 17, No. 3, 184 (1955); L. V. Ivanova-Chumakova and P. A. Rebinder, Colloid J. 18, No. 4, 429 (1956); P. A. Rebinder, Collection Dedicated to the Memory of Academician P. P. Lazarev (Izd. AN SSSR, 1956) p. 113.
- [7] P. A. Rebinder and N. V. Mikhailov, Colloid J. 17, No. 2, 107 (1955).**
- [8] G. V. Vinogradov and K. I. Klimov, Proc. Acad. Sci. USSR 57, 911 (1947); J. Tech. Phys. 18, 355 (1948); G. V. Vinogradov, Colloid J. 15, 371 (1953).**
- [9] N. V. Mikhailov and E. E. Kalmykova, Colloid J. 16, No. 5, 350 (1954); N. V. Mikhailov, Colloid J. 17, No. 1, 68 (1955).**
- [10] A. A. Trapeznikov, Proc. All-Union Conf. on Colloid Chem. Kiev, 1952, p. 175; A. A. Trapeznikov and V. A. Fedotova, Proc. Acad. Sci. USSR 82, No. 1, 97 (1952); 92, No. 6, 1189 (1953).
- [11] J. J. Hermans (Ed.) Flow Properties of Disperse Systems (Amsterdam, 1953).
- [12] G. W. Scott Blair, (Ed.) Foodstuffs, Their Plasticity, Fluidity and Consistency (Amsterdam, 1953).
- [13] M. Reiner, (Ed.) Building Materials, Their Elasticity and Inelasticity (Amsterdam, 1954).
- [14] R. F. Eirich, (Ed.) Rheology. Theory and Application, V. 1 (New York, 1956).
- [15] M. P. Volarovich, Colloid J. 16, No. 6, 474 (1954).**
- [16] M. P. Volarovich and N. N. Kulakov, Bull. Acad. Sci. USSR, Div. Math. and Nat. Sci. 10, 1331 (1935); N. N. Kulakov, Proc. Conf. on Viscosity of Liquids and Colloidal Solutions 1, 391 (1941).*
- [17] N. N. Kulakov and K. I. Samarina, Colloid J. 3, No. 2, 163 (1937).
- [18] M. P. Volarovich and N. V. Lazovskaya, Proc. Acad. Sci. USSR 76, No. 2, 211 (1951); N. V. Lazovskaya, Peat Industry No. 3, 28 (1951).
- [19] M. P. Volarovich and S. N. Markov, Peat Industry No. 10, 23 (1951); Colloid J. 19, No. 4, 401 (1957); I. D. Belovidov, "Plasticity of Worked Crude Peat," Candidate's Dissertation* (Moscow Peat Institute, 1954); A. A. Simonian, Peat Industry No. 10, 22 (1953).
- [20] N. V. Lazovskaya, Trans. Moscow Peat Inst. No. 5, 63 (1957).
- [21] T. Ia. Gorazdovskii, Peat Industry No. 8, 11 (1949).
- [22] V. A. Silin, Colloid J. 13, No. 1, 51 (1951).
- [23] D. M. Tolstoi, Colloid J. 9, No. 6, 450 (1947); 10, No. 2, 133 (1948); Collection Dedicated to the Memory of Academician P. P. Lazarev* (Izd. AN SSSR, 1956) p. 159.

* In Russian.

** Original Russian pagination. See C. B. Translation.

- [24] E. Fukada, J. Phys. Soc. Japan 9, No. 5, 786 (1954).
- [25] P. A. Rebinder, Jubilee Collection for the 30th Anniversary of the Great October Socialist Revolution 1, 533 (1947).*
- [26] M. P. Volarovich, Viscosity of Lubricating Oils at Low Temperatures*(Izd. AN SSSR, 1944); N. N. Kulakov, Introduction to the Physics of Peat*(Gosenergoizdat, 1947).
- [27] M. P. Volarovich, Trans. Inst. Applied Mineralogy No. 66, 1 (1934); M. P. Volarovich and D. M. Tolstoi, J. Phys. Chem. 4, No. 6, 815 (1934).
- [28] N. I. Malinin, Colloid J. 17, No. 4, 332 (1955).**
- [29] T. Alfrey, Mechanical Behavior of High Polymers (Russian translation) (IL, 1952).

The Moscow Peat Institute
Chair of Physics

Received November 13, 1957

INVESTIGATION OF THE TEARING PROCESS IN THE REGION OF TRANSITION FROM THE ELASTIC TO THE BRITTLE STATE

V. E. Gul', L. N. Tsarskii, and S. A. Vil'nits

Recently several papers [1-4] have been published which show convincingly that the tearing of vulcanizates is a process which develops in time. A distinction is made between the slow and rapid stages of the process. The use of high-speed motion pictures has provided clear evidence that in ordinary tensile tests the tearing rate is at first very low, and then increases rapidly and discontinuously. This applies both to tests of specimens without nicks, and to tests of nicked specimens; the influence of the nicking has been studied in detail [5]. Investigations of the tearing of highly elastic materials showed that the tearing of vulcanizates has much in common with the rupture of brittle solids. Nevertheless, the mechanisms of high-elastic and brittle rupture are so different that considerable changes in the course of the rupture in the transition region from the high-elastic to the glassy state are to be expected. The study of these changes forms the subject of the present investigation.

The materials chosen for the study were loaded SKB rubber vulcanizates with 45% carbon black (A), and vulcanizates of SKB and natural rubber in 4:6 ratio, with 10% carbon black (B). All the mechanical tests were carried out in the TsMG and T dynamometer, in which the vulcanizates could be tested at temperatures down to -57° .* In order that the growing nick should traverse a considerable distance through the specimen, and for convenience in the determination of the tearing rate in the course of this process, we used rectangular specimens 50×60 mm, up to 2 mm thick. The tearing region was predetermined by the application of a nick 1 mm long. A white line perpendicular to the direction of extension was marked with paint at this region. The tear spread along this line, and widening of the line at the apex of the tear gave an indication of additional deformation of the material in this zone. The motion pictures were taken with a high-speed 16 mm SKS camera through the glass door of the thermostat. The speed of the photography was determined by means of a neon time indicator type MN-7, which illuminated one edge of the film (at the perforations). When the film was projected at the normal speed of 16 or 24 frames per second, the picture was observed slowed down 10 to 500-fold, according to the speed at which it was taken. When measurements had to be made frame by frame, the frames were projected individually. This allowed of great accuracy in the space and time measurements.

After the specimens had reached the required temperature, the strong external and internal illumination (which was necessary because of the short exposures and the presence of seven glasses in the thermostat) was switched on, the dynamometer was started, the photographs were taken, and the dynamometer readings were taken simultaneously. The films were developed and the photographs analyzed stroboscopically.

The method described above was used for studying the growth of the nick in relation to the test temperature and the deformation rate. More than 300 high-speed films were taken and subsequently analyzed stroboscopically. Typical variations of the tearing rate with time are plotted in Figs. 1-4. Examination of the results shows that the tearing curves follow the course described previously [4, 5] at all the temperatures used. At first the tearing rate is so low that it is probably more convenient to study it by delayed photography. Immediately before the end of the rupture the tearing rate suddenly increases. The maximum tearing rate, under equal conditions, depends on the test temperature. Figs. 1 and 2 show the kinetics of the tearing rate for specimens of SKB and natural rubber vulcanizates. When the temperature is decreased from 22 to 0° , the maximum tearing rate decreases from 2500 to 100 mm/second for vulcanizates based on NR and SKB mixtures. Further

* G. Z. Krasikova took part in the experimental work.

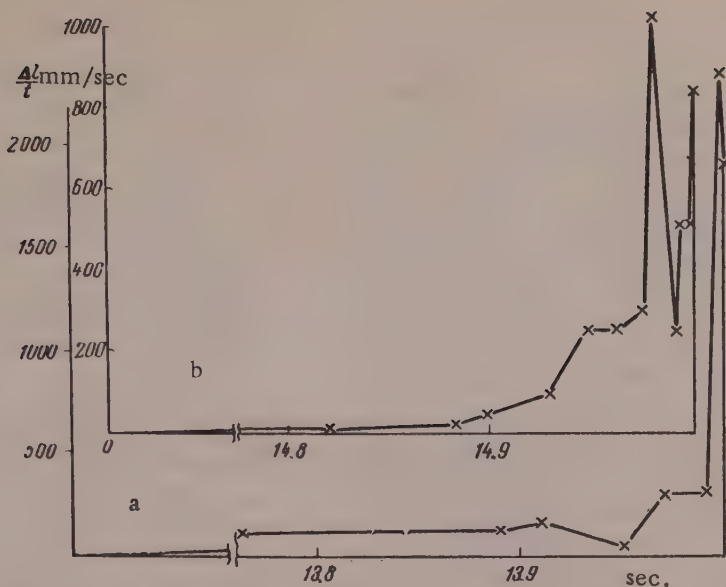


Fig. 1. Variation of the tearing rate of a specimen with time. Mixture based on SKB-50 + NR rubbers (1 : 1); deformation rate 250 mm/minute; temperature: a) 22°; b) 0°.

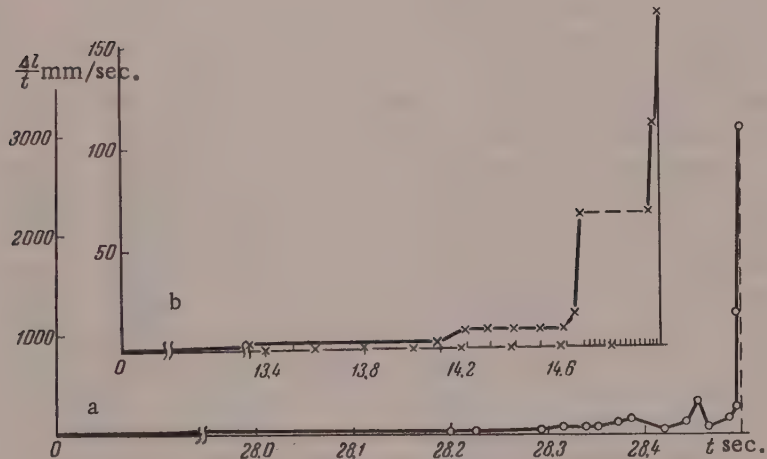


Fig. 2. Variation of the tearing rate of a specimen with time. Mixture based on SKB-50 + NR rubbers (1 : 1); deformation rate 250 mm/minute; temperature: a) 30°; b) 50°.

decrease of temperature results in a further decrease of the tearing rate, but at temperatures of -50° and lower the rate increases again, reaching ~ 3000 mm/second. A similar dependence of the maximum tearing rate on the temperature was found in tests of SKB vulcanizates (A). It follows from Figs. 3 and 4 that the variation of the maximum tearing rate of SKB vulcanizates with decrease of temperature from $+25$ to -50° is also represented by a curve with a minimum. The maximum tearing rates of vulcanizates A and B are plotted against the temperature in Fig. 5. The temperature dependence of the tearing rate depends appreciably on the deformation rate; increase of the deformation rate is generally accompanied by displacement of the kinetic curve for

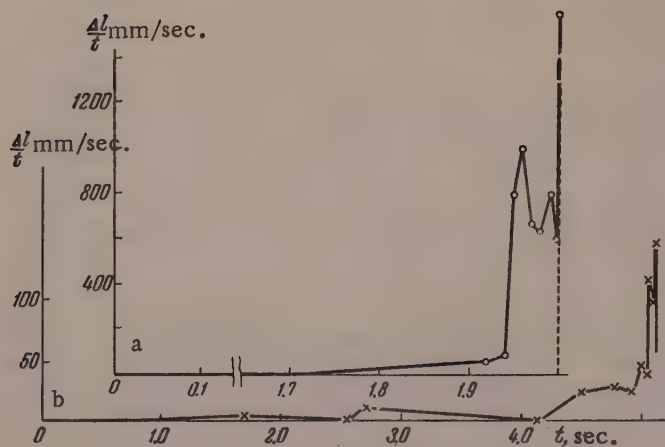


Fig. 3. Variation of the tearing rate of a specimen with time. Mixture based on SKB-50 rubber; deformation rate 500 mm/minute; temperature: a) 50°; b) 30°.

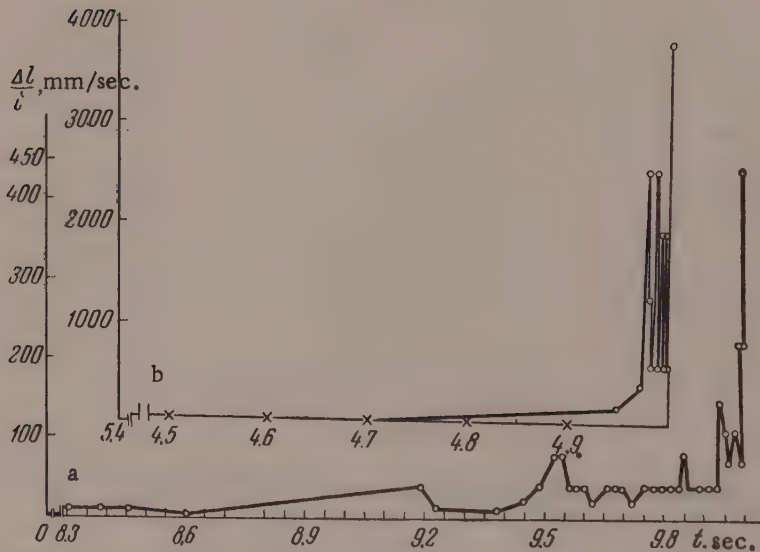


Fig. 4. Variation of the tearing rate of a specimen with time. Mixture based on SKB-50 rubber; deformation rate 500 mm/minute; temperature: a) 0°; b) +25°.

the tearing rate toward higher temperatures. The statistical character of vulcanizate rupture is the reason for the certain amount (small) of scattering of the maximum values for the tearing rate. The values of the average tearing rate vary much more regularly; these are plotted against the temperature for different deformation rates in Fig. 6. It follows from the data in Fig. 6 that the variation of the average tearing rate with the temperature is also represented by a curve with a minimum; the minima on the curves are displaced toward higher temperatures with increase of the deformation rate. The observed change in the course of the

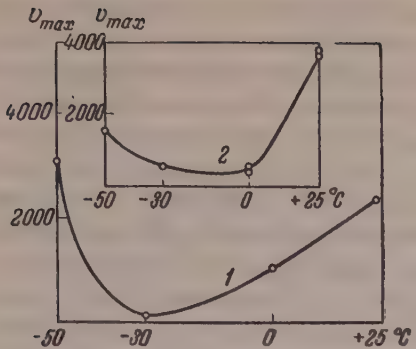


Fig. 5. Variation of the maximum tearing rate with temperature for specimens of carcass rubber: 1) Based on SKB-50 + NR rubbers (1:1); deformation rate 200 mm/minute; 2) based on SKB-50 rubber, deformation rate 500 mm/minute.

creases with fall of temperature, and is 1.2 at -50°C . Naturally, the variation which we detected in the course of the tearing rate cannot fail to influence the mechanical characteristics of the vulcanizates or, more accurately, the tearing characteristics of the vulcanizates.

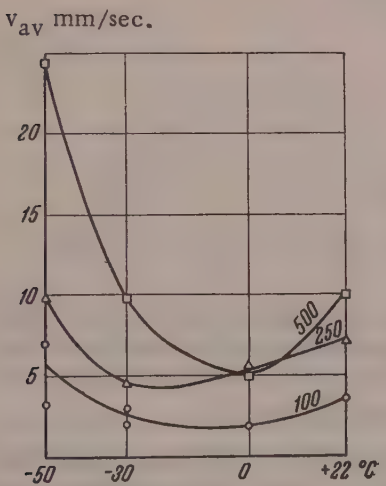


Fig. 6. Variation of the average tearing rate with temperature for a specimen of carcass rubber based on SKB-50; the numbers on the curves represent the deformation rates in mm/minute.

the tensile strengths increase when temperatures are reached at which the tearing rate diminishes appreciably; this is due to changes in the additional orientation. When the growth rate of the tearing region is changed as the result of a change in the deformation rate (if the degree of additional orientation is not altered appreciably), the increase of the tearing rate is accompanied by an increase of tensile strength. Analysis of the effects of

tearing with decrease of temperature is probably associated with the transition from the high-elastic to the brittle state. A decrease of the additional orientation effect of the vulcanize [5] at the site of rupture with decrease of temperature, and with the consequent loss of high-elastic properties, was to be expected. It proved possible to observe this by comparison of the width of the line drawn in the direction of the tear, directly at the apex of the tear and in the middle of the unturned part of the specimen. In Fig. 7 the ratios of the widths of this line at the apex of the tear (d_t) and in the middle of the unturned part of the specimen (d_u) are plotted against time. At first, owing to the small difference between the stress at the apex of the growing tear and the average stress in the specimen, the additional orientation effect was very weak. As the tearing rate increases and exceeds the rate of the relaxation processes which aid dissipation of the stress concentration at the region of tear, the additional orientation effect increases. At $+22^{\circ}\text{C}$ and deformation rate 250 mm/minute the d_t/d_u ratio reaches 2.3 at the instant when tearing ends in (SKB+NR) vulcanize. The final value of d_t/d_u decreases with fall of temperature, and is 1.2 at -50°C .

Naturally, the variation which we detected in the course of the tearing rate cannot fail to influence the mechanical characteristics of the vulcanizates or, more accurately, the tearing characteristics of the vulcanizates. The extension curves of vulcanizates A and B were also studied over the same temperature range. The results for vulcanize B are plotted in Fig. 8. Decrease of the test temperature resulted in a decrease of the relative elongation at break in all cases. Gul' and Farberova showed earlier [6] that the relative elongation at break depends on the temperature in a complex manner, so that cases of increased relative elongation at break with decrease of temperature are possible in principle. It was shown that the temperature dependence of the relative elongation at break is determined by the influence of temperature on the tensile strength (for which suitable expressions have been proposed [1, 2, 7]), and on the deformation properties of the material. Analogously to the nonsteady variation of tensile strength with changes of intermolecular interaction which has been detected in certain cases [8], nonsteady variation of the relative elongation at break with decrease of temperature is also possible. However, in this particular case the relative elongation at break decreased almost continuously, although the tensile strength varied unsteadily. The relative elongation at break is plotted against the temperature in Fig. 9. Figure 10 gives the tensile strength - temperature relationships for vulcanizates of mixtures of SKB and NR. It is significant that

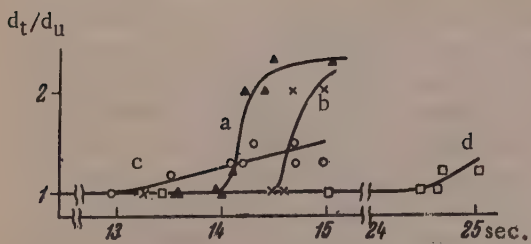


Fig. 7. Variation of the degree of orientation in rubber at the apex of the tear, with time; mixture based on SKB-50 + NR (1:1); deformation rate 250 mm/minute; temperatures: a) 25°; b) 0°; c) -30°; d) -50°.

temperature on relative elongation and tensile strength readily leads to the conclusion that the work of deformation to rupture as a function of the temperature must be represented by a nonsteady curve. Examination of the values of the work of deformation to rupture of specimen A, determined from the extension curves at various temperatures, showed that the values of the work of rupture as a rule increase with decrease of temperature from 22 to 0°. The values of the work of rupture then decrease with further fall of temperature. The work of tearing deformation determined for SKB vulcanizates at different rates of extension is plotted against the temperature in Fig. 11. Comparison of Fig. 11 with Figs. 6 and 7 shows that the values of the work of deformation to rupture increase in the temperature region in which the tearing rate decreases.

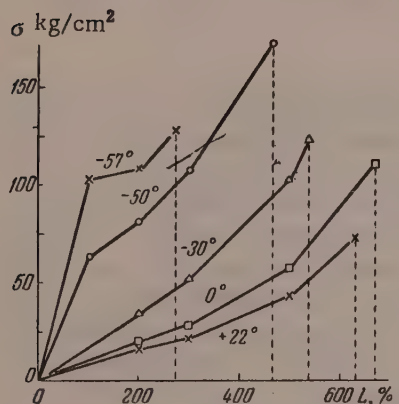


Fig. 8. Curves for extension at constant rate at various temperatures; ring-shaped specimens based on SKB-50 + NR rubbers (1:1); deformation rate 100 mm/minute.

Decrease of temperature is accompanied by an increase in the number of intermolecular bonds which are broken down during deformation and rupture. This occurs in the high-elastic region. Further cooling reduces the mobility of the chain segments. The number of intermolecular bonds broken during deformation and tearing of the specimen also decreases. Deformation of the material in the glassy state does not involve the same degree of breakdown of the intermolecular bonds as is the case in high-elastic deformation, and the additional orientation at the site of rupture decreases. Therefore the work of deformation to rupture decreases in the transition region between the high-elastic and glassy states.

Thus, the transition from the high-elastic to the glassy state is accompanied by a decrease of the tearing rate, of the relative elongation at break, of the tensile strength, and of the work of deformation to rupture. It is important to take these facts into consideration in the solution of certain practical problems relating to mechanical destruction of vulcanizates.

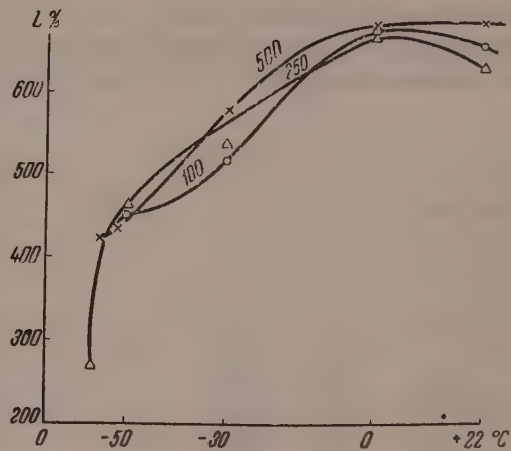


Fig. 9. Variation of relative elongation with temperature for ring-shaped specimens of carcass rubber based on SKB-50 + NR (1:1); the numbers on the curves are the deformation rates in mm/min.

SUMMARY

1. Analysis of high-speed motion pictures of the tearing of vulcanizates, taken in the +22° to -57° range, shows that the tearing rate is initially very low, but it increases rapidly and suddenly immediately before the specimen divides into two parts.

2. The average and maximum tearing rate do not vary steadily with decrease of temperature. In the transition from high-elastic to brittle rupture the tearing rate diminishes at first, owing to an increase in the number of intermolecular bonds which hinder rupture. At the same time decrease of temperature is accompanied by a decrease of the additional orientation of the material at the site of rupture; this has been determined quantitatively. When sufficiently low temperatures are reached the decrease of additional orientation at the site of rupture becomes so considerable that the tearing rate (at a given rate of extension) begins to increase again.

3. This change in the course of the tearing rate with temperature is in harmony with changes in the mechanical properties of the material. Thus, in the transition from high-elastic to brittle rupture the tensile strength varies anomalously with temperature. The tensile strength in this region decreases instead of decreasing with fall of temperature, while the work of rupture first increases and then decreases with fall of temperature.

4. In the temperature regions characterized by definite mechanisms of rupture, either elastic or brittle, decrease of temperature is accompanied by increase of strength. In the transition from elastic to brittle rupture the strength decreases, owing to changes in the structural characteristics of the material.

The authors express their gratitude to Professor B. A. Dogadkin for valuable advice given in the course of discussion of this work.

LITERATURE CITED

- [1] G. M. Bartenev, Progr. Chem. 24, No. 7, 815 (1955).
- [2] S. N. Zhurkov and B. N. Narzulaev, J. Theor. Phys. 23, 10, 1677 (1953).
- [3] W. Späth, Beiträge zur Technologie der Hochpolymeren Gummi und Kunststoffe, Stuttgart (1956).
- [4] V. E. Gul' and G. P. Krutetskaia, Proc. Acad. Sci. USSR 114, No. 5, 973 (1957).*
- [5] V. E. Gul', G. P. Krutetskaia and V. V. Kovriga, Caoutchouc and Rubber 12, 1 (1957).
- [6] V. E. Gul' and I. I. Farberova, Colloid J. 18, No. 6, 660 (1956).

*Original Russian pagination. See C. B. Translation.

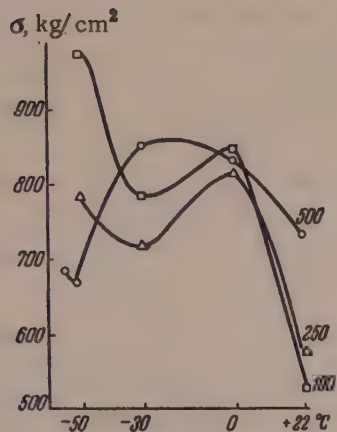


Fig. 10. Variation of true tensile strength with temperature for ring-shaped specimens of carcass rubber based on SKB-50 + NR (1:1); the numbers on the curves are the deformation rates in mm/minutes.

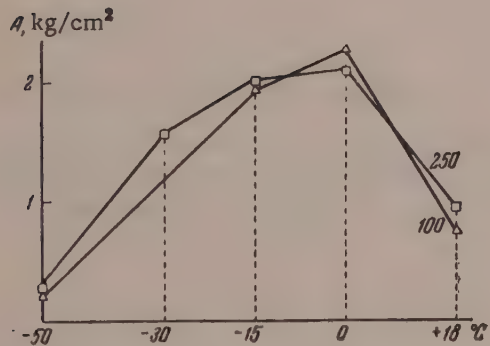


Fig. 11. Variation of the work of rupture with temperature for ring-shaped specimens of carcass rubber based on SKB-50; the numbers on the curves are the deformation rates in mm/min.

[7] V. E. Gul', Proc. Acad. Sci. USSR 96, No. 5, 953 (1954).

[8] V. E. Gul', D. L. Fediukina and B. A. Dogadkin, Colloid J. 15, No. 1, 11 (1953).*

The Moscow Institute of Fine Chemical
Technology
Moscow

Received May 3, 1957

*Original Russian pagination. See C. B. Translation.

METHOD OF CALCULATING THE PRECIPITATION OF DISPERSE PARTICLES FROM A STREAM ON AN OBSTACLE

S. S. Dukhin and B. V. Deriagin

Much attention is devoted in the physics of aerosols to the problem of efficiency of deposition of an aerosol on an obstacle from a stream. To calculate the number of particles deposited on an obstacle in unit time it is sufficient to determine the so-called collection efficiency E , which is the ratio of the cross section of a tube (at a distance from the obstacle) formed by the extreme trajectories of particles of a given size which still impinge on the obstacle, to the midship section of the obstacle. Levin [1] proposed a method for determination of these boundary trajectories, based on qualitative analysis of the differential equation for the motion of a particle for the case when the particle size is so small that the inertia force acting on the particle can be neglected, in comparison with the other forces, in the equation for the motion. Such a simplified equation for the motion of a particle in fact expresses the particle velocity $\vec{v}(r)$ at each point in space in terms of given functions of the coordinates: velocity field of the air stream $\vec{u}(r)$, and the field of external forces $\vec{F}(r)$, acting on the particle.

$$\vec{v}(r) = \vec{u}(r) + \beta \vec{F}(r), \quad (1)$$

where β is the mobility of the particle.

Equation (1) can be used to determine the normal component of the particle velocity at the surface; this provides the most direct method for calculating the flow of the aerosol particles to the surface, if their concentration $n(r)$ at the surface is known

$$I = \iint n(r) [u_n(r) + \beta F_n(r)] ds, \quad (2)$$

Here the integration is performed with respect to the part of the surface on which the particles are deposited. In connection with this calculation method the question arises whether the particle concentration alters along their path.

The expression for the complete derivative of the particle concentration with respect to time, representing the variation of the particle concentration along the path with equilibrium distribution of the particles, is of the form

$$\frac{dn}{dt} = (\vec{v} \nabla n). \quad (3)$$

The right-hand side of Equation (3) should be transformed for convenience, with the use of the equation for the conservation of the number of particles, which may be written as follows:

$$\operatorname{div}(nv) = n \operatorname{div}v + (\vec{v} \nabla n) = 0. \quad (4)$$

Expanding $\operatorname{div} \vec{v}$ by means of Equation (1), and taking into account that $\operatorname{div} \vec{u} = 0$, we have from Equation (4)

$$(\vec{v} \nabla n) = 0, \quad (5)$$

if the following condition is satisfied:

$$\operatorname{div} F = 0. \quad (6)$$

Therefore, if condition (6) is satisfied, then $dn/dt = 0$, which leads to the following theorem.

If the external force field acting on the particles is solenoidal, the concentration of the particles along their trajectory is constant.*

The concentration of particles in an aerosol at a distance from the obstacle, in a region of space the linear dimensions of which are comparable to the dimensions of the obstacle, is usually constant. In a region of space filled with trajectories arriving from infinity and terminating on the obstacle surface, the particle concentration is equal to the concentration at infinity, n_{∞} .

In steady-state conditions, in the region of space filled with trajectories originating at the obstacle surface, the particle concentration should be taken as zero. Accordingly, the concentrations is n_{∞} at the part of the obstacle surface where the trajectories coming from infinity terminate, and is zero at the part of the surface where trajectories originate and also at the part of the surface where the trajectories originating at neighboring regions of the surface terminate. To determine the integration limits in Formula (2), it is necessary to find the boundary line between the part of the surface on which the aerosol is deposited and the part of the surface near which there are no aerosol particles. As this line is the geometrical position of the points lying at the intersection of the boundary trajectories with the obstacle surface, in the general case the proposed method is again reduced to the problem of determination of the boundary trajectories.

It should be pointed out, however, that these difficulties are eliminated if at all points of the obstacle surface the normal component of the velocity vector of the particle is directed along the internal normal. In this case $n = n_{\infty}$ along the whole surface, and there is no need for the complicated procedure of qualitative analysis of differential Equation (1) for calculation of the deposition of the aerosol particles. The particle flow in this case should be calculated from the formula

$$I = n_{\infty} \iint (u_n + \beta F_n) ds, \quad (7)$$

with integration with respect to the whole surface. For example, Equation (7) can be used very simply to derive Levin's known equation [1] for the collection efficiency of small droplets in a mist by a falling electrically charged drop. However, it may be noted that the value of the approach to the calculation of the deposition of particles on an obstacle, described in this paper, is not restricted to the type of problem discussed above. This method is simple and convenient in all cases when it is simpler to find the line of intersection between a bubble surface and the surface formed by the boundary trajectories, than it is to find the latter.

This can be illustrated by a calculation of the sedimentation of particles suspended in water, under the action of gravity, on an ascending bubble. The particles are assumed to be so small that the inertia forces acting upon them in flow around the bubble may be ignored, so that the particle velocity can be expressed by means of the equation

$$\vec{v}(r) = \vec{u}(r) + \vec{v}_d, \quad (8)$$

* It transpired in the course of a discussion with L. M. Levin that he reached an analogous conclusion in the development of a theory of aerosol sampling [1]. It should be pointed out that this theorem has been proved [2] for the special case of a gravitational field.

where v_d is the falling velocity of a particle of diameter d , and the coordinate system carried along by the bubble is taken.

As the normal component of the velocity of the liquid at the bubble surface is zero, the normal component of the particle velocity at the bubble surface, v_n , is determined by sedimentation only

$$v_n = v_d \cos \theta, \quad (9)$$

with θ reckoned from the upper pole of the bubble. It follows from Equation (8) that sedimentation, impossible on the lower hemisphere of the bubble, is possible on the upper hemisphere. It is necessary to prove that the concentration of the aerosol* at the upper hemisphere of the bubble is constant; for this it is enough to show that particle trajectories originating at the lower hemisphere and terminating at the upper hemisphere are impossible. This is the case, because the horizontal component of the particle velocity is directed toward the bubble at each point of the half-space limited at the top by the equatorial plane of the bubble. This follows from the fact that, since the horizontal component \vec{v}_d is zero, the horizontal component of the particle velocity, according to Equation (8), coincides with the horizontal component of the local velocity of the liquid directed toward the bubble at each point of the lower half-space. Consequently, the particle trajectories terminating at the upper hemisphere originate only at infinity, and hence, the particle concentration near the surface points of the upper hemisphere is constant.

The flow of particles onto a bubble of diameter D can be calculated from Equation (7)

$$I = n_\infty \int_0^{\frac{\pi}{2}} v d \cos \theta \frac{\pi D^2}{2} \sin \theta d \theta = \frac{\pi D^2}{4} n_\infty v d. \quad (10)$$

SUMMARY

1. If the inertia of aerosol or colloidal particles in a stream flowing around an obstacle may be neglected, and the external force field is sinusoidal, the numerical concentration of the particles along their trajectories is constant.

2. This theorem can be used in a number of cases for very simple calculation of the rate of deposition on obstacles; for example, for calculation of the collection efficiency of particles by emerging bubbles or falling spheres.

LITERATURE CITED

- [1] L. M. Levin, Proc. Acad. Sci. USSR 94, 3 (1954).
- [2] W. H. Walton, Brit. J. Appl. Phys. No. 3, 29 (1954).

Institute of Physical Chemistry
Academy of Sciences USSR
Moscow

Received January 10, 1958

* As in original — Publisher's note.

THE STRUCTURE OF GELS

14. INFLUENCE OF THE NATURE OF THE PLASTICIZER ON THE PROPERTIES OF FILLED DIVINYL-STYRENE RUBBER

M. P. Zverev, E. A. Eroshkina, and P. I. Zubov

It was shown earlier [1] that unfilled vulcanizates of divinyl-styrene rubber have higher mechanical strength in presence of nonpolar than in presence of polar plasticizers. The question arose whether this is applicable to plasticized divinyl-styrene rubber vulcanizates containing fillers. The strength and deformability of plasticized vulcanizates in presence of a filler were therefore studied. The filler used was a gas channel black with specific surface $110 \text{ m}^2/\text{g}$, with the following composition: C - 93%, H - 1.2%, O - 3.5%. 50 wt. parts of the black per 100 wt. parts of rubber and plasticizer was introduced into the mix. The vulcanizing components, vulcanization conditions, and plasticizers were the same as before [1].

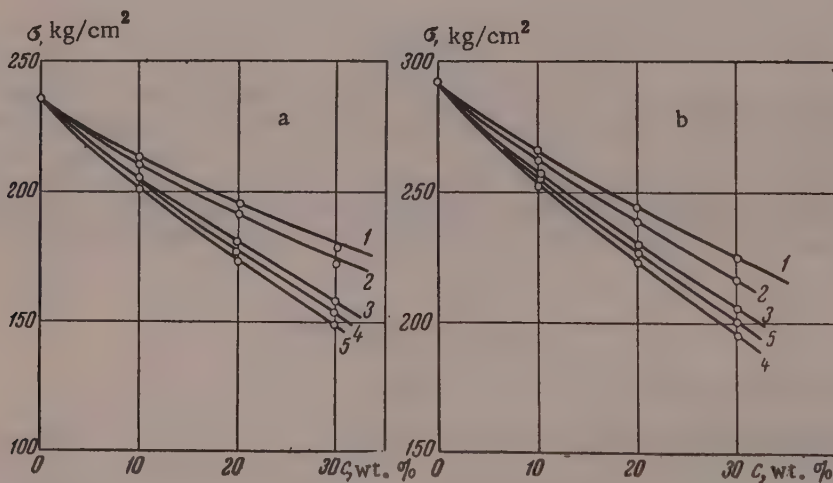


Fig. 1. Variation of the tensile strength of plasticized filled divinyl-styrene rubber vulcanizate with concentration and structure of the plasticizer molecules; Deformation rates: a) 50 mm/min; b) 500 mm/min; 1) Dibutyl phthalate; 2) dibutyl sebacate; 3) ditolylmethane; 4) tetralin; 5) green oil.

Data on the dependence of the tensile strength of filled SKS-30A vulcanizates on the plasticizer concentration and structure at deformation rates 50 and 500 mm/minute are given in Fig. 1. It follows from these data that the mechanical properties of filled plasticized SKS-30A vulcanizates do not vary in the same way as the properties of unfilled vulcanizates. The tensile strength in presence of polar plasticizers is higher than in presence of nonpolar plasticizers at all deformation rates.

Figure 2 shows that the relative elongation of plasticized vulcanizates is greater when nonpolar substances are used.

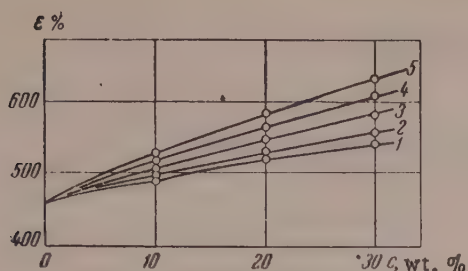


Fig. 2. Variation of the relative elongation of plasticized filled divinyl-styrene rubber vulcanizate with the concentration and structure of the plasticizer molecules. Deformation rate 50 mm/min: 1) dibutyl phthalate; 2) dibutyl sebacate; 3) ditolylmethane; 4) tetralin; 5) green oil.

and samples for viscosity determination were taken at intervals [1]. The amount of rubber adsorbed on the carbon surfaces was estimated from the viscosity change.

In our opinion, this is because changes in the mechanical properties of filled vulcanizates are determined not only by changes in the configuration (flexibility) of the macromolecules, as is the case in unfilled plasticized divinyl-styrene vulcanizates, but also by the degree of interaction of the polymer molecules with the surface of the filler particles.

In presence of polar plasticizers the interaction between the rubber molecules and the surface of the filler particles is apparently greater than in presence of nonpolar plasticizers.

This hypothesis is confirmed by the results of our experiments on the adsorption of rubber molecules on the filler particles in plasticizers (solvents) of different structure. For the adsorption experiments 0.25% solutions of the rubber were prepared in different solvents, and 3.5 g of filler per 100 ml of solution was added.

The rubber solutions were mixed with the carbon black,

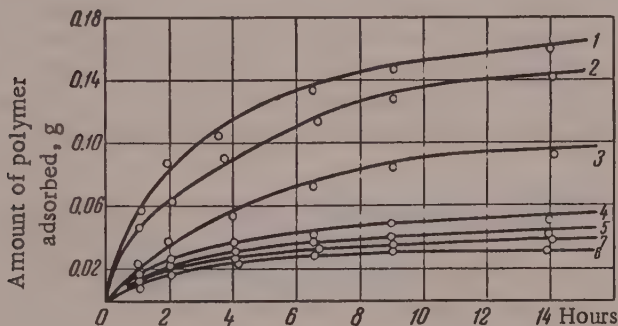


Fig. 3. Adsorption of molecules of divinyl-styrene rubber from solution onto the surface of gas channel black particles in presence of plasticizers: 1) Dibutyl phthalate; 2) dibutyl sebacate; 3) toluene; 4) green oil; 5) ditolylmethane; 6) benzene; 7) tetralin.

The adsorption curves are given in Fig. 3; the time is taken along the abscissa axis, and the amount of rubber in grams, adsorbed on the carbon black surface, along the ordinate axis. It follows from Fig. 3 that the equilibrium adsorption in presence of polar plasticizers is higher than in presence of nonpolar plasticizers. This is probably caused by blocking of the polar groups in the filler particle surface by the molecules of the polar plasticizer.

SUMMARY

1. The tensile strength of filled divinyl-styrene rubber vulcanizates is greater in presence of polar than of nonpolar plasticizers.

2. The explanation for this effect is that the molecules of a polar plasticizer assist better adsorption of the macromolecules on the filler particle surface than do molecules of a nonpolar plasticizer.

LITERATURE CITED

- [1] P. I. Zubov and M. P. Zverev, Colloid J. 18, 679 (1956);^{*} 19, 201 (1957).^{*}

The L. Ia. Karpov Physicochemical Institute
The Dnepropetrovsk Institute of
Chemical Technology

Received November 21, 1957

^{*}Original Russian pagination. See C. B. Translation.

CERTAIN PROPERTIES OF BLOCK COPOLYMERS BASED ON AN EPOXY RESIN AND BUTADIENE-NITRILE RUBBER

V. A. Kargin, N. A. Plate, and A. S. Dobrynina

Much information is available in the literature on different methods for preparation of graft and block copolymers, which are of considerable interest both from the theoretical and the practical aspects. The alternation of long sections of unlike polymeric molecules, joined by chemical bonds, gives new types of polymers, combining the properties of both the individual components involved in the formation of a given graft or block copolymer.

Extensive bibliographies on the subject are given in the reviews by Immergut and Mark [1], Hart [2], and Akutin [3]. However, with a few exceptions, the literature contains no papers dealing with systematic studies of the graft and block copolymers formed. A few communications on certain properties of graft polymers deal with subjects such as the reinforcement of rubbers by the grafting of polystyrene and polymethyl methacrylate [4]. It has also been shown that the block copolymer based on polyethylene terephthalate and polyoxyethylene glycol is more hydrophilic than polyethylene terephthalate; the melting point of the polymer remains constant while the glass transition temperature decreases with increase of the polyoxyethylene glycol content [5]. Graft polymers based on nylon and ethylene oxide have also been studied [6], and it was shown that the moisture absorption of the graft polymer increases with the ethylene oxide content. One of the present authors and his associates [7] studied block copolymers of novolac resin and nitrile rubber and showed that the block copolymer retains the flow properties characteristic of the resin, while its elasticity decreases in comparison with the rubber.

In the present investigation it was desired to study certain properties of the block copolymer formed by cold mastication of an epoxy resin with butadiene-nitrile rubber. The mechanochemical method for the production of graft and block copolymers, proposed and described by a number of authors [7-11], is worthy of attention and study owing to its relative simplicity and possible industrial applications. It was moreover of interest to determine the properties of a block copolymer containing macromolecules of two polar polymers of dissimilar mechanical properties — a hard and brittle epoxy resin and elastic nitrile rubber. This work forms part of a series of investigations of the properties of graft and block copolymers.

Preparation of block copolymers. Block copolymers of ED-15 epoxy resin and SKN-26 butadiene-nitrile rubber were prepared by the mechanochemical method in a flat mill of the "snail" type [11]. * 12 g of a mixture of ED-15 and SKN-26, in the following ratios (by weight): 5:1, 2:1, 1:1, 1:2, 1:5, were treated for 5-7 minutes at room temperature in a nitrogen atmosphere. **

Separation of the mastication products. Isolation of the block copolymers from the mixture obtained after mastication, which contained unreacted resin and rubber in addition to the reaction products, presented

* The term "block copolymers" applied in this paper to the products of mastication of ED-15 with SKN-26, is to some extent conventional, as in addition to true block copolymers a certain proportion of graft polymers is formed in the mixture as the result of mastication. The determination of their relative proportions, and the separation of such copolymers, form the subject of a special investigation, outside the scope of the present paper.

** The authors thank B. M. Kovarskaia for help and advice on the use of the mill.

considerable difficulties owing to the similar solubilities of all three components in many solvents. It was found, however, that a mixture of cyclohexanol with ethylene glycol (65% and 35% by volume) completely dissolves the resin and only 8% of the rubber when the mixture is boiled for 5 hours in 100 ml of the solvent; a mixture of m-xylene and n-heptane (90 and 10% by volume) completely dissolves the rubber and only 1% of the resin in cold treatment of the mixture for 48 hours. Therefore, to separate the block copolymers, the mixture after mastication was treated for 48 hours with a mixture of m-xylene and n-heptane at 18-20°. The undissolved portion was centrifuged off and treated with a boiling mixture of cyclohexanol and ethylene glycol for 5 hours. This two-stage treatment, repeated several times, gave an insoluble residue, which was 12-15% by weight of the mastication product taken, and which consisted of a copolymer of the epoxy resin and nitrile rubber.

Preparation of raw mixtures. To compare the properties of the products obtained after mastication with the properties of a mechanical mixture of the two individual polymers, raw mixtures of epoxide resin and nitrile rubber were prepared. The mixtures were made by evaporation of combined solutions of the two components in chloroform, in the same proportions as in the masticated mixtures.

Turbidimetric titration. To identify the block copolymers [12] and to check the effectiveness of the mastication, we carried out turbidimetric titrations of raw resin-rubber mixtures, of the mixtures obtained directly after the mastication, and of the block copolymers isolated from the mixtures. All the resin-rubber ratios used were taken in all cases. The titration was performed with the aid of the FEK-M photocalorimeter at 19°. The solvent was chloroform, and the precipitant was methanol, which was added from a microburet accurate to within 0.01 ml with an initial volume of 20 ml. For comparison of the titration results, the solution concentrations of the raw resin-rubber mixtures were so chosen that the relative concentration of the rubber did not exceed 0.02%, while that of the resin was not less than 0.02%, as otherwise the rubber coagulated and the resin, because of its higher solubility, did not separate out of solution. The turbidimetric titration curves are given in Fig. 1, where the optical density D_{corr} is plotted against the percentage concentration of methanol in the solution. The values of D_{corr} were calculated by the equation

$$D_{corr} = D \frac{V + v}{v},$$

where D is the experimentally determined value of the optical density of the solution; V is the initial volume of the solution, and v is the volume of the precipitant added [12].

Thermomechanical investigations. The thermomechanical properties of the block copolymers and raw mixtures were studied by means of the dynamometric balance [13] over a wide range of temperatures, with a maximum load of 0.18 kg/cm². The deformation (in arbitrary units) of block copolymers and raw mixtures of the two components is plotted against the temperature in Fig. 2.

DISCUSSION OF RESULTS

First, it is necessary to consider the effectiveness of the mastication process; that is, to determine whether mastication merely produces an intimate mechanical mixture of the two components. It has been shown [12] that this question can be answered by the results of turbidimetric titration. In fact, examination of the titration curves (Fig. 1, a) shows that the curves for mechanical mixtures of epoxide resin and nitrile rubber in different proportions have two distinct bends, corresponding to separation of rubber (with 47.5-48% methanol in the solution) and resin (with 68-69% methanol) from the solution, the two separating out independently of each other. The turbidimetric curves for different mixtures differ somewhat according to the component ratio, but they are all of the same type, corresponding to two-stage titration of the components.

Curves of a totally different form are obtained by titration of isolated block copolymers and of unfractionated mixtures after mastication. Figure 1, b shows the turbidimetric titration curve for an isolated block copolymer with 2:1 ratio of resin to rubber (here and subsequently the component ratio is taken to mean the ratio in which the resin and rubber were taken for mastication; it will be shown that this initial ratio alters in the course of mastication). It is clearly seen that the curve is of a continuous character with a single inflection, corresponding to a one-component system. The polymer begins to separate out of solution at methanol

concentrations not less than 51%, whereas in all mechanical mixtures of rubber and resin in different proportions the rubber begins to separate out at 47.5-48% methanol concentration (Fig. 1). This difference between the initial points of separation of polymers from the solution is well outside the limits of experimental error, as all the titration curves for the block copolymers, without exception, have the same initial point of ascent, corresponding to 51% methanol, whereas separation of rubber begins in all cases at methanol concentrations 3-3.5% below this (Fig. 1, a). This difference between the turbidimetric titration curves, together with other data, indicates that the mastication results in the formation of a new polymer — a block copolymer of the epoxide resin and the nitrile rubber. Figure 1,c also contains a titration curve for an unfractionated mixture of resin and rubber (5:1) after mastication. It is readily seen that the initial portion of this curve completely coincides with the titration curves for the isolated block copolymers, and a second bend, with 69% methanol in the solution, corresponding to separation of the unreacted resin, appears only at the end of the curve.

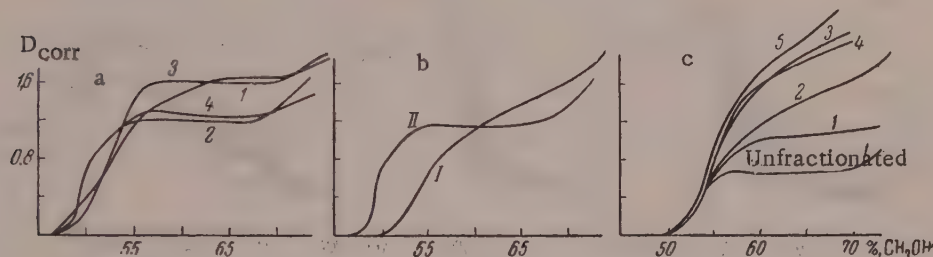


Fig. 1. Turbidimetric titration curves. a) Mechanical mixtures of ED-15 and SKN-26; b) block copolymer (I) and mechanical mixture (II) of samples with 2:1 ratio of ED to SKN; c) block copolymers of ED-15 and SKN-26. Ratios of ED to SKN: 1) 5:1; 2) 2:1; 3) 1:1; 4) 1:2; 5) 1:5.

It was very interesting to study the thermomechanical properties of block copolymers and to compare them with the properties of mechanical mixtures of the two components. Figure 2, a shows deformation-temperature curves for specimens with different ratios of the components, obtained directly after mastication, and Fig. 2, b gives corresponding curves for mechanical mixtures of ED-15 and SKN-26. It is seen that the thermomechanical curves for the raw mixtures are very similar to the curves for the mixtures obtained after mastication. The glass transition temperature of the mixtures increases somewhat with increasing resin content, reaching -10 and +10° at 1:1 and 2:1 ratios of resin to rubber; when the resin content reaches 33% (Curves 5 in Fig 2, a and 2, b) the specimen begins to flow at 70-75°, and with 50% resin (Curves 4) the high-elastic region is almost absent. In this case the polymers pass directly from the glassy into the viscofluid state, i.e., the behavior of the specimens is the same as that of pure epoxide resin. This resemblance of the thermomechanical curves for mechanical mixtures and unfractionated specimens of resin and rubber can be attributed to the relatively low efficiency of the mastication process in this instance, so that the product after mastication still contains appreciable amounts of the unreacted components, which influence the properties of the specimens.

Figure 2, c shows the thermomechanical curves for block copolymers of epoxide resin and nitrile rubber with different ratios of the original components, isolated as described above. It is seen that all the specimens have almost the same glass transition temperature (T_g) which coincides with T_g for pure butadiene-nitrile rubber (-40-20°*). Moreover, all the specimens give thermomechanical curves of similar form, similar to that for pure rubber, i.e., with a fairly distinct region of high elasticity. Both in form and in the height of the high-elasticity plateau, which is inversely proportional to the modulus of high elasticity, all the intermediate block copolymers between the rubber and the resin show progressively increasing strength while retaining the high-elastic properties of the rubber.

We carried out a microanalytical determination of the nitrile group contents of the extreme specimens of the isolated block copolymers — Specimens 2 (ED:SKN = 5:1) and 6 (ED:SKN = 1:5). It was found that the block copolymer becomes relatively richer in nitrile rubber during the mastication. The microanalytical data

*As in original — Publisher's note.

showed that block copolymer 2 contained 39% resin and 61% rubber, and block copolymer 6 contained 8% resin and 92% rubber, whereas the original proportions were 83% resin and 17% rubber in block copolymer 2, and 17% resin and 83% rubber in block copolymer 6. This accounts for the similarity in properties of the rubber and of the block copolymers of different quantitative compositions. It is evident that when the block copolymer is formed, nearly all the rubber and far from all the resin is consumed. It seems likely that the segments of the epoxide resin macromolecules act as rigid regions in the system of the rubber molecules, strengthening and increasing the modulus of the block copolymer, but these reinforcing regions are not large enough to have a significant influence on the flexibility and high elasticity characteristic of butadiene-nitrile rubber. Therefore, even with high resin contents (up to 39%) the products are strengthened somewhat but retain their high elasticity over a wide temperature range.

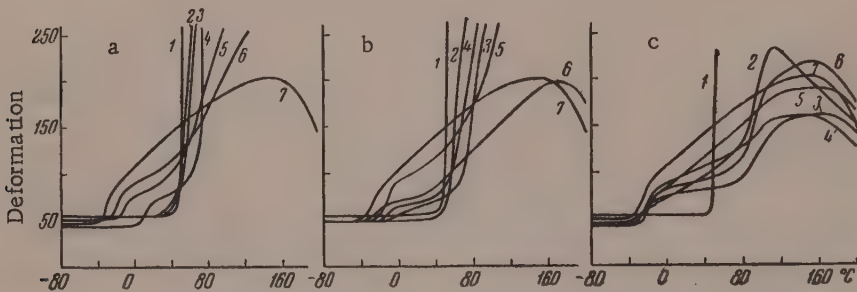


Fig. 2. Deformation-temperature curves: a) for products directly after mastication; b) mechanical mixtures of ED-15 and SKN-26; c) isolated block copolymers of ED-15 and SKN-26. Ratios of ED to SKN taken: 1) ED-15; 2) 5:1; 3) 2:1; 4) 1:1; 5) 1:2; 6) 1:5; 7) SKN-26.

Thus, the mechanical properties of block copolymers of ED-15 and SKN-26 can be considered as formed additively from the properties of the individual components.

SUMMARY

1. Block copolymers of SKN-26 butadiene-nitrile rubber and ED-15 epoxide resin with different proportions of the original components have been prepared by a mechanochemical method.
2. Selective solvents for isolation of the block copolymers from mixtures containing the original individual polymers have been found.
3. The glass transition temperature of the block copolymers formed remains almost constant with variation of the initial component ratio, while the modulus of high elasticity increases relatively to that of the rubber; i.e., mastication results in reinforcement of SKN-26.
4. Mastication produces block copolymers relatively richer in rubber than the original mixtures; despite the considerable resin contents (up to 39%) the block copolymers formed are similar to the rubber in their thermomechanical properties, i.e., the product is reinforced somewhat but retains high elasticity over a wide temperature range.

LITERATURE CITED

- [1] E. Immergut and H. Mark, *Makromolek. Chem.* 18-19, 322 (1956).
- [2] R. Hart, *Ind. chim. belge* 21, 1053, 1193 (1956).
- [3] M. S. Akutin, *Chem. Sci. and Industry* 2, No. 5, 585 (1957).

- [4] J. F. Bloomfield, F. M. Merrett, F. J. Popham and F. M. Swift, *Rubber World* 131, 358 (1954).
- [5] D. Coleman, *J. Polymer Sci.* 14, 15 (1954).
- [6] H. C. Haas, S. J. Cohen, A. C. Oglesby and E. R. Karlin, *J. Polymer Sci.* 15, 427 (1955).
- [7] V. A. Kargin, B. M. Kovarskaia, L. I. Golubenkova, M. S. Akutin and G. L. Slonimskii, *Proc. Acad. Sci. USSR* 112, 485 (1957).*
- [8] W. Watson and D. Wilson, *J. Scient. Instrum.* 31, 98 (1954).
- [9] J. Ayrey, C. Moore and W. Watson, *J. Polymer Sci.* 19, 1 (1956).
- [10] D. Angier and W. Watson, *J. Polymer Sci.* 18, 129 (1955).
- [11] V. A. Kargin, B. A. Kovarskaia, L. I. Golubenkova, M. S. Akutin and G. L. Slonimskii, *Chem. Ind.* No. 2, 77 (1957).
- [12] H. W. Melville and B. D. Stead, *J. Polymer Sci.* 16, 505 (1955).
- [13] V. A. Kargin and T. I. Sogolova, *J. Phys. Chem.* 23, 530 (1949).

The M. V. Lomonosov State University, Moscow
Faculty of Chemistry

Received December 10, 1957

*Original Russian pagination. See C. B. Translation.

ADSORBATE-ADSORBATE INTERACTION IN THE ADSORPTION OF VAPORS ON GRAPHITIZED CARBON BLACKS*

1. THE EQUATION FOR THE ADSORPTION ISOTHERM WITH ADSORBATE-ADSORBATE INTERACTION

A. V. Kiselev

On entering the adsorption layer, the molecules of an adsorbed substance interact with each other. Generally the influence of this interaction is superposed on the influence of surface inhomogeneity, and these factors cannot be separated; this hinders interpretation of experimental data.

However, methods have been recently developed for the production of adsorbents with mainly homogeneous surfaces, suitable for determinations not only of adsorption but also of heats of adsorption. Carbon blacks graphitized above 1500° are of this type. Graphitization of carbon black removes the difficulties caused by surface inhomogeneity, and adsorbate-adsorbate interaction can be detected experimentally, with increasing clarity as such interaction becomes stronger and as adsorbate-adsorbent interaction becomes weaker.

Adsorbate-adsorbate interactions may differ in character. Dispersional forces of attraction, and briefly acting forces of repulsion, appear in all cases. For large nonpolar molecules these are the determining interactions. In the case of small polar molecules electrostatic interaction, and in some cases association with hydrogen bonding, is superposed.

The shape of the vapor adsorption isotherm depends on the relationship of the thermodynamic characteristics of the adsorbate-adsorbent and adsorbate-adsorbate interactions. The methods of statistical thermodynamics can in principle be used for calculation of adsorption equilibria, as of any chemical equilibria. This requires the calculation of the corresponding distribution function for the adsorbate molecules in the force field of the adsorbent and of the previously adsorbed molecules, and the calculation of the fields themselves.

This is one of the most important problems in the modern theory of adsorption [1], but not all the necessary data are available for its complete solution. Therefore in this paper the problem of adsorption equilibria on a homogeneous surface is considered from a purely thermodynamic standpoint by introduction of appropriate constants, the values of which are not calculated theoretically. However, this semiempirical approach makes it possible to compare different methods for the description of adsorption isotherms with each other, and with the results of experiments with graphitized carbon blacks; we have selected for this comparison the simplest equations for vapor adsorption isotherms with adsorbate-adsorbate interaction taken into account.

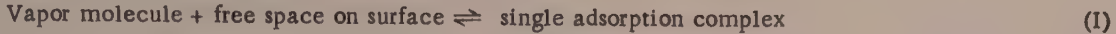
The Brunauer-Emmett-Teller equation. This is a well-known equation, which has been used for the past 20 years;**

$$\theta = \frac{a}{a_m} = \frac{K'_1 h}{(1-h)[1+(K'_1 - 1)h]}, \quad (1)$$

* Presented at the Lomonosov Lectures of the Chemical Faculty of the Moscow State University, October 22, 1957 (Part 1).

** Jones [3] showed that Equation (1) can be derived from the Langmuir equation in multimolecular adsorption [4].

where θ is the fraction of the surface covered; a is the adsorption; a_m is the capacity of the compact monolayer; h is the relative vapor pressure; K'_1 is the equilibrium constant (constant C in the authors notation) of the quasichemical reaction [5]:



Equation (1) takes vertical adsorbate-adsorbate interactions approximately into account, but neglects horizontal interactions.

The BET equation, and its particular case for $h \ll 1$ and $K'_1 \gg 1$ – the usual Langmuir equation – satisfactorily describe the adsorption isotherms of strongly adsorbed substances, such as normal hydrocarbons on graphitized carbon black [5, 6] up to $h \approx 0.3 - 0.4$.* In such cases the isotherm is strongly convex in the monomolecular region and passes through one point of inflection near $\theta = 1$.

Figure 1 shows $\theta(h)$ isotherms calculated from Equation (1) for different values of K'_1 from 1000 to 0.01, and the corresponding positions of the inflection points [3]. An inflection point in the region of positive values of h is found only in isotherms which begin with a convex region ($K'_1 > 2$). At lower values of K'_1 the BET isotherms are concave throughout. It follows from Equation (1) that

$$\theta = \frac{K'_1 h}{1 + (K'_1 - 2)h - (K'_1 - 1)h^2}, \quad (1')$$

therefore in the region of small values of h , even when $K'_1 < 2$

$$\theta \sim \frac{K'_1 h}{1 - (2 - K'_1)h} = \frac{K'_1 h}{1 - Ah} \quad \text{or} \quad \frac{h}{\theta} \approx \frac{1}{K'_1} - \frac{A}{K'_1} \cdot h, \quad (2), (2')$$

where $A = 2 - K'_1 > 0$. In particular, when $K'_1 = 1$ it follows from Equation (1) [3] that $\theta = h / (1 - h)$. Over a wider range of h , when $K'_1 < 1$, it follows from Equation (1) that

$$\frac{h}{\theta(1-h)} = \frac{1}{K'_1} - \frac{1 - K'_1}{K'_1} h = \frac{1}{K'_1} - \frac{B}{K'_1} h, \quad (3)$$

where $B = 1 - K'_1 > 0$. Thus, when $K'_1 < 1$ the BET equation plotted in $\frac{h}{\theta(1-h)}, h$ coordinates gives a straight

line with a negative slope, while at low values of h even when $K'_1 < 2$ it is represented by a straight line with a negative slope in the coordinates of the Langmuir equation $h/\theta; h$ (2'). In the BET theory, the case of low values of K'_1 (weak adsorbate-adsorbent interaction) may be interpreted as spread of the complexes formed by the adsorbate molecules along the surface [9].**

* At higher values of h the calculated values of a or θ begin to exceed the experimental values, as Equation (1) is based on the assumption that the adsorption equilibrium constants are equal in all layers above the first. In reality the adsorption potential decreases in these layers [7, 8], and this always has an effect at $\theta > 1.5 - 2$ [5].

** Dubinin, Zaverina, and Serpinskii [10] proposed the following equation for the adsorption isotherm of water vapor on carbons with an oxidized surface:

$$a = \frac{a_0 ch}{1 - ch}, \quad (4)$$

where a_0 is the number of active centers and c is a constant. This equation is based on the following assumptions: initial adsorption takes place at active centers, the energies of adsorbate-active center and adsorbate-adsorbate interaction are equal, and the surface covering is unrestricted. It follows from Equation (4) that $a = 0$ when $a_0 = 0$ and $a = \infty$ when $h < 1$ (if $c > 1$). For homogeneous surfaces, and equation of the same type (2) is a special case of the BET equation (1') for weakly adsorbed substances ($K'_1 \sim 1$).

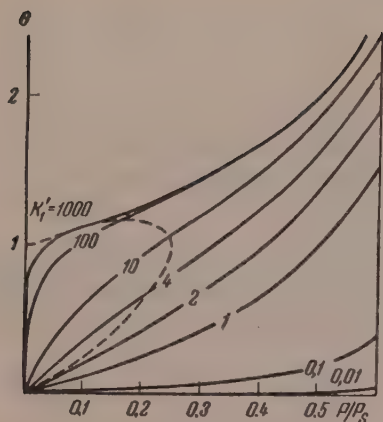


Fig. 1. Vapor adsorption isotherms calculated from the BET equation for various values of K_1' . The dash line represents the positions of the inflection points calculated by Jones [3].

The BET equation (see Fig. 1) is not applicable to known cases of adsorption of vapors of nitrogen [11], argon [11], krypton [12], methanol [13-15], methylamine [16], sulfur dioxide [17] and cyclopentane [18] on graphitized carbon black, when the isotherms commence with a concave region, pass through the first inflection point near $\theta = 0.5$, then become convex, pass through the second inflection point (near $\theta = 1$), and become concave again. In such cases adsorbate-adsorbent and adsorbate-adsorbate interactions are comparable, so that both these interactions must be taken into account in equations for these isotherms, and for concave isotherms for the adsorption of ammonia [16] and water [15] vapors. Equations for adsorption isotherms with adsorbate-adsorbate interaction taken into account may be derived in different ways.

Equation of the van der Waals type. The adsorption isotherm equations of Kobozev and Hill. It is possible to start with equations of state for a two-dimensional layer, analogous to the van der Waals equation of state, with adsorbate-adsorbate repulsion at long and short distances taken into account:

$$\left(\pi - \frac{a'_1}{\omega^2} \right) (\omega - b_2) = kT \quad (5)$$

or with attraction at long distances and repulsion only at short distances

$$\left(\pi + \frac{a''_2}{\omega^2} \right) (\omega - b_2) = kT, \quad (6)$$

where π is the surface pressure of the monolayer; ω is the area per molecule of adsorbate in this layer; a'_1 , a''_2 and b_2 are constants. The connection between the equation of state and the equation for the adsorption isotherm is provided by the Gibbs equation. Substitution of the expression for $d\pi$ from Equation (5) into the Gibbs equation, and integration under the condition that θ is fairly small, gives an equation for the adsorption isotherm of the form [19]*

$$h = \frac{\theta'}{K'_1(1-\theta')} e^{a\theta'}. \quad (7)$$

Kobozev and Gol'dfel'd [19, 20] also derived this equation by introduction of the linear decrease of the adsorption potential as the covering proceeds, into the Langmuir equation; it can also be derived from the expression [20] for the chemical potential of the adsorbate

$$\mu = \mu_0 - \varphi_0 + RT \ln \frac{\theta'}{1-\theta'} e^{a\theta'}, \quad (8)$$

* Subsequently θ' is used to denote the fraction of the monolayer covered.

where φ_0 is the adsorption potential for isolated molecules, and a is a constant. The expression $e^{a\theta'}$ essentially has the meaning of the activity coefficient of the adsorbate in the monolayer. From the condition of equilibrium with the vapor, we obtain Equation (7) for the adsorption isotherm with adsorbate-adsorbate repulsion taken into account.

With the exception of special cases of surfaces bearing charges of the same sign [21, 22], adsorbate-adsorbate attraction generally predominates over a wide range of θ' . Substitution of the expression for π from Equation (6) into the Gibbs Equation (7) and complete integration gives Hill's equation [23] for the monomolecular adsorption isotherm, in the form

$$h = \frac{\theta'}{K'_1(1-\theta')} e^{\frac{\theta'}{1-\theta'} - K_2 \theta'}, \quad (9)$$

where $K_2 = \frac{2a''}{RTb_2}.$

This equation gives an initially concave isotherm. Depending on the ratio of the constants K'_1 and K_2 , it then describes an S-shaped isotherm which starts concave, or an isotherm with a vertical portion, corresponding to two-dimensional condensation [24].

Statistical-thermodynamic expressions for adsorption isotherms with adsorbate-adsorbate interaction. Fowler and Guggenheim [25] considered adsorbed layers from the viewpoint of statistical thermodynamics. The following expression was derived for localized adsorption with mutual attraction of neighboring adsorbate molecules (see also [26]).

$$h = \frac{\theta'}{K'_1(1-\theta')} e^{-a\theta'}, \quad (10)$$

which differs from Equation (7) by the sign in the exponent.

The advantage of the treatment by means of statistical thermodynamics is that the equilibrium constant is expressed in terms of the distribution functions of the adsorbate in the gas phase and on the surface, so that a theoretical calculation is possible in principle.

Barrer and Robins [27] and Barrer and Stuart [28] used statistical thermodynamics [25] to derive isotherms which satisfactorily describe the adsorption of vapors on carbon. This method was used [28] to obtain an equation for the S-shaped isotherms for the adsorption of water and methanol vapors on carbons and graphite over a wide range of h . The equilibrium equation is of the form [25]

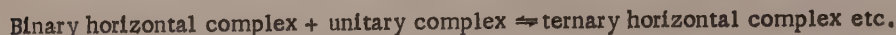
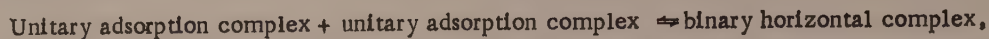
$$h = \frac{\theta'}{K'_1(1-\theta')} \left(\frac{2(1-\theta')}{\beta + 1 - 2\theta'} \right), \quad (11)$$

where $\beta = \left\{ 1 - 4\theta'(1-\theta') \left[1 - \exp - \frac{2w}{ZkT} \right] \right\}^{1/2}$, and $\frac{2w}{Z}$ is the energy of interaction calculated for a pair of molecules at neighboring localization sites; Z is the coordination number of the localization site [4 or 6]. The constants in this equation were found empirically.

Approximate equation for monolayer adsorption with adsorbate-adsorbate interaction. In addition to the primary adsorbate-adsorbent interaction (I) with the equilibrium constant

$$K'_1 = \frac{\theta'_1}{h\theta_0}, \quad (12)$$

where θ'_1 is the fraction of the surface covered by unitary complexes, and θ_0 is the fraction of the surface remaining free, the present author took into consideration the quasichemical reactions of adsorbate-adsorbate interaction [29]:



(II)

The equilibrium constants of Reaction (II) are:

$$K_2 = \frac{\theta'_2}{\theta'_1 \cdot \theta'_1}; \quad K_3 = \frac{\theta'_3}{\theta'_2 \cdot \theta'_1}; \quad K_4 = \frac{\theta'_4}{\theta'_3 \cdot \theta'_1}; \dots \quad (13)$$

Neglecting any possible nonequivalence of the interactions of a unitary complex with different multiple complexes and of interaction between multiple complexes, and assuming as an approximation that

$$K_2 \approx K_3 \approx K_4 \approx \dots = K_n, \quad (14)$$

since the total fraction of the monolayer covered is

$$\theta' = 1 - \theta_0 = \theta'_1 + \theta'_2 + \theta'_3 + \dots, \quad (15)$$

we find [29]

$$\theta'_1 = \frac{\theta'}{1 + K_n \theta'}. \quad (16)$$

Introducing (15) and (16) into (12), we obtain the equation for adsorption in a monolayer with adsorbate-adsorbate interaction approximately taken into account [1, 29]:

$$h = \frac{\theta'}{K'_1 (1 - \theta') (1 + K_n \theta')}, \quad (17)$$

* Taking logarithms, we have from Equation (17)

$$\ln h = -\ln K'_1 + \ln \frac{\theta'}{1 - \theta'} - \ln (1 + K_n \theta'). \quad (18)$$

when $\theta' \ll 1$, $\ln(1 - \theta') \approx -\theta'$ and $\ln(1 + K_n \theta') \approx K_n \theta'$, so that (18) passes into the Williams-Henry equation

$$\ln \frac{h}{\theta'} \approx -\ln K'_1 - (K_n - 1) \theta'. \quad (19)$$

For θ' not greatly different from 0.5, and low values of $K_n \theta'$, Equation (19) becomes the semilogarithmic isotherm [30, 31]

$$\theta' \approx A \ln p + B. \quad (20)$$

where K'_1 is the equilibrium constant of Reaction (I) (adsorbate-adsorbent), and K_n is the equilibrium constant of Reactions (II) (adsorbate-adsorbate). In linear form we have

$$\frac{\theta'}{h(1-\theta')} = K'_1 + K'_1 K_n \theta . \quad (17')$$

This equation can be verified experimentally. When $K_n = 0$, Equations (17) and (17') pass into the Langmuir equation.*

Equation (17) is obtained from Equation (10) by resolution of $e^{a\theta'} \approx 1 + a\theta'$, but this is only possible for small θ' . Thus, Equations (10) and (17) are similar only in the region of small values of θ' , owing to the difference in the functional dependence of the activity coefficient $f_{\theta'}$ of the adsorbate on the fraction covered. In equation (10) $f_{\theta'} = e^{-a\theta'}$, while in Equation (17) $f_{\theta'} = 1/(1 + K_n \theta')$. Both these expressions are approximate, and converge when $a\theta' \ll 1$.

The upper portion of Fig. 2 shows plots of Equation (17) for constant values $K_n = 1$ and $K_n = 10$, at different values of K'_1 , from 1000 to 100 to 0.1, and the lower portion of Fig. 2, corresponding plots for constant $K'_1 = 10$ and $K'_1 = 0.1$, with different values of K_n from 100 and 500 to 0.1 and 0.01. The shape of the adsorption isotherm depends on the magnitude of K'_1 and K_n and on the ratio between them.

With decrease of θ' , Equation (17), like the Langmuir (12), BET (1), Kobozev (7), Fowler and Guggenheim (10), and Hill (9) equations, becomes in the limit the Henry equation $h = \theta'/K'_1$ and $\theta' = K'_1 h$.

The concave or convex nature of the start of the isotherm is determined by the limiting value (for $\theta' = h = 0$) of the second derivative. These values for the various adsorption isotherms are given in the Table.

Initial Values of the Second Derivative for the Different Equations of the Adsorption Isotherms, and the Form of the Initial Ascent of these Isotherms

Equation	Initial value of second derivative	Form of the initial portion of the isotherm $\theta = f(h)$ (relative to the h axis)
$h = \theta'/K'_1(1-\theta')$ (12)	$(d^2h/d\theta'^2)_{\theta=0} = 2/K'_1 > 0$	Convex
$h = \frac{\theta'}{K'_1(1-\theta')} e^{a\theta'}$ (7)	$(d^2h/d\theta'^2)_{\theta=0} = 2/K'_1(1+a) > 0$	Convex
$h = \frac{\theta'}{K'_1(1-\theta')(1+K_n\theta')}$ (17)	$(d^2h/d\theta'^2)_{\theta=0} = (2/K'_1)(1-K_n) \begin{cases} > 0 & \text{Convex if } K_n < 1 \\ < 0 & \text{Concave if } K_n > 1 \end{cases}$	Convex if $K_n < 1$ Concave if $K_n > 1$
$h = \frac{\theta'}{K'_1(1-\theta')} e^{-a\theta'}$ (10)	$(d^2h/d\theta'^2)_{\theta=0} = (2/K'_1)(1-a) \begin{cases} > 0 & \text{Convex if } a < 1 \\ < 0 & \text{Concave if } a > 1 \end{cases}$	Convex if $a < 1$ Concave if $a > 1$
$h = \frac{\theta'}{K'_1(1-\theta')} e^{\frac{\theta'}{1-\theta'} - K_2\theta'}$ (9)	$(d^2h/d\theta'^2)_{\theta=0} = (2/K'_1)(2-K_2) \begin{cases} > 0 & \text{Convex if } K_2 < 2 \\ < 0 & \text{Concave if } K_2 > 2 \end{cases}$	Convex if $K_2 < 2$ Concave if $K_2 > 2$
$\theta = \frac{K'_1 h}{(1-h)[1+(K'_1-1)h]}$ (1)	$(d^2\theta/dh^2)_{h=0} = 2K'_1(2-K'_1) \begin{cases} > 0 & \text{Convex if } K'_1 > 2 \\ < 0 & \text{Concave if } K'_1 < 2 \end{cases} \quad [3]$	Convex if $K'_1 > 2$ Concave if $K'_1 < 2$

It follows from the Table that, of all the isotherms which take into account adsorbate-adsorbate interaction (horizontal or vertical (1)), only the Kobozev isotherm is convex for all values of the constant a . In all other cases the concavity or convexity of the start of the isotherm is determined by the magnitude of the constants K_n (17), a (10), K_2 (9), or K'_1 (1). Thus, even in presence of adsorbate-adsorbate attraction the isotherm may start with either a convex or a concave portion, depending on the values of the relevant interaction constants.*

* In contrast to this, Serpinskii [32] pointed out that "if attraction forces predominate between the adsorbed molecules, this gives rise to (initially) convex adsorption isotherms, whereas if repulsion forces prevail, the isotherms are concave."

The role of the adsorbate-adsorbent equilibrium constant K'_1 is very important. It is clear from Fig. 2 that at high values of K'_1 the shape of isotherm (17) approaches that of the Langmuir isotherm. This is seen if equation (17) is written in the form

$$\theta' = \frac{K'_1 h (1 - \theta')}{1 - K'_1 K_n h (1 - \theta')} . \quad (17'')$$

Large $K'_1 \theta'$ approaches unity even at small h ; therefore the product $h (1 - \theta')$ remains small up to large values of θ' . Therefore the term $K'_1 K_n h (1 - \theta') \ll 1$, and Equation (17'') approaches the Langmuir equation.

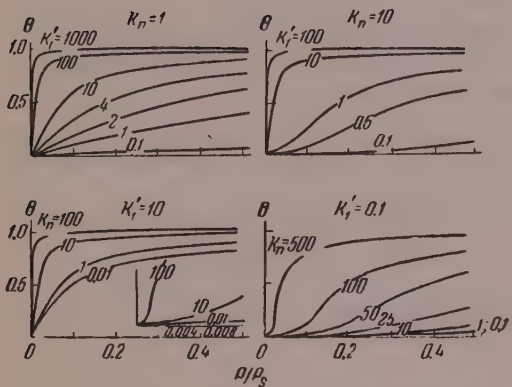


Fig. 2. Monomolecular adsorption isotherms calculated from Equation (17); above) isotherms for constant K_n and different K'_1 ; below) isotherms for constant K'_1 and different K_n .

To obtain the equation of state we differentiate Equation (18), substitute into the Gibbs equation, put $\alpha = \alpha_m \theta'$ (α_m is the capacity of the dense monolayer per unit area) and integrate, obtaining

$$\pi = RT \alpha_m \left[\frac{1}{K_n} \ln (1 + K_n \theta') - \ln (1 - \theta') - \theta' \right] . \quad (21)$$

For small values of $K_n \theta'$ resolution into series after the substitution $\theta' = \frac{\omega_0}{\omega} = \frac{1}{\alpha_m N \omega}$ gives [29]

$$\pi \omega = kT (1 + B_1 / \omega + B_2 / \omega^2 + \dots) , \quad (22)$$

where the coefficients of alternate sign are

$$B_1 = -\frac{K_n + 1}{2} ; \quad B_2 = \frac{K_n^2 + 1}{3} ; \dots \quad (23)$$

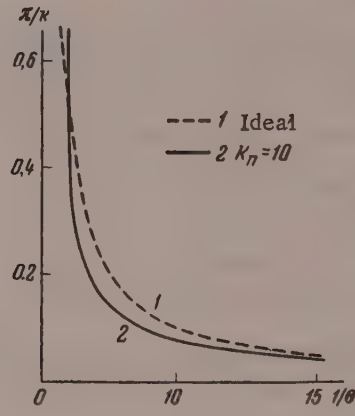
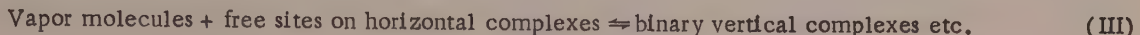


Fig. 3. Plots of the equations of state for an adsorbed film: 1) ideal; 2) conforming to Equation (21) when $K_n = 10$.

The surface pressure π depends, through K_n , on the energy and entropy of the adsorbate-adsorbate interaction. A specimen comparison of the equation of state for a two-dimensional film calculated from Equation (21) for $K_n = 10$ with the ideal equation is given in Fig. 3.

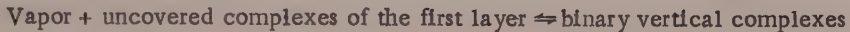
Approximate equation for multimolecular adsorption with adsorbate-adsorbate interaction in the first layer taken into account. In our earlier papers [29, 33] the formation of vertical complexes, in addition to horizontal, was taken into account in terms of quasichemical equilibria for a reaction of the type:



In multimolecular adsorption only uncovered unitary complexes take part in the primary reaction (I) of formation of unitary complexes in adsorbate-adsorbent interaction [33]. Therefore the equilibrium Equation (12) contains, not θ'_1 , the concentration of all (covered and uncovered) unitary complexes, but only the concentration of uncovered unitary complexes, θ'_0 :

$$K'_1 = \frac{\theta'_0}{h\theta_0}. \quad (12')$$

Since we assume that in the reaction:



the adsorbate molecules are distributed uniformly among the different types of uncovered complexes, it follows that

$$\theta'_0/\theta_1 = \theta'_0/\theta_2 = \dots = \theta'_0/\theta', \quad (24)$$

where θ'_0 and θ' are the concentrations of the uncovered and of all the complexes in the first layer. Let us assume that the horizontal interactions in the first layer do not depend on whether the horizontal complexes in this layer carry vertical superstructures of other adsorbate molecules. Then covered and uncovered complexes of the same order in the first layer are indistinguishable with respect to Reactions (II); therefore Equation (16) remains valid. Substituting, into Equation (12'), θ'_1 from Equation (16), θ'_0 from Equation (24), and $\theta'_0 = 1 - \theta'$, we have, instead of (17)

$$K'_1 = \frac{\theta'_0}{h(1-\theta')(1+K_n\theta')}. \quad (25)$$

Next we consider the total fraction θ of the surface covered in multimolecular adsorption. Here we use the same reasoning as in the thermodynamic derivation of the BET equation [5]. We assume [2, 5] that the equilibrium constants for the formation of multiple vertical complexes are equal.*

$$K'' = \frac{\theta''}{h\theta'_0} \approx K''' = \frac{\theta'''}{h\theta''} \approx \dots = K_l, \quad (26)$$

where $\theta'', \theta''', \dots$ are the fractions of the surface covered by binary, ternary, etc. vertical complexes. Since [2] $\theta = \theta'_0 + 2\theta'' + 3\theta''' + \dots$, and $\theta' = \theta'_0 + \theta'' + \theta''' + \dots$, from Equation (26) it follows that [29]

* This assumption in the BET theory restricts the applicability of the equation at large values of h , as in reality the energy and entropy of type (III) interactions later with increase in the size of the vertical complexes (see [7, 8]).

$$\theta = \theta'_0 / (1 - K_l h)^2 = \theta' / 1 - K_l h. \quad (27)$$

From this we find $\theta'_0 = \theta (1 - K_l h)^2$ and $\theta' = \theta (1 - K_l h)$; introducing these expressions into Equation (25) we obtained an approximate equation for multimolecular adsorption of vapors with adsorbate-adsorbate interaction in the first layer taken into account, in the following form [33]:

$$h = \frac{\theta (1 - K_l h)^2}{K'_1 [1 - \theta (1 - K_l h)] [1 + K_n \theta (1 - K_l h)]}. \quad (28)$$

In absence of multimolecular adsorption $K_l = 0$ and Equation (28) becomes the equation for monomolecular adsorption (17). For the case of multimolecular adsorption of vapors of wetting liquids when $h = 1$, $\theta = \infty$ [2]; therefore, from Equation (27) $K_l = 1$ and

$$h = \frac{\theta (1 - h)^2}{K'_1 [1 - \theta (1 - h)] [1 + K_n \theta (1 - h)]} \quad (29)$$

or

$$\frac{\theta (1 - h)^2}{h [1 - \theta (1 - h)]} = K'_1 + K'_1 K_n \theta (1 - h). \quad (29')$$

In absence of adsorbate-adsorbate interaction in the first layer, $K_n = 0$ and Equation (29) becomes the BET equation (1) [33].

In general, Equation (29) represents a curve with two points of inflection. In the particular case when K'_1 is large, adsorbate-adsorbate interaction is relatively small and the equation for multimolecular adsorption approaches the equation [29]

$$\theta = \frac{a}{a_m} = \frac{K'_1 h}{(1 - h)(1 + K'_1 h)}, \quad (30)$$

convenient for determination of the capacity of the dense monolayer a_m and of specific surface. In the case of weak adsorbate-adsorbent interaction, θ remains small over a considerable range of h ; consequently, $\theta (1 - h) \ll 1$ and Equation (29) becomes

$$h \approx \frac{\theta (1 - h)^2}{K'_1 [1 + K_n \theta (1 - h)]} \quad (31)$$

or

$$\frac{h}{\theta (1 - h)} \approx \frac{1}{K'_1} - \frac{K'_1 K_n + 1}{K'_1} \cdot h, \quad (31')$$

i.e., in the coordinates of the BET equation ($h/\theta (1 - h)$, h) the isotherm in this case is represented by a straight line with a negative slope. If K_n is large, the product $K'_1 K_n$ may become considerably greater than unity, and Equation (31') then becomes

$$\frac{h}{\theta (1 - h)} \approx \frac{1}{K'_1} - K_n h. \quad (32)$$

This special case was considered earlier [29]. In the initial region where $h \ll 1$

$$h/\theta \approx \frac{1}{K'_1} - K_n h \quad \text{or} \quad \theta \approx \frac{K'_1 h}{1 - K'_1 K_n h}. \quad (32'), (32'')$$

This equation is similar to Equation (2), which follows from the BET theory, in the form of the functional relationship between θ and h . Thus, in the two extreme cases of large K'_1 and small K'_1 the isotherms are close to the form predicted by the BET theory, but in the latter case the deductions drawn from Equation (29) are more informative, as they indicate the role of horizontal interactions (in terms of K_n).

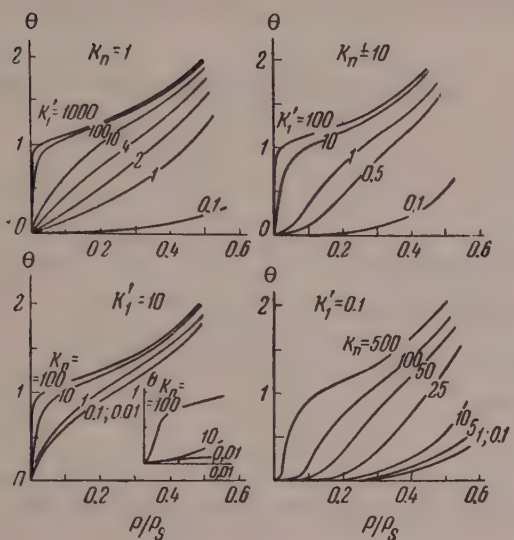


Fig. 4. Isotherms for multimolecular adsorption of vapors, calculated from Equation (29): above) isotherms for constant K_n and different K'_1 ; below) isotherms for constant K'_1 and different K_n .

Plots of Equations (29) for different ratios of the constants K_n and K'_1 are given in Fig. 4. It is seen that with small K_n and large K'_1 the isotherm starts convex and, like the BET isotherm, passes through an inflection point near $\theta = 1$ when $K'_1 \gg 1$. Decrease of K'_1 results in isotherms with concave initial regions and two inflection points. On further decrease of K'_1 the isotherm is concave throughout and has no inflection point, like the BET isotherm when $K'_1 < 2$. The effect of variations of the constant K_n is seen in the lower part of Fig. 4. Large values of K_n make the isotherms initially concave, and they then pass through two inflection points.

It is possible to take similarly into account the superposition of multimolecular adsorption in the other equations, considered above, for monomolecular adsorption with adsorbate-adsorbate interaction in the first layer taken into account. For further refinement of the multimolecular adsorption isotherm it is necessary to take into account horizontal interactions in the second and subsequent layers, the decrease of the vertical equilibrium constants with increasing size of the vertical complexes, and to introduce a more exact relationship between the activity coefficients and the fraction of the layers filled.

Applications of the equations for the adsorption isotherms are described in another paper [34].

SUMMARY

1. Different equations for the isotherms of monolayer adsorption from the gas phase on homogeneous surfaces, with adsorbate-adsorbate interaction taken into account, are examined.
2. Approximate equations for mono- and multimolecular adsorption of vapors, derived by the method of quasichemical equilibria and representing adsorption isotherms with one or two points of inflection, are discussed.
3. The shape of the adsorption isotherm and its initial curvature are determined by the values and ratio of the adsorbate-adsorbent and adsorbate-adsorbate equilibrium constants.

The author is deeply grateful to N. N. Avgul', E. V. Krapova, N. V. Kovaleva, and V. A. Sinitsyn for calculations, plotting of the diagrams, and discussion.*

LITERATURE CITED

- [1] A. V. Kiselev, Bull. Acad. Sci. USSR No. 10, 43 (1958).*
- [2] S. Brunauer, P. H. Emmett and E. Teller, J. Amer. Chem. Soc. 60, 306 (1938).
- [3] D. C. Jones, J. Chem. Soc. 126 (1950).
- [4] I. Langmuir, J. Amer. Chem. Soc. 40, 1361 (1918).
- [5] N. N. Avgul', G. I. Berezin, A. V. Kiselev and I. A. Lygina, J. Phys. Chem. 30, 2106 (1956).
- [6] N. N. Avgul', G. I. Berezin, A. V. Kiselev and I. A. Lygina, Bull. Acad. Sci. USSR, Div. Chem. Sci. 1021 (1957). *
- [7] T. Hill, in the book: Catalysis (Russian translation) (IL, 1955) p. 276.
- [8] J. Halsey, in the book: Catalysis (Russian translation) (IL, 1955) p. 244.
- [9] L. N. Kurbatov, in the book: Surface Chemical Compounds and their Role in Adsorption Phenomena* * (Izd. MGU, 1957) p. 233.
- [10] M. M. Dubinin, E. D. Zaverina and V. V. Serpinskii, Proc. Acad. Sci. USSR 99, 1033 (1954); J. Chem. Soc. 1760 (1955).
- [11] S. Ross and W. Winkler, J. Colloid Sci. 10, 319 (1955).
- [12] S. Ross and W. Winkler, J. Colloid Sci. 10, 330 (1955).
- [13] C. Pierce and R. N. Smith, J. Phys. Colloid Chem. 54, 374 (1950).
- [14] B. Millard, R. A. Beebe and J. Cynarsky, J. Phys. Chem. 58, 468 (1954).
- [15] A. V. Kiselev and V. N. Kovaleva, J. Phys. Chem. 30, 2775 (1956).
- [16] R. M. Dell and R. A. Beebe, J. Phys. Chem. 59, 754 (1955).
- [17] R. A. Beebe and R. M. Dell, J. Phys. Chem. 59, 746 (1955).
- [18] N. N. Avgul', G. I. Berezin, A. V. Kiselev and I. A. Lygina, Bull. Acad. Sci. USSR, Div. Chem. Sci. (in the press).
- [19] Iu. Gol'dfel'd and N. I. Kobozev, J. Phys. Chem. 15, 257 (1941).
- [20] N. I. Kobozev and Iu. Gol'dfel'd, Acta phys.-Chim. USSR 7, 495 (1937).
- [21] D. M. Young, Trans. Faraday Soc., 48, 548 (1952).
- [22] T. Hayakawa, Bull. Chem. Soc. Japan 30, 343 (1957).
- [23] T. Hill, J. Chem. Phys. 14, 441 (1946).
- [24] J. H. de Boer, The Dynamical Character of Adsorption (Oxford, 1953).
- [25] R. Fowler and E. Guggenheim, Statistical Thermodynamics (Russian translation) (IL, 1949).
- [26] T. Hill, J. Chem. Phys. 15, 767 (1947).
- [27] R. M. Barrer and A. B. Robins, Trans. Faraday Soc. 47, 773 (1951).
- [28] R. M. Barrer and W. I. Stuart, J. Chem. Soc. 1956 3307 .
- [29] A. V. Kiselev, Proc. Acad. Sci. USSR 115, 103 (1957). *
- [30] M. I. Temkin, J. Phys. Chem. 15, 296 (1941).
- [31] B. M. W. Trapnell, Chemisorption (London, 1955) p. 124.
- [32] V. V. Serpinskii, article in Russian translation of S. Brunauer: Adsorption of Gases and Vapors (IL, 1948) p. 688.

* Original Russian pagination. See C. B. Translation.

** In Russian.

[33] A. V. Kiselev and D. P. Poshkus, Bull. Acad. Sci. USSR, Div. Chem. Sci. 520 (1958).*

[34] A. V. Kiselev, N. V. Kovaleva, V. A. Sinitsyn and E. V. Krapova, Colloid J. 20, No. 4 (1958). *

Adsorption Laboratory

The M. V. Lomonosov State University, Moscow

Received February 24, 1958

*Original Russian pagination. See C. B. Translation.

HETEROCHAIN POLYAMIDES

10. THE EFFECT OF SOME ORGANIC SUBSTANCES ON THE STABILITY OF ALCOHOLIC POLYAMIDE SOLUTIONS

V. V. Korshak and S. A. Pavlova

The stabilization of concentrated polymer solutions, i.e., the retardation or prevention of the gelation process, is closely associated with polymer solubility. Clearly, from this viewpoint solvent quality depends on the stability of the solutions formed. The solvent power of a liquid with respect to a given polymer is determined by the change of free energy during the solution process [1]. As the change of free energy is the result of changes of the enthalpy and entropy of the system, solution may take place as the result of changes of enthalpy or of the entropy of the system during the process or, most commonly, of changes of both. When a polymer is dissolved in a mixed solvent, the solution mechanism may vary with the solvent composition.

Accordingly the mechanism of the stabilizing action of a second component added to a solvent may vary. Stabilization may take place as the result of formation of a solvate layer which prevents interaction between the molecules and gel formation, or as the result of increased flexibility of the macromolecules and increased entropy of the system. This is favored by desolvation of the macromolecules.

In our study of the stabilizing effects of a number of substances on concentrated solutions of mixed polyamide G-669 in ethanol, it was not our aim to study in detail the mechanism of the stabilizing action of various substances. However, certain conclusions may be drawn from our results.

TABLE 1

Stabilizer Concentrations Required to Stabilize
the Solution for 100 Hours

Stabilizer	Concentration of stabilizer, %
Phenol	9.5
Benzoic acid	14
Formic acid	15
Acetic acid	24

The material chosen was "Anid G-669" * with molecular weight 21,000. 20% solutions of the polyamide in ethanol, containing various amounts of the substances being tested as stabilizers, were heated until quite homogeneous, stirred, and placed in a thermostat. The stabilizing effect of the added substance was judged by the time which elapsed before the solution became turbid, followed by gelation. Complete gelation was taken to be the point when the gel remained immobile with the tube placed in a horizontal position.

Curves for the gelation time against stabilizer concentration are given in Figs. 1-4. The amounts of stabilizers required to protect 20% alcoholic polyamide solution against gelation for 100 hours are given in Table 1.

The polyamide dissolves, without heating, in ethanol containing over 5% aniline and o-chloroaniline or 10% benzyl alcohol.

The results are also given in Table 2. In addition, the stability of 10% polyamide solutions in different alcohols was studied. The results are given in Table 3.

* Anid G-669 is a mixed polyamide obtained by polycondensation of 1 part hexamethylenediammonium adipate, 1 part hexamethylenediammonium azelate, and 2 parts ϵ -caprolactam.

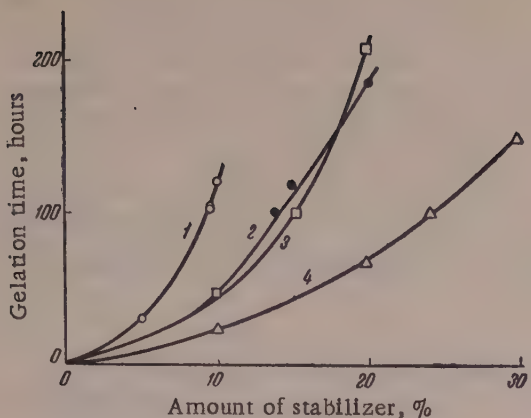


Fig. 1. Effect of stabilizer concentration on the stability of alcoholic polyamide solutions; 1) phenol; 2) benzoic acid; 3) formic acid; 4) acetic acid.

Dissolution of the polyamide is associated with breakdown of hydrogen bonds, and therefore substances which are themselves capable of forming hydrogen bonds, such as acids and phenols, should be solvents for polyamides. Ethyl alcohol is not a sufficiently active solvent from this aspect, and does not dissolve one-component polyamides; it dissolves mixed polyamides only at temperatures above 30°.

TABLE 2

Gelation Times of 20% and 10% Solutions of Polyamide in Ethanol Containing the Stabilizer

Stabilizer	Amount of stabilizer in mixture, %	Time in minutes	
		to turbidity	to gelation
20% Polyamide solutions			
Polyamide without stabilizer	—	35	60
Ethylene glycol	9—10*	165	—
Diglycol	10—11	165	315
Glycerol	10—14	215	—
Octyl alcohol	5	195	390
Ethyl ether	3	75	—
Propionitrile	1	65	80
Urea	5—6	60	95
Dimethylformamide	1	195	270
Pyridine	5	60	270
Water	25	7020	—
10% Polyamide solutions			
Formamide	10—15	70	—
Dichloroethane	30—55	180	—
Chloroform	40—70	No turbidity	

* For some of the stabilizers a concentration range is given in which the stability is approximately constant.

The substances tested as stabilizers may be divided into three groups. The first group includes solvents which, when added to polyamide-ethanol mixtures, steadily increase the solubility of the polyamide in methanol up to its solubility in the pure solvent; it has been shown that they can be compared by the effectiveness of their stabilizing action, which probably depends directly on their solvent power. The second and third groups consist of nonsolvents. Stabilizers of the second group merely lower the solubility of the polyamide in the mixture, while stabilizers of the third group raise the stability of the solution to a certain maximum and then, with further increase of their concentration, precipitate the polyamide or, at high concentrations, cause gel formation. The third group of stabilizers was of the most interest from the practical standpoint, as it included the most effective stabilizers. The optimum concentrations of the added stabilizers and the gelation times of 20% and 10% solutions of polyamides in mixtures containing stabilizer and ethanol are given in Table 2. The diversity of the types of substances which are qualitatively similar in their stabilizing effects should be noted.

TABLE 3
Stability of Polyamide Solutions in Various Alcohols

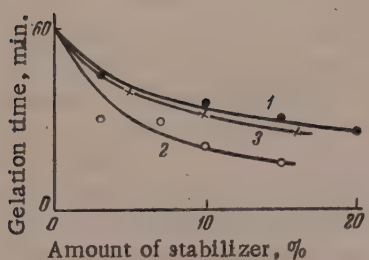


Fig. 2. Effect of stabilizer concentration on the stability of alcoholic polyamide solutions. 1) caprolactam; 2) vinyl butyl ether; 3) acetaldehyde.

Alcohol	Time in minutes before start of	
	turbidity	gelation
Ethyl	—	—
Propyl	75	195
Isopropyl	No turbidity	No gelation
n-Butyl	50	195
Isobutyl	—	195
Benzyl	No turbidity	No gelation

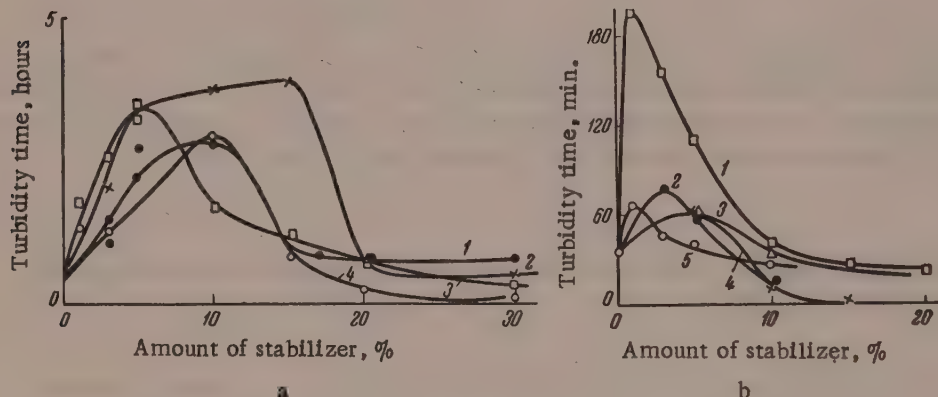


Fig. 3. Effect of stabilizer concentration on the stability of alcoholic polyamide solutions: (a) 1) Ethylene glycol; 2) glycerol; 3) octyl alcohol; 4) diglycol. (b) 1) Dimethylformamide; 2) ethyl ether; 3) pyridine; 4) urea; 5) propionitrile.

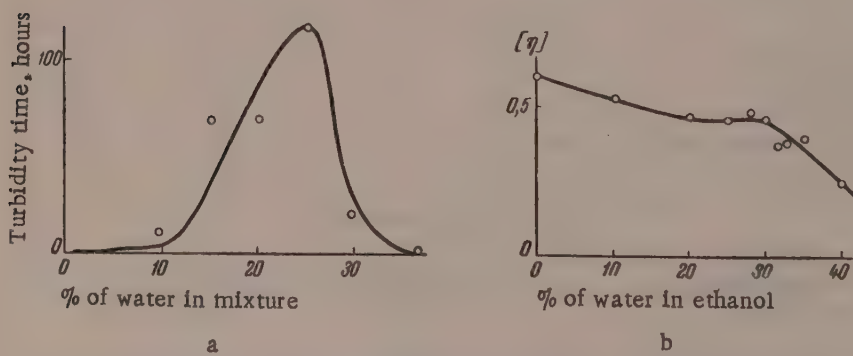


Fig. 4. Effect of water concentration on the stability (a) and the intrinsic viscosity (b) of alcoholic polyamide solutions.

As already stated, the addition of substances forming more stable hydrogen bonds with the polyamide continuously increases the polymer solubility. Substances of the third group are not among these. It seems likely that, for example, the addition of water, which forms aggregates with the alcohol molecules, should favor desolvation of the macromolecules and thus increase their flexibility. The entropy term in the total free energy change of the solution should therefore increase. Figure 4 shows the variation of the intrinsic viscosity of a polyamide solution in ethanol with variations of the water content of the solvent. The decrease of intrinsic viscosity is a sign of a decrease of the hydrodynamic interaction between the polymer macromolecules and the solvent; i.e., there is in fact some decrease in the size of the macromolecular globules, which become more compact (owing to increased flexibility or possibly to the formation of intramolecular hydrogen bonds). The stabilization effect is greatest at 1:1 molecular ratio of water and ethanol. Further addition of water sharply decreases the viscosity and precipitates the polymer.

SUMMARY

The stabilizing effects of certain organic compounds on concentrated solutions of Anid G-669 in ethanol have been studied.

LITERATURE CITED

- [1] A. A. Tager, Progr. Chem. 18, 557 (1949).

Institute of Elementoorganic Compounds
Academy of Sciences USSR

Received July 11, 1957

THE MELTING OF GELATIN GELS

S. I. Meerson and S. M. Lipatov

Our thermochemical investigations showed that the heat of solution of a polymer is a complex function of the temperature and of the nature of the polymer and solvent. It was found that the general thermochemical relationships which were established are associated with the physical state of the polymer and, in a number of cases, with its glass transition temperature. A number of papers have been published by foreign investigators in recent years, dealing with the effect of temperature on the heat of solution of polystyrene in various solvents [1, 2]. The results were in good agreement with our earlier findings for the same polymer [3]. A peculiar feature of the heat of solution of polystyrene in toluene and benzene is the absence of an upper horizontal plateau, which we found for other systems. Schulz and Senckel [1, 2] correlated the observed heat of solution with the heat capacity and the glass transition temperature of the polymer. To explain the result obtained, they suggested that when the polymer dissolves the heat of vitrification (second-order transition) is liberated; the greater the difference between the solution temperature and the glass transition temperature, (T_g) the greater is the heat liberated.

This is made clear in Fig. 1, which shows the dependence of the enthalpy and specific volume of the polymer on the temperature. At low temperatures the polymer is in the glassy state, and its enthalpy and specific volume vary almost linearly with the temperature up to T_g . At T_g the polymer passes into the molten state, which is characterized by a higher temperature coefficient of enthalpy. The authors cited consider that when a polymer is dissolved at a temperature below T_g , such as T_1 , a solution is formed such that its enthalpy (H) and specific volume (V) lie on the continuation of the line for the melt. It follows that dissolution of the polymer at T_1 is accompanied by transition from the glassy state to a solution, with decrease of enthalpy and specific volume ($\Delta H = H_g - H_s$). Therefore heat of vitrification should be liberated when the polymer dissolves ($\Delta H < 0; \bar{Q} > 0$). The amount of heat liberated must decrease with approach to T_g , and at $T_g \bar{Q} = 0$ provided that the heat of mixing of the polymer melt with the solvent is zero.

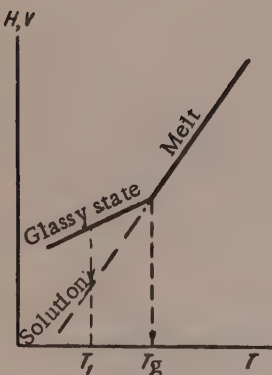


Fig. 1. Effect of temperature on the enthalpy change and the specific volume of the polymer. T_g is the glass transition temperature.

This interpretation can hardly be challenged for the system polystyrene-solvent, especially as it has been shown [2] that the partial specific volume of polystyrene in solution is less than that of the pure polymer, and lies somewhat below the straight line which represents the continuation of the specific-volume line for the melt into the region of lower temperatures.

Therefore, heat of vitrification should be liberated during the solution of polymers if the specific volume and enthalpy of the polymer are lower in solution than in the glassy state.

TABLE 1

Effect of Temperature on the Viscosity of 0.8% Solutions of Gelatin in Water and 3 M Urea Solution

Solvent	η_{rel} at various temperatures, °C					
	8	12.4	20	30	40	50
Water	Gel	4.60	3.64	1.53	1.40	1.38
Urea, 3 M	1.82	1.80	1.74	1.64	1.62	1.55

It is known from the literature that urea lowers the gelation temperature and the viscosity of concentrated gelatin solutions [4]. We also showed that at relatively low temperatures the viscosity of gelatin solutions is lower in urea than in water at the same concentrations; this was in agreement with the findings of other authors. However, at higher temperatures the viscosity of solutions in urea is higher than in water at the same concentrations (Table 1).

TABLE 2

Effect of Temperature and Urea Concentration on Heat of Solution of Gelatin

Temperature of experiment, °C	Heat of solution of gelatin in cal/g		
	water	3M urea solution	8M urea solution
20	22.0	22.6	24.0
50	15.0	17.0	20.0

of water, when dissolved in urea solutions, is the same as in the dissolution of gelatin in water, but the temperature, at which the heat effect ceases to vary with the temperature, decreases (see curve for 87% in Fig. 2).

We used 8 M urea solution for determinations of the heat of solution of gels. The results are plotted in Fig. 2; a totally different situation is seen over a wide range of gel concentrations: the heat of solution increases with temperature. In this case the gel does not melt in the ampoule at relatively low temperatures, and when it dissolves in the urea solution a certain quantity of heat is expended, which is subtracted from the positive heat of interaction of the gelatin with the urea solution. On further increase of temperature the gel melts in the calorimetric ampoule and therefore less heat is absorbed when it dissolves; as a result the total heat effect increases. At a certain temperature (T_m) the gel is completely melted in the calorimetric ampoule, and the observed heat effect is equal to the heat of mixing of the melt with the urea solution. Consequently, $\Delta\bar{Q}$ represents the heat of melting of the gel. It follows from Fig. 2 that the extent of the melting range varies with the gel concentration; the higher the gel concentration, the broader is the melting range and the higher is the melting temperature (T_m).

It is known that on addition of 30% of water to dry gelatin all the polar groups become hydrated (gels of the first type), and such hydrated gelatin does not liberate heat on contact with water. We found that for gels containing less than 30% water the $\bar{Q} = f(t)$ curves for their dissolution in urea solutions are normal, i.e., \bar{Q} decreases with increase of temperature whereas, as follows from Fig. 2, the reverse is true for gels containing over 30% water (gels of the second type).

However, these views appear to us to be incorrect in relation to other systems studied by us (certain polymers which show limited swelling, such as gelatin). We consider the decrease of the heat effect with increase of temperature to be due to absorption of heat of fusion. The controversial nature of this question led us to seek another method, whereby it could be shown that when a polymer of maximum solvation (or gel) passes into solution heat is not liberated but absorbed, and whereby the quantity of heat required for fusion of gels could be determined.

We therefore carried out a series of determinations of the heat of solution of gelatin gels in urea solutions at various temperatures.

These results show not only that urea blocks the active groups [4, 5] which are responsible for structurization and gelation (this effect is especially noticeable in relatively dilute solutions), but also that it causes straightening of the chains.

Preliminary thermochemical investigations showed the heat of solution of gelatin in urea solution, which depends on the solution concentration, as greater than the heat of interaction of gelatin with water. It follows from Table 2 that the heat of solution increases with increasing concentration of urea.

It was also found that the nature of the $\bar{Q} = f(t)$ relationship for dry gelatin and gelatin containing 13%

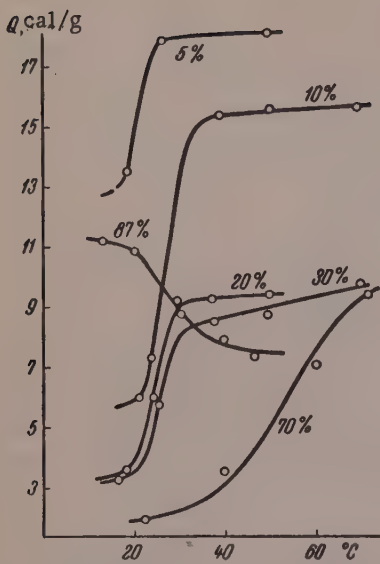


Fig. 2. Effect of temperature on the heat of solution of gelatin gels in 8 M aqueous urea solution; the numbers on the curves represent the percentage concentrations of the gelatin gels.

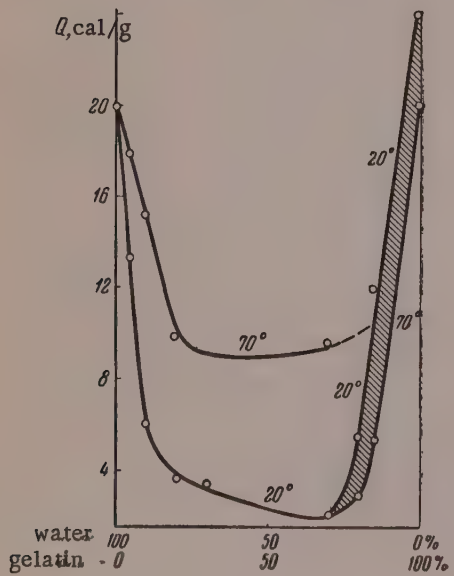


Fig. 3. Effect of gel concentration on the heat of solution of gels in 8 M aqueous urea solution.

The explanation is that there is considerable bonding between the polar groups in gels of the first type, and such gels do not melt in the calorimetric ampoules in the determinations of the $\bar{Q} = f(t^*)$ curves. In gels of the second type the polar groups capable of hydration are completely hydrated and are not joined to each other. The gel structure is maintained either by non-polar groups or by nonhydratable groups; these bonds are weak and the gel melts when the temperature is raised. Nevertheless, there is a certain temperature range when this melting cannot occur, as the heat supplied is less than that required to overcome these bonds. It is not possible to determine this heat of melting in the interaction of gels of the second type with water, as the heat effect is found to be zero over a wide temperature range. (At room temperature the gels do not melt and the heat of hydration is zero, and at higher temperatures the heat of hydration is again zero and the gel is already melted in the ampoule.)

It is quite evident that if a solvent is found in which gels of the second type dissolve at room temperature, the heat of melting can be determined. 8 M aqueous urea solution is such a solvent.

In Fig. 3 the heats of solution of gels in urea solution are plotted against the gel concentrations at 20 and 70°. It is seen that for gels of the first type $\bar{Q}_{20^\circ} > \bar{Q}_{70^\circ}$, and for gels of the second type $\bar{Q}_{20^\circ} < \bar{Q}_{70^\circ}$, i.e., the $\bar{Q} = f(t^*)$ relationship is the reverse of the type found earlier. The difference between the ordinates of the two isotherms gives the heat of melting of a gel of a given composition. Figure 3 can be used to determine the heats of melting of gels of low concentrations; this is important because in experiments with such gels calculations based on dry gelatin content involve large errors.

This new method can be recommended for determinations of the heats of melting of any reversible polymer gels; it is merely necessary to find a solvent in which the gel dissolves spontaneously at all temperatures.

The form of dependence of the heat of solution of gels on the temperature, indicative of melting of the gels, is confirmed by the results of studies of the effect of temperature on the heat capacity of the gels.

The $\bar{C}_p = f(t^*)$ relationship was determined for certain gelatin gels. An adiabatic calorimeter of the S. M. Skuratov type was used. The gels were held for a certain time at each temperature to attain equilibrium. The results for 62% gelatin gel are given in Fig. 4. It is seen that the $C_p = f(t^*)$ passes through a maximum. The same diagram shows the $H = f(t^*)$ relationship calculated from the Kirchhoff law. The

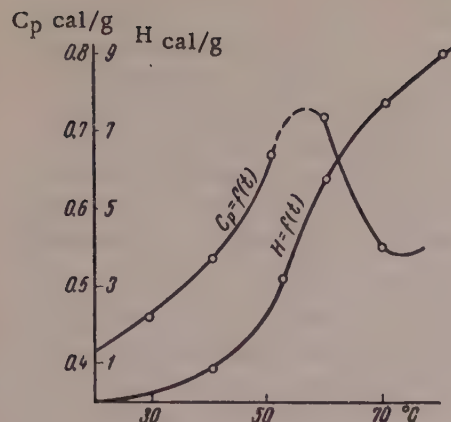


Fig. 4. $C_p = f(t^*)$ and $H = f(t^*)$ relationships for 68% gelatin gel.

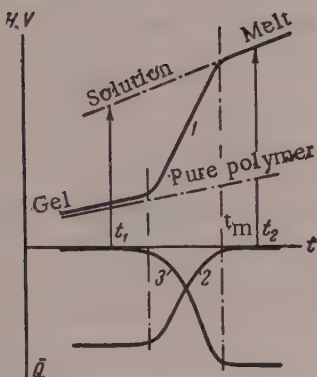


Fig. 5. Schematic plot of the $H = f(t^*)$ and $\bar{Q} = f(t^*)$ relationships (T_m is the melting temperature): 1) $H = f(t^*)$ for gel; 2) $\bar{Q} = f(t^*)$ for gel when dissolved in urea solution; 3) $\bar{Q} = f(t^*)$ for gelatin when dissolved in water.

gelation, must be accompanied by liberation of heat. This result is in agreement with our earlier thermographic investigations [6], with the advantage that the heat of melting can be evaluated quantitatively.

It must be pointed out that thermographic and dilatometric studies of gelation present great difficulties, as the volume and heat effects are very small, especially for relatively dilute gels, as is clear from Fig. 8. However, the nature of the $\alpha = f(t^*)$ and $C_p = f(t^*)$ relationships indicates that a volume effect should also occur in the process. We therefore carried out, jointly with N. N. Puchkova, dilatometric and pycnometric determinations of volume changes in gels over a wide range of temperatures and concentrations. Here we give only one curve, which shows the volume changes of a 60% gel with temperature.*

* More detailed results of studies of the dependence of gel volume on the temperature over a wide range of concentrations will be given in a separate communication.

enthalpy changes of the gel are of the same nature as that found in studies of the heat of solution of gels in urea solution. The same indistinct transition is found, and the heat of melting is 8 cal/g of polymer. The heats of melting found by the two different methods are in fairly good agreement.

These results demonstrate the inapplicability of Senckel's views [2] to the system in question. Figure 5 can be used to account for the increase of the heat effect with increase of temperature when gelatin gels are dissolved in urea solution, and the decrease of the heat effect with increase of temperature when dry gelatin is dissolved in water.

If the enthalpy of the gelatin solution is considered to lie on the continuation of the line for the melt, it is clear that at the transition from gel to solution at t_1 , heat should be absorbed, equal to the heat of melting of the gel. The quantity of heat absorbed should decrease as T_m is approached, and at T_m the heat effect should be zero (or, in this instance, equal to the heat of mixing of the melt with urea solution). This process is represented by Curve 2 (Fig. 5) for the $\bar{Q} = f(t^*)$ relationship.

In explaining the character of the $\bar{Q} = f(t^*)$ relationship for the dissolution of gelatin in water it must not be forgotten that dry gelatin does not melt in the calorimetric ampoule and that the enthalpy changes slightly over the temperature range in question. In this case the melting takes place on contact of the gelatin with water at an elevated temperature. Therefore the enthalpy of dry gelatin must be extrapolated to higher temperatures. The dissolution of gelatin at t_2 is accompanied by absorption of heat. This process is represented by Curve 3 (Fig. 5) for the $\bar{Q} = f(t^*)$ relationship when gelatin is dissolved in water (with the heat of hydration disregarded).

Thus, we were able to show by two independent methods that the transition of a gelatin gel into a melt (gel-sol transition) and the solution of dry gelatin in water over a wide temperature range are accompanied by absorption of heat.

Since melting of the gel is accompanied by absorption of heat, it is clear that the reverse process,

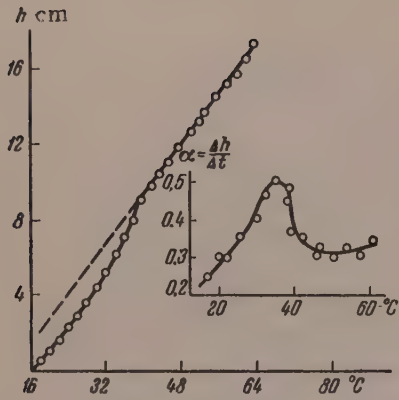


Fig. 6. $h = f(t^\circ)$ and $\alpha = f(t^\circ)$ relationships for 60% gelatin gel.

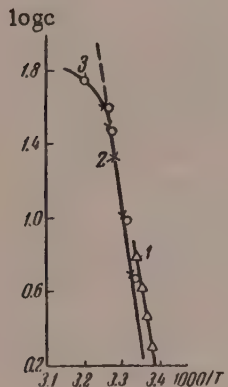


Fig. 7. $\log c = f\left(\frac{1000}{T}\right)$ relationship for gelatin gels; 1) Data of Elridge and Ferry; 2) calorimetric data; 3) dilatometric data.

The ordinates in Fig. 6 represent the height of the mercury in the dilatometer capillary (h) (with a correction for the expansion of mercury). It follows from Fig. 6 that the $h = f(t^\circ)$ curve resembles analogous curves for certain partly crystalline polymers [7]. It is difficult to determine the start of the melting range. However, the end of the melting range is detected fairly clearly from the intersection of the two curves. We denote this point by T_m . This temperature coincides with the melting point determined visually. If the line for the melt is extrapolated to lower temperatures, it is seen that the supercooled melt has a greater volume than the gel at the same temperature.

The variation of the coefficient of volume expansion of the gel (α) with the temperature is also plotted in Fig. 6. It is seen that the $\alpha = f(t)$ curve, like the $C_p = f(t)$ curve, passes through a maximum.

It follows from all these results that the transition of the gel into the liquid state can be regarded as melting.

Since the gels do in fact melt, and T_m is lowered with increasing amount of solvent, it is possible to use the Flory equation [8] for calculation of the heats of melting of the gels. The Flory equation

$$\frac{1}{T} - \frac{1}{T_0} = \frac{2.3R}{\Delta H} \log N_n,$$

may be written in a form more convenient for calculations

$$\frac{1}{T} = -\frac{2.3R}{\Delta H} \log N_n + \text{const}, \quad (1)$$

where $1/T_0 = \text{const}$, T_0 is the melting point of the polymer; T is the melting point of the polymer containing the solvent; N_n is the mole fraction of the polymer. The values of $T_m = T$ were taken from our dilatometric and thermochemical data. We also used the equation

$$\log c = -\frac{\Delta H}{2.3RT} + \text{const}, \quad (2)$$

which had been used both by ourselves [11] and by Elridge and Ferry [9] for calculations. The relationship $\log c = f(1000/T)$ is plotted in Fig. 7. It is seen that Equation (2) is applicable to gels at concentrations not over 40%; above this, calculations based on Equation (1) and on Equation (2) both deviate from linearity.

The values of ΔH are 50 and 57.6 kcal/mole respectively. The values of ΔH calculated by these equations agree with the heats of melting given by Walker [10] and by Elridge and Ferry [9], and also with our values for the heats of melting of gels, calculated from the maximum swelling-temperature relationship [11].

These calculations show that the molar heat of melting cannot be found by mere multiplication of the heat of melting (cal/g of polymer) determined calorimetrically, by the molecular weight.

SUMMARY

1. A calorimetric method for determination of the heats of melting of gels has been developed and used to determine the heats of melting of gelatin gels over a wide range of concentrations.

2. The heat of melting of a gel (in cal/g of polymer), the melting-temperature range, and T_m depend on the concentration of the gel.

3. The dependence of the heat capacity of 62% gelatin gel on the temperature was investigated. It was shown that the $C_p = f(t^\circ)$ curve passes through a maximum.

4. The gel volume-temperature relationship has been studied by a dilatometric method. It was shown that the $h = f(t^\circ)$ curve has an inflection point corresponding to T_m . The $\alpha = f(t^\circ)$ curve passes through a maximum.

5. It may be concluded from all these results that Schulz and Senckel's conclusion concerning the liberation of heat of vitrification during dissolution over a wide temperature range is not valid for all polymers. For the system investigated here, heat of melting is absorbed when gelatin dissolves over a wide temperature range.

LITERATURE CITED

- [1] R. Günner and C. V. Schulz, Naturwissenschaften 40, No. 5, 164, 1953; C. V. Schulz, Z. phys. Chem. 4, 192, 311 (1955).
- [2] E. Senckel and K. Gorke, Z. Naturforschung 7a, 9, 630 (1952).
- [3] S. I. Meerson and S. M. Lipatov, Colloid J. 18, No. 4, 447 (1956).*
- [4] P. I. Zubov, Z. N. Zhurkina and V. A. Kargin, Colloid J. 9, No. 8, 109 (1947).
- [5] J. Bello, H. Riese and S. Vinograd, J. Phys. Chem. 60, No. 9, 1299 (1956).
- [6] S. M. Lipatov and S. I. Meerson, Trans. Moscow Textile Inst. 13, 74 (1954).
- [7] D. Roberts and L. Mandelkern, Problems of Modern Physics No. 2, 69 (1956).**
- [8] P. S. Flory, R. Garrett, S. Neuman and L. Mandelkern, J. Polymer Sci. 12, 97 (1954).
- [9] J. Elridge and J. Ferry, J. Phys. Chem. 58, No. 11, 992 (1954).
- [10] E. Walker, Fibers from Synthetic Polymers (Russian translation) (IL, Moscow, 1957) p. 325.
- [11] S. M. Lipatov and S. I. Meerson, Colloid J. 9, No. 6, 423 (1947).

The Moscow Textile Institute

Received March 2, 1958

* Original Russian pagination. See C. B. Translation.

** Russian translation.

PLASTICOELASTIC PROPERTIES OF SKN-26 RUBBER

A. S. Novikov and F. S. Tolstukhina

The plasticoelastic properties of SKN rubber in the solid phase were studied in relation to the molecular weight, fractional composition, and types of fillers added.

Samples of different molecular weight were obtained by fractionation from solution in benzene-methyl alcohol mixture, by the method of cooling. Seven fractions were isolated, each comprising $12 \pm 2\%$ of the weight of the original polymer. The fractions were stabilized by addition of 2 wt. parts of phenyl- β -naphthylamine per 100 wt. parts of rubber. The first fraction was insoluble. For the soluble fractions, the intrinsic viscosity in benzene at 25° , and the molecular weight (by the osmotic method, in osmometers of Dogadkin's design) were determined. Films were prepared from solutions of the fractions; these were dried to constant weight under 10^{-3} mm Hg residual pressure in the dark at room temperature. Constancy of the molecular structure during the experiments was checked by the solubility and values of the intrinsic viscosity. The results of mechanical tests are given for specimens the molecular weight of which remained unchanged after the experiments.

The kinetics of development of simple shear deformation and of creep after removal of the load [1-4] was studied for the specimens. The shear was effected in a layer of polymer between two plane parallel plates [5]. The displacement was measured by means of a cathetometer to an accuracy of 0.0005 cm; the maximum deformation was 100-150%. The displacement rate was varied between $4.33 \cdot 10^{-2}$ and $1.44 \cdot 10^{-6}$ sec $^{-1}$, according to the material. Rebinder [1] states that this is the most accurate and simplest method for investigation of deformation properties.

At constant stress and temperature, the linear portion of the shear deformation-time curve represents the rate of increase of irreversible deformation, while the high-elastic deformation in conditions of steady flow can be determined from the recovery after removal of the load. The characteristics of the material - the viscosity (η) and equilibrium elasticity modulus (E_2) - were calculated from the expressions

$$\eta = \frac{P}{\dot{\epsilon}} ; \quad E_2 = \frac{P}{\epsilon_m} ,$$

where η is the viscosity in poises; P is the shear stress in dynes/cm 2 ; $\dot{\epsilon}$ is the velocity gradient in sec $^{-1}$; E_2 is the equilibrium elasticity modulus; ϵ_m is the relative high-elastic deformation.

Figure 1 shows a typical rheological curve for a polymer fraction of molecular weight 81,000 at 82° . The curve shows that there are two viscosity regions in the stress range investigated. At low stresses and velocity gradients the polymer behaves as a viscous Newtonian liquid and the viscosity is almost constant in this range. The curves for the recovery after removal of the load show (Fig. 2) that the maximum elastic deformation increases with the stress. Consequently, a change of the molecular chain configuration is not accompanied by a viscosity increase; this, in agreement with P. A. Rebinder's views, is probably the consequence of flow of the polymer under conditions of equilibrium breakdown and restoration of the bonds.

Influence of molecular weight. The viscosities of melts of polymer fractions of different molecular weight were measured at 82° in the first stress region, in which the flow is Newtonian (Table 1).

TABLE 1

Shear Characteristics of Molten Fractions ($t = 82^\circ$)

Fraction No.	(η)	Mol. wt. (osmotic)	η poises	$E_2 \cdot 10^{-3}$ dynes/cm ²
II	2.00	243 000	Partial loss of solubility after experiment	
III	1.56	202 000		334
IV	1.24	112 000		125
V	1.00	81 400		25
VI	0.62	52 000		Low elastic deformation
VII	0.32	$\approx 27\ 000$		No elastic deformation

TABLE 2

Effect of Fractional Composition on the Plasticocelastic Properties of SKN-26 Rubber

Specimen	$\eta \cdot 10^{-3}$ poises		$E_2 \cdot 10^{-3}$ dynes/cm ²
	from slope of curve	from residual deform- ation	
1	—	3.64	97.4
2	1.56	3.17	163
3	2.00	4.83	179

TABLE 3

Shear Characteristics of Raw Loaded Stocks of SKN-26 Rubber ($M = 51,000$) at Constant Stress $P = 4914$ dynes·cm⁻²

Composition of SKN-26 specimen	$\dot{\epsilon} \cdot 10^3$ sec ⁻¹	$\eta \cdot 10^{-6}$ poises	ϵ_m
Without filler	4.70	1.04	0.10
With chalk	1.92	2.55	0.41
With lamp black	1.21	4.06	0.79

It follows from the data in Table 1 that the viscosities of Fraction III and Fraction VII differ by seven tenth-powers.

The viscosities of SKN-26 fractions are higher than those of butadiene-styrene copolymers of the same molecular weights [6].

In Fig. 3 the polymer viscosity is plotted against the molecular weight in logarithmic coordinates. In the molecular-weight range studied (with the exception of Fraction VII) this gives a linear plot, represented by the equation:

$$\log \eta = 8.52 \log M - 34.01.$$

Comparison of data for SKS-30, SKS-30A [4], and SKN-26 for conditions of steady flow shows that the exponent of the molecular weight depends on the flexibility of the polymer chains and the forces of intermolecular interaction.

Effect of fractional composition. The influence of molecular weight distribution on the plasticocelastic properties was tested for three specimens with the same intrinsic viscosity, 1.24.* Specimen 1 was the unfractionated polymer, Specimen 2 was a mixture of Fractions III, IV, and VI, and Specimen 3 was the fairly homogeneous Fraction IV.

The plasticocelastic properties were investigated at the same stress at 82° (Fig. 4). The viscosity was determined from the slope of the steady region of the deformation curve and from the residual deformation after removal of the load, measured after prolonged recovery to an equilibrium value (Table 2).

* For preparation of specimens with intrinsic viscosity 1.24, fractions were mixed in accordance with the principle of additivity of intrinsic viscosities [7]. The experimental values of $[\eta]$ coincided with the values calculated by this rule.

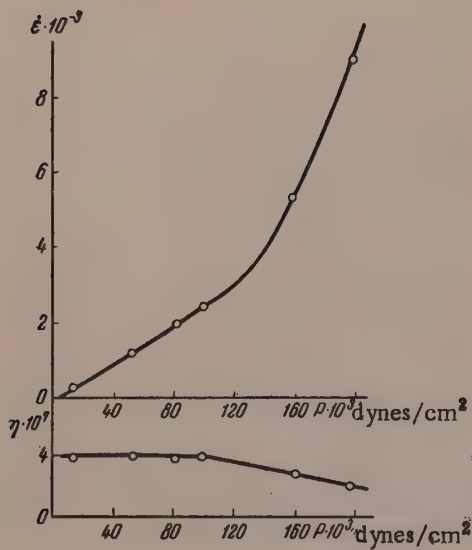


Fig. 1. Effect of shear stress on rate of shear and viscosity in SKN-26 fraction with $M = 81,000$.

dynes \cdot cm² (Fig. 5), for SKN-26 fraction of molecular weight 51 \cdot 10³ (this fraction comprised 12% of the weight of the original polymer), and for mixtures of this fraction with chalk and lamp black show that introduction of fillers not only decreases the rate of irreversible deformation, increasing the viscosity of the mixture, but increases the elastic deformation (Table 3).

It follows from the data in Table 2 that the capacity for viscous flow is almost independent of the molecular weight distribution, and is determined by the intrinsic viscosity. However, polymers of the same intrinsic viscosity and different molecular weight distribution differ by the magnitude of the deformation under constant stress. At similar rates of plastic flow, the most polydisperse specimen has the greatest total deformation. This is because the modulus decreases with increasing molecular weight heterogeneity, i.e., the more homogeneous polymers with narrow molecular weight distributions are harder and less workable.

A dependence of the workability on the molecular weight distribution was also observed for polyisoprene and polybutadiene polymers obtained by polymerization in solution. It follows that the workability of polymers depends not only on the viscosity, but also on the distribution of the relaxation times consequent on the polydispersity.

Effect of loading. The influence of temperature on the viscosity of raw loaded stocks was studied. The fillers were introduced on rolls, 10.9 vol. parts per 100 vol. parts of rubber being added. Curves for the increase of shear deformation at constant stress $P = 4914$

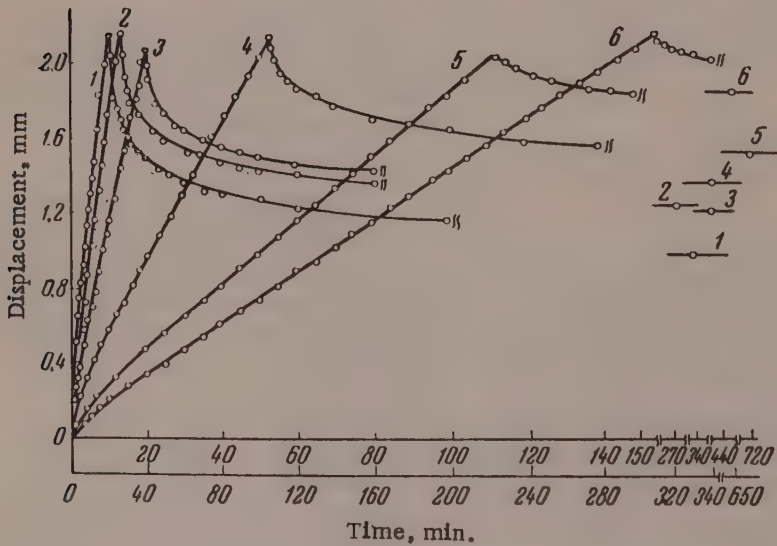


Fig. 2. Shear deformations under different stresses for SKN-26 fraction with $M = 81,000$.

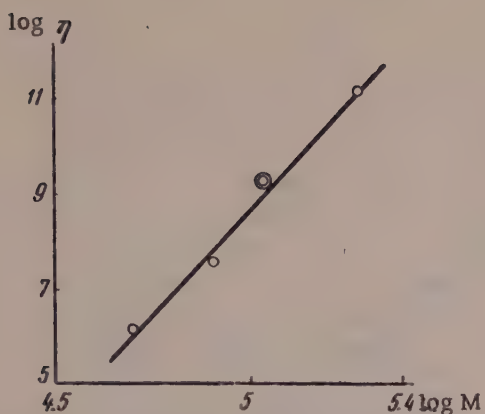


Fig. 3. Logarithmic plot of viscosity against the molecular weight of molten SKN-26 fractions.

TABLE 4

Effect of Temperature on the Shear Properties of Raw Loaded Rubbers at $P = 4914$ dynes \cdot cm $^{-2}$ (SKN Fraction with $M = 51,000$)

Composition of SKN-26 specimen	Temperature, °C	$\epsilon, \text{sec}^{-1}$	$\eta \cdot 10^7$, poises
Without filler	24	$2.69 \cdot 10^{-4}$	1.81
	40	$5.24 \cdot 10^{-4}$	0.935
	60	$1.68 \cdot 10^{-3}$	0.290
	82	$4.70 \cdot 10^{-3}$	0.104
With chalk	24	$1.23 \cdot 10^{-4}$	3.99
	40	$2.48 \cdot 10^{-4}$	1.98
	82	$1.92 \cdot 10^{-3}$	0.255
With lamp black	24	$6.94 \cdot 10^{-5}$	7.08
	40	$1.65 \cdot 10^{-4}$	2.97
	61	$4.74 \cdot 10^{-4}$	1.08
	82	$1.21 \cdot 10^{-3}$	0.406

Thus, the combination of plastic and elastic properties of rubber already changes when the rubber is mixed with the ingredients. The increase of viscosity and high-elastic deformation produced by introduction of a filler is more pronounced with the more "active" fillers. These results are in full harmony with the results obtained by Rebinder et al. [8-10] in studies of structure formation in rubber solutions on addition of fillers.

It was desired to determine whether the flow of loaded mixtures conforms to the temperature relationship established by Eyring [11] for polymers. The data in Table 4 show that when the temperature is raised from 24 to 82°, the viscosity decreases approximately 17-fold.

The results show that the presence of carbon black or chalk in the polymer does not alter the general character of the viscosity-temperature relationship (Fig. 6). The slope of the $\log \eta - 1/T$ lines is almost the same for SKN-26 rubber and loaded mixtures, indicating that the effective activation energy is the same, while the pre-exponential factor increases on addition of fillers, as is shown by the increase of the intercepts cut off along the ordinate axis. This was also found for a polyisobutylene fraction with molecular weight $284 \cdot 10^3$ to which 20 wt. parts of lamp black per 100 wt. parts of rubber was added (Curves 4 and 5, Fig. 6). Thus it may be concluded that at low shear stresses flow in the complex rubber-filler system occurs by displacement of chain segments, as in pure polymers.

The specific influence of the fillers added to the rubber may be due to formation of two types of bonds during the mixing: weak bonds of the type of van der Waals forces between the rubber and filler, which are easily broken down and restored during deformation, forming a kind of mobile structural network; and relatively stable bonds formed by interaction of free polymer radicals, formed during mastication of the rubber, with the filler surface. The formation of such bonds may lead to joining of individual molecular chains through the filler particles up to formation of a continuous network, as is the rubber-carbon black complex [12]. This effect ultimately results in an increase of the elastic deformation of a loaded polymer as compared with the polymer in absence of filler.

The displacement of such an enlarged molecule requires the coordinated displacement of a large number of segments, which is one of the causes of the viscosity increase. Another cause is the increased concentration of mobile contacts between the chains undergoing displacement. The formation of these types of bonds and their relative proportions in a given rubber largely depend on the nature of the filler. The increase of the viscosity and of the elastic deformation can serve as a quantitative measure of filler activity.

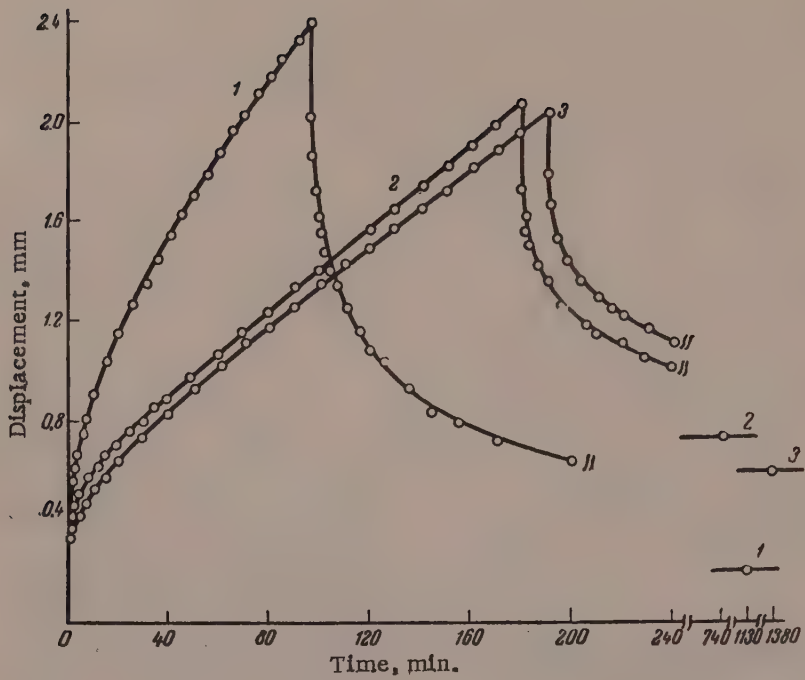


Fig. 4. Effect of molecular weight distribution on the plasticcoelastic properties: 1) Specimen 1; 2) Specimen 2; 3) Specimen 3.

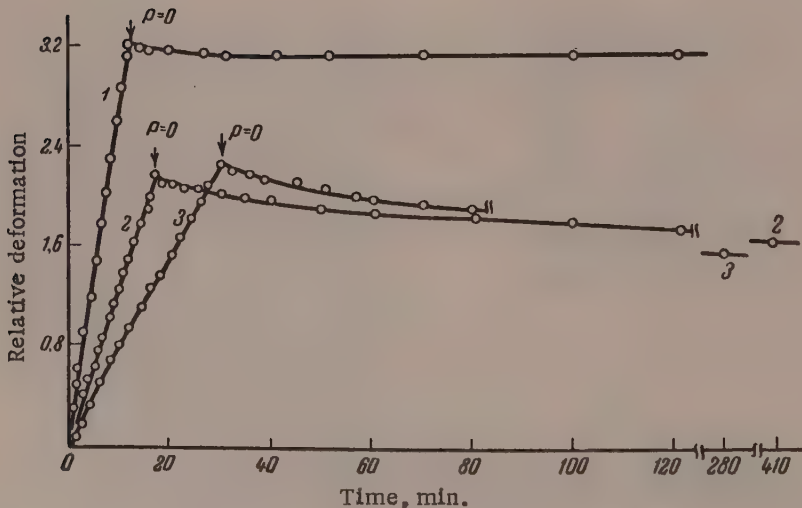


Fig. 5. Growth of shear deformation at $P = 4.9 \cdot 10^3$ dynes/cm 2 , and recovery curve after removal of load ($t = 82^\circ$): 1) SKN-26 fraction; 2) the same, with chalk; 3) the same, with lamp black.

SUMMARY

1. The viscosities of melts of SKN-26 rubber fractions have been determined. The flow law $\log \eta = A \log M + B$ is valid over a wide range of molecular weights.

2. The influence of fractional composition on the plasticoelastic properties of SKN-26 rubber has been studied. For polymers of the same intrinsic viscosity in benzene solution, the viscous flow of the melts is almost independent of the molecular weight distribution. The elastic modulus increases with decreasing polydispersity.

3. Experiments with chalk and lamp black showed that fillers not only increase the viscosity of the mixtures, but also increase the high-elastic deformation.

4. The nature of the viscosity-temperature relationship is not changed by introduction of fillers. This was demonstrated for SKN-26 and polyisobutylene, and confirms that in a complex system, where rubber-carbon complexes may be formed, flow at low shear stresses occurs by the mechanism of segment displacement.

LITERATURE CITED

- [1] P. A. Rebinder, New Methods for Physicochemical Investigation of Surface Phenomena, Trans. Inst. Phys. Chem. (Izd. AN SSSR, 1950). *
- [2] E. E. Segalova and P. A. Rebinder, Colloid J. 10, 233 (1948).
- [3] L. V. Chumakova and P. A. Rebinder, Proc. Acad. Sci. USSR 81, 239 (1951).
- [4] L. V. Chumakova-Ivanova and P. A. Rebinder, Colloid J. 18, 540 (1956). **
- [5] D. M. Tolstoi, Colloid J. 10, 133 (1948).
- [6] A. S. Novikov and F. S. Tolstukhina, Proc. Acad. Sci. USSR 109, 576 (1956). **
- [7] F. T. Wall, J. Am. Chem. Soc. 67, 1929 (1945).
- [8] P. A. Rebinder, G. A. Ab, and S. Ia. Veiler, Proc. Acad. Sci. USSR 33, 444 (1949).
- [9] A. S. Kolbanovskaya and P. A. Rebinder, Colloid J. 12, 194 (1950).
- [10] A. S. Kolbanovskaya, P. A. Rebinder and O. I. Luk'ianova, Colloid J. 12, 208 (1950).
- [11] H. Eyring, J. Chem. Phys. 4, 283 (1936).
- [12] A. S. Novikov, M. B. Khaikina, T. V. Dorokhina and M. I. Arkhangel'skaya, Colloid J. 15, 51 (1953). **

Scientific Research Institute
of the Rubber Industry
Moscow

Received December 26, 1957

* In Russian.

** Original Russian pagination. See C. B. Translation.

EFFECT OF THE COMPOSITION OF RUBBER ON ITS FATIGUE CHARACTERISTICS

M. M. Reznikovskii, L. S. Priss, and M. K. Khromov

In solid and pneumatic tires, in various shock absorbers, clutches, and many other articles rubber is subjected to repeated cyclic stresses. In a number of other articles (gaskets, etc.) the rubber is under continuous static load. In all such cases the most important characteristic of the service quality of the rubber is its capacity for prolonged endurance under mechanical stresses. This quality, which may be termed the fatigue endurance (dynamic or static, according to the applied load) or, in the widely used but inaccurate terminology, the fatigue strength, has recently attracted the close attention of numerous investigators. The results of a large number of investigations in this field are summarized in Dillon's monograph [1], in the review [2] which is appended to the Russian translation.

The present paper deals with a study of the dependence of the endurance of rubbers to dynamic fatigue on the principal formulation factors — type of rubber, degree of vulcanization, loading, and softeners.

Before presentation of the data, let us briefly consider some aspects of terminology and test methods.

The terminology in this field is often very confused and without adequate basis. For example, different authors use the following terms to indicate the number of cycles to cause failure of the rubber: fatigue life, endurance, fatigue resistance, and fatigue strength. Similar ambiguities occur in the literature in English, where the term "fatigue life" is used to denote both the time and the number of cycles to destruction. In a special article on questions of fatigue tests on rubber [3] we proposed a rational terminology, which is used in the present communication. Thus, the number of cycles required to cause failure of the rubber under given dynamic load conditions is denoted by the term fatigue life; the amplitude of the stress causing destruction of the material after a definite number of cycles (corresponding to the given fatigue life) is termed the fatigue stress or fatigue tensile strength. The following terms are introduced for the amplitude of deformation and the energy of the cycle corresponding to a definite fatigue life: fatigue deformation, and fatigue energy.

The fact that fatigue tests on rubber are usually performed at fairly large deformations determines a number of specific features of such tests, as compared with corresponding tests on other materials such as metals. The principal experimental difficulties which arise in fatigue tests on rubber are discussed in our earlier papers [3]; it is shown there that the complications due to relaxation effects, which distort the dynamic conditions, are best overcome by the use of symmetrical alternating stress cycles. It is also shown that the thermal state of the specimens used for dynamic fatigue testing must be taken into consideration. For comparative tests at the same temperature, differences in the hysteresis properties of the specimens must be compensated by variations of the conditions of heat exchange with the surroundings.

The results given below were obtained under conditions of symmetrical alternating load with a pre-determined deformation. These conditions are achieved by rotation of bent specimens, with a cylindrical working portion 8 mm in diameter and 23.5 mm long. The deformation amplitude was varied from 14 to 33%.

The testing frequency was 3000 r.p.m. (50 cycles/second). A test frame was made, consisting of six temperature-controlled sections; four specimens were tested simultaneously in each under the same conditions [3]. The thermostat temperature was chosen so as to ensure an equal temperature in the specimens (120 or 100°) irrespective of the test conditions and the elastic and hysteresis properties. The test temperature was taken to be the surface temperature of the specimens measured by means of a contact thermocouple of special design

when the machine was stopped. This seems to us to be a more correct method than the measurement of temperature in the center of the specimen which is recommended in such tests [4], as failure of the specimen generally begins at the surface.

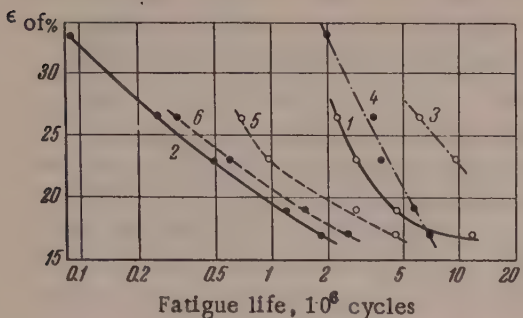


Fig. 1. Variation of fatigue deformation with fatigue life in alternating bend tests: 1) NR (natural rubber) without filler; 2) NR + 40 wt. parts channel black; 3) SKB without filler; 4) SKB + 40 wt. parts channel black; 5) SKS-30 without filler; 6) SKS-30 + 40 wt. parts channel black. Test frequency 3000 cycles/minute; $T = 120^\circ$. Dynamic moduli E of the rubbers: 1) 19.3; 2) 23.6; 3) 14.7; 4) 22.7; 5) 16.6; 6) 31.4 kg/cm².

The dynamic properties of the rubbers were tested on the same specimens and under the same load conditions in a special instrument. A brief description of the frame for fatigue testing and the instrument for determination of the dynamic properties was given earlier [3, 5].

Influence of the type of rubber. Figure 1 shows the variations of the fatigue deformation ϵ_{0f} with fatigue life for unfilled vulcanizates of NR, SKB, and SKS-30 and vulcanizates of the same rubbers, containing 40 wt. parts of channel black per 100 wt. parts of rubber. These results were used to plot the fatigue stress f_{0f} and the fatigue energy W_{0f} against the fatigue life, in Figs. 2. The latter values were calculated from the formulas

$$f_{0f} = E\epsilon_{0f}; \quad W_{0f} = E \frac{\epsilon_{0f}^2}{2}.$$

Examination of the data in Figs. 1 and 2, b reveals the following two facts:

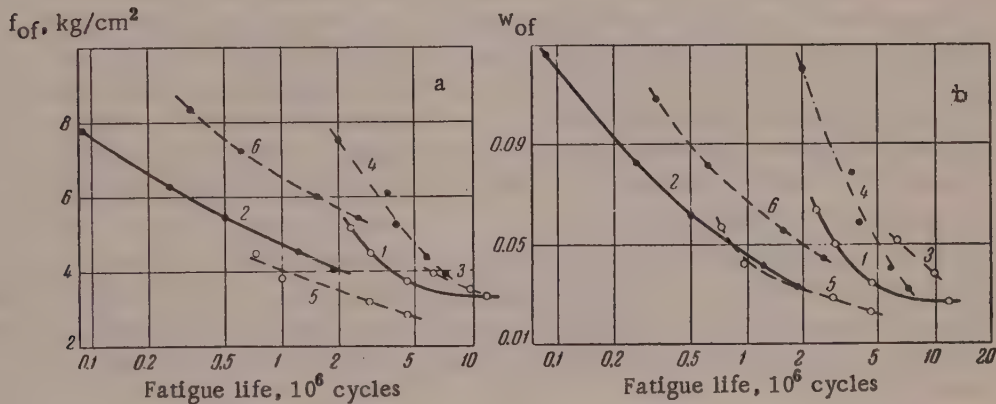


Fig. 2. Variations of fatigue stress (a) and of fatigue energy W_{0f} in joules/cm (b) with the fatigue life in alternating bend tests: 1) NR without filler; 2) NR + 40 wt. parts channel black; 3) SKB without filler; 4) SKB + 40 wt. parts channel black; 5) SKS-30 without filler; 6) SKS-30 + 40 wt. parts channel black. Test frequency 3000 cycles/minute; $T = 120^\circ$.

1. The sequence of the rubbers in order of increasing fatigue life varies considerably under different test conditions. For example, under constant deformation conditions unfilled SKB and SKS-30 vulcanizates have greater fatigue life than the corresponding vulcanizates with carbon black, whereas the reverse is true in constant load tests. These results once again demonstrate the significance of selection of conditions for comparative tests in relation to the use conditions.

2. It follows from these results that loading with channel black, which usually increases the strength characteristics of rubbers (tensile, tearing, and abrasion strengths, etc.), has relatively little effect on the fatigue properties — it decreases the fatigue deformation and raises the fatigue stress somewhat. Hence it may be concluded that the fatigue properties of rubbers are largely determined by the type of rubber. In experiments performed jointly with Z. N. Tarasova we found that the type of the vulcanizing group also has considerably less influence than the nature of the rubber polymer. Curves of the type given in Figs. 1 and 2, obtained for rubbers with different vulcanization accelerators, fall distinctly into separate groups, corresponding to different types of rubber. We also investigated a large number of tire rubbers, which gave the same result.

Therefore, in alternating-load tests at the same temperatures, the fatigue properties are primarily determined by the nature of the rubber. The following sequence (in order of decreasing fatigue life) is found in all cases: vulcanizates based on polybutadiene (SKB), polyisoprene (NR), and butadiene-styrene (SKS-30) rubbers. This result seems unexpected at first sight. The opinion has long been firmly established that NR vulcanizates are considerably superior in fatigue resistance to SKB. This view is supported by the results of laboratory tests and performance characteristics of certain articles, including automobile tires. It is therefore necessary to find why the present tests gave the reverse result. It must first be remembered that laboratory tests are generally performed with the use of repeated stresses of the same sign (either extension or compression), with spontaneous heating of the specimens. Both conditions are more advantageous to natural rubber. With increase of the static component of the load, the fatigue life is increasingly determined by the strength characteristics of the rubber [2], and these are considerably higher for natural rubber. On the other hand, the relatively low internal friction of NR vulcanizates results in more favorable test conditions. To demonstrate this, we carried out comparative tests on NR and SKB vulcanizates with carbon black, in conditions of symmetrical loading and varying asymmetry of the cycle.

The tests were performed with the MRS-2 machine of the "Metallist" factory, on massive specimens with cylindrical working portions; the thickened ends were fixed in special clamps in such a way that the specimens could be tested in conditions either of symmetrical or asymmetrical loading.

The tests were performed at 500 cycles/minute with spontaneous heating of the specimens, at a constant deformation amplitude. Figure 3 shows the variations of the fatigue life of NR and SKB vulcanizates with the degree of asymmetry, determined by the value of the mean deformation of the cycle. The relationships are different for the two rubbers. Whereas the fatigue life of SKB decreases steadily with increase of the static component of the deformation, the fatigue life of vulcanizates based on natural rubber has a minimum when the mean deformation of the cycle is close to zero. This fact has already been reported in the literature [6*]; it is difficult to interpret it conclusively on the basis of the specific properties of natural rubber. It may be said, however, that this type of relationship between the fatigue life and the static component of the deformation can hardly be associated with crystallization, as the latter apparently does not occur at the temperatures and deformations used.

From the differences between the strength characteristics of NR and SKB vulcanizates it might have been expected that increase of the static component of the deformation should lead to a slower decrease of the fatigue life of NR vulcanizates. It is found, however, that fatigue life of the latter even increases, giving rise to a very considerable superiority in the fatigue properties of natural rubber vulcanizates in tests under repeated extension.

The data in Fig. 3 also show that even under conditions of symmetrical alternating load, with spontaneous heating of the specimens, the fatigue life of natural rubber vulcanizates is somewhat higher.

This reveals a second reason for the difference between the generally accepted views on the fatigue properties of rubbers and the result obtained in the present investigation. The data show that comparisons of the fatigue properties of vulcanizates based on polyisoprene (NR) and polybutadiene (SKB) rubbers determined under different test conditions may give directly opposite results. In general, the test conditions should be chosen in relation to the operating conditions of the rubbers in articles for which they are intended. In relation to tire rubbers, including breaker rubbers, it must be pointed out that the apparently better agreement between the service behavior and the results obtained in tests with asymmetric loading cycles does not justify the choice of the latter procedure for laboratory tests. Moreover, existing data indicate that a symmetrical cycle is closer than deformation of constant sign to the operating conditions [3].

* As in original — Publisher's note.

In the choice of a rational method for comparative fatigue tests on tire rubbers it must be remembered that apart from fatigue failure, articles may become unserviceable through a number of other causes. It is probably also significant that, in articles in which the rubber is used under conditions close to a symmetrical cycle, the periodic though irregular action of large asymmetric loads (for example, when a tire rides over an obstacle) is not excluded; this undoubtedly would effect butadiene rubber vulcanizates more adversely.

Without further discussion of this question, we now consider certain other factors which place natural rubber vulcanizates in more favorable conditions in the utilization of a number of articles. In laminated and solid articles the highest temperature develops in the central layers, which are almost completely isolated from access to oxygen. If fatigue failure occurs in these layers, the tests should be performed in an inert atmosphere, for correct laboratory evaluation of the fatigue properties. Further, it is inevitable in the construction of a complex laminated article (such as a tire) that a number of defects arise within it, and these may act as sites of failure. Therefore it is perhaps desirable to test, together with intact specimens, specimens which have previously been damaged.

The influence of these factors on the fatigue life of NR and SKB vulcanizates is illustrated in the Table.

The data in the Table were obtained in alternating bend tests with spontaneous heating of the specimens.

It is seen that the fatigue life of SKB vulcanizates is influenced more strongly by nicking of the specimens. On the other hand, tests in a nitrogen atmosphere on natural rubber vulcanizates give fatigue life values five times as large as those obtained in air, whereas the medium has little influence on the fatigue life of SKB vulcanizates.

Influence of the degree of vulcanization. Rubbers of the following composition were used for studying the effect of the degree of vulcanization: (SKS-30A, heat-softened) 100 wt. parts, sulfur 1.0-12.0 wt. parts; Sulfenamide BT 1.0 wt. part; stearic acid 2.0 wt. parts; zinc oxide 5.0 wt. parts. The following characteristics of the fatigue properties were determined: fatigue strength, fatigue deformation, fatigue energy corresponding to a fatigue life of 10^6 cycles.

For determination of these values, the tests were carried out at two deformation amplitudes, at which the fatigue life was somewhat greater and less than 10^6 cycles. Then, by interpolation in semilogarithmic coordinates (in which the curves become almost linear;

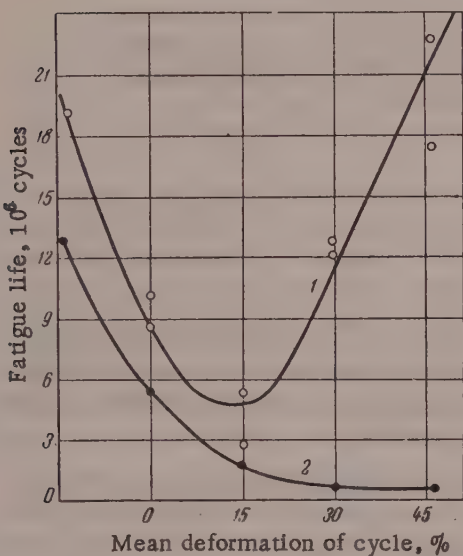
Fig. 3. Variation of fatigue life with the static component of deformation: 1) NR + 40 wt. parts channel black; 2) SKB + 40 wt. parts channel black. Test conditions: deformation amplitude 30%; frequency 500 cycles/minute; $T = 100^\circ$ for 1 and 115° for 2.

see Figs. 1 and 3), the fatigue deformation corresponding to a fatigue life of 10^6 cycles was determined, and then used for calculations of f_{0F} and W_{0F} .

The fatigue characteristics and dynamic properties of the rubbers were determined at 100° .

The effect of total sulfur content on ϵ_{0F} , f_{0F} , and W_{0F} is shown graphically in Fig. 4. The fatigue deformation shows a sharp maximum at 1.8% sulfur content, which corresponds to the amounts used in industrial practice. The fatigue strength increases steadily with the sulfur content, while the fatigue energy increases rapidly up to 3% sulfur and then changes little. Only a few samples, not differing very greatly in their sulfur contents, were used in the studies of the variations of the fatigue characteristics with the fatigue life. The nature of these relationships remained constant within the limits studied.

Influence of loading. The influence of loading on the fatigue properties was studied on SKS-30 vulcanizates containing 0; 2; 5; 10; 15; 20; 30; 40; 60; 80 and 100 wt. parts of filler per 100 wt. parts of rubber.



Channel black was used as the active filler, and lamp black as a less active filler. The stocks had the following composition (in wt. parts): rubber 100, sulfur 2.5, Captax 1.5, stearic acid 2.5, zinc oxide 5.0, carbon black 0-100.

The fatigue and dynamic properties were determined at 100°. The effects of the carbon content on the fatigue characteristics corresponding to a fatigue life of 10^6 cycles are given in Fig. 5. For both series of vulcanizates the fatigue stress increases steadily with the carbon black content. From this and the preceding results the general conclusion can be drawn that, for rubbers subjected to stress at constant amplitude, any increase of hardness owing to vulcanization or filler content has a favorable influence on the fatigue life.

For vulcanizates with channel black the fatigue deformation has a maximum at 15 wt. parts. Because of the scattering of the experimental points for vulcanizates with lamp black, it is not possible to say with certainty whether such a maximum is absent or whether it corresponds to very low carbon contents. In any event, the fatigue deformation decreases with increase of the carbon content over most of the range studied.

Fatigue Life of Vulcanizates with Carbon Black in Alternating Bend Tests

Rubber	Deforma-tion ampli-tude, %	Tempera-ture, °C	Fatigue life, 10^3 cycles		
			in air		in nitrogen
			specimen without nick	specimen with 0.3 mm nick	
NR	26,5	100	780	300	3600
SKB	26,5	115	600	110	780

The fatigue energy of the cycle increases with the carbon black content in vulcanizates with channel black, but changes little with the lamp black content. Investigations of the relationships between the fatigue characteristics and the fatigue life of vulcanizates containing 10, 20 and 40 parts of channel black by weight showed that these relationships were of almost the same character in all cases.

The different effects of loading on the fatigue properties of vulcanizates made from different rubbers must be noted. This was already demonstrated by the data in Figs. 1 and 2. Whereas the fatigue stress of SKS-30 vulcanizates increases with loading, it remains almost unchanged in SKB, and even decreases in NR. Therefore the relationships in Fig. 5 cannot be regarded as illustrating the influence of loading on the fatigue properties of vulcanizates based on every kind of rubber.

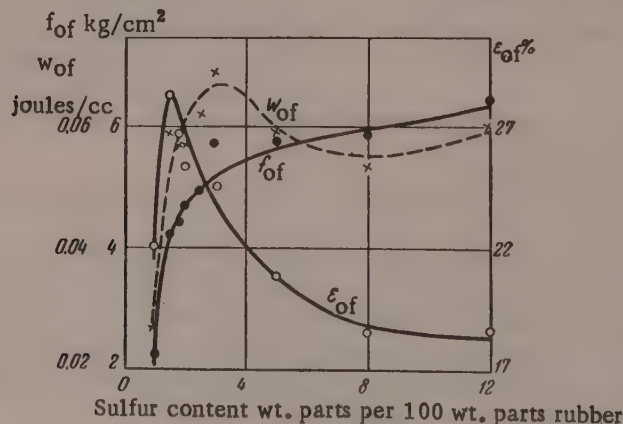


Fig. 4. Fatigue characteristics corresponding to a fatigue life of 10^6 cycles for unfilled SKS-30A vulcanizates with different amounts of sulfur. Test conditions: frequency 3000 cycles /minute; $T = 100^\circ$.

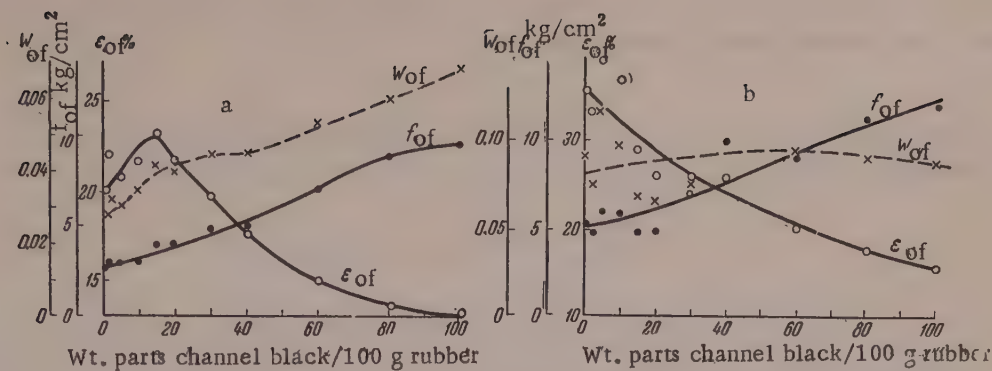


Fig. 5. Fatigue characteristics W_{0f} , joules/cc, corresponding to a fatigue life of 10^6 cycles for vulcanizates with differing contents of channel black (a) and lamp black (b); test conditions: frequency 3000 cycles/minute, $T = 100^\circ$.

Effect of softening. The influence of the degree of softening on fatigue properties was studied on SKS-30A vulcanizates containing different amounts of vaseline oil. The results show that all the fatigue characteristics pass through a maximum corresponding to 20 wt. parts of softener. However, this effect requires further investigation, since the decrease of the fatigue characteristics may have been caused by defects (internal pores) present in many specimens with high softener contents.

This investigation is apparently the first study of the influence of the principal formulation factors on the fatigue properties of vulcanizates, determined under symmetrical alternating load (which eliminates the influence of relaxation effects from the results) at a constant test temperature.

Such results as the superiority of SKB over NR vulcanizates in fatigue properties, and the negative influence of active fillers on the fatigue stress of NR rubber vulcanizates (all these, of course, in the test conditions used) are of undoubtedly interest, and therefore require further study and discussion.

The results obtained in this investigation may serve to illustrate the relationship between the fatigue of rubber and certain other properties, which are simpler and therefore better understood.

SUMMARY

1. The fatigue properties of rubbers under conditions of symmetrical alternating stress have been studied in relation to the principal formulation factors: type of rubber, total sulfur content, amount and type of filler, and softener content.

2. In the test conditions studied, the type of rubber has a significant influence on the fatigue properties, SKB vulcanizates being superior to others (NR and SKS-30) in fatigue resistance.

3. The causes of the loss of the advantages, found in these tests for SKB vulcanizates, under other test conditions and in service are briefly analyzed.

The authors express their gratitude to Prof. B. A. Dogadkin for his interest in the work and for participation in discussion of the results.

LITERATURE CITED

- [1] J. Fillon, in the book: The Fatigue of High Polymers (Russian translation) (Goskhimizdat, 1957) p. 5.
- [2] M. M. Reznikovskii and L. S. Priss, in the book: The Fatigue of High Polymers * (Goskhimizdat, 1957)

p. 119.

*In Russian.

[3] M. M. Reznikovskii, L. S. Priss, M. K. Khromov and E. G. Vostroknutov, Trans. Sci. Res. Inst. Tire Ind. No. 4 (Goskhimizdat, 1957). *

[4] G. Sh. Izraelit, Test Methods for Vulcanizates and Rubber*(Goskhimizdat, 1949).

[5] M. M. Reznikovskii, E. G. Vostroknutov and L. S. Priss, in the book: Aging and Fatigue of Rubbers and Increase of their Stability (Goskhimizdat, 1955) p. 76.

Scientific Research Institute
of the Tire Industry
Moscow

Received February 25, 1958

* In Russian.

THE EFFECT OF THE REGULARITY OF STRUCTURE OF TRIACETYLCELLULOSE
ON ITS SOLUBILITY AND THE PROPERTIES OF ITS SOLUTIONS*

Z. A. Rogovin and D. L. Mirlas

Regularity of the structure of the macromolecules of a polymer is one of the principal factors determining the intensity of intermolecular interaction, and thereby a number of very important properties of the polymer, including the solubility, heat resistance, strength, etc. For example, disturbance of the regular structure of polyamide molecules by synthesis of a copolymer of caprolactam and "AG salt" (adipic acid and hexamethylenediamine) yields a polyamide which, in contrast to polyamides of the same molecular weight but of regular structure (Capron, Anid, Enant), is soluble in ethyl and methyl alcohols containing small amounts (5-10%) of water [1]. Nonpolar polymers of strictly linear structure, without side branches in the macromolecule (stereoregular or isotactic polymers) have much improved properties (polyethylene, polypropylene), with considerably extended fields of application. Disturbance of the structural regularity of polymer macromolecules has a similar effect of increasing the solubility in the case of cellulose derivatives. For example, hydroxyethylcellulose of low degree of substitution, containing the same numbers of the same functional groups in the monomer unit as cellulose, is soluble in dilute NaOH solution and even in water [2]. It is known that cellulose samples of low molecular weight, even with degree of polymerization (DP) 10-20, are insoluble in water. The products of complete acetylation of hydroxyethylcellulose, in contrast to triacetylcellulose, are soluble in acetone [2]. Evidently the anomalous solubility of polymers, including cellulose derivatives, and the formation of strongly structurized solutions which is encountered in industrial conversion of such polymers, can be attributed to variations of the regular structure of the macromolecule (presence or absence of side chains) during synthesis of the polymers or substitution (etherification or esterification) of functional groups in native polymers.

The influence of this factor also probably accounts for the fact, long known to technologists, of the rapid gelation of triacetylcellulose solutions obtained by acetylation of cellulose in a homogeneous medium in presence of HClO_4 catalyst in the acetylation mixture (mixture of acetic anhydride and acetic acid). This process greatly hinders the production of highly stable cellulose triacetates by homogeneous acetylation in a mixture containing acetic acid as solvent. Earlier investigations [3] revealed a number of facts in relation to this interesting effect. It was shown that gelation of triacetylcellulose solutions in the acetylation mixture does not occur in two cases:

1. If the acetic acid in the acetylation mixture is totally or partially replaced by other solvents, such as chlorinated hydrocarbons (dichloroethane, methylene chloride).
2. If relatively large amounts (10-15% on the weight of the cellulose) of sulfuric acid are used as acetylation catalyst in place of perchloric acid. However, the mechanism of this process was not elucidated. The results of our study of this theoretically interesting and practically important question are briefly presented in this paper.

The starting material for acetylation was boiled and bleached cotton cellulose, containing 99.7% α -cellulose. It was activated by treatment with 98% acetic acid (1:1 ratio of cellulose to acetic acid) for 2 hours at 45-50°. The acetylation mixture contained 400% of acetic anhydride and 600% of acetic acid on the weight of the cellulose.

*Communication 70 in the series on the structure and properties of cellulose and its derivatives.

The experiments confirmed that when cellulose is esterified by this acetylation mixture in presence of HClO_4 , H_3PO_4 , or other catalysts which do not react with cellulose under the acetylation conditions used, the acetylcellulose solution congeals either during the esterification process itself or, with triacetylcelluloses of lower molecular weight, a definite time after completion of the esterification. Gelation is most rapid if the acetylation is carried out in presence of HClO_4 . Some experimental results in illustration of this are given in Table 1.

TABLE 1

Acetylation of Cellulose in Acetic Acid in Presence of HClO_4 or H_3PO_4 as Catalyst

Catalyst	% of catalyst on the weight of cellulose	Acetylation temperature, °C	Properties of triacetylcellulose			Gelation time, hours	
			bound acid content, %		specific vis- cosity of 0.25% solution		
			acetic	mineral			
HClO_4	1.5	55	62.5	—	0.28	Immediately after end of acetylation	
HClO_4	10	60	71*	—	0.05		
H_3PO_4	20	75—80	60.9	0.14	0.27	80**	
H_3PO_4	20	80—90	63.2	0.14	0.27	110	

* The high content of bound acetic acid is attributable to the acetolysis which occurs during esterification in presence of large amounts of HClO_4 .

** The probable reason for the slower gelation of triacetylcellulose made in presence of H_3PO_4 is that under such conditions a small amount of phosphoric acid enters the cellulose ester in the form of phosphate esters (1-2 groups per 100 monomer units of the macromolecule).

It must be pointed out that the gelation rate depends, for given process conditions, on the concentration of cellulose in the liquor, i.e., on the liquor ratio. The lower the triacetylcellulose concentration in solution, the less likelihood is there of aggregation of the ester macromolecules, and the slower is the gelation. For example, at 1:10 liquor ratio, when a 16-17% solution of triacetylcellulose is obtained at the end of the acetylation in presence of HClO_4 , gelation of the solution occurs not later than 1-2 hours after the end of acetylation; whereas if the liquor ratio is altered to 1:20 the gelation rate is slowed down considerably, and at 1:35 liquor ratio, when the acetylcellulose concentration in the acetylation mixture is reduced to 5%, gelation of the dope does not occur even after a long time. If cellulose is acetylated in presence of sulfuric acid (10-20% on the weight of the cellulose), gelation of the triacetylcellulose in the acetylation mixture does not occur (see Table 2).

It follows from the data in Table 2 that the composition of the triacetylcellulose gradually changes with increasing keeping-time of the mixture (after formation of the solution) of triacetylcellulose in the acetylation liquor, with saponification of the sulfate groups in the cellulose sulfate-acetates formed in the initial stage of the acetylation, and their gradual replacement by acetyl residues (reesterification). This change in the composition of the cellulose sulfate-acetate, also demonstrated in earlier investigations [4], increases the structural regularity of the triacetylcellulose macromolecules (by increasing the content of one type of functional group in the cellulose ester macromolecules) and thereby alters its solubility.

Triacetylcellulose which does not contain any appreciable amounts of acid radicals other than acetyl, does not dissolve completely at 20° in 98-100% acetic acid (the solubility of triacetylcellulose is still lower in less concentrated acetic acid). This accounts for the rapid gelation of acetylation mixtures containing triacetylcellulose obtained in presence of catalysts which do not react with the OH groups of the cellulose, or in presence of relatively small amounts of catalysts which form the corresponding esters with cellulose.

TABLE 2

Acetylation of Cellulose in Acetic Acid in Presence of H_2SO_4 as Catalyst

% Of catalyst on the weight of cellulose	Time held after formation of solution, hours	Properties of triacetylcellulose			Value of γ for			% Solubility of product	
		% of bound acids		specific viscosity of 0.25% solution	acetyl groups	sulfate groups	OH	in 99.9% acetic acid	in methylene chloride
		H_2SO_4	CH_3COOH						
1*	0.5	0.48	61.3	0.37	291	1.3	8	41.7	—
1	14	0.12	62.0	0.40	296	0.3	4	31.6	—
20	0.5	7.6	53.0	Incompletely soluble	252	22	26	99.0	24.8
20	72	0.62	61.1	0.13	292	1.7	6	80.0	99.3
20	4	6.7	55.7	0.42	272	20	8	99.6	—
20	41	0.2	61.6	0.26	294	0.5	5.5	85.7	—

* With this small amount of catalyst, the triacetylcellulose solution gelates within 1-2 hours in the acetylation mixture. Gelation does not occur with 20% H_2SO_4 .

Therefore the solubility of triacetylcellulose in the acetylation mixture (acetic acid with a small amount of acetic anhydride) decreases during prolonged ripening of the mixture after the end of acetylation, when the reesterification process is completed and the regularity of the macromolecular structure of triacetylcellulose is increased; this may result in gelation of triacetylcellulose solutions obtained in esterification in presence of small amounts of H_2SO_4 .

The solubility of triacetylcellulose in acetic acid can be raised by a considerably decrease of the molecular weight of the cellulose ester, by formation of a mixed ester, such as cellulose sulfate-acetate.

It follows from the data in Table 3 that the presence of over 2% of bound H_2SO_4 (i.e., more than 6 sulfate groups per 100 glucose residues) in a mixed cellulose ester of this type sharply increases the solubility of triacetylcellulose in 99.9% acetic acid.

Table 3 shows that triacetylcellulose of regular structure, free from appreciable amounts of other functional groups, is completely soluble in acetic acid only at DP 40-45. Esters of such low molecular weight are clearly of no practical interest. In products of higher molecular weight, a considerable increase of solubility in acetic acid can be produced, and the risk of gelation of the triacetylcellulose in the acetylation mixture thereby prevented, only by a disturbance of the regularity of molecular structure; as already stated, this can be achieved by the formation of cellulose sulfate-acetates. However, this is not the only possible method for increasing the solubility of triacetylcellulose in acetic acid, and hence retarding or completely preventing gelation of the mixture. If our hypothesis is true that the fundamental method for preventing gelation of triacetylcellulose in the acetylation mixture is by disturbance of the regularity of its structure by way of formation of mixed cellulose esters, then there may be other ways of solving the problem.

1. By formation of cellulose nitrate-acetates by the use of binary catalyst mixtures, such as $HClO_4$ and HNO_3 , in the acetylation process. Nitric acid is not an effective catalyst for the acetylation of cellulose but, like sulfuric acid, it esterifies cellulose. Therefore the use of this catalyst mixture should yield a mixed ester, cellulose nitrate-acetate which, like the sulfate-acetate, contains a small number of other acid residues in addition to acetyl.

TABLE 3

Effect of Degree of Polymerization and Sulfate Group Content in Macromolecules of Cellulose Sulfate-Acetate on its Solubility in Acetic Acid

Specific viscosity of 0.25% sol. in methylene chloride-alcohol mixture (85:15)	DP of ester	Bound H ₂ SO ₄ % on wt. of cellulose ester	Solubility in acetic acid, %
0.05	40	0.29	100
0.25	200	2.88	99.0
0.26	208	0.20	85.7
0.32	256	2.35	99.4
0.37	296	0.48	41.7
0.42	336	6.7	99.6
0.40	320	0.12	31.6
0.64	512	7.0	95.9

If cellulose rather than hydroxyethylcellulose is used, the formation of a fully substituted ester in acetylation under the same conditions takes 3-5 hours. The triacetate formed is completely soluble in acetic acid, methylene chloride, and acetone. These results clearly demonstrate the influence of a disturbance in the regularity of macromolecular structure, and a corresponding decrease in the intensity of intermolecular interaction, both on the solubility of the cellulose ester and on the rate of esterification of the cellulose.

In contrast to triacetylcellulose, partially saponified cellulose acetate with $\gamma = 230-260$ (secondary acetate) is completely soluble in acetic acid. Therefore a solution of secondary cellulose acetate in acetic acid (not only in 99.9% acid, but even in 80-85% solution) is quite stable and does not gelate after prolonged keeping. The partial saponification of triacetylcellulose which occurs in the production of secondary acetate is also essentially a disturbance of the regular structure of the polymer, by the introduction of a small number of other functional groups (hydroxyls) into the triacetylcellulose macromolecule.

If the regularity of the acetylcellulose structure is improved by acetylation of the free OH groups in secondary cellulose acetate, soluble in acetic acid, in presence of HClO₄, it is to be expected that the solution of triacetylcellulose in acetic acid so obtained should gelate rapidly. This was confirmed experimentally. Additional acetylation of secondary acetylcellulose with $\gamma = 240$ dissolved in acetic acid, in presence of various catalysts which do not react with free OH groups (HClO₄, HCl, H₃PO₄), 0.02-1.2% of catalyst on the weight of solution being used, gives a solution of triacetylcellulose in the acetylation mixture, which gelates after some time (0.2-6 days). The solution failed to gelate after additional acetylation only when not less than 1% H₂SO₄ (on the weight of the acetylcellulose) was used as catalyst.

SUMMARY

1. The gelation of solutions of triacetylcellulose in acetylation mixture (acetic acid and acetic anhydride) was studied.
2. The principal factor preventing gelation is decrease of the interaction between the triacetylcellulose macromolecules, achieved by a disturbance of the regularity of macromolecular structure.
3. For prevention of gelation of triacetylcellulose in the acetylation mixture, various methods for reducing the regularity of the macromolecular structure are proposed, involving the formation of mixed cellulose esters containing, in addition to combined acetic acid, small number of other acyl or alkyl groups.

2. By the use of a low-substituted cellulose ether, such as hydroxyethylcellulose, for esterification. Acetylation of this ether, even in presence of HClO₄, gives a mixed cellulose derivative of irregular structure, hydroxyethylcellulose acetate, which should also form stable, nongelating solutions in the acetylation mixture.

These views were confirmed experimentally. If 4-12% HNO₃ and 1.5% HClO₄ (on the weight of the cellulose) are added to the acetylation mixture of the composition given above, the product consists of triacetylcellulose containing 0.25-1% nitrogen, which corresponds to 5-20 nitrate groups per 100 glucose residues in the cellulose nitrate-acetate molecule. Solutions of this cellulose ester do not gelate for 15 days, whereas if HClO₄ (without added HNO₃) alone is used in acetylation under the same conditions, the mixture gelates within 1-2 days after the end of acetylation.

When hydroxyethylcellulose of degree of substitution (γ) 36 is acetylated in presence of HClO₄ catalyst, a syrup is formed within 5-10 minutes, which does not gelate when kept for several weeks.

LITERATURE CITED

- [1] Z. A. Rogovin, Principles of the Chemistry and Technology of Chemical Fiber Production* (State Light Industry Press, 1957).
- [2] Z. A. Rogovin and N. N. Shorygina, Chemistry of Cellulose and Allied Substances* (State Chem. Tech. Press, 1953) p. 486.
- [3] Z. A. Rogovin and M. Ia. Ioffe, J. Gen. Chem. No. 5, 274 (1937); E. Knoevenagel and K. König, Cellulosechemie 3, 113 (1922).
- [4] T. Araki, Text. Research. J. 22, 630 (1952); C. J. Malm and L. J. Tanghe, Ind. Engng. Chem. 45, 995 (1955).

The Vladimir Chemical Works
Central Works Laboratory

Received September 30, 1957

* In Russian.

STRUCTURE STUDIES IN CARBON-BLACK SUSPENSIONS

3. THE EFFECT OF POLYMER ADDITIONS TO CONCENTRATED CARBON BLACK SUSPENSIONS IN A HYDROCARBON MEDIUM

Wu Shu-Ch'iu (U Shu-Tsiu) ** B. Ia. Iampol'skii and S. S. Voiuitskii

It is known that carbon black acts as an active filler in rubber stocks and reinforces the mechanical properties of the rubber. Rebinder and his associates showed that the introduction of relatively small amount of carbon black, corresponding to a small fraction of the volume of the system, results in the formation of a space structure, characterized by structural viscosity and a Bingham yield value. This structure is apparently a spatial network formed by the rubber macromolecules linked by adsorption with the carbon-black particles at the junctions of the network, the carbon particles acting as nuclei for the development of this network [1].

In an earlier investigation, we used suspensions of carbon black in a hydrocarbon medium as models of rubber stocks for studies of structure formation [2]. Dogadkin and others studied structure formation directly in rubber stocks [3-6].

Both in loaded rubber stocks and in model systems — suspensions of carbon black in rubber solutions — the process of structure formation is largely determined by the nature of the interaction between the carbon-black particles and the polymer macromolecules. However, much still remains obscure in this problem. The adsorption of rubber on filler particles has not been studied sufficiently [7-12].

The purpose of the present investigation was to determine how the addition of a small amount of polymer influences structure formation of carbon black in a hydrocarbon medium.*

The mechanical properties of the system were determined in the Shvedov apparatus, with parallel determinations of electrical conductivity [13, 14]. The suspensions were made from lamp black from the Kudinovo works, in pure xylene, containing up to 18% solid phase (by weight).

The added polymers were natural rubber (smoked sheet) of average molecular weight ~200,000, and two samples of polyisobutylene, of molecular weights 70,000 and 200,000. The suspensions were made by the standard method [2], by grinding in a mortar with a pestle for 5 minutes; this gave good reproducibility.

The conductivity of the systems was measured at 1 v with direct current. The suspensions were first left at rest for 30 minutes, to give the additives time to interact with the carbon surface. The conductivity of suspensions in pure xylene and in polyisobutylene solutions became constant in a few minutes. In suspensions containing natural rubber, the conductivity varied at the start of the experiments for 5-8 minutes, and then remained almost constant. The conductivities after 30 minutes were used in our determinations. This time was evidently enough for equilibrium to be established in the systems with additives.

The logarithm of the conductivity (λ) is plotted against the concentration (c) of the carbon-black filler in Fig. 1. The conductivity increases with the carbon-black concentrations, as in the suspensions in petroleum jelly studied earlier [2]. Figure 1 shows that structure formation begins at considerably higher carbon-black concentrations in suspensions containing 1% of natural rubber. In systems with added polyisobutylene, and in pure xylene, structure formation begins at a lower content of the solid phase. The log conductivity-concentration curves for suspensions in pure xylene and in suspensions with added polyisobutylene coincide; therefore polyisobutylene has no appreciable influence on structure formation in carbon black suspended in xylene.

* MGU student A. A. Sokolova took part in the work.

** Transliteration of Russian — Publisher's note.

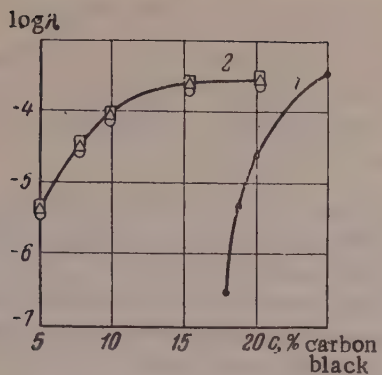


Fig. 1. Variation of conductivity of carbon-black suspensions in xylene with the carbon-black concentration: 1) with addition of 1% natural rubber; 2) with 1% polyisobutylene (molecular weight 70,000 and 200,000) and in pure xylene without additives.

The effect of the amount of polymer added on the conductivity is shown in the graphs in Fig. 2. The carbon-black concentration used was 18%, as this is the minimum concentration required for the formation of a structure which can be detected by conductivity measurements in systems with added natural rubber. It is seen in Fig. 2 that additions of even small amounts of natural rubber sharply lower the conductivity of the suspension, whereas additions of the same amounts of polyisobutylene have no appreciable effect on the conductivity. The explanation for the decrease of conductivity is that the rubber molecules are adsorbed on the carbon-black particles, and therefore the surface of the carbon black becomes more hydrophilic with respect to the medium; introduction of an active additive (natural rubber) increases the solvation of the carbon-black particles, the layers of medium between them become thicker, and the conductivity of the suspension therefore decreases. No adsorption takes place in the case of polyisobutylene, and therefore the conductivity of the suspension does not change on addition of this inactive nonadsorbing polymer.

The mechanical properties were determined in a Shvedov apparatus [13] with two coaxial cylinders. The system to be studied was placed in the annular space between the cylinders. To prevent slippage, rifled cylinders of stainless steel, with sharp vertical grooves 0.75 mm deep and 1.5 mm apart, were used. The inner cylinder was suspended from a tungsten wire fixed to a torsion head. When the torsion head is turned through a definite angle, the concentric layers of the system surrounding the cylinder undergo shearing deformation. The relative shear deformation of the system (ϵ) was found by summation of the deformations in the annular gap [14]

$$\epsilon = \frac{P}{E} = \frac{2\omega}{r^2(1/r^2 - 1/R^2)},$$

where ω is the angle of rotation of the lower end of the wire; r is the radius of the inner cylinder; R is the radius of the outer cylinder.

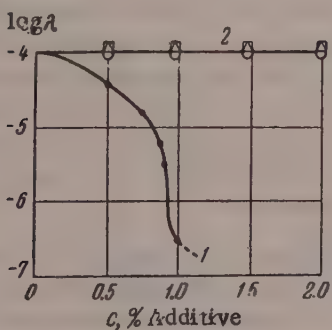


Fig. 2. Variation of conductivity of 18% carbon-black suspension in xylene with concentration of additives: 1) with natural rubber; 2) suspensions with polyisobutylene (molecular weight 70,000 and 200,000) and without additives.

In measurements of the shear stress, the head of the instrument was turned at a constant velocity by means of a Warren motor; this resulted in uniform loading of the system at a low rate, giving more accurate and reproducible results. To prevent evaporation of the dispersion medium, the instrument was placed in a glass box which was saturated inside with xylene vapor. The yield value was first estimated from the sharp displacement of the light spot on the instrument scale and then, more accurately, by a graphical method, from the curves for the deformation rate $d\epsilon/d\tau$ against the shear stress.

It follows from Fig. 3 that the formation and reinforcement of the structure occur at higher carbon-black concentrations in systems with natural rubber than in systems with polyisobutylene or in suspensions without additives. This corresponds to a certain critical value of the volume filling, which depends on the

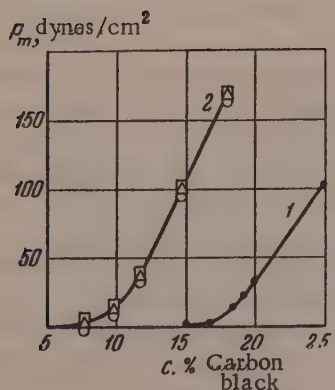


Fig. 3. Variation of yield value of carbon-black suspensions with concentration of carbon black: 1) in 1% solution of natural rubber; 2) in 1% solutions of polyisobutylene (molecular weight 70,000 and 200,000) and in pure xylene.

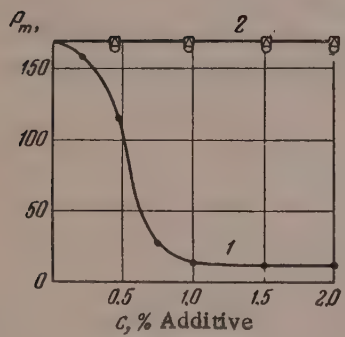


Fig. 4. Variation of yield value of 18% carbon-black suspension with the concentrations of added polymers: 1) with addition of natural rubber; 2) with polyisobutylene (molecular weight 70,000 and 200,000), and in pure xylene.

study. The adsorption of a polymer evidently depends on the structure of the polymer molecule. It is known that the polyisobutylene molecule, unlike that of natural rubber, does not contain double bonds. This may be the reason why polyisobutylene is not an active additive in suspensions of carbon black.

The question may arise whether the results of our experiments are at variance with the fact that carbon black, being an active filler, reinforces rubber mixtures. Kolbanovskaya and Rebiner [14] showed that individual chain molecules of rubber interact at definite points in solution. The number of such interaction increases with increasing polymer concentration, and a continuous network structure of the macromolecules is formed as a result. On addition of a definite critical quantity of active filler to a rubber solution the mechanical characteristics of the system increase sharply owing to formation of a space structure of the rubber macromolecules with the particles of the active filler.

activity of the additive present in the system. It is interesting to note that the curves for systems with polyisobutylene and without additive coincide.

The effects of different concentrations of additives on the value of P_m of suspensions with the same carbon-black content (18%) were then studied. The results are plotted in Fig. 4.

It follows from Fig. 4 that addition of a small amount of polyisobutylene does not change the yield value at any of the concentrations studied. However, the strength of the system falls sharply with increasing amounts of natural rubber added; this is in complete harmony with the conductivity results (Fig. 2). These results show that different polymers have different effects on the structure formation of carbon black in a hydrocarbon medium. This is probably associated with the formation of adsorbed layers on the carbon-black particles, which alter their lyophilicity with respect to the surrounding medium; this is confirmed by determinations of the adsorption of rubber and polyisobutylene on carbon black.

The adsorption was determined gravimetrically. Solutions of natural rubber and polyisobutylene with the following concentrations were carefully prepared: 0.125; 0.25; 0.5 and 1%. (At higher concentrations the suspensions with added carbon black were very difficult to centrifuge because of their high viscosities.) One gram of carbon black was added to each 25 ml lot of solution, the suspensions were thoroughly mixed, placed on the shaker for 30 minutes, and centrifuged for 2 hours at 3000 r.p.m. The solutions were then decanted into weighed bottles, which were weighed again and placed in a vacuum drying oven at room temperature for evaporation of the solvent. After evaporation of the solvent the bottles were kept to constant weight in a vacuum oven at 110°. The adsorption was calculated from the weight loss. The results are given in the Table.

It is clear from these results that polyisobutylene is not adsorbed on carbon black, and it is therefore not an active additive for suspensions of carbon black in xylene. It is still not clear why polyisobutylene is not adsorbed on carbon black; this question requires further

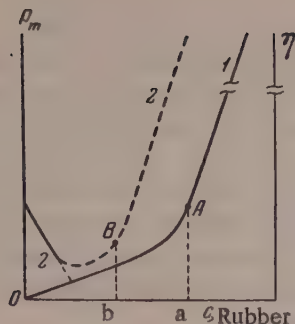


Fig. 5. Variation of mechanical properties of the system with the concentration of polymer adsorbed on the carbon black.

and the polymer concentration can be schematically represented as shown in Fig. 5. In this diagram the rubber concentration is taken along the abscissa axis, and the mechanical properties (the yield value P_M and viscosity η is this instance) are taken along the ordinate axis. Curve 1 (from the previous data [14]) represents the variation of the viscosity of a solution of rubber in xylene with the concentration of rubber. Point A corresponds to the concentration at which a structure is formed in the solution. Curve 2, based on our data, represents the effect of additions of rubber on the strength of the carbon-black structure in 18% suspension of carbon black in xylene. The variation of the strength of the structure in the system rubber solution—carbon black with the concentration can be tentatively represented by the dash region of Curve 2. Before there is any rubber in the system, the carbon-black suspension (if the concentration is adequate) has a definite strength, corresponding to Point B in the diagram. This is the strength of the carbon-black structure itself, formed from the carbon-black particles with thin layers of the medium remaining between them. When small amounts of rubber are added, the strength of the carbon-black structure decreases owing to formation of adsorbed layers on the particles and thickening of the layers of medium as the result of adsorption of the rubber. This decrease of the strength of the carbon-black structure could be continued to zero if the rubber macromolecules did not form their own, "secondary" structure. Subsequently, with increasing concentration of the rubber, its solution becomes more and more structurized and at a definite concentration the mechanical properties increase sharply. Therefore the mechanical strength of the system increases again with increase of the rubber concentration. It is not difficult to see that the sharp increase in the values of the mechanical properties (corresponding to Point B in Fig. 2) of a rubber solution containing carbon black need not necessarily occur just when the concentration of rubber in the solution reaches the level necessary for formation of a structure of rubber molecules in the pure solution (Point A in Curve 1), i.e., the "critical" concentration (b) on Curve 2 should be lower than the "critical" concentration (a) on Curve 1.

Adsorption of Polyisobutylene and Natural Rubber on Carbon Black

Solution concentra- tion, %	Wt. solution, g	Calculated wt. polymer, g	Wt. residue after evapo- ration, g	Wt. solution, g	Calculated wt. rubber, g	Wt. residue after evapo- ration, g	Wt. rubber absorbed in 25 ml solu- tion, g	Adsorp- tion of rubber, % on wt. carbon black
Adsorption of polyisobutylene								
1	7.9802	0.0798	0.0811	8.7112	0.0871	0.0818	0.0152	1.52
0.5	7.4831	0.0374	0.0383	7.2202	0.0361	0.0323	0.0138	1.38
0.25	8.5412	0.02130	0.0220	9.9610	0.0249	0.0225	0.0060	0.60
0.125	7.2104	0.00901	0.0087	10.5605	0.0132	0.0112	0.0047	0.47
Adsorption of natural rubber								

This view is undoubtedly correct. It must be pointed out, however, that the observed formation of a space structure of rubber macromolecules with filler particles [14] occurs in conditions when the rubber solution is itself already structurized (when it is a gel), before addition of the filler. Our experiments, on the other hand, were carried out with low polymer concentrations, when the solution is close to a Newtonian liquid in its properties, i.e., when it is not structurized. It is evident that in this case filler should have a different effect on the mechanical properties of the rubber solution.

If we accept the views [14] concerning the influence of added carbon black on the mechanical properties of rubber solutions, the development of a structure in the system polymer solution—carbon black can be represented as follows:

1. When a polymer (such as rubber) is adsorbed on the surface of carbon-black particles, the relationship between the mechanical properties of the system

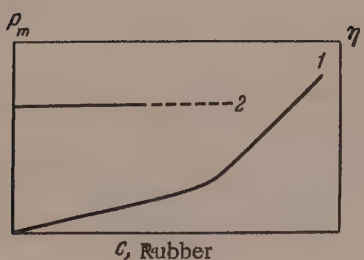


Fig. 6. Variation of the mechanical properties of the system with the concentration of a polymer not adsorbed on carbon black.

black suspensions in solutions of natural rubber (smoked sheet), P_m being determined by the cone-immersion method. The results confirmed that, for a given content of carbon black in the suspensions, the values of P_m pass through a minimum with increase of the rubber concentration.

SUMMARY

1. The influence of added polymers on structure formation in carbon black suspensions in a hydrocarbon medium has been studied.
2. Addition of natural rubber, which is adsorbed on the carbon-black particles, decreases both the conductivity and the strength of the system.
3. Addition of equal amounts of polyisobutylene, which is not adsorbed on the carbon-black particles, has no appreciable effect either on the conductivity or the mechanical strength of the system.

LITERATURE CITED

- [1] P. A. Rebinder, G. A. Ab, and S. Ia. Veiler, Proc. Acad. Sci. USSR 31, 5, 444 (1941); Ia. B. Aron and P. A. Rebinder, Proc. Acad. Sci. USSR 52, 3, 235 (1946); P. A. Rebinder and V. B. Margaritov, Caoutchouc and Rubber 4, 3 (1937).
- [2] U Shu-Tsiu (Wu Shu-Chiu), B. Ia. Iampol'skii and S. S. Voiutskii, Colloid J. 18, 6, 748 (1948).
- [3] B. Dogadkin, K. Pechkovskaia and M. Dashevskii, Colloid J. 10, 256 (1948).
- [4] B. Dogadkin, K. Pechkovskaia and V. Kupriianova, Investigations of the Physics and Chemistry of Rubber* (Goskhimizdat, Moscow, 1950).
- [5] K. A. Pechkovskaia, Ts. Mil'man and B. A. Dogadkin, Colloid J. 14, 250 (1952). **
- [6] A. I. Lukomskaia and B. A. Dogadkin, Colloid J. 15, 259 (1953). **
- [7] A. I. Iurzhenko and I. I. Maleev, Proc. Acad. Sci. USSR 103, 6 (1955). **
- [8] A. I. Iurzhenko and I. I. Maleev, Colloid J. 18, 2, 245 (1956). **
- [9] G. L. Starobinets, Proc. Acad. Sci. USSR 103, 655 (1955). **
- [10] I. M. Kolthoff and Allan Kahn, J. Phys. Chem. 50, 2 (1950).

* In Russian.

** Transliteration of Russian — Publisher's note.

2. If a polymer (such as polyisobutylene) is not adsorbed on the carbon-black particles, the variation of the mechanical properties of the system polymer solution — carbon black with the rubber concentration may be schematically represented by Fig. 6.

Curve 1 in Fig. 6 represents the variation of the viscosity of a solution of an "inactive" polymer with its concentration. Line 2 represents the dependence of the strength of the carbon-black structure on the concentration of the added polymer. This line is parallel to the abscissa axis, as introduction of an inactive polymer into the system does not lead to formation of an independent structure, while the polymer is not adsorbed and cannot form layers around the carbon-black particles, hindering their interaction.

Experiments were recently performed in our laboratory on the determination of the yield value of carbon-

- [11] I. M. Kolthoff and R. G. Gutmacher, *J. Phys. Chem.* 56, 740 (1952).
- [12] M. A. Golub, *J. Polymer Sci.* 11, 583 (1953).
- [13] F. N. Shvedov, *J. de phys.* 8, 341 (1889); 11, 49 (1892).
- [14] A. S. Kolbanovskaya, P. A. Rebinder and O. I. Luk'yanova, *Colloid J.* 12, 3, 208 (1950).

Moscow State University
Chair of Colloid Chemistry

Received July 19, 1957

THE STATES OF AGGREGATION OF HIGH-MOLECULAR COMPOUNDS

2. A STUDY OF THE LINEAR EXPANSION OF GUTTA-PERCHA

R. I. Fel'dman and S. I. Sokolov

A distinctive property of gutta-percha, rather rare in other polymers, is its ability to exist in two modifications (α and β), which can be detected by x-ray and electron diffraction, according to the conditions of preparation. The modifications differ in the spatial arrangement of individual chain segments of the relative arrangement of the chains themselves. However, one of these modifications (β) may not be crystalline in the fullest sense. The α -modification, which has the higher melting point, occurs in plants, in films obtained by slow cooling (0.5° per hour) of melts and in films formed from solutions in ligroine or benzene by slow evaporation of the solvents. The β -modification has been detected in films made from rapidly-cooled melts [1] or from rapidly-evaporated solutions, such as in chloroform [2]. It is believed that at room temperature the β -modification is metastable [1] and the α -modification is stable [3].

Gutta-percha obtained from tropical plants [5] has the same structure as that obtained from Euonymus species in our country, as demonstrated by electron and x-ray diffraction methods [2, 4]. According to electron-diffraction data [2], a film obtained from solution in chloroform contains the orthorhombic β -modification ($a = 7.85 \text{ \AA}$; $b = 11.90 \text{ \AA}$; $c = 4.77 \text{ \AA}$) with a small admixture of the monoclinic α -modification, which gives only one line. Stretched films give typical oriented electron-diffraction patterns. The orientation axis is parallel to the direction of stretch. It has been suggested [6] that stretching of the polymer results in a structural change caused by mechanical "remelting" of the crystals.

Gutta-percha from Euonymus was chosen for our investigations, as it contains less impurities (resins) than gutta-percha from Eucommia. The films were made from solutions prepared at room temperature in chloroform. The solution was separated from the sediment after prolonged settling, and poured onto glass or a mercury surface in a crystallizing dish. The chloroform was evaporated in air at $18-20^\circ$. The films made on glass (gutta-percha G) were transparent and shiny on the side adjacent to the glass, while the films on mercury (gutta-percha M) were opaque. The films on mercury were able to contract freely during evaporation of the solvent, whereas on glass this was not possible and the films became oriented in the horizontal plane; this was revealed by birefringence. Orientation of the palisade type in films $\sim 200 \text{ \AA}$ thick made from Russian gutta-percha on water or aluminum surfaces, similar to that characteristic of monomers [2] and tropical gutta-percha [7], was also detected by electron diffraction. The chains lie with their long axes perpendicular or almost perpendicular to the film surface, with corrugations or coiling in some regions. This type of molecular packing in these films is the most advantageous from the energy aspect, and corresponds to the lowest free energy of the system [2]. Thin films, when the repeat unit is short, are characterized by a few occasional folds which do not have much influence on the general nature of the structure. In gutta-percha films obtained by evaporation of benzene solutions on water, preferential orientation of the c axis of the crystals at right angles to the film plane was observed [4]. Similar results were obtained for polyethylene films made on water surfaces [2]. According to existing data, the turbidity or transparency of the films are associated with formation or disappearance of crystals. Amorphous films of rubber, gutta-percha, balata, and polyethylene are transparent, but in presence of the smallest crystalline formations they become turbid or milk-white [8-11].

It is probable that the films obtained by us on mercury were able to contract freely, and their molecules assumed a configuration with the lowest content of potential energy. The formation of folds with parallel packing of individual chain segments also conforms to this condition. Therefore gutta-percha is in a more stable

state in the form of films made on mercury than in the form of films on glass [12]. Internal stresses were present in the latter, and they could therefore contain two kinds of crystalline regions, characteristic both of unstretched and of stretched β -gutta percha.

Therefore gutta-percha M, gutta-percha G, and additionally stretched gutta-percha are systems of different degrees of stability. The transitions between the different states were investigated by the method of linear dilatometry, which had been applied to other polymers [12, 13] and was described earlier [12]. It was also desired to show, in the case of gutta-percha as an example, that general signs of transitions in high polymer systems exist, manifested in their diffused character, dependence on the kinetics and the previous history of the specimens, and the common occurrence of nonequilibrium states differing in stability.

Gutta-percha M. The results of a series of determinations carried out on a film of gutta-percha M are plotted in Fig. 1 (Curve 1).* Parallel determinations of transparency showed that at 27-33° the edges of the free film become clear, and at 58-62° the film becomes completely transparent. If transparency is regarded as a secondary sign of "complete melting" of the crystals, then 62° must be the temperature at which the transition into the amorphous state is completed. If the film is stressed, the temperature of "complete melting" is lower.

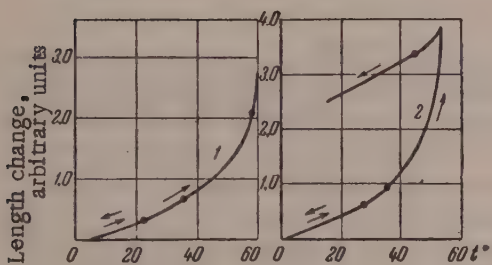


Fig. 1. Effect of temperature on the length of gutta-percha M films: 1) unheated, $P = 10.9 \text{ g/mm}^2$; 2) heated in water at 80°, $P = 13.2 \text{ g/mm}^2$.

be completed. This is probably why the coefficient of linear expansion increases, as it is higher for systems at high than for systems at low temperatures, provided that orientation of the chain molecules in the film plane, which leads to an anomalous course of the length-temperature relationship, is excluded. Analogous results were obtained in experiments on a film of gutta-percha M heated in air to 80°. The length increase after the heating, calculated for 20°, was 0.7%.

Gutta-percha G. The relationship between the temperature and the length of a film of gutta-percha G, plotted in Fig. 2, is of a different form; a possible explanation for the difference is that the specimen was in an oriented unstable state with internal stresses. The total duration of the experiments was seven days. When the film is heated, two competing processes develop as thermal motion in the system increases: contraction and elongation. The contraction is due to the regions oriented lengthwise, and the elongation is due to the unoriented regions. It is probable that at the given degree of orientation in the temperature range 27 to 42° the two processes neutralized each other, and the length of the specimen remained constant while the structure was changing. The disappearance of orientation is indicated by the positive hysteresis observed when the specimens were cooled down from 59°. The next heating-cooling cycle, performed after the specimen had been left at rest for 84 hours, was similar to that described for gutta-percha M. Failure of the specimen (tearing at the clamps) took place at 60°. The coefficient of linear expansion, determined during heating from

*The length-temperature relationships are plotted on an arbitrary scale in all the diagrams. They cannot be used for comparisons of absolute values.

Figure 1 (Curve 2) shows the effect of temperature on the length of a film of gutta-percha M previously heated in water at 80° and rapidly cooled ("quenched") to 15°. Curves 1 and 2 in Fig. 1 are similar in external appearance, but differ somewhat in the transition temperatures and regions, and the coefficients of linear expansion α (in cm/degree · cm) are higher for the quenched film. Under the test conditions described, in the temperature range 5 to 23°, $\alpha_1 = 2.28 \cdot 10^{-5}$ and $\alpha_2 = 3.32 \cdot 10^{-5}$; the value of α determined in cooling of the quenched film down from 46° was $4.41 \cdot 10^{-5}$. It is likely that the packing is more dense in the unheated than in the heated film. Heating of the film to 80° alters the arrangement of the molecular chains and of their individual segments, and completely eliminates the crystalline regions; the system even passes into the viscofluid state. In relatively rapid cooling (quenching), the new packing may be partially retained, as the molecular rearrangement of the system may not

8 to 27°, was between $1.6 \cdot 10^{-5}$ and $1.9 \cdot 10^{-5}$, and the value determined during cooling for 42 to 8° was $2.1 \cdot 10^{-5}$. The length change after the tests, calculated for 25°, was 0.25%.

Gutta-percha M, previously stretched. Films of gutta-percha M were heated in an air thermostat at 80°, cooled rapidly to 13°, and stretched at this temperature to nearly the breaking length on the dynamometer. The films were kept for 48 hours in the stretched condition. They were then stored for 16 days without tension. Although the length almost ceased to alter during this time, the residual elongation was still large. A length-temperature plot determined during heating and cooling of a film with 131% residual elongation is shown in Fig. 3. (Curve 1). The hysteresis in cooling down from 61° was positive. The system after cooling was in a

less stable condition than before cooling. The increase in the length of the specimen during cooling from 61 to 45° is the result of continuing flow, and indicates that the system passed from the viscofluid to the high-elastic state, with a crystalline portion present. The length change on heating and cooling from 59 to 45° was 23%.

According to the available information, the elastic properties of gutta-percha are very slight; if heated to 50° it becomes more extensible, but also plastic. These properties are utilized in the production of articles from gutta-percha. Molding is carried out between 50 and 90° [14].

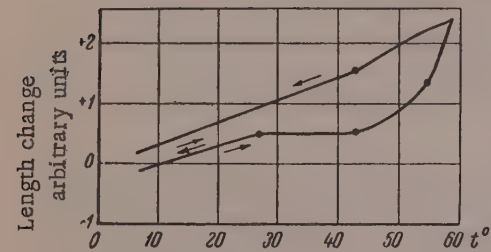


Fig. 2. Effect of temperature on the length of gutta-percha G film, $P = 19 \text{ g/mm}^2$.

Films of previously stretched gutta-percha M differ from films of gutta-percha G by the existence of oriented regions, predominantly parallel to the applied stretching force. Therefore specimens of gutta-percha G remain almost unchanged in length between 27 and 42°, whereas films previously oriented by stretching begin to contract when heated to a certain temperature. When a stretched film is heated to 29-30° the intensity of thermal motion is not yet enough to eliminate the predominant orientation, and the material elongates owing to increase of the distances between the individual regions of the macromolecules. In the temperature range from 2 to 29° the coefficient of linear expansion decreases from $0.8 \cdot 10^{-5}$ to 0. Melting and reorientation continue to 59°; the specimen contracts by 8% between 30 and 59°. The external applied force restrains the reorientation to some extent. Beyond 61° the system becomes plastic and passes into the fluid state. During cooling between 61 and 45° the system returns to the high-elastic state and crystallization begins. The coefficient of linear expansion, determined under the test conditions described during cooling and subsequent heating (after 48 hours) varied from $3.5 \cdot 10^{-5}$ in the range from 45 to 19°, to $3.3 \cdot 10^{-5}$ between 19 and 3°. The length of the specimen, determined at 18°, increased by 18% after the tests. The length-temperature relationship was studied with specimens of different residual elongations. Curve 2 in Fig. 3 represents the results of experiments on a film of gutta-percha M with residual elongation 143%. At this elongation the temperature at which the specimen began to contract fell to 16-18°. The specimen contracted by 9% as the temperature changed from 18 to 56°. The contraction was most rapid starting with 32°. The value of α calculated for the range 49- to 18° was $3.2 \cdot 10^{-5}$. The elongation over the range 56 to 49° was 14%, and after the tests, at 18°, about 3.0%. The temperature at which the stretched specimen begins to contract can be lowered, not only by an increase of the residual elongation, but also by a decrease of the load at which the length determinations are performed. Curve 3 in Fig. 3 represents the results of experiments on a gutta-percha film which had residual elongation of 52% after recovery. The specimen contracted by 21% with increase of temperature from 19 to 63°; on further heating to 64° the specimen stretched by 60% and broke.

An untensioned gutta-percha film, previously stretched to 260% at 12°, begins to contract at 23-24°, and the contraction rate increases from 27°, reaching a maximum at 42°. At 50° the film becomes adhesive. For comparison, transition points for gutta-percha and balata, taken from literature sources, are collected in the Table.

DISCUSSION OF RESULTS

It was concluded in our previous communications [13] that the behavior of crystallizing and noncrystallizing high polymers is similar in many respects. The results presented in this paper provide further illustrations of this. The changes in the linear dimensions of specimens during heating and cooling show that transitions from the

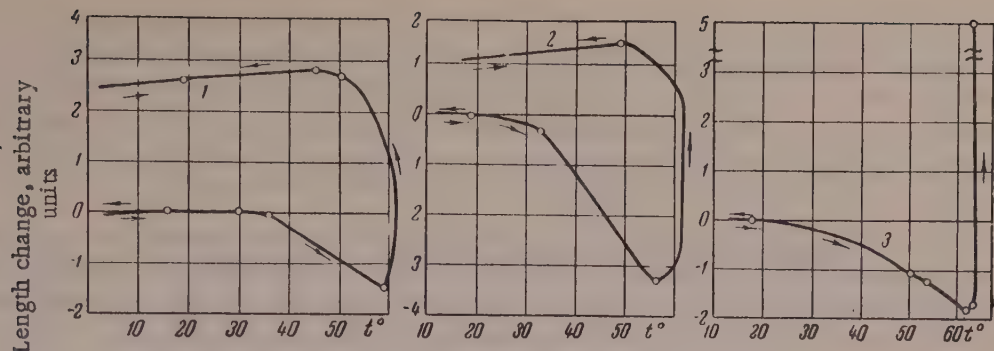


Fig. 3. Effect of temperature on the length of stretched gutta-percha M films: 1) $\epsilon = 131\%$, $P = 32.9 \text{ g/mm}^2$; 2) $\epsilon = 143\%$, $P = 34.1 \text{ g/mm}^2$; 3) $\epsilon = 52\%$, $P = 22.0 \text{ g/mm}^2$.

Transition Temperature Points and Regions

Point, determination method	Temperature, °C	Literature source
Gutta-percha		
T_g , glass transition temperature. Compression	-71	[15]
T_b , brittle point of "paragutta"	-61 to -45	[16]
T_b , brittle point of white gutta-percha	-53.5	[17, 23]
T_b , brittle point of cable gutta-percha	-36 to -23	[16]
T_b , brittle point of Pahang gutta-percha*	-28	[18]
Adhesion strength	16 to 30	[2]
Loss of transparency	below 27	[10]
Melting point of stretched vulcanized gutta-percha	34	[19]
Refractive index		[10]
Stress relaxation	35 to 40	[20]
Disappearance of network structure.	35 to 45	[21]
Ultramicroscopy	45	
Gas permeability		[25]
Disappearance of crystalline interferences.	~50	[14]
X-ray crystallography	50	
Melting point of β -form. Phase diagram		[1, 22]
Melting point under maximum load	56	[19]
Melting point	57	[23, 24]
Melting point of α -form. Phase diagram	60	[1, 22]
Temperature of $\alpha \rightarrow \beta$ transition.	65	[1]
Phase diagram	68	
Transition to mobile liquid	130 to 150	[14]
Balata		
T_b , brittle point of washed and extracted	-67 to -62	[16]
T_b , brittle point of washed	-52 to -44	[16]
T_b , brittle point	-44	[18]
From refractive index	33 to 37	[10]
Commencement of strong turbidity	33	[10]
Start of crystallization	37	[10]
Melting point of β -form	37 to 40	[10]
Softening temperature	60 to 61	[10]
Complete melting. Transparency	above 70°	[10]

* The brittle point rises by 5-10° if the specimen thickness is changed from 1.8 to 1.3 mm [18].

amorphous to the crystalline state, and transitions from one modification to another, do not occur abruptly as in substances of low molecular weight, but gradually over a certain temperature range. The transition points can be displaced along the temperature scale by a great variety of influences, including variations of the heating and cooling rates. As in the examples described previously [12, 13] specimens of gutta-percha may exist in states of varying stability, diverging to various degrees from equilibrium, according to their previous history. Equilibrium states can be reached only in the limit, when ordered packing of the chains with the minimum energy content is possible. In practice, specimens are obtained in states with various deviations from the equilibrium packing of the chains, even if the packing corresponds to the crystalline state.

It is evident from a survey of the literature on gutta-percha that there are no clear ideas concerning the conditions for the transition from one state into another (the α and β modifications, the amorphous state), and, indeed, of the nature of the modifications themselves. The interpretations of the x-ray data are not completely reliable, and they can only be regarded as approximate and probable representations of the chain configuration and packing. Data on the transition temperatures are also very inconsistent and, as the Table shows, illustrate once again the complex behavior of this material during changes of its states of aggregation. The most general conclusion to be drawn from the whole range of facts is that the β -configuration corresponds to the more extended chains. In the α -modification, however, the chain packing is probably closer owing to the greater intermolecular interaction. To obtain the α -modification it is necessary to ensure the appropriate conditions in which relaxation effects can occur more easily and the chains can freely assume the configuration which leads to a minimum energy content. Any influence on the chains favoring their extension favors the formation of the β -modification, and the increased viscosity (due to intermolecular interaction) increases the relaxation time and hinders transition into the α -modification.

Stretching forces may arise in individual regions of the chains not only under the action of external influences, but also during contraction of the specimen during cooling or during rapid removal of the solvent.

The behavior of gutta-percha specimens described in this paper can be interpreted in this light.

SUMMARY

1. Curves have been plotted for the linear expansion of stretched and unstretched gutta-percha films, made on different supports, during heating and cooling.
2. The previous thermal history and previous deformation of the specimens influences the coefficients of linear expansion, hysteresis effects in the establishment of states of varying degrees of stability, and the transition points and regions.
3. The influence of heat treatment on the molecular packing and its relation to the stability of the system is discussed.

LITERATURE CITED

- [1] E. Hauser and G. Susich, Kautschuk 7, 120, 125, 145 (1931).
- [2] B. V. Deriagin and N. A. Krotova, Adhesion*(Izd. AN SSSR, 1949).
- [3] K. H. Meyer, Natural and Synthetic High Polymers, (Interscience, New York, 1942).
- [4] E. E. Rylov and V. L. Karpov, J. Phys. Chem. 27, No. 4, 579 (1953).
- [5] C. W. Bunn, The Chemistry of Large Molecules, Vol 2 (Russian translation) (IL, 1948).
- [6] E. E. Rylov, V. L. Karpov and V. A. Kargin, J. Phys. Chem. 27, No. 4, 572 (1953).
- [7] K. H. Storks, J. Am. Chem. Soc. 60, 1753 (1938).
- [8] L. A. Wood, The Chemistry of Large Molecules Vol. 2 (Russian translation) (IL, 1948) p. 93.
- [9] A. Rossem and J. Lotichius, Rubber Chem. Techn. 2, 378, 1929; Kautschuk 5, 2, 1929.
- [10] A. R. Kemp, Rubber Chem. Techn. 12, No. 1, 475 (1939).
- [11] H. C. Raine, R. B. Richards and H. Ryder, Trans. Faraday Soc. 41, 56 (1945).

*In Russian.

[12] R. I. Fel'dman, *Colloid J.* 20, No. 2, 220 (1958). **

[13] R. I. Fel'dman and S. I. Sokolov, *Chemistry and Physical Chemistry of High-Molecular Compounds** (Izd. AN SSSR, 1952) p. 159; *Summaries of Papers at the IXth Conference on General Questions of the Chemistry and Physics of High-Molecular Compounds** (Izd. AN SSSR, 1957) p. 97.

[14] B. A. Dogadkin, *Chemistry and Physics of Rubber** (Goskhimizdat, 1947).

[15] A. I. Marei, *Chemistry and Physical Chemistry of High-Molecular Compounds** (Izd. AN SSSR, 1952) p. 274.

[16] E. A. Koch, *Kautschuk* 16, 151 (1940); *Rubber Chem. Techn.* 14, 799 (1941).

[17] M. L. Selker, G. G. Winspear and A. R. Kemp, *Ind. Eng. Chem.* 34, 157 (1942); *Rubber Chem. Techn.* 7, 342 (1934).

[18] G. T. Kohman and R. L. Peak, *Ind. Eng. Chem.* 20, 81 (1928).

[19] K. H. Meyer, *Naturwissenschaften* 26, 199 (1938); *Rubber Chem. Techn.* 11, 658 (1938).

[20] S. I. Sokolov and N. A. Krotova, cited in [2]. ***

[21] E. Kirchhof, *Caoutchouc and Rubber* (Russian translation) (IL, 1952) p. 49.

[22] J. N. Dean, *Rubber Chem. Techn.* 6, 76 (1933).

[23] V. L. Simril, *J. Polymer Sci.* 2, No. 2, 142 (1947).

[24] K. Überreiter, *Z. phys. Chem.* B45, 316 (1940).

[25] G. Amerongen, *J. Polymer Sci.* 2, 381 (1947).

The Moscow Technological Institute of the
Light Industry
The Moscow Institute of Chemical Machine
Construction

Received April 15, 1957

* In Russian.

** Original Russian pagination. See C. B. Translation.

*** As in original — Publisher's note.

ELECTRON MICROSCOPE INVESTIGATION OF THE PLASTICIZATION OF A DISPERSION OF VINYL CHLORIDE - VINYLIDENE CHLORIDE COPOLYMER

B. V. Shtarkh and A. P. Pisarenko

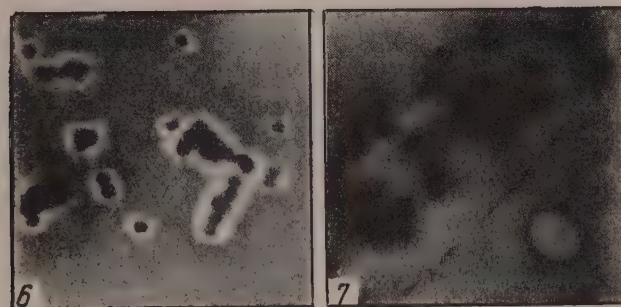
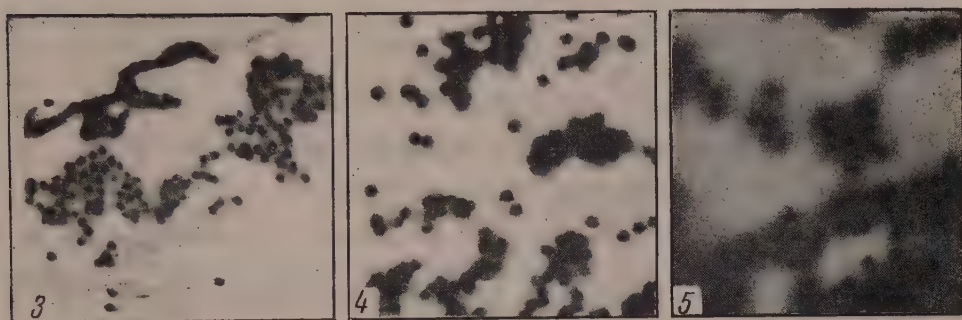
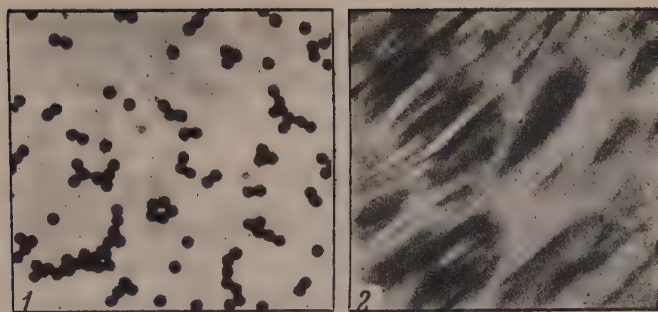
In a number of industries, including the production of artificial leather, a great variety of aqueous polymer dispersions is used. These dispersions are rarely used in their original form. Various substances are generally added to them, according to the purpose for which the dispersion is to be used. Among the components added to dispersions of polymeric plastics are plasticizers, the role of which is particularly important if the polymer present in the dispersion has high hardness, poor autohesion, and therefore poor film-forming power. The use of aqueous dispersions containing rigid polymers such as polyvinyl chloride or Saran is possible in practice only if plasticizers are added [1, 2]. Technological latex mixtures, even if based on such synthetic latexes as SKS-30 or DVKhB-70, intended for fabric impregnation, rubberizing, and coating, also usually contain various amounts of plasticizers.

In our earlier work on determination of the dimensions and shapes of the particles in various latexes and dispersions by means of the electron microscope [3] it was shown that all of them, with the exception of SVKh (vinyl chloride - vinylidene chloride copolymer) dispersion, are polydisperse systems with particles of different shapes.

A classic example of a monodisperse system is provided by SVKh dispersion, which contains copolymer particles of perfect spherical shape, ~ 200 m μ in diameter, with sharp outlines. It is impossible to obtain continuous films from such a dispersion, and it dries on glass in the form of hard scales. We used dibutyl phthalate as plasticizer for SVKh dispersions; 20% of this, calculated on the solid SVKh, was added to the dispersions in the form of a freshly prepared emulsion. The investigations were carried out by the direct preparation method with the EM-3 electron microscope with magnification $\times 7500$.

The control was the original SVKh dispersion, shown in Micrograph 1. Micrograph 2, of the dibutyl phthalate emulsion, shows that the emulsion consists of spreading drops with diffuse outlines. In all probability this is caused by plasticization of the collodion supporting film as the result of drying of the droplets of the plasticizer emulsion on it. Specimens of SVKh dispersion were prepared immediately after addition of the plasticizer and after the plasticized dispersion had been left to stand for 10, 20, 30 and 60 days. In addition, specimens were also prepared from small amounts of dispersions taken from each of these samples and heated for 2 hours at 70° in a thermostat.

Micrograph 3 shows the SVKh dispersion when the specimen was prepared immediately after addition of the plasticizer emulsion. In this case the collodion support is not plasticized, as was the case in specimens prepared directly from the plasticizer emulsion. When dibutyl phthalate emulsion is added to SVKh dispersion, the copolymer particles, owing to their large specific surface, adsorb the plasticizer from the emulsion at a rate which exceeds the plasticization rate of the supporting membrane. It seems likely that the droplets of dibutyl phthalate emulsion are localized near the particles of the SVKh dispersion and thereby assist their aggregation. Despite the fact that the plasticizer was in contact with the copolymer particles for only a short time, the particles lost their individuality. The plasticizer collected in large formations and obscured the outlines of the particles, which began to swell in it. Comparison of micrographs of SVKh dispersions containing the plasticizer and left to stand at room temperature for 10, 20, 30 and 60 days (Micrographs 4, 5, 6 and 7) shows that even after as long as 60 days the elementary copolymer particles retained their original structure. It is also seen that after two months of standing the particle size of the plasticized dispersion increased appreciably (Micrograph 7).



Electron micrographs: 1) Original SVKh dispersion; 2) dibutyl phthalate emulsion; 3) SVKh emulsion immediately after addition of dibutyl phthalate emulsion; 4, 5, 6, and 7) ditto, after 10, 20, 30, and 60 days of standing; 8) ditto, after heating for 2 hours; 9 and 10) ditto, after 30 and 60 days of standing followed by heating for 2 hours.

The joint influence of time and heat treatment on the plasticization of particles in SVKh dispersions by dibutyl phthalate is illustrated in Micrographs 8, 9, and 10; it is seen that heating for 2 hours (Micrograph 8) results in a considerably greater plasticization effect than prolonged standing at room temperature.

Heat treatment is especially effective after plasticized SVKh dispersion has stood for 30 or 60 days (Micrographs 9 and 10). In these cases the globular structure of the dispersion is completely lost, and the field of vision contains dark patches, quite opaque in the electron microscope. This suggests that the coalescence of the copolymer particles was so extensive that a continuous film formed on the collodion support.

SUMMARY

1. An electron microscope investigation was carried out whereby it was possible to observe the changes taking place in an SVKh dispersion containing a plasticizer, after different times of contact between the copolymer particles and plasticizer, and as the result of heat treatment.

2. Prolonged standing or brief heating assists better plasticization of the copolymer particles in SVKh dispersions by the low-molecular plasticizer, dibutyl phthalate.

LITERATURE CITED

- [1] S. S. Voiutskii and K. M. Dziadel', Colloid J. 6, 717 (1940).
- [2] R. E. Dillon, E. B. Brodford and R. D. Andrews, Ind. Engng. Chem. 45, 728 (1953).
- [3] B. V. Shtarkh and A. P. Pisarenko, Light Industry No. 5 (1956).

Central Scientific Research Institute
of the Leather Substitutes Industry
Moscow

Received August 16, 1957

BRIEF COMMUNICATIONS

THE EFFECT OF ELECTRIC CHARGES FORMED DURING REPEATED DEFORMATIONS ON THE FATIGUE RESISTANCE OF VULCANIZATES

B. A. Dogadkin, V. E. Gul', and N. A. Morozova

Electroelastic and triboelastic effects result in the formation of electric charges on articles made from polymers undergoing deformation. It was of interest to determine the effect of the charges formed during deformation on the fatigue resistance of vulcanizates. No convincing experiments clearly demonstrating the role of electric charges arising during friction or deformation had been carried out previously.

Vulcanizates containing different amounts of acetylene black were tested in a machine in which cylindrical specimens with thickened ends were subjected to repeated bending at 1300 cycles/minute.

The stocks had the following composition (in parts by weights): SKS-30A 100, sulfur 2, technical stearin 2, Rubrax 5, black oil 4, Altax 0.6, diphenylguanidine 0.8, zinc white 5, oleic acid 1. Increasing amounts of acetylene black were added to this composition: 6, 12, 18, 20, 22, 30, 40 and 75 wt. parts per 100 wt. parts of rubber.

The experiments showed that specimens containing from 0 to 22 wt. parts of carbon black are nonconducting at 127 v., as a network structure is not formed with these amounts of acetylene black. Vulcanizates containing 30 wt. parts of acetylene black and over are conducting. Specimens of the above composition were tested for fatigue resistance by two methods. In one method, the surface of the vulcanizate specimen was brought in contact with the conducting metal surface of the machine for repeated-deformation tests. In the other method the parts of the specimens placed in the clamps were covered with insulating caps of natural rubber.

The nonconducting specimens, containing up to 22 wt. parts of carbon black, gave the same endurance results by the two methods. The conducting specimens, containing 30 wt. parts of carbon black and over, differed considerably in fatigue endurance according to whether the charges formed could be conducted away. Thus, a specimen containing 30 wt. parts of carbon black failed after 215,000 cycles when tested with insulated ends, whereas when the charges could escape it showed no visible changes after 315,000 cycles. A specimen with 40 wt. parts of carbon black failed after ~23,000 cycles in a test with insulated ends, and after ~48,000 cycles without insulation. A specimen with 75 wt. parts of carbon black failed after 8,000 cycles in the first case, and after ~20,000 cycles in the second.

Thus, the fatigue resistance is more than doubled by the formation of conducting paths of a dispersed filler in the rubber, if the electrical charges produced during repeated deformation are conducted away.

The formation of the charges can hardly be attributed to polarization, as the bound charges formed in the polarization of dielectrics cannot be removed by the method used in these experiments.

The Moscow Institute of
Fine Chemical Technology

Received March 28, 1958

A STUDY OF THE STRENGTH AND HIGH-ELASTIC PROPERTIES OF RUBBER
SOLUTIONS AND THEIR VULCANIZATES AT HIGH
DEFORMATION RATES

A. A. Trapeznikov and T. V. Assonova

Investigations of the strength and high-elastic properties of rubber solutions [1] and of vulcanizates are of interest in relation to studies of the formation and character of the structures in rubber solutions. We carried out such determinations with the aid of an elastoviscosimeter for oscillographic recording of $P(\epsilon)$ curves at high values of $\dot{\epsilon}$ [2], and also an elastorelaxometer [3] designed for direct measurements of elastic deformations in flowing systems at high values of $\dot{\epsilon}$. ($P(\epsilon)$ curves for 6% solution of rubber in decalin are given in Fig. 1).

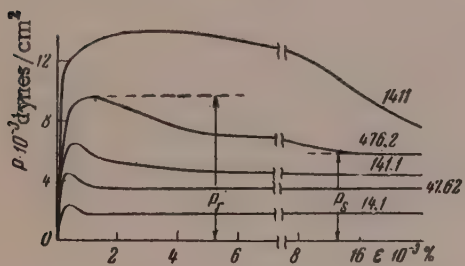


Fig. 1. $P(\epsilon)$ curves for different values of $\dot{\epsilon}$ (numbers on the curves) for 6% solution of rubber in decalin.

It was found that, in agreement with earlier findings [1], the $P(\epsilon)$ curves for solutions of rubber (pale crepe) in decalin at 4, 6, and 10% concentrations, in the range $\dot{\epsilon}$ from 14 to 5000 sec⁻¹, pass through a maximum $P = P_r$, the position of which along the ϵ axis shifts with increasing $\dot{\epsilon}$ in the direction of increasing ϵ_r , reaching 5000% at high values of $\dot{\epsilon}$. The $\epsilon_r(\dot{\epsilon})$ relationship is linear.

Measurements of the elastic deformation by means of the elastorelaxometer for $\dot{\epsilon} = 143$ and 1142 sec⁻¹ at $c = 4\%$ showed that the $\epsilon_e(\epsilon)$ curves also pass through a maximum, but this lies at $\epsilon_m \gg \epsilon_r$. The highest values of ϵ_e are 770 and 1100%.

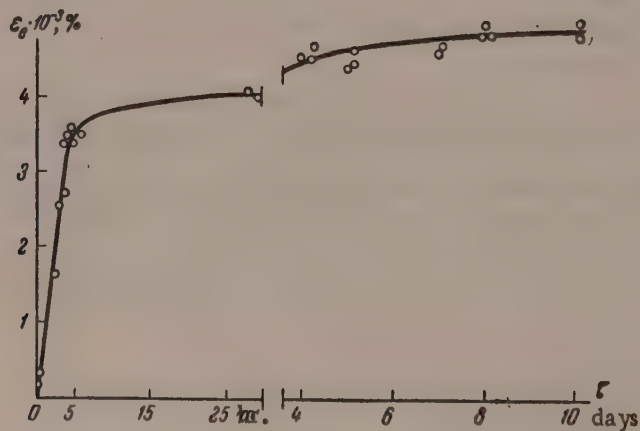


Fig. 2. Time variation of the elastic deformation of 2% solution of rubber in decalin after addition of 10% S_2Cl_2 (fixed $\epsilon = 5400\%$; $\dot{\epsilon} = 286$ sec⁻¹).

Vulcanization of 2% rubber solution with 10% of S_2Cl_2 (on the weight of the rubber) sharply increases the relaxation time of the system. Therefore at $\dot{\epsilon} = 286 \text{ sec}^{-1}$ and total fixed $\epsilon = 5400\%$, the elastic deformation ϵ_e may reach 4000-5000% (1-2 days after the start of vulcanization of the solution (Fig. 2). These results show that the chain regions between the junctions of the network may be deformed to 40 to 50 times their own length.

The discrepancies between the positions of ϵ_r and ϵ_m on the $P(\epsilon)$ and $\epsilon_e(\epsilon)$ curves, and the shift of P_r in the direction of higher ϵ_r with increase of $\dot{\epsilon}$ show that the deformation and strength characteristics of rubber solutions are determined by a range of bonds in the system, characterized by different ϵ_{ki} and θ_i [3]. Therefore with increase of $\dot{\epsilon}$ the strength maximum is transferred to longer bonds, which relax at a higher rate.

LITERATURE CITED

- [1] A. A. Trapeznikov, Proc. Second All-Union Conference on Colloid Chemistry^{*}(Izd. AN SSSR, 1952) p. 175; A. A. Trapeznikov and V. A. Fedotova, Proc. Third All-Union Conference on Colloid Chemistry^{*}(Izd. AN SSSR, 1956) p. 65.
- [2] T. G. Shalopalkina and A. A. Trapeznikov, Proc. Acad. Sci. USSR 118, 994 (1958).^{**}
- [3] A. A. Trapeznikov, Colloid J. 18, 496 (1956);[†] Proc. Acad. Sci. USSR 102, 1177 (1955).

Institute of Physical Chemistry
Academy of Sciences USSR, Moscow

Received March 25, 1958

^{*}In Russian.

^{**}Original Russian pagination. See C. B. Translation.

NEW PROBLEMS OF COLLOID CHEMISTRY

A Plenary Session of the Central Committee of the Communist Party of the Soviet Union was held May 6-7, 1958; as a consequence of N. S. Khrushchev's address, a resolution was adopted "On acceleration of the development of the chemical industry and especially of the production of synthetic materials and articles made from them, in order to satisfy the needs of the population and the demands of the national economy." The resolution provides for a steep rise in the production and processing of polymers. For example, by the end of 1956 the production of artificial and synthetic fibers should be 4.6 times, the production of plastics and synthetic resins 8 times, and of synthetic rubber, 3.4 times the 1957 production.

This increase in the output of synthetic polymer materials can be possible only if scientific research work is developed correspondingly. Soviet research workers are confronted with the serious, honorable, and responsible task of developing the branches of chemical knowledge on which the production of polymer materials depends. This primarily applies to specialists in the field of colloid chemistry. High polymers are colloidal in nature; many technological processes in their production and processing are based primarily on the phenomena and laws of colloid chemistry and physics.

The first process to attract attention from this aspect is emulsion polymerization — the main process used in the production of synthetic rubbers and a number of plastics and coatings. Therefore the whole range of physicochemical problems associated with the stability of aqueous dispersions, searches for new emulsifiers and stabilizers, their effects on the polymerization kinetics and properties of polymers, etc., should form the focus of attention in colloidochemical research. Equally worthy of attention are technological processes for the production of articles directly from aqueous dispersions of polymers (the production of foam rubbers and foam plastics, and of microporous ebonite from natural and synthetic latex), anticorrosion coatings, and coloration of synthetic resins in aqueous suspensions. These processes have been developed very extensively abroad; a considerable expansion of research is needed for their acceleration and for the development of principles of continuous mechanized production.

Most materials and articles made from polymers are produced in conjunction with other materials, usually in a state of high dispersion (fillers, dyes, fibrous substances, etc.). Rubber stocks, plastics, reinforced plastics, etc., are multiphase and multicomponent systems, the properties of which depend on colloidochemical phenomena characteristic of interphase boundaries. Therefore the rational development of technological processes for the conversion of polymer materials requires the competent participation of colloid chemists and colloid physicists, who are confronted with numerous research problems relating to polymer systems.

Another specific characteristic of polymers is that their mechanical properties, and therefore their behavior in use, greatly depend on the chemical processes which take place during their production and utilization; in turn, mechanical influences may induce or activate chemical changes in polymers. This situation has led to the development of the new field of mechanochemistry, the successful growth of which may have a favorable influence on polymer technology and on improvements in the properties of polymers. Determination of the laws which relate the physical and mechanical properties of polymer materials to the conditions of their processing is an important scientific task in physicochemical mechanics; wide circles of Soviet scientists, specialists in colloid chemistry, must take part in the fulfillment of this task.

Research into a number of problems of the chemistry and physics of adhesives, the adhesion process, and film formation, is of great practical significance. The role of colloidochemical phenomena is predominant in these processes. The fruitful researches of Soviet scientists in this field must be subordinated to the tasks posed by the resolution of the May Plenary Session.

We have named only a part of the scientific colloidochemical problems which must be intensively studied

in order to develop the production of synthetic materials. The Plenary Session of the Central Committee of the CPSU calls upon scientists to mobilize their efforts "in order to increase the output of chemical products, to develop new progressive technological processes and highly productive types of equipment, to solve important technological problems, and to seek the most effective methods and means for the production of new chemical materials. The accelerated development of the chemical industry must be the aim of the whole nation."

The Editorial Board of "Colloid Journal" is firmly confident that Soviet specialists in the field of colloid chemistry will take the most active part in measures for the realization of the resolution of the Central Committee of the Communist Party of the Soviet Union.

THERMAL DEGRADATION OF POLYMETHYL METHACRYLATE

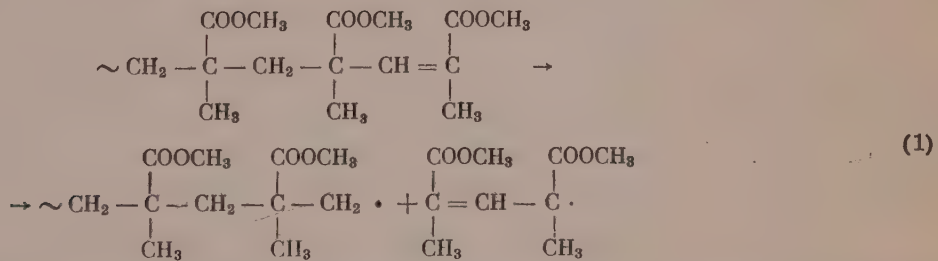
S. E. Bresler, A. T. Os'minskaia, A. G. Popov, E. M. Saminskii
and S. Ia. Frenkel'

In recent years there have been a number of investigations of the thermal degradation of polymers in connection with the preparation of high-temperature macromolecular compounds. After the work of Votinov, Kobeko, and Marei [1], the degradation of methyl methacrylate polymer (PMMA) in vacuum was studied in great detail by Melville and his co-workers [2], and by Madorsky [3], who showed that the thermal degradation of PMMA proceeds smoothly down to the monomer. Melville, Grassie et al., used PMMA of relatively low molecular weight ($M < 200,000$); they found that:

- a) at about 200° the degradation of about 50% of the polymer proceeds smoothly and at a constant relative rate. The remaining half is considerably more stable, and must be heated to about 300° ;
- b) the molecular weight (number-average) remains constant during degradation;
- c) the activation energy of degradation of half the PMMA is 32 kcal./mole of monomer.

These results show that thermal degradation under vacuum is a chain reaction in which monomer units are detached from macromolecular radicals, i.e., it is the reversal of the radical-polymerization reaction. The primary activation of the macromolecule occurs at the end, and the whole macromolecule is broken down completely, i. e., the kinetic chain is equal to the material chain; hence the molecular weight and the degradation rate per unit weight of the material being depolymerized remain constant.

In the polymerization of methyl methacrylate, chain termination usually occurs by disproportionation [4], and therefore half the macromolecules have a double bond at one of their ends. It is natural to assume that the primary activation consists of the removal of an allyl radical from the end of the chain.



This process requires the expenditure of much less energy than the rupture of an ordinary C-C bond, as conjugation energy, which may reach 23 kcal./mole, is liberated in the removal of the relatively stable allyl radical [5]. In order to prove that a double bond is needed for end initiation, Melville and his co-workers used different methods of polymerization (photochemical activation, polymerization with chain transfer) whereby it was possible to regulate the number of molecules with terminal double bonds. It was found that only the macromolecules containing double bonds are degraded at $200-250^\circ$. Finally, Brockhaus and Jenckel [6] confirmed this by direct chemical experiment — by permanganate determination of the number of double bonds in the polymer in parallel with determinations of the degradation rate.

This is not the only reaction in the degradation of PMMA. The other half of the PMMA, without terminal

double bonds, is degraded only at temperatures of 280° and over. Similar behavior is shown by a polymer with the chain ends blocked (for example, by diphenylcyanomethyl [2] or OH [7] groups). The activation energy in the degradation of such a polymer is 47 kcal./mole [2]. The kinetics of the degradation of high-molecular PMMA ($M = 6 \cdot 10^6$) [8] differs considerably from that studied by Melville. The degradation proceeds with difficulty, requires temperatures of the order of 300° and over, and its activation energy, according to Madorsky [8] is 55 kcal./mole. According to Hart [9], the process is accompanied by a sharp decrease in the molecular weight of the polymer, i.e., internal chain rupture takes place.

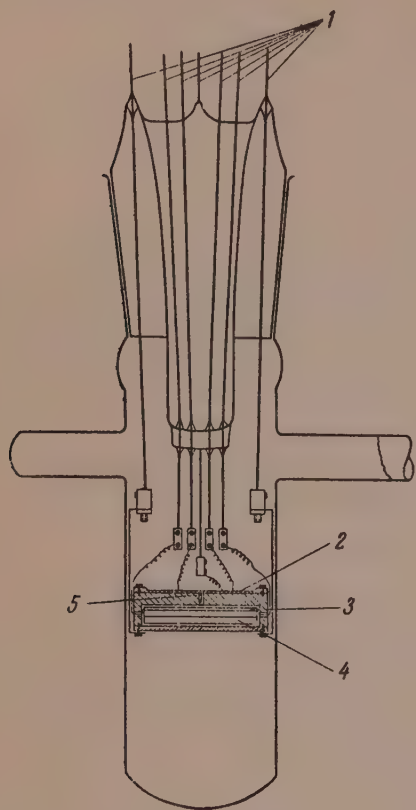


Fig. 1. Vacuum reaction vessel.

- 1) Molybdenum leads; 2) cup with polymer; 3) resistance thermometer;
- 4) heater; 5) thermocouple.

and its area was compared with the decrease in the weight of the polymer at the end of the experiment. The independent calibrations usually did not differ from each other and from the calibration against the monomer by more than 3%. This seemed to us a better method than the use of the McBain balance [3, 8], as it is possible to use thin layers of polymer, with elimination of diffusion effects and better temperature control.

In addition to the degradation kinetics, changes in the molecular weight of the polymer, and also the molecular-weight distribution in some cases, were studied. The determinations were carried out in ethyl acetate solutions by means of the ultracentrifuge at 40,000 r.p.m.; the calculation methods developed in our laboratory [10] were used. In the case of ethyl acetate, the molecular weight is calculated from the sedimentation constant S_0 by means of the formula $S_0 = -0.06 \pm 0.026\sqrt{M}$ (S_0 in Svedberg units).

Two types of polymer were studied; high-molecular PMMA ($M_0 = 3,700,000$) obtained by block polymerization with benzoyl peroxide at 50° (polymerization time about 7 days), and low-molecular PMMA ($M_0 = 250,000$).

RESULTS AND DISCUSSION

In the kinetic graphs in Fig. 2 the degradation rate (rate of evaporation of the monomer) is plotted as a function of the percentage degradation of the polymer at temperatures up to 300°. It is seen that degradation stops at

The present investigation consisted of a detailed study of the degradation kinetics of high-molecular PMMA ($M = 4 \cdot 10^6$) which is now used in technology. In addition, the influence of oxygen, monomer, and various admixtures on the degradation was studied, in order to link the simplest model experiments in vacuum with the degradation of the polymer in practice; possible methods of inhibiting degradation were studied.

The apparatus used for the kinetic studies of the degradation of polymethyl methacrylate was the same in principle as that used by Melville and Grassie [2]. The vacuum vessel (Fig. 1) contained a suspended shallow brass or nickel cup 2, the temperature of which could be kept constant by means of the heater 4 and the resistance thermometer 3. The temperature of the cup was measured by means of the thermocouple 5. A thin layer of polymer in the form of dust (30-50 mg in all) was put on the surface of the cup. The thickness of the layer ($2-3 \text{ mg/cm}^2$) was such that diffusion of the monomer through the polymer did not interfere with the kinetics of the process. The course of degradation was studied by means of a Pirani manometer, which was used to measure the pressure of monomer vapor in the vessel. The liberated monomer was collected in a trap cooled in liquid nitrogen. The resistance of the tubes between the reaction vessel and the trap was such as to give a vapor pressure of the order of $10^{-2} - 10^{-4}$ mm in the vessel. The Pirani manometer was calibrated against a stream of monomer, and the readings were recorded by means of a recording potentiometer. In addition, an independent calibration was carried out in each experiment. The kinetic curve was integrated,

36% in the case of the low-molecular, and at 5-10% in the case of the high-molecular PMMA. This is undoubtedly degradation at the chain ends, or the first mechanism considered by Melville. The probable reason why 50% degradation, which is to be expected from the data of Melville et al. [2], was not reached is that for our relatively long macromolecules the kinetic chain is shorter than the material chain.

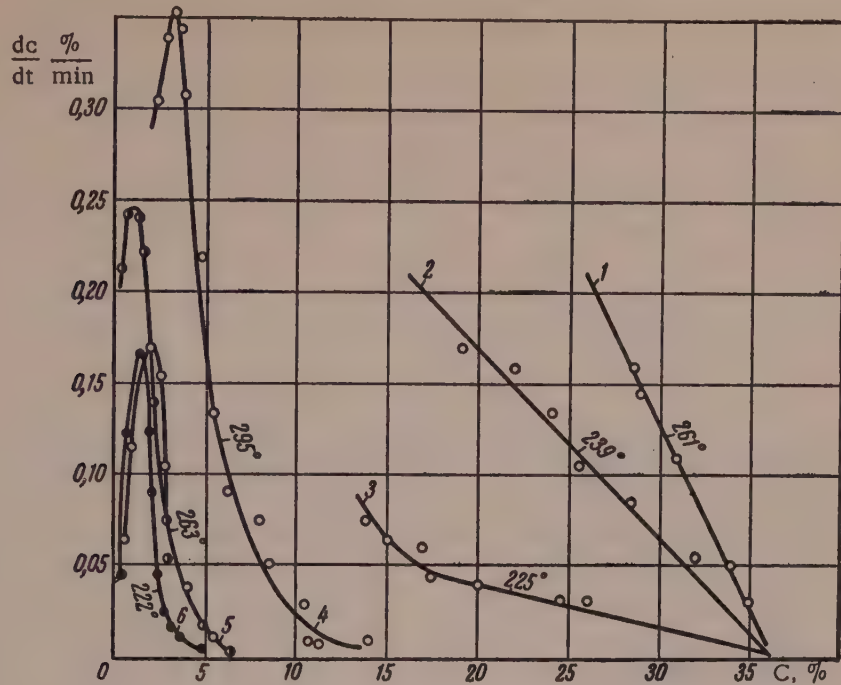


Fig. 2. Degradation rate of PMMA in vacuum, calculated on the original weight of the polymer, as a function of the percentage degradation at temperatures below 300°;
1, 2, 3) low-molecular PMMA; 4, 5, 6) high-molecular PMMA.

Let us consider the process of chain depolymerization in greater detail. Initiation occurs at the end of the macromolecule containing a double bond. This is a monomolecular process which conforms to the equation

$$dn / dt = - k_1 n, \quad (2)$$

where k_1 is the initiation rate constant; n is the number of molecules which are capable of activation (in this case, with double bonds at the ends).

The rate calculated on the original weight of the polymer is

$$\frac{dc}{dt} = - a \frac{dn}{dt}, \quad (3)$$

where a is the amount of monomer evaporating as the result of each act of initiation.

Elimination of time from Equations (2) and (3) gives

$$n = \frac{an_0 - c}{a}, \quad (4)$$

where c is the amount of evaporated monomer relative to the initial weight of the polymer (degree of degradation).

Substitution of (4) into (3) gives

$$dc / dt = - k_1 (an_0 - c). \quad (5)$$

This accounts for the linear course of Curves 1, 2 and 3 (Fig. 2). When all the molecules with double bonds have been consumed, i.e., when the degree of degradation reaches the value $c = an_0$, degradation ceases ($dc / dt = 0$). However, this occurs only at constant chain length, i.e., when the material and kinetic chains are equal. In the

case of the high-molecular sample, macroradicals are formed during initiation of degradation, and a chain reaction develops. The rate of the over-all process per unit weight of polymer at time t is

$$\frac{dv}{dt} = k_2 v, \quad (6)$$

where v is the macroradical concentration; k_2 is the rate constant of chain growth. However, the macroradicals are continuously lost as the result of disproportionation (as was shown by Bamford and Jenkins [4]; recombination of PMMA macroradicals is improbable). The concentration is determined by the quasi-equilibrium condition

$$k_3 v^2 = k_1 n, \quad (7)$$

where k_3 is the termination (disproportionation) rate constant. Hence

$$v = \sqrt{k_1 n / k_3}$$

and

$$\frac{dv}{dt} = k_2 \sqrt{\frac{k_1}{k_3}} n. \quad (8)$$

The activation energy of the over-all process is given by the expression

$$u = \frac{u_1 - u_3}{2} + u_2. \quad (9)$$

The activation energy of the termination reaction u_3 is known from Melville's experiments [11]; its value is 1-2 kcal./mole. The activation energy of chain propagation u_2 was measured in the same investigation and

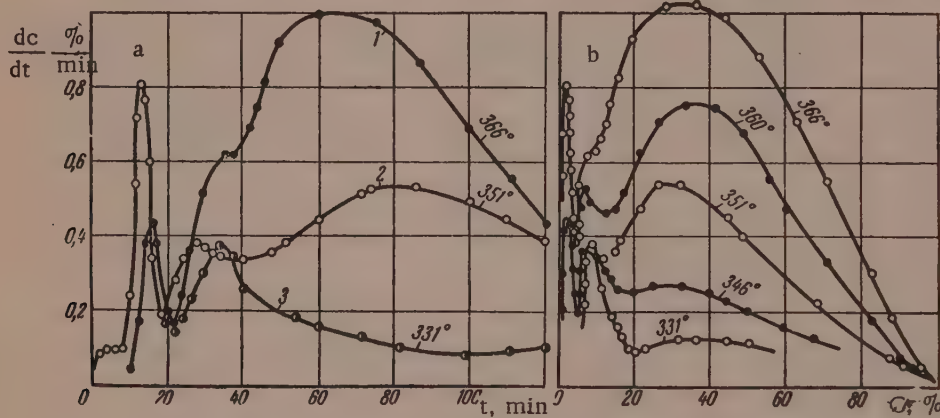


Fig. 3. Variations of the degradation rate of high-molecular PMMA in vacuum, calculated on the original weight of the polymer, with time (a) and degree of degradation (b) at temperatures above 300°.

also by Hajime Miyama [12]; its value for the polymerization of methyl methacrylate is 6.5 kcal./mole. It is clear that in the reverse reaction of depolymerization, the activation energy of chain growth must have the same value plus the heat of reaction (13 kcal./mole). Hence $u_2 = 20$ kcal./mole. Therefore the energy of initiation is

$$u_1 = 2(u - u_1) + u_3 = 2(u - 20) + 2 = 2(u - 19) \text{ kcal/mole.} \quad (10)$$

The macromolecules with double bonds are completely depolymerized, or in other words exactly 50% of the polymer is degraded by the first mechanism, only if disproportionation has no time to take place (with short material chains). If the material chain is long, each act of disproportionation results in the formation of one active chain end from two; i.e., the number of ends capable of activation gradually diminishes and the process dies down rapidly without producing much effect; this accounts for the fact that only 36% of low-molecular and 5-10% of high-molecular PMMA is degraded by the first mechanism (Fig. 2). The activation energy of chain depolymerization calculated from our data is 28 kcal./mole, which is 4 kcal./mole less than the values given by Melville [2]. This is evidently because of the higher molecular weight of our samples, and the correspondingly more prominent role of the termination reaction.

We now consider the second mechanism of PMMA degradation. Data for high-molecular PMMA at temperatures above 300° are plotted in Fig. 3, a and b. The variation of the molecular weight of the same sample with the degree of degradation is plotted in Fig. 4; the given degrees of degradation were reached at 280 and 400° respectively, in correspondingly different times.

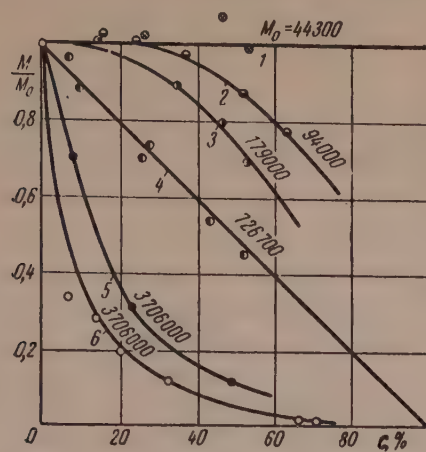


Fig. 4. Relative variations of the molecular weight of PMMA with the degree of degradation (in vacuum):
1, 2, 3, 4) from the data of Grassie and Melville [2]; 5) degradation of PMMA at 280°; 6) ditto, at 400°.

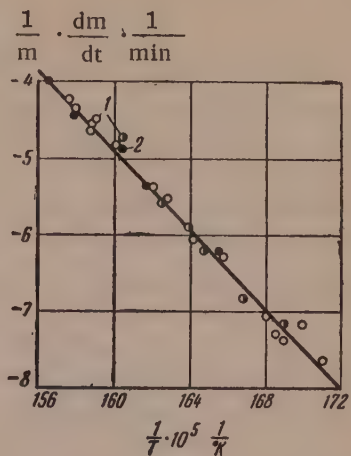


Fig. 5. Graph for calculation of the activation energy of degradation of high-molecular PMMA in vacuum at temperatures above 300°. Points found by the method of least squares:
1) by the step method; 2) from the maximum rates (Fig. 8).

The degradation rate increases for 1-1.5 hours to a maximum, when it reaches 15-30 times its initial value (Fig. 3, a), if the first maximum on the kinetic curves, resulting from rapid chain depolymerization to a maximum degree of degradation of only 5-10%, is ignored. This maximum is reached on all the curves approximately at the point at which about 25-30% of the polymer has been degraded by the second mechanism under consideration (Fig. 3, b). The degradation rate then decreases smoothly. Near the point of total depolymerization (100% breakdown) the kinetic curves become linear and all cross the abscissa axis at 100% degradation. This characteristic picture can be correlated with the course of the molecular-weight variation. It may be asserted that chain depolymerization down to the monomer by the second mechanism, namely, at higher temperatures, also commences at the ends of the molecules, although without unsaturated bonds. The slow development and acceleration of the process in the high-molecular polymer as its internal bonds are broken (Fig. 3, a) i.e., as chain ends accumulate, is sufficient to show that the hypothesis of initiation at the chain ends is highly probable. If the reaction is frozen at a particular instant, and then brought back to the same temperature, the kinetic curve always continues from the point at which the process was halted.

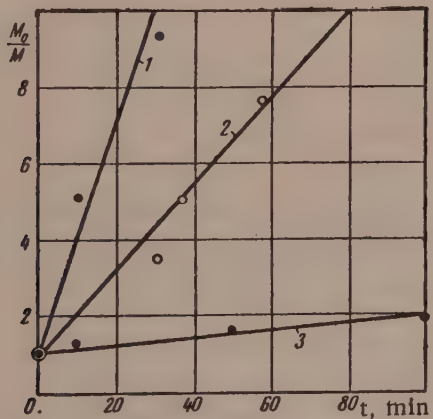


Fig. 6. Variation of the reciprocal relative molecular weight with time:
1) $M_0 = 5,030,000$ at 320° [9];
2) $M_0 = 3,700,000$ at 400°;
3) $M_0 = 146,000$ at 150° [9].

Further, low-molecular PMMA is degraded more rapidly than the high-molecular polymer at high temperatures. The difference in the rate approximately corresponds to the difference of molecular weights at the given degree of degradation.

It was of interest to determine the activation energy of the high-temperature degradation. Because of the complex nature of the over-all kinetics, the following procedure was used. In our apparatus the temperature be-

comes equalized in 4-5 minutes. At the end of this period a constant degradation rate became established. If we waited tens of minutes or several hours, the rate would vary according to the curves already discussed. However, we did not wait for these changes but raised the temperature again; this gave a new step in the increase of the rate, etc. The ordinary $\ln(dv/dt) = f(1/T)$ graph of the Arrhenius type is plotted in Fig. 5. The calculated activation energy $u = (53 \pm 2)$ kcal./mole is in good agreement with Madorsky's results [8]. It is clear that this method cannot be very accurate, since we are dealing with an over-all process with complex kinetics. However, the value obtained is very interesting and can be analyzed to some extent. Substitution of this value in Equation (10) gives $u_1 = 68$ kcal./mole, which is close to the energy of rupture of the C-C bond. A similar conclusion was reached by Simha [13] in his analysis of the degradation of polystyrene — a process with very short kinetic chains (kinetic chain length 4-5). This is highly important in relation to possible inhibition of polymer degradation. It is clear that spontaneous rupture of C-C bonds cannot be prevented by any means. It is only possible to attempt to interfere with the growth of the chain reaction which follows the rupture of the C-C bond.

Analysis of the reaction kinetics. For quantitative analysis of the kinetics of high-temperature degradation, we introduce certain simplifications into the kinetic equations. In the consideration of the change of molecular weight, it is sufficient as a first approximation to consider only the rupture of internal bonds in the chains, chain degradation down to the monomer being ignored. Fig. 5 shows that at 50% degradation the molecular weight is decreased 20-fold. Therefore chain depolymerization is by no means the main and basic cause of the decrease of molecular weight. Let us consider a macromolecule of the original polymer with molecular weight M_0 . The number of molecules in 1 g of polymer is $1/M$ (M is the average molecular weight at time t). Each time a C-C bond is broken, a new molecule appears. The number of broken bonds is

$$l = 1/M - 1/M_0.$$

Since $1/M_0 \ll 1/M$ (in our case $1/M = 0.05/M$),

$$l = 1/M. \quad (11)$$

The number of unbroken bonds is $1/M - l \approx 1/M$, as $l = 1/M \ll 1/\mu$, where μ is the molecular weight of the monomer. The number of broken bonds is given by the kinetic equation

$$\frac{dl}{dt} = k_0 \frac{1}{\mu}, \quad (12)$$

the solution of which is

$$l = \frac{k_0}{\mu} t + \frac{1}{M_0}$$

or

$$\frac{M}{M_0} = 1 + \frac{k_0}{\mu} t. \quad (13)$$

Fig. 6 shows that this theoretical conclusion is confirmed experimentally, i.e., M/M_0 is a linear function of time. The second theoretical conclusion relates to the nature of the molecular-weight distribution. It is known from the work of Kuhn and from many subsequent investigations that random breakdown of bonds in the chain should result in a Poisson distribution

$$q_w(M) = \frac{dw}{dM} = \beta^2 M e^{-\beta M}, \quad (14)$$

where $q_w(M)$ is the weight distribution function; dw is the relative weight of the macromolecules in the range from M to $M + dM$; β is a distribution parameter, equal, for a function of the form of (14), to the reciprocal number-average molecular weight. Fig. 7 shows that the initial distribution is very far from this. As degradation proceeds, the distribution becomes very close to that expected. Therefore the concept of random rupture of internal bonds in the chain is confirmed by experimental data.

Kinetic equations for monomer yield. Consider the expression for the degradation rate per 1 g of polymer. Since in high-temperature degradation initiation also occurs at the chain ends, although the ends no longer contain double bonds (i.e., every molecule can be activated), it follows that $n = 1/M$ or $n = l$, and in accordance with Equations (11) and (12) the expression becomes

$$\frac{dn}{dt} = \frac{k_0}{\mu}. \quad (12a)$$

Eliminating time from Equations (8) and (12a), we find

$$\frac{dv}{dn} = \frac{k_0 k_3}{\mu} \sqrt{\frac{k_1}{k_3}} n^{3/2}. \quad (15)$$

If instead of the degradation rate per 1 g of polymer we use the rate determined by direct experiment, relative to the initial weight of the polymer, we have

$$\frac{dc}{dn} = (1 - c) \frac{dv}{dn} = K (1 - c) n^{3/2} \quad (16)$$

or

$$\ln(1 - c) = -\frac{2}{3} K (n^{3/2} - n_0^{3/2}). \quad (17)$$

Since $n_0 \ll n$,

$$(1 - c) = e^{-\frac{2}{3} K n^{3/2}}.$$

We then have the following expression for the degradation rate:

$$\frac{dc}{dn} = K e^{-\frac{2}{3} K n^{3/2}} n^{3/2}, \quad (16a)$$

i.e., a curve with a maximum.

Differentiation readily shows that at the point of the maximum rate $n^{3/2} = 1/2K$, and the degree of degradation is

$$c_{\max} = 1 - \frac{1}{e^{1/2}} = 0.285. \quad (18)$$

This position of the maximum along the c axis is independent of the kinetic constants, i.e., of the temperature. Therefore the maxima on the kinetic curves should always be found in the same value of $c = 0.285$. The

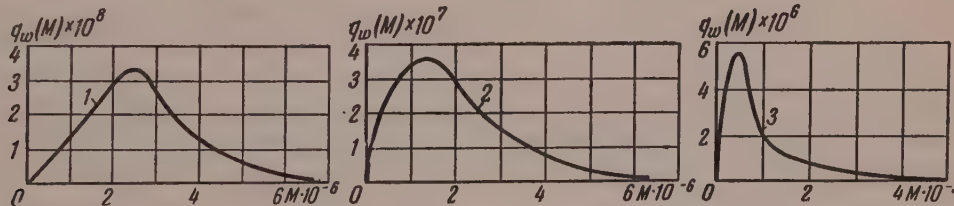


Fig. 7. Variation of the molecular-weight distribution of high-molecular PMMA as degradation proceeds:

1) original sample; 2) 24.4% degradation; 3) 65.4% degradation.

difference between the theroretically predicted and experimental values (Fig. 3, b) is not significant if the value of the degradation by the first mechanism, which is 5-10% according to Fig. 2, is subtracted. The activation energy of the over-all process has already been considered. It can also be calculated by another method, from the maximum rate of degradation $(dv/dt)_{\max}$. Points corresponding to the maximum rates on the curves in Fig. 8 are plotted in Fig. 5. These points evidently correspond to our value of the activation energy.

Effect of oxygen on the degradation of PMMA. It is known that oxygen greatly influences polymerization, accelerating it in some cases [14, 15] and retarding it in other [16]. Madorsky [8] refers to only one experiment in presence of oxygen. It was therefore of interest to study the effect of oxygen on the degradation of PMMA in greater detail.

Fig. 9 shows relative weight loss — temperature ($^{\circ}\text{C}$) curves for PMMA powder (grain size ~ 0.1 mm) and a block specimen (~ 5 mm), after the specimens had been heated in an air thermostat for 6 hours. A curve for

the degradation of the powder in vacuum is given for comparison. Several experiments were also performed with an inert gas (argon). As usual, the relative weight loss is taken as the degradation rate (in the case of PMMA in block form this may give a low value for the degradation rate, if the monomer cannot all escape from the block during the experiment for any reason).

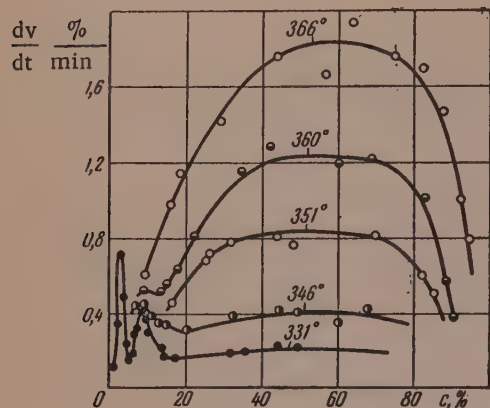


Fig. 8. Variation of the degradation rate of high-molecular PMMA in vacuum, calculated for the weight of polymer at each given instant, with the degree of degradation at temperatures above 300°.

In absence of oxygen there is no significant difference between the degradation kinetics of PMMA in powder and in block form, whereas in the degradation of PMMA in air (at 200°, Fig. 9) oxygen has a strong inhibiting effect on the degradation of PMMA powder and accelerates the degradation of the block specimen; i.e., oxygen displays its dual character in degradation also. It was found in experiments with air circulated under various conditions that when PMMA powder is degraded in air, volatile products are formed which greatly accelerate the degradation. Oxygen inhibits degradation almost completely if these volatile products are totally removed.

TABLE 1

Molecular Weights of PMMA Samples
(degradation at 180° in air)

Type of polymer	Rupture of molecular chains (%)	Molecular weight
Original polymer	—	3,706,000
Powder	1.6	863,000
Block	10.0	284,000
Block	59.4	38,000

peratures used. When PMMA is degraded in presence of oxygen, peroxides are continuously formed and continuously give rise to new radicals, capable of breaking the polymer chains [17], i.e., of initiating degradation. In conditions of free circulation of air, when the volatile products are removed from the polymer surface, the role of oxygen reduces merely to termination of the kinetic chains, with a consequent very sharp decrease of the depolymerization rate (Curve 3, Fig. 9). Table 1 gives the molecular weights of PMMA heated in air; it is seen that the average degree of polymerization of a sample which lost almost no weight (powder), decreases. In other words, in presence of oxygen the molecular chains are ruptured internally, but this is not accompanied by appreciable depolymerization.

Oxygen is almost insoluble in PMMA, and therefore penetrates only slightly into a block specimen; its

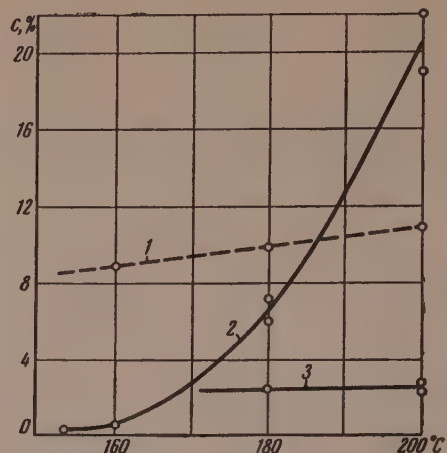


Fig. 9. Variation of degradation of high-molecular PMMA in 6 hours with the temperature;
1) powder in vacuum; 2) block in air;
3) powder in air.

It has been shown in studies of polymerization [14-16] that molecular oxygen terminates the kinetic chains by reacting with free radicals. However, this results in formation of peroxides and hydroperoxides which can themselves decompose and initiate new chains. In a number of experiments we deliberately introduced peroxides and hydroperoxides into PMMA; the polymer was dissolved together with benzoyl peroxide or isopropylbenzene hydroperoxide, films were cast from the solutions, and subjected to degradation in vacuum. Introduction of hydroperoxides increases the degradation rate only during the first instant, as these substances are unstable at the experimental tem-

peratures used.

Inhibiting effect is confined to a thin surface film, where its concentration is relatively high. On the other hand, peroxide catalysts dissolve, diffuse into the specimen, and result in violent degradation of the block. It is therefore not surprising that the degradation of a block of PMMA depends on its linear dimensions (Fig. 10). So long as the specimen is fairly thin, its breakdown is independent of the dimensions, and the breakdown rate is very low, as oxygen inhibits degradation and the substances which initiate it volatilize. If the size of the specimen is such that not enough oxygen is present in its center for termination of the kinetic chains, inhibition is replaced by acceleration. Degradation then increases in proportion to the volume, as the region into which the catalysts can penetrate, but where not enough oxygen is present to terminate the reaction chains, increases. Finally, if the block is quite large, the degradation occurs mainly near the surface, i.e., the weight loss is proportional to the square of the linear dimensions of the block. Therefore the degradation rate (weight loss/total weight \times time) should decrease linearly with increase of the size for fairly large blocks (Fig. 10).

Influence of monomer on the degradation kinetics. Quasi-equilibrium. In the investigations of the influence of the monomer on the rate of thermal degradation, definite known amounts of monomer were added to the polymer. For this, small blocks of the polymer ($5 \times 5 \times 8$ mm) were sealed together with the monomer in glass bulbs, and left to swell in the monomer (in absence of air) at 120° for 24 hours.

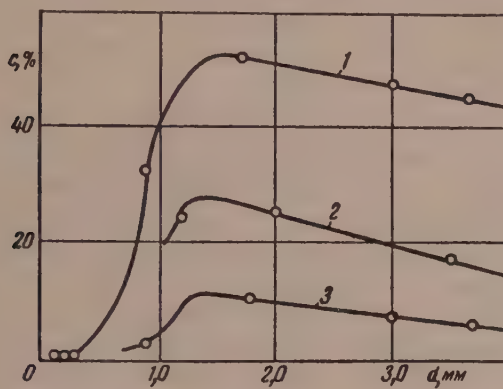


Fig. 10. Effect of block size on the degradation of high-molecular PMMA on heating in air;
1) 6 hours at 200° ; 2) 4 hours at 200° ;
3) 6 hours at 180° .

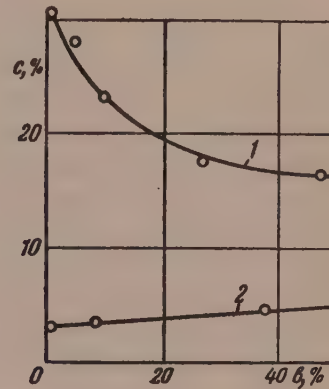


Fig. 11. Effect of monomer on the degradation of high-molecular PMMA;
1) block in air 7 hours at 216° ; 2) block in vacuum, 6 hours at 264° .

When PMMA is degraded in air at 216° a substance which initiates kinetic chains is formed, while the monomer present in the polymer inhibits degradation (Fig. 11, Curve 1) by combining with the free radicals, thus directing the reaction toward polymerization. Moreover, these experiments show that during the swelling of the specimens the monomer remained as such, i.e., it did not polymerize. In the degradation of PMMA in vacuum (Fig. 11, Curve 2), the rate of loss of volatile products remains almost unchanged by addition of monomer. The only possible explanation is that the added monomer is completely polymerized at 264° before the polymer undergoes appreciable degradation, and is subsequently degraded in the same way as the rest of the polymer.

Therefore, if polymerization proceeds at an appreciable rate together with depolymerization at high temperatures in the system polymer-monomer, a state of quasi-equilibrium should exist in a closed system; i.e., a constant concentration m of the monomer should be established at which the polymerization rate is equal to the rate of monomer removal from the polymer

$$a\lambda = b\lambda m, \quad (19)$$

where λ is the concentration of the macroradicals, and a and b are rate constants; hence

$$m = \frac{a}{b} = \frac{\alpha_1}{\alpha_2} e^{-\frac{u_1 - u_2}{RT}} = \text{const}, \quad (20)$$

where $u_1 - u_2$ is the heat of polymerization.

Experiments to test this conclusion were carried out in airtight stainless-steel ampoules in absence of air; the results are given in Table 2. The ampoules were kept in a thermostat at $180-280^\circ$. For determination of the

monomer concentration, films of the polymer (not more than 0.1 mm thick) cast from benzene solution on glass were dried in air at 105°.

Table 2 clearly shows that the final concentration of monomer in the system is independent of the initial monomer-polymer ratio.

TABLE 2

Degradation of PMMA ($M = 250,000$) in Stainless-Steel Ampoules in 24 Hours

Before heating		temperature in °C	After heating		molecular weight	
relative amounts (%) of			monomer	polymer		
monomer	polymer					
0	100	183.6	11.7	88.3	120,000	
0	100	183.6	11.6	88.4	100,000	
60	40	183.6	11.1	88.9	150,000	
0	100	210	19.9	80.1	55,000	
0	100	210	23.5	76.5	80,000	
40	60	210	15.8	84.2	130,000	
50	50	210	35.2	64.8	85,000	

Therefore "quasi-equilibrium" was attained because degradation predominated in some ampoules and polymerization in others. The variation of the "quasi-equilibrium" concentration of monomer with the temperature does not correspond to that expected on thermodynamic grounds. Ivin [18], who studied this type of equilibrium with continuous photochemical activation of the system, plotted true equilibrium curves and determined the real heat of reaction $u_1 - u_2$. In the quasi-equilibrium under consideration, only a relatively small "live" proportion of the polymer with double bonds at the chain ends capable of activation of the temperature of the experiment, participates in the polymerization-depolymerization processes. Therefore the thermodynamic relationships derived for true equilibria in which the system as a whole participates are inapplicable in principle to this instance.

Inhibition of degradation. Suppression of the thermal degradation of PMMA is a question of practical importance. Our experiments permit a planned approach to the problem of inhibition of PMMA degradation. Since the thermal degradation of PMMA is a chain reaction which proceeds as the result of formation of unstable free radicals, substances which form stable compounds with the macroradicals formed may inhibit the process. Nonpolymerizing [19] compounds* of the vinyl series were tested for this purpose: diphenylmethacrylamide, methylphenylmethacrylamide, dimethylmethacrylamide pentachlorostyrene, p-methoxyphenylmethacrylamide, and p-epoxyphenylmethacrylamide [20]. It was presumed that these substances should give rise to stable radicals by combining with the free radicals. In addition, the effects of phenanthrene, triphenyltin, tetraallyltin, and tetraphenyltetrazene on the degradation of PMMA were investigated; it was presumed that they are capable of forming inactive radicals which would trap the macroradicals.

The effects of these substances on the thermal degradation of the polymer were studied under conditions in which the degradation of the polymer is particularly rapid: the polymer was taken in block form and heated in air. Pieces of PMMA of equal size (about $4 \times 4 \times 2.5$ mm) were first put into glass ampoules with various amounts of the substances to be tested. The ampoules were sealed and kept for a week in a thermostat at 120-130°; the percentage of inhibitor absorbed was then determined by weighing. After this the specimens were placed in a thermostat heated to 200° (the temperature was 245° in the investigation of the effect of tetraphenyltetrazene on degradation), and the course of the degradation of PMMA was determined. The results of these experiments are given in Table 3.

The results of the experiments show that additions of 2-4% of methylmethacrylamide, p-ethoxyphenylmethacrylamide, and p-methoxyphenylmethacrylamide decrease degradation 6- to 7-fold. Phenanthrene also decreases thermal degradation to a considerable extent.

* We take the opportunity of expressing our sincere thanks to T. A. Sokolova for supplying these substances.

TABLE 3

Inhibition of the Degradation of PMMA in Air

Inhibitor	Amount of inhibitor	Weight loss of PMMA, %			
		in 6 hr.	in 12.5 hr.	in 17 hr.	in 23 hr.
Polymer without inhibitor	—	32,2	50,5	59,5	66,5
Diphenylmethacrylamide	2,8	8,4	14,8	20,6	28,8
	6,7	8,8	10,6	11,6	12,0
	11,8	8,4	10,2	11,1	11,3
Methylphenylmethacrylamide	1,7	4,7	7,2	9,2	11,2
	6,2	6,2	8,3	10,3	12,3
	11,4	7,2	8,6	10,1	11,5
Dimethylmethacrylamide	1,5	21,2	40,4	51,0	57,3
	5,3	7,8	13,5	19,0	26,6
	9,1	6,8	8,1	9,5	10,8
p-Methoxyphenylmethacrylamide	3,9	6,0	8,0	9,0	—
	5,1	6,9	7,9	8,5	—
	12,5	9,8	10,7	11,3	—
p-Ethoxyphenylmethacrylamide	2,8	6,9	9,2	10,2	—
	6,3	8,1	9,2	9,6	—
	12,6	10,1	10,9	11,9	—
Pentachlorostyrene	2,2	27,2	45,1	56,0	63,5
	5,3	20,5	38,8	49,2	58,5
	6,1	16,5	36,9	46,3	55,0
Phenanthrene	3,1	6,36	10,6	17,0	26,4
	5,8	7,05	8,3	9,4	—
	11,8	8,9	10,2	11,1	16,4
Triphenylallyltin	1,66	17,6	38,6	49,4	56,2
	7,8	9,3	13,8	18,2	21,4
Tetraallyltin	1,4	26,0	44,0	53,5	59,0
	3,3	6,8	—	—	—
		in 18 hours		in 24 hours	
Tetraphenyltetrazene	0,0	95,0		96,5	
	0,53	84,6		88,0	
	2,48	23,9		67,8	

Determinations of molecular weight showed that despite the low degree of degradation (in terms of weight loss) the molecular weight falls sharply during breakdown of the polymer with added inhibitors. This is a very significant result, as it demonstrates directly that inhibitors only prevent chain depolymerization but cannot prevent rupture of the molecular chains.

SUMMARY

- There exist two mechanisms in the degradation of polymethyl methacrylate (PMMA) in vacuum — a low-temperature mechanism ($T < 300^\circ$), with an activation energy of 28 kcal./mole, which is a simple reversal of the polymerization process with chain depolymerization starting at chain ends carrying double bonds; and a high-temperature mechanism ($T > 300^\circ$), with an activation energy of 53 ± 2 kcal./mole, involving random rupture of internal C-C bonds. This process leads to the formation of new ends at which chain depolymerization starts again.
- Oxygen accelerates degradation on the one hand, probably by the formation of peroxides and hydroperoxides, decomposition of which initiates degradation. On the other hand, oxygen acts as a deactivator of free radicals, terminates the kinetic chains, and inhibits degradation.
- At $180\text{--}280^\circ$ both depolymerization and polymerization take place in the polymer-monomer system; i.e., quasi-equilibrium is established in a closed system, when the depolymerization rate equals the polymerization rate.
- The monomer suppresses degradation of PMMA in presence of oxygen, as it directs the reaction toward polymerization by combining with radicals formed by decomposition of the catalysts.
- The degradation of PMMA can be suppressed by addition of certain nonpolarizing compounds of the vinyl series (p-methoxyphenylmethacrylamide, p-ethoxyphenylmethacrylamide, diphenylmethacrylamide, etc.) capable

of yielding inactive radicals which trap the macroradicals.

Institute of High-Molecular Compounds
Academy of Sciences USSR Leningrad

Received October 21, 1957

LITERATURE CITED

- [1] A. P. Votinov, P. P. Kobeko, and F. I. Marei, *J. Phys. Chem.* 15, 106 (1942).
- [2] N. Grassie, H. W. Melville, *Discuss. Faraday Soc.* 348, No. 2, (1947); *Bull. Soc. chim. belges* 57, 142, 1948; *Proc. Roy. Soc., A* 199, 1 (1949); N. Grassie and E. Vance, *Trans. Faraday Soc.* 49, 184 (1953).
- [3] S. D. Madorsky, *J. Polymer Sci.* 9, 133 (1952).
- [4] C. Bamford and A. D. Jenkins, *Nature* 176, 78 (1955); S. E. Bresler and S. Ia. Frenkel*, *J. Tech. Phys.* 25, 2163 (1955).
- [5] N. N. Semenov, *Some Problems of Chemical Kinetics and Reactivity* (Izd. AN SSSR, 1954) p. 41.*
- [6] A. Brockhaus, and E. Jenckel, *Die Makromolek. Chem.* 18-19, 262, (1956).
- [7] S. Bywater, *J. Phys. Chem.* 57, 879 (1953); J. H. Baxendale, S. Bywater and M. G. Evans, *Trans. Faraday Soc.* 42, 675 (1946).
- [8] S. L. Madorsky, *J. Polymer Sci.* 11, 491, (1953).
- [9] V. E. Hart, *J. Research, Nat. Bur. Standards* 56, 67 (1956).
- [10] S. E. Bresler and S. Ia. Frenkel*, *J. Tech. Phys.* 25, 2163 (1955); S. Ia. Frenkel*, *J. Tech. Phys.* 24, 2169 (1954); *Progr. Phys. Sci.* 53, 161 (1954).
- [11] H. W. Melville, *Proc. Roy. Soc.* 237, 149 (1956).
- [12] Hajime Miyama, *Bull. Chem. Soc. Japan* 29, 711 (1956).
- [13] R. Simha, L. Wall, *J. Phys. Chem.* 56, 707 (1952); *J. Polymer Sci.* 6, 39, (1951); R. Simha, L. Wall and P. Blatz, *J. Polymer Sci.* 5, 615 (1950).
- [14] H. Staudinger and E. Urech, *Helv. Chim. Acta* 12, 1127 (1929); R. Ditmar, *Modern Plastics* 14, 3, 40 (1936); *Ind. Eng. Chem.* 28, 1160 (1936).
- [15] G. V. Schulz and F. Blashke, *Z. Phys. Chem.* 50B, 305 (1941); *Z. Electrochem.* 47, 747 (1941).
- [16] H. Staudinger and H. W. Kohlschütter, *Ber. ges. Biol.* 64B, 2091 (1931); H. Staudinger and A. Schwabach, *Justus Liebigs Ann. der Chemie* 488, 33 (1931); B. N. Rutovskii and G. S. Goncharov, *J. Appl. Chem.* 26, 426 (1953).**
- [17] S. E. Bresler, B. A. Dolgoplosk, V. A. Krol', and S. Ia. Frenkel*, *J. Gen. Chem.* 26, 2201 (1956).**
- [18] K. G. Ivin, *Trans. Faraday Soc.* 51, 1273 (1955).
- [19] T. A. Sokolova and V. N. Nikitin, *Bull. Acad. Sci. USSR, Div. Chem. Sci.* (1958) (in the press).**
- [20] T. A. Sokolova, *J. Gen. Chem.* 27, 2205 (1957); M. M. Koton, T. A. Sokolova, M. N. Savitskaia and T. M. Kiseleva, *J. Gen. Chem.* 27, 2239 (1957); T. A. Sokolova and L. A. Ovsiannikova, *J. Gen. Chem.* (1958) (in the press).**

* In Russian.

** Original Russian pagination. See C. B. Translation.

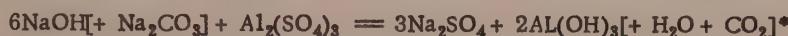
NATURE OF THE REACTION OF ALUMINUM NAPHTHENATE FORMATION

2. PREPARATION OF ALUMINUM NAPHTHENATE BY THE MIXING OF A SUSPENSION OF ALUMINUM HYDROXIDE WITH AN EMULSION OF NAPHTHENIC ACIDS

D. F. Vasil'ev

Conductometric and potentiometric investigations [1] showed that the so-called exchange reaction between potassium or sodium naphthenates and aluminum sulfate comprises the following processes:

- 1) neutralization of the alkalinity of the naphthenate soap according to the equation:



- 2) formation of aluminum hydroxide and an emulsion of naphthenic acids;
- 3) mutual adsorption of particles of Al(OH)_3 suspension and naphthenic acid emulsion;
- 4) precipitation of the adsorption complex, an emulsosuspensoid, in the pH range 7-6.**

From this it was concluded that aluminum naphthenate (AlNp) can be made by the mixing of Al(OH)_3 suspension with an emulsion of naphthenic acids.

Preparation of aluminum naphthenate. The following materials were used for the preparation of AlNp: 1) a solution of naphthenate soap containing 7.2% naphthenic acids, with total alkalinity 2.8% [1]; 2) a mixed solution of H_2SO_4 and HCl containing 0.75 g-equiv./liter, made by dilution of a mixture of the composition 3.2% H_2SO_4 , 8.92% HCl; 3) a suspension of aluminum hydroxide, made by the addition of caustic soda solution to aluminum sulfate solution. For purification of the suspension the Al(OH)_3 precipitate was washed repeatedly with distilled water until its specific conductance fell to $\chi = 2 \cdot 10^{-5} \text{ ohm}^{-1}\text{cm}^{-1}$ (pH 5.6). The suspension contained 12.4 g of Al(OH)_3 per liter.

For preparation of AlNp by the new method, about 0.7 liter of the mixed acid solution was added carefully to 1 liter of the naphthenate soap solution with stirring at room temperature. Partial neutralization of the naphthenate soap of pH 7.8-7.5 gave a highly disperse emulsoid sol of a milky yellow color, containing 4.5 to 5% of naphthenic acids. This sol was mixed with 2 liters of thoroughly suspended aluminum hydroxide. A milk-white emulsosuspensoid sol was formed; the mixed acid solution was added to it in small portions until the system was coagulated (to pH 6.0). Coagulation of the system by the acid mixture is best carried out with short interruptions; it is found that the almost monodisperse sol gives rise to a system containing aggregates of uniform size if the mixture is thoroughly stirred on addition of the acids. The gradual growth of particle size during the coagulation is easily regulated by control of the rate at which the acid is added.

When the aggregates reached 1-1.5 mm in size (at pH 7.0-6.5), they began to coalesce, joining by their surfaces to give a spongy mass in the form of lumps, which readily disintegrated into aggregates of the former size when pressed lightly with a glass rod. This completed the actual preparation of AlNp.

The emulsosuspensoid is completely precipitated as the result of the gradual decrease of pH by the addition

* As in original $[\text{Na}_2\text{CO}_3]$ should probably be $[\text{H}_2\text{CO}_3]$ — Publisher.

** Trapeznikov and Belugina [2] also admit the possibility of formation of adsorption compounds of aluminum hydroxide with organic acids, as well as the formation of compounds by the ordinary ionic double decomposition.

of acid, forming a flocculent soft porous precipitate in a completely clear liquid.

If this precipitate is boiled for 20-30 minutes in the dispersion medium at pH 6, a very porous product in the form of a brittle sponge is easily obtained. If the boiling in the dispersion medium is omitted and the product is washed with cold water, it shows some tendency to cake. It is then less spongelike in structure, but can also be easily powdered when dried to constant weight at 85-90°. The weight of the dried powder is almost exactly equal to the sum of the weights of the sesquioxide and the naphthenic acids (within the limits of experimental error).

Samples made by this method, and additionally boiled or washed with cold water, differ from samples made by the method of double decomposition in giving solutions of excessive viscosity (which form gels). For studies of viscosity changes in the systems the AlNp concentration must not exceed $\frac{1}{3}$ of the concentrations used with samples made by the usual method.

The following analytical data were obtained for a sample made by the method described:

Ash	21.8%	Residual SO ₄	0.39%
Moisture	1.9%	Al	11.2%
		Cl ⁻	absent

It is seen that Cl⁻ was not detected in the product, although the acid mixture contained a considerable amount of HCl when used for coagulation of the system. It is likely that if hydrochloric acid alone is used for neutralization of naphthenate soap the AlNp samples obtained would be quite free of residual SO₄. The ash obtained from the powder consists almost entirely of Al₂O₃.

Aluminum naphthenate is used in various branches of industry [3]. Its ability to form viscous and stable solutions and gels in mixtures with hydrocarbons is often used as a measure of its quality. We compared the viscosities and stabilities of AlNp samples made by double decomposition and by the new method. The samples were made with great care in the laboratory and dried to equal moisture contents. A light petroleum fraction was used as solvent. A high-quality industrial sample made by double decomposition was taken for comparison.

The Table shows that the sample made by the new method compares favorably with the samples obtained by double decomposition.

Properties of 2% Solutions of Aluminum Naphthenate Made by Different Methods

Sample	Method of preparation	Viscosity in poises	Stability of systems
Industrial	Double decomposition	0.25	System broke down after 20 days
Laboratory	Double decomposition	2.0	System broke down after 30 days
Laboratory	Coagulation of a mixture of Al(OH) ₃ suspension and naphthenic acid emulsion	7.0	Viscosity fell to 1.13 poises after 90 days

Advantages of the new method for preparation of AlNp over the method of double decomposition. When AlNp is precipitated by Al₂(SO₄)₃ solution from naphthenate soap by the double-decomposition reaction, the precipitate formed is inevitably polydisperse. At the start of the precipitation, at high pH, very fine particles of Al(OH)₃ and emulsified naphthenic acids are formed; their mutual adsorption gives a very fine suspension of AlNp. As the pH of the medium decreases, the precipitate particles increase very irregularly in size. At the points where fresh portions of the aluminum sulfate enter, rapid local coagulation occurs, which inevitably leads to formation of lumps in which both the naphthenate soap and the Al₂(SO₄)₃ solution are trapped. It is therefore very difficult to obtain a product of reasonably uniform composition, especially under production conditions. The relative proportions of Al(OH)₃ and naphthenic acids, and the amounts of impurities (electrolytes) in individual flakes and lumps, both vary considerably. The individual particles, flakes, and lumps also vary considerably in size. There are particles of microscopic dimensions and lumps up to several centimeters in diameter. The formation of lumps, often very large, is common in production; it often leads to breakdowns of rapidly rotating stirrers.

All these difficulties and disadvantages of the physicochemical formation of the precipitate are eliminated in the production of AlNp by the new method. First, if the Al(OH)_3 is thoroughly purified ($\text{pH} \sim 6$), it is completely free of impurities such as basic salts of aluminum, and sodium sulfate. Much smaller amounts of sodium sulfate are formed in this method from naphthenate soaps of the same alkalinity. Therefore the amounts of contaminating salts can be reduced to a minimum. The second advantage of the new method is that the particles of the precipitated AlNp are very uniform in size. The mixing solutions (emulsion and suspension) are not polydisperse, and the interaction between the particles is more complete. The grains or nuclei of the emulsosuspensoid retain their initial size during the coagulation of the whole product, and become joined into a porous sponge.

The product formed by this method of mixing of the original solutions is incomparably more uniform in composition than the product made by the usual method. If two highly disperse colloidal systems — an emulsion of naphthenic acids, and a suspension of Al(OH)_3 , are mixed, a new colloidal system consisting of an emulsosuspensoid with aggregates of fairly uniform size is formed. Each individual particle of the new colloidal system can be regarded as a nucleus which, by surface adhesion with other such nuclei, forms a lump externally reminiscent of a soft sponge. The individual lumps may vary in size according to the rate of stirring, the time of lump formation, and the rate of change of pH. Nevertheless, the primary nuclei remain of the same size in each lump. This accounts for the unusually high porosity of the precipitate and its brittleness when dry, if the relative amounts of Al(OH)_3 and naphthenic acids are suitably chosen.

In the final coagulation of the emulsosuspensoid by the mixed acid solution it is easy to control the formation of particles of a definite size, as the new method is free from the complicating factor found in the old method — additional precipitation with decrease of pH, and formation of excess $\text{Al}_2(\text{SO}_4)_3$. The less contaminated and porous product is much easier to wash. For example, three washings of the precipitate, even in cold water, reduced the specific conductance (X_{20°) of the wash waters from 0.018 to $0.4 \cdot 10^{-4} \text{ ohm}^{-1}\text{cm}^{-1}$. The water used for the washing had $X_{20^\circ} = 0.1 \cdot 10^{-4} \text{ ohm}^{-1}\text{cm}^{-1}$.

A final important advantage is that this method not only gives products which form solutions of increased stability and viscosity, but the powder is free from caking.

SUMMARY

1. Products of predetermined ash content and properties can be easily obtained when suspensions of aluminum hydroxide and of naphthenic acids are mixed.
2. This method for the preparation of aluminum naphthenate gives a product of uniform composition, of high purity and porosity.

Moscow

Received April 2, 1957

LITERATURE CITED

- [1] D. F. Vasil'ev, Colloid J. 11, 377 (1949).
- [2] A. A. Trapeznikov and G. V. Belugina, Proc. Acad. Sci. USSR 87, No. 4, 635 (1952); 87, No. 5, 825 (1952); 94, No. 1, 97 (1954).
- [3] A. F. Dobrianskii and E. V. Malinovskaia, J. Appl. Chem. 20, 837 (1947).

STUDY OF THE FOAMING OF MOLASSES

T. I. Vlasova

The principal raw material in yeast production is final molasses. A copious and stable foam is formed in molasses during the growth of yeast owing to the presence of surface-active substances and to aeration of the molasses. Because of foaming, the capacity of the fermentation vats cannot be completely utilized in yeast production, and, moreover, because of the abundant foaming, the amount of air necessary for vigorous growth of the yeast cannot be blown through. Therefore oleic acid is used for suppression of foaming in yeast production. Despite the considerable practical interest of this question, there have been very few studies of foam formation in yeast production [1].

Therefore the present investigation was carried out with the following objects: study of the foaming of molasses solutions; tests of the effects of individual surface-active colloids present in molasses on its foaming; determination of the foaming power of a number of colloids.

Foaming of molasses solutions. The properties of the system were represented graphically on a triangular diagram, which shows the regions of maximum and minimum foaming and foam stability for solutions of different compositions [2].

As the foam is a three-component system, the relative amounts of each of the three components (air, water, and foam former) were varied in the investigations of foam properties, the total amount being kept constant.

The foam former was a solution of molasses containing 10% solids. Foaming was determined by the shaking method. A cylinder with a ground glass stopper, 250 ml in capacity, was filled with calculated volumes (in ml) of the three components and shaken by hand for 1 minute, similarly in all cases. The amounts of foam formed were measured in milliliters. The results were used to plot the diagram (Fig. 1).

Fig. 1 shows that the "isofoam" lines, representing equal quantities of foam, have maxima on the "molasses-air" side of the triangle and on all sections of the triangle parallel to this side; the line A-A is drawn through the maximum values. The amount of foam formed increases with increasing supply of air, reaches a maximum (the line A-A), and then decreases with further increase of the amount of air.

Fig. 2 represents variations in the stability of the foam with changes in the relative proportions of the three components. The most stable foam is formed at low concentrations of molasses.

From the technological conditions of the fermentation process in yeast production (density of molasses mash 1-2%, air blown through at about 100 m^3 per 1 m^3 of mash per hour) and the data in the triangular diagram it may be concluded that the fermentation process in yeast production approximately corresponds to Points 44 and 50 in the triangular diagram; this means that fermentation takes place outside the zone of maximum foaming, but in the region of high foam stability.

Foaming power of the surface-active colloids present in molasses. According to the literature [3, 4], the colloids in molasses include mainly the following surface-active substances which act as foaming agents — caramel, acids of colloidal nature (glucinic, apoglucinic, and melasic acids), melanoids, araban, and nitrogenous compounds (presumed to be peptones).

We prepared caramel [5], colloidal acids [6] and melanoids [3]; araban was obtained from sugar-beet pulp [7]. These colloids were very similar to molasses in color. The foaming power of each artificially prepared molasses colloid was determined separately, and also jointly, by the pneumatic method [8]. 10 ml samples of

5% solutions of the colloids were foamed directly; the foam was measured in milliliters. The results are given in Table 1.

TABLE 1

Foaming Power and Foam Stability of Individual Colloids of Molasses

Colloids	Foam formation, ml	Foam stability, seconds	Colloids	Foam formation, ml	Foam stability, seconds
Caramel	80	4	Caramel, colloidal acids, and araban	125	11
Colloidal acids	70	3	Caramel, colloidal acids and melanoids	60	8
Melanoids	10	4	Caramel, colloidal acids, melanoids and araban	120	11
Araban	10	up to 30 minutes	Caramel, colloidal acids, melanoids, and araban	190	16
Caramel and colloidal acids	85	5	Caramel, colloidal acids, melanoids, and araban; acidified to pH 4.5		
Melanoids and araban	10	28			

The influence of sucrose, the main component of molasses, on the foaming power of these colloids was studied. Of all the colloids tested, only caramel was influenced by the presence of sucrose (up to 50%) in the solution, the foaming being decreased somewhat.

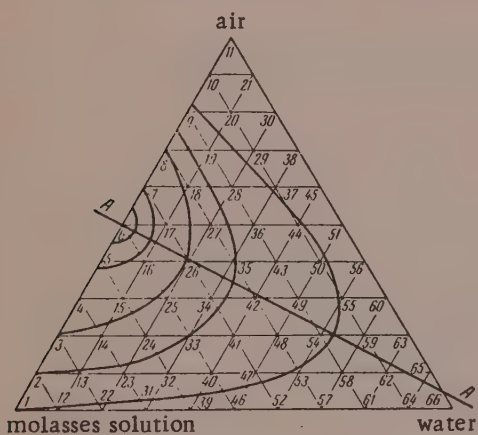


Fig. 1. Triangular diagram for foaming of molasses solutions.

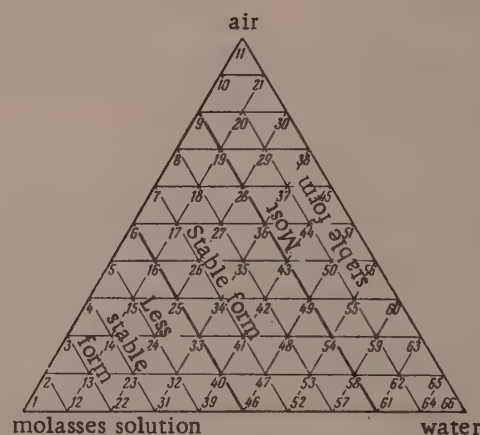


Fig. 2. Triangular diagram for foam stability in molasses solutions.

The foaming of these colloids was studied directly in molasses solution. To 100 ml of molasses solution, containing 5% solids, 5 ml of an aqueous solution of the artificially prepared colloid was added, the solutions were mixed and foamed as in the preceding series of experiments. The results of tests of the foaming power of molasses solution with additions of the various colloids are given in Table 2.

It follows from Tables 1 and 2 that caramel and colloidal acids are the most powerful foaming agents of all the colloids studied. Foaming is increased in their simultaneous presence, probably because the colloids exert a mutual stabilizing effect. A pure solution of melanoids is a poor foaming agent. When mixed with good foam formers (caramel and colloidal acids) melanoids somewhat decrease foaming, exerting some measure of antagonism to the other colloids. It should be noted that the highly colored transparent solution of melanoids had surface tension almost equal to that of water, in agreement with Kharin's results [3]. The low surface tension may account for the poor foaming power of melanoids.

It was found, however, that when the melanoid solution was stored under sterile conditions it acquired foaming power, probably as the result of aging of the colloid.

Araban is of considerable interest with regard to foaming. A solution of araban gives rise to a stable foam of small volume. When mixed with other foaming agents (caramel, colloidal acids) it considerably increases foam stability and also foam formation.

TABLE 2

Foaming Power of Individual Colloids in Presence of Molasses

Addition to molasses solution	Foam formation, ml	Foam stability, seconds
No addition (molasses solution)	90	9
Caramel solution	95	7
Solution of colloidal acids	90	6
Solution of melanoids	70	9
Solution of araban	140	17
Solution of caramel and colloidal acids	90	6
Solutions of caramel, colloidal acids, and melanoids	80	8
Solutions of caramel, colloidal acids, and araban	135	13
Solutions of caramel, colloidal acids, melanoids, and araban, after acidification with sulfuric acid to pH 4.5	210	19

This is evidently an example of stabilization in a mixture of colloids, influencing their foam stability and foaming power. The effect is especially prominent if the solution is acidified to pH 4.5-4.0.

SUMMARY

1. The amount of foam formed on shaking in a molasses solution increases with the amount of air up to a certain maximum, and then decreases again. The volume of foam also decreases with decreasing concentration of the molasses solution.
2. The most stable foams are formed at low concentrations of molasses in the solution.
3. The fermentation of molasses mash in yeast production takes place outside the region of maximum foaming, but in the region of maximum foam stability.
4. The colloidal substances present in molasses can be arranged in the following series of decreasing foaming power:
Caramel > colloidal acids > melanoids > araban.

Scientific Research Institute for
Agriculture and Animal Husbandry of the
Western Regions of the Ukrainian SSR, L'vov

Received December 3, 1956

LITERATURE CITED

- [1] B. D. Metiushev and S. E. Kharin, in the book: Technological Processes and Control in the Food Industry in the Light of Colloid Science (Voronezh Institute of Chemical Technology Press, 1938).*
- [2] A. V. Dumanskii, Bull. State Sci. Res. Inst. Colloid Chem. No. 1 (1934).
- [3] A. V. Dumanskii, E. M. Silaeva and S. E. Kharin, Bull. State Sci. Res. Inst. Colloid Chem. No. 1 (1934).
- [4] P. M. Silin, Technology of Sugar Substances (Food Industry Press, 1950).*
- [5] G. S. Benin and E. E. Shnaider, Sugar Industry No. 7 (1951).

* In Russian.

- [6] M. I. Barabanov, Dissertation: "Coloring Substances in Products of the Sugar Industry" (Kiev, 1952).*
- [7] T. K. Gaponenkov, Colloid J. 2, No. 7 (1936).
- [8] B. Tiutiunnikov and N. Kas'ianova, Oil and Fat Ind, No. 2 (1930).

* In Russian.

A STUDY OF THE LAWS OF POLYANIONIC EXCHANGE

A. T. Davydov and R. Z. Davydova

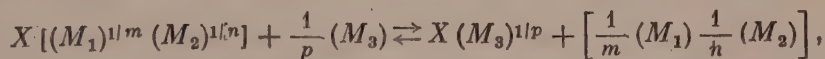
The practical applications of ion-exchange chromatography must be based on a knowledge of the quantitative laws of both cation and anion exchange to an equal degree. Despite the similarity in the exchange behavior of cations and anions, and despite the fact that it has been proved that anions and cations conform to the same laws [1-3], there have been few investigations of anion exchange. The probable explanation for this situation is that investigations of the exchange sorption of anions, in contrast to cations, could be performed only with synthetic anion-exchange resins, as no natural anion exchangers which might be of industrial importance have yet been found.

Various theoretical investigations ([4-7] and others) have greatly influenced the growth of our knowledge of the sorption of anions by soils of various compositions. However, physicochemical studies of anion exchange in soils were of less value in the development of a theory on anion exchange than corresponding studies of exchange sorption of cations.

The extensive use of anion exchange in industrial practice represents a further stage in the development of the science of anion exchange, and requires the development of a modern theory based on new experimental data obtained in investigations of various types of anion exchangers. As in cation-exchange reactions, anion exchange in soils or in industrial practice does not consist of exchange reactions between two kinds of anions; several ions are involved in the exchange, and the reaction is one of polyanionic exchange. Therefore investigations of the quantitative laws of polyanionic exchange are of great practical as well as theoretical interest.

The purpose of the present investigation was a study of the quantitative laws of the exchange of three anions on MMG anion-exchange resin, and a verification of the applicability of the equation for the exchange isotherm for several cations to anion exchange.

Our study of the quantitative laws governing the exchange of three anions was based on Gapon's equation [8] and his fundamental hypothesis that the displacement of ion M_1 is entirely independent of the displacement of ion M_2 when the surfaces occupied by M_1 , M_2 , and M_3 are in thermodynamic equilibrium with a solution containing these ions in the concentrations C_1 , C_2 , and C_3 . On the assumption of the independent exchange of the ions in their simultaneous presence, the process may be schematically represented as follows:



where X is the adsorbent, and m , n , and p are the valences of the exchanging ions M_1 , M_2 , and M_3 .

The derivation of the equation for the exchange of three ions was based on the assumption that the forward and reverse reactions proceed at equal rates at equilibrium; this may be represented by the following equations for each pair of exchanging ions:

$$K_1 \Gamma_1 c_3^{1/p} = K_2 \Gamma_3 c_1^{1/m}, \quad (1)$$

$$K_3 \Gamma_2 c_3^{1/p} = K_4 \Gamma_3 c_2^{1/n}, \quad (2)$$

where Γ_1 , Γ_2 , and Γ_3 are the amounts of the adsorbed cations M_1 , M_2 , and M_3 in meq; c_1 , c_2 , and c_3 are the concentrations of the cations M_1 , M_2 , and M_3 , in terms of normalities, in the equilibrium solution.

The above equations can be used to find two constants for each pair of exchanging ions: M_1 , M_3 and M_2 , M_3 as follows:

$$\frac{\Gamma_1}{\Gamma_3} = \frac{K_2}{K_1} \frac{c_1^{1/m}}{c_3^{1/p}} = K' \frac{c_1^{1/m}}{c_3^{1/p}}, \quad (3)$$

$$\frac{\Gamma_2}{\Gamma_3} = \frac{K_4}{K_3} \frac{c_2^{1/n}}{c_3^{1/p}} = K'' \frac{c_2^{1/n}}{c_3^{1/p}}. \quad (4)$$

Division of Equation (3) by Equation (4) gives the expression:

$$\frac{\Gamma_1}{\Gamma_2} = \frac{K'}{K''} \frac{c_1^{1/m}}{c_3^{1/p}} = K''' \frac{c_1^{1/m}}{c_2^{1/n}}. \quad (5)$$

Equation (5) shows that the ratio of the amounts of ions adsorbed by the solid phase is proportional to the ratio of the concentrations of these same ions, raised to the corresponding powers, in the equilibrium solution (i.e., this equation is analogous to the expression for the isotherm for the exchange of two ions):

$$\Gamma_1 = \Gamma_{1\infty} - mc_1; \quad \Gamma_2 = \Gamma_{2\infty} - nc_2,$$

where $\Gamma_{1\infty}$ is the initial adsorbed amount of ion M_1 ; $\Gamma_{2\infty}$ is the initial adsorbed amount of ion M_2 (i.e., the amounts of ions M_1 and M_2 in the solid phase before the start of interaction with M_3).

Substitution of these values of $\Gamma_{1\infty}$ and $\Gamma_{2\infty}$ into Equation (5) gives the expression in its final form:

$$\frac{\Gamma_{1\infty} - mc_1}{\Gamma_{2\infty} - nc_2} = K''' \frac{c_1^{1/m}}{c_2^{1/n}}. \quad (6)$$

Equation (6) was verified experimentally by Gapon with the aid of numerical data obtained in a study of the exchange of calcium and magnesium ions with ammonium ions in soils, and by Levitskii [9] in a study of polycationic exchange on sulfonated coal and wofatite. Equation (6) is used in studies of complex compounds, when complex cations or several complex anions are formed in solution [10].

Experimental verification of Equation (6) showed that its applicability is quite satisfactory. The values of $\Gamma_{1\infty}$ and $\Gamma_{2\infty}$ used by Gapon for the verification were found by extrapolation and not by direct experiment. Levitskii found these values experimentally from the differences of the ion concentrations in the original and equilibrium solutions after saturation of the adsorbent. In both cases the values of $\Gamma_{1\infty}$ and $\Gamma_{2\infty}$ used for verification of Equation (6) were obtained from the sorption capacities found for each exchanging ion separately, and not in mixtures with other ions.

We considered that it would be more rational to use values of $\Gamma_{1\infty}$ and $\Gamma_{2\infty}$ obtained by direct experiment for each of the anions taking part in the exchange, i.e., the values of the exchange capacity for each anion present in a mixture with the others. With this approach, the values of $\Gamma_{1\infty}$ and $\Gamma_{2\infty}$ should represent the true exchange behavior of each exchanging anion, with the influence of the other ions involved in the exchange taken into account.

It was found that Eqaution (6) is not applicable to our experimental data for the exchange of three anions when the concentration of the displacing anion was in the range of 0.1 to 1 N. The inapplicability of the equation is shown by the fact that down to 0.1 N concentration of the displacing ion twice the amount of the anion desorbed was greater than its exchange sorption value, and calculations of the term $\frac{\Gamma_{1\infty} - mc_1}{\Gamma_{2\infty} - nc_2}$ in the equation gave negative values for the sorption, especially in the exchange of multivalent anions. It was therefore decided to test its validity at low concentrations of the displacing anion, in the range from 0.1 to 0.03 N. In these experiments the synthetic MMG anion-exchange resin was saturated with a mixture containing equal concentrations (0.5 N) of carbonate and sulfate ions. The saturated resin was dried and sifted through a sieve of 0.2 mm mesh. 5 g lots of the resin were put into flasks, followed by 100 ml of a solution containing the displacing cation (KNO_3). The

flasks were shaken and the contents left to settle for 48 hours; the flasks were then put into a thermostat at 25°, and samples were taken for analysis of the desorbed anions. The results are given in the Table.

Calculation of the Tri-Anionic Exchange Constant for the System MM. $-\text{[CO}_3^{2-}, \text{SO}_4^{2-}] + \text{NO}_3\text{K}$

KNO ₃ concentration, N	Anions displaced in meq per 100 g of resin		$\frac{c_1^{1/2}}{c_2^{1/2}}$	$\frac{\Gamma_{2\infty} - 2c_1}{\Gamma_{1\infty} - 2c_1}$	K'''
	$c_1 (\text{CO}_3^{2-})$	$c_2 (\text{SO}_4^{2-})$			
0,100	90,0	52,6	1,315	0,5875	0,7726
0,050	75,7	44,4	1,306	0,5707	0,7480
0,050	60,0	34,7	1,315	0,5830	0,7666
0,040	47,6	29,7	1,266	0,5510	0,7000
0,030	37,4	23,0	1,270	0,5624	0,7140

$$\Gamma_{1\infty} = 237,3 \text{ meq. } \Gamma_{2\infty} = 137,8 \text{ meq.}$$

of double this value from the sorption capacity gives negative values up to 0.25 N concentrations, and in some cases at 0.1 N. This was found for all the systems studied, irrespective of the charge on the ion.

Analysis of these results suggests that Equation (6) is probably valid at higher concentrations of the displacing anion if a considerable amount of undisplaced ions remains in the resin owing to nonequivalence of its active groups; further, it may be applicable to the exchange of a large number of ions, when the desorption of each is not large, with considerable differences between the values of the desorption and the sorption capacity for the given ion. It must also be pointed out that Equation (6) can be applicable only to mixtures in which there is no interaction between the ions, such as complex formation, association, etc.

SUMMARY

1. The exchange sorption of three anions differing in valence on MMG anion-exchange resin has been studied at different concentrations of the displacing anion; it was confirmed that the exchange of individual anions from mixtures proceeds independently.
2. The investigation showed that E. N. Gapon's equation for the exchange of three ions is applicable only over a limited range; it is valid at low concentrations of the displacing ions.
3. Equation (6) was applicable to data obtained for anion exchange in the concentration range from 0.03 to 0.01 N, in which satisfactory values were obtained for the constants.
4. Investigation of the weakly basic MMG anion-exchange resin showed that its sorption capacity for the carbonate ion is almost double its capacity for the sulfate ion; this may be due to selectivity of this resin with respect to carbonate ions.

The A. M. Gor'kii State University, Khar'kov
The V. V. Dokuchaev Agricultural Institute,
Khar'kov

Received June 2, 1956

LITERATURE CITED

- [1] A. T. Davydov, Sci. Mem. Khark'kov University 23, 139 (1946).
- [2] I. I. Zhukov and N. I. Brodskaya, Colloid J. 11, 327 (1949).
- [3] B. P. Nikol'skii and V. I. Paramonova, Sci. Mem. Leningrad State Univ. 163, 119 (1955).
- [4] K. K. Gedroits, J. Experimental Agronomy 19, 6, 294 (1918).
- [5] B. P. Nikol'skii and V. I. Paramonova, Z. Phys. Chem. A 159, 1 (1932).

These results show that Equation (6) is quite satisfactorily applicable at low concentrations of the displacing anion. Our results indicate that the equation is valid for solution concentrations not above 0.1 N.

If values of the total sorption capacity with respect to a given anion, and not the limiting sorption, i.e., the exchange capacity for each exchanging ion, are used in verification of Equation (6), it still remains inapplicable at concentrations above 0.1 N. For example, the sorption capacity of the resin for the carbonate ion is 250 meq per 100 g of resin, and the desorption under the action of 1 N solution of the displacing anion is 133 meq per 100 g of resin; subtraction

[6] S. Mattson, "The laws of soil colloidal behavior, X" Soil Sci. 34, 459 (1932).

[7] N. I. Antipov-Karataev, A. P. Vishniakov, and V. G. Sochevanov, Trans. Leningrad Section, Lenin All-Union Acad. Agric. Sci. No. 23 (1933).

[8] E. N. Gapon, J. Gen. Chem. 3, 6, 667 (1933).

[9] I. Ia. Levitskii, Dissertation (Khar'kov, 1953).*

[10] V. V. Fomin, Progr. Chem. 24, 1014 (1955).

* In Russian.

SPECTROSCOPIC INVESTIGATION OF THE SORPTION OF METAL CATIONS BY OXIDIZED CELLULOSES

I. N. Ermolenko and R. G. Zhbankov

Cellulose materials are always oxidized to some extent; carboxyl groups are found not only in fibers which have been bleached or subjected to other treatments, but also in purified samples. Artificial cellulose fibers have approximately 10 times the carboxyl group contents of native fibers [1]. The presence of cations has a significant influence on the properties of celluloses — dyeability, viscosity, strength, electrical-insulation properties, heat stability, etc. [2-5]. Native cellulose which has not been subjected to any treatments contains: Ca^{2+} , Mg^{2+} , Fe^{3+} , Al^{3+} [2, 6, 7]. Sorption of cations by oxidized celluloses from aqueous solutions [8] is characteristic of acid oxidized celluloses, and involves mainly an ion-exchange reaction between the carboxyls of the oxidized celluloses and the metal ions [9]. The course of the reaction depends on the cation concentration, the solution pH, and the nature of the ions — radius, charge, and degree of hydration. Series characterizing the affinity of cations for oxidized celluloses have been published [9-11].

The sorption of cations by oxidized celluloses as the result of ion exchange between carboxyl hydrogen and metal was confirmed by spectroscopic investigations of cation exchange on oxidized celluloses [12]. The extent of the long-wave displacement of the carboxyl $\text{C}=\text{O}$ band increases with increasing mass of the sorbed cation. The carbonyl $\text{C}=\text{O}$ band is not displaced as the result of sorption. This suggests that carbonyl groups are not involved in the sorption of cations.

This paper deals with the interaction of oxidized celluloses with dilute salt solutions, including solutions containing mixtures of cations, and with differences in the sorption by carboxyls in different positions in the monomer unit in the macromolecule.

In practice, cations are most commonly sorbed by cellulose materials from dilute solutions formed by contact with equipment (Cu, Fe), from town water (Ca, Fe), etc. Sorption from dilute solutions is equivalent to purification of water by ion-exchange resins. The use of oxidized celluloses as cheap cation exchangers has already been claimed in patents [13]. Cation exchange on fiber carboxyls is important in paper technology [14].

The materials studied were cotton celluloses in gauze form, oxidized by periodic acid, sodium chlorite, and nitrogen dioxide (kindly supplied by Professor V. I. Ivanov). The oxidation by NaIO_4 was carried out with 0.1 M solution at pH 5, and by NaClO_2 , at pH 2-3. The oxidation by nitrogen dioxide (tetroxide) vapor was carried out in static conditions at room temperature.

Carboxyl groups in the samples were determined by the known calcium acetate method, aldehydes were determined iodometrically, and carbonyl groups were determined by the hydroxylamine method. The celluloses were treated in the solutions under static conditions at room temperature in vessels with ground-glass stoppers. The liquor ratio was 1 : 1000. The products were washed with distilled water and dried at room temperature in vacuum desiccators.

The absorption spectra were measured by the method used previously [15] by means of the IKS-II infrared recording spectrometer with an NaCl prism under constant conditions: amplifier tube filament voltage 1.5 v; current in radiation source (Nernst filament) 0.5 amp.; speed ratio of wave length and photographic paper recording drums, $\frac{3}{4}$. The slit width was 0.15 mm in the 200-1500 cm^{-1} region, and 0.25 mm in the 1500-1160 cm^{-1} region. To reduce the errors introduced in determinations of the specimen thickness, and instrumental errors, the

absorption coefficients in the 2000-2300 cm⁻¹ region were reduced by calculation to a single value for all the spectra being compared. The eventual error in comparisons of the absorption coefficients of different specimens did not exceed 3-5%.

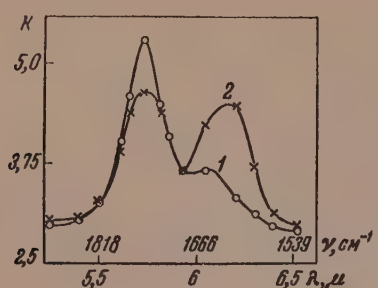


Fig. 1. Absorption spectra of dicarboxy cellulose (6.8% COOH):
1) before sorption; 2) after sorption of Ca²⁺.

For determination of the effect of cation concentration, the sorption of uranyl cations from uranyl nitrate solutions of different concentrations by dicarboxy cellulose was studied (Fig. 2). The results show that considerable variations of the concentration have little effect on the degree of substitution; this indicates that the energy of sorption is high. Several methods have been proposed in recent years for determination of carboxyl groups in oxidized celluloses, based on estimations of the sorption of multivalent cations: gravimetric determination of the sorption of uranyl [17], radiochemical determination of the sorption of radioactive cerium isotope [18], etc. Although the hydrolysis of uranyl [19] and other cellulose salts introduced considerable errors, the high affinity of heavy metals for carboxyl groups in oxidized celluloses is an undoubted advantage of these methods. In contrast to the sorption of univalent cations, in this case a definite hypothesis on the mechanism of sorption by carboxyls must be adopted for calculations of the carboxyl contents from the degree of sorption.

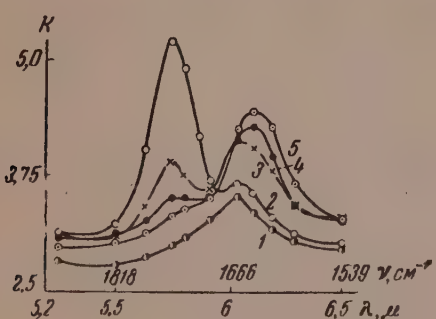


Fig. 2. Absorption spectra:
1) unoxidized cellulose, treated with 0.1 N UO₂(NO₃)₂ solution; 2) dicarboxy-cellulose (6.8% COOH) treated with water; 3) ditto, treated with 0.001 N UO₂(NO₃)₂ solution; 4) ditto, treated with 0.01 N UO₂(NO₃)₂ solution; 5) ditto, treated with 0.1 N UO₂(NO₃)₂ solution.

presence of sorbed water in the samples and by the considerable absorption by the cellulose hydroxyls in this region. It is preferable to study these compounds by the absorption bands associated with deformational vibrations of the hydroxyls. In such cases it is advisable to check that the samples do not contain precipitated metal hydroxides.

Fig. 1 shows the spectra of dicarboxy cellulose (Curve 1), and of the same oxidized cellulose after treatment with 0.001 N calcium acetate solution (Curve 2). The spectra show that very active sorption occurs in this dilute solution. A considerable proportion of the carboxyl hydrogens entered ion exchange with calcium — the intensity of the C=O band at 1740 cm⁻¹ decreased considerably, while at 1590 cm⁻¹ the C=O band of the calcium carboxylate group appeared, as was observed previously in concentrated solutions.

The weak band at 1650 cm⁻¹ observed in the spectrum was caused by sorbed water present in the samples. Our experiments were performed at low moisture contents. The weak water band at 1650 cm⁻¹, constant in all the experiments, did not interfere with the results, in agreement with earlier findings [16].

When multivalent cations are bound by carboxyl groups, each cation may interact with one, two, or more carboxyls. In the first case basic salts (of the type cell-COO, UO₂-OH) or mixed salts (of the type cell-COO--UO₂-NO₃) are formed. Most investigators consider that each cation reacts with one carboxyl group [3, 9, 20]. Experimental evidence to the contrary is available for some cellulose materials — there are data on the binding of cations by more than one carboxyl in ion exchange [21-24]. Mixed salts of oxidized celluloses are detected most easily by the characteristic bands for anion sorption (for example, by the 1350 cm⁻¹ band for the NO₃ anion [25] for a salt of the type cell-C-O-Ca-NO₃). Analysis of the structure of basic cellulose salts of the type cell-C-O-Me-OH by the hydroxyl va-

lence vibrations in the 3 μ region is made difficult by the presence of sorbed water in the samples and by the considerable absorption by the cellulose hydroxyls in this region. It is preferable to study these compounds by the absorption bands associated with deformational vibrations of the hydroxyls. In such cases it is advisable to check that the samples do not contain precipitated metal hydroxides.

Fig. 1 shows the spectra of dicarboxy cellulose (Curve 1), and of the same oxidized cellulose after treatment with 0.001 N calcium acetate solution (Curve 2). The spectra show that very active sorption occurs in this dilute solution. A considerable proportion of the carboxyl hydrogens entered ion exchange with calcium — the intensity of the C=O band at 1740 cm⁻¹ decreased considerably, while at 1590 cm⁻¹ the C=O band of the calcium carboxylate group appeared, as was observed previously in concentrated solutions.

The weak band at 1650 cm⁻¹ observed in the spectrum was caused by sorbed water present in the samples. Our experiments were performed at low moisture contents. The weak water band at 1650 cm⁻¹, constant in all the experiments, did not interfere with the results, in agreement with earlier findings [16].

When multivalent cations are bound by carboxyl groups, each cation may interact with one, two, or more carboxyls. In the first case basic salts (of the type cell-COO, UO₂-OH) or mixed salts (of the type cell-COO--UO₂-NO₃) are formed. Most investigators consider that each cation reacts with one carboxyl group [3, 9, 20]. Experimental evidence to the contrary is available for some cellulose materials — there are data on the binding of cations by more than one carboxyl in ion exchange [21-24]. Mixed salts of oxidized celluloses are detected most easily by the characteristic bands for anion sorption (for example, by the 1350 cm⁻¹ band for the NO₃ anion [25] for a salt of the type cell-C-O-Ca-NO₃). Analysis of the structure of basic cellulose salts of the type cell-C-O-Me-OH by the hydroxyl va-

lence vibrations in the 3 μ region is made difficult by the presence of sorbed water in the samples and by the considerable absorption by the cellulose hydroxyls in this region. It is preferable to study these compounds by the absorption bands associated with deformational vibrations of the hydroxyls. In such cases it is advisable to check that the samples do not contain precipitated metal hydroxides.

In the 7-8 μ region the spectrum of cellulose contains absorption bands at 1360, 1340, and 1325 cm^{-1} , which relate, as in alcohols [26], to primary hydroxyls and which decrease in intensity when the cellulose is oxidized. The same region, near 7 μ , contains absorption bands of carboxylate groups (symmetrical vibration of the O-C-O group [27]) which give an indication of the ionization of carboxyls in the course of salt formation as the result of sorption.

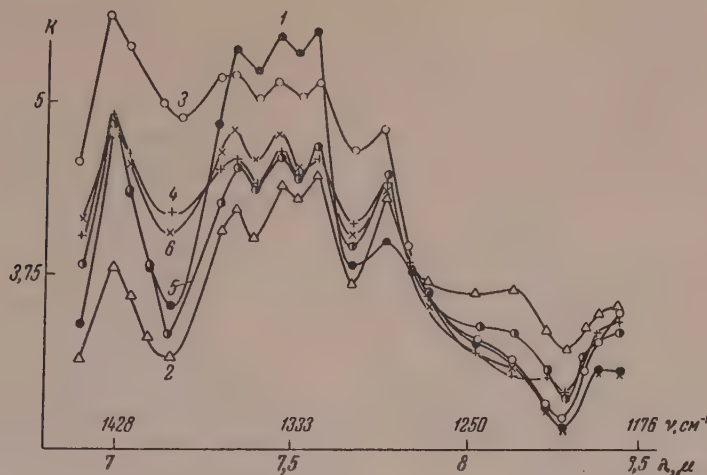


Fig. 3. Absorption spectra in the 1550-1170 cm^{-1} region:

- 1) unoxidized cellulose; 2) monocarboxycellulose containing 12% COOH; 3) ditto, after sorption of Pb^{2+} ; 4) ditto, with UO_2^{2+} ;
- 5) ditto, with Ca^{2+} ; 6) ditto, with Ag^+ . 0.01 Nitrate solutions were used for the sorption.

Fig 3 shows our absorption spectra of unoxidized cellulose, monocarboxycellulose containing 12% COOH, and the same oxidized cellulose treated with Ag^+ , Ca^{2+} , Pb^{2+} and UO_2^{2+} . The absorption in this spectral region is increased considerably as the result of cation sorption. With lead, the absorption extends into the 1290 cm^{-1} region, which contains the symmetrical valence vibrations of the N=O nitro ester groups present in cellulose oxidized by nitrogen oxides. The observed increase of intensity in the region of the absorption band at 7 μ is not associated with the CH_2 groups which absorb in this region, but is caused by ionization of the carboxyls after sorption. However, the increased absorption in the region of the primary hydroxyl bands ($1320-1360 \text{ cm}^{-1}$), where considerably greater changes are observed than in the region near 7 μ as the result of sorption of UO_2^{2+} and Ca^{2+} , may be caused not only by superposition of absorption due to carboxyl groups on the bands of the primary hydroxyls, but also by formation of basic salts of cellulose, the hydroxyls of which may show absorption near this region, or by formation of mixed salts of cellulose. Such structures are obviously not formed on sorption of univalent cations. Our measurements of the spectra of mono- and dicarboxycellulose treated with Ag^+ showed increased absorption in the 7 μ region, greater in the case of dicarboxycellulose, with almost no changes in the region of the primary hydroxyl bands.

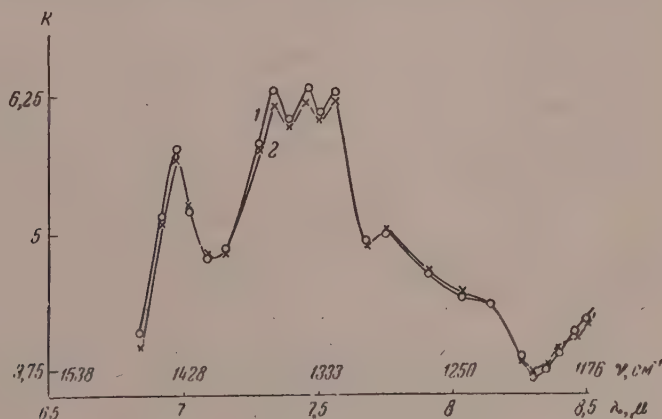


Fig. 4. Absorption spectra of dialdehydecellulose (12% CHO):

- 1) before treatment; 2) after treatment.

As solutions of uranyl, lead, and calcium nitrates were used for the sorption of these bivalent cations, if mixed salts are formed, the products should contain NO_3^- anions, absorbing in the $1340-1410 \text{ cm}^{-1}$ region; another and less intense band due to NO_3^- is found at $800-860 \text{ cm}^{-1}$ [25].

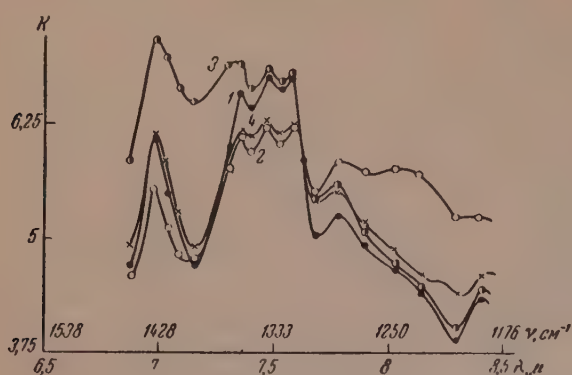


Fig. 5. Absorption spectra in the $1550-1170 \text{ cm}^{-1}$ region:

- 1) unoxidized cellulose; 2) dicarboxycellulose (14.7% COOH); 3) ditto, after sorption of Pb^{2+} ;
- 4) ditto, after sorption of Ca^{2+} .

results for dialdehydecellulose containing 12% CHO are given in Fig. 4. It is seen that no appreciable changes take place in this region of the spectrum after cation treatment of the celluloses. Cation treatment of dicarboxy-celluloses leads to spectral changes similar to those found as the result of sorption by monocarboxycellulose. The results obtained after sorption of Ca^{2+} and Pb^{2+} are given in Fig. 5.

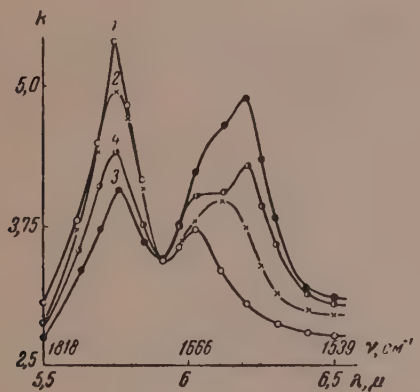


Fig. 6. Absorption spectra of dicarboxycellulose containing 6.8% COOH:

- 1) before treatment; 2) treated with 0.001 N LiNO_3 solution; 3) treated with 0.001 N $\text{Cu}(\text{NO}_3)_2$ solution; 4) treated with a 1 : 1 mixture of 0.002 N $\text{Cu}(\text{NO}_3)_2$ and LiNO_3 solutions.

considerably in their affinity for carboxyl groups were used in these experiments, sorption from dilute equimolar solutions is competitive in character. This is also shown by the characteristic form of the broad absorption band in the 1590 cm^{-1} region in the spectrum of the product after sorption from the mixture. The presence of Li^+ ions in the solution decreases the sorption of Cu^{2+} not only as the result of a decrease of the negative charge of the fiber surface owing to suppression of the ionization of the carboxyls by the lithium ions in solution, but also because of the simultaneous sorption of lithium ions together with copper ions.

Measurement of the spectrum of the products of ion exchange of lead with monocarboxy-cellulose showed that absorption at $800-860 \text{ cm}^{-1}$ decreases owing to nonplanar vibration of the carboxyl OH groups [27].

It has been suggested that in an alkaline medium the hydroxyls of neighboring macromolecules in unoxidized cellulose may bind metals by hydrogen bonding, in the form of hydroxo anions of the type $[\text{PB}(\text{OH})_3]^-$, $[\text{Cu}(\text{OH})_4]^{2-}$, $[\text{Sb}(\text{OH})_4]^-$ [28, 29].

To confirm that the observed spectral changes in this region are the result only of processes accompanying the interaction of cations with carboxyl groups, and not of sorption by hydroxyl groups, we measured the absorption spectra of unoxidized cellulose and of dialdehydecellulose, before and after treatment with cations. The

Comparison of Figs. 3 and 5 shows that there are greater differences in the region of carboxylate group absorption ($1400-1350 \text{ cm}^{-1}$) as the result of sorption of lead and calcium respectively by dicarboxycellulose, than in the sorption of these cations by monocarboxycellulose. The course of ion exchange between fibers and solutions containing mixtures of cations depends on the relative affinities of the cations for carboxyl groups, and the concentrations of the cations.

Sorption experiments were carried out with dilute (0.001 N) solutions of Li^+ and Cu^{2+} salts and with an equinormal mixture of these salts at the same concentrations. Dicarboxycellulose containing 6.8% carboxyl groups was used for the experiments. The spectra of the products and the spectrum of the original dicarboxy-cellulose are given in Fig. 6. The degree of substitution by cations as the result of sorption from the mixture, a measure of which is provided by the weakening of the 1740 cm^{-1} band, is less than the degree of substitution in the case of copper, but greater than in the case of lithium. Thus, despite the fact that cations differing

Another cause of decreased sorption of copper in presence of lithium may be the formation of compounds of higher order in solution [30]. In such cases the multivalent cation forms part of a complex anion of the type $[\text{Cu}(\text{NO}_3)_2]^-$, and therefore its participation in ion exchange on oxidized cellulose decreases.

SUMMARY

1. Changes in the infrared spectra, associated with ionization of carboxyl groups, of the products formed by the sorption of cations by oxidized celluloses have been determined. The greatest differences are found when the sorption takes place at uronic and nonuronic carboxyls. The absorption depends on the nature of the cation.
2. The sorption of cations from dilute aqueous solutions by oxidized celluloses proceeds actively by a mechanism of ion exchange with carboxyl groups; both cations, irrespective of their affinities for carboxyl groups, are sorbed from mixtures of cations.

The authors thank Professor B. I. Stepanov and Professor V. I. Ivanov for their interest and valuable advice.

Institute of Physics and Mathematics
Academy of Sciences, Belorussian SSR
and the Belorussian State University

Received December 20, 1957

LITERATURE CITED

- [1] J. Farrar and S. M. Neale, *J. Colloid. Sci.* 7, 186 (1952).
- [2] D. A. McLean, and L. Wooten, *Ind. Engng. Chem.* 37, 1138 (1939).
- [3] H. F. Chuck, *J. Soc. Chem. Ind.* 66, 221 (1947).
- [4] T. Kleinert and W. Wincor, *Textile Rundschau* 9, 201 (1954).
- [5] D. A. McLean, *Paper Trade J.* 118, 31 (1944).
- [6] A. C. Walker and M. H. Quell, *J. Text. Inst.* 24, T 123, 131 (1933).
- [7] A. M. Sookne and M. Harris, *J. Res. Nat. Bur. Standards* 35, 47 (1930); *J. Text. Res.* 10, 405 (1940); *Amer. Dyestuff Reporter* 29, 333, (1940).
- [8] G. Witz, *Bull. soc. Ind. Rouen* 11, 169 (1883).
- [9] E. Ott, H. M. Spurlin and M. W. Grafflin, *Cellulose and Cellulose Derivatives, part I* (Interscience, New York), 140, 557, 1954.
- [10] A. J. Ultee and J. Hartel, *Analyt. Chem.* 27, No. 4, 557 (1955).
- [11] G. F. Davidson, *Shirley Inst. Mem.* 21, 47, 69 (1947).
- [12] I. N. Ermolenko and R. G. Zhbakov, *Summaries of Papers at the IXth Conference on General Chemistry and Physics of High Polymers* (Izd. AN SSSR, 1957) p. 91; *J. Phys. Chem. (in the press)*.
- [13] British Patent, *J. Text. Inst.* 45, No. 12, A866 (1954).
- [14] S. G. Mason, *Tappi* 33, 413 (1950).
- [15] R. G. Zhbakov and I. N. Ermolenko, *Bull. Acad. Sci. Belorussian SSR, Ser. Tech. Sci.* No. 1, 15 (1956).
- [16] H. Sobue and Y. Tabata, *J. Polymer Sci.* 20, No. 96, 567 (1956).
- [17] I. Farrar, S. M. Neale and G. R. Williamson, *Nature* 168, No. 1274, 566, (1951).
- [18] P. Valls and A. M. Venet, *J. de La Microanalyse* 106 (1953).
- [19] O. Ant-Wuorinen, *Paperi ja puu* 35B, No. 4 (1953).
- [20] H. Ruth, H. Dometsch, *Klepzig's Textile-Z.* 41, 475 (1938).
- [21] A. M. Sookne, and M. Harris, *J. Res. Nat. Bur. Standards* 26, 205 (1947).

* In Russian.

- [22] O. G. Efremova and I. K. Kosyreva, Scientific Annual for 1954, Saratov State University (1955) p. 552.*
- [23] G. Torok, Magyar tud akad. kem tud oszt. kozl. 3, No. 1, 83, 83, 1953.
- [24] S. I. Orlov and S. A. Glikman, Scientific Annual of the Saratov State University (1956) p. 446.*
- [25] Miller and Wilkins, Analyt. Chem. 24, 1253, 1952.
- [26] B. I. Stepanov, J. Phys. Chem. 19, 497 (1945).
- [27] L. J. Bellamy, The Infrared Spectra of Complex Molecules (London, 1956), p. 149.
- [28] R. H. Roschier and Kaisekola, Paperi ja puu 36, No. 2, 27 (1954); No. 17, 37039 (1955).
- [29] R. H. Roschier, Simo Hyvarinen Anveli Ahola paperi ja puu, 36, No. 4, 181 (1953); Referat. Zhur. Khim. No. 3, 14, 551 (1954).
- [30] N. F. Ermolenko and Kh. Ia. Levitman, J. Inorg. Chem. 1, No. 6, 1162 (1956).

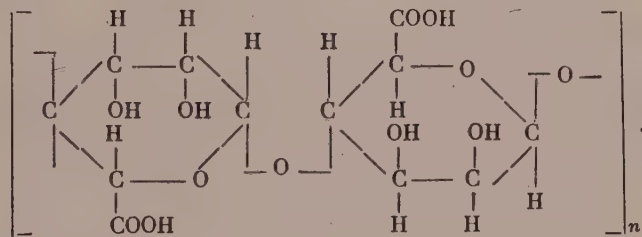
* In Russian.

THE MECHANISM OF STABILIZATION OF CLAY SUSPENSIONS BY AN ALGAL
EXTRACT

N. A. Zavorokhina and V. G. Ben'kovskii

One of the important factors influencing the speed and quality of oil-well drilling is the drilling fluid. The drilling fluid, which consists of a suspension of clay in water, must, like any other colloid system, have definite physicochemical properties. The waters and clays used for making the drilling fluids often contain large amounts of electrolytes, and this leads to flocculation of the drilling fluids, i.e., to loss of the necessary technological properties. To protect drilling fluids against electrolyte flocculation they are subjected to chemical treatment with various stabilizers. Among the stabilizers used in the oil industry are protective colloids such as starch and its derivatives, humic substances from brown coal and peat, paper-industry wastes, carboxymethylcellulose, etc. A stabilizer made from seaweed has recently come into use in France [1] and the USSR. However, the mechanism of stabilization of clay suspensions by this new stabilizer has not been studied.

The seaweed stabilizer, which is an alkaline extract, is not a homogeneous substance; it contains various compounds, principally sodium alginate and fucoidin. Alginic acid is considered to be a polymer of hexuronic acid [2, 3]:



It is insoluble in alcohol, benzene, acetic acid, xylene, ligoine, and water; it is partially soluble (up to 10%) in pyridine and in alkaline solvents. Sodium, potassium, ammonium, and magnesium alginates are readily soluble in water. It has been shown [3] that alginic acid forms salts of constant composition, and its salts with alkali metals resemble salts of strong acids.

The formula of fucoidin has not been finally established, but it is known that fucoidin is a polymeric sulfate ester of a carbohydrate, with the general formula $(ROSO_2OMe)_n$, where R is a radical containing 60% fucose [4]. The metal may be potassium, sodium, magnesium, or calcium. The ash content of such preparations is 25–30%. 63–64% of sulfate was found in the ash; this corresponds to about 17–19% of sulfate in fucoidin. Moreover, these authors showed that fucoidin is not a calcium salt, as was formerly thought. Fucoidin isolated from brown algae [5] contained from 43.9 to 48.4% fucose, 32.4% sulfate, 6.9% metals, and 22.6% ash.

The discrepancies in the data on the composition of fucoidin may be attributed to the use of different methods for its isolation and analysis, and also to the use of algae from different seas. Moreover, the harvesting time of the algae, which also influences the chemical composition of algal extracts, was not taken into consideration.

The purpose of the present investigation was to study the effects of these components of the extract on the colloidal properties of clay suspension, and to determine which substance acts as the stabilizer. Alginic acid

and fucoidin were isolated from the seaweed *Fucus vesiculosus* ("F.V."), and aqueous solutions of their sodium salts were prepared.

Alginic acid was isolated in the form of sodium alginate by a method described previously [6].

The seaweed was steeped in cold dilute hydrochloric acid. It was then separated from the acid and washed in water; this was followed by alkaline extraction to convert alginic acid into soluble sodium alginate. The alkaline extract was separated from the seaweed and treated with concentrated hydrochloric acid, which was added in small portions (0.5-1 ml) with continuous stirring of the solution. The alginic acid, which separated out in the form of brown colloidal flakes, was filtered off, washed with distilled water until free from chloride ions, and dried in air. For preparation of sodium alginate, the alginic acid was dissolved in alkaline solution (NaOH). Excess of alginic acid was used. The aqueous solution of sodium alginate was filtered to remove excess alginic acid, and used for the experiments.

Fucoidin was isolated by the method described previously [7]; 100 g of the dry seaweed, ground in a roller mill and sifted through a sieve of 0.25 mm mesh, was stirred for an hour with 1000 ml of 0.1 N HCl, the mixture being heated on the water bath at 70°. The extract was centrifuged, neutralized by alkali, and evaporated to dryness under vacuum at 40°. The residue was dissolved in 30% ethyl alcohol and centrifuged to remove insoluble impurities. Fucoidin was isolated by precipitation by 60% ethyl alcohol. The product was washed with alcohol and ether and dried in a desiccator. As in the case of sodium alginate, aqueous solutions of the sodium salt of fucoidin were used for the investigations.

Numerous investigations by Soviet scientists [8] indicate that stabilizers are adsorbed on the clay particles and form structured protective films which prevent flocculation of the clay suspensions. We therefore studied the adsorption of sodium alginate and fucoidin by various clays, the viscosities of their aqueous solutions, and the effects of sodium alginate, fucoidin, and their mixtures on the properties of clay suspensions. A comparison of the results should give an indication of the roles played by sodium alginate and fucoidin in stabilization.

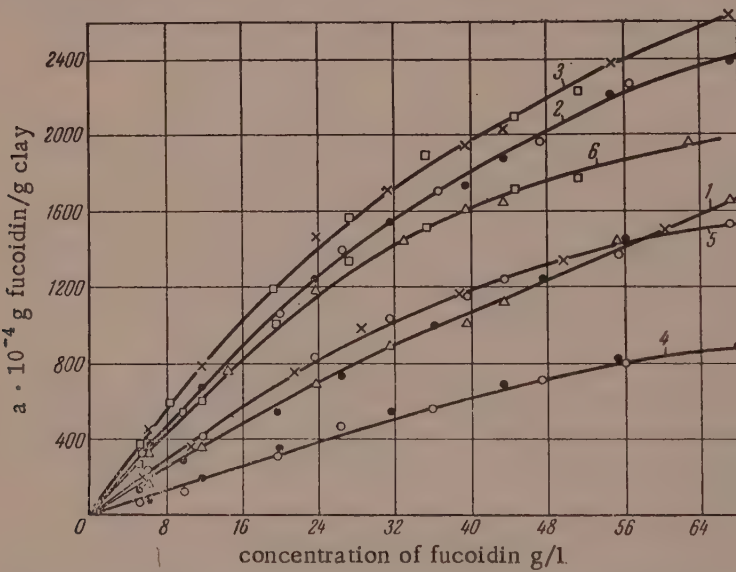


Fig. 1. Adsorption of fucoidin on clays as a function of its concentration in solution:

1, 2, and 3) Makat, Kulsary, and Novobogatinskoe native clays (soaked and dry); 4, 5, 6) the same clays after dialysis.

The adsorbents used were Makat, Novobogatinskoe, and Kulsary clays (native and dialyzed), previously ground and passed through a sieve of 0.25 mm mesh. The chemical composition of these clays is given in the literature [9]. In order to eliminate the influence of adsorption of the solvent and of variations in the degree of dispersion of the clays during adsorption, the experiments were performed with dry clays and also with clays previously saturated with distilled water. The adsorption was measured at 18-20°. The magnitude of the adsorption was given by the difference between the concentrations of sodium alginate and fucoidin in the solutions before

and after adsorption. The concentrations of sodium alginate and fucoidin in solution were determined by precipitation of the copper salts and iodometric titration of excess copper ions in the solution [10].

A Höppler viscosimeter was used for determinations of the viscosities of aqueous sodium alginate and fucoidin solutions.

The properties of the clay suspensions were determined by the methods generally used in the oil industry [11].

It follows from Fig. 1 and 2 that the adsorption of sodium alginate and fucoidin is considerably less on dialyzed than on native clays. The reason is that water-soluble salts, up to 6.5% of which is present in native clays, are removed by dialysis, and as a result the observed adsorption capacity of the clays is decreased considerably. The following is the most likely explanation: the clay particles containing water-soluble salts are always surrounded by a diffuse layer of solvent with a higher concentration of electrolytes than the bulk of the solution. The high electrolyte concentration lowers the solubility of the protective colloid, and this favors increase of its adsorption on the clays.

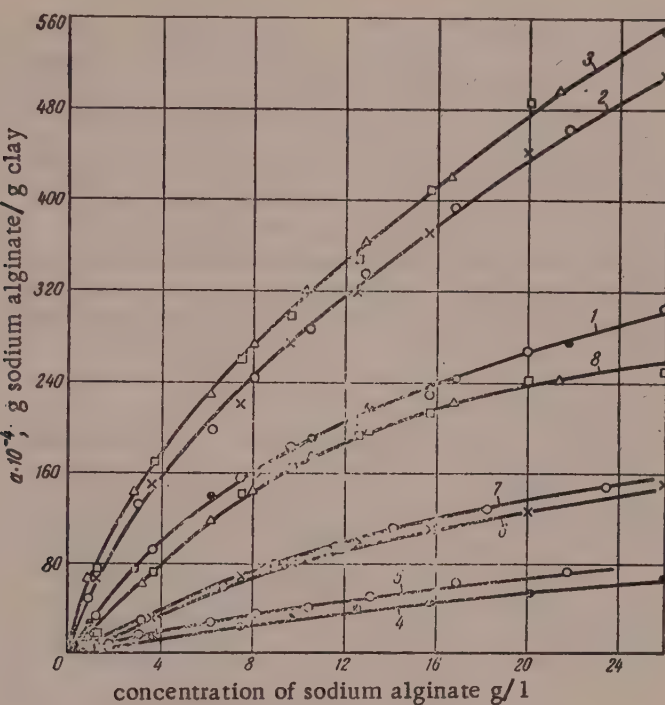


Fig. 2. Adsorption of sodium alginate on clays as a function of its concentration in solution:

- 1, 2, and 3) Makat, Kulsary, and Novobogatinskoe native clays (soaked and dry); 4) dialyzed Makat clay, not soaked;
- 5) ditto, soaked; 6) dialyzed Kulsary clay, not soaked;
- 7) ditto, soaked; 8) Novobogatinskoe clay, dialyzed, soaked and not soaked.

Novobogatinskoye clay has the greatest adsorptive power for sodium alginate and fucoidin, and Makat clay has the least. Adsorption of the solvent influences the adsorption only in the case of adsorption of sodium alginate on dialyzed Makat and Kulsary clays. The adsorption isotherms of sodium alginate on these clays after preliminary soaking lie somewhat above the corresponding isotherms for clays without preliminary soaking (Fig. 2, Curves 4, 5, 6, and 7). If the solvent has no influence, the adsorption isotherms for the soaked and unsoaked clays completely coincide (Figs. 1 and 2, Curves 1, 2, and 3). The adsorption of the solvent becomes more prominent with decreasing adsorbability of the solute [12].

The influence of sodium and magnesium chlorides on the adsorption of sodium alginate and fucoidin by Kulsary clay is shown in Figs. 3 and 4. The adsorption of sodium alginate by native Kulsary clay gradually increases with increasing concentration of sodium chloride in the solution (Fig. 4, Curve 1), and passes through a maximum

with increasing concentration of magnesium chloride (Curve 2). The adsorption of fucoidin on Kulsary clay (native and dialyzed) passes through a maximum with increase of sodium or magnesium chloride concentration in solution (Fig. 3).

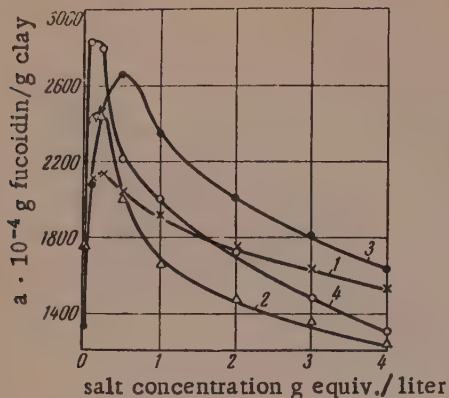


Fig. 3. Adsorption of fucoidin on Kulsary clay in presence of salts:

- 1) Native clay and NaCl; 2) native clay and MgCl₂; 3) dialyzed clay and NaCl;
- 4) dialyzed clay and MgCl₂.

through minima. With further increase in the concentrations of these salts the viscosity curves of sodium alginate and fucoidin pass concave toward the abscissa axis. The viscosity of aqueous sodium alginate solution in presence of sodium chloride is exceptional; it increases continuously with the salt concentration.

TABLE 1

Effects of Fucoidin, Sodium Alginate, and Their Mixtures on the Properties of Clay Suspensions

clay	Composition of suspension, %			Properties of suspension						
	fucoidin	alginate	NaCl	sp. gr.	Viscosity by SPV-5, sec.	filtration rate in cc (cc/min.)	thickness of clay crust, mm	static yield value, mg/cm²		24-hr. sedimentation, %
								1 min.	10 min.	
22	—	—	—	1,12	17,2	40/10	5	0	0	50,3
22	1,5	—	—	1,13	20,0	7/30	0,5	0	0	4
22	2,5	—	—	1,13	24,0	5/30	0,5	0	0	3
22	1,5	—	10	1,20	17,0	24/30	6	0	0	12,6
22	2,5	—	10	1,23	22,0	11,5/30	2,5	0	0	5
22	—	1,5	—	1,13	147,0	11/30	2	63	75	7
22	—	2,5	—	1,30	does not flow	5,5/30	1	273	345	0
22	—	1,5	10	1,20	46,0	15/30	2	42	45	4
22	—	2,5	10	1,23	230,0	12/30	2,5	171	180	0
22	1,5	1,5	10	1,19	42,0	13,5/30	1,5	24	33	3
22	2,5	1,5	10	1,16	49,0	6,5/30	1	42	45	1

The probable cause of the decrease of viscosity on addition of small amounts of salts is partial dispersion of the sodium alginate and fucoidin micelles [14]. The subsequent increase of the viscosity, followed by a decrease, is caused by coagulation of the sodium alginate and fucoidin; this passes from latent coagulation (in the region of viscosity increase) to visible coagulation (in the region of viscosity decrease). Visible coagulation of sodium alginate does not occur in presence of sodium chloride.

The properties of suspensions of native Kulsary clay stabilized by fucoidin, sodium alginate, and mixtures of the two, are given in Table 1.

The increased adsorption of sodium alginate and fucoidin in presence of salts may be attributed not only to a surface salting-out process [13], but also to dispersion of the clay particles by the action of sodium chloride, to ion exchange between magnesium ions and the ions in the ionogenic clay complex, and to a probable chemical reaction between magnesium and sodium alginate and fucoidin [3]. The decreased adsorption on further addition of magnesium chloride is caused by coagulation of the clay particles, i.e., a decrease of the adsorbing surface, and in the case of fucoidin also by coagulation of the protective colloid itself.

Fig. 5 shows the viscosity variations of aqueous solutions of sodium alginate and fucoidin with concentration. It is seen that the viscosity of aqueous sodium alginate solutions is 3.5 times that of fucoidin solutions. In presence of small amounts (up to 1 g-equiv./liter) of sodium and magnesium chlorides the viscosity curves of aqueous solutions of sodium alginate and fucoidin pass

Figs. 1 and 2 show that the adsorption of fucoidin by clays is approximately 3 times the adsorption of sodium alginate by the same clays. The adsorption of these substances completely corresponds to their stabilizing properties. Clay suspensions stabilized by equal amounts of sodium alginate and fucoidin (1.5% on the weight of the suspension) differ considerably in properties. Table 1 shows that a suspension stabilized by fucoidin has better water loss and sedimentation properties, but has zero static yield value. The explanation of the stabilization of clay suspensions by fucoidin is that as the result of its considerable adsorption by the clay particles fucoidin assists their solvation, acting as an intermediate layer between the clay and the aqueous phase; this is confirmed by the almost complete absence of enforced or free separation of the liquid phase. A suspension stabilized by sodium alginate has worse water loss and sedimentation properties, but it has a considerable viscosity and fairly good structural and mechanical properties. Clay suspensions stabilized by large amounts of fucoidin or sodium alginate (2.5% on the weight of suspension) have approximately the same water loss, while no sedimentation at all occurs in the suspension stabilized by sodium alginate. The explanation is that sodium alginate forms very viscous solutions, in which a considerable part of the water is bound between the stabilizer molecules. As a result, the system sodium alginate-water is capable of retaining clay particles in a suspended state; this is an additional stabilizing factor.

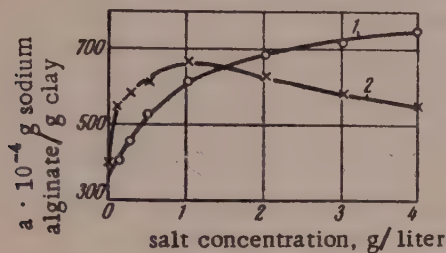


Fig. 4. Adsorption of sodium alginate on native Kulsary clay in presence of NaCl (1) and MgCl_2 (2).

Sodium alginate, two stabilizing factors operate: increase of the bonding of the medium by the clay particles (the result of adsorption of the sodium alginate on the clay particles), and structure formation by the bonding of water by sodium alginate micelles. It follows that the stability of suspensions to electrolyte flocculation should be greater in presence of sodium alginate than of fucoidin. Viscosity data for aqueous solutions of sodium alginate and fucoidin in presence of sodium chloride also indicate that sodium alginate is more stable than fucoidin to the action of electrolytes. The viscosity curve for sodium alginate solution in presence of sodium chloride has no region of visible coagulation. However, clay suspensions stabilized by a mixture of fucoidin and sodium alginate has quite satisfactory properties in presence of sodium chloride. Clay suspensions stabilized by an alkaline extract of F. V. algae are also quite stable in presence of sodium chloride (Table 2).

Thus, the stabilizing action of F. V. extract is mainly due to the formation of surface adsorbed films of fucoidin, which protect the clay particles from coagulation, and to the structural and mechanical properties conferred on the suspensions by sodium alginate.

However, in presence of sodium chloride the properties of suspensions stabilized by fucoidin deteriorate to a considerably greater extent than the properties of suspensions stabilized by sodium alginate. The explanation is that the solvate layers formed around the clay particles as the result of adsorption of fucoidin are compressed on addition of electrolytes, and the system gradually loses its stability. When clay suspensions are stabilized by so-

dium alginate, two stabilizing factors operate: increase of the bonding of the medium by the clay particles (the result of adsorption of the sodium alginate on the clay particles), and structure formation by the bonding of water by sodium alginate micelles. It follows that the stability of suspensions to electrolyte flocculation should be greater in presence of sodium alginate than of fucoidin. Viscosity data for aqueous solutions of sodium alginate and fucoidin in presence of sodium chloride also indicate that sodium alginate is more stable than fucoidin to the action of electrolytes. The viscosity curve for sodium alginate solution in presence of sodium chloride has no region of visible coagulation. However, clay suspensions stabilized by a mixture of fucoidin and sodium alginate has quite satisfactory properties in presence of sodium chloride. Clay suspensions stabilized by an alkaline extract of F. V. algae are also quite stable in presence of sodium chloride (Table 2).

TABLE 2

Effects of Coal-Alkali Regent (CAR), Algal Extract (AE), and Sodium Alginate on the Properties of Kulsary Clay Suspensions

clay	Composition of suspension, %				sp. gr.	viscosity by SPV-5, sec.	filtration rate in cc (cc/min.)	Properties of suspension			24-hr. sedimentation, %
	CAR	AE	alginate	NaCl				thickness of clay crust, mm	static yield value, mg/cm²	1 min.	
22	— — — —			10	1,22	16,5	40/14	3	6	6	23,5
22	— — — —		1,5	10	1,20	46,0	15/30	2	42	45	4
22	— — — —		1,5	10	1,19	20,0	40/18	5	12	12	19
20	— — — —		1,5	10	1,19	24,0	24/30	4	15	21	11,8
18	— — — —		1,5	10	1,19	321,0	6/30	0,5	18	45	0
22	— — — —	2	1,5	10	1,23	35,0	7/30	1	21	24	0
18	— — — —	2	—	10	1,20	40,0	4/30	0,5	6	12	0

Note. CAR is in % calculated as coal; AE is in % calculated as dry seaweed.

These results suggest that sodium alginate protects fucoidin from coagulation by sodium chloride. The protective action of alginic acid and its salts on gold salts has been reported [2]. In addition, we found that sodium alginate and alkaline extract of F. V. algae protect sodium humate solutions from coagulation by sodium chloride. Data on the stabilization of Kulsary clay suspensions by coal-alkali reagent, algal extract, sodium alginate, and their mixtures are given in Table 2.

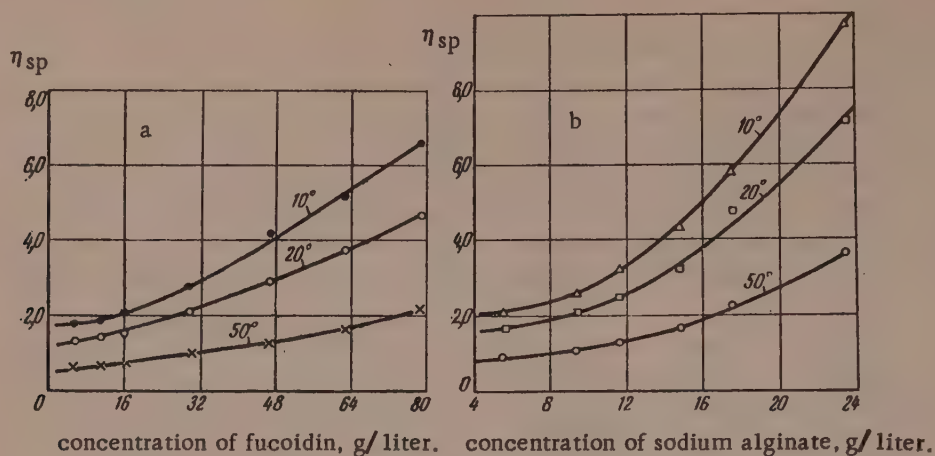


Fig. 5. Viscosity of aqueous solutions of fucoidin (a) and sodium alginate (b).

The foregoing examples show that clay suspensions can be stabilized successfully even if the stabilizer consists of a mixture of two or more substances which are not adequate stabilizers if used separately.

SUMMARY

1. The adsorption of fucoidin and sodium alginate is considerably greater on native than on dialyzed clays.
2. The solvent has almost no influence on the nature of the adsorption of fucoidin and sodium alginate on clays.
3. The adsorption of fucoidin and sodium alginate on clays passes through a maximum with increasing magnesium chloride concentration, whereas in presence of sodium chloride the adsorption of fucoidin passes through a maximum while the adsorption of sodium alginate increases steadily with the salt concentration.
4. The mechanism of stabilization of clay suspensions by extract of F. V. algae consists of the formation of protective surface films, mainly by adsorption of fucoidin, and of structure formation by the action of sodium alginate.
5. It is suggested that sodium alginate protects fucoidin from coagulation by sodium chloride.
6. The use of mixed protective colloids for the stabilization of drilling fluids with high electrolyte contents in the aqueous phase is of considerable practical interest.

Institute of Petroleum, Academy of Sciences
Kazakh SSR, Gur'ev

Received June 10, 1957

LITERATURE CITED

- [1] M. I. Dupic, Bull. de l'association Francaise des Techniciens du Petrole, 30, No. 102, 51, 1953.
- [2] Iu. K. Novodranov, Sci. Mem. Leningrad State Univ., Chem. Ser., 1, 58 (1935); 11, 29 (1952).
- [3] N. A. Pribytkova and V. A. Rozhina, Coll. Trans. Arkhangel'sk Seaweed Inst. (Arkhangel'sk, 1936).
- [4] G. Lunde, E. Heen, and E. Oy, Hoppe - Seyler's Zeitschrift für Physiologische Chemie, 247, 4-5, 189 (1937).
- [5] E. G. V. Percival and A. G. Ross, J. Chem. Soc., 717 (1950).

- [6] A. I. Vedrinskii, Trans. Arkhangel'sk Seaweed Inst. 1 (Arkhangel'sk, 1938).
- [7] W. A. P. Black, E. T. Dewar and F. N. Woodward, J. of the Science of Food and Agriculture, 3, 3, 123 (1952).
- [8] P. A. Rebinder and A. A. Trapeznikov, Proc. Acad. Sci. USSR 18, 7, 421 (1938); J. Phys. Chem. 12, 5-6, 573 (1938); A. A. Trapeznikov and P. A. Rebinder, Proc. Acad. Sci. USSR 18, 3, 185 (1938); S. E. Bresler and P. F. Pokhil, Bull. Acad. Sci. USSR, Div. Math. Nat. Sci., Chem. Ser. 2, 413 (1927).
- [9] V. G. Ben'kovskii, K. A. Kaganskaia, and S. S. Sukharev, Trans. Inst. Petroleum Acad. Sci. Kazakh SSR, 1 (Alma-Ata, 1956).
- [10] M. A. Sobolev and A. A. Krestinskaia, Textile Ind. 7, 39 (1954).
- [11] V. S. Branov, Clay Suspensions for Oil-Well Drilling in Difficult Conditions (State Fuel Tech. Press, 1955); *E. A. Demlianova, Properties of Bentonite Suspensions and their Use in Prospecting (State Geol. Tech. Press, 1954).*
- [12] I. I. Zhukov, Colloid Chemistry (Leningrad, 1949) p. 209; *W. Lewis, L. Squires, and G. Broughton, Chemistry of Colloidal and Amorphous Materials (Russian translation) (Moscow, 1948) p. 101.
- [13] V. K. Semenchenko, J. Appl. Chem. 7, 4, 75 (1930); V. K. Semenchenko and E. A. Davidovskaia, J. Phys. Chem. 6, 1, 37 (1935); V. K. Semenchenko and A. F. Gracheva, J. Phys. Chem. 6, 1, 45 (1935).
- [14] N. V. Mikhailov and V. A. Kargin, J. Phys. Chem. 9, 6, 805 (1937).*

* In Russian.

ADSORBATE-ADSORBATE INTERACTION IN THE ADSORPTION OF VAPORS ON
GRAPHITIZED CARBON BLACKS

2. APPLICATION OF THE EQUATIONS FOR THE ADSORPTION ISOTHERMS TO EXPERIMENTAL DATA*

A. V. Kiselev, N. V. Kovaleva, V. A. Sinitsyn, and E. V. Krapova

The equations given in the preceding paper [1] for the unimolecular (Equations 1-3) and multimolecular (Equation 4) adsorption isotherms of vapors with adsorbate-adsorbate interaction in the first layer are applied in this paper to experimental adsorption isotherms for different vapors on graphitized carbon blacks.

1) The approximate equation derived by one of the present authors [1-4]

$$h = \frac{\theta'}{K'_1(1-\theta')(1+K_n\theta')} , \quad (1)$$

where $h = p/p_s$ is the relative vapor pressure; θ' is the fraction of the surface covered by the monolayer; K'_1 is the adsorbate-adsorbent equilibrium constant; K_n is the adsorbate-adsorbate equilibrium constant.

2) The Hill equation [5]

$$h = \frac{\theta'}{K'_1(1-\theta')} e^{\frac{\theta'}{1-\theta'}} - K_2\theta' , \quad (2)$$

where $K_2 = \frac{2a_2}{b_2RT}$, and a_2 and b_2 are constants in an equation of state of the van der Waals type for the monolayer.

3) The Fowler-Guggenheim equation [6]

$$h = \frac{\theta'}{K'_1(1-\theta')} e^{-a\theta'} , \quad (3)$$

where a is a constant characterizing the interaction of neighboring pairs of adsorbate molecules.

The approximate equation [1, 7] which combines the equation for monolayer adsorption (1) and the BET equation [8]

$$h = \frac{\theta(1-h)^2}{K'_1[1-\theta(1-h)][1+K_n\theta(1-h)]} , \quad (4)$$

where θ is the total fraction of the surface covered.

In this paper Equations (1-4) are applied to experimental isotherms, published by various authors, for the adsorption of different vapors on graphitized carbon blacks.**

*Presented at the Lomonosov Lectures of the Chemical Faculty of Moscow University, October 22, 1957, part 2.

** In the literature the adsorption isotherms are given only in graphical form; we used these graphs for determination of the values of adsorption and vapor pressure, required for the calculations. We take this opportunity of thanking Drs. Ross and Paltz for supplying numerical data for nitrogen and argon.

Adsorption of normal alkanes. The adsorption isotherms of normal alkanes on graphitized carbon black give a good fit with the Langmuir equation (over the initial region) and the BET equation [9-10]. This is in accordance with the high values of K_1' (strong interaction between n-alkane and graphite [9-11], high net heats of monolayer adsorption) and relatively low values of K_n . In such cases Equations (1) and (4) approximate to the Langmuir and BET equations [1, 2, 7].

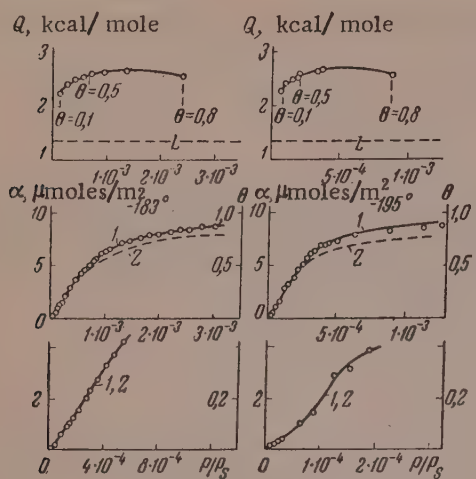


Fig. 1. Adsorption of nitrogen vapor on P-33 carbon black graphitized at 2700°. Points represent experimental data [12]. Above — differential heat of adsorption as a function of \underline{h} ; here and subsequently L is the heat of condensation. Below — adsorption isotherms at -183° and -195° . Calculated isotherms: 1) from Equation (1), 2) from Equation (2).

For $\theta < 0.1$ the adsorption isotherms of nitrogen, argon, and krypton vapors on this carbon conform to the Henry equation, then, from $\theta \approx 0.1$ to $\theta \approx 0.5$, to the Hill equation (2), and at higher values, to the Langmuir equation. The constant K_1' in the Hill equation is also the constant of the Henry equation for low values of θ [1], and therefore the Hill isotherm should pass continuously into the Henry isotherm. The different regions of θ found by the authors [12] for these isotherms are the results of somewhat high values for the adsorption at low \underline{h} owing to residual heterogeneity [14]. This is clear from Fig. 2, where breaks can be seen in these isotherms, plotted in h/α , \underline{h} , coordinates, so that the "Henry region" does not pass smoothly into the region of applicability of the Hill isotherm, while the constancy of h/α in the "Henry region" can be attributed to somewhat high values of α at low \underline{h} .

It follows from Fig. 1 that the adsorption isotherms of nitrogen vapor calculated from Hill's equation (the constants for this equation are given in [12]) coincide with the experimental isotherms up to $\theta \approx 0.4$, after which they deviate downward. It was found [12] that at higher values of θ the isotherms conform to the Langmuir equation, and it was suggested that up to $\theta > 0.5$ the adsorbate molecules are localized and the energy of adsorption remains constant.

In the light of our Equation (1), the S-shaped character of these isotherms may be explained by the magnitude and the ratio of the equilibrium constants for adsorbate-adsorbant and adsorbate-adsorbate interaction. In Fig. 3 the adsorption isotherms of nitrogen vapor (Fig. 1) are plotted in the coordinates of the linear form of Equation (1):

$$\frac{\theta'}{h(1-\theta')} = K'_1 + K'_1 K_n \theta'. \quad (1')$$

* In the paper cited [12] the isosteric heats of adsorption of nitrogen and argon vapors are given for the average temperature -189° .

Adsorption of cyclopentane. In this case [4] the value of K_1' is considerably less than for normal pentane, and therefore Equations (1) and (4) do not approximate to the Langmuir and BET equations; the isotherm commenced with a concave region and passes through two points of inflection. Equation (4) gives a satisfactory fit with this isotherm [4].

Adsorption of nitrogen, argon, and krypton vapors. The points in Fig. 1 denote the experimental isotherms and heats of adsorption of nitrogen vapor determined at two temperatures* [12] on P-33 carbon black graphitized at 2700°. The values of the heats of adsorption Q obtained by the authors [12] from two isotherms are here expressed as a function of \underline{h} , for comparison with the isotherms; the adsorption α is calculated per unit surface. At -183° the initial net heat of adsorption is ~ 0.8 kcal/mole, i.e., it exceeds the heat of condensation by $\sim 60\%$. As \underline{h} increases to $1 \cdot 10^{-3}$ the net heat of adsorption increases, and reaches a maximum of 1.3 kcal/mole at this value \underline{h} . This increase of the heat of adsorption is caused by adsorbate-adsorbate interaction. The adsorption isotherms of nitrogen vapor in the monolayer region are S-shaped; they are initially concave, then pass through the first point of inflection near $\theta = 0.4$, and become convex.

The authors [12, 13] concluded that in the range of

For $\theta < 0.1$ the adsorption isotherms of nitrogen, argon, and krypton vapors on this carbon conform to the Henry equation, then, from $\theta \approx 0.1$ to $\theta \approx 0.5$, to the Hill equation (2), and at higher values, to the Langmuir equation. The constant K_1' in the Hill equation is also the constant of the Henry equation for low values of θ [1], and therefore the Hill isotherm should pass continuously into the Henry isotherm. The different regions of θ found by the authors [12] for these isotherms are the results of somewhat high values for the adsorption at low \underline{h} owing to residual heterogeneity [14]. This is clear from Fig. 2, where breaks can be seen in these isotherms, plotted in h/α , \underline{h} , coordinates, so that the "Henry region" does not pass smoothly into the region of applicability of the Hill isotherm, while the constancy of h/α in the "Henry region" can be attributed to somewhat high values of α at low \underline{h} .

It follows from Fig. 1 that the adsorption isotherms of nitrogen vapor calculated from Hill's equation (the constants for this equation are given in [12]) coincide with the experimental isotherms up to $\theta \approx 0.4$, after which they deviate downward. It was found [12] that at higher values of θ the isotherms conform to the Langmuir equation, and it was suggested that up to $\theta > 0.5$ the adsorbate molecules are localized and the energy of adsorption remains constant.

In the light of our Equation (1), the S-shaped character of these isotherms may be explained by the magnitude and the ratio of the equilibrium constants for adsorbate-adsorbant and adsorbate-adsorbate interaction. In Fig. 3 the adsorption isotherms of nitrogen vapor (Fig. 1) are plotted in the coordinates of the linear form of Equation (1):

$$\frac{\theta'}{h(1-\theta')} = K'_1 + K'_1 K_n \theta'. \quad (1')$$

Curves 1 and 2 in Fig. 3 were used to determine the constants K_1' and K_n of this equation (see Table) for the adsorption of nitrogen, when the capacity of a dense nitrogen monolayer $\alpha_m = 10.2 \mu \text{ moles}/\text{m}^2$ ($\omega_0 = 1000/6.02 \alpha_m = 16.2 \text{ A}^2$). (The value of α_m is needed for calculation of $\theta = \alpha/\alpha_m$). These constants were used to calculate the adsorption isotherms denoted by continuous lines in Fig. 1. Fig. 1 shows that Equation (1) satisfactorily describes almost the whole region up to completion of the monolayer. This is also confirmed by the work of Graham [14], who found that the "equilibrium function" $\frac{\theta}{h(1-\theta)}$ for the adsorption of nitrogen vapor on a homogeneous graphitized carbon black surface increases linearly with θ . This follows from Equations (1), (1').*

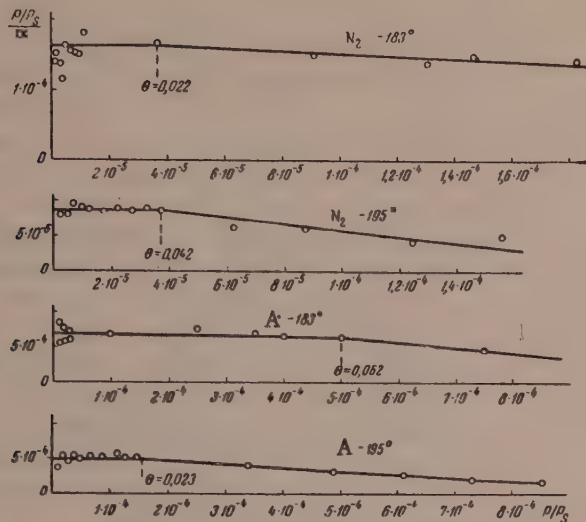


Fig. 2. Initial regions of the adsorption isotherms of N_2 and A on graphitized P-33 carbon black, plotted from the data of Ross et al. in h/α coordinates.

at -195° . It is clear from Fig. 4 that the isotherms calculated from Equation (1) coincide with the experimental values over a wider range of θ than those calculated from Equation (2). The applicability region of Equation (1) may be extended if it is assumed that the packing of the adsorbate molecules in the adsorbed layer alters as the adsorption proceeds, passing from a predominantly hexagonal to a predominantly cubic packing. Simple cubic packing of argon molecules corresponds to $\omega_0 = 14.7 \text{ A}^2$, and hexagonal packing, to $\omega_0 = 12.8 \text{ A}^2$ [12]. Reference is made to such a change of the molecular packing of argon in the paper in question [12].

Round Values of the Constants in the Equations for the Adsorption Isotherms of Vapors on Graphitized Carbon Blacks

Adsorbate	Tempera-ture ($^\circ\text{C}$)	Value of ω_0 taken, in A^2	$Q_{\max-L}/L$	Constants in absorption isotherm equations						
				Equation (2)		Equation (1)		Equation (4)		
				K_1'	K_1	K_1'	K_n	K_1'	K_n	K_n/K_1'
n-Pentane	20	45	0,65	—	—	—	—	165	0,45	0,003
Cyclopentane	20	38,2	0,35	—	—	—	—	20	2,5	0,12
Nitrogen	-195	16,2	1,0	1150	4,3	1000	6,0	—	—	0,006
Nitrogen	-183	16,2	1,0	580	3,5	550	2,65	—	—	0,005
Argon	-183	12,8	0,72	105	4,6	90	6,3	—	—	0,07
Krypton	-183	14,5	1,0	80	6,2	(30)	(30)	—	—	(1)
Sulfur dioxide	0	13,8	0,26	1,2	5,1	1,2	8,4	—	—	7,0
Methylamine	0	16,0	0,31	1,2	5,1	—	—	0,75	9,5	13
Ammonia	-78,8	11,4	0,0	0,19	6,3	—	—	0,094	4,6	50
Methanol	20	16,0	(0,2)	0,27	7,5	—	—	0,10	35	350
Water	30	10,6	<0	—	—	(0,005)	(250)	—	—	(50000)

* The experimental data cited [12-14] refer to low values of h , and therefore when K_1' is large the Equation (4) for multimolecular adsorption in this region reduces to Equation (1) for monolayer adsorption.

Fig. 4 shows the heats of adsorption of argon vapor, and the adsorption isotherms determined experimentally [12] and calculated from Equations (1) and (2). The initial net heats of a adsorption are $\sim 0.7 \text{ kcal/mole}$, exceeding the heat of condensation by about 45%. The net heats of adsorption increase with increasing h , reach a maximum value of 1.2 kcal/mole at $\theta = 0.6$, and then decrease. Interaction between adsorbate molecules produces an increase of 0.5 kcal/mole in the net heat of adsorption, $\sim 70\%$ of its initial value. The adsorption isotherms in the monolayer region are S-shaped. In Fig. 3, Curves 3 and 4, the experimental points of these isotherms are plotted in coordinates of Equation (1'); they are almost linear, although the agreement is less good than in the adsorption of nitrogen vapor (Fig. 3, Curves 1 and 2). Fig. 3, Curves 1 and 2, were used to find the constants K_1' and K_n given in the Table for the values $\omega_0 = 12.8 \text{ A}^2$ at -183° and 11.5 A^2

Fig. 5 shows experimental points [13] of the adsorption isotherms of krypton vapor at -183° and -195° , and also the calorimetric heats of adsorption at -183° [15]. The initial net heat of adsorption is ~ 1.5 kcal / mole; it then increases and at $h = 1.75 \cdot 10^{-3}$ ($\theta \approx 0.75$) reaches a maximum of 2.2 kcal / mole, after which it decreases.

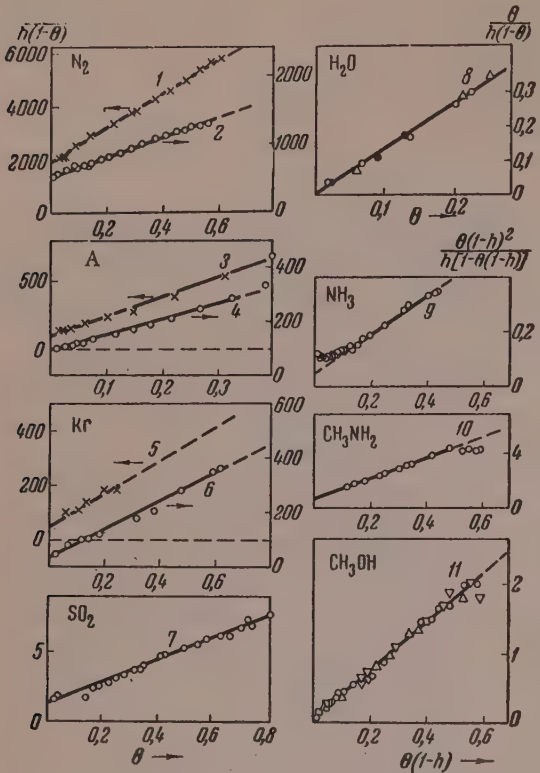


Fig. 3. Experimental data on the adsorption of vapors on graphitized carbon blacks, plotted in coordinates of Equations (1') and (4):
1 and 2) nitrogen at -195 and -183° ; 3 and 4) argon at -195 and -183° ; 5 and 6) krypton at -195 and -183° ; 7) sulfur dioxide at 0° ; 8) water at 30° ; 9) ammonia at -78.8° ; 10) methylamine at 0° ; 11) methanol at 20° .

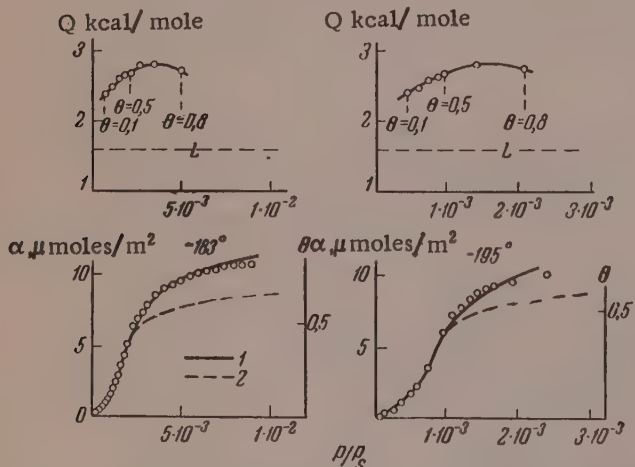


Fig. 4. Adsorption of argon vapor on P-33 graphitized carbon black.

Designations as in Fig. 1.

This increase of the net heat of adsorption is also the result of adsorbate-adsorbate interaction.

According to the papers cited [13, 15], the critical temperature of a two-dimensional krypton layer is about -190° . The adsorption isotherm is S-shaped at -183° (i.e., above the critical temperature) in the unimolecular region. It follows from Fig. 3, Curve 5 and from Fig. 5 that Equation (1), like Equation (2), represents the experimental isotherms for the adsorption of krypton vapor at this temperature over a narrow range of θ only. The constants of Equation (1), which is represented by a continuous line, were found from Curve 5, Fig. 3, for $\omega_0 = 14.5 \text{ \AA}^2$. Equation (1) does not correspond to the experimental isotherms over a wider range of θ in this case owing to the proximity to the critical temperature of the two-dimensional layer. In this case better results are given by Equation (3) with $K_1^* = 95$ and $a = 4$. The temperature -195° is below the critical value, and the adsorption changes discontinuously (Fig. 5); this indicates a first-order phase transition in the krypton monolayer. Equations (1) (see Fig. 5) and (2) (see [13]) do not describe this effect. Equation (3) indicates the existence of a phase transition in this case. Plots of this equation for the values $K_1^* = 50$; $a = 7$ and $K_1^* = 72.5$; $a = 8.3$ are given in Fig. 5, Curves 3 and 4.

In all other cases Equation (3) proved to be inapplicable: the experimental points for the adsorption of nitrogen, argon, and other substances studied did not fit on straight lines when plotted in $\ln \frac{\theta^*}{h(1-\theta^*)}$ and θ^* coordinates.

Fig. 6 shows curves of state for two-dimensional layers of krypton at -183 and -195° (above and below the critical temperature), calculated from the experimental adsorption isotherms by means of the Gibbs equation (see [1]). For comparison, a plot of the equation of state of an ideal gas monolayer at -183° is also given. Fig. 6 shows that krypton undergoes a two-dimensional phase transition at -195° .

Fig. 7 gives the adsorption isotherms for vapors of nitrogen [16], [17], argon [17], and krypton [15] in the region of higher h , where multimolecular adsorption is already appreciable in the case of nitrogen and argon. Calculation of the isotherms from Equation (4) with the values of the constants determined from the graphs (Fig. 3) for the region of monolayer filling gave a curve

close to the experimental points in the case of adsorption of nitrogen vapor. For adsorption of argon vapor, the calculated adsorption for $\omega_0 = 11.5 \text{ \AA}^2$ was considerably greater than the experimental values. However, if it is assumed that the packing of argon is looser in the second layer, then the calculated values for the adsorption are close to the experimental values with the same values of K_1' and K_n , when $\omega_0 = 14.7 \text{ \AA}^2$ (simple cubic packing). This confirms the hypothesis [12] relating to the change in the packing of the argon molecules in the adsorbed layer on carbon black.

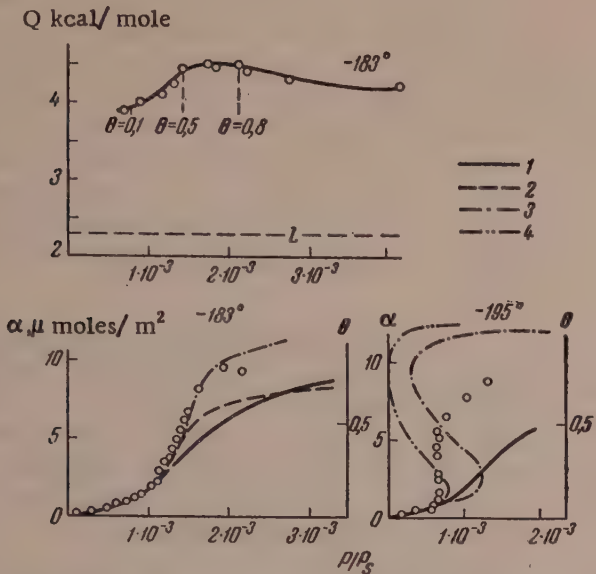


Fig. 5. Adsorption of krypton vapor on P-33 graphitized carbon black.

Above — differential heat of adsorption as a function of h at -183° [15]. Below — adsorption isotherms; the points represent experimental data [13], 1, and 2) calculated from Equations (1), (2); 3 and 4) calculated from Equation (3).

$$K_1' = 50; a = 7 \text{ and } K_1' = 72.5; a = 8.3.$$

(1) and (4), given in the Table, were found from Fig. 3, Curve 7, and the constants of Equation (2) were found from Fig. 9* for the value $\omega_0 = 13.8 \text{ \AA}^2$ **. It follows from Figs. 8 and 9 that the experimental data are in good agreement with Equations (1) and (2), since in this region of the isotherm $\theta < 1$. Calculation by Equation (4) gives high values for the adsorption when $h > 0.15$. It is probable that in this case, up to $h \approx 0.4$, multimolecular adsorption does not play any significant role. This allows of the use of different equations of state for the monolayer.

Fig. 10 shows the relationship between the surface pressure π of the monolayer and the area ω per molecule of SO_2 in the monolayer. It is seen that the curve calculated from the experimental isotherm by means of the Gibbs equation is close to the curve calculated from the equation of state [1]

$$\pi = RT\alpha_m \left[\frac{1}{K_n} \ln(1 + K_n\theta) - \ln(1 - \theta) - \theta \right], \quad (5)$$

which corresponds to the equation for the adsorption isotherm (1), and to the curve calculated from the equation

* Equation (2) gives a linear plot in W and h coordinates, where

$$W = \theta' / (1 - \theta') + \ln \theta' / (1 - \theta') - \ln h = \ln K_1' + K_2 \theta'. \quad (2')$$

** Calculation of a simple cubic packing by the formula $\omega = (M/\delta N)^{2/3}$, where M is the molecular weight; δ is the density; N is the Avogadro number, gives $\omega_0 = 13.0 \text{ \AA}^2$; better agreement with experimental data is obtained if θ is calculated with $\omega_0 = 13.8 \text{ \AA}^2$.

The adsorption isotherm for krypton on graphitized carbon black at low temperatures has a well-defined stepwise character [15, 18]. There is no smooth transition from adsorption in one layer to adsorption in the next. Accordingly, the experimental points between the first and second stepwise ascents of the isotherm are closer to the curve calculated from Equation (3) for monolayer adsorption. Equation (4), with constants K_1' and K_n determined from Fig. 3, Curve 6 for the monomolecular region, gives the best results for $\omega_0 = 16.5 \text{ \AA}^2$ which corresponds to less close packing.

Adsorption of sulfur dioxide vapor. Fig. 8 shows the heat of adsorption and adsorption isotherms of SO_2 vapor at 0° determined [19] for Spheron-6 carbon black graphitized at 2700° . The points denote the experimental data. The initial net heat of adsorption of SO_2 is close to the heat of condensation; it then increases sharply and reaches the maximum value of 1.5 kcal./mole at $h \approx 0.2$. The adsorption isotherm is S-shaped; it is concave at low values of h , passes through a point of inflection at $h \approx 0.15$, and becomes convex. Isotherms calculated from Equations (1), (2), and (4) are given in the same diagram. The constants of Equations

$$(\pi + a_2/\omega)(\omega - b_2) = kT, \quad (6)$$

in which the constant $a_2 = 0.48 \cdot 10^{-20}$ erg.cm²/(mole)² was found from the constant $K_2 = 2a_2/b_2 RT$ in the Hill adsorption isotherm equation (2) for $b_2 = \omega_0 = 13.8 \text{ \AA}^2$. For comparison the ideal condition Curve $\pi \omega = kT$ is shown in figure 10. The real curve lies below the ideal curve at high values of ω (forces of attraction predominate in the adsorbate-adsorbate interaction), crosses it near $\omega_0 = 20 \text{ \AA}^2$, and then lies above it (repulsion forces predominate). It is interesting that the maximum on the heat of adsorption curve (Fig. 9) corresponds to the similar value $\omega = 24 \text{ \AA}^2$. Since in this case the adsorption remains almost monomolecular, the increase and decrease of the heat of adsorption correspond to the predominance first of attraction and then of repulsion forces between the SO_2 molecules in the monolayer.

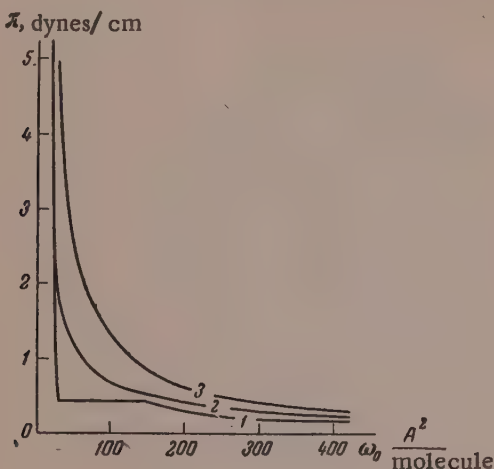


Fig. 6. Curves of state for krypton monolayers on graphitized carbon black.

1) At -195° ; 2) at -183° ; 3) calculated for the ideal state of the monolayer at -183° .

convex, passes through the second inflection point, and becomes concave again. A noteworthy fact is the very low adsorption of ammonia vapor (net heat of adsorption is roughly zero), and the sharp increase of adsorption on introduction of a methyl group into the molecule (the net heat of adsorption of methylamine increases with increasing adsorption, passing through a maximum when the monolayer is completed).

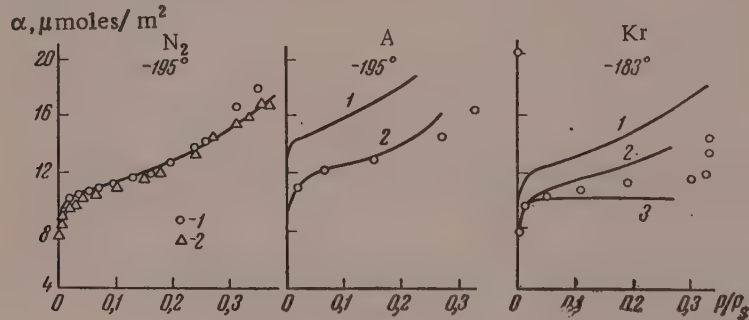


Fig. 7. Adsorption isotherms of vapors on graphitized carbon blacks in the region of h up to 0.4.

Points represent experimental values. Nitrogen: 1) [16]; 2) [17], curve calculated from Equation (4). Argon: points from [17], 1 and 2) from Equation (4) for $\omega_0 = 11.5$ and 14.7 \AA^2 . Krypton: points from [15], 1 and 2) from Equation (4) for $\omega = 14.5$ and 16.5 \AA^2 , 3) from Equation (3).

Curves 10 and 11 in Fig. 3 were used to find the constants K_1 and K_n in Equation (4) for $\omega_0 = 11.4 \text{ \AA}^2$ for ammonia,* and $\omega_0 = 16 \text{ \AA}^2$ ** for methylamine. Fig. 11 shows that Equation (4) fits the concave experimental

* Calculated for simple cubic packing.

** In accordance with the van der Waals dimensions of the CH_3 group and data for adsorption of methanol on graphite [21].

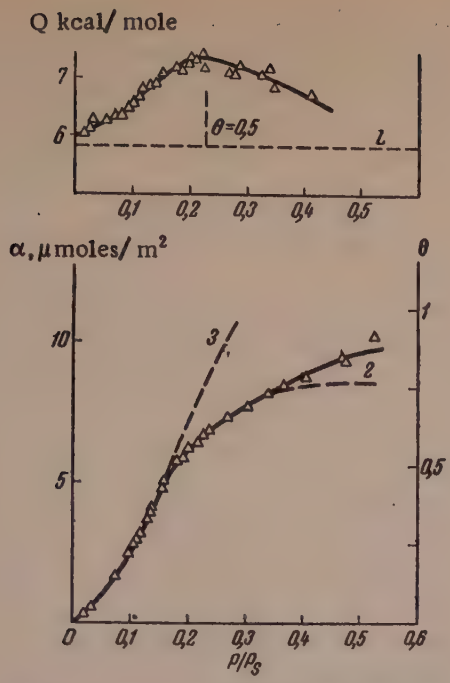


Fig. 8. Adsorption of SO_2 vapor on graphitized black.

Points represent experimental values [19]. Above — differential heat of adsorption as a function of h . Below — adsorption isotherms. 1, 2, 3) calculated from Equations (1), (2) and (4).

concave up to saturation. The net heats of adsorption of water vapor on graphitized carbon black are apparently

isotherm for adsorption of ammonia vapor up to $h \approx 0.55$, and the adsorption isotherm of methylamine vapor, with two inflection points, up to $h \approx 0.2$; subsequently the calculated values for the adsorption deviate from the experimental data because of the inaccuracies introduced by the assumptions that the equilibrium constants of the horizontal interactions [1] and vertical interactions in the second and subsequent layers [9] retain constant values. The Hill equation gives a satisfactory fit with the initial regions of these isotherms (Figs. 9 and 11).

It was shown earlier [1, 2] that when the constant K'_1 is small, Equation (4) approximates to the equation

$$\frac{h}{\theta(1-h)} \approx \frac{1}{K'_1} - \frac{K'_1 K_n + 1}{K'_1} h, \quad (7)$$

which is represented by a straight line with a negative slope in the coordinates of the linear form of the BET equation. The experimental adsorption isotherm of ammonia [20] is plotted in these coordinates in Fig. 12. Calculation of the constant K'_1 from this equation gives 0.095, which is close to the value found from Fig. 3, Curve 9, and Equation (4).

The adsorption of water vapor [22] (Fig. 11) is even less than that of ammonia; the isotherm remains

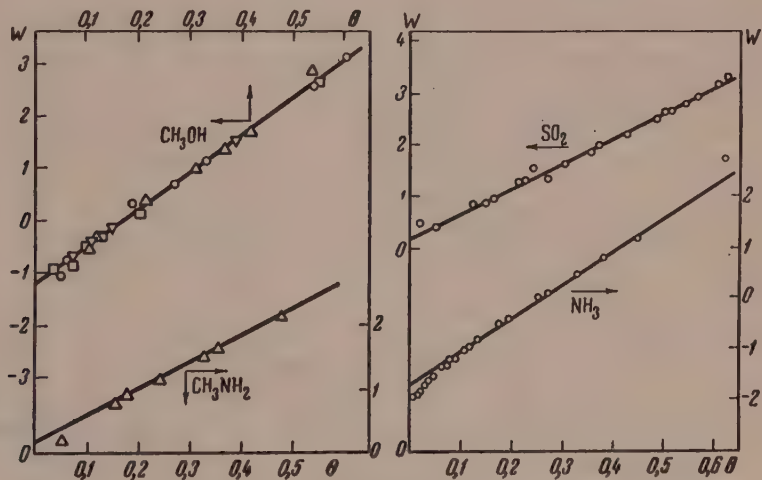


Fig. 9. Adsorption isotherms of vapors of CH_3OH , CH_3NH_2 , SO_2 and NH_3 on graphitized carbon blacks, in $W = \theta'/(1-\theta) + \ln \theta'/(1-\theta') - \ln h$ and θ' coordinates. Points represent experimental values.

initially negative [23, 24]. The values of θ are less than unity in all cases. Therefore the adsorption isotherm of water vapor is satisfactorily represented by Equation (1) for monolayer adsorption (Fig. 3, Curve 8). The value of w_0 was taken as 10.6 Å^2 for water ($\alpha_m = 15.5 \mu \text{ mole}/\text{m}^2$) [25]. The introduction of a methyl group into the water molecule (as into the ammonia molecule) greatly increases adsorption on graphite. The adsorption isotherm of methanol vapor [21, 22, 26] is concave at low values of h , passes through the first inflection point near $h \approx 0.2$,

and then becomes convex. At $h \approx 0.5$ ($\theta \approx 1$) it passes through the second inflection point and becomes concave again. The relationship between h and the heat of adsorption of methanol vapor on graphitized carbon black, plotted in Fig. 11, was calculated from the data of Millard et al. [26]. The experimental points are not given in their paper. In our opinion, the portion of the curve represented by the dash line is too high. The variation of the heat of adsorption of methanol with h should be analogous to the corresponding variation in the adsorption of methylamine [20].

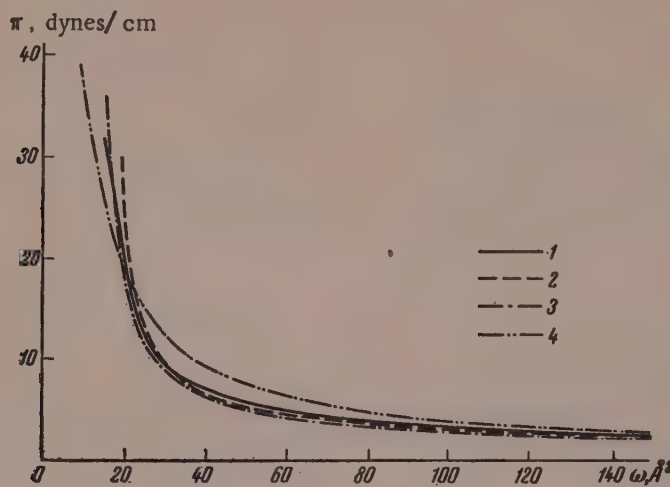


Fig. 10. Curves of state of a monolayer of SO_2 on graphitized carbon black: 1) from experimental isotherm; 2) from Equation (2); 3) from Equation (1); 4) for the ideal state.

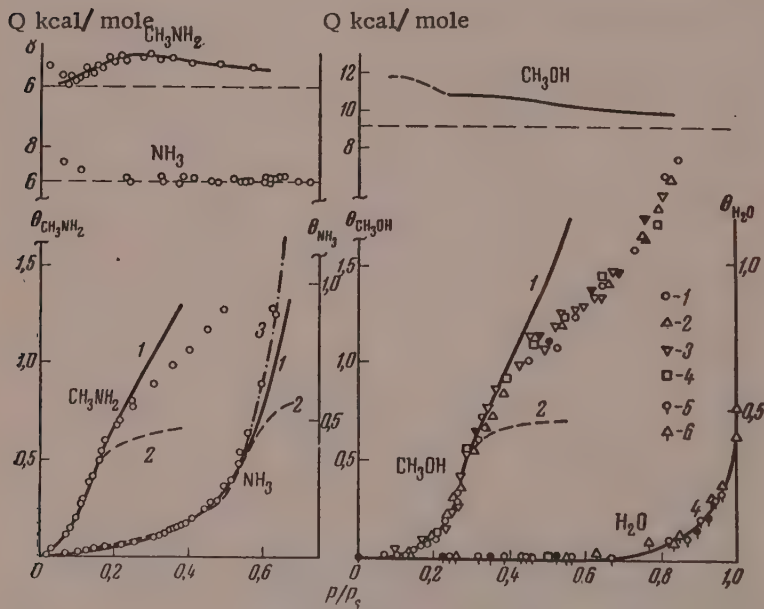


Fig. 11. Adsorption of NH_3 , CH_3NH_2 , H_2O , and CH_3OH vapors on graphitized carbon blacks.

Above — differential heats of adsorption as functions of h ; below — adsorption isotherms. Points represent experimental values for NH_3 [20], CH_3NH_2 [20], H_2O — 5, 6 [22] and CH_3OH — 1, 2 [21], 3 [22], 4 [26]. Curves 1 and 2 calculated from Equation (4) and (2); Curve 3, from Equation (7); Curve (4), from Equation (1).

Adsorption isotherms of methanol vapor calculated from Equations (4) and (2) are plotted in Fig. 11. The constants of these equations, given in the Table, were determined graphically (Fig. 3, Curve 11, and Fig. 9), ω_0 for methanol being taken as 16 A^2 [21].*

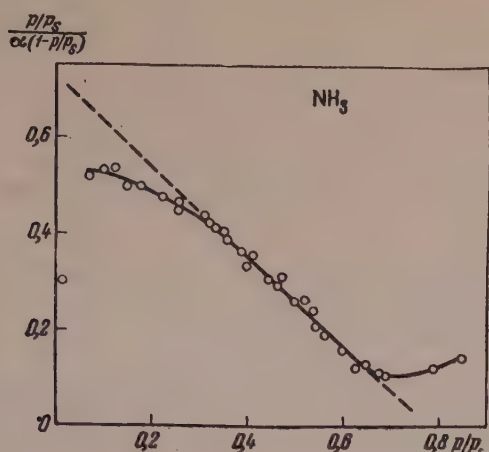


Fig. 12. Isotherms for the adsorption of NH_3 vapor on graphitized carbon black, in coordinates of Equation (7). The points represent experimental values [20].

It follows from Fig. 11 that the experimental adsorption isotherm of methanol vapor gives a satisfactory fit with the equation for multimolecular adsorption (4) up to $h \approx 0.4$. At higher values of h the calculated isotherm lies above the experimental curve for the same reasons as in the case of methylamine. Moreover, in the adsorption of methylamine and methanol, complications may arise owing to changes of their molecular orientation [28].**

The round values of the constants in Equations (1), (2), and (4) for the cases under consideration are given in the Table. Since the equilibrium constants depend very much on the temperature, their values can be compared only for groups of substances studied at similar temperatures. Nevertheless, the general course of the K_{B}/K_1^* ratio in the transition from adsorption of hydrocarbons and nitrogen, to the adsorption of ammonia and water, is quite clear.

SUMMARY

1. Equations for isotherms for uni- and multimolecular adsorption on homogeneous surfaces, with adsorbate-adsorbate interaction in the first layer taken into account, were applied to literature data on the adsorption of various vapors on graphitized carbon blacks.
2. The approximate Equations (1) and (4) agree satisfactorily with these experimental isotherms in the region of unimolecular adsorption and at the start of multimolecular adsorption (above the critical temperature of the monolayer).
3. As adsorbate-adsorbent interaction weakens and adsorbate-adsorbate interaction relatively increases, the isotherms change their shape, from convex in the initial region, with one point of inflection (normal alkanes), to initially concave with two points of inflection (nitrogen, argon, krypton, sulfur dioxide, methylamine, methanol), and then to concave throughout, without inflections (water). The adsorption isotherm of ammonia is concave over a considerable range of relative vapor pressures.

The authors express their deep gratitude to N. N. Avgul' for help in the calculations and for valuable advice in the discussion of the results.

The M. V. Lomonosov State University, Moscow
Adsorption Laboratory and Institute of Physical
Chemistry, Academy of Sciences USSR
Laboratory of Sorption Processes

Received February 24, 1958

LITERATURE CITED

- [1] A. V. Kiselev, Colloid J. 20, 338 (1958).***

* The values of ω_0 for water and methanol (as for other similar molecules) greatly depends on the nature of the adsorbent; with a hydrated silica surface, the values of ω_0 for water and methanol is determined by the positions of the hydroxyl groups, and is $\sim 25 \text{ A}^2$ [27].

** Barrer and Stuart [29] represented the adsorption of methanol on graphite by an equation, derived by methods of statistical thermodynamics, for localized adsorption with mutual coordination of the adsorbate molecules.

*** Original Russian pagination. See C. B. Translation.

- [2] A. V. Kiselev, Proc. Acad. Sci. USSR 117, 103 (1957).*
- [3] A. V. Kiselev, Vestnik Akad. Nauk SSR 43, No. 10 (1957).
- [4] N. N. Avgul', G. I. Berezin, A. V. Kiselev, and I. A. Lygina, Bull. Acad. Sci. USSR, Div. Chem. Sci. (in the press).**
- [5] T. Hill, J. Chem. Phys. 14, 441 (1946).
- [6] F. Fowler and E. Guggenheim, Statistical Thermodynamics (Russian translation) (IL, 1949).
- [7] A. V. Kiselev and D. P. Poshkus, Bull. Acad. Sci. USSR, Div. Chem. Sci. No. 3, 520 (1958).*
- [8] S. Brunauer, P. H. Emmett and E. Teller, J. Amer. Chem. Soc. 60, 309 (1938); S. Brunauer, The Adsorption of Gases and Vapors (Russian translation) (IL, 1948).
- [9] N. N. Avgul', G. I. Berezin, A. V. Kiselev, and I. A. Lygina, J. Phys. Chem. 30, 2106 (1956).
- [10] N. N. Avgul', G. I. Berezin, A. V. Kiselev, and I. A. Lygina, Bull. Acad. Sci. USSR, Div. Chem. Sci. No. 9, 1021 (1957).*
- [11] N. N. Avgul', A. A. Isirikian, A. V. Kiselev, I. A. Lygina, and D. P. Poshkus, Bull. Acad. Sci. USSR, Div. Chem. Sci. No. 11, 1314 (1957).*
- [12] S. Ross, W. Winkler, J. Colloid Sci. 10, 319 (1955).
- [13] S. Ross, W. Winkler, J. Colloid Sci. 10, 330 (1955).
- [14] D. Graham, J. Phys. Chem. 61, 1310 (1957).
- [15] C. H. Amberg, W. B. Spencer and R. A. Beebe, Canad. J. Chem. 33, 305 (1955).
- [16] A. V. Kiselev, and E. V. Khrapova, Bull. Acad. Sci. USSR, Div. Chem. Sci. No. 4, 389 (1958).*
- [17] M. H. Polley, W. D. Shaeffer and W. R. Smith, J. Phys. Chem. 57, 469 (1953).
- [18] H. Clark, J. Phys. Chem. 59, 1068 (1955).
- [19] R. A. Beebe, and R. M. Dell, J. Phys. Chem. 59, 746 (1955).
- [20] R. M. Dell, R. A. Beebe, J. Phys. Chem. 59, 754 (1955).
- [21] C. Pierce, and R. N. Smith, J. Phys. Coll. Chem. 54, 374 (1950).
- [22] A. V. Kiselev and N. V. Kovaleva, J. Phys. Chem. 30, 2775 (1956); A. V. Kiselev and N. V. Kovaleva, Bull. Acad. Sci. USSR, Div. Chem. Sci. (in the press).**
- [23] C. J. Young, J. J. Chessick, F. H. Healey and A. C. Zettlemoyer, J. Phys. Chem. 58, 313 (1954).
- [24] B. Millard, E. G. Gaswell, E. E. Leger, and D. R. Mills, J. Phys. Chem. 59, 976 (1955).
- [25] N. N. Avgul', O. M. Dzhigit, and K. D. Shcherbakova, Proc. Acad. Sci. USSR 92, 105 (1953).
- [26] B. Millard, R. A. Beebe, and J. Cynarsky, J. Phys. Chem. 58, 468 (1954).
- [27] L. N. Soboleva and A. V. Kiselev, J. Phys. Chem. 32, 49 (1958).
- [28] N. N. Avgul', O. M. Dzhigit, A. V. Kiselev and K. D. Shcherbakova, Proc. Acad. Sci. USSR 92, 1185 (1953).
- [29] R. M. Barrer, and W. J. Stuart, J. Chem. Soc. 3307 (1956).

*Original Russian pagination. See C. B. Translation.

**See C. B. Translation.

SECONDARY EFFECTS ON PRECIPITATION CHROMATOGRAMS OF VARIOUS COMPOUNDS

V. D. Kopylova and K. M. Ol'shanova

Changes in the chromatograms with time are more common in precipitation chromatography than in other types of chromatographic analysis [1]. These changes, which have been termed secondary effects, consist mainly of the following effects: zone boundaries become leveled out, new zones are formed, in some cases the zones move down and sometimes up the column; the initial zone splits into a number of rings; the color intensity increases, and the colors of the zones may change in some cases, etc. The nature of the changes in precipitation chromatograms in the course of time depends on the experimental conditions, including the concentration of the precipitant, the concentration of the test solution, the presence of impurities in it, the method used for formation of the chromatogram, and the temperature.

Time changes are more common in precipitation chromatograms than in other types of chromatograms (molecular, ion-exchange chromatograms) because the columns used in precipitation chromatography are more complex in composition, consisting of a mixture of two mutually inert substances — carrier and precipitant [2]. Therefore the formation of a chromatogram in a column of this type depends on numerous factors, and side effects are liable to be more frequent and more complex than in other forms of chromatographic analysis.

No data are available in the literature which would account for the changes in precipitation chromatograms with time, although this question is important both from the practical and from the theoretical standpoints.

For a detailed elucidation of the laws governing the changes in precipitation chromatograms with time, a study was made of secondary effects in the precipitation chromatograms of phosphates, chromates, and hydroxides of various cations, and of a number of other precipitates, in relation to the experimental conditions (composition of the column, composition and concentration of the test solution and precipitant, method used for preparation of the chromatogram, and the temperature of the experiment). Changes in the precipitation chromatograms and variations of the distribution of the precipitated ion and precipitant along the column, as functions of the above-named factors, were studied visually. The most important of the results obtained are presented in this paper.

METHOD

With the use of radioactive tracers. A mixture of carrier and precipitant was packed carefully into a tube of transparent water-impermeable polyvinyl chloride film, ~0.1 - 0.2 mm thick, 12 cm long, and 0.5-0.6 cm in diameter, blocked with cotton wool at the lower end. 0.2 ml of distilled water was introduced into the column, followed by a definite volume of the test solution. Primary chromatograms were obtained in 6-8 columns simultaneously. The radioactive isotope was introduced either into the precipitant or into the test solution, according to the problem under investigation. The distribution of the tracer isotope along the column was observed 2, 24, 48, 72, 96, and 144 hours after the end of percolation of the test solution. The chromatogram was cut into portions 2-3 mm long. Each portion was dried to constant weight, weighed to the nearest 0.001 g, transferred to an aluminum plate, powdered thoroughly, and spread over an area of 1.5 cm^2 . The radiation intensity of each layer of the column was measured by means of a counter. The results were used to calculate the number of meq of the tagged substance per 100 mg of dry column material, and the amounts of substance (in meq per 100 mg of column material) were plotted against the weight of the zone (in mg), to give distribution curves of the substance along the column, with the top of the column corresponding to the coordinate origin.

Without radioactive tracers. In a number of cases the investigations were performed without the use of radioactive isotopes. The experimental procedure was the same as with the use of tracers, but the chromatograms were not cut; the lengths of the zones of colored precipitates were measured to the nearest 0.5 mm, and the color of the zone was recorded (usually by drawing).

The time changes in precipitation chromatograms of hydroxides, phosphates, chromates, and other compounds were studied for most of the individual cations of the 3rd and 4th analytical groups, and for mixtures of two or more cations from these groups.

The first series of experiments showed that the following are the most characteristic time changes in the majority of the precipitation chromatograms.

1. Leveling of the zone boundaries in the chromatograms.

2. Increase of the initial zone length. This is often accompanied by the appearance of a new zone under the lower boundary of the chromatogram, with a similar color (but somewhat lighter or darker) to the color of the zone in the primary chromatogram.

3. Change of the color of the chromatogram as the result of various oxidation-reduction reactions (this is especially characteristic of hydroxides).

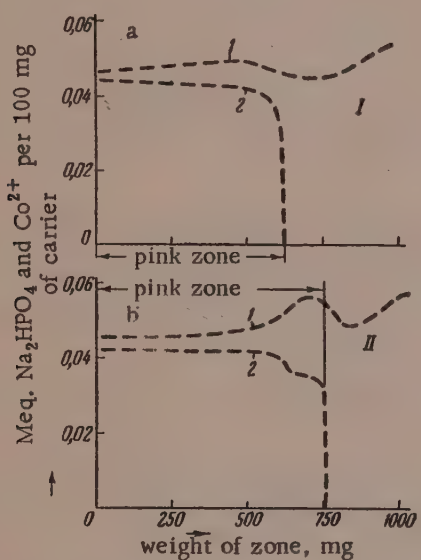


Fig. 1. Time changes in the distribution of precipitant (Na_2HPO_4) and precipitated ion (Co^{2+}) along the column, after the end of percolation of the solution:
I) distribution of the precipitant, HPO_4^{2-} (0.5 meq/1 g of carrier); II) distribution of the Co^{2+} ion (0.2 g-equiv./liter);
1) after 4 hours; 2) after 48 hours.

3. Changes in the precipitation chromatograms become more rapid with increase of temperature.

For elucidation of the mechanism by which the precipitation chromatograms change, tagged P^{32} , Co^{65} , Fe^{59} , Hg^{203} atoms were used to determine the course of the distribution of precipitant and precipitated ion along the column with time, as functions of the concentrations of the precipitant and the precipitated ion, and of the experimental temperature.

The experimental results show that:

1. The distributions of the precipitated ion and precipitant along the column vary with time (Fig. 1). These variations directly depend on the experimental conditions and produce the visible changes in the precipitation chromatograms.

In some instances the precipitate moves down the column. If a precipitate in the upper zone migrates, a zone of pure carrier is formed at the top of the chromatogram; if a precipitate occupying an intermediate or the lowest position in the chromatogram migrates, a zone of pure carrier is formed between the precipitates. In our experiments, zones of pure carrier were formed only in the precipitation chromatograms of the hydroxides of the following cations: Fe^{2+} , $\text{Fe}^{2+}-\text{Cu}^{2+}$, $\text{Fe}^{2+}-\text{Hg}^{2+}$. In the first and second cases the $\text{Fe}(\text{OH})_2$ zone moved downward and a zone of pure carrier was formed in the upper part of the chromatogram; in the third case the lower $\text{Fe}(\text{OH})_2$ zone moved down the column, while the HgO zone remained at the top of the chromatogram, so that zone of pure carrier was formed between them.

The results showed that the experimental conditions influence the time changes in the precipitation chromatograms as follows.

1. As the precipitant concentration increases, the rate of change of the initial zone length and the rate of leveling of the zone boundaries both decrease; the rate of change of the color of the chromatogram increases.

2. Increase of the concentration of the test solution increases the rates of boundary leveling and change of zone length in the primary chromatogram.

2. The variation of the distribution of the precipitant along the column usually consists of its movement (diffusion) up the column. Increases of the precipitant concentration and temperature usually accelerate migration of the precipitant (Fig. 2).

3. The concentration of the precipitated ion decreases with time along the zone (roughly uniformly along the whole length of the zone), so that the length of the initial zone increases. The newly-formed part of the zone may be more dense (with amorphous precipitates) or less dense (with crystalline precipitates) than the initial zone (Fig. 3). Thus, the visible changes in precipitation chromatograms are directly related to the processes taking place within the column (displacement of the precipitant and the precipitated ion, migration of the precipitate). In our opinion, the leveling of the boundaries and increase of the zone lengths in the initial chromatograms are mainly the results of diffusion of the precipitated ion present in the pores of the carrier, and of partial creeping of the precipitate down the column. This is shown by the time decrease of the concentration of the ion in the initial zone, and its presence in the newly-formed part of the zone (Figs. 1 and 3).

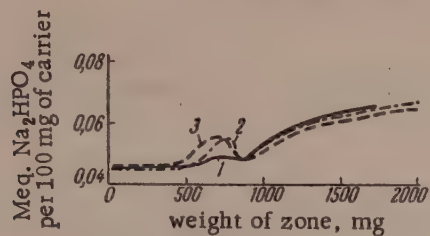


Fig. 2. Effect of temperature on displacement of the precipitant along the column:

- 1) after 4 hours; 2,3) after 48 hours;
- 2) at 20°; 3) at 40°. Precipitant — Na_2HPO_4 (0.5 meq/1 g of carrier).
- Precipitated ion — Co^{2+} (0.2 g-equiv./liter).

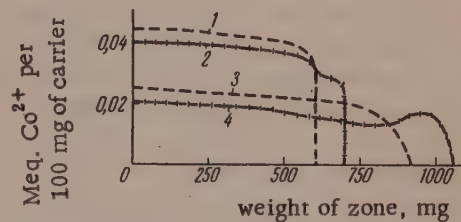


Fig. 3. Time variations of the distribution of different precipitates along the column:

- 1, 2) precipitate of $\text{Co}_3(\text{PO}_4)_2$; 3, 4) precipitate of cobalt rubeanate; 1, 3) 4 hours after end of percolation of the solution; 2, 4) after 48 hours.

The microstructure of the precipitate determines which of these factors prevails. Thus, if the precipitates are colloidally dispersed, their adhesion to the carrier is low, and they creep down the column (as in the precipitation chromatograms of hydroxides, ferricyanides, and some other precipitates). The density is usually higher in the newly-formed part of the zone than in the initial zone, and the former is considerably brighter in color. The first factor is predominant in the formation of precipitation chromatograms with crystalline precipitates (chromates, phosphates, and some other compounds). Moreover, recrystallization of crystalline precipitates is of great significance. The density of the precipitate is usually less in the newly-formed part of the zone than in the primary zone. The occasional creeping of the precipitate and formation of a zone of pure carrier are generally characteristic of amorphous precipitates, and are in all probability the consequence of low "adhesion" of the colloidal precipitate to the carrier.

In addition to the above factors, diffusion of the precipitant and the precipitated ion along the column is of great significance (Fig. 1). The rate and direction of diffusion are determined by Fick's first and second laws, and depend on the nature of the precipitant, its concentration, and the temperature. Diffusion of the precipitant is especially important when it is present in high concentrations, and at high temperatures. The time variations in the color of the zones in the chromatogram are caused by various oxidation-reduction processes.

The rates at which the zone length varies and the boundaries are leveled decrease with increasing concentration of precipitant, as for a given concentration of the test solution the density of the precipitate formed increases and its tendency to migrate diminishes. Diffusion of the test solution downward out of the pores of the carrier leads to leveling of the lower boundary and to lengthening of the zone, the latter being greater at lower precipitant concentrations. Moreover, as the precipitant concentration increases, its ions diffuse at a greater rate in a direction opposite to the displacement of the precipitate and the test solution, so that these processes are retarded and the zone length changes at a lower rate.

Increase of the concentration of the test solution results in an increase in the number of ions of this solution present in the carrier pores. Downward diffusion of the ions results in leveling of the boundary and increase of the

zone length, at increasing rates with increasing concentration of these ions in the solution, as this increases the amount of precipitate formed from the solution present in the carrier pores. In the case of colloidal precipitates, increase of the rate of diffusion of the ions being precipitated results in their creeping down the column more rapidly, which also increases the zone length. With crystalline precipitates, the higher the concentration of the test solution, the smaller are the crystals initially formed. In the course of time, recrystallization of the precipitates takes place in the chromatogram, and as a result the newly-formed crystals are distributed over a considerably greater length than in the primary chromatogram. The increase of zone length as the result of this process is proportional to the concentration of the test solution. Variations of the temperature cause changes in the rates of diffusion and the chemical reactions, which naturally influence the time variations in the precipitation chromatograms.

In conclusion, it must be pointed out that the results of these investigations not only reveal the nature of the processes which cause secondary effects in precipitation chromatograms in a number of cases, but also make it possible to regulate these processes by variation of the conditions for the formation of precipitation chromatograms. Furthermore, the above considerations may often be used to account for secondary effects in molecular and ion-exchange chromatograms. Thus, leveling of zone boundaries and lengthening of the zones with time can be attributed to diffusion of the solution present in the carrier pores, and to changes of the equilibrium conditions of adsorption or ion exchange along the column. If the development of an ion-exchange chromatogram involves the formation of a precipitate, then in many cases the time changes in such (developed) chromatograms are analogous to the changes observed in precipitation chromatograms.

SUMMARY

1. The changes which occur in time in precipitation chromatograms of hydroxides, phosphates, chromates, and other compounds in relation to the experimental conditions (temperature, concentrations of precipitant and test solution) have been studied.

2. As a rule, changes in the precipitation chromatograms occur as the result of diffusion of the solution down the column, partial creeping and recrystallization of the precipitate, and various oxidation-reduction reactions.

The Moscow Technological Institute
of the Meat and Dairy Industries

Received February 25, 1957

LITERATURE CITED

- [1] E. N. Gapon and I. M. Belen'kaia, Colloid J. 14, 323 (1952).*
- [2] V. D. Kopylova, Trans. Moscow Technol. Inst. Meat and Diary Ind. 8, 149 (1958).

*Original Russian pagination. See C. B. Translation.

EFFECT OF THE DENSITY OF POLYTRIFLUOROCHLOROETHYLENE ON DIELECTRIC LOSS

G. P. Mikhailov, B. I. Sazhin, and V. S. Presniakova

In studies of the influence of the crystallization of polymers on their physical properties, use is generally made of the concept of the "degree of crystallinity," which represents the volume or weight fraction of the substance present in the crystalline regions. The degree of crystallinity (X) is a very arbitrary characteristic; for example, for dilatometric determination of X it is necessary to know the densities of the amorphous and crystalline regions of the polymer, and the first region is often determined by linear extrapolation, to room temperature, of the melt volume - temperature relationship, while the latter is determined from x-ray and electron diffraction data. Both these methods are often inaccurate and unreliable. Indeed, the $V = \phi(X)$ relationship may be nonlinear over a wide range of temperatures. On the other hand, the formal application to polymers of the theory of x-ray scattering, developed for low-molecular crystals, sometimes leads to erroneous conclusions concerning polymer structure. Moreover, in calculations of X it is generally assumed that the polymer may be regarded as a mechanical mixture of amorphous and crystalline regions, and the existence of regions of intermediate degrees of order is not taken into consideration. All this shows that the so-called degree of crystallinity is a conventional characteristic which does not reflect a number of details of polymer structure; nevertheless, this concept is widely used in studies of polymer properties and in their practical utilization.

The dilatometric, optical, and x-ray methods are used for determination of the degree of crystallinity. The use of heat capacity and nuclear magnetic resonance methods for this purpose has been reported. In all these methods determination of X depends on the fact that crystallization changes many physical properties of polymers.

It has been shown in a number of papers [1, 2] that polymer crystallization has a significant influence on dielectric loss and the dielectric constant, and also on the variations of these quantities with temperature and frequency. However, the influence of crystallinity on dielectric properties was investigated only qualitatively. The literature contains no reports of studies of the quantitative relationships between the dielectric properties and the crystallinity of polymers. However, the question is one of considerable interest. If a definite relationship exists between the degree of crystallinity of a polymer and, say, the dielectric loss, the degree of crystallinity could be determined by means of relatively simple dielectric measurements; i.e., the degree of crystallinity could be determined by a dielectric method.

The present paper deals with a study of the influence of the density of polytrifluorochloroethylene (F-3) on its dielectric loss, carried out in order to determine the possibility of using a dielectric method for determination of the degree of crystallinity of this polymer.

It was shown earlier that two types of relaxation dielectric loss occur in F-3: high-frequency relaxation loss (HFR), at temperatures below t_g , and medium-frequency relaxation loss (MFR), at $t > t_g$ [1]. It was also shown that $\tan\delta$ decreases in both loss regions in chilled specimens after annealing; i.e., that crystallization of F-3 is accompanied by a decrease of $\tan\delta$. In studies of the effect of density on the dielectric loss it is possible in principle to measure $\tan\delta$ in both the HFR and the MFR regions. However, in the latter case it proved necessary to heat the specimens above t_g . This might have resulted in additional crystallization in specimens of low crystallinity. Therefore $\tan\delta$ for F-3 specimens of different densities was measured in the HFR region, and the temperature of the specimens during the experiments did not exceed 110-120°. There were no appreciable changes in the degree of crystallinity of the specimens under these conditions.

The degree of crystallinity (X) of F-3 was calculated from the formula:

$$X = \frac{V_a - V}{V_a - V_c} = \frac{\rho_c (\rho - \rho_a)}{\rho (\rho_c - \rho_a)}, \quad (1)$$

where V , V_a , and V_c are the specific volumes of the specimen and of the amorphous and crystalline phases of the polymer respectively; ρ , ρ_a , and ρ_c are the corresponding densities.

The densities of the specimens were determined by the hydrostatic-weighing method. An analytical balance type ADV-200 was used; specimens in the form of films 18 or 100 μ thick and 1-3 g in weight were weighed in distilled water at room temperature.

The Table includes the results of repeated determinations of the density of Specimen 4; it is seen that the absolute error in determinations of ρ is ± 0.0006 g/cc, i.e., that the relative error in determinations of $\Delta\rho/\rho$ is approximately $\pm 0.03\%$.

Calculations of the Degree of Crystallinity. Values of (X) for Specimens of Polytrifluorochloroethylene of Different Density at 19°

Specimens	ρ , g/cc	$\Delta\rho$, g/cc	$\tan \delta_m \cdot 10^2$	X , %	Specimens	ρ , g/cc	$\Delta\rho$, g/cc	$\tan \delta_m \cdot 10^2$	X , %
1	2,0886	0,0001	5,55	29	5	2,1200	0,0005	4,66	43,5
2	2,0906	0,0004	5,48	30	6	2,1237	0,0001	4,63	45
3	2,1004	0,0002	5,38	34	7	2,1270	0,0020	4,18	46,5
4	2,1110	0,0003			8	2,1398	0,0005	3,77	52,5
	2,1121	0,0014			9	2,1420	0,0020	3,84	53
	2,1107	0,0000			10	2,1465	0,0005	3,58	55
	2,1101	0,0006			11	2,1497	0,0003	3,53	57
	2,1114	0,0007	5,06	39	12	2,1511	0,0005	3,44	57,5
	2,1097	0,0010			13	2,1511	0,0006	3,34	57,5
	2,1102	0,0005			14	2,1614	0,0005	3,20	62
	2,1107	0,0000			15	2,1645	0,0005	3,20	64

F-3 was subjected to special heat treatment to give specimens of different densities, the density difference being up to 3%, so that the hydrostatic-weighing method was suitable for recording density variations of the specimens with a large margin of sensitivity.

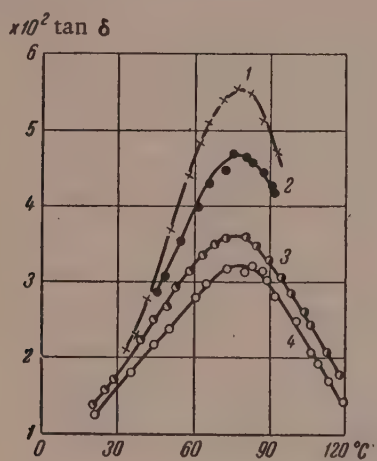


Fig. 1. Variation of the high-frequency relaxation dielectric loss of F-3 with temperature at 80 kilocycles; 1) Specimen 1, $\rho = 2,0886$ g/cc; 2) Specimen 5, $\rho = 2,1200$ g/cc; 3) Specimen 10, $\rho = 2,1465$ g/cc; 4) Specimen 15, $\rho = 2,1645$ g/cc.

The values of $\rho_a = 2.03$ g/cc and $\rho_c = 2.25$ g/cc, required for calculations of crystallinity with the aid of Formula (1), were taken from published papers [3].

The variations of $\tan \delta$ with temperature for four specimens of F-3 of different densities are plotted in Fig. 1. It is seen that at a frequency of 80 kilocycles all the specimens show maximum dielectric loss at 78°. $\tan \delta$ decreases with increasing density, this decrease being most prominent in the region of maximum $\tan \delta$. For example, whereas for Specimen 1 $\tan \delta_m = 5.5 \cdot 10^{-2}$, for Specimen 15 $\tan \delta_m = 3.2 \cdot 10^{-2}$. These data apply to the specimens with the greatest crystallinity difference. The results of determinations of density and $\tan \delta_m$ for thirteen other specimens with intermediate values of ρ and X are given in the Table, and some also in Fig. 1.

Fig. 2 (Curve 1) shows the variation of $\tan \delta_m$ with the density of F-3 in the region of maximum HFR at 80 kilocycles. It is seen that $\tan \delta_m$ decreases regularly with increasing density. For most of the specimens the deviations do not exceed 2% of $\tan \delta$ or 0.1% of the density. These results show that the dielectric loss in

the region of maximum HFR bears an almost definite relationship to the density of the polymer.

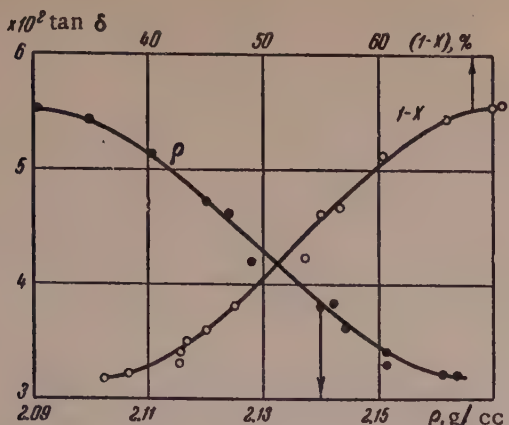


Fig. 2. Variations of $\tan \delta_m$ in the region of maximum high-frequency relaxation loss of F-3 at 80 kilocycles, with the density ρ and the content of the amorphous phase $(1 - X)$.

dielectric method could probably be used for determination of the degree of crystallinity of rubber, polyethylene terephthalate, etc. Indeed, it has been shown that the values of ϵ' and $\tan \delta$ in these polymers decrease on crystallization, so that the densities and crystallinities of these polymers may be determined for measurement of $\tan \delta$ with the aid of calibration graphs similar to Fig. 2. Of course, this method would be most successful for polar polymers, in which impurities have less influence on ϵ' and $\tan \delta$ than in nonpolar substances.

SUMMARY

1. It was shown by determinations of the density and dielectric loss of polytrifluorochloroethylene that in the region of maximum dielectric loss $\tan \delta$ decreases regularly with increasing density, and is almost directly proportional to the content of the amorphous substance.

2. The dielectric method can be used for determinations of the degree of crystallinity of this and some other polymers.

The M. I. Kalinin Polytechnic Institute
Leningrad

Received April 3, 1957

LITERATURE CITED

- [1] G. P. Mikhailov and B. I. Sazhin, J. Theoret. Phys. 26, 1723 (1956).
- [2] G. P. Mikhailov, J. Theoret. Phys. 21, 1395 (1951); G. P. Mikhailov and B. M. Fainshtein, J. Theoret. Phys. 22, 5 (1952); G. P. Mikhailov, A. M. Liubanov, and B. I. Sazhin, J. Theoret. Phys. 24, 1553 (1954).
- [3] Sasamu, Povuga, Masakasa and Honda, J. Polymer Sci. 20, 96, 587, (1956); J. Nichdes, J. Appl. Phys. 25, 840 (1954).

Curve 2 in Fig. 2 represents the variations of $\tan \delta_m$ with the content of the "amorphous" phase $(1 - X)$ in F-3. The degree of crystallinity was calculated from Equation (1), with the values of ρ , ρ_a and ρ_c given above; the calculated values of X are given in the Table. It follows from the data in Fig. 2 that the dielectric loss of F-3 is roughly in direct proportion to the content of the amorphous phase. This, together with earlier data [1], shows that the HFR loss in F-3 is due to processes in the amorphous regions. The decreases of ϵ' and $\tan \delta$ of F-3 on crystallization are probably the results of transition of some macromolecular segments from the amorphous into the crystalline regions, with corresponding changes in the relaxation times for these regions.

It follows from our results that the degree of crystallinity of F-3 can be determined by means of relatively simple measurements of dielectric loss. The

SOME EXPERIMENTAL STUDIES OF THE PHYSICAL CHEMISTRY OF STARCH

V. I. Nazarov, N. P. Silina, and T. P. Tikhomirova

The effects of temperature and of electrolyte solutions on the behavior of starch grains are considered in this paper. It is known that starch grains consist mainly of polymeric carbohydrate chains of varying degrees of branching. A number of starch properties, such as the gelatinization temperature, depend on the internal structure of the grains and on the nature and stability of the bonds between the individual components of the starch grain. Hydrogen bonds play an important part in the formation of a stable internal structure in starch grains [1, 2].

Effect of temperature on the properties of starch. Without considering the question of gelatinization of aqueous starch suspensions, let us examine certain data on the influence of preliminary heating of air-dry potato starch on the gelatinization temperature.

Effect of Time of Heating at 100° on the Gelatinization Temperature of Potato Starch

Heating time, hours	0	1	2	3	4	5
t_{gel} , degrees	72.0	71.5	70	68.5	64.0	63

curves which was observed by Rakovskii was undoubtedly caused by changes in the stability of the intermolecular bonds which determined the original internal structure and the physicochemical properties of the starch grains. We studied the effect of the time for which air-dry potato starch was heated at 100°, on its gelatinization temperature (t_{gel}). The heating curves of aqueous suspensions, recorded by means of the Kurnakov pyrometer, show (Fig. 1) that the gelatinization temperature decreases with increase of the duration of the preliminary heating (see Table).

The temperature chosen for the preliminary heating of starch was 100°, so that deeper changes in the inner structure of the grain were unlikely. It was assumed that the effect of the heating was to weaken the bonds in the internal structure of the starch grains, with a consequent lowering of the gelatinization temperature.

After removal of almost the last traces of water at 120°, further increase of temperature produces more serious changes in the internal structure of starch grains, accompanied by a number of diverse chemical processes (including dextrinization). This has been clearly shown, for example, by Ulmann [5].

Effect of electrolytes on the properties of starch. The question of interaction of ions with starch is of great theoretical and practical interest. The nature of the ions bound with starch often has a distinct influence on some of its physicochemical properties. For example, Dumanskii [6] showed that the water-binding capacity of starch depends on the nature of the cations present. It is also known that starch is an ion exchanger. Ion exchange in starch can be clearly demonstrated [7].

To prepare starch containing definite cations, it is first necessary to treat it with acid in order to exchange the cations in it for hydrogen ions, and then to treat it with a solution of a salt in order to replace the hydrogen ions by the cations in question.

The results of filtration analysis lead to the following conclusion. Although the number of ions bound with the starch is very small, their influence on filtration and moisture retention is quite clear. Ions of metals of the

Rakovskii [3] considered that 120° is a certain limiting temperature at which starch, without changing visibly, is capable of losing all the water contained in it. It was shown by one of us (jointly with Nikolaev) [4] by a thermographic method that most of the bond water in starch is lost at about 107°. The displacement of the hydration and dehydration

second group had a more definite effect than those of the first.

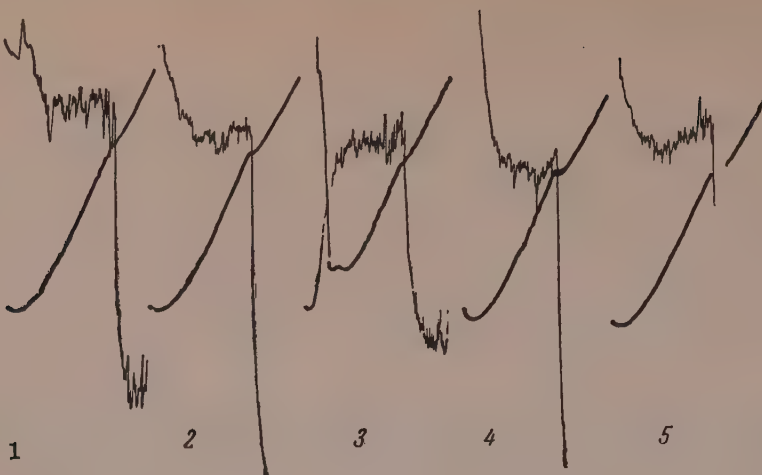


Fig. 1. Thermograms of samples of potato starch previously heated at 100° for:
1) 1 hour; 2) 2 hours; 3) 3 hours; 4) 4 hours; 5) 5 hours.

The cations formed the following series in order of their influence on the water retention of starch:



The water retention of native starch is always higher than that of starch after acid treatment ("acid" starch).

Adsorptive capacity of starch. The adsorptive capacity of starch has been studied very little [8]. Our investigations showed that the adsorptive capacity of starch depends on the cations present in it. The adsorbate chosen was the dye methylene blue, which is adsorbed well by starch. As previously, hydrogen ions in "acid" starch were replaced by the cations under consideration, and the adsorptive capacity of these specimens was then studied. The cations form the following series in order of their influence on the adsorption of methylene blue:

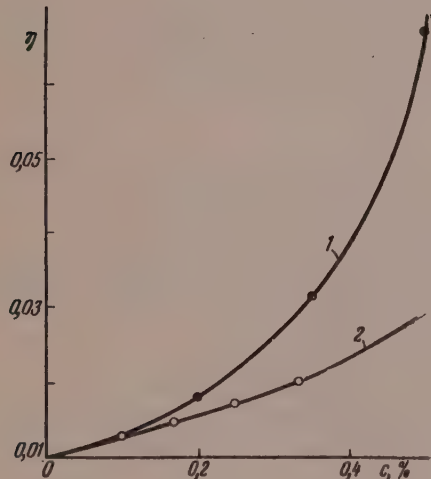
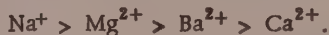


Fig. 2. Viscosity - concentration graphs for solutions of native (1) and acid (2) starch.

of the starch depends on their location and the nature of the bonding to the individual elements of the internal structure of the starch grain. The situation is different if the starch is present in an electrolyte solution, where the force fields of the ions have a considerable influence on the physicochemical properties of the starch grains; this

Viscosity of solutions of "ionic" starches. The ions bound with the starch carbohydrates may influence the stability of the bonds between the components of the starch grains, and aqueous solutions of starch prepared under similar conditions but with different ions present may differ in viscosity. For example, it should be noted that the viscosity of "acid" starch is always lower than the viscosity of native starch, as shown in Fig. 2.

The viscosities of solutions of "cationic" starches are closer to the viscosity of native starch. We have the following series for the solution viscosities of "cationic" starches:



If a starch has been treated with a solution of an electrolyte and then washed thoroughly, the eventual number of ions bound with the starch is relatively low, and their influence on the properties

was demonstrated by a number of authors some time ago [9, 10]. The ions penetrate into the grains and interact with the polar regions of the internal structure; this influences its strength and therefore a number of physicochemical properties of the grain. This is confirmed by our data which show the existence of a linear relationship between ionic refraction and gelatinization temperature of starch in solutions of different electrolytes* (Fig. 3).

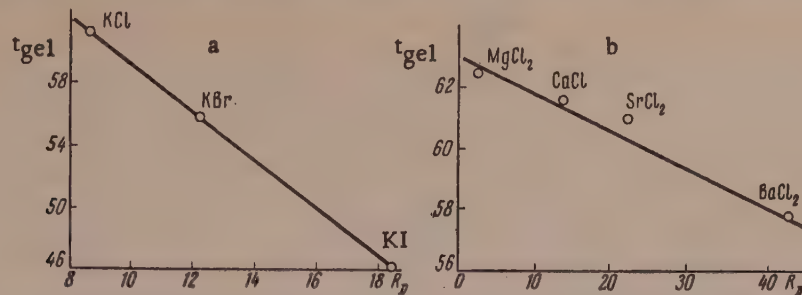


Fig. 3. Gelatinization temperature of starch as a function of the ionic refraction of anions (a) and cations (b).

The mechanism of the influence of ions on the properties of starch is not the same when they are bound with the carbohydrate components of starch as when the grains interact with an electrolyte solution. The work of Rugeberg [11] on the influence of ions on the properties of starch paste is of some interest in this respect. This author regards starch as an electrolyte, with ion-exchange properties, and explains the action of ions on the properties of starch paste on this basis.

SUMMARY

1. Heating curves of aqueous suspensions of potato starch were obtained by means of the Kurnakov pyrometer; it was found that the gelatinization temperature is lowered if samples of air-dry starch are subjected to preliminary heating. This is the consequence of a decrease in the stability of the internal bonds in starch grains under the action of heat.

2. Ions bound with starch influence some of its properties; they can be arranged in the following series according to their influence on:

a) filtration



b) adsorption of methylene blue



c) solution viscosity



3. There is a linear relationship between the ionic refractions and the gelatinization temperature of starch in solutions of the corresponding electrolytes.

The Moscow Technological Institute
of the Food Industry
Laboratory of Physical and Colloid Chemistry.

Received April 1, 1957

LITERATURE CITED

- [1] M. Samec, Die Starke 5, 105 (1953).

* The data of Samec [9] were used for the gelatinization temperatures in presence of anions, and our own results for the gelatinization temperatures in presence of cations.

- [2] R. W. Kerr, Chemistry and Industry of Starch (Russian translation) (Food Industry Press, 1956) p. 209.
- [3] A. V. Rakovskii, The Science of Adsorption (Moscow, 1913).*
- [4] V. I. Nazarov and A. V. Nikolaev, Proc. Acad. Sci. USSR 23, 264 (1939).
- [5] M. Ullmann, Kolloid. Z. 130, 31, 33 (1953).
- [6] A. V. Dumanskii, Bull. Acad. Sci. USSR, Chem. Ser. 1189 (1937).
- [7] V. I. Nazarov and A. B. Luk'ianov, Colloid J. 17, 302 (1955).**
- [8] V. I. Nazarov, Proc. Conf. on Adsorption, on the 200th Anniversary of MGU (Izd. MGU, 1957) p. 268.*
- [9] M. Samec, Kolloidchemie der Starke, (1927) p. 173.
- [10] J. R. Katz, and F. Muschter, Biochemische Z. 257, 385, 1933.
- [11] H. Rüggeber, Starke 5, 109, 1953.

* In Russian.

** Original Russian pagination. See C. B. Translation.

THE TOPOCHEMISTRY OF DROP POLYMERIZATION OF VINYL CHLORIDE

B. F. Teplov and P. M. Khomikovskii

Two kinds of emulsion polymerization are known: 1) polymerization in emulsions stabilized by soaps, which takes place in small polymer-monomer particles [1-5], and which leads to formation of latexes. 2) Polymerization in emulsions stabilized by protein emulsifiers or polymers, under the influence of initiators soluble in the monomer. In this case the polymer is obtained in the form of a relatively coarse suspension. Comparisons of the rates and activation energies of polymerization in bulk and in emulsions, of the average molecular weights of the polymers, and of the effects of peroxide concentration and nature of the emulsifier on the polymerization rates, showed that the process takes place within drops of the monomer (and can therefore be described as drop polymerization) and does not differ from polymerization in the mass of the monomer in its molecular mechanism [4, 6, 7]. Similar conclusions concerning the topochemistry of the process were reached by Rutowskii et al. [8] as the result of their observations of color changes in the particles on addition of an oil-soluble dye to the monomer.

It is known that appreciable amounts of organic substances can be dissolved in gelatin solutions. The question therefore arises whether polymerization takes place in miscelles of gelatin containing dissolved monomer, and if so, at what rate this process takes place.

Reliable data on the topochemistry of drop polymerization can be obtained from comparisons of the rates of the process in water, in emulsifier solutions, and in emulsion.

The present work consisted of a study of the polymerization of vinyl chloride in water and in 2% solution of photographic gelatin under the influence of benzoyl peroxide (BP) and azobisisobutyronitrile (ABN).

Solubility of initiators and vinyl chloride. For determination of the solubilities of benzoyl peroxide and azobisisobutyronitrile, these substances were shaken with water or gelating solution in sealed bulbs, and the undissolved residues were weighed. Saturation was reached after 5-6 hours. For determination of the solubility of vinyl chloride, it was fed in the gas phase from a glass measuring vessel containing the liquid monomer into an autoclave containing 4 liters of water or of gelatin solution. Saturation of the aqueous phase resulted in a constant value of the vapor pressure, corresponding to the vapor pressure of vinyl chloride at the given temperature. The results are given in the Table.

Solubilities of Benzoyl Peroxide (BP), Azobisisobutyronitrile (ABN), and Vinyl Chloride (VC) in Water and in 2% Photographic Gelatin Solution

Solute	Temperature (deg)	Solubility in g/liter	
		in water	in 2% photo- graphic gelatin solution
BP	20	less than	0.001
ABN	20	0.40	0.41
VC	50 (pressure 7.5 atm.)	10	11

It follows from these results that benzoyl peroxide is almost insoluble in water and in gelatin solution. Azobisisobutyronitrile is appreciably soluble in water. Vinyl chloride is somewhat more soluble in gelatin solutions than in water.

For estimation of the distribution of azobisisobutyronitrile between water and the monomer, a solution of this initiator in dichloroethane (0.4 g/liter) was shaken with an equal volume of water for 40 hours at 20° until a stable emulsion was formed. The ABN concentrations in dichloroethane and water were determined by weight after removal of the solvents by evaporation under vacuum. It was found that 92% of the ABN was in the dichloroethane and 8% in the water.

Polymerization. The polymerization was performed in absence of air at 50°. Vinyl chloride was added to water or to 2% solution of photographic gelatin by the method described. The monomer and the initiator solution were connected through the vapor phase in the apparatus shown in Fig. 1. The vessel was totally immersed in a thermostat and shaken vigorously in a horizontal direction. The polymerization rate was found from changes in the monomer volume in the graduated tube B. Before the start of the experiment the vessel was repeatedly filled with oxygen-free nitrogen and evacuated to 1 mm residual pressure in order to remove air. A solution of the initiator in water or in gelatin solution was then introduced into the vessel A. Dissolved air was removed from the solution by freezing and thawing under vacuum. Vinyl chloride was introduced into the tube B, and the apparatus was sealed under vacuum.

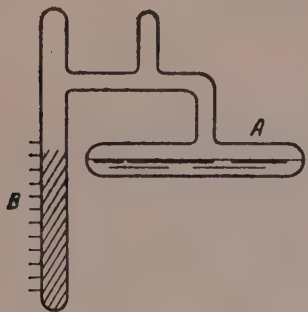


Fig. 1. Polymerization vessel.

The sorption of vinyl chloride by the polymer was determined under the same conditions (the polymer instead of the aqueous phase was introduced into the vessel A). It was found (Fig. 2) that 1 g of polyvinyl chloride absorbs 0.25 g of monomer (at 50°, under 7.5 atm. vapor pressure of vinyl chloride). A similar value is reported for the sorption of ethyl chloride by polyvinyl chloride [9]. For the polymerization experiments, the water and gelatin solution were previously saturated with the initiator. In some experiments a fabric bag containing solid initiator (0.1 g) was placed in the aqueous solution in order to maintain a constant concentration of the initiator. When the monomer was added to the aqueous phase without monomer, the absorption of monomer in 24 hours did not exceed its solubility at the given temperature. The monomer concentration in the polymerization system with the use of ABN (in the constant-rate region) was 0.12-0.13 g per 1 g of polymer.

The polymerization rate in presence of benzoyl peroxide is very low (Curve 1, Fig. 3). In presence of ABN polymerization proceeds at a constant rate after a period of acceleration, until a considerable amount of polymer has accumulated in suspension, regardless of whether a saturated solution is used or the initiator is present in the solid phase. The polymerization rate is somewhat higher in the latter case, probably because saturation of the aqueous phase with the initiator was effected at 50°.

The polymer yield time curves obtained in our experiments are similar to those obtained in polymerization in emulsions stabilized with gelatin. The polymerization rates (in the linear regions of the curves) when the monomer is supplied through the gas phase and when it is present in emulsion, with 1 : 4 ratio of vinyl chloride to emulsifier solution, are similar (Fig. 3). The average molecular weights of the polymers obtained in water and in gelatin solution are equal (Fig. 4), and are somewhat greater ($[\eta]^* = 1.4$) than the molecular weights of emulsion polymers ($[\eta] = 1.2$), probably because of the lower concentration of ABN.

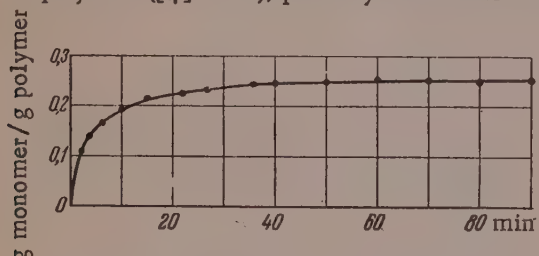


Fig. 2. Absorption of vinyl chloride by the polymer at 50°.

The polymerization proceeds at equal rates in solutions containing 0.4 and 1 g of potassium persulfate per liter. In polymerization with BP, the polymer is formed in the volume of the liquid and on the surface of the bag containing the initiator. The particles of polymer formed in presence of ABN are distributed uniformly through the whole liquid phase. In presence of potassium persulfate a latex is formed.

Particle size. The particle-size distributions of the suspensions were determined by direct microscopic measurements, by a method described in detail earlier [10]. A drop of suspension was placed on a slide, and the number of particles of each given size range was counted with the aid of a micrometer eyepiece. 1500-2000 particles were counted in each sample of suspension. Micro-

* $[\eta]$ is the intrinsic viscosity measured in cyclohexanone at 25°. The polymer concentration is given in g/100 ml.

scopic examination showed that all the polymer particles or, more correctly, aggregates, consist of transparent particles of irregular shape and differing in size, firmly stuck together. Particles obtained by polymerization through the vapor phase and by emulsion polymerization with gelatin are microscopically similar. The maximum on the size distribution curves of particle aggregates obtained by emulsion polymerization is independent of the degree of conversion, and lies in the $15\text{--}25\ \mu$ region. All the particles lie in the range of 1 to $100\ \mu$. The contents of small particles ($\sim 5\ \mu$) increase somewhat with increase of the degree of conversion (in %). In polymerization through the vapor phase, the commonest particle aggregates are somewhat larger ($\sim 50\ \mu$).

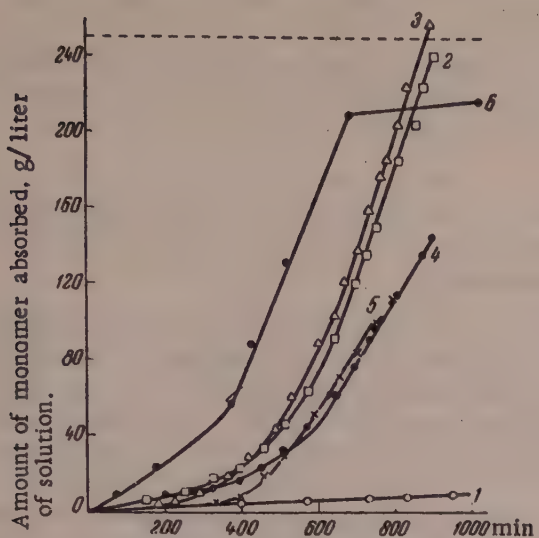


Fig. 3. Absorption of vinyl chloride when supplied through the gas phase:

- 1) 2% solution of photographic gelatin saturated with BP, with 0.1 g of solid BP;
- 2) ditto, saturated with ABN at 20° , with 0.1 g of solid ABN;
- 3) water saturated with ADN at 20° , with 0.1 g of solid ABN;
- 4) ditto, without solid initiator;
- 5) 2% solution of photographic gelatin, with 0.1% of potassium persulfate;
- 6) emulsion polymerization: 250 g of monomer (c_{M_0}) per liter of 1% gelatin solution. 0.5% of ABN on the weight of monomer. (The graph for this experiment gives the amounts of polymer formed in g, per 1 liter of aqueous phase of the emulsion).

molecules to the primary radicals, and also to polymeric radicals formed in the particles.

c) Chain termination. This reaction may be effected in two ways: interaction between polymeric and primary radicals, and combination or disproportionation of pairs of polymeric radicals. Since the mobility of polymeric radicals in the particles is very low, the first route of the termination reaction is the more probable.

d) Chain transfer through monomer and polymer molecules. In the case of vinyl chloride the rate constants of these reactions are very considerable [7, 12]. As the result of chain transfer through polymer molecules, polymeric radicals fixed in the solid polymer are formed; this increases the over-all reaction rate and the average molecular weight, in comparison with polymerization in homogeneous systems [7, 12, 13].

* The average molecular-chain length (\bar{p}) was calculated from the intrinsic viscosities (Fig. 4) by means of the equations: $[\eta] = 1.16 \cdot 10^{-4} (62.5 \cdot \bar{p}_n)^{0.85} (100 \text{ ml/g})$ or $[\eta] = 2.4 \cdot 10^{-4} (62.5 \cdot \bar{p}_n)^{0.77}$. These equations, which give similar values of \bar{p}_n , were found by correlation of the average molecular weights of nonfractionated vinyl chloride polymers obtained under various conditions, with intrinsic viscosities of solutions of the polymer in cyclohexanone [11].

The particle size and shape are not affected by the manner in which the vinyl chloride is supplied for the polymerization — either through the vapor phase into an aqueous solution of ABN, or into a solution of gelatin saturated with the initiator.

From these results certain inferences may be drawn concerning the topochemistry of polymerization of vinyl chloride in presence of gelatin under the influence of azobisisobutyronitrile.

1. The polymer yield — time curves, and the average molecular weights of the polymers formed, are the same for polymerization in water and in gelatin solutions. This indicates that polymerization does not occur in gelatin aggregates (micelles) (in which 5 g of vinyl chloride per 100 g of gelatin dissolves).

2. Polymerization begins in a molecular aqueous solution containing ABN (0.4 g/liter) and VC (10 g/liter). Polymeric molecules several monomer units long, and polymeric radicals of the same chain length, are precipitated and form aggregates of polymeric particles in which the polymerization proceeds. Since the average chain length of the polymer* is about 1000, it is evident that most of the polymer is formed in these particles.

3. The following reactions may occur in the polymer particles:

a) Initiation of polymerization by ABN molecules absorbed by the polymer particles, and also by free radicals from the aqueous solution.

b) Chain growth by addition of monomer molecules entering the particles from the aqueous solution.

4. From the instant of formation of the polymer particles (indicated by the instant at which the aqueous phase becomes turbid) there are two sites of polymerization: in the aqueous solution, and in the polymer particles.

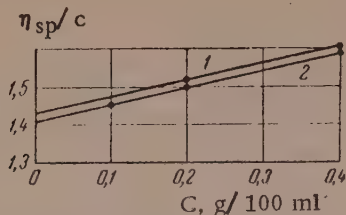


Fig. 4. Variation of η_{sp}/c with c , in cyclohexanone at 25°, for polymers made by supply of monomer through the gas phase into:

- 1) 2% gelatin solution, 2) water, both saturated with azobisisobutyronitrile.

The increase in the absorption rate of the monomer at the start of the process is probably caused by an increase of the rate of the process in the polymer particles.

The rate of the process is higher in the polymer particles than in water, for two reasons: a) because the average monomer concentration is 13% in the particles and 1% in water; the concentration of ABN in water is 0.04%, and if all the initiator enters the polymer $c_{ABN} \approx 0.3\%$; b) because of the decreased rate of chain termination in the polymer particles [3, 4, 14].

5. After a certain amount of polymer has accumulated, the polymerization rate remains constant, evidently because the process takes place almost entirely in the polymer particles.

The following causes may determine the constancy of the over-all polymerization rate in the particles:

- 1) the process may occur in a certain constant volume near the surface of the polymer particles, as postulated by some authors [5]. The over-all polymerization rate may depend in different ways on the surface area, depending on which of the elementary stages (initiation, growth, or termination of the chains) are influenced by the surface [15]; 2) constant amounts of primary and polymeric radicals may be present in the system.* The growth of each radical proceeds at a constant rate, as a constant concentration of monomer is maintained in the particles. If two or more radicals were present in a particle simultaneously, the rate of chain termination should decrease with time owing to an increase of the reaction volume, and the over-all rate should increase in consequence. Therefore it may be assumed that in the conditions of our experiments each particle contains one free radical at any time. A second radical, entering the particle or forming in it as the result of decomposition of the initiator, causes chain termination, as is probably the case in the latex polymerization of styrene in presence of potassium persulfate [16].

Enough experimental data are not yet available for more definite conjectures concerning the mechanisms of the elementary reactions in the polymerization of vinyl chloride in heterogeneous systems.

6. Since the rates of polymerization (Fig. 3) in presence of ABN in gelatin-stabilized emulsions and in the conditions of our experiments are equal, and since the particles in the suspensions are of the same shape and size in both cases, it follows that the mechanism and topochemistry of the process are the same in both cases: most of the polymer is formed in the polymer particles irrespective of the location of the initiator at the start of the reaction. The time required to reach a constant rate is less in emulsion polymerization. The reason is that in an emulsion the polymerization begins mainly in monomer droplets, as their monomer and initiator contents are considerably higher, and less time is required for the formation of the quantity of polymer which is sufficient for the process to continue almost entirely in the particles.

7. The considerably higher rates of polymerization of vinyl chloride in heterogeneous systems (in bulk, in emulsion, in precipitant media) as compared with polymerization in media in which polymer solutions are formed, are the consequence of peculiarities of the reactions in the polymer particles — decreased rate of chain termination in the solid, slightly swollen polymer (at temperatures close to the glass transition temperature), and the formation by chain-transfer reactions, of long-lived radicals fixed in the polymer particles [17, 18, 19].

Latex polymerization of vinyl chloride usually proceeds at higher rates than drop polymerization, and yields a product of higher molecular weight. However, there are no reliable data which would make it possible to decide whether this is caused only by an increase of the initiation rate (by the use of more active initiators), or also by an additional decrease in the rate of chain termination in small particles, as is the case in the formation of latex polymers soluble in their own monomers (styrene, methyl methacrylate [14]).

* In our experiments the process was continued for 5 hours at constant rate. During this time, at 50°, the ABN concentration fell by only 5-6%.

SUMMARY

1. The polymerization kinetics of vinyl chloride has been studied under conditions such that the monomer passes through the gas phase into water or a solution of gelatin, saturated with initiator (azobisisobutyronitrile). The reaction rates, the molecular weights of the polymers, and the size of the polymer particles are almost the same in both cases, and are close to the corresponding values found in polymerization in gelatin-stabilized emulsions.

2. The polymerization of vinyl chloride in the bulk of the monomer and in emulsions proceeds predominantly in the polymer, which forms a new phase in the course of the reaction, or at its surface.

This investigation was carried out at the suggestion of A. S. Shevliakov in connection with problems which arise in the development of a method for the continuous polymerization of vinyl chloride in suspension. The authors are indebted to S. S. Medvedev and Kh. S. Bagdasar'ian for valuable advice given in the course of discussion of polymerization kinetics in heterogeneous systems.

Dzerzhinsk

Received April 13, 1957

LITERATURE CITED

- [1] A. I. Iurzhenko, J. Gen. Chem. 16, 1171 (1946); A. I. Iurzhenko and N. S. Tsvetkov, Proc. Acad. Sci. USSR 85, 1099 (1952); 90, 421 (1953); Colloid J. 15, 136, 308 (1953);* 18, 362 (1956);* A. I. Iurzhenko and V. P. Gusiakov, Proc. Acad. Sci. USSR 86, 129 (1952); Colloid J. 14, 140, 414 (1952);† 16, 72 (1954);* A. I. Iurzhenko and R. V. Kucher, Proc. Acad. Sci. USSR 85, 1337 (1952); Colloid J. 14, 219, 283 (1953); 15, 442 (1953);*
- [2] W. Harkins, J. Am. Chem. Soc. 69, 1428 (1947); J. Polymer Sci. 5, 217 (1950).
- [3] P. M. Khomikovskii, Proc. Acad. Sci. USSR 60, 615 (1948); P. M. Khomikovskii, E. V. Zabolotskaya, and S. S. Medvedev, Papers at the 6th Conference on High-Molecular Compounds (1949) p. 45; Z. N. Markina, P. M. Khomikovskii, and S. S. Medvedev, Proc. Acad. Sci. USSR 75, 243 (1950).
- [4] P. M. Khomikovskii and S. S. Medvedev, Proc. 3rd Conf. on Colloid Chem. (Izd. AN SSSR, 1956) p. 440.*
- [5] A. P. Sheinker and S. S. Medvedev, Proc. Acad. Sci. USSR 97, 111 (1954); J. Phys. Chem. 29, 250 (1955); E. V. Zabolotskaya, I. G. Soboleva, N. V. Makletsova and S. S. Medvedev, Proc. Acad. Sci. USSR 94, 81 (1954); Colloid J. 18, 420 (1956);* G. V. Tkachenko and P. M. Khomikovskii, Proc. Acad. Sci. USSR 72, 543 (1950); Colloid J. 13, 217 (1951).
- [6] W. Hohenstein and H. Mark, J. Polymer Sci. 1, 127 (1947); W. Kaghan, R. Shreve, Ind. Engng. Chem. 45, 292 (1953).
- [7] G. V. Tkachenko, Dissertation, MKhTI (Moscow, 1951).**
- [8] B. N. Rutovskii, G. S. Goncharov, and Ia. G. Muravin, Chem. Ind. No. 3, 11, 75 (1949); Trans. Moscow Inst. Chem. Machine Construction 1 (9) 36 (1950).
- [9] V. A. Kargin and T. V. Gatovskia, J. Phys. Chem. 30, 2051 (1956).
- [10] P. M. Khomikovskii, Trans. Sci. Res. Inst. Polygraphic Ind. No. 5, 121 (1937); Colloid J. 2, 737 (1936).
- [11] J. Breitenbach, E. Forster, and A. Renner, Kolloid-Z. 127, 1 (1952); F. Danusso, G. Maraglio and S. Gazzera, Chimica e Industria 36, 883, (1954).
- [12] G. V. Tkachenko, P. M. Khomikovskii, and S. S. Medvedev, J. Phys. Chem. 25, 823 (1951).
- [13] W. Bengough, R. Norrish, Nature 163, 325 (1949); Proc. Roy. Soc. 200, 301 (1950).
- [14] P. M. Khomikovskii and S. S. Medvedev, Paper at the 9th Conference on High-Molecular Compounds (January 1957).**
- [15] S. S. Medvedev, L. Gindin, and M. Lazarev, J. Phys. Chem. 13, 1389 (1939).
- [16] W. Smith, R. Ewart, J. Chem. Phys. 16, 592, 1948; P. Flory, Principles of Polymer Chemistry (N.Y., 1953); E. Bartholome, H. Gerrens, R. Herbek and H. Weitz, Z. Elektrochem. 60, 334 (1956); H. Gerrens, ibid. 60, 400 (1956).

*Original Russian pagination. See C. B. Translation.

**In Russian.

- [17] G. V. Tkachenko, P. M. Khomikovskii, A. D. Abkin and S. S. Medvedev, *J. Phys. Chem.* **31**, 242 (1957).
- [18] A. Schindler, J. Breitenbach, Simposio intern. chim. macromolecolare. Supplemento a "La Ricerca Scientifica", 1955, p. 35; F. Danusso, *ibid*, p. 46; J. Breitenbach, A. Schindler, *J. Polymer Sci.* **18**, 435 (1955).
- [19] M. Magat, *J. Polymer Sci.* **16**, 491 (1955); **19**, 583 (1956).

RELAXATION OF DEFORMATION AND REPEATED DEFORMATION OF ALUMINUM NAPHTHENATE GELS

A. A. Trapeznikov

Relaxation is one of the most important components of the complex of rheological properties of a structurized colloidal system. Despite the numerous investigations on this subject [1-7], there have been no systematic investigations of the variation of the relaxation rate of a system with the magnitude of the deformation along the stress-deformation $P(\epsilon)$ curve. Neither have any investigations been carried out with repeated deformations of the system, with measurements of elastic recovery at various fixed deformations ϵ along the $P(\epsilon)$ curve.

We showed earlier [8] that one of the most effective methods for studying the properties of structurized systems is by means of $P(\epsilon)$ curves when $\dot{\epsilon} = \text{const}$. If $\dot{\epsilon}$ is not too small, the $P(\epsilon)$ curve has a maximum $P = P_r$, indicating breakdown of the structure. It was found that the relaxation rate greatly increases when $P = P_r$ and subsequently when $P = P_s$ [9].

In studies of relaxation phenomena a distinction should be made between relaxation of stress and relaxation of deformation. The two kinds of relaxation are, of course, closely related, but in a fairly complex manner; they depend in different ways on the range of structural elements in the system with different relaxation times Θ_i and different critical deformations ϵ_{ki} . Therefore it is in general necessary to investigate both kinds of relaxation jointly.* However, as the transition from elastic to residual deformation is fundamental in the process of irreversible relaxation, investigation of relaxation of deformation is often the more direct method.

The elastic recovery measured by us in highly elastic gels of the aluminum naphthenate type includes the so-called instantaneous and the after-effect deformations. In rapidly relaxing systems, especially at high values of ϵ and with large $\dot{\epsilon}$, it is almost impossible to separate these two types of deformation, especially because, as was shown earlier [5], separation of these types of deformation in such systems is purely arbitrary, and depends on the instant of time chosen.

The term "relaxation rate" is often used without a quantitative definition of this concept. In analyzing the behavior of a Maxwell body, we defined [10] this quantity as the rate of increase of the residual deformation relative to the acting elastic deformation

$$V_{\text{rel}}^e = \frac{1}{\epsilon_e} \frac{d\epsilon_v}{d\tau}.$$

If the total deformation $\epsilon = \text{const}$, the decrease of elastic deformation is equal to the increase of residual deformation [9], and then

$$V_{\text{rel}}^e = -\frac{1}{\epsilon_e} \frac{d\epsilon_e}{d\tau}$$

It was shown that this definition is valid both when $\epsilon = \text{const}$ and when $\dot{\epsilon} = \text{const}$, and the relaxation time

* This is possible in principle with the instrument used in this investigation, but for measurements of stress relaxation it is necessary to have automatic recording, such as that used in our large instrument [14].

$$\vartheta^e = \frac{1}{V_{\text{rel}}^e} = \frac{\epsilon_e}{d\epsilon_v / d\tau}$$

may be defined as the time in which all the existing elastic deformation would disappear if the rate of its conversion into residual deformation remained constant.

Usually when relaxation processes are considered the relaxation time ϑ of the system is defined only on the basis of a Maxwell (or Kelvin) law, i.e., a purely exponential law. However, in most cases these laws are not obeyed and then ϑ or V_{rel} remain unknown. In some cases the Maxwell law is arbitrarily assumed and ϑ is defined as the time in which P decreases by a factor of e [4]. However, a defect of such calculation methods is that they ignore variations of the time or rate of relaxation during the course of the whole relaxation process. However, great interest attaches to the magnitude of the relaxation times at any particular instant of the relaxation process, irrespective of model concepts. Such values are useful for interpretation of the mechanism of the process, even if they are not differentiated with respect to the constituent types of deformation, and are aggregate values.

The advantage of the above definitions of V_{rel} and ϑ is that they are valid for any stage of the relaxation process, irrespective of its exponentiality. A corresponding definition can also be introduced for stress relaxation in the condition that $\epsilon = \text{const}$

$$V_{\text{rel}}^P = -\frac{1}{P} \frac{dP}{d\tau} \quad \text{and} \quad \vartheta^P = -\frac{P}{dP/d\tau}.$$

For a process which conforms to an exponential law, the values of V_{rel} and ϑ remain constant throughout the process, i.e., at any values of ϵ and P . Therein lies the characteristic peculiarity of a classic Maxwell (or Kelvin) body.

Relaxation of Deformation

Our elastorelaxometer [11] is convenient for investigations of relaxation of deformation in highly elastic gels which relax relatively rapidly, with the total deformation $\epsilon = \text{const}$. In relaxation measurements, the upper magnet, which releases the inner cylinder, is switched on by hand, instead of automatically, after the system has been held for various times after the outer cylinder has been stopped. Relaxation takes place during this time, and the elastic recovery decreases.

In the relaxation curves in Fig. 1, θ_e is plotted against τ_{hold} (the holding time) for different fixed values of θ expressed in degrees of rotation of the outer cylinder ($R_2 = 1.5$ cm) relative to the inner cylinder ($R_1 = 1.396$ cm), with moment of inertia $M = 121.5 \text{ g} \cdot \text{cm}^2$. These curves are used for graphical determination of $d\theta_v / d\tau = -d\theta_e / d\tau$ or $d\epsilon_v / d\tau = -d\epsilon_e / d\tau$ * respectively for different values of θ_e or ϵ_e along the $\theta_e(\tau_{\text{hold}})$ curve, and V_{rel} and ϑ are calculated (Table 1). The values of V_{rel} as a function of θ_e for different values of θ are given in Fig. 2 (on two scales); it follows from these curves that at low values of $\theta_e = 90^\circ - 120^\circ < \theta_{e \text{ max}} = 165^\circ$, in particular at low θ , the values of V_{rel} are almost constant and least; at high θ_e the values of V_{rel} are very large. Constancy of V_{rel} and ϑ in the region of small θ_e is also a consequence of the linearity of the lower portions of the $\log \theta_e = f(\tau_{\text{hold}})$ curves in Fig. 3. In these ranges of θ_e the relaxation process becomes exponential, $\theta_e = \theta_{e0} e^{-\tau/\vartheta}$ [9].

However, the extents and slopes of the linear regions differ for different θ . It follows from Table 2 that initially the values of θ_{e0} , corresponding to the beginning of the linear regions, increase with θ (up to $\theta = 90^\circ$), but later decrease sharply. The values of ϑ decrease continuously, starting even at small values of θ .

The $V_{\text{rel}}(\theta)$ relationship is illustrated particularly clearly by the curve in Fig. 4, plotted for the least $\theta_e = 40^\circ$. The $\theta_e(\theta)$ curve is plotted in the same diagram. The values of V_{rel} remain roughly constant up to $\theta = \theta_m$, and then begin to increase. This clearly shows that at $\theta > \theta_m$ (and therefore at $\epsilon > \epsilon_m$) intensive breakdown of the structure begins. However, it is only at low values of θ that V_{rel} begins to increase only when $\theta \geq \theta_m$. It follows from the curves in Fig. 2 that for $\theta > 90^\circ$ V_{rel} begins to increase even when $\theta_e = 90^\circ$ and less, that is, still in the region of $\theta < \theta_m = 165^\circ$.

The fact that ϑ is constant, i.e., that the $\log \theta_e = f(\tau_{\text{hold}})$ curves are linear, indicates that the state of the

* For the cylinder used in this case, $\epsilon = 0.262 \theta^\circ$.

TABLE I

Relaxation Rates V_{rel} and Times δ for a 2% Gel. Calculated from the Curves in Fig. 9 ($\tau^{tagging} = 16$ days)

system remains unchanged in this deformation range. This is possible when the particles attain some definite established configuration, for example a more or less globular form, corresponding to minimum deformations. The higher rate of relaxation at large deformations of the globules may be associated with elongation of the globules. This elongation, however, is not enough to account for the positions of the curves in Fig. 2. When the particles contract in the course of relaxation to some smaller degree of deformation, the values of V_{rel} should become equal, irrespective of the degree of the initial deformation. In other words, changes of V_{rel} , in consequence of elongation only, presuppose complete reversibility of the system. This is not the case in reality. For example, V_{rel} at fixed $\theta = 42^\circ$ for $\theta_e < \theta_{e0}$ is 0.0176 sec.⁻¹ and at $\theta = 90^\circ$ V_{rel} in the range $\theta_e \leq \theta_{e0}$ is 0.208 sec.⁻¹, whereas for $\theta = 142^\circ$ and $\theta = 160^\circ$, with subsequent contraction down to the same small values of $\theta_e < \theta_{e0}$, V_{rel} is 0.0236 and 0.0253 sec.⁻¹ respectively. This "hysteresis of V_{rel} " shows that the deformation process is not reversible, even in the range of elastic deformations $\theta_e < \theta_{e max}$. The structure of the system evidently alters. This change in the structure of the system should be attributed to breakdown of some of the bonds in the course of large deformations. Evidently, when the deformations are small, the relatively short, the most rigid, slowly-relaxing elements of the structure are broken down; when the deformations are large, the breakdown occurs in the longer, more flexible, and rapidly-relaxing structural elements, with larger critical deformations ϵ_{ki} , and lower ϑ_i , which are restored more rapidly after removal of the stress or in conditions of steady flow (the experiments on repeated deformation of the gels demonstrate their rapid restoration after removal of the stress).

Thus, as the result of measurements of V_{rel} along the whole $P(\epsilon)$ curve it may be concluded that the structure breaks down at different degrees of deformation. It is seen that breakdown occurs when $\epsilon < \epsilon_m$, and also, and to a greater extent, when $\epsilon > \epsilon_m$. Direct proof of the latter is provided by the decrease of ϵ_e when $\epsilon > \epsilon_m$ [9].

It should be noted that whereas at large θ the exponential course of the relaxation process (the linear region when $\theta_e < \theta_{e0}$) is rela-

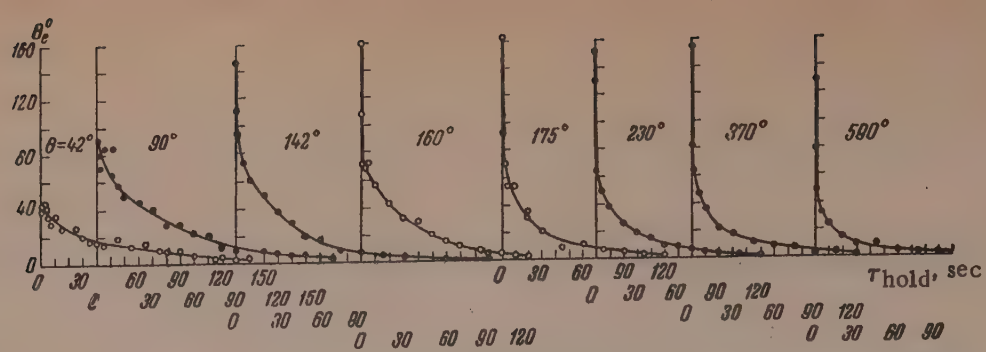


Fig. 1. $\Theta_e(\tau_{\text{hold}})$ relaxation curves for different values of θ in 2% aluminum naphthenate gel.

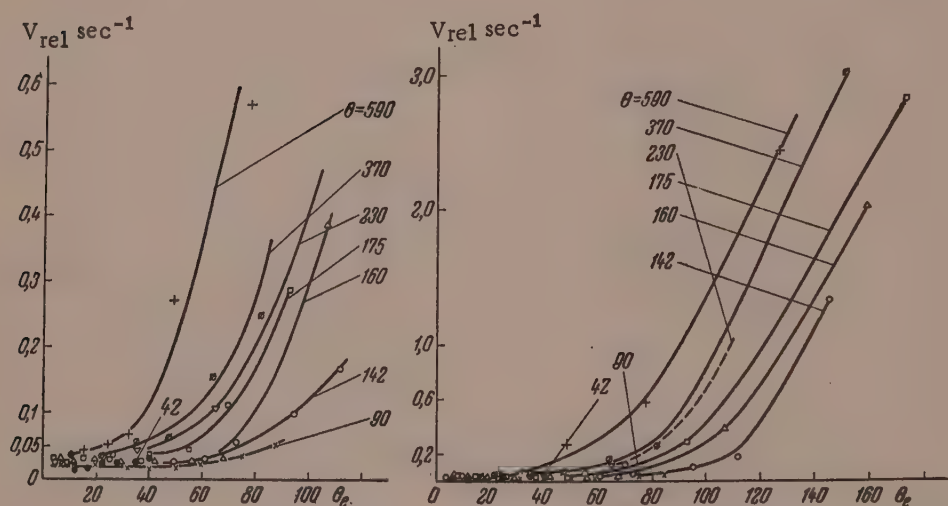


Fig. 2. $V_{\text{rel}}(\theta_e)$ curves in two different scales.

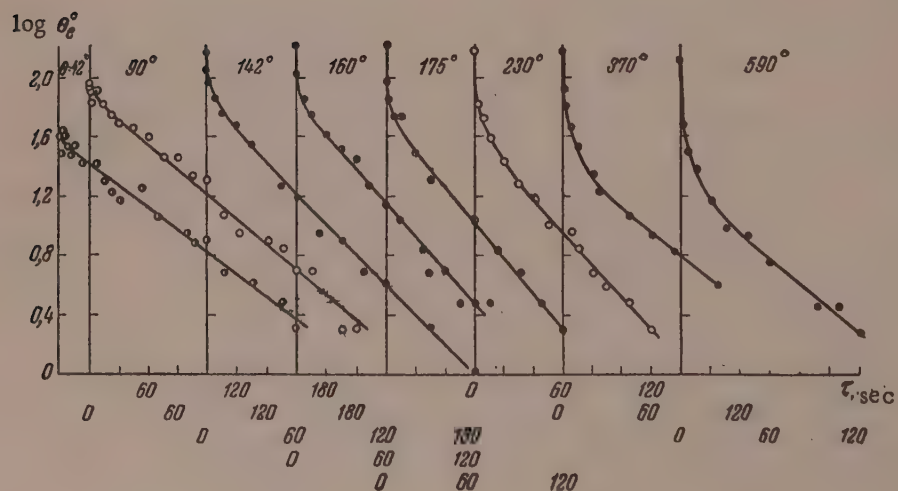


Fig. 3. $\log \Theta_e = f(\tau_{\text{hold}})$ curves for different values of θ .

TABLE 2

Values of θ Calculated from the Linear Regions of the $\theta_e = f(\tau_{\text{hold}})$

θ°	θ , sec.	θ_e° beginning of linear region
42	57.6	22
90	49.4	43
142	42.2	37
160	39.5	33
175	35.0	30
230	40.6	18
370	54.3	15
590	53.6	8

Repeated Deformation of Gels, and Their Thixotropic Properties in Relation to the Range of Structural Elements

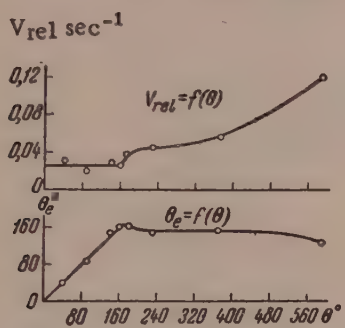


Fig. 4. $V_{\text{rel}}(\theta)$ curve for $\theta_e = 40^\circ$, and $\theta_e(\theta)$ curve.

Changes in the structure of a colloidal system in the course of deformation, along the $P(\epsilon)$ or the $\epsilon_e(\epsilon)$ curve, may be studied by methods involving repeated deformation of the system to different values of ϵ . There are two variations of the method:

1. The gel is repeatedly deformed to a certain ϵ at definite relatively short intervals, for example at $\tau = 1$ minute (or less), known to be insufficient for complete restoration of the structure. Each time the value of P corresponding to the given ϵ is measured (if $\epsilon > \epsilon_m$ and is sufficiently large, only the maximum values of $P = P_1$, i.e., the extreme deflections of the light spot on scale, are recorded when P is read off visually). The elastic recovery ϵ_e is measured at the same time.

2. The gel is first deformed to a certain small degree of deformation $\epsilon = \epsilon_1$, and then, after a short time, $\tau = 1$ minute, it is again deformed to a greater degree $\epsilon = \epsilon_2$. P and ϵ_e are measured at each deformation.

The use of these methods, especially the first, has led to certain new conclusions, and provided direct confirmation that breakdown of the structure occurs along the entire $P(\epsilon)$ curve, along both its ascending and its descending branches, and predominantly along the latter.

Fig. 6 shows typical curves for shear stress and elastic recovery as functions of the time interval between repeated deformations to fixed ϵ , for 3% and 4% aluminum naphtenate gels in decalin ($\dot{\epsilon} \approx 100 \text{ sec.}^{-1}$), with aging times (τ_{aging}) of 20 and 30 days respectively (the values of τ along the abscissa axis are not to scale).

It follows from the curves in Fig. 6 that P decreases considerably even at the second deformation, and subsequently, with the same intervals $\tau = 1$ minute, it either remains roughly constant or continues to decrease. P

tively short, and corresponds only to the ends of the $\theta_e(\tau_{\text{hold}})$ curves, at small θ it forms about half of the total deformation.

The values of θ_e for different τ_{hold} , corresponding to the curves in Fig. 1, can be used to plot $\theta_e(\theta)$ curves for different τ_{hold} (Fig. 5). Such curves correspond, as it were, to different deformation rates and to different times required to reach a given θ . It follows from Fig. 5 that the general form of the curves remains the same, but the values of θ_e deviate increasingly from θ with increase of τ_{hold} . This clearly demonstrates the role of the deformation rate in studies of the magnitude of elastic deformations in rapidly-relaxing systems.

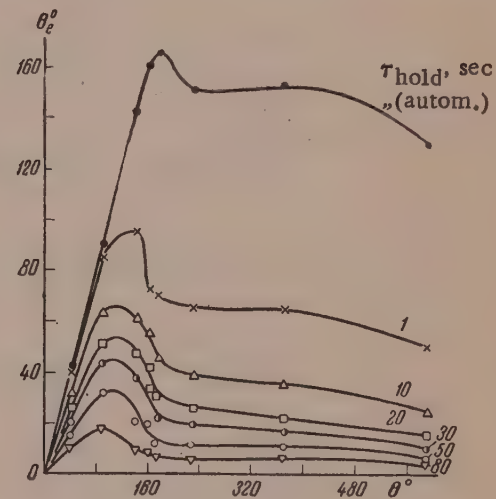


Fig. 5. $\theta_e(\theta)$ curves for different τ_{hold} , plotted from the curves in Fig. 1.

increases and reaches its initial value with increase of τ . The curves relate both the $\epsilon < \epsilon_m$ and $\epsilon > \epsilon_m$ regions. The difference between them lies in the duration and extent of the decrease of P . In the region $\epsilon > \epsilon_m$ each repeated deformation (at 1-minute intervals) produces additional breakdown of the structure. This means that in a single deformation of the system to a fixed ϵ not all the bonds (not all the structural elements) which can be broken down at the given deformation and at the given $\dot{\epsilon}$ are destroyed. This gradual character of the structural breakdown can evidently account for many details of the deformation properties of colloidal systems, and in particular for the length of the descending region of the $P(\epsilon)$ curve in the $\epsilon > \epsilon_r$ region until $P = P_s$ is reached, in the usual $P(\epsilon)$ determination by the method of constant $\dot{\epsilon}$.

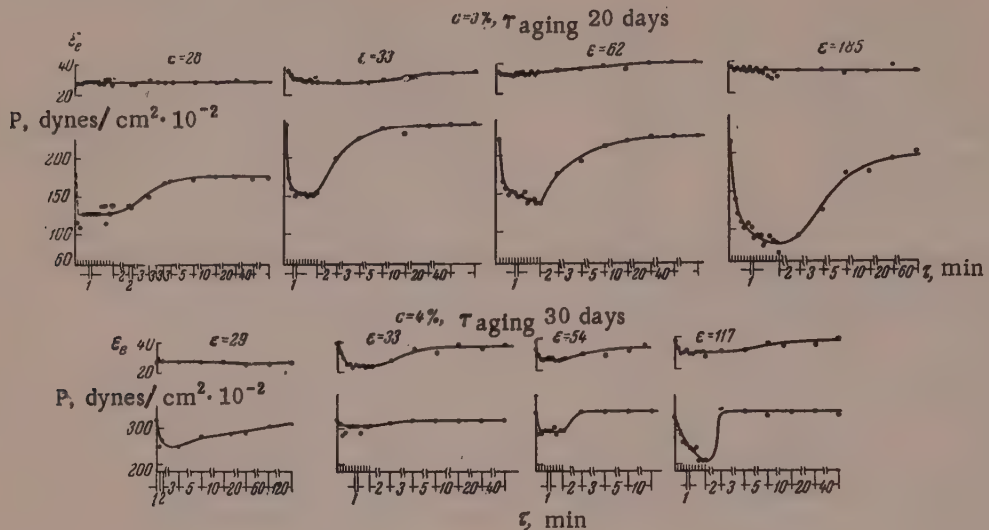


Fig. 6. Typical $P(\tau_{\text{rep}})$ and $\epsilon(\tau_{\text{rep}})$ curves for 3% and 4% gels for different values of ϵ .

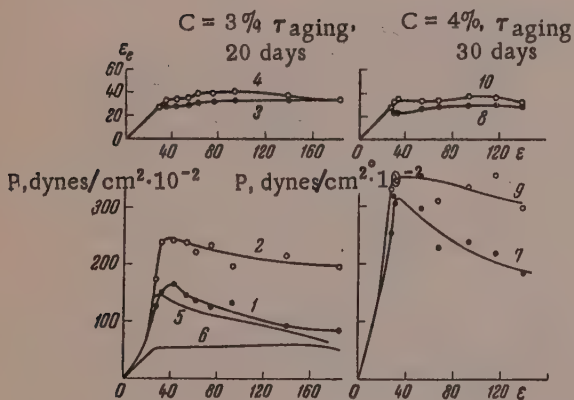


Fig. 7. $P(\epsilon)$ and $\epsilon_e(\epsilon)$:

a) For 3% aluminum naphthenate gel, plotted from the minimum (1 and 3) and limiting (2 and 4) values of the curves in Fig. 6. Curves 5) $P(\epsilon)$ and 6) $\epsilon_e(\epsilon)$ were obtained by means of consecutive deformations at 1-minute intervals with continuously increasing ϵ (the scale of Curve 6 corresponds to the scales of Curves 3 and 4); b) for 4% gel, plotted from the minimum (7 and 8) and limiting (9 and 10) values of the curves in Fig. 6.

Fig. 7, a and b, gives $P(\epsilon)$ and $\epsilon_e(\epsilon)$ curves plotted from the minimum values of P and ϵ_e , corresponding to the greatest influence of repeated deformation (lower curves), and from the maximum (limiting) values corresponding to complete restoration of the structure (upper curves). The sections of the ordinates between the corresponding curves represent the greatest decreases of P and ϵ_e as the result of repeated action on the system. Fig. 7, a, also shows $P(\epsilon)$ and $\epsilon_e(\epsilon)$ curves obtained by deformation of the gel with consecutively increasing deformations at 1-minute intervals. It follows from the curves in Figs. 6 and 7 that the highest values of $P = P_r$ are reached at $\epsilon = \epsilon_r = 41.5$ for the 3% gel, and at $\epsilon = \epsilon_r = 31.5$ for the 4% gel. These values are given by both the lower and the upper curves.

Data on the elastic recovery ϵ_e in repeated deformations, determined in parallel with P , are of interest. It follows from Figs. 6 and 7 that at the lowest values of ϵ studied the values of ϵ_e remain almost constant during all the consecutive deformations, although the values of P decrease. As ϵ is increased, repeated deformations give lower values of ϵ_e , because of the breakdown of a certain number of bonds which cause elastic deformation. Therefore the break-

down of these bonds, still in the $P < P_r$ region, results in a residual deformation $\epsilon_v = \epsilon - \epsilon_e$. Since a second deformation reflects the changes which took place in the first deformation of the original system, it follows that a similar breakdown of structure and development of residual deformation may occur in the usual $P(\epsilon)$ determinations. Therefore deviations of $\epsilon_e(\epsilon)$ curves from linearity may be the results of structural breakdown, apart from relaxation.

An interesting fact is that the region of ϵ close to ϵ_r the decrease of ϵ_e on repeated deformation (Fig. 6) is greatest. The decrease of ϵ_e is relatively small with large deformations of the system to $\epsilon \gg \epsilon_r$. The only possible explanation is that at high values of ϵ the elastic recovery is determined by a certain part of the structural elements which remains almost unchanged in repeated deformations, or, at least, is restored very rapidly, and that this part of the structural elements depends very little on the remaining part, broken down before the given ϵ is reached. The influence of gel concentration on these effects produced in repeated deformation is of interest.

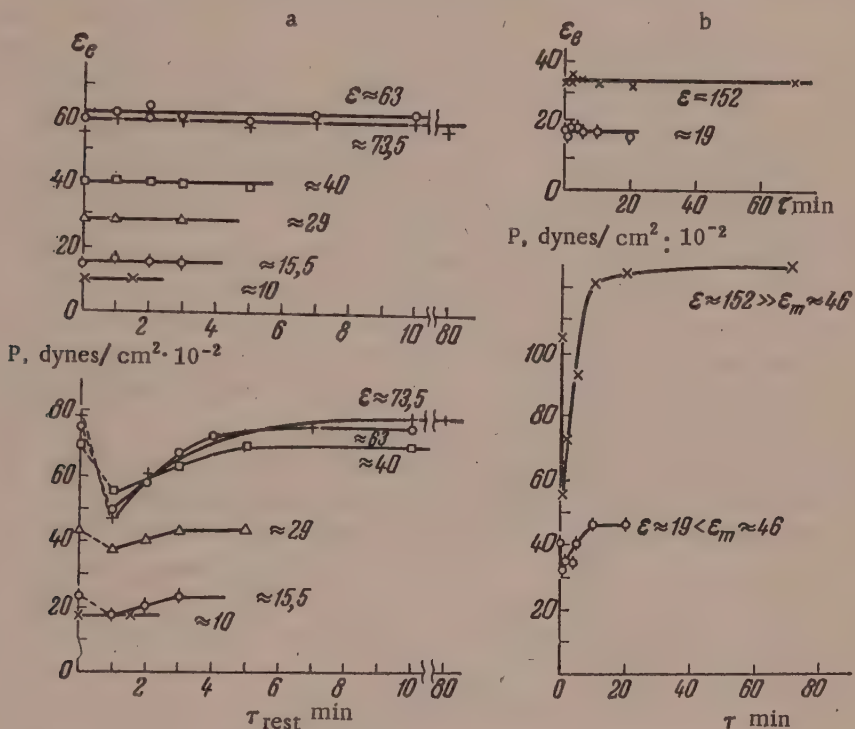


Fig. 8. $P(\tau_{\text{rep}})$ and $\epsilon_e(\tau_{\text{rep}})$ curves:

a) For 2% aluminum naphthenate gel in decalin at different ϵ , $\tau_{\text{aging}} = 74$ days; b) for 2% aluminum naphthenate gel in decalin, with 0.25% polyisobutylene, $\tau_{\text{aging}} = 70$ days, at different ϵ .

The influence of repeated deformation on P is quite distinct in a 2% gel (Fig. 8, a, $\tau_{\text{aging}} = 74$ days), and in other systems of low concentrations (1.5 and 1.0%). Deformation after 1 minute results in a large decrease of P , and if τ_{rest} is increased, P rises to the original value. On the other hand, the values of ϵ_e remain constant at all the values of ϵ , both less and greater than ϵ_m , in all repeated deformations. Therefore, despite breakdown of part of the structure (the values of P being lower), the deformation may remain completely elastic, and $\epsilon_e = \epsilon$. In other words, complete reversibility of the deformation does not exclude partial breakdown of the structure. The explanation is that the stress maximum and the deformation maximum are associated with different structural elements of the system, in agreement with the concept of the existence of a range of structural elements with different critical ϵ_{ki} and ϑ_i [10, 12]. When the system is deformed to a given ϵ , the latter proves to be greater than ϵ_{ki} for a certain group of bonds. These bonds are therefore broken down, but bonds with higher ϵ_{ki} remain intact; these are the bonds which ensure complete reversibility of the deformation, such that $\epsilon_e = \epsilon$.

The concept of a range of structural elements with critical values of ϵ_{ki} , ϑ_i and ϵ_{ki} was developed in the course of consideration of $\epsilon_r(P_r)$ relationships and $\eta(P)$ or $\eta(\dot{\epsilon})$ curves [13]. Indeed, the present results confirm

that a considerable part of the shear stress at each value of ϵ influences the shortest, slowly-relaxing bonds, which break down at the earliest stages of deformation, at low $\dot{\epsilon}$, leaving the more rapidly relaxing longer structural elements with smaller θ_i and larger ϵ_{ki} and $\dot{\epsilon}_{ki}$. It follows that the various deformational and viscous properties of colloidal systems are associated with the distribution of the structural elements by their values of ϵ_{ki} and θ_i .

The probable explanation for the difference between gels with $c \leq 2\%$ and $c \geq 3\%$ is that in the less concentrated gels* the structure is relatively free, there is little intertwining of the particles, and the elastic recovery is greatest. Therefore, the breakdown of a certain part of the structural elements which, at the given deformation ϵ , are "short" and have $\epsilon_{ki} < \epsilon$, does not affect the longer structural elements which determine total $\epsilon_e = \epsilon$. In a dilute gel of this type the short and long structural elements act fairly independently of each other. In more concentrated gels, with more intertwining in the structure, the breakdown of the short structural elements, manifested in a decrease of P , also affects the longer structural elements responsible for ϵ_e , so that ϵ_e decreases simultaneously. In concentrated gels the distribution of bonds probably lies within a narrower range of ϵ_{ki} , and is displaced toward smaller values of ϵ_{ki} . Hence it follows that in systems with much intertwining of the particles changes of P and ϵ_e are closely interrelated, whereas in systems with a free structure these changes may be almost entirely independent of each other, although, of course, in such cases the different structural elements interact, and breakdown of some leads to redistribution of stresses and deformations to other structural elements.

In 2% aluminum naphthenate gels made with additions of 0.25, 0.5, and 1% polyisobutylene ($M \approx 200,000$), the influence of repeated deformations of P and ϵ is qualitatively the same as in 2% aluminum naphthenate gel without these additions, but quantitatively it is much more pronounced. On repeated deformation the values of ϵ_e remain unchanged, whereas P decreases, and to a much greater extent than for gels consisting of aluminum naphthenate only, and the value is restored much more slowly (Fig. 8, b). This shows that the viscosity of the system increases under the influence of polyisobutylene, which hinders the formation of the "short" part of the structure from the aluminum naphthenate particles. On the other hand, this does not prevent rapid restoration (within 15 seconds) of the rapidly-relaxing, longest structural elements, which determine the maximum ϵ_e , although the absolute value of the maximum ϵ_e is less in these gels than in pure aluminum naphthenate gels.

These results show that both the maximum ($P = P_r$) and the intermediate ($P < P_r$) shear stresses and the values of the elastic deformation $\epsilon_p = \epsilon$ are not necessarily or directly interrelated. For example, it follows from the Curves in Fig. 2, and also the curves in Fig. 9, obtained for a 2% aluminum naphthenate gel by deformation at 1-minute intervals with gradually increasing ϵ , i.e., in conditions in which P does not have enough time for complete

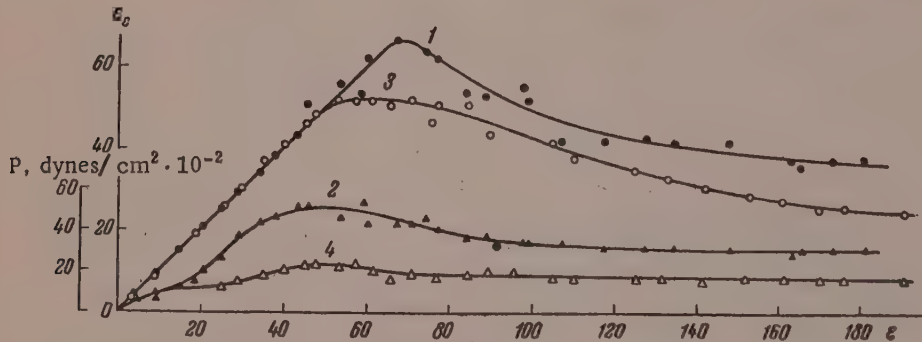


Fig. 9. $P(\epsilon)$ and $\epsilon_e(\epsilon)$ curves for 2% aluminum naphthenate gel in decalin, determined at 1-minute intervals for consecutive fixed values of ϵ :

1) $\epsilon_e(\epsilon)$; 2) $P(\epsilon)$; $\tau_{\text{aging}} = 62$ days; 3) $\epsilon_e(\epsilon)$; 4) $P(\epsilon)$; $\tau_{\text{aging}} = 152$ days.

restoration, that not only $\epsilon = \epsilon_m$, but also $\epsilon_e = \epsilon_{e \max}$ are definitely greater than $\epsilon = \epsilon_r$, corresponding to maximum $P = P_r$. It follows that even $P = P_r$ for a completely restored structure does not, in principle, necessarily correspond to maximum elastic deformations and the longest (highly elastic) structural elements. This stress corres-

* The 2% gel discussed here was studied after relatively long aging. Its behavior after short aging times should be closer to that of a 3% gel.

pounds to the maximum of a certain function of stress distribution by the number and strength of the structural elements, including viscous resistance when the given deformation $\epsilon = \epsilon_r$ is reached. The maximum elastic deformation $\epsilon = \epsilon_{e\ max}$ can be even greater than the deformation corresponding to the maximum shear stress, $\epsilon = \epsilon_r$, and it is then determined by a relatively small number of long flexible structural elements. At the same time, even the experimentally determined $\epsilon_{e\ max}$ may not reflect the longest structural elements present in the system. If they are present in small numbers, they may be incapable of causing motion of the inner cylinder in the opposite direction to the resistance arising as the result of broken-down structure in the medium.

The above results relating to the separate action of "short" and "long," slowly and rapidly restoring structural elements, which influence P_r and $\epsilon_{e\ max}$ in different ways, are of interest in relation to general questions of rheology of colloidal systems, and also in relation to the problem of thixotropic breakdown and buildup of structure; they show that thixotropic properties may be characterized in terms of ϵ_e as well as of P_r .

SUMMARY

1. The elastic recovery and relaxation of elastic deformation has been studied in aluminum naphthenate gels at various fixed deformations, along the course of the stress-deformation curve.
2. The rate of relaxation of deformation greatly depends on the values of the fixed and elastic deformations, owing to changes in the configuration of the particles and also to breakdown of the structure. It is shown that the latter process is closely associated with transition through the structural strength maximum.
3. The system was studied by the method of repeated deformation at various deformations along the stress-deformation curve. It was found that in general the stress and the elastic deformation depend on the time interval between consecutive deformations.

Two deformation regions were found for 3% and 4% gels: a region of small deformations, in which the shear stress depends on the time interval but the deformation does not; and a region of large deformations, in which the stress and elastic recovery depend on the time interval between consecutive deformations. It was found that in gels containing 2% and less of aluminum naphthenate in decalin, and in gels containing polyisobutylene, repeated deformation has a strong influence on the shear stress but not on the elastic recovery over the whole deformation range. It was found that the maxima on the $P(\epsilon)$ and $\epsilon_e(\epsilon)$ curves need not necessarily coincide.

4. It follows from these results that these systems contain a range of structural elements, characterized by different critical deformations and different relaxation times. In dilute gels these structural elements act relatively independently, while in more highly concentrated gels breakdown of the short structural elements affects also the long structural elements.

It is shown that breakdown of a certain part of the structure is possible in the range of completely reversible deformations.

It is noted that the maximum shear stress $P = P_r$ on the $P(\epsilon)$ curve represents the maximum of the function of particle distribution by bond strength, which need not coincide with the maximum elastic deformation on the $\epsilon_e(\epsilon)$ curve, which corresponds to the maximum of the distribution function of the particles by critical deformations.

In conclusion, the author thanks laboratory assistant L. S. Meshcheriakova for performing the determinations.

Institute of Physical Chemistry
Academy of Sciences USSR
Moscow

Received July 24, 1957

LITERATURE CITED

- [1] Th. Schwedoff, J. de Phys. (2) 3, 341 (1889).
- [2] E. Hatscheck, R. S. Jane, Kolloid.-Z. 89, 300 (1926).
- [3] R. K. Schofield, G. W. Scott Blair, Proc. Roy. Soc., Lond. A 138, 707, (1932); 139, 557; 141, 72 (1948).

- [4] M. P. Volarovich and R. A. Branopol'skaia, *Colloid J.* 10, 406 (1948).
- [5] A. A. Trapeznikov, *Colloid J.* 12, 67 (1950); in the book: *New Methods of Physicochemical Investigation of Surface Phenomena* 1 (1950) p. 20; A. A. Trapeznikov and E. M. Shlosberg, *ibid*, p. 39.*
- [6] A. S. Kolbanovskaia and P. A. Rebinder, *Colloid J.* 12, 194 (1950).
- [7] J. G. Oldroyd, D. J. Strawbridge and B. A. Toms, *Proc. Phys. Soc. B* 64, 44, (1951); B. A. Toms and D. J. Strawbridge, *Trans. Far. Soc.* 49, 1224 (1953).
- [8] A. A. Trapeznikov and V. A. Fedotova, *Proc. Acad. Sci. USSR* 81, 1001 (1951); 82, 97 (1952); *Proc. 3rd All-Union Conf. on Colloid Chemistry* in Minsk (Izd. AN SSSR, Moscow, 1956).*
- [9] A. A. Trapeznikov and T. G. Shalopalkina, *Proc. Acad. Sci. USSR* 111, 380 (1956).**
- [10] A. A. Trapeznikov, *Proc. Acad. Sci. USSR* 102, 1177 (1955).
- [11] A. A. Trapeznikov, *Colloid J.* 10, 398 (1958).**
- [12] A. A. Trapeznikov, *Colloid J.* 18, 496 (1956).**
- [13] A. A. Trapeznikov, *Doctoral Dissertation* (Moscow, 1955).*
- [14] T. G. Shalopalkina and A. A. Trapeznikov, *Proc. Acad. Sci. USSR* 118, 994 (1958).**

* In Russian.

** Original Russian pagination. See C. B. Translation.

ELECTROCHEMICAL STUDY OF BENTONITE SUSPENSIONS

2. THE PROGRESSIVE ACTION OF SODIUM HYDROXIDE ON SUSPENSIONS OF ELECTRODIALYZED ASKANGEL

I. A. Uskov and E. T. Uskova

The question of the origin and nature of acid bentonites has attracted considerable attention recently. Large quantities of acid-treated clays are used in the oil-refining industry and as catalysts for clarification of oils in the food industry. Acid soils often contain minerals of the montmorillonite group, which have high exchange capacity. A knowledge of the properties of montmorillonite is necessary for studies of such soils. Finally, studies of the nature of acid aluminosilicates are of considerable theoretical interest, since they give a deeper insight into their structure.

Despite the large number of investigations of acid clays and soils, the problem of the nature of their acidity has not been finally solved. Acid clays are experimentally studied either by analysis of salt extracts [1-4], or by potentiometric [5-9] and, less frequently, conductometric [6, 8] titrations. The advantage of electrochemical methods applied without preliminary additions of large amounts of neutral electrolytes is that the suspensions are not subjected to the coagulating action of extraneous electrolytes.

Most of the investigators who performed electrometric titrations of acid soils with bases concluded that the process involves neutralization of exchangeable hydrogen, adsorbed on the surface of the clay particles [5-9]. However, it is difficult to reconcile this conclusion with the presence of aluminum ions in salt extracts [1, 2] and with the similarity between potentiometric titration curves of acid clay suspensions in presence of concentrated solutions of neutral electrolytes, and titration curves of aluminum salts [8].

In this connection it is useful to compare the curves obtained by Harward and Coleman [8] in potentiometric titrations, with sodium hydroxide, or bentonite suspensions after electrodialysis, leached with dilute (0.1 N) and concentrated (1.0 N) hydrochloric acid, saturated with aluminum, and passed through a column with a cation-exchange resin in the H form [10]. It was found that the titration curves for Al-substituted bentonite leached with 0.1 N HCl, and for electrodialyzed bentonite are similar, and are typical of the potentiometric titration of a weak acid by a strong base. The bentonite treated with the cation exchanger in the H form, and the bentonite treated with 1 N HCl, gave curves typical of strong acids. It was concluded from this that clay treated by the first group of methods are Al-substituted, and those treated by the second group are H-substituted. This conclusion was confirmed by thermochemical data: the heats of neutralization of Al-bentonite and of H-bentonite were found to be 5.4-6.4 and 13.4-13.6 kcal./equiv. respectively. It must be noted, however, that different bentonite fractions were a "clay" fraction, with particles smaller than 2 μ , and a "sand" fraction, consisting of water-resistant aggregates 0.17-0.25 mm in diameter.

It is to be expected that the potentiometric curves for Al-bentonites should have a second inflection in the strongly alkaline region, characteristic of aluminum salts [11, 12] and aluminum hydroxide sols [12, 13]. Mitra [7] found a second inflection for kaolinite clay, and attributed it to the presence of OH groups differing in accessibility in the kaolinite. Titration curves with a single inflection are known for montmorillonite. However, when the potentiometric curve of electrodialyzed bentonite was determined on the 7th day after addition of alkali, we found that there is an inflection at pH 10.5 [14].

In all the papers on potentiometric titrations of acid clays it is usually tacitly assumed that equilibrium is

established relatively rapidly after addition of alkali. Marshall [15] noted that equilibrium is established slowly, but he left the suspension with the alkali for 24 hours only.

Dietzel and Schmidt [9] found that the reaction of clay with alkali is completed in 20 minutes.

We found earlier that several days are required for equilibrium to be established after addition of alkali to electrodialyzed bentonite [14]. The manner in which the equilibrium is established, and the causes of this effect, were not determined. This question is of undoubted interest both for the development of our understanding of the neutralization of acid clays by alkalies, and in relation to problems associated with the definition of the term "cation-exchange capacity," and its practical determination.

The neutralization of electrodialyzed bentonite by a strong base is considered in this paper. The potentiometric and conductometric titration curves were determined at different intervals after the addition of alkali.

The Russian bentonite, askangel, was used for the investigations. The preparation of the suspension was described earlier [14]. The 7% suspension was electrodialyzed, kept for a year, and then again electrodialyzed at a potential gradient of ~40 v/cm in the middle compartment. After the second electrodialysis the suspension was diluted 10-fold and kept for 4 months more. 25 ml lots of the 0.7% electrodialyzed bentonite suspension were put into Pyrex flasks with ground-glass stoppers. Water was added to the suspension in each flask so that after addition of the required volume of 0.1 N sodium hydroxide the total volume was always 40 ml.

For the pH determinations, antimony and saturated calomel electrodes were used, the vessels with the suspension being continuously rotated at 60 rpm. The antimony electrode had a constant area in the determinations. For this, an antimony rod cast in a tube 4.9 mm in diameter was inserted in a glass tube of 5 mm internal diameter. The tube with the inserted antimony rod was sealed with picein, and the end of the electrode was then ground flat. The electrode was ground by means of 000 abrasive paper and rubbed with dry filter paper before each series of determinations. The surrounding glass tube and the antimony were ground down simultaneously, so that the exposed end of the antimony always had the same area. The potential of this electrode became constant fairly rapidly. It was assumed that equilibrium had been reached when the electromotive force did not change by more than a few units in the fourth significant figure after 1 minute.

However, the system proved to be very unstable in the region of the second inflection on the curve, and deviations up to 1 mv were permitted there.

The conductivities were measured by means of immersed platinum electrodes; the cell constant was 0.152. The measurement circuit included a plug resistance box and two standard resistances of 1000 ohms each; the sonic-frequency generator was tuned to 500 cycles; the null instrument was an electronic oscillograph. The error did not exceed 1%.

The successive series of determinations were performed 5 minutes, 24 hours, 8 days, and 14 days after addition of the alkali to the electrodialyzed bentonite suspension. The results of the conductometric and potentiometric determinations are given in Figs. 1 and 2.

The potentiometric curve determined immediately after addition of the alkali is similar to the titration curve of a weak monobasic acid by a strong base; it has one inflection at pH ~8.3, corresponding to 730 microequiv. of alkali per g. After 24 hours, a second inflection appeared in the high-pH region. After 8 days the first inflection was displaced to 810 microequiv./g, and the second became more distinct. The neutralization point in the curve in Fig. 2 corresponds to 855 microequiv./g. A horizontal plateau appeared in the region preceding the second inflection, and the inflection itself became extremely distinct.

The conductometric titration curves consist of three linear regions, and resemble the titration curves of mixtures of two weak acids by strong bases. The points of intersection of these regions and the slopes of the straight lines remained almost unchanged with time. The amount of alkali taken in the titration up to the first break in the curve is ~770 microequiv./g.

DISCUSSION OF RESULTS

All the potentiometric titration curves show a rapid increase of pH with small additions of alkali, followed by a slow increase in the middle region of the curve, and a fairly distinct equivalence point at pH 8.2-8.4. The curves also show considerable differences. First, attention should be drawn to the form of the curve obtained im-

mediately after addition of alkali; this differs from the others in not having a second inflection at pH 10-10.5. The entire curve shifts downward and to the right in the course of time, and the second inflection becomes more pronounced.

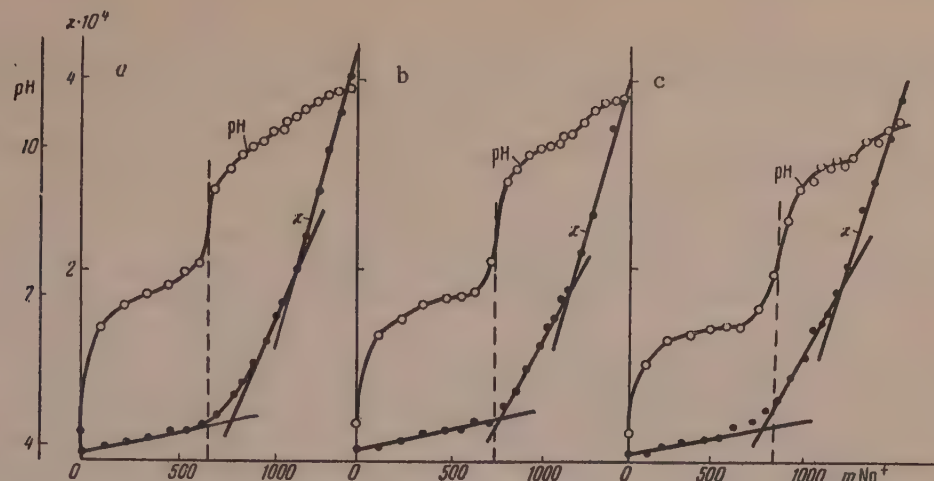


Fig. 1. Variations of pH and conductivity (κ) of electrodialyzed askangel suspension with the amount of sodium hydroxide added (m) in microequiv./g; times after addition of alkali:
a) 5 minutes; b) 24 hours; c) 8 days.

Not every possible measure to prevent the action of atmospheric carbon dioxide was taken in our experiments. The only step taken was to boil the distilled water used for dilution of the suspension. The decrease of pH, found in all the suspensions, may have been caused by the action of CO_2 .

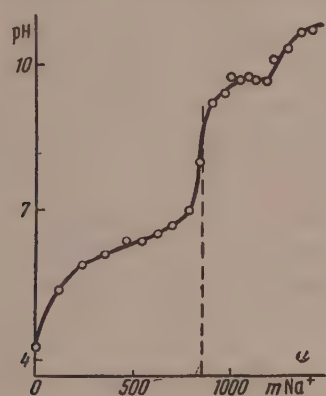


Fig. 2. Variation of pH of electrodialyzed askangel suspension with the amount of sodium hydroxide added (m) in microequiv./g; 14 days after addition of alkali.

A special experiment was performed to test this. Two flasks contained electrodialyzed bentonite suspension to which 688 microequiv./g of NaOH had been added, and the other two flasks contained the suspension with the addition of 1001 microequiv./g of NaOH. One of each pair of flasks was left for two weeks, while the contents of the other two flasks were tested by the procedure used in this investigation. On the 14th day the determinations were performed on all the suspensions, and after that only the contents of the flasks which had previously been closed were tested. The results, plotted in Fig. 3, show that atmospheric carbon dioxide did not have any appreciable influence on the pH of the suspension to which a considerable amount of alkali had been added.

We were previously inclined to attribute the second inflection on the potentiometric titration curve to the existence of two kinds of ions adsorbed on the particles of electrodialyzed bentonite — silicic acid, HSiO_3^- , and aluminum hydroxide residues $\text{Al}(\text{OH})_2^+$. The shift of the equivalence point with time is difficult to explain if it is assumed that H ions formed as the result of dissociation of silicic acid are present on the surface of the clay particles. There is no reason to believe that neutralization of these ions should take such a long time. The observed effect is satisfactorily explained if it is assumed that mainly adsorbed aluminum ions are present on the surface of electrodialyzed bentonite particles.

In the case of Al-substituted bentonite the equilibrium dispersion medium contains Al ions which, being hydrolyzed to a considerable extent, make the suspension medium acid. Addition of alkali first suppresses the hydrolysis of Al^{3+} ,^{*} with a sharp decrease of acidity, and the medium enters the neutral pH region. At the same time

* As in original. — Publisher.

the Al ions on the surface are replaced by Na ions, with formation of aluminum hydroxide. This evidently assists the replacement of multivalent aluminum ions by univalent sodium ions. Neutralization of the exchanged aluminum ions leads to the formation of equivalent amounts of aluminum hydroxide. The aluminum hydroxide formed creates steric hindrance to further interaction of the adsorbed Al^{3+} ions with sodium hydroxide, and therefore the over-all process is slow in time.

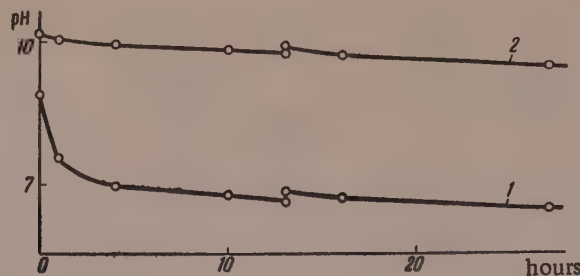


Fig. 3. Variations of the pH of dialyzed askangel suspensions with time; amounts of added alkali:
1) 688 microequiv./g; 2) 1001 microequiv./g.

The second inflection on the potentiometric curve is associated with dissolution of aluminum hydroxide and its conversion into aluminate. This inflection first appears after 24 hours and becomes distinct after two weeks;

at first it lies in the region of fairly high pH, but subsequently shifts into the region of lower pH and larger amounts of alkali. The dissolution of aluminum hydroxide is slow right from the start, otherwise the second inflection would appear immediately on addition of alkali. The probable cause is that the aluminum hydroxide formed "clogs" the interparticle spaces and sterically hinders access of alkali, so that the conversion of aluminum hydroxide into aluminate is retarded.

This study of the course of neutralization of electrodialyzed bentonite by sodium hydroxide therefore showed that the process is a complex one. The observed effects are satisfactorily explained on the assumption that electrodialyzed bentonite is mainly Al-substituted.

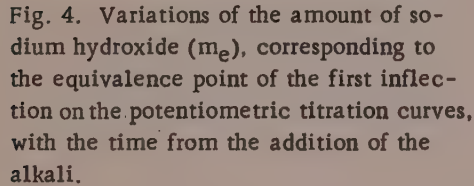


Fig. 4. Variations of the amount of sodium hydroxide (m_e), corresponding to the equivalence point of the first inflection on the potentiometric titration curves, with the time from the addition of the alkali.

The results of conductometric titrations confirm the conclusions drawn from the potentiometric determinations. The conductivity increases appreciably after the first additions of alkali, owing to the higher dissociation of sodium bentonite in comparison with electrodialyzed bentonite. The subsequent large increase of conductivity is caused by the appearance of sodium aluminate in the solution. The even greater increase after the second break is caused by the appearance of free alkali in the system.

Our experiments showed that neutralization of electrodialyzed bentonite by alkali proceeds slowly. Fig. 4 shows the time variation of the amount of sodium hydroxide corresponding to the equivalence point at the first inflection of the potentiometric titration curve. It is seen that further considerable amounts of alkali are absorbed during the first 24 hours; this absorption gradually decreases, but does not cease even on the 15th day. The limit of sodium hydroxide absorption is indicated on the curve in Fig. 4, but unfortunately it was not reached. Nevertheless, the course of the curve shows that the binding of alkali by electrodialyzed bentonite is not limitless; this agrees with the view that aluminosilicates have definite sorption capacities. The interaction of bentonite with sodium hydroxide ceases when the aluminum ions have been completely replaced by sodium ions. Only then can quantitative conclusions be drawn concerning the ion-exchange capacity of bentonite. Determinations of the sorption capacity of bentonite by means of potentiometric titration may be used provided equilibrium is reached in the system; this requires a very long time if the experiment is performed at room temperature.

SUMMARY

1. The course of the interaction of electrodialyzed bentonite with sodium hydroxide was studied by means of potentiometric and conductometric titration.
2. Potentiometric determinations showed that immediately after the addition of alkali electrodialyzed bentonite gives a titration curve similar to the titration curve of a weak acid by a strong base, the equivalence point being at pH 8.3.
3. It was found that in the course of time a second inflection appears at pH 10.4, due to formation of aluminate, on the potentiometric titration curve (recorded 24 hours later).
4. The potentiometric curves become displaced in the course of time in the direction of larger amounts of absorbed alkali. This is attributed to the presence of exchangeable aluminum ions in electrodialyzed bentonite; these ions react with alkali to yield aluminum hydroxide. The latter causes steric hindrance and thereby retards the interaction of bentonite with alkali.
5. The second inflection on the potentiometric titration curve becomes more distinct in the course of time. It is also displaced in the direction of larger amounts of absorbed alkali and lower pH values. The retardation of this process is also the consequence of steric hindrance caused by the presence of aluminum hydroxide in the spaces between the particles.
6. The results of conductometric titrations confirm the conclusions drawn from the potentiometric curves concerning the presence of exchangeable aluminum ions in electrodialyzed bentonite.

The T. G. Shevchenko State University, Kiev
The Ukrainian Academy of Agricultural Sciences

Received April 7, 1957.

LITERATURE CITED

- [1] V. A. Chernov, *The Nature of Soil Acidity* (Izd. AN SSSR, Moscow-Leningrad, 1947).*
- [2] K. G. Miesserov, *Pochvovedenie* No, 3, 17 (1955).
- [3] B. Chatterjee and M. Paul, *Indian J. Agric. Sci.* 12, 113 (1942).
- [4] J. N. Mukherjee and B. Chatterjee, and A. Ray, *J. Colloid Sci.* 3, 437 (1948).
- [5] C. E. Marshall and C. A. Krinbill, *J. Phys. Chem.* 46, 1077 (1942).
- [6] R. Mitra and K. Rajagopalan, *Indian J. Phys.* 22, 129 (1948).
- [7] R. Mitra and K. Rajagopalan, *Soil Sci.* 73, 349 (1952).
- [8] M. E. Harward and N. T. Coleman, *Soil. Sci.* 78, 181 (1954).
- [9] A. Dietzel and O. Schmidt, *Ber. Dtsch. Keram. Ges.* 31, 77 (1954).
- [10] W. H. Slabough, *J. Amer. Chem. Soc.* 74, 4462 (1952).
- [11] W. Blum, *J. Amer. Chem. Soc.* 35, 1500 (1913).
- [12] B. P. Nikol'skii and V. I. Paramonova, *J. Phys. Chem.* 2, 687 (1931).
- [13] M. E. Shishniashvili and A. L. Batsanadze, *Colloid J.* 15, 130 (1953).**
- [14] I. A. Uskov and E. T. Uskova, *Colloid J.* 19, 361 (1957).**
- [15] C. E. Marshall and W. E. Bergman, *J. Amer. Chem. Soc.* 63, 1911 (1941).

* In Russian.

** Original Russian pagination. See C. B. Translation.

DISPERSION OF A STREAM OF SUPERHEATED LIQUID

V. A. Fedoseev

The dispersion of liquids into drops by means of atomizers (spray jets, pulverizers, etc.) is accompanied by two processes, the combined effects of which in practice set definite limits to the application of the method of mechanical dispersion. When a liquid is dispersed in a spray, the dispersion of jets and films is accompanied by a process of the opposite character — mutual coalescence of the drops. After a certain definite degree of dispersion has been reached, further expenditure of energy for dispersion is not justified, as coalescence leads to growth of the droplets. The influence of coalescence in the spray may be diminished by two methods: either by a decrease of the number of droplets per unit volume, or by the establishment of conditions in the spray such that the droplets are mutually repelled. The first method is mainly suitable for use in dispersion of gas streams, and the second may be used, for example, if the stream is electrified, and the strong like charges cause mutual repulsion of the droplets.

Deriagin and Prokhorov [1] discovered a remarkable relationship between moisture deficiency and observed noncoalescence of droplets even after prolonged contact; it follows from this that the greater the evaporation of the droplets, the more is their coalescence hindered. The present author [2] measured the repulsion force between two evaporating drops suspended from the arms of a torsion balance. It was found that this force increases with increasing temperature of the evaporating drops; this is entirely in accordance with increased evaporation of higher temperatures.

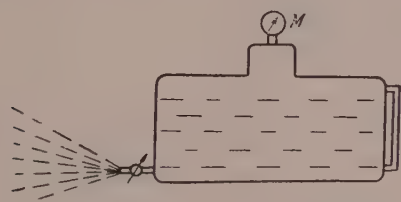


Fig. 1. Principle of device for dispersion of a superheated liquid.

Therefore if conditions are created in the spray such that the droplets evaporate fairly rapidly, a higher degree of dispersion of the liquid may be attained. It is found in practice that such conditions exist in the spray if a superheated liquid is dispersed. If a liquid is heated to above its boiling point under normal pressure (760 mm Hg) and released into a space at atmospheric pressure, this liquid is in a superheated condition and disintegrates into fine droplets without any external influence. This kind of dispersion is relatively simple to bring about. The liquid is

heated in a boiler (Fig. 1) to above its boiling point at atmospheric pressure, as shown by the equilibrium vapor pressure of the liquid, recorded by the manometer. The pressure gives an indication of the temperature of the liquid. If this liquid is released into a space where the pressure is atmospheric, a stream of superheated liquid is obtained; vapor bubbles extending the liquid into thin films are formed in the stream, and bursting of these bubbles leads to the formation of numerous small droplets. The process of dispersion in the stream of superheated liquid is accompanied by vigorous evaporation of the droplets owing to the excess heat provided by the superheating. This evaporation leads to strong mutual repulsion of the droplets, and yields fine droplets without the use of any special devices. Thus, in this method for the dispersion of a liquid the heated liquid but not its vapor is released from a boiler; it is a peculiar thermomechanical method for dispersing a liquid, but not a method for the formation of a disperse system by condensation of vapor.

The processes which take place in a stream of superheated liquid disintegrating into droplets differ considerably from the processes accompanying the disintegration of an unheated liquid. Whereas a stream of unheated liquid, released from the vessel at the same pressure as the heated liquid, has an extended undispersed portion, a stream of superheated liquid begins to break up immediately after leaving the nozzle. This distinction applies

even if the surface tension of the unheated liquid is decreased, by addition of alcohol, to the surface tension of the heated liquid.

Fig. 2 shows photographs of a stream of unheated liquid with added alcohol (a), and a stream of heated liquid (b), undergoing dispersion as the result of superheating.



Fig. 2. Liquid stream emerging from a nozzle:

- a) unheated water with added alcohol, at 3 atm.; b) water heated to a temperature at which the equilibrium vapor pressure is 3 atm.

The size of the drops formed in the dispersion of a stream of superheated liquid depends very little on the shape of the outlet nozzle. Under constant conditions, the dispersity of the aerosol formed depends only on the cross-sectional area of the nozzle. Different nozzles of equal cross-sectional area but differing in shape (round, triangular, and rectangular nozzles), and nozzles with a screw configuration for rotation of the emerging liquid, all give aerosols of the same degree of dispersion when the liquids are under the same pressure, i.e., at equal superheating. This shows that the processes which occur in the stream as the result of superheating of the liquid occur at a greater intensity than the processes determined by the hydrodynamic conditions in the emerging liquid. For a given cross-sectional area of the nozzle, the degree of dispersion of the aerosol formed depends only on the degree of superheating of the liquid. The higher the temperature of the liquid in the boiler, the greater will be its degree of superheating when it leaves the boiler, and the finer will be the aerosol formed.

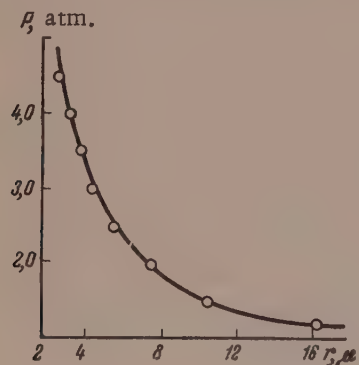


Fig. 3. Variation of the size of droplets formed during dispersion with the equilibrium vapor pressure of the superheated liquid.

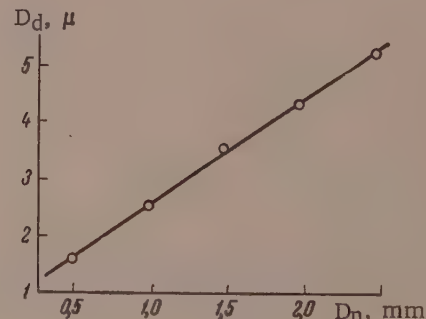


Fig. 4. Variation of the size of droplets formed during dispersion with the diameter of the nozzle through which the superheated liquid is released.

As the temperature of the liquid in the boiler is related to its equilibrium vapor pressure, the degree of dispersion of the aerosol formed is a function of the vapor pressure in the boiler. As it is much easier in practice to measure the pressure than the temperature in the boiler, the relationship in Fig. 3 is preferable for practical purposes. Fig. 3 shows that the droplet size decreases with increase of pressure.

Experiments showed that the relationship between droplet size and vapor pressure in the boiler is hyperbolic; i.e., for a given nozzle

$$Pr = \text{const.}$$

where P is the vapor pressure in the boiler; r is the average droplet radius.

Since the form of the nozzle has little effect on the degree of dispersion of the aerosol formed, for practical purposes it is possible to use a simple round nozzle in the form of a piece of pipe attached to the outlet valve. It was found that for a round nozzle a linear relationship exists at constant pressure between nozzle diameter and droplet size (see Fig. 4); here D_d is the diameter of the droplets formed, and D_n is the diameter of the nozzle.

As already stated, the dispersion of a stream of superheated liquid begins immediately as the liquid emerges from the nozzle. However, this process is not instantaneous; it continues as the liquid travels away from the nozzle and terminates at some distance from it, according to the power of the stream. Fig. 5 shows size distribution curves of droplets in a stream of spray formed from a superheated liquid leaving a nozzle 1.2 mm in diameter at 3 atm.

Curve 1 shows the dispersity of the aerosol in immediate proximity to the outlet nozzle. In this region there are droplets of a great variety of sizes, as the dispersion is not complete. Curve 22 represents the size distribution of the droplets at a distance of 3 m 70 cm from the origin of the stream. It is seen that the dispersion process is almost complete; the number of droplets is at its maximum, and their size is in the range of 17 to 45 μ . Curve 3 is for half way along the stream; it is seen that the dispersion process is continuing here.

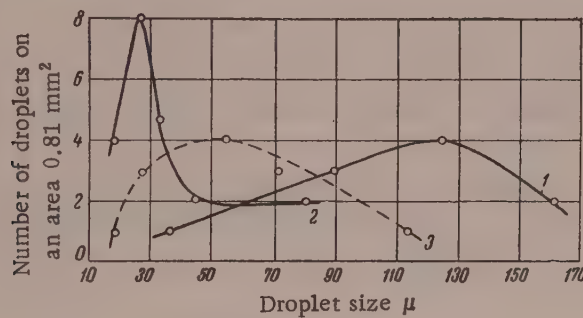


Fig. 5. Size distribution curves for droplets in a stream of superheated liquid at different distances from the exit nozzle.

The most interesting feature of this dispersion method is that it is possible, in a given time, to disperse a quantity of liquid which, if unheated, would require tens or even hundreds of horse power for its dispersion.* In some of our experiments 100 liters of liquid was converted into aerosol through a single nozzle in 1-1.5 minutes, yielding powerful waves of aqueous aerosol. The pressure in the boiler remained constant until all the liquid had passed through the exit valve. It is quite clear that the movement of such powerful aerosol waves would differ from that of aerosol waves created by ordinary aerosol machines. As confirmed in practice, these powerful aerosol waves can travel considerable distances; waves of aqueous aerosols were sent over more than 500 meters.

The action of the boiler may be regarded as follows. While the liquid is being heated, it stores heat; this heat is then expended rapidly for dispersion of the liquid.

This method is the most economical from the standpoint of power consumption, as all the heat is utilized in aerosol formation, while evaporation is beneficial, as it decreases coalescence.

It is the author's pleasant duty to thank Corresponding Member (AN SSSR), Professors A. S. Predvoditelev and B. V. Deriagin, for their interest, valuable advice, and helpful discussions.

* V. A. Fedoseev, B. A. Manakin, A. I. Polianskii, V. D. Korneichuk, and L. P. Latonina used aerosols made by dispersion of superheated liquids for control of agricultural pests; suitable equipment was designed and tested at the collective farms of the Odessa province. The purpose of this work was to study the physical principles of dispersion of superheated liquids and to provide a basis for the proposed method of aerosol production.

SUMMARY

1. A liquid heated to above its boiling point under normal conditions (760 mm Hg) and released into a space where the pressure is atmospheric disintegrates, as the result of its superheating, into fine droplets without the influence of any external forces or special devices (attachments, pulverizers, etc.).
2. The size of the droplets formed depends only on the degree of superheating of the liquid and the size of the exit nozzle. The shape of the nozzle has no appreciable influence on the droplet size.
3. It is convenient to use a relationship between droplet size and the equilibrium vapor pressure in the boiler. This relationship is hyperbolic in character, i.e., P_r is constant for a given nozzle.
4. For simple round nozzles a linear relationship exists between nozzle diameter and the diameter of the droplet formed.
5. The dispersion of a superheated liquid is completed only at a considerable distance from the nozzle. The distance at which the process terminates depends on the power of the stream, and may be several meters.
6. With this method of dispersion it is possible to disperse, in unit time, amounts of liquid the dispersion of which by the usual methods requires hundreds of horse power. When the liquid is heated, it stores heat, which is then expended rapidly for dispersion.

The I. I. Mechnikov State University
Odessa

Received July 24, 1956

LITERATURE CITED

- [1] B. V. Deriagin and P. S. Prokhorov, in the book: New Ideas in the Study of Aerosols, edited by B. V. Deriagin.*
- [2] V. A. Fedoseev and A. I. Polianskii, in the collection: Experiments on the Application of the Torsion Balance to the Measurement of Small Forces in the Interaction of Drops, Phys.-Math. Faculty, Sci. Res. Inst. Physics and Odessa State University, vol. 5 (1954).*

* In Russian.

THE STABILIZATION OF CARBON-BLACK SUSPENSIONS IN VASELINE OIL-DRYING OIL MIXTURES

B. N. Shakhkel'dian

The oil dispersion media used in the production of printing inks consist of film-forming vehicles of the polymerized drying oil type, and solutions of resins or bitumens in mineral oils. Mixtures of drying oils and nondrying mineral oils are also used. Finally, the printing properties of inks are sometimes modified by the addition of mineral oil to the finished inks made with drying oil.

It is clear that differences in the physicochemical nature of the dispersion medium should result in different physicomechanical properties and printing behavior of the inks, owing to differences in the adsorption of surface-active substances, which protect the pigment from agglomeration and structurization, on the pigment surface. The stabilizing effects of different vehicles in relation to a given pigment may be evaluated in terms of relative viscosity $\eta_{rel} = \eta / \eta_0$, i.e., the ratio of the viscosity of the ink to the viscosity of the dispersion medium, at a definite constant concentration of the pigment in all the systems [1]. It has been shown that the stabilizing effect is much greater with drying oils obtained by polymerization of linseed oil than with raw linseed oil; i.e., the effect increases with increased contents of polymer in the oil.

The object of the present investigation was a study of the influence of mixtures of drying oil and mineral oil in the stabilizing power of vehicles.

Solutions were prepared containing from 0 to 100% of polymerized drying oil ($\eta_{30} = 10.4$ poises, $d_{30} = 0.930$) in vaseline oil ($\eta_{30} = 0.767$ poises, $d_{30} = 0.871$, surface tension at the water interface 50.9 ergs/cm²). The pigment used was gas black, repeatedly extracted with hot benzene in order to remove polar substances which might influence adsorption of the surface-active components in the vehicle. Each of the solutions was blended into an ink containing 11.9% carbon black by volume, corresponding to 20 wt.% for an ink made with pure drying oil. The prepared inks were kept for a week before the tests so that wetting of the pigment particles, which continues after the mixing, could be completed and the inks acquired stable properties which did not change with time [2].

The viscosities were determined by means of a rotational viscosimeter, the outer cylinder of which was rotated by means of a motor, and the inner cylinder was suspended from a torsion arm. With cylinders 1.1 and 1.05 cm radius, a stress heterogeneity of the order of 8-9% arises in the annular gap. Therefore, to increase the accuracy in calculations of the flow curves, it was decided to determine the variations of the true velocity gradient with the stress at the wall on the inner cylinder, by the method described by Krieger, Elro, and Maron [3-5], who derived the following formula for calculation of the velocity gradient $\dot{\epsilon}$:

$$\frac{\dot{\epsilon}}{P} = \Phi \left[1 + K_1 \frac{d \log \Phi}{d \log P} + K_2 \left(\frac{d \log \Phi}{d \log P} \right)^2 \right], \quad (1)$$

$$\text{where } K_1 = \frac{S^2 - 1}{2S^2} \left(1 - \frac{2}{3} \ln S \right) \text{ and } K_2 = \frac{S^2 - 1}{6S^2} \ln S$$

are constants which depend on the viscosimeter parameters (the ratio of the cylinder radii $S = r_2/r_1$); P is the stress at the wall of the inner cylinder; Φ is the fluidity calculated from the original experimental data; the angular velocity ω and the torque M , by the usual formula $\Phi = \frac{4\pi r_1^2 r_2^2 L \omega}{M(r_2^2 - r_1^2)}$, valid for calculations of viscosity

and fluidity of true viscous liquids. The expression in the square brackets of Equation (1) is a correction introduced into the value of the fluidity or calculated velocity gradient for structurized liquids. For determination of this correction, Φ is first found, P is calculated from the formula $P = M / 2\pi r^2 L$, and $\log \Phi$ is plotted against $\log P$. The derivative $d \log \Phi / d \log P$ is then found by graphical differentiation for each point corresponding to the experimental stresses. For true viscous liquids, in which the fluidity and viscosity are independent of the stress, $d \log \Phi / d \log P = 0$, and the correction factor is unity. For structurized liquids the derivative is not zero, but increases with increasing deviation from the Newtonian law of flow. The constants of our viscosimeter were $K_1 = 0.0485$ and $K_2 = 0.00074$. As K_2 is small, the term containing the second power of the derivative may be ignored when the latter is itself small: $d \log \Phi / d \log P \ll 1$. In practice, this term was only taken into account in our calculations at low velocities and stresses. The correction factor was then as much as 1.5-2.0, which introduced a substantial correction into the calculated value of the velocity gradient. At higher deformation rates, when a considerable proportion of the structure was broken down, the term $K_2(d \log \Phi / d \log P)^2$ became negligibly small, and the correction factor as a whole decreased, reaching unity in the region of flow with completely broken-down structure. Thus the calculation method introduces considerable corrections into the values of the velocity gradient, and therefore into the $\dot{\epsilon} = f(P)$ relationship in its nonlinear region.

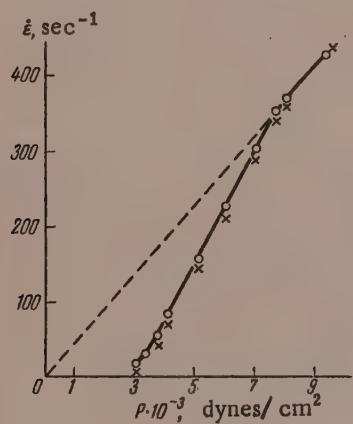


Fig. 1. Rheological curve for a carbon-black suspension in vaseline oil.

all the systems studied, is based on data obtained on the downward curve after the maximum structural breakdown had been reached, and therefore constitutes an independent rheological characteristic, not complicated by thixotropy, reproducible on increase or decrease of the deformation rate. Because of the great viscosity differences between the solutions used as dispersion media, it was not possible to draw conclusions concerning structure formation in relation to the composition of the dispersion medium merely from the $\dot{\epsilon} = f(P)$ or $\eta_{eff} = f(\dot{\epsilon})$ rheological curves. However, such conclusions can be drawn if the test results are represented in the form of the influence of the deformation rate on the relative increase of consistency (viscosity) produced by the addition of equal amounts of carbon black to media of different composition.

These relationships are plotted in Fig. 2; it is seen that the relative viscosity, corresponding to maximum structural breakdown, is highest in the system based on pure vaseline oil, and decreases with progressive additions of polymerized drying oil. Therefore, although increase of the velocity gradient breaks down the structural network in the nonpolar oil medium to such an extent that Newtonian flow takes place as the result of bond disruption between individual kinetic particles, and of deformation and orientation of the latter in flow, these particles themselves consist of aggregates the shape and size of which may vary according to the composition of the dispersion medium. It is evident that in systems containing polymerized drying oil the adsorption of its polymeric fractions on the pigment surface stabilizes the pigment, prevents aggregation, and thereby lowers the consistency. The relative viscosity corresponding to maximum structural breakdown decreases with increasing concentration of drying oil in the dispersion medium, tending to a limiting constant value $\eta_{eff}/\eta_0 = 12-13$ with 30% of drying oil and over in the dispersion medium. This shows that the adsorption reaches its limiting value at this concentration of drying oil, and in systems with high contents of drying oil complete structural breakdown occurs at

The rheological curve for one of the paints studied is given, as an example, in Fig. 1; this shows the velocity gradients calculated by the method described above, with corrections for deviations from Newtonian behavior, and the velocity gradients calculated on the assumption that the inks are Newtonian fluids, by means of the formula $\dot{\epsilon} = 2r_2^2 \omega / r_2^2 - r_1^2$.

It follows from Fig. 1 that the maximum possible structural breakdown is reached in the ink; this is shown by the existence of a linear region at high velocities and stresses. When extrapolated, this region passes exactly through the coordinate origin, showing that the viscosity is independent of the velocity and of the applied stress, i.e., that the fluid conforms to Newton's law. The substantial differences between the results given by the two methods, found in the region of anomalous viscosity, gradually disappear in the transition into the region of minimum constant viscosity. This rheological curve, which is typical of

high deformation rates, when the shape and size of the structural aggregates become independent both of the velocity gradient and of the composition of the dispersion medium.

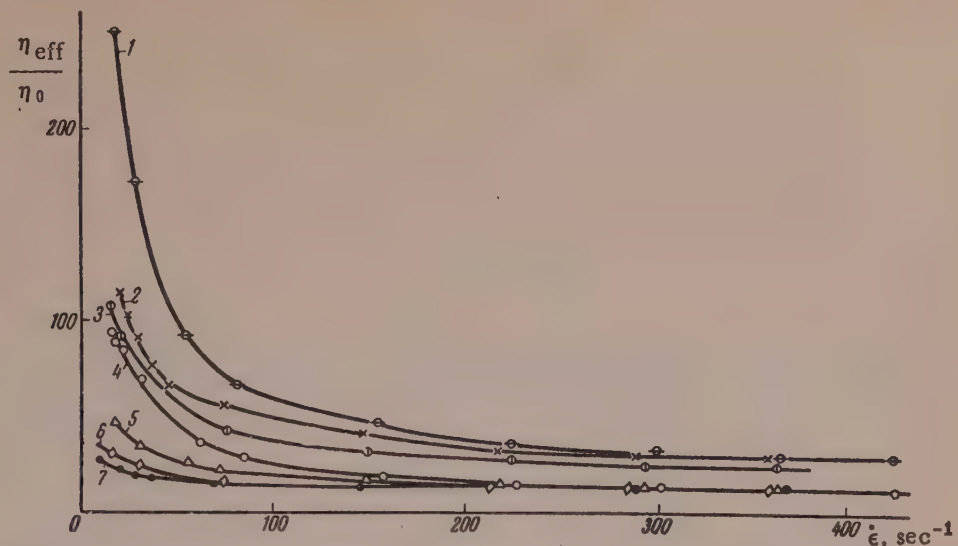


Fig. 2. Effects of deformation rate and composition of the dispersion medium on the relative viscosity of suspensions.

Composition of dispersion medium: 1) 100% vaseline oil ($\eta_0 = 0.755$ poise);
2) with 10% drying oil ($\eta_0 = 0.985$ poise); 3) with 20% drying oil ($\eta_0 = 1.32$ poises);
4) with 30% drying oil ($\eta_0 = 1.59$ poises); 5) with 40 % drying oil ($\eta_0 = 2.18$ poises);
6) with 80% drying oil ($\eta_0 = 5.12$ poises); 7) 100% drying oil ($\eta_0 = 10.4$ poises).

SUMMARY

1. Suspensions of carbon black in mixtures of vaseline oil and polymerized drying oil have structural viscosity; at high shear rates they undergo maximum structural breakdown and flow like Newtonian liquids.

2. The consistency increase (relative viscosity) corresponding to maximum structural breakdown is greatest in suspensions made with pure vaseline oil, and decreases with increasing contents of drying oil; this is indicative of the stabilizing effect of the drying oil. With 30% and more of drying oil in the dispersion medium, the relative viscosities of all systems with equal concentrations of carbon black tend to a constant value with increase of shear rate; therefore the limiting degree of adsorption is reached at this concentration of the drying oil.

The Moscow Polygraphic Institute

Received April 8, 1957

LITERATURE CITED

- [1] B. N. Shakhkel'dian, Colloid J. 18, 111 (1956).*
- [2] B. N. Shakhkel'dian, Sci. Trans. Moscow Polygraphic Inst. 4, 137 (1956).
- [3] J. M. Krieger and H. Elro, J. Appl. Phys. 24, 134 (1953).
- [4] J. M. Krieger and S. H. Maron, ibid. 25, 72, (1954).
- [5] W. Fritz, and H. Kroepelin, Kolloid.-Z. 140, 213, 149 (1955).

*Original Russian pagination. See C. B. Translation.

A TRADITIONAL ERROR IN THE THEORY OF CAPILLARITY

L. M. Shcherbakov

The theory of capillarity was largely formulated during the past century [1, 2]. It is based on two laws, generally known as Laplace's laws of capillarity. The first of these defines the excess pressure resulting from the curvature of the liquid surface:

$$K = K_0 + \sigma \left(\frac{1}{R_1} + \frac{1}{R_2} \right), \quad (1)$$

where R_1 and R_2 are the principal radii of curvature of the liquid surface, and σ is the surface tension. Laplace's second law defines the equilibrium conditions at the periphery of wetting, i.e., at the common interface of the three media in contact. The mathematical theory based on these laws satisfactorily accounted for most known experimental facts. However, until recently it involved an erroneous physical interpretation of the term K in Equation (1). It must be pointed out that Laplace himself did not consider the physical interpretation of the quantities used in this theory, and it was only later, in particular after the work of Van der Waals [2] and Bakker [3], that K came to be identified with the molecular pressure of the liquid,* while Equation (1) came to be interpreted as an equation for the variation of the molecular pressure with curvature of the liquid surface. Several objections have been raised in recent years [4, 5] to this interpretation of the Laplace equation.

1. It is extremely doubtful whether the molecular pressure of a liquid, which is an "internal" property ("an internal bond" in the language of analytical mechanics) can influence the mechanical equilibrium of the system. Ordinary hydrostatic pressure is more likely to exercise this function.

2. If K is identified with molecular pressure, the Laplace equation (1) is incorrect. This is confirmed by the following considerations. According to Equation (1), the molecular pressure should increase with decrease of the drop radius r . However, in the light of the molecular kinetic theory the decrease of the specific surface of the drop which accompanies decrease of r should be accompanied by an increase in the number of "surface" molecules at the expense of "internal" molecules; this cannot fail to decrease the degree of force discompensation in the molecules of the surface layer, and hence the molecular pressure. Therefore the Laplace equation is at variance with the molecular kinetic theory.

It is not difficult to find direct contradictions between the Laplace equation and experimental facts. It is true that owing to lack of methods for determination of molecular pressure a direct experimental test of this equation is not possible. However, it may be tested indirectly by comparison of experimental facts with the consequences of application of the Laplace equation to the question of saturated vapor pressure over a curved liquid surface. As an interface develops, the properties of the two contacting phases change. The Laplace equation defines the magnitude of the change in one of the properties of the liquid phase — its molecular pressure. As the phases are in equilibrium, variations in the properties of the liquid phase must be associated with variations in the properties of the gaseous phase. In particular, it follows that the change in the saturated vapor pressure brought about by curvature of the interface may be calculated from the corresponding change in the molecular pressure of the liquid.

It is known from thermodynamics that if the phases in a system are under different pressures, the pressure

* This was the consequence of a certain error in Laplace's reasoning; this is discussed below.

changes in the phases are interrelated as follows:

$$v' dp' = v'' dp'' \quad (2)$$

(v is the molar volume). Applying this relationship to the system in question, we can write for the change in the saturated vapor pressure:

$$dp = \frac{v_1}{v_g} dP, \quad (3)$$

where dP is the change of the (hydrostatic) pressure of the liquid phase. The latter can be calculated from the change of molecular pressure, given by the Laplace equation. If we apply the known thermodynamic identity

$$K = T \frac{\partial P}{\partial T} - P \quad (4)$$

to the case in which the liquid is bounded by a curved interface, and to a flat interface, we have after subtraction

$$\Delta K = T^2 \frac{\partial}{\partial T} \left(\frac{\Delta P}{T} \right).$$

Substituting the value of ΔK from the Laplace equation and integrating with respect to T , we have:

$$\Delta P = -(\sigma + \beta) \cdot \left(\frac{1}{R_1} + \frac{1}{R_2} \right),$$

where β is a real positive quantity, determined by the expression:

$$\beta = T \int_0^T \frac{1}{T} \left(-\frac{d\sigma}{dT} \right) dT.$$

Hence we have for the saturated vapor pressure over a curved liquid surface:

$$p = p_0 - \frac{v_1}{v_g} (\sigma + \beta) \left(\frac{1}{R_1} + \frac{1}{R_2} \right). \quad (5)$$

This expression is a direct consequence of the Laplace equation; apart from that equation, only the strict thermodynamic equations (3) and (4) were used in its derivation. Therefore Equation (5) will agree with experimental data to the same extent as the Laplace equation itself. However, according to Equation (5) (and therefore, according to the Laplace equation) the saturated vapor pressure should be less over a convex meniscus and greater over a concave meniscus than over a plane liquid surface. This conclusion is in complete contradiction to all theoretical conclusions (including the well-known Kelvin equation), and to experimental data; this shows that both Equation (5) and the Laplace equation from which it was derived are erroneous.

Despite the erroneous nature of the Laplace equation itself, individual relationships which formally follow from it, such as the Juring law, the equation for pressure in bubbles, etc., are in accord with experience. However, these relationships deal only with the second term of Equation (1), the excess pressure $\sigma(1/R_1 + 1/R_2)$, while the term K is eliminated during their derivation. Since liquid equilibrium is determined by the hydrostatic and not the molecular pressure, the term $\sigma(1/R_1 + 1/R_2)$ should be regarded as the excess hydrostatic pressure. In that case, however, the Laplace equation would be a formal combination of two entirely unlike terms: molecular pressure of the liquid with a plane interface, and change of the hydrostatic pressure caused by curvature of the liquid surface. It would be more logical to include these terms in two different relationships.

Thus, we may postulate the existence of two relationships of the Laplace type [4], one of which determines the change of molecular pressure with increase of the liquid surface, and the other represents changes of hydrostatic pressure, and the theory of capillarity must be based on the second relationship, as is the case in the classical work of Gibbs.

To derive these expressions, we consider the system "liquid (denoted by ') — saturated vapor (denoted by '')" with a developed interface. For the virtual change of the latter, we have on geometrical considerations:

$$\delta S = (1/R_1 + 1/R_2) \delta Y' = 2G \delta Y'.$$

The free energy of this system is: $F = F' + F'' + \sigma S$, where the surface tension σ is regarded as a function of the temperature T and of the average radius of curvature $R = 1/G$. Variation of this expression, for the supplementary conditions*:

$$T' = T_S = T'' = \text{const}, \quad V' + V'' = \text{const}, \quad m' + m'' = \text{const}$$

with the variation of F taken as zero, gives the equilibrium conditions for the system:

$$\mu'(p', T) = \mu''(p'', T), \quad p' = p'' + 2\sigma G + \frac{\partial \sigma}{\partial (1/G)}. \quad (6)$$

We differentiate these conditions with respect to G , taking into account that the derivative of the chemical potential μ with respect to the pressure p gives the molar volume v ; this gives the differential equation for the hydrostatic pressure in the liquid (denoted henceforth by P):

$$\frac{\partial P}{\partial G} = \frac{v''}{v'' - v'} \cdot \frac{\partial}{\partial G} \left[2\sigma G + \frac{\partial \sigma}{\partial (1/G)} \right] \approx \frac{\partial}{\partial G} \left[2\sigma G + \frac{\partial \sigma}{\partial (1/G)} \right].$$

Hence, integration with respect to G in the limits $G = 0$ to $G = G$ gives the following expression for the hydrostatic pressure under the curved liquid surface:

$$P = P_0 + 2\sigma G + \frac{\partial \sigma}{\partial (1/G)}. \quad (7)$$

This is the first of the expressions of the Laplace type, giving the relationship between the hydrostatic pressure and the extent of the liquid surface. To find the second equation, we substitute the value of P into the thermodynamic Equation (4). We then obtain, taking into account the expression: $\epsilon = \sigma - T \frac{\partial \sigma}{\partial T}$, which connects the specific total surface energy ϵ with the surface tension σ , the following expression for the molecular pressure of the liquid:

$$K = K_0 - 2\sigma G - \frac{\partial \epsilon}{\partial (1/G)}. \quad (8)$$

For a liquid drop this equation becomes:

$$K = K_0 - \frac{2\epsilon}{r} - \frac{\partial \epsilon}{\partial r}.$$

In discussing these results, we note that Equation (8) differs from the classic Laplace Equation (1) by the sign and the coefficient of the second term, and by the introduction of a third term for the variation of ϵ with r . The decrease of molecular pressure with decreasing drop size, which follows from Equation (8), is in harmony with elementary considerations of molecular kinetics. The presence of the coefficient ϵ in Equation (8), in place of the coefficient σ in the Laplace equation, is quite justifiable from the physical standpoint; since the molecular pressure is expressed thermodynamically as the derivative of the total energy of the liquid, changes of the molecular pressure caused by increase of the surface should be expressed in terms of the derivative of the total (and not the free) surface energy. It should also be noted that Equations (7) and (8) are in accord with the Kelvin equation, as the latter can be derived from them.

In conclusion, we consider the point in Laplace's paper [1] which led to the erroneous interpretation of his Equation. In the first section of this paper Laplace defines the force with which a liquid sphere attracts an external

* Corresponding to constant temperature and mechanical isolation of the system.

column of liquid normal to its surface, and gives it as*

$$K - H/b \quad (9)$$

(b is the radius of the sphere). In the modern view, the forces of attraction considered by Laplace are nothing but the molecular pressure of the liquid. In particular, K corresponds to the molecular pressure with a plane liquid surface. Therefore Laplace's intermediate Equation (9) is analogous to our Equation (8). However, Laplace goes further, and in the second section proceeds to calculate the force with which a liquid sphere attracts a liquid column contained within it. He obtained the following final expression for this force:

$$S = K + H/b, \quad (10)$$

here K and H are constants which, according to Laplace, have the same meaning as previously. It is here that Laplace's error lies.

Indeed, as was pointed out earlier, the force with which the liquid attracts an external liquid column corresponds, in modern terminology, to the molecular pressure of the liquid. The liquid as a whole exerts no influence** on the column directed inward, so that the total force acting on such a column is equal to the external (hydrostatic) pressure. Therefore the physical meaning of K in Equation (10) is not the same as in Equation (9). This was not taken into account by Laplace, and he therefore obtained the erroneous Equation (10), when he should have obtained the Equation:

$$P = P_0 + H/b,$$

analogous to Equation (7).

It should be noted that the constants H in Equations (9) and (10) also have different values. This could not have been taken into consideration by Laplace, as he did not take account of the thermal motion of the particles.

SUMMARY

1. It is shown that the Laplace equation:

$$K = K_0 + \sigma \left(\frac{1}{R_1} + \frac{1}{R_2} \right),$$

which determines the dependence of the molecular pressure on the curvature of the liquid surface, is erroneous.

2. Two equations of the Laplace type are derived:

$$K = K_0 - 2\sigma G - \frac{\partial \sigma}{\partial (1/G)}, \quad P = P_0 + 2\sigma G + \frac{\partial \sigma}{\partial (1/G)}$$

(where G is the mean curvature of the surface), which determine the variations of the molecular pressure K and the hydrostatic pressure P of the liquid with increase of its surface.

In conclusion, the author thanks Corresponding Member (AN SSSR) B. V. Deriagin and Professor O. M. Todes for valuable discussions.

The Mechanical Institute, Tula

Received April 2, 1957

LITERATURE CITED

- [1] P. S. Laplace, *Oeuvres completes*, Paris, 4, 1880.
- [2] C. F. Gauss, *Werke*, Gottingen, 5, 1867; S. D. Poisson, *Nouvelle theorie de l'action capillaire*, Paris, 1831; A. Davidov, *Theory of Capillary Effects* (Moscow, 1851); *** I. Gromeka, *Theory of Capillary Effects* (Kazan').
- * In the original notation.
- ** Because the individual forces are mutually balanced (for details, see [4,e]).
- *** In Russian.

1886);* Van der Waals, Z. Phys. Chem. 13, 657 (1894).

[3] G. Bakker, Z. Phys. Chem. 104, 10 (1923).

[4] L. M. Shcherbakov, Sci. Mem. Kishinev University, 1, No. 2, 23 (1949); L. M. Shcherbakov, Dissertation, Inst. Phys. Chem. Acad. Sci. USSR (1950);* L. M. Shcherbakov and V. I. Rykov, Sci. Mem. Kishinev University 5, 131 (1952).

[5] Great Soviet Encyclopedia, vo. 20, p 44 "Capillary Effects" (1953).*

* In Russian.

MICROSCOPICAL DETERMINATION OF DROPLET SIZE IN OIL MISTS

Z. M. Iuzhnyi

One of the commonest methods for determination of the dispersity of oil mists is microscopical measurement of droplets deposited on glass plates coated with special substances. The substance used must ensure a constant contact angle of the oil droplets.

If the contact angle is constant, the droplets are of regular lens shape, and the ratio of the lens diameter to the diameter of a free droplet remains constant.

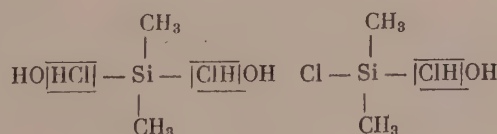
The commonest substance used for this purpose was basic lead stearate [1], probably because its preparation, the technique of applying it to glass, and the values of the spreading coefficients of different oils on it have been detailed fairly fully [2]. However, the coatings so formed had a number of disadvantages which hindered microscopic investigation, especially at high magnifications (the granular structure of zinc stearate interfered with the visibility of the finer droplets, the transparency was appreciably reduced by the thickness of the coatings, the coatings were irregular, etc.).

Moreover, zinc stearate is very inconvenient to use for covering curved surfaces (spheres, cylinders, etc.), necessary in certain investigations [3].

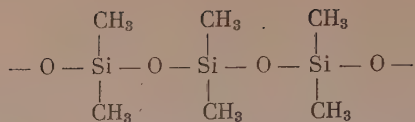
Several types of coatings have been reported in the literature for this purpose: octadecylamine [4], 1% alcoholic solution of mannitan monolaurate [5], a liquid organosilicon compound (Dri-Film 9987) [6], etc.

According to reports [6, 7], the most successful of these materials was the silicone oil, but the literature contained no information on the chemical composition of the substance (Dri-Film 9987), the method of its preparation, contact angles of different oils on the coating, etc. We therefore tested certain silicones and developed a technique for the use of one of them, namely dimethyldichlorosilane, $(\text{CH}_3)_2\text{SiCl}_2$. The standard commercial product, technical grade dimethyldichlorosilane (Technical Specification of the Ministry of Chemical Industry 3317-52) containing $\sim 80\%$ $(\text{CH}_3)_2\text{SiCl}_2$ and 20% of other methylsilanes of similar boiling point, was used. The technical product was further fractionated through a laboratory column, $(\text{CH}_3)_2\text{SiCl}_2$ containing 55.1% Cl_2 being collected at 69-71°.

10% solutions of $(\text{CH}_3)_2\text{SiCl}_2$ in benzene or in a light ligoine fraction (petroleum ether) were prepared for coating the glass. The glass plates, previously washed and dried (in air) were immersed in a beaker containing $(\text{CH}_3)_2\text{SiCl}_2$ solution, removed, and dried (for 5-10 minutes). The glasses were then rubbed dry (with cotton cloth) on each side. The films formed consisted of polymerized dimethyldichlorosilane. The mechanism of formation of these films is as follows: alkylchlorosilanes undergo hydrolysis and condensation at the hydroxyl groups [8] on contact with the surface, which always contains moisture (in varying amounts). In the case of dimethyldichlorosilane the hydrolysis proceeds as follows (at ordinary temperatures):



and yields a product of the following composition



The coatings formed were extremely thin, the transparency of the glass was quite unchanged, and the treated glasses were indistinguishable from the untreated in appearance. The films were quite heat-resisting (the coatings were unchanged after several treated glass plates had been kept for several hours in a drying oven at $\sim 200^\circ$) and mechanically strong (they were quite unaffected by vigorous rubbing of the surface). Oil drops on the coated glasses were of quite regular lens shape.

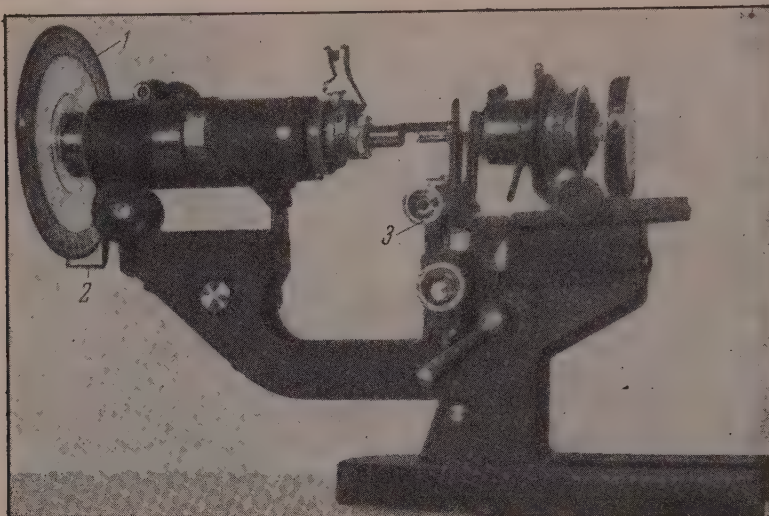


Fig. 1. Apparatus for determination of contact angles.

For determination of the spreading coefficient, the contact angles of different oils on these coatings were measured. The method described in the literature [6] was used, with somewhat different apparatus. The apparatus is shown in Fig. 1. The tube of a petrographic microscope, used as an ordinary microscope, was fixed horizontally. A graduated circular scale 1, with a pointer 2 attached below, was fixed in a special manner at the end of the eyepiece mount (containing an eyepiece grating). The usual stage was replaced by a moving guide (type ST-12, commercially available), by means of which the object can be moved very smoothly in two directions perpendicular to the microscope axis. The glass surface was fixed horizontally and parallel to the microscope axis.

TABLE 1

Contact Angles and Spreading Coefficients of Drops of Certain Oils

Oil	Lens size, mm	Contact angle	Spreading coefficient D/d
Transformer	2,2; 0,85; 0,7; 0,362	38,5	1,96
Diesel fuel	1,44; 0,88; 0,6; 0,333	32,5	2,05
Industrial "12"	1,16; 0,84; 0,24	39	1,92
Industrial "20"	1,72; 0,84; 0,42	40	1,94
Anthracene oil	1,84; 0,84; 0,64	50,5	1,74
"DEFO"*	2; 1,36; 0,8; 0,37	46,0	1,82

* DEFO is a distillation extract produced in the dephenolization of distillate oils in a number of oil refineries.

The drops were placed on the glass by contact with a needle moistened with the oil.

As in the investigation cited [6], the eyepiece hairlines were adjusted consecutively parallel to the glass surface, parallel to the tangents at the right and left base of the lens-shaped drop, and the corresponding angles were read off (to the nearest 0.5°). Almost the same values were obtained for α_R and α_L , so that after the first few measurements, which confirmed the equality of α_R and α_L , merely the value of 2α was measured. The measurements were performed with different oils, with drops of three or four different sizes, 3 measurements being made for each drop (a 10° eyepiece and 3°, 9°, and 20° objectives were used). Since the contact angle was the same for drops of different sizes (of the same oil), an average value of α from 9-12 measurements was taken for each oil. The results of the measurements are given in Table 1.

The following formula is used for determination of the drop diameter d from the lens diameter D (assumed spherical):

$$\frac{D}{d} = \sqrt{\frac{4 \sin^3 \alpha}{2 + \cos^3 \alpha - 3 \cos \alpha}}.$$

A graph based on this formula is given in Fig. 2. The results of the contact-angle measurements (see Table 1 and Fig. 2) were used to determine the spreading coefficient (ratio of lens diameter to drop diameter, D/d) of certain oils on the silicone coating.

The fractional compositions and certain physical properties of these oils are given in Table 2.

TABLE 2

Fractional Composition, Density, and Viscosity of the Oils Tested

Oil	Density d_{20}^*	Kinematic viscosity η (seconds)	Under 1 mm residual pressure								
			Start of boiling, °C	% by weight distilled off							
				up to 50°	from 50° to 100°	from 100° to 150°	from 150° to 200°	from 200° to 250°	from 250° to 300°	300° C	
Solar	0.846	5 (20°)	39	3,03	27,5	46,6	15,3	7,57	—	—	
Transformer	0.88	22,5 (20°)	89	—	1,15	33,25	56,6	9	—	—	
Industrial "12"	0.91	12 (50°)	98	—	—	15,9	59,4	21,2	3,5	—	
Industrial "20"	0.92	20 (50°)	106	—	—	23,8	48,2	23,2	4,8	—	
Anthracene oil	1,115	38,5 (50°)	64	—	22,4	25,7	35,6	16,3	—	—	
DEFO	0.95	15 (100°)	163	—	—	—	15,1	49,6	30,1	5,2	

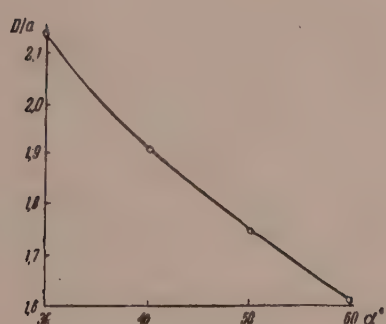


Fig. 2. Variation of spreading coefficient D/d with the contact angle α .

It follows from Table 1 and 2 that the spreading coefficient (D/d) varies little (roughly between 1.8 and 2) for oils differing greatly in fractional composition, physical properties, and chemical composition (such as Diesel fuel, transformer oil, and distillation extract containing up to 85% aromatics); it may be taken as 1.9 for most oils with sufficient accuracy for practical purposes.

Our most recent experiments showed that it is possible to use (with the same technique) technical dimethyl-dichlorosilane, $(CH_3)_2SiCl_2$, for formation of the silicone films; the spreading coefficient of oils on these films does not differ appreciably from that on films made from purified $(CH_3)_2SiCl_2$. This simplifies the use of this silicone considerably.

SUMMARY

1. Dimethyldichlorosilane is recommended for use as a coating for glass plates in microscopical determinations of droplet size in oil mists. The quality of these coatings is considerably higher than that of coatings made from basic zinc stearate. These coatings may also be used for studies of aqueous mists, as the films are water-repellent.

2. A very simple technique for the production of these coatings has been developed, and the contact angles of different oils on them have been measured.

The Moscow Station of the All-Union
Institute of Plant Protection (VASKhNIL)

Received February 28, 1957

LITERATURE CITED

- [1] N. A. Fuks, Progr. Chem. 19, 2 (1950); A. G. Amelin and M. I. Beliakov, Factory Labs. No. 12 (1955); V. F. Dunkskii, Z. M. Iuzhnyi, and D. N. Khokhlov, Factory Labs. No. 5 (1955).
- [2] N. A. Fuks, Colloid J. 11, No. 4, 280 (1949).
- [3] A. G. Amelin and M. I. Beliakov, Colloid J. 18, 385 (1956). *
- [4] R. E. Anderson, J. Econom. Entomol. 41, 974 (1948).
- [5] A. H. Yeomans, U. S. Dept. Agric. Min. Bull. El-267, p. 7, (1947).
- [6] K. R. May, J. Sci. Instrum. 22, 187 (1945).
- [7] J. R. De Jong, Ann. Appl. Biol. 37, No. 3, 316 (1950).
- [8] K. A. Andrianov and O. I. Gribanova, Organosilicon Compounds for Industry, part II (Central Office of Technical Information, Ministry of the Electrical Industry Press, 1946). **

*Original Russian pagination. See C. B. Translation.

** In Russian.

ANNOUNCEMENT

By the decision of the Presidium of the Academy of Sciences USSR, the 1957 Lomonosov Prize of 20,000 rubles has been awarded to the research group consisting of Doctor of Physico-Mathematical Sciences E. M. Lifshits, Corresponding Member (AN SSSR) B. V. Deriagin, and Candidate of Physico-Mathematical Sciences I. I. Abrikosova for their combined theoretical (E. M. Lifshits) and experimental (B. V. Deriagin and I. I. Abrikosova) investigations of molecular forces of attraction between solids.



PORTRAIT OF P. A. REBINDER

The Editorial Board of Colloid Journal warmly congratulates Academician Petr Aleksandrovich Rebinder, the eminent research worker in the field of the physical chemistry of disperse systems, on his 60th birthday, and wishes him health, happiness, and new successes in his work.

THE WORK OF P. A. REBINDER AND HIS SCHOOL ON SURFACE PHENOMENA IN DISPERSE SYSTEMS, AND ON PHYSICO- CHEMICAL MECHANICS

(On the 60th birthday of Academician P. A. Rebinder, and on his completion of
35 years of scientific activity)

The scientific and technological community of our country celebrates this year the 60th birthday of the eminent Soviet physical chemist, Academician P. A. Rebinder (born October 3, 1898), and his completion of 35 years of scientific activity.

This activity reflects the characteristic features of the Soviet era in the development of physical chemistry — its progressive character, its versatility, and its extensive and living connection with practice. Rebinder's fruitful activity has opened new frontiers in science, which have provided the scientific basis of many important industrial processes.

P. A. Rebinder graduated at the Physico-Mathematical Faculty of Moscow University as a physicist in 1923, and while still a student commenced scientific research on surface phenomena. His first experimental paper, entitled "The thermodynamics and physical chemistry of surface phenomena," dealt with a study of the relationship between temperature and the surface tension of aqueous solutions of surface-active substances in relation to the associated anomalies due to the influence of adsorption.

At the same time he showed that the coefficient of the Duclaux-Traube rule, for the increase of surface activity in homologous series with increasing length of the hydrocarbon chain, decreases rapidly and continuously with increase of temperature. The experimental results of these early studies of P. A. Rebinder are now included in reference books and physicochemical tables. In these investigations the method of maximum pressure of bubble and drop formation was used, with the aid of a convenient and simple apparatus constructed by Rebinder, which is now extensively used in research and works laboratories for measurement of surface tension at various interfaces (liquid-vapor and liquid-liquid). This apparatus was used by Rebinder and his associates (A. B. Taubman, K. F. Zhigach) to establish the relationship between surface tension and the time of formation of the absorption layer in solutions of higher homologs and surface-active semicolloids such as soaps, proteins, and saponin (the surface tension decreases exponentially to a static value). The development of his research in this field enabled Rebinder to determine the connection between surface activity and the molecular nature of the phases forming the liquid interface (the rule of equalization of polarities, etc.) and, in particular, to show that surface activity, i.e., the ability to form adsorption layers, usually increases sharply in the transition from a water-air (vapor) interface to a water-nonpolar liquid (hydrocarbon) interface, and that therefore substances which have no surface activity under the conditions of the usual determinations may be strongly adsorbed at interphase boundaries in organisms. These results were of great interest in relation to the biological role of surface activity in physiologically active substances. The discussion with the distinguished German scientist L. Traube which followed the publication of this work resulted in considerable modifications of some of the views held by Traube and his school.

In his research on "Water as a surface-active substance" (1926) Rebinder measured the surface tensions of aqueous solutions of highly soluble salts, including the double nitrate of silver and thallium, which has limited solubility in water at the melting point (82.5°), over the entire concentration range, and obtained data for

estimation of the structure of the adsorption layer of water and the dimensions of its oriented molecules. As the result of this work, the tension at different interfaces has become an important characteristic in the evaluation of various liquid media in a number of branches of science and industry — solutions of detergents, oils, and petroleum products (lubricants) etc. Included in this group are also researches into surface activity in mixed solvents (for example, of isoamyl alcohol in mixtures of water with ethylene glycol), studies of the influence of surface tension on the critical solubility temperatures of pairs of liquids, etc.

This work was developed further by A. B. Taubman in his studies of the structure of adsorption layers in aqueous and nonaqueous solutions.

1928 marked a new stage in Rebinder's work, which then became closely associated with technology and industry; numerous pupils and associates became attracted by the topical nature of the interesting and varied subjects studied.

Investigations of surface activity at various liquid interfaces in relation to their molecular nature guided Rebinder into the main direction of his scientific activity, successfully developed by himself and his numerous pupils and associates for 30 years. This work consisted of elucidation of the role of surface phenomena in the origin of properties characteristic of various disperse and colloidal systems, and of the specific processes taking place in such systems. Particular attention was devoted to variations in the nature of interfaces as the result of formation of oriented adsorption layers of surface-active substances on them. The role of surface effects and adsorption layers in the formation of disperse systems both by condensation (with formation of a new disperse phase) and by dispersion, in the aggregative stability of disperse systems, and in processes of breakdown (coagulation, coalescence) and structure formation in such systems was studied.

His work on one of the basic problems of colloid chemistry — the aggregative stability of lyophobic disperse systems — was founded on the concept of the kinetic nature of this stability, which was measured in terms of the reciprocal of the breakdown (phase separation) rate of a definite column of a given system (emulsion or foam), i.e. of its "life."

Rebinder measured the life of bubbles considered as elements of foams, or of droplets considered as elements of emulsions, in contact with each other and with the interface in solutions of surface-active substances and thereby determined the mechanism of formation and stabilization of emulsions and foams, and the phase inversion in emulsions. He showed jointly with E. K. Venstrem, N. N. Serb-Serbina, and A. M. Smirnova that emulsions of both types are formed when a system of two liquid layers is emulsified, but the only one to "survive" is the one which corresponds to the longer life of the droplets in relation to the nature of the stabilizing emulsifier layer. Some remarkable experiments were performed for the first time, in which a layer of mercury was cut by means of a glass rod under water with addition of a surface-active emulsion stabilizer; such cuts can exist for any length of time. These cuts form equilibrium plane-face figures, the analogs of Plateau's spatial figures of soap films and bubbles. This makes it possible to demonstrate experimentally the consequences of the "two-dimensional" theory of capillarity. At the same time, the life of such cuts in relation to the concentration of the surface-active substance can be used for evaluation of its effectiveness as an emulsion stabilizer. L. Ia. Kremnev's extensive research on emulsion stabilization is related to this work.

This work on the stability of disperse systems led Rebinder and his associates to develop methods of dispersion analysis. A convenient instrument (elastic microbalance and Figurovskii sedimentometer) has been designed in his laboratory for the continuous sedimentometric analysis of suspensions and emulsions, and is widely used in scientific laboratories, for students' practical work, and in industry.

Rebinder's work on foam formation has provided formulations for very stable fire-extinguishing foams (work by L. M. Rozenfel'd and E. M. Savitskaia) and for cellular heat-insulating materials (foam concretes, foam plastics).

Determinations of the structural and mechanical properties of monolayers on water surfaces, and of adsorption layers formed on solution surfaces under various conditions, continued by A. A. Trapeznikov, yielded important results relating to the structure of such layers and to the relationship between the mechanical properties and stabilizing action of adsorption layers.

The first papers in this series appeared in print before the results obtained in the laboratories of Langmuir and Harkins in the U.S.A.

As the result of further work in this field, Rebinder postulated the existence of two types of stabilization of lyophobic disperse systems: 1) stabilization which may be effected by nonstructurized molecular adsorption layers or diffuse ionic double layers or, as in liquid films and foams, as the result of local differences of surface tension, preventing attenuation of the film (the Marangoni-Gibbs effect) and 2) stabilization caused by a structuromechanical barrier localized in the surface adsorption layer of the dispersion medium or throughout its volume. This second stabilization factor, which operates in protective colloids, prevents close approach of the particles and ensures almost complete stability even in concentrated disperse systems which cannot be stabilized by other methods. When the interfacial tension is very low, two-phase colloidal systems are lyophilic, as in the case of semicolloids of the soap type, or of critical or solubilized emulsions. Such disperse systems are formed spontaneously and are thermodynamically stable, not requiring additional stabilization. That is why many suspensions and sols of the intermediate type have fairly high stability even in absence of a structuromechanical barrier (aqueous clay suspensions, hydroxide sols, and suspensions in hydrocarbon media, the stabilization of which by surface-active substances has been studied in detail by Rebinder and his associates). Subsequently Rebinder has devoted much attention to lyophilic disperse systems, which he regards as true spontaneously-forming colloids, and which constitute a continuous transition from true solutions to coarsely dispersed two-phase systems — stabilized suspensions or emulsions. In this connection he studied the laws of solubilization — the colloidal solution (within the micelles) of liquids insoluble in the dispersion medium itself. In 1936, independently of Hartley, Rebinder introduced the concept of the structure of thermodynamically stable spheroidal soap micelles with lyophobic nuclei and lyophilic outer shells. This work was extended further (jointly with K. A. Pospelova and Z. N. Markina), in relation to the conversion of the spheroidal micelles into flat laminar micelles and microcrystals of soap, as the result of coagulation and then crystallization structure formation with increase of concentration and decrease of temperature. An interesting effect was discovered in these investigations: soap gels became greatly liquefied when used for solubilization of hydrocarbons, the maximum viscosity becoming thousands of times less, evidently as the result of reconversion of laminar into spheroidal micelles. Work on solubilization in connection with polymerization in emulsions was continued by A. I. Iurzhenko and his associates, and by P. M. Khomikovskii.

Related to this group of investigations are Rebinder's studies (jointly with N. N. Petrova, A. B. Taubman, and others) of the wetting and detergent action of surface-active substances. In his work on the physicochemical principles of detergent action, in association with specialists on the technological production and applications of detergents (D. A. Rozhdestvenskii, A. Iu. Rabinovich), Rebinder showed that high detergency is determined by an optimum combination of surface activity (adsorptive power) and colloidal properties (tendency to structure formation) in the detergent, especially in surface layers. This ensures stable emulsification and solubilization of liquid (oily) dirt, and peptization of solid dirt when washed from the surfaces of fabrics, etc. In studies of the stabilization of aqueous suspensions (jointly with N. N. Serb-Serbina) it was shown that soaplike surface-active substances at low concentrations, present in true solution and adsorbed as oriented monolayers, make the surfaces of the solid particles water-repellent and flocculate suspensions, causing the particles to float by adhesion to air bubbles. At higher concentrations, corresponding to micelle formation, the adsorption layers acquire a gel structure and exert a stabilizing action characteristic of soaps, with total suppression of flotation.

The researches of Rebinder on the wetting of solid surfaces, and the influence of oriented adsorption layers and of the molecular nature of the contacting phases on wetting, are of great scientific and practical importance. These results, presented by him together with data on the adsorptional lowering of strength at the 6th Congress of Russian physicists in 1928, represented the first physicochemical investigation of the quantitative laws of wetting, based on contact-angle measurements, under various condition. He introduced the concept of selective wetting of solid surfaces by pairs of liquids of opposite polarity (water and heptane) in conditions of their mutual displacement from the surface. He was thus able to classify solid surfaces as hydrophobic and hydrophilic, according to the molecular nature and structure of the solid and the ratio of the heats of wetting. Jointly with M. E. Lipets, M. M. Rimskaya, and A. B. Taubman, he studied the influence of oriented adsorption layers of surface-active substances on selective wetting and on hysteresis of wetting at the water-air interface under different formation conditions of the three-phase perimeter. The mechanism of action of flotation and collecting agents was elucidated as the result of this work. Together with A. N. Frumkin's well-known work on the mechanism of formation of the contact angle, where the wetting interlayer of the aqueous medium is disrupted and a thin residual layer of the medium forms a new film phase, Rebinder's work laid the foundation of modern physicochemical concepts of the nature of the elementary act in flotation — the adhesion of mineral particles to gas bubbles.

It was demonstrated in this work that in froth flotation sufficiently sharp hydrophobization of the solid surface by the action of the oriented adsorption layer can be induced only by chemisorption, i.e., by chemical fixation of polar groups at the appropriate regions of the solid surface. This fixation of polar groups reinforces the orientation of the adsorption layers of hydrocarbon chains perpendicular to the surface.

These concepts were later applied by A. B. Taubman in studies of the mechanism and principles of the dust-collecting action of surface-active substances added to water for prevention of silicosis in mine workers.

A consequence of Rebinder's work was the general principle of the inversion of wetting of solid surfaces when adsorbed layers of oriented molecules of surface-active substances are formed on them. This effect, which is especially pronounced in conditions of selective wetting, was extensively utilized by D. L. Talmud and his associates in the so-called "molecular welding" for intensification of adhesive action, and by N. N. Korotkevich, A. F. Mutul, and others for reinforcement of the bonding between bitumen and mineral fillers and gravel in road surfaces. Associated with this trend was the work of P. A. Rebinder and his associates (V. B. Margaritov, A. P. Pisarenko, et al.) on adsorptive activation of fillers in rubber stocks, on disperse pigment structures in oil paints, and on the scientific principles of lithographic printing processes. This work helped to clarify the mechanism of interaction between printing ink and the form and paper (L. A. Kozarovitskii et al.) and led to the development of new methods for evaluation of the quality of printing inks and paper, considered as disperse structures, and to improvements in printing technology.

Rebinder's work has been widely developed in the food industry, and has resulted in the clarification of the physicochemical principles of a number of processes in the industry. This was furthered by a special course of lectures organized and presented by Rebinder jointly with A. V. Lykov in the Moscow Technological Institute of the Food Industry. Among the results obtained, mention should be made of research into processes of conversion of chocolate pastes, considered as structurized suspensions, and elucidation of the action of liquefiers — surface-active substances such as lecithin; the production of food emulsions such as margarine (N. A. Petrov) and butter (I. N. Vlodavets); studies of gelation processes in the confectionery industry and evaluation of gelating power, by V. S. Griuner and his associates; influence of moisture and water distribution in the grain on flour milling (Ia. N. Kuprits and his associates); studies of the elasticoviscous and relaxational properties of flour dough (B. A. Nikolaev et al.).

Rebinder's work on the form of bonding between moisture and disperse bodies during drying has acquired special importance in relation to the work of A. V. Lykov and his school on the theory of drying. Rebinder stresses that the bond between moisture and the material should be characterized by its free energy, and points out that, apart from chemical (constitutional) and adsorptive bonding (including chemical hydration) in solutions, it is necessary to take into account that the rest of the solvent (osmotically bound water) is held not by molecular forces but as the result of entropy, i.e., in consequence of the entropy increase during the uniform distribution of the components in the solution. The role of immobilized water, not bound, but held mechanically in a coagulatory or condensational structure, was demonstrated.

It was thus established as the result of all these investigations that the fundamental properties of disperse systems — the stability of various types of emulsions, foams, and suspensions, and the tendency to structure formation in suspensions — like the formation of disperse systems by dispersion and condensation processes are determined by the origin, nature, and structure of the adsorption layers at the interface between the dispersion medium and the disperse phase.

30 years ago Rebinder studied the forces required to split calcite crystals along the cleavage planes in various liquid media, and discovered adsorptive lowering of strength (hardness).

This effect is caused by lowering of the surface energy (work of formation) of the new surfaces which develop in a deformed solid body at its structural defects under the influence of adsorption from the external medium. As these surfaces originate and develop, they become covered with adsorptive layers as the result of two-dimensional diffusion. The very general effect of adsorptive strength lowering and easier deformations of various types has been extensively studied both here and abroad, in metals (poly- and monocrystalline), graphite, ionic crystals (mica, gypsum, calcite, quartz, etc.), glasses, rocks, and concretes, and has been named the Rebinder effect. This work forms the basis of a large new branch of science — physicochemical mechanics. These adsorption effects are especially large under prolonged loading under conditions of creep or prolonged

strength (stability) of the solid, and under periodic loading which weakens its structure at weak points (under condition of fatigue strength). The work of P. A. Rebinder and V. I. Likhtman and their co-workers, G. I. Logginov, M. S. Aslanova, and others, has demonstrated that the new surfaces which develop in microcervices (cracks) in the elastic deformation region disappear again after removal of the load, as if healed by molecular cohesion; the adsorptive action of the medium can be completely reversible, and the body gradually recovers its properties after removal of the load, displacing the adsorption layers which had penetrated at the weak points in its structure. Solid bodies undergoing deformation may change qualitatively as the result of adsorption, being converted from the elasticobrittle to the plasticofluid state or vice versa. These adsorption effects can be used to facilitate and improve mechanical treatment of metals by pressing and cutting, to accelerate processes of fine grinding (particularly vibratory grinding), and drilling of hard rocks (L. A. Shreiner and K. F. Zhigach). The action of surface-active lubricants consists largely of adsorptional softening (plastification) of the surface layer of the metal; this was demonstrated by P. A. Rebinder with V. I. Likhtman and S. Ia. Veiler. Active lubricants therefore accelerate running-in of machines by easing the leveling of surface irregularities. Subsequently, when the running-in process is complete, local stresses in the surface layers are reduced and the same lubricants greatly decrease wear. Strength loss in metals occurs not only as the result of corrosion, but sometimes to an even greater extent as the result of reversible adsorptional action of the medium. Thus, in addition to corrosion fatigue, there is adsorption fatigue (G. V. Karpenko) and adsorption creep of metals.

In further development of this work, P. A. Rebinder, jointly with E. K. Venstrem and V. I. Likhtman, discovered and studied the electrocapillary lowering of metal strength, the decrease in the resistance of metals to deformation and destruction on polarization of the metal surface in electrolytes.

In full harmony with the electrocapillary curves for the surface tension of liquid metals, the maximum strength is found at the point of zero charge, the significance of which was discovered by the well-known work of A. N. Frumkin and his school. Near this maximum (at weaklycharged solid surfaces) the introduction of surface-active substances into electrolytes results in an additional decrease of strength as the result of adsorption. This work of Rebinder was developed further by the well-known German metal physicist Masing and his associates in Gottingen.

In recent papers by P. A. Rebinder, V. I. Likhtman, and their associates, it is shown that the greatest adsorptional lowering of the strength of single metal crystals is produced, not by typical surface-active substances, but by fusible surface-active metals, in the form of melted coatings or admixtures, which greatly decrease the surface energy of the solid metal undergoing deformation. Such admixtures are widely used as adsorptive modifiers in casting. By retarding the growth of crystallization centers, they confer a much finer structure to alloys and so increase their strength at normal temperatures. However, at high operating temperatures these same admixtures of surface-active metals become harmful, and considerably reduce the heat resistance of the alloys; this has been shown by a number of metallographers (S. T. Kishkin et al.).

Adsorption effects can be used for control of the mechanical properties of substances, not only by decreasing their strength in mechanical treatment, but also by indicating ways of increasing strength. This can be achieved by elimination of surface-active media and impurities, which are especially dangerous at high temperatures and stresses, and cause the development of surface defects. On the other hand, the adsorptive action of the medium can be used to intensify surface strengthening of solids by internal dispersion of metal in the surface layer. Thus, the mechanical properties of solids and treatment processes can be controlled by the simultaneous influence of physicochemical factors, stress, and temperature. The physicochemical influence of the medium often proves decisive here: pressure treatment of metals, especially at high temperatures with the use of powerful presses, is impossible without the use of active lubricants, the choice of which is a complex problem which is solved as the result of the above-mentioned researches. Fine (colloidal) dispersion of valuable components of solid alloys, refractories, dyes, and fillers is impossible in absence of surface-active additives.

The work of Rebinder and his associates has also indicated the path to a scientific solution of the opposite problem - the production of solid materials with predetermined mechanical properties and structure by the formation of a new solid phase by crystallization from a melt or solution, or by pressing and sintering of powders. The principal types of spatial structure in disperse systems - coagulational, condensational, and crystallizational structures - have been defined and the mechanism and kinetics of structure formation has been elucidated in close relation to the resulting mechanical properties (strength synthesis).

P. A. Rebinder and his associates (N. N. Serb-Serbina, K. F. Zhigach, E. E. Segalova, and L. A. Abduragimova) have studied the formation and characteristic properties of thixotropic coagulation structures in suspensions and sols (in relation to the sol \rightleftharpoons gel transition) and showed that all these properties (relatively low strength, very pronounced plasticity and creep, and reversible restoration of the initial strength after structural breakdown) are determined by thin residual interlayers of liquid medium at the points of contact between the particles forming the structure.

L. A. Abduragimova showed that in such solidlike structures the maximum viscosity in the quasi-elastic region (at low shear stresses) is 8-9 orders of magnitude greater than the minimum viscosity of the totally destroyed structure.

P. A. Rebinder and N. V. Mikhailov succeeded, by the use of delicate methods, in determining complete flow curves for the transition from fluidlike to solidlike structures, i.e., in obtaining the complete picture of the decrease of effective viscosity from the upper limit to the minimum value, and thereby established a general relationship between the equilibrium degree of breakdown of a thixotropic structure in steady flow and the acting shear stress (or velocity gradient). This made it possible to introduce the concepts of the maximum viscosity of the virtually intact structure and the minimum viscosity of the completely broken-down structure as new invariant characteristics of substances such as bitumens, cement-sand mixes, and concretes used in building and road making, in the place of the indefinite concepts of structural viscosity used in colloid chemistry. The maximum viscosity characterizes the creep or mechanical strength of the material under various service conditions, while the minimum viscosity characterizes the transportability, workability, or moldability of the structurized mass in concreting processes or in the formation of constructional parts under works conditions.

Rebinder's concepts of coagulation and condensation structures (formed during consolidation and drying of clay soils), and of their rheological characteristics, have been extensively applied in soil science and engineering geology (I. M. Gor'kova, N. Ia. Denisov) in studies of the mechanism of soil subsidence, the behavior of quicksands, etc.

In further development of Rebinder's work on structure formation, K. F. Zhigach and co-workers developed a number of optimum formulations for thixotropic colloidal solutions and suspensions to be used in modern technological processes of deep drilling under various oil field conditions. These structurized drilling fluids can be used for increasing drilling speeds under difficult conditions, prevent accidents, and are widely used in the oil industry.

Rebinder's studies of the mechanical properties of coagulation structures and polymer solutions in relation to the spatial networks formed in them provided the basis for a relational system of quantitative characteristics of the elasticoviscous (relaxational) properties of various structures. This involves studies of the course of development of deformation in homogeneous shear under the action of a constant tangential force in a narrow gap between two coaxial cylinders or parallel plates. Rebinder used simple relaxational models to derive theoretically the law of elastic relaxation of shear stress, which was confirmed experimentally for coagulatory structures such as aqueous suspensions of bentonite clays, and aluminum oxide and vanadium pentoxide hydrogels (in relation to the discovery that they exhibited elasticity - clearly defined retarded resilience). A simple relationship was derived for the kinetics of development of elastic shear deformation and elastic relaxation in polymers and solutions, with the use of a single constant characterizing the maximum viscosity (L. V. Ivanova-Chumakova).

Rebinder's work has assisted in the development of the scientific principles of conversions of polymers into materials and articles of predetermined structure and mechanical properties (by the production of disperse structures in rubbers and plastics by the introduction of active fillers, under the simultaneous influence of plasticizers and surface-active additives).

Rebinder studied (in 1934) the modification of crystallization at the initial stages of formation of solid-phase nuclei from undercooled melts or supersaturated solutions. He noted that the development of the new phase must pass through a colloidal stage, and it is at this initial stage that the further development of the new phase can be regulated by means of physicochemical factors - degree of undercooling of supersaturation, the action of added adsorbable substances (modifiers of the 1st kind) or of dispersed additives consisting of suspended particles which have favorable conditions for the formation of crystallization nuclei on their surfaces.

(modifiers of the 2nd kind). Surface-active additions (modifiers of the 1st kind) usually produce a very fine structure in polycrystalline metals and alloys, by suppressing the growth of crystallization centers as they arise; as the result of adsorption on their surfaces, these modifiers favor the formation of a large number of micro-crystals in unit volume in a given time. If their growth is suppressed completely, a colloidal system may be formed. If a modifier of this type is also a stabilizer, such as a protective colloid in aqueous solution, the colloidal system which results is quite stable to coagulation. By being absorbed to different degrees on different faces of the forming crystallization centers, modifiers of the 1st kind can not only make the polycrystalline structure finer, but are capable of greatly changing the crystal form, usually making them more anisometric, but with an unchanged crystal lattice. The greatest superficial growth is found in those crystal faces the surface tension of which is decreased owing to selective adsorption, and whose linear growth rate is the most retarded. These changes of crystal form also alter the conditions for their concretion and at the same time, in view of the much finer structure formed, can greatly improve the mechanical properties; for example, by increasing the strength of alloys, or of hardened cement, during crystallization of new compounds in the course of hydration hardening, etc. T. P. Zhuze used Rebinder's theories in his studies of surface-active substances used as depressants which lower the pour point of petroleum products such as lubricating oils at low temperatures, by their influence on the crystallization of paraffins. This work was continued by P. I. Sanin.

The researches of P. A. Rebinder with E. E. Segalova, O. I. Luk'ianova, and others, on crystallizational structure formation in the hydration-hardening of mineral cementing materials (aluminate-silicate cements, plaster of Paris, lime) have acquired special significance. This work has given rise to a general physicochemical theory of hardening, with the action of surface-active additives and electrolytes taken into consideration, which can be used for control of the formation and growth of crystallizational structures in the production of very strong and durable building materials and structural parts with predetermined properties, and with the minimum consumption of cement.

The work of P. A. Rebinder and his associates on structure formation has provided the basis of a new concrete technology, developed by N. V. Mikhailov and co-workers, in which mechanical vibrations and physico-chemical factors are utilized in the production of concrete and ferroconcrete articles.

As the result of Rebinder's activities, a number of new important problems in colloid chemistry have been raised and studied; this has led to the reorganization of several of its main divisions in the light of the physical chemistry of surface phenomena. The work of Rebinder and his associates on structure formation in disperse systems, and physicochemical studies of the deformation, predestruction, and dispersion of solids, led to the growth of a new boundary region of science — physicochemical mechanics. The development of this region has enriched the physical chemistry of disperse systems by correlating it with molecular physics, the physics of solids, the mechanics of materials, soil science, problems of engineering geology and building, the technology of constructional materials, and a number of other branches of technology of primary importance in the national economy. It is in this direction, in all of P. A. Rebinder's work, that the special characteristics of his activity as a Soviet scientist were revealed, manifested in a close, organic bond between scientific theory and the most important problems and demands of modern technology. Rebinder's original approach to new important scientific problems stems from a generalization of the demands of technology and of its development under the conditions of our socialist economy. Work on such scientific problems has united many formerly unrelated branches of technology on a common scientific basis. For example, research into the wetting of solid surfaces and of the influence of adsorption layers on wetting has provided a common theory for flotation processes, printing, activation of fillers in materials based on polymers, and of pigments in varnish and paint systems. Theories of coagulational and condensational-crystallizational structure formation now form the basis of production of new constructional materials such as concrete, ceramics, and sintered metals, and the conversion of polymers containing active fillers into various articles. The development of the scientific principles of technological processes has made it possible to determine their optimum conditions and to introduce new and rational technological methods.

P. A. Rebinder and his associates work in close cooperation with the industrial institutes and directly with industry. The extensive consultant work of Rebinder and the leading representatives of his school in industry has acquired great importance in this respect. This has forged close scientific bonds with numerous centers of our land.

A characteristic feature of Rebinder's work is the breadth and diversity of its applications in the most varied branches of science and technology. At the same time, all the branches of the scientific and practical activity of Rebinder and his school are united by a common idea — the control of properties of disperse systems by action on interfacial layers — for radical improvement of various processes. The significance of these researches is also seen in the fact that they have demonstrated more clearly than ever before the importance of surface phenomena in the most diverse branches of natural science and modern technology.

All the activities of P. A. Rebinder — the originator of a number of trends in the physical chemistry of surface phenomena and disperse systems — is characterized by a desire to place science at the service of industry, to provide a scientific basis for new technological processes, and thereby to enrich science by the solution of urgent problems raised by the demands of industry.

The work of P. A. Rebinder in his new fields has also been widely recognized abroad.

In 1929 he was confirmed in the title of professor; in 1933 he was elected Corresponding Member, and in 1946, a full Member of the Academy of Sciences USSR. In 1934 he was awarded the degree of Doctor of Physicomathematical Sciences, and in 1935, Doctor of Chemical Sciences, for his research on surface phenomena in relation to the dispersion of solids.

In 1934-1935 he organized the Division of Disperse Systems, of which he is the head, first in the Institute of Physics of the Academy of Sciences USSR, and subsequently in the Colloidal and Electrochemical Institute, now the Institute of Physical Chemistry, Academy of Sciences USSR. Since 1942 he has been head of the Chair of Colloid Chemistry of Moscow University, where he presents each year a course of general colloid chemistry for students of the Chemical Faculty, and also gives special course of lectures on the special trends of his work (physicochemical mechanics, theory of structure formation, theory of the formation of new phases, surface effects in disperse systems). Many qualified research workers are being trained in the laboratories under his guidance; during the past 30 years about 80 scientists have originated from his team, of whom 60 have been awarded candidate's degrees, and 18 have presented doctorate dissertations. Rebinder's pupils have performed and published over 300 researches under his general guidance.

The Soviet Government showed its high esteem of the achievements of P.A. Rebinder in the development of Soviet science and technology by the award of the Stalin Prize for chemistry, for his discovery of the adsorptive lowering of strength of solids (1942), and by the award of the Order of Lenin, the Order (1st Class) of the Patriotic War, and medals.

In 1953 P. A. Rebinder was awarded (with E. E. Segalova) the A.N. Bakh prize for physicochemical studies of structure formation in cement suspensions.

Rebinder has always combined his scientific work with extensive teaching activity. He is a brilliant lecturer, with a deep affection for his science; he does much scientific and social work by the presentation of papers and popular lectures in Moscow and other centers. He has been a member of the Editorial Board of Colloid Journal since its foundation, and has always taken part in the organization of the All-Union Conferences on Colloid Chemistry.

At the present time P. A. Rebinder is actively developing his scientific activity and is at the height of his creative powers. We confidently expect that the researches of Rebinder and his school will continue to enrich Soviet science and technology with new and important achievements.

Editorial Board

SELECTED WORKS OF P. A. REBINDER

"The surface activity of solutions," Z. phys. Chem. 111, 5/6, 447, (1924); J. Appl. Phys. 1, 1/4, 153 (1924); Bull. Inst. Phys. and Biophys. 3, 1/2, 74 (1925).

"Water as a surface-active substance," Z. Phys. Chem. 121, 1/2, 103, (1926); in the book: Molecular Forces and their Electrical Nature (State Press, Moscow-Leningrad, 1928), p. 135. *

"Measurements of surface energy and surface activity of solutions and biological fluids at various interfaces," J. Exp. Biol. Med. 4, 14, 939 (1927).

*In Russian.

"Surface activity and structure of polar molecules" (jointly with A. B. Taubman), *J. Appl. Phys.* 7, 2, 3 (1930); *Z. phys. Chem. A*, 147, 3, 188, (1930).

"Stabilization of suspensions by surface-active substances" (jointly with E. K. Venstrem), *J. Phys. Chem.* 1, 2, 163 (1930); *Z. phys. Chem. A*, 146, 1, 63 (1930).

"The stabilizing action of adsorption layers, stability of bubbles and drops" (jointly with E. K. Venstrem), *J. Phys. Chem.* 2, 6, 754, 764, 768, 776 (1931); *Koll.-Z.* 53, 2, 145 (1930).

"Decrease of hardness by adsorption of surface-active substances. Sclerometry and physics of disperse systems," *J. Tech. Phys.* 2, 7/8, 726 (1932); *Z. Phys.* 72, 3/4, 191 (1931).

Physical Chemistry of Flotation Processes (jointly with M. E. Lipets, M. M. Rimskaia and A. B. Taubman) (Metallurgy Press, Moscow-Leningrad-Sverdlovsk, 1933), p. 230; * *Koll.-Z.* 65, 3, 268 (1933); 66, 1, 40; 66, 2, 212; 66, 3, 273 (1934).

Physical Chemistry of Detergent Action (Food Industry Press, Leningrad, 1935), 160 pp. *

Investigations in the Field of Surface Phenomena (ONTI, Moscow-Leningrad, 1936), 300 pp. *

Molecular surface phenomena in printing processes and the scientific principles of lithography (State United Press, Moscow, 1936), 148 pp.*

"Adsorption layers and their influence on the properties of disperse systems", *Bull. Acad. Sci. USSR, Chem. Ser. No. 5*, 639 (1936).

"Adsorption layers in wetting and flotation processes," *Bull. Acad. Sci. USSR, Chem. Ser. No. 5*, 707 (1936); *Mining J. No. 2*, 17 (1937).

Physicochemical studies of printing inks and interaction with printing surfaces (*Coll. Trans. of Laboratory*), *Trans. Sci. Res. Inst. State United Press*, 5, part 1 (United State Press, Moscow, 1937), 206 pp.*

"Influence of the medium and adsorption layers on plastic flow of metals," (jointly with E. K. Venstrem), *Bull. Acad. Sci. USSR, Phys. Ser. No. 4/5*, 531 (1937).

"Surface phenomena and the significance of small additions of adsorbable substances in the technology of constructional materials. Physicochemical principles of the production of foam concrete," *Bull. Acad. Sci. USSR, Div. Tech. Sci. No. 4*, 593 (1937).

"Mechanical properties and stabilizing action of adsorption layers in relation to their degree of saturation. Part 1" (jointly with A. A. Trapeznikov), *J. Phys. Chem.* 12, 5/6, 573 (1938); *Acta phys.-chem. USSR*, 9, No. 2, 257 (1938); *Proc. Acad. Sci. USSR* 18, 3, 185; 18, 7, 421; 18, 7, 425 (1938).

"Surface activity of hydrophilic colloids" (jointly with K. F. Zhigach), *J. Phys. Chem.* 13, 1, 94 (1939).

"Wetting and flotation in relation to the problem of the intermediate layer," *Trans. Faraday Soc.* 36, 1, 295 (1940).

"Significance of physicochemical processes in the mechanical destruction and treatment of solids in technology," *J. Acad. Sci. USSR No. 8/9*, 5 (1940).

"Spontaneously forming emulsions. Mechanism of formation of soluble oils, in the series: adsorption layers in disperse systems" (jointly with K. A. Pospelova), *Acta phys.-chim. USSR*, 16, 1-2, 71, 1942.

"Electrocapillary effects in the reduction of the hardness of metals" (jointly with E. K. Venstrem), *J. Phys. Chem.* (1944); *Acta phys.-chim. USSR* 19, 1, 36, (1944).

Softeners for Use in Drilling (jointly with L. A. Shreiner and K. F. Zhigach) (Izd. AN SSSR, Moscow-Leningrad, 1944), 200 pp. approx.; English edition (Melbourne, Australia, 1947).*

"The theory of emulsions," *Colloid J.* 8, 3, 157 (1946).

"Physicochemical studies of the deformation of solids" in the book: Jubilee Volume on the 30th Anniversary of the October Socialist Revolution, part 1 (Izd. AN SSSR, Moscow-Leningrad, 1947), p. 535.*

*In Russian.

"Structure formation in aqueous suspensions of bentonite clays" (jointly with N. N. Serb-Serbina), *Colloid J.* 9, 5, 381 (1947).

"Investigation of structuromechanical properties and thixotropy in oleocolloidal systems" (jointly with E. E. Segalova), *Colloid J.* 10, 3, 223 (1948).

Influence of Surface-Active Media on Processes of Metal Deformation (jointly with V. I. Likhtman and G. V. Karpenko) (Izd. AN SSSR, Moscow-Leningrad, 1954).*

"Coagulation and thixotropic structure formation," *Discuss. Faraday Soc.* 18, 151, (1954).

"Physicochemical investigations of structure formation in cement suspensions" (jointly with E. E. Segalova and O. I. Luk'yanova), *J. Moscow Univ.* 2, 17 (1954).

"Elasticoviscous properties of thixotropic structures in aqueous suspensions of bentonite clays" (jointly with L.A. Abduragimova and N. N. Serb-Serbina), *Colloid J.* 17, No. 3, 184 (1955).**

"Structure formation and spontaneous dispersion in suspensions," Proc. 3rd All-Union Conf. on Colloid Chemistry, Minsk, Nov. 21, 1953 (Izd. An SSSR, Moscow, 1956), p. 7.

"Investigation of structure formation in aqueous gypsum suspensions" (jointly with E. E. Segalova and V. N. Izmailova), *Proc. Acad. Sci. USSR* 107, 3, 425; 110, 5, 808 (1956).

"Physicochemical concepts of the mechanism of setting and hardening of mineral cements," Proc. Conf. on Theory of Concrete Technology (Acad. Sci. Armenian SSR Press, Erevan, 1956); *Proc. Conf. on Cement Chemistry (Ind. Construction Press, Moscow, 1956), p. 125.*

"Elasticoviscous properties of polyisobutylene solutions" (jointly with L. V. Ivanova-Chumakova), *Colloid J.* 18, 4, 429 (1956).**

"Laws of the development of shear deformation and stress relaxation in elastomers and their solutions" (jointly with L. V. Ivanova-Chumakova) *Colloid J.* 18, 5, 540 (1956).**

"Adsorptional decrease of strength of single metal crystals and spontaneous dispersion in a liquid medium" (jointly with V. I. Likhtman and L. A. Kachanova), *Proc. Acad. Sci. USSR* 111, 6, 1278 (1956).

"Effect of additions of a hydrophilic plastifier on the properties of concentrated cement suspensions" (jointly with O. I. Luk'yanova and E. E. Segalova), *Colloid J.* 19, 1, 82; 19, 4, 459 (1957); *Proc. Acad. Sci. USSR* 117, 6, 1034 (1957).*

"Some results of the development of physicochemical mechanics," *Bull. Acad. Sci. USSR, Div. Chem. Sci.* No. 11, 1284 (1957).**

Physicochemical Mechanics - a New Branch of Science (Knowledge Press, Moscow, 1958); *J. Acad. Sci. USSR* No. 10, 32 (1957).

"Influence of surface-active media on the deformation and destruction of solids" (jointly with V. I. Likhtman), *Proc. 2. Intern. Congress Surface Activity*, (1957), p. 563.*

"Structure formation in processes of hardening of mineral cements" (jointly with E. E. Segalova), *Proc. 2. Intern. Congress Surface Activity*, (1957) p. 492. *

*In Russian.

**Original Russian pagination. See C.B. Translation.

MODERN PROBLEMS OF COLLOID CHEMISTRY*

I. FORMATION AND AGGREGATIVE STABILITY OF DISPERSE SYSTEMS

P. A. Rebinder

In the light of the modern theory of lyophobic and lyophilic systems [1], all two-phase disperse systems, including systems of the maximum dispersity (colloidal systems), can be divided into two groups according to the magnitude of the specific free interfacial energy σ (surface tension), which may be greater or less than the boundary value σ_m . This value is determined by the commensurate value of the mean kinetic energy of thermal (Brownian) motion

$$\sigma_m = \gamma \frac{RT}{N\delta^2}, \quad (1)$$

where δ is the average size of the particles involved in the Brownian motion ($\delta \sim 10^{-8}$ cm); γ is a dimensionless factor ($\gamma \sim 30$ [2]); $R = 8.31 \cdot 10^7$ ergs/mole · degree, the gas constant; $N = 6 \cdot 10^{23}$, the Avogadro number ($R/N = k$ is the Boltzmann constant); T is the absolute temperature. At normal temperatures ($T \sim 300^\circ$ K), $\sigma_m \sim 0.1$ erg · cm⁻².

The first group includes lyophobic systems with high interfacial tension $\sigma > \sigma_m$, and therefore with clearly defined interphase boundaries. The free molecular forces on the surfaces of lyophobic particles, not balanced by the surrounding medium, caused well-defined coagulation or coalescence, unidirectional processes which are a manifestation of the aggregative instability of these essentially irreversible thermodynamically nonequilibrium disperse systems. The stability of such systems must be regarded in a purely kinetic sense [3] as the time of their existence in terms of "half life" (time required for half-demixing of a column of emulsion or foam).

The aggregative instability of a lyophobic system increases with decrease of particle (droplet) size and with increase of their number per unit volume (particle concentration), i.e., with increase of the intensity of Brownian motion and of the probability of effective collisions. This is why the degree of dispersion of lyophobic systems of the emulsion type, especially highly concentrated, cannot be high and is determined by the conditions of stabilization. The stability of emulsions and foams, even of the maximum concentration, can be estimated from the decrease of dispersity (the course of the coalescence of droplets or bubbles). In the case of suspensions and sols, observations of the course of aggregation (coagulation) are possible only in the dilute systems which are normally studied. In concentrated dispersions (which are the ones of most practical interest, for example, in soil science, and in construction work - not model systems but real suspensions and disperse materials), aggregation as a whole can be assessed only by the formation and development of coagulation structures with their characteristic mechanical strength. In highly disperse systems, because of the intense Brownian motion of the particles the strength of the structure increases thixotropically after breakdown, i.e., it is reversibly restored. This effect is most pronounced in suspensions of optimum dilution, and considerably less so in concentrated dispersions, which already have high initial strength.

In lyophobic dispersions, formed by mechanical subdivision of solids, the dispersity is determined by the conditions of mechanical destruction, which becomes more difficult as the particles become small enough,

*Paper at the 4th All-Union Conference on Colloid Chemistry, Tbilisi, May 13, 1958.

because of the so-called scale reinforcement which occurs after all the defects (weak spots) of the solid structure, which are the sites of destruction, have been utilized and the formation of new defects is needed for further subdivision.

In lyophobic emulsions, further dispersion of the droplets is hindered by intensification of the reverse processes of coalescence and even with complete stabilization, the average size of the droplets obtained by dispersion processes remains above $1-1.0 \mu$ (even with the so-called homogenization of the emulsions [4]). Therefore, highly disperse lyophobic systems (sols) are made not by dispersion, but by condensation methods, by formation of new phases in which the growth of the initial particles is arrested at the nucleation stage, for example, by stabilization effected by adsorption layers.

Lyophilic disperse systems which retain their two-phase nature are characterized by very low interfacial surface energies, below the boundary values determined by the energy of thermal motion (σ_m). Such systems are therefore formed spontaneously by colloidal dissolution, analogously to true dissolution, under the influence of the entropy factor; the increase of entropy due to the more uniform distribution of the substance in the disperse phase more than compensates for the increase of free surface energy with increase of the interfacial area. The dispersity of such lyophilic systems is characterized by equilibrium distribution curves, in the case of spontaneously formed emulsions, as was first shown by Volmer [5]. In the case of spontaneous or almost spontaneous formed is characterized by the size distribution of the structural defects or "mosaic blocks." Therefore, dispersity in lyophilic systems is not an accidental quantity which depends on the conditions of formation and stabilization, but is determined by the molecular nature of the two phases forming the system, and by their state, i.e., primarily the temperature.

Lyophilic disperse systems formed after sufficiently long coexistence of the two phases cannot be coarsely or arbitrarily disperse, and both routes - condensation and dispersion - lead to the same ultimate result. Lyophilic systems are semicolloids in the sense that they contain appreciable amounts of the substance of the colloidal phase in true solution in the surrounding dispersion medium. At the same time, it is such reversible systems that are the true colloids - two-phase, ultramicroheterogeneous systems of maximum dispersity, in thermodynamic equilibrium or quasi-equilibrium; the concept of aggregative instability is not applicable to them, and they do not require stabilization.

Differences between lyophobic and lyophilic systems are most pronounced in systems with liquid interfaces - emulsions or semicolloids. Aqueous soap solutions which solubilize, i.e., absorb in their micelles, definite amounts of hydrocarbons, are such systems. Only systems with liquid interfaces can be regarded as being in thermodynamic equilibrium. With solid disperse phases such equilibrium is attained only as the result of alternate formation and dissolution of nuclei of the new phase, ultramicrocrystallites.

Lyophobic emulsions consisting of pairs of pure liquids are most generally converted into lyophilic ones, i.e., spontaneously forming, when the temperature approaches the critical temperature of phase mixing (critical emulsions).

Lyophilic (spontaneous) emulsions or semicolloids may be formed continuously from ordinary lyophobic emulsions of the "oil in water" type by the introduction of sufficient amounts of a surface-active component such as soap. The interfacial tension then falls below the critical value, and emulsification proceeds spontaneously, as we showed jointly with Pospelova [6], as the result of a peculiar type of phase inversion: the external medium, water, is absorbed by the oil phase containing a large amount of acid soap colloidally dissolved in it. The water, in becoming dispersed, is solubilized in the soap oleomicelles (reverse solubilization). Gradual increase of the water content in the oil phase results in a sharp inversion of phases, which may be detected by a sudden increase of electrical conductivity; the oil phase becomes a maximum-concentration lyophilic colloidal emulsion of oil in water, distributed in the form of thin films between oil cells. A gel-like system of this type, sometimes described as an emulsol or soluble oil, can be spontaneously diluted with any large quantity of equilibrium aqueous medium [6]. The reverse solubilization of water in oil thereby passes into direct solubilization of oil in water.

Solutions of surface-active substances with hydrophilic polar groups and sufficiently long hydrocarbon chains in aqueous media are lyophilic colloids of this type. These soaplike substances may be ionogenic or nonionogenic in their polar groups; they are typical protective colloids - stabilizers, emulsifiers and foaming agents, wetting agents and detergents. All the properties of such semicolloids are closely associated with

their two specific characteristics — adsorbability at various interfaces, and the ability to form spatial coagulative structures, especially in surface layers but also in the solution volume.

If the polar group is insufficiently hydrophilic, as in the series of saturated alcohols, the true solubility falls sharply with lengthening of the hydrocarbon chain, while colloid formation is very weak.

Thus, by appropriate choice of the polarity of the mixed solvent, the hydrocarbon chain length, chemical nature, and the hydrophily of the polar group, and by introduction of additives such as solubilizable substances, it is possible, by decrease of temperature or increase of concentration, to effect a remarkable continuous transition from a true solution or one-phase system to a two-phase lyophilic colloidal system, i.e., a micellar semicolon, and ultimately to a lyophobic suspension of soap crystallites or an emulsion. This last case is specially characteristic — it corresponds to the introduction into a soap solution of an excess of hydrocarbon above the amount which can be solubilized. An excess of nonpolar liquid forms suddenly, but with a continuous increase of its quantity, a coarsely emulsified phase, stabilized by adsorption layers of soap as in ordinary direct emulsions.

Thus, the general principles of formation and stability of colloid systems of different types are demonstrated by solutions of typical surface-active substances in water and in liquids of varying polarities.

We now return to lyophobic systems, which require stabilizing layers for adequate stability, i.e., for prolonged existence.

Let us consider all the three possible stabilization factors [3, 4]:

1. In systems with liquid interfaces, and especially in foams and individual films (bubbles) attenuation of the film is prevented by local instantaneous differences of surface tension due to extension of the adsorption layers covering the film (the Marangoni-Gibbs effect). These differences are equalized by surface and volume diffusion of the adsorbed stabilizer, and therefore they can ensure only short lives; hence the Marangoni-Gibbs effect can be only a weak factor in stabilization.

2. The formation of double layers of ions and, equally, of molecular adsorption layers, stabilizes the particles in lyophobic systems if the layers themselves are lyophobic on their external surfaces. This means that at fairly large distances, when the van der Waals cohesion between the particles is weak, these cohesion forces are also weak between the outer boundaries of the layers, which may be interpreted as low residual surface tensions at these boundaries.

Such stabilization may be termed thermodynamic, irrespective of whether it is caused by an ionic or by a molecular stabilizer, i.e., whether the particles are charged or not. Such thermodynamic stabilization is very common, and has already been studied by us in detail [3] in the case of reversible oriented adsorption of typical surface-active substances on hydrophilic particles of suspensions in hydrocarbon media.

3. Thermodynamic stabilization is also a weak stabilization factor. Particles may approach each other at fairly high instantaneous velocities as the result of the kinetic factor, not controlled by thermodynamics. Therefore under conditions of high particle concentration and dispersity, considerable stabilization, of the maximum degree, may be attained only if the protective adsorption-solvation layer is structurized, i.e., if it has structural viscosity at low velocity gradients, much higher than the viscosity of the medium, and thus serves as a structuromechanical barrier [7-9].

However, the existence of such a barrier, which is a necessary condition for virtually complete stabilization of lyophobic systems is sufficient only if the surface energy at the outer boundary is low and does not increase sharply in the approach to the particle. Otherwise, in the presence of a lyophobic and not a lyophilic, even if structurized, layer, coagulation — secondary flocculation — takes place by cohesion of the layers at their external surfaces.

In their simplest form, such effects were studied by us in the chemical adsorption of surface-active substances by polar groups at the surfaces of hydrophilic solid particles [10]. The outwardly directed hydrocarbon chains become bound with each other in a peculiar local coalescence of the hydrophobic layers. Later this type of particle flocculation became widely used in practice not only in flotation processes, but also for increasing the rate of filtration.

II. STRUCTURE FORMATION IN DISPERSE SYSTEMS

Coagulation structures are formed by cohesion of the particles by weak van der Waals forces through thin residual interlayers of the medium [1, 11-13]. If the volume content of the solid phase is small, such coagulation structures are formed only when the dispersity is high, i.e., at high particle concentrations, if the particles are sufficiently anisometric, and if the surface is sufficiently lyophilic, i.e., if the number of coagulation centers, generally localized at the ends and edges of the particles, is small.

Stabilization allows a considerable increase of the volume content of the solid disperse phase, i.e., of the degree of filling, with the strength of the coagulational structure remaining unchanged. Only powerful stabilization, due to the formation of a structuromechanical barrier in the liquid interlayers, is effective. For example, the addition of surface-active protective colloids, such as humates or sulfolignates, is the only method for the liquefaction of concentrated or weighed clay suspensions used as drilling fluids.

It must be pointed out that at the highest particle-packing densities, which can be attained only as the result of maximum stabilization, the system retains high plastic strength despite such stabilization, and this strength is largely due to structure formation of the stabilizing protective colloid itself in the interlayers between the particles. The thin interlayers of the medium at the regions of contact between the particles of a coagulational structure determine all its remarkable properties — the power of reversible breakdown and restoration (thixotropy), low strength, plasticity, and creep at any shear stress, no matter how small, corresponding to slow flow at the maximum viscosity of the almost intact structure, 9 or even 10 orders of magnitude greater than the minimum (Newtonian) viscosity of the structure at maximum breakdown, which is only a little greater than the viscosity of the medium (solvent) [13, 14].

This also accounts for a remarkable property common to all coagulation structures, their high elasticity and very pronounced elastic aftereffects. All these properties are properties of the coagulation structure as a whole, and not of its constituent particles [1, 11, 13].

Condensation-crystallization structures, in contrast to coagulation structures, are formed by the action of chemical principal valence forces, as in spatial polymerization (or vulcanization by means of bridge bonds), or by direct coalescence of crystallites of the new phase being formed.

The development kinetics of crystallization structures, based on primary concentrated coagulation structures, is of special significance in the theory of hardening of mineral binders in building materials — cement pastes and concretes. Condensation-crystallization structures are characterized by extremely high strength, breakdown of essentially irreversible nature, and absence of thixotropic properties.

Coagulation structures may in principle have relatively high thermodynamic stability: in the course of thixotropic buildup, characteristic of fairly dilute suspensions, and in spontaneous condensation — syneresis in concentrated suspensions — with attenuating of the liquid interlayers between the particles, coagulational structures tend to thermodynamically more stable equilibrium states; this is in harmony with the increase of their mechanical strength.

In contrast, crystallization structures or concretions of crystallites are formed from supersaturated solutions only at quite high supersaturations, and are thermodynamically unstable owing to the nonequilibrium nature of the coalescence regions of the crystallites. Therefore, as Segalova [15] has shown, the subsequent tendency of crystallization structure to reach thermodynamic equilibrium is manifested in dissolution of the coalescence contacts with a decrease of the mechanical strength to zero as the result of isothermal transfer of the solid-phase substance — the transfer of the substance from the coalescence regions to the free crystallite surfaces, with the formation of free, nonconcreted crystals.

Intermediate colloidal systems, near to lyophilic, even with low contents of the disperse phase, readily form coagulation thixotropic structures or gels; both in the case of solutions of soaplike surface-active substances, and in the case of colloidal suspensions of clays. This is due to the high dispersity — large number of particles — of micelles or microcrystallites per unit volume, their anisometric character, and the location of the coagulation centers at individual border regions of the particle surfaces. In contrast to this, crystallizational structures are characteristic of more lyophobic systems with fairly high interfacial tensions. Because of this, sufficiently high supersaturations can arise in the formation and development of the new phase, which is necessary for coalescence of the crystallites.

The mechanical properties of coagulation structures can be regulated by increase of the degree of filling of the system with the solid disperse phase, by control of its primary dispersity, and by addition of stabilizers and coagulants. This is the primary importance in modern soil science, and particularly for control of the properties of soils from the geological-engineering (constructional) standpoint, as has been demonstrated by Serb-Serbina, Denisov [16], Gor'kova [17], and Liubimova [18]. These considerations apply also to processes of working and molding of clays in the ceramic industry, as was shown by Nichiporenko [19]. By decrease of the thickness of the liquid interlayers between the particles of the disperse phase, for example by slow drying of extremely dense clay pastes, it is possible to effect a continuous transition from soft, highly plastic coagulation structures to very strong brittle structures with the strength and properties of monolithic stone. However, such structures differ from crystallization structures in being unstable to the action of water, and they liquefy reversibly on adsorption of even small quantities of water, corresponding to the limiting adsorptioinal strength decrease - spontaneous dispersion in the given liquid medium, with respect to which the solid phase is lyophilic (hydrophilic).

The strength of crystallization structures can be controlled at the first stages of formation and growth of the new phase, in the induction period of structure formation, by variation of the dispersity of the crystal nuclei by means of adsorptioinal modification [20] and, for example, by termination of their growth as the result of blocking by adsorption layers, and by variation of the conditions for further coalescence of the crystals and the formation of a framework [15].

One important example of coagulation structure formation is the action of active fillers, especially in polymers and their solutions.

The filler particles, which form a suspension in the filled medium, favor the development of a spatial structure in it even when their volume fraction is low, and greatly raise the strength of this structure by forming junctions - centers of structure growth - by virtue of adsorption forces on the surface of the filler particles [21]. We showed long ago [22] that if an original system consists of a polymer (for example, rubber) solution of such low concentration that a structural network cannot be detected in it by the usual methods, the introduction of small amounts of filler, in themselves insufficient for the development of a coagulation structure, results in the formation of a network structure of appreciable strength (limiting static shear stress) in the solution.

As the amount of filler is increased, its particles begin to form a secondary coagulation structure, interacting with each other through the thin residual interlayers of the medium - the polymer or its solution. This produces a further increase of strength, and, correspondingly, an increase of the maximum limiting viscosity of the virtually intact structure [23, 24]. These are the optimum degrees of filling used in rubber, plastics, and bitumen technology.

The presence of thin interlayers of a medium (dielectric) between the particles of electron-conductive active filler (such as carbon black in rubber), which form a coagulation structure by cohesion into chains and frameworks, is proved by the fact that the conductivity of such systems does not remain constant, but rises sharply over a definite range with increasing potential difference, in accordance with the breakdown mechanism [25].

If the surface of the filler particles is not sufficiently lyophilic with respect to the medium, the filler is inactive; if small amounts are added, the particles do not assist the development of a network in the polymer, while at higher filler contents they undergo compact coagulation, i.e., they are not dispersed in the polymer and therefore cannot form a coagulation structure in it. Therefore, inactive (lyophobic) fillers do not cause reinforcement or improvement of the mechanical (strength) properties. We have shown [21, 22] that inactive fillers of this kind can be activated by oriented adsorption of surface-active substances, which results in inversion of the selective wetting of the particle surfaces [26]. Hydrophilic fillers can be made "carbo-phobic" (wetted by rubber) by surface adsorption of surface-active substances with sufficiently long hydrocarbon chains, provided that chemical fixation (chemisorption) of the polar groups takes place [26]. This chemical fixation at definite regions of the surface of the crystal lattice results in fixed orientation of the water-repellent hydrocarbon chains outward, making the solid surfaces stably hydrophobic, as is found in the action of flotation collectors. Hydrophilic fillers which are compounds of alkaline earth metals (calcium and magnesium carbonates, barium sulfate, etc.), can thus be activated by carboxylic acids or soaps, while hydrophilic fillers

such as silica, silicates, and aluminosilicates are activated by cationic reagents (amines, salts of quaternary ammonium bases, pyridine derivatives).

The oriented adsorption layers of the activator intensify the molecular bonding between the polymer and filler, the particles of which thus become centers in the spatial network formed by the polymer macromolecules. At the same time, the activating adsorption layers peptize and stabilize the filler particles in the polymer or its solution, which favors the development of coagulation structures at sufficiently high filler contents by preventing compact coagulation, and makes it possible and advisable to use higher contents of filler, corresponding to the optimum properties of the material. Such adsorptive activation of disperse pigments in paints and varnishes corresponds to a sharp decrease of the oil capacity, i.e., formation of coagulation structures at higher volume contents of the pigment. It is therefore clear that the pigment in a varnish system must play the role of a filler, not only ensuring good color and covering power, but also improving the mechanical properties of the coating — its strength and hardness.

As is known, vulcanization consists of the formation of a spatial network in linear polymers by means of chemical cross links (bridges) at the unsaturated regions of the macromolecules. This gives rise to a typical condensation structure, analogous to the structure of a space polymer, as in silicic acid gels. Such condensation structures have high strength, break down irreversibly, and are devoid of thixotropic properties. However, it is evident from the foregoing that van der Waals (adsorption) bonds which arise on the introduction of active fillers can serve as bridges. The spatial structures so formed are coagulational, have thixotropic properties, and are easily regenerated, i.e., they are restored spontaneously after breakdown. It follows from Pisarenko's work that it is possible to effect a continuous transition from coagulation structures which arise in polymers with the participation of active fillers, to condensation structures resulting from vulcanization. This transition is effected in industrial practice in the form of rubbers with high carbon-black contents, vulcanized with very small amounts of vulcanization agent (sulfur) for very short times at high temperatures. The vulcanizates so formed have peculiar thixotropic properties, with easy regenerability of structures.

The theory of structure formation in colloid chemistry provides a solution to the principal problem of physicochemical mechanics [28], the production of materials of predetermined structure and mechanical properties. These include a great variety of materials, from fluidlike and then solidlike plastic structures to various high-strength solids such as concretes, asphaltic concretes, plastics, vulcanized rubbers, metallic alloys, sintered metals, glass, and ceramics.

In the solution of such problems special significance attaches to the simultaneous influence of physicochemical factors and of mechanical (especially vibrational) forces in the dispersion and maximum breakdown of structure at the initial stage, and therefore in the uniform distribution of particles and maximum condensation of the structure; this has been demonstrated by Mikhailov [29] in relation to the scientifically substantiated concrete technology which is being developed by him.

III. DISPERSION. BREAKDOWN AND PREDESTRUCTION OF SOLIDS

We have seen that structure formation in disperse systems is one fundamental problem of physicochemical mechanics. Its second fundamental problem, the converse of the first, is also closely associated with the development of colloid chemistry. This is the problem of fine grinding or dispersion of various solids and also, more generally, the problem of deformation regarded as predestruction, and of the actual destruction of solids, i.e., the formation of new interfaces with the surrounding medium.

As was to be expected, destruction processes of solids, and the preceding deformation processes, are highly sensitive to physicochemical factors [30]: the reversible influence of the medium and of additions of adsorbable substances, which decrease the work of formation of new surfaces, together with the optimum mechanical influences and variations of temperatures, make it possible to regulate deformation processes and to achieve a continuous transition from adsorptive lowering of strength in the mechanical breakdown of solids to spontaneous colloidal dispersion with formation of two-phase lyophilic systems of the maximum possible degree of dispersion.

All solids have structural defects — weak places, distributed in such a way that the solid regions between them are, on the average, of colloidal dimensions (of the order of 10^{-6} cm) — and on the average there is one defect for every 100 regular interatomic (or intermolecular) spacings.

Structural defects develop under the influence of stressed states induced in solids by external forces (if these stressed states are such that they lead to destruction of the body when they increase in intensity). Structural defects therefore act as nuclei of new surfaces in ultramicrocrevices which develop at the boundary with the surrounding medium or with layers of the adsorbed substance, which are able to cover these surfaces, by two-dimensional diffusion, in the course of their development. Therefore the deformation process itself, under the influence even of small stresses, which inevitably involves the development of new surfaces in a given solid at the boundary with the surrounding medium, is a predestruction process – a process of internal or latent dispersion [30, 31]. At the same time, deformation processes and the breakdown in which they culminate, especially in surface-active media, must be regarded from the kinetic aspect; in the case of crystals having definite plasticity, in the light of the dislocation theory [2]. In fine grinding, for example, under the action of vibrations at sufficiently high frequencies, leading to brittle destruction, the work of dispersion per unit volume $dA/dv = H$ is approximately proportional, by Rittinger's law, to the product of the specific free surface energy σ and the dispersity of the product $S_1 = S/v$. The dimensionless proportionality factor $K = H/\sigma S_1$ is very considerable; only a small proportion ($1/K$) of all the surfaces which develop in unit volume of the deformed solid becomes completely opened up during the destruction, while the other surfaces, after the stress is released in the course of the breakdown, are closed again under the action of the cohesion forces in the deformed body, and the corresponding part of the work of destruction is dissipated in the form of heat [31].

The process of destruction, i.e., the formation of new surfaces with the corresponding surface energy, is activated by the energy of elasticity stored in the body during the preceding deformation. The condition for breakdown as the result of loosening of the structure at the weak spots or defects may be written as [32, 33]

$$\beta P_m v = \sigma S - \gamma kT, \quad (2)$$

where P_m is the strength, i.e., the highest (limiting) stress which the body can withstand; $S \sim \delta^2$ and $v = \delta^3$ are the average surface area and average volume of the mosaic block; β and γ are dimensionless coefficients.

When $P_m = 0$, Equation (1) becomes the condition for spontaneous dispersion (1):

$$\sigma \ll \sigma_m = \gamma kT/S. \quad (3)$$

If the strength of the body in the given medium is fairly considerable (the lyophobic case $\sigma \gg \sigma_m$

$$\beta P_m \delta = \sigma, \quad (4)$$

and if the surface formed by brittle destruction is the same (which in the simplest case corresponds to the development of one, the weakest, spot, as in the brittle fracture of a crystal into two parts), the relative decrease of strength $\frac{(P_m)_0 - (P_m)_A}{(P_m)_0}$ produced by the given active medium, as compared with the strength in vacuum or an inactive medium, is determined by the corresponding relative decrease of surface energy.

We showed, for a variety of destruction conditions, that under the same mechanical conditions the surface area formed, i.e., the dispersity of the product, is considerably greater in a surface-active than in an inactive medium. This is the direct consequence of the complete development of a large number of weak spots of different kinds during brittle destruction, and of a number of slippage planes which come into operation during the plastic deformation of a single crystal in an active medium.

If the interfacial surface energy is decreased very considerably under the influence of the external medium, i.e., in the lyophilic case, the true strength of a solid (with its defective structure taken into account) can be decreased so much that even small residual internal stresses cause dispersion in a given medium. This type of transition to spontaneous dispersion can be effected, for example, in bentonite or even subbentonite clays, the strength of which in the compacted and dried state is very high, but which falls almost to zero under the influence of moisture. This corresponds to spontaneous colloidal dispersion of the clay in water as the result of the opening (in the wetted state) of all the weak spots localized at the cleavage planes and layer lattices of clay minerals of the montmorillonite group. At the same time, the true solubility of these metals in water is virtually zero.

We have briefly considered three problems, specific for modern colloid chemistry, analysis of which is based on the theory of surface phenomena – the problems of stability, structure formation, and dispersion.

All three problems are characterized by remarkable and, moreover, to some extent continuous, transitions from one-phase systems (true solutions) to two-phase (microheterogeneous) disperse systems, from lyophobic to lyophilic disperse systems, from weak to strong stabilization factors, from coagulation to condensation-crystallization structures, and from mechanical destruction to spontaneous dispersion in a given medium. These peculiar transitions clearly characterize the individuality of colloidal systems as transitional systems; and thereby reveal the peculiar nature of the field of science concerned with them - the physical chemistry of disperse systems and of surface phenomena in these systems.

SUMMARY

1. Disperse two-phase (microheterogeneous) systems are divided into two groups: a) lyophobic systems with high interfacial tension above a certain critical value $\sigma > \sigma_m$, and b) lyophilic systems of low $\sigma (0 < \sigma < \sigma_m)$.

Lyophobic systems are unstable, and are characterized by a certain "life" (time of half-demixing of a column of emulsion or foam); their dispersity is arbitrary and relatively low if they are made by dispersion methods. In the formation of lyophobic systems by condensation methods, their dispersity can in practice be kept high if the further growth of the particles and their coagulation or coalescence is prevented by means of stabilizing (protective) adsorption layers.

Lyophilic two-phase systems (critical and spontaneously-formed emulsions, semicolloids) are thermodynamically stable and are formed spontaneously; they have quite definite high dispersity, characterized by the size distribution curve for the droplets or micelles in the colloidal region.

The limiting lyophilic system corresponds to unlimited mutual solubility ($\sigma = 0$), i.e., to the formation of a one-phase system - a true solution of an ordinary or polymeric substance in the given medium. Continuous transitions from lyophobic to the limiting lyophilic systems, i.e., from coarsely disperse systems, through semicolloids, to true solutions, may be effected in various ways.

2. Weak stabilization factors are inadequate for the production of almost complete aggregative stability in concentrated lyophobic disperse systems, and it is necessary to use a strong stabilization factor - the structuromechanical barrier which arises in the structurized surface layer of the dispersion medium, or in its volume.

3. The development of spatial coagulation and crystallization structures makes it possible to effect a continuous transition from true viscous liquids to solidlike thixotropic plastic structures and to brittle solids of high strength. Thus, consideration of structure formation in disperse systems leads to a solution of the fundamental problem of physicochemical mechanics - the production of technical materials, solids and structurized systems, of predetermined disperse structure and mechanical properties (as in the hardening of mineral cements), by the development of crystallization structures and transition from coagulation to condensation (vulcanization) structures in polymers and their solutions under the action of active or activated fillers.

4. Studies of dispersion processes of solid bodies, with consideration of their defective (disperse) structure and the kinetics of predestruction in a surface-active medium, make it possible to effect a continuous transition from mechanical destruction (fine grinding), facilitated by the adsorptive action of the medium and admixtures, to spontaneous dispersion.

Institute of Physical Chemistry USSR

Division of Disperse Systems

University of Moscow

Chair of Colloid Chemistry

Received June 16, 1958

LITERATURE CITED

- [1] P. A. Rebinder, Proc. 3rd All-Union Conf. Colloid Chem. (Izd. AN SSSR Moscow, 1956) p. 7; Discuss. Faraday Soc. No. 18, 151 (1954).
- [2] E. D. Shchukin and P. A. Rebinder, Colloid J. 20, 5, 645 (1958).*

*Original Russian pagination. See C.B. Translation.

- [3] P. A. Rebinder and E. K. Venstrem, J. Phys. Chem. 1, 2, 163, 4-5, 533 (1930); Z. Phys. Chem. A 146, 1, 63 (1930); P. A. Rebinder, J. Phys. Chem. 2, 6, 764, 754, 768 (1931); P. A. Rebinder and E. K. Venstrem, Koll.-Z. 53, 2, 145 (1930); P. A. Rebinder, Bull. Acad. Sci. USSR, Div. Math. Nat. Sci. Chem. Ser. No. 5, 639, 707 (1936).
- [4] P. A. Rebinder, Colloid J. 8, No. 3, 157 (1946).
- [5] M. Volmer, Z. phys. Chem. A 155, 281 (1931).
- [6] P. A. Rebinder and K. A. Pospelova, Introduction to the translation of W. Clayton's Emulsions (IL, Moscow, 1950) p. 11; K. A. Pospelova and P. A. Rebinder, Acta Phys. Chim. URSS 16, 1-2, 71 (1942); Z. N. Markina and P. A. Rebinder, Proc. Acad. Sci. USSR 109, 6, 156 (1956).
- [7] L. Ia. Kremnev, Colloid J. 20, 5, 546 (1958).*
- [8] A. B. Taubman and A. F. Koretskii, Colloid J. 20, 5, 676 (1958).*
- [9] E. M. Natanson, Colloid J. 20, 5, 556 (1958).*
- [10] P. A. Rebinder, in the book: Role of Gases and Reagents in Flotation Processes (Proc. Conf. on the Theory of Flotation Beneficiation) (Izd. AN SSSR, Moscow-Leningrad, 1950) p.13.**
- [11] P. A. Rebinder, Proc. Conf. on Eng.-Geol. Properties of Rocks and Methods of their Investigation (OGGI Acad. Sci. USSR Moscow, 1956) p. 31;** N. N. Serb-Serbina and P. A. Rebinder, Colloid J. 9, 5, 381 (1947); in the book: The Geology, Mineralogy, and Utilization of Clays in the USSR (papers at the International Conference on Clays, Brussels, 1958) (Izd. AN SSSR, Moscow, 1958); p. 115;** N. N. Serb-Serbina, Colloid J. 20, 5, 563 (1958).*
- [12] E. E. Segalova and P. A. Rebinder, Colloid J. 10, 3, 223 (1948); 13, 6, 461 (1951).
- [13] L. A. Abduragimova, P. A. Rebinder, and N. N. Serb-Serbina, Colloid J. 17, 3, 184 (1955).*
- [14] L. A. Abduragimova, Colloid J. 20, 6 (1958).*
- [15] P. A. Rebinder and E. E. Segalova, Proc. 2. Internat. Congress on Surface Activity, (London, 1957) p. 492;** E. E. Segalova, O. I. Luk'ianova, and P. A. Rebinder, J. Moscow Univ. 2, 17, (1954); E. E. Segalova, V. N. Izmailova, and P. A. Rebinder, Proc. Acad. Sci. USSR 110, 5, 808; 107, 3, 425 (1956); 114, 3 (1957);* O. I. Luk'ianova, E.E. Segalova, and P. A. Rebinder, Colloid J. 19, 1, 82; 4, 459 (1957);* E. E. Segalova, E. S. Solov'eva, and P. A. Rebinder, Proc. Acad. Sci. USSR 113, 1; 117, 5 841 (1957).**
- [16] N. Ia. Denisov, Constructional Properties of Clays (Gosenergoizdat, Moscow-Leningrad, 1956).**
- [17] I. M. Gor'kova, Colloid J. 20, 5, 585 (1958);* Proc. Conf. on Eng.-Geol. Properties of Rocks and Methods of Their Investigation (OGGI, Acad. Sci. USSR, Moscow, 1956) p. 98.**
- [18] T. Iu. Liubimova, Colloid J. 20, 6 (1958).
- [19] P. A. Rebinder, Bull. Acad. Sci. USSR, Div. Chem. Sci. 11, 1284 (1957); *S. P. Nichiporenko, Colloid J. 20, 5, 575 (1958).*
- [20] P. A. Rebinder, High-Quality Steel 3, 31 (1934).
- [21] P. A. Rebinder, and V. V. Margaritov, J. Rubber Ind. 11, 991 (1935); Caoutchouc and Rubber 4, 3 (1937).
- [22] P. A. Rebinder, G. A. Ab, and S. Ia. Veiler, Proc. Acad. Sci USSR 31, 5, 444 (1941); A. B. Aron and P. A. Rebinder, Proc. Acad. Sci. USSR 52, 3, 235 (1946); A. S. Kolbanovskia, P. A. Rebinder, and O. I. Luk'ianova, Colloid J. 12, 3, 208 (1950).
- [23] N. V. Mikhailov and P. A. Rebinder, Colloid J. 17, 2, 107 (1955).*
- [24] S. Ia. Shalyt, N. V. Mikhailov, and P. A. Rebinder, Colloid J. 19, 2, 244 (1957).*
- [25] Wu. Shu-ch'iu, B. Ia. Iampol'skii, and S. S. Voiutskii, Colloid J. 18, 6, 748 (1956);* 20, 3, 382 (1958).*

*Original Russian pagination. See C.B. Translation.

**In Russian.

- [26] P. A. Rebinder et al., Physical Chemistry of Flotation Processes (Metallurgy Press, Moscow-Leningrad-Sverdlovsk, 1933). *
- [27] A. P. Pisarenko and P. A. Rebinder, Proc. Acad. Sci. USSR 73, 1, 129 (1950).
- [28] P. A. Rebinder, "Physicochemical Mechanics" Knowledge (series 4, Mo 39-40), (Moscow, 1958); * J. Acad. Sci. USSR 10, 32 (1957).
- [29] N. V. Mikhailov, Physicochemical Theory of Concrete and the Basic Principles of a New Theory of Concrete and Ferroconcrete (As and Arkh. USSR, Moscow, 1958). **
- [30] P. A. Rebinder, Jubilee Vo. on 30th Anniversary of the October Socialist Revolution, 1 (Izd. AN SSSR, Moscow-Leningrad, 1947), p. 535; * V. I. Likhtman, P. A. Rebinder, and G. V. Karpenko, Influence of Surface-Active Media on Metal Deformation (Izd. AN SSSR, Moscow-Leningrad, 1954). *
- [31] P. A. Rebinder, L. A. Shreiner, and K. F. Zhigach, Substances for Lowering Hardness in Drilling (Izd. AN SSSR, Moscow-Leningrad, 1944). *
- [32] P. A. Rebinder and V.I. Likhtman, Proc. 2. Internat. Congress on Surface Activity, (1957) , p. 563. *
- [33] P. A. Rebinder, V. I. Likhtman, and L. A. Kachanova, Proc. Acad. Sci. USSR, 111, 6, 1278 (1956).
- [34] G. M. Bartenev, L. V. Iudina, and P. A. Rebinder, Colloid J. 20, 5, 655 (1958). ***

* In Russian.

** Not identified. Translator's note.

*** Original Russian pagination. See C.B. Translation.

SOME CHARACTERISTICS OF THE ADSORPTION OF SURFACE-ACTIVE SUBSTANCES IN NONAQUEOUS MEDIA

A. B. Taubman and S. I. Burshtein

1. Surface Activity in Formamide and at the Hydrocarbon - Water Interface

In a series of investigations of surface tension of solutions of surface-active substances, Rebinder [1] established relationships between surface activity and the molecular properties of the interface; these relationships are extremely important not only in relation to the general laws of adsorption at liquid interfaces, but also with regard to the practical production of stable technical emulsions, foams, suspensions, active lubricating fluids, etc. These investigations have been extended further by one of the present authors [2], especially in relation to nonaqueous solutions.

In this communication we consider data which, in conjunction with earlier results, can be used for the formulation of the most important laws of adsorption from nonaqueous media. Because of the different molecular properties of water and nonaqueous solvents, these laws should differ significantly for their solutions. Because of the dipolar structure of these compounds, their adsorption properties are influenced by the individual parts of the molecules, the hydrocarbon chains and the functional polar groups; this influence can be evaluated separately in the over-all effect.

Presented below are the results of a study of the surface activity of molecularly soluble surface-active substances - organic acids, alcohols, amines, and others - in two nonaqueous solvents showing extreme differences in their polar properties: in formamide, at the solution-vapor interface, and in a hydrocarbon medium, at the solution-water interface, for substances insoluble in water (higher homologs).

The method consisted of measurements of the surface tension of solutions by the maximum bubble or drop-pressure method, and cryoscopic determinations of their thermodynamic activity. The solutions were studied in the range of low concentrations, so that in calculations of the adsorption of the surface-active component (Γ) and of its maximum value (Γ_M) it was possible to use the Gibbs equation in its normal application to binary solution, adsorption of the solvent being equated to zero (the Gibbs condition):

$$\Gamma = - \frac{d\sigma}{d\mu} = - \frac{1}{RT} \frac{\partial\sigma}{\partial \ln(fc)},$$

where σ , μ , c and f are the surface tension, chemical potential, concentration, and activity coefficient respectively; since adsorption from the aqueous phase at the interface between the two liquids was excluded in absence of partition of the solute, this equation could also be applied to three-component systems. All the compounds studied (normal members of homologous series) and solvents were thoroughly purified.

The results obtained reveal a number of features in the adsorption behavior which distinguish nonaqueous solvents from water.

Formamide solution-vapor interface. Among nonaqueous solvents of different molecular nature, formamide is especially suitable to use in investigations of adsorption behavior, as it has well-defined polar properties (dielectric constant $\epsilon = 84$, dipole moment $\mu = 3.2$ D, with a weak dipolar character, owing to the absence of a hydrocarbon chain in the molecule) and relatively high surface tension ($\sigma_{20^\circ} = 58.35$ ergs/cm²).

Surface tension isotherms for solutions of some intermediate homologs in the aliphatic alcohol, acid, and amine series in formamide are shown in Fig. 1. It is seen that the adsorption of these compounds is fairly pronounced, and increases rapidly along the homologous series. The coefficient of the Traube rule, $\beta = G_0(n+1)/G_0(n)$, calculated from the maximum surface activities $G_0 = \frac{\partial \Delta \sigma}{\partial c} = \frac{b}{a}$, where b and a are the constants of the Shishkovskii equation, is $\beta = 1.8$. This value corresponds to the work of adsorption of the hydrocarbon chains $W = RT \ln \beta = 345 \text{ cal/mole of } \text{CH}_2 \text{ groups}$.

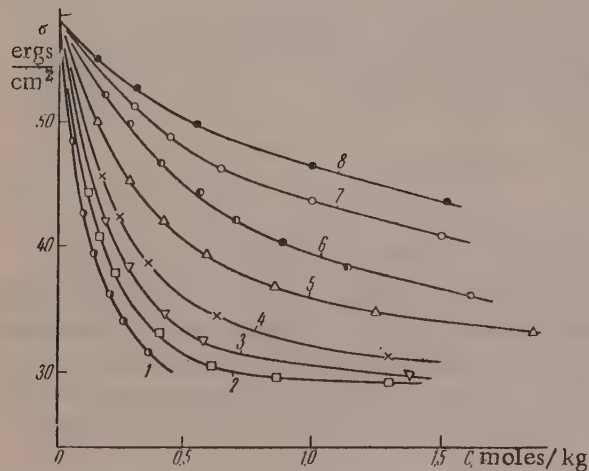


Fig. 1. Surface activity in formamide at the solution-vapor interface at 20°: 1) Heptyl alcohol; 2) caprylic acid; 3) heptylamine; 4) heptylic acid; 5) caproic acid; 6) butyl alcohol; 7) butylamine; 8) butyric acid.

It is important to note that these molecular interactions also influence the structure of the adsorption layers.

The table contains calculated values of the maximum adsorption (Γ_M) and the minimum area (S_M) occupied by each adsorbed molecule in saturated adsorption layers in the substances studied.

Structure of Adsorption Layers in Formamide Solutions

Surface-active substance	c in moles/kg	σ in ergs/cm²	$\Gamma_M \cdot 10^{10}$ in moles/cm²	S_M in Å²
Butyl alcohol	1.0	39.0	5.65	29.4
Heptyl alcohol	0.2	36.5	5.70	29.2
Butylamine	2.0	38.1	5.80	28.7
Heptylamine	0.35	35.9	6.05	27.5
Caproic acid	0.7	37.9	4.80	34.7
Heptylic acid	0.5	35.7	5.00	33.2
Caprylic acid	0.25	35.9	5.25	31.7

from nonpolar hydrocarbon media, which have the lowest surface tensions of all organic compounds ($\sigma \sim 20 \text{ ergs/cm}^2$), adsorption layers can be formed only at interfaces of hydrocarbons with polar liquids.

The interfacial tension is greatest ($\sigma_{12} \sim 50 \text{ ergs/cm}^2$) at the water interface, so that the surface activities of any substances soluble in hydrocarbons can be investigated in hydrocarbon solution. Figure 2 shows

However, the surface activity in formamide is much lower than in water ($\epsilon = 80$, $\mu = 1.8 \text{ D}$), for which $\beta = 3.5$ and $W = 730 \text{ cal/mole}$ [1]; thus, for butyl and heptyl alcohols G_0 is 240 and 10,000 absolute units, respectively, in water, and 48 and 300 absolute units in formamide. Thus, the adsorption of surface-active molecules depends only slightly on the dielectric properties of the medium from which they are adsorbed, and is determined mainly by the nature and degree of the interaction of individual portions of the dipolar molecules with the corresponding groups of the solvent molecules.

Alcohols have greater activity in formamide than amines or acids of the same chain length; in contrast, the activity in water is virtually the same for substances of all three series. This result is evidently due to the greater differences in the energy of interaction of the polar groups of these substances with formamide, the molecule of which essentially consists of a single polar group, than with water in the hydration of the same groups in aqueous solutions.

It follows from these results that the molecular packing density in saturated adsorption layers in formamide solutions does not correspond to the actual dimensions of the oriented adsorbed molecules. As in aqueous solutions [3], S_M is considerably greater than their cross-sectional areas; this indicates that a factor considered earlier — the solvating effect of the medium, which prevents maximum packing of the molecules [4] — is operative.

It is clear that in formamide solutions, at the liquid-vapor interface, solvation affects only the polar groups of the dissolved molecules, which can readily interact with the solvent by hydrogen bonding.

Hydrocarbon-water interface. In adsorption

isotherms for the lowering of the interfacial tension $\Delta\sigma_{12} - c$ for members of different homologous series in adsorption from n-octane; it is seen that the surface activity of diphilic molecules is determined primarily by the work of adsorption of the polar groups and not of the hydrocarbon chains, the influence of chain length being very weak.

Comparison of the isotherms for the C₁₂ and C₁₈ homologs in the alcohol series, and C₁₂ and C₁₈ homologs in the acid series, indicates that the surface activity increases very little in the series; the value of the Traube coefficient $\beta = 1.1-1.2$, which corresponds to a very low value of the work of adsorption $W \sim 50-100$ cal/mole of CH₂ groups.

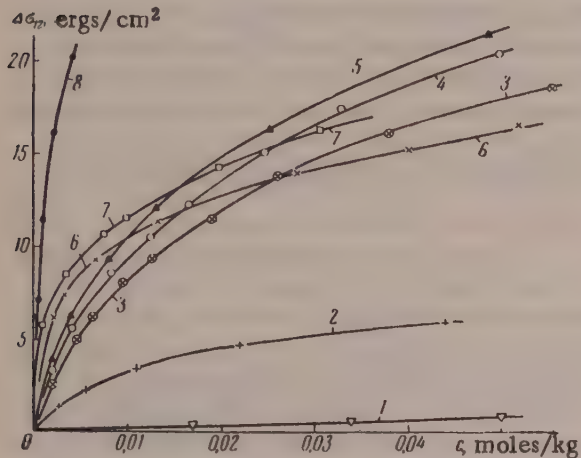


Fig. 2. Surface activity at the octane-water interface at 20°: 1) Heptyl iodide; 2) methyl laurate; 3) laurylamine; 4) lauryl alcohol; 5) cetyl alcohol; 6) lauric acid; 7) stearic acid; 8) oleic acid.

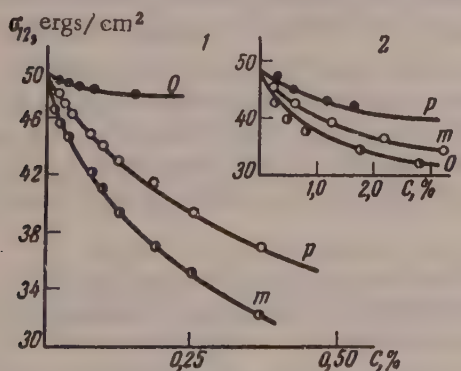


Fig. 3. Surface activity at the hexane-water interface: 1) Nitrophenols; 2) hydroxyphenols.

neighboring NO₂ and OH groups [7]. Because of this utilization of the acceptor properties of hydrogen, the compound loses its polar groups and therefore the properties which are determined by their presence in the molecule, in contrast to the other two isomers, which cannot form intramolecular hydrogen bonds for steric reasons. This is clear from Fig. 3, which shows the $\sigma_{12} - c$ isotherms for the o-, m-, and p-isomers of nitrophenol and hydroxyphenol respectively, at the hexane-water interface. Since the surface activity (G) increases symbatically with increase of molecular asymmetry, it follows [8] that the following series is valid for hydroxy-

It is interesting to note in this connection that the surface activities of diphilic molecules in adsorption from hydrocarbons and from water respectively differ by many orders of magnitude; for example, the values of the maximum surface activity G₀ for stearic acid are 10⁸ and 10¹⁰ absolute units, respectively.* Clearly, the value of β may be considered as one of the characteristics of the polar properties of the medium from which adsorption takes place.

For a given chain length, the functional groups can be arranged in the following series in order of adsorption capacity: OH \geq COOH \geq NH₂ \geq COOR $>$ I = Cl. This series corresponds with the series for the force of adhesion to water, which indicates the ability of these groups to form monolayers, differing in stability, of insoluble long-chain homologs of surface-active substances [5].

It may be noted in illustration that according to our calculations the work of adsorption, say of carboxyl group, in adsorption from octane is ~ 2500 cal/mole.

It is also interesting to note that this series likewise represents the effectiveness of adsorptive action of surface-active substances on the deformation behavior of solids — single metallic crystals — in hydrocarbon media; here this influence is determined only by the specific properties of the functional groups in the molecules [6].

Clear confirmation of this decisive role of polar groups in adsorption was obtained in our studies of surface activity of three isomers of nitrophenol at the hydrocarbon-water interface. It is known that o-nitrophenol forms an intramolecular hydrogen bond in nonpolar solvents, by ring closure between

*The value for stearic acid in aqueous solution was found from values of G₀ for average water-soluble fatty acid homologs and from $\beta = 3.5$.

phenols at the aqueous solution-vapor interface: $G_0 > G_m > G_p$. We found the same sequence for the hexane-water interface (Fig. 3, 2), as, because of the insolubility of hydroxyphenols in hydrocarbons, they are adsorbed almost entirely from the aqueous phase only.

The sequence for nitrophenols is different (Fig. 3, 1). While the activities of the p- and m-isomers are considerable, and the $G_m > G_p$ sequence is normal, the activity of the o-isomer is negligibly low; because of its anomalously high relative solubility in hydrocarbons* it is adsorbed predominantly from the organic solvent as the result of distribution between the two phases.

This role of the polar groups readily accounts for the position of the surface-tension isotherm for oleic acid in Fig. 2 (Curve 8). Its exceptionally high surface activity, relative to that of stearic acid, is the consequence of the presence of a double bond in the molecule; this acts as a weak polar hydrophilic group, which greatly intensifies the action of the principal functional group in a nonpolar solvent (similarly, in aqueous solutions it greatly lowers the surface activity of unsaturated compounds). This conclusion follows also from the considerable value of the dipole moment and the easy polarizability of the double bonds, and also from the differences between the spreading coefficients $K = W_a - W_c$ (where W_a and W_c are the work of adhesion and cohesion respectively) of saturated and unsaturated hydrocarbons; for example, K for octane is 0.3 erg/cm^2 , and for octylene it is 28.2 ergs/cm^2 . This latter value is comparable to the values for polar compounds (for example, K for octyl alcohol is $36.7 [10]$).

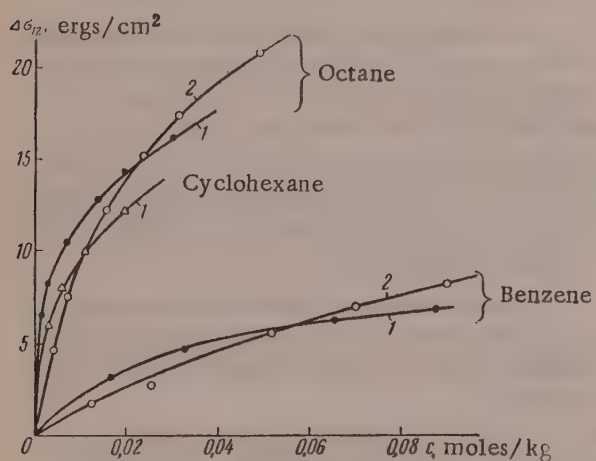


Fig. 4. Surface activity at hydrocarbon-water interfaces in adsorption from n-octane, cyclohexane, and benzene at 20° : 1) Stearic acid; 2) lauryl alcohol.

the hydrocarbon solvent, which greatly weakens such interaction.

This solvation effect can be characterized quantitatively by the value of the cohesion constant in the equation of state for the adsorption layer; this is close to unity, irrespectively of the length of the hydrocarbon chains of the adsorbed molecules, corresponding to almost complete elimination of cohesion forces [4].

These considerations are also confirmed by a certain experimental criterion. It is known that the maximum bubble pressure method used in the present investigation is applicable to determinations of surface tension of solutions at interfaces with vapors of only the lower and intermediate homologs of surface-active substances. Beyond the C_7 to C_8 homologs the results are no longer reproducible. However, in the present investigation this method of maximum pressure of drop formation at interfaces between two liquid phases could be used for determinations in solutions of any homologs (up to the C_{22} homolog in our experiments), strictly quantitatively and quite reproducibly.

It may be assumed that lack of reproducibility is a consequence of surface micelle formation, as first reported by Frumkin [11] and later by Langmuir, as the result of which structural uniformity of the adsorption

*The solubilities of the p-, m-, and o-isomers of nitrophenol in benzene at room temperature are 1.0, 1.8, and 104 g in 100 g, respectively [9].

It follows from the foregoing that the adsorption of surface-active molecules should be greatly influenced by differences between the polar properties of hydrocarbon solvents. In fact, it is clear from Fig. 4 that the adsorption of surface-active substances is much less from the readily polarized benzene than from the difficultly polarized octane and cyclohexane.

The structure and properties of the adsorption layers are also influenced by the hydrocarbon medium in a number of characteristic ways.

All the $\Delta\sigma_{12} - c$ isotherms (Fig. 2) differ characteristically from isotherms for aqueous solutions; there is no S-shaped bend in the initial region of the curves, caused by interaction between the hydrocarbon chains of the adsorbed molecules. This change in the shape of the isotherms is the result of solvation of the hydrocarbon chains in the adsorption layers by

layers is disturbed, and regions with different adsorption layers and hence differing in surface tension arise at the bubble surface. As a result, escape of the bubble may occur at indefinite and accidental values of external pressure.

At the hydrocarbon-water interface the measurement conditions are very different. Because of chain solvation and of the high mobility of the adsorbed molecules, surface micelle formation is prevented and the bubble is uniformly covered.

It follows that, at the octane-water interface, adsorption layers of long-chain homologs of surface-active substances of any chain length are in a gaseous state (and not in a condensed state, as in monolayers on water surfaces), in harmony with their structure [4].

Whereas determinations of surface potential and of direct gradual adsorptional filling of the water-air interface [12] for monolayers of stearic acid give $S_M = 21 - 23 \text{ A}^2$, for the minimum surface area per molecule for a saturated layer, the value for the adsorption layer at the octane solution-water interface is 30.7 A^2 , and the value for lauric acid is 31.0 A^2 . It is known that these values are also characteristic for adsorption layers of the lower and intermediate water-soluble homologs of surface-active substances in aqueous media [3].

It is interesting to note that the molecular packing of the adsorption layer of oleic acid at saturation is more compact, and corresponds to $S_M \sim 24 \text{ A}^2$, probably because of the higher energy of dispersion interaction of the hydrocarbon chains containing double bonds, as the result of which the solvation effect of the hydrocarbon solvent is greatly weakened.

SUMMARY

1. The surface activity of fatty acids, alcohols, amines, and other substances dissolved in formamide and in n-octane has been studied; it was found that these solvents differ considerably from water in a number of adsorptional characteristics.
2. The adsorption of surface-active substances in nonaqueous media is determined by the nature and energy of molecular interaction of the polar and nonpolar parts of the diphilic molecules with the corresponding groups in the solvent molecules.
3. In polar formamide, the solvating effect of the solvent at the solution-vapor interface influences only the polar groups of the absorbed molecules; as in aqueous solutions, the surface activity is associated with the work of adsorption of the hydrocarbon chains, although its magnitude is less in this case.

In hydrocarbon solvents, which do not contain dipoles, the surface activity at the water interface is largely determined by the work of adsorption of the functional groups, the influence of chain length being very weak. Here the unsaturated bonds must also be regarded as weak polar groups; this accounts for the much higher surface activity of unsaturated as compared with saturated compounds, and for the sharp differences in surface activity in adsorption of polar substances from paraffinic and aromatic hydrocarbons respectively.

4. Solvation of the hydrocarbon chains of the adsorption layers by the solvent converts these chains into the gaseous state, with correspondingly less dense molecular packing, and prevents the formation of condensed adsorption layers at the interface between two liquids.

Institute of Physical Chemistry, Academy of Sciences USSR,
Division of Disperse Systems
The Mechnikov University, Odessa

Received June 2, 1958

LITERATURE CITED

- [1] P. A. Rebinder, J. Appl. Phys. 1, 153 (1924); Z. phys. Chem. 121, 103 (1926); 129, 161, (1927); Biochem. Z., 187, 19 (1927).
- [2] A. B. Taubman, Doctorate Dissertation, Institute of Physical Chemistry, Acad. Sci. USSR (Moscow, 1948).*
- [3] A. B. Taubman, J. Phys. Chem. 26, 389 (1952).
- [4] A. B. Taubman and E. K. Venstrem, Proc. 2nd All-Union Conf. Colloid Chem. (Izd. AN SSSR, 1952) p. 52.*

*In Russian

- [5] N. K. Adam, Physics and Chemistry of Surfaces (State Tech. Press, 1947) p. 126 [Russian translation].
- [6] A. B. Taubman and E. K. Venstrem, Proc. 3rd All-Union Conf. Colloid Chem. (Izd. AN SSSR, 1956), p. 52.*
- [7] Sidgwick, J. Chem. Soc. 979 (1929).
- [8] W. Harkins and Grafton, J. Amer. Chem. Soc. 47, 1329 (1925).
- [9] A. Seidell, Solubilities of Organic Compounds, (1941), V. II., 365.
- [10] W. Harkins, G. Clark and L. Roberts, J. Amer. Chem. Soc. 42, 702, (1920).
- [11] A. N. Frumkin, Trans. Karpov Chem. Inst. 4, 56 (1925); I. Langmuir, J. Chem. Phys. 1, 756 (1933).
- [12] A. N. Frumkin, Trans. Karpov Chem. Inst. 4, 75 and 88 (1925).

*In Russian.

GELATINIZED EMULSIONS

16. THE INFLUENCE OF NEUTRAL INORGANIC SALTS ON EMULSIFICATION. ANTAGONISTIC EMULSIFIERS

L. Ia. Kremnev

The thickness of the protective adsorption-solvation layers which prevent droplet coalescence in emulsions of maximum concentration first decreases with increase of emulsifier concentration in the dispersion medium, and then reaches a minimum and constant value in the high-concentration range. For example, in O/W emulsions with sodium oleate as emulsifier, the minimum layer thickness is $\delta_{cr}^* = 1 \cdot 10^{-2} \mu$ [1]; in W/O emulsions with the same emulsifier $\delta_{cr}^* = 0.6 \cdot 10^{-2} \mu$ [2] (Fig. 1, a and b). When δ_{cr}^* is greater than $\delta_{cr}^* : \gamma = \delta_{cr}^*/\delta_{cr}^* > 1$, an O/W emulsion is formed; if $\gamma = \delta_{cr}^*/\delta_{cr}^* < 1$, the reverse emulsion is stabilized [3]. If an alkali soap is used as emulsifier, the latter condition is favored by introduction into the aqueous phase of neutral inorganic salts which do not react chemically with the emulsifier. Kremnev and Kuibina [3] also used this method for effecting phase reversal in less-concentrated emulsions (less than 74% by volume).

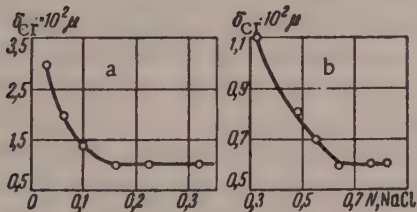


Fig. 1. Variation of the thickness of protective layers with sodium oleate concentration in concentrated O/W (a) and W/O (b) emulsions: a) Benzene as the disperse phase; b) 2N NaCl solution as the disperse phase.

A noteworthy fact for which there is no satisfactory explanation is that, in a narrow range of electrolyte concentrations in water, stable emulsions are not formed at all. Neither is it clear how the type of emulsion formed is related to the salt concentration in the aqueous medium. Evidently, further investigation of the influence of neutral salts on emulsification is required. We therefore studied concentrated emulsions with sodium oleate emulsifier, to which NaCl in a large range of concentrations was added (the nonaqueous liquid in the emulsions was benzene). The results of the δ_{cr} determinations are given in Fig. 2, the right-hand side of which contains data published earlier [2].

Figure 2 reveals 5 regions of NaCl concentrations, with different effects on emulsification and emulsion properties. The peculiar influence of NaCl is due to salting-out of the soap from the aqueous medium, which increases with increasing salt concentration (Fig. 3). The salted-out sodium oleate under these conditions acts as an oleophilic stabilizer for W/O emulsions.

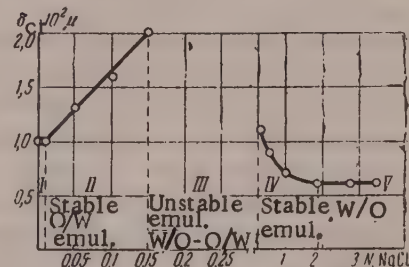


Fig. 2. Variation of the thickness of protective layers in direct and reverse concentrated emulsions with the NaCl concentration.

It should be emphasized that when the soap is partially salted out, the system contains two emulsifiers simultaneously: oleophilic (salted out) and hydrophilic (dissolved in water) sodium oleate; the latter is capable as before of stabilizing O/W emulsions. Antagonism arises between these two varieties of soap, of the same chemical composition and structure, because of their respective tendencies to convert benzene and water into the disperse phase of the emulsion.

We assume that the emulsifying effects of the hydrophilic and oleophilic emulsifiers are mutually nullified in equimolecular amounts, as the emulsion is stabilized by the formation of adsorption monolayers of the soap. If this is so, only excess of hydrophilic or oleophilic stabilizer (above the amount neutralized)

can exert emulsifying power, provided that its concentration is sufficient for the formation of a stable emulsion; this determines the result of the emulsification. The experimental confirmation of these views is provided by a closer scrutiny in Fig. 2.

In Region I, at low salt concentrations ($5 \cdot 10^{-4} - 1 \cdot 10^{-2}$ N), O/W emulsions are formed, and the protective layers are of the same thickness as in emulsions with sodium oleate without added electrolyte: $\delta_{cr}^* = 1 \cdot 10^{-2} \mu$ (Fig. 1,a). Under such conditions the soap is not salted out to any appreciable extent (Fig. 3), so that δ_{cr}^* remains constant, although the electrolyte added to the soap solution compresses the diffuse layers in the surfaces of the benzene droplets. It is clear that, in agreement

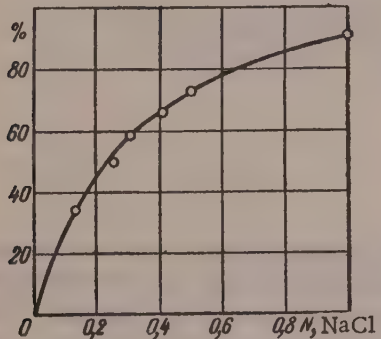


Fig. 3. Salting-out effect of NaCl on sodium oleate.

with Rebinder's views [4], electrostatic repulsion of the diffuse layers is not an important factor in the stability of concentrated emulsions.

In Region II, with increase of NaCl concentration, there is an increase of δ_{cr}^* due to salting-out of the stabilizer. For example, 0.05 N NaCl solution salts-out 16% of the soap (Fig. 3), and an equal amount of hydrophilic sodium oleate in aqueous solution is antagonistic with respect to it. Consequently 32% of the total amount of soap in the system is devoid of emulsifying action. Above the amount so neutralized, the water contains an additional 68% of soap, and it is easy to show that only this amount can stabilize an O/W emulsion. In these experiments (Regions I-III) 0.16 N sodium oleate solution was used; therefore the amount remaining in solution corresponds to 0.11 N sodium oleate. However, a sodium oleate solution of this concentration should stabilize an O/W emulsion by means of protective layers $\delta_{cr}^* = 1.3 \cdot 10^{-2} \mu$ thick (Fig. 1,a). In fact, in the case of 0.05 N NaCl solution (Fig. 2) δ_{cr}^* has precisely this value: $\delta_{cr}^* = 1.3 \cdot 10^{-2} \mu$; this confirms that only the hydrophilic soap present in excess above the amount exerting an antagonistic effect has emulsifying power. Satisfactory agreement of the values of δ_{cr}^* is also found for other salt concentrations.

The concept of the antagonistic effect of the emulsifiers makes it quite clear why only unstable emulsions are formed in Region III. For example, 0.2 N salt solution salts-out 45% of the soap (Fig. 3), and its emulsifying action is neutralized by an equal amount of soap dissolved in water. This leaves 0.016 N sodium oleate solution, which, according to our experiments, cannot stabilize a direct concentrated emulsion.

The antagonistic effect is especially prominent in the case of 0.25 N salt solution. At this concentration 50% of the soap is salted out (Fig. 3); all the hydrophilic soap remaining in solution is used to neutralize it, and, as was found in our experiments, the formation of a stable emulsion becomes impossible.

In the range of 0.25-0.3 N NaCl solutions, oleophilic sodium oleate begins to predominate, but its excess over the hydrophilic oleate is insufficient for the formation of a concentrated W/O emulsion, just as the formation of a stable O/W emulsion is impossible at NaCl concentrations somewhat below 0.25 N (see above).

Emulsifier antagonism also determines the course of the right-hand part of the curve in Fig. 2, which refers to concentrated W/O emulsions formed at higher NaCl concentrations. 0.64 N sodium oleate solution was used for these experiments [2].

At salt concentrations up to 1.8 N (Region IV), the oleophilic oleate increasingly predominates over the hydrophilic. For example, 0.6 N NaCl solution salts-out 78% of the sodium oleate (Fig. 3). Consequently, 44% of the soap is involved in antagonistic action, while the 56% excess of oleophilic (salted-out) soap forms a 0.36 N solution which should stabilize a concentrated reverse emulsion by means of protective layers of thickness $\delta_{cr}^* = 0.9 \cdot 10^{-2} \mu$ (Fig. 1,b). It is seen in Fig. 2 that in presence of 0.6 N salt solution the reverse emulsion is stabilized by layers of just this thickness: $\delta_{cr}^* = 0.9 \cdot 10^{-2} \mu$; this confirms that only the excess of oleophilic stabilizer, after subtraction of the quantity acting antagonistically, has an emulsifying effect. The values of δ_{cr}^* are also in satisfactory agreement for other salt concentrations.

Finally, in Region V reverse concentrated emulsions continue to be formed, but the thickness of the protective layers remains constant at $\delta_{cr}^* = 0.6 \cdot 10^{-2} \mu$. There is nothing unexpected in this. At high NaCl concentrations virtually all the sodium oleate is salted out of aqueous solution, and takes part in the stabilization of the reverse emulsions. However, at high soap concentrations δ_{cr}^* reaches precisely this minimum constant value: $\delta_{cr}^* = 0.6 \cdot 10^{-2} \mu$ (Fig. 1,b).

We must point out in conclusion that the questions considered above are not only of theoretical interest, but are of practical significance, for example, for the production of emulsions of water in organic binders used in road building.

SUMMARY

1. The action of a neutral salt on aqueous solutions of sodium oleate has been studied, and the conditions for formation of O/W and W/O emulsions have been determined.
2. The soap dissolved in water (hydrophilic emulsifier) and the salted-out soap (oleophilic emulsifier) have a mutually antagonistic effect.
3. The emulsifying effects of the hydrophilic and the oleophilic sodium oleate neutralize each other in equivalent amounts. If a sufficient excess (over the amount neutralized) of one of these types of soap is present, it acts as an independent stabilizer of either an O/W or a W/O emulsion.

The Lensoviet Technological Institute
Leningrad

Received April 8, 1957

LITERATURE CITED

- [1] L. Ia. Kremnev and S. A. Soskin, Colloid J. 9, 269 (1947).
- [2] L. Ia. Kremnev and N. I. Kuibina, Colloid J. 16, 358 (1954).*
- [3] L. Ia. Kremnev and N. I. Kuibina, Colloid J. 17, 34 (1955).*
- [4] P. A. Rebinder, Colloid J. 8, 3, 157 (1946).

*Original Russian pagination. See C.B. Translation.

THE INFLUENCE OF ETHYLENE GLYCOL ON THE COLLOIDAL PROPERTIES OF AQUEOUS SODIUM OLEATE SOLUTIONS

A. I. Iurzhenko and G. F. Storozh

It was shown in the preceding paper [1] that the turbidity of aqueous solutions of sodium oleate increases and passes through a maximum on addition of alcohols (methyl, ethyl, n-butyl, and isoamyl). The viscosity of the systems shows analogous changes. We attributed this effect of the alcohols to their dehydrating and dispersing action on the soap micelles and molecules in solution. The present paper deals with a study of light scattering, viscosity, and electrical conductivity of aqueous sodium oleate solutions in presence of ethylene glycol. Our choice of ethylene glycol is relevant to determination of the influence of the number of hydroxyl groups in the alcohol molecule on the colloidal properties of the systems.

The methods used for the synthesis of sodium oleate and measurements of light scattering and viscosity were described earlier [1]; these properties were studied in 0.05; 0.1; 0.2; 0.3 and 0.5 M solutions of sodium oleate in glycol-water mixtures. The glycol concentrations are given in molar percentages. All the determinations were performed at $25 \pm 0.1^\circ$.

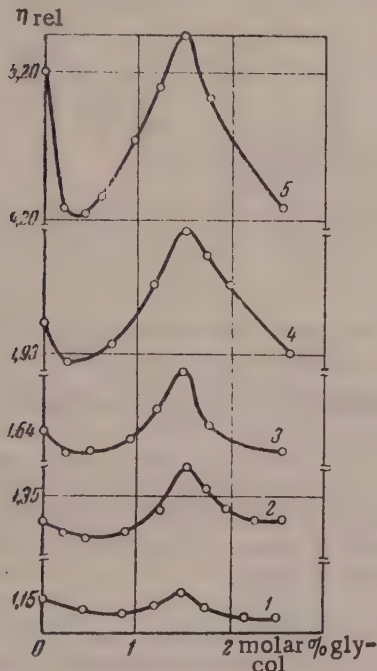


Fig. 1. Relative viscosity of aqueous glycol solutions of sodium oleate: 1) 0.05 M; 2) 0.1 M; 3) 0.2 M; 4) 0.3 M; 5) 0.5 Moleate.

sodium oleate solutions, found that with polar additives, such as octyl alcohol, there is also a concentration optimum at which these properties of soap solutions are at their maximum values.

Curves for the variation of the relative viscosity of 0.1 M sodium oleate solution with the concentrations of ethanol and ethylene glycol respectively are compared in Fig. 2, a. It is seen that at low concentrations of the two alcohols the curves almost coincide. When the concentration of the additives reaches 0.9 molar %, the η_{rel} - calc curves diverge appreciably, and the maximum for the system sodium oleate-ethanol-water lies below the maximum for the system sodium oleate-glycol-water. Therefore, increase of the number of hydroxyl groups in the alcohol molecule raises the viscosity maximum and shifts it in the direction of lower concentrations, although, as is clear from Fig. 2,b, aqueous glycol solutions have lower viscosities than aqueous

ethanol solutions. It may be noted that the viscosity of pure glycol is almost 17 times that of ethanol [5]. We attribute this action of glycol to the fact that its dehydrating power is greater than that of ethanol.

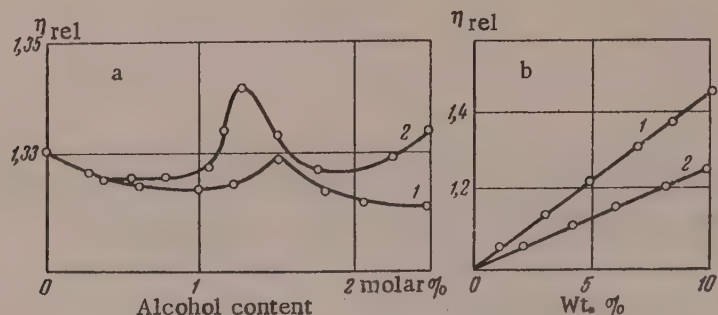
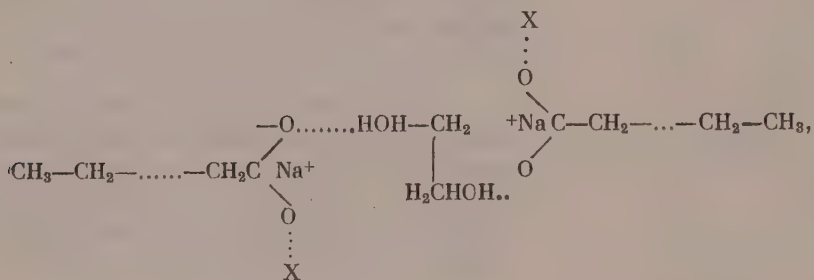


Fig. 2. Relative viscosities: a) 0.1 M aqueous alcohol solutions of sodium oleate: 1) with ethanol; 2) with ethylene glycol; b) Aqueous solutions of: 1) ethanol; 2) ethylene glycol.

From 2.13 molar % of the alcohols in the solutions, the viscosity of the system sodium oleate-ethanol-water continues to decrease, whereas for the system sodium oleate-glycol-water it begins to increase. As already stated, in both cases dispersion of the soap micelles occurs, with formation of various complexes, such as



which increase the total viscosity of the system in the range of glycol concentrations studied (X represents a molecule of alcohol or water).

The results of the conductivity determinations are plotted in Fig. 3. It is seen that additions of ethylene glycol in general decrease the conductivity, and in the region of ethylene glycol concentration which corresponds to the viscosity maximum the decrease of conductivity is retarded considerably almost to zero. Similar results were obtained by Passinen and Ekvall [5] for the system sodium oleate-decanol-water.

Figure 4 represents variations of the product $\eta \cdot \kappa$ with glycol concentration for 0.05, 0.1, and 0.2 molar solutions of sodium oleate. It is clear from Fig. 4 that the $\eta \cdot \kappa - c_{\text{glyc}}$ curves are analogous in form to the $\kappa - c_{\text{glyc}}$ curves. In our view, this confirms the hypothesis that, at low glycol concentrations, dehydration and partial coalescence of the soap micelles takes place (at their exposed portions), and the charge on the particles therefore decreases. This corresponds to the initial viscosity decrease. In the region where the conductivity is approximately constant, further growth of the micelles is accompanied by some solvation by the glycol (with a viscosity increase). On further increase of the glycol concentration the colloidal solution is converted into a system containing particles of higher dispersity.

The results of the light-scattering studies are plotted in Fig. 5. It is seen that small amounts of the glycol first decrease considerably the solution turbidity; the turbidity then passes to a maximum and decreases again with increase of the glycol content. The turbidity maximum corresponds to the sharp viscosity change; this is in agreement with the hypothesis that the first portions of glycol have a dehydrating effect. The solution turbidity decreases with further increase of glycol concentration; this must be attributed to subsequent dispersion of the micelles. This conclusion is in harmony with the viscosity and conductivity data.

The soap concentration has a considerable influence on the turbidity of such systems. The turbidity maximum decreases with increase of oleate concentration; this is evidently due to decreased hydrolysis of the soap on the one hand, and to changes of the micellar structure on the other.

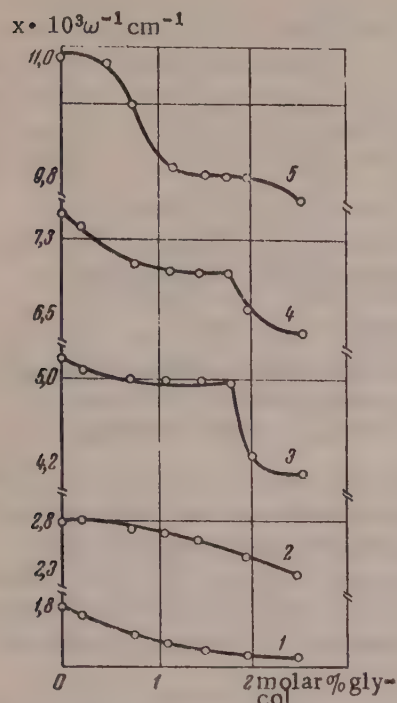


Fig. 3. Conductivity of aqueous glycol solutions of sodium oleate: 1) 0.05 M; 2) 0.1 M; 3) 0.2 M; 4) 0.3 M; 5) 0.5 M oleate.

when the alkali concentration reaches 0.0005 M the hydrolysis of the oleate is totally suppressed. It is seen in Fig. 6 (Curve 1) that appreciable hydrolysis of sodium oleate begins when the soap concentration falls below 0.0015 M. This value almost coincides with the critical concentration of micelle formation (CCM) for sodium oleate. Similar values were found by Flockhart and Graham [6] in conductivity determinations on aqueous sodium oleate solutions, and by other workers [7].

Variations of turbidity with sodium oleate concentration in presence of different amounts of ethanol and glycol are plotted in Fig. 7. It follows from Fig. 7 that in the concentration range studied these alcohols decrease the turbidity of the soap solutions without suppressing hydrolysis. Comparison of these curves with the curves in Fig. 6 shows that the alcohols have a similar effect to alkali on the turbidity of soap solutions. These curves have two concentration regions. The first region, with the higher turbidity maximum (the first maximum is not shown in full in the graphs because the turbidities are very high), which probably corresponds to hydrolysis, corresponds to very low oleate concentrations. The second region, with a lower maximum, is found at higher soap concentrations. At oleate concentrations corresponding to the second maximum the micelles begin to aggregate, with resultant changes in their form. The oleate concentration corresponding to the boundary between these two regions, should be regarded, as stated earlier, as the critical concentration of micelle formation.

Ekwall et al. [8] found an analogous relationship between turbidity and soap concentration in studies of light scattering in aqueous solutions of some salts of fatty acids in presence of decanol. These authors consider that the first boundary concentration (limiting association concentration - LAC), corresponds to the start of interaction between the soap molecules and the molecule of its related acid (formation of acid soaps), or molecules of decanol.

It may be noted, however, that this first boundary concentration (like the first maximum) is found even in absence of additions (Curve 1 in Figs. 6 and 7). The above-named workers added excess alkali to the soap

To determine the influence of hydrolysis on the turbidity of sodium oleate solution, we also determine light scattering in such solutions in relation to the soap concentration with different alkali contents. The $\tau - c_{\text{ol}}$ relationship is plotted in Fig. 6; it is seen that the turbidity decreases with increasing NaOH content, and

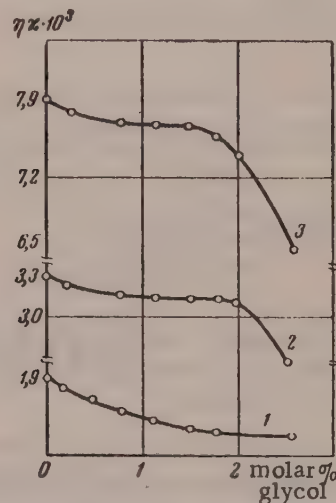


Fig. 4. $\eta \cdot \kappa - c_{\text{glyc}}$ curves for different sodium oleate contents: 1) 0.05 M; 2) 0.2 M; 3) 0.3 M sodium oleate.

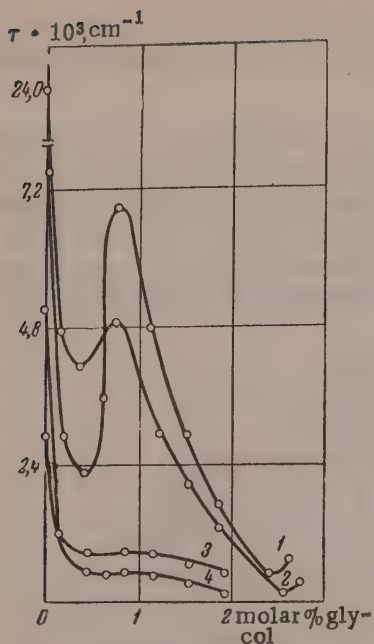


Fig. 5. Light scattering in aqueous glycol solutions of sodium oleate: 1) 0.05 M; 2) 0.1 M; 3) 0.2 M; 4) 0.3 M; 5) 0.5 M oleate.

tration must be insufficient to suppress hydrolysis, owing to partial neutralization of this acid. Therefore, we consider that the definition of LAC is not very apt and to some extent even arbitrary.

Neither do we agree with their definition [8] of the critical concentration of micelle formation (CCM). In their opinion, CCM is defined as the concentration at which micelle aggregation increases sharply (the maxi-

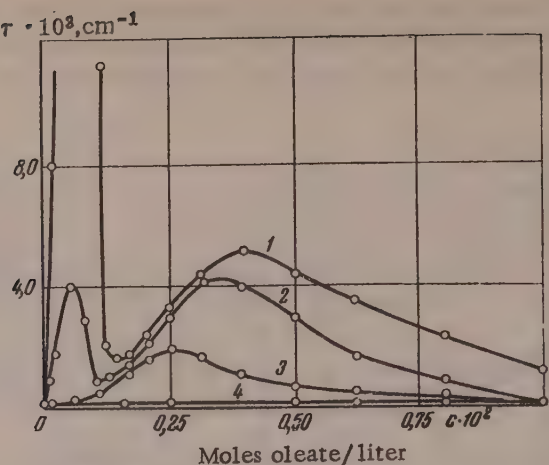


Fig. 6. Effect of concentration on the turbidity of alkaline sodium oleate solutions: 1) 0.0 M; 2) 0.0002 M; 3) 0.0005 M; 4) 0.001 M NaOH.

solutions to prevent hydrolysis. In such cases, as our results show, critical effects are not found at all when a definite NaOH concentration is reached (Fig. 6, Curve 4). It is evident that when its related acid is added to an alkaline soap solution, the alkali concen-

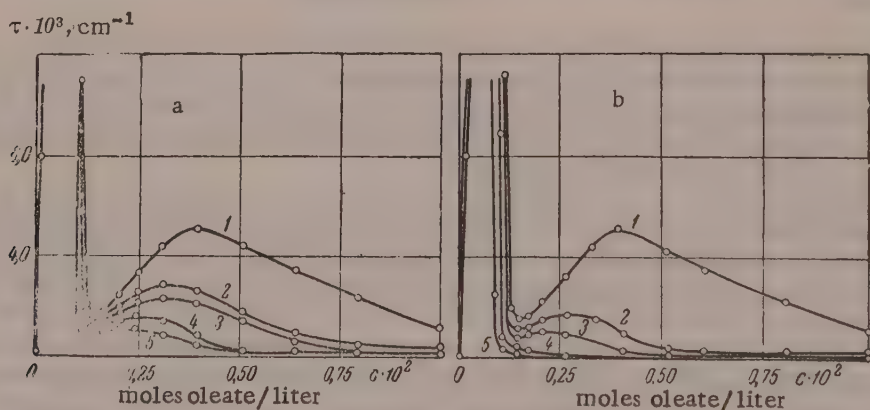
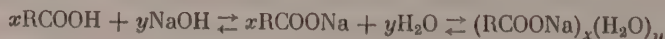


Fig. 7. Effect of concentration on the turbidity of sodium oleate solution ($\tau \cdot 10^3 \text{ cm}^{-1}$ along the ordinate axis) containing ethanol (a) and ethylene glycol (b): 1) 0%; 2) 1%; 3) 3%; 4) 7%; 5) 10%, by weight.

mum of the second concentration region). We hold the opinion that the critical concentration of micelle formation is the concentration at which micelles begin to form. This concentration corresponds to the boundary between the two concentration regions. Below this boundary the equilibrium



is shifted to the left, and above it, to the right.

With regard to the effect of alcohols on the critical concentrations of sodium oleate, our data show that these values decrease with increasing ethanol and glycol contents, owing to their partial dehydrating action.

SUMMARY

1. The viscosities of aqueous sodium oleate solutions with different concentrations of ethylene glycol and soap were studied.

It was found that the viscosity of the system passes through a maximum and then decreases with increasing glycol concentration. The position of the maximum corresponds to 1.5 molar % of glycol, irrespective of the oleate content. This effect must be attributed to a dual action of ethylene glycol - dehydrating and dispersing effects. The viscosity maximum increases with increasing soap concentration. Increase of the number of hydroxyl groups in the alcohol molecule increases the viscosity of the system, because of the greater dehydrating power.

2. The turbidity of the sodium oleate-glycol-water system varies analogously to the viscosity, but the turbidity maximum is found at lower glycol concentrations.

3. The conductivity of sodium oleate solutions decreases with increasing ethylene glycol concentration.

4. Alcohols (ethanol and glycol), at the concentrations studied, like NaOH, lower the boundary concentrations (critical concentrations of micelle formation) of sodium oleate.

The I. Franko University, L'vov

Received December 24, 1957

LITERATURE CITED

- [1] A. I. Iurzhenko and G. F. Storozh, Sci. Mem. L'vov Univ.* (in the press).
- [2] Angelescu, Kolloid.-Z. 82, 164, 1938; 82, 304 (1938).
- [3] A. J. Hyde et al., Disc. Faraday Soc. 18, 239 (1954).
- [4] Z. N. Markina and P. A. Rebinder, Proc. Acad. Sci. USSR 109, 1156 (1956).
- [5] K. Passinen and P. Ekwall, Acta Chem. Scand. 9, 1438 (1955).
- [6] B. D. Flockhart and H. Graham, J. Coll. Sci. 8, 105 (1953).
- [7] Per Ekwall, Kolloid.-Z. 136, 37 (1954).
- [8] Per Ekwall et al., Acta Chem. Scand. 10, 227 (1956).
- [9] Landolt-Bornstein, 1, 126, 130 (1923).

*LDY - Transliteration from Russian. Probably L'vov Univ. Translator's note.

FORMATION AND STABILITY OF METAL SOLS*

E. M. Natanson

The disperse phases of many metal and alloy sols have extremely valuable catalytic, pyrophoric, lubricant, antidental, and ferromagnetic properties. For this reason they are coming into extensive use in chemical industry, electrical and radio engineering, machine construction, and other branches of industry. Many urgent problems of modern technology involve detailed studies of the formation of the disperse phases of metal sols and determination of their stability; these questions are also of considerable scientific interest in general.

The formation of colloidal metal particles is based on either of two principles: condensation of metal atoms to particles of colloidal size, or dispersion of particles of the given metal.

These principles apply to the formation of colloidal particles of any substance, but they have their specific features in relation to metals, in connection with the structure of the crystal lattice and the modern electronic theory of metal structure.

Metal sols are extremely unstable, and cannot be obtained in concentrations higher than 0.1-0.2% in absence of stabilizers. Formation of concentrated and stable metal sols is possible only in the presence of stabilizing compounds of high molecular weight.

As the result of the researches of P. A. Rebinder and his school [1, 2] on the influence of adsorption layers on interaction of contacting phases in disperse systems and on the stabilization of such systems, it is now possible to elucidate theoretically the extensive experimental data available on the formation of metal sols and their stability, and also to point the way to further research in this direction.

An important defect of colloidochemical research into the production of metal sols by dispersion methods is lack of due attention to the mechanical properties and physical state of the metals undergoing dispersion. The plasticity and strength of the metal and the presence in it of microcrevices and various defects of crystal structure determine its resistance to destruction and have a decisive influence in dispersion processes.

As disintegration proceeds, when the metal particles become of microscopic size and the specific surface is therefore very large, the predominant factor is hardness of the metal, characterized by the work of formation of unit new surface area [2]. The same applies to processes of fine grinding.

The work of Rebinder and his school [2] has shown that the physicochemical nature of the medium in which the dispersion takes place can, as the result of adsorptional action, greatly facilitate the dispersion process (adsorptional lowering of strength as the result of decreased surface energy or the work of formation of new surfaces; this is often known as the Rebinder effect).

These researches have provided new potentialities in the fields of dispersion and mechanical treatment of metals.

The addition of surface-active substances which sharply lower the hardness of metals, i.e., facilitate their dispersion, to the liquids used in the dispersion process has a much more favorable effect on the formation of colloidal particles than the use of the most advanced mechanical devices.

Many years of experience in the use of the so-called colloid milis, of a great variety and of the most advanced design, have shown that these devices mainly produce highly disperse suspensions, and the yields of colloidal fractions are usually slight [3].

*Paper at the IVth All-Union Conference on Colloid Chemistry, Tbilisi, May 1958.

The possibility of metal dispersion by means of ultrasonic waves has been investigated by many workers [4].

It was found that pure metals in the form of macroscopic particles are not dispersed at all under the action of ultrasonic waves in liquid media. In general, only the oxide films, present on almost every metal surface, are dispersed in the process. The ultrasonic dispersion of metals at the instant of their liberation at the cathode has been studied in considerable detail [5]. Under such conditions, the cathodic deposits are disintegrated in the surrounding medium, forming highly disperse suspensions or unstable metal sols.

A method worthy of special attention is the dispersion of certain metals, such as tungsten, molybdenum, zirconium, etc., by repeated consecutive treatments of coarse powders of these metals with solutions of various acids and bases [6].

Although this is a very old method, its mechanism still remains quite obscure; it involves not only peptization, but also breakdown of the individual crystals formed as the result of the adsorptive action of the medium, in agreement with Rebinder's theories [1].

For avoidance of oxidation, the formation of colloidal metal particles by this method must take place in an indifferent gas without access of oxygen.

Our detailed experimental studies of the formation of colloidal metals by condensation methods have led to the following conclusions.

1. The known electrical methods for the production of metal sols have a number of defects: considerable oxidation of the colloidal metal particles, decomposition of the dispersion medium, and the impossibility of obtaining concentrated and stable sols in hydrocarbon media. Such methods are now used very little and are mainly of interest in relation to questions of techniques.

2. Thermal methods for the production of sols by the simultaneous condensation of vapors of the metal and the dispersion medium are free from some of the above defects. However, at present these methods can be used only for the production of stable organosols of easily fusible metals such as mercury and the alkali metals.

3. The production of metal sols by thermal dissociation of metal compounds, especially carbonyls, is now coming into use on the industrial scale, especially for the production of ferromagnetic colloidal metals - iron and nickel.

4. Investigations of the possible formation of metal organosols by reduction of metal compounds in various organic media have so far not given positive results, as the metal sols obtained by this method are contaminated with decomposition products of the dispersion medium.

5. The formation of colloidal metals by reduction of ions by means of various organic reducing agents has long been known, but the process is used widely only for the production of hydrosols of platinum, gold, silver, bismuth, and other metals which are readily reduced in aqueous media.

6. The most general method is the electrolytic method, developed by us [7] in A. V. Dumanskii's laboratory, for the formation of colloidal metal particles by cathodic reduction of the appropriate ions, followed by production of metal organosols. This method is based on the electrolytic liberation of metals from aqueous solutions of their salts, in the form of highly disperse cathodic deposits, which immediately enter the organic medium and are dispersed in it in presence of surface-active additives.

The process is carried out in a two-layer bath. The lower layer consists of the electrolyte solution, while the upper layer is a dilute solution of a specially selected surface-active substance in a hydrocarbon medium. The anode is fixed, and is separated by a diaphragm from the disk-shaped cathode rotating at the interface. This method is of fairly universal applicability. With suitable choice of conditions, any metal can be obtained in the colloidal state by this method.

The basic principles and the optimum conditions for the production of metal sols and alloys by this method are detailed in a number of published papers [7]. The process is now used industrially; the technological procedure, developed by us jointly with Barabash and Veneraki, is as follows (Fig. 1).

The principal apparatus is the electrolytic cell 1 with a rotating or rocking multidisk cathode. A 2-3% electrolyte solution is fed from the tank 3 through the valve 2 into the cell, and fills it to the level of the cathode shaft. The electrolyte solution is covered, from the tank 4, with the dispersion medium containing ~1% of oleic acid or other surface-active substance, in a layer 10-15 cm thick.

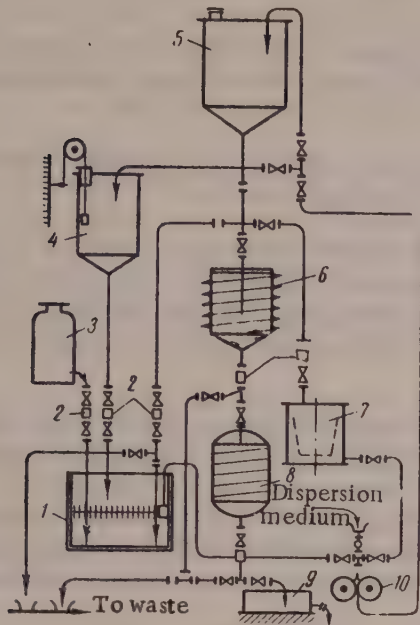


Fig. 1. Process for the production of metal organosols.

crease of cathode polarization. The curves obtained by Kozachek [8] for cathode polarization in the formation of lead-tin alloy organosols are shown in Fig. 2. This effect favors the simultaneous deposition of different metals at the cathode, and the formation of the corresponding alloys. The production of colloidal organosols of lead-tin, nickel-chromium, and nickel-iron by this method is described in detail in our papers [9].

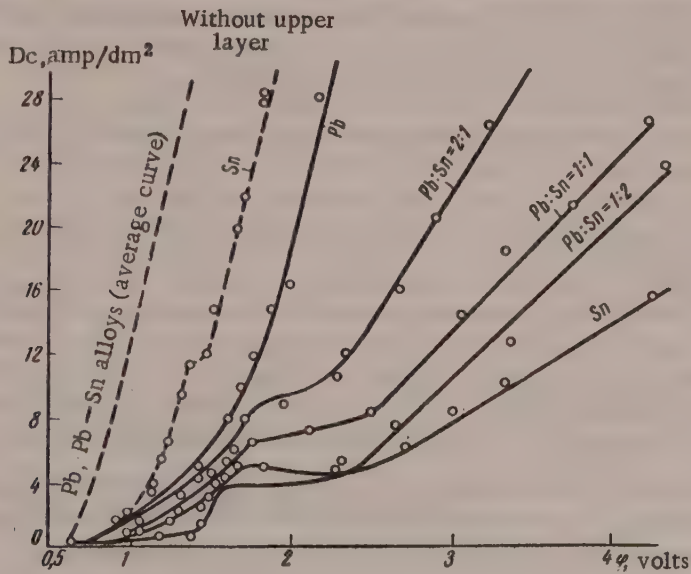


Fig. 2. Cathode polarization curves for the formation of lead-tin alloy organosols.

The electrolysis is performed at 20-30° in the current density range 16-30 amp/dm², usually until the metal concentration in the organosol reaches 5-7%. The sol is pumped by means of the pump 10 into the centrifuge 7 and the tank 5, where it is washed with distilled water to remove electrolyte impurities. The washed organosol passes into the electrically heated vessel 6, where it is left to settle and undergoes preliminary dehydration at a temperature not above 50°. The lower aqueous layer which forms as the result of demixing is carefully removed. The organosol after preliminary dehydration is passed into the vacuum drier 8 in order to remove as much moisture as possible. The finished organosol is collected in the tank 9.

Among the numerous factors which determine the size and structure of the colloidal particles formed by the electrolytic method, the most important are cathode polarization and current density.

It must be noted that when the electrolysis is performed in a two-layer bath, the rotating cathode is continuously passivated, with a resultant considerable in-

It was found that if the colloidal particles of one of the alloy components are microdendritic in form, it is possible to use the electron microscope to follow the course of formation of the colloidal particles of the alloy in relation to the cathodic current density, electrolyte composition, electrolysis temperature, nature of the cathode and its rotation rate, and a number of other factors.

It was found by x-ray investigations of the structure of the disperse phase in lead-tin and nickel-chromium alloy organosols, obtained with different ratios of the alloy components in the aqueous layer of the bath and at different current densities, that alloys of a eutectic character are formed in the simultaneous deposition of lead and tin at the cathode from two-layer baths.

Solid solutions are formed in the simultaneous deposition of nickel and chromium from ammonium tartrate electrolytes from acid baths containing mixtures of nickel and chromium chlorides.

Microcinematography of the formation of the disperse phase in organosols of lead-tin and other alloys under various electrolytic conditions in two-layer baths shows that at low voltages, from 0.9 to 1.5 volts, there is an initial delay, a sort of "induction period" of the electrocrystallization process [8], the duration of which depends mainly on the degree of passivation of the cathode surface, largely determined by the composition of the upper layer of the bath.

The electrocapillary polarization effects studied by A. N. Frumkin and his associates [10] play a significant role in the mechanism of formation of metal and alloy colloidal particles by the electrolytic method; they determine the desorption of surface-active substances when the surface of the rotating cathode is in the aqueous layer of the bath, and readsorption of the same substances when the surface enters the organic layer. The ratio of the rates of these two processes largely determines the total fraction of the active cathode surface, consisting of individual islets, not protected by layers of surface-active substances, at which the metal ions are discharged.

The current density becomes particularly high at these regions, with a corresponding increase in the discharge rate of the metal ions, leading to the formation of very fine particles with a disordered structure.

If surface-active substances are present in the hydrocarbon medium during the formation of these particles, their surfaces become partially covered with water-repellent adsorption layers and the particles can thus be detached more readily from the cathode surface. This is not only the cause of the slight cohesion between the colloidal metal particles formed and the cathode surface, but it also protects the particles from mutual aggregation and to a considerable extent retards their oxidation.

The nature of the bonding between the adsorbed surface-active substances and the surface of the colloidal particles, their interaction with the medium and with the macromolecules of the polymers used for stabilization of the sol, are very important factors in the stability of the metal sols.

Our studies of the adsorption of surface-active substances on the surfaces of colloidal tungsten, molybdenum, and zirconium particles formed in hydrocarbon media, and measurements of the heats of wetting of the disperse phases in metal organosols [11] are in full agreement with Rebinder's views [1] on the significance of chemical fixation of the adsorption layers for strong hydrophobization of the particle surfaces in the production of stable and concentrated sols.

In fact, we were able to show that the surface-active substances used for stabilization of metal organosols in hydrocarbons media form chemically bonded adsorption layers on the particle surfaces. For example, cinchonine and quinine proved to be effective stabilizers for tungsten sols, o-hydroxyquinoline for molybdenum sols, and phenylhydrazine for zirconium sols. These substances are used in analytical chemistry for quantitative determination of tungsten, molybdenum, and zirconium, respectively, and form complex compounds with them.

In view of the irreversibility of the adsorption, and of the high values of the molar heats of adsorption, of quinine, o-hydroxyquinoline, and phenylhydrazine on the surfaces of W, Mo, and Zr particles, there is reason to assume that surface compounds are formed on the oxidized surfaces of these particles:

- 1) $\equiv W = O + 2C_{20}H_{24}N_2O_2 \rightarrow \equiv W (C_{20}H_{23}N_2O_2)_2 + H_2O,$
- 2) $\equiv Mo = O + 2C_9H_7ON \rightarrow \equiv Mo (C_9H_6ON)_2 + H_2O,$
- 3) $= Zr = O + C_6H_5 - NH - NH_2 \rightarrow = Zr (C_6H_5N_2H_3)_2 + H_2O.$

The formation of chemically fixed adsorption layers on the surface of metallic sol particles determines their high lyophilicity toward hydrocarbon media, and is a necessary condition for the stability of such sols. For example, such hydrophobization of the metal particles in the formation of organosols decreases the hydrophilicity coefficient, calculated from heats of wetting, from 2.3 to 0.48 for tungsten and from 3.5 to 0.56 for molybdenum.

In addition to lyophilization, the presence of polymeric compounds is necessary for a sharp increase in the stability of metal organosols; this is in full agreement with Rebinder's view [1] of the structuromechanical barrier as a powerful factor in the stabilization of disperse systems.

In this connection it is necessary to take into account that because of the high dispersity of the organosols only individual segments of the macromolecules are adsorbed on the surfaces of the colloidal metal particles. Each macromolecule may be bound simultaneously to many colloidal metal particles, so leading to the formation of chainlike aggregates differing in shape and length in the dispersion medium. Colloidal metal particles also serve as junctions at which segments of different or the same molecules are linked together [12]. In organosols of this kind, the stabilized colloidal particles of the disperse phase are contained in the spatial network consisting of the macromolecules of the protective polymer.

We have carried out, jointly with N. N. Kozachek, numerous investigations on the stability, structural viscosity, and structural strength of numerous metal and alloy organosols. It was found that metal sols with pronounced anomalous viscosity and yield stress are the most stable [13].

These views are also confirmed by the results of electron microscope studies of the disperse phase of tungsten organosols protected by means of rubber. It was found that the colloidal particles in these systems are arranged in groups, and often form chains of various shapes and lengths.

This mechanism of the protective action of polymers on metal sols has not only been established experimentally, but has also to some extent been justified theoretically by Simha, Frisch, and Eirich [14]. As a result of statistical analysis of the adsorption of flexible macromolecules, they concluded that only a certain proportion of the total segments in the macromolecule is adsorbed on the surface of the colloidal particles.

It must also be pointed out that in recent years similar views on adsorptional interaction between lyophobic colloidal particles and polymer macromolecules have been put forward by Heller et al. [15], who consider that this type of interaction in the system gives rise to the so-called "steric protection."

The extensive factual material accumulated in the course of several decades shows that a very significant and universal criterion of hydrosol and organosol stability is the presence of structurized adsorption-solvation layers on colloidal particle surfaces, irrespective of the mechanism by which they are formed on these surfaces. In the case of very stable concentrated sols, especially metal organosols, the formation of lyophilizing adsorption layers is always accompanied by the development of a spatial structure in the entire system, because of the inevitable presence of a suitable polymer as an additional stabilizer.

SUMMARY

1. Consideration of various methods for the preparation of metal organosols shows that the most general, convenient, and technically suitable method is by formation of the colloidal metal particles by electrolysis at a rotating cathode, with continuous transfer of the particles into an organic medium in contact with the electrolyte.

2. Stabilization of the metal particles in the resultant organosol, to virtually the maximum possible stability, is effected by the simultaneous action of two types of stabilizers:

a) hydrophobizing ("carbophilizing") surface-active substances, which are fixed chemically when adsorbed on the metal particle surfaces covered with oxide films;

b) polymers, which form loose spatial structures throughout the sol volume, the colloidal metal particles being included in the form of junctions in the network.

LITERATURE CITED

- [1] P. A. Rebinder, Bull. Acad. Sci. USSR, Chem. Ser. 5, 639 (1936); Physical Chemistry of Flotation Processes (Moscow-Leningrad, Metallurgy Press, 1933); * Investigations in the Field of Applied Physical Chemistry of Surface Phenomena (Moscow-Leningrad, Izd. AN SSSR, 1936). *
- [2] P. A. Rebinder, L. A. Shreiner, and K. F. Zhigach, Softeners in Drilling (Moscow-Leningrad, Izd. AN SSSR, 1944); * P. A. Rebinder, July Session, Academy of Sciences USSR (1946); P. A. Rebinder, Jubilee Volume on the 30th Anniversary of the Great October Socialist Revolution (Moscow-Leningrad, Izd. AN SSSR 1947), p. 535; * P. A. Rebinder and V. P. Likhtman, Proc. Acad. Sci. USSR 56, 723 (1947); 32, 2 (1941); V. I. Likhtman, P. A. Rebinder, and G. V. Karpenko, Influence of Surface-Active Media on Metal Deformation (Moscow-Leningrad, Izd. AN SSSR, 1954). *
- [3] G. F. Hüttig, H. Soles, and O. Stangeberger, Monats. Chem. 85, 3, (1954); M. L. Morgulis, Vibratory Grinding of Materials (Industrial Construction Press, 1957); * V. I. Akunov, Modern Vibratory Grinders Without Pebbles or Balls (Industrial Construction Press, 1957). *
- [4] L. Bergmann, Ultrasound and its Applications in Science and Technology (1956), p. 472 [Russian translation].
- [5] B. Claus, Z. techn. Phys. 16, 201, (1935); Kolloid. Beihefte, 45, 41 (1936).
- [6] H. Kuzel. Oest.**Pat. 2572/06; 2573/06 (1906); E. Wedekind, Z. anorgan. Chem. 45, 365 (1905).
- [7] E. M. Natanson, Mem. Inst. Chem. Acad. Sci. Ukrainian SSR 7, 314 (1940); Colloid J. 9, 191 (1947). Proc. 2nd All-Union Conf. Colloid Chem. (Acad. Sci. Ukrainian SSR Press, 1952), p. 113.*
- [8] N. N. Kozachek, Candidate's Dissertation, Inst. General and Inorganic Chem., Acad. Sci. Ukrainian SSR (1958).
- [9] E. M. Natanson, V. P. Chalyi, N. N. Kozachek, and A. P. Kaban. Colloid J. 19, 319 (1957); *** E. M. Natanson and N. N. Kozachek, Colloid J. 19, 698 (1957). ***
- [10] A. N. Frumkin, Electrocapillary Phenomena and Electrode Potentials (Odessa, 1919); * Ergebn. Exakt. Naturw. 7, 235 (1928); A. N. Frumkin, V. S. Bagotskii, A. V. Iofe and B. M. Kabanov. Kinetics of Electrode Processes (Izd. MGU, 1952). *
- [11] E. M. Natanson, Ukrain. Chem. J. 16, 508 (1950).
- [12] P. A. Rebinder and S. Ia. Veiler, Proc. Acad. Sci. USSR 31, 444 (1941); Ia. B. Aron and P. A. Rebinder, Proc. Acad. Sci. USSR 52, 235 (1946); A. S. Kolbanovskaya and P. A. Rebinder, Proc. Acad. Sci. USSR 49, 354 (1945); Colloid J. 12, 205 (1950).
- [13] E. M. Natanson, Proc. Acad. Sci. USSR 74, 517 (1950); E. M. Natanson and N. N. Kozachek, Ukrain. Chem. J. 20, 364 (1954); Colloid J. 18, 724 (1956). *
- [14] R. Simha, H. Frisch, and R. Eirich, J. Phys. Chem. 57, No. 6, 584 (1953).
- [15] W. Heller and T. Pugh, G. Chem. Phys. 22, No. 10, 1778 (1954); W. Heller and W. Tanaka, Phys. Rev., 82, 301 (1951).

*In Russian.

** Austrian

*** Original Russian pagination. See C.B. Translation.

PHYSICOCHEMICAL PRINCIPLES OF THE REGULATION OF MECHANICAL PROPERTIES OF THE STRUCTURES IN CLAY-WATER SYSTEMS

N. N. Serb-Serbina

The work of P. A. Rebinder and his associates [1] has shown that clay dispersions in water, with various clay contents (from highly concentrated clay pastes, made by the grinding of clays with the minimum amounts of water, down to dilute suspensions) form coagulation structures — spatial networks of varying strength. All the mechanical properties of these coagulation structures, and their thixotropy, i.e., the reversible breakdown of the structure and its gradual restoration, are determined by the fact that the clay particles are always separated by thin residual layers of the aqueous medium at the points of contact. The van der Waals forces of molecular attraction, greatly weakened by distance, act through these layers. These forces determine the strength of the coagulation structures, which is much less than the maximum strength attained at the same density (weight per unit volume) with direct cohesion of the particles at all the points of contact, as in the concretion of fine crystals in the formation of a crystallization structure when a new solid phase crystallizes from an undercooled melt or supersaturated solution. The residual aqueous layers at the points of contact between the particles forming a coagulation structure also serve as lubricating layers and thereby determines the relative mobility of the individual structural elements — the ability of the structure to withstand considerable residual deformations without loss of continuity and its plasticity and creep, even at very low shear stresses [2].

In addition to the plasticity and thixotropy, i.e., the reversible restoration after breakdown, of these coagulation structures, another remarkable feature is their peculiar high elasticity, similar to that found in flexible-chain polymers and their solutions. Such shear deformations, which develop slowly and slowly disappear after removal of the load, and which are reversible in magnitude, are characteristic not of the particles themselves, which are rigid microcrystals, but of the spatial network formed by them, with liquid interlayers at the points of contact. The kinetics of the elastic aftereffect, i.e., the development of retarded elastic deformation at constant shear stress and its decrease after removal of the stress, is represented in Fig. 1; it is seen that the equilibrium shear modulus is roughly $\frac{1}{2}$ of the nominal-instantaneous modulus.

The presence of the lubricating aqueous interlayers also accounts for the steady creep found by Abduragimova [2] in coagulation structures, of maximum thixotropic buildup, in dilute aqueous bentonite suspensions in the region of very low constant shear stresses; the flow is unaccompanied by any appreciable breakdown of the structure (see Curve 1, Fig. 2).

For example, in the case of a 10% suspension of Oglanli^{*} bentonite (with a small admixture of alkaline-earth carbonates), the maximum viscosity of the virtually intact structure ($\eta_m = 10^7$ poises) is 10^8 times the minimum viscosity of the structure at maximum breakdown ($\eta_m = 0.1$ poise). Therefore the stress region below the nominal flow limit (strength limit) is the region in which such a virtually intact structure behaves like an elastic solid. Over a relatively narrow stress range, near the flow limit, further increase of the shear stress or, what is the same thing, of rate of shear in steady flow, produces a sharp decrease of viscosity by 7-8 orders of magnitude, corresponding to sudden breakdown of the structure.

It has been shown by Gor'kova [3] that the ratio of the two constant viscosities $\eta_0 / \eta_m = \gamma$, i.e., the viscosity ratio of the virtually intact structure and the structure at maximum breakdown, together with the kinetic characteristics of thixotropic buildup (i.e., the variation of the limiting shear stress, regarded as the strength of the structure, with the time of its restoration), are adequate for the complete characterization of the stability of clays and soils to water and mechanical destruction.

*Transliteration of Russian — Publisher's note.

The strength of the coagulation structures formed in dilute suspensions is determined by the number of points of cohesive contact or by the number of free particles formed in the spontaneous dispersion of the clay, i.e., in the disruption of the larger particles in peptization by water. Moreover, the structural strength decreases

(for a constant number of contacts or constant contact area) with increasing thickness of the water interlayer, i.e., with increasing thickness of the diffuse layer of the ionic double layer. This is of particular significance in compact structures of pastes with high clay contents, where considerable contact areas arise at cleavage planes carrying exchange cations.

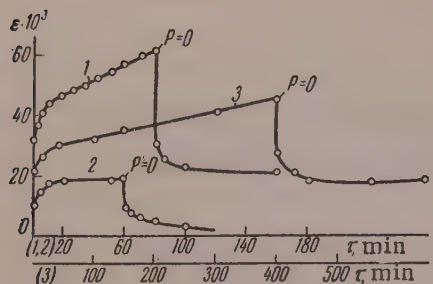


Fig. 1. Deformation kinetics of thixotropically reinforced aqueous suspensions of Oglanli bentonite (ϵ , τ) at constant load ($P = \text{const}$) and after removal of the load: 1) 10% natural bentonite, sample 1, at $P = 13$ dynes \cdot cm^{-2} ; 2) ditto, sample 2, at $P = 100$ dynes \cdot cm^{-2} ; 3) 45% Ca-bentonite at $P = 1080$ dynes \cdot cm^{-2} .

On the other hand, the main factor which determines the mechanical properties of the structure in dilute suspensions is the number of contacts per unit volume, n_1 (or per unit surface, $n_1^{\frac{1}{2}}$), as the nature of the contacts of the apex-apex, apex-edge, or edge-edge types may be independent, over a fairly wide range, of the composition of the cation-exchange complex, i.e., of the degree of hydration of the cleavage planes.

The maximum diffuse ionic layers, of the greatest thickness, are formed at the cleavage planes if all the cations are replaced by univalent cations (Na, Li), in absence of excess (especially multivalent) ions in the

aqueous medium. Such layers stabilize these surfaces, and prevent compact coagulation of the particles at them not only by mutual repulsion of similarly-charged counter ion atmospheres (the disjoining action of the ionic layers, in Derjaguin's terminology) but also because of the high hydrophily, i.e., very low surface tension at the external surface of the clay particle lyospheres (in this instance the two effects are intimately associated). However, as the clay content increases (with increase of the density of the structure) and the surfaces approach closer together, coagulative cohesion begins, with formation of a residual quasi-equilibrium interlayer; as this becomes thinner, the strength and density of the structure in the mass continuously increases. The plastic and high-elastic properties of such pastes still remain pronounced, and disappear only after complete drying, when (as in I. M. Gor'kova's experiments) the compact structure is no longer coagulatory and acquires a condensational character, approaching crystallization structures. This means that direct contact is established between the parti-

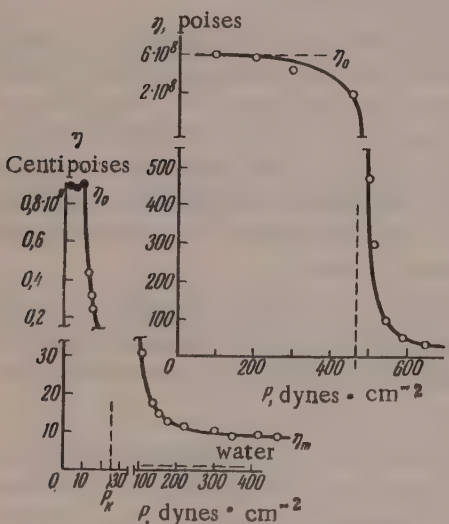


Fig. 2. Viscosity of 10% (in centipoises, below) and 20% (in poises, above) aqueous suspensions of Oglanli bentonite as a function of the shear stress (η , P).

cles over quite considerable regions of the surface; this corresponds to maximum strength and brittle destruction.

The interaction between water and the solid phase in clay-water systems is extremely important. Various contradictory views exist on this object. In relativity, the bound water (apart from water of constitution, bound

in the crystal lattice), is the absorbed water of the first monomolecular layer; this has been evaluated correctly from the heats of wetting by Ovcharenko [4]. In general, the only true criterion of the bound state of water is the value of the free binding energy. The water of the diffuse double ionic layers, which forms the so-called hydration hull, is very weakly bound or virtually free. Water immobilized in the coagulation structure is also free, although it is displaced with difficulty because of the high dispersity of such structures. In hydrophobic suspensions in which coagulation is compact, with formation of large aggregates which do not give rise to thixotropic structures, the amount of immobilized water is relatively small. With more hydrophilic disperse phases, which include clays, especially of the montmorillonite type, it increases as shown schematically in Fig. 3, because of the abrupt increase of the number of particles in the transition from compact coagulation to the continuous coagulation structure of a gel. It is known [4] that Ca-bentonites bind water more strongly than Na-bentonites, being more hydrophilic, as shown by the magnitude of the binding energy, i.e., by the heats of wetting. However, their diffuse double layers are not as thick as in Na-bentonites, and therefore peptization of their particles does not occur and they undergo compact coagulation through very thin water interlayers. This means that in this case also, all the available clay surface interacts with water, but this interaction is not accompanied by liberation of the particles and a consequent increase of their number per unit volume, as is the case with Na-bentonite. In this last instance, the particles are bound together much more weakly at the points of contact, and are linked by their corners and edges and not by planes covered with cations, but their number, and therefore the number of contact points, is considerably larger. At the limit, when the exchange ions have been completely replaced by Na, the diffuse ionic layers are so extensively developed that the peptization of the particles, and their stabilization in dilute suspensions, are complete, i.e., the strength of the structure in such suspensions falls to zero, and the thixotropic properties of the system become weak (Fig. 4). Such a suspension of Na-bentonite becomes, instead of a solidlike structurized system, a highly viscous, almost structureless liquid, the viscosity of which is much higher than that of water because of the considerable filling of the volume (by the Einstein theory) with a large number of free particles surrounded by extensive ionic layers or hydration hulls.

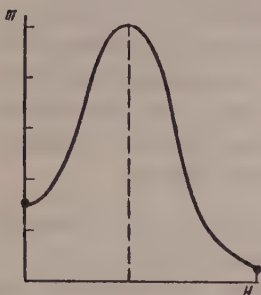


Fig. 3. Relationship between the amount of immobilized water (m) in aqueous highly disperse clay suspensions, and the molecular nature of their particles (H is an arbitrary measure of hydrophilicity).

Li-bentonite is even more hydrophilic than Na-bentonite, and resembles Ca-bentonite because of the high hydration of the Li ions. However, as these ions are univalent, the diffuse layers on the surface of Li-bentonite particles are as extensive as in Na-bentonite; this leads to total peptization and coagulation-structure formation in dilute suspensions at intermediate degrees of substitution. In concentrated suspensions or pastes, however, complete substitution by Li or Na does not prevent the formation of strong structures, such as are formed, for example, in gradual and regular evaporation of water; i.e., it does not prevent a decrease in the thickness of the layers at all points of contact between the particles. On the contrary, the structures so formed are the strongest because of the maximum cohesion at the greatest proximity of the particles, i.e., at the highest packing density. However, these strong structures are completely devoid of resistance to water, and are readily broken down when soaked.

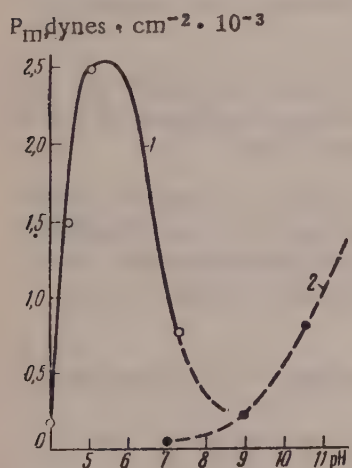


Fig. 4. Structural strength (limiting shear stress, P_m) of bentonite suspensions as a function of pH: 1) 10% electrodialyzed Oglanli bentonite with addition of 15, 30, and 60 meq of NaOH; 2) 4% Na-bentonite (from askangel) at equilibrium pH in presence of NaOH at various concentrations.

By control of peptization (dispersion) and coagulative cohesion, which may be effected by addition of electrolytes, surface-active substances, and protective colloids of various kinds in order to vary the interaction between water and clay, it is possible to regulate, in wide limits, the structure and mechanical properties of soils and disintegrated clays; their compaction may be facilitated by various mechanical influences, especially vibration, and they can be reinforced by the formation of crystallization structures on addition of the appropriate reagents or by means of electrolysis.

As an example of such modification of the strength properties of clay pastes and suspensions, we may quote the results obtained by Chiang Lung in our laboratory, in a study of the effects of humus substances and electrolytes on these systems. He studied the variations of structural strength and the invariant characteristics of the structure as a function of the concentration of humates from brown coal in alkaline coal reagent (ACR) relative to the amount of solid phase, and established the existence of three qualitatively distinct regions: I, the region of slight strength decrease, when the concentration of Na humates does not exceed 0.01-1% relative to the solid phase; II, the strengthening region with a sharp maximum in the range of Na humate concentrations from 2 to 6%; and III, the region of a sharp decrease of strength when the Na humate concentration exceeds 9%. The probable explanation of this result is that at low concentrations of Na humates, far from saturation of the adsorption layer, the humates exert a flocculant effect and decrease somewhat the strength of the coagulation structure; at higher concentrations the strength and viscosity of the coagulation structure increase owing to the stabilizing action of the micellar adsorption layer of humate, in which part of the Na^+ is exchanged for Ca^{++} from the bentonite exchange complex, so that the surface layer is in the nature of a mosaic. At high concentrations of Na humates, the bentonite is peptized and stabilized, and at the same time their particles themselves assist the development of a coagulation humate structure which develops in the dispersion medium.

The rheological characteristics of these systems change accordingly. The thixotropically reinforced systems in the first two regions exhibit the highest creep viscosity, of the order of 10^{11} poises and over, over a very considerable range of shear stresses. In the third region, at high ACR concentrations, the rheological curve changes sharply, and reveals structural breakdown with a decrease of the effective viscosity from 10^{10} to 10^5 poises and less, over a narrow range of relatively low shear stresses. In this case the elasticity of the system [2] increases from 0.4-0.5 to 0.7 at sufficiently high absolute values of the shear modulus.

SUMMARY

1. Aqueous dispersions (pastes and suspensions) of clay form coagulation network structures varying in strength according to the number of free particles per unit volume and the cohesion of the particles through residual thin layers of the aqueous phase. These structures, in addition to their plasticity and thixotropy, have well-defined retarded elasticity — peculiar high-elastic properties characteristic of the spatial coagulation network rather than of the clay particles themselves.

2. The presence of thin aqueous interlayers at the points of contact between the clay particles also determines the steady-state creep of these systems, virtually unaccompanied by residual breakdown of the structure in the region of relatively low shear stresses. The maximum viscosity of the virtually intact structure is 5-9 orders of magnitude greater than the effective viscosity when the structure is broken down to the limit at sufficiently high shear stresses (velocity gradients).

3. The effect of the composition of the exchange complex on the strength characteristics of the structures has been demonstrated in the case of bentonite suspensions. It was found that the strength maximum for Oglanli bentonite suspensions lies in the range of 50-75% substitution of the exchange cations by Na^+ .

4. The structuromechanical properties of clay suspensions can be regulated within wide limits by control of peptization, spontaneous dispersion, and coagulative cohesion by the introduction of various electrolytes, surface-active substances, or protective colloids. For example, by variations of the amount of sodium humate (ACR) added, it is possible to effect either liquefaction or fairly effective reinforcement of structure in clay dispersions in water.

I offer my deep gratitude to P. A. Rebinder for his general guidance of these researches for many years.

Institute of Physical Chemistry, Academy of Sciences USSR
Division of Disperse Systems
Moscow

Received June 20, 1958

LITERATURE CITED

- [1] P. A. Rebinder, in the symposium: Viscosity of Liquids and Colloidal Solutions, I (Izd. AN SSSR, 1941), p. 361; *N. N. Serb-Serbina, ibid, p. 361; P. A. Rebinder, Colloid J. 9, No. 5 (1947); P. A. Rebinder, in the symposium: Physicochemical Methods for the Investigation of Surface Phenomena (Izd. AN SSSR, 1950), p. 5; *N. N. Serb-Serbina and T. M. Plonskii, Proc. Acad. Sci. USSR 96, No. 1 (1954).

*In Russian.

[2] P. Rehbinder, Disc. Faraday Soc. 18, 151 (1954); A. A. Abduragimova, P. A. Rebinder, and N. N. Serb-Serbina, Colloid J. 17, No. 3, 184 (1955); *P. A. Rebinder, Proc. 3rd All-Union Conf. on Colloid Chem. (Izd. AN SSSR, 1956) p. 7; **E. M. Kobakhidze, M. E. Shishniashvili and N. N. Serb-Serbina, Colloid J. 19, No. 3 (1957).**

[3] I. M. Gor'kova, Proc. Conf. on Engineering and Geological Properties of Rocks and Methods of their Investigation (Izd. AN SSSR, 1958), p. 115.**

[4] F. D. Ovcharenko, The Geology, Mineralogy, and Utilization of Clays in the USSR (Izd. AN SSSR, 1958), p. 115.**

*Original Russian pagination. See C.B. Translation.
**In Russian.

RHEOLOGICAL INVESTIGATION OF STRUCTURIZED SUSPENSIONS OF
ASKANGEL AND SOME OF ITS DERIVATIVES

O. M. Mdivnishvili and G. V. Vinogradov

During the past 10 or 15 years P. A. Rebinder, K. F. Zhigach, and their associates [1-3] have carried out extensive investigations on clay suspensions and pastes, and have elucidated many important characteristics of their mechanical properties. However, up to the present not enough attention has been paid to the influence of the nature of the cations present in the exchange complex of clay minerals of the montomorillonite type on the mechanical properties of their suspensions and pastes, or to the distinction between this question and the question of the coagulant action of added electrolytes. Comparisons of the properties of systems broken down to their limits and of systems of the same nature, but with a strongly developed structure, should also prove informative. An allied problem is determination of the thickening action of the disperse phase at different concentrations in relation to difference in the nature of the exchange cations, etc., apart from the influence of anomalous viscosity. It is of great interest to correlate the thixotropic properties of such systems with their strength characteristics, especially as in such investigations it is possible to approach the problem with the aid of methods developed recently by Soviet investigators for systems of a different type.

The experiments here described were performed at room temperature in a rotational elastoviscosimeter with concentric cylinders, at stress heterogeneity of $\sim 10\%$. The instrument used was the type described previously [4]. The rates of load were in the range of $3.9 \times 10^{-5} - 7.0 \times 10^{-3} \text{ g} \cdot \text{cm}^{-2} \cdot \text{second}^{-1}$.

The materials studied were aqueous suspensions and pastes of askangel, and aqueous systems prepared from askangel, by the Gedroits method, by the treatment of monosubstituted Na-, Ca-, and Al-bentonites and of mixed Na-, Ca-bentonites with NaCl, CaCl₂, and AlCl₃ solutions. Suspensions of all these derivatives were made from askangel suspensions which did not pass through the stage of total drying. This resulted in better peptization of the specimens. Details of the exchange complex of askangel and its monosubstituted derivatives are given in the table.

Composition of Bentonite Exchange Complexes *

Specimen	Total ex-change capacity	Composition of exchange complex					Soluble salts			
		Na ⁺	Ca ⁺⁺	Mg ⁺⁺	Al ⁺⁺⁺	H ⁺	Na ⁺	Ca ⁺⁺	Mg ⁺⁺	H ⁺
Askangel	82	47	28	7	—	—	26	3	—	—
Na-bentonite	82	77	5	—	—	—	—	—	—	—
Ca-bentonite	82	8	74	—	—	—	—	—	—	—
Al-bentonite	82	—	5	—	70	8	—	—	—	19

The yield values (τ_m) of the systems were determined as the maximum values of the shear stress (τ) on $\tau - \gamma$ curves, determined after prolonged breakdown of the systems at high velocity gradients (D), when the minimum viscosity of the structures broken down to the limit (η_{min}) is reached, and also after prolonged rest of such structures.

*All numerical values are given in meq per 100 g of bentonite.

In contrast to the $\tau - \gamma$ curves for askangel pastes and suspensions of the type well-known in the literature, in the case of Na-bentonite the values of τ_m are found to be close to the equilibrium shear stresses (τ_e) reached at high values of γ in experiments on the determination of $\tau - \gamma$ curves at continuously increasing shear stresses [5]. The $\tau - \gamma$ curves in Fig. 1, for specimens not previously tested and kept for a long time at rest before the experiments, show that as the concentration (c) of the bentonite increases, the monotonic curves pass into smooth curves with distinct maxima (at $c = 8\%$), while at still higher concentrations ($c > 10\%$) the curves have breaks which mark the boundary between the region of elastic deformation and the regions of structural breakdown and viscous flow.

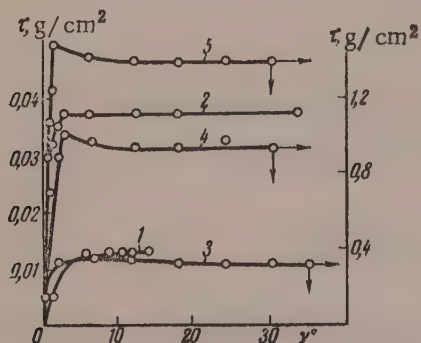


Fig. 1. Shear stress-deformation curves for Na-bentonite suspensions: contents of Na-bentonite: 1) 4%; 2) 6%; 3) 8%; 4) 10%; 5) 11.5%.

which were hitherto kinetically independent, form aggregates (which we shall term secondary particles); these, in their turn, interact and participate in the formation of a three-dimensional structure in the disperse system. It may be assumed that the average bond strength between the aggregates may be less than their own structural strength. The shear strength of the system should decrease with increasing compactness of the structure of the secondary particles and with decrease of their concentration in the system (for a given weight concentration of the disperse phase). The shear strength of coagulation structures should increase with increasing concentration of the primary particles and the extent of their aggregation. At the same time, the greater the spatial homogeneity of the bonds between these particles, the higher this strength should be. The greatest shear strength should be found in coagulation structures with the least variations between the packing density of the primary particles in the individual aggregates and the aggregates in the three-dimensional structural network embracing the whole system. Thus, in Na-bentonite, with a low content of Ca ions in the exchange complex, τ_m increases particularly rapidly with increasing concentration of the disperse phase, as the condition of maximum spatial homogeneity of the structure should be satisfied in this case. In contrast, Ca- and Al-bentonite pastes and suspensions are coagulation structures in which the density of the primary-particles aggregates is high, i.e., the number of secondary particles per unit volume is relatively low, and the bonds between them are therefore easily broken by small shear stresses. Ca- and Al-bentonite pastes, not previously subjected to mechanical breakdown, give $\tau - \gamma$ curves with relatively weak maxima or inflection points similar to those in Fig. 1 for concentrated aqueous Na-bentonite pastes.

The foregoing accounts for the peculiarities on the shear strength-concentration curves in Fig. 2. Here Fig. 2, a refers to systems after prolonged rest and not tested previously; Fig. 2,b represents systems tested immediately after maximum breakdown.

In the studies of thixotropic structure formation in aqueous suspensions and pastes of bentonites, the systems were previously broken down to the limit in a uniform stress field in a rotational viscosimeter. This results in strictly uniform mechanical treatment of all the systems, which cannot be achieved with such preparation methods, commonly used, as grinding, stirring, etc., followed by charging of the system into the apparatus. After maximum breakdown, the values of τ_m were determined as a function of time. Systems containing askangel and Na-bentonite showed rapid restoration of structure. In relatively dilute pastes of Ca- and Al-bentonites (containing about 8% of the solid phase), maximum breakdown was followed by appreciable decrease of τ_m , because of settling of the disperse-phase particles. In more highly concentrated Ca-bentonite pastes, the shear strength did not change with time. Concentrated Al-bentonite pastes showed some increase of τ_m with time. However, the substitution of the exchange ions by Al ions in Al-bentonite is incomplete, and it is not quite free from hydrogen ions (see table).

At low concentrations, aqueous Na-bentonite systems are fairly well-peptized systems with low τ_m . Much higher strength at low concentrations is found for suspensions of native askangel, which has a considerable content of calcium ions (over 40%) in its exchange complex, and a certain amount of electrolyte in the dispersion medium, causing partial coagulation in the system.

When coagulation occurs, the primary particles,

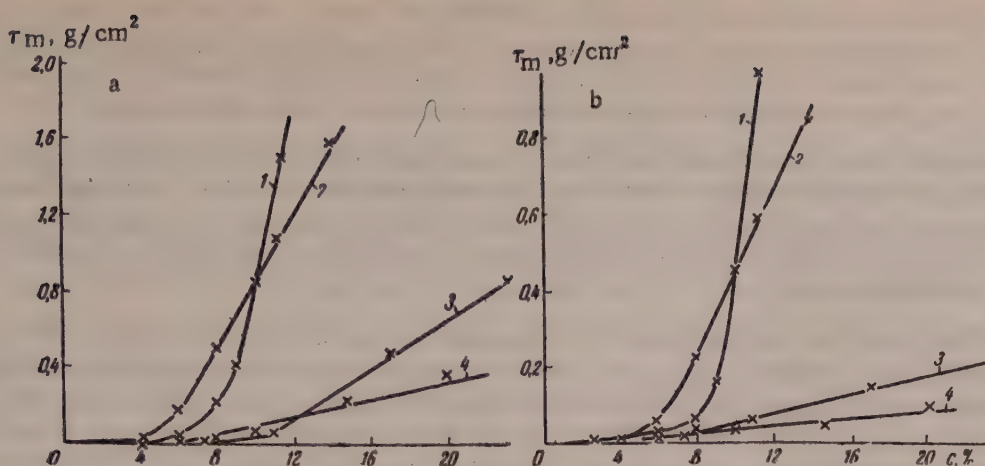


Fig. 2. Effect of concentration of yield value: a) suspensions of askangel and its monosubstituted derivatives, left at rest for a long time after preparation; b) suspensions of askangel and its monosubstituted derivatives, after maximum breakdown; 1) Na-bentonite; 2) askangel; 3) Ca-bentonite; 4) Al-bentonite.

In connection with the influence of the nature of the ions in the exchange complex on the mechanical properties of bentonite pastes and suspensions, the relationship between these properties and the ratio of the amounts of Na and Ca ions in the exchange complex is of interest. Typical results for 8% bentonite suspension are given in Fig. 3. Here the composition of the exchange complex is taken along the abscissa axis, while the ordinates of the left give values of τ_m , τ_e , and τ_{res} (residual shear stress). The ordinates on the right correspond to values of $\Delta\tau = \tau_{24} - \tau_0$, where τ_{24} is the shear strength of the systems determined 24 hours after maximum breakdown. The values of $\Delta\tau$ represent the tendency of the systems to thixotropic restoration. The divergence of the maxima on the $\Delta\tau$ -concentration curves from the maxima on the curves for τ_m , τ_e , and τ_{res}

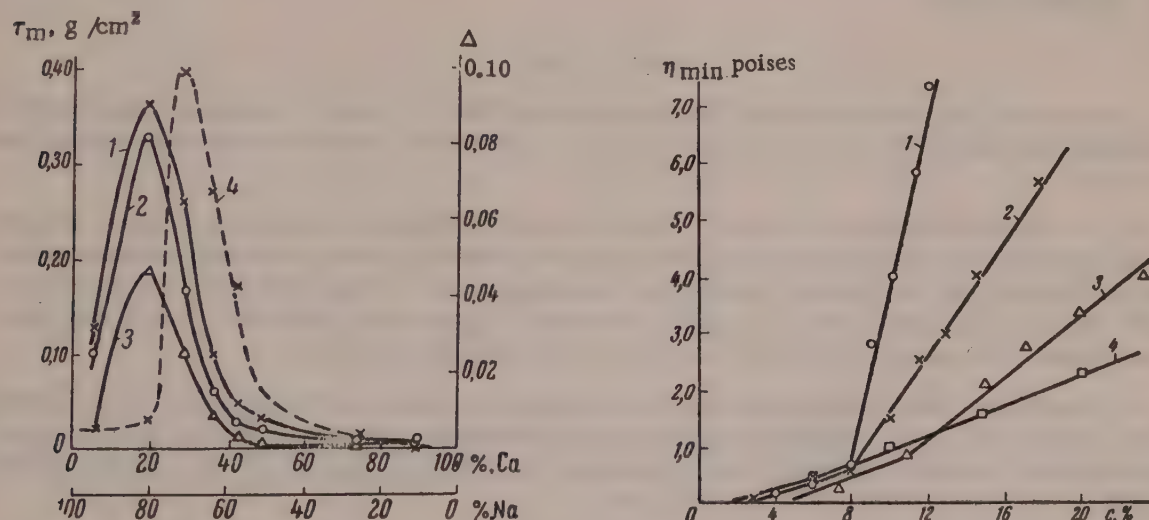


Fig. 3. Variations of yield value (1), equilibrium shear stress (2), residual shear stress (3), and 24-hour increase of yield value in structures after maximum breakdown (4) with the Na-Ca ion ratio in 8% bentonite suspension.

correspond to maximum structure formation, which hinders the thixotropic restoration of the systems. At the same time, it is clear from Fig. 3 that in the region of maximum values of τ_m and τ_e their difference is least; the difference increases with increase of c , reaches a maximum, then decreases again. It is easy to show from the data in Fig. 3 that the maximum values of $\Delta\tau$ and $\tau_m - \tau_e$ correspond to the same region of

Fig. 4. Effect of concentration on the viscosity of systems after maximum breakdown: 1) Na-bentonite; 2) askangel; 3) Ca-bentonite; 4) Al-bentonite.

as functions of concentration is due to the fact that the highest structural strengths under these conditions

the Na-Ca ion ratio in the exchange complex. This is in agreement with Trapeznikov's [6] views in relation to fluid systems (in the usual terminology for non-Newtonian liquids); namely, that the value of $\tau_m - \tau_e$, which determines the breakdown of the systems in the course of deformation under continuously increasing shear stress, also characterizes the tendency of these systems to thixotropic transformations. Hence the results of the present investigation can be used to extend Trapeznikov's views to plastic disperse systems.

In studies of the viscous properties of these systems, the variation of the effective viscosity (η_{eff}) with D was first determined, and the ascending branch of the viscosity curve was thus found; D was then decreased and the descending branch of the viscosity curve was obtained. It was found that in test under conditions of nearly uniform stress at all the above concentrations, maximum breakdown and hence η_{min} are reached at D of the order of 200-300 seconds⁻¹.

For dilute askangel systems, the ascending and descending branches of the $\eta_{eff} - D$ curves coincide. As the concentration increases, hysteresis loops appear, due to the fact that restoration of structure is more difficult at high concentrations of the disperse phase, and therefore at high viscosities. In Na-bentonites hysteresis effects are found at low concentrations, while the ascending and descending branches of the $\eta_{eff} - D$ curves tend to coincide at higher concentrations. These viscosity characteristics of Na bentonites are the consequence of the relatively low rate of structure formation in dilute systems. The most pronounced hysteresis loops are found for concentrated Ca- and Al-bentonite pastes.

The $\eta_{min} - c$ relationships for different systems are plotted in Fig. 4 in the form of broken straight lines. The breaks correspond to the critical concentrations at which η_{min} begins to depend to a much greater extent on c ; this occurs when the relative volume filled by the particles of the disperse phase is such that the particles can remain in continuous contact in a flowing system after maximum breakdown.

Comparison of the $\eta_{min} - c$ and $\tau_m - c$ curves leads to the important conclusion that there is a qualitative correspondence between the structure-formation conditions and the strength and viscosity properties respectively. This is particularly noteworthy because the shear strength limits are close to the characteristics of structure formation in static conditions, whereas the viscosity of a structure after maximum breakdown is its typical dynamic characteristic. This leads to the interesting possibility that the structure-forming tendency of the disperse phase in a clay suspension can be evaluated from the Newtonian viscosity determined at sufficiently high deformation rates.

SUMMARY

1. Suspensions and pastes of askangel, its monosubstituted Na-, Ca-, and Al-derivatives, and mixed Na-, Ca-bentonites were studied at room temperature by means of a rotational elastoviscoimeter in a uniform shear stress field.
2. The shear stress-deformation curves for these systems exhibit some characteristic features. The most pronounced maxima, and the greatest differences between the yield values and equilibrium shear stresses corresponding to steady flow, are found for askangel and disubstituted Na-, Ca-bentonites with Na and Ca ions in 4:1 ratio. When concentrated pastes of Ca- and Al-bentonites, not previously subjected to mechanical breakdown, are deformed to maximum breakdown, the yield values decrease irreversibly.
3. The greatest power of thixotropic restoration in bentonites containing Ca and Na ions in the exchange complex is found at a degree of coagulation higher than that corresponding to their maximum shear strength. For plastic disperse systems this greatest power of thixotropic restoration corresponds to the maximum difference between the yield value and the equilibrium shear stress.
4. Maximum breakdown in flow is readily attained in all the systems studied. The viscosity-concentration relationships for systems after maximum breakdown are represented by intersecting straight lines. The points of intersection evidently correspond to critical concentrations of the disperse phase above which the particles are in continuous contact.
5. A qualitative correlation has been established between the strength properties of systems after prolonged rest and their viscosity properties after maximum breakdown.

LITERATURE CITED

- [1] P. A. Rebinder, in the symposium; Viscosity of Liquids and Colloidal Solutions, 1 (1941) p. 361.*
- [2] N. N. Serb-Serbina and P. A. Rebinder, Colloid J. 9, 381 (1947).
- [3] P.A. Rebinder, Disc. Faraday. Soc. No. 18, 151 (1954); Proc. 3rd All-Union Conf. on Colloid Chemistry (Izd. AN SSSR, 1956), p. 7; *L. A. Abduragimova, P. A. Rebinder, and N. N. Serb-Serbina, Colloid J. 17, 3 (1955). **
- [4] G. V. Vinogradov, V. G. Lebedev, and V. A. Protod'iakonov, Colloid J. 18, 633 (1956). **
- [5] K. I. Klimov, Dissertation: Elasticoplastic Properties of Greases (Moscow, 1950). *
- [6] A. A. Trapeznikov and V. A. Fedotova, Proc. 3rd All-Union Conf. on Colloid Chemistry (Izd. AN SSSR, 1956), p. 65. *

*In Russian.

**Original Russian pagination. See C.B. Translation.

PHYSICOCHEMICAL MECHANICS OF DISPERSE SYSTEMS IN CERAMIC TECHNOLOGY*

S. P. Nichiporenko

Hitherto, it has not been possible to evaluate the suitability of ceramic bodies - concentrated dispersions of clays in water - for plastic handling and forming, to determine the optimum process parameters and the quality of the treatment, and hence to select the appropriate processing and forming equipment and to design the production line on a rational basis.

However, the fundamental principles of physicochemical mechanics of disperse systems, developed by Rebinder and his school [1-14], can be successfully applied to the development of a theoretical basis for the plastic processing and forming of ceramic bodies.

According to Rebinder's concepts, the technological properties of structurized dispersion, which include ceramic bodies, are primarily characterized by their structuromechanical properties; their capacity to exhibit both retarded-elastic (high-elastic) deformations, reversible in magnitude, which have been discovered in such systems by the Rebinder school [4, 11], and also residual deformations. The strength and elasticoviscous properties of ceramic bodies determine the nature of the deformation and breakdown processes which occur in these disperse structures.

These concepts, and some very effective investigation methods, have provided the basis for a study of the structuromechanical properties of ceramic bodies over a wide range of shear stresses, carried out in order to establish the theoretical principles of the plastic processing and forming of ceramic bodies.

Plastic strength of ceramic bodies. Determinations of plastic strength by the cone-plastometer method [5, 6] showed that when a cone is immersed in a ceramic mass, the mass undergoes plastic flow, and that constant values are obtained in determinations of yield values with cones of vertical angles 30 to 60°, over a wide range of loads.

Investigations of the relationship between yield value and the moisture content of ceramic bodies (Fig. 1) provided the basis for a method of determination of the principal parameters of the forming process - the optimum moisture content and its permissible limits [15, 16].

In this method, the optimum moisture content is determined by average pressure (2 kg/cm^2) exerted on the mass in the band press [17], and is calculated directly from the yield value-moisture content ($P_m - C$) graph. The permissible limits of moisture content are found from the slope of the $P_m - C$ curves on the assumption that the pressure may vary in the range of $1.5-2.5 \text{ kg/cm}^2$.

The optimum moisture contents and their permissible limits are given in Table 1. The minimum value of the permissible variation limits is 2%.

Determination of the yield value P_m by the cone plastometer is 5-10 times as sensitive as other methods. This made it possible to use determinations of the yield value P_m for evaluation of the quality of body treatment and of the performance of the equipment [15, 16]. The methods of mathematical statistics were used to evaluate the performance of each machine in the production line, and of the line as a whole, from the consecutive changes in the homogeneity of the body in its passage through the machine.

*Paper at the 4th All-Union Conference on Colloid Chemistry in Tbilisi, May 1958.

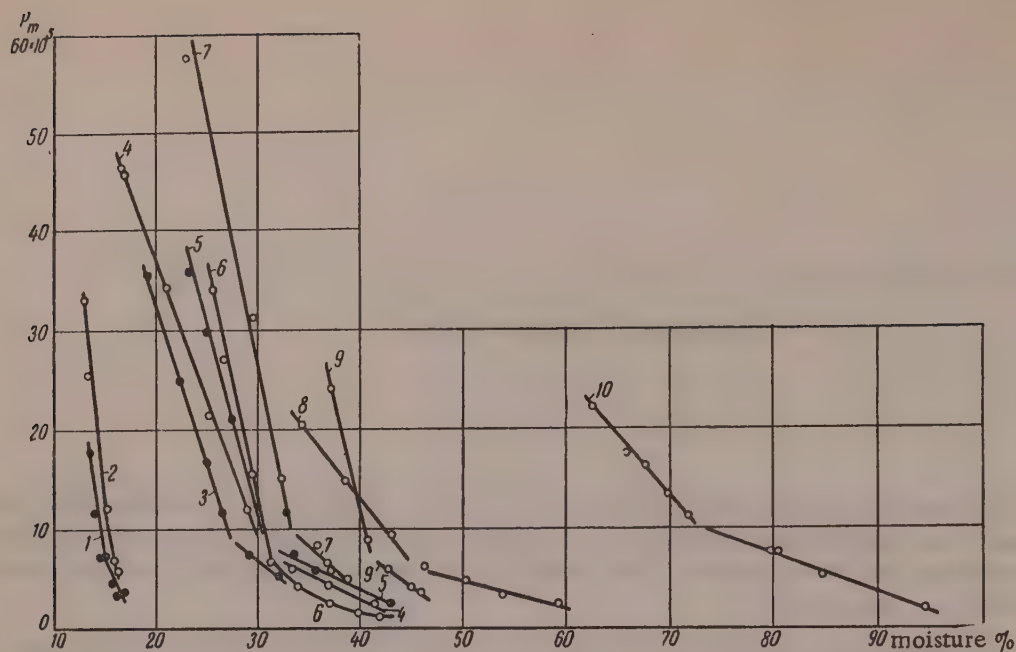


Fig. 1. Variations of yield value P_m with moisture content for bodies made from: 1) Novomaiachka loam; 2) Golaia Pristan* loess; 3) Frunze clay; 4) Novomaiachka clay; 5) Nikiforovo clay; 6) Kiev loam; 7) Kiev spondylic* clay; 8) Chasov Iar clay; 9) Glukhov kaolin; 10) Pyzhev bentonite.

Analysis of the results led to the following conclusions.

The principle on which the production line operates, with simultaneous processing of a restricted volume of material under conditions of considerable fluctuations in the composition of the initial charge and the moisture content, makes complete homogenization of the finished body impossible. As a result, the optimum conditions for drying and firing of the ware cannot be established and the quality of the production from brick works is characteristically uneven.

TABLE 1

Optimum Forming Moisture and Permissible Moisture Limits for Ceramic Bodies

Clays	Optimum moisture content, %	Permissible moisture fluctuations, $\pm \Delta\%$	Clays	Optimum moisture content, %	Permissible moisture fluctuations, $\pm \Delta\%$
Novomaiachka loam	13	0,8	Nikiforovo clay	29	1,6
Golaia Pristan* loess	14	0,5	Kiev loam	29	0,9
	24	1,5	Kiev spondylic clay	31	1,1
Novomaiachka clay	26	1,7	Chasov Iar clay	35	3,8
			Glukhov kaolin	38	1,1
			Pyzhev bentonite	64	4,8

A decisive improvement in the quality of the product can be achieved by preliminary equalization of the charge composition and by the creation of reserves which would make it possible to operate with a charge of constant composition for considerable periods.

*Not translator verified.

The production lines in operation in the Kiev brick works are not the best possible. In some cases certain individual machines, such as crushers and fine grinders, are ineffective and do not increase the homogeneity of the body. The position of the blade mixers in which the mass is humidified immediately before the band press is unsatisfactory. It eliminates all the preceding units from the processing cycle. Because of the absence of kneading machines, the main burden of the treatment is borne by the band press, the proper function of which is forming of the ware. We have recommended the following procedure for the Kiev brick works: feed → fine grinding → two-rollblade mixer with steam humidification → pug mill → fine-grinding roll-mill band press.

The yield value, determined by the cone plastometer method, considered as the principal characteristic of plastic strength, provides an explanation of the processes occurring in the body during manipulation, makes it possible to determine the optimum moisture content and its permissible fluctuation limits by a laboratory method and to investigate the performance of operating units and production lines, and can be used as an experimental basis for the planning of new production lines in relation to the structuromechanical properties of the bodies.

Investigations of plastic working and forming of ceramic bodies based on determinations of the yield value P_m by means of the cone plastometer have been carried out extensively by L. K. Petrov (Belorussian Institute of Constructional Materials, Minsk) and by M. G. Lundina and L. L. Koshliak (Scientific Research Institute of Construction Ceramics, Moscow).

Elasticoplasticoviscous properties of intact structures in ceramic bodies. A parallel-plate instrument of the Tolstoi [18, 19] type was used for investigations of the elasticoplasticoviscous properties of intact structures in ceramic bodies. The investigations showed (Fig. 2) that the form of the deformation-time ($\epsilon - \tau$) curves at constant load P , qualitatively corresponds to the Maxwell-Shvedov-Kelvin mechanical model; as was shown by Rebinder and Segalova [3], this function can be represented by the equation:

$$\epsilon' = \frac{P}{E_1} + \frac{P - P_{k1}}{\eta_1^*} \tau + \frac{P}{E_2} \left(1 - e^{-\frac{\tau E_2}{\eta_2}} \right) \quad (1)$$

According to Equation (1), the behavior of the mass under a load which causes virtually no structural breakdown can be characterized by five independent constants, determined from the $\epsilon - \tau$ curves: the initial (nominal-instantaneous) elastic shear modulus E_1 ; the elasticity modulus E_2 ; the maximum plastic (Shvedov) viscosity η_1^* ; the elastic aftereffect viscosity η_2 ; and the nominal static flow limit P_{k1} . These values are invariant in the stress region where there is no structural breakdown. Their interrelationships may be represented in the form of the following three fundamental characteristics: elasticity λ , Volarovich plasticity P_{k1}/η_1^* , and true relaxation time θ_1 .

Investigations of the structuromechanical properties of ceramic bodies which exhibit different behavior during plastic working and molding made it possible to establish the relationships between their behavior and the fundamental characteristics: elasticity λ , plasticity P_{k1}/η_1 , and true relaxation time θ_1 [20-23].

Table 2 gives the fundamental characteristics and the nominal specific deformation power $N_{\epsilon \cdot \text{nom}}$ for nine clays. ($N_{\epsilon \cdot \text{nom}}$ is the power required for deformation of 1 cc of the body at a rate of $0.001 \text{ second}^{-1}$).

Semiproduction trials of clays, carried out at the Kiev Experimental Works, and trials carried out in 1951 at the Institute of Constructional Materials of the Academy of Building and Architecture of the Ukrainian SSR showed that Glukhov kaolin and Kiev loess give rise to lean bodies, of poor cohesion and bad formability; bodies made from Zolochev loess and Vinogradov clay form well and show no streakiness; bodies from Frunze clay and Pavlograd loam have good cohesion, are difficult to form, and have a tendency to streakiness; Novomaiachka, Chasov Jar, and Druzhkovka clays give bodies with good forming properties but with a pronounced tendency to streakiness.

Comparison of the process behavior of the clays with the data in Table 2 leads to the following conclusions.

Clays with good forming properties, without a tendency to streakiness, have the following fundamental characteristics: elasticity λ not less than 0.6-0.65, plasticity P_{k1}/η_1 not less than $2.0-2.5 \cdot 10^{-6} \text{ second}^{-1}$, and relaxation time θ_1 not less than 300-350 seconds.

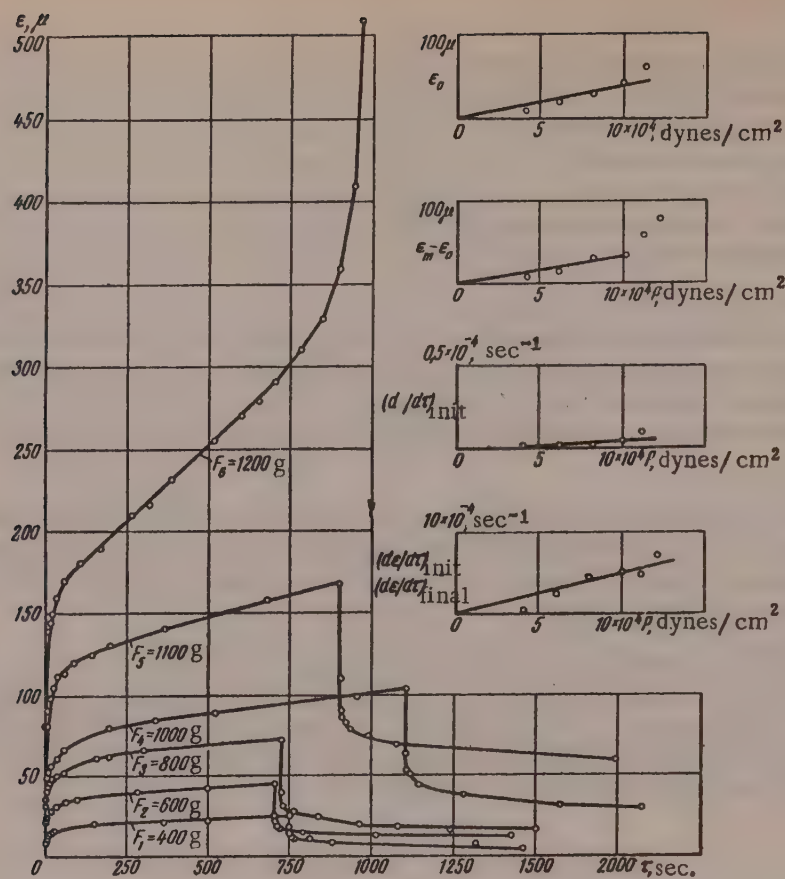


Fig. 2. Deformation-time ($\epsilon - \tau$) curves under constant load for Pyzhev bentonite with 82.6% moisture content.

TABLE 2

Fundamental Characteristics, Nominal Deformation Power, and Types of Ceramics Bodies

Clays	Elasticity $= \frac{E_1}{E_1 + E_2}$	Plasticity $P_{k1}/\eta_1 \cdot 10^6$, sec ⁻¹	True relax- ation time θ_1 , seconds	Nominal specific de- formation power $N \times 10^{-5}$ erg. sec ⁻¹	Type of body
Glukhov kaolin	0,67	1,43	1120	13,9	
Kiev loess	0,65	1,46	960	18,4	I
Zolochev loess	0,68	2,19	780	34,9	
Vinogradov clay	0,73	2,24	391	118	II
Frunze clay	0,37	2,39	360	141	
Pavlograd loam	0,37	2,71	252	151	III
Novomaiachka clay	0,43	7,22	101	68,5	
Chasov Iar clay	0,47	9,20	208	41,1	IV
Druzhkovka clay	0,40	13,7	298	30,6	

Clays of the Kiev loess and Glukhov kaolin type yield elastic bodies, with a long relaxation time, but of low plasticity and low nominal deformation power.

Bodies from clays of the Frunze and Pavlograd type have normal plasticity, low elasticity, sometimes a somewhat shorter relaxation time, and the highest nominal deformation power.

Chasov Iar, Druzhkovka, and Novomaiachka clays form highly plastic bodies of low elasticity, short relaxation times, and moderate nominal deformation power.

Thus, ceramic bodies can be classified in four types according to the fundamental characteristics of their structuromechanical properties (Table 2): I) low plasticity (Glukhov kaolin, Kiev loess), II) good formability (Zolochev loess, Vinogradov clay), III) low elasticity (Frunze clay, Pavlograd loam), and IV) low elasticity and short relaxation time (Chasov Iar, Druzhkovka, and Novomaiachka clays).

The data in Table 2 also provide an explanation of the physical significance of the molding properties of ceramic bodies.

We compared the values of relative deformation, calculated from the equation for the Maxwell-Shvedov and Kelvin models [3] for shear stress $P_m = 20 \cdot 10^5$ dynes/cm² and deformation time $\tau = 1000$ seconds.

In this time, in addition to the elastic instantaneous deformation ϵ_0 , the elastic deformation ϵ_2 and a definite plastic deformation $\epsilon_1\tau$ also develop.

In the case of Glukhov kaolin and Kiev loess (Type 1), the relatively weak development of plastic deformation in conjunction with the general easy deformability of the bodies determines their poor formability.

In Chasov Iar, Druzhkovka, and Novomaiachka clays (Type IV), with moderate values of the nominal specific deformation power, plastic deformation develops to the greatest extent, and this is the principal cause of streakiness in clays of this type.

Deformation of Frunze clay and Pavlograd loam (Type III) requires considerable forces; in view of the high values of the instantaneous elastic deformation and the weak development of elastic deformation ϵ_2 , clays of this type have a tendency to streakiness as the result of brittle breakdown of their structures.

The development of all the types of deformation, as expressed by definite relationships between the fundamental characteristics, predetermines the good formability of the bodies (Type II) irrespective of the power required for the deformation.

Consequently, the behavior of ceramic bodies in working and forming, or their molding properties, are determined by the manner in which the deformation process develops: by the values of the instantaneous-elastic deformation, the rates of the elastic and plastic deformations over a certain interval of time, and the ratios of these deformations.

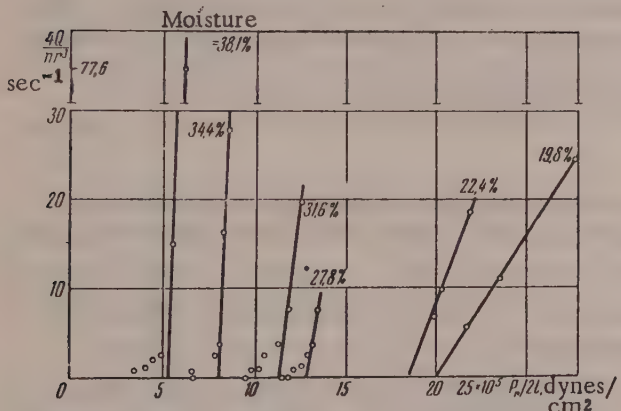


Fig. 3. Velocity gradient-shear stress curves for Kiev spondylic clay.

direction in which the parameters characterizing the elasticoplasticoviscous properties of the body should be varied.

Rheological properties of ceramic bodies. The analogy between the motion of a ceramic body in the band press and the flow of a plasticoviscous fluid in a pipe of variable cross section is now generally accepted [17, 24, 25]. Despite this, existing methods for calculations of band press design are based exclusively on kinematic (geometric) considerations, without regard to the properties of the bodies being formed.

A study was therefore carried out on the structuromechanical properties of flowing ceramic bodies, with the aid of the Volarovich viscosimeter [26].

Investigation of the relationship between effective viscosity and moisture content of ceramic bodies [16, 27] showed (Fig. 3) that at low shear stresses the variations of the velocity gradient are represented by a curve. With increasing shear stress, from body velocities of about 1 cm/second, the velocity gradient-shear stress relationship $4Q/\pi r^3 = f(P_r/2l)$ becomes linear; this means that under these conditions the structure of the mass undergoes virtually ultimate breakdown. In this region a ceramic body may be characterized by two constants: the minimum plastic (Bingham) viscosity η_m^* and the nominal dynamic flow limit P_{k_2} . The values of η_m^* and P_{k_2} are constant for heads 2.50–4.85 cm long and the radius 0.250–0.525 cm, over a wide range of loads on the viscosimeter piston.

On the basis of the results reported by numerous workers [17, 24, 25] it was assumed as a first approximation that the body in a band press flows at the minimum plastic viscosity.

Analysis of the experimental data, with the aid of the similarity theory, revealed the existence of a relationship between the principal parameters of the clay bodies and the power and output of the band press; it was thus possible to eliminate the indeterminate coefficients generally used in design calculations relating to such presses.

This relationship shows that the pressure in the clay body increases very little with increase of press output (velocity of body). Most of the energy is expended to overcome resistance and therefore to maintain steady flow at the required velocity. Decrease of the compression ratio of the press greatly lowers the pressure on the clay. It follows that it is advantageous to operate band presses at higher flow rates and to design band presses with lower compression ratios.

Further extensive studies on the rheology of ceramic bodies are being conducted by V. B. Chernogorenko and M. S. Komskaia (Kiev).

Complete rheological curves of ceramic bodies. Abduragimova, Rebinder, and Serb-Serbina [11], who studied the elasticoviscous properties of thixotropic structures in aqueous clay suspensions, drew attention to the great importance of complete rheological curves, and established that at shear stresses below the nominal flow limit these systems exhibit slow flow of the creep type.

We therefore studied the structuromechanical properties of a thixotropically reinforced body of spondylic clay, with 33.5% moisture, over a wide range of shear stresses (P from $3 \cdot 10^4$ to $2 \cdot 10^6$ dynes/cm²), and obtained the complete picture for the flow of the body at various degrees of structural breakdown, including the stresses which arise in ceramic bodies during working and molding in production machines [28, 29].

The log $\eta - P$ curve is shown in Fig. 4.

At shear stresses below the nominal flow limit $P_{k_1} = 4.8 \cdot 10^4$ dynes/cm², produced in a parallel-plate instrument, the body has maximum (Newtonian) viscosity [10, 11] of the order of 10^{13} poises, and exhibits flow of the creep type almost without structural breakdown.

Increase of the shear stress from $4 \cdot 10^4$ to $5 \cdot 10^4$ dynes/cm², i.e., above the nominal flow limit, results in a sharp decrease of viscosity by about two orders of magnitude.

When the shear stress is increased from $5 \cdot 10^4$ to $1.5 \cdot 10^5$ dynes/cm², the body exhibits plastic flow with virtually intact structure, i.e., with simultaneous breakdown and restoration of the structure. The viscosity remains constant, of the order of 10^{10} poises, and corresponds to the maximum plastic (Shvedov) viscosity [11].

Further increase of stress from $1.5 \cdot 10^5$ to $2.1 \cdot 10^5$ dynes/cm² leads first to partial breakdown on the structure and then to rupture of the sample, and is accompanied by a decrease of viscosity. The least measurable effective viscosity in this instance was of the order of 10^8 poises.

At shear stresses of $8 \cdot 10^5 - 1.6 \cdot 10^6$ dynes/cm² (in a capillary viscosimeter), the body flows with a gradual increase of structural breakdown and a simultaneous decrease of effective viscosity from 10^6 to 10^4 poises.

A shear stress of $1.6 \cdot 10^6$ dynes/cm² produces almost total breakdown of the structure in the body. On further increase of the shear stress to $2 \cdot 10^6$ dynes/cm² the viscosity remains constant and corresponds to the minimum plastic (Bingham) viscosity of the order of 10^4 poises [11].

Rheological viscosity - shear stress ($\eta - P$) curves have very great practical importance, as they determine the fundamental principles of the technological processes of molding and working ceramic bodies and of machine design by providing a direct connection between the nature of the flow, the degree of structural breakdown, and the shear stress.

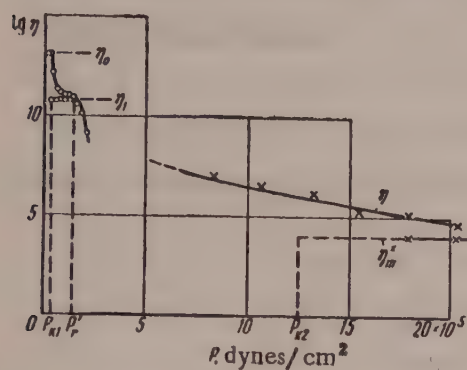


Fig. 4. Rheological ($\log \eta - P$) curve for spondylic clay body; moisture content 33.5%.

required, either stresses of the order of the nominal limit of the virtually intact structure P_1 , at which flow occurs at the maximum plastic viscosity, or stresses of the order of the nominal dynamic flow limit P_{k2} , at which streakiness does not yet occur; it also make it possible to determine these values directly, so providing the basic calculation data relating to the forming process and equipment.

The stipulated conditions may be fulfilled and the required press output maintained, by a considerable decrease in the resistance to the flow of the body. This can be effected by a decrease of the press body diameter and an increase of shaft thickness, by conditions for smooth flow of the body in the head and mouthpiece of the press, and by a general decrease of the compression ratio of the press [30].

Examination of the $\eta - P$ curves for ceramic bodies also leads to the conclusion that the plastic forming process is economically most efficient at shear stresses which result in maximum breakdown of the structure.

New design principles for molding machines used for plastic working of ceramic bodies must be developed. Maximum structural breakdown throughout the flowing ceramic body can be effected by means of vibrations at sonic or ultrasonic frequencies. The instantaneous thixotropic build-up characteristic of highly concentrated suspensions such as ceramic bodies, fixes the form of the ware.

Maximum structural breakdown can also be effected in the boundary layers of the flowing mass only; this is equivalent to creation of wall slip. This result can be attained either by vibration of the head and mouthpiece of the band press, or by electroosmosis, as proposed by P. M. Rudenko.

SUMMARY

1. Application of the physicochemical mechanics of disperse systems to studies of plastic working and forming of ceramic bodies gives very useful results.
2. Studies of the plastic strength of ceramic bodies led to the development of methods for determination of optimum moisture content and homogeneity of the clay bodies, and for evaluation of equipment performance.
3. Studies of the elasticplasticoviscous properties of intact structures have given rise to criteria for evaluation of the molding properties of ceramic bodies, and make it possible to predict their behavior during working and forming, and to modify their properties accordingly.

4. Investigations of the performance of band presses by means of structuromechanical analysis have revealed a relationship between the press parameters and the clay properties. Analysis of this relationship leads to important practical recommendations.

5. Rheological curves for ceramic bodies have been used to determine the permissible pressure limits in forming. Operating conditions for band presses have been formulated and suggestions made for improvements in their design. New principles for the design of machines for the plastic forming of ceramic bodies have been put forward.

Research into the physicochemical mechanics of ceramic bodies provides the scientific basis for studies, planning, the selection of the optimum process conditions in plastic working and forming of ceramic bodies.

Institute of Constructional Material and Articles
Kiev

Received June 16, 1958

LITERATURE CITED

- [1] P. A. Rebinder, in the symposium: Viscosity of Liquids and Colloidal Solutions (Moscow-Leningrad, Izd. AN SSSR, 1941) p.1.*
- [2] S. Ia. Veiler and P. A. Rebinder, Proc. Acad. Sci. USSR 49, 5, 354 (1945).
- [3] E. E. Segalova and P. A. Rebinder, Colloid J. 10, 3, 223 (1948).
- [4] N. N. Serb-Serbina and P. A. Rebinder, Colloid J. 9, 5, 384 (1947).
- [5] B. Ia. Iampol'skii and P. A. Rebinder, Colloid J. 10, 6, 466 (1948).
- [6] P. A. Rebinder and N. A. Semenenko, Proc. Acad. Sci. USSR 64, 6, 385 (1949).
- [7] P. A. Rebinder and E. E. Segalova, Proc. Acad. Sci. USSR 71, 1, 85 (1950).
- [8] P. A. Rebinder, Trans. Inst. Phys. Chem. Acad. Sci. USSR (1950), p. 5.
- [9] E. E. Segalova, P. A. Rebinder, and A. N. Sentiurikhina, Colloid J. 13, 6, 462 (1951).
- [10] N. V. Mikhailov and P. A. Rebinder, Colloid J. 17, 2, 107 (1955). **
- [11] L. A. Abduragimova, P. A. Rebinder, and N. N. Serb-Serbina, Colloid J. 17, 3, 184 (1955). **
- [12] P. A. Rebinder, Proc. 3rd All-Union Conf. on Colloid Chemistry (Izd. AN SSSR, 1956), p. 7.*
- [13] P. A. Rebinder, in the symposium: To the Memory of Academician P. P. Lazarev (Izd. AN SSSR, 1956), p. 113.*
- [14] P. A. Rebinder, Bull. Acad. Sci. USSR, Div. Chem. Sci. 11, 1284 (1957). **
- [15] S. P. Nichiporenko, in the symposium: Advances in Building Technology (Acad. Archit. Ukrainian SSR Press, 1953) 4, p. 50.
- [16] S. P. Nichiporenko, Theory of the Processing of Plastic Ceramic Bodies (Acad. Archit. Ukrainian SSR Press, 1955).
- [17] M. Ia. Sapozhnikov, Apparatus and Machines for the Production of Constructional Materials (1948). *
- [18] D. M. Tolstoi, Colloid J. 9, 6, 450 (1947).
- [19] D. M. Tolstoi, in the symposium: to the Memory of Academician P. P. Lazarev (Izd. AN SSSR, 1956), p. 159. *
- [20] S. P. Nichiporenko, in the symposium: Advances in Building Technology (Acad. Archit. Ukrainian SSR Press, 1956), 8, p. 60. *
- [21] S. P. Nichiporenko and S. A. Dikova, in the symposium: Advances in Building Technology (Acad. Archit. Ukrainian SSR Press, 1956), 8, p. 73.

*In Russian.

**Original Russian pagination. See C.B. Translation.

- [22] S. P. Nichiporenko, Proc. Acad. Sci. Ukrainian SSR 3, 267 (1956).
- [23] S. P. Nichiporenko, Proc. Acad. Sci. Ukrainian SSR 5, 554 (1958).
- [24] V. S. Kvitko, "Band presses" part 1, Trans. Inst. Refractories, 43 (1938).
- [25] R. Haefeli and G. Amberg, Schweizerische Tonwaren Industrie, No. 1-5 (1949).
- [26] M. P. Volatovich, In the symposium: Viscosity of Liquids and Colloidal Solutions 2 (1944) p. 192.*
- [27] S. P. Nichiporenko, Proc. Acad. Sci. Ukrainian SSR 3, 186 (1954).
- [28] S. P. Nichiporenko and S. A. Dikova, Proc. Acad. Sci. Ukrainian SSR 3, 290 (1957).
- [29] S. P. Nichiporenko, Proc. Acad. Sci. USSR 118, 4, 785 (1958).
- [30] S. P. Nichiporenko, Glass and Ceramics 2, 16 (1950).

*In Russian.

DEFORMATION CHARACTERISTICS OF NATURAL AND DISPERSED STRUCTURES OF SOME CLAYS

I. M. Gor'kova

Native clays are natural, structurized disperse systems. The development of a spatial structural network and its reinforcement with time under the influence of molecular cohesion forces, confers definite mechanical properties on the clays. Studies of the structuromechanical properties of clays in the light of modern views of the most recent branches of colloid chemistry — the theory of structure formation in disperse systems, and physico-chemical mechanics — are of great theoretical and practical interest; they assist in the elucidation of the nature of the strength of natural structures, and in a scientifically-based engineering and geological characterization of the clays.

The present communication deals with certain results obtained in studies of the structuromechanical properties of clays of various genetic types, containing weak structural bonds and bonds which have been reinforced to various degrees.

The samples studied were glauconite, hydromica, and kaolinite Jurassic and Quaternary sandy-colloidal materials * from the Moscow and Salekhard regions, with their natural moisture content; recent, early Black Sea and neo-Euxinian hydromica-kaolinite and montmorillonite deposits from the Black Sea, with their natural moisture content; hydromica Khvalynsk clays of the Volga region and hydromica-kaolinite Jurassic clays from the Moscow and KMA** regions, with their natural structure and in paste form; and pastes of certain other clays.

The theory and methods of the quantitative characterization of the rheological and strength properties of structurized disperse systems are detailed in the publications of P. A. Rebinder and his associates [2].

The Maslov, Veiler-Rebinder and Tolstoi shear instruments were used, by the appropriate methods, for investigations of clay samples with their natural structure and of concentrated pastes.

The composition and properties of the samples, and full details of the methods and results, are given in earlier papers [3].

Studies of the development and decay of deformation in natural and dispersed structures of the clays at various constant shear stresses showed that the structuromechanical properties can be determined quantitatively only for clays at relative humidity $W/W_f < 0.5 - 0.6$ (W is the percentage moisture content of the clay; W_f is the percentage moisture content of the paste at the lower yield value, in Atterberg's terminology) in the stress region where the elastic shear modulus E is independent of the acting stress P (i.e., in the region of virtually intact structures).

*Sandy-colloidal materials, true quicksands in Lebedev's terminology, contain up to 90% by weight of coarse inert filler (sand and large dusty fractions $> 10 \mu$), with a colloidal complex of highly disperse clay minerals, sols and gels of silica, alumina, and iron compounds, mineral organic compounds, and humic acids of high molecular weight; they have a very low electrolyte content — 0.02 to 0.006 %.

The organomineral colloidal complex of these materials is highly hydrophilic and in a state of maximum peptization. Therefore, they may be regarded as highly plasticized and hydrophilic varieties of clay.

**Not identified. Translator's note.

The natural structures of Jurassic clays at their natural relative humidity ~0.40 have a high yield value ($P_{k1} = 5.8 \cdot 10^5$ dynes/cm²), high strength ($P_m = 1.9 \cdot 10^6$ dynes/cm²), high values of the elasticity moduli (E_1 of the order of 10^6 dynes/cm²; E_2 of the order of 10^7 - 10^8 dynes/cm²). These structures have low deformability ($1/E = 4 \cdot 10^{-7}$ cm²/dyne), low elasticity ($\gamma = 0.03$ - 0.10) and high maximum viscosity in the virtually intact state ($\eta_0 = 2 \cdot 10^{11}$ poise). The deformation of these structures disappears almost completely on instantaneous removal of load. Slight residual deformations develop in them as the result of slow flow of the creep type in the region of $P_{k1} - P^*r$, i.e., in the region of virtually intact structures (Fig. 1).

The natural structures in the clays studied are similar in their properties to elasticobrittle condensation structures, but allow of slow flow of the creep type owing to the presence of residual hydration layers at the points of contact between the particles. Thus, clay with their natural structure are nominally elasticoplastic

systems which have become reinforced as the result of dehydration, orientation, and condensation of the Jurassic sea deposits.

The natural structures of Jurassic clays, like those of the Khvalynsk clays studied earlier [5], must be regarded as aged coagulation structures in clay deposits. They can therefore be classified as a group of coagulation structures strengthened as the result of syneresis, with properties intermediate between those of crystallization-condensation and recent coagulation structures.

Sandy-colloidal materials, sediments, and freshly prepared clay pastes, with moisture contents varying over a wide range, are much less strong coagulation (dispersion) structures, with pronounced plasticoviscous and elastic properties; they exhibit considerable residual deformations and restore their strength rapidly after structural breakdown.

A characteristic feature of the pastes and clays

Fig. 1. Deformation kinetics of the natural structure of Jurassic clay, KMA, Oboian', from a depth of 478 m at $W/W_f = 0.39$.

at relative humidities above 0.5-0.6 is their orientational reinforcement in shear deformation. This is shown by the increase of the equilibrium modulus E (From 2 to 20-fold, with decreasing concentration of the solid phase) as the deformation decays after removal of load, and by the considerable increase in the relative proportion of the residual deformations (Fig. 2). Similar orientation of kaolinite clays in flow was observed by Raitburd et al. [6].

Comparative studies of the course of deformation in dispersion structures of these clays at various constant shear stresses revealed the existence of two types of structures. The first type includes natural structures and concentrated pastes of KMA Jurassic clays ($W/W_f < 0.6$), natural structures of neo-Euxinian sediments, pastes of Far Eastern and Khvalynsk bentonite clays (up to $W/W_f = 2.50$), for which the shear modulus E is

independent of the action stress P over a definite stress region (up to $P^* = 1.2 \cdot 10^6$; $3 \cdot 10^3$; $4.1 \cdot 10^5$; $1.3 \cdot 10^6$; $5.6 \cdot 10^4$; $2.4 \cdot 10^3$ dynes/cm² respectively).

The elasticity moduli of 10% bentonite clay suspensions were found to be similarly independent of P in the stress region up to 19.8 - 500 dynes/cm² [2]. Therefore, these structures are characterized by the existence of a pronounced nominal-elastic region.

The second type of structure includes moister pastes of Jurrassic clays ($W/W_f > 1.0$) and, in particular, sandy-colloidal materials and upper sedimentary layers. They are characterized by a pronounced dependence of E on P , even at low shear stresses, and by high elasticity; this shows that their structural bonds are weak

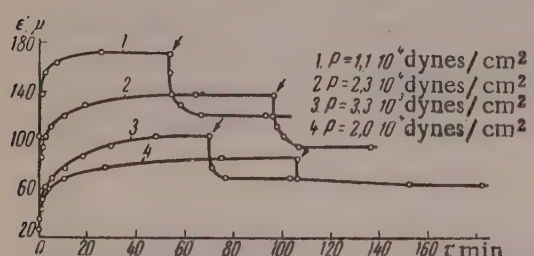


Fig. 2. Deformation kinetics of natural structures in early Black Sea sediments at different depths: 1) 60-80 cm; 2) 155-170 cm; 3) 654-680 cm; 4) 1052-1075 cm; $W/W_f = 1.2$.

and that the structural network is broken down in the course of testing (Fig. 3).

There is no doubt that these differences in the deformation behavior of clays of different origins are primarily due to the nature of the adsorption layers through which the particles interact in the course of structure formation.

Coagulation structures in clays are formed by cohesion of the particles as the result of spontaneous sudden thinning of the ionic hydration layers [7]. The structures formed have high viscosity and elasticity over a definite stress range. In this nominal-elastic region, corresponding to the solidlike state of the coagulation structures, the elasticity $\lambda = E_1/(E_1 + E_2)$ may serve as a characteristic of the rigidity of their structural bonds in relation to hydration of the particles at their points of contact. Values of $\lambda < 0.5$ indicate that the clays have solid-like properties, and are characteristic of clays with moisture contents below the adhesion limit (such as the Jurassic clays studied), or clays in which contacts between the particles are reinforced in presence of considerable amounts of free water in the pores, as in Khvalynsk and other highly porous clays, in sediments, in bentonite suspensions [2], etc.

In sandy-colloidal materials and in upper sediment layers, containing considerable amounts of organic matter (0.31 to 4% C), particle interaction occurs mainly through extensive, highly hydrophilic, mechanically strong, and therefore very stable molecular adsorption layers. Such protective layers of organic surface-active substances make the particles kinetically and aggregatively stable because of their weak cohesion and confer mobility, high deformability, and elasticity to the materials in the moist state. Jurassic clays, containing up to 2.2-4% of organic matter, have considerably higher deformability than Khvalynsk and bentonite clays.

The highest deformability ($1/E = 10^{-4} \text{ cm}^2/\text{dyne}$) and fluidity ($1/\eta = 0.05-0.01$) are found in moist sandy-colloidal materials containing colloidally dispersed minerals of the montmorillonite and glauconite types, which form the most stable mineral organic compounds. On drying, these materials form brittle irreversible condensation structures as the result of cementing by organic matter and by the oxides of silicon and iron.

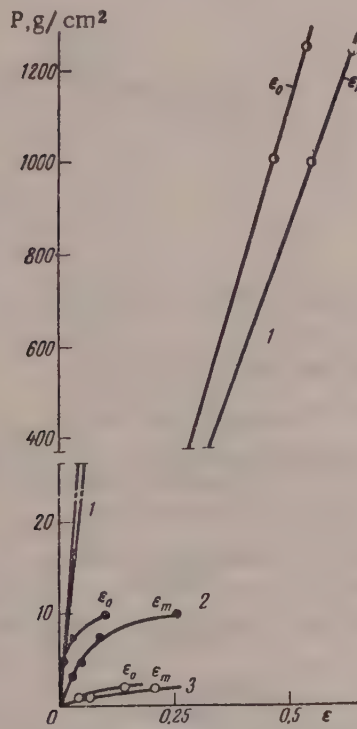


Fig. 3. Variations of the instantaneous elastic deformation ϵ_0 and maximum elastic deformation ϵ_m with shear stress P for natural structures in Jurassic clay (1), early Black Sea sediments (2), and Jurassic sandy-colloidal material (3).

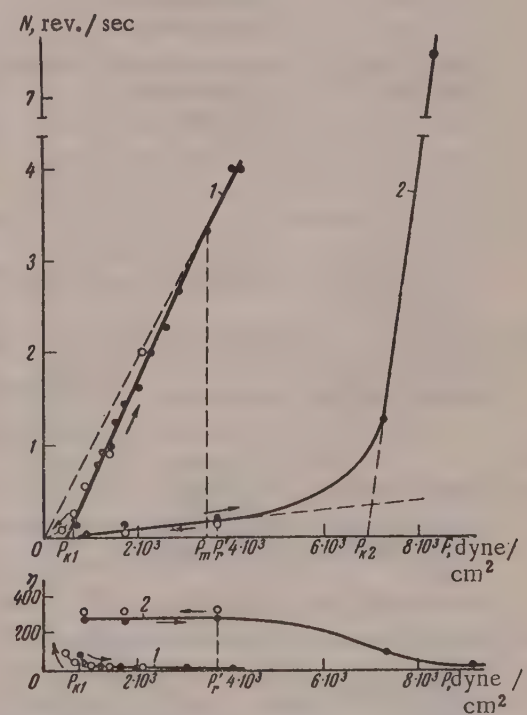


Fig. 4. Rheological curve (N) and variations of effective viscosity (η) with acting stress for Jurassic sandy-colloidal material (1) from a depth of 79 meters, with $W/W_f = 1.2$, and recent sediment (2) from a depth of 0-10 cm, with $W/W_f = 1.43$. White circles represent the down branches of the curves.

Characteristics of Dispersion Structures of Certain Clays

Materials	Mineral composition of fraction $< 1 \mu$	$W, \%$	W/W_f	$P_{k=1}^{\infty}$, dynes/cm ²	η_0 , poises	η^m , poises	η_e/η_m	Variation of effective viscosity with decrease of acting stress
Sandy-colloidal material								
Jurassic, Moscow, 79 m	Glauconite	33	1,2	$6 \cdot 10^2$	81	17	4,4	Branches of curves coincide
Quaternary, Salekhard, 49 m	Hydromica, kaolinite	31	—	$7 \cdot 10^2$	250	50	5	The same
The same, 52 m	Hydromica, kaolinite	34	—	$3 \cdot 10^2$	160	10	16	»
Black Sea sediments								
Recent, 0-10 cm	Highly disperse hydromica and kao-linite	57,8	1,43	0	280	20	14	»
The same, 30-35 cm	The same	54,2	—	$1 \cdot 3 \cdot 10^4$	1000	76	13	Branches of curves almost coincide
The same, 122-153 cm	»	66,0	1,20	$8 \cdot 5 \cdot 10^3$	$8 \cdot 2 \cdot 10^3$	153	53	Hysteresis loop
Early Black Sea, 60-80 cm	Highly disperse hydromica and mont-morillonite	98,5	1,02	$2 \cdot 10^4$	$4 \cdot 10^4$	40	1000	Very large hysteresis
Neo-Euxinian, 654 cm	Highly disperse hydromica and kao-linite	41,9	0,62	$2 \cdot 4 \cdot 10^4$	$2 \cdot 10^4$	171	117	Large hysteresis loop
Clay pastes								
Khvalynsk clay, Volga region, 7.75 m	Hydromica	46	0,77	$7 \cdot 2 \cdot 10^4$	$7 \cdot 10^4$	572	122	Hysteresis loop
The same	The same	66,5	1,12	$7 \cdot 4 \cdot 10^3$	$5 \cdot 5 \cdot 10^4$	21	2620	Very large hysteresis loop
The same, 9.25 cm	»	92,0	1,53	$1 \cdot 7 \cdot 10^4$	$1 \cdot 7 \cdot 10^4$	148	115	Large hysteresis loop
»	»	24,7	0,89	$8 \cdot 10^3$	$3 \cdot 4 \cdot 10^5$	343	1000	Very large hysteresis loop
Chistopol* clay	Montmorillonite	59,8	0,94	$3 \cdot 10^4$	$1 \cdot 2 \cdot 10^5$	311	400	Hysteresis loop
Jurassic clay, KMA, Oboian*, 464 m	Hydromica, kaolinite	40,0	0,93	$3 \cdot 6 \cdot 10^4$	$2 \cdot 10^4$	$2 \cdot 10^3$	10	Branches of curve coincide
The same, 478 m	The same	65	1,27	$8 \cdot 10^3$	$3 \cdot 3 \cdot 10^3$	140	23	Branches of curves almost coincide
The same, 478 m	»	83	1,62	$1 \cdot 9 \cdot 10^3$	$4 \cdot 10^3$	40	100	Branches of curve coincide
Jurassic clay, KMA, Glinki, 4.05 m	»	62	0,91	$3 \cdot 10^4$	$1 \cdot 1 \cdot 10^4$	534	20	Branches of curve coincide
Glukhov kaolin	Kaolinite	29,6	1,57	$6 \cdot 10^3$	$3 \cdot 10^3$	129	23	Branches of curves almost coincide

The structures which arise in clays when particle cohesion is weakest as the result of stabilization by extensive hydrated ionic layers and mechanically strong, highly stable molecular adsorption layers cannot be regarded as coagulational; they are strongly stabilized in character, and fluidlike in structure.

Investigations of the characteristics of stabilized and coagulation structures in these materials with the aid of the Volarovich viscosimeter [8] fully confirmed this distinction in their deformation behavior. As the result of these investigations, clays can be classified in the following groups according to the rheological characteristics of their dispersion structures (see Table).

1. The group of fluidlike materials of the type of sandy-colloidal quicksands and certain of the most recent sediments. Dispersed structures of these materials are characterized by virtual absence of a nominal yield value of the ratio η_0/η_m [4-16], mainly owing to the low values of initial viscosity η_0 . The rheological curves and the curves for the variations of effective viscosity with acting stress, determined for increasing and decreasing stress, coincide in this group (Fig. 4). In other words, these materials are only weakly thixotropic because of the presence of extensive adsorption layers and of the dense packing of the particles, which allow of rapid restoration of the weak structure; they have the highest fluidity, elasticity, and deformability.

2. Group of materials with a loose structure, with solidlike properties due to strengthened cohesion of the particles at the points of contact in coagulation structure formation and in the course of diagenesis — this group includes early Black Sea and neo-Euxinian sediments and especially highly disperse Khvalynsk light and heavy clays.

These materials have a nominal yield value and are characterized by the highest values of the ratio of initial viscosity to the viscosity of structures broken down to the limit η_0/η_m (100-2600). The magnitude of this ratio is a measure of the solidlike properties of coagulation structures. Khvalynsk highly disperse hydromica

clays have the most pronounced solidlike properties and high viscosities in the region of virtually intact structures ($P_{k1} - P'_{k1}$). However, they liquefy abruptly as the result of brittle breakdown of their structure at stresses above the Bingham dynamic yield value P_{k2} . These clays exhibit pronounced thixotropic recovery of the initial paste viscosity with time, at stresses below P_{k1} . This is shown by the large hysteresis loop and by the restoration of viscosity on decrease of the acting stress (Fig. 5, Curve 1).

3. The earliest group studied, KMA Jurassic clays have the highest nominal yield value but relatively low values of the ratio η_0/η_m (10-100), because of the high viscosities of the structures after ultimate breakdown, η_m . The materials of this group are weakly thixotropic, because cohesion between the weakly hydrated and closely packed particles is rapidly restored.

The extremely high density of the structure in Jurassic clays is the consequence of their

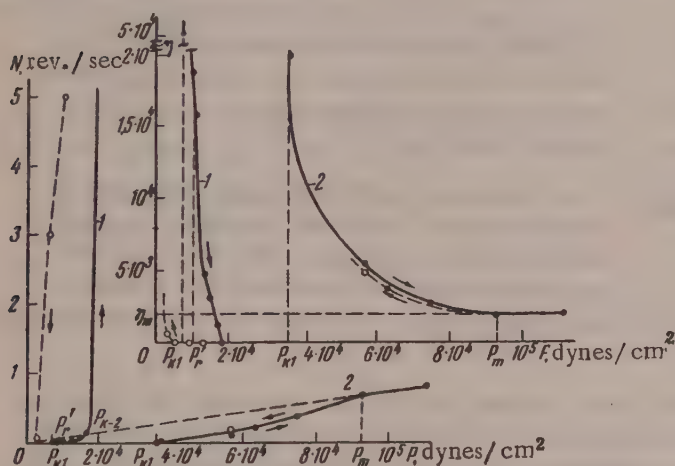


Fig. 5. Rheological curves (N) and variations of effective viscosity (η) with acting stress for Khvalynsk clay of the Volga region (1) with $W/W_f = 1.12$, and Jurassic KMA clay (2) with $W/W_f = 0.93$. White circles represent the down branches of the curves.

hydromica-kaolinite composition, the predominant content of sorbed Ca, growth of the clay mineral crystals with time, the presence of considerable amounts of dust and sand particles and of organic matter, which favors close packing of the particles stabilized by it, and the prolonged consolidation of clays at great depths. At stresses above the flow limit these clays behave like very viscous liquids and show a tendency to unlimited deformation with flow of the creep type (Fig. 5, Curve 2).

Thus, a high affinity for water and the presence of extensive adsorption layers, by favoring peptization of the particles, produces a relatively higher degree of compactness in clay materials, together with high mobility because of their low viscosity and very weak cohesion between the particles. This accounts for the fluidity of true quicksands and the most recent sediments. Such materials have little or no thixotropy, but

have a tendency for unlimited deformation owing to flow with continuous restoration of the structure. Analogous structures are found in the denser Jurassic clays, but these have much higher strength and viscosity owing to the considerable dehydration of the particles with time.

Structures of this compact type [9], corresponding to maximum volume filling and contact between the particles by solvation hulls developed to various degrees, are found mainly in clays of the kaolinite type, and also in other materials with particles effectively stabilized, especially by organic substances (such as true quick-

sands, fresh-water and recent marine sediments, early deposits, marsh and lagoon formations, gleys, northern running clays, etc.). Because of the compact packing of the particles and therefore a low content of free water, materials with such structures (in absence of large amounts of plant remains) usually have low moisture capacity. Such structures are characterized by low values of the η_0 / η_m ratio.

Structures of the loose type, i.e., coagulation structures proper, are formed predominantly in clays with anisodiametric particles (i.e., in montmorillonites or hydromicas), at definite concentrations of the solid phase, and if the electrolyte content is adequate; more often in marine media. They have high moisture capacity because of the retention of large amounts of free water in the pores, as the cohesion of the highly disperse particles takes place predominantly at corners and edges. Such structures strengthen rapidly as the result of spontaneous dehydration of the particles during syneresis at the points of contact. Such structures have great variability of strength and viscosity over a narrow stress range; they have high η_0 / η_m ratios (Fig. 6).

Thixotropy is intimately associated with the characteristics of these loose structures. Reversible restoration of the structures and of their solidlike

Fig. 6. Variations of η_0 / η_m with W/W_f for dispersed structures of some clay materials: 1) Neo-Euxinian hydromica-kaolinite sediment; 2) Khvalynsk hydromica clay; 3) light Khvalynsk hydromica clay; 4) early Black Sea hydromica-montmorillonite sediment; 5) Chistopol' montmorillonite clay; 6) Jurassic hydromica-kaolin clay; 7) Jurassic sandy-colloidal glauconite; 8) recent hydromica-kaolinite sediments from Shallow Black Sea waters; 9) Glukhov kaolin.

properties after liquefaction of the clays occurs in consequence of the sudden penetration of the hydration layer at the points of contact of the particles on collision (at stresses below the flow limit).

It must be noted that it is virtually impossible to draw a dividing line between thixotropic and syneretic reinforcement of clays, as both processes often occur simultaneously, and both favor strengthening of the structure by increase of the number and area of contacts between the particles and increased bonding between them with time.

SUMMARY

1. The structuromechanical properties and characteristics of natural dispersed structures of certain clay minerals of various origins have been studied.

2. Natural coagulation structures in clays, reinforced as the result of syneresis effects, are intermediate in their properties between crystallization-condensation and recent coagulation structures.

3. The structures studied are classified in the following groups: a) fluidlike structures of organomineral sandy-colloidal materials and recent sediments; these have the highest fluidity, elasticity, and deformability; b) solidlike loose structures in Khvalynsk clays and early Black Sea and neo-Euxinian sediment, the viscosity of which falls rapidly over a narrow stress range, with thixotropic recovery of the solidlike properties; c) compact structures of the most highly dehydrated and dense Jurassic materials, with a tendency to slow plastic flow of the creep type.

4. The deformation and strength characteristics of clays must be investigated by rheological methods in order to provide a sound basis for clay characterization from the engineering and geological aspects and for calculations in construction planning.

The F. P. Savarenskii Laboratory of Hydrogeological Problems
Academy of Sciences USSR

Received December 4, 1957

LITERATURE CITED

- [1] P. A. Rebinder, J. Acad. Sci. USSR, No. 2. (1955)
- [2] E. E. Segalova, P. A. Rebinder, and L. N. Sentiurikhina, Colloid J. 13, No. 6, 462 (1951); N. V. Mikhailov and P. A. Rebinder, Colloid J. 17, No. 2, 107 (1955); A. A. Abduragimova, P. A. Rebinder, and N. N. Serb-Serbina, Colloid J. 17, No. 3, 184 (1955); P. A. Rebinder, Proc. Conference on Engineering and Geological Properties of Rocks and Methods of their Investigation (Moscow, Izd. AN SSSR, 1956). **
- [3] V. A. Priklonskii, I. M. Gor'kova, N. A. Oknina et al., Trans. Lab. Hydrogeol. Problems Acad. Sci. USSR 13 (1956); I. M. Gor'kova, V. F. Chepik and K. N. Riabicheva, Trans. Lab. Hydrogeol. Problems Acad. Sci. USSR 15 (1957). **
- [4] I. M. Gor'kova, Proc. Conference on Engineering and Geological Properties of Rocks and Methods of their Investigation, 1 (Moscow, 1956). **
- [5] I. M. Gor'kova, Colloid J. 18, No. 1, 27 (1956). *
- [6] Ts. M. Raitburd, Proc. Conference on Engineering and Geological Properties of Rocks and Methods of their Investigation, 1 (Moscow, 1956); W. R. Buessem and B. Nardy, Clays and Clay Minerals (Washington, D. C., 1954).
- [7] B. V. Deriagin, Kolloid-Z. 69, 155 (1937); A. D. Malkina and B. V. Deriagin, Colloid J. 12, No. 6 (1950).
- [8] M. P. Volarovich and D. M. Tolstoi, J. Phys. Chem. 4, No. 6 (1933); M. P. Volarovich and M. F. Nikitina, Colloid J. 12, No. 3 (1950).
- [9] P. A. Rebinder, Proc. Conference on the Viscosity of Liquids and Colloidal Solutions, 1 (Izd. AN SSSR, 1941), p. 361. **

*Original Russian pagination. See C.B. Translation.

**In Russian.

THE ROLE OF PLASTIFICATION AND HYDROPHOBIZATION IN THE COMPACTION OF SOILS

T. Iu. Liubimova and T. V. Iagodovskaya

The hydrophobization of soils used in building, in order to decrease their water permeability and tendency to soaking, in contrast to waterproofing effected by filling of the open pores with insoluble substances, is achieved by decrease of the wettability of the particle surfaces as the result of chemisorption of surface-active substances, in harmony with Rebinder's theory [1].

Water-repellent surface-active additives can probably exert a direct plastifying effect in the course of strong compaction of the soil, similar to the effect discovered by Khigerovich [2] in the waterproofing of lean concrete mixes and building materials.

There have been several studies of the hydrophobizing action of various surface-active substances on soils, but the effect was not considered in relation to subsequent compaction of the soils and variations of their mechanical properties under the action of moisture and in the course of time [3].

In investigations related to road engineering problems [4], hydrophobizing surface-active substances were introduced into soils immediately before compaction, but the possible plastifying effect of the adsorption layers and their influence on structure formation in compacted soils were not considered; neither are there any reports of comparative studies of the changes of mechanical properties of compacted hydrophobized and non-hydrophobized soils under this action of moisture.

The hydrophobizing agents used in the above-mentioned investigations [3, 4] were mainly the sodium soaps of saturated and unsaturated higher fatty acids, and sodium sulfonaphthalene and abietate. Water imbibition was greatly retarded by these additives, both in compacted and in noncompacted soils.

The aim of the present work was to study the hydrophobizing and plastifying effects of technical soap wastes, containing alkali soaps of higher saturated and unsaturated fatty acids as their surface-active components, on soils. The material used contained ~67% of sodium oleate (on the dry substance). The results of experiments on the influence of adsorption layers of sodium oleate on structure formation in compacted soils will be presented in a separate paper.

Rebinder [1] showed that stable hydrophobization of mineral particle surfaces is possible only if the adsorption layers are bound chemically. Therefore, the most pronounced water-repellent effect should be found in carbonate soils and mineral powders. It appears that chemical binding of the water-repellent adsorption layers is not essential for their plastifying effect in the course of soil compaction.

The test samples were prepared as follows. The air-dry soils and mineral powders were sifted through a screen of 0.8 mm mesh and mixed with definite amounts of water or solution of surface-active agent. The samples were compacted by tamping in the apparatus for standard compaction of soils [8] in cylindrical metal cases, in which the samples were subjected to various tests.

It is known that in the mechanical compaction of soils of different moisture contents, near the lower plastic limit, the density of the soil (bulk density of the framework) γ as a function of the water content W is represented by a curve with a characteristic sharp maximum, the position of which for a given soil corresponds to the so-called "optimum moisture content," which represents the maximum possible densification of

the soil by the mechanical treatment used. The plastifying effect of the adsorption layers in the course of compaction was studied by determinations of the optimum moisture contents of the soils for different concentrations of the surface-active additives.

The mechanical properties of the compacted samples were characterized by their plastic strength P_m , determined by means of the lever-type cone plastometer devised in the Department of Colloid Chemistry of Moscow University.

Figure 1 shows typical curves for the effects of moisture content at mixing on the plastic strength and bulk density immediately after compaction. It is seen that the $P_m = f(W)$ curve has an inflection point, the abscissa of which (extremal on the differential curve $dP_m/dW = \varphi(W)$) coincides with the abscissa of the maximum on the $\gamma = F(W)$; this was the case for all the samples studied. This property of the curves for the

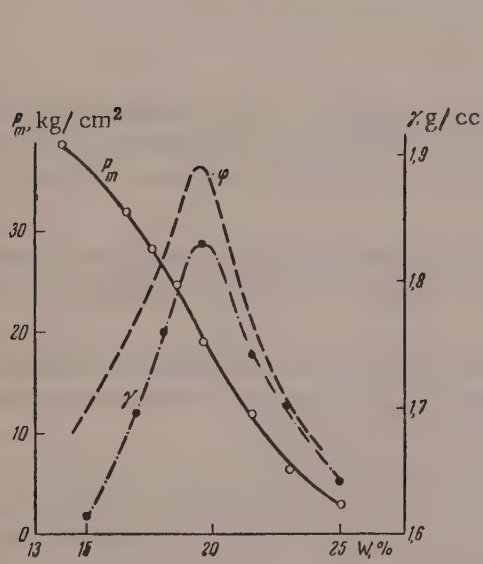


Fig. 1. Effects of moisture content at mixing on the plastic strength and bulk density of soil after compaction, $P_m = f(W)$; $\frac{dP_m}{dW} = \varphi(W)$; $\gamma = F(W)$.

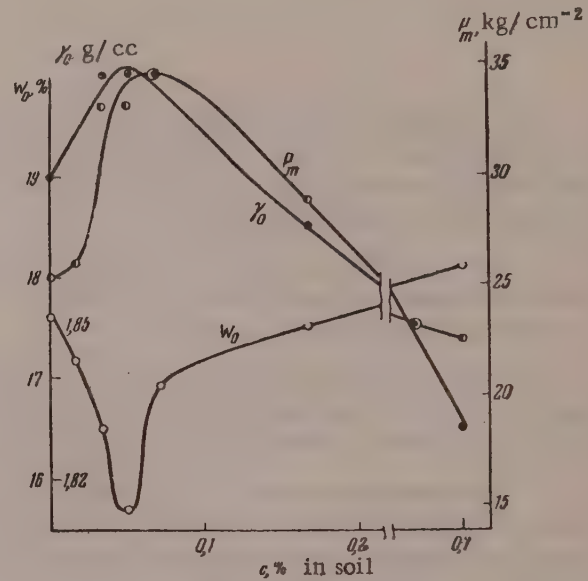


Fig. 2. Effects of sodium oleate concentration (c) on the optimum moisture content W_0 , plastic strength P_m , and the bulk density of the compacted soil framework (γ_0) in Cheremushki clay.

plastic strength of compacted soils as a function of the moisture content during compaction can therefore also be used for determination of the optimum moisture content. Data on the effects of sodium oleate concentration on the optimum moisture content, plastic strength, and maximum bulk density of the soil framework at the state of maximum compaction are presented in Figs. 2 and 3 and in Table 1.

Aqueous soap solutions are the most extensively studied class of surface-active semicolloids. Rebinder and his associates [1] have shown that the nature of the adsorption layer on the solid surface in contact with soap solution depends on the concentration of the solution: in adsorption from dilute solutions, ionic and ionic-molecular layers of a hydrophobic character are formed, and cause dehydration of the surface and flocculation of the dispersed particles; in adsorption from concentrated solutions, micellar hydrophilizing and stabilizing adsorption layers are formed, and peptize the disperse phase. Serb-Serbina [5] determined the following concentration ranges for sodium oleate: the range of flocculating concentrations 0.05-0.15%; the range of peptizing and stabilizing concentrations, 0.5-1%.

The data in Table 1 reveal the distinct plastifying action of hydrophobic adsorption layers, as shown by the decrease of the optimum moisture contents for Leningrad clay and Khar'kov Loess (a neutral and a weakly alkaline soil, respectively) over a narrow range of flocculating concentrations of sodium oleate; in the case of the more acid Cheremushki clay, probably as the result of increased hydrolysis of the soap with decrease of pH, the range of flocculating concentrations is shifted somewhat toward higher values [6].

The decrease of the optimum moisture content is accompanied by an increase of strength of the compacted soils, over the same range of sodium oleate concentration; the simultaneous increase of density, although regular, is small in absolute terms. For the soils studied the decrease of the optimum moisture content $\sim 10\%$ (1.5-2.0 absolute %); The strength increase after compaction varies from 30 to 90%; the density increase is 1-3%.

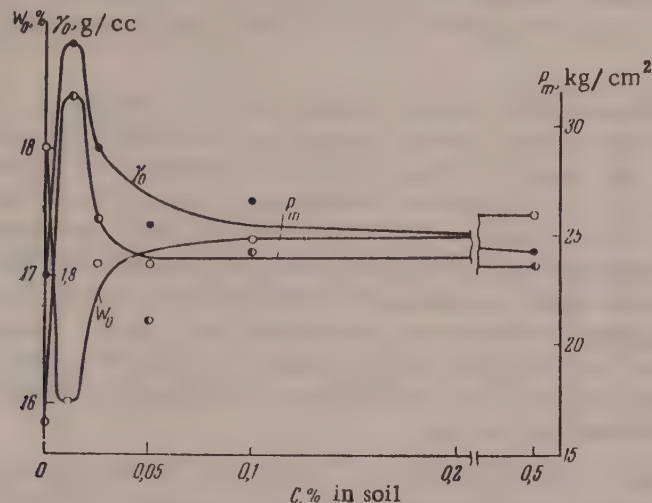


Fig. 3. Effects of sodium oleate concentration (c) on the optimum moisture content W_0 , plastic strength P_m , and the bulk density of the compacted soil framework (γ_0) in Khar'kov loess.

TABLE 1

Effect of Sodium Oleate Concentration on the Optimum Moisture Content, Plastic Strength, and Bulk Density of the Soil Framework at Maximum Compaction

Soils	Sodium oleate concentration, %		Optimum moisture content W_0 , % on the soil	P_m in kg/cm^2	γ in g/cc
	on the weight of soil	in solution at mixing			
Cheremushki (surface, carbonate-free) clay	—	—	17.6	25.0	1.88
	0.017	0.10	17.2	25.9	—
	0.034	0.21	16.5	33.1	1.90
	0.05	0.33	15.7	33.1	1.90
	0.07	0.43	16.9	34.6	1.90
	0.17	0.98	17.5	28.8	1.87
	0.34	2.00	17.3	23.0	1.85
Leningrad (surface) clay	0.70	4.00	18.1	22.5	1.83
	—	—	17.9	24.7	1.81
	0.01	0.06	16.7	31.1	1.83
	0.025	0.15	16.5	28.8	1.82
	0.075	0.44	17.0	23.4	1.81
Khar'kov loess	0.25	1.50	17.3	24.7	1.80
	—	—	18.0	16.4	1.80
	0.01	0.06	16.0	31.1	1.89
	0.025	0.15	17.1	25.6	1.85
	0.05	0.30	17.1	21.0	1.82
	0.10	0.60	17.3	24.1	1.83
	0.50	2.60	17.5	23.6	1.81

Only the fine-grained soils – a number of clays and loess – showed decreases of the optimum moisture content and increases of strength and density on addition of small amounts of sodium oleate. There was no effect on heavy sandy clays and loams. Similar results were obtained by Lambe [6] in a study of the effect of addition of sodium tetraphosphate as a "dispersing agent" on soils undergoing compaction; the peptizing action of this addition increases plasticity, decreases the optimum moisture content, and raises the density, but does not increase the strength. Further increase of the sodium oleate concentration again raises the optimum moisture content and lowers the strength and density to their initial values; in the range of stabilizing concentrations (for Cheremushki clay) the optimum moisture content rises above the initial value, and the density and strength decrease.

The physical significance of the optimum moisture content evidently lies in maximum peptization of the relatively weak structural contacts in the soil aggregates and stabilization of the soil particles by the adsorbed hydration layers. It is known [7, 8] that increase of the specific work of compaction is accompanied by appreciable and regular decrease of the optimum moisture content and increase of the corresponding values of maximum soil density. This suggests, first, that a high degree of compaction of moist soil can be attained by the action of external mechanical forces even with incomplete stabilization of the solid particles, in absence of fully developed hydration layers; second, that a limiting factor in maximum compaction is the presence in the soil mass of microaggregates which are only weakly peptized by water – fragments of the natural structure, to the breakdown of which the increase of density with increasing work of compaction must be attributed. This hypothesis is confirmed by the above data on the influence of hydrophobic adsorption layers on the compaction of soils and their optimum moisture contents.

The decrease of optimum moisture content in the region of flocculating concentrations of sodium oleate with the simultaneous regular, if slight, increase of density, is evidently the consequence of the lubricating action of the adsorption layers, which facilitate sliding of solid particles under the action of external compressive forces during compaction of the soil [2].

The strength increase of newly compacted soil in the region of plastifying (flocculating) sodium oleate concentrations can be attributed, in addition to the decrease of the moisture content, also to the formation of a larger number of structural contacts because of the thinning or removal of the stabilizing hydration layers; the effect should be especially prominent in conjunction with compacting forces. The introduction of a hydrophobizing additive is thus analogous to the application of a greater force or the expenditure of more work in compaction.

At higher concentrations of sodium oleate, with a transition to thick micellar hydrophilic adsorption layers of the gel type, the effect of decreased optimum moisture content vanishes, while at very high concentrations the optimum moisture content may even increase in accordance with the greater hydrophily of the solid surface.

The strength and density decreases in the region of stabilizing (peptizing) concentrations may also be caused by strong retardation or total inhibition of structural contact formation between the soil particles under such conditions, and possibly by the cushioning action of the strong gel-like structurized adsorption layers during compaction.

The effectiveness of the hydrophobizing action of sodium oleate was determined by the rate of capillary rise of water, the rate of water impregnation by Volkova's method [9], and by variations of the plastic strength in the dry and saturated states.

The impregnation rate was characterized by the value of K in Equation (1) for the volume of imbibed water as a function of time

$$V^2 = K \tau \quad (1)$$

The values of K were found graphically from the linear relationship between the impregnation rate and $1/\tau$

$$\frac{dV}{d\tau} = A \frac{1}{V \tau}, \quad (2)$$

where $A = \sqrt{K}/2$.

TABLE 2

Effect of Sodium Oleate on the Water Resistance and Water Absorption of Soils and Mineral Powders Compacted at the Optimum Moisture Content

Soil or mineral powder	Sodium oleate, % on the material	W*, in %	P _m , kg/cm ²			$\frac{P''_m}{P'_m} \cdot 100$	$\frac{P''_m(c)}{P''_m(0)} \cdot 100$	K × 10 ² , cm ⁶ /min
			after compaction P _m	after drying P [*] _m	in saturated state P ^{**} _m			
Kaolinite	—	39,6	13,0	144,0	0,9	0,6	100	289
	0,01	38,4	10,8	147,6	1,8	1,2	200	—
	0,1	37,5	11,0	144,0	1,4	1,0	155	134
Surface clay	—	17,8	24,5	57,6	2,0	3,5	100	2,6
	0,18	13,8	30,8	77,4	9,7	11,2	435	1,2
	0,36—0,72	14,5	31,0	73,8	8,1	11,0	405	1,3
	1,2	16,0	34,6	72,0	12,1	16,8	605	1,0
	2,4	17,0	30,6	54,0	7,4	13,7	370	—
Loess	—	15,1	19,0	111,0	6,1	5,5	100	15
	0,1	15,0	18,0	111,0	6,5	5,9	107	10
	0,25	14,7	18,9	111,0	8,1	7,3	132	3
	0,50	15,1	19,3	129,6	8,1	6,2	113	6
	1,0	16,8	22,0	129,6	5,4	4,1	74	10
Loam with a high carbonate content	—	21,5	11,5	111,0	0,4	0,4	100	1,3
	0,25	20,5	7,2	115,2	2,0	1,7	425	1,3
	0,5	19,4	9,0	115,0	2,5	2,1	525	0,5
	1,0	19,6	9,0	111,0	2,3	2,1	525	1,0
Kaluga limestone	—	11,5	31,0	115,0	25,4	22,1	100	100
	0,5	9,8	39,8	115,2	36,9	32,0	145	4—5
	1,0	8,5	—	130,0	57,1	43,9	199	5
	2,0	8,0	27,9	130,0	113,4	87,2	395	0,1

* W is the maximum saturation by capillary imbibition, in per cent on the dry soil;
P^{**}_m (c) is the plastic strength of the hydrophobized soil in the saturated state; P^{**}_m (0) is the corresponding value for nonhydrophobized soils.

TABLE 3

Characteristics of the Soils Tested

Soil	Fraction composition, in weight % of fraction of particle size				pH	Plasticity limits, %		Optimum moisture content in %
	<5μ	5—50μ	50—250μ	>250μ		upper	lower	
Surface carbonate-free clay from Cheremushki	40,8	38,3	20,4	0,5	6,0	40,2	18,4	17,0—17,5
Khar'kov loess	42,9	38,1	19	—	7,8	37,3	17,5	19,8
Leningrad clay from "Krasnaia								
Zvezda* site	48,1	75,9	6,0	—	7,0	30,0	19,8	17,9
Loam from Shurichi	9,2	82,31	8,5	—	7,6	29,3	20,0	17,3
Kaluga limestone		4,8	39,3	55,9	8,2	—	—	11,0

The experiments showed that the greatest decrease of the rate and amount of water imbibition occurs at sodium oleate concentrations above those corresponding to the maximum decrease of the optimum moisture content; therefore the samples for studies of the hydrophobizing action of sodium oleate were prepared at the same moisture content, corresponding to the optimum value for soil without additives. The strengthening effect of the surface-active additive is also observed in this concentration region, and it becomes particularly appreciable in the course of time, during subsequent structure formation, especially in a saturated-vapor atmosphere, rather than directly after compaction.

The results of tests on a number of soils and mineral powders are given in Tables 2 and 3. The samples were tested for water absorption and impregnation rate in the air-dry state after preliminary exposure for 2-3 months to an atmosphere of constant humidity ($\varphi = 80\%$), until their strength ceased to increase with time as the result of structure formation.

It is clear from the results that addition of sodium oleate to soils or mineral powders before compaction at optimum moisture content decreases their rate of water impregnation; this is especially prominent for carbonate materials. The hydrophobizing influence of sodium oleate also manifests itself in increased water resistance of the compacted soils.

SUMMARY

1. The plastifying and hydrophobizing effects of sodium oleate, introduced into soils before composition, were studied.

2. In the case of fine-grained soils, the optimum moisture content is decreased by about 10% (1.5-2.0% absolute) in the concentration range corresponding to the formation of ionic-molecular adsorption layers of sodium oleate, and the strength of the compacted soils increased (by 30 to 90%), for the same work of compacting.

3. The hydrophobizing action of sodium oleate consists of retardation of water absorption and an increase of the water resistance of the compacted soils; these effects are more stable in carbonate soils and mineral powders owing to the formation of chemically bound adsorption layers of calcium soaps.

These results are in accordance with the theories of P. A. Rebinder and his school concerning the mechanism of structure formation in soils and the significance of the nature of the adsorption layers on the particles of the disperse phase in compaction and improvement of their constructional characteristics.

The All-Union Road Scientific Research Institute
Moscow

Received March 10, 1957

LITERATURE CITED

- [1] P. A. Rebinder et al., *Phys. Chem. of Flotation Processes*, Moscow-Leningrad, Goskhimizdat, 1935); *
P. A. Rebinder, *Bull. Acad. Sci. USSR, Chem. Ser. No. 5* (1936); D. L. Talmud and S. E. Bresler, *Surface Phenomena* (GTTI, 1933). *
- [2] M. I. Khigerovich, *Hydrophobic Cement and Hydrophobizing and Plastifying Additives* (Constructional Materials State Press, 1957). *
- [3] F. E. Koliasev and M. P. Lyseuko, *Colloid J.* 13, 3, 188 (1951); S. D. Sukhovol'skaya, *Collected Papers on Agricultural Physics*, No. 3, 81 (1941); I. A. Kuz'michev, *Chemicalization of Socialist Agriculture* No. 7-8, 106 (1936); M. T. Kostriko, *Theory of Soil Hydrophobization* (Leningrad, Military Supply and Transport Academy, 1957). *
- [4] 10th International Road Congress (Moscow, Scientific Technical Press for the Automobile Transport Industry, 1957); * *Soil mechanics for road engineering*, Road research Laboratory, (London, 1955).
- [5] N. N. Serb-Serbina, *J. Phys. Chem.* 10, 625, 813 (1937)
- [6] W. Lambe, *J. Boston Soc. of Civil Engin.* 41, 2, 184 (1954).

*In Russian.

[7] A. A. Arsen'ev, V. A. Bochin, and N. N. Ivanov, Construction of Motorways, Part I (Moscow, Automobile Transport Press, 1955), p. 116; *M. Ia. Telegin, Methods of Compaction of Road Embankments (Road Press, 1952). *

[8] Z. V. Volkova, Mineral Raw Materials No. 7 (1934); Z. Volkowa, Koll.-Z., 67, 280, 1934; Acta Physicochemica 4, 635 (1936).

*In Russian.

STRUCTURE FORMATION IN THE COURSE OF HYDRATION HARDENING OF CALCIUM SULFATE HEMIHYDRATE (PLASTER OF PARIS)

E. E. Segalova and V. N. Izmailova

Plaster of Paris, considered as an individual cementing material, is of special interest in studies of the physicochemical basis of setting and hardening processes, and in clarification of the mechanism of these processes, which is still obscure, even for the simplest monomineral cements. Hydration hardening, i.e., hardening under the influence of water, essentially depends on the conversion of a primary cement containing little or no water into a new hydrated substance. The existing theories of hardening are largely concerned with the mechanism of the hydration reaction itself, and with the cause of the high supersaturations found in cement-water systems [1, 2].

Most workers [2] agree with the founder of the first theory of gypsum hardening, Le Chatelier, that supersaturation on the system plaster of Paris-water arises by dissolution of the original plaster, the solution of which is supersaturated with respect to the stable hydrate, gypsum. These concepts have been developed most fully by Zabzhinskii, Ratinov, and Rozenberg [3], who showed that the duration of the hydration reaction depends on the degree of supersaturation in the plaster suspensions, while the accelerating or retarding influence of electrolytes, which had not been conclusively explained previously [4], consists of their effect on the solubilities of the original unstable hemihydrate and of the dihydrate formed. These investigations showed that the concept of the dissolution of plaster with formation of stable supersaturated solutions, the plaster content of which can be regarded as the conventional "solubility" of the original compound, is a very valuable concept which can be used for quantitative description of the hydration process and for control of its rate.

However, studies of the hardening process should not be confined to clarification of the hydration mechanism, as crystallization of the new hydrate need not lead to the formation of a strong product, which is the direct goal in cement hardening in building technology. Unfortunately, the question of the origin and course of development of the crystallization structure has not been studied from the physicochemical aspect. The only publications in the literature deal with microscope studies of the structure of hardened gypsum [5], and with attempts to correlate its hardness with the dimensions of the dihydrate crystals formed. The information available is contradictory; increase of strength has been attributed both to increase [4] and to decrease [6] of crystal size.

The question of crystal concretion, the nature of the contacts between the crystals in the formation of a crystallization structure, and of the influence of the conditions under which the dihydrate crystallizes on the strength of the structure, were first studied by P. A. Rebinder and his associates [7-10].

The purpose of the present investigation was to determine the laws and mechanism of formation of the crystallization structure formed in the hardening of plaster.

The material studied was the β -form of calcium sulfate hemihydrate, containing 99.7% $\text{CaSO}_4 \cdot \frac{1}{2} \text{H}_2\text{O}$. The experiments were performed with suspensions containing a large amount of inert filler and finely ground quartz sand, in addition to the plaster. In the presence of an inert filler in the plaster suspension it is possible to obtain high values of the water-plaster (W/P) ratio without demixing of the suspensions, and thereby to retard structure formation, so that the mechanism of the process is much easier to study.

In accordance with the usual procedure in our laboratory, the course of structure formation was studied by determinations of the increase in the plastic strength of the structure forming in the suspension. A cone plastometer [7] was used for the purpose. The prepared samples (30% of plaster and 70% of ground quartz sand, with 50% water on the weight of the dry mixture) were kept in desiccators over saturated calcium sulfate solution.

Figure 1 shows that structure formation in plaster suspensions proceeds in three stages: at the first stage the plastic strength of the system is very low ($\sim 1.5 \text{ g/cm}^2$), and increases relatively slowly. 4 or 5 minutes after the mixing the second stage begins; this is a very rapid increase of strength, which reaches its maximum value (15 kg/cm^2), tens of thousands of times as high as the original, after 30 minutes. Then, if the suspension is kept in presence of moisture, the strength decreases slowly (third stage). The different nature of the structures formed in plaster suspensions at the first and second stages is clearly revealed in studies of the influence of mechanical forces on the properties of these structures.

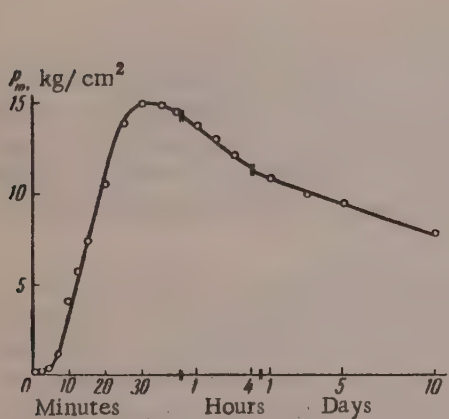


Fig. 1. Course of structure formation in a suspension containing 30% plaster, 70% sand, and 50% water on the dry mixture.

The course of structure formation in plaster suspensions subjected to additional stirring at different stages of structure formation is shown in Fig. 2. Mechanical breakdown (stirring) of the structure formed at the first stage does not affect either its strength or the strength of the crystallization

structure which subsequently developed in the suspension (Fig. 2, Curve 1). At this stage the suspension contains a coagulation structure of particles of plaster, sand, and of nuclei of the new dihydrate phase, but as yet there is no continuous crystallization framework; its formation and growth are associated with the rapid increase of plastic strength. If the suspension is now stirred again, the crystallization structure now present in it is broke down irreversibly, and the structure formed during subsequent hardening is much weaker (Fig. 2, Curves 2 and 3).

It must be noted that stirring of the suspension 12-15 minutes after it is mixed not only causes irreversible breakdown of the crystallization structure formed by that time, but also prevents the development of such a structure later (Fig. 2, Curve 4), although the hydration process at the second stirring of the suspension (after 12-15 minutes) is far from complete. Therefore in this case, also, the continuing hydration of plaster is unaccompanied by hardening.

Under normal conditions, when a crystallization structure forms in plaster suspensions, the instant when this structure reaches its maximum strength coincides with the end of hydration, i.e., the conversion of all the plaster into the dihydrate. This was demonstrated by parallel determinations of the course of strength increase and of hydration (as shown by the evolution of heat) [8]. Figure 3 shows the results of one such experiment,

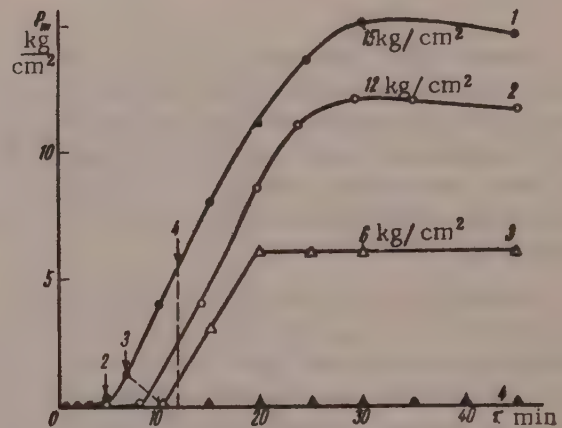


Fig. 2. Increase of plastic strength P_m of the structure in suspensions of 30% plaster, 70% ground quartz sand, and 50% water on the dry mixture ($W/S = 0.5$), with breakdown of the structure at different stages of its formation: 1) original suspension ground for 1-3 minutes when mixed; 2) the structure was again stirred for 2 minutes at the end of 5 minutes; 3) ditto, at the end of 7 minutes; 4) ditto, at the end of 12-14 minutes.

for a suspension containing 30% plaster, 70% sand, and 50% water on the dry mixture. This result is in full agreement with earlier data [11] and shows that the strength increase of the crystallization structure is caused by crystallization of the dihydrate, and ceases when that process is completed. The usual prolonged hardening of plaster samples, which led Baikov [1] to conclude that the end of hydration and the end of hardening do not coincide in time, is in reality due to the increase in the hardness of the gypsum structure during drying.

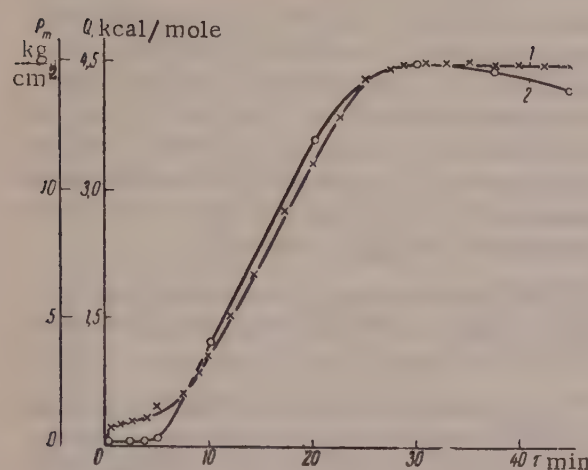


Fig. 3. Parallel determinations of the course of heat liberation (1) and of structure formation as indicated by the increase of plastic strength (2), in suspensions of the same composition as in Figs. 1 and 2.

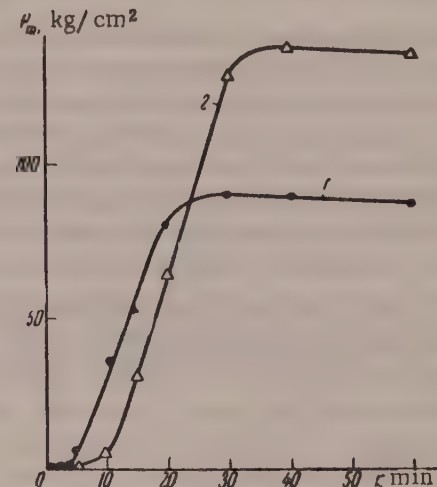


Fig. 4. Course of structure formation in plaster suspensions: 30% plaster, 70% ground quartz sand, and 50% water on the dry mixture; 1) at 25°; 2) at 70°.

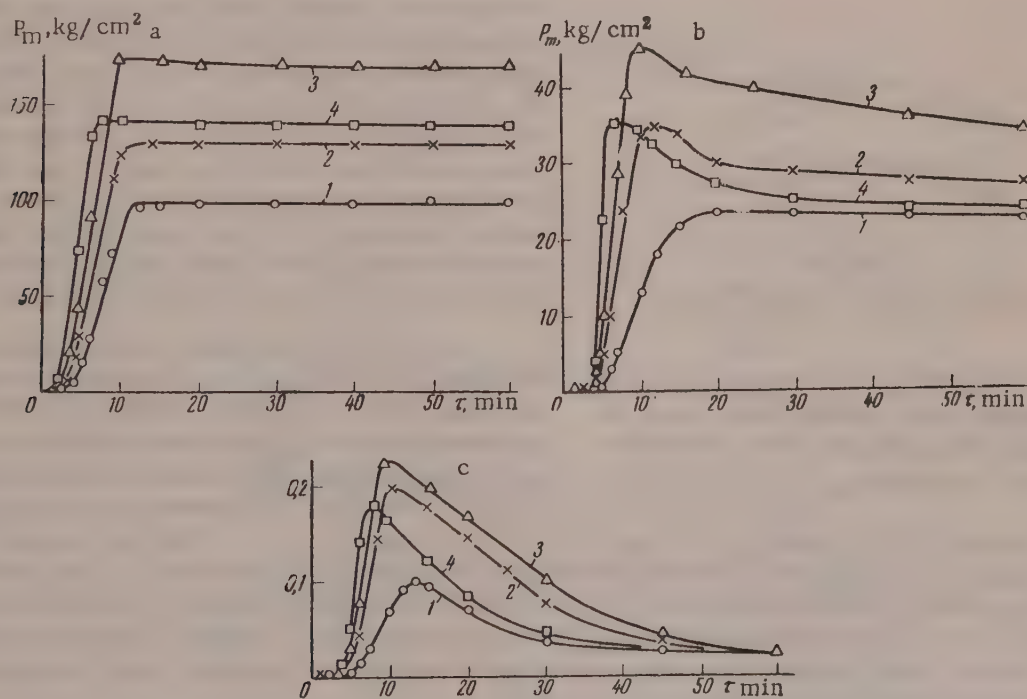


Fig. 5. Course of structure formation in plaster suspensions as a function of the nominal specific surface of the original plaster; 1) 3060 cm²/g; 2) 7180 cm²/g; 3) 12000 cm²/g; 4) 15000-18600 cm²/g. Water content (W/S ratio); a) 0.3; b) 0.6; c) 2.0. Composition of suspension: 30% plaster + 70% ground quartz sand + water.

The influence of conditions of crystallization of the dihydrate on the strength of its crystallization structure was studied in experiments in which the temperature and the dispersity of the original plaster were varied, and dihydrate was added to the suspension.

It is known [4] that much higher supersaturations are reached in the hydration of plaster at 25° than at 70°, and therefore larger dihydrate crystals are formed at 70°. This was confirmed by direct microscopic observations, and also by sedimentation analysis of the dihydrates formed at 25 and 70°. Figure 4 shows that under these conditions large crystal size corresponds to high strength of the crystallization structure.

For determination of the influence of particle size, the original plaster was ground in a 3-liter vibratory 4M-10 mill (at 3000 vibrations per minute). The course of structure formation was studied at different W/S ratios. The results for three of these are given in Fig. 5. It should be noted that hydration of the plaster was complete in all the experiments; this was confirmed by parallel determinations of heat evolution in these suspensions. It follows from Figs. 5 and 6 that the strength of the crystallization structure as a function of the dispersity of plaster of Paris [9] passes through a maximum at $S_{nom} = 1200 \text{ cm}^2/\text{g}$, irrespective of the water content of the suspension. Further increase of the dispersity of the plaster to $15000 \text{ cm}^2/\text{g}$ and over results in a decrease of strength, but the value remains higher than the strength of the structure at $S_{nom} = 3060 \text{ cm}^2/\text{g}$.

Observations under the microscope showed that the size of the dihydrate crystals decreases with increasing dispersity of the original plaster. Thus in these experiments, in contrast to the preceding, strength increase of the crystallization structure is associated with a decrease of the crystal size.

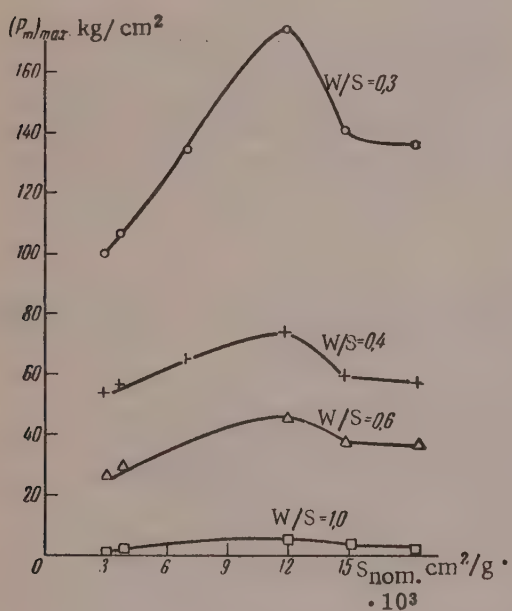


Fig. 6. Variation of maximum strength of structure with the dispersity of the original plaster in suspensions containing 30% plaster and 70% ground quartz sand at various W/S ratios.

accelerate hardening without lowering the strength of the crystallization structure. On further increase of the dihydrate content in the suspensions, acceleration of the process is accompanied by a sharp decrease in the strength of the hardening structure. When half or all of the sand is replaced by dihydrate, the strength of the crystallization structure is decreased 30- to 60-fold as compared with the normal strength of hardened plaster with sand, without added dihydrate. Hydration of the hemihydrate was complete in all cases; this was confirmed by determinations of heat evolution.

These experiments demonstrate most convincingly that hydration of plaster, even in fairly concentrated suspensions, need not result in the formation of a hardening structure; this requires the formation of stable crystallization contacts — sites of direct concretion — between the individual dihydrate crystals. It seems that in

The experiments revealed very clearly the characteristics of the strength decrease of the crystallization structure of gypsum when stored under moist conditions. The process was characterized by the ratio of the strength of the structure 45 minutes after preparation, $(P_m)_{45}$, to the maximum strength $(P_m)_{max}$.

The higher the water content of the suspension, i.e., the more porous the crystallization structure and the higher the dispersity of the original plaster, the more rapid is the spontaneous strength decrease of the crystallization structure (Fig. 7); for $S_{nom} = 3060$, at $W/S = 2.0$, $(P_m)_{45}/(P_m)_{max}$ is 0.4, whereas for $S_{nom} = 7180$ the value decreases to 0.2. This strength decrease is irreversible, and persists after drying. These experiments provide an explanation of the fact, known from practical experience [4], that gypsum samples kept under moist conditions have lower strength after drying than samples dried immediately after hydration.

For studies of the influence of added gypsum (dihydrate) on the strength of the structure formed in hardening, mixtures containing different amounts of ground quartz sand and gypsum were added to a standard suspension containing 30% of hemihydrate. It is clear from Fig. 8 that small amounts of the dihydrate merely

presence of large amounts of added dihydrate in the plaster suspension the conditions necessary for the formation of such contacts do not arise. The presence of the dihydrate should influence the magnitude and the variation of the supersaturation in suspensions of calcium sulfate hemihydrate.

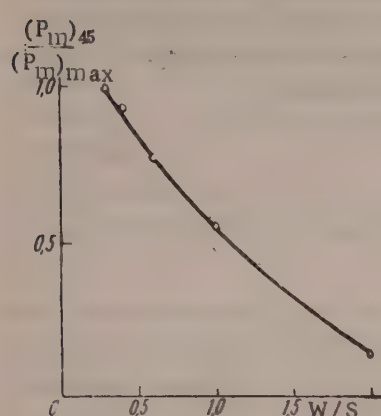


Fig. 7. Variation of $(P_m)_{45} / (P_m)_{\text{max}}$ ratio with the water-solid ratio.

The particles are held together by van der Waals forces, the strength of crystallization structures is determined by the formation of stable crystallization contacts between individual crystals. The experimental data presented in Figs. 9 and 10 show that such contacts can be formed if a definite degree of supersaturation is maintained in the suspension for long enough. This occurs in concentrated suspensions of plaster of Paris or other mineral cements which interact with water to form solutions supersaturated with respect to the stable hydrates of the

Figure 9 shows the course of variations of supersaturation, as shown by changes in the conductivity, in a suspension of hemihydrate in presence of added dihydrate.

The conductivity was determined by the usual method, with the use of alternating current, at the optimum stirring rate (400. r.p.m.). The dihydrate was introduced into the suspension during its preparation. Crystals of the dihydrate, which are capable of acting as crystallization centers, accelerate the crystallization of gypsum from the supersaturated solutions present in the suspensions, and thereby accelerate the whole hydration process. It is clear from Fig. 9 that the time during which maximum stable supersaturation persists in the suspension decreases with increase of the amount of dihydrate added, and when the amounts added are large, the upper limit of supersaturation is not reached at all and the supersaturation of the suspension decreases rapidly.

Analysis of the experimental results leads to the following conclusions. In contrast to the unstable coagulation structures,

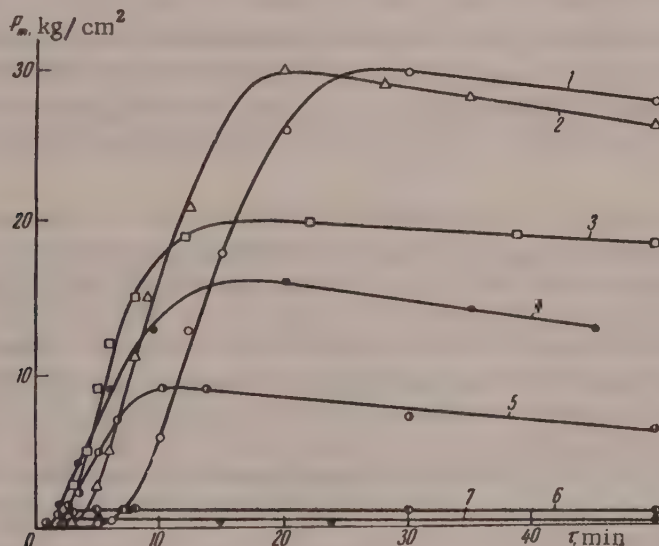


Fig. 8. Course of structure formation in suspensions containing 30% hemihydrate and various amounts of sand and dihydrate, $W/S = 0.6$.

Curves	1	2	3	4	5	6	7
Sand, %	70	68	65	60	50	20	0
Dihydrate, %	0	2	5	10	20	50	70

respective compounds. If no appreciable supersaturation arises in the suspension, or if the supersaturation persists for only a short time, as, for example, in the presence of large amounts of added dihydrate, a crystallization structure is not formed and hydration merely leads to growth of free crystals of the dihydrate.

This is the case in the experiments represented in Fig. 2. Additional stirring of the suspension 12-15 minutes after its preparation almost completely prevents further structure formation, although the hydration process is not yet complete. The explanation is that by the time of the second stirring and suspension already contains so much newly formed dihydrate that further dissolution of the hemihydrate in the suspension cannot maintain appreciable supersaturation. Therefore under these conditions only the existing dihydrate crystals grow, but crystallization contacts between them are not formed, i.e., a hardening structure does not form. If, however, the suspension is not stirred again (Fig. 2, Curve 1), its strength continues to increase rapidly, and the process terminates only when all the hemihydrate has been converted into the dihydrate.

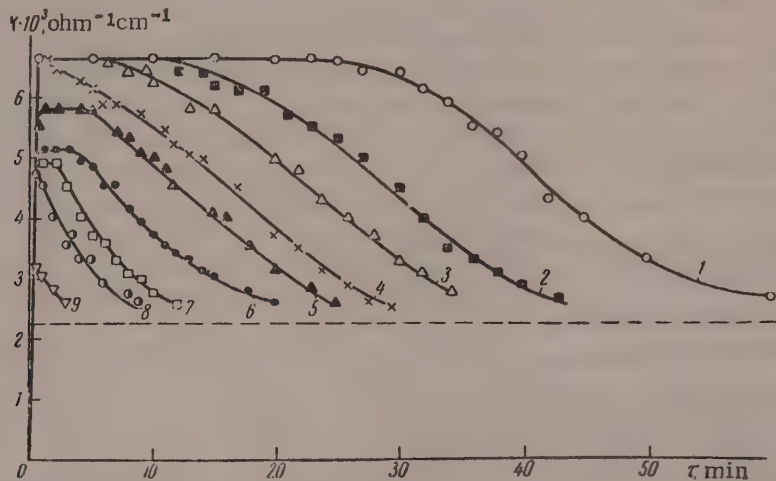


Fig. 9. Variations of conductivity in suspensions containing 25 g of hemihydrate in 500 ml of water with additions of dihydrate: 1) 0; 2) 1 g; 3) 3 g; 4) 10 g; 5) 20 g; 6) 25 g; 7) 50 g; 8) 75 g; 9) 100 g.

This means that at the beginning, when a high degree of supersaturation is still maintained in the plaster suspension and crystallization contacts can be formed, the skeleton of the crystallization structure is formed; subsequently, when the degree of supersaturation is not high, the individual crystals of dihydrate forming the skeleton grow. It is found experimentally that this process is also accompanied by strengthening of the crystallization structure.

High degrees of supersaturation are maintained in the liquid phase of the suspension so long as the loss of substance from solution as the result of crystallization is balanced by dissolution of the original substance. The higher the dispersity of the plaster, the greater is its total solution rate and the greater is the time (as a fraction of the total hydration time) during which a high degree of supersaturation is maintained in the suspension, with favorable conditions for the formation of crystallization contacts. Therefore the strength of the crystallization structure increases with increasing dispersity of the original plaster. However, the strength of the hardened structure increases with the dispersity of the original plaster only up to a certain limit, 12000 cm^2/g for the plaster studied, beyond which the strength decreases. This shows that if a high degree of supersaturation is maintained too long, as in this instance, conditions become unfavorable for crystallization-structure formation, probably because of the formation of a large number of very fine crystals of dihydrate in conditions unfavorable for their growth.

Crystallization contacts, which are regions of direct concretion of the newly formed crystals, must inevitably have a deformed crystal lattice, as they join crystals of completely random orientation. It is known that crystals with deformed, stressed lattices have excess free energy, and therefore, higher solubility than correctly formed, unstressed crystals [12]. Therefore crystallization contacts, which are not in thermodynamic equilibrium and have higher solubility, cannot be in equilibrium with correctly formed and not excessively-small crystals of the dihydrate. Therefore, when the structure is kept under moist conditions, recrystallization processes occur, in which the contacts dissolve and free crystals grow. These processes are accompanied by an irreversible decrease in the strength of the crystallization structure of the gypsum, the decrease being more rapid at higher porosities of the structure and higher initial dispersities of the hemihydrate, i.e., with greater

densities of the crystallization contacts in the structure. Such spontaneous breakdown of crystallization structures is more difficult to observe in ordinary plaster samples without filler, where the process is very slow because of the relatively low porosity. To accelerate the recrystallization processes, samples of hardened plaster were subjected to repeated alternate wetting and drying (without leaching of the gypsum). It was assumed that when the samples were wetted, the crystallization contacts should dissolve first, and on drying the substance should crystallize on the regular crystal faces, with a consequent decrease of strength. The results of the experiments confirmed this assumption (see table). After the first wetting the drying the strength increased somewhat, probably because of the dissipation of possible stresses on moistening. Subsequently the strength fell continuously and irreversibly.

Effect of the Number of Repeated Wettings on the Compressive Strength of Plaster Samples ($2 \times 2 \times 2$; W/P = 0.6)

Number of wettings	0	1	5	10	20	40
Compressive strength, kg/cm ²	200	210	150	90	60	20

irreversible decrease of strength caused by such recrystallization must be distinguished from the reversible lowering of plaster strength caused by adsorption.

The enormous role of stable supersaturation in the formation of the hardening structure shows that crystallization hardening in suspensions of highly disperse calcium sulfate dihydrate, which has been recommended as a peculiar type of bonding material [13], is impossible, because the degrees of supersaturation which might be reached in the suspension from the colloidal fraction cannot be achieved because of the enormous amount of dihydrate present. Therefore recrystallization of the colloidal particles cannot lead to the formation of crystallization contacts under such conditions. The strength of such systems, as of clays, if their density is high enough is the consequence of removal of water during drying, and the resultant strengthening of coagulation contacts between the crystals when they are very close together.

It is known that such structures, in contrast to crystallization structures, have no water resistance, i.e., they lose strength completely when wet.

SUMMARY

1. A study was made of structure formation in suspensions of plaster of Paris, and the influence of the crystallization conditions on the strength of the crystallization structure of the dihydrate.

Structure formation in plaster suspensions proceeds in the following three stages:

- a) the induction period, during which a coagulation structure composed of small crystals of the original hemihydrate and of newly formed dihydrate crystals is formed in the suspension;
- b) formation and growth of a dihydrate crystallization structure; this, in contrast to the primary coagulation structure, is irreversibly broken down by mechanical forces;
- c) strength decrease of the crystallization structure during storage under moist conditions, as the result of recrystallization effects.

2. The crystallization structure is formed as the result of recrystallization of dihydrate from supersaturated solution, with formation of stable crystallization contacts or points of direct concretion between the crystals. The strength of the crystallization structure ceases to increase when the hydration process, i.e., the crystallization of the dihydrate, is complete.

3. Crystallization structures, i.e., hardened structures, are thermodynamically unstable and break down spontaneously and irreversibly in presence of moisture as the result of crystallization processes which lead to dissolution of the crystallization contacts - the regions of crystal concretion.

Similar results are obtained when plaster samples are kept for a long time in their own saturated solution.

Thus, the low water resistance of plaster articles, which is usually wrongly attributed to the high solubility of gypsum, is in reality observed even when dissolution does not occur, and is the consequence of recrystallization of crystallization contacts which are not in a state of thermodynamic equilibrium. The

4. The strength decrease as the result of recrystallization processes is greater at higher porosity (higher W/S ratio) of the structure and higher dispersity of the original plaster (higher density of crystallization contacts in the structure).

5. The strength of the crystallization structure as a function of the specific surface of the original plaster passes through a maximum; for the plaster studied, this is found at $S_{nom} = 12000 \text{ cm}^2/\text{g}$. The strength increase is the result of better conditions for formation of crystallization contacts, as high degrees of supersaturation can be maintained for longer periods in the suspension with increase of the dispersity of the original plaster. The fall of strength on further increase of dispersity is the consequence of the excessively small size of the dihydrate crystals formed.

6. Additions of dihydrate, which act as crystallization centers, accelerate dihydrate crystallization and therefore the hardening process. Small amounts of added dihydrate, which have hardly any effect on the extent and duration of the supersaturation, shorten the induction period of structure formation without decreasing the strength of the structure formed. Large amounts decrease the strength of the crystallization structure, as the degree and duration of the supersaturation decrease in their presence, and the conditions for formation of crystallization contacts are therefore worse.

University of Moscow
Faculty of Chemistry
Chair of Colloid Chemistry

Received April 18, 1958

LITERATURE CITED

- [1] W. Michaelis, Chem. Z. 982 (1893); A. A. Baikov, Collected Works 5 (Izd. AN SSSR, 1948); *V. Khakimov, Trans. Chem. Inst. Kirghiz Branch, Acad. Sci. USSR 3 (1950); Wo. Ostwald and W. Wolski, Kolloid Z. 27, 78 (1920); V. V. Konstantinov, Bull. Acad. Sci. Kazakh SSSR 126, 78 (1954); H. G. Fischer, ASTM Bull. 192, 43, (1953); J. A. Muray, and H. G. Fischer, Proc. Amer. Soc. Test. Mater. 51, 1197, (1951); V. F. Zhuravlev, Chemistry of Cements (Leningrad-Moscow, 1951); *O. P. Mchedlov-Petrosian, Proc. Acad. Sci. USSR 89, 1, 137 (1953); Proc. Conference on Cement Chemistry (1956), p. 63.*
- [2] J. A. A. Ketelaar and D. Hejman, Roc. trav. chim. 73, 279 (1954); G. Becherer, Silikat Technik 6, 7, 292 (1955); G. Becherer, Naturwissenschaften 2, 41 (1954); P. P. Budnikov and Ia. K. Syrkin, Bull. Ivanovo-Voznesensk Polytech. Inst. 6, 235 (1922); I. I. Korol'kov and A. V. Krupnova, J. Appl. Chem. 26, 907 (1953).**
- [3] Ia. L. Zabechinskii, V. B. Ratinov, and T. I. Rozenberg, Proc. Acad. Sci. USSR 108, 6, 1137 (1956); B. V. Ratinov, Ia. L. Zabechinskii, and T. I. Rozenberg, Proc. Acad. Sci. USSR 109, 5 (1956).
- [4] P. P. Budnikov, Calcium Sulfate, its Investigation and Use (Stroizdat, 1943). *
- [5] B. Tavasci, Chim. industria 24, 309 (1942); C. L. Haddon, Trans. Faraday Soc. 20, 337 (1924); W. A. Cunningham, R. R. Kunham, and L. L. Antes, Ind. Eng. Chem. 44, 10, 2402, (1952); M. I. Strelkov, Proc. Conference on Cement Chemistry (1956), p. 183.*
- [6] Iu. M. Butt and T. M. Berkovich, Cements with Surface-Active Additives (Industrial Construction Press, 1953).*
- [7] V. N. Izmailova, E. E. Segalova, and P. A. Rebinder, Proc. Acad. Sci. USSR 107, 3, 425 (1956).
- [8] E. E. Segalova, V. N. Izmailova, and P. A. Rebinder, Proc. Acad. Sci. USSR 110, 808 (1956).
- [9] E. E. Segalova, V. N. Izmailova, and P. A. Rebinder, Proc. Acad. Sci. USSR 114, 594 (1957).
- [10] P. A. Rebinder and E. Segalova, Proc. 2. Internat. Congress of Surface Activity, (London, April, 1957).*
- [11] O. V. Kuntsevich, P. E. Aleksandrov, V. B. Ratinov, T. I. Rozenberg et al., Proc. Acad. Sci. USSR 104, 4 (1956).
- [12] F. M. Lea and R. M. Nurse, Disc. Faraday Soc. 5, 345 (1948).
- [13] L. G. Gulinova and V. A. Ipat'eva, Unfired Gypsum Cement and Articles Made from It (Kiev, Acad. Architect. Ukrainian SSR Press, 1954); *I. I. Rivlin and L. P. Papkova, Trans. Khar'kov Polytech. Inst., Chem. Technol. Ser., 8, No. 3, 219 (1956).

*In Russian.

**Original Russian pagination. See C.B. Translation.

EFFECT OF ADDITIONS OF A HYDROPHILIC PLASTIFIER*ON THE
KINETICS OF STRUCTURE FORMATION IN THE
HARDENING OF CEMENT **

E. E. Segalova, R. R. Sarkisian, and P. A. Rebinder

Extensive and diverse experimental and production data are available on the influence of hydrophilic organic surface-active substances such as sulfite alcohol waste liquor (SSB) on the properties of cement mixes, pastes, and concretes. These data indicate that small amounts of added SSB are highly effective for improvement of the technological and service properties of cements and concretes; in a number of cases it is possible to increase the strength, density, and durability, with considerable savings of cement [1].

However, the existing industrial and experimental data are often very contradictory. In a number of cases the effect of the additive was not the expected liquefaction and decrease of the water retention of the cement paste, but an increase; setting was greatly accelerated rather than retarded, and the mixes sometimes lost mobility so rapidly that they could not be used. Under such conditions a normal cement is converted into the so-called "bystriak" (quick-setting cement) by the addition of SSR [2].

Accordingly, Shestoporov [3] classified high-alumina cements, which usually showed adverse results on addition of SSB, as unplastifiable.

These contradictory results in the action of SSB on cements of different mineral composition may be explained in the light of our studies of the influence of surface-active additives on structure formation in suspensions of mineral cements [4]. It was shown that a Portland cement suspension passes through three stages during mixing.

Stage I, the formation of a coagulation structure of cement particles and newly formed hydrates (this stage is generally very short in absence of a hydrophilic stabilizer);

Stage II, the development of a continuous loose crystallization structure consisting of hydroaluminate; this causes rapid thickening of the paste;

Stage III, where mechanical breakdown of the hydroaluminate crystallization structure is followed by formation of hydrate crystals in the suspension.

When the hydrophilic SSB additive is introduced, the first stage in the life of the cement suspension, before a crystallization structure of hydroaluminate is formed in it, is greatly prolonged. Mechanical breakdown of the crystallization structure formed in presence of SSB is followed by thickening of the cement suspension in consequence of the great reduction in size of the newly formed substance (mainly hydro and sulfo-aluminate) owing to their adsorption of SSB during crystallization. This suggests that the water capacity of cement in presence of this additive depends on which stage the cement paste is at, and this in its turn depends on the conditions of preparation and the manner in which the additive is introduced.

The mechanical properties of the cement suspensions were characterized by the plastic strengths as determined by means of the cone plastometer, while the water capacity was characterized by the value of the water-cement ratio (W/C) at which the cement pastes had the same initial plastic strength.

* "Plastifier", "plastification", etc., are special terms, and are not to be confused with "plasticizer", "plasticization", which refer to softeners added to plastics. These terms are repeatedly used in papers by P. A. Rebinder.

** Paper at the 4th All-Union Conference on Colloid Chemistry in Tbilisi, May 1958.

Two clinkers were used in the experiments: a low-aluminate clinker from the Komsomolets factory (KMS), and a high-aluminate clinker from the Armenian factory (ARM); their calculated mineral composition and specific surface (calculated from the air permeability) are given in Table 1.

Table 1

Clinker	Mineral contents, %				Specific surface cm ² /g
	C ₃ S	C ₂ S	C ₃ A	C ₄ AF	
ARM	51.6	20.4	10.3	12.5	4000
KMS	48.5	33.8	4.4	12.6	3500

The clinkers were ground in a laboratory ball mill; 5% of gypsum (dihydrate) was added during the grinding.

To obtain cement paste in Stage I, it was mixed for 1-2 minutes, so that there was not enough time for a crystallization hydroaluminate structure to form, while to obtain Stage III paste it was stirred until the crystallization structure was broken down completely. The duration of stirring was greater with larger amounts of SSB added with the mixing water,

and the stirring was ended only when the plastic strength reached a constant value, which remained without appreciable change on further stirring. Continuous rubbing of the suspension is not necessary, and it might lead to additional dispersion of the cement particles; it is merely necessary to prevent mechanically the formation of a continuous crystallization structure in the suspension.

In the preparation of Stage I and III cement pastes, the SSB was always added with the mixing water. Another method, introduced by S. V. Shestoporov to prevent quick setting, is to add the SSB after previous hydration of the cement. The cement is first mixed with somewhat less water than required for the given W/C ratio, and the rest of the water containing the SSB is added to the paste after 25-30 minutes of stirring.

The course of structure formation in cement paste depends on the stage at which stirring of the system (mixing of the cement paste) ceases. If the stirring is stopped at Stage I, a crystallization hydroaluminate structure is formed very rapidly; this corresponds to the formation of a quick-setting cement. If the stirring is continued to Stage III, i.e., if the hydroaluminate crystallization structure is broken down completely, further increase of plastic strength is gradual, and is due mainly to hydrosilicate hardening, and the product is a normal-setting cement.

The increase of plastic strength in cement pastes obtained after different times of stirring in presence of SSB is shown graphically in Fig. 1.

The plastic strength of Stage I cement paste first falls sharply as the result of a lengthening of the induction period of structure formation in presence of SSB, but this decrease is succeeded by a sharp increase of plastic strength as the result of the formation of a crystallization hydroaluminate structure (Curve 2).

If the SSB is introduced after previous hydration, the structure formation in the cement paste is greatly retarded (Curve 4).

The plastic strength of cement paste at Stage III (Curve 3) is high at first because of the thickening influence of the finely divided newly formed substances, but after 3-4 hours the retarding effect of the additive on the hydration of silicate minerals prevails; structure formation in the latter largely determines the further course of the strength increase. The thickening effect of the additive on Stage III cement paste increases with the concentration of the additive up to a certain value which depends on the aluminate content of the cement. Figure 2 shows that the higher the SSB content, the greater is the plastic strength of the paste during the first 2-3 hours after mixing, but after this the position of the curves is reversed.

It follows from Fig. 3 that the plastifying effect of the additive is greatest at Stage I, when the suspension is almost completely liquefied. The increase of plastic strength with > 1.0% SSB can be attributed to the formation of adsorption layers of considerable thickness on the cement particles. When cement paste is made in presence of SSB in Stage III, its plastic strength increases continuously with SSB content. Despite the wide range of SSB contents, no plastifying effect on the coagulation structure of the hydroaluminate could be detected.

This mechanism of the action of hydrophilic additives on structure formation in cement pastes can be used in solution of problems relating to the optimum utilization of SSB as an additive to cement pastes and

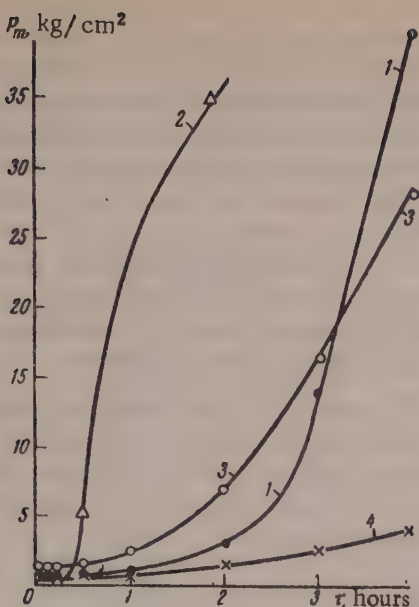


Fig. 1. Course of structure formation in cement pastes made by different methods: 1) Without additive, stirred for 5 minutes; 2) with SSB, Stage I, stirred for 1 minute; 3) with SSB, Stage III, stirred for 20 minutes; 4) SSB added after previous hydration of the cement; ARM clinker; W/C = 0.27; 0.3% SSB added on the weight of cement.

concrete. In particular, it provides an explanation of the occasional acceleration of setting and of the increase of the water capacity of cement pastes resulting from the introduction of the additive.

Setting is accelerated because a crystallization hydroaluminite structure is formed in presence of SSB in the cement paste, when Stage I is brief but longer than the time of stirring.

The water capacity increases in cement suspensions for which Stage I is so brief that the crystallization structure which forms is broken down during the preparation of the paste, so that at the end of the mixing the paste is at Stage III.

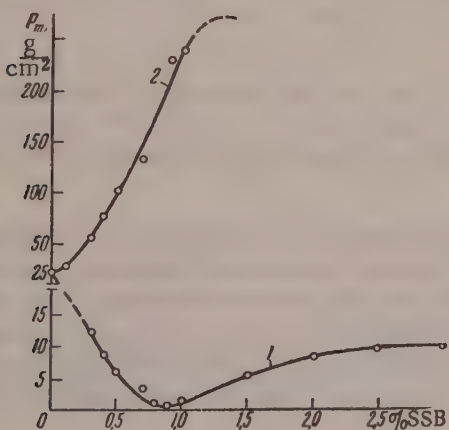


Fig. 3. Effect of amount of SSB added on the plastic strength of cement paste: 1) At Stage I; 2) at Stage III. ARM Clinker W/C = 0.26.

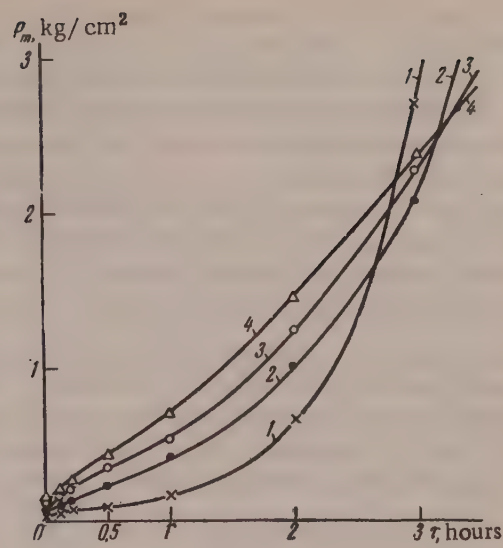


Fig. 2. Course of structure formation in Stage III cement pastes with various amounts of added SSB: 1) Without SSB; 2) 0.3% SSB; 3) 0.4% SSB; 4) 0.5% SSB. ARM Clinker; W/C = 0.26.

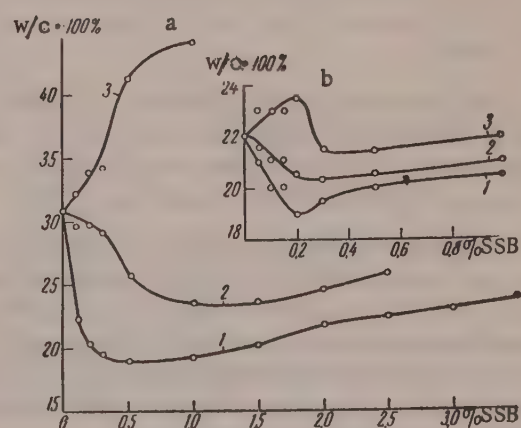


Fig. 4. Water-cement ratios required for production of cement pastes of equal plasticity made by different methods in presence of SSB: 1) At Stage I; 2) SSB added after previous hydration of the cement paste; 3) at Stage III; a) ARM clinker; b) KMS clinker; $(P_m)_{init} = 27 \text{ g/cm}^2$.

The water-cement ratios required for the production of ARM and KMS cement pastes of equal plasticity in presence of SSB are given in Fig. 4. The cement paste was made at Stages I and III, and also by introduction of SSB after previous hydration. The initial plastic strength was 27 g/cm² for all the systems. The greatest plastifying effect, i.e., the greatest decrease of the water-cement ratio, is found when the cement paste is made at Stage I; the minimum W/C ratio obtainable with complete stabilization of the suspension is independent of the mineral composition of the cement, and is 19% for both clinkers. The water-cement ratio can also be decreased by previous hydration (Curve 2), but fairly large amounts of SSB are required to produce any substantial decrease. This is the consequence of the considerable differences between the cement paste at Stage I and the paste obtained with addition of SSB after previous hydration. The former is a fairly coarse suspension, and therefore small amounts of surface-active substance are sufficient to stabilize it completely. In the latter case, the paste already contains large amounts of highly disperse new material, so that the total surface of the disperse phase is much greater. Evidently very much more of the additive is required to stabilize such a suspension.

The production of a cement paste of equal plasticity at Stage III in presence of SSB requires an increase of the water-cement ratio (Curve 3). In the case of ARM clinker it was not possible to reach the amount of additive which would lower the water-cement ratio at stage III. This was possible in the case of KMS clinker (Fig. 4,b, Curve 3). Addition of up to 0.2% SSB increased the water-cement ratio required for the formation of cement paste of equal plasticity, whereas additions of over 0.2% SSB decreased it.

TABLE 2

Duration of Stage I in Presence of Different Amounts of SSB in Pastes from ARM and KMS Clinkers, for Initial $P_m = 27 \text{ g/cm}^2$

Clinker	Duration of stage I in minutes, with different additions of SSB (% on weight of cement)						
	0,1	0,2	0,3	0,5	1,0	1,5	2,0
ARM	—	5—8	15	20	40	50	100
KMS	20	30	50	75	200	—	—

The duration of Stage I (time from the start of mixing to the crystallization of newly-formed aluminates) for cement pastes made from ARM and KMS clinkers with different amounts of SSB is given in Table 2.

The duration of Stage I is much greater, with equal amounts of SSB, for the low-aluminate KMS cement than for ARM cement. Stage I in the high-aluminate cement can be prolonged by an increase of the amount of SSB added.

For investigation of the influence of different amounts of SSB, and different methods of their introduction, on the hardening of cement, cement specimens were prepared with the W/C ratios indicated in Fig. 4, with constant initial plastic strength of 27 g/cm², and their strength was determined after 3, 28, and 90 days. The results of these tests are given in Figs. 5 and 6.

The greatest strength increase, relative to the control specimens, was found in the specimens prepared at Stage I. However, this increase occurs only on addition of SSB up to a certain limit. Further increase of the amount of SSB results in a sharp fall of strength; the SSB content at which this occurs increases with increasing age of the specimens. In the case of cement made from KMS clinkers (Fig. 5,b) decreases of strength occur at much smaller additions of SSB than in the specimens made from the high-aluminate cement. The strength decrease during the induction period is replaced by a rapid increase, which ultimately results in the formation of a product of higher strength.

The mechanism of the action of SSB is the same in both cements; the only difference is that the retarding effect of the additive is more pronounced, and occurs with considerably smaller amounts of SSB, in KMS cement. Whereas in the case of KMS cement 0.3% of SSB completely inhibits the strength increase of three-day specimens, 2.0% of SSB is required to produce the same effect in ARM cement of the same age.

The explanation is that SSB is strongly adsorbed by newly-formed aluminate minerals in the course of crystallization, and therefore the higher the aluminate content of the cement, the less of the additive is available for the silicate minerals. Indeed, if 3% of tricalcium aluminate (C_3A) is added to the low-aluminate KMS clinker, considerably larger amounts of SSB must be added to decrease the cement strength (Table 3).

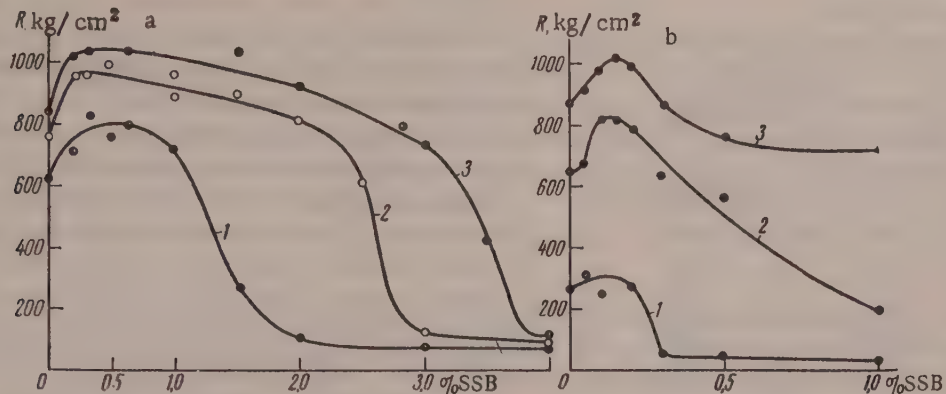


Fig. 5. Effect of amount of SSB added on the strength of cement (R , kg/cm^2) prepared at Stage I. Ages of cement specimens: 1) 3 days; 2) 28 days; 3) 90 days; a) ARM clinker; b) KMS clinker.

Table 3 shows that after 3 days 0.3% of SSB inhibits the strength increase of cement made from KMS clinker without added C_3A . The strength in this case is $50 \text{ kg}/\text{cm}^2$. Cement containing 3.0% of C_3A has a strength of $665 \text{ kg}/\text{cm}^2$ at the same age with the same amount of added SSB. The strength is similarly increased in presence of 0.5% of SSB.

The curves for the variations of cement strength with the amount of SSB added after previous hydration (Fig. 6) are similar to the curves for Stage I cements, but they begin to descend at much lower SSB contents.

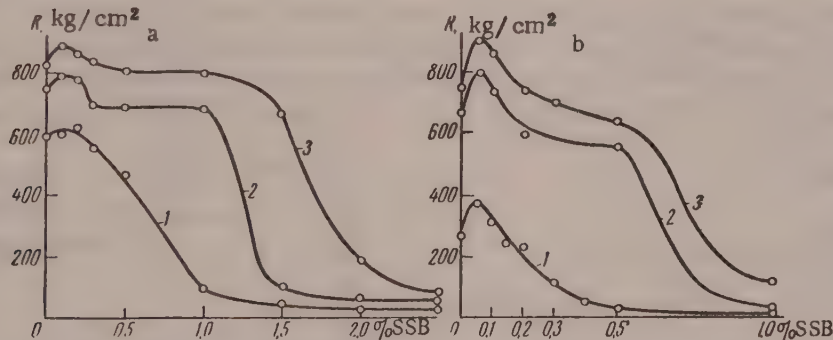


Fig. 6. Effect of amount of SSB added on the strength of cement (R , kg/cm^2) made by addition of SSB after previous hydration; ages of cement specimens: 1) 3 days; 2) 28 days; 3) 90 days; a) ARM clinker; b) KMS clinker.

The addition of SSB after previous hydration produces almost no strength increase in cement made from high-aluminate clinker; it was for this type of clinker that this method was recommended by S. V. Shestopalov.

Studies of the course of structure formation in cement pastes based on determinations of plastic strength, followed by compressive tests on hardened specimens, make it possible to follow the entire process of cement hardening from its earliest stages. In Figs. 7 and 8 the plastic strengths of the same specimens are conventionally plotted in the same graphs, which thus represent the effects of SSB on the general kinetics of cement hardening.

The course of structure formation in cements made with equal water-cement ratios ($W/C = 0.25$) is plotted in Fig. 7. Figure 8 shows corresponding data for cements of equal initial plasticity (initial $P_m = 27 \text{ g/cm}^2$). The cement paste with added SSB was made at Stage I, i.e., before the hydroaluminate crystallization structure was formed. The strength in kg/cm^2 is plotted against the time of hardening; the plastic strength values determined by the cone plastometer are followed by compressive strengths of blocks. The transitions between the two systems of determinations are represented by dash lines. The hardening curves for systems without added SSB each have a single S-bend. In these systems the crystallization structure of the aluminate minerals was broken down during the mixing. Appreciable increase of strength begins after 2-3 hours, mainly as the result of structure formation in the silicate component of the cement clinker. Curves for systems with added SSB have two S-shaped bends. Addition of SSB lengthens the induction period of structure formation in the aluminate minerals, so that the first rapid increase of strength is caused by crystallization of the newly-formed aluminates. The formation of the crystallization structure of the hydroaluminate is largely complete after 3-4 hours. The second rapid increase of strength is caused by structure formation in the silicate component of the cement clinker.

TABLE 3

Effect of Added C_3A on the Strength of Cement Made from KMS Clinker in Presence of Added SSB, $(P_m)_{\text{init}} = 27 \text{ g/cm}^2$

Amount added, % on cement weight	C ₃ A	SSB	Compressive strength in kg/cm^2 at age of		
			W/C • 100%	3 days	28 days
—	0,0	—	22,0	275	650
—	0,3	—	19,5	50	640
—	0,5	—	19,5	44	570
—	1,0	—	20,5	3	200
3	0,3	—	19,5	665	850
3	0,5	—	19,5	540	762
3	1,0	—	20,5	52	400

At constant W/C ratio (Fig. 7), Curve 2 lies above Curve 1 only at the earliest stages of structure formation; the curves then intersect and the final strength of the hardened cement with added SSB is always lower than that of cement without the additive, for the same W/C ratio.

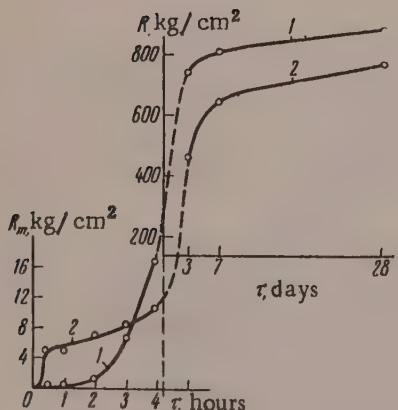


Fig. 7. Strength increase during hardening of cement, for constant $W/C = 0.25$; ARM clinker: 1) Without added SSB; 2) 0.5% SSB; P_m) plastic strength of cement paste; R) compressive strength of set cement.

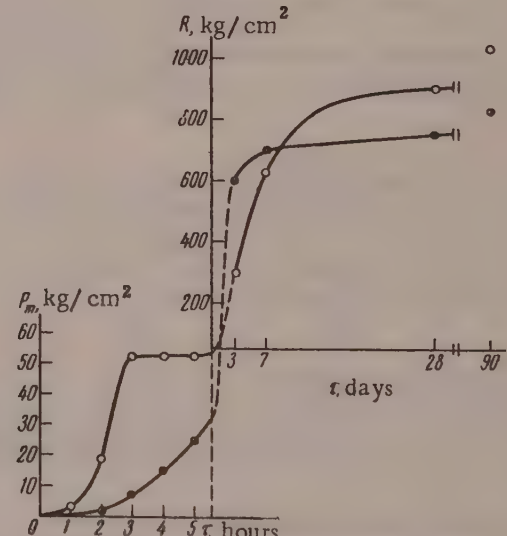


Fig. 8. Strength increase during hardening of cement, for constant initial plasticity; ARM clinker, initial $P_m = 27 \text{ g/cm}^2$; O) Without additive; $W/C = 0.305$; O) 1.5% SSB; $W/C = 0.215$; P_m) plastic strength of cement paste; R) compressive strength of set cement.

At constant initial plasticity (Fig. 8), addition of SSB increases cement strength. The lower 3 and 7-day strengths can be attributed to the retarding effect of the additive on structure formation of the silicate component of the cement clinker. It should be noted that if the amount of SSB added to the high-aluminate ARM

cement is not large (0.3-0.5%), it is all adsorbed during the crystallization of newly-formed aluminate minerals and the silicate minerals harden normally, as if in absence of the additive. The data presented in Fig. 7 and 8 emphasize once again that in presence of added SSB the strength of cement can be increased only by condensation of the structure, i.e., by decrease of the W/C ratio. At a given W/C ratio, added SSB lowers the strength of cement as the result of retarded structure formation and additional entrainment of air.

SUMMARY

1. Cement paste passes through three stages in the course of mixing, the stages being more pronounced in presence of hydrophilic plastifier: I, an induction period before the formation of a crystallization structure of newly formed aluminates derived from the aluminate component of the Portland cement clinker (tricalcium hydroaluminate); II, formation and development of the crystallization structure of the hydroaluminate, manifested in the rapid thickening of the cement paste as the result of strengthening of this structure, which arises during the mixing; III, complete mechanical breakdown of the hydroaluminate crystallization structure during mixing. Crystallization of the newly formed compounds (i.e., hydration) continues, but the crystals do not coalesce.

2. For a constant initial plasticity, the greatest decrease of the amount of mixing water can be obtained if the plastifier (SSB) is introduced with the mixing water and the cement paste is laid down at Stage I. The duration of this stage increases with decrease of the aluminate content and with increase of the amount of SSB added.

3. If the cement paste, containing plastifier added with the mixing water, is at Stage III during the mixing, the water capacity of the cement paste for a given initial plasticity increases with the dispersity and the aluminate content of the cement.

4. The water-cement ratio can also be lowered by the addition of SSB after previous hydration, at Stage III, but the decrease is less than that produced at Stage I.

5. For a given water-cement ratio, the strength of cement with added plastifier is always somewhat lower than that of cement without the additive. An increase of cement strength in presence of SSB is achieved by decrease of the water-cement ratio, with constant initial plasticity. The highest strength increase is obtained if the cement paste is laid down at Stage I.

6. In the case of high-aluminate cements, considerable increases of the amount of SSB from 0.2 to 0.5-1% do not lower the final strength of the cement, as the additive is adsorbed by the newly formed aluminates on crystallization. It is therefore possible to lower the water-cement ratio and to increase the strength of cement pastes and concretes based on high-aluminate cements with larger amounts of added SSB than usual.

University of Moscow
Faculty of Chemistry
Chair of Colloid Chemistry

Received April 18, 1958

LITERATURE CITED

- [1] E. I. Arieli, Bull. Constr. Techn. No. 14 (1946); Iu. M. Butt and T. M. Berkovich, Cements with Surface-Active Additives (Moscow, 1953);* B. D. Trinker, Use of Plastified Cement and Plastifying Additions to Concrete (Moscow, 1952);* S. V. Shestoporov, Durability of Concrete (Moscow, 1953).*
- [2] E. I. Arieli, Bull. Constr. Techn. No. 10 (1947); E. A. Galabutskaia, Bldg. Industry No. 11 (1948); B. D. Trinker, Collected Papers on Building No. 6 (1950).
- [3] S. V. Shestoporov, F. M. Ivanov, and T. Iu. Liubimova, Cement No. 6 (1952).
- [4] P. A. Rebinder and E. E. Segalova, Nature No. 12 (1952); P. A. Rebinder, E. E. Segalova, and O. I. Luk'ianova, J. Moscow Univ. No. 2 (1954); E. E. Segalova and E. S. Solov'eva, Proc. Conf. on Cement Chemistry (Moscow, 1956). *

*In Russian

KINETICS OF CRYSTALLIZATIONAL STRUCTURE FORMATION IN THE HYDRATION HARDENING OF TRICALCIUM ALUMINATE*

E. S. Solov'eva and E. E. Segalova

Studies of structure formation in suspensions of tricalcium aluminate $3\text{CaO} \cdot \text{Al}_2\text{O}_3(\text{C}_3\text{A})$ are of interest primarily because this mineral determines the behavior of Portland cement suspensions during the first few hours after mixing. The literature on tricalcium aluminate deals largely with its hydration products, their composition, stability, solubility, etc. [1]. The mechanism of hardening of C_3A has not been studied as such.

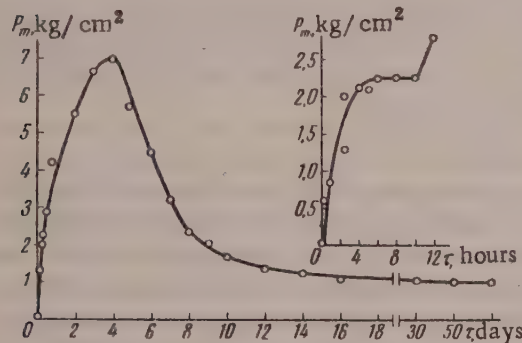


Fig. 1. Course of crystallizational structure formation in a suspension containing 5% C_3A , 95% ground quartz sand, and 50% water on the dry mixture; $t = 16-17^\circ$.

the cone plastometer [2]. Figure 1 shows that the induction period of structure formation, during which a coagulation structure of the original particles and newly formed crystals is formed in the C_3A suspensions, is very short [3, 4]. The formation and development of a crystallization structure of tricalcium hydroaluminate results in a rapid increase of plastic strength. It must be noted that the strength curve generally shows a peculiar inflection during the first few hours; this is clearly seen in Fig. 1 on an enlarged scale. A continuous crystallization structure is formed in C_3A suspensions as the result of direct concretion of tricalcium hydroaluminate crystals, deposited from the supersaturated solution formed in the suspension, with the formation of a loose framework [5]. The hardened structure reaches its maximum strength simultaneously with the conversion of all the anhydrous aluminate into the hydrate, as is clear from Fig. 2.

For determination of the amount of chemically bound water, a sample of suspension was covered with alcohol and thoroughly ground in a mortar. The resultant suspension was filtered and washed again with alcohol, and then with ether. The sample was dried at 105° and then heated at $800-900^\circ$.

Figure 3 shows the variation of the strength of the structure with the amount of tricalcium hydroaluminate formed in the suspension. The plastic strength and hydroaluminate content are expressed as percentages of their maximum values in the suspension at the end of hydration.

It is to this problem — crystallizational structure formation in suspensions of tricalcium aluminate — that this paper is devoted; it represents one of the investigations performed in P. A. Rebinder's laboratory [2-9] on the physicochemical mechanics of cements.

The solid phase of the suspensions studied consisted of 1-5% C_3A and 99-95% of finely ground quartz sand used as an inert filler. The processes of structure formation in such suspensions are determined by the C_3A , while the large amount of inert filler makes investigation of these systems easier. The prepared suspensions were put into special vessels and stored in a desiccator over water.

For studies of the course of structure formation in these suspensions and of their changes with time, their plastic strength was determined by means of

the cone plastometer [2]. Figure 1 shows that the induction period of structure formation, during which a coagulation structure of the original particles and newly formed crystals is formed in the C_3A suspensions, is very short [3, 4]. The formation and development of a crystallization structure of tricalcium hydroaluminate results in a rapid increase of plastic strength. It must be noted that the strength curve generally shows a peculiar inflection during the first few hours; this is clearly seen in Fig. 1 on an enlarged scale. A continuous crystallization structure is formed in C_3A suspensions as the result of direct concretion of tricalcium hydroaluminate crystals, deposited from the supersaturated solution formed in the suspension, with the formation of a loose framework [5]. The hardened structure reaches its maximum strength simultaneously with the conversion of all the anhydrous aluminate into the hydrate, as is clear from Fig. 2.

*Paper at the 4th All-Union Conference on Colloid Chemistry in Tbilisi, May 1958.

It follows from Figs. 2 and 3 that the strength increase is not proportional to the amount of hydroaluminate present in the suspension. The formation of hydroaluminate is very rapid at first, but the strength of the crystallization structure is relatively low. Thus, about 70% of the hydroaluminate is formed in the first 30 minutes, but the strength of the structure at this stage is only 30% of the maximum value. The hydration, very rapid at first, slows down (Fig. 2), and the gradual crystallization of the remaining 30% of the hydroaluminate results in a considerable strengthening of the initial weak crystallization.

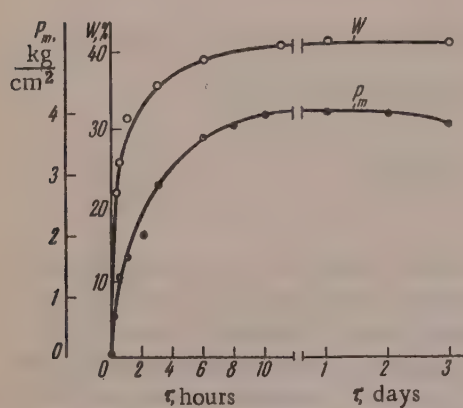


Fig. 2. Course of crystallizational structure formation and hydration of C_3A in a suspension containing 5% C_3A , 95% ground quartz sand, and 37% H_2O on the dry mixture; W is the amount of chemically bound water, as a percentage on the weight of C_3A .

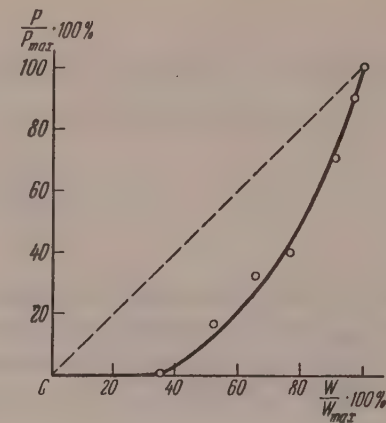


Fig. 3. Variation of the plastic strength of the crystallization structure with the amount of hydroaluminate formed in a suspension of 5% C_3A , 95% ground quartz sand, and 38% H_2O .

It was shown earlier [6, 7] that the formation of the crystallization structure, i.e., of the hardened structure, proceeds in two stages. During the first stage a fairly high degree of supersaturation is maintained in the suspension, and the newly formed crystals coalesce to form the framework of the crystallization structure. During the second stage the degree of supersaturation is not high, new crystallization nuclei and crystallization contacts are not formed, and the crystals forming the framework of the crystallization structure increase in size. The ratio between the lengths of the first and second stages of structure formation is determined most easily by direct measurements of the course of supersaturation in the suspension with time, or by determination of the time at which mechanical breakdown (stirring) of the hardening suspension completely prevents the formation of a crystallization structure in it.

After additional stirring, a crystallization structure can be formed again only if the degree of supersaturation required for formation of crystallization contacts still exists in the suspension [6, 8]. It is clear from Fig. 4 that if the suspension is stirred 30 minutes after its preparation, the formation of a crystallization structure is prevented. The fairly high plastic strengths of suspensions stirred again after 30 minutes, or later, can be attributed to the thickening effect of hydroaluminate microcrystals formed in the suspensions by this time. These results show that the first stage of structure formation, during which the formation of crystallization contacts is possible, is brief in these suspensions. If the suspensions were not stirred again, the strength increases would continue for a long time, and would be complete only after 24 hours.

Our determinations of the degree and variations of supersaturation in the aqueous medium of C_3A suspensions [5] showed that when C_3A dissolves, the nuclei of newly formed hydroaluminate crystals begin to form in the suspension at supersaturation below the maximum possible value, corresponding to the nominal solubility of anhydrous C_3A . The hydroaluminate crystals form protective coatings on the surface of the original C_3A particles, and the rate of solution of the latter is thereby greatly decreased. The transition between the first stage of structure formation, when a high degree of supersaturation is maintained in the suspension, to the second stage, when the supersaturation is no longer high, is associated with the formation of these protective films, which lower the solution rate of C_3A and thereby decrease the degree of supersaturation in the suspension. Before the formation of the protective films the rate of solution of C_3A is very high; a high degree of super-

saturation is maintained in the suspension and very fine crystals of hydroaluminate are formed; these crystals coalesce to form the framework of the crystallization structure. Because of the very small size of the crystals constituting this structure, its strength is low, but increases greatly during the second stage of structure forma-

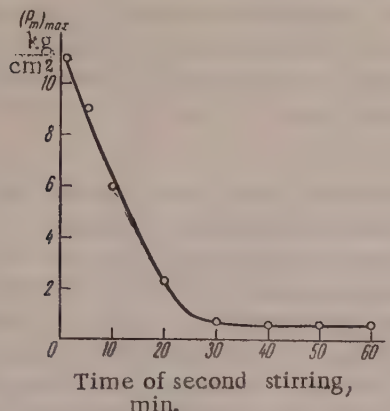


Fig. 4. Variation of the final strength of the crystallization structure with the time between the preparation and the second stirring of the suspension. Composition of suspension: 5% C₃A, 95% ground quartz sand, 26% water.

tion, when the crystals forming the framework of the crystallization structure grow at low degrees of supersaturation. The inflection in the strength curve (Fig. 1) represents the formation of the framework of the crystallization structure, the strength of which then slowly increases as the result of crystal growth. This is seen particularly clearly in Fig. 5; the inflection on the strength curve shows that the formation of the framework of the crystallization structure is completed after about 1 hour. In fact, if the suspension is stirred at this stage (Fig. 5, Curve 3), the crystallization structure breaks down irreversibly and the strength does not increase after this, despite the continuing hydration. In this case, because of the low degree of supersaturation, the free crystals already present in the suspension increase in size, but crystallization contacts are not formed between them. By the time framework of the crystallization structure has been formed, the hydration is 75% complete, while the strength is 40% of the final strength, which is reached after about 10 hours in this case. It must be pointed out that the final stages of structure formation, like the strength increase, are accelerated appreciably by even a small increase of temperature.

After the strength of the crystallization structure has reached its maximum value, it begins to decrease if the specimen is kept in presence of moisture (Fig. 1), and a slow decrease of strength continues for a fairly long time. This strength decrease is caused by slow recrystallization of thermodynamically unstable crystallization contacts arising during the formation of the crystallization structure; this was demonstrated for suspensions of plaster of Paris [6, 8].

The course of structure formation in C₃A suspensions with different water-solid (W/S) ratios is shown in Fig. 6. As W/S increases, i.e., as the structure becomes more porous, recrystallization becomes more rapid, and therefore the strength decrease under moist storage conditions is accelerated. For example, if the ratio of the plastic strength of the crystallization structure after 15 days of storage under moist conditions (P₁₅) to the maximum strength reached at the end of hydration (P_{max}) is taken as a measure of the rate of strength decrease, it follows from Table 1 that this ratio decreases appreciably with increase of W/S.

The strength of the hydroaluminate crystallization structure after the maximum value has been reached (at the end of hydration) can be raised by drying. Strength increase of drying, and strength decrease on moistening, as the result of adsorptional decrease of strength, are reversible processes in coagulation structures [9] and in individual crystals [10]. In the case of the crystallization structure of tricalcium hydroaluminate, alternate

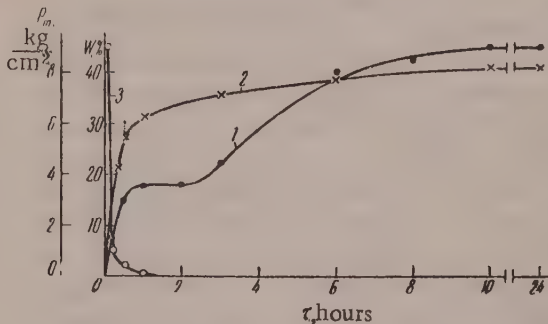


Fig. 5. Course of crystallization structure formation in a suspension containing 5% C₃A, 95% ground quartz sand, and 37% water (1); course of the chemical binding of water in the same suspension (2) (the amount W of chemically bound water is expressed as a percentage on the weight of C₃A); variation of the final strength of the crystallization structure with the time between the preparation and the second stirring of the suspensions (3).

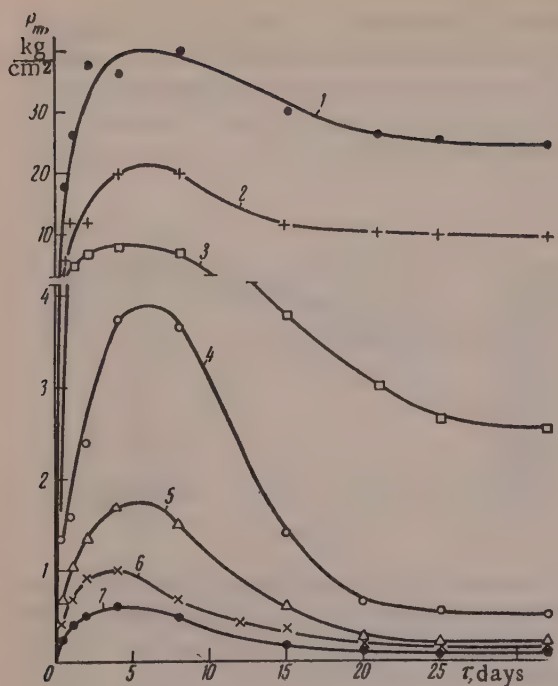


Fig. 6. Course of structure formation in suspensions containing 5% C_3A and 95% ground quartz sand at different W/S ratios: 1) 0.3; 2) 0.4; 3) 0.5; 4) 0.6; 5) 0.7; 6) 0.8; 7) 0.9.

wetting and drying results in partially irreversible decrease of strength owing to recrystallization effects — dissolution of crystallization contacts and growth of regularly formed hydroaluminate crystals (Table 2).

In the experiments the results of which are given in Table 2, the specimens were dried in a vacuum desiccator to constant weight, and the wetting was performed in such a way as to avoid leaching of the hydroaluminate.

The results in Table 2 show that the strength both of wet and of dry specimens decreases with increasing number of wetting and drying cycles. This effect is less pronounced at higher cement contents in the suspension or at lower W/S ratios, i.e., when the structure is denser. It also follows from Table 2 that the effect of wetting is to decrease the strength of the hydroaluminate structure approximately 2.5-fold. The greater decrease of strength on wetting observed by Shestoporov and Liubimova [11] can be accounted for by the fact that in their experiments the crystallization structure of the hydroaluminate was broken down into a considerable extent even while the suspensions were being prepared. In such cases the coagulation structure is responsible for a greater proportion of the strength, and that is why the strength fell sharply on wetting.

TABLE 1

Effect of W/S Ratio on the Rate of Strength Decrease in the Crystallization Structure of Tricalcium Hydroaluminate (composition of solid phase: 5% C_3A + 95% sand)

W/S	0.3	0.4	0.5	0.6	0.7	0.8	0.9
P_{15}/P_{\max}	0.775	0.548	0.423	0.368	0.333	0.286	0.266

TABLE 2

Effect of Alternate Wetting and Drying on the Strength of the Crystallization Structure of Tricalcium Hydroaluminate (composition of suspension: 5% C_3A + 95% quartz sand, W/S = 0.36)

Wet and drying cycles	P_m , kg/cm ²	
	wet specimen	dry specimen
1	19	50
2	17	45
3	16	40
4	14	35

This irreversible breakdown of the crystallization-structure framework during prolonged stirring of the suspension in the course of preparation introduced errors into the results of many workers who studied the hardening of C_3A in suspensions without inert fillers [11, 12]. It follows from Figs. 1 and 6 that the strength decreases very rapidly as the result of dissolution of the crystallization contacts in the crystallization structure of tricalcium hydroaluminate, despite the relatively low solubility of the latter. It was therefore natural to assume that recrystallization effects are accelerated in this instance as the result of transition of the unstable hexagonal tricalcium hydroaluminate, which is the direct hydration product of C_3A , into stable form-cubic tricalcium aluminate hexahydrate. The solubility of hexagonal

hydroaluminate has been determined by a number of workers; the average value is 0.67 g C₃A per liter. The solubility of stable cubic hydroaluminate at various temperatures was determined by Peppler and Wells [13]; their value for 21° was 0.34 g C₃A per liter.

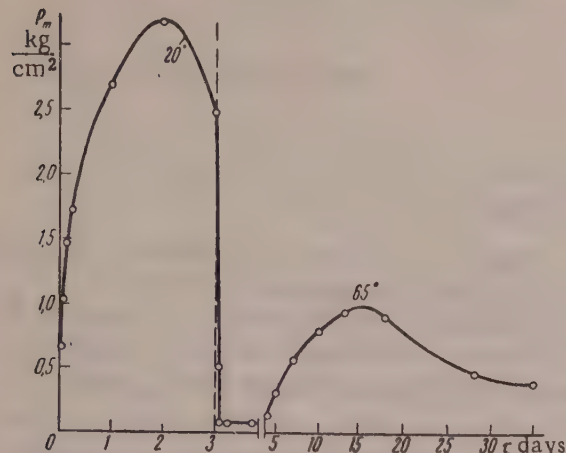


Fig. 7. Course of crystallization-structure formation in a suspension containing 15% C₃A, 85% of ground quartz sand, and 70% water on the dry mixture. The suspension was kept at 20° for the first 3 days, then at 65°.

dissolution of the crystallization contacts, which are thermodynamically unstable and therefore have higher solubility than the regular crystals of hexagonal hydroaluminate.

Further increase in the amount of cubic hydroaluminate results in the development of a new crystallization structure, which reaches its maximum strength in the given suspension (Fig. 7) in 15 days. After the strength of this new hardened structure has reached its maximum value, it begins to decrease when stored under moist conditions as the result of recrystallization processes and dissolution of nonequilibrium crystallization contacts.

The recrystallization processes are much slower in this case, as supersaturation is due only to the nonequilibrium character of the crystallization contacts, while in the former instance a high degree of supersaturation was ensured by the difference between the solubilities of the stable and unstable forms of the hydroaluminate.

The formation of hexagonal hydroaluminate when the first crystallization structure is formed, and of cubic hydroaluminate when the secondary hardened structure arises in C₃A suspensions, is confirmed by (Fig. 8).

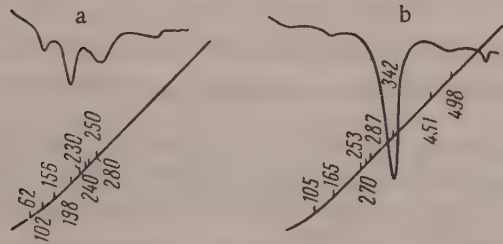


Fig. 8. Thermograms of samples taken from suspensions during the course of structure formation of which is given in Fig. 7: a) Sample taken after 24 hours; b) sample taken after 15 days.

strength increase in the course of crystallizational structure formation in tricalcium aluminate (C₃A).

2. Hydration processes, i. e., dissolution of anhydrous C₃A and crystallization of the hydrate, give rise to a crystallization structure consisting of hexagonal crystals of tricalcium hydroaluminate.

3. Recrystallization and transition of the unstable hexagonal hydroaluminate into the stable cubic form under moist storage conditions leads to spontaneous breakdown of this initial crystallization structure and to formation of a new structure consisting of the cubic form of tricalcium hydroaluminate. This process is considerably accelerated at higher temperatures.

SUMMARY

1. A study has been made of the kinetics and

strength increase in the course of crystallizational structure formation in tricalcium aluminate (C₃A).

4. There are two distinct stages in the formation of the initial crystallization structure. First a weak framework of the crystallization structure is formed, and later, when the dissolution rate of C_3A is retarded owing to formation of protective hydroaluminate films on its surface, the framework is built up. Most of the substance ($\sim 70\%$) becomes hydrated during the first stage, but the strength is increased mainly during the second stage of structure formation.

Moscow State University
Faculty of Chemistry
Chair of Colloid Chemistry

Received March 18, 1958

LITERATURE CITED

- [1] T. Thorvaldson and N. S. Grace, Canad. J. Res. 1, 36, 1929; 1, 201, (1929); G. Assersson, Z. anorgan. und allgem. Chem. 200, 385 (1931); 205, 335, (1932); 214, 158 (1933); R. Nacken, and R. Mosebach, Z. anorgan. und allgem. Chem. 225, 289 (1935); E. P. Polheim, Zement 24, 41-43, 643 (1935); L. S. Wells, W. F. Clarke and H. F. McMurdie, J. Res. Nat. Bur. Standards 30, 367 (1943); V. M. Moskvin and T. V. Rubetskaia, Research of the All-Union Sci. Res. Inst. of Construction. Concretes and Cements (Moscow, 1955), p. 120; T. V. Rubetskaia, ibid, p. 95.
- [2] E. E. Segalova, P. A. Rebinder, and O. I. Luk'yanova, J. Moscow Univ. No. 2 (1954); P. A. Rebinder and E. E. Segalova, Nature No. 12 (1952).
- [3] E. E. Segalova and E. S. Solov'eva, Proc. Conf. on Cement Chemistry (Moscow, 1956).*
- [4] E. E. Segalova, E. S. Solov'eva, and P. A. Rebinder, Proc. Acad. Sci. USSR 113, 1 (1957).**
- [5] E. E. Segalova, E. S. Solov'eva, and P. A. Rebinder, Proc. Acad. Sci. USSR 117, 5 (1957).
- [6] E. E. Segalova, V. N. Izmailova, and P. A. Rebinder, Colloid J. 20, No. 5, 601 (1958).**
- [7] E. E. Segalova and P. A. Rebinder, Abstracts of Papers at the 4th All-Union Conference on Colloid Chemistry (Moscow, Izd. AN SSSR, 1958).*
- [8] V. N. Izmailova, E. E. Segalova, and P. A. Rebinder, Proc. Acad. Sci. USSR 107, 3 (1956); E. E. Segalova, V. N. Izmailova, and P. A. Rebinder, Proc. Acad. Sci. USSR 110, 5 (1956); 115, 3 (1957).**
- [9] P. A. Rebinder, Jubilee Volume of the Academy of Sciences USSR on the 30th Anniversary of the October Revolution (Moscow-Leningrad, 1947).*
- [10] G. I. Logginov and M. P. Elinzon, Materials and Construction in Modern Architecture (Moscow, 1948).*
- [11] S. V. Shestoporov and T. Iu. Liubimova, Proc. Acad. Sci. USSR, new series 36, No. 6 (1952).
- [12] P. H. Bates and A. A. Klein, Techn. Papers Bur. Standards, 78 (1917); S. D. Okorokov, Interaction of the Minerals in Portland Cement Clinker During Hardening of Cement (Moscow-Leningrad, Peoples' Commissariat for Building Construction Press, 1945);* Iu. M. Butt, "Investigation of hydration and corrosion of cements and their constituent compounds" Doctorate Dissertation (Moscow, 1945).*
- [13] R. Peppler and L. Wells, J. Res. Nat. Bur. Standards, 52, 2, 75 (1954).

*In Russian

**Original Russian pagination. See C.B. Translation.

MECHANISM OF THE ACTION OF MIXED ADDITIVES FOR CEMENT, BASED ON A HYDROPHILIC PLASTIFIER

O. I. Luk'ianova and S. A. Dariusina

It is known [1-6] that the setting time of cement can in a number of cases be successfully regulated by means of small amounts of surface-active substances, such as SSB lignosulfonates. It has been shown in P. A. Rebinder's laboratory by E. E. Segalova, R. R. Sarkisian, one of the present authors, and others that the decisive factor in this action is the induction period of hydration and structure formation in the cement suspension (paste), produced by the added SSB. However, this induction period is too short even with relatively high SSB contents; this is particularly true of high-aluminate, highly disperse cements which are being increasingly used in the production of prefabricated parts and constructions from quick-setting concrete.

We found that the induction period is lengthened 5 to 10-fold if the mixing water contains, in addition to the hydrophilic SSB additive, small amounts (up to 1% on the weight of the cement) of alkali metal or ammonium salts with anions giving rise to sparingly soluble calcium salts. Not only does the cement retain its ability to set and harden at the end of the induction period, but in a number of cases these processes are intensified.

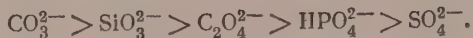
The purpose of this investigation was to study the physicochemical mechanism of the action of mixed additives of this type, in order to determine the optimum conditions for their use. The studies were performed with highly disperse high-aluminate cement from the "Gigant" factory, of the following mineral composition: $C_3S - 49.1\%$; $C_2S - 25.2\%$; $C_3A - 12.1\%$; $C_4AF - 12.2\%$. The nominal specific surface of the cement determined by the air-permeability method, was $0.45 \text{ m}^2/\text{g}$.

For elucidation of the mechanism of action of the mixed additives, a study was made of the hydration and structure-formation kinetics in concentrated cement suspensions containing various amounts of the mixed additives and their individual components; the course of variation of their contents in the liquid phase of the suspensions was also studied. The course of hydration was studied calorimetrically at a constant rate of heat transfer. Kiselev's [7] calorimeter with an automatically regulated adiabatic jacket was used. The course of structure formation was studied by the cone plastometer method, described earlier [1, 2]. The concentrations of the components of the mixed additive in the aqueous phase of the suspensions were determined colorimetrically (in the case of hydrophilic SSB additive) and by other analytical methods (for the inorganic salts used as the second component of the mixed additive).

The second components of the mixed additive used for increasing the length of the induction period of hydration and structure formation were carbonates, oxalates, silicates, phosphates, and sulfates of alkali metals and ammonium. Since the anions of all these salts precipitate equivalent amounts of calcium from SSB solutions, in a number of experiments it was convenient to express the amounts of these additives in terms of equivalents of calcium lignosulfonates. The calcium in the SSB lignosulfonates was determined by conductometric titration [8]. The mixed additives were always introduced with the mixing water, and the contents of the individual components were varied between 0.1 and 2.0% of SSB on the weight of cement, and between 0.5 and 10-15 equivalents of salts, relative to SSB. The expression of SSB concentration relative to the weight of cement is justified on physicochemical grounds [3].

The duration of the induction period of hydration and structure formation in cement is increased in presence of the mixed additives, as described below.

Variations of the length of the induction period (τ_0) with the inorganic salt content, with the same amount of SSB, are plotted in Fig. 1. In this instance the length of the induction period is taken to be the time from the preparation of the suspension to the start of the rapid increase of plastic strength P_m on the curves for the kinetics of structure formation. It is clear from Fig. 1 that salts with different anions have different effects on the length of the induction period. The anions can be arranged in the following series in order of their effectiveness:



The nature of the cation is much less significant, as is clear from a comparison of Curves 1 and 2 in Fig. 1. Replacement of Ca^{2+} ions in the SSB solution by equivalent amounts of alkali metal or ammonium ions has no significant effect on the strength of the induction period; Fig. 1 shows that this increases over the initial

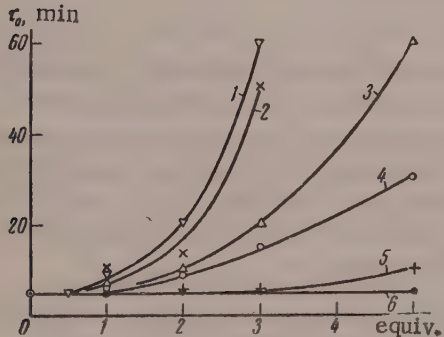


Fig. 1. Length of the induction period of structure formation in cement suspensions ($W/C = 0.3$; 1% SSB on the weight of cement) containing mixed additives: 1) Na_2CO_3 ; 2) K_2CO_3 ; 3) NaSiO_3 ; 4) $\text{K}_2\text{C}_2\text{O}_4$; 5) $(\text{NH}_4)_2\text{HPO}_4$; 6) Na_2SO_4 .

value (5 minutes for the given SSB content) only if the precipitant salt is added in excess. For example, introduction of three equivalents of K_2CO_3 results in a tenfold increase of τ_0 .

With further increase of the amount of precipitant salt, the induction period begins to decrease again after reaching a maximum value, as shown in Fig. 2. This behavior was found with all the amounts of added SSB studied; it was also found that the maximum induction period is reached at lower contents of the precipitant salt if the amount of SSB is decreased, and its absolute value becomes less.

It has been shown [1, 2] that most of the SSB lignosulfonates introduced into a cement suspension during its preparation are adsorbed irreversibly on the original cement particles within a few minutes. Further adsorption, which proceeds at a considerably lower rate, is adsorption of SSB by the hydration products of the cement clinker minerals; this occurs slowly during the induction period. It is also known that the end of the induction period of structure formation and the start of the rapid increase of the plastic strength of the cement coincides in time with almost complete binding of the lignosulfonates. The length of the induction period therefore depends on the SSB content of the aqueous phase in the cement suspension.

To determine the causes of the increase of the induction period in presence of the mixed additives, the changes of SSB lignosulfonate concentration in a cement suspension containing various amounts of potassium carbonate in addition to SSB were investigated. The effect of K_2CO_3 on the course of binding of SSB is shown in Fig. 3; the primary effect is a decrease of the initial adsorption (a_0) of SSB on the original cement particles, with a consequent sharp increase in the time required for complete binding of the SSB. The dash line represents the adsorption corresponding to complete binding of the SSB from the aqueous phase at the given SSB content.

The decrease of a_0 in presence of K_2CO_3 is greater with increase of the salt content, reaching a certain limit when the latter reaches K_2CO_3 on the weight of cement. In Fig. 4, a the variations of a_0 are plotted

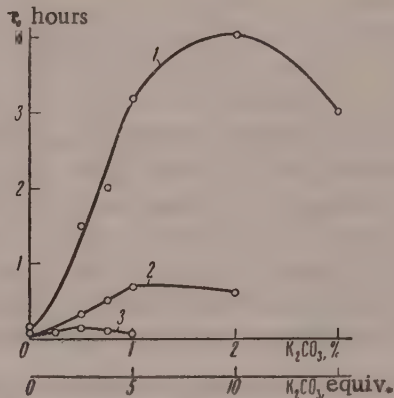


Fig. 2. Length of the induction period of structure formation in cement suspensions ($W/C = 0.26$) containing mixed additives: 1) 0.5% SSB; 2) 0.25% SSB; 3) 0.1% SSB.

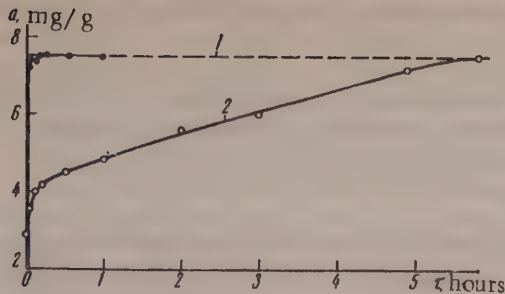


Fig. 3. Binding of SSB lignosulfonates from the aqueous phase in cement suspensions ($W/C = 0.5$; 0.75% SSB); 1) without K_2CO_3 ; 2) 1% K_2CO_3 .

against the amount of K_2CO_3 present in suspensions containing different amounts of solid phase; it is seen that a_0 depends only on the amount of K_2CO_3 relative to cement, and is not influenced, within the limits of experimental error, by the water-cement ratio of the suspension. The abscissa axis in Fig. 4 shows the K_2CO_3 contents after subtraction of the amount used in precipitation of Ca^{2+} from SSB solutions. Therefore the direct cause of the increase of the induction period of hydration and structure formation in cement suspensions containing SSB additive is the decreased adsorption of SSB on original cement particles under the influence of K_2CO_3 , and the corresponding increase of the lignosulfonate content of the aqueous phase in the suspension.

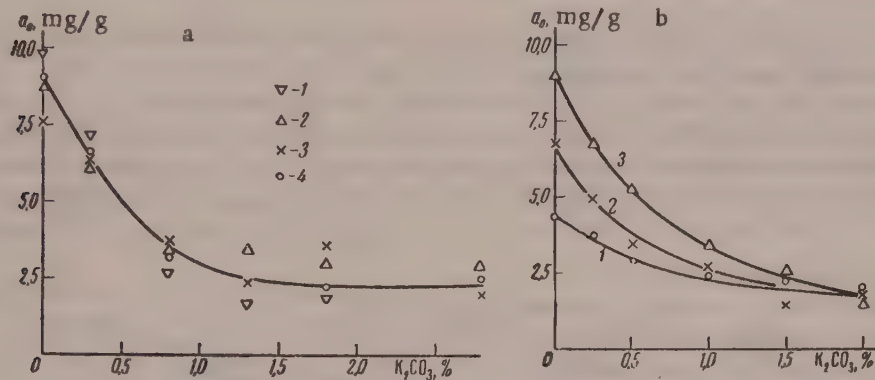


Fig. 4. Initial adsorption of SSB (a_0) in presence of K_2CO_3 : a) 1% SSB; 1) $W/C = 2$; 2) $W/C = 3$; 3) $W/C = 4$; 4) $W/C = 5$; b) $W/S = 5$; 1) 0.5% SSB; 2) 0.75% SSB; 3) 1% SSB.

The decrease of the initial adsorption of SSB, in its turn, is probably caused by adsorption of CO_3^{2-} ions on the original cement particles, which changes the nature of their surface and their adsorption capacity for lignosulfonates. In particular, it is seen in Fig. 4,b that the adsorption of SSB lignosulfonates on cement particles coated with a carbonate layer, in contrast to adsorption of fresh cement surfaces, reaches a limit even with relatively small amounts of SSB (less than 0.5% on the weight of cement). Figure 5 represents the course of binding of CO_3^{2-} ions from the aqueous phase of cement suspensions, based on determinations of the carbonate concentration by the volumetric gas method. The course of the curves in Fig. 5 shows that a certain quantity of CO_3^{2-} ions, corresponding to about 1% K_2CO_3 on the cement weight, is taken up almost instantaneously. The limit of the decrease of the initial adsorption of lignosulfonates, caused by K_2CO_3 , is reached at the same K_2CO_3 content (1-1.5% or $\approx 5 \cdot 10^{-5}$ g-ion CO_3^{2-} per g); this quantity corresponds to the specific surface of the cement if a monoionic layer is formed.

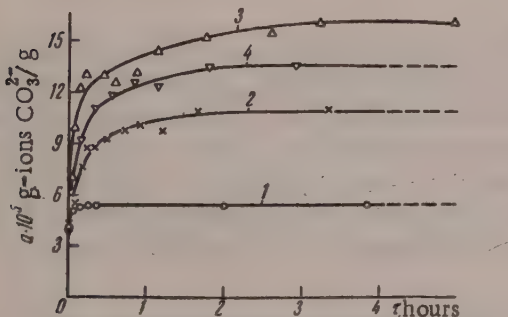


Fig. 5. Binding of CO_3^{2-} from the aqueous phase of cement suspensions ($W/C = 5.0$; 1% SSB): 1) 1% K_2CO_3 ; 2) 2% K_2CO_3 ; 3) 3% K_2CO_3 ; 4) 2% SSB and 3% K_2CO_3 .

These facts, and the fact that a_0 is independent of the water-solid ratio, indicate that in this case a protective $CaCO_3$ phase film is not formed on the cement particles. In particular, if a phase film is formed, its thickness depends on the concentration

of the reagent solution [9, 10]; this is not so in the present instance. Only the surface of the cement grains is involved in the initial binding of CO_3^{2-} , so that the process is adsorptive in character. The mechanism of formation of the adsorption layer is probably similar to that of formation of protective films of salts, and is a limiting case of the latter.

Other salts which are capable of lengthening the induction period produced by addition of SSB also decrease the adsorption of SSB by cement, but to a lesser extent than carbonates. This property is probably associated with their adsorption capacity for SSB, and decreases in proportion to the decrease of their ability to lengthen the induction period.

The foregoing results suggest that the components of the mixed additives under consideration have the following functions. The salt anion, which forms an insoluble compound with calcium, is adsorbed on the original cement particles, and their adsorption capacity for SSB is thereby decreased. The SSB lignosulfonates present in the aqueous phase of the cement suspension inhibit hydration and structure formation, being adsorbed on the cement hydration products. Decrease of the initial adsorption a_0 with increasing content of K_2CO_3 (or any other salt in which the anion is adsorbed by cement better than SSB is) has the same influence on the length of the induction period as an increase of the total SSB content in the cement suspension. The induction period is lengthened in both cases, as the time required to take up the SSB from the aqueous phase of the suspension is greater [11].

The length of the induction period depends not only on the lignosulfonate content of the aqueous phase, but also on the rate of binding of the lignosulfonates by the cement hydration products; this rate, in its turn, depends on the hydration rate of cement in presence of SSB and the adsorption capacity of its hydration products for SSB. To obtain an idea of the hydration rate of cement in presence of mixed additives during the induction period, the course of hydration was studied calorimetrically. The heat liberation in the hydration of high-aluminate cement was determined in presence of 0.1 to 1.0% of SSB and of 0.1 to 0.5% of K_2CO_3 , on the weight of cement.

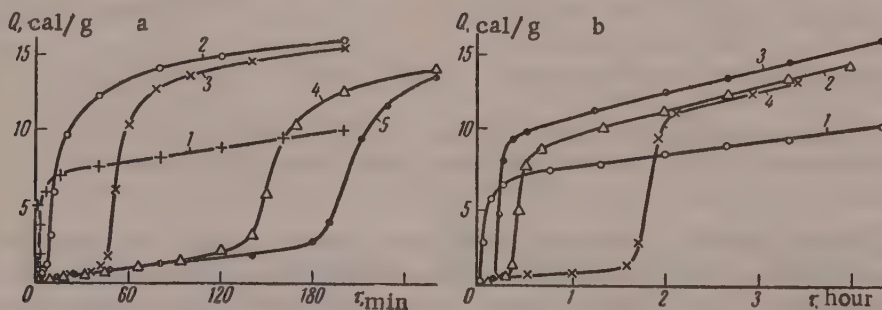


Fig. 6. Heat liberation in the hydration of cement with mixed additives:
a) 0.5% SSB: 1) without additives; 2) SSB only; 3) SSB and 0.15% K_2CO_3 ; 4) SSB and 0.35% K_2CO_3 ; 5) SSB and 0.5% K_2CO_3 ; b) 0.1 and 0.25% SSB: 1) 0.1% SSB; 2) SSB and 0.4% K_2CO_3 ; 3) SSB and 1% K_2CO_3 ; 4) 0.25% SSB and 0.5% K_2CO_3 .

The kinetics of heat evolution in the hydration of cement containing 0.5% SSB and various amounts of carbonate is plotted in Fig. 6,a. The shape of Curve 1, for cement without additives, indicates that the hydration in this case commences virtually without an induction period and at a high rate, which gradually decreases to a constant value. Addition of 0.5% SSB produces a short induction period (Curve 2), after which the hydration is very rapid. The heat evolution is greater in this case than in absence of additives. This effect was reported by us earlier [11]; the explanation is that formation of protective films of hydration products on the cement particles is prevented. The length of the induction period increases with increased K_2CO_3 content (Curves 3, 4, and 5 in Fig. 6,a).

The induction period again becomes shorter when the K_2CO_3 content exceeds the optimum value; this is illustrated by Fig. 6,b (Curve 3), and is in harmony with the data on the kinetics of structure formation in Fig. 2. Comparison of Curves 3-5 (Fig. 6,a) and the Curves 2-4 (Fig. 6,b) shows that the quantity of heat

liberated during the induction period increases roughly linearly with time, and is similar for all systems. The same effect is produced by increase of the total SSB content of the cement suspension. The total quantity of heat liberated in the hydration of cement during the induction period increases with increasing SSB and K_2CO_3 content. Since the hydration of cement at the initial stages is largely determined by its aluminate component the quantity of heat liberated is proportional to the quantity of hydroaluminate formed in the hydration of the tricalcium aluminate in the clinker.

As already noted, the binding of SSB from the aqueous phase of the cement suspension during the induction period depends on the quantity of hydration products formed; more precisely, on the quantity of hydroaluminate. The adsorption of a surface-active substance dissolved in a liquid medium in which crystallization is taking place may occur on the crystalline substance at various stages of its formation, both on the crystallization nuclei, which are generally passivated as a result, and on the formed crystals of the new phase.

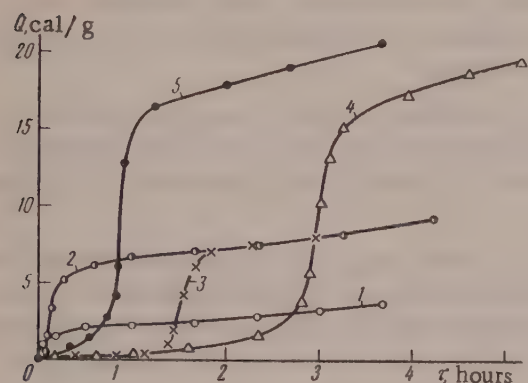


Fig. 7. Heat liberation in the hydration of cement ($W/C = 0.4$; 6% $CaSO_4 \cdot 2H_2O$) with mixed additives:
1) Without additives; 2) 0.25% SSB; 3) SSB and 0.4% K_2CO_3 ; 4) SSB and 1% K_2CO_3 ; 5) SSB and 2% K_2CO_3 .

The lower the SSB content of the system, the less is the absolute increase of the lignosulfonate concentration in the liquid phase of the cement suspension, caused by displacement of lignosulfonates from the adsorption layers on the original cement particles. Accordingly, the amount of K_2CO_3 , which served as a hydration accelerator, required for binding of SSB and shortening of the induction period is also less. This accounts for the displacement of the τ_0 maximum in the direction of lower K_2CO_3 contents with decrease of the amount of SSB added (Fig. 2). The mechanism of the action of alkali-metal carbonates as hydration and hardening accelerators for cement is not yet fully understood. However, this is an independent problem which is not considered in this paper.

High-aluminate clinker without gypsum was used for our investigations of the action of mixed additives on the initial stages of hydration and structure formation in cement. In view of the practical importance of cement containing the normal amounts of gypsum, an additional series of experiments was performed with such cement; it was found that the mixed additives have the same effect as in the cement without gypsum. Figure 7 shows the course of heat liberation in the hydration of cement with a normal gypsum content (6% $CaSO_4 \cdot 2H_2O$). As in the case of cement without gypsum, addition of SSB (Curve 2) results in an increase of heat liberation and the appearance of an induction period, which is longer in presence of K_2CO_3 (Curve 3,4). In addition to the lengthening of the induction period in presence of the mixed additives, cement with a normal gypsum content shows a strong increase of the hydration rate after the end of the induction period (Curve 4,5). This effect, but less pronounced, was also observed in cement without gypsum (Fig. 6,b, Curve 3). In both cases the additional increase of heat evolution, above that produced by additions of SSB, is found only at high carbonate contents, after the maximum of the induction period has been passed. As already stated, in such systems some CO_3^{2-} ions remain in the liquid phase of the suspension. Together with the formation of adsorption layers of SSB on the surface of the original cement particles, this favors the hydration-accelerating effect

From the results of our experiments on heat liberation and the data on the kinetics of the binding of SSB it is possible to give a more precise picture of the mechanism of SSB adsorption, based on the hypothesis that SSB lignosulfonates are adsorbed on the crystallization nuclei of the hydroaluminate, which are formed slowly and at a constant rate during the entire induction period.

This hypothesis also readily accounts for the shortening of the induction period of hydration and structure formation if the amount of added potassium carbonate is increased above the optimum.

Alkali-metal carbonates, which act as accelerators of cement hydration and hardening under certain conditions, thereby assist accelerated binding of SSB lignosulfonates from the aqueous phase of the suspension by the cement hydration products, and hence shorten the induction period.

of carbonates. Under such conditions the formation of protective films of microcrystalline hydration products, or of reaction products of cement with carbonates, on the cement particles is unlikely.

The mixed additives based on the hydrophilic plastifier are therefore of practical interest both for regulation of the setting time of high-aluminate cement, and for acceleration of cement hardening.

SUMMARY

1. Mixed additives, consisting of small amounts of hydrophilic SSB plastifier with alkali metal or ammonium carbonates (or of silicates, oxalates, and other salts which precipitate calcium), added to cement with the mixing water, give rise to an induction period of hydration and structure formation; the length of this period passes through a maximum with increase of carbonate content.

2. The length of the induction period in presence of the mixed additives is determined by two factors: the SSB content in the aqueous phase of the suspension (the length increases with increase of SSB content), and the rate of binding of SSB during the induction period.

3. The initial adsorption of calcium lignosulfonates on the cement particles, which determines the lignosulfonate content of the aqueous phase, decreases sharply in presence of carbonates down to a limiting value at relatively high carbonate contents (1-1.5% on the weight of cement).

4. CO_3^{2-} ions, and probably also SiO_3^{2-} , $\text{C}_2\text{O}_4^{2-}$ ions, are adsorbed from the aqueous phase of the cement suspensions in presence of SSB by the cement surface, forming monoionic layers; this lowers the adsorptive capacity of the cement for lignosulfonates. The excess of CO_3^{2-} ions, initially remaining in the aqueous phase, is slowly bound during the induction period.

5. The rate of binding of SSB during the induction period, and the rate of cement hydration (as indicated by heat evolution) are low and almost constant during the induction period, with different contents of SSB and K_2CO_3 in the cement suspensions. This is due to the adsorption of SSB from the aqueous phase of the suspension on the hydraluminate crystallization nuclei as the latter are formed; this accounts for the induction period of hydration.

6. Increase of the K_2CO_3 content in the mixed additive is equivalent to increase of the initial SSB content in the aqueous phase of the suspension, and after the limit of CO_3^{2-} adsorption has been reached it is also tantamount to an increase of the rate of binding of SSB during the induction period.

The existence of a maximum induction period is the result of the combined influence of these factors.

University of Moscow
Faculty of Chemistry
Chair of Colloid Chemistry

Received December 23, 1957

LITERATURE CITED

- [1] E. E. Segalova, P. A. Rebinder, and O. I. Luk'ianova, J. Moscow Univ. 2, 17(1954); O. I. Luk'ianova, E. E. Segalova, and P. A. Rebinder, Colloid J. 19, 1, 82 (1957).*
- [2] S. V. Shestoporov, T. Iu. Liubimova, and F. M. Ivanov, Proc. Acad. Sci. USSR 70, 6 (1950).
- [3] Iu. M. Butt and T. M. Berkovich, Cements with Surface-Active Additions (Industrial Construction Press, 1953).**
- [4] Ts. G. Ginzburg, Plastifying Additions in Hydraulic Concrete (Hydraulic Power Press, 1956).**
- [5] L. H. Tuthill and W. A. Cordon, J. Amer. Concrete Inst. 27, No. 3, 273 (1955).
- [6] R. R. Sarkisian, Effect of Sulfite-Alcohol Waste Liquor on Cement Pastes and Concretes (Erevan, Acad. Sci. Armenian SSR Press, 1957).**
- [7] V. F. Kiselev, Proc. Conf. on Cement Chemistry (Industrial Construction Press, 1956), p. 243.**
- [8] V. K. Nizovkin and O. I. Okhrimenko, Trans. All-Union Sci. Res. Inst. of Sulfite Alcohol and Hydrolysis Ind. 2 (1947).

*Original Russian pagination. See C.B. Translation.

**In Russian.

[9] A. V. Nikolaev and E. I. Feigina, in the symposium: Protective Films on Salts (Izd. AN SSR, 1944), p. 83, 99. *

[10] T. I. Rozenberg and V. B. Ratinov, Coll. Trans. All-Union Sci. Res. Inst Ferroconcrete, No. 1 (1957), p. 49.

[11] O. I. Luk'yanova, E. E. Segalova, and P. A. Rebinder, Proc. Acad. Sci. USSR 117, 6,1034 (1957). **

*In Russian.

**Original Russian pagination. See C. B. Translation.

INFLUENCE OF SURFACE-ACTIVE SUBSTANCES ON THE
CRYSTALLIZATION OF TRICALCIUM
HYDROALUMINATE *

N. G. Zaitseva and A. M. Smirnova

The use of the tracer-atom method for determinations of the specific surfaces of powder involves a number of difficulties. One of the chief difficulties lies in distinguishing between surface and internal exchange. This is especially true in determinations of the specific surface of cements, when hydration, i.e., dissolution of the original substance and crystallization of the newly formed hydrate, results in complete exchange of calcium ions between the solid phase and solution [1] at a rate proportional to the hydration rate, which is very high in a number of binding materials (lime, tricalcium aluminate). In such cases exchange within the depth of the solid phase is insignificant, because of the low rate of diffusion in solids. This is also confirmed by the fact that complete ion exchange is not found in newly formed hydrates, i.e., completely hydrated cements [2, 3]. If the recrystallization process could be greatly retarded, exchange within the bulk of the solid phase should be virtually excluded, so that it should be possible to determine more correctly the extent of surface exchange, and hence the specific surface. Crystallization can be retarded either by considerable dilution, or by introduction of various surface-active substances [4]. In the present investigation the surface-active additives used were saponin and lignosulfonates (SSB).

As in our previous investigations, the radioactive tracer used as the Ca^{45} ion in the form of calcium chloride; concentration of the calcium chloride solution was 0.125%.

The mineral was finely powdered and sifted through a screen of 250 mesh. The W/S ratios were 80, 40, and 5. The amount of exchanged calcium was estimated from the difference of activity between the original solution and the filtrate after it had been in contact with the powder for time τ .

The course of the isotope exchange is plotted in Fig. 1. The amount of exchanged calcium in the solid phase A_{Ca} in mg/g is plotted against the time in minutes. Curve 1 was determined without surface-active additions, while the other curves were obtained in presence of various concentrations of SSB calcium lignosulfonates and saponin. Each curve has two characteristic regions — a region of rapid exchange, and a region of slower exchange; these regions are more distinct in presence of surface-active substances.

The initial region of the curve corresponds to rapid exchange of surface ions; this proceeds at the same rate in all cases, both without additives (Curve 1) and in presence of additives (Curves 2-6), and is virtually complete after one minute. Exchange within the solid, which we consider to be caused by recrystallization of all the original substance in the form of hydrate, also proceeds at a fairly high rate in absence of additives (Curve 1), and in presence of 0.5% saponin (Curve 2), so that its separation from surface exchange must be arbitrary. In presence of sufficiently large amounts of surface-active substances the exchange slows down sharply after 1 minute, and for a considerable time Curves 2-6 lie parallel to the abscissa axis. Sharp breaks therefore appear on the curves, so that it is possible to determine more reliably the amount of calcium corresponding to surface exchange.

The absence of exchange associated with crystallization of the hydroaluminate may be attributed to suppression of the growth of the forming nuclei by the adsorption layers of the surface-active additives.

*Paper at the 4th All-Union Conference on Colloid Chemistry Tbilisi, May 1958.

The retardation of nucleus formation and growth by additions of lignosulfonates (SSB) and saponin increases with concentration of the additive. For example, with 0.01% of the additive (at W/S = 80) the exchange is retarded by 1-2 minutes. With 0.10% of the additive the crystallization is delayed by 2-3 minutes, and with 0.15%, by 5 minutes, after which the rate increases again. This provides satisfactory confirmation for

the results of Luk'ianova, Segalova, and Rebinder [5], who showed that in presence of added SSB a cement suspension remains in its initial state for a period which depends on the amount of additive, and which they defined as the induction period of hydration.

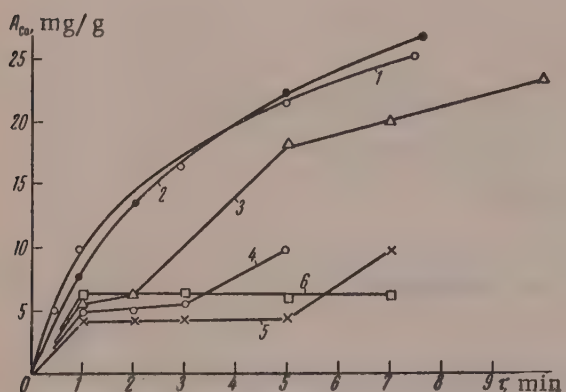


Fig. 1. Isotope exchange of calcium ions between tricalcium aluminate powder and calcium chloride solution, in mg/g: 1) Without additives; 2) with 0.05% saponin; 3) with 0.01% SSB; 4) with 0.02% SSB; 5) with 0.15% SSB; 6) with 0.1% saponin.

The maxima on Curves 1 and 2 correspond to 45 minutes of hydration time, while in Curve 3 it corresponds to a later time. The maximum specific surface $S = 7 \text{ m}^2/\text{g}$ with a small amount of additive is lower than the maximum for hydration in water ($S = 10 \text{ m}^2/\text{g}$), but with a high concentration of additive it is higher than in water ($S = 13 \text{ m}^2/\text{g}$). Moreover, when the specific surface has reached its maximum value, it remains unchanged

for a long time in presence of a high concentration of SSB. Thus, at W/S = 5 the surface decreases appreciably only after 48 hours of hydration, whereas in water the specific surface decreases from 10 to 8 m^2/g after 4 hours.

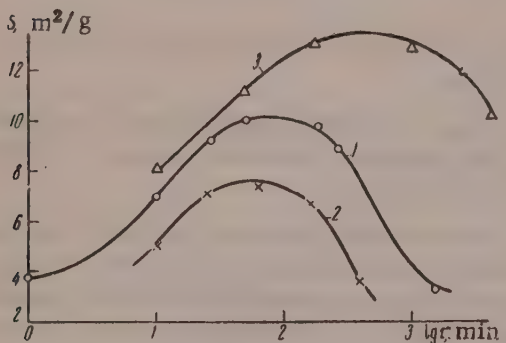


Fig. 2. Variation of the active specific surface of tricalcium aluminate in the course of hydration; 1) In water; 2) with 0.3% SSB; 3) with 1% SSB.

after this, concretion and recrystallization of the crystals begins to prevail, with a decrease of specific surface.

The inhibiting effect of surface-active substances of the SSB type on the formation of nuclei increases with concentration. Therefore the maximum development of the specific surface takes longer to reach at high concentrations. The increase of supersaturation observed in presence of surface-active substances also influences the number of nuclei formed and their rate of growth, with a consequent change of the specific surface.

The solid phase in tricalcium aluminate suspensions was also studied by microphotography, in parallel with the determinations of the specific surface. The results are in good agreement with the specific-surface data.

With small amounts of SSB (Fig. 3, photographs taken after 3.5-4 hours of hydration), there are some very large as well as small crystals (Fig. 3,c). There are no large crystals if the hydration takes place in pure water (Fig. 3, a). At higher SSB concentrations small crystals are formed (Fig. 3,b).

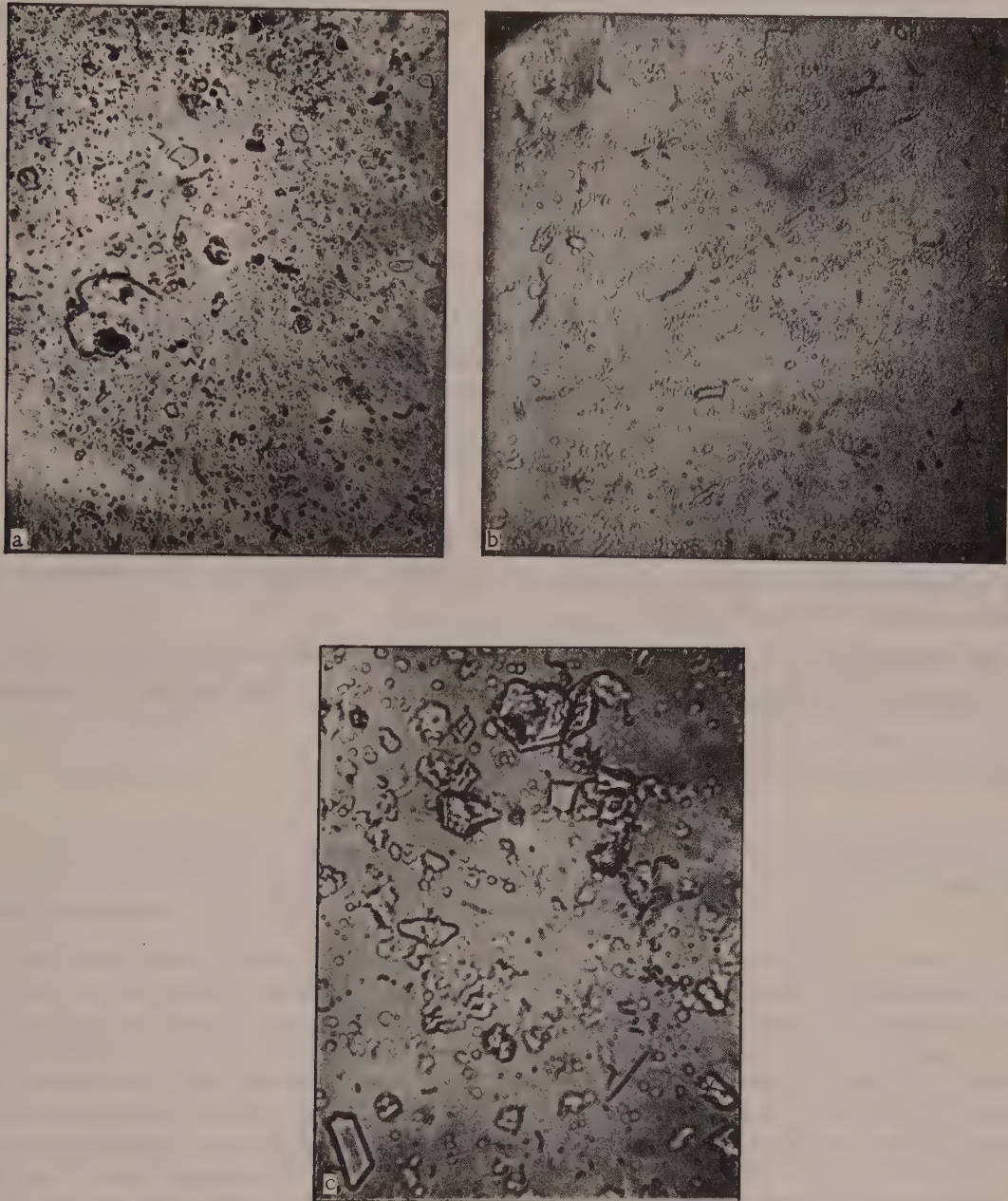


Fig. 3. Microphotographs of tricalcium aluminate crystals formed after 4 hours of hydration (magnification $\times 300$): a) In water; b) with 0.3% SSB; c) with 1% SSB.

Evidently in presence of small amounts of surface-active substances the degrees of supersaturation are such that the rate of crystal growth exceeds the rate of nucleus formation. As the result of the retarded rate of the latter, the crystals formed at the start of the process can grow to a considerable size and are of regular form. The crystals formed later remain small. At high SSB concentrations the inhibition of nucleus growth lasts longer, so that highly supersaturated hydroaluminate solutions arise in the system; after the end of the inhibitory period this leads to the formation of large numbers of very small crystals.

SUMMARY

1. Surface and volum isotope exchange can be easily distinguished in presence of surface-active additives; this principle was used for a reliable determination of the specific surface of tricalcium aluminate.

2. The action of surface-active substances is essentially to delay the formation and growth of the nuclei of the new tricalcium hydroaluminate phase; this alters the supersaturation of the system and hence influences crystal growth.

Institute of Physical Chemistry,
Acad. Sci. USSR
Division of Disperse Systems
Moscow

Received June 9, 1957

LITERATURE CITED

- [1] A. M. Smirnova and P. A. Rebinder, Proc. Acad. Sci. USSR, 4, 319 (1946).
- [2] A. M. Smirnova, N. G. Zaitseva and V. P. Sukhova, Coll. Proc. 2nd Conference on Methods of Investigating the Structure of Highly Disperse and Porous Substances (Izd. AN SSSR, 1958). *
- [3] J. A. A. Ketelaar, and D. Hejman, Recueil trav. chim. 73, No. 4, 240 (1954).
- [4] A. Langer, J. Chem. Phys. 10, 321 (1942).
- [5] O. I. Luk'ianova, E. E. Segalova, and P. A. Rebinder, Colloid J. 19, 1, 82 (1957). **
- [6] P. A. Rebinder and E. E. Segalova, Nature No. 12, 45 (1952); E. E. Segalova, P. A. Rebinder, and O. I. Luk'ianova, J. Moscow Univ. No. 2 (1954).
- [7] A. M. Smirnova, N. G. Zaitseva and P. A. Rebinder, Colloid J. 18, 94 (1956). **
- [8] V. L. Izmailova, E. E. Segalova and P. A. Rebinder, Proc. Acad. Sci. USSR, 107, No. 3, 425 (1956).

* In Russian.

** Original Russian pagination. See C.B. Translation.

THE RHEOLOGY OF METALS IN SURFACE-ACTIVE MEDIA *

V. S. Ostrovskii and V. I. Likhtman

Plastic metals behave like viscous bodies in many treatment and deformation processes, and it is therefore very useful to know the rheological characteristics of metals, especially in studies of creep effects and work hardening. By their structure metals can be included, in P. A. Rebinder's classification [1], among the structurized systems with dense crystallization structures. Such structures, if their individual elements have plastic properties, are capable of undergoing plastic deformation and have high viscosity at low stresses; the viscosity decreases sharply over a narrow stress range, which corresponds to the practical yield value.

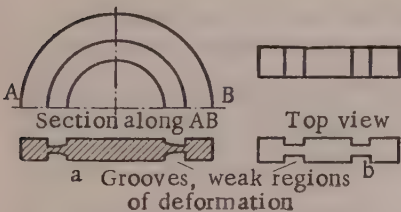


Fig. 1. Test specimens.

The available data on the principal rheological characteristic of metals, the effective viscosity $\eta = P / \frac{d\epsilon}{d\tau}$, are very contradictory [2]; results differing by several orders of magnitude are obtained in attempts to determine its value. Neither the Newton nor the Bingham equation (i.e., with the creep limit P_0 taken into account) gives positive results, as deformation of the metal produces changes which influence its mechanical properties, including the creep limit. The latter increases with increasing deformation, whereas values of P_0 determined at low stresses and correspondingly low deformation are used for determinations of viscosity.

For investigation of the rheological behavior of metals, and the influence of certain physicochemical factors on it, we performed creep tests on polycrystalline tin and lead in conditions approximating to uniform shearing deformation. The shape of the test specimens is shown in Fig. 1.

The flow curves of metals under constant stress (the stress remains constant, as the area on which the force acts does not change during the deformation, at least until the appearance of predestruction cracks) have three regions: 1) nominally-instantaneous deformation, measurable in ~1 second; 2) nonsteady creep at a gradually decreasing rate; 3) steady creep at a constant minimum rate $v_m = d\epsilon / d\tau$, where ϵ is the relative shear deformation. The decrease of deformation (elastic recovery on removal of load in the region of steady creep) is considerably less than the instantaneous deformation. This means that relaxation of elastic stresses takes place during the plastic flow. The region of nonsteady creep is relatively small, and is followed by the region with a steady minimum creep rate. The creep curves for tin are given in Fig. 2; Curves 4 and 5 both refer to the same stress, but Curve 5 represents creep in a surface-active medium. It follows from the slope of the curves in Fig. 2 that the rate of steady creep increases with the stress. The rheological curves for tin are given in Fig. 3. At low stresses, the rheological curve for 20° contains a region in which the relationship between the stress P and the steady flow rate v_m is linear. Extrapolation of this region of the curve to the abscissa axis gives the intercept P_0 , which may be regarded as the creep limit for the given experimental conditions. At higher stresses the curve is no longer linear, and v_m increases more and more steeply with P , so that at high stresses the rheological curve becomes asymptotic to a straight line parallel to the ordinate axis. The intersection of this line with the abscissa axis gives the intercept P_m , which should be regarded as the yield value in the Bingham region. The product $\eta v_m = P_m$ is virtually constant in this region. This region

* Paper at the 4th All-Union Conference on Colloid Chemistry, Tbilisi, May 1958.

is approached in our experiments. The rheological curve can be used to calculate the effective viscosity of the metal, but the effective viscosity varies continuously with the stress, and cannot serve as a physical characteristic of a metal. Viscosity calculations for flow at constant rate, with the creep limit taken into account, show that the plastic viscosity may be regarded as a constant which defines the properties of a metal at fairly low stresses (Fig. 4), where v_m is a linear function of P . At high stresses the breaking stress $P_m = \eta v_m$ [3].

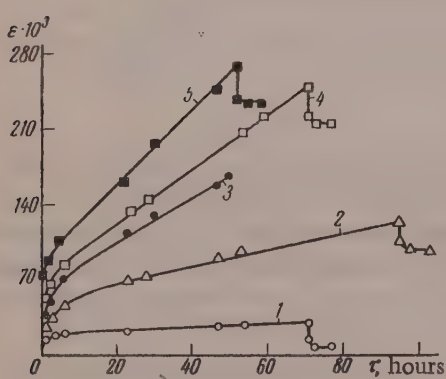


Fig. 2. Creep curves for lead at stresses: 1) 0.095; 2) 0.15; 3) 0.20; 4 and 5) 0.26 mg/mm^2 .

The creep of tin and lead under shear was studied at various temperatures, and in a surface-active medium. The rheological curves for tin at 89 and 122° are presented in Fig. 3. It is seen that the curves have the same course at elevated temperatures also, i.e., v_m is a linear function of P in the low-stress region. The

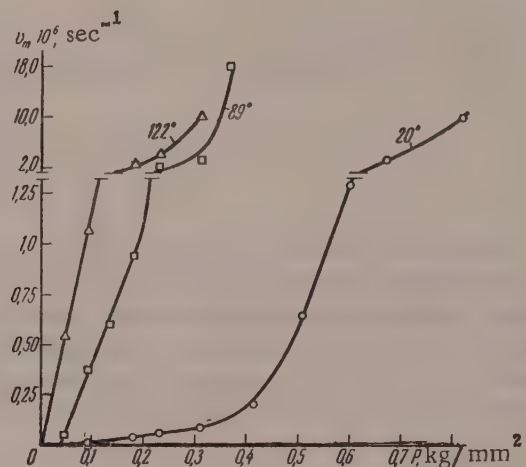


Fig. 3. Variation of the rate of steady flow of tin with the stress at various temperature.

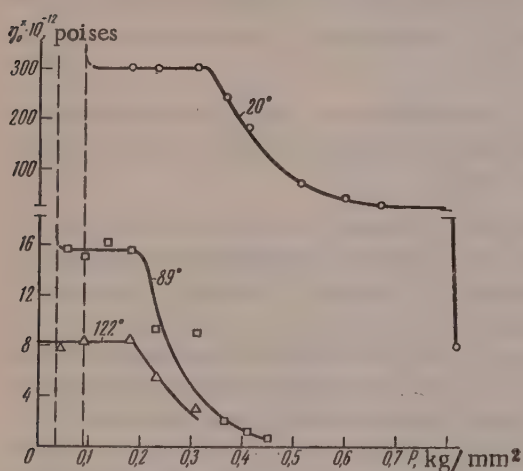


Fig. 4. Plastic viscosity-stress curves for tin at various temperatures.

TABLE 1

$\eta_0^* \cdot 10^{12}$ poises	Temperature in °C	Medium
Tin		
300	20	air
15.6	89	"
8.2	122	"
232	20	surface-active medium
Lead		
265	20	
15.9	86	
13.2	116	

higher the test temperature, the lower is the stress at which the linear portion of the rheological curve passes into a curve. Thus, the rheological curves are displaced toward lower stresses with increase of temperature. The creep limit decreases continuously, and becomes zero above a certain temperature. The maximum plastic viscosity (η_0^*) decreases correspondingly (Fig. 4, Table 1), and the region of the abrupt decrease of viscosity (practical yield value) is found at lower stresses. The $v_m - P$ curves for the high-stress region at 20 and 86 are given in Fig. 5. At these temperatures the flow rates increase rapidly over a narrow range, so that the Bingham equation is applicable in this region: $P - P_m = \eta^*_1$ or $\eta - \eta^*_1 = P_m/v_m$; if $\eta^*_1 \ll \eta$, which is indeed the case, then $\eta v_m = P_m$. Therefore a metal can be characterized by its maximum plastic viscosity

at low stresses, and by the breaking stress at high stresses, at high temperatures also.

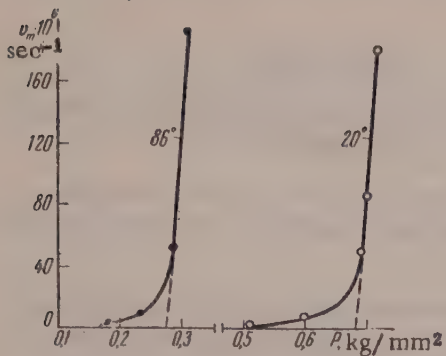


Fig. 5. Rheological curves for tin in the high-stress region.

The influence of a surface-active medium on the course of the rheological curve was of interest. The surface-active medium was a 0.2% solution of oleic acid in nonpolar vaseline oil. It was found in control experiments that the nonpolar vaseline oil itself had no effect on the mechanical properties of tin or lead. The surface-active medium has a significant influence on the creep curves. The rate of steady flow increases, and the whole tensile curve lies above the tensile curve in air at the same load. Accordingly, the rheological curve is displaced to the left along the stress axis, toward lower stresses, and a higher flow rate than that found in air corresponds to each stress (Fig. 6, Curve 2). However, the relationship is still linear in the low-stress region. The creep limit decreases appreciably. The maximum plastic viscosity also decreases, but only slightly (Fig. 6, Curve 4).

TABLE 2
Variation of the Effect of the Surface-Active Medium with the S/V Ratio for Tin

Shape of specimen	Cylindrical		Specimens used for shear tests	
	d = 0.5 mm (single crystal)	d = 2 mm	flat, Fig. 1,b	round, Fig. 1,a
S/V, cm ⁻¹	82	20	13	8
E, %	190	-	150	150

The effect of the surface-active medium may be evaluated in terms of the ratio, expressed as a percentage, of the difference between the steady flow rates in the surface-active medium and air to the steady rate in air, $E = 100 [v_{ma} - v_m]/v_m$. The effect E of the surface-active medium has a well-defined maximum on the E-P curves at stresses of ~ 400 g/mm² for tin, and 480 g/mm² for lead. The maximum effect of the surface-active medium corresponds to the stresses near the upper boundary of the region of constant plastic viscosity (Fig. 7). The effect for lead (275%) is approximately double the effect for tin (150%). These values are in good agreement with the results obtained for these metals by a number of investigators [4]. It is interesting to note that the specimens used in our experiments were rather massive in comparison to those

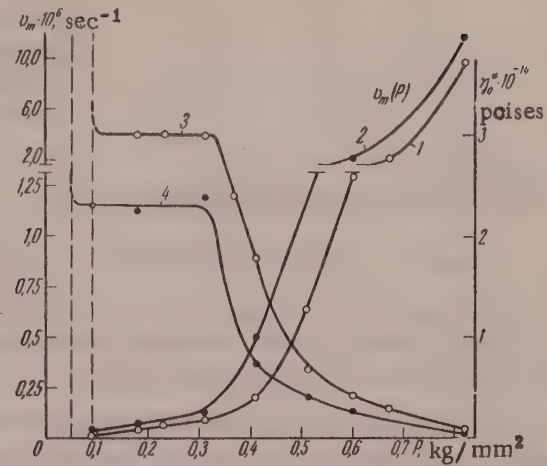


Fig. 6. Rheological curves and plastic viscosity curves for tin in air (1, 3) and in a surface-active medium (2, 4).

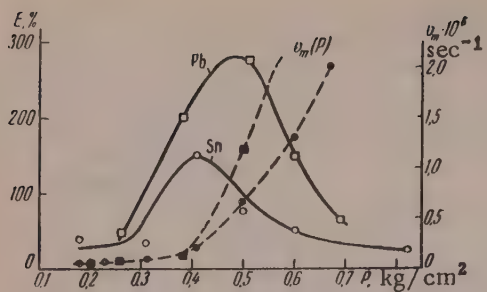


Fig. 7. Effect of the surface-active medium.

2. The plastic viscosity has constant maximum value, independent of the stress, at low stresses (above the creep limit). At high stresses the plastic viscosity falls sharply with increasing shear rate, so that the breaking stress is independent of the deformation rate.

3. Creep of lead and tin is considerably facilitated by a surface-active medium. The creep limit and the maximum plastic viscosity are lower in a surface-active medium. The maximum adsorption effect corresponds to shear stresses at the upper limit of the region of constant viscosity.

4. The plastic viscosity decreases regularly with increase of temperature as the result of an increased rate of flow of the metal and of a lowering of the creep limit.

Institute of Physical Chemistry
Academy of Sciences USSR
Division of Disperse Systems
Moscow

Received June 16, 1958

used by others. The effects of surface-active substances on specimens with different S/V ratios (S is the surface area; V is the volume of the specimen) are compared in Table 2. It is seen that the S/V ratio in our specimens was 1/8 of the ratio for the specimens used in most other experiments, but, as Table 2 shows, the magnitude of the effect is almost the same.

SUMMARY

1. The laws of plastic flow of lead and tin under shear over a wide stress range were studied.

LITERATURE CITED

- [1] P. A. Rebinder, Summaries of Papers at the Tectonophysical Conference (Moscow, 1957);^{*} Colloid J. 20, No. 5, 527 (1958).**
- [2] V. D. Kuznetsov, Physics of Solids, Vol. 4 (Tomsk, 1947).*
- [3] V. I. Likhtman and V. S. Ostrovskii, Proc. Acad. Sci. USSR 119, No. 3 (1958).**
- [4] V. I. Likhtman, P. A. Rebinder, and G. V. Karpenko, Influence of Active Media on Metal Deformation (Moscow, Izd. AN SSSR, 1954).*

* In Russian.

** Original Russian pagination. See C.B. Translation.

FORMATION OF NEW SURFACES IN THE DEFORMATION AND
DESTRUCTION OF A SOLID IN A SURFACE-ACTIVE
MEDIUM *

E. D. Shchukin and P. A. Rebinder

It has long been known that adsorption of surface-active substances by a solid undergoing deformation may have a decisive influence on the deformation and strength properties of the solid [1, 2]. Systematic investigations of this effect showed that it is very general; the accumulated experimental data laid the foundation of a new branch of science — physicochemical mechanics of solids. These extensive experimental data show convincingly that the influence of a surface-active medium on the mechanical properties of solids may result in a number of very diverse effects [14]; depending on the conditions, a body may become more plastic, or very brittle, or it may tend to undergo spontaneous dispersion into particles of colloidal size. The present paper deals with some aspects of these three effects.

I. Numerous experimental results [3, 5, 7] show convincingly that the effect of plastification of solids as the result of reversible adsorption of extremely small amounts of surface-active substances from the surrounding medium is very general. In particular, this effect is very distinctive in the deformation of single crystals of tin, zinc, and other metals in media such as solutions, in nonpolar vaseline oil, of a number of organic substances with a polar group and a long hydrocarbon chain in the molecule (oleic acid, etc.). When single crystals are extended at a constant rate, the effect of the surface-active medium is to lower the yield point; in tests under constant load the rate of plastic flow is increased. The following facts are noteworthy in analysis of these effects.

1. Since diffusion of large organic molecules into the lattice of a single crystal of a metal is impossible, the effect must depend on purely surface interaction between the specimen and the medium. This interaction lowers the free surface energy σ of the specimen as the result of reversible adsorption from the surroundings [1-3].

2. The decrease of free surface energy observed in these experiments on the adsorption of organic substances is small, of the order of a few tens of ergs per cm^2 , relative to the free surface energies of the metal single crystals used ($\sim 500\text{-}1000 \text{ ergs/cm}^2$); i.e., the decrease does not exceed 1/10 of the initial value of σ .

3. The plastification effect is observed within definite limited ranges of temperature and deformation rates [3, 13]; it is therefore caused by some thermally activated process. The temperature corresponds to the optimum deformation rate with regard to the magnitude of the effect.

Since the plastic flow of a crystal consists of displacement of dislocations in the slip planes and their emergence on the surface, while the plastification effect is caused by purely surface phenomena, the principal cause of the observed effect must evidently be interaction of the dislocations with the free surface of the crystal [15].

Being a thermodynamically unstable defect (having excess free energy), a dislocation tends to emerge to the surface. The force of attraction of an edge dislocation, to a surface situated parallel to it, has been determined by an approximation of the theory of elasticity; this force (termed the "mirror-image force") is inversely proportional to the distance from the surface, i.e., it is determined by a slowly changing logarithmic

*Paper at the 4th All-Union Conference on Colloid Chemistry in Tbilisi, May 1958.

potential [16]. At the same time, the emergence of a dislocation (i.e., the completion of shear in a given slip plane) is accompanied by the appearance of a step, the width of which, at the given point of the slip plane contour, is equal to the component of the Burgers dislocation vector lying in the slip plane parallel to the contour. The formation of each new surface cell requires the expenditure of an amount of work $\leq b^2\sigma$, where b is the Burgers vector (unit translation). This potential barrier extends into the crystal to a distance of only about half the width of the dislocation (of the order of a few b), i.e., it is rather steep, and in the immediate proximity to the surface the force determined by it, preventing the emergence of the dislocation, is greater than the "mirror-image force" [15] tending to push it out.

Consider a point M on the contour of an active slip plane, at which the Burgers dislocation vector is perpendicular to the contour and the step reaches its maximum width $\sim b$. During plastic flow of the crystal y , dislocations pass through this point in one second, and as each passes through, a new surface $\sim b^2$, with free energy $\sim b^2\sigma$, is formed in the region of point M. This free energy is probably the value to be ascribed to the activation energy of the processes in absence of applied stresses.

The condition of equality of the incoming and outgoing dislocation at the point M is given by the equation $v = \nu \exp(-U/kT)$, where $\nu \sim 10^{12} - 10^{13} \text{ sec}^{-1}$ is the Debye vibration frequency of the lattice, and U is equal to $b^2\sigma$, less the work of external forces A. Then the temperature defined by this expression, $T_1 = b^2\sigma/k\ln(\nu/v)$ corresponds to the "upper boundary temperature" of the existence of the potential barrier in question: when $T > T_1$, the application of any significant forces is not required for emergence of the dislocations to the crystal surface; at lower temperatures work must be done by external forces. It is to be expected that near T_1 , when A is small, even a small decrease of σ , by lowering A to zero, would have the greatest influence on the plastic properties of the crystal; i.e., from the point of view of the plastification effect, the optimum temperature $T_{\text{opt}} \approx T_1$.

The parameter y is determined by the rate and microheterogeneity (localization of shears in the series of slip lines) of the deformation, and with average crystal orientations it may be estimated [15] as follows: $v \sim \dot{\epsilon}hu/b$; here $\dot{\epsilon}$ is the relative rate of extension; h is the average distance between the slip lines, while the factor of deformation-microheterogeneity u has the meaning of the ratio of the total number of slip lines to the number of active slip lines at any given instant (in general, hu may vary in fairly wide limits, say from 10^{-1} to 10^{-3} cm).

Thus, the optimum temperature of the plastification effect for the model under consideration can be estimated as

$$T_{\text{opt}} \sim \frac{b^2\sigma}{k \ln(vb/shu)} \quad (1)$$

For $\dot{\epsilon} = 10\% \text{ min}^{-1}$ the logarithmic term in the denominator is $\sim 20-25$, while substitution of $b = 3 \cdot 10^{-8} \text{ cm}$ and $\sigma = 10^3 \text{ ergs/cm}^2$ gives $\sim 0.5-0.6$ electron-volts for the activation energy; this means that under the given conditions $T_{\text{opt}} \sim 300^\circ \text{ K}$; increase of $\dot{\epsilon}$ by two orders of magnitude should displace T_{opt} to about 400° K .

This result is in good agreement with experimental data on the yield value [13], according to which the plastification effect of adsorption is at a maximum at room temperature if the extension rate $\dot{\epsilon} = 5-10\% \text{ min}^{-1}$ and at 100° if $\dot{\epsilon} \sim 500\% \text{ min}^{-1}$.

A considerable role in the plastification effect may be played by subsurface sources of dislocation (anchored at a single point), which begin to operate at considerably lower stresses than sources anchored at two points [17]. It is known that a thin polycrystalline film, by hindering the operation of such sources, can raise appreciably the yield point of a single crystal [18-20]. Conversely, decrease of σ should increase the activity of the subsurface sources and lower the yield point. Since the interaction of such a source with the surface consists of consecutive "tracing" of a dislocation segment on the crystal surface by the second (free) end, i.e., of the formation of a step on the surface, Expression (1) remains completely valid; the parameter y remains of the same order of magnitude and acquires the meaning of the number of rotations of the subsurface source per second (a dislocation spiral in the Frank-Read mechanism [16]).*

*The mechanism of the action of a surface-active medium may also be associated with generation of dislocation sources. However, the question of generation of these sources, and of the influence of σ on this process, is still not clear.

However, the above model cannot be applied directly to the recently discovered case of plastification of metal single crystals under the influence of melted metallic coatings at elevated temperatures and very low extension rates [11]; in this case the activation energy of the process is considerably greater than $b^2\sigma$. The principal role here is evidently played by interaction of dislocations with surface defects blocking individual points on the contour of the slip plane; the potential barrier is higher and is described by a different expression, but it remains of short range and significantly dependent on σ .

Thus, the plastification effect, which is only one instance of the influence of surface-active media on the mechanical properties of solids, is in itself complex and diverse, is associated with the existence of a whole spectrum of activation energies, and may be manifested over different ranges of temperature and deformation rate.

We have considered some aspects of the plastification of solids in surface-active media. We now examine the directly opposite effect: the production of extreme brittleness and a sharp decrease of strength.

II. Extreme brittleness and a sharp decrease of strength may be produced in metal single crystals in presence of a very thin melted coating of a more easily fusible metal; for example, in zinc in presence of liquid tin [8] or mercury [9, 10].

This effect has the following characteristic features.

1. The decrease of surface free energy at the boundary between the metal and its saturated solution in another liquid metal may be very considerable [4, 8], some hundreds of ergs/cm².

2. The effect is observed over a wide temperature range, of which the lower limit is the melting point of the coating T_m , and the upper limit is the melting point of the metal T_M (for the zinc-tin system [8]), or the temperature of brittle transition T_C ; in this region, in a relatively narrow range ΔT , peculiar "partial brittleness" (in the system zinc-mercury [9]) is observed.

3. Since the effect involves the development of cracks within the crystal, it is a volume effect which requires rapid penetration of surface-active atoms to the surfaces of the internal microcavities by nonregular diffusion (two-dimensional migration) along the defects of the crystal structure.

Elucidation of the mechanism of this effect must evidently be based on an analysis of the conditions in which "dangerous" microcracks originate and develop in the course of brittle breakdown: sharp decrease of σ at the internal microcavities facilitates this process and renders it independent of thermal activation over a wide temperature range.

Investigations of the conditions for the brittle rupture of pure-zinc single crystals along the basal planes at low temperature [10] showed that failure is always preceded by some plastic deformation. The tensile stress p_c , normal to the cleavage plane, is by no means constant for differently oriented single crystals: the less the angle between the axis of the specimen and the basal plane, the greater is the limiting plastic shear, the higher is the shearing force τ_c reached at failure, and the lower is p_c ; the Zonke law ($p_c = \text{const}$) is totally inapplicable in this instance.

It is known that the actual ultimate tensile stresses at the cleavage planes are several orders of magnitude less than the calculated values for an ideal lattice; this discrepancy is due to the presence of microcrevices in the crystal. It is natural to assume that if tensile rupture is due to presence of a microcrevice, the magnitude ζ of which becomes dangerous at a given p_c , the formation and development of the microcrevice to the dangerous dimensions must be related to the magnitude of the applied shearing stress τ and the plastic deformation process in the course of which nonuniformity of shear leads to sharp local stress concentrations and the formation of microcavities [12].

In agreement with Mott and Stroh [21-23], we consider the main sites of high stress concentration to be piled-up dislocations (incomplete local shears) formed at various strong obstacles in the slip plane. Analysis of the course of formation of the dislocation accumulations shows that even at low values of τ the head dislocations may coalesce and form a hollow nucleus (such hollow dislocation nuclei, giving rise to pores in the crystal, are able to ensure rapid penetration of the surface-active substance into the crystal even at the early stages of deformation). The accumulation develops with increase of τ and of specific crystallographic shear, and in its leading region, at a certain angle Θ to the slip plane, an equilibrium microcrevice develops, the

limiting size of which is of the order of $c \sim \tau^2 L^2 / G\sigma$; here G is the shear modulus and L has the meaning of the effective dimensions of the slip plane (in the case of polycrystals it is the grain size, and for not very thick single crystals, ≤ 1 mm, the diameter) [12, 22].

On the other hand, if a tensile stress p is applied perpendicularly to the plane of a crack of width c , according to Griffith [24] the crack ceases to be in equilibrium if the condition $p_c \sim (G\sigma/c)^{1/2}$ is satisfied.

Substituting the maximum possible magnitude of the crack $c(\tau)$ into the expression $p_c(c)$, we obtain, instead of the Sohnke law $p_c = \text{constant}$, a new expression

$$p_c \tau_c = \text{const} = K^2, \quad (2)$$

where $K = \gamma \sqrt{G\sigma} / L$; here the dimensionless coefficient γ is close to unity. Expression (2) may be defined as the "condition that the product of the normal and shearing stresses is constant" in brittle rupture [12].

The stresses p_c and τ_c in Equation (2) are in general applied to different planes, intersecting at an angle Θ . However, in the case of zinc single crystals, in which the same basal plane is the sole slip plane and the sole well-defined cleavage plane under the given conditions, it may be assumed that $\Theta \approx 0$, i.e., p_c and τ_c may be referred to the basal plane. Then the following expressions are obtained in conjunction with the geometrical condition $p_c/\tau_c = \tan \chi$, where χ is the angle between the basal plane and the axis of the specimen at the instant of rupture:

$$p_c = K \sqrt{\tan \chi}; \quad \tau_c = K \sqrt{\cot \chi}. \quad (3)$$

The experimental values of $p_c(\chi)$ and $\tau_c(\chi)$ for brittle rupture of zinc single crystals along basal planes, at the temperature of liquid nitrogen [10] are in good agreement (Fig. 1) with the theoretical curves for $p_c(\chi)$ and $\tau_c(\chi)$ calculated from Equations (3) at $K = 200 \text{ g/mm}^2$ [12] (the constant K was chosen for the best agreement of the experimental points and the theoretical curves). On the assumption that, for zinc, $G = 3 \cdot 10^{11} \text{ dynes/cm}^2$, $\sigma = 10^3 \text{ ergs/cm}^2$, and $L = \phi = 0.1 \text{ cm}$, we have $\gamma = K/(G\sigma/L)^{1/2} \approx 0.4$.

For analogous data on the brittle rupture of amalgamated single crystals of zinc at room temperature [10], the experimental points again coincide with the curves based on Equations (3), but the constant K is found to be $\sim 80 \text{ g/mm}^2$ [12], evidently as the result of the great decrease of the free surface energy of zinc in presence of mercury [4, 6, 8, 9]. This relative change of σ is $(K_{Zn}/K_{Zn-Hg})^2 \sim 6$ (somewhat lower, to be exact, if the dependence of the modulus G on temperature is considered), i.e., in presence of

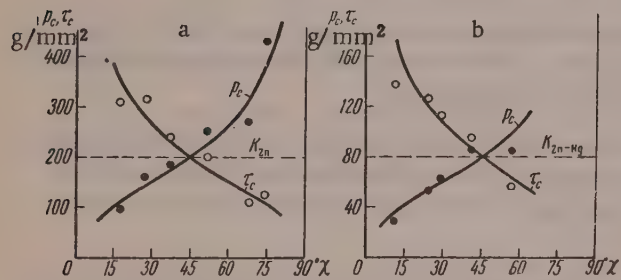


Fig. 1. Normal stresses p_c and shearing stresses τ_c in the rupture of differently oriented zinc single crystals along the basal planes: a) Single crystals of pure zinc at -196° ; b) amalgamated single crystals of zinc at 20° .

mercury, the free surface energy of the rudimentary microcavities was approximately $150-200 \text{ ergs/cm}^2$ in these experiments.

Since the constant K depends little on the temperature, whereas plastic flow of crystals is a pronounced thermally activated process, it is to be expected that at a certain temperature T_c , and at not excessively high deformation rates, the yield value and the work-hardening coefficient should be so low that Condition (2) is not satisfied even on considerable decrease of σ and at the most extensive deformations, so that the single crystal would become plastic again.

According to an equation [9] derived for amalgamated single crystals of zinc, at $\dot{\epsilon} = 15\% \text{ min}^{-1}$ and $\chi_0 \sim 45^\circ$ the transition from the brittle to the plastic state occurs at about $T_c = 420^\circ \text{ K}$, in the range $\Delta T = 40-50^\circ$, (in this range the $\epsilon_{\max}(T)$ curve rises from a few per cent to 500-600%, see Fig. 2).

If plastic flow is regarded as a thermally activated process in which dislocations overcome obstacles in the slip plane, and if the maximum accumulation of dislocations possible under the given conditions is compared with the "dangerous" value leading to the development of a nonequilibrium crack, it is possible to derive

a criterion for the deformability of a crystal in relation to T , $\dot{\epsilon}$, and σ [15], and to determine the "probability of plastic flow"

$$W = 1 - \exp \{ - \exp [- (U_c/k) \cdot (1/T - 1/T_c)] \} \quad (4)$$

and the critical transition temperature

$$T_c = U_c/k \ln (\nu \lambda b / \dot{\epsilon} h u); \quad (5)$$

here $U_c = U_c(\sigma)$ is the activation energy for overcoming an obstacle by a dislocation at the stress at which brittle failure occurs, and λ is the number of points along the dislocation line at which rupture is possible; on the whole, the logarithmic term in the denominator > 30 .

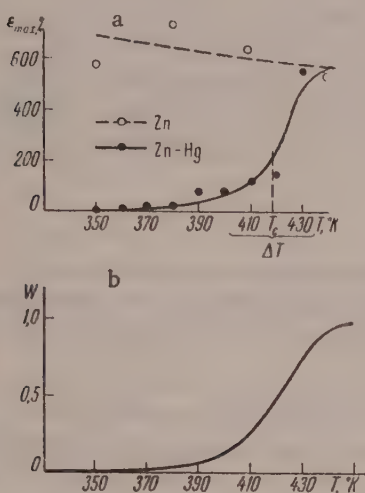


Fig. 2. Variation of the deformation at rupture ϵ_{\max} with temperature for pure and amalgamated single crystals of zinc at $\dot{\epsilon} = 15\% \text{ min}^{-1}$ and $\chi \sim 45^\circ$ (a), and the theoretical relationship between "the probability of plastic flow" and the temperature for amalgamated single crystal (b).

into the zinc, and because of the formation of a surface "casting" of polycrystalline mercury [20]. At higher temperatures the strengthening effect (i.e., additional retardation of the dislocations by point defects — foreign atoms) disappears.

Changes in the deformation and strength properties as the result of adsorption have also been found in glasses [27, 28]. It has been found that the presence of surface-active substances (including water vapor) lowers the tensile strength of glass fibers, especially in prolonged strength tests. At the same time, adsorption from the surrounding medium may lead to pronounced elastic lag, which in especially-active media passes into residual deformations increasing with time.

The dislocation mechanism described above is inapplicable to noncrystalline bodies — other concepts are necessary to account for these effects in glasses. However, here also the decisive role is probably played by easier development of microdefects as the result of a lowering of the free surface energy.

III. Finally, we consider the case when adsorption from the surrounding medium lowers the free surface energy of a solid to extremely low values, tenths of one erg per cm^2 and less. In such cases, if the true solubility is low, as the medium penetrates along the structural flaws of the body (boundaries of the microblocks), spontaneous dispersion of the body into particles of colloidal size $\delta_m \sim 10^{-6} \text{ cm}$, i.e., of the same order as the structural microblocks [4, 8, 14, 25] may take place.

Consider a body with linear dimensions L . Neglecting small numerical coefficients, we assume its surface area to be $A_0 \sim L^2$ and its volume $V_0 \sim L^3$. The total number of microblocks on the surface is approxi-

Experimental data [9] on ϵ_{\max} as a function of T give $U_c \approx 3.3kT_c^2/\Delta T \sim 1.1 \pm 0.1$ electron-volts, and $\ln (\nu \lambda b / \dot{\epsilon} h u) \approx 3.3T_c / \Delta T \sim 31 \pm 3$. The plot of W as a function of T based on these estimates gives good agreement with the experimental $\epsilon_{\max} - T$ relationship [9, 6].

The above considerations are confirmed by experiments on the brittle failure of single crystals of zinc coated with melted tin [8]. At the usual extension rates of $\sim 10\% \text{ min}^{-1}$ the effect is observed from T_m up to T_M (i.e., $T_c > T_m$). If the rate is decreased by 4-5 orders of magnitude, as in experiments on the rate of steady creep [11], brittleness disappears over the entire $T_m - T_M$ range (T_c is now lower than T_m); moreover, a plastification effect is observed, as described in the first section of this paper.

The effect of critical embrittlement and strength decrease may be accompanied even by some elevation of the $P - \epsilon$ curve, as the result of alloying of the specimen with atoms of the coating metal as they diffuse into the crystal lattice. This is clearly revealed in the rupture of such specimens in liquid nitrogen (i.e., below T_m); in this case amalgamated single crystals of zinc are stronger than pure crystals, both because of diffusion of mercury

mately L^2/δ_m^2 , and the probability of separation of each is proportional to $\nu \exp(-U_A/kT)$, where U_A is the activation energy of the process, and ν is the frequency of the thermal vibrations of the block.

The number of particles detached from the surface per second is $q \approx (L^2/\delta_m^2) \times \nu \exp(-U_A/kT)$. We assume that the body can be dispersed if its subdivision is completed in time $t^* \sim 1$ year = $3 \cdot 10^7$ seconds. Then the average number of particles detached per second must be $q^* \approx L^3/\delta_m^3 t^*$. The probability of dispersion or, more accurately, the "measure of the dispersibility of the body" may be defined as the ratio $M_D = q/q^* = (\nu t^* \delta_m/L) \cdot \exp(-U_A/kT)$. The tendency to dispersion evidently corresponds to the condition $M_D \geq 1$, or, which is the same thing, the condition $Di \leq 1$, where the dimensionless criterion Di is

$$Di = U_A/kT \ln(\nu t^* \delta_m/L). \quad (6)$$

In general, the activation energy U_A of the process is determined by the work of formation of a new surface, less, first, the work of external forces (or internal elasticity fields caused by local stress concentrations near the defects) and second, the term $T\Delta S$, where ΔS is the increase in the entropy of a particle when it passes into a colloidal solution. We suppose, however, that dispersion proceeds in absence of external force (spontaneously); we also neglect the work of the internal elasticity fields and the entropy increase; this results in some revaluation of U_A , which can now be written as $U_A \sim \sigma \delta_m^2$. Then we have the following approximate condition for spontaneous dispersion

$$Di_0 = \sigma \delta_m^2/kT \ln(\nu t^* \delta_m/L) \leq 1. \quad (7)$$

The logarithmic term in the denominator can be readily estimated on the following considerations. The order of magnitude of the vibration frequency ν is determined by the particle size δ_m and the velocity of sound c_s : $\nu \sim c_s/\delta_m$. Therefore $\ln(\nu t^* \delta_m/L) = \ln(c_s t^*/L) = \ln(10^5 \cdot 3 \cdot 10^7/1) \approx 30$ [14]. Evidently the numerical values of t^* or L are not very critical.

At room temperature Equation (7) leads to the condition $\sigma \leq 4 \cdot 10^{-14} \cdot 30/\delta_m^2$ or, roughly, $\sigma \leq 10^{-12}/\delta_m^2$ ergs/cm². This means that the body can undergo dispersion, in the sense postulated, into particles of $\delta_m \sim 10^{-6}$ cm, if σ is increased to 1 ergs/cm² or less.

However, this condition refers only to the kinetics of the process if it is thermodynamically possible; that is, if the dispersion process is thermodynamically advantageous, then it will proceed at a sufficient rate if Condition (7) is satisfied.

We now consider qualitatively the free energy change ΔF of the system when a solid is dispersed in a liquid into particles of colloidal size: $\Delta F = \sigma \Delta A - T \Delta S$, where ΔA is the increase in the free surface of the particles, and ΔS is the increase in the entropy of the system. Neglecting, as before, small numerical coefficients, we can write ΔA as $\Delta A \sim n \delta_m^2$, where $n = V_0/\delta_m^3$, the number of colloidal particles in the solution.

Suppose that N_1 moles of the solid is dissolved in N_2 moles of liquid. Then the entropy of mixing is

$$\Delta S = -kN_A(N_1 + N_2) \{[N_1/(N_1 + N_2)] \ln[N_1/(N_1 + N_2)] + [N_2/(N_1 + N_2)] \ln[N_2/(N_1 + N_2)]\},$$

where N_A is the Avogadro number. When $N_1 \ll N_2$, we have $\Delta S = +kN_A N_1 \times \{\ln(N_2/N_1) + 1\}$. In this case the product $N_A N_1$ is the number n of the particles of the solid phase, while the logarithmic term is not very critical, and is about 10-15. Hence $\Delta S \approx (10-15)nk$.

For the change of free energy, we have $\Delta F = n\sigma\delta_m^2 - (10-15)kT$; this becomes negative if

$$\sigma \leq (10-15) \cdot kT/\delta_m^2, \quad (8)$$

for room temperatures, this gives approximately $\sigma \leq 0.5 \cdot 10^{-12}/\delta_m^2$ ergs/cm². Therefore, in order that the dispersion into particles of $\delta_m \sim 10^{-6}$ cm should be thermodynamically advantageous, σ must be decreased at least down to some tenths of 1 ergs/cm². Since this condition is more critical than the Criterion (6), it is justifiable to write the latter in the roughly approximate form of Condition (7).

Nevertheless, even the more rigid Condition (8) is not yet a sufficient condition of the possibility of the process. Indeed, at very low values of δ_m the situation is changed considerably by considerations of equilibrium between the colloidal particles and substance in true solution, and also of the change of the particles. As δ_m decreases, ΔF begins to increase again; it may not have a minimum at all, and then the colloidal state is unattainable under the given conditions; it is possible that despite the fact that the condition $\Delta F = 0$ cannot be satisfied there might be a minimum, but with a positive value, when the colloidal state is metastable; only if the condition $\Delta F = 0$ is satisfied can ΔF have a negative minimum, corresponding to a stable colloidal state at some even smaller value of δ_m .

The microstructure of the particular solid also places considerable limitations on the possibility of dispersion: the process does not occur in practice if the structure is too coarse in comparison with the thermodynamically possible value of δ_m , or if the nature of the defects between the blocks of the microstructure is such that the surface-active molecules cannot penetrate to even a small depth. (In the latter case, however, it is possible to consider the consecutive, cell-by-cell, development of the particle surface δ_m^2 , as was done by Bartenev [26]). It must be stressed that in crystalline bodies the microstructure is nothing else but a dislocation structure; its nature is determined by the growth conditions of the single crystal or the polycrystalline aggregate, and by the plastic deformations to which it has been subjected.

On the other hand, Conditions (6) and (8) are more easily satisfied if we take into account the liberation of elastic energy associated with the existence of a microstructure (dislocation horizontal rows, vertical walls of dislocations, etc.) when the body breaks up into colloidal particles.

Indeed, in heavily cold-worked metal the dislocation density may reach $\sim 10^{11} - 10^{12} \text{ cm}^{-2}$, and the corresponding stored elastic energy may be $\sim 10^8 \text{ ergs/cm}^3$ and over [23]. This corresponds to up to 10^{-10} erg for each element of the volume of linear dimensions $\delta_m \sim 10^{-6} \text{ cm}$. If all this elastic energy could be utilized in the formation of a new surface, dispersion would be possible even at relatively high values of $\sigma \sim 10 \text{ ergs/cm}^2$ and over.

SUMMARY

Several distinctive effects are observed in adsorption on surfaces of solids undergoing deformation.

1. Small decreases of free surface energy, of a few tens of ergs per cm^2 , caused by adsorption of some organic substances may result in considerable plastification of a strained crystal. In the light of the dislocation theory this effect is attributed to a lowering of the potential barrier, associated with the formation of a new surface and preventing emergence of the dislocations to the crystal surface; in agreement with experimental results, it is possible to determine theoretically the temperatures and deformation rates at which the optimum effect is obtained.

2. If the adsorbed substance decreases the surface energy of the crystal considerably, to a half of its initial value or less, and if it can migrate rapidly into the crystal along the hollow dislocation nuclei and other structural flaws, adsorption may result in brittleness and a sharp decrease of strength. The reason for this is easier development of internal microsurfaces, and the formation of "dangerous" cracks in regions with high local stress concentrations resulting from dislocation accumulations. A theoretical expression is derived for the probability of plastic flow of a body, and an expression in agreement with experimental data, for the transition from brittle failure to plastic flow in a definite temperature range; the theory also provides a correct evaluation of normal and shearing stresses in brittle failure.

Analogous experimental data are known for glasses. The mechanism of such effects must be explained on different considerations.

3. If the free surface energy of a body is decreased very greatly — to fractions of 1 erg/cm^2 or less — spontaneous dispersion of the body into colloidal particles may occur. By consideration of thermal fluctuations with microblocks separated by structural defects, both in absence and in presence of external forces or local stressed states, it is possible to determine the rate of growth of the free surface of the separating particles, i.e., the rate of the dispersion process, and to estimate quantitatively the value of the preexponential term in the expression for the probability of spontaneous separation of a colloidal particle; the criterion for the spontaneous dispersion of a solid, derived from this expression, is obtained in more precise form. Consideration of the

conditions for the thermodynamic possibility of the dispersion process give similar results.

Institute of Physical Chemistry,
Academy of Sciences SSR
Division of Disperse Systems
Moscow

Received June 16, 1958

LITERATURE CITED

- [1] P. A. Rebinder, *Z. Phys.* 72, 191 (1931).
- [2] P. A. Rebinder, Jubilee Volume on the 30th Anniversary of the Great October Socialist Revolution, 1 (Izd. AN SSSR, 1947), p. 123. *
- [3] V. I. Likhtman, P. A. Rebinder, and G. V. Karpenko. Effect of Surface-Active Media on the Deformation Processes of Metals (Izd. AN SSSR, 1954). *
- [4] P. A. Rebinder, "New problems of physicochemical mechanics." Paper at the Permanent Colloquium on Solid Phases of Variable Composition, jointly with the Moscow Colloid Colloquium, January 26, 1956; * *J. Acad. Sci. USSR* No. 10, 32 (1957). *
- [5] V. I. Likhtman, *Progr. Phys. Sci.* 37, 3 (1949); 54, 6 (1954).
- [6] P. A. Rebinder, *Bull. Acad. Sci. USSR, Div. Chem. Sci.* 11, 1284 (1957). **
- [7] P. A. Rebinder and V. I. Likhtman, Proc. of the 2nd Internat. Congress of Surface Activity, (London, 1957) p. 563.
- [8] P. A. Rebinder, V. I. Likhtman, and L. A. Kochanova, *Proc. Acad. Sci. USSR* 111, 1278 (1956).
- [9] V. N. Rozhanskii, N. V. Pertsov, E. D. Shchukin, and P. A. Rebinder, *Proc. Acad. Sci. USSR* 116, 769, (1957). **
- [10] V. I. Likhtman, L. A. Kochanova, and L. S. Briukhanova, *Proc. Acad. Sci. USSR* 120, No. 4 (1958).
- [11] V. A. Labzin and V. I. Likhtman, *Proc. Acad. Sci. USSR* (1958), in the press.
- [12] E. D. Shchukin and V. I. Likhtman, *Proc. Acad. Sci. USSR* (1958), in the press.
- [13] V. I. Likhtman, P. A. Rebinder, and L. P. Ianova, *Proc. Acad. Sci. USSR* 56, 8 (1947).
- [14] E. D. Shchukin and P. A. Rebinder, Summaries of Papers at the 4th All-Union Conference on Colloid Chemistry, Tbilisi, May 1958 (Moscow, Izd. AN SSSR, 1958), p. 128. *
- [15] E. D. Shchukin, *Proc. Acad. Sci. USSR* 118, 1105 (1958). **
- [16] A. H. Cottrell, *Dislocation and Plastic Flow in Crystals* (Metallurgy Press, 1958) [Russian translation].
- [17] J. S. Fischer, *Trans. AIMME* 194, 531 (1952).
- [18] V. I. Likhtman and V. S. Ostrovskii, *Proc. Acad. Sci. USSR* 93, 105 (1953).
- [19] G. V. Greenough, *J. Inst. Metals*, No. 12, 467 (1956).
- [20] L. S. Briukhanova and E. D. Shchukin, *Engineering Physics Journal* (1958) (in the press).
- [21] N. F. Mott, *Proc. Phys. Soc. B* 64, 729 (1951); *Philos. Mag.* 43, 1151 (1952); *Proc. Roy. Soc. A* 220, 1 (1953); *J. Phys. Soc. Japan* 10, 650 (1955).
- [22] A. N. Stroh, *Proc. Roy. Soc. A* 218, 391 (1953); A 223, 404 (1954); *Philos. Mag.* 46, 968 (1955).
- [23] A. N. Stroh, *Philos. Mag.* 2, 1 (1957).
- [24] A. A. Griffith, *Philos. Trans. Roy. Soc., London, A* 221, 163 (1920).
- [25] M. Volmer, *Z. Phys. Chem.* 125, 151, (1927); A 155, 281 (1931).

*In Russian.

**Original Russian pagination. See C.B. Translation.

- [26] G. M. Bartenev, Bull. Acad. Sci. USSR, OTN No. 9 (1955).
- [27] M. S. Aslanova, Proc. Acad. Sci. USSR 95, 1215 (1954).
- [28] M. S. Aslanova and P. A. Rebinder, Proc. Acad. Sci. USSR 96, 299 (1954).

THE THEORY OF SPONTANEOUS DISPERSION OF SOLIDS *

G. M. Bartenev, I. V. Iudina, and P. A. Rebinder

The adsorptional lowering of strength of solids has been studied in detail [1-5].

The cause of the decrease of strength of a solid in a surface-active medium is decrease of surface energy at the body-medium interface. Media similar in molecular nature to a given body (fusible metals and alloys are such media in relation to metals) decrease its surface tension to very low values, and brittle rupture occurs even at small tensile stresses. The surface energy of a body can be decreased so much that the colloidal state becomes thermodynamically more stable than the condensed state, and the body begins to break down spontaneously, in absence of external forces, into particles the dimensions of which correspond to the mosaic blocks in the case of single crystals, to individual grains in polycrystals, and to macrostructural regions in glasses. The kinetics of this type of breakdown is determined by the existence of structurally weakened boundaries between the microregions (blocks of the mosaic structure of a single crystal, grains of polycrystal, macrostructural regions in glass, etc.) and internal stresses of the second kind [6] at these boundaries.

Disintegration of the body occurs along complex planes, intersecting in all directions, and passing along the most weakened boundaries. Such spontaneous dispersion differs substantially from ordinary destruction under the action of external forces, when rupture occurs in the plane of the greatest tensile force, extending not only along the boundaries, but through the microregions themselves.

Breakdown of the boundaries may be regarded as brittle, apart from slight plastic deformation at the vertices of the microcrevices, as the internal stresses are generally small and do not reach the plastic limit. This is another significant distinction from destruction under external load, when the rupture of metals is accompanied by appreciable plastic deformation. The role of dislocations in single crystals reduces to the formation of microdefects which form the block boundaries, and which may be characterized by a certain average "surface tension" α_b at the boundaries. The formation of new dislocations does not play any significant role in the spontaneous dispersion process itself, as plastic deformation is virtually absent.

The growth of cracks under external stress proceeds at an increasing rate, as the stress on the remaining cross section of the specimen increases. Spontaneous dispersion proceeds at a certain average rate, usually very low; small variations of this rate are due, not to the development of the process as a whole, but to fluctuations of the magnitude of the internal stresses and the degree of structural weakening from boundary to boundary of the microregions. This constitutes the third distinctive feature of such processes.

Here we consider the spontaneous dispersion of a single crystal, but the general reasoning is also applicable to polycrystals, where the individual grains play the part (and possibly more actively) of the mosaic blocks, and to glasses with well-defined macrostructural regions [7].

This discussion does not represent a final theory of spontaneous dispersion, but rather consists of an examination of the physical nature of the process, its causes, the influence of various factors on it and, finally, it includes the derivation of certain criteria.

The mechanism of brittle destruction. Since the mechanism of crack growth is important in relation to the dispersion of solids, the concepts of crack growth on which the subsequent discussion is based must first be considered.

*Paper at the 4th All-Union Conference of Colloid Chemistry in Tbilisi, May 1958.

The molecular mechanism of crack growth is considered in a paper by one of the present authors [8]. The influence of a surface-active medium was not considered but we shall show that this additional influence on the kinetics of crack growth can be taken into account.

As destruction is a nonequilibrium process, it cannot be examined by the methods of classical thermodynamics. All the theories based on thermodynamic relationships (including the theory of Griffiths) can only be used to determine the instant when equilibrium breaks down. Investigation of the rupture process itself demands a kinetic approach, such as that proposed by one of the authors [8]. We shall consider it briefly here.

Whereas simple cleavage of bonds between pairs of atoms or molecules does not always involve the surmounting of a potential-energy barrier, cleavage of any type of bonds in a solid with subsequent formation of new surfaces at the apex of the growing microcrevice must involve transition across a barrier. In the paper cited [8] the growth of one, the most dangerous, crack was considered, as this provides a basis for the interpretation of the whole complex rupture process, which evidently involves interaction of the individual cracks.

The concepts of the reversibility of microcrevice development in time, the form of the microcrevices [1] (Fig. 1), and the role of thermal fluctuations were used by the author to derive an equation for the rate of rupture, and the latter was used as the basis of a number of experimental relationships.

If we consider the group of particles at the vertex of the crack, then the left-hand minimum of potential energy (Fig. 2) corresponds to the stable state of the particles within the body, and the right-hand minimum, to their stable state at the new free surface. In absence of extension (and of an active medium) the barrier U_1 is always higher than U_2 , and the crack does not grow. Moreover, in absence of corrosion processes and internal stresses the crack closes up to the defect at which it originated, as it is more probable that the particles are at the left-hand rather than the right-hand minimum of the potential curve.

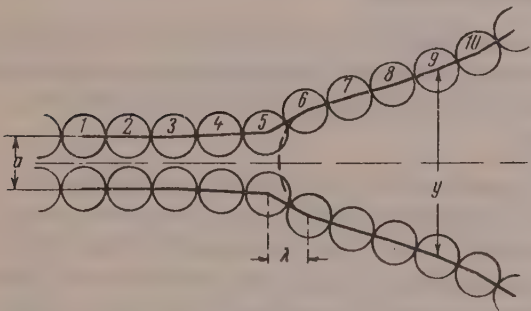


Fig. 1. Schematic representation of a longitudinal section of a crack under tensile load. The radius of the spheres represents the molecular radius; a is the interparticle distance away from the crack. The dash line is the edge of the crack; particles before rupture are shown to the left, and after rupture, to the right of this line.

left and right along the potential curve (Fig. 2). It may be assumed that the Particles 6 are already on the surface, while Particles 5 are still in the volume. The bonds are broken mainly during the 5-6 transition, when the particles are moved apart to a distance of 10-20% greater than the normal. At the moment of rupture, the quasi-elastic force reaches its maximum value, corresponding to the theoretical strength calculated from the approximate formula $\Sigma_* \approx 0.1 - 0.2 E$, where E is Young's modulus. The interparticle distance changes suddenly as the result of bond rupture (Fig. 1), and the vertex of the crack moves a distance λ , corresponding to one interparticle distance. It follows that the atoms (or molecules) do not approach each other asymptotically, as was formerly believed in relation to crack configuration, but there is a quite definite physical boundary for the transition from continuity to a crack.

With a single fluctuation, which results in the advance of the crack front by one "step," the groups of the particles simultaneously affected by the fluctuations ("rupture segments" in the terminology used previously [8]),

The tensile stress Σ at the vertex of the crack lowers the barrier U_1 and raises the barrier U_2 ; this increases the probability of transition from the left-hand to the right-hand minimum, and decreases the probability of the reverse transition. At a definite stress Σ_0 , corresponding to the safe load P_0 , the barriers and probabilities of the two states are equal. Σ_0 corresponds to an instant of unstable equilibrium, and is the stress below which rupture is impossible in principle. Crack growth occurs at stresses above the safe value, and crack closure at stresses below it. Σ_0 is an equilibrium parameter in the physical sense.

In reality, the molecular picture of crack growth and closure is more complex than suggested earlier [8]. Several particles to the left and right of the crack vertex are in an intermediate position between the two equilibrium states, and are maintained there owing to interaction with their neighbors to the

shown as points in Fig. 2, pass along the potential curve, to the right in rupture and to the left in crack closure. Fig. 2 represents the process of crack closure after removal of the load ($\Sigma = 0$). In this, process Segment 2 takes the place of Segment 1, Segment 3 takes the place of Segment 2, 4 takes the place of 3, etc. As a result, there is one segment more at the left-hand minimum, and one segment less at the right-hand minimum.

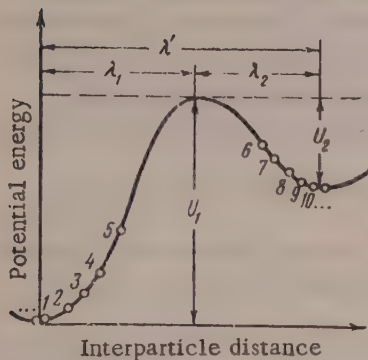


Fig. 2. Schematic representation of the dependence of the potential energy on the interparticle distance as the particles pass from the crack surfaces into the volume during crack closure after removal of the load ($\Sigma = 0$).

medium which lowers its surface tension is caused primarily by a decrease of the stress at which crack growth begins, i.e., the safe stress Σ_0 .

It is interesting to note that Equation (1) for the safe stress exactly coincides with the Polanyi [9] equation for the critical stress which, according to Polanyi, corresponds to complete conversion of the work done by external force (stress) into the energy of the newly formed free surfaces. In reality the elementary stress energy at the crack vertex is converted completely into energy of the new surfaces only at stress Σ_0 , when the crack grows (or closes) infinitely slowly. At stresses above the safe value (including the critical stress), when the growth rate of the crack is not zero, part of the elastic energy is converted into heat and part is expended in the formation of additional unevenness of the new surfaces — roughness which increases with increase in the crack-growth rate and with transition into the rapid stage of rupture (the mirror zone becomes rough).

Spontaneous dispersion. Any real crystal contains, in addition to the spatial network of mosaic blocks bounded by weak regions, surface defects or microcrevices which form partially even during the growth of the crystal. The subsequent history of the crystals, involving mechanical damage to the surface, plastic deformations, corrosion processes, and the action of surface-active media, increases the number and the dangerous nature of the microcrevices and other surface defects. In spontaneous dispersion, the active medium penetrates along these surface cracks into the depth of the single crystal, and then spreads along the boundaries of the mosaic blocks.

The structural weakness of the boundaries is characterized by a certain average surface tension α_p . Structurally, all the boundaries are weakened, but internal tensile stresses weaken the boundaries, while compressive stresses strengthen them.

Internal stresses can be characterized by a certain distribution function, analogous to the distribution function proposed by Volkov [10] for polycrystals. Cracks do not grow along compressed boundaries, forming strengthened regions. However, as the numbers of weakened and strengthened boundaries are equal (the distribution function is symmetrical with respect to extension and compression), a crack can always find a "detour," and spontaneous dispersion does not stop. Moreover, because of branching of the cracks during their growth, it will be a chain process, which is not considered in this paper.

We now consider the influence of a surface-active medium on crack growth.

Instead of this scheme, an equivalent scheme [8] may be used: in each single act of closure (or rupture), one segment passes from the right-hand (or left-hand) minimum to the other. It is probably necessary to introduce a correction factor into the calculations; however, since the constants in the formulas are found from experimental data, the correction factor is applied automatically.

The safe stress Σ_0 is

$$\Sigma_0 = 2e/\lambda', \quad (1)$$

where e is the potential energy of 1 cm^2 of the surface, determined from the Gibbs-Helmholtz equation; $e = \alpha - T \partial \alpha / \partial T$; α is the surface tension of the bond in a given medium, in vacuum in the particular case; T is the absolute temperature; $\lambda' = \lambda_1 + \lambda_2$; the meaning of λ_1 and λ_2 is clear from Fig. 2, where λ_1 is reckoned from the left-hand and λ_2 from the right-hand minimum.

Thus, the strength decrease of a body in a surface-active

medium which lowers its surface tension is caused primarily by a decrease of the stress at which crack growth begins, i.e., the safe stress Σ_0 .

The strength decrease of solids in an active medium [1-5] is mainly due to two factors: decrease of the free surface energy α , and two-dimensional pressure of the adsorbed layer on the steric obstacle at the vertex of the crack (the influence of solvation layers is not considered because of the low rate of capillary penetration; their role in crack growth is insignificant).

Decrease of surface energy raises the barrier U_2 , but does not affect the barrier U_1 , determined by the energy of interparticle bond cleavage; therefore the critical stress Σ^* remains unchanged. However, the safe stress, which is determined by Equation (1), by the surface tension α of the body in the given medium, decreases in an active medium. The minimum value of α is zero, when $\Sigma_0 = 0$, and the barrier U_2 becomes equal to the barrier U_1 , and the probabilities of the two equilibrium states (in the volume and on the surface) become equal. For rupture to occur (which is possible if the probability that the particle is on the surface is higher), decrease of the surface tension is by itself insufficient — a tensile stress Σ at the crack vertex is also necessary. This stress consists of two parts:

$$\Sigma = \Sigma^* + \Sigma'', \quad (2)$$

where Σ^* is the consequence of internal stresses of the 2nd kind on the block boundaries, and the additional stress Σ'' is the consequence of two-dimensional pressure of the adsorbed layer. We assume Σ^* constant along any one boundary; the stress Σ'' is assumed constant, and equal[5] to

$$\Sigma'' = A(\alpha_0 - \alpha), \quad (3)$$

where the difference $(\alpha_0 - \alpha)$ is the two-dimensional pressure of the adsorbed layer, applied to unit length of the crack front; α_0 and α are the surface energies of the body in vacuum and the given medium respectively; the surface energy near the crack vertex depends on the interparticle distance y (Fig. 1), but in virtually all the regions of the crack accessible to the relatively large molecules of the active medium, α is constant [2]; hence A is constant.

Thus, the role of the active medium in colloidal breakdown consists of: 1) lowering the safe stress; 2) appearance of the additional stress Σ'' . The role of the dislocations and the mosaic structure of a single crystal consists of: 1) the existence of internal stresses at the block boundaries; 2) structure weakening of the boundaries, which may be characterized by a certain average "surface tension" α_b at the boundaries.

At low surface tension α , characteristic of spontaneous dispersion, α_b is comparable to α and plays an appreciable role, lowering the safe stress:

$$\Sigma_0 = \frac{2}{\lambda'} \left(\alpha - T \frac{\partial \alpha}{\partial T} - \alpha_b \right), \quad (4)$$

where $T \frac{\partial \alpha}{\partial T}$ is a correction * which we henceforth neglect.

The derivation of an expression for the rate of crack growth in an active medium is analogous to the earlier derivation [8], and gives:

$$v = \lambda v \left[\exp \left(\frac{\omega \Sigma_1}{kT} \right) - \exp \left(- \frac{\omega' \Sigma_1}{kT} \right) \right], \quad (5)$$

where $v = v_0 \exp(-\frac{U_0}{kT})$; v_0 is the thermal-vibration frequency of the group of particles involved in a single fluctuation; U_0 is the magnitude of the barriers on the left and right "equalized" at the safe stress; λ is the advance of the crack front during one fluctuation; $\Sigma_1 = \Sigma - \Sigma_0$; Σ_0 is the safe stress in the medium; ω and ω' are the volumes of the fluctuations in the growth and closure of the crack.

The lower applicability limit of Equation (5) is the condition $\Sigma = \Sigma_0$ and the upper, the condition

*For example, for liquid metals, α for which has been measured fairly accurately, the correction term $T \frac{\partial \alpha}{\partial T}$ is a small fraction of α .

$\Sigma = \Sigma_M$, where Σ_M is the growth rate of the crack, equal to the migration rate of the surface-active molecules. If the growth rate becomes greater than the migration rate, the front along which the monomolecular layer of the surface-active molecules extends lags behind the front of crack growth. The medium then ceases to influence the disintegration process, which stops or slows down until the surface-active molecules again reach the crack vertex. Since the internal stresses do not exceed the safe stress in vacuum (otherwise the body would undergo spontaneous dispersion in vacuum), spontaneous dispersion cannot proceed at a rate exceeding the migration rate. The internal stresses at the great majority of the boundaries are so small that it is possible to assume that the rate of crack growth along the boundaries is very low, less than the migration rate, which is measurable in meters/second, and Equation (5) can therefore be used.

Criteria of spontaneous dispersion. The condition for spontaneous dispersion of a solid either in the stressed or in the unstressed state is given in an earlier paper [3].

The probability of the process is taken to be

$$W \approx \exp\left(\frac{\delta V\sigma - s\alpha}{kT}\right), \quad (6)$$

where σ is the stress; δ is a dimensionless term, not greater than 0.1–0.5 for rupture of brittle bodies (for tensile stresses $\delta > 0$, for compressive stresses $\delta < 0$); $V \approx b^3$; $s \approx b^2$; b is the average linear dimension of a colloidal particle.

In absence of stresses, the surface tension α in the medium, for spontaneous dispersion, must be below a certain limiting value α'_m , which is equal to

$$\alpha'_m \approx \frac{kT}{b^2}, \quad (7)$$

At greater values of α , dispersion can take place only under the influence of stresses, and the limiting surface tension α''_m is

$$\alpha''_m \approx \frac{kT}{b^2} + \delta b\sigma. \quad (8)$$

In accordance with our reasoning, spontaneous dispersion is possible when the total stress Σ at the vertex of the microcrack is greater than the safe stress Σ_0 in the given medium. If one additional stress Σ'' proves sufficient to bring about the process ($\Sigma'' > \Sigma_0$), the process will take place even in absence of internal tensile stresses; the latter can merely accelerate it. All the foregoing is valid both in the presence of internal stresses and for the particular case of their absence.

Thus, the limiting value α'_m corresponds to the case in which the safe stress Σ_0 in the medium is equal to the additional stresses Σ'' ; then at $\alpha < \alpha'_m$ $\Sigma'' > \Sigma_0$, and breakdown can proceed in absence of internal stresses. From Equations (3) and (4) it follows that

$$\alpha'_m = \frac{\alpha_0 A\lambda' + 2\alpha_b}{2 + A\lambda'}, \quad (9)$$

In the stressed state, the limiting value α''_m corresponds to the surface tension at which the safe stress Σ_0 in the medium is equal to the sum of the additional stress Σ'' and the stress Σ' :

$$\Sigma_0 = A(\alpha_0 - \alpha''_m) + \Sigma',$$

and hence

$$\alpha''_m = \frac{\alpha_0 A\lambda' + 2\alpha_b + \lambda'\Sigma'}{2 + A\lambda'}. \quad (10)$$

If $\Sigma' < 0$ (compressive stress), then $\alpha''_m < \alpha'_m$. This means that a more active medium, i.e., a medium which decreases the surface tension to lower values, is needed for spontaneous dispersion.

Equations (9) and (10) provide an absolute criterion for the occurrence of the process. It is of interest to derive a criterion for the occurrence of spontaneous dispersion at a definite, appreciable rate. For this, we use Equation (5) for the rate of crack growth v along the block boundaries. Let v have a definite value, sufficient to make the second exponent negligible, so that we may assume

$$v = \lambda v_0 \exp\left(\frac{\omega \Sigma_1}{kT}\right). \quad (5')$$

It has been shown [8] that the second exponent may be rejected, and in practice we may start with velocities of 10^{-7} cm/second and over.

Taking logarithms in Equation (5), and taking into account that $U_0 \approx \omega(\Sigma_* - \Sigma_0)$ (see [8]), we have

$$\alpha = \alpha_0 + \frac{\ln \frac{\lambda v_0}{v}}{\omega A} kT + \frac{\Sigma'}{A} - \frac{\Sigma_*}{A}, \quad (11)$$

where $\lambda v_0 = v_*$ (the critical rate of crack growth).

Equation (11) provides the criterion for spontaneous dispersion of a single crystal in the stressed state, at a definite rate v . Since the stress Σ' varies from boundary to boundary, the rate of crack growth also varies from boundary to boundary.

It should be noted that Equations (7) and (8) are given in the earlier paper [3] as approximate criteria associated with a definite probability of destruction. Therefore they must be compared with Equation (11) and not (9) and (10).

The difference between Equations (11) and (8) (equations which refer to the stressed state, and which are therefore more general, are being compared) lies primarily in the fact that Equation (11) contains two additional terms. The dimensions of the coefficients of the corresponding terms in the two equations coincide, although the coefficients themselves have different meanings; in the earlier paper [3], a whole block was taken as the kinetic unit, whereas here we assume that each block boundary is broken down as the result of consecutive fluctuations.

We shall now show that Equations (11) and (8) are not mutually contradictory in the mathematical sense. If the probability of breakdown W is assumed proportional to the breakdown rate v , we can write

$$W = C_0 v.$$

Then, if $\Sigma = \Sigma_0$, there is no breakdown and $W = 0$, which is in agreement with $v = 0$; if $\Sigma = \Sigma_*$, breakdown always occurs at the maximum rate $v_* = \lambda v_0$ and $W = 1$, these statements are in agreement if $C_0 = 1/\lambda v_0$. If we consider the case $(\omega \Sigma_1/kT) > 1$ ($\omega^* \approx \omega$), we can reject the second exponent, and we then have, after rearrangement

$$W = \exp\left(-\frac{\omega \Sigma_*}{kT}\right) \exp\left(\frac{\omega A \alpha_0}{kT}\right) \exp\left(\frac{\omega \Sigma' - \omega A \alpha}{kT}\right).$$

The first two factors are constants for the given substance, independent of the medium. Denoting their product by C , and remembering that ω has the dimensions of volume, and ωA of area, we obtain an expression analogous to (6) in structure and dimensions of its constituent terms, although different in physical content.

Therefore the mathematical difference between Equations (11) and (8) (the presence of two additional terms) is due to the fact that the expression for the probability in the earlier paper [3], the term C , associated with constants for a given substance, was not taken into account.

We now return to Equations (10) and (11); they can be considered from two different standpoints.

If it is known that N_1 block boundaries have internal stresses $\sigma_1 N_2 - \sigma_2$, $N_3 - \sigma_3$, etc. (i.e., if the distribution function is known), and if the surface tension α in the medium is also known, it is possible to

estimate the degree of dispersion of the body in this medium. Equations (10) and (11) then give the limiting value Σ'_{\lim} , equal to the product of the internal stress σ_{\lim} and the stress-concentration coefficient β at which the boundary of two blocks breaks down (infinitely slowly, by Equation (10), or at a definite and appreciable rate, by Equation (11)). All the boundaries with internal stresses greater than σ_{\lim} also break down, and at a higher rate. The number of boundaries broken down characterizes the degree of dispersion (theoretically, i.e., over a infinite time, by Equation (10), or over a definite time interval by Equation (11)). The problem can be stated in another way: what surface-active medium can ensure a given degree of dispersion? Here we are given the number of boundaries which must be broken down (either theoretically, or over a definite time interval), and therefore the limiting value of the internal stress σ_{\lim} and $\Sigma_{\lim} = \beta \sigma'_{\lim}$. The equations are used to find the corresponding surface tension α . Any medium which decreases the surface tension to a lower value will give a higher degree of dispersion under the same conditions.

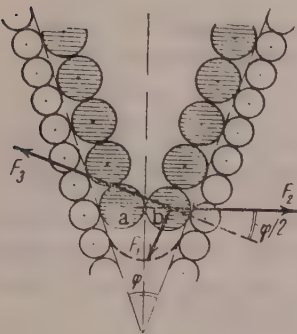
It is of interest to estimate the small values of surface tension at which spontaneous dispersion occurs (in absence of internal stresses, which facilitate the process).

For the calculation it is necessary to know the numerical value of A in the expression for the additional stress $\Sigma'' = A(\alpha_0 - \alpha)$; it can be estimated as indicated in Fig. 3, where a and b are the two "end" molecules of the monomolecular layer of surface-active medium. The angle φ of the crack in a solid is probably between 1 and 10° .

Each of the molecules a and b is acted upon by three forces: $F_1 = (\alpha_0 - \alpha) D$, where $(\alpha_0 - \alpha)$ is the two-dimensional pressure per unit length of the boundary of the steric obstacle and D is the diameter of the active molecules, and the elastic reactions F_2 and F_3 . The required additional stress $\Sigma'' = F_2/S$, where S can be assumed to be one order of magnitude greater than the cross section of a molecule of the solid. Since spontaneous dispersion occurs only in media similar in molecular nature to the solid, i.e., the diameter D of an active molecule is approximately equal to the diameter of a molecule in the solid, then

$$\Sigma'' = \cot \frac{\varphi}{2} \cdot \frac{\alpha_0 - \alpha}{10D}.$$

Fig. 3. Origin of an additional stress Σ'' at the crack vertex as the result of two-dimensional pressure of the surface-active molecules.



For φ between 1 and 10° , and $\cot \varphi$ between 30 and 3, we have $K \frac{\alpha_0 - \alpha}{D} = \Sigma''$ where K is roughly between 3 and 0.3.

If Σ'' is equal to the safe stress $\Sigma_0 = 2\alpha/\lambda'$ in the medium, spontaneous dispersion is possible in absence of internal stresses, and

$$K \frac{\alpha_0 - \alpha}{D} = \frac{2\alpha}{\lambda'}.$$

Since $\lambda' \approx D$, it follows that the surface tension in the medium must be decreased, relative to its value in vacuum, by about one order of magnitude (for metals this gives $\approx 10 \text{ ergs} \cdot \text{cm}^{-2}$) for spontaneous breakdown to be possible (at an infinitely-low rate) even in absence of internal stresses [11]. The process occurs at a finite rate at which lower values of α .

For example, the rate of crack growth in metals may be found from Equation (11), with the following assumptions: $\alpha_0 = 500 \text{ dynes/cm}^2$; $E = 10000 \text{ kg/mm}^2$; $\lambda_1 = \lambda_2 = 2.5 \text{ Å}$; $\lambda_p = 2.5 \text{ Å}$. Since $\Sigma_* \approx 0.2E = 2 \cdot 10^{11} \text{ dynes/cm}^2$, the safe stress in vacuum is $\Sigma_{ov} = 2\alpha_0/\lambda' = 2 \cdot 10^{10} \text{ dynes/cm}^2 = 0.1\Sigma_*$, and the additional stress Σ'' , even in the most active media ($\alpha \approx 0$) does not exceed the safe stress in vacuum ($\Sigma'' < K\alpha_0/D$, where $D \approx \lambda'$, and K is between 3 and 0.3), it follows that the critical stress is greater by at least one order of magnitude than the additional stress, and the product $A(\alpha_0 - \alpha)$ in Equation (11) may be ignored; $\Sigma' = 0$, there are no internal stresses.

Under these conditions the equation for the crack growth rate assumes the simple form:

$$v = v_* \exp\left(-\frac{U_1}{kT}\right).$$

Substitution of numerical data into this formula, when $U_1 \approx \omega \Sigma_*$, shows that $v \approx 10^{-28}$ cm/second; as the second exponent in the rate equation cannot be ignored at such rates, in reality v is even smaller.

Therefore in absence of internal stresses spontaneous dispersion of metals, already possible in principle when the surface tension is lowered by about one order of magnitude, is an infinitesimally slow process even in the most active media. It follows that internal stresses play an important role in the spontaneous dispersion of metals under real conditions.

SUMMARY

1. The physical principle of the spontaneous dispersion of a single crystal are considered. The main conclusions and the method are also applicable to polycrystals and to glasses with clearly defined macro-structural regions.

2. Two criteria for spontaneous dispersion have been derived: a thermodynamic criterion, which gives the condition for the start of breakdown of a solid, and a kinetic criterion, which determines the conditions for the occurrence of the process at an appreciable rate.

3. The results of the present investigation are of special interest in relation to the problem of heat resistance, because of the great decrease in the strength of high-melting alloys under the influence of small amounts of fusible impurities at the grain boundaries (the impurities act as a very active medium).

The authors offer their thanks to V. L. Likhtman and E. D. Shchukin for active discussion of this paper.

The Potemkin Pedagogic Institute, Moscow
Chair of Theoretical Physics
Institute of Physical Chemistry, Academy of Sciences USSR
Division of Disperse Systems

Received June 16, 1958

[1] P. A. Rebinder, Jubilee Volume on the 30th Anniversary of the October Revolution (Izd. AN SSSR, 1947), p. 535; * J. Tech. Phys. 2, 7/8 (1932).

[2] V. L. Likhtman, P. A. Rebinder, and G. V. Karpenko, Effect of Surface-Active Media on the Deformation Processes of Metals (Izd. AN SSSR, 1954). *

[3] P. A. Rebinder, V. L. Likhtman, and L. A. Kochanova, Proc. Acad. Sci. USSR 111, No. 6 (1956).

[4] P. A. Rebinder, "New problems of Physicochemical Mechanics." Paper at the Permanent Colloquium on Solid Phases of Variable Composition, jointly with the Moscow Colloid Colloquium, January 26, 1956 (Moscow, 1956); J. Acad. Sci. USSR No. 10, 32 (1957). *

[5] S. T. Kishkin, Proc. Acad. Sci. USSR 95, No. 4, 789 (1954); Ia. M. Potak and L. M. Shcheglakov, J. Tech. Phys. 25, 897 (1955).

[6] N. N. Davidenkov, in the symposium: Applications of X-ray Analysis to Metal Testing (Moscow-Leningrad, ONTI, 1936), p. 393.

[7] G. V. Spivak, A. L. Krokhina, and L. V. Lazareva, Proc. Acad. Sci. USSR 104, No. 4 (1955).

[8] G. M. Bartenev, Bull. Acad. Sci. USSR, OTN No. 9 (1955).

[9] F. Seitz, The Physics of Metals (Moscow - Leningrad, State Tech. Press 1947) [Russian translation].

[10] S. D. Volkov, J. Tech. Phys. 23, No. 11 (1953).

[11] E. D. Shchukin and P. A. Rebinder, Colloid J. 20, No. 5, 645 (1958). See C.B. Translation.

* In Russian

SOME FEATURES OF THE COMMINUTION OF GRAPHITE IN AN AQUEOUS MEDIUM*

E. B. Matskevich and P. Iu. Butiagin

The influence of the medium is strong and often decisive in the grinding of graphite. By variations of the medium in fine grinding it is possible to obtain graphites differing sharply in adsorptive capacity, electrical conductivity, granulometric composition, and technical properties. Atmospheric oxygen, water, or surface-active substances are adsorbed on the newly formed clean graphite surfaces in different media. This fact alone partially accounts for the differences in the properties of the ground material. However, in addition to direct adsorptive modification of the graphite surface, adsorption leads to a number of important consequences.

In the grinding of dry graphite the finest particles join to form stable aggregates [1]. The aggregation of graphite is comparable to the granulation of carbon black in drums; this process was studied by Voiutskii, Zaionchkovskii, and Rubina [2]. At the first stage, the individual particles of carbon black join at the points of contact, as in the formation of a coagulation structure in a liquid medium. Such nuclei grow in size and become more compact as they travel through the layers of material, and the freshly added particles become oriented along the granule surfaces. The granulation of carbon black proceeds more intensively in vacuum; additions of hydrocarbons have the reverse effect.

In the grinding of graphite, granule formation and growth is accompanied by granule breakdown under the action of the grinding balls. It is possible that the primary particles constituting the granules are also broken down. Feigin [1], who ground dry graphite in a vibratory mill, obtained a product with primary particles $\sim 100 \text{ \AA}$ in size, with a greater specific surface (up to $600 \text{ m}^2/\text{g}$) than ordinary carbon blacks.

The rate of comminution of graphite falls sharply in presence of water vapor. Feigin and Rozhanskii [3] showed that if a monomolecular layer of water (or of some organic substances) is formed on the graphite surface, the growth rate of new surfaces is decreased 10 to 20-fold. These authors attribute this interesting effect to the lubricant action of the adsorption layers, on the assumption that friction forces between the particles are decisive in the dispersion of dry graphite.

The comminution rate of graphite is higher in solutions of surface-active substances than in an aqueous medium. This is a manifestation of the effect discovered by Rebiner [4], in which dispersion is facilitated by adsorption. The commonest active additive in the case of graphite is sulfite liquor [5].

Graphite grains are broken down in aqueous suspensions if they come between colliding grinding bodies. With this mechanism, analysis of the process kinetics becomes much easier if the comminution of individual narrow fractions comprising a polydisperse material is considered independently. Zagustin [6], and later Huttig and others [7] applied a first-order reaction equation to the kinetics of comminution, on the assumption that the destruction rate of the grains of each fraction is directly proportional to its content in the whole material, and is independent of the quantitative proportions of the other fraction or of the final products of grinding.

As an example, we may consider a very simple, ideal mechanism of the process; the original mono-disperse material consists of grains 1 in size; destruction of the original grains results in formation of particles

*Paper at the 4th All-Union Conference on Colloid Chemistry in Tbilisi, May 1958.

of size r_1 ; destruction of these yields secondary products with particle size r_2 , etc. The final product consists of particles of size r_f . The material undergoes comminution by collisions of the grinding bodies; provided that each collision is sufficiently effective, we have

$$-\frac{dn_r}{d\tau} = \alpha'_r \beta_r N, \quad \text{or with } \alpha'_r = \alpha_r n_r : \left(-\frac{dn_r}{d\tau} \right) = \alpha_r \beta_r N n_r, \quad (1)$$

where n_r is the number of particles of diameter r in the material; N is the number of collisions of the grinding bodies per unit time; α'_r is the probability of location of particles of diameter r between the grinding bodies during their collision; α_r is the corresponding probability for one particle of diameter r ; β_r is the probability of destruction of a particle under impact of the grinding bodies.

From the number of grains n_r we can pass to their volume V_r , and then to their volume concentration $c_r = V_r / V$ in the material:

$$-\frac{dc_r}{d\tau} = \alpha_r \beta_r N c_r \quad \text{or} \quad -\frac{dc_r}{d\tau} = k_r c_r, \quad (2)$$

where $k_r = \alpha_r \beta_r N$ is the destruction-rate constant (hour⁻¹).

Changes of the volume concentration c_r of the fractions $r_0, r_1, r_2, \dots, r_k$ are represented by equations of the form:

$$-\frac{dc_n}{d\tau} = k_{n-1} c_{n-1} - k_n c_n, \quad (3)$$

where always $k_0 > k_1 > \dots > k_n > \dots > k_f = 0$, and $c_0 + c_1 + \dots + c_n + \dots + c_f = 1$.

The specific surfaces S of the material at any instant is given by the sum:

$$S = \frac{1}{r_0} (F_0 e^{-k_0 \tau} + F_1 e^{-k_1 \tau} + \dots + F_n e^{-k_n \tau} + \dots + F_f), \quad (4)$$

where $F = F(k, r)$.

The exponential functions in the right-hand side of Equation (4) can be resolved into series by power of $k\tau$; then, if only the first two terms of the series are taken (which is permissible at small values of τ , so long as $k\tau \leq 0.2$) for any values of k_r and r_n we have

$$S = S_0 \left(1 - k_0 \frac{r_0 - r_1}{r_1} \tau \right) \quad \text{or} \quad S - S_0 = k_0 \Delta S_1 \tau, \quad (5)$$

where S_0 is the specific surface of the original material, and ΔS_1 is the increase of specific surface in the formation of the primary destruction products from the original grains.

Equation (5) connects the rate of growth of fresh surface with the destruction-rate constant, calculated from changes in the particle-size composition, for an ideal simplest case of volume destruction of a monodisperse material.

Equation (5) can be used in the derivation of an equation for the initial growth rate of the specific surface in the comminution of a polydisperse material:

$$\left(\frac{dS}{d\tau} \right)_{\tau \rightarrow 0} = \int_{r_{\min}}^{r_{\max}} c_r k_r \Delta S_1 dr. \quad (6)$$

For integration of Equation (6) it is necessary to know the dependence of k_r and ΔS_1 on the particle size, and the particle-size distribution function of the original material.

The destruction-rate constants in the grinding of quartz sand and glass powder in ball mills were determined by Zagustin [6] and Huttig [8]. The rate constants for the grinding of graphite in an aqueous medium in ball mills were calculated from Morachevskaia and Figurovskii's experimental data [9]. It was found that in all cases, for very different materials, the rate constant is directly proportional to the square of the grain diameter. This quadratic relationship is probably the consequence of the fact that the probability that the grains will be found between the grinding bodies (the quantity α_r in Equation (2)) is proportional to their cross-sectional area.

In our experiments on the comminution of graphite in vibratory mills, the rate of the process was estimated from the destruction-rate constants and the rate of increase of the specific surface; the adsorption of the active additive on the newly formed graphite surface was determined at the same time.*

For determinations of the adsorption of the active additive on the newly formed graphite surface, a technique was developed whereby the concentration of the additive in aqueous solutions was found from the electrical conductivity of standard graphite suspensions. Conductivity was determined by the usual method with a high-frequency tube oscillator and Wheatstone bridge. The conductivity cell was semicircular in cross section, with 4 mm radius; the platinum electrodes were placed at the ends 40 mm apart.

Figure 1 shows the results obtained in conductivity determinations with Taiga graphite ($S = 12 \text{ m}^2/\text{g}$; heated at 380° before the experiments), in aqueous solutions containing different concentrations of sulfite liquor. The graphite-solution ratio was 1:1. With increase of the sulfite liquor concentration in the original

solution to 9 mg/cc, the conductivity of the suspension is decreased almost 10-fold. This effect is caused by weakening of the contacts in the coagulation structure by adsorption of the active additive on the graphite surface.

The curve in Fig. 1 was used as a calibration graph for determination of the sulfite liquor concentrations in the solutions. The test solution and standard graphite were made into a paste, its conductivity was measured, and the concentration of the additive was found from the curve. The measurements and calculations take about 10 minutes, while the accuracy is roughly 20%. In determinations of the sulfite liquor concentration in the aqueous phase, most of the graphite should first be separated by means of a centrifuge.

The specific surface of the graphites was determined by adsorption of methylene blue from aqueous solutions. Before the determinations, all the specimens were heated in presence of atmospheric oxygen at $360-380^\circ$, to clean the graphite surface. This treatment burns out the organic substances (flootation reagents and surface-active additives), and the graphite surface is oxidized.

Fig. 1. Conductivity of graphite suspensions in sulfite liquor solutions of various concentrations.

The adsorption isotherms of methylene blue on graphite have horizontal regions at equilibrium concentrations of 0.02 mg/cc and over. Adsorption of 1 mg of methylene blue under saturation conditions corresponds to the covering of 1 m^2 of the carbon surface. For comparison, the specific surfaces of several graphite samples were determined by the BET method from the adsorption isotherms of nitrogen and water vapor. All three methods gave similar results when the specific surface of the graphite was less than $20 \text{ m}^2/\text{g}$.

The particle-size composition of the graphites was determined sedimentometrically, either by the pipet or by the areometer method. Both methods give reproducible results, in agreement with each other. Sulfite liquor was used for stabilization of the graphite suspensions in the determinations.

The specific surfaces of ground graphite and of the sediment collected after a 4% suspension had settled for 1 hour are given in Table 1.

When dry graphite is ground, the comminuted material and the sediment have equal specific surfaces, i.e., aggregates and not individual large particles settle out of the suspension, and sedimentation analysis is

*S. S. Koriagina took part in the experimental work.

unsuitable for determination of the primary-particle size of the graphite. The use of other stabilizers (Leukanol, bentonite), repeated rolling of the material, treatment with sulfuric-hydrochloric acid mixture, vacuum "conditioning" before stabilization, and other methods did not give satisfactory results. It is interesting to note that in sieve analysis the residue on a 0060 sieve has almost the same specific surface as the unsifted graphite; i.e., it consists of stable granules which are not broken down when the moist material is rubbed through a fine sieve.

TABLE 1

Test on Separation of Graphite by Sedimentation

Grinding method	Specific surface, m ² /g	
	graphite af- ter grinding	sediment
Dry	11	11
In aqueous solution of sulfite liquor	11 - 11.5	5.5

of graphite was 4 g, and the molding pressure was 500 kg/cm². This technique was developed by Morachevskaya [10].

The original Taiga graphite (KT brand) contained 97% carbon; its specific surface was 4-8 m²/g, with up to 2% residue on a 0060 sieve. The granulometric composition of the original graphite is satisfactorily represented by the Rosin-Rammler equation:

$$100 - Q = 100e^{-br^n} \quad \text{or} \quad c_r = \frac{dQ}{dr} = 100 b(n-1)r^{n-1}e^{-br^n}, \quad (7)$$

where Q is the percentage content of grains of diameter r and less, and b and n are constants. For different batches of the original graphite the constant n was always 2, while the constant b varied from $1.1 \cdot 10^{-3}$ to $3.4 \cdot 10^{-3} \mu^{-2}$; the maximum on the particle-size distribution curve corresponds to the 15-30 μ range.

In most of the experiments the graphite was ground in M200- 1.5 and M10-3.0 vibratory mills. The grinding medium consisted of steel balls from 8 to 16 mm in diameter. Samples for analysis were taken from the mill at definite time intervals from the start of the experiment. From 2 to 5 duplicate grindings were performed under the same conditions for each experiment. The experimental conditions are given in Table 2.

TABLE 2

Experimental Conditions in the Grinding of Graphite in Vibratory Mills.

Expt. No.	Type of mill	Medium	Ball charge,kg	Graphite charge, kg	Vibration amplitude, mm	Duration of experiment, hours
1	M10	Air	30	2	2,2	6
2	M10	Water	28-30	1,8-2,0	1,3-1,5	5
3-4	M10	Aqueous solution of sulfite liquor	28-30	1,8-2,0	1,3-1,5	3,5-24,5
5	M200		640-680	20-25	1,9-2,2	2,5-3,0
6	M200		640-680	20-25	1,5-1,7	3,0-3,5

In grinding in water and in sulfite liquor solution, the moisture content of the graphite suspension was 50-60% (by weight). The contents of sulfite liquor were up to 4% in Experiment 3, and up to 15% in Experiment 4 (on the weight of graphite).

Variations of the granulometric composition of graphite during prolonged grinding in an aqueous solution of sulfite liquor are shown in Fig. 2 (Experiment 4). In Fig. 3, a and 3,b the contents of grains of different sizes in the graphite are plotted against the grinding time. All the curves in Fig. 3,a and 3,b can be classified into three groups according to the nature of their initial regions, and the material of the curves. The first group (1st fraction, $r > 15 \mu$) includes Curves 30, 20, and 15. The content of this fraction decreases continuously. The second group includes Curves 12, 5 and 4 (2nd fraction, $15 > r > 3 \mu$). The curves of this group first ascend steeply, then pass through a maximum. The third group includes Curves 3 (3rd fraction, $r < 3 \mu$); its ascending region is S-shaped.

Variations of the quantitative proportions of the three fractions in the course of grinding are shown in Fig. 3,c. During the first few hours mainly grains of the 1st fraction are broken down, with formation of the primary products — grains of the 2nd fraction. After 5 hours the content of the 2nd fraction reaches 80%, and this is followed by rapid formation of secondary destruction products — particles smaller than 3μ .

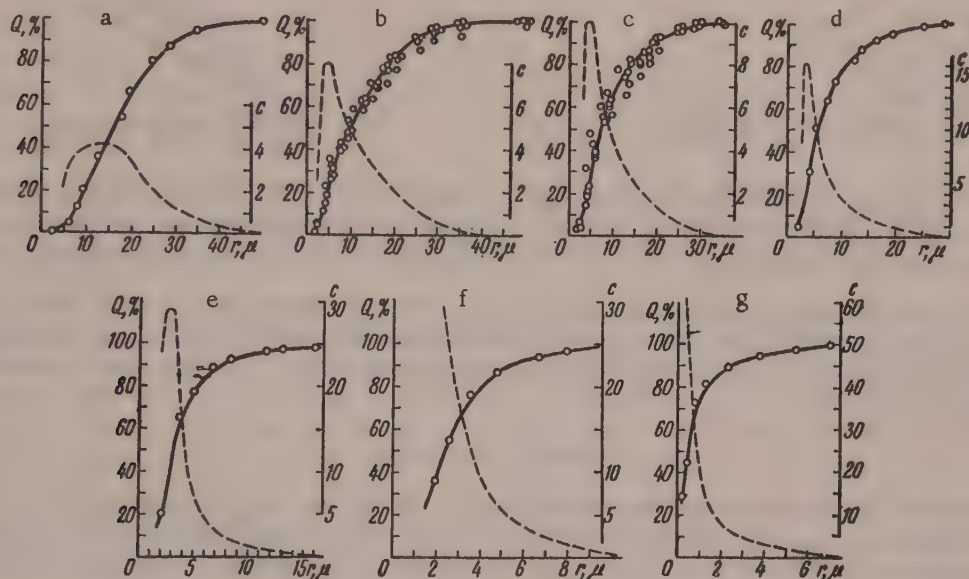


Fig. 2. Particle-size composition of graphite after grinding (Experiment 4): a) Original; b) 1.5 hours; c) 3 hours; d) 5.2 hours; e) 10.5 hours; f) 15.5 hours; g) 24 hours.

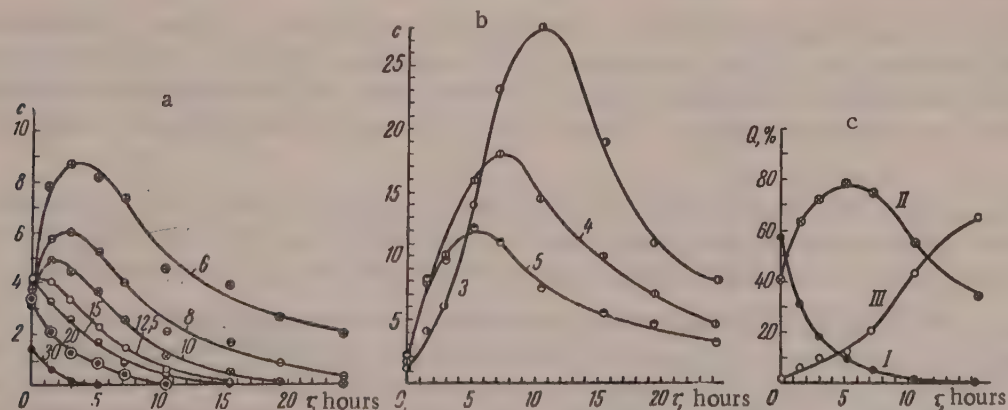


Fig. 3. Variation of the concentrations of graphite grains of different sizes during grinding (Experiment 4): In Figures a and b, the numbers on the curves represent the grain sizes in μ ; in Figure, c: I) fraction of 15μ and over; II) fraction of $3-15 \mu$; III) fraction of 3μ and less.

The destruction rates of the grains in the 1st and 2nd fractions are satisfactorily represented by Equation (2) (see Fig. 4). The variations of the destruction-rate constant with the grain size in different experiments are plotted in Fig. 5. As in the grinding of graphite and other materials in ball mills, the rate constant is directly proportional to the square of the grain diameter. The proportionality coefficient $a = k / r^2$ is a direct measure of the destruction rate of the material under the given conditions.

The quadratic relationship between the rate constant and grain size accounts for the accumulation of considerable amounts of intermediate destruction products in the material, and for the existence of a practical limit of comminution.

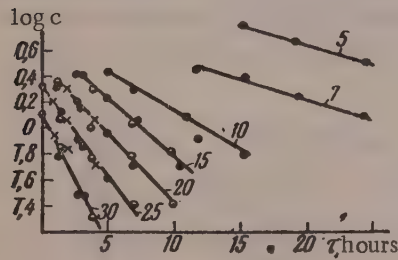


Fig. 4. Effect of grinding time on the concentration of graphite grains of different sizes (numbers on the curves). Calculated from Equation (2).

In the experiment under consideration, the initial growth rate of the specific surface (see Fig. 6, Curve 4) is approximately $1.8 \text{ m}^2/\text{g} \cdot \text{hour}$. The $k(r)$ and $c(r)$ relationships are known. It may be assumed in the first approximation that ΔS_1 is inversely proportional to the grain diameter, i.e., $\Delta S_1 = m/r$. Then integration of Equation (6) gives

$$(dS/d\tau)_{\tau \rightarrow 0} = Iam, \quad (8)$$

where I depends only on the granulometric composition of the material. In the present instance $I = 24$, $a = 0.54 \cdot 10^{-3}$, $(dS/d\tau)_{\tau \rightarrow 0} = 1.8$; hence $m = 150$. Therefore, with original grains 30μ in diameter the increase of specific surface in the formation of the primary destruction products is approximately $5 \text{ m}^2/\text{g}$.

When graphite was ground in water without surface-active additive (Fig. 5, Experiment 2), the lowest destruction-rate constants were found, and $a = 0.24 \cdot 10^{-3} \mu^{-2} \cdot \text{hour}^{-1}$, i.e., the destruction rate of the graphite grains increased almost 2.5-fold in presence of the surface-active additive.

In the third experiment, 3-4% of sulfite liquor was added to the graphite suspension. The decrease in the concentration of particles 20μ in size is represented by the broken Line 3 (Fig. 6,a). Initially this line coincides with the straight line for Experiment 4 (excess of sulfite liquor), but after about 2 hours the destruction rate decreased; the second region of Line 3 is parallel to Line 2, which represents grinding without the active additive.

Analogous results were obtained in determinations of specific surface (see Fig. 6,b); in Experiment 3 the first point is close to Curve 4, while all the others lie considerably lower. The ratio of the increases of specific surface in Experiments 2 and 4, like the ratio of the rate constants, is approximately 2.5.

Curves for the variations of the sulfite liquor concentration in Experiments 3 and 4 are given in Fig. 6,c. In Experiment 3 the concentration of the active additive fell to $3-5 \text{ mg/cc}$ after 2 hours. This was the time at the end of which the decrease in the rate of the process, as shown by changes in the granulometric composition and specific surface, was noted; the rate of the process is greatest while the comminution proceeds in sulfite liquor solution, i.e., while the active additive can be adsorbed on the graphite surface as soon as the latter is formed. As soon as the concentration of sulfite liquor falls to a few mg/cc , the rate of the process drops to a level corresponding to comminution in absence of active additive.

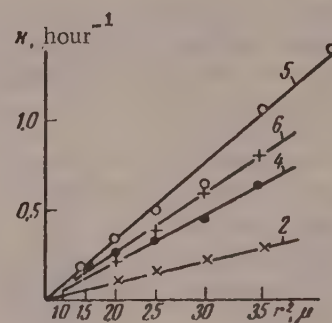


Fig. 5. Variation of destruction-rate constant with graphite grain size. The numbers on the curves correspond to the numbers of experiments (Table 2).

In a number of experiments on the comminution of graphite, the sulfite liquor concentration in each sample was determined twice: once immediately after sampling, and the second time after two hours of shaking. The results coincided in every case, so that it may be assumed that the equilibrium concentrations of the sulfite liquor were determined. The concentration decreases as the result of adsorption on the newly formed graphite surfaces. The amount adsorbed can be found from the difference between the concentrations of the active additive in the original suspension and in each sample (if the volume of the system is known).

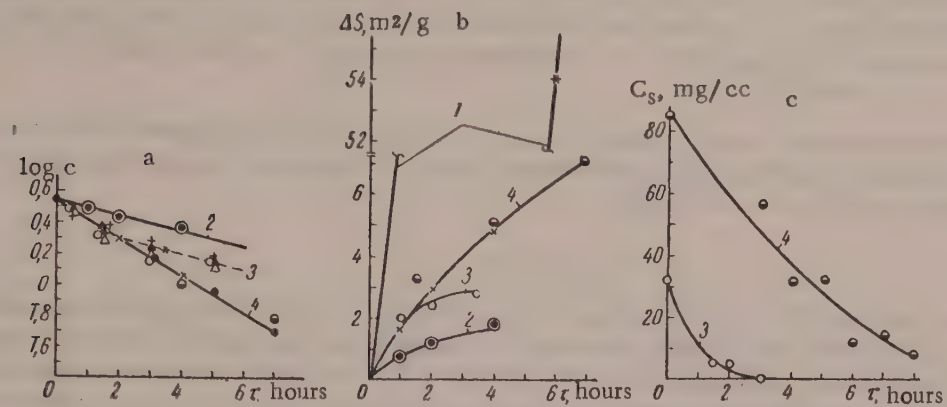


Fig. 6. Variations of the concentration of $20\text{ }\mu$ particles (a), specific surface (b), and sulfite liquor concentration in the aqueous phase of the graphite suspension (c) during grinding. The numbers on the curves correspond to the experiment number (Table 2).

The experimental and calculated results are plotted in Fig. 7. The adsorption of the active additive, in mg per g of graphite, is plotted against the increase of the specific surface of the graphite. The results of 8 experiments performed under different conditions are given in the graph. All the points are ranged around one straight line. The absolute adsorption of the active additive per 1 m^2 of newly formed graphite surface was calculated from the slope of this line; the value was found to be $14 \pm 3\text{ mg/m}^2$.

In the grinding of dry graphite (see Line 1, Fig. 6,b) the rate of increase of specific surface is constant, and is 10 times the rate in an aqueous medium (Experiment 2). This result is in good agreement with Feigin's data [3]. The rate constants could not be calculated for this experiment, as comminution of dry graphite is accompanied by its granulation, and sedimentation analysis is unsuitable for determination of the particle-size distribution curve.

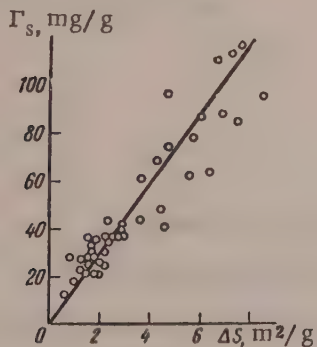


Fig. 7. Adsorption of active additive on newly formed graphite surface.

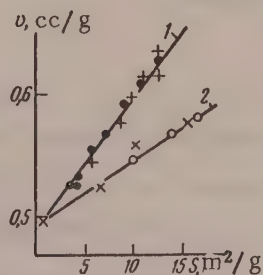


Fig. 8. Specific volume of pressed graphites:
1) Graphites ground in aqueous media; 2) graphites ground dry.

For comparison of the particle-size composition of graphites comminuted in different media, the specific volume of the pressed powders was determined. In Fig. 8 the specific volume of the briquets is plotted against the specific surface of the graphite. The specific volume is always less graphites ground dry (Line 2)

than for graphites ground in water or in a solution of sulfite liquor (Line 1). The two lines meet at a point close to the specific volume of graphite crystals.

Figure 8 also contains the results of tests on graphites with their particle-size composition modified artificially: the black circles represent the specific volumes of classified graphites with narrow ranges of grain size, and the white circles represent the specific volumes of classified powdered graphite to which 5, 10 and 15% of a fine fraction with particles smaller than $0.5\text{ }\mu$ and specific surface $38\text{ m}^2/\text{g}$ had been added. The black circles lie around Line 1, and the white, around Line 2; i.e., the density of the briquets was increased by addition of the fine fraction. It is likely that the higher density of the briquets resulting from dry grinding is also due to heterogeneity of the particle-size composition of the graphite, and the presence of fine fraction formed as the result of friction [3].

Thus, comminution of dry graphite not only results in a sharp increase in the growth rate of the specific surface, but also alters the properties of the comminuted product - its secondary structure (granulation effect, see Table 1), and the particle-size composition.

SUMMARY

1. The use of different media (water, surface-active solutions, air) for the fine grinding of graphite results in variations of the rate of the process, its kinetics, the particle-size composition, and the secondary structure of the breakdown products. The influence of the medium is associated with adsorption of water or surface-active substances on the newly-formed graphite surface, the adsorptinal decrease of strength (Rebinder effect), and the stabilizing and lubricating action of the adsorption layers.

2. When graphite is ground in an aqueous medium, the rate of grain destruction is directly proportional to the square of the grain diameter and to the grain content in the material. Breakdown of original grains $10-50\text{ }\mu$ in diameter yields primary destruction products with particles $3-15\text{ }\mu$ in size. The content of this fraction in the material gradually increases and reaches 80% by volume; this stage is followed by predominant formation of secondary destruction products with particles of $3\text{ }\mu$ and less. The increase of specific surface in the formation of primary destruction products from the original grains is roughly $4-6\text{ m}^2/\text{g}$.

3. The rate of increase of the specific surface and the rate of breakdown of the graphite grains in grinding on aqueous solutions of sulfite liquor are roughly 2.5 times the corresponding rates in water. The increase of the comminution rate is due to adsorption of the active additive on the graphite surface at the instant of its formation, i.e., adsorptinal facilitation of the dispersion process. The absolute adsorption of the active additive on the newly formed graphite surface is independent of the comminution conditions, and is $14 \pm 3\text{ mg/m}^2$.

The authors express their sincere gratitude to Academician P. A. Rebinder for his constant attention and interest.

Scientific Research Institute
of the Chemical Industry
Moscow

Received June 1, 1958

LITERATURE CITED

- [1] L. A. Feigin, Chem. Science and Industry 1, 210 (1956).
- [2] S. S. Voiutskii, A. D. Zaionchkovskii and S. I. Rubina, Colloid J. 14, 28 (1952). *
- [3] L. A. Feigin and V. N. Rozhanskii, Proc. Acad. Sci. USSR 115, No. 5, 946 (1957). *
- [4] P. A. Rebinder, Jubilee Volume on the 30th Anniversary of the Great October Socialist Revolution, 1 (Izd. AN SSSR, 1947), p. 533 [in Russian].
- [5] L. V. Liutin and G. V. Zakharova, Mineral Raw Materials 8, 58 (1933).
- [6] A. L. Zagustin, 15 Years in the Service of Socialist Construction, Jubilee Volume, Sci. Res. Inst. for Mechanical Concentration of Minerals, 1 (ONTI, 1935) [in Russian].
- [7] G. F. Huttig and H. Sales, Monatsh. Chem. 85, No. 3, 588 (1954).

*Original Russian pagination. See C.B. Translation.

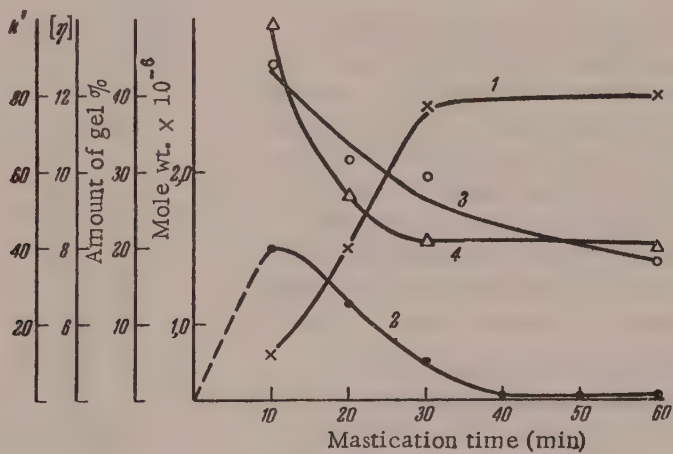
- [8] G. F. Huttig, W. Simm, and G. Glawitsch, Monatsh. Chem. 85, No. 5, 1124(1954).
- [9] N. A. Figurovskii, Sedimentometric Analysis (Izd. AN SSSR, 1948), p. 297 [in Russian].
- [10] A. V. Morachevskaia, Trans. Sci. Res. Inst. Chem. Ind. No. 1, 33 (1954).

LETTERS TO THE EDITOR

GEL FORMATION IN THE MASTICATION OF NATURAL RUBBER, AND ITS INFLUENCE ON VULCANIZATE STRENGTH

B. A. Dogadkin and V. N. Kuleznev

Angier and Watson observed formation of spatial structures (gels) in polychloroprene rubber [1], certain GRS fractions, and butadiene-acrylonitrile rubber [2], under the influence of powerful shearing forces during treatment in a specially designed scroll-type masticator [3]. This gel formation was considered to be a specific characteristic of synthetic rubbers; no one has reported gel formation in the mastication of natural rubber (NR). In our experiments, described below, an insoluble gel was formed in NR. Weighed samples of extracted smoked sheet were masticated in an argon atmosphere containing not more than 0.05% oxygen, on specially designed rolls [4], with 0.12 mm gap between the rolls cooled intensively with water.



Molecular changes in natural rubber during mastication in argon:

- 1) Molecular weight by light scattering; 2) amount of gel; 3) intrinsic viscosity; 3) Huggins constant.

The formation of an insoluble fraction (gel) at the early stages of mastication was established in repeated experiments. Its maximum content (after 10 minutes of mastication) reaches 20%, and further milling results in mechanical dispersion of the gel fraction, so that after 60 minutes of mastication the rubber is again completely soluble in the common solvents. However, the masticated rubber contains formations branched to such an extent that most of them (~80%) are precipitated from octane solution by centrifugation at 12000 r.p.m. for an hour. Molecular weight determinations, based on changes in the light scattering of the solutions at an angle of 90°, showed that the molecular weights of the sol fractions of the masticated samples increase during mastication, reaching 2,500,000 after 60 minutes. The true molecular weight of the particles is apparently of major significance, as a correction for the asymmetry of the scattering particles was not applied.

Gel formation is not observed if the argon contains more than 0.1% of oxygen, which stabilizes the free radicals formed in the mechanical rupture of the molecular chains of the rubber.

In absence of oxygen, secondary reactions of the radicals lead to the formation of branched molecules, which are more compact particles offering less resistance to shearing deformations, and therefore the intrinsic

viscosity (and hence the average molecular weight determined from the viscosity) decreases in the course of mastication. The slope of the η_{sp}/c curves, which is a measure of the Huggins constant k' , decreases during mastication; this suggests that the structural fragments in microgel form are spherical, with a higher density of the rubber substance in the molecular coil.

A very important fact is that the presence of branched formations (microgel) in natural rubber masticated under the conditions described lowers the tensile strength of unfilled sulfur vulcanizates to 20-40 kg/cm², i.e., to values typical for unfilled vulcanizates of noncrystallizing synthetic rubbers. It is known that the strength of vulcanizates of natural rubber, masticated normally in presence of air, reaches 200-250 kg/cm². Thus, the mechanical strength of rubber vulcanizates depends not only on the molecular structure, which is determined by the composition, relative positions, and sequence of the atomic groups, but also on the degree of branching of the molecules,* and in particular on the presence of microgels in the rubber.

The M. V. Lomonosov Institute of Fine
Chemical Technology, Moscow

Received June 10, 1958

LITERATURE CITED

- [1] D. J. Angier and W. F. Watson, *J. Polymer Sci.* 18, 87, 129 (1955).
- [2] D. J. Angier and W. F. Watson, *IRI Trans.* 33, 1, 22, (1957).
- [3] W. F. Watson and D. J. Wilson, *J. Sci. Instr.* 31, 3 98 (1954).
- [4] B. A. Dogadkin et al., *Colloid J.* 19, 421 (1957).**

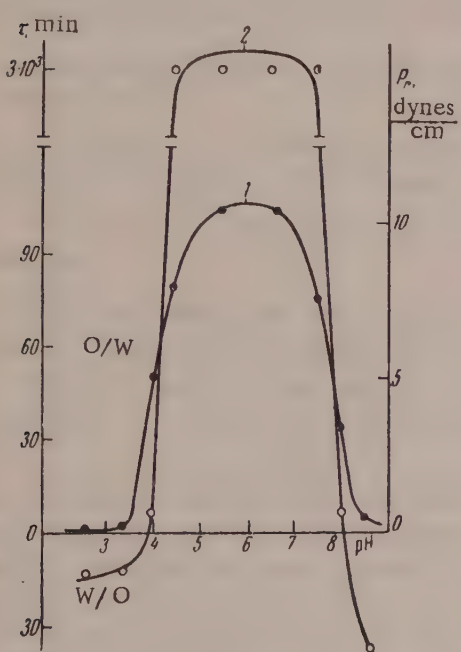
*The influence of branching on the mechanical properties of vulcanizates is considered in detail in the papers by B. K. Karmin et al.

**Original Russian pagination. See C.B. Translation.

THE ROLE OF THE STRUCTUROMECHANICAL FACTOR IN EMULSION STABILITY *

A. B. Taubman and A. F. Koretskii

We found in a study of the stabilizing action of bentonite clay on emulsions of hydrocarbon liquids in water, that stable emulsions can be obtained with the aid of solid-emulsifier monolayers only in the presence of adsorption layers of metal soaps formed in the bentonite particles during emulsification by the interaction of Al^{3+} ions and stearic acid, present in the aqueous and oil phases, respectively [1].



Effect of pH on the yield stress of adsorption layers of aluminum soaps (1) and the stability of emulsions of CCl_4 containing 0.1% of stearic acid, in 0.1 N aqueous AlCl_3 solution (2).

formed, because of its diphilic nature (hydrophilic-hydrophobic structure), has the optimum mosaic characteristics for firm fixation on the interface, resulting in reliable "armoring" of the emulsion droplets, which are thereby protected against coalescence.

Institute of Physical Chemistry, Academy of Sciences
USSR, Moscow
Division of Disperse Systems

Received June 15, 1958

*Paper at the 4th All-Union Conference of Colloid Chemistry in Tbilisi, May 1958.

LITERATURE CITED

- [1] A. B. Taubman and A. F. Koretskii, Proc. Acad. Sci. USSR, 120, No. 1, 126 (1958).*
- [2] J. A. Spink and J. V. Sanders, Trans. Faraday Soc. 51, 1156 (1955); H. Kimizuka, Bull. Chem. Soc. Japan 29, 123, (1956); A. A. Trapeznikov and G. V. Belugina, Proc. Acad. Sci. USSR 87, No. 4, 625 (1952).

* Original Russian pagination. See C. B. Translation.

CURRENT EVENTS

THE FOURTH ALL-UNION CONFERENCE ON COLLOID CHEMISTRY

From May 12 to 16, 1958, the Fourth All-Union Conference on Colloid Chemistry was held in Tbilisi, to summarize the results obtained by Soviet workers in this field during the past four years (the Third Conference was held in Minsk in December 1953).

This conference was convened in Tbilisi by the Division of Chemical Sciences, Academy of Sciences USSR, and the Academy of Sciences, Georgian SSR. Because of the significance of the work on colloid chemistry which is being successfully carried out by Georgian physical chemists.

The conference consisted of five sections (I — surface phenomena and stability of disperse systems, II — adsorption, formation and destruction of aerosols, III — physicochemical mechanics, processes of structure formation, IV — colloid chemistry of clays and peat, and V — disperse systems in polymers, and semicolloids).

More than 150 papers and communications were presented at the conference; 10 of these were given at plenary sessions.

The conference was attended by about 360 delegates, representing most of scientific centers of the Soviet Union in which research is done on colloid chemistry.

Scientists and representatives of industry of Tbilisi, and senior students took part in the meetings of the conference.

It is interesting to note that at the preceding conference, the Third All-Union Conference in Minsk, 200 delegates were present and only 62 papers were given.

These figures clearly demonstrate the rapid growth of research in colloid chemistry, in full accord with its significance in science and the national economy of the USSR.

The importance and topicality of the physical chemistry of colloids and surface phenomena lie in the fact that the substances studied in this field include the most important technological materials — metals and alloys, ceramics, sintered metals, all building and road materials, clays and soils, polymeric materials, food products, detergents, and other surface-active substances. Therefore the work of the conference acquired special importance in relation to the decisions of the May Plenum of the Central Committee of the CPSU on the development of our chemical industry, and also in relation to the decisions of the 2nd All-Union Conference of Builders, held in the Kremlin in March of this year.

It is to be reported with satisfaction that, as the result of the extensive work by the Organizing Committee, the summaries of the papers were printed before the opening of the conference. This was of great help in discussions, and made it possible to include in the program, after the main communications, additional addresses which are noted in the "Summaries." Therefore in this brief survey we confine ourselves to enumeration of the most important research trends and the names of the authors.

At the opening of the conference, our oldest colloid chemist A. V. Dumanskii was unanimously elected Honorary Chairman. In his introductory address, A. V. Dumanskii briefly outlined the history of colloid research in the USSR.

In papers at three plenary sessions, P. A. Rebinder, V. A. Kargin, B. V. Deriagin, M. E. Shishniashvili, and M. P. Volarovich reviewed a number of new fundamental trends represented in the work of the sections.

Work on polymers, polymer solutions, and semicolloids was widely represented at the conference. Papers were presented by V. A. Kargin and his associates; by V. N. Tsvetkov, S. M. Lipatov and their associates, and

others, on the structure of polymer solutions and the mechanism of gel formation; by A. I. Iurzhenko et al. and by P. M. Khomikovskii on the mechanism of emulsion polymerization; by B. A. Dogadkin et al. on the formation and properties of interpolymers of natural and butadiene-styrene rubber; by P. I. Zubov on the mechanism of polymer film formation in adhesion processes; by S. S. Voiutskii and D. M. Sandomirskii on the colloidal properties of latex systems; by A. S. Kuz'minskii and A. P. Pisarenko on the properties of rubber solutions; by V. A. Pchelin on the structural and mechanical properties of gelatin gels; by A. V. Dumanskii et al. on new methods for studying soap and gel structures; and by N. A. Demchenko on solubilization in soap solutions.

Particular attention was devoted to the work of the section on physicochemical mechanics and structure formation.

This included the presentation and discussion of papers by P. A. Rebinder and his school (E. E. Segalova, Tu Yu-ju, Z. N. Markina, E. Stoklosa, A. M. Smirnova and others) on structure formation during hardening of mineral cements (building materials) and on the physicochemical principles of a new concrete technology (N. V. Mikhailov et al.). The paper by O. P. Mchedlov-Petrosian was also concerned with this group of subjects.

The papers by A. A. Trapeznikov, S. S. Voiutskii and B. Ia. Iampol'skii, and G. V. Vinogradov dealt with rheology and structure formation in oleophilic systems (greases, printing inks, hydrocarbon suspensions, etc.). The mechanism of printing processes and the influence of the rheological properties of printing inks on these processes were considered in L. A. Kozarovitskii's paper.

A number of papers — by I. N. Vlodavets, P. A. Rebinder, and others — were concerned with structure formation in food products.

The influence of adsorption on deformation processes, rheological behavior, and destruction of solids and metals was discussed in papers by V. I. Likhtman, G. M. Bartenev, E. D. Shchukin, and P. A. Rebinder. P. A. Thiessen (Democratic German Republic) reported on surface dispersion of solids, and Linde (Democratic German Republic) presented a theory of the influence of surface layers on the kinetics of heterogeneous diffusion exchange.

Structure formation was also the main theme at the section of the colloid chemistry of clays and peat, at which Georgian physical chemists (M. E. Shishniashvili and his associates), and M. P. Volarovich et al., N. N. Serb-Serbina, N. Ia. Denisov, Z. Ia. Berestneva, A. S. Korzhuev, S. P. Nichiporenko, G. V. Kukolev, F. D. Ovcharenko, L. N. Antipov-Karataev and others used new concepts in this field for the interpretation of the technological and constructional (engineering and geological) properties of soils, rocks, clays, and peats.

At the section devoted to surface phenomena and stability of disperse systems, one of the most important problems of colloid chemistry — the mechanism and theory of colloid stability and coagulation — was considered in a large number of papers by B. V. Deriagin and his school, and a number of other authors. These included the paper by B. V. Deriagin (jointly with B. N. Kabanov) on the interaction of crossed metal threads in electrolyte solutions. In addition to the papers by B. V. Deriagin and his associates, papers by the Bulgarian physical chemist A. D. Sheludko and by M. B. Radvinskii were on the subject of the stability of free films and foams, and S. V. Nerpin's paper dealt with the hydromechanics and thermodynamics of thin films, and their influence on soil properties. Catalytic processes in foams were considered in S. Iu. Elovich's paper. The paper by Iu. M. Glazman et al. was devoted to the first mathematical theory of ionic antagonism.

The papers by O. N. Grigorov, D. A. Fridrikhsberg, and S. G. Teletov were concerned with the electro-kinetic properties of colloids in relation to their coagulation by electrolytes.

E. M. Nanobashvili presented a paper on her researches on radiation colloid chemistry.

The section of surface phenomena included papers by B. A. Dogadkin on activated adsorption of sulfur and rubber on carbon blacks, by S. G. Mokrushin on the formation of thin colloidal films, and by N. A. Krotova on the influence of electric fields on the dispersing of liquids.

The papers by E. M. Natanson, V. G. Levich, L. Ia. Kremnev, and A. B. Taubman were concerned with investigations of emulsion and suspension stability in relation to the stabilizing action of the structuromechanical properties of protective surface layers.

Papers on the influence of adsorption of vapors by condensation nuclei on the formation of aqueous aerosols were presented by P. S. Prokhorov, B. V. Deriagin, G. I. Izmailova, and S. S. Dukhin. The kinetics of aerosol formation and destruction was considered by R. I. Kaishev (Bulgaria) and O. M. Todes, and thermophoresis effects, by N. A. Fuks.

Results of studies of kinetic wetting in the collection of dust by surface-active solutions were reported by A. B. Taubman and P. I. Ermilov.

In the adsorption section, mention must be made of the papers by A. N. Frumkin et al., M. M. Dubinin, B. P. Bering, V. V. Serpinskii, V. M. Luk'ianovich, L. V. Radushkevich, G. V. Tsitsishvili, N. F. Ermolenko, and a number of other authors, on adsorption from vapors and from liquid media.

Active part was taken in the conference by eminent scientists from the People's Democracies: member of the Bulgarian Academy of Sciences Professor R. Kaishev, Assistant Professor of Sofia University A. A. Sheludko; member of the Berlin Academy of Sciences Professor P. A. Thiessen, and Dr. Linde, from the German Democratic Republic; Professor of Lublin University, A. Waksmundzki from Poland; Dr. Spurny from Czechoslovakia.

Animated discussions on current problems of colloid chemistry took place at the meeting of the sections. Among these discussions, which have helped in the development of new scientific trends, special mention must be made of the discussion on the problem of the stability of disperse systems, in connection with the papers by B. V. Deriagin et al., V. G. Levich, Iu. M. Glazman, and others.

The work of the sections was efficiently organized. Nevertheless, the conference program was somewhat overloaded, and this hindered discussion in a number of cases.

The work of the conference attracted the attention of many sections of the community in the Georgian capital, and was reported in the periodical press.

The Tbilisi group of the Organization Committee, in cooperation with the Academy of Sciences, Georgian SSR and the leading Georgian institutions, did much preparative work which ensured the success of the conference.

It may be stated in conclusion that the work of the Fourth Colloid Conference was at a high level, and assisted in uniting the efforts of Soviet colloid chemists in the fulfillment of their honorable task — to take creative part in the solution of the important problems raised by the party and Government, in relation to the production of new synthetic materials based on polymers, and of new building materials.

A. B. Taubman

THE VISCOSITY OF TOTALLY DESTRUCTURIZED CLAY SUSPENSIONS,
AND THE EFFECT OF SODIUM HYDROXIDE ON IT*

L. A. Abduragimova and N. G. Alekperova

It has been shown [1] that aqueous suspensions of bentonite clays have a pseudoelastic region at low shear stresses, in which they flow at a virtually constant very high viscosity η_0 , of the order of 10^9 - 10^8 poises. Increase of the shear stress leads to a sharp drop of viscosity, by 8-9 orders of magnitude, when the practical yield value is exceeded. The region of minimum constant viscosity, corresponding to ultimate breakdown of the structure, was determined by means of the Ubbelohde capillary viscosimeter in fairly dilute suspensions of bentonite clays (4,7, and 10% suspensions of Oglanli clay).

In the present investigation of the viscosity of totally destructureclay suspensions, a capillary viscosimeter was used, whereby the rheological properties of clay suspensions of any concentration could be studied at a relatively high shear stresses. The clay suspension was pumped from a storage vessel 1 liter in capacity, through a capillary in a vertical position, into a receiver, under the influence of a pressure difference at the capillary ends, produced by a vacuum pump. The viscosity of the clay suspensions was calculated from the Poiseuille equation [2]; the volume of the suspension passing through the capillary was found from its density and the weight which flowed through the capillary in the given time.

The viscosimeter was tested by determination of the viscosity of water at 28° in streamline flow (Fig. 1). The viscosity behavior of clay suspensions was studied over a wide range of velocity gradients and shear stresses. Slippage along the capillary walls is possible in the flow of clay suspensions [3], but as the experiments were performed at considerably higher shear stresses, in the region of maximum structural breakdown or close to it, when the viscosity of clay suspensions is between 0.1 and 1 poise, slippage of the system should be slight if it occurs at all.

The results were plotted in the form of rheological curves representing the velocity gradient ($\dot{\epsilon} = d\epsilon/d\tau$) as a function of the stress (P). The Newtonian viscosity of the system was calculated from the cotangent of the slope of the linear region of the rheological curve, the continuation of which passes through the coordinate origin (Figs. 1,2).

The Newtonian viscosity of a clay suspension remains constant up to stresses corresponding to transition from laminar to turbulent flow. In the rheological curves the turbulent-flow region is represented by straight lines the continuation of which cuts the ordinate axis. If wide capillaries are used with dilute suspensions, it is possible to reach turbulent flow before maximum structural breakdown, i.e., before the minimum constant viscosity is reached.

Newtonian viscosity, unlike anomalous viscosity, does not depend on the capillary radius or on the time of efflux through the capillary (Fig. 3).

In the region of anomalous viscosity, on the other hand, the lower the efflux rate, the greater are the viscosity changes in relation to the efflux time at constant shear stress (Fig. 3).

Figs. 1 and 2 present rheological curves for ten-day 35, 40, 45, 50, and 55% suspensions of Zykh (kaolin) clay. The Newtonian viscosities of ten-day suspensions of Ramanin (kaolin) and Gekmalin (bentonite) clays, calculated from the rheological curves, are given in the Table.

It follows from Figs. 1 and 2 and the Table that the viscosity of the clay suspensions increases sharply with

*Paper at the IVth All-Union Conference on Colloid Chemistry in Tbilisi, May 1958.

increase of the solid-phase concentration. The experimental values of the minimum constant viscosity for all the systems studied are at least 10 times the values calculated from the Einstein equation [2].

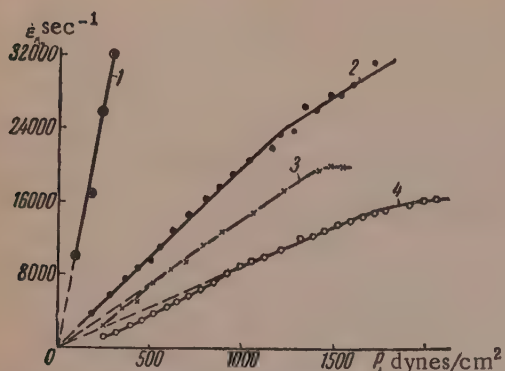


Fig. 1. Rheological curves:

- 1) Water, $\eta_m = 0.089$ poise; suspensions of Zyk clay: 2) 35%, $\eta_m = 0.049$ poise; 3) 40%, $\eta_m = 0.071$ poise. 4) 45% $\eta_m = 0.119$ poise.

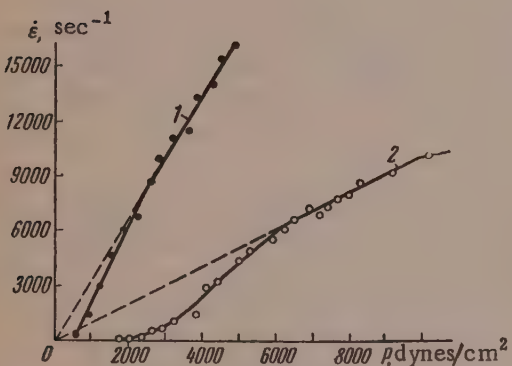


Fig. 2. Rheological curves for Zyk clay suspensions:

- 1) 50%, $\eta_m = 0.3$ poise; 2) 55% $\eta_m = 1.0$ poise.

The probable cause of the deviations of the Newtonian viscosity of these systems from the Einstein equation, apart from the particle shape, degree of particle hydration, and their spontaneous dispersion, mainly lies in the fact that in the η_m region the system consists, not of individual primary particles, but of particle aggregates (structural fragments) which do not undergo further breakdown, and the cavities of which contain water in the immobilized state. According to Rebinder [4], the strength of such aggregates is due to cohesion of the particles at the corners and edges, through very thin hydration layers. The structure of the suspension formed by cohesion of the particles through relatively thick hydration layers, is weak, and is broken down completely when the maximum shear stress P_m is reached.

The Newtonian viscosity of bentonite clay suspensions depends on their age (time from the moment of preparation). The viscosity of 15% Gekmalin clay suspension increases from 0.193 to 0.342 poise in 10 days; that of a 15% askangel suspension, from 0.200 to 0.660 poise (Fig. 4). The Newtonian viscosity of an askangel suspension continues to change after 10 days; after 30 days the viscosity of a 15% askangel suspension rises to 0.940 poise. The Newtonian viscosity of kaolin clays changes very little with time. The Newtonian viscosity of 45% Zyk clay suspension increases from 0.104 to 0.119 poise in 10 days. The increase of the Newtonian viscosity of bentonite clays with time is in all probability caused by increase in the size of the aggregates (structure fragments) as the result of hydration and spontaneous dispersion of the particles, and also by slow attenuation of the thin interlayers between the particles [5], i.e., as the result of strengthening of the bonds between the particles.

The influence of alkali on the viscosity of totally destruc-
tured bentonite and kaolin clay suspensions is a subject of great interest. It is known that small amounts of surface-active electrolytes can be used for active regulation of the colloidal properties of disperse systems, and are used widely for this purpose in technology. The technical properties of

Effect of Solid-Phase Content on η_m of Clay Suspensions

Concentration of Ramanin clay suspension, %	η_m , poises	Concentration of Gekmalin clay suspension, %	η_m , poises
40	0.106	10	0.130
45	0.189	12	0.240
50	0.450	15	0.342
55	1.320	20	1.300

disperse systems (cements, concretes, clay suspensions, etc.) can be deliberately controlled if the mechanism of the action of various substances on their structural and mechanical properties is known. The properties of clay suspensions used in oil-well drilling are improved by such additives as carbon-alkali reagent, sulfite waste liquor, carboxymethylcellulose, etc.; NaOH is a constant component of all chemically-treated drilling muds. We studied the effect of alkali on the Newtonian viscosity of Zykh, Ramanin, and Gekmalin clays. Fig. 5 shows graphs of the Newtonian viscosity against the percentage of alkali in the liquid phase in 10-day suspensions, calculated from the rheological curves. Fig. 5 shows that the first additions of alkali increase the Newtonian viscosity of the clay suspensions, but further additions reduce it.

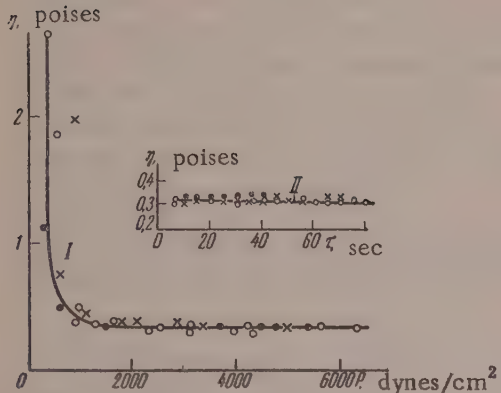


Fig. 3. (I) Effect of capillary radius on the Newtonian viscosity of 12% Gekmalin clay suspension;

$r=0.11$ cm, $r_1=0.09$ cm, $r_q=0.083$ cm.

(II) Effect of efflux time on the Newtonian viscosity of 50% Zykh clay suspension:
 $P = 2580.2$ dynes/cm²; $P_1 = 3911.7$ dynes/cm²; $P_2 = 4312.4$ dynes/cm².

One factor causing changes of Newtonian viscosity when alkali acts on a clay suspension is alteration of the composition of the exchange complex of the clay owing to ion exchange between the clay and the alkali. The influence of changing composition of the exchange complex may be eliminated if pure Na kaolin and Na bentonite clays are used. We therefore prepared Na Ramanin, Na Zykh, and Na Gekmalin clays by the Gedroits method [5].

Curves for the Newtonian viscosity of ten-day suspensions of Na clays against the alkali concentration are presented in Fig. 6. As in the case of native clays, the first additions of alkali increase the Newtonian viscosity of Na clays, but further additions decrease it.

It is also interesting to note that replacement of the exchange complex by Na produces a sharp increase of Newtonian viscosity in bentonite clays, but only a slight one in kaolin clays. The Newtonian viscosity of a 15% suspension of native Gekmalin clay is 0.342 poise, and that of a 15% suspension of Gekmalin Na bentonite is 6.2 poises. Replacement of the exchange complex by Na in Zykh and Ramanin clays changes the viscosity of 40% suspensions of these clays from 0.071 and 0.106 poises to 0.150 and 0.216 poises respectively.

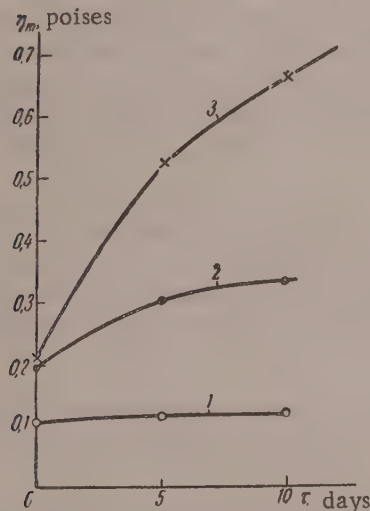


Fig. 4. Effect of age on the Newtonian viscosity of clay suspensions:

1) Zykh, 45%; 2) Gekmalin, 15%; 3) askangel, 15%.

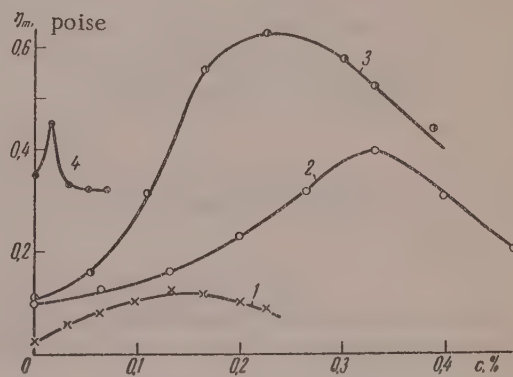


Fig. 5. Effect of alkali concentration on the Newtonian viscosity of clay suspensions:

1) Ramanin, 25%; 2) Zykh, 40%; 3) Ramanin, 35%; 4) Gekmalin, 15%.

For elucidation of the role of the alkali added to clay suspensions, we studied the sorption of alkali by both native and Na clays. The sorption of alkali by the clays was determined by titration of filtrates from suspensions of 5 g of bentonite and 10 g of kaolin clays in 100 ml of water, by hydrochloric acid in presence of methyl orange.

The suspensions were filtered and the filtrates titrated 24 hours after preparation, i.e., after the equilibrium concentration (c) had become established.

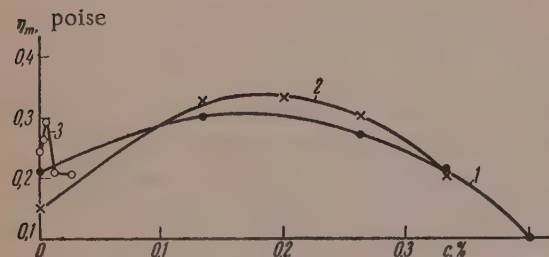


Fig. 6. Effect of alkali concentration on the Newtonian viscosity of clay suspensions:

- 1) Na Ramanin, 40%; 2) Na Zykh, 40%; 3) Na Gekmalin, 8%.

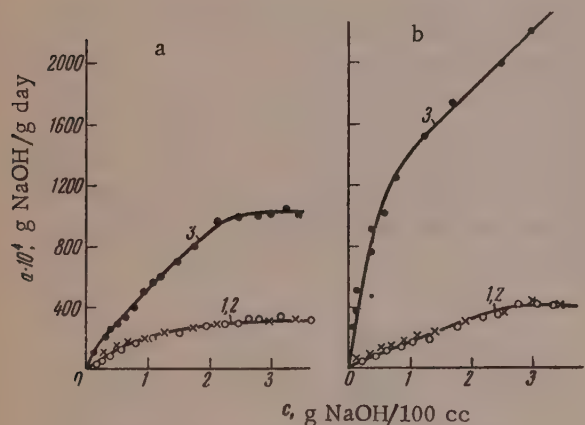


Fig. 7. Isotherms for the adsorption of alkali on clays:

- a) 1) Zykh; 2) Ramanin; 3) Gekmalin;
b) 1) Na Zykh; 2) Na Ramanin; 3) Na Gekmalin;
a) not washed; b) washed free of electrolytes.

considerable increase of the capacity of the clay for alkali. In the case of Na Gekmalin clay the maximum sorption of alkali was not reached, probably because of further spontaneous dispersion of the particles with increase of the alkali concentration.

Nearly all the alkali (80–90%) adsorbed by the clays can be removed by water as the result of very prolonged repeated washings, or by dialysis for two months or more. The fact that the alkali can be washed out by water suggests that the adsorption is of a physical character.

Adsorption of caustic soda by the particle surfaces in clay suspensions results in the formation of diffuse hydration layers of different thickness, which depends on the concentration of the added NaOH. At low concentrations of NaOH in solution, such additions result in increases of these layers and this favors spontaneous dispersion and formation of loose aggregates (fragments of the structural network) with a large amount of immobilized

To eliminate the influence of water sorbed by the clays, the clays were previously soaked for 3–4 days in definite amounts of water, corresponding to their swelling. In the case of Zykh and Ramanin clays, the swelling of which is 100 and 120% respectively, preliminary soaking has hardly any effect on the sorption of alkali. In the case of Gekmalin clay, and especially of Na Gekmalin clay, the swelling of which is 600 and 1000% respectively, preliminary soaking results in higher values of alkali sorption. The cause of the difference between the amounts of alkali taken up by bentonite clay without and with previous soaking is that in absence of previous soaking the volume of the filtrate is considerably less, because of the considerable swelling of the clay, and this distorts the results.

Curves for the sorption of alkali by previously soaked Zykh, Ramanin, and Gekmalin clays are plotted in Fig. 7.

Fig. 7 shows that Gekmalin clay takes up the most alkali.

In the case of native clays, decrease of the amount of alkali in solution (i.e., sorption) may be caused by: 1) ion exchange between the alkali and the clay, to a certain extent, 2) reactions between the alkali and salts present in the clay, and 3) adsorption.

In order to eliminate the influence of the exchange reaction between the alkali and clay, and of reactions between the alkali and the soluble salts present in the clay, the sorption of alkali was also studied for Na-substituted kaolin and bentonite clays washed free of electrolytes. The Na clays can take up alkali by adsorption only.

It follows from Fig. 7 that substitution of the exchange complex of Gekmalin clay by Na results in a considerable increase of the capacity of the clay for alkali. In the case of Na Gekmalin clay the maximum sorption of alkali was not reached, probably because of further spontaneous dispersion of the particles with increase of the alkali concentration.

water, with an increase in the volume of the "solid phase" (in the Einstein equation [2]), and therefore an increase of η_m .

When an amount of alkali causing compression of the diffuse layer is added, the bonds at the points of contact are strengthened, the aggregates become more compact, and immobilized water is liberated; this leads to a decrease of η_m .

SUMMARY

1. The rheological properties of suspensions of native and of Na Ramanin, Na Zykh, and Na Gekmalin clays, with and without additions of alkali, have been studied at relatively large shear stresses. Newtonian viscosity, independent of the capillary radius and efflux time, has been detected in all the clay suspensions.

2. Deviations of the Newtonian viscosity (η_m) from the values predicted by the Einstein equation are probably caused, apart from the particle shape, their hydration, and spontaneous dispersion, by the fact that in the η_m region the system consists not of primary disconnected particles but of aggregates (fragments of the structural network), which are not broken down further, and the cavities of which contain immobilized water. The strength of such aggregates is due to cohesion of the particles at their corners and edges through very thin interlayers of the dispersion medium.

3. Curves for the adsorption of alkali by native and Na clays have been plotted. It is shown that bentonite clays, and in particular Na bentonites, have the greatest adsorption capacity for alkali.

4. The influence of added alkali in the Newtonian viscosity (η_m) of native and Na clays has been studied. The first additions of alkali increase η_m , and subsequent additions decrease it.

In conclusion, we offer our sincere gratitude to Academician P. A. Rebinder and to N. N. Serb-Serbina for valuable advice and guidance in the work and in analysis of the results.

LITERATURE CITED

- [1] L. A. Abduragimova, P. A. Rebinder and N. N. Serb-Serbina, *Colloid J.* 17, 184 (1955).*
- [2] I. I. Zhukov, *Colloid Chemistry* [in Russian] (Leningrad State University Press, 1952).
- [3] D. M. Tolstoi, Doctorate Dissertation (Moscow, 1954). [In Russian].
- [4] P. A. Rebinder, *Faraday Society Discussion*, No. 18 (1954).
- [5] B. V. Deriagin, Proc. Conference on Engineering and Geological Properties of Rocks and Methods for their Investigation [in Russian] (Moscow, 1956).
- [6] K. K. Gedroits, *The Sorptional Capacity of Soils* [in Russian] (State Agricultural Press, 1933).

Institute of Chemistry, Academy of
Sciences, Azerbaijan SSR, Baku

Received September 17, 1957

*Original Russian pagination. See C. B. translation.

INFLUENCE OF TEMPERATURE ON THE EXCHANGE OF COBALT AND COPPER CATIONS ON ORGANIC CATION-EXCHANGE RESINS

L. S. Aleksandrova and S. Iu. Elovich

Ion exchange has been the subject of intensive study for 60 years. In view of the growing use of ion-exchange chromatography, with the aid of organic ion exchangers, interest in various aspects of the action of ion exchangers has been growing continuously in recent years.

The use of ion exchangers at elevated temperatures for accurate separation of ions has been described [1].

However, very little work has been done on the influence of temperature on ion-exchange adsorption in relation to various properties of the adsorbents. There have only been some isolated studies of the influence of temperature on the rate at which equilibrium is reached. The equilibrium itself, and the effect of temperature on its characteristics, have been studied very little. Boyd, Schubert, and Adamson [2] studied the temperature effect of ion-exchange adsorption for the system sodium-potassium on Amberlite IR-1 resin. The determinations were performed over a limited temperature range, from 13.5 to 30°. The heat of adsorption was roughly estimated as 2 ± 2 kcal/mole. Kressman and Kitchener [3] found that the heat of adsorption on a sulfonated-phenol cation exchanger in the exchange of potassium and hydrogen ions is 1.95 kcal/mole. The temperature range of the investigation was between 1.5 and 40°.

Duncan and Listrer [4] studied ion-exchange equilibrium between sodium and hydrogen ions, and also between barium and hydrogen ions. The cation exchanger was Dowex-50, which contains the functional group HSO_3^- . The effect of temperature on sorption was studied at 20 and 87°, and the heat of sorption for the system $\text{Na}^+ - \text{H}^+$ was found to be 525-720 cal/mole.

According to Duncan's calculations [5] the heat of adsorption for the system barium-hydrogen varied greatly in the range of 2000-6000 cal/mole.

Mention must also be made of the work of Dickel and Nieciecki [6], who studied the kinetics of ion-exchange equilibrium of the alkali elements in relation to cation exchangers in the hydrogen form. The resins used were Levatites S100 and KS, which are sulfonated-styrene adsorbents, and Wofatit KS, which belongs to the class of phenol-formaldehyde resins. The exchange constant was determined from only one point of equilibrium concentration, at 0, 25, 50 and 75°. The determinations were performed in the concentration region of about 0.005 N. The temperature coefficient of adsorption was found to be small.

Certain published data [7] indicate that the exchange capacity of inorganic ions on certain organic and inorganic cation exchangers increases with temperature. It has been shown [8] that temperature has no appreciable influence on exchange on glauconite. Several workers [9] have also found that increase of temperature has no appreciable influence on the equilibrium distribution of ions of the same valence.

Walton [10] found that the temperature effect of ion-exchange sorption should not exceed 2 kcal/mole, and can be considerable only for weakly acidic cation exchangers.

However, the influence of temperature on ion exchange has not been studied sufficiently: the experimental data are fragmentary and unsystematic.

We studied the ion-exchange equilibrium of Cu^{2+} and Co^{2+} ions on two organic cation exchangers in the range from 20 to 75°.

The resins were: KU-2, which is a sulfonated-styrene resin with a strongly acid HSO_3^- functional group, and RF, containing the $\text{PO}(\text{OH})_2$ functional group, much less acid than the sulfo group. The resins were crushed to 20-50 mesh and converted into the hydrogen form. The capacity of KU-2 was 4.18 meq/g, and of RF, 1.79 meq/g, calculated on the dry resin. The swelling of KU-2 was 262.5%, and of RF, 161.4%.

The time for equilibrium to be reached was ~1 hour for KU-2 resin, and 4-5 hours for RF resin. The original solutions contained cobalt and copper at the following concentrations: 0.005; 0.01; 0.02; 0.03; 0.04; 0.05 and 0.1 N. The equilibrium determinations were performed at approximately constant ionic strength, which was maintained by additions of 0.2 N HCl solution.

Method. 1 g of resin in a flask was covered with 20 ml of the appropriate salt solution. The flasks with the solutions were then placed in a thermostat and shaken for 5 hours at the required temperature. The equilibrium concentration of Cu^{2+} ions was determined iodometrically; the Co^{2+} concentration was determined by means of the nitroso R salt, and the Co^{60} isotope was also used. The volume changes caused by increase of temperature were taken into account in the determinations of the initial and equilibrium concentrations.

The equilibrium was calculated by means of the Nikol'skii equation

$$\frac{q_{\text{Me}}^{1/2}}{q_{\text{H}}} = K \frac{a_{\text{Me}}^{1/2}}{a_{\text{H}}},$$

where q_{Me} and q_{H} are the amounts of bivalent ions and hydrogen ions adsorbed; a_{Me} and a_{H} are the equilibrium activities of these ions. The determinations were carried out at approximately constant ionic strength. The ionic strength of the equilibrium solutions varied in the 10-15% range.

The principal data on the exchange isotherms are given in Table 1.

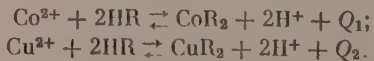
TABLE 1

Data on Exchange Isotherms

t°C	KU-2 resin				RF resin			
	Co^{2+}		Cu^{2+}		Co^{2+}		Cu^{2+}	
	equilibrium concentration in meq/ml	amount adsorbed in meq/g	equilibrium concentration in meq/ml	amount adsorbed in meq/g	equilibrium concentration in meq/ml	amount adsorbed in meq/g	equilibrium concentration in meq/ml	amount adsorbed in meq/g
20	0.00027	0.0970	0.0003	0.1321	0.00214	0.0655	0.0019	0.066
	0.00042	0.1950	0.0007	0.2582	0.00489	0.1215	0.0038	0.130
	0.00115	0.3857	0.0013	0.5165	0.01490	0.2304	0.0086	0.237
	0.00263	0.5600	0.0032	0.7459	0.01743	0.2878	0.0145	0.327
	0.00382	0.740	0.0043	0.9813	0.0242	0.3657	0.0196	0.433
	0.00510	0.919	0.0067	1.1537	0.03037	0.4680	0.027	0.479
	0.01710	1.6923	0.0249	2.0925	0.07241	0.632	0.0674	0.708
	0.00028	0.1380	0.0004	0.164	0.00475	0.1245	0.0053	0.118
40	0.00333	0.6660	0.00405	0.774	0.0322	0.4195	0.0310	0.471
	0.01076	1.4680	0.0140	1.452	0.0742	0.6044	0.0722	0.701
	0.00028	0.1370	0.00049	0.1623	0.0533	0.0881	0.0058	0.1052
75	0.0030	0.6659	0.00457	0.765	0.0310	0.375	0.0333	0.400
	0.01126	1.4571	0.0163	1.419	0.0769	0.5046	0.0745	0.632

The data are plotted in the coordinates of the Nikol'skii equation in Figs. 1 and 2. The points fit on straight lines passing through the origin. The lines for adsorption on RF resins lie lower with increase of temperature (Fig. 1). This means that the adsorption of cobalt and copper ions, relative to the adsorption of hydrogen ions, decreases with increase of temperature.

The exchange of cobalt and copper on RF resin may be represented as:



Here Q_1 and $Q_2 > 0$. The reaction of exchange adsorption proceeds from left to right, with a positive heat effect.

A different result is obtained for KU-2 resin (Fig. 2). The points representing adsorption of cobalt ions at 20, 40, and 70° lie on the same straight line.

The adsorption of Cu^{2+} ions has a small temperature effect; the adsorption of Cu^{2+} ions decreases with increase of temperature.

The exchange constants at different temperatures are given in Table 2.

In Fig. 3,a the logarithm of the exchange-adsorption constant is plotted against the reciprocal absolute temperature. The experimental points fit satisfactorily on straight lines. The heats of adsorption (Q) for the systems $\text{Cu}^{2+}-\text{H}^+$ and $\text{Co}^{2+}-\text{H}^+$ on RF resin are 1260 and 1040 cal/mole respectively.

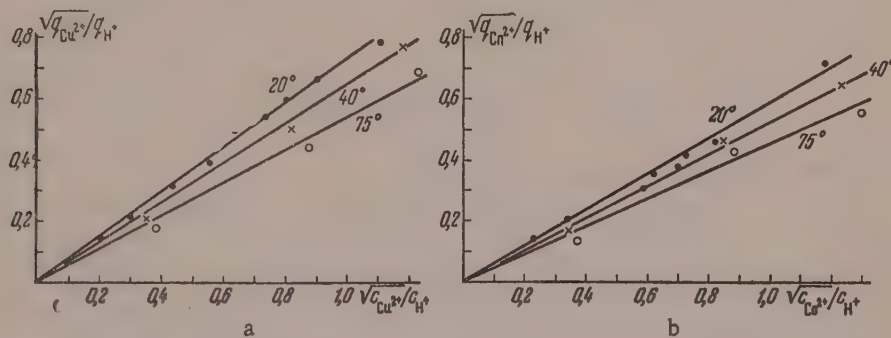


Fig. 1. Adsorption of copper (a) and cobalt (b) ions on RF resin at 20, 40, and 75°.

In the case of the system $\text{Cu}^{2+}-\text{H}^+$ on KU-2 resin the heat of adsorption (Q) is only ~600 cal/mole (Fig. 3,b), while for the system $\text{Co}^{2+}-\text{H}^+$ the heat of adsorption cannot be calculated. In calculations of the heats of adsorption it was assumed that the activity coefficients depend little on the temperature; this is known to be the case for a number of ions.

TABLE 2

Exchange Constants

Tempera- ture, °C	RF resin		KU-2 resin	
	system $\text{Cu}^{2+}-\text{H}^+$	system $\text{Co}^{2+}-\text{H}^+$	system $\text{Cu}^{2+}-\text{H}^+$	system $\text{Co}^{2+}-\text{H}^+$
20	0.74	0.62	1.1	1.0
40	0.65	0.54	1.03	1.0
75	0.54	0.47	0.96	1.0

A number of authors have shown [11] that, if swelling adsorbents are used, changes in the distribution of ions between the adsorbent and solution may lead to water being taken up by or displaced from the resin, and hence to changes in the degree of hydration of the ions in the adsorbent. This factor should influence the energy of adsorption. We studied the swelling of the resins used in our experiments. The degree of swelling was determined under the same conditions as were used for the adsorption experiments. The results are presented in Tables 3 and 4.

It follows from Tables 3 and 4 that the volume of the adsorbent remains almost unchanged during adsorption at all the temperatures used. The slight systematic volume change does not exceed 2.5%. In most instances the changes do not exceed 1% of the initial volume. In view of the rough method used for estimation of swelling,

and because of lack of data on the coefficient of thermal expansion of the resins used, we cannot attach any significance to these changes, and we assume that within the accuracy limits of our experiments the degree of swelling of the resins is virtually constant. Consistent values for the exchange constants were therefore obtained, as resins of constant properties were used for the adsorption.

TABLE 3

Swelling of RF Resin, as % of Initial Volume

Tempera- ture °C	Cu(NO ₃) ₂		Co(NO ₃) ₂		0,4N HCl	H ₂ O
	0,1NCu ²⁺ in 0,2NHCl	0,05NCu ²⁺ in 0,2NHCl	0,1NCo ²⁺ in 0,2NHCl	0,01NCo ²⁺ in 0,2NHCl		
20	164,8	164,0	163,4	166,3	159,6	161,4
40	164,8	163,1	162,2	164,8	159,6	161,4
75	162,2	161,4	161,4	163,1	159,6	161,4

TABLE 4

Swelling of KU-2 Resin, as % of Initial Volume

Tempera- ture °C	Cu(NO ₃) ₂		Co(NO ₃) ₂		0,4N HCl	H ₂ O
	0,1NCu ²⁺ in 0,2NHCl	0,02NCu ²⁺ in 0,2NHCl	0,1NCo ²⁺ in 0,2NHCl	0,01NCo ²⁺ in 0,2NHCl		
20	243,7	247,3	247,3	251,7	252,6	262,5
40	247,5	250,0	250,0	253,5	254,4	262,2
75	248,2	251,7	253,5	252,6	251,8	268,7

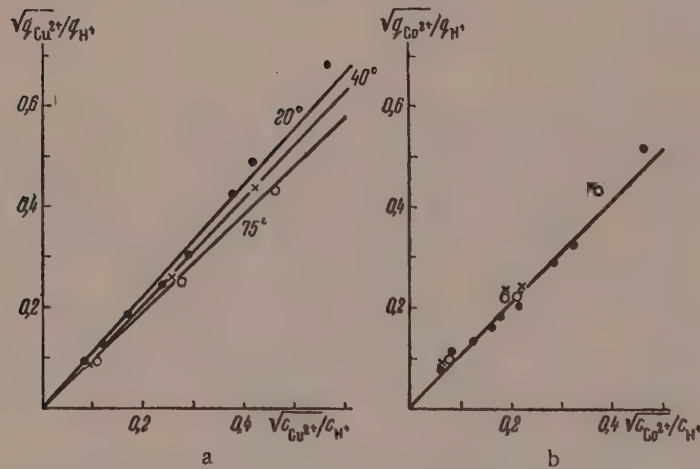


Fig. 2. Adsorption of copper (a) and cobalt (b) ions on KU-2 resin at 20, 40, and 75°.

Our results confirm the views of many of the workers cited above, concerning the low value of the temperature coefficient of ion-exchange adsorption.

The heat of sorption of Co²⁺ on KU-2 resin was found to be almost zero. The equilibrium constant K may

be represented as follows:

$$K = K_0 e^{Q/RT},$$

where Q is the heat of sorption. For adsorption of cobalt on KU-2 resin, $Q \approx 0$. This means that the value of the exchange constant for Co^{2+} on KU-2 is determined only by the entropy term K_0 . The fact that no heat is evolved in ion-exchange adsorption shows that replacement of two hydrogen ions by a cobalt ion does not alter the state of the ions in the adsorbent as compared with their state in solution.

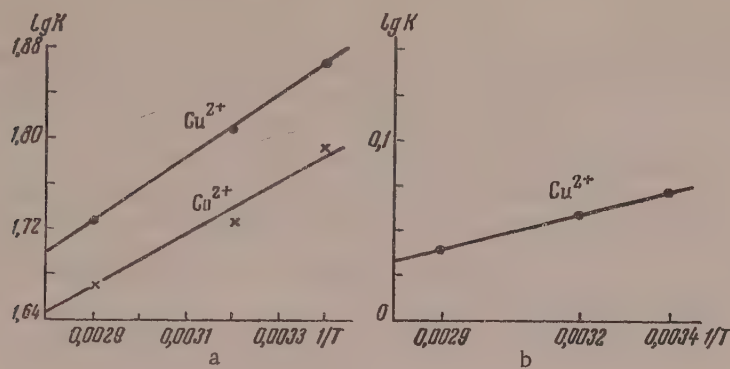
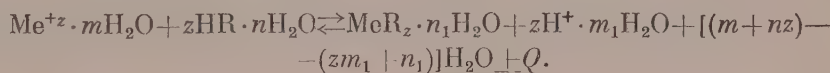


Fig. 3. Temperature coefficients of adsorption:
a) of copper and cobalt on RF resin; b) copper on KU-2 resin.

The degree of hydration of the ions evidently remains unchanged. This is consistent with the well-known rule that the adsorption series of ions in relation to a given resin coincides with the series of ions in order of their hydrated radii in solution. The sole exception is sorption of hydrogen ions by adsorbents with weakly acidic functional groups. In such a case the hydrogen ion, being stably held by the anion of the functional group, readily displaces other ions; as the hydrogen ion passes from solution to the site of adsorption, the weakly acidic functional group, the state of the hydrogen ion, and in particular its degree of hydration, is greatly changed, and some water molecules are therefore displaced from the hydration zone into the solution. The heat of formation of an undissociated molecule of a weak acid may be considerable. For example, for the second stage of dissociation of phosphoric acid $Q \approx 4000$ cal [12].

When a hydrogen ion in the weakly acidic functional group is displaced by some cation, transhydration of the ions usually takes place, and this determines the heat of ion-exchange adsorption. The absolute value of the exchange constant is also determined by the entropy term.

In the light of these considerations, the cation-exchange equation may be written as follows:



The heat effect may be either positive or negative. However, the more weakly-acidic the resin used, the more probable it is, under the same conditions, that the temperature coefficient of the above reaction is negative.

Our resins, RF and KU-2, belong to groups of resins differing in their degree of swelling. However, calculation of the number of molecules of water per functional group within the resin shows that in the conditions of our adsorption experiments this number is 19.6 for KU-2 resin, and 20.0 for RF resin. The two adsorbents are therefore approximately the same with regard to the structure of the solution within the resin. Therefore the main difference between them must be attributed to differences in the acidity of the functional groups. As our experiments were performed in an acid medium, the dissociation of the second hydroxyl group of the phosphoric acid in the resin was disregarded.

For a strongly swollen adsorbent of low capacity it may be assumed that the structure of the electrolyte within the adsorbent does not differ from the structure outside the resin. In the case of not very concentrated electrolytes, there is a short-range and a long-range order of water molecules. Samoilov [13] introduced the

concept of short-range coordination, corresponding to a definite number of water molecules bound directly to the electrolyte ion. Beyond these water molecules there is a much larger number of water molecules, held much less strongly by the central electrolyte ion. If this structure is retained, then interaction between the adsorbed ion and the functional group occurs at relatively large distances, and therefore small differences in the hydrated ion radii have very little influence on their adsorption. The hydrated radii of cobalt and copper ions, determined by Stokes' law, are 3.56 and 3.37 Å respectively [14]. The crystallographic radius of the Co^{2+} ion is 0.82 Å, and of the Cu^{2+} ion, 0.79 Å [14]. The ionic radii remain similar in solution [15].

The numbers of water molecules in the hydration layers, determined by Stokes' law, differ somewhat; the value is 8 for Co^{2+} , and 7 for Cu^{2+} .

With resins of a lower degree of swelling and relatively high capacity the structure of the solution described above is no longer retained. It then corresponds to the structure of concentrated solutions, with a more uniform arrangement of water molecules, and gradual elimination of the "long-range order" of the water molecules. Interaction between the adsorbed ions and the functional groups then occurs at shorter distances, and the differences between the ions become more prominent. These effects were observed by Samuelson [16] for two sulfonated polystyrene resins of different degrees of swelling. The less-swollen resin proved to be the more selective.

In a paper cited above [11], the author modified the equation for the ion-exchange isotherm by allowing for the change of the resin volume in adsorption.

In the present instance we evidently determined the heat effect without the interfering effect of swelling during adsorption.

SUMMARY

1. Isotherms for the adsorption of bivalent cobalt and copper ions on two adsorbents have been determined: on KU-2 sulfonated-polystyrene resin, and on RF resin containing the $\text{PO}(\text{OH})_2$ functional group.
2. Isotherms at 20, 40, and 75° at approximately constant ionic strength have been determined. The temperature effect for KU-2 resin was very slight. The temperature effect in adsorption on the weakly acidic RF resin was ~1000 cal/mole.
3. The temperature effect of adsorption is largely associated with the degree of acidity of the functional groups of the resins.

LITERATURE CITED

- [1] B. Ketelle and G. Boyd, J. Am. Chem. Soc. 69, 2800 (1947).
- [2] G. Boyd, J. Schubert and A. W. Adamson, J. Am. Chem. Soc. 69, 2818 (1947).
- [3] T. R. E. Kressman and J. A. Kitchener, J. Chem. Soc. (London), 1190 (1949).
- [4] J. F. Duncan, B. A. J. Listrer, J. Chem. Soc. (London), 3285 (1949); Disc. Farad. Soc. 7, 104 (1949).
- [5] J. F. Duncan, Austral. J. Chem. 8, 1 (1955).
- [6] G. Dickel, L. v. Nieciecki, Z. Elektrochem. 57, 901 (1913).
- [7] I. A. Apel'tsin, V. A. Kliachko, Iu. A. Lur'e, and A. S. Smirnov, Ion Exchangers and their Applications [in Russian] (State Standards Press, 1949), p. 68.
- [8] E. A. Materova, Sci. Mem. Leningrad State Univ., Chem. Ser., No. 79, issue 7, 15 (1945).
- [9] V. Rothmund and G. Kornfeld, Z. anorg. Chem. 103, 129, 1918; 108, 215, 1919; I. R. Patton, I. V. Ferguson, Cancer. Res. B 15, 103, 1937; L. P. Vanselow, Soil Sci. 33, 95, 1932; O. C. Magistad, M. Fireman, B. Marby, Soil. Sci. 57, 371, 1944.
- [10] H. Walton, in the book: Ion Exchange (F. Nachod, ed.) (Moscow, IL, 1951), p. 24 [Russian translation].
- [11] G. V. Samsonov, Colloid J. 18, 592 (1956).
- [12] R. A. Robinson and R. H. Stokes, Electrolytic Solutions (1955), p. 496.

- [13] O. Ia. Samoilov, Proc. Acad. Sci. USSR 58, 1073 (1947); 83, 447 (1952).
- [14] E. Darmois, J. Chim. Phys. 43, I (1946).
- [15] A. F. Kapustinskii, S. I. Drakin and B. M. Iakushevskii, J. Phys. Chem. 27, 433 (1953).
- [16] O. Samuelson, Dissertation, cited through H. Walton, in the book: Ion Exchange (F. Nachod, ed.) (Moscow, 1951) [Russian translation].

Institute of Physical Chemistry
Academy of Sciences USSR, Moscow

Received May 6, 1957.

STUDIES OF THE PHYSICOCHEMICAL PROPERTIES OF TIRE-CORD FIBERS

1. HEATS OF SOLUTION OF CAPRON FIBERS

V. A. Berestnev, T. V. Gatovskaia, V. A. Kargin, and E. Ia. Iaminskaia

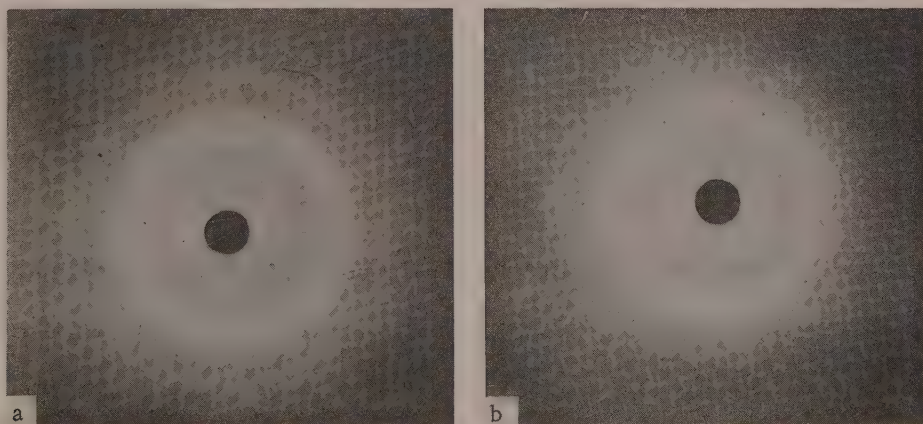
It is known that many valuable properties of cords deteriorate during production and use of tires. This is caused mainly by the action of heat and mechanical forces, and may be determined either by changes of fiber microstructure, i.e., changes in the flexibility of the molecular chains, their packing density, crystallinity of the polymer, etc., or by changes in the macrostructure, associated with growth of macroscopic defects in the fiber (microscopic cracks, voids, etc.).

The purpose of the present work was to study changes in the microstructure of capron cord caused by different treatments. Changes of polymer structure may be studied by means of thermodynamic methods. The method used in this investigation was determination of the integral heats of solution, which gave an indication of changes in the degree of crystallinity of polycaprolactam [1].

Samples of standard capron cord fiber were used in the investigation. The samples were subjected to heat and mechanical treatments. For the heat treatment, the samples were heated in air or in water. For the mechanical treatment, the fibers were stretched on a metal frame under a load of 10.5 kg, which is ~80% of the breaking load. The elongation was 22%. The fiber fixed in the frame was either heated in air or water, or left in the stretched state at room temperature. Another form of mechanical treatment was repeated extension under a load of about 50% of the breaking load, to induce dynamic fatigue. Finally, for evaluation of changes in the cord microstructure on total destruction of the fiber, the original cords were milled at room temperature for 1 hour. This yielded a "milled" sample, which had the appearance of a fibrous powder.

The heats of solution of different samples of capron cord fiber in concentrated (95%) formic acid were determined in an adiabatic calorimeter [2]. The accuracy was 0.1 cal.

The results of the determinations are given in the Table. Comparison of the heat of solution of the original sample and of heat-treated samples shows that the heat of solution decreases as the result of heat treatment; this can be due only to increased crystallinity of the polymer. The increase of crystallinity is less in the sample heated in air than in the sample heated in water.



Rotation x-ray patterns of original (a) and milled (b) capron cord.

The data in the Table show that the decrease of the heat of solution produced by the action of boiling water differs for two fiber samples (Nos 2 and 4), whereas it is the same for samples heated in air. Since the effects of heat on the original and stretched samples are the same (the heat of solution is decreased to the same extent when the samples are heated in air), it follows that the difference between the heats of solution of Samples Nos 2 and 4 must be due to differences in the plasticizing effect of water. This hypothesis is confirmed by data on the sorption of water by capron fibers at high vapor pressures [3]. The dependence of hygroscopicity on the degree of orientation of the polymer is especially prominent in that region. According to those data, the difference between the sorption capacities of stretched and unstretched fibers in the saturation region is 50%. In our case the difference between the changes in the heats of solution is only 0.77 cal/g, or only 25% of 2.81 kcal/g. which is the total difference between the heats of solution of Samples 1 and 2. The discrepancy between the sorption and the calorimetric data is easily explained if it is remembered that our original cord sample had already been stretched during manufacture of the fiber, and that the treatment was carried out at a high temperature, when the hygroscopicity is lower.

Effect of Different Treatments on the Heat of Solution of Capron Fibers in 95% Formic Acid

Sample No.	Treatment	Heat of solution	Deviation from original	
			cal/g	%
1	Original sample (standard cord)	10.35	0	0
2	Heated 3 hrs in boiling water, not stretched	7.54	-2.81	27
3	" " " air at 100°, not stretched	9.07	-1.28	12.5
4	Stretched under 80% breaking load and then heated for 3 hrs in boiling water	8.31	-2.04	20
5	The same, with subsequent heating at 100° for 3 hrs in air	9.11	-1.24	12
6	The same, left without heating for 6 days	10.35	0	0
7	Repeated extension (to failure)	10.62	+0.27	2.6
8	Milling for 1 hour at 20°	12.87	+2.52	24.5

Thus, if capron cord is heated, especially in presence of water, its heat of solution in formic acid is decreased considerably; this indicates an increase of the crystallinity of the polymer. Naturally, this lowers the elasticity of the fiber and the performance characteristics of the cord deteriorate.

Samples Nos 6 and 7 were subjected to mechanical action only, without heat. Sample No. 6 was in a stretched state on the frame for six days. Sample No. 7 was subjected to repeated cyclic extension to failure. The experimental data show that there is no significant difference between the heats of solution of the original and the fatigued samples. There are two possible explanations of this experimental fact. The first is, that two opposing factors are mutually compensated. On the one hand, extension of the fiber decreases the flexibility of the polymer chains and therefore loosens the polymer structure [4], so that intermolecular forces are weakened and the heat of solution increases. On the other hand, extension may cause the chains to assume certain configurations which are advantageous from the energy aspect, which would lead to local increases of the structural density, increases of intermolecular forces, and therefore a decrease of the heat of solution. If the influence of the two factors balances out, the heat effect may remain unchanged. However, the probability of such compensation is very low.

However, there is another possible explanation. If the applied mechanical force causes tension in the molecular chains which is considerably less than the intermolecular forces, the molecular structure of the fiber may not undergo any changes, so that the heat of solution remains unaltered. In this case mechanical treatment, in contrast to heat treatment, has no effect on the microstructure of the capron cord. Fiber breakdown as the result of fatigue, on the other hand, probably occurs as the result of the presence of macroscopic defects, i.e., defects considerably larger than the elements of the molecular structure.

It is interesting to note that the heat of solution of the "milled" sample is considerably higher (by 24.5%)

than that of the original sample. This leads to the conclusion that milling results in a considerable decrease of polymer crystallinity. This is confirmed by the x-ray pattern of the milled cord, in which the interference rings are clearly seen to be diffuse. Hence the increase of the heat of solution of the "milled" sample, caused by decrease in the crystallinity of the capron fiber, is fully consistent with our views concerning the influence of the phase state of polycaprolactam on the heat of solution.

SUMMARY

1. The heats of solution of capron cord fibers subjected to different treatments have been determined.
2. Heat treatment of capron fibers increases their crystallinity; this effect is especially pronounced after heat treatment in water, because of its plasticizing action.
3. Stretch treatment does not affect the changes of fiber crystallinity caused by heating, but it weakens the plasticizing action of water.
4. Purely mechanical treatment does not alter the heat of solution of capron cord, and therefore does not alter its crystallinity.
5. Fatigue failure of cord fibers is probably due to the presence of macroscopic defects which develop in the course of fatigue.

The authors are deeply grateful to N. V. Mikhailov and E. Z. Fainberg for the opportunity of carrying out these experiments.

LITERATURE CITED

- [1] N. V. Mikhailov and E. Z. Fainberg, *Colloid J.* 18, 315 (1956).*
- [2] N. V. Mikhailov and E. Z. Fainberg, *Colloid J.* 18, 44 (1956); N. V. Mikhailov, E. Z. Fainberg, and S. M. Skuratov, *Colloid J.* 15, 271 (1953). *
- [3] E. S. Fainberg, Dissertation (1956). **
- [4] V. A. Kargin and T. V. Gatovskaya, *Proc. Acad. Sci. USSR* 100, No. 1, 105 (1955).

The L. Ia. Karpov Institute of Physical Chemistry
Scientific Research Institute of the Tire Industry
Moscow

Received October 5, 1957

*Original Russian pagination. See C. B. Translation.

**In Russian.

INFLUENCE OF THE DISPERSE PHASE ON THE RESULTS OF HYDROGEN-ION
ACTIVITY DETERMINATIONS IN SALT SOLUTIONS

R. V. Voitsekhovskii and A. M. Vovnenko

In determinations of the activities of hydrogen and other ions the results obtained differ in the series: ultrafiltrate, sol, residue from ultrafiltration; or: centrifugate (filtrate), suspension, precipitate [1-3]. The pH difference between the dispersion medium and the suspension may sometimes reach several units (Table 1).

TABLE 1
Values of Suspension and Dispersion Medium pH
(based on Wiegner and Pallmann's data [1])

Disperse phases of aqueous suspensions	pH of suspension	pH of dispersion medium	Suspension effect $\text{pH}_0 - \text{pH}$
H-permutite	4,27	4,63	+0,36
H-clay	4,47	5,64	+1,17
Palmitic acid	4,50	5,11	+0,61
Sulfur (Raffo)	4,30	5,48	+1,18
Acid blood char	4,12	6,30	+2,18
$\text{Ca}(\text{HPO}_4)_2$	6,21	6,52	+0,31
Aluminum hydroxide, positively charged	5,11	5,82	+0,71
Ca-permutite	8,65	7,94	-0,71
$\text{Ca}_3(\text{PO}_4)_2$	8,62	7,74	-0,88
Ferric hydroxide, negatively charged	8,57	8,33	-0,24
Aluminum hydroxide, negatively charged	8,88	8,35	-0,53
Ca-soil	7,58	7,34	-0,24

This phenomenon, which is described in the literature as the Wiegner or the Pallmann suspension sol effect, has been studied little as yet. The view has been put forward that it can be explained in terms of the Donnan theory of membrane equilibrium [2].

If this theory is applied to the distribution of ions between the precipitate and the clear liquid (filtrate or ultrafiltrate)

$$ka = k_0 a_0; \quad (1)$$

$$ha = h_0 a_0, \quad (2)$$

then the result, and the electroneutrality principle

$$e\zeta' + k + h = a + oh; \quad (3)$$

$$a_0 + oh_0 = k_0 + h_0, \quad (4)$$

can be used to derive an equation for the dependence of the suspension effect on the concentration of the suspension, and the magnitude and sign of the charge on its particles:

$$\frac{e\xi'}{k+h} + 1 = \frac{a+oh}{a_0+oh_0} \cdot \frac{a}{a_0}, \quad (5)$$

where h , oh , a , and k are the respective concentrations of the hydrogen ions, hydroxyl ions, anions, and cations in the suspension or the precipitate; h_0 , oh_0 , a_0 , k_0 are the corresponding concentrations in the dispersion medium; ξ , ξ' are the concentration of the electronegative and electropositive particles respectively in the suspension; e is the average electric charge on the particles. If we neglect the values of oh and oh_0 , which are small in absolute magnitude as compared with a and a_0 in a medium of $pH < 7$, we obtain the following, after transformation:

$$h - h_0 = \left(1 - \sqrt{\frac{e \cdot \xi'}{k+h} + 1}\right)h. \quad (6)$$

The dependence of the suspension effect on the concentration and charge of the electronegative particles is derived analogously

$$h - h_0 = -\left(1 - \sqrt{\frac{e \cdot \xi'}{a+oh} + 1}\right)h. \quad (7)$$

Equation (7) shows that the positive suspension effect $h-h_0$ (increase of hydrogen-ion activity under the influence of the electronegative particles in the suspension) increases with the concentration of the suspension (ξ) and with the particle charge (e), and decreases with increases of the electrolyte concentration (a) and of pH of the dispersion medium.

In some instances experimental data have shown that this relationship is qualitatively valid. For example, Gatovskaya and Vasil'ev [3] showed with the aid of a glass electrode that after dialysis of tungsten trioxide, titanium dioxide, and vanadium pentoxide sols the hydrogen ion activity increases in the series: ultrafiltrate, sol, residue from ultrafiltration.

In experiments with thoroughly-dialyzed iron sol the hydrogen-ion activity decreases in the same series, whereas the activity of chloride ions, which are the counter ions in this instance, increases [4]. The magnitude of the suspension effect increases with the concentration of the suspension [1].

However, facts which contradict Equations (6) and (7) are also known. For example, Table 1 shows that the negatively charged hydroxides of iron and aluminum decrease hydrogen-ion activity ($pH > pH_0$), whereas positively charged aluminum hydroxide has the opposite effect ($pH < pH_0$). For elucidation of the causes of these contradictions, and for a more detailed study of the effect, we investigated the dependence of the suspension effect on pH , electrolyte concentration in the dispersion medium, nature of the disperse phase, and others factors.

The present communication contains the results of determinations of hydrogen-ion concentration, performed with the aid of the quinhydrone electrode. The following experimental procedure was used. A definite hydrogen-ion concentration was established in the suspension, containing 14% of the disperse phase, by means of HCl and NaOH solutions. The suspension was first acidified to $pH \sim 0.5$; alkali was then added stepwise, the suspension effect was determined, and variations of this effect with the pH of the dispersion medium were studied in the same suspension sample.

The effect of the suspension concentration on the suspension effect was studied by a similar procedure. In this case calculated amounts of dry salt were added successively to the suspension sample. The pH determinations were performed in a calibrated centrifuge tube 8-10 ml in capacity. The sample with quinhydrone was centrifuged from 3 to 5 minutes, according to the stability of the suspension. The pH determinations were performed with the platinum electrode in two different positions. In one instance the platinum electrode was located above the precipitate, and in the other, it was immersed in the precipitate to a depth of 5 mm from the boundary (Fig. 1).

The results of e.m.f. determinations for the cell: calomel electrode - quinhydrone electrode were used for

calculation of the change in potential of the quinhydrone electrode, in millivolts, when its position was altered:

$$\Delta E = E - E_0,$$

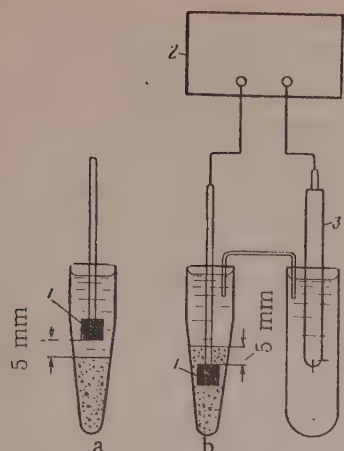


Fig. 1. Determination of suspension pH by means of the quinhydrone electrode:

1) quinhydrone electrode; 2) potentiometer; 3) calomel electrode.

for the system $\text{Fe}_2\text{O}_3-\text{H}_2\text{O}$ in the pH ranges from 0.7 and 2.1, and 7.7 to 8.6; for the system $\text{Al}_2\text{O}_3-\text{H}_2\text{O}$ in the pH ranges from 4.25 to 6.8 and 8.25 to 9.4; and for the system SiO_2 -4.5 M NaCl solution in the pH range from 5.45 to 9.1 (Table 2).

Under these conditions the suspension effect must be taken into account in determinations of suspension pH.

Comparison of the suspension effects for the same disperse phase but with different dispersion media shows that the variations of the suspension effect with pH for water and for 4.5 M NaCl solution are qualitatively similar. A considerable suspension effect is also observed in concentrated electrolyte solutions. For estimation of the reproducibility of the results, three series of determinations of the suspension effect were performed with the systems: $\text{Al}_2\text{O}_3-\text{H}_2\text{O}$ and Al_2O_3 -4.5 M NaCl solution. The suspensions were prepared separately for each series of determinations. Fig. 2, a and b, shows that there is some scattering of the experimental points, both for the aqueous suspension and for the suspension in concentrated NaCl solution. Results of experiments on the influence of electrolyte concentration showed that with increase of the sodium chloride concentration in the dispersion medium an appreciable decrease of the suspension effect is observed only in some isolated instances; namely, for Fe_2O_3 suspensions at pH 2.0, and for Al_2O_3 suspensions at pH 4.2, while for the other suspensions the pH values do not conform to this relationship (Table 3).

As has already been stated, the suspension effect depends strongly on the nature of the disperse phase; as regards the nature of the electrolyte used in concentrated solution as the dispersion medium, the relationship remains qualitatively unchanged. Replacement of an electrolyte with a univalent cation by one with a bivalent cation (3.5 M MgCl_2 solution) (Table 4) had a somewhat greater effect.

The theory of the membrane equilibrium leads to a definite relationship between the charge of the disperse phase and the sign of the suspension effect. This relationship was not confirmed by our experiments. In the case of iron and aluminum oxides the sign of the charge changes at pH ~ 8.0 [5], whereas the sign of the suspension effect changes in the pH range between 3.1 and 4.5. It is known that the membrane-equilibrium theory is based on the assumption of thermodynamic equilibrium of the components in the system in question. To test how far this assumption may be extended to the systems under investigation, we carried out experiments to determine how the sequence in which the pH becomes established influences the suspension effect. The suspension effect was determined for different sequences of pH variation: from the acid to the alkaline region, from the alkaline to the acid region, and from a neutral to an acid medium.

where E_0 is the potential of the quinhydrone electrode in the dispersion medium (position a), and E is its potential in the precipitate (position b, Fig. 1).

The experiments showed that the magnitude and sign of the suspension effect vary with the nature of the disperse phase, the pH of the dispersion medium, and the electrolyte concentration in the latter (Table 2).

In the case of ferric oxide and sulfur the suspension effect changes with increase of pH from positive to negative values, while in the case of alumina, silica, and silicon the reverse is true.

It was found that conditions may be established, dependent on the nature of the disperse phase and the pH of the dispersion medium, in which the suspended disperse phase has very little or no influence on the potential of the quinhydrone electrode. This suggests that under such conditions hydrogen-ion activities of suspensions may be determined without separation of the suspended particles. In other cases the disperse phase has a considerable influence on the potential of the quinhydrone electrode in certain pH ranges. This is true

TABLE 2

Variations of Suspension Effect with pH of the Dispersion Medium and Nature of the Disperse Phase

Composition of suspension: disperse phase - dispersion medium		Suspension effect ΔE in mv, and pH of dispersion medium									
Fe ₂ O ₃ - H ₂ O	-	23,0 0,7	23,0 1,0	16,0 1,3	13,5 2,1	-	10,0 4,3	-	-	-36,0 7,7	-
Fe ₂ O ₃ -NaCl (4,5 M)	-	-	13,0 1,2	11,0 1,7	-4,0 2,8	-6,0 3,3	-	-10,0 5,5	-	-43,5 7,7	-47,0 8,0
Flowers of sulfur - H ₂ O	-	1,0 0,9	0 1,05	-1,0 1,38	-2,8 2,55	-3,2 3,2	-3,0 4,0	-	-3,0 6,9	-	-4,2 8,36
Flowers of sulfur - NaCl (4,5 M)	-	-	2,2 1,24	-	0 2,29	-4,0 3,5	-7,0 4,87	-	-6,0 6,5	-	-3,7 8,18
Al ₂ O ₃ - H ₂ O	-	1,2 0,64	-2,5 0,85	-10,0 1,1	-9,0 2,2	3,0 3,63	14,0 4,25	15,0 5,8	14,0 6,8	3,0 7,3	-33,5 8,25
Al ₂ O ₃ -NaCl (4,5 M)	-	-4,0 0,8	-11,0 1,4	-	-	-2,0 3,75	5,0 4,3	22,5 6,0	-	33,0 7,4	18,0 7,9
SiO ₂ - H ₂ O	-	-3,0 0,8	-1,0 1,1	-2,0 1,57	-3,0 2,62	2,0 3,35	7,0 4,0	18,5 5,6	35,0 6,5	29,5 7,4	16,5 7,9
SiO ₂ -NaCl (4,5 M)	-	-3,0 0,45	-2,0 1,2	-	-2,0 2,75	4,0 3,56	10,0 4,35	27,0 5,45	24,0 6,75	22,0 7,0	25,0 7,9
Si - H ₂ O	-	-8,0 0,7	-3,2 1,1	-5,0 1,5	-4,2 2,2	-3,5 3,5	-	-	-11,0 6,4	-23,0 7,2	-
Si - NaCl (4,5 M)	-	-4,2 1,2	-	-5,0 2,4	-3,0 3,5	-6,0 4,9	-	-	-10,2 7,0	2,8 8,8	-

TABLE 3

Variation of the Suspension Effect with Electrolyte Concentration in the Dispersion Medium

Composition of suspension: disperse phase-dispersion medium	Suspension effect ΔE in mv, and electrolyte concentra- tion k in moles/liter									
$\text{Fe}_2\text{O}_3 - \text{NaCl}$ (pH 2,0)	ΔE	44,5	6,0	—	4,0	0	-4,0	-8,0	-2,0	
	k	0	0,1	—	1,0	2,0	3,0	4,0	4,5	
$\text{Fe}_2\text{O}_3 - \text{NaCl}$ (pH 7,6)	ΔE	-16,9	-37,5	—	-29,0	-23,4	-23,5	-16,0	-16,0	
	k	0	0,1	—	1,0	2,0	3,0	4,0	4,5	
$\text{Al}_2\text{O}_3 - \text{NaCl}$ (pH 3,8)	ΔE	3,0	3,0	0	-1,0	-1,0	-1,5	-2,0	-2,5	
	k	0	0,1	0,5	1,0	2,0	3,0	4,0	4,5	
$\text{Al}_2\text{O}_3 - \text{MgCl}_2$ (pH 4,2)	ΔE	19,0	14,0	10,0	4,0	-3,0	-5,5	-2,0	—	
	k	0	0,1	0,5	1,0	2,0	3,0	3,5	—	
$\text{SiO}_2 - \text{NaCl}$ (pH 2,4)	ΔE	-2,5	-2,5	-2,0	-2,0	-2,0	-2,0	-2,0	-2,0	
	k	0	0,1	0,5	1,0	2,0	3,0	4,0	4,5	
Flowers NaCl (pH 0,7) of sulfur	ΔE	0	0	1,5	1,2	1,0	1,0	1,0	0,5	
	k	—	0,1	0,5	1,0	2,0	3,0	4,0	4,5	

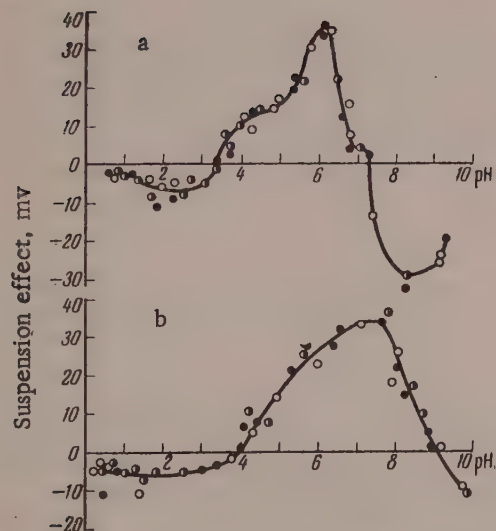


Fig. 2. Variation of the suspension effect with the pH of the dispersion medium for the systems: $\text{Al}_2\text{O}_3 - \text{H}_2\text{O}$ (a) and $\text{Al}_2\text{O}_3 - 4.5 \text{ M NaCl}$ solution (b).

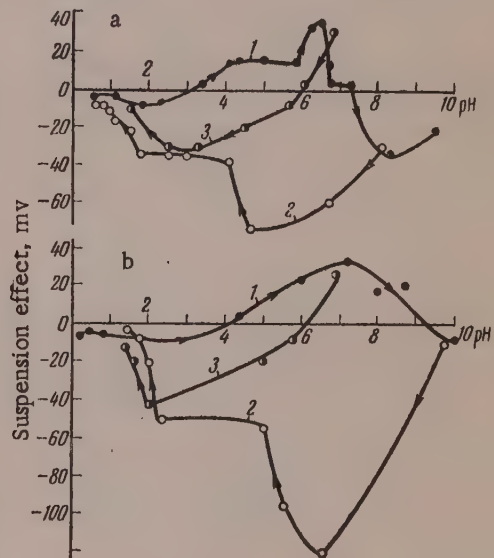


Fig. 3. Variation of the suspension effect with the pH of the dispersion medium for systems: $\text{Al}_2\text{O}_3 - \text{H}_2\text{O}$ (a) and $\text{Al}_2\text{O}_3 - 4.5 \text{ M NaCl}$ solution (b), with different sequences of acidity variation.

If an Al_2O_3 suspension is first acidified, and alkali is then gradually added, then the suspension effect is negative in the region of low pH, whereas it is positive in the pH range from 3.3 to 7.3 for the system $\text{Al}_2\text{O}_3 - \text{H}_2\text{O}$ and from 4.0 to 9.3 for the system $\text{Al}_2\text{O}_3 - 4.5 \text{ M NaCl}$ solution.

In a weakly alkaline medium the suspension effect becomes negative again (Fig. 3, Curve 1).

When the pH is changed in the reverse direction, from the alkaline to the acid region, the curve representing the relationship between the suspension effect and pH follows a different course, without a region of positive values (Fig. 3, Curve 2). An interesting feature is the existence of large negative suspension effects, with maxima at pH 4.8 for the system $\text{Al}_2\text{O}_3 - \text{H}_2\text{O}$, and at pH 6.6 for the system $\text{Al}_2\text{O}_3 - 4.5 \text{ M NaCl}$ solution. The points on the

TABLE 4

Variations of the Suspension Effect with pH and Composition of the Dispersion Medium

Composition of suspension: disperse phase-dispersing medium		Suspension effect ΔE in mv, and pH of dispersion medium									
Al ₂ O ₃ — H ₂ O	—	-1,0 0,95	-2,5 1,1	-10,5 -1,8	-9,0 2,2	3,0 3,63	36,5 7,3	-33,5 8,25	—	-20,0 9,4	—
Al ₂ O ₃ — LiCl (4,5 M)	ΔE pH	-9,0 0,23	-5,0 0,70	-3,0 1,1	-8,0 1,62	-11,0 2,06	1,0 3,65	21,5 4,12	-	38,0 7,4	6,0 8,3
Al ₂ O ₃ — NaCl (4,5 M)	ΔE pH	-5,0 0,2	-4,0 0,8	-	-11,0 1,4	-	-2,0 3,75	5,0 4,3	22,5 6,0	33,0 7,1	9,5 7,9
Al ₂ O ₃ — Na ₂ SO ₄ (1 M)	ΔE pH	-	-	-2,5 1,1	-2,0 1,45	-4,0 1,95	-2,5 3,9	8,5 4,45	-	-	—
Al ₂ O ₃ — MgCl ₂ (3,5 M)	ΔE pH	-9,5 0,1	-4,5 0,5	-2,0 1,45	-	-43,5 3,9	-72,0 2,2	-2,0 4,45	-18,0 4,95	26,0 6,5	-14,0 7,0

different curves coincide in the acid and the weakly alkaline regions. The curve for the suspension effect as a function of pH, determined in experiments with suspensions the pH of which was changed from the neutral point to the acid range (Fig. 3, Curve 3), occupies an intermediate position between Curves 1 and 2. These experiments demonstrate the irreversibility of the suspension effect; this is evidently due to the nonequilibrium state of the system.

Observations over periods of time showed that the positive or negative suspension effects, dependent on the order of acidification, persist for an indefinite time in the region close to neutrality. This indicates that the electric charges acquired by the suspension particles have a high potential barrier. The fact that the points on the curves coincide in the acid region suggests that the potential barrier is surmounted more easily by mobile hydrogen ions.

All the foregoing considerations show that the definite relationship between the suspension effect and the charge of the disperse phase which follows from the theory of membrane equilibrium is inadequate for even a qualitative description of all the variations of the magnitude and sign of the suspension effect. Apart from the nonuniform distribution of the ions between the precipitate and the clear liquid, the suspension effect is evidently strongly influenced by certain other factors. It is probably necessary to take into consideration the nature of the ions constituting the electrical double layer, their mobilities, and the associated value of the adsorption potential, which varies with the degree of saturation of the adsorbent in question.

It is known that under certain conditions the disperse phase firmly retains a previously-acquired charge during various changes in the composition of the dispersion medium [6].

In the light of these views the following qualitative description may be offered for the observed variations of the suspension effects of aluminum and iron oxides with changes of pH. According to published data, Al₂O₃ and Fe₂O₃ are positively charged in acid media. According to Equation (6), they should exhibit a negative suspension effect in that region. In reality this is true for Al₂O₃ only; the suspension effect is positive in the pH region from 0.7 to 0.3 for the system Fe₂O₃—H₂O and from 1.2 to 3.3 for the system Fe₂O₃—4.5 M NaCl solution (Table 2).

The deviation of the suspension effect of ferric oxide from Equation (6) must evidently be attributed to the nature of the ions in the inner electrical layer.

In the case of ferric oxide these are the very mobile positively charged hydrogen ions [7], whereas the positive charge of aluminum oxide is due to Al(OH)₂⁺, firmly bound to the particles [8]. In the former case the hydrogen ions of the inner layer of ferric oxide have a direct influence on the

adsorbent in an acid medium. A diametrically opposite situation arises at higher pH values. With a considerable decrease of the hydrogen-ion concentration their content in the inner electrical layer of ferric oxide decreases correspondingly. The surface of the ferric oxide retains hydrogen ions at the most active points of higher adsorption potential. Positively charged ferric oxide influences the potential of the quinhydrone electrode in accordance with the membrane-equilibrium mechanism in the pH range from 4.3 to 8.6 for the system $\text{Fe}_2\text{O}_3-\text{H}_2\text{O}$ and from 2.8 to 8.6 for the system $\text{Fe}_2\text{O}_3-4.5 \text{ M NaCl}$ solution (Table 2).

The positive electric charge acquired by aluminum oxide in the region of low pH is retained, but it evidently becomes excessive in regions of higher pH 3.63 for the system $\text{Al}_2\text{O}_3-\text{H}_2\text{O}$ and ~4.3 for the system $\text{Al}_2\text{O}_3-4.5 \text{ M NaCl}$ solution (Table 2); in consequence under these new conditions the aluminum oxide particles become capable of accepting electrons when in contact with the electrode, and hence of raising the potential of the quinhydrone electrode. This is manifested as a considerable positive suspension effect. When aluminum oxide is brought into an alkaline medium, of pH~8.25 for the system $\text{Al}_2\text{O}_3-\text{H}_2\text{O}$ and ~9.1 for the system $\text{Al}_2\text{O}_3-4.5 \text{ M NaCl}$ solution, the suspension effect of aluminum oxide becomes positive again (Table 2). Although the positive charge of aluminum oxide is replaced by a negative charge in an alkaline medium, according to the theory of membrane equilibrium the suspension effect should be positive. This change is probably due to the predominant effect of the highly mobile negative hydroxyl ions, adsorbed by the aluminum oxide in the alkaline medium, which have a direct influence on the potential of the quinhydrone electrode.

The return of an aluminum oxide suspension from high to low pH by progressive acidification is accompanied by a negative suspension effect along the entire curve. This effect may be attributed to hysteresis of the electric charge of the particles in the aluminum oxide suspension during acidification. The negative charge acquired by Al_2O_3 at high pH is retained on acidification, but in consequence of the discrepancy which arises between the particle charge and the medium the particles in the suspension become capable of giving up electrons at the instant when the electrode is immersed.

Therefore the explanation of the contradictions found in relation to the suspension effect in the literature is that the authors concerned did not make due allowance for the influence of the medium, the nature of the ions, and hysteresis effects in the particle charges.

Determinations of the suspension effect can undoubtedly be used in studies of the structure of the electrical double layer in disperse systems.

SUMMARY

1. The magnitude and sign of the suspension effect depend on the nature of the disperse phase, the pH, and the concentrations of the suspension and the electrolyte in the dispersion medium.
2. The suspension effect is also associated with hysteresis phenomena in the charge of the disperse-phase particles, and it is therefore influenced by the method used for preparation of the suspensions.

LITERATURE CITED

- [1] H. Pallmann, Kolloid. Beihefte 30, 334 (1930); G. Wiegner, Kolloid.-Z. 51, 49 (1930).
- [2] B. P. Nikol'skii, J. Phys. Chem. 5, 266 (1934).
- [3] T. V. Gatovskaya and P. S. Vasil'ev, J. Phys. Chem. 7, 697 (1936).
- [4] P. S. Vasil'ev, T. V. Gatovskaya, and A. I. Rabinovich, J. Phys. Chem. 7, 674 (1936).
- [5] I. M. Kolthoff and E. B. Sandell, Quantitative Analysis (1948) [Russian translation].
- [6] V. M. Gortikov, Colloid J. 2, 429 (1936).
- [7] A. I. Rabinovich, V. A. Kargin, Z. phys. Chem. 133, 203 (1928).
- [8] V. A. Kargin and N. A. Organdzhanova, J. Phys. Chem. 10, 782 (1937).

THE SECONDARY (DIFFUSIONAL) ELECTRICAL DOUBLE LAYER

S. S. Dukhin and B. V. Deriagin

A secondary electrical double layer arises at a mobile interface; in view of the great practical importance of flotation, we shall consider the surface of a moving bubble as an example of such an interface.

Let Γ^+ and Γ^- represent the adsorption of positive and negative ions respectively in the surface layer, and let v_t be the velocity distribution along the surface. Movement of the surface is accompanied by convective transfer of positive and negative ions, the convective-flow densities of which, $\Gamma^+ v_t$ and $\Gamma^- v_t$, respectively, vary along the surface. The difference between the ions entering and leaving the double layer at each region of the surface, consequent upon the convective flow of the ions, must be balanced by the corresponding component of the volume flow of the ions, which serves in this instance as the source or receiver of ions in convective flow

$$\operatorname{div}_s \Gamma^+ v_t = j_n^+, \quad \operatorname{div}_s \Gamma^- v_t = j_n^-. \quad (1)$$

The normal components of the ion streams j_n^+ and j_n^- are determined by diffusion of the ions and their migration in an electric field; hence, writing in full the right-hand sides of Equations (1), we have

$$\operatorname{div}_s \Gamma^+ v_t = j_n^+ = \left(-D^+ \frac{\partial c^+}{\partial r} + \frac{F}{RT} D^+ z^+ c^+ E_{1r} \right)_a, \quad (2)$$

$$\operatorname{div}_s \Gamma^- v_t = j_n^- = \left(-D^- \frac{\partial c^-}{\partial r} - \frac{F}{RT} D^- z^- c^- E_{1r} \right)_a, \quad (3)$$

where \vec{E}_1 is the field intensity; F is the Faraday number; T is the absolute temperature; R is the gas constant; c^+ and c^- , D^+ and D^- , z^+ and z^- respectively are the concentrations, diffusion coefficients, and electrovalences of the positive and negative ions in a binary electrolyte; a is the bubble radius. With a high content of ions, the charges of the positive and negative ions should largely balance out*, so that we may disregard the relatively negligible concentration of electrically-uncompensated ions, and write the conditions for electroneutrality of the solution and the surface

$$z^+ c^+ - z^- c^- = 0, \quad z^+ \Gamma^+ - z^- \Gamma^- = 0, \quad (4)$$

and we can then introduce the volume molar concentration c and the surface molar concentration Γ

$$c = c^+ / z^+ = c^- / z^-, \quad \Gamma = \Gamma^+ / z^+ = \Gamma^- / z^-.$$

With the aid of Conditions (4) it is easy to find the boundary conditions for $c(r, \theta)$ from Equations (2) and (3), and to determine the intensity of the electric field at the surface.

* If the reverse is assumed, then at high ionic concentrations there would be enormous electric fields, which would eliminate themselves spontaneously owing to the conductivity of the electrolyte.

To determine the electric field* within the volume of the electrolyte we must use the continuity equations for the volume, which become considerably simplified in electroneutrality, and become [1]:

$$D_{eff} \Delta c = \vec{v} \text{ grad } c, \quad (5)$$

$$\frac{F}{RT} (z^+ D^+ + z^- D^-) c \vec{E} + (D^+ - D^-) \text{ grad } c = \frac{\vec{i}}{F z^+ z^-}, \quad (6)$$

where D_{eff} is the effective diffusion coefficient [1]; $\vec{I}(r, \theta)$ is the electric current density. It can be shown that under the conditions of complete electroneutrality of the surface and absence of current at infinity $\vec{I}(r, \theta)$ is everywhere zero, and it follows that the electric field is determined by the molar-concentration distribution

$$\vec{E}(r, \theta) = \frac{RT}{F} \frac{D^+ - D^-}{z^+ D^+ + z^- D^-} \text{ grad } \ln c. \quad (7)$$

The order of magnitude of the Peclet group $Pe = av_0/D_{eff}$ for freely ascending bubbles 1-2 mm in diameter is 10^5 - 10^6 , and therefore a thin diffusional boundary layer of thickness $\delta \sim a/Pe^{1/2} \sim 10^{-3}a$, is formed at the bubble surface. The concentration gradient and electric field are localized within the diffusional boundary layer. When the electric field has been found, it is possible to determine the density distribution of the uncompensated electric charges within the volume of the solution, $\rho_v = (z^+ c^+ - z^- c^-) F$, and at the bubble surface $\sigma_s = (z^+ c^+ - z^- c^-) F$. σ_s is determined from the boundary condition for \vec{E} undergoing rupture at the boundary of two dielectrics, $(\epsilon_1 E_{1r} - \epsilon_2 E_{2r}) = 4\pi \sigma_s$, where ϵ_2 is the dielectric constant of air and E_r is the electric field intensity in air. The Poisson equation $\text{div } E_i = \frac{4\pi}{\epsilon_1} (z^+ c^+ - z^- c^-) F$ can also be used to find ρ_v ; from the mean value of this for the thickness of the layer in which the volume charges are distributed we can find the total volume charge σ_v per unit bubble surface. Calculation shows that any region of the bubble surface and the adjacent solution volume are electrically neutral as a whole: $\sigma_s + \sigma_v = 0$. It is therefore convenient to introduce the concept of an electrically neutral double layer; one layer of this is the bubble surface, and the other, a region of the solution adjacent to this surface, several δ thick. In distinction from the ordinary diffuse double layer, formed at a stationary interface owing to differences in the adsorptional properties of the ions, this double layer is formed only during the motion of an interface, owing to differences between the diffusion coefficients of the ions, and it may be termed the diffusional double layer. Just as in the usual double layer the outer layer is diffuse because of the thermal motion of the ions, in the double layer under consideration the charge density in the outer layer gradually diminishes in a direction away from the surface as the result of diffusion, and it may be conveniently termed the diffusional layer. Similarly to an equilibrium double layer, the two layers of the diffusional double layer constitute a single system of charges in the sense that any change of charge distribution in one of the layers must inevitably be accompanied by a change of charge distribution in the other. The diffusional double layer may be regarded as being formed in the motion of an ordinary double layer, and it can therefore be described as secondary.

SUMMARY

1. If the interface between two media, at least one of which is an electrolyte, is mobile, then in consequence of the difference between the diffusion coefficients of the ions there arises, in addition to the usual (diffuse) electrical double layer formed as the result of interaction of diffusion and ionic migration in the electric field, a secondary (diffusional) electrical double layer, formed as the result of interaction of processes of convective diffusion and ionic migration in the electric field.

2. The charge of the inner layer of the secondary double layer is determined by deviations from the electrical neutrality of the ordinary double layer; the charge of the outer layer, equal to it in magnitude but opposite in sign, is located in the electrolyte layer adjacent to the interface; the thickness of this layer is of the same order of magnitude as the thickness of the diffusional boundary layer.

* If the absence of an electric field is postulated, i.e., if it is assumed that $E_T = 0$, Equations (2) and (3) become incompatible with the electroneutrality Conditions (4). This means that the electric field arises owing to the necessity to maintain approximate electroneutrality of the solution; it is directed so as to hinder the motion of rapidly-diffusing ions and to accelerate slowly-diffusing ions, so that the flows of positive and negative charges on the bubble surface become equalized, ensuring its electroneutrality.

LITERATURE CITED

- [1] V. G. Levich, Physicochemical Hydrodynamics [in Russian] (Izd. AN SSSR, 1952), p. 191.

The Caucasian Institute of Mineral
Raw Materials

Received May 12, 1958

FACTORS DETERMINING THE STRUCTUROMECHANICAL PROPERTIES OF VISCOSE SOLUTIONS

N. N. Zav'ialova and N. V. Mikhailov

Work on improvement of methods of viscose production and fiber properties is being carried on in several directions: by increase of the cellulose concentration in the viscose solution [1], by increase of the degree of polymerization of cellulose in the fiber [2], and by searches for new extrusion conditions [3]. It should be noted that most work in this field relates to viscose solutions of high viscosities, 800-1000 poises and over. The production of fibers from such solutions is difficult because of the hight viscosities.

With the aim of reducing the viscosity of spinning viscoses, we had performed investigations of the influence of the following factors on the viscosity of viscose solutions: NaOH/cellulose ratio [4], degree of xanthation [5], temperature [5], and various additives. Increase of the NaOH/cellulose ratio from 0.5 to 1 lowers the viscosity 2.5- to 3-fold. Increase of temperature from 20 to 50° lowers the viscosity 2.5-fold. With increase of the degree of xanthation (γ_{CS_2}) from 35 to 65, the viscosity of the xanthate falls more than 1.5-fold.

The present paper, which represents a continuation of the earlier work, contains the results of studies of the structuromechanical properties of viscose solutions of different α -cellulose concentrations, NaOH/ cellulose ratios, and ripeness, which may be of interest for production purposes.

The aim of the work was to find means of producing fibers with improved properties from such solutions.

For this purpose a study was made of the structuromechanical properties of viscoses of different ripeness, with cellulose concentrations of 10 and 12%, and with NaOH/ cellulose ratios of 1.06 and 0.55 in the first case, and 0.53 and 0.86 in the second.

The structure of the viscose solutions was studied with the aid of a coaxial rotational elastoviscosimeter of the Shvedov type, as used by Rebinder et al. [6]. In such determinations the course of deformation in time, under constant torque applied by means of a twisted thread, is usually investigated [6, 7].

These determinations yielded curves for the relative shear deformation as a function of time for all the above-named solutions, at different shear stresses.

The relative shear deformation $\epsilon = 2R^2 \omega / (R^2 - r^2)$, where R and r are the radii of the inner and outer cylinders, and ω is the angular deformation in radians.

Some of these curves for 10 and 12% viscose solutions of different ripeness are given in Fig. 1. The other curves are not shown, as they are similar in character. In nearly every instance the deformation was a linear function of time at the shear stresses used, i.e., the deformation developed at a constant rate throughout each experiment. Only in rare instances, in prolonged experiments, were there slight deviations from linearity. However, during such long periods (2 hours and over) the ripeness and therefore the structure of the viscose changes; therefore all the deformation curves are plotted for relatively short periods (up to 20 minutes).

Curves similar to these were obtained by Ivanova-Chumakova and Rebinder [7] for polyisobutylene solutions below 40% concentration, and by I. A. Dumanskii, A. V. Dumanskii, and L. V. Khailenko [8] for viscose solutions of the usual cellulose concentrations. However, these workers also obtained curves of a different type for solutions of polyisobutylene above 40% concentration and for ripe viscose solutions after 300 hours of ripening (close to coagulation); these curves were characterized by an initial sharp increase of deformation (nominal-instantaneous

elastic deformation) followed by a gradual increase of deformation until a constant rate was established. These results suggest that the solutions under investigation, characterized by curves of the first type, do not have elastic properties.

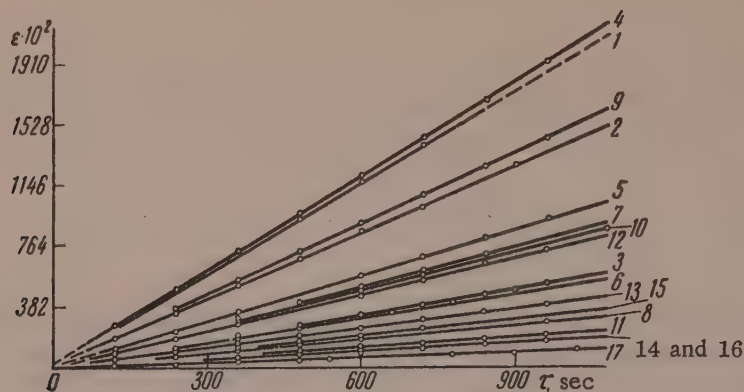


Fig. 1. Development of relative shear deformation:
10% solutions of α -cellulose: 1-3) ripeness 18 cc, $P = 3.9, 2.8$,
and 1.3 dynes/cm² respectively; 4-6) ripeness 14.65 cc,
 $P = 4.3, 2.0$, and 1.5 dynes/cm² respectively; 7,8) ripeness
7.5 cc, $P = 3.8$ and 1.35 dynes/cm².
12% solutions of α -cellulose: 9-11) ripeness 13.95 cc, $P = 8.0$,
4.6, and 1.5; 12-14) ripeness 7.5 cc, $P = 8.0, 4.0$, and 2.0;
15-17) ripeness 5.0 cc, $P = 8.2, 4.0$, and 2.1.

However, Ivanova-Chumakova and Rebinder [7] showed that if the experimental conditions are changed and larger torques (higher velocity gradients) are used, these properties can also be detected in relatively dilute polyisobutylene solutions. With the usual experimental procedure the use of large torques is difficult owing to the impossibility of observing the course of deformation. Further, they showed that at relatively small shear stresses the magnitude of the elastic deformation is very small (a few tenths of one percent). Therefore in our experiments these small elastic deformations could not be determined quantitatively.

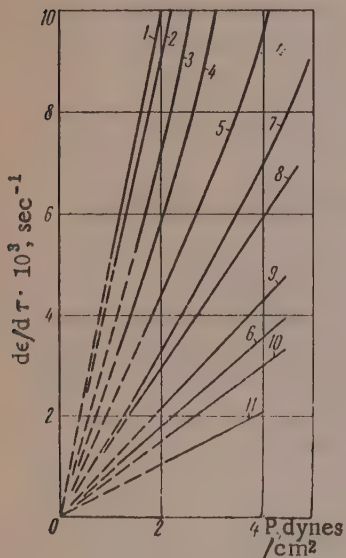


Fig. 2. Variation of $d\epsilon/d\tau$ with the shear stress P : 1-6) α -cellulose concentration 10%; 7-12) 12%.

Thus, our curves evidently do not prove the absence of elasticity in the viscose solutions studied, but merely indicate that the method is not sensitive enough in the experimental conditions used. Indeed, Fig. 1 shows that an initial intercept along the ordinate axis, corresponding to elastic deformation, is also present in our curves, but it is very small. We were therefore unable to characterize the structure of the viscose solutions in terms of the elasticity moduli. An attempt was therefore made to characterize the structomechanical properties of the solutions in terms of the flow rate and the corresponding viscosity, given by the ratio $P/(d\epsilon/d\tau)$ calculated from the curves for $d\epsilon/d\tau$ as a function of shear stress, which were in turn derived from the experimental deformation-time curves (see curves in Fig. 1). The corresponding $d\epsilon/d\tau = f(P)$ curves are presented in Fig. 2.

It must be noted that the curves for $d\epsilon/d\tau$ as a function of the shear stress P for 10 and 12% viscose solutions deviate from linearity at high shear stresses. However, this deviation is of the reverse sign in some instances. A positive deviation is to be expected owing to the commencing structural breakdown, whereas a deviation of negative sign is unexpected, and cannot be explained, as the data are inadequate. Therefore only the linear portions of the curves are given in this case.

The curves for the rate of change of the relative shear deformation as a function of the acting stress for stresses below those used in our experiments are assumed to pass through the origin (dash lines).

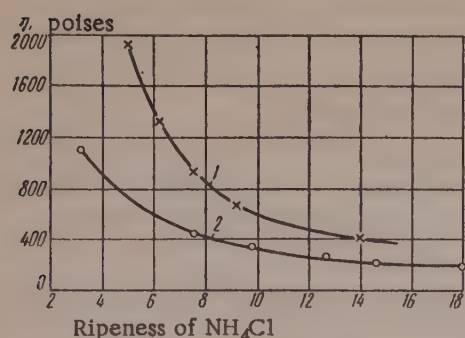


Fig. 3. Effect of viscose age on the effective viscosity $\eta' = P/(d\epsilon/d\tau)$
1) α -cellulose concentration 12%; 2) 10%

effective viscosity (η') of the viscose solutions is in good agreement with their ripeness, whereas the ball-fall viscosity of viscoses with different NaOH / cellulose ratios does not always vary consistently with the ripeness figure. Therefore the calculated effective viscosity is a more precise characteristic of the structure of viscose solutions than the ball-fall viscosity.

Increased ripeness of a viscose solutions is directly related to changes in the chemical composition of the cellulose xanthate, leading to formation of new intermolecular bonds. The density of the structural network in solution should increase in the process.

Effect of the Ripeness of Viscose Solutions on Their Structure

Curve No. in Fig. 2	Cellulose concentration, %	NaOH / cellulose ratio	Ball-fall viscosity, sec	Ripeness, cc NH_4Cl	$P/(d\epsilon/d\tau) = \eta'$
1	10	1,06	144	18	200
2	10	1,06	140	14,6	218
3	10	1,06	150	12,6	276
4	10	1,06	—	9,7	350
5	10	0,55	275	7,5	455
6	10	0,55	583	3,2	1110
7	12	0,86	387	13,9	413
8	12	0,86	480	9,2	675
9	12	0,53	680	7,5	935
10	12	0,86	615	6,2	1330
11	12	0,53	808	5,0	1920

Thus the value of η' is a measure of the structural strength of the solution, which depends on the number of intermolecular bonds; also, as will be shown later, it probably depends on changes of their strength. In some instances the ripeness of the viscose solutions has a greater influence than the ball-fall viscosity on the slope of the curves. For example, Curves 1, 2, and 3 in Fig. 2, corresponding to viscose solutions of almost the same ball-fall viscosity (144, 140, and 150 seconds) but of different ripeness, have slopes which depend on their ripeness. In the same way Curves 9 and 10 and 9 and 6, which represent viscose solutions of different and the same concentrations respectively, but of different viscosities, are found to be in order of ripeness, despite the fact that their viscosities are not consistent with the values of the modulus (in this instance viscose solutions of higher ball-fall viscosity have lower values of η'). These cases of discrepancy between the effects of ripeness and ball-fall viscosity on the structuromechanical properties of viscose solutions do not refute but rather emphasize the predominant role of ripeness in the structurization of viscose solutions.

The effective viscosity was calculated from these initial regions as $\eta' = P/(d\epsilon/d\tau)$. This calculation method is arbitrary because our method did not allow of measurements in the region of very small loads (because of the large experimental error in the visual readings), but the general course of the curves does not give any reason to expect any significant changes of the effective viscosity η' in this region. The effects of viscose ripeness on the effective viscosity are given in the Table and Fig. 3.

The curves in Fig. 2 are in sequence of the ripeness and effective viscosity of the viscose solutions; i.e., the greater the age of the viscose solutions (the lower the ripeness figure) the higher is the effective viscosity (see Table) and therefore the higher is the mechanical strength of the solution structure.

It follows from the Table and Fig. 3 that the calculated

Indeed, it is found for viscose solutions represented by Curves 9 and 10, and by Curves 9 and 6, that despite the higher content of NaOH in the former case, and the lower content of α -cellulose in the latter, structurization of these solutions is more pronounced and is consistent with their ripeness. Yet both these factors, which favor the solubility of cellulose xanthate, should lead to decreased structurization of the solutions. Hence the influence of ripeness in some cases masks the influence of the NaOH/cellulose ratio and of the α -cellulose concentration on the structuromechanical properties of viscose solutions; this must evidently be attributed not only to increased density of the intermolecular-bond network, which also depends on the above-named factors, but also to the formation of stronger bonds, characteristic of gels formed from solutions of this type.

This conclusion is of great practical importance, as the structural strength of spinning viscose should have a direct influence on the conditions of fiber formation. The higher the structural strength of the spinning solution, the more difficult it is to obtain a well-oriented fiber in spinning. This leads to the conclusion that viscoses of low ripeness should be spun if fibers of high strength are required.

The patent literature indicates that in foreign practice viscous viscoses (800-1000 poises) are in fact being spun at low ripeness (infinity by the NH_4Cl test, or 5.0-7.0 or higher by the NaCl test).

We are studying the influence of solution structure on thread formation and strengthening of viscose fibers in spinning, and the results will be reported in the next communication.

SUMMARY

1. The effective viscosity η' , calculated from the ratio of the shear stress to the development rate of relative shear deformation, can be used as a measure of the structure of spinning viscoses.
2. Viscose ripeness has a greater influence on the structure of viscose solutions than the NaOH/cellulose ratio or, in some instances, than the concentration or the ball-fall viscosity.
3. It is postulated that not only the number but also the strength of the intermolecular bonds increases with increasing ripeness of viscose solutions.

LITERATURE CITED

- [1] N. Drish, British Patent 709,700 (1954); E. Torke and W. Matthoes, Federal German Patent 904,893 (1954); Australian Patent 175,660 (1953).
- [2] N. Drish, Textil-Praxis 8, No. 8, 710 (1953); Text. Res. J. 23, No. 8, 512-521 (1953); Modern Text. Mag. 34, No. 7, 67-88 (1953).
- [3] German Patent 2323 (1953); R. Klein, Democratic German Patent 916,347 (1954); Swiss Patent 299,328 (1954).
- [4] N. V. Mikhailov and N. N. Zav'ialova, J. Appl. Chem. 28, No. 1, 97 (1956).*
- [5] N. V. Mikhailov and N. N. Zav'ialova, Sci. Res. Trans. All-Union Sci. Res. Inst. Synthetic Fibers No. 2, 30 (1955).
- [6] A. S. Kolbanovskaya and P. A. Rebinder, Colloid J. 12, No. 3, 194 (1950).
- [7] L. V. Chumakova and P. A. Rebinder, Proc. Acad. Sci. USSR 81, 239 (1951); L. V. Ivanova-Chumakova and P. A. Rebinder, Colloid J. 18, No. 4, 429 (1956); *T. I. Samsonova and L. V. Ivanova-Chumakova, Colloid J. 19, No. 3, 343 (1957).*
- [8] I. A. Dumanskii, A. V. Dumanskii, and L. V. Khailenko, Proc. Acad. Sci. USSR 92, No. 6, 1189 (1953).

Scientific Research Institute
for Synthetic Fibers Mytishchi

Received July 18, 1957

*Original Russian pagination. See C. B. Translation.

CERTAIN PROPERTIES OF CALCIUM OXALATE PRECIPITATES IN ELECTROLYTE SOLUTIONS

G. G. Kandilarov

It is known that precipitates in which the particles are closely packed are relatively more difficult to pep-tize than precipitates of more or less loose structure [1]. One of the factors determining the structure of precipitates is the nature and concentration of the electrolytes present during the precipitation. The volume of the precipitate gives an indication of the nature of the packing. A subject of theoretical and practical interest is study of the influence of various ions on the volume of the precipitates formed in polydisperse suspensions of calcium oxalate. Observations of this type were performed by us earlier on suspensions of $\text{Ca}_3(\text{PO}_4)_2$ [2] and kaolin [3]. The results of these observations may prove useful in studies of the formation and dissolution of analogous precipitates in the human organism. Experiments were therefore carried out on suspensions of calcium oxalate in presence of electrolytes differing in concentration and valence of their ions. The following types of electrolytes were used: 1) containing univalent, bivalent, and trivalent cations (sodium, calcium, and aluminum chlorides); 2) containing univalent and bivalent anions (sodium chloride, sulfate, phosphate, and oxalate); 3) sodium hydroxide and hydrochloric acid.

EXPERIMENTAL

Calcium oxalate was prepared by precipitation from calcium chloride (chemically pure, Main Administration of Chemical Reagents) by addition of a saturated solution of pure oxalic acid.* After filtration the precipitate was shaken mechanically with a large volume of distilled water. The suspension was left to settle, and the clear liquid was decanted off. The crystalline precipitate was washed repeatedly with a large amount of distilled water for several weeks to a completely negative reaction for chloride and calcium ions. The precipitate was dried at 110° for 6 hours and then ground in a mortar. The grinding in the mortar was difficult, as the crystals were hard. The product was used for the experiment one year after preparation. The same method was used to prepare another sample of calcium oxalate, but this was dried at 140-150° and used immediately after preparation.

Samples of this calcium oxalate, weighing 1.25 g or 1.0 g, were taken and mixed with 10 ml lots of electrolyte solutions. The precipitate was shaken with the solution in two stages: for 3 minutes in the first stage, and for 2 minutes in the second. The liquids were left to settle for 24 hours at 25°. The experiments were performed in triplicate.

It was found by electrophoresis that the calcium oxalate particles were almost neutral electrically. However, in presence of certain electrolytes (NaCl , CaCl_2 , AlCl_3 , Na_2SO_4 and others) they acquire a positive charge, and a certain degree of stability is conferred on them by uni-, bi-, and trivalent cations.

Calcium oxalate-sodium chloride. The suspensions were prepared from 1 g of calcium oxalate shaken with 10 ml of solution. The sedimentation volumes measured after 24 hours were calculated for 1.25 g weights of precipitate. Fig. 1 shows that as the sodium chloride concentration increases, the sedimentation volume first increases, reaches a maximum, and then tends to decrease. The volume of the precipitate, calculated for 1.25 g of calcium oxalate, varies between 5.30 and 5.98 cc.

Calcium oxalate-calcium chloride. These suspensions were prepared from 1.25 g of calcium oxalate with 10 ml of CaCl_2 solution. In most cases the precipitates formed after 24 hours of sedimentation had a smooth and

* Oxalsäure krist. p. a. V. E. B.

even surface, so that the volume of the precipitate could be determined more precisely. Nearly all the suspensions remained more or less turbid even after 24 hours of sedimentation; the maximum turbidity was found with a calcium chloride concentration of ~50 millimoles/liter. However, the turbidity was so slight that it could hardly affect the volume of the precipitate significantly. At high concentrations (1000 and 2000 millimoles/liter) the liquid above the precipitate was quite clear.

It is seen from Fig. 1 that with increase of the CaCl_2 concentration to 100 millimoles/liter the volume of the calcium oxalate precipitate decreases sharply; it is reduced by almost one half (from 5.09 to 2.79 cc) over the range from 0.2 to 100 millimoles/liter. The volume of the precipitate increases with increase of the CaCl_2 concentration above 100 millimoles/liter. Therefore the volume of the calcium oxalate precipitate in CaCl_2 solutions differs appreciably from that in NaCl solutions, both in absolute magnitude and in the nature of its variation.

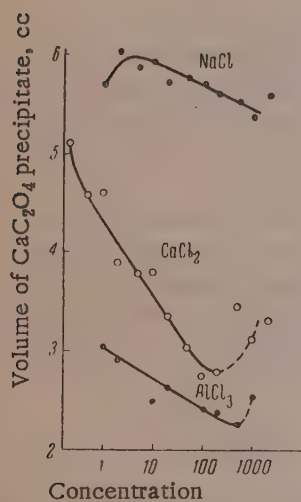


Fig. 1. Variation of the volume of CaC_2O_4 precipitate with the concentrations of NaCl , CaCl_2 , and AlCl_3 present during sedimentation.

Calcium oxalate-aluminum chloride. Suspensions were prepared from 1 g samples of aged and 1.25 g samples of freshly precipitated calcium oxalate. With AlCl_3 concentrations of 1, 2, 10, and 20 millimoles/liter the liquid over the precipitate was turbid even after 24 hours of sedimentation, and contained a small amount of suspended particles. At concentrations of 100, 200, and 500 millimoles/liter the solution was clear at the top and opalescent below.

Fig. 1 shows that, as compared with suspensions in NaCl and CaCl_2 solutions, the volume of the calcium oxalate precipitate in AlCl_3 is least (2.25-3.03 cc) at AlCl_3 concentrations from 1 to 500 millimoles/liter; this is a sign of closer packing of the particles in the precipitate. The volume of the calcium oxalate precipitate decreases with increase of the AlCl_3 concentration, and reaches a minimum at 500 millimoles of AlCl_3 per liter. The minimum lies further to the right than is the case for suspensions made in CaCl_2 solutions.* The volume of the calcium oxalate precipitate decreases with increasing valence of the cations (Na^+ , Ca^{2+} , Al^{3+}). The volume of the precipitate decreases rather rapidly with increase of the CaCl_2 concentration, and the curve descends more steeply than the curves for NaCl and AlCl_3 . This may be associated with the higher adsorption of calcium ions, as they are involved in the formation of the crystal lattice of the precipitate. Because of this the suspensions formed are relatively more stable.

It may be assumed that the electric charge of the particles in the suspension increases with increasing concentrations of calcium and aluminum ions, so that the precipitate is more closely packed and the volume is therefore less.

Calcium oxalate-sodium oxalate. These suspensions were prepared from 1.25 g of freshly prepared calcium oxalate and 10 ml of solution. After 24 hours of sedimentation the solution over the precipitate was absolutely clear at all the concentrations of sodium oxalate taken. It follows from Fig. 2 that in solutions of sodium oxalate the average volume of the calcium oxalate precipitate is approximately the same (3.83 cc) as that found for CaCl_2 over the same concentration range of 0.2-200 millimoles/liter (3.76 cc). However, in presence of CaCl_2 the volume of the calcium oxalate precipitate decreases from 5.09 to 2.79 cc, or almost by one half, with increase of solution concentration, whereas in the case of sodium oxalate the volume changes little, with only a weak minimum at 20 millimoles/liter.

Calcium oxalate-sodium sulfate. The suspensions were prepared from 1.25 g of calcium oxalate in 10 ml of solution. With a few exceptions the precipitates formed after 24 hours had a relatively even and smooth surface. The solutions over the precipitates were completely clear.

* In experiments with negatively charged kaolin suspensions under the same conditions, the minimum was shifted to the left under the influence of multibasic acids.

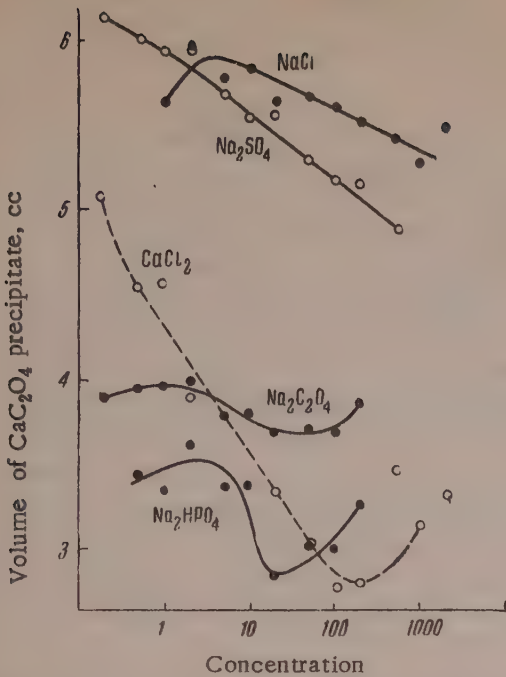


Fig. 2. Variation of the volume of CaC_2O_4 precipitate with the concentrations of NaCl , Na_2SO_4 , $\text{Na}_2\text{C}_2\text{O}_4$, Na_2HPO_4 and CaCl_2 .

containing $\text{Na}_2\text{C}_2\text{O}_4$. This minimum is shifted to the left relative to the minimum for suspensions with CaCl_2 solutions; this may be associated with differences in the valence of the ions.

Calcium oxalate-sodium hydroxide. The suspensions were prepared from 1.25 g of freshly prepared calcium oxalate. Fig. 3 shows that in the range of NaOH concentrations from 2 to 1000 millimoles/liter the volume of the calcium oxalate precipitate decreases rapidly from 4.60 to 3.21 cc, and then increases again, possibly because of the increase in solution viscosity. Here the volume of the calcium oxalate precipitate corresponds to a closer packing of the particles in the precipitate.

Volumes of Precipitates Formed in Polydisperse Calcium Oxalate Suspensions in Electrolyte Solutions

Electrolyte concentration in millimoles/liter	Volumes of CaC_2O_4 precipitates in ml, formed in presence of					
	HCl	NaCl	Na_2SO_4	$\text{Na}_2\text{C}_2\text{O}_4$	CaCl_2	AlCl_3
1	6.36	5.66	5.94	3.96	4.58	3.03
2	—	5.98	5.95	3.99	3.90	2.90
200	6.07	5.54	5.18	3.86	2.79	2.36
500	6.20	5.45	4.90	—	3.44	2.25
1000	6.99	5.30	—	—	3.12	2.53

oxalate precipitate found in our systems. Hence in an alkaline medium (NaOH) the calcium oxalate particles are closely packed, whereas hydrogen ions favor the formation of precipitates with a relatively loose structure. This

Fig. 2 shows that with increase of the sodium sulfate concentration in the range of 0.2-200 millimoles/liter the volume of the precipitate changes from 6.11 to 5.18 cc. In this respect the influence of sodium sulfate solutions on the volume of the precipitate is very similar to the influence of sodium chloride; in the latter case the volume of the calcium oxalate precipitate changes from 5.66 to 5.54 cc in the concentration range from 1 to 200 millimoles/liter.

Calcium oxalate-disodium hydrogen phosphate. These suspensions were prepared from 1.25 g of freshly prepared calcium oxalate in 10 ml of solution. After 24 hours of sedimentation the liquid above the precipitate was completely clear, while the precipitates had a relatively even and smooth surface. The surface was uneven only at high concentrations.

It follows from Fig. 2 that the volume of the CaC_2O_4 precipitates in Na_2HPO_4 solutions is less than that found in suspensions formed from NaCl , Na_2SO_4 , and $\text{Na}_2\text{C}_2\text{O}_4$ solutions; it varies from 3.60 to 2.82 cc in the concentration range from 0.5 to 200 millimoles/liter. This shows that the packing of the particles in these precipitates is denser. With increase of the Na_2HPO_4 concentration the volume of the CaC_2O_4 precipitates reaches a weak minimum at 20 millimoles/liter; this corresponds to the minimum for suspensions

Calcium oxalate-hydrochloric acid. The suspensions were prepared from aged calcium oxalate. The suspensions were centrifuged immediately after sedimentation, and the pH of the solutions was determined potentiometrically by means of quinhydrone and calomel electrodes.

Fig. 3 shows that the volume of the calcium oxalate precipitate exhibits very large fluctuations with increase of the hydrochloric acid concentration, with a maximum at 10 and a minimum at ~ 1000 millimoles/liter. The volume of the calcium oxalate precipitate reaches a higher value in hydrochloric acid (from 6.16 to 6.84 cc in the HCl concentration range from 0.2 to 10 millimoles/liter) than in sodium hydroxide, where the average volume of the precipitate is 4.38 cc in the range of NaOH concentrations from 2 to 10 millimoles per liter.

This value is one of the greatest volumes of the calcium

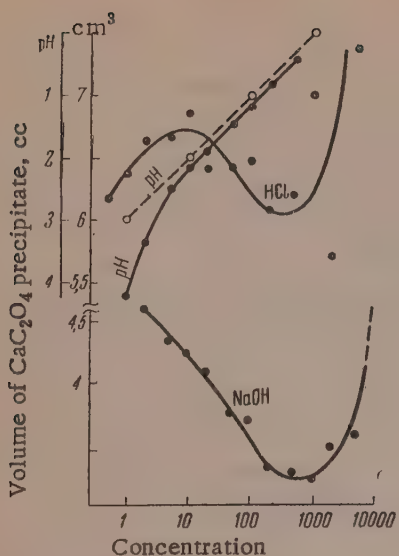


Fig. 3. Variation of the volume of CaC_2O_4 precipitate with the concentrations of NaOH and HCl , and with pH of HCl solutions.

studies of the formation of calcium oxalate precipitates in the human organism, and in work on methods for the prevention of this effect.

In conclusion, we may compare the nature of the variations of the volume of calcium oxalate precipitates with the variations found earlier in the volumes of $\text{Ca}_2(\text{PO}_4)_3$ [2] and kaolin [3] suspensions with changes in the concentrations of NaOH , AlCl_3 , and HCl solutions. It is seen that with increase of electrolyte concentration the changes in the volumes of precipitates in calcium oxalate, $\text{Ca}_2(\text{PO}_4)_3$, and kaolin suspensions proceed partially in opposite directions. This is probably associated with the opposite electric charges of the particles in these suspensions.

SUMMARY

The following results were obtained in experiments on suspensions of calcium oxalate in solutions of NaCl , CaCl_2 , AlCl_3 , $\text{Na}_2\text{C}_2\text{O}_4$, Na_2SO_4 , Na_2HPO_4 , NaOH and HCl :

1. The volume of the calcium oxalate precipitate decreases with increasing valence of the cations in solution.
2. The volume of the calcium oxalate precipitate reaches highest values in: a) dilute solutions of the electrolytes studied; b) NaCl and Na_2SO_4 solutions (in presence of the univalent sodium cation); c) an acid medium.
3. Multivalent cations (Ca^{2+} and Al^{3+}), especially at high concentrations, favor close packing of the calcium oxalate precipitate. Dilute solutions of NaCl and Na_2SO_4 (in absence of multivalent cations) favor the formation of bulky precipitates of a looser structure, which are probably broken down more easily. These observations are of interest in relation to the formation of calcium oxalate precipitates in the human organism, and in development of methods for its prevention.
4. In an alkaline medium (NaOH solutions) the volume of calcium oxalate precipitates is at a minimum in the NaOH concentration range from about 200 to 1000 millimoles/liter.
5. The particles in calcium oxalate suspensions in water are electrically almost neutral. However, uni-, bi-, and trivalent cations (Na^+ , Ca^{2+} , and Al^{3+}) confer positive charges and thereby definite stability on them.
6. Concentration-precipitate volume curves for $\text{Ca}_2(\text{PO}_4)_3$, calcium oxalate, and kaolin in NaOH , AlCl_3 ,

is confirmed by the almost symbiotic variation of the volume of the calcium oxalate precipitate with the hydrogen-ion concentration in the range from 0.2 to 10 millimoles/liter.

For comparison, the Table contains some of our data on the volumes of the precipitates formed in polydisperse suspensions of calcium oxalate in electrolyte solutions. Comparison of the data in the Table with the curves in Figs. 1, 2, and 3 shows that in dilute solutions of NaCl , Na_2SO_4 , and HCl the volumes of the calcium oxalate precipitates are almost double the volumes of the precipitates in suspensions formed on CaCl_2 and AlCl_3 solutions. This shows that whereas calcium or aluminum ions favor the formation of relatively close-packed precipitates, dilute solutions of NaCl , Na_2SO_4 , and HCl favor the formation of bulky precipitates of a looser structure.

It is known that close-packed precipitates are peptized layer by layer, so that the breakdown of the precipitates is hindered considerably. If a precipitate with a loose structure is formed, the area of contact between the precipitate and the liquid phase is considerably greater, and the conditions therefore favor, to some extent, breakdown of the precipitate.

Some of the ions discussed in this paper are present in human urine, and evidently the results can be used to some extent in

and HCl solution lie partially in opposite directions; this is probably because of the opposite electric charges of the suspensions.

LITERATURE CITED

- [1] H. R. Kruyt, *Colloid Science*, 1 (1955), p. 469. [Russian translation].
- [2] G. G. Kandilarov, *Colloid J.* 19, 435 (1957); **Sci. Trans. VIKhVPROM*, 3 (1956), p. 15.
- [3] G. G. Kandilarov, *Kolloid, Z.* 90, 320, 1940; 91, 56, 1940; *Colloid J.* 13, 357 (1951); 18, 293 (1956); *Sci. Trans. VSI*, 1 (1952), p. 1; *Bull. Chem. Inst. Bulgarian Acad. Sci.* 4, 287 (1956).

Chair of Inorganic, Analytical, Colloid, and
Physical Chemistry, VIKhVPROM
Plovdiv, Bulgaria

Received May 31, 1957.

*Original Russian pagination. See C. B. Translation.

STRUCTURE FORMATION IN COMPACTED SOILS

T. Iu. Liubimova

When soils are used as constructional materials, their natural structure which arises under natural conditions is destroyed during the excavation work; subsequently the soils undergo intensive compaction during construction of embankments. A state of the maximum compaction possible for the particular mechanical working conditions is reached at an optimum moisture content, specific for each given soil [1].

The mechanical strength of a freshly-compacted moist soil increases for some time after compaction, as the result of structurization processes in the soil; the kinetics and extent of these processes are determined for each given soil by the external conditions — the moisture content of the surroundings.

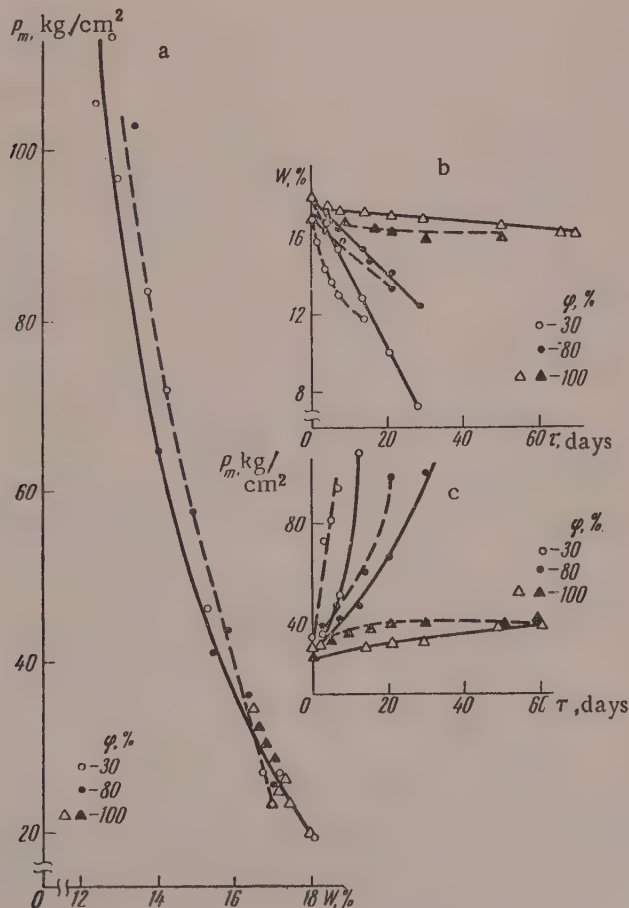


Fig. 1. Effect of residual moisture on plastic strength (a), and variations of the moisture content (b) and plastic strength (c) during drying of soils in air of different relative humidities (φ , %):
 —) Kar'kov loess; - - -) Cheremuskhi clay.

Investigations of structure formation in artificially compacted soils, and elucidation of the influence of the conditions of structure formation on the mechanical properties of the soil and on their stability to external influences are both of theoretical interest for extension of our knowledge of structure formation in disperse systems, and of practical importance in relation to the influence of local, climatic, and seasonal conditions in the planning of various constructions.

A soil compacted at the optimum moisture content is a disperse system of the maximum possible concentration, in which the dispersion medium is present to a considerable extent in the form of hydration layers. Simple calculations show that when a soil is compacted to the maximum and all the spaces between the particles are filled with water ~20% of all the water is present in the form of hydration layers (if their thickness is assumed to be 10^{-6} cm), if the nominal mean particle diameter is of the order of 1μ . In a dusty soil (average particle diameter $\sim 10\mu$) ~2% of all the water is contained in hydration layers, etc. The conditions in such a system appear to be especially favorable for formation of structural bonds between the particles of the solid phase.

In the light of the views developed by Rebinder and his school [2], the primary act of any structure formation in a disperse system is the formation of a coagulational spatial network of the finest particles of the solid phase, contact between which is a consequence of collisions in thermal motion; such contact may be effected through the hydration (solvation) layers if they do not fully block the intermolecular forces. Such structures are characterized by low strength, high plasticity, creep, and thixotropy.

The formation of coagulational contacts through the hydration layers on the soil-particle surfaces occurs in compacted soils probably during the compaction process, not only spontaneously but also under the influence of external forces. The concept of a spontaneously-formed spatial structural coagulational network becomes meaningless here, as the packing density of the solid phase is determined by the external mechanical forces during compaction.

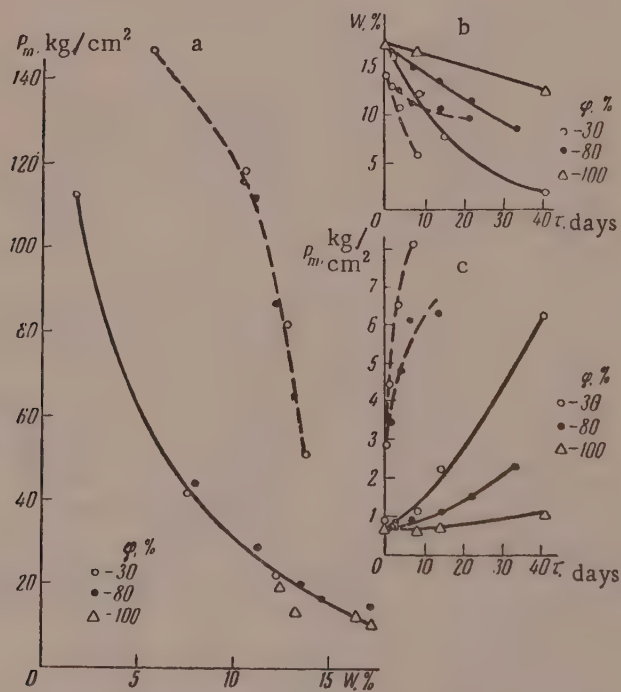


Fig. 2. Effect of residual moisture on plastic strength (a), and variations of the moisture content (b) and plastic strength (c) during drying of soils in air of different relative humidities ($\varphi, \%$):

—) Central Asian loam; ---) Moscow loam.

Subsequent structure formation after compaction may proceed in two ways: 1) with removal of the dispersion medium (water) by free evaporation into the surroundings; 2) without removal of water, when the surroundings are saturated with water vapor, and moisture does not evaporate.

According to Rebinder [3], when a soil dries, condensational structures arise by formation of direct cohesive bonds, both as the result of a direct approach between the particles when the water layers between them become thinner or disappear, and by the formation and growth of a new phase cementing the soil particles together. Evaporation of water from the soil facilitates the action of the molecular cohesion forces which tend to bring the solid particles closer together against the separating action of the hydration layers. In this way dehydration of concentrated coagulational structures strengthens them and gradually converts them into condensational structures, characterized by high strength, brittleness, and irreversible breakdown.

It is evident that mechanical properties of soils at any given instant during drying depend wholly on the rate of evaporation of the moisture, and are determined by the residual moisture of the soil.

The presence of elements of plasticity and thixotropy should be evidence of the predominant influence of mobile reversible coagulational contacts. If the rigid condensational bonds formed in the course of drying begin to play the predominant role, the soil acquires the properties of a brittle solid.

In the other possible case — in absence of free evaporation of water from the soil — gradual strengthening of the coagulational contacts and the corresponding strengthening of the structure can evidently occur only as the result of aging — syneresis of the coagulational structure and spontaneous packing of the solid phase by the action of molecular cohesion forces which squeeze out the liquid interlayers between the particles.

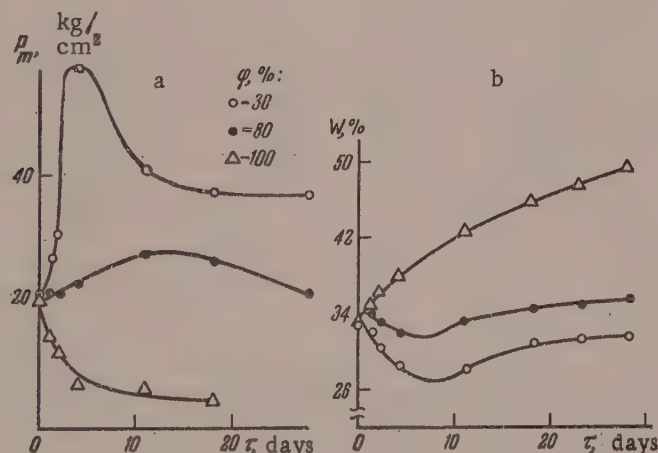


Fig. 3. Variations of plastic strength (a) and moisture content (b) with time for Oglanli bentonite during exposure to air of different relative humidities (φ , %).

In such a case the increase of soil strength must evidently be attributed not to removal but merely to redistribution of water in the three-phase system: soil-air-water (or pore liquid).

The conversion of coagulational into condensational structures in natural soils and clay pastes has been studied in detail by Gor'kova [4].

The present communication contains the results of experiments on structure formation in compacted soils. The compaction was effected at optimum moisture content by the tamping method; the compaction conditions were so chosen that the degree of compaction was close to that produced by the corresponding modern equipment under industrial conditions [1]. The air-dry soils were sifted through a sieve with hole 0.8 mm in diameter before compaction.

The mechanical properties of the compacted soils were characterized in terms of their plastic strength, measured by means of a cone plastometer of the lever type. The plastic strength was first determined immediately

after compaction, and then at various time intervals during exposure of the compacted specimens to air of different but constant humidities (the relative humidity φ of the air was 30, 80, and 100%). The moisture contents of the soils were determined together with the plastic strength.

The experiments showed that the strength of a compacted soil during drying is a definite function of its residual moisture content, irrespective of the evaporation kinetics (determined by the humidity of the surroundings). Fig. 1 shows data for Khar'kov loess and carbonate-free surface clay (from Cheremushki), and Fig. 2 shows analogous data for two loams: a dusty type, with a high carbonate content (light Central Asian, from Shurchi), and a heavy surface loam (from the Moscow region).

It follows from these results that the course of strength increase when there is free evaporation of moisture from the soil (i.e., when $\varphi < 100\%$) is determined entirely by the evaporation kinetics.

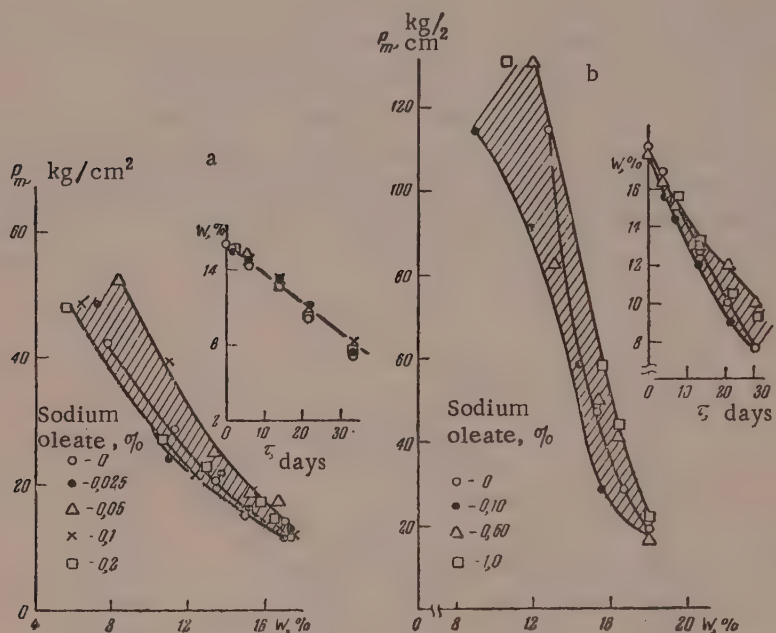


Fig. 4. Effects of added sodium oleate (% on the dry soil) on the relationship between plastic strength and residual moisture content, and on the kinetics of moisture evaporation during drying:

a) Central Asian loam, $\varphi = 80\%$; b) Khar'kov loess, $\varphi = 30\%$.

Similar experiments were also performed with monomineral clays — Prosianaia kaolinite and Oglanli bentonite, compacted at the optimum moisture content. In the case of the kaolinite there was a definite relationship between plastic strength and residual moisture at different rates of drying. In the case of the bentonite, in harmony with the existing views on the highly hydrophilic nature of this mineral, when it was exposed to air of relative humidity 30 % and over in all cases there was a progressive loss of strength of the structure formed during compaction, owing to sorption of water vapor. At relative air humidities $< 100\%$ there was initially some increase of strength, corresponding to a slight decrease in the moisture content of the system, and then the moisture content increased again as the result of sorption, with a consequent persistent decrease of strength in the course of time (Fig. 3).

The definite relationship between the strength and residual moisture content of a compacted soil no longer holds when a surface-active substance is introduced into the soil. Under such conditions the strength increase — formation and reinforcement of new structural contacts — is determined not only by removal (evaporation) of water from the system, but also by the state of the particles of the solid phase, i.e., of the structural elements. If the adsorption layers formed when the surface-active agent is introduced make the solid particles hydrophobic, structure formation is accelerated and facilitated; if stabilizing adsorption layers of the gel type are formed, structure formation is retarded to a degree which depends on the extent of stabilization.

It was shown by Rebinder and his associates [5] that in the adsorption of higher fatty acids of the saturated and unsaturated series from aqueous soap solutions the nature of the adsorption layers formed (hydrophobization and flocculation, or stabilization, of the particles of the disperse phase) is determined only by the concentration of the surface-active agent solution. We carried out experiments in order to study the effects of sodium oleate on structure formation in compacted soils and mineral powders; the sodium oleate was added in various concentrations in the form of soap stock wastes containing 67% of the surface-active component. The surface-active additive was introduced into the soil with the mixing water.

The results for Central Asian loam and Ukrainian loess are presented in Fig. 4. In the case of the loam the rate of evaporation of water is unchanged with additions of up to 0.2% sodium oleate, although the points representing the strength as a function of residual moisture are considerably scattered, and at the later stages of structure formation there is a tendency for a greater strength increase in the specimens containing the surface-active additive. In the carbonate soil (loess) partial formation of chemically fixed monomolecular hydrophobizing layers of calcium soaps on the surfaces of the particles is to be expected. The results (Fig. 4) show that in this case also the points for the strength as a function of residual moisture are considerably scattered. The effect of a gradual transition from ionic-molecular hydrophobizing adsorption layers (formed in adsorption from dilute sodium oleate solutions) to stabilizing and hydrophilizing adsorption layers of the gel type (formed in adsorption from concentrated solutions) can be more conveniently observed with a pure carbonate material. Experiments were therefore performed with powdered Kaluga limestone, also compacted at the optimum moisture content.

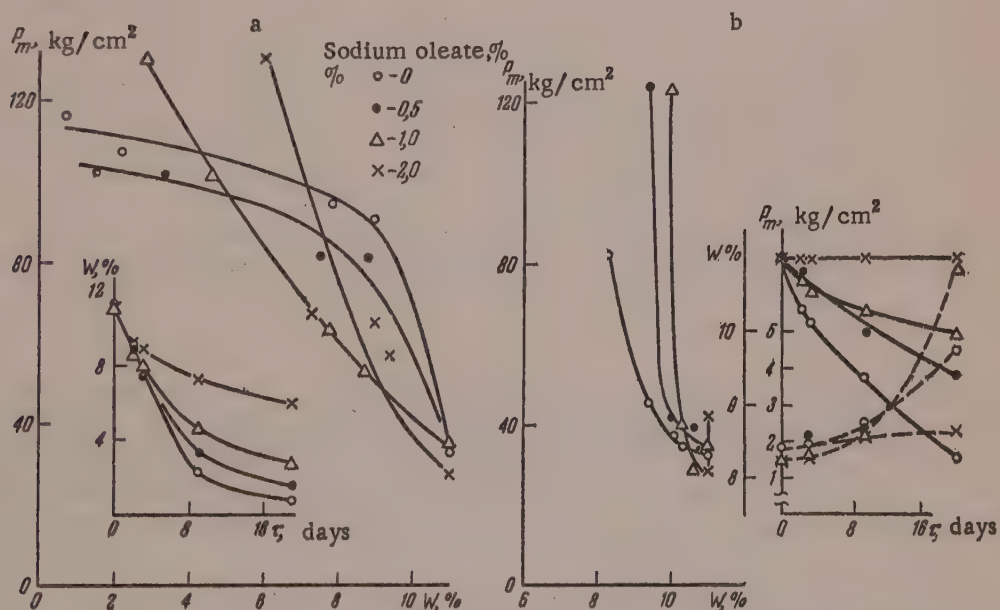


Fig. 5. Effect of added sodium oleate (% on the dry material) on the relationship between plastic strength and residual moisture content, and on the variation of the moisture content of Kaluga limestone when exposed under different conditions:

a) at $\varphi = 30\%$; b) at $\varphi = 100\%$; — $W\%$; - - P_m

The results (Fig. 5,a) show that when specimens of compacted limestone are dried at $\varphi = 30\%$ there is a regular decrease in the rate of water evaporation with increasing concentration of sodium oleate, probably owing to retardation of the migration of water in a capillary system with a water-repellent surface. The relationship between strength and residual moisture content of the system differs at different stages of drying; at relatively high moisture contents the strength varies in accordance with the residual moisture: the lower the moisture content, the higher is the strength. At low moisture contents the reverse relationship holds, and the strength is higher with larger amounts of added sodium oleate.

The probable explanation of this last result is that when the system is greatly dehydrated as the result of drying the presence of colloidal adsorption layers results in additional reinforcement of the contacts because of their cohesion and condensation.

For studies of the influence of adsorption layers on structure formation in compacted soils without superposition of dehydration during drying of the system, the specimens were exposed to an atmosphere of saturated vapor.

The water pressed out under these conditions during syneretic compaction of the soil, which appeared on the open surfaces of the samples, apparently flowed out to some extent spontaneously under gravity; the "sweated" surfaces were carefully dried immediately before determinations of the plastic strength and residual moisture.

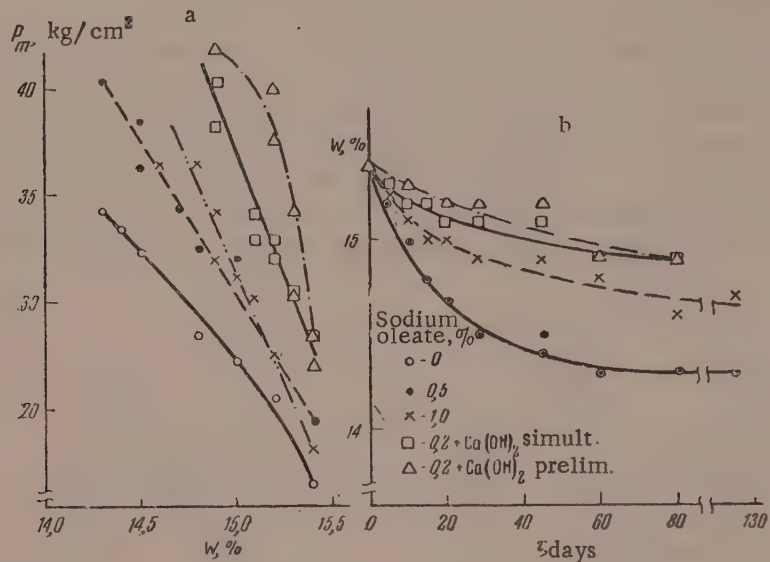


Fig. 6. Effect of added sodium oleate (% on the dry soil) on the relationship between plastic strength and moisture content (a), and the course of moisture variation (b) during synergetic reinforcement of Cheremushki clay.

Thus, the slight decrease in the moisture contents of compacted soils and mineral materials which takes place in saturated vapor accompanies an increase of their strength, but is a consequence and not the cause of the latter. The strength may increase even if the total moisture content of the system remains unchanged, if the reinforcement of the coagulation contacts which takes place is not accompanied by the pressing out of considerable amounts of water. It is the latter effect which apparently occurs in presence of a hydrophobizing agent which, by decreasing the thickness of the hydration layers or by removing them entirely, favors more rapid approach between the particles of the solid phase and formation of direct contacts between them, as shown by the more rapid increase of strength with small changes of moisture content or even without alteration in the moisture content of the system.

In the case of the limestone specimens studied (Fig. 5, b) additions of up to 1% of sodium oleate are evidently still hydrophobizing in their action, as with retarded separation of water the strength increase is more intensive because of the larger number of structural contacts formed, or of their higher strength. An addition of 2% of sodium oleate has a strong stabilizing effect on the system and retards the strength increase by preventing the formation of structural contacts; neither the strength nor the moisture content of the system show any appreciable changes throughout the experiment (20 days).

The influence of hydrophobizing adsorption layers on syneresis is even more pronounced in compacted soils. Figs. 6 and 7 show the results of certain experiments with surface clay (from Cheremushki) and Khar'kov loess. The experiments with clay were performed in three variants: 1) with addition of sodium oleate only; 2) with

simultaneous addition of sodium oleate and of an amount of calcium hydroxide corresponding to the sorption capacity of the clay (0.6% on the soil), and 3) with preliminary prolonged saturation (for 10 days) of the clay with the same amounts of $\text{Ca}(\text{OH})_2$, followed by mixing with sodium oleate solution. The purpose of the lime treatment was to ensure subsequent chemical fixation of the water-repellent adsorption layers on the surfaces of the soil particles. The results show that in the case of clay the strongest structuring influence is exerted by chemically fixed adsorption layers of calcium soaps. In the case of the carbonate soil — loess — the strength increase on introduction of 1% sodium oleate takes place at unchanged moisture content.

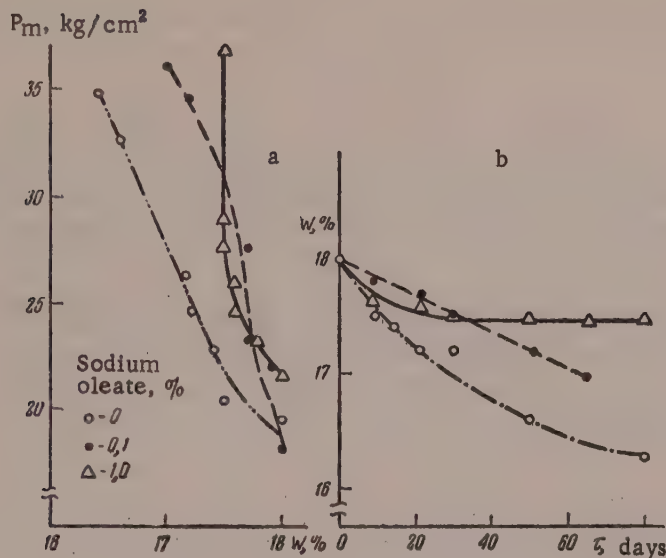


Fig. 7. Effect of sodium oleate (% on the dry soil) on the relationship between plastic strength and moisture content (a), and the course of moisture variation (b) during synergistic reinforcement of Khar'kov loess.

SUMMARY

1. Structure formation in soils during drying, with gradual transformation of coagulational into condensational contacts by thinning or complete disappearance of interlayers of the dispersion medium at the points of contact (in accordance with P. A. Rebinder's theory), is characterized by:

a) different rates of evaporation of moisture under different conditions, dependent on the humidity of the surroundings;

b) different rates of strength increase under different conditions, dependent on the rate of evaporation of the moisture;

c) a definite relationship between the plastic strength and the residual moisture content of the soil (irrespective of the rate and conditions of moisture evaporation).

2. The definite relationship between plastic strength and residual moisture content of a compacted soil during drying breaks down on introduction of a surface-active substance (sodium oleate); the adsorption layers formed are capable of influencing the course of structure formation differently at different stages, with the same concentration of sodium oleate in the soil; at relatively high residual moisture contents the strength increase may be retarded owing to a retardation of moisture evaporation. The strength increase is accelerated at low residual moisture contents, owing to the additional cohesive action of the colloidal adsorption layers during their dehydration.

3. In an atmosphere of saturated vapor, when the coagulational contacts are reinforced only as the result of

pressing out of the boundary (aqueous) phase by the action of molecular forces (self-condensation, syneresis), the introduction of a surface-active substance (sodium oleate) in the concentration range corresponding to the formation of hydrophobizing ionic-molecular adsorption layers intensifies the strength increase, owing to attenuation or removal of the hydration layers from the surfaces of the soil particles.

4. The formation of micellar adsorption layers, stabilizing the particles of the solid phase, at high concentrations of sodium oleate retards or even inhibits structure formation.

LITERATURE CITED

- [1] A. A. Arsen'ev, V. A. Bochin, and N. N. Ivanov, Construction of Highways, part 1 [in Russian] (Moscow Motor Transport Press, 1955), p. 116; M. Ia. Telegin, Compaction Methods for Road Embankments [in Russian] (Road Press, 1952).
- [2] E. E. Segalova and P. A. Rebinder, Colloid J. 10, No. 3, 223 (1948); P. A. Rebinder and E. E. Segalova, Nature No. 12, 45 (1952); E. E. Segalova, P. A. Rebinder and O. I. Luk'ianova, J. Moscow Univ. No. 2, 17 (1954); V. N. Izmailova, E. E. Segalova and P. A. Rebinder, Proc. Acad. Sci. USSR 107, No. 3, 425 (1956);* N. V. Mikhailov and P. A. Rebinder, Colloid J. 17, No. 2, 107 (1955);* L. A. Abduragimova, P. A. Rebinder and N. N. Serb-Serbina, Colloid J. 17, No. 3, 184 (1955).*
- [3] P. A. Rebinder in Proceedings of Conference on the Engineering and Geological Properties of Rocks and Methods for Their Investigation, 1 [in Russian] (Izd. AN SSSR, 1956), p. 31.
- [4] I. M. Gor'kova, Colloid J. 18, No. 1, 26 (1956); I. M. Gor'kova, in Proceedings of Conference on the Engineering and Geological Properties of Rocks and Methods for Their Investigation, 1 [in Russian] (Izd. AN SSSR, 1956), p. 98.
- [5] P. A. Rebinder et al., Physical Chemistry of Flotation Processes (collected papers) [in Russian] (Moscow-Leningrad-Sverdlovsk, 1933); P. A. Rebinder et al., Physical Chemistry of Detergent Action (collected papers) [in Russian] (Moscow-Leningrad, 1935); N. N. Serb-Serbina, J. Phys. Chem. 10, No. 4-5, 6 (1937).

All-Union Road Scientific Research Institute

Received March 10, 1957.

*Original Russian pagination. See C. B. Translation.

DETERMINATION OF THE ADSORPTION OF SOLUTES ON HYDROGELS

P. S. Meleshko

Determination of the Adsorption of One Solute on a Hydrogel

The usual method for determination of the adsorption of a solute on the surface of a solid adsorbent consists of measurements of the concentration of the solute before immersion of the adsorbent into the solution and after adsorption equilibrium has been reached. The amount of solution must also be known. The amount of substance adsorbed is usually referred to unit mass of adsorbent. In determinations of adsorption in a system in which the concentration of the original solution is not known the adsorbent is separated from excess solid phase and analyzed together with the solution adhering to it. A weighed sample of this mixture of liquid and solid phases (LS mixture) is analyzed for the percentage content of the anhydrous adsorbent (a), the total contents of the adsorbate, adsorbed and remaining in solution (b), and the concentration of the equilibrium solution (c).

Suppose that 100 g of LS mixture contains i grams of adsorbed substance; then the amount of solute is $b - i$, and the amount of solution is $100 - a - i$. Since the concentration of the equilibrium solution is c , the weight of solute is $(100 - a - i)c / 100$. The amount i of substance adsorbed is equal to the difference between the total content of the adsorbate in the LS mixture and the amount remaining in solution:

$$i = b - \frac{(100 - a - i)c}{100} \quad \text{or} \quad i = \frac{ac - 100(c - b)}{100 - c}.$$

The number of grams of adsorbate per 1 g of adsorbent, Γ_1 , is:

$$\Gamma_1 = \frac{ac - 100(c - b)}{a(100 - c)}. \quad (1)$$

Formula (1) can be used for calculation of Γ_1 , irrespectively of whether a dry or moist adsorbent was taken for the experiment. The determination of adsorption is somewhat different if the adsorbent is a hydrogel. Hydrogels usually contain chemically bound water, and to calculate the adsorption of a solute on a colloidal hydrate it is necessary to know its content of chemically bound water.

Let the percentage content of the anhydrous substance (An) in the hydrate be x ; then the number of grams of the hydrate in the LS mixture is $100a/x$. If, as before, we denote the amounts of substance adsorbed by i , then the weight of solution is $100 - 100a/x - i$, and the amount of solute is $(100 - 100a/x - i)c / 100$. It follows that the amount of substance adsorbed must be $i = b - \frac{(100a/x - i)c}{100}$ or, after rearrangement

$$i = \frac{100ac - 100x(c - b)}{x(100 - c)}. \quad (2)$$

Since i is adsorbed by $100a/x$ grams of hydrate, we have

$$\Gamma_1 = ix / 100a. \quad (3)$$

Substituting the value of i from Equation (2) into (3) we have

$$\Gamma_1 = \frac{ac - x(c - b)}{a(100 - c)}. \quad (4)$$

If the colloidal adsorbent is not a hydrate but is anhydrous and $x = 100$, Equation (4) becomes Equation (1) after the substitution.

As for an anhydrous adsorbent the determination of the adsorption of a solute on a colloidal hydrate is a problem which can be solved in two ways: by analysis of the LS mixture and equilibrium solution, and by determination of the concentration of the adsorbate solution before and after immersion of the adsorbent in it. It should be noted that the latter method may have certain advantages in the experimental sense in certain cases. However, if Formula (4) is to be used for calculation of the results in this instance, the values of \underline{a} and \underline{b} must first be calculated from the formulas

$$a = P_1 A / (P + P_1) \quad (5)$$

and

$$b = P c / (P + P_1), \quad (6)$$

where P_1 and P are the weights of the colloidal adsorbent and the original solution respectively; \underline{c} is the concentration of the original solution; and \underline{A} is the content of the anhydrous substance in the hydrogel.

The adsorption on the surface of a hydrogel can also be determined if the amount of chemically bound water in the colloidal hydrate is unknown. In this case, however, it is necessary to determine the composition of the adsorbent (colloidal hydrate) simultaneously with the determination of adsorption. Neither of the required quantities can be found independently of the other. The simultaneous determination of the adsorption of a solute on the surface of a hydrogel and of the amount of chemically bound water in a colloidal hydrate is carried out by the third-component method of Danil'chenko [1-2]. The third-component method is an extension of the Schreinemakers [3] indirect method for determination of the composition of the solid phase in a ternary system to the case in which the substance in question is capable of adsorbing the solute.

Determination of the Adsorption of Two Solutes Present Simultaneously in a Solution

The determination of the adsorption of several solutes by a hydrogel, when they are present simultaneously in a solution, presents a special problem. If the solution contains two substances, each of which can be separately adsorbed on the given hydrogel, it may be assumed that joint (simultaneous) adsorption of both substances will take place. Thus, to solve the problem in general form, it is necessary to find formulas for calculation of Γ_1 and Γ'_1 when both these quantities are greater than zero. We return to Formula (4) for this purpose.

We denote the total quantity of the two adsorbed substances by $\Gamma_1 + \Gamma'_1$; the total concentration on the solutes in the equilibrium solution is $c + c'$; the total contents of the two adsorbates in the LS mixture is $b + b'$. Substituting the corresponding total values for the two adsorbates for Γ_1 , \underline{c} , and \underline{b} in Equation (1) we have:

$$\Gamma_1 + \Gamma'_1 = \frac{a(c + c') - x[(c + c') - (b + b')]}{a[100 - (c + c')]} \quad (7)$$

To calculate the adsorption of each of the substances separately, we again use Formula (4), but we first transform it by recalculation of the values of \underline{c} , \underline{b} , and \underline{a} in Equation (4), obtaining the new values c_2 , b_2 , and a_2 . It is shown below that this recalculation has the effect of eliminating one of the solutes from the equilibrium solution and the LS mixture.

The equilibrium solution of our system contains $c\%$ of Solute I (SI) and $c'\%$ of Solute II (SII). To find the new value c_2 for the concentration of the first solute, we take $100 - c'$ of the solution as 100%. This gives

$$c_2 = 100c / (100 - c'). \quad (8)$$

The LS mixture contains $b\%$ of substance I, $b'\%$ of substance II, and $a\%$ of the anhydrous adsorbent substance. Taking $100 - b'$ in the LS mixture as 100%, we find the new values of b_2 and a_2 :

$$b_2 = 100b / (100 - b'); \quad (9)$$

$$a_2 = 100a / (100 - b'). \quad (10)$$

Replacing in Equation (4) the values of \underline{c} , \underline{b} , and \underline{a} by c_2 , b_2 , and a_2 , we find, after rearrangement, the formula for calculation of Γ_1 for one of the substances:

$$\Gamma_1 = \frac{100ac - x[c(100 - b') - b(100 - c')]}{100a[100 - (c + c')]} . \quad (11)$$

To derive an equation for calculation of Γ_1' for the second adsorbate, we calculate c_2' , b_2' and a_2' similarly, but this time we "eliminate" the first solute from the system:

$$c_2' = 100c' / (100 - c), \quad (8a)$$

$$b_2' = 100b' / (100 - b); \quad (9a)$$

$$a_2' = 100a' / (100 - b). \quad (10a)$$

We now replace c, b, and a in Equation (4) by the values of c_2' , b_2' , and a_2' :

$$\Gamma_1' = \frac{100ac' - x[c'(100 - b') - b'(100 - c)]}{100a[100 - (c + c')]} . \quad (11a)$$

Summation of the right and left-hand sides of Equations (11) and (11 a) and appropriate rearrangement gives equation (7). This result confirms the validity of these equations, since different approaches were used for the derivation of Equation (7) on the one hand, and of Equations (11) and (11 a) on the other. For the use of Equations (11) and (11 a) the content of anhydrous substance (x) in the colloidal hydrate must be known. If it is not known, it must be found by the third-component method in a parallel experiment.

After the composition of the colloidal hydrate has been found, there are no obstacles to the calculation of the required values of Γ_1 and Γ_1' for substances I and II. It must be remembered, however, that for calculation of either of these values it is necessary to determine the concentration c and c' of the two solutes in the equilibrium solution, and their contents (b and b') in the LS mixture; the content of the anhydrous substance (a) in the same mixture must also be determined.

It is seen that the principle of this method consists of a virtual conversion of each of the adsorbed substances from the four-component system $An-H_2O-SI-SII$ into a three-component system $An-H_2O-S$.

It must be added that the procedure for calculation of the adsorption of one of the solutes remains the same if the other solute is not adsorbed. In such a case either Γ_1 or Γ_1' will be found to be zero when Formulas (11) and (11 a) are used.

Determination of the Adsorption of Several Solutes Present Simultaneously in a Solution

The method for determination of the adsorption of two solutes, present simultaneously in a solution, on a hydrogel may be extended to systems with several solutes. Here again the method of "component elimination" must be used, but in the presence of several solutes not one, but $n-1$ components, where n is the total number of solutes, must be "eliminated."

Let us consider the simplest case, the simultaneous adsorption of three solutes. Suppose that each or any of the solutes present in the system $An-H_2O-SI-SII-SIII$ can be adsorbed on the hydrogel surface. To find the adsorption Γ_1 of one of the three solutes, the following conversion formulas must be used:

$$c_3 = \frac{100c}{100 - c' - c''}; \quad (12)$$

$$b_3 = \frac{100b}{100 - b' - b''}; \quad (13)$$

$$a_3 = \frac{100a}{100 - b' - b''}, \quad (14)$$

and the values of c_3 , b_3 , and a_3 must be substituted into Equation (4). To find Γ_1' and Γ_1'' , the values of c'_3 , b'_3 , a'_3 , and c''_3 , b''_3 , a''_3 must be calculated in the same way, and substituted in turn into Equation (4).

The same method can be used for calculation of the adsorption of a larger number of solutes. In principle, the applicability of the method is not limited by the number of solutes. The sole condition for determination of the adsorption of any one adsorbate is determination of the concentrations of each solute in the solution and the LS mixture.

The adsorption of a solute on a hydrogel surface can also be determined graphically. The graphical method for determination of adsorption is very convenient, as the required value is rapidly found. The same experimental data are used as in the calculation of adsorption by Formula (4). These data are plotted in a Rooseboom triangular diagram [4]. In the diagram of Fig. 1 the vertices of the right-angled triangle correspond to the three components of the system $\text{An}-\text{H}_2\text{O}-\text{S}$, where An is the anhydrous substance and S is the solute. The sides of the triangle correspond to the three binary systems: water-solute, water-anhydrous substance, and anhydrous substance-solute.

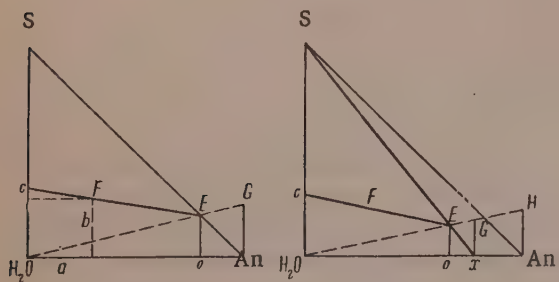


Fig. 1

Fig. 2.

ordinate of the point E represents the percentage content of the adsorbate in the adsorption product. To find the amount of adsorbate per 100 g of adsorbent, a straight line must be drawn from the H_2O vertex of the triangle through the point E to its intersection with the perpendicular through the point An . The intercept GAn is the required amount.

If the adsorbent is a colloidal hydrate with a known content of chemically bound water, before the analytical data are plotted on the diagram (Fig. 2) the percentage content of anhydrous substance in the hydrate is marked on the horizontal side of the triangle (point x), and this point is joined to the point S . Each point of the line Sx corresponds to a constant $\text{An} : \text{H}_2\text{O}$ ratio, representing the composition of the hydrate. Any point representing the composition of the adsorption product must lie on this line, regardless of the degree of adsorption. The points c and F are plotted by the same method, but the straight line through these points is drawn to its intersection of the "hydrate-composition hypotenuse" Sx , where the point E must now lie. Here again the intercept EO represents the percentage of adsorbate in the adsorption product, but in this case it gives the adsorption of the solute on the hydrate and not the anhydrous substance. We denote this adsorption by y_E ; then the amount of hydrate in the adsorption product is $100 - y_E$. The number of grams of adsorbate per 100 g of hydrate is: $y = 100 y_E / (100 - y_E)$. Finally, the amount of substance adsorbed by the hydrate, per 100 g of anhydride, is $y_{\text{An}} = 100 y/x$.

To find the two values y and y_{An} graphically (Fig. 2), a straight line is drawn from the H_2O vertex through E to its intersections with the perpendiculars through the points x and An . The intercepts Gx and HAn represent y and y_{An} respectively. It must be remembered that $y = \Gamma_1 \cdot 100$.

We now consider a third case: the adsorbent is a colloidal hydrate with an unknown content of chemically bound water. If we plot the analytical data for one sample of LS mixture on the diagram and draw a composition line through the points c and F , we cannot in this case find the position of the point E , which must be given by the intersection of two straight lines. As was shown by Danil'chenko [2], in this case analytical data for at least two samples of LS mixture must be used.

The points c and c' in the diagram (Fig. 3) represent the concentrations of equilibrium solutions and points F and F' give the compositions of two samples of LS mixtures.

Straight lines are drawn through the pairs of points c and F and c' and F' to intersect at the point E , but this point represents the composition of the adsorption product only if the adsorbent surface is saturated with adsorbate molecules in both samples. Any other straight line based on analytical data for an LS mixture of the same system, with a concentration of the equilibrium solution different from the first two, will pass through this

To plot the analytical data in the diagram, the percentage content of the solute in the equilibrium solution is marked off on the vertical side of the triangle at the point c . By marking the content of the anhydrous substance in the LS mixture on the abscissa axis (point a), and the total content of solute and adsorbed substance in this mixture along the ordinate axis (point b), we find the second point, F , representing the composition of the LS mixture. A straight line is drawn through the points c and F . If the adsorbent is anhydrous, the composition of the adsorption product is given by the point of intersection of the straight line cF with the side SAn of the triangle, the point E . The

point, provided that this concentration is sufficient for maximum adsorption of the adsorbate molecules on the hydrogel surface.

By drawing a straight line from the vertex S through the point E to its intersection with the horizontal side of the triangle, we find the point x , which represents the composition of the colloidal hydrate as percentages of anhydrous substance and chemically bound water. Now, as before, it is easy to find the degree of adsorption even in samples in which the maximum adsorption of solute molecules on the hydrogel surface has not been reached. All the points for the compositions of the adsorption products below maximum saturation must also lie on the line Sx , but below the point E.

The straight line $c''F'$ (Fig. 3) cuts the "hydrate-composition hypotenuse" Sx at the point E' , which is below the point E. The point E' , like E, represents the composition of the product formed by adsorption of solute molecules on the colloidal hydrate, but in contrast to the latter it corresponds to a product with an unsaturated layer of adsorbed molecules. Evidently the concentration c'' of the equilibrium solution is insufficient for formation of the adsorption product of limiting composition. Finally, by drawing straight lines from the H_2O vertex of the triangle through the points E and E' to their intersections with the perpendicular drawn from the point x , we find the two values y and y' .

The graphical method is inferior to the analytical method of calculation in the accuracy of the results obtained, but because of its simplicity and convenience it is useful in all determinations of the degree of adsorption on hydrogels.

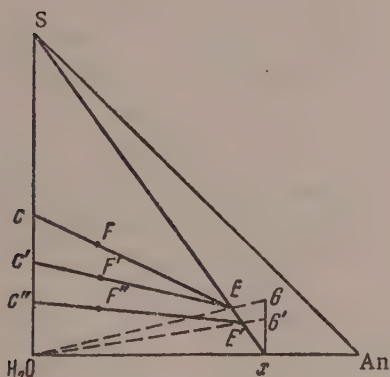


Fig. 3.

For graphical determination of the adsorption of two adsorbates in the system $An-H_2O-SI-SII$, as for a three-component system, we use a triangular diagram. While two vertices of the triangle (Fig. 4), as before, represent the anhydrous substance (An) and H_2O respectively, the third now corresponds to the sum of two solutes, SI and SII. We represent the content of anhydrous substance in the colloidal hydrate by the point x in the horizontal side H_2O-An of the triangle. We join the point x to the vertex $SI + SII$ by a straight line, which should contain the point corresponding to the product formed by joint adsorption of two solutes, SI and SII, on a hydrate with a content x of anhydrous substance. The concentrations of the two solutes in the equilibrium solutions are now marked off in such a way that the concentration of one, c , is taken from the coordinate origin, while the concentration of the other, c' , is taken from the point c , and the intercept between the H_2O vertex to " $c + c'$ " represents the sum of the concentrations of the two solutes. We then mark the content of anhydrous substance in the LS mixture by the point a along the abscissa axis and plot the contents of substances I and II in the LS mixture on the ordinate axis in the same order as the equilibrium concentrations. We thus find the points b and " $b + b'$ ". We draw a straight line through the points " $c + c'$ " and " $b + b'$ " to its intersection with the hypotenuse " $SI + SII - x$ " at the point E. The ordinate of E (the intercept OE) gives the total content of the two adsorbates in the adsorption product, but gives no indication of the degree of adsorption of either of the substances separately. If a straight line is now drawn through the points c and b to its intersection with the hypotenuse " $SI + SII - x$ ", point J likewise does not give the degree of adsorption of either of the adsorbates. The point E' ; which is the point of intersection of the line cb , with the perpendicular OE dropped from the point E to the abscissa axis, has a different significance. The point E' divides OE into two parts, which represent the contents of the two adsorbates in 100 parts of the adsorption product: OE' represents the content of substance I, and EE' , the content of substance II.

To express the adsorption of each of the substances in terms of parts per 100 weight parts of hydrate, we proceed as described for the construction of the preceding diagrams; i.e., we draw straight lines from the H_2O vertex of the triangle through the points E and E' to their intersections with the perpendicular through the point x . The intercepts xG' and GG' represent the required values y and y' .

This method of graphical determination of the adsorption of two solutes is not the only one possible. For example, the problem may be solved in stages, the adsorption of each adsorbate being found by means of a separate diagram. For example, to determine the adsorption of solute I (y), the values of c , b , and a recalculated

SI + SII

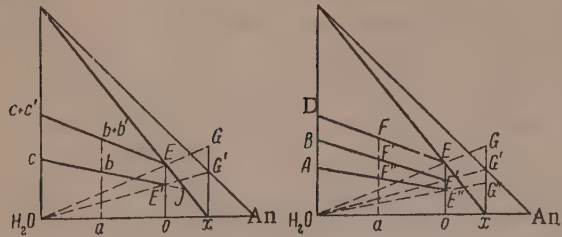


Fig. 4.

SI + SII + SIII

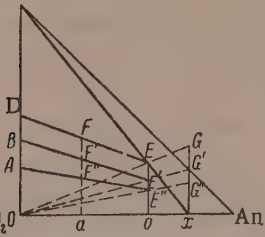


Fig. 5.

by means of Formulas (8), (9), and (10) are plotted in the triangular diagram (Fig. 2). Here the ordinate of the point \underline{c} is $c_2 = 100c/(100-c')$, while the ordinate and abscissa of the point F are respectively $b_2 = 100b/(100-b')$ and $a_2 = 100a/(100-a')$. The vertex S of the triangle now represents 100% SI. The intercept xG gives the required value of \underline{y} . For determination of the adsorption of substance II, the values of c' , b' , and a' are recalculated by Formulas (8 a), (9 a), and (10 a), and a triangular diagram is plotted from the results. If the same Fig. 2 is used, then the vertex S of the triangle corresponds to 100% SII; the ordinate of the point \underline{c} is c'_2 , and the coordinates of the point F are b'_2 and a'_2 .

Finally, the intercept xG in this case represents the adsorption \underline{y} of substance II.

The graphical method for determination of the adsorption of two substances may be applied to systems with a larger number of solutes. Analytical data for the system $\text{An}-\text{H}_2\text{O}-\text{SI}-\text{SII}-\text{SIII}$ are plotted in the diagram (Fig. 5) in the same way as for two adsorbed substances (Fig. 4).

In this diagram (Fig. 5) the point A corresponds to \underline{c} , the concentration of SI; the point B represents the sum of the concentrations of SI and SII, i.e., $c + c'$; the point D represents the total concentration of all three solutes, $c + c' + c''$. Similarly, the ordinate of F'' represents \underline{b} ; the ordinate of F' represents $b + b'$, and the ordinate of F, the sum of $b + b' + b''$. Straight lines are drawn through each pair of points, D and F, B and F' , and A and F'' . Only the line DF must be drawn to the intersection with the "hydrate-composition hypotenuse." The other lines are drawn only to their intersections with the perpendicular from the point E to the abscissa axis. Straight lines are drawn from the H_2O vertex through the points E, E', and E'' to cut the perpendicular from the point \underline{x} ; this gives the required values of \underline{y} , \underline{y}' , and \underline{y}'' .

Finally, the method of "component elimination" can be used in this case also. It is possible to find \underline{y} by the usual construction method if the values of c_3 , b_3 , and a_3 are calculated by means of Formulas (12), (13), and (14) and plotted on a triangular diagram. Similarly, it is necessary to calculate c'_3 , b'_3 , a'_3 , and c''_3 , b''_3 , a''_3 , in order to find \underline{y}' and \underline{y}'' . To determine the adsorption of each adsorbate by this last method, it is necessary to plot as many separate diagrams as there are solutes in the system.

SUMMARY

1. The method for determination of the adsorption of a solute on a hydrogel from analytical data for the solution and the mixture of the liquid and solid phases has been extended to systems with several solutes.
2. It is shown how the adsorption of each of several jointly adsorbed substances may be determined, whatever their contents in the solution; calculation formulas are derived for this purpose.
3. For determination of the adsorption of any one of several jointly adsorbed substances it is necessary to determine the concentrations of each solute in the solution and in the mixture of liquid and solid phases.
4. A graphical method is described for determination of the adsorption of one or several solutes adsorbed on a hydrogel.

LITERATURE CITED

- [1] P. T. Danil'chenko, J. Analyt. Chem. 2, 299 (1947).
- [2] P. T. Danil'chenko, Bull. Crimean Pedagogic Inst. 12, 5 (1947).
- [3] F. Schreinemakers, Z. Phys. Chem. 59, 641 (1907).
- [4] Rooseboom, Z. phys. Chem. 12, 367 (1893).

KINETICS OF PHASE SEPARATION IN PROTECTED EMULSIONS

S. G. Mokrushin and V. I. Borisikhina

The kinetics of phase separation in emulsions may be represented by the Lederer equation [1].

$$dV/dt = k(1 - V)V^{0.5}, \quad (1)$$

where dV/dt is the rate of phase separation in the emulsion; k is the rate constant for phase separation; V is the relative volume of the separated oil (the initial volume of the oil being taken as unity). The integral form of Equation (1) is

$$k = \frac{1}{t} \lg \frac{1 + \sqrt{VV}}{1 - \sqrt{VV}}. \quad (2)$$

We took numerical values of the constant k as a measure of the stability of emulsions stabilized by emulsifiers consisting of organic dyes.

Phase Separation Constants of Benzene Emulsions in Water Protected by Various Dyes

Dyes	t, sec	V_n , ml	V , ml	k , sec ⁻¹
Congo Red	180	3,0	0,12	0,0016
	240	4,4	0,17	0,0016
	300	5,2	0,21	0,0014
	360	6,3	0,25	0,0013
	420	7,2	0,29	0,0012
	480	7,8	0,31	0,0011
	540	8,6	0,34	0,0011
	600	9,7	0,38	0,0011
Methyl Violet	240	11,5	0,40	0,00298
	300	13,5	0,54	0,00272
	360	16,0	0,64	0,00265
	420	18,0	0,72	0,00259
	480	20,0	0,80	0,00261
	540	21,5	0,86	0,00262
	600	22,5	0,90	0,00263
	40	7,0	0,28	0,012
Methyl Green	60	13,0	0,52	0,013
	80	15,8	0,61	0,010
	100	18,0	0,72	0,010
	120	20,0	0,80	0,010
	140	22,0	0,88	0,010

According to Rebinder and his associates [2,3] the most powerful and universal stabilizers are substances which cover the emulsion droplets by protective gel-like films with structural properties which prevent coalescence of the droplets. Dyes, which have the properties of colloids and are dipolar in character, form protective films which stabilize the emulsion droplets. Similar films formed by dyes were observed by Nakagaki [4] in the preparation of stable foams.

In the present investigation * o/w emulsions were prepared from freshly distilled water and benzene in 3:1 ratio. The emulsifiers were 0.01% aqueous solutions of the following dyes: Congo Red, Methyl Green, and Methyl Violet. The emulsification was performed by the method of shaking in a closed cylinder, as described by Briggs [5].

The variation of emulsion stability with the concentration of the emulsifier (Congo Red) is shown in Fig. 1. It follows from Fig. 1 that the stability of the emulsion increases, i.e., the amount of benzene separating out decreases, with increase of the amount of dye added. The experimental data for calculation of the rate constant (k) of phase separation in an emulsion made from 72 ml of distilled water, 25 ml of benzene,

*Student A. N. Torokin took part in the experimental work.

and 3 ml of dye solution are given in the Table. The initial volume of benzene (25 ml) is denoted by V_0 ; the volume of benzene separated out of the emulsion in t seconds is denoted by V_n ; the relative volume V is

$$V = V_n / V_0.$$

The variation of the rate constant with the amount of added emulsifier (dye) is plotted in Fig. 2.

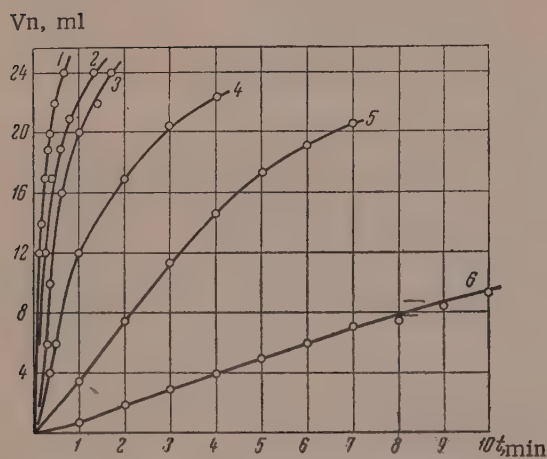


Fig. 1. Kinetics of phase separation of emulsions, with different amounts of added 0.01% Congo Red solution:
1) without addition; 2) with 0.1 ml of Congo Red; 3) with 0.2 ml; 4) with 0.5 ml; 5) with 1 ml; 6) with 3 ml.

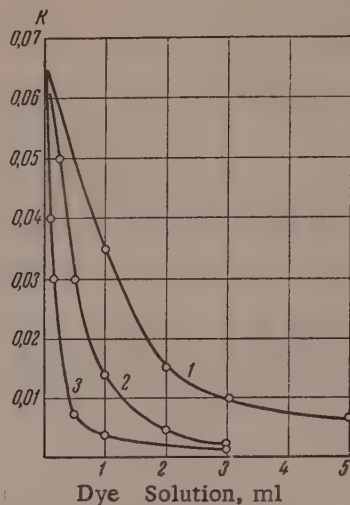


Fig. 2. Variation of the rate constant of phase separation with the amount (ml) of 0.01% solutions of the following dyes:
1) Methyl Green; 2) Methyl Violet; 3) Congo Red.



Fig. 3. Microphotographs of an emulsion stabilized by Congo Red:
a) during the first minutes after formation; b) 48 hours after formation.

Fig. 2 shows that the constant decreases with increasing concentration of the dyes in the emulsions, and that Congo Red has a greater emulsifying power than Methyl Violet or Methyl Green. The differences in the stabilizing power of the dyes diminish with increase of the amounts added; for example, the ratio of the rate constants for

Methyl Violet and Congo Red is 4.0 with 0.5 ml of dye, 3.6 with 1 ml, and 2.0 with 3 ml.

Fig. 3, a, is a microphotograph of an emulsion stabilized by Congo Red, during the first few minutes after its formation, and Fig. 3, b shows the same emulsion after 48 hours of standing. Fig. 3,b shows that fine droplets 10-20 μ in diameter are attached to the surfaces of large droplets of average diameter $\sim 100\mu$.

For the formation of stable emulsions, the amount of dye emulsifier should be not less than 1 g per 100 ml of emulsion; this is necessary for formation of ultrathin structurized films [6, 7]. The tendency of a dye to form a gel-like structure on the surface of the emulsion droplets depends on the colloidal properties of the dye. Congo Red has more pronounced colloidal properties than Methyl Violet or Methyl Green, and it therefore has a greater stabilizing effect.

SUMMARY

1. The stability of benzene-water emulsions stabilized by Congo Red, Methyl Violet, and Methyl Green can be characterized by the constant for the rate of phase separation in the emulsion, from the Lederer equation.
2. The Lederer constant decreases with increase of dye concentration in the benzene-water emulsion.
3. Microphotographs of stabilized emulsions clearly show the stages of their formation and breakdown.

LITERATURE CITED

- [1] E. L. Lederer, *Kolloid-Z.* 71, 61 (1935).
- [2] P. A. Rebinder, *Colloid J.* 8, 158 (1946).
- [3] P. A. Rebinder and K. A. Pospelova, introductory chapter to W. Clayton's *Theory of Emulsions and Their Technical Treatment* (Moscow, IL, 1950), p. 21 [Russian translation].
- [4] M. Nakagaki, *Bull. Chem. Soc. Japan* 22, 5, 200 (1949).
- [5] T. R. Briggs, *J. Phys. Chem.* 24, 120 (1930).
- [6] L. Ia. Kremnev and N. I. Kuibina, *Colloid J.* 17, No. 1, 36 (1955).
- [7] S. G. Mokrushin and T. P. Avilova, *Colloid J.* 16, No. 1, 45 (1954).

The S. M. Kirov Polytechnic
Institute of the Urals

Received June 3, 1957.

STUDIES OF ALUMINUM HYDROXIDE HYDROSOLS

4. THIXOTROPIC GELATION OF SOLS IN METHYL ALCOHOL-DIOXANE MIXTURES

P. V. Rufimskii

It was shown in an earlier paper [1] that ethyl alcohol is an effective structurizing agent for aluminum hydroxide hydrosols. Our experiments showed that methyl alcohol, in contrast to ethyl alcohol, does not cause thixotropic gelation of aluminum hydroxide sols. The purpose of the present investigation was to study the thixotropic gelation of aluminum hydroxide sols in dioxane-water and dioxane-methyl alcohol mixtures over a wide range of sol and additive concentrations, as it appears that determinations of this type have never been performed.

Aluminum hydroxide sol was prepared, as before, by Crum's method [2]; methyl alcohol (commercial) was dehydrated by boiling with methyl alcohol followed by two distillations; the dioxane was left to stand over solid caustic potash, distilled, boiled for a long time with metallic sodium, distilled off, and frozen out at 7-8°.

The properties of the methyl alcohol and dioxane used in the experiments are given in Table 1.

TABLE 1

Properties of Methyl Alcohol and Dioxane

Substance	Boiling point °C	Refractive index		Specific gravity	
		from tables	experimental	from tables	experimental
Methyl alcohol	64.5-55.0	1.33057	1.3307	0.7913	0.7915
Dioxane	101.3	1.4224	1.4221	1.0337	1.0335

The region of thixotropic gelation of the sol was determined, as in the case of electrolytes and ethyl alcohol, by the Rabinerson method [3] in conjunction with Dumanskii's [4] concentration-triangle method.

For determination of the region of thixotropic gelation, the aluminum hydroxide sol of maximum concentration was mixed with dioxane and water or with the alcohol and dioxane in volume proportions corresponding to definite compositions on the concentration triangle. The components were mixed in glass test tubes 7-8 mm in diameter and 6-7 cm long, which are convenient for visual observations of thixotropic systems. The total volume of the mixture in each experiment was 1 ml. The solution volumes were measured by means of a previously calibrated microburet. The experiments were performed at 21-23°.

Fig. 1,a represents the state of the system: Al_2O_3 sol ($c = 10.04 \text{ g/liter}$) $\text{C}_4\text{H}_8\text{O}_2-\text{H}_2\text{O}$ 24 hours after the reagents were mixed. Here I is the region of thixotropic gelation of the alumina sol; II is the region of lumpy gels; III is the region of unchanged sol. Alumina sol becomes thixotropic in presence of dioxane; thixotropic gelation may be observed with Al_2O_3 and $\text{C}_4\text{H}_8\text{O}_2$ contents in the mixture from 0.19 to 0.39 wt. % for Al_2O_3 , and from 60.53 to 60.66 wt. % for $\text{C}_4\text{H}_8\text{O}_2$. It should be noted that the alumina gel formed is typically thixotropic: when shaken, it liquefies instantly and becomes a sol, but the latter sets into a gel after a few seconds.

It is also noteworthy that after the gels have been kept in inverted tubes for only two or three days a "tongue" is formed, a clear exudate separates out, and the gel decreases considerably in volume, leaving a very thin film on the tube walls.

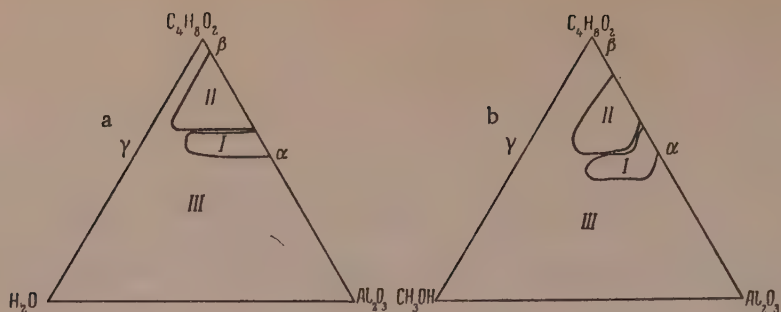


Fig. 1. Diagram for the thixotropic gelation of Al_2O_3 sol with a concentration of 10.04 g/liter in presence of dioxane (a) and methyl alcohol (b).

Al_2O_3 sols also undergo structurization in methyl alcohol-dioxane mixtures. The state of the sol 24 hours after addition of methyl alcohol is represented in Fig. 1,b. The component ratios (Region I, Fig. 1,b) in volume and weight percentages in the system: Al_2O_3 ($c = 10.04$ g/liter) - $\text{C}_4\text{H}_8\text{O}_2$ - CH_3OH are given in Table 2.

TABLE 2

Component Ratios in the System Al_2O_3 - $\text{C}_4\text{H}_8\text{O}_2$ - CH_3OH

Composition of mixture in ml (vol. %)			Composition of mixture in wt. %			
Al_2O_3	$\text{C}_4\text{H}_8\text{O}_2$	CH_3OH	Al_2O_3	$\text{C}_4\text{H}_8\text{O}_2$	CH_3OH	H_2O
40	60	-	0.39	60.56	-	39.05
40	50	10	0.40	51.67	7.91	40.02
30	50	20	0.31	52.81	16.18	30.70

Since the compositions of the mixtures represented in the concentration triangles (Figs. 1,a and 1,b) varied over wide limits, systems were made up in "extended" concentration triangles, which differed from the previous ones by covering narrower concentration ranges (they are denoted by, α , β , and γ in Figs. 1,a and 1,b). The state of the system in these cases is represented by Figs. 2,a and 2,b, where I is the region of thixotropic gelation of the alumina sol; III is the region of unchanged sol.

The composition of the "corner" solutions are given in Table 3.

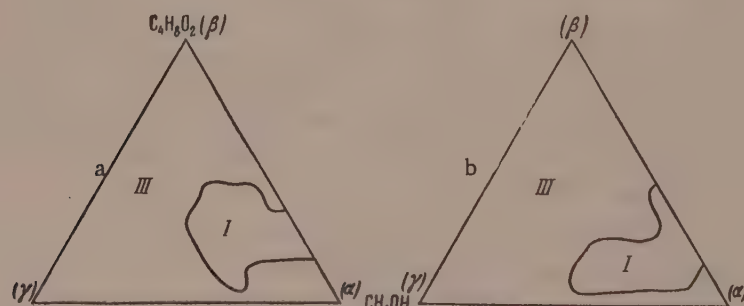


Fig. 2. Diagram for the thixotropic gelation of Al_2O_3 in the α , β , γ region (Fig. 1,a) 24 hours after addition of dioxane.

TABLE 3

Composition of Systems Represented in Figs. 2,a and 2,b

Corner of triangle	Concentration in wt. % (Fig. 2,a)			Concentration in wt. % (Fig. 2,b)			
	Al ₂ O ₃	C ₄ H ₈ O ₂	H ₂ O	Al ₂ O ₃	C ₄ H ₈ O ₂	CH ₃ OH	H ₂ O
Solution α	0.45	67.29	32.26	0.37	50.70	—	48.92
Solution β	0.20	80.45	19.35	0.38	50.00	—	49.62
Solution γ	0.20	60.73	39.07	0.24	62.18	16.47	31.11

SUMMARY

1. Aluminum hydroxide sol prepared by Crum's method undergoes thixotropic gelation on addition of dioxane, and in dioxane-methyl alcohol mixtures.
2. The qualitative aspects of the thixotropic gelation of alumina sols in presence of dioxane and in dioxane-methyl alcohol mixtures have been studied.
3. In addition to typical thixotropic gels, lumpy gels are also formed in presence of dioxane and in dioxane-methyl alcohol mixtures.
4. In the case of dioxane the region of thixotropic gelation is wider and is shifted in the direction of maximum concentration of the latter; the probable explanation is that methyl alcohol does not influence thixotropic gelation of alumina sols.

I am grateful to Professor, Doctor of Chemical Sciences A. F. Bogoliavenskii for his scrutiny of this paper.

LITERATURE CITED

- [1] P. V. Rufimskii, Colloid J. 18, No. 3, 332 (1956).*
- [2] M. Aschenbrenner, Z. phys. Chem. 127, 416 (1927).
- [3] A. I. Rabinerson, Trans. Leningrad Chem. Tech. Inst. 3, 67 (1935).
- [4] A. V. Dumanskii, J. Gen. Chem. 62, 1649 (1930); Progr. Chem. 1, 290 (1930); Bull. State Sci. Res. Inst. Colloid Chem., Voronezh, No. 1, 5 (1934).

The Ul'ianov-Lenin State University, Kazan'
Faculty of Chemistry

Received April 25, 1957.

*Original Russian pagination. See C. B. translation.

SEDIMENTATION OF A MAGNESIUM HYDROXIDE SUSPENSION IN AN ULTRASONIC FIELD

N. I. Soboleva, A. G. Bol'shakov, and A. V. Kortnev

Much attention has been devoted in recent years to applications of ultrasonics in physical and colloid chemistry; for example, for dispersion of liquids and solids in various media by the action of an ultrasonic field [1-3], sedimentation of aerosols and coagulation in hydrosols [1,3-5], liquefaction of thixotropic gels [9], activation of oxidation processes [10], acceleration of hydrolysis reactions [11], etc.

An ultrasonic field may have both a dispersing and a coagulating effect on a colloidal system; the experimental conditions determine which of these processes predominates. For example, Sollner [12] attributes the existence of a concentration limit in an aqueous emulsion of mercury made by the ultrasonic method to the fact that during prolonged exposure under given conditions (constant power and frequency of the ultrasound) coagulation begins to proceed at a higher rate than dispersion. Urazovskii and Polotskii [13] suggested that there is an optimum power (and exposure time) for successful dispersion of solids in liquids; if this is exceeded, the sol formed subsequently coagulates. Gilling [14] considers that coagulation requires less energy than dispersion, where a definite minimum is required to produce cavitation. The coagulation rate under the influence of ultrasonics also depends on the particle size of the disperse system. In coarsely disperse systems (suspensions and emulsions) orientation, accumulation, and coagulation of particles in an ultrasonic field is readily observed [3]. Hermans [5] studied the coagulation of AgI sols by electrolytes; the process was accelerated considerably in an ultrasonic field. In absence of electrolytes AgI sols were stable both in the ultrasonic field and outside it.

The mechanism of ultrasonic action on colloidal systems is not yet fully understood. Of all the effects accompanying the action of ultrasonic waves on aqueous solutions, many authors attach most importance to cavitation and the agitation effect. Much importance is attached to cavitation in explanations of the chemical action of ultrasonic waves (activation of molecules), whereas the physicochemical processes accompanied by changes in the state rather than of the properties of a substance are predominantly influenced by the agitating effect of ultrasonic waves (instantaneous powerful accelerations in the liquid microlayers).

In this investigation we studied the sedimentation kinetics of $Mg(OH)_2$ suspensions of various concentrations in a wide range of frequencies. The separation of amorphous precipitates such as $Mg(OH)_2$ or $Al(OH)_3$ in industrial practice is a very lengthy process which requires a large volume of equipment. Therefore acceleration of the sedimentation process and improvement of the structure of precipitates for easier filtration are of great importance for intensification of technological processes of this type.

The object chosen for the investigation was the system: $MgCl_2-NaOH-Mg(OH)_2-NaCl$ under approximately the conditions of brine purification in soda ash manufacture.

The ultrasonic source was a piezoelectric quartz ultrasonic generator of ~350 watt power. Its circuit diagram is given in Fig. 1. The ultrasonic oscillators were quartz plates with natural vibration frequencies of 300, 450, 600, 950, 1500 and 2000 kilocycles/second. The high-frequency oscillator was of the Hartley type, with self-excitation in the GK-3000 oscillator tube. The rectifier circuit was of the full-wave type with four VG-129 gas rectifiers. The high-tension oscillator feed was 3000 v. Changes of frequency range in the operation of the generator were effected by changes of circuit coils, while the generator was tuned to the required frequency by means of a variable capacitor and, in some instances, by the connection of an additional fixed capacitor.

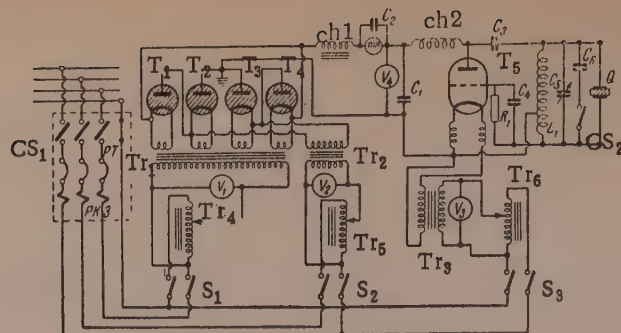


Fig. 1. Circuit diagram of ultrasonic generator:
 T₁, T₂, T₃, T₄) VG-129 gas rectifiers; T₅) GK-3000 tube;
 Tr₁) rectifier tube filament transformer; Tr₂) high-tension
 transformer; Tr₃) tube filament transformer; Tr₄, Tr₆)
 LA TR-2 autotransformers; Tr₅) LATR-1 autotransformer;
 Ch₁) low-frequency choke; Ch₂) high-frequency choke;
 C₁) smoothing-filter capacitor; C₂) shunt capacitor; C₃)
 coupling capacitor; C₄) tube supply-line capacitor; C₅)
 variable capacitor for oscillatory circuit; C₆) supplement-
 ary capacitor; R₁) 2000-ohm resistance; L₁) inductance
 coil of oscillatory circuit; Q) quartz oscillator.

Circular X-cut piezoelectric quartz plates of two sizes were used: for frequencies of 300, 450, and 600 kc the diameter was 35 mm; for frequencies of 950, 1500, and 2000 kc, it was 20 mm.

The holders for the 35 mm quartz plates were made from Plexiglas, with an air gap under the lower brass electrode. The upper electrode was a brass ring pressed against the quartz plate by means of spring clamps. The thickness of the lower electrode was strictly determined by the natural frequency of the quartz plate. This type of holder design ensures maximum supply of the ultrasonic power into the medium under investigation. The holders for the 20 mm quartz plates were constructed on the same principle, but porcelain plates served as the bases of the holders.

The experiments were performed in an ordinary 1-liter beaker fitted with a special lid and a Plexiglas insert to keep the quartz holder and the tubes with the solution stationary. The solution was put into test tubes with ground-glass bottoms, which ensured the maximum possible transfer of sonic energy into the system. A circulation cooling system was provided for the experimental vessel in order to maintain a constant temperature ($\pm 2^\circ$) during each experiment.

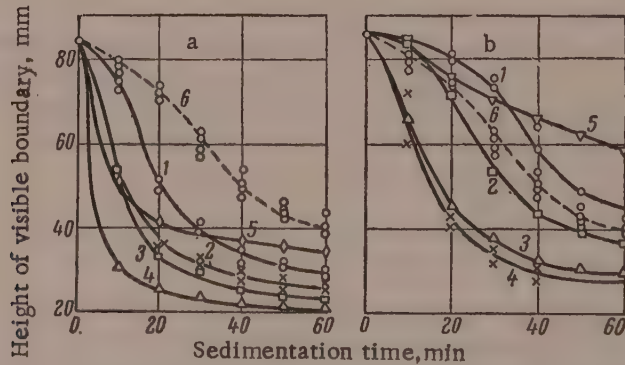


Fig. 2. Effect of ultrasonic vibrations on sedimentation of magnesium hydroxide from a solution containing 6.61 g MgCl₂/liter.

Solution No. I, ultrasonic frequencies: a) 1500 kc; b) 450 kc; exposure times: 1) 0.5 minutes, 2) 1 minute, 3) 3 minutes, 4) 5 minutes, 5) 10 minutes; 6) control experiment.

The ultrasonic generator was first switched on and tuned, and the feed voltage, anode current, and anode voltage were checked. A frequency meter was also switched in to check the tuning of the generator to the required frequency. Stable operation of the generator was indicated by the shape and size of an oil fountain, which reached a height of 5-7 cm for a maximum output of sonic energy.

10 ml of the $MgCl_2$ solution was mixed with the same volume of NaOH solution and placed in the ultrasonic field. The duration of the exposure time was measured by means of a stop watch. At the end of the exposure the test tube with the solution was fixed in a clamp and the height of the $Mg(OH)_2$ precipitate, which was used as a measure of the sedimentation rate was measured every 10 minutes after the end of the exposure.

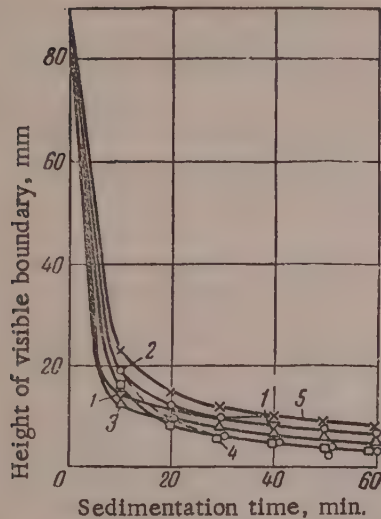


Fig. 3. Effect of ultrasonic vibration on sedimentation of magnesium hydroxide from a solution containing 0.86 g $MgCl_2$ /liter.

Solution No. 5; ultrasonic frequency 1500 kc, exposure times: 1) 0.5 minutes, 2) 1 minute, 3) 3 minutes, 4) 5 minutes, 5) 7 minutes. The curve for the control experiment coincides with Curve 2.

Cities. The ultrasonic frequencies were 300, 450, 600, 950, 1500 and 2000 kc.

The anode potential of the generator tube varied from 2200 to 2800 v, and the anode current was 100-120 ma.

Figs. 2, 3, and 4 show that the general character of the curves is the same for all the solutions studied. It follows from Fig. 2 that the sedimentation rate of $Mg(OH)_2$ is greatest under the influence of an ultrasonic field for 5 minutes, whereas exposure for half a minute has little effect on the sedimentation of $Mg(OH)_2$. With prolonged action of the ultrasonic field on this suspension the dispersion process prevails over coagulation, and the precipitate, consisting of finer particles, entrains a larger mass of solution and so occupies a greater volume.

The curves for solutions of low concentration (Fig. 3) almost coincide, but nevertheless it may be seen that during the initial period (10 minutes of sedimentation time) Curve 4 lies below the others, although its further course indicates that the sedimentation of $Mg(OH)_2$ is accelerated in comparison with the control experiment.

The relationship between the ultrasonic frequency and the sedimentation of $Mg(OH)_2$, plotted in Fig. 4, indicates that at 450 kc dispersion of the precipitate takes place in all the solutions (the numbers marked along the ordinate axis represent the values for control experiments). For most of the solutions the least layer height is obtained at 1500 kc. This is probably the most favorable frequency for acceleration of the sedimentation of $Mg(OH)_2$ suspensions from these solutions.

During the first few seconds of exposure the solution became deaerated in all the experiments; gas bubbles were formed along the entire liquid column in the tube, rose to the surface, and vanished.

Control experiments were performed simultaneously with the same $MgCl_2$ and NaOH solutions which had not been exposed to ultrasonic vibrations. The height of the $Mg(OH)_2$ precipitate was measured at 10-minute intervals after the solutions had been mixed.

During the operation of the ultrasonic generator part of the sonic energy is absorbed by the transformer oil and the test solution and is converted into heat. In our experiments the maximum temperature rise for 300 cc of transformer oil without cooling was 12-13° in 7 minutes. With the use of the cooling system the temperature increase was 2-3° in 7 minutes of exposure. The sonic energy emitted by 1 cm^2 of the quartz plate can be determined calorimetrically. In our experiments it was found to be 5 watts/ cm^2 at 2000 kc.

The sonic power calculated from the electrical characteristics of the generator was 8.4 watts/ cm^2 at 2000 kc and 3.4 watts/ cm^2 at 300 kc.

The choice of the concentration of the original magnesium chloride solution was based on the values met in industrial practice. The magnesium chloride solutions used contained 6.61, 5.53, 3.31, 1.69, 0.86 and 0.43 g of $MgCl_2$ per liter of solution. Each solution was exposed for 0.5, 1, 3, 5, and 7 minutes to ultrasonic vibrations of different frequencies.

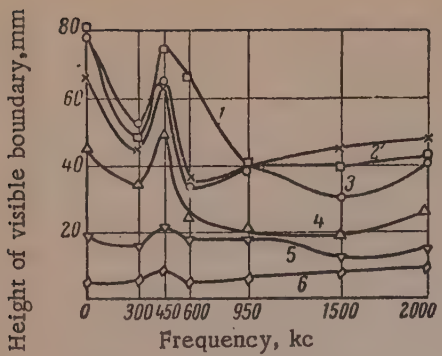


Fig. 4. Effect of ultrasonic frequency on the sedimentation of $\text{Mg}(\text{OH})_2$. Exposure time 5 minutes, sedimentation time 10 minutes: solutions: 1) No. 1; 2) No. 2; 3) No. 3; 4) No. 4; 5) No. 5; 6) No. 6 (20 minutes).

Solutions of different concentrations exhibit different behavior in the ultrasonic field. The influence of ultrasonic vibrations is most prominent in solutions containing 6.61, 5.83, and 3.31 g MgCl_2 per liter (Fig. 5).

The curves for dilute solutions differ very little from each other, and in most cases lie above the curve for the control experiment; i.e., ultrasonic vibrations cause only a slight dispersion of the precipitate and do not accelerate sedimentation.

The graphical data can be used for determination of the average sedimentation rate of $\text{Mg}(\text{OH})_2$ suspensions and for comparison of the particle radii in suspensions exposed to an ultrasonic field with the particle radii in untreated suspensions. On the assumption that the suspension is mono-disperse, that the particles are spherical, and that the sedimentation proceeds at average velocity v , the particle radius can be calculated from the formula [15]:

$$r = \frac{3}{\sqrt{2}} \sqrt{\eta v / (D - d)} g,$$

where η is the viscosity of the suspension; D is the density of the solid phase; d is the density of the liquid phase; g is the acceleration due to gravity. For the suspension in question $r = 0.008 \sqrt{v}$.

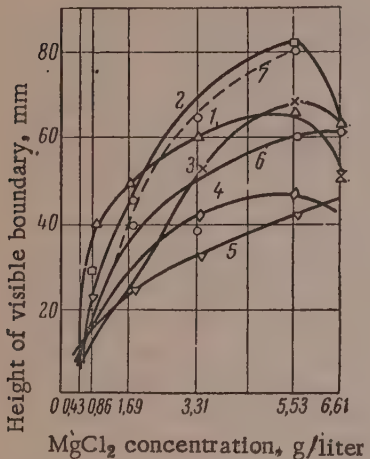


Fig. 5. Effect of concentration of the MgCl_2 solution on the sedimentation of $\text{Mg}(\text{OH})_2$. Exposure time 3 minutes, sedimentation time 10 minutes, frequencies: 1) 300 kc, 2) 450 kc, 3) 600 kc, 4) 950 kc, 5) 1500 kc, 6) 2000 kc, 7) control experiment.

The values given in the Table correspond to experiments in which the greatest increases in the sedimentation rate of $\text{Mg}(\text{OH})_2$, in comparison with the control experiments, were observed for the given solution. The different effects of ultrasonic vibrations on the sedimentation of $\text{Mg}(\text{OH})_2$ from solutions of different concentration can evidently be attributed to differences in the particle sizes of the suspensions formed. Particles of different sizes vibrate differently in the ultrasonic field. The natural vibration frequency of the particles in the suspension, which is related to their size, may coincide with the frequencies of the forced vibrations caused by the ultrasonic field. In that case the vibration amplitude may increase so much as to exceed the distances between the particles. Increased collisions between the particles in the suspension leads to their growth, and the sedimentation rate of the suspension increases accordingly.

Large particles in solutions of low MgCl_2 concentration settle so rapidly that any appreciable influence of the ultrasonic field cannot be detected. In concentrated solutions, on the other hand, a fine suspension of $\text{Mg}(\text{OH})_2$ is formed; these fine particles vibrate under the influence of the ultrasonic field, collide, and form large aggregates which settle much more rapidly than the original particles.

A frequency of 1500 kc, in the range investigated, proved favorable for acceleration of the settling of an $\text{Mg}(\text{OH})_2$ suspension containing particles $\sim 1 \mu$ in size. In the other cases the particles apparently did not follow the vibrations of the medium and therefore did not increase in size.

Solu- tion No.	Untreated		Exposed to ultrasound				Relative in- crease of particle radius %
	sedimenta- tion veloci- ty, mm/sec	particle radius, μ	frequency kc	duration of treatment in min	sedimenta- tion velocity, mm/sec	particle radius, μ	
1	0,0128	0,90	1500 2000	5	0,0916	2,42	170
2	0,0141	0,94	950 2000	5	0,0750	2,19	133
3	0,0350	1,49	1500 1500	7	0,0833	2,30	54
4	0,0666	2,06	950	5	0,1083	2,64	28
5	0,1166	2,72	1500	5	0,1216	2,78	2,2
6	0,1333	2,92	1500	1	0,1333	2,92	0

SUMMARY

1. An ultrasonic piezoelectric quartz unit operating over a wide range of frequencies at ~350 watts has been designed and constructed.
2. The sedimentation of magnesium hydroxide suspensions in an ultrasonic field was studied at frequencies of 300, 450, 600, 950, 1500 and 2000 kc, with exposure times of 0.5, 1, 3, 5, and 7 minutes. The concentrations of the original $MgCl_2$ solutions were 6.61, 5.53, 3.31, 1.69, 0.86 and 0.43 g/liter.
3. An ultrasonic field has two effects on the sedimentation of $Mg(OH)_2$: in some conditions the sedimentation of $Mg(OH)_2$ suspensions is accelerated (frequency 1500 kc, exposure time 5 minutes, $MgCl_2$ concentrations 6.61, 5.53 and 3.31 g/liter), while in other conditions the precipitate undergoes dispersion and the sedimentation time of $Mg(OH)_2$ increases (frequency 450 kc, exposure times 0.5 and 7 minutes, $MgCl_2$ concentrations 1.69, 0.86, and 0.43 g/liter).

LITERATURE CITED

- [1] Bergmann, Ultrasonics (IL, 1956) [Russian translation].
- [2] S. N. Rzhevkin and E. P. Ostrovskii, J. Phys. Chem. 6, 73 (1935).
- [3] Söllner, Colloid Chemistry, Edited by J. Alexander, V. 5, (1944), pp 337-373.
- [4] D. Thompson, Chem. Eng. Progress 46, 1, 3-6 (1950).
- [5] J. J. Hermans, Rec. trav. chim. Pays-Bas 58, 139 (1939).
- [6] A. P. Kapustin, J. Tech. Phys. 20, 10 (1950).
- [7] A. P. Kapustin, J. Tech. Phys. 22, 5 (1952).
- [8] A. I. Berlaga, J. Exp. Theoret. Phys. 16, No. 7, 647 (1946).
- [9] B. B. Kudriavtsev, Application of Ultrasonic Methods in Physicochemical Investigations (GITTL, 1952). *
- [10] I. G. Polotskii, J. Gen. Chem. 17, 4 (1947).
- [11] O. S. Stepanova, Trans. Odessa State Univ. 21, 15, coll. Chem. Faculty, vol. 2 (1952), p. 191.
- [12] Söllner, Bondy, Trans. Faraday Soc. 32, 616 (1936).
- [13] S. S. Urazovskii and I. G. Polotskii, Colloid J. 6, No. 9, 779 (1940).
- [14] D. Gilling, Chem. Prod. 7, 11, 69 (1944).

*In Russian.

[15] I. I. Zhukov, Colloid Chemistry [in Russian] (Leningrad State University Press, 1949).

The Odessa Polytechnic Institute

Received April 13, 1957.

INVESTIGATION OF BOUNDARY FRICTION AND ADHESION, IN RELATION
TO STUDIES OF THE INTERACTION OF FINELY DISPERSED PARTICLES

1. CERTAIN BOUNDARY PROPERTIES OF SOLUTIONS IN NARROW PLANE
GAPS BETWEEN SOLID SURFACES

G. I. Fuks

Friction and adhesion of solids in liquids are usually determined in order to study the lubricating action of the latter and to select lubricating oils for machines and instruments. However, such measurements can also be used in modeling of particle interaction in suspensions and colloidal solutions [1]. The nature and magnitude of the forces acting between the particles determine the stability of disperse systems [2, 3] and have a very significant influence on their structuromechanical properties [4, 5]. Studies of these forces constitute one of the important problems of colloid chemistry.

Whereas important results have recently been obtained in the development of a theory of particle interaction (for reviews, see [3, 6, 7]), the number of experimental investigations in this field is not large. Information of the influence of various factors on the strength of bonds between particles is mainly based on indirect and incomplete data, such as the values of the electrokinetic potential.

The binding force between two colloidal or microscopic particles in a supermicellar structure is so small that it has not yet been measured directly, by mechanical methods.*

The strength and nature of the bonds between like particles may differ [9, 10]. Under such conditions dimensional modeling becomes of great significance.

Constancy of the numerical values of dimensionless characteristics is a necessary and sufficient condition of mechanical similarity between an object and its model [11]. Either of two postulates may be used in the modeling of bonding between particles of disperse systems in liquid dispersion media: 1) a bond arises in consequence of the resistance of the liquid to relative displacement of the particles; 2) particle interaction results in an elastic bond, the breakdown of which requires the application of a critical stress.

The first, hydrodynamic modeling method is based on investigations of the flow of a liquid into a gap between solids, and of shear of solids separated by a liquid layer. Dimensional analysis shows that the resistance force W exerted by a liquid on a body moving in it is given by the expression:

$$W = \rho l^2 V^2 f(\alpha, R), \quad (1)$$

where ρ is the density; l are the linear dimensions (not less than two); V is the average velocity; α is the angle of direction of the velocity; R is the Reynolds number. For motion characterized by low Reynolds numbers (creep motion) the value of ρ , which represents inertia, may be disregarded (see [11, 12] for fuller details), and Expression (1) then becomes:

*The force of adhesion of a quartz particle 3μ in size to a quartz plate in water is between 0.02 and 0.90 micro-dyne, according to the purity of the water and the time of contact [8].

It follows from Equation (2) that the model must be geometrically similar to the particles under investigation, and the rate of bond rupture is low. Real highly-disperse particles have very diverse and often irregular shapes. However, there are adequate grounds for assuming that, on the average, microscopic particles are geometrically similar to highly disperse particles of the same composition and structure [13]. This justifies the modeling of coagulation and structure formation by investigation of the adhesion of microscopic particles to plates [8, 14], whereby it is possible to study the influence of contact time, surface inhomogeneity of the particles and certain other factors on the interaction.

The modeling of elastic bonds arising between particles is of interest in relation to the rheology of disperse systems. In this case the model and the object are mechanically similar if the following three dimensionless characteristics coincide: $\mu; E/\rho gl; P/EI^2$, where E is a measure of rigidity (in the case of a homogeneous system it is its elasticity modulus), μ is the Poisson ratio, $\gamma = \rho g$ is the specific gravity, and P is the load. The critical stress τ_{cr} which breaks the bond has the same dimensions as E , the ratio τ_{cr}/E is dimensionless, and

$$\tau_{cr}/E = f(\mu, E/\rho gl, P/EI^2). \quad (3)$$

μ varies within relatively narrow limits, the difference between the specific gravities of the disperse particles and the dispersion medium is usually not very large, and therefore the main condition of similarity is constancy of P/EI^2 . Estimation of E for the object is the most difficult problem in modeling of the bond between two particles.

Elastic and, to a smaller degree of accuracy, incompletely elastic bonds can be regarded as similar if they have equal stress-concentration ratios, i.e., equal ratios of maximum to mean stress [15, 16], but the contact area must be known for this method of modeling. If the bond is not completely elastic and does not break instantaneously, which is the case in real disperse systems (see below and also [8]), then the modeling conditions include a time factor; for Newtonian liquids it is proportional to their viscosity.

Deragin [17] has developed a general phenomenological theory of adhesion, from which it follows that the following relationship holds between the adhesion force F_a between two bodies, the energy of interaction U between plane surfaces of these bodies in the same medium, the gap h between their surfaces, and a geometrical factor Ω

$$F_a = \Omega U f(h), \quad (4)$$

where Ω is determined by the shape of the gap near its minimum width, and is expressed in terms of the radii of curvature of the two surfaces

$$U f(h) = \int_h^\infty P_r(H) dH, \quad (5)$$

where P_r is the disjoining pressure [18] and H is the thickness of the plane-parallel gap.

Analysis of similarity conditions shows that either geometrically similar bodies or bodies of simple shape must be used for modeling of particle interaction. In the latter case it is possible to verify the laws which follow from hydrodynamics and the theory of elasticity. The same analysis also shows that the most important factors in modeling are the distance between the particles and between the elements of the model, the interaction time, and the properties of the dispersion medium.

The present communications contain the results of determinations of forces of interaction between solids of simple geometrical form, with plane and convex contact surfaces, in aqueous electrolyte solutions, mineral oils and hydrocarbons, and solutions of surface-active substances. Adhesion experiments were used for studies of

*This equation is one statement of Stokes' law. Substitution for a sphere: $f(\alpha) = \text{const} = 6\pi$ gives the usual expression of this law. It may be shown by means of hydrodynamics that if the inertia terms in the Navier-Stokes equation are disregarded, Stokes' law is valid for bodies of any shape.

normal forces of interaction, and friction experiments for tangential forces. The first communication describes certain specific boundary effects detected in the separation and approach of plane-parallel circular disks in the liquids studied. These effects were used to characterize the boundary properties of solutions and lubricating oils in narrow gaps between solids.

Method. According to Stefan and Reynolds [19], the time t of approach or separation of plane-parallel circular disks in a liquid of viscosity η is given by the equation

$$t = \frac{3\pi r^4 \eta}{4F} \left(\frac{1}{h_1^2} - \frac{1}{h_2^2} \right), \quad (6)$$

where r is the disk radius; h_1 and h_2 are the initial and final distances between them; F is the normal force. This equation has a strict theoretical basis [19, 20] and has been verified experimentally for wide gaps by a number of workers [21, 22], including the present author [23]. If $h_2 \gg h_1$, then Equation (6) may be written:

$$t = 3\pi r^4 \eta / 4Fh_1^2. \quad (7)$$

Transferring the liquid flow characteristics η and F to the left-hand side of the equation, dividing through by the disk area S , and denoting the specific force F/S by σ , we have:

$$t\sigma / \eta = 3\pi r^4 / 4h^2 S = \psi. \quad (8)$$

The product $t\sigma$ has the dimensions of viscosity, and $t\sigma/\eta$ is a dimensionless coefficient. Derived on the basis of somewhat different considerations [23], this coefficient was termed the coefficient of boundary thickening and denoted by the symbol ψ .

In the previous communication [24] a method was described for determination of the approach and separation times of plane-parallel disks to an accuracy of 0.01 second, and of the gap between them, 20μ and over in width, to an accuracy of 0.02-0.04 μ . Disks from 2 to 18 mm in diameter were made from U10 steel, quartz, and synthetic ruby; they were polished to Class 14 finish and ground against each other. The enlarged image in the Linnick interference microscope showed that almost all the microheterogeneities ($H_{av} < 0.03\mu$) were directed into the disks. A special device was used for keeping the disks strictly parallel in approach and separation (under forces from 0.0 to 8 kg/cm²).

The disks were completely immersed in the liquid, and steps were taken to remove dust and air from the space between them. The liquid was kept at constant temperature (within $\pm 0.1^\circ$).

The gap between the disks, and its variations, were read off from the scale of a mirror galvanometer included in a capacitance bridge. One of the arms of the bridge consisted of the separable plates of a plane capacitor, the distance between which varied in proportion to the gap between the disks. The galvanometer scale was calibrated by direct measurement of the distance between the disks by means of a horizontal microscope and an Uverskii interferometer. The distance between the disks pressed against each other under the given load in air was taken as zero. The disks were first washed repeatedly in the distilled solvents and rubbed over three times with powdered activated charcoal. The quartz and ruby were heated strongly. The liquids used were filtered before the determinations.

Approach of plane-parallel disks. A pressure which forces the liquid out of the gap arises between plane-parallel disks approaching each other. In streamline flow of a Newtonian liquid, under conditions such that wall slippage may be disregarded, the pressure P at a point x is given by the following expression [25]

$$P_x = 3\eta V (r^2 - r_x^2) / h^3, \quad (9)$$

where V is the approach velocity of disks of radius r ; r_x is the distance from the disk center. Hence the maximum pressure at the disk center is

$$P_{max} = 3\eta V r^2 / h^3. \quad (10)$$

A parabolic velocity distribution is established along the radius. Simple geometrical considerations show that the average flow velocity \bar{v} and the maximum rate of shear of the liquid S_{max} conform to the following relationships:

$$\bar{v} = rV / 2h, \quad (11)$$

$$S_{\max} = 3rV / h^2. \quad (12)$$

TABLE I

Dynamic Parameters of Liquids in Gaps Between Approaching Disks, Calculated from Equations (10-12) for Experiments of Fig. 1.

Liquid	Disks	Normal load, kg/cm ²	Start of measurement				Decrease of disk displacement				
			initial gap, μ	time interval, min	$V \cdot 10^8$, cm/sec	P_{\max} , kg/cm ²	$\bar{v} \cdot 10^4$, cm/sec	S_{\max} , sec ⁻¹	initial gap/ μ	time interval, min	
2	0,01 N NaCl	0,2	0,46	1-5	6,7	7,4	4,4	54	0,18	10-30	0,33
5	The same	4,0	0,24	5-40	4,7	55	6,8	192	0,07	20-30	0,17
1	Transformer oil	0,2	0,55	0,5-1	13,3	180	6,1	61	0,18	45-60	0,22
r = 5 mm	Steel										
4	The same	4,0	0,45	1-10	6,3	156	3,5	47	0,10	30-45	0,07
3	The same + 0,05% of stearic acid	4,0	0,43	1-10	6,0	169	3,5	49	0,15	10-30	0,24
	Quartz										
	$r = 6$ mm										

It follows from Equation (7) that at a steady velocity the gap between approaching disks must be inversely proportional to the square root of the contact time. Fig. 1 shows the results obtained in measurements of the rate of approach of disks separated by turbine oil and NaCl solution. The calculated dynamic parameters of the liquids for these experiments are given in Table 1. The measurements were started 60 to 300 seconds after the start of each experiment, as reliable results could not be obtained after shorter intervals.

The initial regions of the curves in Fig. 1 show that during the first period the flow of the liquids is represented, to some degree of approximation, by Equation (6). The calculated and experimental values for the approach velocity of the disks coincide in order of magnitude; for example, for the experiment represented by Curve 1 the theoretical time required for the gap to decrease from 0.55 to 0.51 μ is 90 seconds, while the experimental value is 65 seconds. With increasing approach of the disks the velocity diminishes and there are sharp deviations from Equation (6). For the same experiment the theoretical time required for the gap to decrease from 0.20 to 0.19 μ is 46 seconds, while the experimental value is 900 seconds. Variations of the maximum pressure between the disks in their approach are given in Table 1.

The mutual approach of the disks ceases before all the liquid between them has been displaced (horizontal regions of the curves in Fig. 1). One half of the layer retaining a constant thickness during the experiment (up to 24-30 hours) is termed the residual or minimum layer, and its thickness is denoted by h_{\min} .

The deviations from the Stefan-Reynolds law in our experiments were not the consequence of the disks not being parallel; if this was so, the approach velocity and the effective specific contact pressure would increase [1]. Neither can this effect be due to roughness of the disk surfaces. The height of the crests of the surface microirregularities is considerably less than the distance between the disks at which a viscosity increase and the presence of a residual boundary layer are observed. Microroughness is taken into account by determination of the "zero" gap in contact of the disks in air. Finally, the effect between any one pair of disks depends very much on the composition of the liquid. No residual layers of benzene or cyclohexane were observed on quartz at pressures of 40 g/cm² and over, or of isoctane and cyclohexane on steel at pressures above 1000 g/cm². *

*Dow [22] found that an appreciable correction for disk roughness must be introduced into the Stefan-Reynolds equation. For his glass disks the correction was 15 μ . However, disks with surface crest 7.5 μ high are not polished but coarsely ground (Class

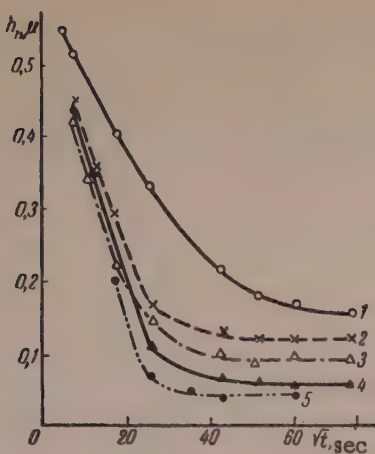


Fig. 1. Variation of the gap h_1 between plane-parallel quartz (2 and 5) and steel (1, 3 and 4) circular disks with the contact time t : 1, 2) normal pressure 0.2 kg/cm^2 , 3, 4, and 5) 4.0 kg/cm^2 . Liquids between disks: 2, 5) 0.01 NaCl solution; 1, 4) transformer oil; 3) 0.01% solution of stearic acid in transformer oil.

h , the $h = f(1/\sqrt{t})$ curves become more nearly linear although the approach velocity still diminishes at very small gap widths.

On the assumption that the boundary properties of a liquid are manifested by the difference between its surface and volume mechanical properties, the thickness of the boundary layer can be found by estimation of the gap width at which the linear relationship between h and $t^{-1/2}$ breaks down. Some of these results are given in Table 2; they show that the thickness of the boundary layer is not constant but depends on the properties of the liquid, and it may be influenced by the temperature and flow velocity, and also by the properties of the solid.

The residual layer. The approach (and separation) velocity of the disks is strongly dependent on their radius, but the thickness of the residual layer remains constant, with the limits of experimental error, for disks of different diameters (Table 3). The value of h_{\min} is determined by the composition of the liquid, the disk material, the specific normal pressure, and the temperature.

TABLE 2
Thickness of Boundary Liquid Layers, Measured by the Disk Approach Method
($h_b = h/2$, at which the linear relationship between h and $t^{-1/2}$ breaks down)

Liquid	Disks	Temperature, °C	$\bar{V} \cdot 10^6$, cm/sec	h_b, μ
Transformer oil fraction	Steel	20	1,40	0,14
$\nu_{20} = 39,7$ centistokes	The same	80	1,70	0,08
	"	20	0,85	0,18
0,05 N NaCl	Quartz	20	1,60	0,12
	The same	20	0,79	0,11
	"	50	0,70	0,09
	Ruby	90	0,64	0,09
		20	0,80	0,10

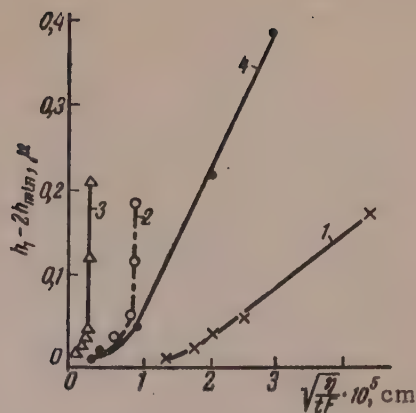


Fig. 2. Experimental relationship between the parameters of the Stefan-Reynolds equation and the gap between the disks, with a correction for the residual liquid layer (curve numbers as in Fig. 1).

Evidently the decrease of the approach velocity may be the consequence of a diminution of the effective gap owing to formation of a quasisolid residual layer. Indeed, the results in Fig. 2 show that, if h_{\min} is subtracted from

6 finish). The large correction is more likely to indicate that the determinations were not sensitive enough or that the apparatus had technical defects.

As the temperature increases, h_{\min} for mineral oils and solutions of fatty acids in them remains unchanged at first, but later drops sharply (Fig. 3). The fall of h_{\min} occurs over a certain temperature range (extending over $10-15^\circ$ and more), which may be regarded as the region of partial disorientation of the boundary layer ("fusion"). This region differs for different liquids; it is below the melting point of the boundary layer measured at high contact pressures [25, 26]. It follows that formation of the residual layer depends not only on chemisorption, which determines adsorption of the first layer of fatty acid molecules on the metal surface, but also on the structural factors of the boundary layer.

TABLE 3

Thickness of Residual Liquid Layers

Liquid	Disks	Specific pressure σ_n , g/cm ²	Temperature, °C	h_{\min} , μ			
				disk diameters, mm			
				2	10	12	17
Vacuum-distilled fraction of transformer oil $v_{20} = 35.3$ centistokes	Steel	2000	20	0,05	0,07	0,07	0,06
	Quartz	2000	20	—	0,03	0,04	0,04
	Ruby	2000	20	—	0,04	0,05	—
	Steel	200	80	0,08	0,10	0,10	0,09
The same + 0.3 % stearic acid	Steel	200	20	0,27	0,31	0,32	0,32
	Quartz	200	20	—	0,20	—	0,20
0.1 N LiCl solution	Quartz	200	20	—	0,18	0,20	0,18
	Quartz	2000	20	—	0,09	0,09	0,09
	Ruby	200	20	—	0,16	0,16	—

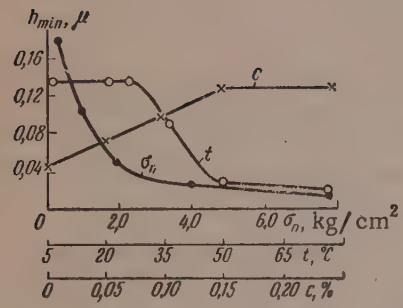


Fig. 3. Variations of the thickness of the residual layer h_{\min} of a vacuum-distilled fraction of "L" turbine oil with the stearic acid concentration c , temperature t , and specific load σ_n .

sistance of the residual layer to thinning. Most of the determinations were performed in the $0.2-2.0$ kg/cm² load range. The value of $E_{0.2-2.0}$ varies in the range of $0.8-12$ kg/cm², in accordance with the composition of the liquid and its content of surface-active substances (Fig. 4). The resistance of thinning of a residual layer more than 0.02μ thick is several orders of magnitude less than the compression modulus of solids.

For a given sample of mineral oil or solution of fatty acid in oil $\bar{E}_{\sigma'_n-\sigma''_n}$ increases with decrease of h_{\min} or, correspondingly, with increase of σ'_n . This shows that the bond strength between the components of the residual layer increases with increasing approach to a solid surface.

For elucidation of the nature of the residual layer it is important to estimate the reversibility of its thickness on removal of load. Fig. 5 shows variations of h_{\min} for 0.05 N LiCl solution between quartz disks on alternate loading and unloading. At instant τ_1 the load was increased from 80 to 2000 g/cm², and at instant τ_2

The thickness of the residual layer decreases with increase of specific pressure (Fig. 3 and Table 3); its dependence on the pressure diminishes with decrease of h_{\min} [23]. For a constant narrow range of specific loads we can calculate, by analogy with the compression modulus, the ratio of the thinning of the residual layer to the increase of load:

$$\bar{E}_{\sigma'_n-\sigma''_n} = \frac{h'_{\min}(\sigma''_n - \sigma'_n)}{h'_{\min} - h''_{\min}}, \quad (13)$$

where $\bar{E}_{\sigma'_n-\sigma''_n}$ is a measure of the resistance of h_{\min} to attenuation. Although $\bar{E}_{\sigma'_n-\sigma''_n}$ is a conventional

measure, it is convenient for characterization of the re-

sistance of the residual layer to thinning. Most of the determinations were performed in the $0.2-2.0$ kg/cm² load range. The value of $E_{0.2-2.0}$ varies in the range of $0.8-12$ kg/cm², in accordance with the composition of the liquid and its content of surface-active substances (Fig. 4). The resistance of thinning of a residual layer more than 0.02μ thick is several orders of magnitude less than the compression modulus of solids.

For a given sample of mineral oil or solution of fatty acid in oil $\bar{E}_{\sigma'_n-\sigma''_n}$ increases with decrease of h_{\min} or, correspondingly, with increase of σ'_n . This shows that the bond strength between the components of the residual layer increases with increasing approach to a solid surface.

For elucidation of the nature of the residual layer it is important to estimate the reversibility of its thickness on removal of load. Fig. 5 shows variations of h_{\min} for 0.05 N LiCl solution between quartz disks on alternate loading and unloading. At instant τ_1 the load was increased from 80 to 2000 g/cm², and at instant τ_2

it was decreased from 2000 to 80 g/cm². The results show that part of the residual layer is in equilibrium.

The equilibrium effect is, in all probability, equivalent to the disjoining pressure discovered by B. V. Deriagin et al. [18] in experiments on the adhesion of gas bubbles to solids in liquids. From this viewpoint the observed increase of $E_{\sigma_n' - \sigma_n}$ with decrease of h_{min} should be interpreted as an increase of the disjoining pressure with decrease of the distance between the disks.

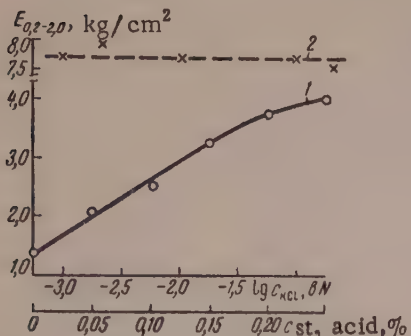


Fig. 4. Variations of $E_{0.2-2.0}$ for a vacuum-distilled fraction of turbine oil between steel disks with concentration of stearic acid (1) and KCl solution between quartz disks (2).

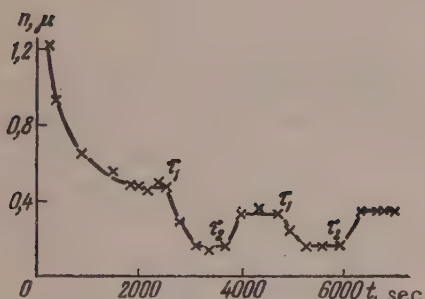


Fig. 5. Effect of alternate loading and unloading on the gap between quartz disks separated by 0.05 N LiCl solution (temperature 20°, initial load 80 g/cm²).

Separation of plane-parallel disks. The separation time of disks in solutions of electrolytes and surface-active substances increases with increasing time of previous contact and with the compressing load. The coefficient of boundary thickening varies similarly (Fig. 6). The explanation of this effect is evidently that the gap between the disks persists and partially decreases in width with time and under the action of the load. This effect is not observed in the separation of quartz disks in benzene or isoctane. As was noted earlier, these liquids do not form residual layers on quartz.

Proof that boundary layers of liquid persist between the disks is also provided by experiments on the time required for their separation. If the gap between the disks is assumed to be equal to the lower sensitivity limit of the method (0.02μ), Equation (7) shows that the time of separation should be 10^3 - 10^6 seconds. However, the experimental value for the separation time of disks in low-viscosity liquids does not exceed 20-30 seconds, while in viscous oils it is between 10^2 and 10^3 seconds. However, if h_1 in Equation (7) is taken to be the thickness of the residual layer, the theoretical time of separation becomes close to the experimental value (Table 4). The theoretical time of separation is considerably in excess of the experimental value only with viscous liquids, if the duration of preliminary contact is insufficient.

The factors influencing disk separation are not confined to the geometry of the gap and the viscosity of the liquid. After a contact time sufficient for the formation of the residual layer, ψ increases with increasing concentrations of fatty acid in mineral oil and of electrolytes in water, although it might be expected to remain constant or even to decrease. Fig. 7 shows that the coefficient of boundary thickening of LiCl solution in the gap between disks the same distance apart increases with increasing concentration of the solution. This may be interpreted as an effect caused by increase of viscosity in the boundary layer. The mechanism of this effect will be considered in future communications.

After the disks had been calibrated by means of a liquid which forms virtually no boundary layer, and the separation time of the disks and the width of the gap between them had been determined by independent methods, Equation (8) was used for calculation of the viscosities of certain solutions and oils in the boundary layer (Table 5). The integral values of the boundary viscosity η_b of the solutions studied are not more than 6 times the values of the volume of viscosity; * this coincides in order of magnitude with the latest determinations of boundary viscosity by the blow-off method [27]. Fig. 1 suggests that the viscosity in the boundary layer depends on its thickness.

* In our earlier papers on the separation kinetics of plane-parallel disks [23, 24] the values given for the boundary viscosity of bone oil and instrument oils are roughly 1.5 times the correct values, because of the inaccurate correction for the residual layer.

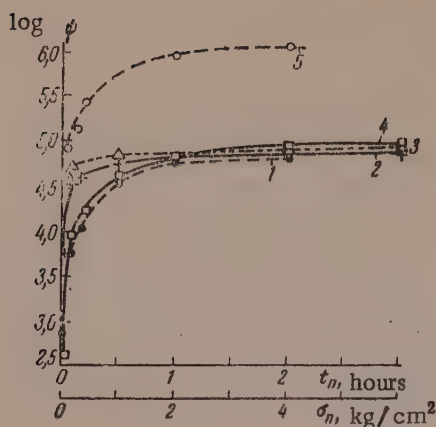


Fig. 6.

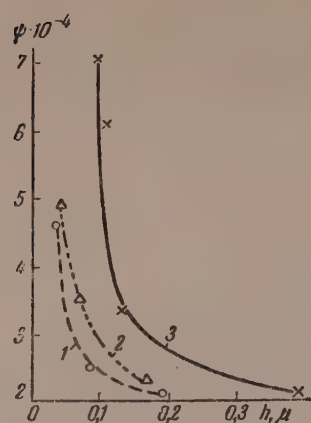


Fig. 7.

Fig. 6. Effects of contact time t_n (1, 2, 3) of disks in liquids, and of the applied load σ_n (4, 5), on the coefficient of boundary thickening ϕ at 20°.

Liquids: 1) vacuum-distilled fraction of turbine oil; $\eta_2 = 2.3$; 2,4) 0.25% solution of stearic acid in this fraction; 3,5) 0.05 N aqueous NaCl solution; 1, 2, 4) steel disks, 17 mm in diameter; 3, 5) quartz disks, 8 mm in diameter.

1) $\sigma_n = \sigma_{sep} = 80 \text{ g/cm}^2$; 2) $\sigma_n = 200 \text{ g/cm}^2$, $\sigma_{sep} = 400 \text{ g/cm}^2$; 3) $\sigma_n = 4000 \text{ g/cm}^2$, $\sigma_{sep} = 80 \text{ g/cm}^2$; 4) $\sigma_{sep} = 80 \text{ g/cm}^2$, $t_n = 60 \text{ seconds}$; 5) $\sigma_{sep} = 80 \text{ g/cm}^2$, $t_n = 1800 \text{ seconds}$.

Fig. 7. Variation of the coefficient of boundary thickening of electrolyte solutions in water with the gap width between quartz disks (determined by N. I. Kaverina):

1) 0.01 N NaCl; 2) 0.001 N LiCl; 3) 0.01 N LiCl.

TABLE 4

Separation Time t_{sep} for Plane-Parallel Disks in Liquids (Disk radius 0.6 cm, separation force 80 g/cm² at 20°)

Liquid	Disks	Time of preliminary contact, min	t_{sep} , sec		
			theoretical		experimental
			$h_1 = 0.02 \mu$	$h_1 = 2h_{min}$	
0.1 N NaCl solution	Quartz	120	$8.6 \cdot 10^8$	19	12
0.1 N LiCl solution	"	60	$8.6 \cdot 10^8$	9.6	3.4
Isooctane + 0.01% palmitic acid	Steel	60	$4.3 \cdot 10^8$	30.0	14.5
Naphthenic fraction of MS 20 Groznyi oil + 0.005% butyric acid	"	30	$8.1 \cdot 10^8$	2200	1680
"L" turbine oil	"	150	$2.6 \cdot 10^8$	620	595

TABLE 5
Increase of Boundary Layer Viscosity Compared with Volume Viscosity
Measured by Means of Plane-Parallel Disks, at 20°

Disks	Liquid	Volume viscosity, η , centipoises	Initial gap, μ	η_b / η
Quartz	Benzene	0,65	0,02	1,9
Steel	Vacuum distilled fraction of turbine oil	35,3	0,15	4,1
Steel	The same	35,3	0,20	2,9
Quartz	" "	35,3	0,15	2,4
Steel	Bone Oil	84,2	0,14	4,9
Quartz	0,05 N NaCl solution . . .	1,0	0,11	2,5
Quartz	0,05 N LiCl solution . . .	1,0	0,11	3,1

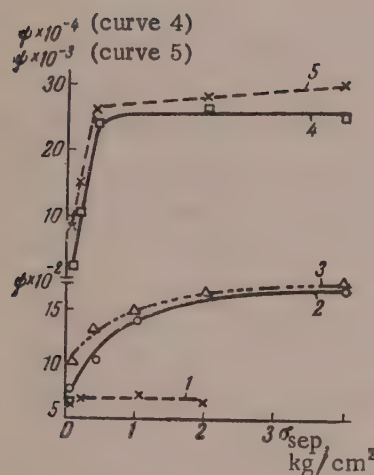


Fig. 8. Influence of the separation force σ_{sep} on the coefficient of boundary thickening of a turbine oil fraction of $\eta = 2.3$ at 20°:
1, 2, 3) quartz disks, 12 mm in diameter; 4, 5) steel disks, 5 mm in diameter; 1) $\sigma_n = 80 \text{ g/cm}^2$, $t_n = 300 \text{ seconds}$; 2) $\sigma_n = 80 \text{ g/cm}^2$, $t_n = 3600 \text{ seconds}$; 3) $\sigma_n = 1000 \text{ g/cm}^2$, $t_n = 3600 \text{ seconds}$; 4) $\sigma_n = 4000 \text{ g/cm}^2$, $t_n = 300 \text{ seconds}$; 5) $\sigma_n = 4000 \text{ g/cm}^2$, $t_n = 3600 \text{ seconds}$.

3. The thickness of the boundary layers of the liquid studied does not exceed $0.3\text{--}0.4\mu$, and depends on the solution composition, the disk material, temperature, and the applied force. The thickness of the residual layer depends on the composition of the liquid and the solid material.

The thickness of the residual layer in mineral oils and solutions of fatty acids in them decreases sharply over a definite narrow range of temperature. The resistance to the thinning of the residual layer increases with approach to the solid surface.

4. The thickness of the residual layer of LiCl solution in water is partially reversible upon variation of the normal load. The equilibrium character of part of the residual layer may be regarded as a manifestation of the disjoining pressure of the boundary liquid layers.

5. The mean effective boundary viscosity of the wall layer of a liquid is 1-6 times the volume viscosity.

The activation energy of liquid flow is higher in the boundary layer than in the volume of the liquid, and it increases as the residual layer is approached [1]. The value of ψ remains unchanged, increases, or decreases with the temperature in accordance with the ratio of the temperature coefficients of the separation time and volume viscosity [23].

The values of ψ and η_b / η decrease with increase of the separation force, and hence the separation velocity, in mineral oils (Fig. 8). This is an indication of anomalous viscosity in the boundary layer. Since the viscosity in the boundary layer is high and anomalous, the values of P_{max} (Table 1 and other data), which were calculated with the use of viscosity values, are approximate.

SUMMARY

1. Studies of adhesion and friction of plane and convex solids of simple geometrical shape in liquids can be used for modeling of the interaction of colloidal and microscopic particles in disperse systems.

2. Oils and solutions of fatty acids and electrolytes contained in narrow gaps between approaching or separating plane-parallel steel or quartz disks have higher effective viscosities in these gaps than in the volume of the liquid. These liquids leave residual layers between the disks; these layers are not squeezed out by pressures up to 8 kg/cm^2 . These boundary properties are not found in benzene or cyclohexane and are very weak in isoctane.

It seems likely that it increases in the boundary layer with decreasing distance from the residual layer. The boundary viscosity depends on the same factors as the thickness of the residual layer.

LITERATURE CITED

- [1] G. I. Fuks, Proc. 3rd All-Union Conference on Colloid Chemistry [in Russian] (Izd. AN SSSR, 1956), p. 301; B. V. Deriagin, N. I. Moskvitin and M. F. Futran, *ibid*, p. 285.
- [2] A. D. Malkina and B. V. Deriagin, *Colloid J.* 12, 431 (1950).
- [3] H. R. Kruyt (ed.), *Colloid Science* (IL, 1955), Chapters II and VI [Russian translation edited by V. P. Mishin].
- [4] P. A. Rebinder, Proc. Conference on the Viscosity of Liquids and Colloidal Solutions [in Russian] (Izd. AN SSSR, 1941), pp. 1, 368.
- [5] G. I. Fuks, *Colloid J.* 12, 228 (1950).
- [6] B. V. Deriagin, Proc. 3rd All-Union Conference on Colloid Chemistry [in Russian] (Izd. AN SSSR, 1956), p. 225.
- [7] E. J. W. Verwey and J. Th. G. Overbeek, *Theory of the Stability of Lyophobic Colloids* (Amsterdam, 1948).
- [8] G. I. Fuks, V. M. Klychnikov, and E. V. Tsyganova, Proc. Acad. Sci. USSR 65, 307 (1949); G. I. Fuks and V. M. Klychnikova, Trans. All-Union Inst. Fertilizers, Soil Science, and Agricultural Engineering, No. 28, 215 (1948); G. I. Fuks and E. V. Tsyganova, in the book: *Investigation and Uses of Petroleum Products* [in Russian] No. 1 (1948), p. 171.
- [9] P. A. Rebinder and N. A. Semenenko, Proc. Acad. Sci. USSR 64, 835 (1949); E. E. Segalova and P. A. Rebinder, *Colloid J.* 10, 223 (1948).
- [10] A. I. Rabinerson and G. I. Fuks, *Structure of Soil Colloids* [in Russian] (Leningrad Branch of the All-Union Institute for Fertilizers, Soil Science, and Agrotechnics, 1933), No. 22.
- [11] L. I. Sedov, *Similarity and Dimensional Methods in Mechanics* [in Russian], 2nd edn. (State Tech. Theoret. Press, 1951).
- [12] G. I. Fuks, *Viscosity and Plasticity of Petroleum Products* [in Russian] (State Fuel Tech. Press, 1951).
- [13] S. G. Gregg, *The Surface Chemistry of Solids* (London, 1951), Chapters VII and VIII.
- [14] A. Buzagh, *Kolloid.-Z.* 47, 370 (1929); 51, 105, 230 (1930) *J. phys. chem.* 43, 1003 (1939).
- [15] N. A. de Bruyne and R. Houwink (eds.), *Adhesion and Adhesives* (IL, 1954) [Russian translation].
- [16] C. Mylonas, Proc. VIIth Intern. Congr. Appl. Mechanics. 4 (London, 1948) p.137.
- [17] B. V. Deriagin, *J. Phys. Chem.* 6, 1306 (1935).
- [18] B. V. Deriagin and E. V. Obukhov, *Colloid J.* 1, 385 (1935); B. V. Deriagin and M. M. Kusakov, *Bull. Acad. Sci. USSR, Chem. Ser.* No. 5, 471 (1936); No. 5, 1119 (1937); *J. Phys. Chem.* 26, 1536 (1952); B. V. Deriagin, *Colloid J.* 17, 207 (1955). *
- [19] W. Stefan, *Z. ber. Akad. Wissen.* 69, 713 (1874) O. Reynolds, *Philos. Trans. Roy. Soc.*, 177, 157 (1886).
- [20] J. Bikerman, *J. Colloid Sci.* 2, 163 (1947).
- [21] E. Ormandy, *Engineer* 143, 362, 393 (1927); Iu. L. Margolina and S. S. Votskii, *Factory Labs.* 14, 321 (1948).
- [22] Aero Research, Technical Notes, *Bull.* No. 24, 3, 1944 (cited through [15]).
- [23] G. I. Fuks, Lubricating Power of Instrument Oils, in the book: *Watch Mechanisms* [in Russian] (Mashgiz, 1955), p. 186.* *

*Original Russian pagination. See C. B. Translation.

**In Russian.

[24] G. I. Fuks, Factory Labs. 21, 1445 (1955).

[25] F. Bowden, and D. Tabor, Friction and Lubrication of Solids (Oxford, 1950).

[26] M. M. Khrushchev and R. M. Matveevskii, Bull. Machine Construction No. 1, 12 (1954); R. M. Matveevskii, Temperature Method for Estimation of the Limiting Lubricating Power of Machine Oils [in Russian] (Izd. AN SSSR, 1956); J. W. Mentor, and J. Tabor, Proc. Roy. Soc. A. 204, 514 (1951); K. G. Brummage, *Ibid.* A. 191, 243 (1947).

[27] B. V. Deriagin and V. V. Karasev, Proc. Acad. Sci. USSR 101, 281 (1955); V. V. Karasev and B. V. Deriagin, Colloid J. 15, 365 (1953).

Scientific Research Institute of the
Horology Industry

Received May 27, 1957.

LETTERS TO THE EDITOR

CALCULATION OF THE WORK OF HOMOGENEOUS NUCLEUS-FORMATION IN VAPOR CONDENSATION

L. M. Shcherbakov

The dependence of surface tension on drop radius cannot be taken into account by simple replacement of the tabulated value of σ_{∞} in the Kelvin equation by the modified value $\sigma = \sigma(r)$. The precise conditions of equilibrium in the system drop (1) — vapor (2) are [1]:

$$\mu_1(P_1, T) = \mu_2(P_2, T), \quad P_1 - P_2 = \frac{2\sigma}{r} + \frac{\partial\sigma}{\partial r}. \quad (1)$$

Hence for the saturated vapor pressure of the drop we have

$$P = P_s \exp \left\{ \frac{v_1}{kT} \left(\frac{2\sigma}{r} + \frac{\partial\sigma}{\partial r} \right) \right\}.$$

The work of formation of a nucleus in a homogeneous medium of vapor pressure P can be expressed [2] in terms of the change of potential Ω :

$$A = \Omega - \Omega_0,$$

where

$$\Omega = -P \left(V - \frac{4}{3} \pi r^3 \right) - P_1 \cdot \frac{4}{3} \pi r^3 + 4\pi r^2 \sigma.$$

From Equation (1) we have

$$A = \frac{4}{3} \pi r^2 \left(\sigma - r \frac{\partial\sigma}{\partial r} \right). \quad (2)$$

By Equation (2), the work of nucleus formation becomes zero not when $r = 0$, but at a finite value r^* , determined by the condition

$$\sigma / r^* = \partial\sigma / \partial r^*,$$

and this happens before σ becomes zero.

When $r \leq r^*$, nuclei are formed without expenditure of work. Therefore supersaturation

$$S^* = (P / P_s)^* = \exp \left\{ \frac{v_1}{kT} \left(\frac{2\sigma}{r^*} + \frac{\partial\sigma}{\partial r^*} \right) \right\} = \exp \left(\frac{3\sigma v_1}{kTr^*} \right),$$

corresponds to the start of spontaneous condensation. However, when $S = S^*$, the rate of nucleus formation is negligible, so that somewhat higher supersaturation is required in practice.

It has been shown [3] that in absence of active centers spontaneous condensation begins at a definite and reproducible critical supersaturation S_c . S_c is theoretically defined as the supersaturation at which the rate of nucleus formation becomes considerable. The foregoing considerations eliminate the arbitrary character of

calculation of S_C , as the latter is correlated with the lower limit of the region of spontaneous condensation S^* , which can be found on thermostatical considerations.

For comparison of the results with experimental data, we use the following formula [4] as a first approximation of the relationship between σ and r :

$$\sigma = \sigma_\infty (1 - 2/\alpha r),$$

where $\alpha = -1/(\partial\sigma/\partial P)_T$, an empirical coefficient. Then $r^* = 4/\alpha$, which is of the order of 10^{-7} cm. S^* then becomes

$$S^* = \exp\left(\frac{3\sigma_\infty v_1 \alpha}{8kT}\right).$$

Taking a published value of α [5], we find for C_2H_5OH $S^* = 2.09$, whereas the experimental value [3] of $S_C = 2.34$.

LITERATURE CITED

- [1] L. M. Shcherbakov, Trans. Tula Mechanical Ins. 7, 17 (1955).
- [2] L. Landau and E. Lifshits, Statistical Physics [in Russian] (Moscow-Leningrad, 1951), p. 469.
- [3] M. Volmer and H. Flood, Z. phys. Chem. (A) 170, 273 (1934).
- [4] L. M. Shcherbakov., Colloid J. 14, 379 (1952).*
- [5] A. Kundt, Ann. Phys. 12, 538 (1881).

The Tula Mechanical Institute

Received June 2, 1958.

*Original Russian pagination. See C. B. translation.

DISCUSSION

VERIFICATION OF THE APPLICABILITY OF HIGH-FREQUENCY ANALYSIS TO COLLOIDOCHEMICAL STUDIES

N. F. Ermolenko

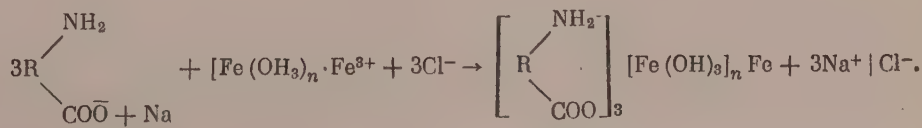
(With reference to the paper by V. I. Ermakov, V. N. Maslov, and O. G. Stolarov,
Colloid J. 19, 198, 1957)

On the basis of the hypothesis, advanced by Eristavi and Barnashvili [1], that the structure of the diffuse electrical double layer in micelles is changed under the influence of a high-frequency electromagnetic field, Ermakov, Maslov, and Stolarov [2] concluded that, conversely, changes in the electrical double layer in micelles in colloidal processes should produce changes in the dispersion of conductivity, which may be detected by means of high-frequency analysis. They designed an apparatus for high-frequency analysis and tested the possibility of determining, with its aid, changes in the structure of the electrical double layer on particles of ferric hydroxide sols under the coagulating action of $(\text{NH}_4)_2\text{SO}_4$; the expected effect was observed.

We consider that the choice of the second system for the verification is unfortunate. They used gelatin mixed with ferric hydroxide and expected extensive interaction to occur, accompanied by changes in the electrical double layer in the ferric hydroxide sol micelles; however, they did not detect a visible effect (incidentally, this result was to be expected). Gelatin is a complex organic amino acid which dissociates only slightly, and therefore neither extensive chemical interaction with ferric hydroxide nor changes of the electrical double layer in the micelles of the latter could occur. In this case gelatin acts as a protective substance which has virtually no effect on the diffuse character of the electrical double layer of the ferric hydroxide micelles. However, if air is blown through this system, ferric hydroxide is carried out to the surface with the protein foam (by flotation), and it is only in the surface layer that changes in the double layer of the ferric hydroxide micelles, owing to the increase of concentration, are possible; this may lead to coagulation. We have termed this effect laminar coagulation [3]; it was used extensively by Mokrushin [4] in his work on foam chromatography. Similar changes in the micellar double layer may occur on sedimentation of weakly charged particles of a suspension, as described by us earlier in relation to sedimentational thixotropy [5].

The authors [2] state that by using gelatin as the other component with ferric hydroxide they confirmed our interpretation [3] of the interaction of the protein with ferric hydroxide. Here they are guilty of a dual error.

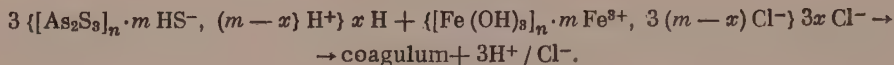
1. In the investigation cited we did not use gelatin but a vegetable protein in an alkaline medium. Gelatin, being a degraded protein, is soluble in water, is weakly dissociated, and is not precipitated from aqueous solution even in the isoelectric state. Our vegetable protein is almost insoluble in water but is readily soluble in alkalies. In the latter case the protein macromolecules are in salt form and are readily dissociated, and therefore they are negatively charged, as is shown in our scheme. Hence such macromolecules can interact more readily with the positively charged micelles of ferric hydroxide as follows:



It is easily seen that such an equation is not applicable to gelatin in a neutral medium.

2. Careful study of our paper should have shown that, as we emphasized, deeper interaction between the protein micelles and ferric hydroxide, up to coagulation, would take place in the surface adsorption layer during foaming of the system. That is why we described this type of coagulation as laminar. The fact that a protein foam holding ferric hydroxide is more stable than a pure protein foam indicates that there is extensive bonding of the components in the surface layer. Thus, the greatest changes in the electrical double layer in our system should be detected in the surface adsorption layer.

If we wished to test the applicability of high-frequency analysis to detection of changes in the electrical double layers of micelles, we would use a system without protective substances, of the type



This would be a "pure system, not influenced by side factors (protective effects), and changes in the electrical double layer of the micelles would lead to visible coagulation, not in the surface adsorption layer, but in the volume, where the authors cited performed their determinations.

LITERATURE CITED

- [1] D. M. Eristavii and D. Barnashvili, Proc. Acad. Sci. USSR 25, No. 7, 606 (1939).
- [2] V. I. Ermakov, V. N. Maslov, and O. G. Stoliarov, Colloid J. 19, No. 2, 198 (1957).*
- [3] N. F. Ermolenko and G. N. Plenina, Colloid J. 5, No. 3, 194 (1939).
- [4] S. G. Mokrushin, Colloid J. 12, No. 6, 448 (1950); Nature No. 4544, 1244 (1956).
- [5] N. F. Ermolenko, Sci. Mem. Belorussian Univ., Chem. Ser. 30, 79 (1937); A General Discussion of the Faraday Soc. 18, 145 (1954).

Received July 28, 1957

*Original Russian pagination. See C. B. translation.

ERRATA

Volume 20, Number 4

<u>Page</u>	<u>Line</u>	<u>Reads</u>	<u>Should read</u>
382	6 from bottom	$S_0 = -0.06 \pm 0.026 \sqrt{M}$	$S_0 = -0.06 + 0.026 \sqrt{M}$
383	2 " "	$ac/dt = 0$	$dc/dt = 0$
385	(Units on y-axis) Fig. 5	$\frac{1}{m} \cdot \frac{dm}{dt} \cdot \frac{1}{min}$	$\ln \left(\frac{1}{m} \cdot \frac{dm}{dt}, \frac{1}{min} \right)$
386	21 "	$1/M - l \approx 1/M$	$1/\mu - l \approx 1/\mu$
386	15 "	$\frac{M}{M_0} = 1 + \frac{k_0}{\mu} t$	$\frac{M_0}{M} = 1 + \frac{M_0 k_0}{\mu} t$
386	14 "	M/M_0	M_0/M
386	Last sentence	Since in high-temperature degradation initiation also occurs at the chain ends, although the ends no longer contain double bonds (i.e. every molecule can be activated), it follows that $n = 1/M$ or $n = l$, and in accordance with Equations (11) and (12) the expression becomes	Since in high-temperature degradation initiation also occurs at the chain ends, although the ends no longer contain double bonds (i.e. every molecule can be activated), it follows that $n = 1/M$ or $n = l$, in accordance with Equation (11). In Equation (12) the expression becomes
387	3 from top	$\frac{dv}{dn} = \frac{k_0 k_2}{\mu} \sqrt{\frac{k_1}{k_3}} n^{1/2}$	$\frac{dv}{dn} = \frac{\mu k_2}{\sqrt{k_3}} \sqrt{\frac{k_1}{k_3}} n^{1/2}$

- Index -

COLLOID JOURNAL

Volume 20, 1958

CONTENTS

	RUSS. PAGE	PAGE
Influence of the Preparation Conditions of Aluminum Soaps of Naphthenic Acids on the Properties of their Oleogels. <u>G. V. Belugina and A. P. Trapeznikov</u>	1	3
Investigation of the Dispersity of Sapropels by Means of the Sedimentometer and the Electron Microscope. <u>M. P. Volarovich and V. P. Tropin</u>	9	13
Compatibility of Nitrocellulose with Butadiene-Acrylonitrile Copolymers. 4. Relaxation Properties of Binary Mixtures. <u>S. S. Voiutskii, V. I. Alekseenko and L. E. Kalinina</u>	15	20
The Heats of Hydration of Some Cations and the Effect of Their Adsorption on the Structure of Silica Gels. <u>Z. Z. Vysotskii and V. V. Shalia</u>	23	29
Thermomechanical Investigation of Epoxide Resins. <u>L. I. Golubenkova, B. M. Kovarskaia, M. S. Akutin and G. L. Slonimskii</u>	29	34
The Structure and Phase State of Polyethylene Terephthalate Fibers. <u>V. O. Gorbacheva and N. V. Mikhailov</u>	33	38
The Formation and Properties of Interpolymers of Natural and Butadiene-Styrene Rubbers. <u>B. A. Dogadkin, V. N. Kuleznev and Z. N. Tarasova</u>	39	43
Electron Microscopic and Adsorption Studies of Silica Sols and Silica Gels. <u>A. V. Kiselev, V. I. Lygin, I. E. Neimark, I. B. Sliniakova and Chen' Ven'-han</u>	47	52
Investigation of the Nature of the Adhesion Bond in the Bonding of Two High-Molecular Compounds. <u>L. P. Morozova and N. A. Krotova</u>	55	59
The Hydrodynamic Characteristics and Polydispersity of Some Ethylcellulose Specimens. <u>T. I. Samsonova and S. Ia. Frenkel'</u>	63	67
Investigation of the Coagulation of Rubber Latexes with the Aid of Radioactive Isotopes. <u>D. M. Sandomirskii and M. K. Vdovchenkova</u>	75	80
The Structure and Adsorptive Properties of Silica Gels Prepared From Alkaline Media. <u>I. B. Sliniakova and I. E. Neimark</u>	79	84
Processes of Structure Formation in Milk Fat and Their Significance in the Production of Butter. <u>A. I. Titov, I. N. Vlodavets and P. A. Rebinder</u>	87	92
The Hydrophilic Properties of Montmorillonite Clay. <u>E. T. Uskova</u>	95	102
The Effect of Plasticizer Additions on the Mechanical Properties of Vinyl Chloride-Vinylidene Chloride Copolymer and Polyvinyl Chloride. <u>R. I. Fel'dman, A. K. Mironova and S. I. Sokolov</u>	99	106
The Effect of the Acetyl Group Content of Acetylcellulose on the Properties of its Solutions. <u>V. P. Kharitonova and A. B. Pakshver</u>	103	110

CONTENTS (continued)

PAGE	RUSS. PAGE
------	---------------

Brief Communications

Swelling of Silicate Melts and Blistering of Enamel Coatings on Steel. <u>K. P. Azarov</u>	111	118
An Apparatus for Determining the Dispersity of Emulsions. <u>B. M. Babanov and V. V. Kafarov</u>	115	121
Determination of the Bound Water Content in Peat by the Method of the Negative Adsorption of a Radioactive Tracer. <u>M. P. Volarovich, F. D. Sysoeva, V. V. Cherniavskia and</u> <u>N. V. Churaev</u>	117	122
The Action of Metal Oxides in the Vulcanization of Rubber by Tetramethylthiuram Di- sulfide. <u>B. A. Dogadkin and V. A. Shershnev</u>	119	124

COLLOID JOURNAL

Volume 20, Number 2

March -April, 1959

CONTENTS

	RUSS. PAGE	PAGE
Theory of the Optical Recording of Mixture Compositions by an Inclined Cylindrical Lens Arrangement. <u>Ia. M. Bikson</u>	123	129
Character of the Relaxation of Nonvulcanized Rubber Mixes. <u>K. Weber</u>	129	135
Investigation of the True Fluidity and Elasticity of Rubbers and Raw Rubber Mixes. <u>B.I. Gengrinovich and G.L. Slonimskii</u>	137	143
The Coagulation of Lyophobic Sols by the Action of Mixtures of Electrolytes. Communication II. <u>Iu. M. Glazman, I.M. Dykman and E.A. Strel'tsova</u>	143	149
The Formation of Ultrathin Layers of Disperse Phase at the Hydrosol — Organic Liquid Interface. <u>T.A. Degtiareva and S.G. Mokrushin</u>	153	159
Binding of Water by Finely Divided Sediments. 1. Calculation of the Amount of Bound Water From the Electrolyte Concentration in the Equilibrium Solution. <u>O.I. Dmitrenko</u>	157	163
The Surface Tension of Disperse Systems. <u>S.N. Zadumkin</u>	163	170
Gelatinized Emulsions. 15. Limiting-Concentration Emulsions of Paraffin Wax in Water. Structure of Protective Layers. <u>L.Ia. Kremnev and A.I. Perelygina</u>	167	174
Effect of the Structure of Certain Surface-Active Substances on the Foaming of Aqueous Gelatin Solutions. <u>S.M. Levi and O.K. Smirnov</u>	173	179
The Structural and Mechanical Properties of Clay Suspensions Used in Difficult Drilling Conditions. <u>A.K. Miskarli and T.G. Gasanova</u>	179	184
The Effect of Cations on the Properties of Black Sea Agaroid. <u>A.A. Morozov and S.N. Stavrov</u>	187	194
The Structure of Gels. 12. Preparation of Gels from Solutions of Methyl Methacrylate — Methacrylic Acid Copolymer. <u>N.F. Proshliakova, P.I. Zubov and V.A. Kargin</u>	191	199
The Structure of Gels. 13. Investigation of the Properties of Gels of Methyl Methacrylate — Methacrylic Acid Copolymer Containing Univalent Metals. <u>N.F. Proshliakova, P.I. Zubov and V.A. Kargin</u>	195	202
Equation for the Sorption Isotherm of Amino Acids on Ion Exchange Resins in the Hydrogen Form. <u>G.V. Samsonov and N.P. Kuznetsova</u>	201	209
A Radioactive Isotope Study of the Ionic Deposition of Rubber from Latex. <u>D.M. Sandomirskii and M.K. Vdovchenkova</u>	205	214
The States of Aggregation of High Polymers. 1. Study of the Linear Expansion of Polymethyl Methacrylate, Polystyrene, Polyvinyl Chloride, and Vinyl Chloride — Vinyl Acetate Copolymer. <u>R.I. Fel'dman</u>	211	220

CONTENTS (continued)

	RUSS. PAGE	PAGE
Fractionation of Amylose According to the Degree of Polymerization. <u>J. Hollo and J. Szejtli</u>	219	229
Influence of Electrolytes on the Coagulation of Colloidal Particles at the Liquid-Gas Interphase. <u>R.V. Shveikina and S.G. Mokrushin</u>	223	233
The Site of Polymerization of Unsaturated Compounds in Systems Containing Protective Colloids. <u>A.S. Shevliakov and K.S. Minsker</u>	227	237
The Adsorption of Similarly Charged Ions in the Coagulation of Sols by Electrolytes. 1. Radiometric Measurements. <u>A.M. Shkodin and L.D. Shaposhnikova</u>	231	242
Ivan Platonovich Losev (on his 80th birthday), <u>O.V. Smirnova</u>	235	246
Discussion		
The Fluidity and Strength of Structurized Disperse Systems. <u>G.V. Vinogradov and V.P. Pavlov</u>	237	248
Brief Communications		
Influence of the Ratio of Free to Bound Alkali in the Precipitation of Aluminum Soaps on their Thickening Properties. <u>A.A. Trapeznikov, G.V. Belugina and F.M. Rzhavskaya</u> ..	243	254

COLLOID JOURNAL

Volume 20, Number 3

May-June, 1958

CONTENTS

	RUSS. PAGE	PAGE
On the Sixtieth Birthday of Boris Aristarkhovich Dogadkin. <u>S. M. Lipatov, S. S. Voiutskii, and V. E. Gul'</u>	245	257
The Structure and Properties of Rubbers Produced in Irradiation Vulcanization. <u>B. A. Dogadkin, Z. N. Tarasova, M. Ia. Kaplunov, V. L. Karpov, and N. A. Klauzen</u>	248	260
The Chemical Interaction of Sulfur and Carbon Black. <u>B. A. Dogadkin, Z. V. Skorodumova, and N. V. Kovaleva</u>	259	272
The Mechanism of Vulcanization in Presence of 2-Mercaptobenzothiazole. <u>B. A. Dogadkin and I. A. Tutorskii</u>	266	279
The Vulcanizing Action of Certain Heterocyclic Disulfides. <u>M. S. Fel'dshtein, I. I. Eitington, D. M. Pevzner, and B. A. Dogadkin</u>	274	288
Ionic Deposition from Carboxylic Divinyl-Styrene Reflexes. <u>D. M. Sandomirskii, Iu. L. Margolina, B. A. Dogadkin and L. S. Krokhina</u>	279	293
The Heat of Adsorption of Hydrocarbons on Carbon Blacks of Different Degrees of Graphitization. <u>N. N. Avgul', G. I. Berezin, A. V. Kiselev, and A. Ia. Korolev</u>	283	298
The Gas Permeability and Structure of Vulcanized Rubbers. <u>G. M. Bartenev</u>	290	305
A Study of the Rheological Properties of Low-Moisture Peats. <u>M. P. Volarovich and N. I. Malinin</u>	295	311
Investigation of the Tearing Process in the Region of Transition from the Elastic to the Brittle State. <u>V. E. Gul', L. N. Tsarskii and S. A. Vil'nits</u>	302	318
Method of Calculating the Precipitation of Disperse Particles from a Stream on an Obstacle. <u>S. S. Dukhin and B. V. Deriagin</u>	309	326
The Structure of Gels. 14. Influence of the Nature of the Plasticizer on the Properties of Filled Divinyl-Styrene Rubber. <u>M. P. Zverev, E. A. Eroshkina, and P. I. Zubov</u>	312	329
Certain Properties of Block Copolymers Based on an Epoxy Resin and Butadiene-Nitrile Rubber. <u>V. A. Kargin, N. A. Plate, and A. S. Dobrynina</u>	315	332
Adsorbate-Adsorbate Interaction in the Adsorption of Vapors on Graphitized Carbon Blacks. <u>A. V. Kiselev</u>	320	338
Heterochain Polyamides. 10. The Effect of Some Organic Substances on the Stability of Alcoholic Polyamide Solutions. <u>V. V. Korshak and S. A. Pavlova</u>	332	349

CONTENTS (continued)

	PAGE	RUSS. PAGE
The Melting of Gelatin Gels. <u>S. I. Meerson and S. M. Lipatov</u>	336	353
Plasticoelastic Properties of SKN-26 Rubber. <u>A. S. Novikov and F. S. Tolstukhina</u>	342	361
Effect of the Composition of Rubber on its Fatigue Characteristics. <u>M. M. Reznikovskii, L. S. Priss, and M. K. Khromov</u>	348	368
The Effect of the Regularity of Structure of Triacetylcellulose on its Solubility and the Properties of its Solutions. <u>Z. A. Rogovin and D. L. Mirlas</u>	355	376
Structure Studies in Carbon-Black Suspensions. 3. The Effect of Polymer Additions to Concentrated Carbon Black Suspensions in a Hydrocarbon Medium. <u>Wu Shu-Chiu (U Shu-Tsiu), B. Ia. Iampol'skii, and S. S. Voiutskii</u>	360	382
The States of Aggregation of High-Molecular Compounds. 2. A Study of the Linear Expansion of Gutta-Percha. <u>R. I. Fel'dman and S. I. Sokolov</u>	366	388
Electron Microscope Investigation of the Plasticization of a Dispersion of Vinyl Chloride-Vinylidene Chloride Copolymer. <u>B. V. Shtarkh and A. P. Pisarenko</u>	372	395
Brief Communications		
The Effect of Electric Charges Formed During Repeated Deformations on the Fatigue Resistance of Vulcanizates. <u>B. A. Dogadkin, V. E. Gul', and N. A. Morozova</u>	375	397
A Study of the Strength and High-Elastic Properties of Rubber Solutions and Their Vulcanizates at High Deformation Rates. <u>A. A. Trapeznikov and T. V. Assanova</u>	376	398

CONTENTS

	PAGE	RUSS. PAGE
New Problems of Colloid Chemistry.....	379	401
Thermal Degradation of Polymethyl Methacrylate. <u>S. E. Bresler, A. T. Os'minskaia, A. G. Popov, E. M. Saminskii, and S. Ia. Frenkel'</u>	381	403
Nature of the Reaction of Aluminum Naphthenate Formation. 2. Preparation of Aluminum Naphthenate by the Mixing of a Suspension of Aluminum Hydroxide with an Emulsion of Naphthenic Acids. <u>D. F. Vasil'ev</u>	393	417
Study of the Foaming of Molasses. <u>T. I. Vlasova</u>	397	421
A Study of the Laws of Polyanionic Exchange. <u>A. T. Davydov and R. Z. Davydova</u>	401	425
Spectroscopic Investigation of the Sorption of Metal Cations by Oxidized Celluloses. <u>I. N. Ermolenko and R. G. Zhbankov</u>	405	429
The Mechanism of Stabilization of Clay Suspensions by an Algal Extract. <u>N. A. Zavorokhina and V. G. Ben'kovskii</u>	411	436
Adsorbate—Adsorbate Interaction in the Adsorption of Vapors on Graphitized Carbon Blacks. 2. Application of the Equations for the Adsorption Isotherms to Experimental Data. <u>A. V. Kiselev, N. V. Kovaleva, V. A. Sinitsyn, and E. V. Khrapova</u>	419	444
Secondary Effects on Precipitation Chromatograms of Various Compounds <u>V. D. Kopylova and K. M. Ol'shanova</u>	429	456
Effect of the Density of Polytrifluorochloroethylene on Dielectric Loss. <u>G. P. Mikhailov, B. I. Sazhin, and V. S. Presniakova</u>	433	461
Some Experimental Studies of the Physical Chemistry of Starch. <u>V. I. Nazarov, N. P. Silina, and T. P. Tikhomirova</u>	437	465
The Topochemistry of Drop Polymerization of Vinyl Chloride. <u>B. F. Teplov and P. M. Khomikovskii</u>	441	469
Relaxation of Deformation and Repeated Deformation of Aluminum Naphthenate Gels. <u>A. A. Trapeznikov</u>	447	476
Electrochemical Study of Bentonite Suspensions. 2. The Progressive Action of Sodium Hydroxide on Suspensions of Electrodialyzed Askangel. <u>I. A. Uskov and E. T. Uskova</u>	457	487
Dispersion of a Stream of Superheated Liquid. <u>V. A. Fedoseev</u>	463	493
The Stabilization of Carbon-Black Suspensions in Vaseline Oil—Drying Oil Mixtures. <u>B. N. Shakhkel'dian</u>	467	498
A Traditional Error in the Theory of Capillarity. <u>L. M. Shcherbakov</u>	471	502

CONTENTS (continued)

	PAGE	RUSS. PAGE
Microscopical Determination of Droplet Size in Oil Mist. <u>Z. M. Iuzhnyi</u>	477	507
Announcement	481	512

CONTENTS

	RUSS. PAGE	PAGE
The Work of P. A. Rebinder and His School on Surface Phenomena in Disperse Systems, and on Physicochemical Mechanics.	483	515
Modern Problems of Colloid Chemistry. I. Formation and Aggregative Stability of Disperse Systems. <u>P. A. Rebinder</u>	493	527
Some Characteristics of the Adsorption of Surface-Active Substances in Nonaqueous Media. <u>A. B. Taubman and S. I. Burshtein</u>	503	539
Gelatinized Emulsions. 16. The Influence of Neutral Inorganic Salts on Emulsification. Antagonistic Emulsifiers. <u>L. Ia. Kremnev</u>	509	546
The Influence of Ethylene Glycol on the Colloidal Properties of Aqueous Sodium Oleate Solutions. <u>A. I. Iurzhenko and G. F. Storozh</u>	513	550
Formation and Stability of Metal Solns. <u>E. M. Natanson</u>	519	556
Physicochemical Principles of the Regulation of Mechanical Properties of the Structures in Clay-Water Systems. <u>N. N. Serb-Serbina</u>	525	563
Rheological Investigation of Structurized Suspensions of Askangel and Some of Its Derivatives. <u>O. M. Mdivnishvili and G. V. Vinogradov</u>	531	569
Physicochemical Mechanics of Disperse Systems in Ceramic Technology. <u>S. P. Nichiporenko</u>	537	575
Deformation Characteristics of Natural and Dispersed Structures of Some Clays. <u>L. M. Gor'kova</u>	547	585
The Role of Plastification and Hydrophobization in the Compaction of Soils. <u>T. Iu. Liubimova and T. V. Iagodovskaia</u>	555	594
Structure Formation in the Course of Hydration Hardening of Calcium Sulfate Hemihydrate (Plaster of Paris). <u>E. E. Segalova and V. N. Izmailova</u>	563	601
Effect of Additions of a Hydrophilic Plastifier on the Kinetics of Structure Formation in the Hardening of Cement. <u>E. E. Segalova, R. R. Sarkisian, and P. A. Rebinder</u>	571	611
Kinetics of Crystallizational Structure Formation in the Hydration Hardening of Tricalcium Aluminate. <u>E. S. Solov'yeva and E. E. Segalova</u>	579	620
Mechanism of the Action of Mixed Additives for Cement, Based on a Hydrophilic Plastifier. <u>O. I. Luk'ianova and S. A. Dariusina</u>	585	628
Influence of Surface-Active Substances on the Crystallization of Tricalcium Hydroaluminate. <u>N. G. Zaitseva and A. M. Smirnova</u>	593	636

CONTENTS (continued)

	PAGE	RUSS. PAGE
The Rheology of Metals in Surface-Active Media. <u>V. S. Ostrovskii and V. L. Likhtman</u>	597	640
Formation of New Surfaces in the Deformation and Destruction of a Solid in a Surface-Active Medium. <u>E. D. Shchukin and P. A. Rebinder</u>	601	645
The Theory of Spontaneous Dispersion of Solids. <u>G. M. Bartenev, L. V. Iudina, and P. A. Rebinder</u>	611	655
Some Features of the Comminution of Graphite in an Aqueous Medium. <u>E. B. Matskevich and P. Iu. Butiagin</u>	619	665
Letters to the Editor		
Gel Formation in the Mastication of Natural Rubber, and Its Influence on Vulcanizate Strength. <u>B. A. Dogadkin and V. N. Kuleznev</u>	629	674
The Role of the Structuromechanical Factor in Emulsion Stability. <u>A. B. Taubman and A. F. Koretskii</u>	631	676
Current Events		
The Fourth All-Union Conference on Colloid Chemistry	633	677

Volume 20, Number 6

November-December 1958

CONTENTS

	RUSS. PAGE	PAGE
The Viscosity of Totally Destructurized Clay Suspensions, and the Effect of Sodium Hydroxide on it. <u>L. A. Abduragimova and N. G. Alekperova</u>	637	681
Influence of Temperature on the Exchange of Cobalt and Copper Cations on Organic Cation-Exchange Resins. <u>L. S. Aleksandrova and S. Iu. Elovich</u>	643	687
Studies of the Physicochemical Properties of Tire-Cord Fibers. 1. Heats of Solution of Capron Fibers. <u>V. A. Berestnev, T. V. Gatovskaya, V. A. Kargin, and E. Ia. Iaminskaya</u>	651	694
Influence of the Disperse Phase on the Results of Hydrogen-Ion Activity Determinations in Salt Solutions. <u>R. V. Voitsekhovskii and A. M. Vovnenko</u>	655	697
The Secondary (Diffusional) Electrical Double Layer. <u>S. S. Dukhin and B. V. Deriagin</u>	663	705
Factors Determining the Structuromechanical Properties of Viscose Solutions. <u>N. N. Zav'ialova and N. V. Mikhailov</u>	667	708
Certain Properties of Calcium Oxalate Precipitates in Electrolyte Solutions. <u>G. G. Kandilarov</u>	671	713
Structure Formation in Compacted Soils. <u>T. Iu. Liubimova</u>	677	719
Determination of the Adsorption of Solutes on Hydrogels. <u>P. S. Meleshko</u>	685	728
Kinetics of Phase Separation in Protected Emulsions. <u>S. G. Mokrushin and V. I. Borisikhina</u>	691	736
Studies of Aluminum Hydroxide Hydrosols. 4 Thixotropic gelation of sols in methyl alcohol-dioxane mixtures. <u>P. V. Rufimskii</u>	695	739
Sedimentation of a Magnesium Hydroxide suspension in an Ultrasonic Field. <u>N. I. Soboleva, A. G. Bol'shakov and A. V. Kortnev</u>	699	742
Investigation of Boundary Friction and Adhesion, in Relation to Studies of the Interaction of Finely Dispersed Particles. 1. Certain Boundary Properties of Solutions in Narrow Plane Gaps Between Solid Surfaces. <u>G. I. Fuks</u>	705	748
Letters to the Editor		
Calculation of the Work of Homogeneous Nucleus-Formation in Vapor Condensation. <u>L. M. Shcherbakov</u>	717	759
Verification of the Applicability of High-Frequency Analysis to Colloidochemical Studies. <u>N. F. Ermolenko</u>	719	761

CONTENTS (continued)

RUSS.
PAGE PAGE

Errata

721

Index for 1958

Table of Contents

723

Author Index

735

AUTHOR INDEX

1958

- Abduragimova, L. A., and N. G. Alekperova. The Viscosity of Totally Destructurized Clay Suspensions, and the Effect of Sodium Hydroxide on it - 681
- Akutin, M. S., see Golubenkova, L. L. - 29
- Alekperova, N. G., see Abduragimova, L. A. - 681
- Aleksandrova, L. S. and S. Iu. Elovich. Influence of Temperature on the Exchange of Cobalt and Copper Cations on Organic Cation-Exchange Resins - 687
- Alekseenko, V. I., see Voiutskii, S. S. - 15
- Assanova, T. V., see Trapeznikov, A. A. - 376
- Avgul', N. N. G. I. Berezin, A. V. Kiselev and A. Ia. Korolev. The Health of Adsorption of Hydrocarbons on Carbon Blacks of Different Degrees of Graphitization. - 283
- Azarov, K. P. Swelling of Silicate Melts and Blistering of Enamel Coatings on Steel - 111
- Babanov, B. M., and V. V. Kafarov. An Apparatus for Determining the Dispersity of Emulsions - 115
- Bartenev, G. M. The Gas Permeability and Structure of Vulcanized Rubbers - 290
- Bartenev, G. M., L. V. Iudina and P. A. Rebinder. The Theory of Spontaneous Dispersion of Solids - 611
- Belugina, G. V., see Trapeznikov, A. A. - 243
- Belugina, G. V., and A. P. Trapeznikov. Influence of the Preparation Conditions of Aluminum Soaps of Naphthenic Acids on the Properties of their Oleogels - 1
- Ben'kovskii, V. B., see Zavorkhina, N. A. - 411
- Berestnev, V. A., T. V. Gatovskaya, V. A. Kargin and E. Ia. Iaminskaia. Studies of the Physicochemical Properties of Tire-Cord Fibers. 1 Heats of Solution of Capron Fibers - 694
- Berezin, G. I., see Avgul', N. N. - 283
- Bikson, Ia. M. Theory of the Optical Recording of Mixture Compositions by an Inclined Cylindrical Lens Arrangement - 123
- Boi'shakov, A. G., see Soboleva, N. L. - 742
- Borisikhina, V. I., see Mokrushin, S. G. - 736
- Bresler, S. E., A. T. Os'minskaya, A. G. Popov, E. M. Saminskii, and S. Ia. Frenkel'. Thermal Degradation of Polymethyl Methacrylate. - 381
- Burshtein, S. L., see Taubman, A. B. - 503
- Butiagin, P. Iu., see Matskevich, E. B. - 619
- Chen'Ven'-han, see Kiselev, A. V. - 47
- Cherniavskaya, V. V., see Volarovich, M. P. - 117
- Churaev, N. V., see Volarovich, M. P. - 117.
- Dariusina, S. A., see Luk'ianova, O. L. - 585
- Davydov, A. T. and R. Z. Davydova. A Study of the Laws of Polyanionic Exchange - 401
- Davydova, R. Z., see Davydov, A. T. - 401
- Derilagin, B. V., see Dukhin, S. S. - 309
- Derilagin, B. V., see Dukhin, S. S. - 705
- Degtiareva, T. A. and S. G. Mokrushin. The Formation of Ultrathin Layers of Disperse Phase at the Hydrosol - Organic Liquid Interface - 153
- Dogadkin, B. A., see Fel'shtein, M. S. - 274
- Dobrynina, A. S., see Kargin, V. A. - 315
- Dogadkin, B. A., V. E. Ful', and N. A. Morozova. The Effect of Electric Charges Formed During Repeated Deformations on the Fatigue Resistance of Vulcanizates. - 375
- Dogadkin, B. A., and V. N. Kuleznev. Gel Formation in the Mastication of Natural Rubber, and Its Influence on Vulcanizate Strength - 629
- Dogadkin, B. A., V. N. Kuleznev, Z. N. Tarasova. The Formation and Properties of Interpolymers of Natural and Butadiene-Styrene Rubbers - 39
- Dogdakin, B. A., see Sandomirskii, D. M. - 279
- Dogadkin, B. A., and V. A. Shershnev. The Action of Metal Oxides in the Vulcanization of Rubber by Tetramethylthiuram Disulfide - 119
- Dogadkin, B. A., Z. V. Skorodumova and N. V. Kovaleva. The Chemical Interaction of Sulfur and Carbon Black - 259
- Dogadkin, B. A., Z. N. Tarasova, M. Ia. Kaplunov, V. L. Karpov and N. A. Klauzen. The Structure and Properties of Rubbers Produced in Irradiation Vulcanization - 248
- Dogadkin, B. A. and L. A. Tutorskii. The Mechanism of Vulcanization of Presence of 2-Mercapto-benzothiazole - 260
- Dukhin, S. S. and B. V. Derilagin. Method of Calculating the Precipitation of Disperse Particles from a Stream on an Obstacle. - 309
- Dukhin, S. S. and B. V. Derilagin. The Secondary (Diffusional) Electrical Double Layer - 705
- Dykman, I. M., see Glazman, Iu. M. - 143
- Eitington, I. I., see Fel'shtein, M. S. - 274
- Elovich, S. Iu., see Aleksandrova, L. S. - 687
- Ermolenko, I. N. and R. G. Zhabankov. Spectroscopic Investigation of the Sorption of Metal Cations by Oxidized Celluloses - 405
- Ermolenko, N. F. Verification of the Applicability of High-Frequency Analysis to Colloidochemical Studies - 761

- Eroshkina, E. A., see Zverev, M. P. - 312
- Fedoseev, V. A. Dispersion of a Stream of Superheated Liquid - 463
- Fel'dman, R. I. The States of Aggregation of High-Polymers. 1. Study of the Linear Expansion of Polymethyl Methacrylate, Polystyrene, Polyvinyl Chloride, and Vinyl Chloride - Vinyl Acetate Copolymer - 211
- Fel'dman, R. I., A. K. Mironova, and S. L. Sokolov. The Effect of Plasticizer Additions on the Mechanical Properties of Vinyl Chloride-Vinylidene Chloride Copolymer and Polyvinyl Chloride - 99
- Fel'dman, R. I. and S. L. Sokolov. The States of Aggregation of High-Molecular Compounds. 2. A Study of the Linar Expansion of Gutta-Percha - 366
- Fel'shtein, M. S., I. I. Eitington, D. M. Pevzner and B. A. Dogadkin. The Vulcanizing Action of Certain Heterocyclic Disulfides - 274
- Frenkel', S. Ia., see Bresler, S. E. - 381
- Frenkel', S. Ia., see Samsonova, T. I. - 63
- Fuks, G. I. Investigation of Boundary Friction and Adhesion, in Relation to Studies of the Interaction of Finely Dispersed Particles. 1. Certain Boundary Properties of Solutions in Narrow Plane Gaps between Solid Surfaces - 748
- Ful', V. E., see Dogadkin, B. A. - 375
- Gasanova, T. G., see Miskarli, A. K. - 179
- Gatovskaya, T. V., see Berestnev, V. A. - 694
- Gengrinovich, B. I. and G. L. Slonimskii. Investigation of the True Fluidity and Elasticity of Rubbers and Raw Rubber Mixes - 137
- Glazman, Iu. M., I. M. Dykman and E. A. Strel'tsova. The Coagulation of Lyophobic Sols by the Action of Mixtures of Electrolytes. Communication II. - 143
- Golubenkova, L. L., B. M. Kovarskaia, M. S. Akutin and G. L. Slonimskii. Thermomechanical Investigation of Epoxide Resins - 29
- Gorbacheva, V. O., and N. V. Mikhailov. The Structure and Phase State of Polyethylene Terephthalate Fibers - 33
- Gor'kova, I. M. Deformation Characteristics of Natural and Dispersed Structures of Some Clays - 547
- Gul', V. E., see Lipatov, S. M. - 245
- Gul', V. E., L. N. Tsarskii and S. A. Vil'nits. Investigation of the Tearing Process in the Region of Transition from the Elastic to the Brittle State - 302
- Hollo, J. and J. Szejtli. Fractionation of Amylose According to the Degree of Polymerization - 219
- Iagodovskaia, T. V., see Liubimova, T. Iu. - 555
- Iaminskaia, E. Ia., see Berestnev, V. A. - 694
- Iampol'skii, B. Ia., see Wu-Shu-Chiu- (U Shu-Tsiu) - 360
- Iudina, I. V., see Bartenev, G. M. - 611
- Iurezhenko, A. I., and G. F. Storozh. The Influence of Ethylene Glycol on the Colloidal Properties of Aqueous Sodium Oleate Solutions - 513
- Iuzhnyi, Z. M. Microscopical Determination of Droplet Size in Oil Mist - 477
- Izmailova, V. N., see Segalova, E. E. - 563
- Kafarov, V. V., see Babanov, B. M. - 115
- Kalina, L. E., see Voiutskii, S. S. - 15
- Kandilarov, G. G. Certain Properties of Calcium Oxalate Precipitates in Electrolyte Solutions - 713
- Kaplunov, M. Ia., see Dogadkin, B. A. - 248
- Kargin, V. A., see Berestnev, V. A. - 694
- Kargin, V. A., N. A. Plate and A. S. Dobrynina. Certain Properties of Block Copolymers Based on an Epoxy Resin and Butadiene-Nitrile Rubber - 315
- Kargin, V. A., see Proshliakova, N. F. - 191
- Kargin, V. A., see Proshliakova, N. F. - 195
- Karpov, V. L., see Dogadkin, B. A. - 248
- Kharitonova, V. P., and A. B. Pakshver. The Effect of the Acetyl Group Content of Acetyl-cellulose on the Properties of Its Solutions - 103
- Khomikovskii, P. M., see B. F. Teplov - 441
- Khrapova, E. V., see Kiselev, A. V. - 419
- Khromov, M. K., see Reznikovskii, M. M. - 348
- Kiselev, A. V. Adsorbate-Adsorbate Interaction in the Adsorption of Vapors on Graphitized Carbon Blacks - 320
- Kiselev, A. V., see Avgul', N. N. - 283
- Kiselev, A. V., N. V. Kovaleva, V. A. Sinitsyn, and E. V. Khrapova. Adsorbate - Adsorbate Interaction in the Adsorption of Vapors on Graphitized Carbon Blacks. 2. Application of the Equation for the Adsorption Isotherms to experimental Data - 419
- Kiselev, A. V., V. I. Lygin, I. E. Neimark, I. B. Sliniakova and Chen' Ven'-han. Electron Microscopic and Adsorption Studies of Silica Sols and Silica Gels - 47
- Klauzen, N. A., see Dogadkin, B. A. - 248
- Kopylova, V. D. and K. M. Ol'shanova. Secondary Effects on Precipitation Chromatograms of Various Compounds - 429
- Koretskii, A. F., see Taubman, A. B. - 631
- Kovaleva, N. V., see Kiselev, A. V. - 419
- Kovarskaia, B. M., see Golubenkova, L. L. - 29
- Krokhina, L. S., see Sandomirskii, D. M. - 279
- Krotova, N. A., see Morozova, L. P. - 55
- Korolev, A. Ia., see Avgul', N. N. - 283

- Korshak, V. V. and S. A. Pavlova. Heterochain Polyamides. 10. The Effect of Some Organic Substances on the Stability of Alcoholic Polyamide Solutions. - 332
- Kortnev, A. V., see Soboleva, N. I. - 742
- Kovaleva, N. V., see Dogadkin, B. A. - 259
- Kremnev, L. Ia. Gelatinized Emulsions. 16. The Influence of Neutral Inorganic Salts on Emulsification. Antagonistic Emulsifiers - 509
- Kremnev and A. I. Perelygina. Gelatinized Emulsions. 15. Limiting-Concentration Emulsions of Paraffin Wax in Water. Structure of Protective Layers - 167
- Kuleznev, V. N., see Dogadkin, B. A. - 39
- Kuleznev, V. N., see Dogadkin, B. A. - 629
- Kuznetsova, N. P. see Samsonov, G. V. - 201
- Levi, S. M. and O. K. Smirnov. Effect of the Structure of Certain Surface-Active Substances on the Foaming of Aqueous Gelatin Solutions - 173
- Likhtman, V. I., see Ostrovskii, V. S. - 597
- Lipatov, S. M., see S. I. Meerson - 336
- Lipatov, S. M., S. S. Voiutskii and V. E. Gul' On the Sixtieth Birthday of Boris Aristarkhovich Dogadkin - 245
- Liubimova, T. Iu. Structure Formation in Compacted Soils - 719
- Liubimova, T. Iu. and T. V. Iagodovskaia. The Role of Plastification and Hydrophobization in the Compaction of Soils - 555
- Losev, Ivan Platonovich (on his 80th birthday) - 235
- Luk'ianova, O. I. and S. A. Dariusina. Mechanism of the Action of Mixed Additives for Cement, Based on a Hydrophilic Plastifier - 585
- Lygin, V. L., see Kiselev, A. V. - 47
- Malinin, N. I. Volarovich, M. P. - 295
- Margolina, Iu. L., see Sandomirskii, D. M. - 279
- Matskevich, E. B. and P. Iu. Butiagin. Some Features of the Comminution of Graphite in an Aqueous Medium - 619
- Mdivnishvili, O. M., and G. V. Vinogradov. Rheological Investigation of Structurized Suspensions of Askangel and Some of Its Derivatives - 531
- Meerson, S. I. and S. M. Lipatov. The Melting of Gelatin Gels - 336
- Meleshko, P. S. Determination of the Adsorption of Solutes on Hydrogels - 728
- Mikhailov, G. P., B. I. Sazhin, and V. S. Presniakova. Effect of the Density of Polytrifluorochloroethylene on Dielectric Loss - 433.
- Mikhailov, N. V., see Gorbacheva, V. O. - 33
- Mikhailov, N. V., see Zav'ialova, N. N. - 708
- Minsker, K. S., see Shevliakov, A. S. - 227
- Mirlas, D. L., see Rogovin, Z. A. - 355
- Mironova, A. K., see Fel'dman, R. I. - 99
- Miskarli, A. K. and T. G. Gasanova. The Structural and Mechanical Properties of Clay Suspensions Used in Difficult Drilling Conditions - 179
- Mokrushin, S. G., and V. I. Borisikhina. Kinetics of Phase Separation in Protected Emulsions - 736
- Mokrushin, S. G., see Degtiarvea, T. A. - 153
- Mokrushin, S. G., see Shveikina, R. V. - 223
- Morozov, A. A. and S. N. Stavrov, The Effect of Cations on the Properties of Black Sea Agaroid - 187
- Morozova, L. P., and N. A. Krotova. Investigation of the Nature of the Adhesion Bond in the bonding of Two High-Molecular Compounds - 55
- Morozova, N. A., see Dogadkin, B. A. - 375
- Natanson, E. M. Formation and Stability of Metal Sols - 519
- Nazarov, V. I., N. P. Silina, and T. P. Tikhomirova. Some Experimental Studies of the Physical Chemistry of Starch - 437
- Neimark, I. E., see Kiselev, A. V. - 47
- Neimark, I. E., see Sliniakova, I. B. - 79
- Nichiporenko, S. P. Physicochemical Mechanics of Disperse Systems in Ceramic Technology - 537
- Novikov, A. S. and F. S. Tolstukhina. Plasticcoelastic Properties of SKN - 26 Rubber - 342
- Ol'shanova, K. M., see Kopylova, V. D. - 429
- Os'minskaya, A. T., see Bresler, S. E. - 381
- Ostrovskii, V. S., and V. I. Likhtman. The Rheology of Metals in Surface Active Media - 597
- Pakshver, A. B., see Kharitonova, V. P. - 103
- Pavlov, V. P., see Vinogradov, G. V. - 237
- Pavlova, S. A., see Korshak, V. V. - 332
- Perelygina, A. I., see Kremnev, L. Ia - 167
- Pevzner, D. M. see Fel'shtein, M. S. - 274.
- Pisarenko, A. P., see Shtarkh, B. V. - 372
- Plate, N. A., see Kargin, V. A. - 315.
- Popov, A. G., see Bresler, S. E. - 381
- Presniakova, V. S., see Mikhailov, G. P. - 433
- Priss, L. S., see Reznikovskii, M. M. - 348
- Proshliakova, N. F., P. I. Zubov and V. A. Kargin. The Structure of Gels. 12. Preparation of Gels from Solutions of Methyl Methacrylate - Methacrylic Acid Copolymer - 191
- Proshliakova, N. F., P. I. Zubov, and V. A. Kargin. The Structure of Gels. 13. Investigation of the Properties of Gels of Methyl Methacrylate - Methacrylic Acid Copolymer Containing Univalent Metals - 195

- Rebinder, P. A. Modern Problems of Colloid Chemistry. I. Formation and Aggregative Stability of Disperse Systems - 493
 Rebinder, P. A., see Bartenev, G. M. - 611
 Rebinder, P. A., see Segalova, E. E. - 571
 Rebinder, P. A., see Shchukin, E. D. - 601
 Rebinder, P. A., see Titov, A. I. - 87
 Reznikovskii, M. M., L. S. Priss, and M. K. Khromov. Effect of the Composition of Rubber on its Fatigue Characteristics - 348
 Rogovin, Z. A. and D. L. Mirlas. The Effect of the Regularity of Structure of Triacetylcellulose on its Solubility and the Properties of its Solutions - 355
 Rufimskii, P. V. Studies of Aluminum Hydroxide Hydrosols - 739.
 Rzhavskaya, F. M., see A. A. Trapeznikov - 243
 Saminskii, E. M., see Bresler, S. E. - 381
 Samsonov, G. V. and N. P. Kuznetsova. Equation for the Sorption Isotherm of Amino Acids on Ion Exchange Resins in the Hydrogen Form - 201
 Samsonova, T. I. and S. Ia. Frenkel'. The Hydrodynamic Characteristic and Polydispersity of Some Ethylcellulose Specimens - 63
 Sandomirskii, D. M., Iu. L. Margolina, B. A. Dogadkin and L. S. Krokhina. Ionic Deposition from Carboxylic Divinyl-Styrene Reflexes - 279
 Sandomirskii, D. M., and M. K. Vdovchenkova. Investigation of the Coagulation of Rubber Latexes with the Aid of Radioactive Isotopes - 75
 Sandomirskii, D. M. and M. K. Vdovchenkova, A Radioactive Isotope Study of the Ionic Deposition of Rubber from Latex - 205
 Sarkisian, R. R., see Segalova, E. E. - 571
 Sazhin, B. I., see Mikhailov, G. P. - 433
 Segalova, E. E. and V. N. Izmailova. Structure Formation in the Course of Hydration Hardening of Calcium Sulfate Hemihydrate (Plaster of Paris) - 563
 Segalova, E. E., R. R. Sarkisian and P. A. Rebinder. Effect of Additions of a Hydrophilic Plastifier on the Kinetics of Structure Formation in the Hardening of Cement - 571
 Segalova, E. E., see Solov'eva, E. S. - 579
 Serb-Serbina, N. N. Physicochemical Principles of the Regulation of Mechanical Properties of the Structures in Clay-Water Systems - 525
 Shakhel'dian, B. N. The Stabilization of Carbon-Black Suspensions in Vaseline Oil - Drying Oil Mixtures - 467
 Shalia, V. V., see Vysotskii, Z. Z. - 23
 Shaposhnikova, L. D., see Shkodin, A. M. - 231
 Shcherbakov, L. M. A traditional Error in the Theory of Capillarity - 471
 Shcherbakov, L. M. Calculation of Work of Homogeneous Nucleus-Formation in Vapor Condensation - 759
 Shchukin, E. D. and P. A. Rebinder. Formation of New Surfaces in the Deformation and Destruction of a Solid in a Surface-Active Medium - 601
 Shershnev, V. A., see Dogadkin, B. A. - 119
 Sheviakov, A. S. and K. S. Minsker. The Site of Polymerization of Unsaturated Compounds in Systems Containing Protective Colloids. - 227
 Shkodin, A. M. and L. D. Shaposhnikova. The Adsorption of Similarly Charged Ions in the Coagulation of Sols by Electrolytes. 1. Radiometric Measurements - 231
 Shtarkh, B. V. and A. P. Pisarenko. Electron Microscope Investigation of the Plasticization of a Dispersion of Vinyl Chloride-Vinylidene Chloride Copolymer - 372
 Shveikina, R. V. and S. G. Mokrushin. Influence of Electrolytes on the Coagulation of Colloidal Particles at the Liquid - Gas Interphase - 223
 Silina, N. P., see Nazarov, V. I. - 437
 Sinitysyn, V. A., see Kiselev, A. V. - 419
 Skorodumova, Z. V., see Dogadkin, B. A. - 259
 Sliniakova, L. B., see Kiselev A. V. - 47
 Sliniakova, L. B., and L. E. Neimark. The Structure and Adsorptive Properties of Silica Gels Prepared from Alkaline Media - 79
 Slonimskii, G. L., see Gengrinovich, B. I. - 137
 Slonimskii, G. L., see Golubenkova, L. I. - 29
 Snirnov, O. K., see Levi, S. M. - 173
 Smirnova, A. M., see Zaitseva, N. G. - 593
 Soboleva, N. L., A. G. Bol'shakov and A. V. Kortnev. Sedimentation of Magnesium Hydroxide Suspension in an Ultrasonic Field - 742
 Sokolov, S. I., see Fel'dman, R. I. - 99
 Sokolov, S. I., see Fel'dman, R. I. - 366
 Solov'eva, E. S., and E. E. Segalova, Kinetics of Crystallizational Structure Formation in the Hydration Hardening of Tricalcium Aluminate - 579
 Stavrov, S. N., see Morozov, A. A. - 187
 Storozh, G. F., see Iurzhenko, A. I. - 513
 Strel'tsova, E. A., see Dykman, I. M. - 143
 Sysova, F. D., see Volarovich, M. P. - 117
 Szejtli, J., see Hollo, J. - 219
 Tarasova, Z. N., see Dogadkin, B. A. - 39
 Tarasova, Z. N., see Dogadkin, B. A. - 248

- Taubman, A. B. and S. I. Burshtein. Some Characteristics of the Adsorption of Surface-Active Substances in Nonaqueous Media - 503
- Taubman, A. B. and A. F. Koretskii. The role of the Structuromechanical Factor in Emulsion Stability - 631
- Teplov, B. F. and P. M. Khorikovskii. The Topochemistry of Drop Polymerization of Vinyl Chloride - 441
- Tikhomirova, T. P., see Nazarov, V. I. - 437
- Titov, A. I. and I. N. Vlodavets and P. A. Rebinder. Processes of Structure Formation in Milk Fat and Their Significance in the Production of Butter - 87
- Tolstukhina, F. S., see Novikov, A. S. - 342
- Trapeznikov, A. A. Relaxation of Deformation and Repeated Deformation of Aluminum Naphthenate Gels - 447
- Trapeznikov, A. A. and T. V. Asanova. A Study of the Strength and High-Elastic Properties of Rubber Solutions and Their Vulcanizates at High Deformation Rates - 376
- Trapeznikov, A. A., G. V. Belugina and F. M. Rzhavskaya. Influence of Ratio of Free to Bound Alkali in the Precipitation of Aluminum Soaps on their Thickening Properties - 243
- Trapeznikov, A. P., see Belugina, G. V. - 1
- Tropin, V. P., see Volarovich, M. P. - 9
- Tsarskii, L. N., see Gul', V. E. - 302
- Tutorskii, I. A., see Dogadkin, B. A. - 260
- Uskov, I. A. and E. T. Uskova. Electrochemical Study of Bentonite Suspensions. 2. The Progressive Action of Sodium Hydroxide on Suspensions of Electrodialyzed Askan-gel - 457
- Uskova, E. T. The Hydrophilic Properties of Montmorillonite Clay - 95
- Uskova, E. T., see Uskov, I. A. - 457
- Vasil'ev, D. F. Nature of the Reaction of Aluminum Naphthenate Formation. 2. Preparation of Aluminum Naphthenate by the Mixing of a Suspension of Aluminum Hydroxide with an Emulsion of Naphthenic Acids - 393
- Vdovchenkova, M. K., see Sandomirskii, D. M. - 75
- Vdovchenkova, M. K., see Sandomirskii, D. M. - 205
- Vil' nits, S. A., see Gul', V. E. - 302
- Vinogradov, G. W., see Mdivnishvili, O. M. - 531
- Vinogradov, G. V. and V. P. Pavlov. The Fluidity and Strength of Structurized Disperse Systems - 237
- Vlasova, T. I. Study of the Foaming of Molasses - 397
- Vlodavets, I. N., see Titov, A. I. - 87
- Voitsekhovskii, R. V. and A. M. Vovnenko. Influence of the Disperse Phase on the Results of Hydrogen-Ion Activity Determination in Salt Solutions - 697
- Voiutskii, S. S., V. I. Alekseenko and L. E. Kalinina. Compatibility of Nitrocellulose with Butadiene-Acrylonitrile Copolymers. 4. Relaxation Properties of Binary Mixtures - 15
- Voiutskii, S. S., see Lipatov, S. M. - 245
- Voiutskii, S. S., see Wu-Shu-Chiu (U Shu-Tsiu) - 360
- Volarovich, M. P. and N. I. Malinin. A Study of the Rheological Properties of Low-Moisture Peats - 295
- Volarovich, M. P., F. D. Sysoeva, V. V. Cherniav-skaia and N. V. Churaev. Determination of the Bound Water Content in Peat by the Method of the Negative Adsorption of a Radioactive Tracer - 117
- Volarovich, M. P., and V. P. Tropin. Investigation of the Dispersity of Sapropels by Means of the Sedimentometer and the Electron Microscope - 9
- Vovnenko, A. M., see Voitsekhovskii, R. B. - 697
- Vysotskii, Z. Z., and V. V. Shalia. The Heats of Hydration of Some Cations and the Effect of Their Adsorption on the Structure of Silica Gels - 23
- Weber, K. Character of the Relaxation of Non-vulcanized Rubber Mixes - 129
- Wu-Shu-Chiu (U Shu-Tsiu), B. Ia. Iampol'skii and S. S. Voiutskii. Structure Studies in Carbon-Black Suspensions. 3. The Effect of Polymer Additions to Concentrated Carbon Black Suspensions in a Hydrocarbon Medium - 360
- Zadumkin, S. N. The Surface Tension of Disperse Systems - 163
- Zaitseva, N. G. and A. M. Smirnova. Influence of Surface-Active Substances on the Crystallization of Tricalcium Hydroaluminate - 593
- Zav'ialova, N. N. and N. V. Mikhailov. Factors Determining the Structuromechanical Properties of Viscose Solutions - 708
- Zavorkhina, N. A. and V. G. Ben'kovskii. The Mechanism of Stabilization of Clay Suspensions by an Algal Extract - 411
- Zhbankov, R. G., see Ermolenko, I. N. - 405
- Zubov, P. I., see Proshliakova, N. F. - 191.

Zubov, P. I., see Proshliakova, N. F. - 195

Zubov, P. I., see Zverev, M. P. - 312

Zverev, M. P., E. A. Eroshkina, and P. I. Zubov.

The Structure of Gels. 14. Influence of the
Nature of the Plasticizer on the Properties of
filled Divinyl-Styrene Rubber - 312

